pharmaceutics

Special Issue Reprint

Therapeutic Drug Monitoring and Pharmacokinetics-Based Individualization of Drug Therapy

Edited by
Barna Vasarhelyi and Gellért Balázs Karvaly

mdpi.com/journal/pharmaceutics

MDPI

Therapeutic Drug Monitoring and Pharmacokinetics-Based Individualization of Drug Therapy

Therapeutic Drug Monitoring and Pharmacokinetics-Based Individualization of Drug Therapy

Editors

Barna Vasarhelyi
Gellért Balázs Karvaly

MDPI

Basel • Beijing • Wuhan • Barcelona • Belgrade • Novi Sad • Cluj • Manchester

Editors

Barna Vasarhelyi
Semmelweis University
Budapest
Hungary

Gellért Balázs Karvaly
Semmelweis University
Budapest
Hungary

Editorial Office
MDPI AG
Grosspeteranlage 5
4052 Basel, Switzerland

This is a reprint of articles from the Special Issue published online in the open access journal *Pharmaceutics* (ISSN 1999-4923) (available at: https://www.mdpi.com/journal/pharmaceutics/special_issues/drug_monitoring_pharmacokinetics).

For citation purposes, cite each article independently as indicated on the article page online and as indicated below:

Lastname, A.A.; Lastname, B.B. Article Title. *Journal Name* **Year**, *Volume Number*, Page Range.

ISBN 978-3-7258-2021-4 (Hbk)
ISBN 978-3-7258-2022-1 (PDF)
doi.org/10.3390/books978-3-7258-2022-1

Contents

About the Editors

Barna Vasarhelyi

Barna Vasarhelyi has been the director of the Department of Laboratory Medicine, Semmelweis University, Budapest, the largest clinical laboratory department of Hungary, since 2011. He supervises the operation of nine laboratories which house all of the laboratory specialties currently known. Barna has also been acting as the chief clinical laboratory specialist in Hungary since 2019. He graduated from Semmelweis University as a medical doctor in 1992, and obtained his Ph.D. and D.Sc. degrees in 1998 and 2009 in nephrology and pediatrics, respectively. He has invented tests for clinical chemistry and immunology, performed research in translational medicine, and conducted population studies in pediatric patients.

Gellért Balázs Karvaly

Gellért Balázs Karvaly is the head of the Laboratory of Mass Spectrometry and Separation Technology, Department of Laboratory Medicine, Semmelweis University, Budapest, Hungary. He graduated as a pharmacist (Pharm.D.) from the University of Szeged, Hungary, in 2001, and received his Ph.D. degree from the Miklós Zrínyi National Defense University, Budapest, in 2008 for his research conducted in the field of military toxicology. Gellert founded the Laboratory of Mass Spectrometry and Separation Technology with Barna Vásárhelyi in 2017, and has been devoted to managing and developing it with a special focus on therapeutic drug monitoring. He is keen on the processing of the results of bioanalysis with pharmacokinetic and biostatistics tools to generate laboratory data which can be implemented directly into clinical practice. In his spare time, Gellért eagerly pursues activities with his family, his spouse Szilvi, his son Sebestyén, and his daughter Patrícia.

Preface

Until approximately 2015, the idea of linking therapeutic drug monitoring (TDM) to pharmacokinetic interpretation was incepted only by a handful of dedicated professionals. In the past years, the world has turned, and development in TDM has been tightly linked to clinical pharmacokinetics and pharmacometrics. This change has taken place very fast as the result of considerable improvements in digital technology. Recently, the power of machine learning and artificial intelligence has also been discovered, and efforts are already underway to guide drug therapies using these tools.

Nevertheless, the idea has been around for over fifty years, and suitable computer software has been available for a substantial part of this period. Experiencing the hesitation to implement the findings in healthcare facilities, as well as seeing that the clinical utility of TDM is not yet accepted in all medical fields, one may have several questions: are we advancing in the right direction? Will this recent leap into the future spark enthusiasm soon, or shall conservative concepts, including the "one dose fits all" approach, prevail until marketed precision pharmacotherapy software platforms with user-friendly graphical interfaces will be available, providing full assistance for clinical decision making and eliminating the need to gain insight into the underlying theory and processes in order to come to the correct conclusions? Who can be expected to be in possession of the knowledge required to apply the software tools properly in healthcare facilities—pharmacists? The clinical laboratory? Bioinformatics experts? Clinicians? Will the precision pharmacotherapy approach ever be implemented in minor facilities, or will it remain within the ivory towers of academic institutions?

The more research performed, the more answers that can be provided to these and other related questions. The chapters of this reprint provide insight into studies performed by renowned experts in a broad range of clinical fields, showing that the distinct level of evidence provided by TDM is important from ophthalmology to transplantation surgery and from the treatment of adults to the therapy of pediatric patients. It is demonstrated that parametric and nonparametric modeling could equally work, and that a broad range of software applications are available to aid clinical decision making. We expect that understanding the approaches and the findings of these studies will contribute to the constructive interpretation of TDM results.

We would like to thank the contributors of the manuscripts published in the Special Issue "Therapeutic drug monitoring and pharmacokinetics-based individualization of drug therapy" of the journal *Pharmaceutics* for submitting their works and for cooperating with the managing editors and guest editors tirelessly until publication was completed. We express our deepest gratitude to the reviewers who devoted their time to perform the peer review of the manuscripts. We are indebted to the editors of *Pharmaceutics*, especially Ms. Lovia Hu, for their proactive cooperation, patience, and eagerness to look for a solution whenever we were in need of them. Finally, we are thankful to our families for allowing us time to work on the submissions and on the compilation of this reprint.

We hope that the readers will find the compilation useful and will gain inspiration for their research and efforts in healing. Patients belonging to one of the populations covered are often in grave need of state-of-the-art medical care, and we sincerely hope that the information conveyed by the chapters will take healthcare providers closer to the optimized treatment of individuals diagnosed with any of the conditions discussed in the reprint.

Barna Vasarhelyi and Gellért Balázs Karvaly

Editors

pharmaceutics

MDPI

Editorial

Therapeutic Drug Monitoring and Pharmacokinetics-Based Individualization of Drug Therapy

Gellert Balazs Karvaly * and Barna Vásárhelyi

Department of Laboratory Medicine, Faculty of Medicine, Semmelweis University, 4 Nagyvárad Square, 1089 Budapest, Hungary; vasarhelyi.barna@semmelweis.hu

* Correspondence: karvaly.gellert.balazs@semmelweis.hu

1. Introduction

The philosophy, practice, and clinical impact of therapeutic drug monitoring (TDM) has changed profoundly with the appearance of widely available and, in a technical sense, commonly applicable modeling, simulation, and dosing software tools in the past decade. As a result, TDM, once a marginal field of clinical chemistry, has grown into a multidisciplinary branch of clinical medicine, allowing laboratory and pharmacometrics professionals to deliver highly relevant clinical information for supporting the management of pharmacotherapy. The newborn discipline has been given the name "model-informed precision dosing", and is progressing to become a game changer in medicine as it lends itself to being boosted in performance and utility by machine learning and artificial intelligence tools. The eventual scope of the revolution model-informed precision dosing is bringing about is to implement individualized, patient-centric treatments [1].

TDM-guided therapies are most promising to patients with outstanding vulnerability and with atypical properties in terms of the pharmacokinetic fate of the drugs administered. Examples include oncology patients, the critically ill, those receiving donated organs, or those who have undergone major surgery. In addition, entire populations, such as children or the obese, must also be viewed as subjects to special dosing strategies. Importantly, people who are different from the majority of patients due to having atypical biological features, such as a pharmacogenetic mutation or a liver disease, will also require individual therapeutic approaches.

The nineteen research articles and the five review papers appearing in this Special Issue cover vulnerable patient populations, unique scenarios, and novel methodologies to demonstrate the utility of TDM and the pharmacokinetic processing of measurement results. Several works focus on improving the administration of anti-infective agents. On this list, one can find novel antibiotics (cefiderocol and dalbavancin) as well as ones employed globally (gentamicin, piperacillin, rifampicin, tobramycin, and vancomycin). Treatment with the antifungal isavuconazole, as well as with the antivirals ganciclovir and the cabotegravir–rilpivirine combination, are discussed. Articles focusing on immunosuppressant therapy, which is ever more often based on TDM, explore the clinical pharmacokinetics of busulfan, methotrexate, mycophenolate, and tacrolimus. Other entities, mentioned less often in the related literature, include haloperidol, omeprazole, and the combination of the antidiabetics dapagliflozin and linagliptin. Finally, this volume contains five review papers related to four different fields of clinical medicine.

2. Overview of the Published Works

2.1. Immunosuppressants

The optimization of tacrolimus dosing regimens is one of the core areas of TDM and pharmacokinetics-based treatment. Contribution (1) demonstrated the applicability of this approach in patients undergoing heart transplants. This study spans a year after receiving the organ and delivers in-depth information on the relationship between tacrolimus levels

Citation: Karvaly, G.B.; Vásárhelyi, B. Therapeutic Drug Monitoring and Pharmacokinetics-Based Individualization of Drug Therapy. *Pharmaceutics* **2024**, *16*, 792. https://doi.org/10.3390/pharmaceutics16060792

Received: 27 May 2024
Accepted: 5 June 2024
Published: 11 June 2024

measured in whole blood and endomyocardial biopsies. An important conclusion from this study is that tacrolimus concentrations attained in the target graft organ cannot be safely estimated by determining systemic drug levels.

Methotrexate is widely administered as an immunosuppressant in pediatric oncology for the treatment of acute lymphoblastic leukemia. The remarkable interindividual variability in its pharmacokinetic properties merits model-informed precision dosing for optimized treatments. In contribution (2), six population pharmacokinetic models, published earlier, are compared with an independent external evaluation patient dataset compiled by the authors. The message obtained from this study is that pharmacokinetic models should be validated by each healthcare facility prior to their adoption.

In a retrospective monocentric study, the impact of the co-administration of calcineurin inhibitors on the twelve-hour area under the concentration–time curve of mycophenolic acid, its primary pharmacokinetic marker related to clinical efficacy, is investigated in 21 adults who have undergone a heart transplant. The follow-up had lasted at least 12 months following the transplant and the beginning of mycophenolate mofetil therapy. Exposure to mycophenolic acid, as well as its peak and trough concentrations, have been considerably lower in cases where acute cellular rejection (ACR) of the implanted organ has occurred. In addition, in comparison to the co-administration of tacrolimus, co-medication with cyclosporine A has resulted in a substantially higher proportion of cases with ACR (contribution (3)).

2.2. Anti-Infectives

The clinical pharmacokinetics of ganciclovir have been explored in patients diagnosed with cystic fibrosis (CF) who have undergone lung transplants using Bayesian modeling, with the findings being compared to those observed in non-cystic fibrosis patients. The clearance of this antiviral appears to be higher in the CF population, leading to lower systemic exposure. Nomograms are provided for administering loading and maintenance doses by taking the height of the patients and the estimated glomerular filtration rates into account (contribution (4)).

The preliminary pharmacokinetic results of a nationwide multicenter study with the scope of following up HIV-positive patients receiving a combined long-acting injectable formulation of cabotegravir–rilpivirine by therapeutic drug monitoring are presented in contribution (5). This work was the first to test pharmacokinetic models for the real patient population, with the aim of defining a trough therapeutic range.

Isavuconazole is a relatively new agent effective against systemic fungal infections. It was approved for the treatment of invasive aspergillosis and invasive mucormyosis in December 2023, but, prior to that date, it had been used off-label for the treatment of immunocompromised pediatric patients. Contribution (6) described the retrospective pharmacokinetic evaluation of the TDM program of isavuconazole conducted in a pediatric hospital and offers a methodology for the optimized, model-informed precision dosing of isavuconazole in this especially vulnerable patient population.

Cefiderocol is a new cephalosporin active against Gram-negative strains, including those producing beta-lactamase and carbapenemase. The authors of contribution (7) investigated its population pharmacokinetics in critically ill adults for the first time. They revealed that serum albumin concentration and chronic kidney disease are predictors of the proportion of the unbound fraction of cefiderocol in the circulation.

A novel approach to estimating individual piperacillin concentrations by constructing nonparametric artificial population pharmacokinetic (PK) quasi-models is described in contribution (8). The number of volunteers included in a population pharmacokinetic study is often low, which results in limited utility, including the comparability of findings. The authors of this study demonstrated that the quasi-models are efficient for augmenting population PK models and could provide a tool for generating individual concentration estimates when the population PK model has been obtained by including data from a small set of subjects.

The efficient guidance of vancomycin dosing is an especially complex task in pediatric patients, considering the variability of the physiological properties of different age groups and of various individuals in each age group. The authors of contribution (9) presented population pharmacokinetic models by evaluating renal function using urinary and blood cystatin C and neutrophil gelatinase-associated lipocalin (NGAL) concentrations. Three modeling approaches were compared in this study, and it was demonstrated that their performance cannot be associated with the complexity of the model, favoring the consideration of simpler models for clinical use.

Dalbavancin is one of the very few new entities available for the treatment of serious Gram-positive bacterial infections. It has an unusual pharmacokinetic profile, including an elimination half-life of over 400 h. The strategy of its administration, as well as the monitoring of the course of therapy, is substantially different from that applied to most drugs. In contribution (10), the associations and correlations of four dosing regimens with the characteristics of patients, the pathogen, and the clinical situation are discussed, including the analysis of the relationship between individual dalbavancin pharmacokinetics and therapeutic outcomes.

In contribution (11), the authors demonstrate that the implementation of model-informed precision dosing of tobramycin for treating pulmonary exacerbations caused by *Pseudomonas aeruginosa* in cystic fibrosis results in the administration of higher doses and is also associated with success in therapy. They also show that, in spite of dose elevations, renal function improves by the end of the treatment.

The external validation of population pharmacokinetic models may not necessarily demonstrate their broader utility. For such cases, the re-estimation of gentamicin model parameters is proposed in contribution (12). Four parametric models, published earlier, are applied to two datasets obtained by the authors in critically ill populations in the framework of TDM conducted at their facility. It was shown that none of them is capable of making acceptable predictions of pharmacokinetic–pharmacodynamic targets, but their performance is improved substantially when model parameters are re-estimated using the new datasets. In the future, this re-estimation strategy may prevent the construction of redundant models, with the incorporation of new data increasing the robustness of existing ones.

An account was given by contribution (13) concerning treatment with 10 mg/kg rifampicin based on TDM to take initiative against the high prevalence of tuberculosis in native Paraguayans in comparison to non-natives. In this study, a realistic procedure was elaborated for collecting dried blood samples from tuberculosis patients across the country. The probabilities of pharmacokinetic–pharmacodynamic target attainment were calculated. When individual minimal inhibitory concentration (MIC) values were not available, the attainment of targets depended solely on the hypothetical MIC considered. The authors of this study concluded that administering an increased dose (35 mg/kg) of rifampicin warrants investigation for improving outcomes.

2.3. Miscellaneous Drugs

Contribution (14) is the first clinical study to describe the pharmacokinetics of busulfan in patients diagnosed with neurofibromatosis, a condition that can currently be cured only by hematopoietic stem cell transplantation. This was also the first effort to include the metabolite sulfolane in a busulfan population pharmacokinetic model. Total body weight was identified as the main covariate. The findings were expected to allow the individualized dosing of busulfan to neurofibromatosis patients, restricting the development of irreversible liver impairment.

Anticoagulant therapy has changed dramatically since the introduction of direct-acting oral anticoagulants. Although the relationship between the pharmacokinetics and the pharmacodynamic effects of these drugs is still unclear, it is now understood that the interindividual variability of exposure is high and overexposure may cause adverse effects. Population pharmacokinetic models based on real-life therapeutic drug monitoring as well

as simulations are presented in contribution (15) to compare the exposure to rivaroxaban, administered to Thai adults diagnosed with non-valvular atrial fibrillation based on renal function, or in standard dosages. It is shown that in this population, renal function and body weight are covariates, and the prescription of standard 20 mg dosages will likely lead to overexposure.

The impact of C-reactive protein (CRP) on exposure to haloperidol following the administration of low haloperidol doses in critically ill adults was described in contribution (16). By constructing its parametric Bayesian model and by performing Monte Carlo simulations, the authors showed that the clearance of haloperidol is negatively correlated with increasing CRP up to approximately 50 mg/L, pointing to the utility of individualized dosing at the intensive care unit to overcome delirium.

In contribution (17), the pharmacokinetics and safety of the antidiabetics dapagliflozin and linagliptin, given as an experimental combination product formula, were compared to those recorded during the separate administration of the two substances in a randomized, open-label, single-dose study conducted with healthy male volunteers. The bioequivalence of the two formulations was demonstrated, providing important evidence that the combined administration of these pharmacologically complementary entities is a rational, patient-centric approach.

Gastrectomy can alter the absorption of drugs from the gastrointestinal system profoundly. Laparoscopic sleeve gastric surgery (LSG), a widely employed bariatric intervention, leads to a considerable reduction in gastric capacity and, as a result, increased acid reflux, which is countered by the prolonged administration of proton pump inhibitors (PPIs). In contribution (18), it is shown that the faster absorption of omeprazole, a well-known PPI, takes place after surgery has been performed. The results of the comparison of omeprazole exposure among normal, intermediate, and poor cytochrome P2C19 metabolizer obese patients who have undergone LSG are also presented. The authors concluded that 20 mg of omeprazole given once daily is sufficient for this population.

One of the key advantages of pharmacokinetics-based individualized drug therapy is that, given a population pharmacokinetic model relying on rich data, individual pharmacokinetic information can be inferred by measuring drug concentrations in a small number of samples (referred to as a *limited sampling strategy*). An approach is provided in contribution (19) to evaluating the robustness of such strategies by assessing the elimination of iohexol, a gold standard in characterizing glomerular filtration rates, from the circulation by enforcing pre-planned deviations from planned sampling times.

2.4. Reviews

In this work, timely topics related to cystic fibrosis, oncology, ophthalmology, and psychiatry are reviewed. Westra et al. discussed pharmacological approaches to increasing exposure to protein kinase inhibitors (contribution (20)). In another article, an overview is provided of current knowledge regarding the therapeutic monitoring of these substances in peripheral fluid spaces (contribution 21). Comprehensive updates are presented on the monitoring of cystic fibrosis transmembrane conductance regulators (CFTCRs) as well as of biological therapy substances applicable against non-infectious uveitis in contributions (22) and (23). Finally, a review of the most recent literature of TDM in psychiatry, starting with the publication of the latest update of the widely accepted guidelines of the Arbeitsgemeinschaft fur Neuropsychopharmakologie und Pharmakopsychiatrie, is delivered [2].

3. Future Perspectives

Claiming that we have entered a golden era of TDM is perhaps not an exaggeration. The diversity and outstanding importance of the topics, the multitude of software employed, and the long road that lies ahead in implementing the approaches described clearly highlight the perspectives of this exciting and versatile field. It is also evident that multidisciplinarity is of key significance; the structures, procedures, and infrastructure maintaining

the efficiency of the multidisciplinary clinical teams must be elaborated and continuously improved to support the translation of the knowledge that emerges into clinical protocols. These challenges raise a plethora of scientific questions, which will certainly keep the topics of therapeutic drug monitoring and pharmacokinetics-based individualized treatment current for years to come.

Author Contributions: Conceptualization, G.B.K. and B.V.; writing—original draft preparation, G.B.K.; writing—review and editing, B.V. All authors have read and agreed to the published version of the manuscript.

Funding: This editorial received no external funding.

Conflicts of Interest: The authors declare no conflicts of interest.

List of Contributions:

1. De Gregori, S.; De Silvestri, A.; Cattadori, B.; Rapagnani, A.; Albertini, R.; Novello, E.; Concardi, M.; Arbustini, E.; Pellegrini, C. Therapeutic drug monitoring of tacrolimus-personalized therapy in heart transplantation: new strategies and preliminary results in endomyocardial biopsies. *Pharmaceutics* **2022**, *14*, 1247.
2. Wang, S.; Yin, Q.; Yang, M.; Cheng, M.; Xie, F. External evaluation of population pharmacokinetic models of methotrexate for model-informed precision dosing in pediatric patients with acute lymphoid leukemia. *Pharmaceutics* **2023**, *15*, 569.
3. Lo Re, F.; Angelini, J.; Sponga, S.; Nalli, C.; Zucchetto, A.; Biasizzo, J.; Livi, U.; Baraldo, M. Therapeutic drug monitoring of mycophenolic acid as a precision medicine tool for heart transplant patients: results of an observational pharmacokinetic pilot study. *Pharmaceutics* **2022**, *14*, 1304.
4. Dvorácková, E.; Sima, M.; Petrus, J.; Klapková, E.; Hubácek, P.; Pozniak, J.; Havlín, J.; Lischke, R.; Slanar, O. Ganciclovir pharmacokinetics and individualized dosing based on covariate in lung transplant recipients. *Pharmaceutics* **2022**, *14*, 408.
5. Thoueille, P.; Alves Saldanha, S.; Schaller, F.; Munting, A.; Cavassini, M.; Braun, D.; Günthard, H.F.; Kusejko, K.; Surial, B.; Furrer, H.; et al. Real-Life Therapeutic concentration monitoring of long-acting cabotegravir and rilpivirine: preliminary results of an ongoing prospective observational study in Switzerland. *Pharmaceutics* **2022**, *14*, 1588.
6. Elhence, H.; Mongkolrattanothai, K.; Mohandas, S.; Neely, M.N. Isavuconazole pharmacokinetics and pharmacodynamics in children. *Pharmaceutics* **2023**, *15*, 75.
7. Zahr, N.; Urien, S.; Llopis, B.; Noé, G.; Tissot, N.; Bihan, K.; Junot, H.; Marin, C.; Mansour, B.; Luyt, C-E.; Bleibtreu, A.; Funck-Brentano, C. Total and unbound pharmacokinetics of cefiderocol in critically ill patients. *Pharmaceutics* **2023**, *15*, 2786.
8. Karvaly, G.B.; Vincze, I.; Neely, M.N.; Zátroch, I.; Nagy, Zs.; Kocsis, I.; Kopitkó, Cs. Modeling pharmacokinetics in individual patients using therapeutic drug monitoring and artificial population quasi-models: a study with piperacillin. *Pharmaceutics* **2024**, *16*, 358.
9. Downes, K.J.; Zuppa, A.F.; Sharova, A.; Neely, M.N. Optimizing vancomycin therapy in critically ill children: a population pharmacokinetic study to inform vancomycin area under the curve estimation using novel biomarkers. *Pharmaceutics* **2023**, *15*, 1336.
10. Stroffolini, G.; De Nicoló, A.; Gaviraghi, A.; Mula, J.; Cariti, G.; Scabini, S.; Manca, A.; Cusato, J.; Corcione, S.; Bonora, S.; Di Perri, G.; De Rosa, F.G:; D'Avolio, A. Clinical effectiveness and pharmacokinetics of dalbavancin treatment-experienced patients with skin; osteoarticular; or vascular infections. *Pharmaceutics* **2022**, *14*, 1882.
11. Reverchon, J.; Tuloup, V.; Garreau, R.; Nave, V.; Cohen, S.; Reix, P.; Durupt, S.; Nove-Josserand, R.; Durieu, I.; Reynaud, Q.; Bourguignon, L.; Charles, S.; Goutelle, S. Implementation of model-based dose adjustment of tobramycin in adult patients with cystic fibrosis. *Pharmaceutics* **2022**, *14*, 1750.
12. Duong, A.; Simard, C.; Williamson, D.; Marsot, A. Model re-estimation: an alternative for poor predictive performance during external evaluations? Example of gentamicin in critically ill patients. *Pharmaceutics* **2022**, *14*, 1426.
13. Ghimire, S.; Molinas, G.; Battaglia, A.; Martinez, N.; Paciello, L.G.; Aguirre, S.; Alffenaar, J-W.C.; Sturkenboom, M.G.G.; Magis-Escurra, C. Dried blood spot sampling to assess rifampicin exposure and treatment outcomes among native and non-native tubercolosis patients in Paraguay: an exploratory study. *Pharmaceutics* **2023**, *15*, 1089.

14. Dadkhah, A.; Wicha, S.G.; Kröger, N.; Müller, A.; Pfaffendorf, C.; Riedner, M.; Badbaran, A.; Fehse, B.; Langebrake, C. Population pharmacokinetics of busulfan and its metabolite sulfolane in patients with myelofibrosis undergoing hematopoietic stem cell transplantation. *Pharmaceutics* **2022**, *14*, 1145.
15. Singkham, N.; Phrommintikul, A.; Pacharasupa, P.; Norasetthada, L.; Gunaparn, S.; Prasertwitayakij, N.; Wongcharoen, W.; Punyawudho, B. Population pharmacokinetics and dose optimization based on renal function of rivaroxaban in thai patients with non-valvular atrial fibrillation. *Pharmaceutics* **2022**, *14*, 1744.
16. Li, L.; Sassen, S.D.T.; van der Jagt, M.; Endeman, H.; Koch, B.C.P.; Hunfeld, N.G.M. Pharmacokinetics of haloperidol in critically ill patients: is there an association with inflammation? *Pharmaceutics* **2022**, *14*, 549.
17. Park, J.-W.; Kim, J.-M.; Noh, J.H.; Kim, K.-A.; Chung, H.; Kim, E.; Kang, M.; Park, J.-Y. Pharmacokinetics of a fixed-dose combination product of dapagliflozin and linagliptin and its comparison with co-administration of individual tablets in healthy humans. *Pharmaceutics* **2022**, *14*, 591.
18. Chen, K.; Luo, P.; Zhu, S.; Lin, Y.; Yang, N.; Huang, S.; Ding, Q.; Zhu, L.; Pei, Q. Effect of laparoscopic sleeve gastrectomy on the pharmacokinetics of oral omeprazole using a population approach. *Pharmaceutics* **2022**, *14*, 1986.
19. Hovd, M.; Robertsen, I.; Woillard, J.-B.; Åsberg, A. A method for evaluating róobustness of limited sampling strategies—exemplified by serum iohexol clearance for determination of measured glomerular filtration rate. *Pharmaceutics* **2023**, *15*, 1073.
20. Westra, N.; Touw, D.; Lub-de Hooge, M.; Kosterink, J.; Oude Munnink, T. Pharmacokinetic boosting of kinase inhibitors. *Pharmaceutics* **2023**, *15*, 1149.
21. Köllő, Z.; Garami, M.; Vincze, I.; Vásárhelyi, B.; Karvaly, G.B. Therapeutic monitoring of orally administered, small-molecule anticancer medications with tumor-specific cellular protein targets in peripheral fluid spaces—a review. *Pharmaceutics* **2023**, *15*, 239.
22. Choong, E.; Sauty, A.; Koutsokera, A.; Blanchon, S.; André, P.; Decosterd, L. Therapeutic drug monitoring of ivacaftor, lumacaftor, tezacaftor, and elexacaftor in cystic fibrosis: where are we now? *Pharmaceutics* **2022**, *14*, 1674.
23. Busto-Iglesias, M.; Rodríguez-Martínez, L.; Rodríguez-Fernández, C.A.; González-López, J.; González-Barcia, M.; de Domingo, B.; Rodríguez-Rodríguez, L.; Fernández-Ferreiro, A.; Mondelo-García, C. Perspectives of therapeutic drug monitoring of biological agents in non-infectious uveitis treatment: a review. *Pharmaceutics* **2023**, *15*, 766.
24. Pennazio, F.; Brasso, C.; Villari, V.; Rocca, P. Current status of therapeutic drug monitoring in mental health treatment: a review. *Pharmaceutics* **2022**, *14*, 2674.

References

1. Poweleit, E.A.; Vinks, A.A.; Mizuno, T. Artificial intelligence and machine learning approaches to facilitate therapeutic drug management and model-informed precision dosing. *Ther. Drug Monit.* **2023**, *45*, 143–150. [CrossRef] [PubMed]
2. Hiemke, C.; Bergmann, N.; Clement, H.W.; Conca, A.; Deckert, J.; Domschke, K.; Eckermann, G.; Egberts, K.; Gerlach, M.; Greiner, C.; et al. Consensus guidelines for therapeutic drug monitoring in neuropsychopharmacology: Update 2017. *Pharmacopsychiatry* **2018**, *51*, 9–62. [PubMed]

pharmaceutics

MDPI

Article

Therapeutic Drug Monitoring of Tacrolimus-Personalized Therapy in Heart Transplantation: New Strategies and Preliminary Results in Endomyocardial Biopsies

Simona De Gregori [1,*], Annalisa De Silvestri [2], Barbara Cattadori [3], Andrea Rapagnani [4], Riccardo Albertini [1], Elisa Novello [1], Monica Concardi [5], Eloisa Arbustini [5] and Carlo Pellegrini [6]

1 U.O.C Laboratorio Analisi Chimico Cliniche, Fondazione IRCCS Policlinico San Matteo, 27100 Pavia, Italy; r.albertini@smatteo.pv.it (R.A.); elisa.novello1996@gmail.com (E.N.)
2 U.O.S Epidemiologia Clinica e Biostatistica, Fondazione IRCCS Policlinico San Matteo, 27100 Pavia, Italy; a.desilvestri@smatteo.pv.it
3 U.O.C. di Cardiochirurgia, Fondazione IRCCS Policlinico San Matteo, 27100 Pavia, Italy; b.cattadori@smatteo.pv.it
4 Unità di Chirurgia Cardiaca, Dipartimento di Scienze Clinico Chirurgiche, Diagnostiche e Pediatriche, Università degli Studi di Pavia, 27100 Pavia, Italy; andrea.rapagnani01@universitadipavia.it
5 Centro Malattie Genetiche Cardiovascolari, Fondazione IRCCS Policlinico San Matteo, 27100 Pavia, Italy; m.concardi@smatteo.pv.it (M.C.); e.arbustini@smatteo.pv.it (E.A.)
6 Unità di Chirurgia Cardiaca, Dipartimento di Scienze Clinico Chirurgiche, Diagnostiche e Pediatriche, Università degli Studi di Pavia—U.O.C. di Cardiochirurgia, Fondazione IRCCS Policlinico San Matteo, 27100 Pavia, Italy; carlo.pellegrini@unipv.it
* Correspondence: s.degregori@smatteo.pv.it; Tel.: +39-0382-503647

Citation: De Gregori, S.; De Silvestri, A.; Cattadori, B.; Rapagnani, A.; Albertini, R.; Novello, E.; Concardi, M.; Arbustini, E.; Pellegrini, C. Therapeutic Drug Monitoring of Tacrolimus-Personalized Therapy in Heart Transplantation: New Strategies and Preliminary Results in Endomyocardial Biopsies. *Pharmaceutics* **2022**, *14*, 1247. https://doi.org/10.3390/pharmaceutics14061247

Academic Editor: Federico Pea

Received: 28 April 2022
Accepted: 10 June 2022
Published: 12 June 2022

Abstract: Tacrolimus (TAC) is an immunosuppressant drug approved both in the US and in the EU, widely used for the prophylaxis of organ rejection after transplantation. This is a critical dose drug: low levels in whole blood can lead to low exposure and a high risk of acute rejection, whereas overexposure puts patients at risk for toxicity and infection. Both situations can occur at whole-blood concentrations considered to be within the narrow TAC therapeutic range. We assumed a poor correlation between TAC trough concentrations in whole blood and the incidence of acute rejection; therefore, we propose to study TAC concentrations in endomyocardial biopsies (EMBs). We analyzed 70 EMBs from 18 transplant recipients at five scheduled follow-up visits during the first year post-transplant when closer TAC monitoring is mandatory. We observed five episodes of acute rejection (grade 2R) in three patients (2 episodes at 0.5 months, 2 at 3 months, and 1 at 12 months), when TAC concentrations in EMBs were low (63; 62; 59; 31; 44 pg/mg, respectively), whereas concentrations in whole blood were correct. Our results are preliminary and further studies are needed to confirm the importance of this new strategy to prevent acute rejection episodes.

Keywords: heart transplantation; acute rejection; therapeutic drug monitoring; tacrolimus; endomyocardial biopsies

1. Introduction

Heart transplant (HTx) remains the gold standard treatment for end-stage heart failure. Survival has significantly increased up to 12 years [1] and improvements in immunosuppressive therapies are one of the factors that has contributed considerably to better outcomes. Tacrolimus (TAC), the primary immunosuppressive drug for HTx recipients, has proven to be superior to cyclosporine (CyA) in both the prevention and treatment of rejection [2]. The two drugs differ in their chemical structure (CyA is a cyclic endecapeptide, whereas TAC is a macrocyclic lactone) but they act in a similar way. They are calcineurin inhibitors and although their main mechanism of action is similar, TAC produces therapeutic effects at concentrations 100 times lower than CyA and, consequently, has a reduced risk of toxicity.

Tacrolimus administered orally is rapidly absorbed with a mean time to maximal concentration (t_{MAX}) of 1–2 h, but the composition of food may highly influence its absorption. The highly lipophilic character of TAC largely explains this phenomenon. Another factor regulating TAC bioavailability is P-glycoprotein (Pgp), an efflux pump that is situated in the apical membrane of mature epithelial cells, in hepatocytes, in renal tubular cells, in the leucocytes, and also in the blood–brain barrier. When TAC passes Pgp and enters the enterocyte, it is metabolized by the cytochrome P-450 CYP3A. The expression of Pgp is influenced by genetics. The bioavailability of TAC has been found to be approximately 15% but may vary between 4 and 89%. TAC is highly bound to erythrocytes. It's binding to plasma proteins varies between 72 and 98% depending on the methodology used. Because of the extensive partitioning of tacrolimus into erythrocytes, its apparent volume of distribution (Vd) based on blood concentrations is much lower (1.0 to 1.5 L/kg) compared with values based on plasma concentrations (about 30 L/kg). Patients treated with a calcineurin inhibitor (CNI) are at high risk of developing kidney injury; nephrotoxicity is manifested either as acute kidney injury (AKI), which is largely reversible after reducing the dose, or as chronic progressive kidney disease, which is usually irreversible. Other kidney effects of CNI include tubular dysfunction and, rarely, thrombotic microangiopathy (TMA) that can lead to acute kidney allograft loss after kidney transplantation.

Tacrolimus is a critical dose drug; low levels in whole blood can lead to low exposure and a high risk of acute rejection, whereas overexposure puts patients at risk for both toxicity (as reported above) and infections. Both situations can occur at whole-blood concentrations considered to be within the narrow TAC therapeutic range. Moreover, data from three randomized controlled trials did not find an association between TAC pre-dose concentrations (trough: C_0), the reference parameter for therapeutic drug monitoring, and the incidence of acute rejection [3,4].

Tacrolimus demonstrates large pharmacokinetic inter-individual variability, partially due to pre-systemic metabolism by the intestinal cytochrome P450 (CYP3A4/5) [5], which may be affected by other CYP3A substrates, inducers, inhibitors, demographic characteristics, hepatic dysfunction, and hematocrit. High variability in TAC trough levels has been related to worse outcomes both in kidney transplant recipients [6] and in HTx populations [7–9], mostly during the first year after transplantation when closer TAC monitoring is mandatory (range: 5–20 ng/mL).

Rejection continues to be one of the leading causes of death during the first year after HTx [10]; the role and usefulness of endomyocardial biopsy (EMB) in routine surveillance during this period remain controversial. EMB should be performed to detect any evidence of graft rejection when non-invasive tests, such as cardiac magnetic resonance imaging (MRI) or positron emission tomography (PET) scans, cannot provide a diagnosis. Nevertheless, the need for frequent monitoring makes cumbersome the use of non-invasive tests.

We assumed a poor correlation between TAC trough concentrations in whole blood and incidence of acute rejection; therefore, we propose to study TAC concentrations in EMBs. To the best of our knowledge, we believe this is the first work showing preliminary results of TAC-concentration profiles (pg/mg vs. time) in EMBs of HTx patients at six scheduled follow-up visits during the first post-transplant year.

We want to share our preliminary results, although our study is ongoing and further analysis is required before drawing conclusions.

2. Materials and Methods

2.1. Patients

The aim of our study "Therapeutic Drug Monitoring of Tacrolimus Personalized Therapy in Heart Transplantation: new strategies" (cod. 08073421), approved by the ethics committee of "Fondazione IRCCS Policlinico San Matteo" and supported by 5×1000 donations, is to evaluate possible correlations between TAC concentrations in EMBs and acute rejection episodes in order to find an accurate, specific, and predictive marker.

The entire study, which started in 2020 and is ongoing,", requires the enrollment of at least 25 de novo transplant recipients, male and female, aged 18 to 70, who receive TAC twice-daily dosing (BID) in combination with steroids and antiproliferative drugs (Mycophenolate Mofetil, Sodium Mycophenolate). To date, 33 patients (9F/24M) have been screened; 18 of them (6F/12M; median age 57 years old, max 69–min 23) underwent HTx and were enrolled in the study, whereas the other 15 are still on the waiting list. Within the group of patients who received the graft, 10 completed the follow-up period, 2 completed the sixth month, 4 completed the third month, and 2 died between the first and the third months. Each patient was anonymized and identified by the alphanumeric code TAC-XX, where XX is a consecutive number assigned during the enrollment.

All participants signed informed-consent forms, authorizing the use of their samples for the study. At each of the study time points (15 days, 1 month, 3 months, 6 months, and 12 months after transplantation), two whole blood samples (5 mL each) were collected in EDTA-containing tubes for TAC quantification both in whole blood and in the peripheral blood monocytes cells (PBMC—data not reported). EMBs from the transplanted heart were also obtained both for histopathological analysis and for TAC quantification (one EMB/each study time-point).

2.2. Sample Preparation

Tacrolimus whole-blood concentration was measured by antibody-conjugated magnetic immunoassays (ACMIAs) (Dimension instrument) from Siemens Healthcare Diagnostics, according to the manufacturer's specifications and the clinical practice guidelines of the laboratory. Tacrolimus quantitation in cardiac biopsies was analyzed by a combined enzymatic-digestion/mass spectrometry assay based on an analytical method that we validated and published in September 2020 [11]. Briefly, the obtained EMBs were properly weighted and then incubated in 50 µL of digestion buffer (10% Proteinase K solution in TAC-free ATL buffer) at 55 °C for 90 min. In the end, the tissue was completely solubilized and was added with 20 µL of internal standard (FK-506-$^{13}CD_2$: 100 ng/mL), 300 µL of water, and 1 mL of tert-butyl methyl ether into the same cryovial for reaction. To promote the TAC extraction into the organic phase, samples were gently mixed for 15 min on a rotary mixer at room temperature to avoid an emulsion between the aqueous and organic layers and then centrifuged at 10,400× *g* for 10 min. In the end, the organic phase was evaporated to dryness under a gentle flow of nitrogen (room temperature). Dry residues were reconstituted by adding 60 µL of methanol and injected into the liquid chromatography–mass spectrometry (LC–MS/MS) system.

2.3. HPLC-MS/MS Assay

After the cleanup procedure, the extracted samples underwent an online solid phase extraction (SPE) coupled to liquid chromatography–tandem mass spectrometry; the required trap column and the analytical column (heated and maintained at 50 °C) were purchased from Chromsystems (REF 93110 and 93100, respectively). Elution was carried out in gradient mode at a flow rate of 0.5 mL/min with ammonium acetate 2 mM (acidified with 0.1% HCOOH) in water (mobile phase A) and ammonium acetate 2 mM (acidified with 0.1% HCOOH) in CH_3OH (mobile phase B).

Ammonium acetate and formic acid promote the formation of the ammoniated precursor ions ($[M + NH_4]^+$, TAC *m*/*z* 821.3; $^{13}CD_2$-TAC *m*/*z* 824.3) that can be easily fragmented. Multiple-reaction monitoring (MRM) mode was used to simultaneously detect TAC and its isotopic analog ($^{13}CD_2$-TAC), chosen as the internal standard; the optimal instrument parameters and MS/MS transitions (*m*/*z* 821.3→768.0; *m*/*z* 824.3→771.0) were determined by direct infusion at a flow rate of 7 µL/min for TAC and $^{13}CD_2$-TAC separately into the mass spectrometer at a concentration of 1 µg/mL in mobile phase B.

2.4. Calibration Standards and Quality Controls (Qc)

Calibration curves were prepared by spiking the target analyte (TAC) into a matrix that has been judged to be representative of the real samples' matrix. We bought a swine heart in a butcher's shop and cut it into many small pieces (0.5–5 mg); each section was added with 50 µL of digestion buffer standard solution containing TAC at known concentrations (standard solutions). Five calibrators and 3 quality controls have been prepared and used to obtain the daily calibration curve; the peak area ratios of TAC to IS ($Area_{TAC}/Area_{IS}$) were plotted as a function of the quantity of TAC (ng) added to the pieces of swine heart (TAC [ng] = standard solution concentration [ng/mL] $\times$ 50 $\times$ 10^{-3} mL).

We prepared calibration standards and quality controls containing 0.033, 0.065, 0.130, 0.260, 0.520 ng and 0.070, 0.208, 0.416 ng of TAC, respectively. The deviation of standards from their nominal values could not exceed 15% (20% for the Lower Limit of Quantification: LLOQ, 0.033 ng).

2.5. Data Analysis

The Xcalibur 2.07 and LCquan 2.5.6 software (Thermo Fisher Scientific, San Francisco, CA, USA) were used for LC–MS/MS system control, data acquisition, and data analysis; the calibration curves were established by plotting the peak area ratio (analyte/IS) versus the TAC nominal concentrations or nominal added quantity in blood or in EMBs respectively, using a weighted (1/x) linear regression curve. Analyte peaks were identified with a combination of retention times and the specific MRM transition.

The amount of TAC (ng) in patients' biopsies was back-calculated from the daily calibration curve equation; the TAC concentration in EMBs was expressed as the ratio between the measured TAC amount and the initial EMB weight (mg) (Equation (1)).

$$[\mathrm{TAC}]_{\mathrm{EMB}} = \frac{\text{Amount of TAC (ng)}}{\text{weight of EMB (mg)}} \times 1000 = \left[\frac{\mathrm{pg}}{\mathrm{mg}}\right] \quad (1)$$

2.6. Rejection Surveillance

2.6.1. Technical Considerations

Protocol-based EMBs are performed in the first year after HTx for acute rejection surveillance, according to our institute's good clinical practice.

Each EMB is assessed for acute cellular rejection (ACR) and antibody-mediated rejection (AMR) as stated by the International Society for Heart and Lung Transplantation (ISHLT) guidelines. The presence of circulating donor-specific antihuman leukocyte antigen (HLA) antibodies (DSAs) is considered a mandatory criterion for AMR after HTx. DSAs are known as prognostic biomarkers of outcome; recipients with de novo DSA have a threefold increased risk of mortality [12].

Endomyocardial biopsy (EMB) is a valuable diagnostic tool for myocardial disease, for monitoring cardiac allograft rejection, and for diagnosing inflammatory and infiltrative cardiomyopathies. At our center, an experienced cardiothoracic surgeon uses a disposable rigid bioptome inserted through the right internal jugular vein and guided into the right atrium to cross the tricuspid valve and reach the right ventricular septum under echocardiographic guidance. The benefit of this new biopsy catheter was adequate endomyocardial sampling without procedure-related complications [13].

The interventricular septum is the preferred biopsy site for its thickness, compared to the free wall of the right ventricle for its continuity with the left ventricle and for its location in the natural path of the blood flow, which facilitates access. The drawback is that repeated EMB sampling results in a restricted region of the endocardium being assessed and may result in interpretive errors.

The tissue sample procured is usually a 1–2 mm cube of endocardium and myocardium. After extraction of the tissue fragment, the cardiovascular surgeon was careful not to remove the specimen with forceps, but rather to gently "move it" with a needle from the biopsy catheter and place it directly into 10% neutral-buffered formalin. The fixative was

kept at room temperature to prevent additional contraction band artifacts. Histological preparation, embedding, staining, reading, and reporting of the diagnosis within 24 h are standard procedures.

The cardiovascular surgeon used the same careful approach for the biopsies intended for the determination of the TAC concentration; he placed them in empty cryovials and immediately called the laboratory for the subsequent standardized procedures (weighing and storage at −80 °C until analysis).

2.6.2. Histological Preparation

The microscopic description of acute cellular rejection in the cardiac allograft is generally accepted as the presence of a myocardial mononuclear infiltrate, hemorrhage, myocyte injury or necrosis, and vascular endothelial lesions, which includes endothelial disruption and platelet fibrin deposition. The sensitivity of detecting transplant rejection can approach 98% with five adequate biopsy fragments, yet more than six samples do not appear to increase diagnostic yield [14]. The greatest potential limitation to EMB interpretation is sampling error. The adequacy of tissue fragments is very important for correct diagnostic accuracy and interpretation.

Standard histological preparation requires paraffin-wax embedding followed by ribbons of 4 µm thick sections mounted on glass slides. Slides are numbered sequentially and stained with hematoxylin and eosin for histomorphological characterization.

Evaluation of sample adequacy for the International Society of Heart and Lung Transplantation grading scheme requires a minimum of four good endomyocardial tissue fragments, with less than 50% of each fragment being fibrous tissue, thrombus, or other non-interpretable tissue fragments (such as crush artifacts or poorly processed fragments).

2.7. Statistical Analysis

Medians are presented in graphs showing a single outcome measured at several points over time. Points are connected by straight lines. Error bars show an interquartile range (IQR). Joint modeling would be more appropriate considering the association between time-to-event (acute rejection episode) and the measured longitudinal data (TAC concentrations). However, in our opinion, the limited sample size (5 events, 3 patients) is not adequate for estimating the effects of the longitudinal process in joint modeling [15].

3. Results

3.1. Concentration–Time Profiles

Figures 1–4 show the concentration–time profiles and the median concentration time-profiles of TAC in EMBs and whole blood samples, respectively, from each of the 18 transplant recipients.

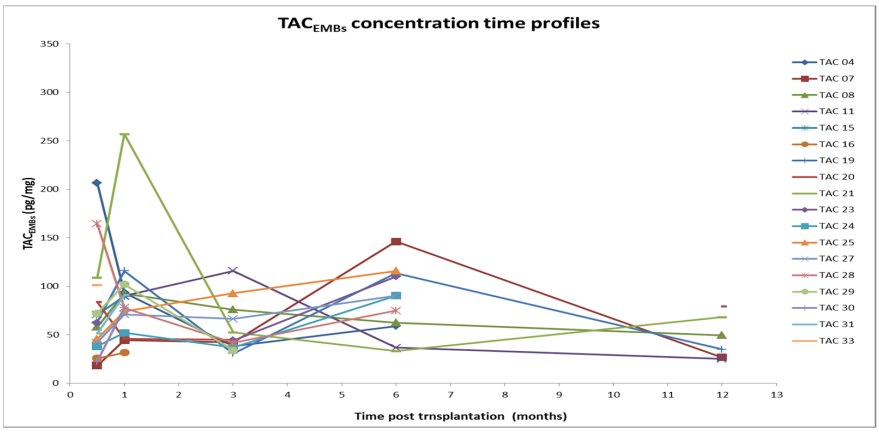

Figure 1. Concentration–time profiles of TAC in EMBs (18 patients). TAC: Tacrolimus; EMB: Endomyocardial biopsy.

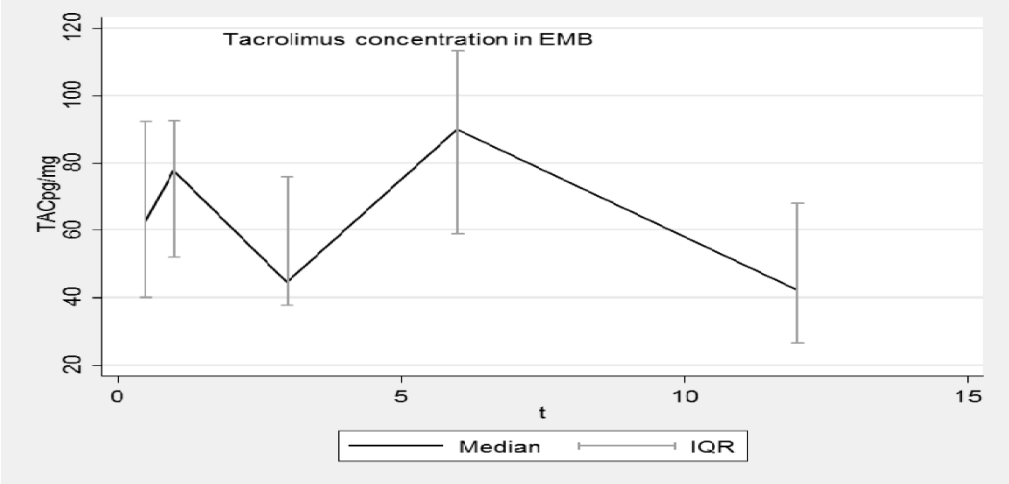

Figure 2. Median concentration–time profile of TAC in EMBs. TAC: Tacrolimus; EMB: Endomyocardial biopsy; IQR: interquartile range.

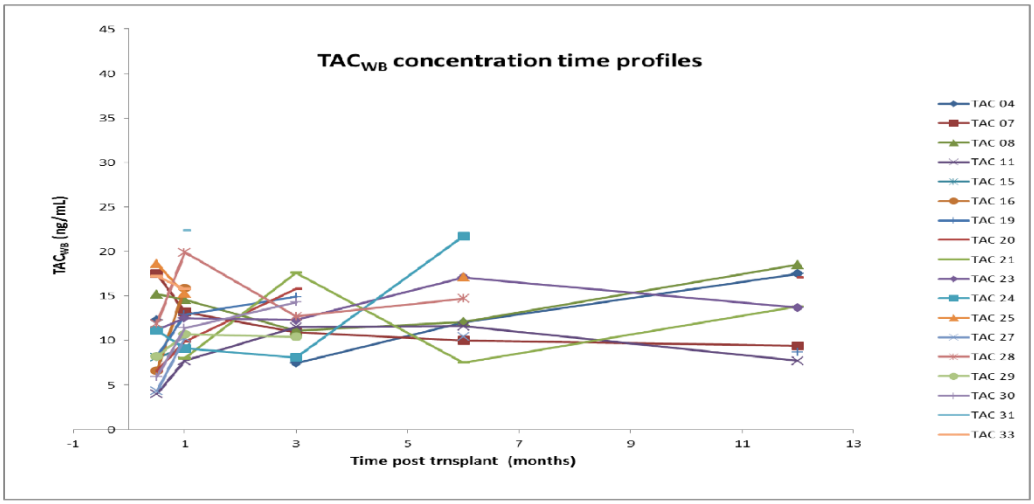

Figure 3. Concentration–time profiles of TAC in whole blood (18 patients). TAC: Tacrolimus; WB: whole blood.

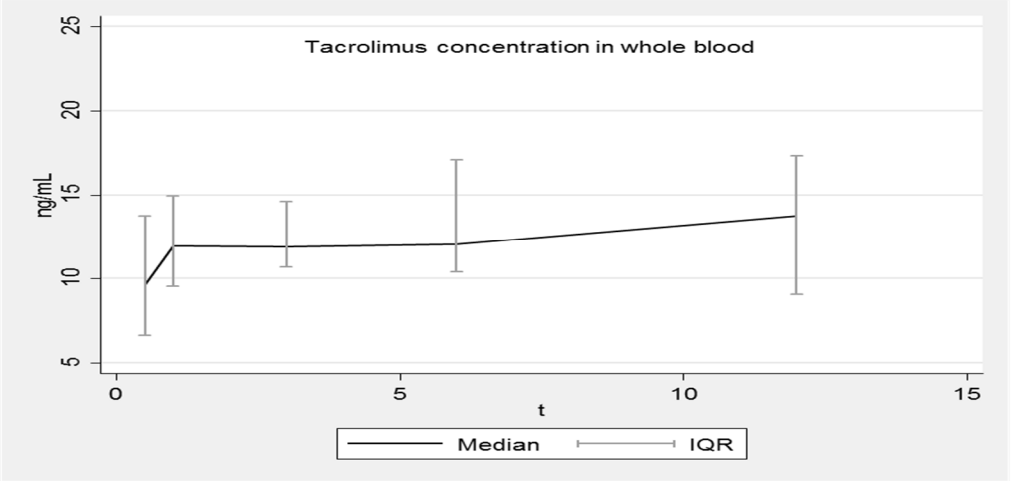

Figure 4. Median concentration–time profile of TAC in whole blood. IQR: interquartile range.

The analysis in the two different matrices was always performed on the same day to reduce possible and unexpected interferences.

TAC concentrations in EMBs were variable, especially during the first months after transplantation; at the first (15 days) and second follow-up visits (1 month), TAC_{EMB} of patients TAC-04 and TAC-21 were unexpectedly elevated (207 and 257 pg/mg, respectively) but over the next few months their values dropped to conform to the others.

The maximum concentration value was detected around 1 month after transplantation (257 pg/mg; patient TAC-21), whereas the minimum level (18 pg/mg) was observed 15 days after HTx (18 pg/mg; patient TAC-11), as reported in Table 1.

Table 1. TAC median concentrations in EMBs during the first year post-HTx.

Time Post-HTx	N° Analyzed EMBs	TAC Conc. pg/mg Median (Min–Max)
15 days	17	62 (18–207)
1 month	17	86 (31–257)
3 months	16	45 (31–119)
6 months	11	90 (33–146)
12 months	9	66 (25–112.5)

TAC: Tacrolimus; EMB: Endomyocardial biopsy; HTx: Heart transplant.

At the third evaluation (3 months), some TAC_{EMB} profiles reached a minimum and then increased again in the following months. The results corresponding to 1 year post-transplantation come from a low number of samples (Table 1: N = 9) but a decreasing trend is plausible. At this time point, the dispersion of data appears minimal but only half of the patients completed the observation period. All these results are better summarized in Figure 2, where the median concentration–time profile of TAC_{EMB} and the related interquartile range (IQR) are reported as time functions (months). Although the pattern is very irregular, the IQR is overlapping.

In contrast, the concentration–time profiles of TAC_{WB} during the entire first year post-HTx were more regular for all patients (Figure 3), as required by the universally accepted therapeutic drug monitoring guidelines.

The corresponding calculated median concentration–time profile shows a continuous slight increase (8.2–13.8 ng/mL), although the interquartile ranges (IQR) are overlapping (Figure 4). Fluctuations are limited and always within the expected therapeutic range (5–20 ng/mL).

When the study started, the potential concentration range for TAC in EMBs was unknown; Capron and colleagues [16] found TAC levels ranging from less than 5 up to 387 pg/mg in liver biopsies. The tissue levels displayed an excellent correlation with the liver histopathologic BANFF rejection score, whereas the blood levels did not.

Even though the liver and heart are obviously different organs, Capron's work was a good starting point for the present study; to date, similar concentrations were found in EMBs ranging from 18 to 257 pg/mg.

3.2. Acute Rejection Episodes

Five acute rejection episodes (grade 2R) [17] were observed in three patients, whose characteristics are summarized in Table 2; 1 episode occurred at 0.5 months, 3 at 3 months, and 1 at 12 months, when the TAC concentrations in EMBs were low (63; 62; 59; 31; 44 pg/mg, respectively).

Table 2. Patients' characteristics.

Patient ID	M/F	Age (Year)	Blood Type		Total Ischemic Time	Cold Ischemia Time	Warm Ischemia Time
			Donor	Recip			
TAC-23	M	57	A-	A-	140 min	77 min	63 min
TAC-19	F	54	A-	A-	95 min	50 min	45 min
TAC-04	F	58	AB+	AB+	188 min	130 min	58 min

The highest ratio of TAC_{WB}/TAC_{EMBS} was reached 3 months after HTx, when TAC_{WB} was always in the expected therapeutic range, whereas the TAC_{WB}/TAC_{EMBs} ratio was the lowest in the presence of acute rejection (Table 3).

Table 3. Tacrolimus concentration–time profiles in whole blood and EMBs.

	Median				
Months after HTx	0.5	1	3	6	12
N° analyzed EMBs	17	17	16	11	9
Whole blood (ng/mL)	8.2	12.0	12.5	13.4	13.8
EMB (pg/mg)	62.0	85.9	45.0	90.0	66.0
Ratio WB/EMB	0.13	0.14	**0.28**	0.15	0.21

EMB: Endomyocardial biopsy; HTx: Heart transplant; WB: whole blood.

Despite the small sample size, TAC concentrations were analyzed in both EMBs and whole blood by considering the results of rejecting (RPs) and non-rejecting patients (NRPs) separately; for the second time, the conclusions are different depending on the specific matrix.

The median TAC concentrations in EMBs (Figure 5) and whole blood (Figure 6) of RPs and NRPs were plotted; in both situations the IQRs overlap, but in Figure 5 the median concentration of the RP group is lower, whereas in Figure 6 the opposite situation occurs.

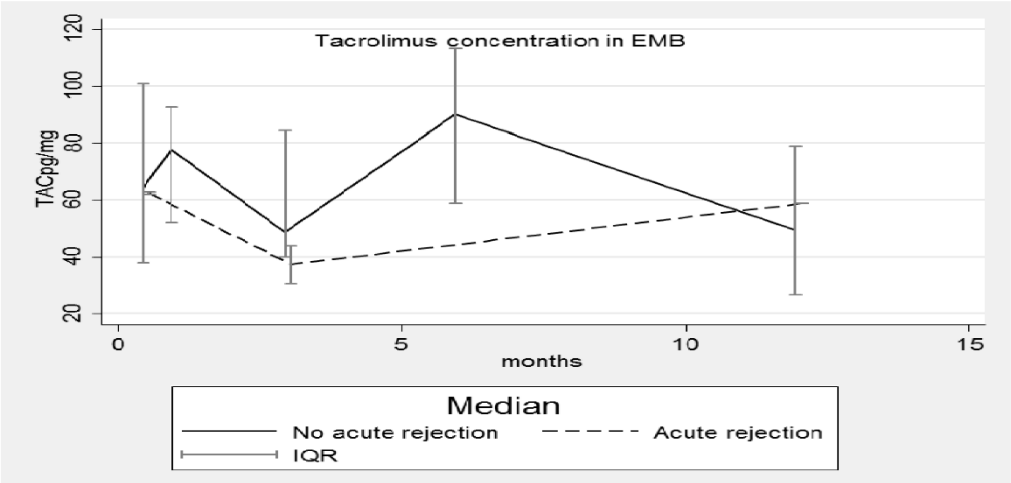

Figure 5. Median concentration–time profile of TAC in EMBs with and without acute rejection episodes. TAC: Tacrolimus; EMB: Endomyocardial biopsy; IQR: interquartile range.

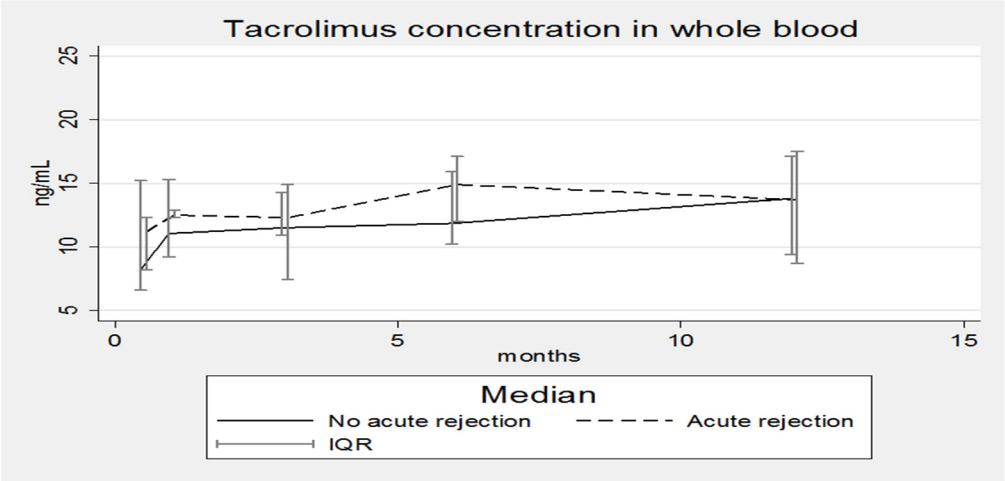

Figure 6. Median concentration–time profile of Tacrolimus in whole blood with and without acute rejection episodes. IQR: interquartile range. No correlation was found between TAC concentrations in EMBs and whole blood, considering all patients together as a single group and as subgroups of RPs or NRPs.

4. Discussion and Conclusions

Despite the progress and improved overall outcomes, acute allograft rejection (AR) remains the Achilles' heel of heart transplantation. The manifestations of rejection can occur as early as intraoperatively to many years after transplant. The timing of AR plays a significant role in establishing cause and diagnosis. Acute rejection can either be responsible for early graft dysfunction, occurring in the first days after surgery, or late graft dysfunction developing weeks to years after transplantation.

Acute allograft rejection is an important contributor to graft failure, which remains a leading cause of death (10%) within the first three years after HTx; low TAC levels in whole blood can lead to low exposure and an increased risk of acute rejection, but, unfortunately, an acceptable correlation between these two factors has never been demonstrated.

Episodes of acute rejection can also occur when TAC concentrations fall within their narrow therapeutic range. The unbound concentration has been shown to be a crucial factor in cellular uptake and may increase glomerular vasoconstriction leading to nephrotoxicity in the early days after transplantation. From a mechanistic point of view, the plasma concentration of unbound TAC is a more reasonable parameter to monitor to achieve optimal TAC dosing in transplant patients, especially in the early days after HTx, but current assays used for routine TAC monitoring lack the sensitivity to adequately measure it [2].

From 1995 to 2021, many clinical studies [18] investigated whole blood, PBMC, and allograft TAC concentrations and their association with clinical outcomes, to evaluate an evident clinical benefit with respect to the prediction of rejection. All the studies were conducted on liver- or kidney-transplanted patients; none involved HTx patients. The results are controversial; well-designed and powered prospective clinical trials are still needed to determine whether TAC therapeutic drug monitoring (TDM) in alternative matrices offers a significant clinical benefit over the current TDM based on whole blood determinations.

In order to collect initial data from HTx patients, preliminary results on TAC concentration-time profiles both in whole blood and in EMBs during the first year after transplantation are presented. Each specialized center normally determines the minimum levels of the appropriate immunosuppressant drug in whole blood to prevent AR episodes; in general, target TAC concentrations are highest soon after HTx and slowly decrease over the first year, eventually settling on the lowest maintenance levels of immune suppression that are compatible with AR prevention and the attenuation of drug toxicities. Another general

principle is to favor the use of low doses of multiple drugs without overlapping toxicities over the use of higher doses of fewer drugs whenever feasible. A third principle is that excessive immunosuppression is undesirable because it leads to a high incidence of side effects such as infections and malignancies. Finding the right balance between over- and under-immunosuppression in an individual patient is truly an art that requires science. The reason for the therapeutic choice by our center was poor post-operative peripheral perfusion, which requires a lower dosage of nephrotoxic drugs to not overload the kidneys. As summarized in Table 3, TAC_{WB} concentrations were maintained as constant throughout the observation period and, although the median was significantly lower than the others 15 days after HTx, it was still within the expected therapeutic range (5–20 ng/mL).

Nonetheless, five AR episodes occurred and were classified as grade 2R by the pathological characterization. Concurrent with the AR episodes, TAC concentrations in the EMBs were low at the three-month post-transplant time point (when three of the five episodes occurred); indeed, the corresponding median TAC_{EMB} concentration reached the lowest value (Figure 5). Patients' blood-type mismatches and total ischemic times cannot be considered confounding factors, as reported in Table 2; transplantation with blood-type mismatch is never performed even in emergency cases and the total ischemic time was shorter than 4 h for all three patients. Figure 5 also confirms that the median concentration–time profiles of TAC in EMBs in the rejecting and non-rejecting patient groups are different with the median concentrations being lower for patients suffering from rejection. Completely different and unexpected results were obtained by analyzing data from whole blood (Figure 6).

Two patients died 1 and 3 months after transplantation, respectively. The cause of death was related to HTx in the first patient who died from multiple organ failure (MOF). The cause of the second death was instead intracerebral hemorrhage that occurred in a patient without hypertension.

As the transplanted patients and the corresponding donors are different individuals with different genetics, investigations of the role of the polyglycol protein (P-gp) directly in the graft will be carried out at this center next year. P-glycoprotein is a transmembrane glycoprotein that is directly encoded by the human ABCB1 gene. It is responsible for the efflux of many harmful compounds inside the cell to the extracellular space, but on the other hand, it also favors the removal of many drugs from the cells leading to a substantial reduction in their activity. P-glycoprotein controls drug absorption, distribution, and elimination in the body. Previous recent studies report that both TAC and CyA are substrates of P-gp; this has been demonstrated mainly for liver and kidney transplant recipients [19,20]. In 2002, Messner and colleagues described the expression and localization of the P-gp in fifteen left ventricular samples and observed a very wide inter-individual variability [21]. Future areas of investigation will address the characteristics of the donors in terms of the expression and localization of P-gp in the myocardial tissue to confirm or improve on Messner's results.

We have not reported our results on tacrolimus concentrations in peripheral blood mononuclear cells because the trend is often in good agreement with its corresponding concentrations in whole blood.

In our opinion, all our future data combined with standardized pharmacokinetic analysis will be a requirement to achieve personalized therapy. Some individual characteristics could be strongly related to the mechanism of action of the drug and may reflect the personal response to the treatment; the synthesis of clinical signs and biological and histological parameters would allow both the minimization of immunosuppressive therapy and an improvement in the outcomes.

To the best of our knowledge, this is the first work reporting results of TAC concentrations in EMBs from HTx patients.

This study argues that TAC tissue concentrations in the allograft cannot be accurately predicted based on the blood level and that this is a possible mechanism underlying the AR occurrence. However, further studies and a larger population are needed to confirm these findings. In consideration of the need for cardiac transplant recipients to

be closely monitored with clinical and imaging methods to early diagnose AR despite whole blood immunosuppressant concentrations within the therapeutic range, the routine implementation of analytical procedures to identify low allograft tissue levels will allow for more personalized therapeutic regimens, a step forward to AR defeat and a reduction of drug toxicities.

Author Contributions: Conceptualization, S.D.G. and C.P.; methodology, S.D.G., M.C., C.P. and A.D.S.; software, A.D.S. and A.R.; validation, S.D.G. and A.D.S.; formal analysis, S.D.G. and A.D.S.; investigation, B.C., C.P. and E.N.; data curation B.C., R.A. and A.D.S.; writing—original draft preparation, S.D.G.; writing—review and editing, S.D.G., R.A., C.P. and E.A.; supervision, R.A. and C.P.; project administration, S.D.G.; funding acquisition, S.D.G. All authors have read and agreed to the published version of the manuscript.

Funding: This research was approved by Fondazione IRCCS Policlinico San Matteo, Pavia (cod. 08073421) and was funded by a 5 × 1000 (five by one thousand) tax donation.

Institutional Review Board Statement: The study was conducted in accordance with Good Clinical Practice guidelines and the ethical principles that have their origins in the Declaration of Helsinki. The protocol and informed consent form were approved by the Ethics Committee of Pavia (protocol code 0009010/22).

Informed Consent Statement: All patients gave written informed consent before any procedure related to this study was performed, and to publish related scientific results.

Data Availability Statement: Not applicable.

Acknowledgments: We want to deeply thank all patients who donated their EMBs for this research.

Conflicts of Interest: The authors declare no conflict of interest.

References

1. Lund, L.H.; Edwards, L.B.; Dipchand, A.I.; Goldfarb, S.; Kucheryavaya, A.Y.; Levvey, B.J.; Meiser, B.; Rossano, J.W.; Yusen, R.D.; Stehlik, J. International Society for Heart and Lung Transplantation. The Registry of the International Society for Heart and Lung Transplantation: Thirty-third Adult Heart Transplantation Report-2016; Focus Theme: Primary Diagnostic Indications for Transplant. *J. Heart Lung Transplant.* **2016**, *35*, 1158–1169. [CrossRef] [PubMed]
2. Skima, M.A.; van Maarseveen, E.M.; van de Graaf, E.A.; Kirkels, J.H.; Verhaar, M.C.; Donker, D.W.; Kesecioglu, J.; Meulenbelt, J. Pharmacokinetics and toxicity of tacrolimus early after heart and lung transplantation. *Am. J. Transplant.* **2015**, *15*, 2301–2313. [CrossRef] [PubMed]
3. Costanzo, M.R.; Dipchand, A.; Starling, R.; Anderson, A.; Chan, M.; Desai, S.; Fedson, S.; Fisher, P.; Gonzales-Stawinski, G.; Martinelli, L.; et al. The International Society of Heart and Lung Transplantation Guidelines for the care of heart transplant recipients. *J. Heart Lung Transplant.* **2010**, *29*, 914–956. [CrossRef]
4. Bouamar, R.; Shuker, N.; Hesselink, D.A.; Weimar, W.; Ekberg, H.; Kaplan, B.; Bernasconi, C.; van Gelder, T. Tacrolimus predose concentrations do not predict the risk of acute rejection after renal transplantation: A pooled analysis from three randomized-controlled clinical trials. *Am. J. Transplant.* **2013**, *13*, 1253–1261. [CrossRef] [PubMed]
5. Woillard, J.B.; Mourad, M.; Neely, M.; Capron, A.; van Schaik, R.H.; van Gelder, T.; Lloberas, N.; Hesselink, D.A.; Marquet, P.; Haufroid, V.; et al. Tacrolimus Updated Guidelines through popPK Modeling: How to Benefit More from CYP3A Pre-emptive Genotyping Prior to Kidney Transplantation. *Front. Pharmacol.* **2017**, *8*, 358. [CrossRef] [PubMed]
6. Seibert, S.R.; Schladt, D.P.; Wu, B.; Guan, W.; Dorr, C.; Remmel, R.P.; Matas, A.J.; Mannon, R.B.; Israni, A.K.; Oetting, W.S.; et al. Tacrolimus trough and dose intra-patient variability and CYP3A5 genotype: Effects on acute rejection and graft failure in European American and African American kidney transplant recipients. *Clin. Transplant.* **2018**, *32*, e13424. [CrossRef] [PubMed]
7. Gueta, I.; Markovits, N.; Yarden-Bilavsky, H.; Raichlin, E.; Freimark, D.; Lavee, J.; Loebstein, R.; Peled, Y. High tacrolimus trough level variability is associated with rejections after heart transplant. *Am. J. Transplant.* **2018**, *18*, 2571–2578. [CrossRef]
8. Wallemacq, P.; Armstrong, V.W.; Brunet, M.; Haufroid, V.; Holt, D.W.; Johnston, A.; Kuypers, D.; Le Meur, Y.; Marquet, P.; Oellerich, M.; et al. Opportunities to optimize tacrolimus therapy in solid organ transplantation: Report of the European consensus conference. *Ther. Drug Monit.* **2009**, *31*, 139–152. [CrossRef]
9. Brunet, M.; van Gelder, T.; Åsberg, A.; Haufroid, V.; Hesselink, D.A.; Langman, L.; Lemaitre, F.; Marquet, P.; Seger, C.; Shipkova, M.; et al. Therapeutic Drug Monitoring of Tacrolimus-Personalized Therapy: Second Consensus Report. *Ther. Drug Monit.* **2019**, *41*, 261–307. [CrossRef] [PubMed]
10. Subherwal, S.; Kobashigawa, J.A.; Cogert, G.; Patel, J.; Espejo, M.; Oeser, B. Incidence of acute cellular rejection and non-cellular rejection in cardiac transplantation. *Transplant. Proc.* **2004**, *36*, 3171–3172. [CrossRef]

11. Molinaro, M.; Pellegrini, C.; Cattadori, B.; De Gregori, S. Development and validation of a combined enzymatic-digestion/mass spectrometry assay for Tacrolimus quantitation in cardiac biopsies. *J. Chromatogr. B* **2020**, *1152*, 122215. [CrossRef] [PubMed]
12. Barten, M.J.; Zuckermann, A. The meaning of donor-specific antibodies after heart transplant. *Curr. Opin. Organ. Transplant.* **2019**, *24*, 252–258. [CrossRef] [PubMed]
13. Cunningham, K.S.; Veinot, J.P.; Butany, J. An approach to endomyocardial biopsy interpretation. *J. Clin. Pathol.* **2006**, *59*, 121–129. [CrossRef] [PubMed]
14. Zerbe, T.R.; Arena, Z. Diagnostic reliability of endomyocardial biopsy for assessment of cardiac allograft rejection. *Hum. Pathol.* **1988**, *19*, 1307–1314. [CrossRef]
15. Chen, L.M.; Ibrahim, J.G.; Chu, H. Sample size and power determination in joint modeling of longitudinal and survival data. *Stat. Med.* **2011**, *30*, 2201–2340. [CrossRef]
16. Capron, A.; Lerut, J.; Verbaandert, C.; Mathys, J.; Ciccarelli, O.; Vanbinst, R.; Roggen, F.; De Reyck, C.; Lemaire, J.; Wallemacq, P.E. Validation of a liquid chromatography-mass spectrometric assay for tacrolimus in liver biopsies after hepatic transplantation: Correlation with histopathologic staging of rejection. *Ther. Drug Monit.* **2007**, *29*, 340–348. [CrossRef]
17. Stewart, S.; Winters, G.L.; Fishbein, M.C.; Tazelaar, H.D.; Kobashigawa, J.; Abrams, J.; Andersen, C.B.; Angelini, A.; Berry, G.J.; Burke, M.M.; et al. Revision of the 1990 working formulation for the standardization of nomenclature in the diagnosis of heart rejection. *J. Heart Lung Transplant.* **2005**, *24*, 1710–1720. [CrossRef]
18. Sallustio, B.C. Monitoring Intra-cellular Tacrolimus Concentrations in Solid Organ Transplantation: Use of Peripheral Blood Mononuclear Cells and Graft Biopsy Tissue. *Front. Pharmacol.* **2021**, *12*, 733285. [CrossRef]
19. Masuda, S.; Inui, K. An up-date review on individualized dosage adjustment of calcineurin inhibitors in organ transplant patients. *Pharmacol. Ther.* **2006**, *112*, 184–198. [CrossRef]
20. Ogasawara, K.; Chitnis, S.D.; Gohh, R.Y.; Christians, U.; Akhlaghi, F. Multidrug resistance-associated protein 2 (MRP2/ABCC2) haplotypes significantly affect the pharmacokinetics of tacrolimus in kidney transplant recipients. *Clin. Pharmacokinet.* **2013**, *52*, 751–762. [CrossRef]
21. Meissner, K.; Sperker, B.; Karsten, C.; Schwabedissen, H.M.; Seeland, U.; Böhm, M.; Bien, S.; Dazert, P.; Kunert-Keil, C.; Vogelgesang, S.; et al. Expression and localization of P-glycoprotein in human heart: Effects of cardiomyopathy. *J. Histochem. Cytochem.* **2002**, *50*, 1351–1356. [CrossRef] [PubMed]

pharmaceutics

MDPI

Article

Therapeutic Drug Monitoring of Mycophenolic Acid as a Precision Medicine Tool for Heart Transplant Patients: Results of an Observational Pharmacokinetic Pilot Study

Francesco Lo Re [1], Jacopo Angelini [1], Sandro Sponga [2,3], Chiara Nalli [3], Antonella Zucchetto [4], Jessica Biasizzo [5], Ugolino Livi [2,3] and Massimo Baraldo [1,2,*]

[1] Clinical Pharmacology and Toxicology Institute, University Hospital Friuli Centrale ASU FC, 33100 Udine, Italy; francesco.lore@asufc.sanita.fvg.it (F.L.R.); jacopo.angelini@asufc.sanita.fvg.it (J.A.)
[2] Department of Medical Area (DAME), University of Udine (UNIUD), 33100 Udine, Italy; sandro.sponga@uniud.it (S.S.); ugolino.livi@uniud.it (U.L.)
[3] Department of Cardiothoracic Surgery, University Hospital Friuli Centrale ASU FC, 33100 Udine, Italy; chiara.nalli@asufc.sanita.fvg.it
[4] Scientific Directorate, Centro di Riferimento Oncologico di Aviano (CRO), Istituto di Ricovero e Cura a Carattere Scientifico (IRCCS), 33081 Aviano, Italy; azucche@libero.it
[5] Institute of Clinical Pathology, University Hospital of Friuli Centrale ASU FC, 33100 Udine, Italy; jessica.biasizzo@asufc.sanita.fvg.it
* Correspondence: massimo.baraldo@uniud.it

Abstract: In the clinical practice management of heart transplant (HTx), the impact of calcineurin inhibitors co-administration on pharmacokinetics (PKs) of mycophenolic acid (MPA), mycophenolate mofetil (MMF) active drug, is not adequately considered. This retrospective study investigated full MPA-PK profiles by therapeutic drug monitoring (TDM) in 21 HTx recipients treated with MMF combined with cyclosporine (CsA) or tacrolimus (TAC) at a median time of 2.6 months post-transplant. The two treatment groups were compared. We described the main MPA-PK parameters in patients developing acute cellular rejection (ACR) and those who did not. Median dose-adjusted MPA-trough levels and MPA-$AUC_{0–12h}$ were higher in patients co-treated with TAC than with CsA ($p = 0.0001$ and $p = 0.006$, respectively). MPA-C_{max} and T_{max} were similar between the two groups, whereas the enterohepatic recirculation biomarker of MPA (MPA-$AUC_{4–12h}$) was higher in the MMF and TAC group ($p = 0.004$). Consistently, MPA clearance was higher in the MMF and CsA group ($p = 0.006$). In total, 87.5% of ACR patients were treated with MMF and CsA, presenting a lower MPA-$AUC_{0–12h}$ ($p = 0.02$). This real-world study suggested the CsA interference on MPA-PK in HTx, evidencing the pivotal role of MPA TDM as a precision medicine tool in the early phase after HTx. A prospective study is mandatory to investigate this approach to HTx clinical outcomes.

Keywords: therapeutic drug monitoring; pharmacokinetic interactions; heart transplant; precision medicine; clinical practice

Citation: Lo Re, F.; Angelini, J.; Sponga, S.; Nalli, C.; Zucchetto, A.; Biasizzo, J.; Livi, U.; Baraldo, M. Therapeutic Drug Monitoring of Mycophenolic Acid as a Precision Medicine Tool for Heart Transplant Patients: Results of an Observational Pharmacokinetic Pilot Study. *Pharmaceutics* **2022**, *14*, 1304. https://doi.org/10.3390/pharmaceutics14061304

Academic Editor: Antonello Di Paolo

Received: 12 May 2022
Accepted: 18 June 2022
Published: 20 June 2022

Publisher's Note: MDPI stays neutral with regard to jurisdictional claims in published maps and institutional affiliations.

1. Introduction

Mycophenolate mofetil (MMF) represents a cornerstone for the treatment of heart transplant (HTx) [1]. Standard immunosuppressive maintenance protocols include its administration combined with calcineurin inhibitors (CNIs), such as cyclosporine (CsA) or tacrolimus (TAC), and corticosteroids.

After oral administration, MMF is rapidly metabolized to mycophenolic acid (MPA), which is a selective and noncompetitive inhibitor of inosine-5′-monophosphate dehydrogenase (IMPDH) that causes the arrest of the proliferation of T- and B-cells [2]. When orally administered, the time to reach MPA plasma maximum concentration (T_{max}) occurs after approximately 1–2 h. Frequently, MPA exhibits a secondary peak due to enterohepatic recirculation (EHC), occurring 6–12 h after drug administration [2]. Indeed, uridine diphosphate

glucuronosyltransferase (UDP-GT) enzyme family metabolized MPA into its main inactive metabolite 7-O-MPA-glucuronide (MPAG), which is mainly excreted in the urine and into the bile by multi-drug resistance protein 2 (MRP-2). Hence, MPAG can be hydrolyzed into MPA by gastrointestinal flora and then reabsorbed by EHC [2]. Since CsA inhibits MRP-2, in the case of MMF and CsA co-administration MPA secondary peak is suppressed [2]. In renal transplant patients, Cattaneo et al. evidenced a decrease in MPA concentrations, occurring 4–12 h from MMF administration, as suggested by the corresponding biomarker represented by the area under the concentration–time curve from 4 to 12 h ($AUC_{4–12h}$) [2–4]. Consistently CsA administration increases MPA clearance (Cl) [5].

From a pharmacokinetic (PK) point of view, MPA exposure, in terms of its area under the 12 h concentration–time curve ($AUC_{0–12h}$), represents the major prognostic PK parameter for this immunosuppressive treatment [6]. MPA-$AUC_{0–12h}$ is characterized by a relevant inter- and intra-subject variability [7]. It has been reported a >10-fold variation in dose-adjusted MPA-$AUC_{0–12h}$ among patients in heart and renal transplants [8]. Some authors also suggested a relationship between MPA plasma concentration and incidence of cardiac rejection [9,10]. For this reason, the therapeutic drug monitoring (TDM) of MPA is recommended to maximize the efficacy of treatment, especially in the first period after transplant and in patients with high immunological risk [6].

A therapeutic MPA-$AUC_{0–12h}$ target, ranging from 30 to 60 mg·h/L, was prospectively validated in renal transplant patients [6,11]. In the Htx setting, similar thresholds were identified [12,13], although supported by low strength of recommendation and scarce quality of evidence [6].

This retrospective observational monocentric pilot study was designed to compare the effect of CsA or TAC administration on MPA-PK in a cohort of HTx recipients. Patients were treated according to the standard clinical practice of our University Hospital Center. In particular, we primarily sought to compare the 12-h MPA-PK profiles in both groups in the first period after transplant and to examine the effect of CsA on MPA EHC.

Secondarily, we only exploratively described the main MPA-PK parameters in patients reporting acute cellular rejection (ACR) and in those who did not (NACR).

2. Materials and Methods

2.1. Patients

In total, 21 adult patients who underwent primary HTx were included in our analysis. All patients had been previously treated at the University Hospital of Udine following the internal protocol with MMF and CsA (Group 1) or MMF and TAC (Group 2) and prednisone [14]. From 1 January 2011 to 31 December 2019, TDM of immunosuppressive drugs was performed for each patient during a minimum follow-up period of 12 months. All consecutive HTx recipients in the study period who met these criteria were included in the analysis. Patients treated with prokinetic drugs, resins, or other drugs interfering with MPA-PK, except for prednisone, were excluded. Patients treated with other immunosuppressive agents than MMF, CsA, and TAC or subjects with relevant missing data in the clinical records or without informed consent for clinical, epidemiological research, training, and study of pathologies were excluded from the study.

CsA and TAC were administered according to the clinical condition and renal function. CsA and TAC doses were adjusted to reach different blood concentration targets, according to our clinical practice adapted from literature: 150–250 ng/mL and 100–200 ng/mL for CsA; 10–15 ng/mL and 5–10 ng/mL for TAC, <3 months and >3 months post-transplant, respectively [15,16].

MMF was administered with a median dose of 750 mg twice daily, and dose-adjustments were performed according to blood leucocyte count, clinical conditions, drug tolerability, or adverse effects. The TDM of MPA was executed at a median time of 2.6 months post-transplant, setting an $AUC_{0–12h}$ target range at 30–60 mg·h/L [6].

2.2. Study Design and Pharmacokinetic Measurements

This is a pilot, observational, retrospective cohort study.

Pharmacological, hematological, and biochemical analyses were performed according to routine clinical practice. PK analyses were required when the expected steady state was reached for all drugs. In particular, PK analysis consisted of the 12 h MPA-PK profile, CsA, and TAC pre-dose measurement. Patients were asked to take their usual morning dose of MMF, CsA, or TAC after having a standard meal.

For the 12 h MPA-PK profile, written informed consent had been obtained, and 8 venous blood samples had been taken at 0 (pre-dose), 0.5, 1.25, 2, 4, 6, 8, and 12 h after MMF morning dose. Each patient executed a single PK profile one time only. Separation of plasma was performed immediately in a centrifuge at 4 °C. Plasma MPA concentrations were measured by high-pressure liquid chromatography with UV detector (HPLC/UV) using a reference method published in literature [17]. Our laboratory reported the following parameter for the HPLC/UV method used: limit of detection: 0.1 μg/mL; linearity between 0.1 and 40 μg/mL (coefficient of determination, R^2: 0.9988); intra-batch imprecision expressed as coefficient of variation (CV): 3.15%, 1.55%, and 1.76% at MPA plasma concentrations of 1.5, 5.0, 15.0 μg/mL, respectively; inter-batch imprecision (CV): 3.41%, 3.21%, and 1.92% at MPA plasma concentrations of 1.5, 5.0, 15.0 μg/mL, respectively; overall inaccuracy (% bias) of the procedure: ranged from 8.7% to 13.6%. TAC and CsA trough levels were determined in whole blood for all patients by an affinity column-mediated immunoassay (ACMIA) method using a Dimension Vista 1500® Analyzer (Siemens Healthcare Diagnostics, Berlin, Germany). Our laboratory reported the following parameter CsA: assay range (25–500 ng/mL); linearity from 25 to 200 ng/mL; limit of detection 25 ng/mL; within-run precision (CV): 5.2%, 4.3%, and 4.3% at CsA concentrations of 65, 151, 400 ng/mL, respectively; within laboratory precision (CV): 8.2%, 5.4%, and 4.8% at CsA concentrations of 65, 151, 400 ng/mL, respectively. For TAC the parameter reported were the followings: assay range (1–30 ng/mL); linearity from 1 to 30 ng/mL; limit of detection 0.7 ng/mL; within-run precision (CV): 3.8%, 2.3%, and 3.1% at TAC concentrations of 4.4, 11.4, 27.4 ng/mL, respectively; within laboratory (CV): 6.9%, 4.5%, and 5.1% at TAC concentrations of 4.4, 11.4, 27.4 ng/mL, respectively.

MPA PK was evaluated by a non-compartmental model after oral administration using the PK solver software® [18], according to similar studies in the literature [4,19,20]. MPA-$AUC_{0–12h}$ was calculated by means of the linear trapezoidal rule.

According to Cattaneo et al. [4], we investigated the possible impact of TAC or CsA on MPA bioavailability, taking into consideration the area under the concentration–time vurve from 0 to 2 h ($AUC_{0–2h}$), as a surrogate marker of absorption, the MPA peak plasma concentration (C_{max}) and the T_{max}. Furthermore, we evaluated the MPA-$AUC_{4–12h}$ as a surrogate marker of EHC. MPA apparent clearance (Cl/F) was evaluated by this formula for both groups:

$$\text{MPA Cl/F} = (\text{MPA morning dose})/(\text{MPA AUC}_{0–12h}) \quad (1)$$

MPA-PK parameters were assessed and compared between patient groups.

Secondarily, as explorative analysis, we described MPA-$AUC_{0–12h}$ values, all the drug serum concentration sampling points, C_{max} absolute and dose-adjusted values in ACR and NACR patients.

To exclude the confounding factor of different MMF drug doses, MPA-PK parameters were normalized for the daily MMF dose according to the following formula [4]:

$$\text{MPA PK parameter dose} - \text{adjusted} = (\text{MPA PK parameter})/(\text{MMF daily dose}) \quad (2)$$

2.3. Rejection Assessment

The incidence of ACR was evaluated by endo-myocardial biopsies executed as per standard clinical practice [14] and classified according to the International Society for Heart and Lung Transplantation (ISHLT) standardized grading method [21]. ACR was defined

as an ISHLT grade greater than or equal to 1 at the time of observation after transplant on endomyocardial biopsy specimens.

2.4. Statistical Analysis

Categorical variables were presented as absolute value and relative frequency (percentage) and continuous variables as the median and interquartile range (IQR). Normality was assessed using Shapiro–Wilk test. Categorical variables were compared using the Fisher's exact test, whereas continuous variables were compared using Mann–Whitney test, according to the distribution of the data. The non-parametric Mann–Whitney test was used to compare MPA PK values between the study groups and between male and female patients. *p*-values of a 2-sided test lower than 0.05 were considered statistically significant. Analyses were performed using MedCalc (Statistical Software version 20.106, Ostend, Belgium; http://www.medcalc.org accessed on 1 March 2022). Correlation among multiple variables with nonparametric distribution data was performed by Spearman test, considering r > 0.6 as strong correlation.

The ratio between the median value of each MPA-PK parameter we measured in Group 1 and Group 2 was used to estimate the degree of the differences between the two groups according to the following formula:

$$\text{RATIO} = \text{ median PK parameter Group 2/Group 1} \quad (3)$$

The same evaluation was assessed among NACR and ACR patients as follows:

$$\text{RATIO} = \text{ median PK parameter NACR patients/ACR patients} \quad (4)$$

3. Results

3.1. Patients Characterization

Twenty-one patients were included in the analysis, fourteen men (67.0%) and seven (33.0%) women. Twelve of them (57.1%) were included in Group 1, whereas nine (42.9%) were in Group 2. Treatment groups were balanced in terms of relevant clinical characteristics, as shown in Table 1.

Table 1. Patients' baseline demographical and clinical data are reported as overall and according to the immunosuppressive treatment.

Parameter	Total	Group 1	Group 2	
	Median (IQR)	**Median (IQR)**	**Median (IQR)**	***p*-Value**
Number of patients (N, %)	21 (100%)	12 (57.1%)	9 (42.9%)	-
Males (N, %)	14 (67%)	10 (83%)	4 (44%)	0.09 [a]
Age (years)	56.0 (42.0–62.9)	58.3 (49.8–60.5)	43.1 (41.0–65.6)	0.57
MMF dose (mg/day)	1500 (1500–2000)	1500 (1500–2000)	1500 (1500–2000)	1.00
MMF dose (mg/kg/day)	26.3 (20.5–29.7)	24.7 (19.9–28.1)	26.3 (20.8–29.7)	0.72
Post-transplant time (months)	2.6 (1.9–6.1)	2.8 (1.1–6.7)	2.6 (2.3–5.6)	0.67
BMI (Kg/m^2)	22.7 (19.9–28.7)	22.7 (19.9–29.2)	22.7 (20.2–26.8)	0.86
RBCs ($\times 10^6/\mu L$)	3.9 (3.6–4.2)	4.0 (3.6–4.4)	3.8 (3.5–4.0)	0.23
Hb (g/dL)	11.6 (10.3–12.8)	11.6 (10.5–12.5)	11.6 (10.3–12.8)	0.7
WBCs ($\times 10^3/\mu L$)	7.9 (6.2–9.2)	8.0 (6.7–10.1)	6.5 (5.2–8.5)	0.21
Neutro ($\times 10^3/\mu L$)	5.3 (3.9–7.4)	6.1 (4.4–7.7)	4.3 (3.7–6.2)	0.14
Lymph ($\times 10^3/\mu L$)	1.0 (0.6–1.5)	0.9 (0.5–1.3)	1.1 (0.9–1.5)	0.41
Mono ($\times 10^3/\mu L$)	0.6 (0.5–0.8)	0.6 (0.5–0.8)	0.7 (0.6–0.7)	0.43

Table 1. *Cont.*

Parameter	Total	Group 1	Group 2	
	Median (IQR)	**Median (IQR)**	**Median (IQR)**	***p*-Value**
Eos ($\times 10^3/\mu L$)	0.09 (0.02–0.12)	0.09 (0.02–0.11)	0.09 (0.03–0.12)	0.86
Bas ($\times 10^3/\mu L$)	0.04 (0.01–0.06)	0.05 (0.02–0.05)	0.04 (0.01–0.07)	0.91
Plt ($\times 10^3/\mu L$)	219.0 (195.0–299.0)	206.0 (173.0–214.5)	255.0 (221.0–311.0)	0.04 *
ALT (IU/L)	19.3 (17.0–30.0)	21.5 (17.8–31.0)	18.0 (17.0–19.3)	0.31
AST (IU/L)	19.0 (14.6–30.0)	19.5 (15.5–24.3)	19.0 (14.6–20.0)	0.52
Albumin (mg/dL)	42.4 (36.0–44.7)	37.5 (34.9–43.9)	44.4 (41.4–47.8)	0.05
Bilirubin (mg/dL)	0.7 (0.4–1.1)	1.0 (0.7–1.3)	0.4 (0.4–0.6)	0.01 *
CrCl (mL/min) [b]	56.0 (48.0–80.0)	60.5 (37.0–83.8)	55.0 (52.0–68.0)	0.83
GFR (mL/min/1.73 m^2) [c]	60.0 (50.5–81.0)	61.5 (38.3–88.5)	60.0 (51.0–65.0)	0.89
Prednisone (mg/day)	15.0 (7.5–20.0)	12.5 (9.4–15.0)	20.0 (7.5–25.0)	0.26
Prednisone (mg/kg/day)	0.2 (0.1–0.3)	0.2 (0.1–0.2)	0.3 (0.1–0.4)	0.14
CsA dose (mg/day)	-	200.0 (168.8–250.0)	-	-
CsA dose (mg/kg/day)	-	2.9 (2.5–3.5)	-	-
CsA C_0 (ng/mL)	-	184.6 (171.7–209.4)	-	-
TAC dose (mg/day)	-	-	4.0 (4.0–5.0)	-
TAC dose (mg/kg/day)	-	-	0.1 (0.1–0.1)	-
TAC C_0 (ng/mL)	-	-	11.4 (9.9–12.0)	

Data are expressed as median and inter-quartile range (Q1–Q3), if not otherwise indicated. * Statistical difference between Group 1 and Group 2, $p < 0.05$ of Mann–Whitney test for continuous variables. [a] Fisher's exact test for dichotomous variables. [b] Evaluated by Cockcroft–Gault adjusted for body weight. [c] Evaluated by CKD-EPI Equation; ALT—alanine aminotransferase; AST—aspartate aminotransferase; Bas—basophils; BMI—body mass index; C_0—pre-dose drug concentration; CsA—cyclosporine; Eos—eosinophils; CrCl—creatinine clearance; GFR—glomerular filtration rate; Group 1—(MMF + CsA group); Group 2—(MMF + TAC group); Hb—hemoglobin level; IQR—interquartile range; Lymph—lymphocytes; Mono—monocytes; MMF—mycophenolate mofetil; Neutro—neutrophils; Plt—platelets; RBCs—red blood cells; TAC—tacrolimus; WBCs—white blood cells.

3.2. Analysis of Patients' Primary Outcome: PK Analysis

The results of the 12-h MPA-PK analysis performed at a median time of 2.8 months (IQR; 1.1–6.7 months) in Group 1 and at 2.6 months post-transplant (IQR: 2.3–5.6 months) in Group 2 are shown in Table 2.

Table 2. Patients' mycophenolic acid pharmacokinetics data in Group 1 and Group 2.

Parameter	Group 1		Group 2			
	Median	**IQR**	**Median**	**IQR**	***p*-Value**	**Ratio**
MMF dose (mg/day)	1500	1500–2000	1500	1500–2000	1	1
MPA-C_0 (μg/mL)	1.20	0.66–1.75	2.83	2.08–5.83	0.0014 *	2.35
MPA dose-adjusted C_0 (μg/mL/g)	0.78	0.44–0.89	2.11	1.27–2.95	0.0014 *	2.70
MPA-C_{max} (μg/mL)	12.05	3.84–14.27	14.06	11.50–18.07	0.1769	1.16
MPA dose-adjusted C_{max} (μg/mL/g)	5.55	3.15–9.40	9.52	5.58–14.41	0.1021	1.72
T_{max} (min)	75	52.50–120.00	75	63.75–120.00	0.8806	1
MPA Cl/F (L/h)	24.63	18.85–32.12	12.28	10.18–18.34	0.0056 *	0.50
MPA-$AUC_{0–12h}$ (mg·h/L)	36.05	22.95–47.85	67.60	52.75–80.30	0.0036 *	1.88

Table 2. *Cont.*

Parameter	Group 1		Group 2			
	Median	**IQR**	**Median**	**IQR**	***p*-Value**	**Ratio**
MPA dose-adjusted $AUC_{0–12h}$ (mg·h/L/g)	20.40	15.57–26.58	40.73	27.50–50.63	0.0056 *	2.00
MPA-$AUC_{0–2h}$ (mg·h/L)	13.80	3.67–19.55	16.31	14.97–29.23	0.1021	1.18
MPA dose-adjusted $AUC_{0–2h}$ (mg·h/L/g)	7.28	3.63–10.51	12.92	7.94–21.67	0.1021	1.77
MPA-$AUC_{4–12h}$ (mg·h/L)	12.12	8.48–17.40	27.91	16.09–42.17	0.0230 *	2.30
MPA dose-adjusted $AUC_{4–12h}$ (mg·h/L/g)	8.10	5.84–9.25	17.77	11.67–24.46	0.0036 *	2.19

* Statistical difference between Group 1 and Group 2, $p < 0.05$ of Mann–Whitney test. $AUC_{0–2h}$—area under the 0–2-h concentration–time curve; $AUC_{4–12h}$—area under the 4–12-h concentration–time curve; $AUC_{0–12h}$—area under the 12-h concentration–time curve; C_{max}—peak drug plasma concentration; Cl/F—apparent clearance; Group 1—(MMF + CsA group); Group 2—(MMF + TAC group); IQR—interquartile range; MMF—mycophenolate mofetil; MPA—mycophenolic acid; Ratio—degree of the differences between the Group 2 vs. Group1; T_{max}—time to reach the maximum drug plasma concentration.

Absolute and dose-adjusted MPA-C_0 values were significantly higher in Group 2 ($p = 0.001$), and the ratio between median values of the two groups was 2.35 and 2.70, respectively.

The T_{max}, absolute, and dose-adjusted MPA-C_{max} and $AUC_{0–2h}$ results did not show a statistically significant difference between the two groups of treatment.

MPA-$AUC_{0–12h}$ absolute and dose-adjusted values were significantly higher in Group 2 ($p = 0.04$; $p = 0.06$, respectively) as shown in Figure 1a,b, and the ratio between median values were 1.88 and 2, respectively (Table 2). On the other hand, MPA Cl/F (L/h) in the Group 1 was higher than in Group 2 ($p = 0.006$) (Figure 1c).

The main difference in the MPA-PK profiles between the two immunosuppressive treatments was observed at the MPA-$AUC_{4–12h}$. In Group 1, MPA absolute and dose-adjusted $AUC_{4–12h}$ were significantly reduced compared to Group 2 ($p = 0.023$, $p = 0.0036$, respectively), as shown in Figure 2a,b. The absolute and dose-adjusted MPA-$AUC_{4–12h}$ ratios between Group 2 and Group 1 median values were 2.30 and 2.19, respectively (Table 2).

We investigated whether other parameters such as age, sex, renal function, drug clearance, weight and BMI could interfere with the PK differences observed, according to cotreatments, but no correlations were found by Spearman Correlation ($r < 0.6$) and Mann-Whitney tests ($p > 0.05$). It was highlighted only a difference in terms of the MPA–$AUC_{0–2h}$ among female and male patients (median values: 25.9; IQR: 15.8–29.4 vs. 13.7; IQR: 4.6–17.1 respectively; $p = 0.03$).

3.3. Descriptive Analysis of Patients Reporting Acute Cellular Rejection

Out of twenty-one treated patients, eight (38.1%) experienced ACR (six males and two females). Their daily median MMF dose was 1750 mg (IQR: 1375.0–2000.0), corresponding to 24.1 mg/kg/day (IQR: 19.4–30.7). Seven of them (87.5%) were co-treated with CsA, and we investigated the impact of CNIs co-treatments on ACR (Table 3).

The grade of rejection ranged from mild to severe (grade 1R–3R, as shown in Table 4). It occurred at a median time of 3.0 months (IQR: 2.5–10.1) after HTx.

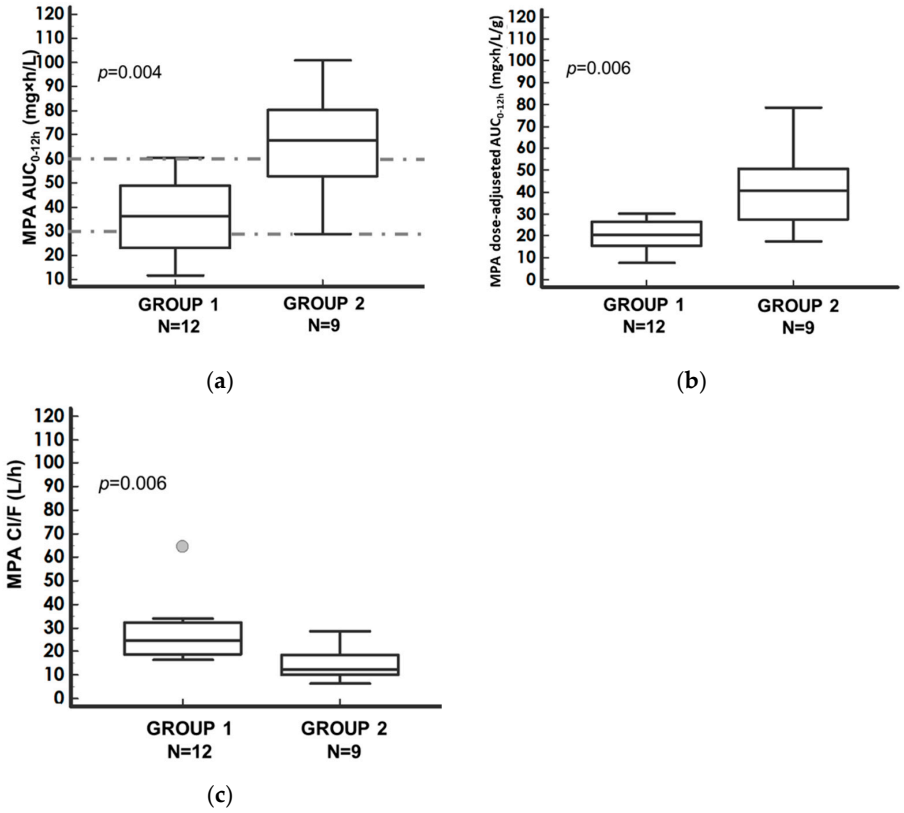

Figure 1. Comparison of (**a**) MPA–$AUC_{0–12h}$; (**b**) dose-adjusted MPA–$AUC_{0–12h}$; (**c**) MPA–CL/F, between Group 1 (MMF + CsA group) and Group 2 (MMF + TAC group) and corresponding *p*-value of the Mann–Whitney test. Median values with the corresponding 95% confidence intervals (bars). Dots represent the outliers. In (**a**), the interval between the dotted lines represents the therapeutic range (30–60 mg·h/L). Nomenclature: $AUC_{0–12h}$—area under the 12 h concentration–time curve; Cl/F—apparent clearance; CsA—cyclosporine; MPA—mycophenolic acid; MMF—mycophenolate mofetil; TAC—tacrolimus.

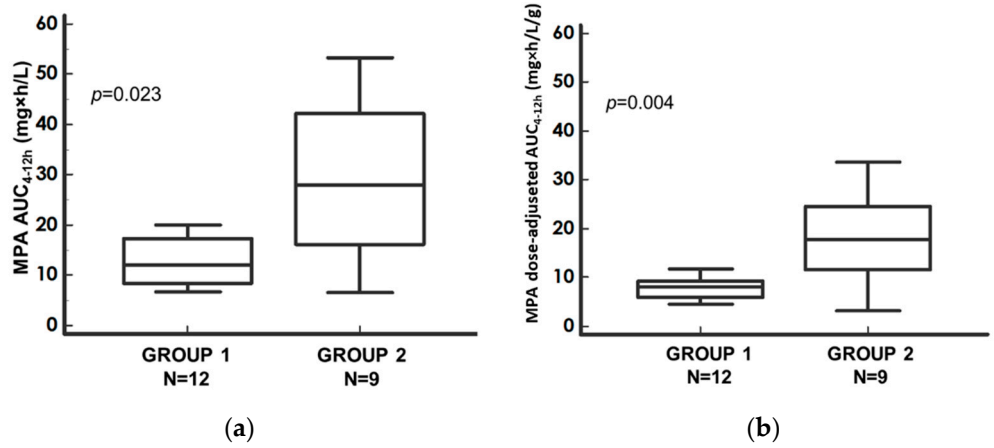

Figure 2. Comparison of (**a**) MPA–$AUC_{4–12h}$; (**b**) dose-adjusted MPA–$AUC_{4–12h;}$ between Group 1 (MMF + CsA group) and Group 2 (MMF + TAC group) and corresponding *p*-value of the Mann–Whitney test. Median values with the corresponding 95% confidence intervals (bars). Dots represent the outliers. Nomenclature: $AUC_{4–12h}$—area under the 4–12-h concentration–time curve; CsA—cyclosporine MPA—mycophenolic acid; MMF—mycophenolate mofetil; TAC—tacrolimus.

Table 3. The impact of cyclosporine and tacrolimus co-treatments in patients with and without acute cellular rejection (ACR).

	CsA-Treated Patients N (%)	TAC-Treated Patients N (%)	Total N (%)	Fisher's Exact Test *p*-Value
ACR Patients	7 (58.3)	1 (11.1)	8 (38.1)	0.067
NACR Patients	5 (41.7)	8 (88.9)	13 (61.9)	
Total	12 (100)	9 (100)	21 (100)	

ACR—acute cellular rejection; CsA—cyclosporine; NACR—not acute cellular rejection; TAC—tacrolimus.

Table 4. Patients' acute cellular rejection (ACR) grading.

Parameter	N (%)
Patients reporting ACR ISHLT 1R (N, %)	5 (62.5%)
Patients reporting ACR ISHLT 2R (N, %)	2 (25.0%)
Patients reporting ACR ISHLT 3R (N, %)	1 (12.5%)

The percentage is referred to the total of ACR patients. ACR—acute cellular rejection; ISHLT—International Society for Heart and Lung Transplantation; 1R—mild grade; 2R—moderate grade; 3R—severe grade.

The TDM was performed at a median time of 1.04 months (IQR: −1.91–3.36) from ACR assessment. To investigate the presence of potential bias due to a different intake of CNIs, we compared NACR and ACR patients according to the CsA or TAC daily dose co-treatment. No differences in terms of daily dose for each CNIs were found with regard to CsA ($p = 0.56$), with a median CsA daily dose equal to 200 mg/kg/day (IQR: 168.75–212.5) among NACR vs. 200 mg/kg/day (IQR: 162.5–343.75) among ACR patients. Due to just a single case of ACR in the TAC-treated group, the test could not be performed.

MPA PK parameters in NACR and ACR patients are reported in Table 5.

Table 5. Pharmacokinetics description in NACR and ACR patients.

Parameter	NACR Pts		ACR Pts			
	Median	IQR	Median	IQR	*p*-Value	Ratio
MMF dose (mg/day/kg)	26.32	20.14–29.46	24.09	18.21–34.04	0.86	0.91
MPA-$AUC_{0–12h}$ (mg·h/L)	60.60	40.45–72.10	31.85	22.95–47.10	0.0248 *	1.90
MPA dose-adjusted $AUC_{0–12h}$ (mg·h/L/g)	29.53	21.57–43.17	20.40	16.57–23.98	0.0298 *	1.45
MPA-C_0 (μg/mL)	2.11	1.62–2.95	1.35	0.70–2.10	0.3106	1.60
MPA dose-adjusted C_0 (μg/mL/g)	1.10	0.73–2.13	0.84	0.60–1.14	0.4257	1.31
MPA-C_{max} (μg/mL)	14.06	11.88–16.02	8.95	3.88–11.56	0.0074 *	1.60
MPA dose-adjusted C_{max} (μg/mL/g)	8.89	5.45–12.89	4.48	3.15–5.96	0.0357 *	1.98
MPA-C_{12} (μg/mL)	2.14	1.74–3.29	0.91	0.77–1.21	0.0030 *	2.36
MPA dose-adjusted C_{12} (μg/mL/g)	1.33	0.99–2.29	0.63	0.49–0.91	0.0059 *	1.60

* Statistical difference between NACR and ACR patients, $p < 0.05$ of Mann–Whitney test. Nomenclature: $AUC_{0–12h}$—area under the 12-h concentration–time curve; ACR—acute cellular rejection; ACR pts—patients who developed ACR; NACR pts—patients who did not develop ACR; C_0—pre-dose drug plasma concentration; C_{12}—12 h post-dose drug plasma concentration; C_{max}—peak drug plasma concentration; IQR—interquartile range; MPA—mycophenolic acid; Ratio—degree of the differences between the NACR vs. ACR patients.

MPA-$AUC_{0–12h}$ median value in NACR patients was higher than in ACR patients ($p = 0.02$), as shown in Figure 3a, and the ratio between median values was 1.9 (Table 5). These results were also confirmed for the dose-adjusted parameter (Table 5). No statistically significant difference in MPA-C_0 between the two groups of patients was found (Table 5).

On the contrary, NACR recipients presented a higher MPA-C_{max} ($p = 0.007$), as shown in Figure 3b, than ACR, and the ratio between the median values was 1.6 (Table 5). Significantly increased values were evidenced for MPA-C_{12h} ($p = 0.003$), as shown in Figure 3c, and the ratio between NACR and ACR recipients was 2.4 (Table 5).

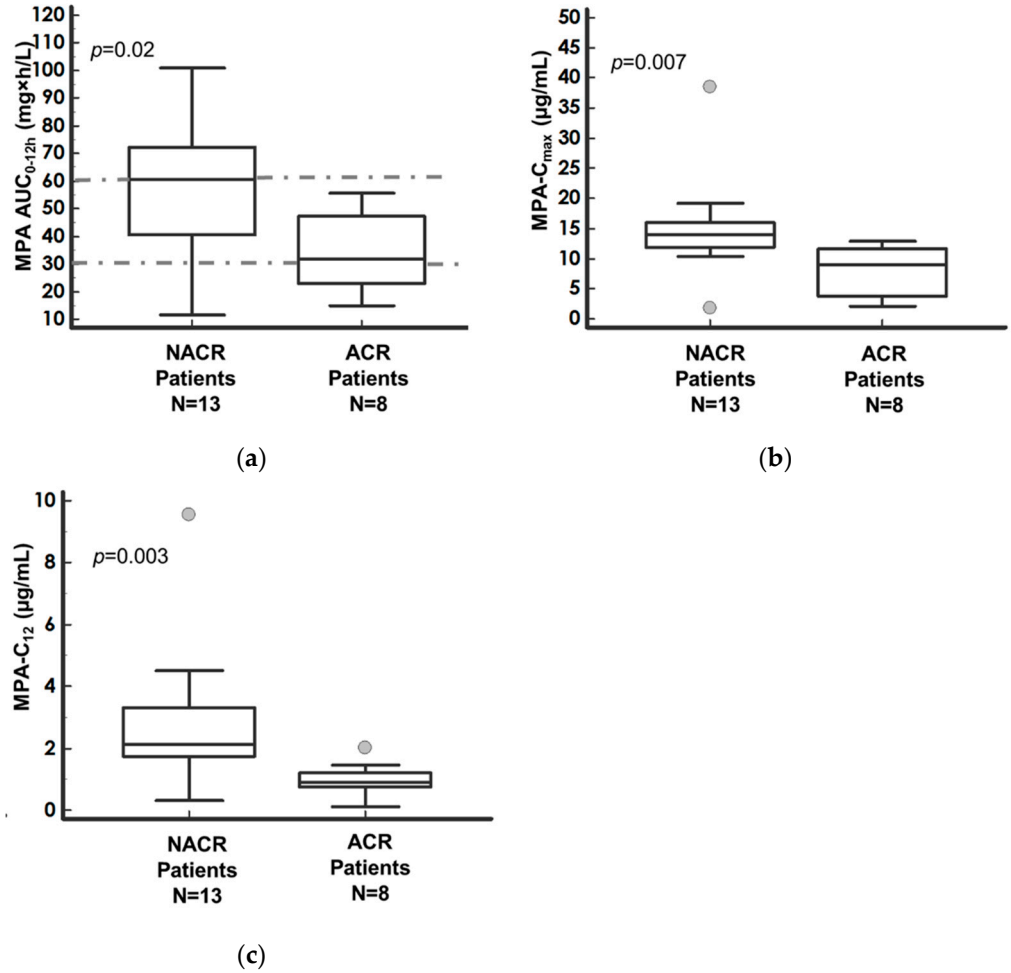

Figure 3. Comparison of (**a**) MPA–$AUC_{0–12h}$, (**b**) MPA–C_{max}, and (**c**) MPA–C_{12} between NACR and ACR patients and corresponding *p*-value of the Mann–Whitney test. Median values with the corresponding 95% confidence intervals (bars). In (**a**), the interval between the dotted lines represents the therapeutic range (30–60 mg·h/L). Dots represent the outliers. Nomenclature: $AUC_{0–12h}$—area under the 12-h concentration–time curve; C_{max}—peak drug plasma concentration; C_{12}—12 h post-dose drug plasma concentration, ACR pts—patients who developed acute cell rejection; NACR pts—patients who did not develop acute cell rejection.

All these differences were confirmed by the analysis of the corresponding dose-adjusted parameters, as shown in Table 5.

4. Discussion

MPA-PK profile can be influenced by the CNIs co-treatment, as evidenced by the effect of CsA on MPA EHC [6]. Due to the critical conditions of patients in the early post-HTx period [15] and the possible pharmacological interaction of the co-administration of immunosuppressive agents, the TDM of MPA could play a pivotal role in the context of precision medicine in clinical practice. In this study on HTx recipients treated with MMF, we found marked differences in MPA-$AUC_{0–12h}$, which were influenced by the co-administered CNI, resulting in a two-fold higher exposure in patients co-treated with TAC. No influences of CsA or TAC were observed on both MMF adsorption and bioavailability, as

supported by our data on MPA $AUC_{0–2h}$, C_{max} and T_{max}. On the contrary, we evidenced a higher dose-adjusted MPA-$AUC_{4–12h}$ in Group 2 than in Group 1 and a higher MPA-Cl/F in Group 1. These results suggest the inhibition of EHC by CsA in HTx recipients. The higher MPA trough levels observed in Group 2 (Table 2) could be explained by the interference of CsA on MPA EHC since it frequently occurs from 6 to 12 h after MMF administration. Considering the confounding factor of MMF administered dose, MPA-PK parameters were adjusted for daily dose. This approach presumed linearity between MMF doses and MPA exposure. By comparing the absolute and dose-adjusted MPA PK parameters, linearity between dose and concentration was confirmed, as suggested by Cattaneo et al. in renal transplant patients [4].

These data are aligned to a similar study involving 62 HTx recipients, where patients co-treated with CsA and MMF showed higher MPA exposure and pre-dose levels than patients co-treated with sirolimus, confirming the effect of CsA on MPA exposure as evidenced in our study [22]. Previous studies have already shown that CsA could influence MPA-$AUC_{0–12h}$ affecting MPA EHC [2] and MPA-Cl [5]. Nevertheless, this PK interaction has been well documented in renal transplant recipients [4,22,23], whereas there is a paucity of data from studies investigating not-renal transplant recipients, where renal clearance and drugs half-life should be less involved.

The impact of MPA TDM on HTx has been less studied, differently from renal transplant. Two reviews resumed the previous clinical trials in the HTx setting, investigating a relationship between MPA-PK parameters and therapy outcomes [24,25]. Although the prevention of ACR in HTx patients is not totally defined, it has been suggested that MPA-$AUC_{0–12h}$ monitoring represents a more effective strategy to prevent rejection than a single-time point model [24]. For this reason, in this pilot study, we exploratively described the PK parameters in NACR and ACR patients, obtaining results in terms of absolute and dose-adjusted MPA-$AUC_{0–12h}$ ($p < 0.03$), which are aligned with the main relevant data in the literature. De Nofrio et al. showed in 38 Htx recipients that patients with a grade 2 or 3 rejection had a lower mean total MPA-$AUC_{0–12h}$ (26.1 ± 6.6 vs. 42.8 ± 14.0 mg·h/L, $p < 0.08$), while no effect of MPA trough level was found [26]. According to the last Consensus Report by the International Association of Therapeutic Drug Monitoring and Clinical Toxicology on MMF, different thresholds have been proposed [6]. Figurski et al. showed in 21 HTx patients that an MPA-$AUC_{0–12h}$ < 36.2 mg·h/L in the first two weeks post-transplant was associated with a higher risk of ACR, with high sensitivity (0.8) and specificity (0.8), although the statistical significance was not reached [13]. Woillard et al. identified for MPA-$AUC_{0–12h}$ a threshold of 50 mg·h/L, below which there was a higher risk of rejection, stratifying patients for CNI exposure ($p = 0.002$) [12].

In this study, since no MMF dose changes occurred, we supposed that ACR patients were less exposed to immunosuppressive maintenance treatment than NACR patients. Due to the higher prevalence of ACR recipients in Group 1 compared to Group 2, this clinical outcome could also be attributable to the influence of CsA on MPA-$AUC_{0–12h}$. The Fisher exact test we performed to explore this hypothesis showed only a trend (p-value 0.067), probably due to a limited number of patients included in our analysis. Furthermore, we evidenced a statistically significant difference between NACR and ACR patients not only on MPA-C_{max} ($p = 0.01$) but also on MPA-C_{12} ($p = 0.003$), which previous studies demonstrated an acceptable correlation to the entire MPA-$AUC_{0–12h}$ [7,27,28]. These data confirmed the strong relationship between total drug exposure and immunosuppressive efficacy. On the contrary, MPA-C_0 does not statistically discriminate between ACR and NACR patients in our analysis, resulting in a weak surrogate marker of total drug exposure and efficacy. Hence, the estimation of MPA-$AUC_{0–12h}$ by a limited sampling scheduled should be preferred to a pre-dose determination. Alternatively, if only one sample can be obtained, Kaczmareck et al. showed that MPA-C_{12} could be a better efficacy biomarker than MPA-C_0 due to the scheduled sampling time strongly linked to dose administration [29].

In our analysis, we excluded possible PK interpretation biases such as the interference of glucocorticoids in MPA exposure and bilirubinemia. Glucocorticoids induce the expres-

sion of UDP-GT, the inactivating enzyme of MPA [2]. Nevertheless, all patients received the same mg/kg/day dose of prednisone, not representing a confounding variable. On the other hand, MPA-$AUC_{0–12}$ could be affected by bilirubinemia, which was different in Group 1 and Group 2 [23]. High plasmatic bilirubin levels could displace MPA from albumin binding sites, thus affecting its total exposure [30]. We excluded this possible influence since our patients did not show clinically relevant high levels of plasmatic bilirubin, and hyperbilirubinemia does not significative affect the free active MPA concentration [27]. We did not consider the different baseline platelet levels in Group 1 and Group 2 since no data in the literature show possible influence on immunosuppressive treatments.

Due to the small number of patients and the retrospective and observational nature of this study, MPA-$AUC_{0–12h}$ was measured by a single PK profile analysis per patient which was not executed at the same time for all the enrolled patients and not strictly close to ACR, as it was executed by clinical practice, not following a specific study protocol. Hence, no conclusive results can be obtained. However, we assumed that MPA-PK parameters were most likely stable during the observational time since physicians did not observe any clinical conditions requiring a dose adaptation of the standard immunosuppressive regimen. Furthermore, MPA PK prospective studies on heart and renal transplants did not show relevant variability of these parameters during the first year of treatment, considering both absolute and dose-adjusted data [4,13]. This misalignment between PK measurements and clinical assessments could represent the major source of bias that prevented us from assessing whether there was a meaningful clinical relation between ACR and low MPA exposure. Nevertheless, the PK parameters we found in our analyses were consistent with other similar PK studies in terms of (a) increased Cl/F in Htx recipients co-treated with CsA compared to TAC, (b) two-fold increased $AUC_{0–12h}$ in TAC than in CsA co-treated patients, and (c) identification of a relevant MPA-EHC in TAC co-treated recipients [4,20]. Another source of bias in this study could be related to the overall study group composition, mainly represented by men, whereas Group 2 included a high percentage of women. However, MPA-PK generally is not influenced by gender [2,31], although it was recently suggested for MPA and MPAG PK in stable renal transplant recipients receiving enteric coated mycophenolate sodium combined with TAC [32]. Interestingly, in our analysis, we did not observe any relevant PK differences, except for the MPA-$AUC_{0–2h}$, suggesting a better absorption of MMF in female patients than in male patients.

Due to the aforementioned limitations, our findings cannot be transferred into clinical practice. A prospective study with homogeneous scheduled serial measurements per subject, from the enrolment up to the development of rejection, is required.

5. Conclusions

This pilot study evidenced that TAC or CsA co-administration could affect MPA exposure in HTx recipients. This effect is attributable to MPA EHC suppression and consequent MPA-Cl augmentation by CsA. These results have to be prospectively validated in order to support a precision medicine approach in routine clinical practice. MPA TDM represents a relevant supporting tool for clinicians, especially in the early post-transplant period, when MMF is administered at a fixed dose. In this context, the estimation of the MPA-$AUC_{0–12}$ by a few sampling points (i.e., limited sampling strategies) is a more effective approach than a single sample point model (i.e., C_0). This method could optimize MMF efficacy and minimize adverse effects, especially when recipients are switched from CsA to TAC or vice versa. The findings of our explorative study can be used in order to design a future prospective trial aiming to identify the optimal thresholds for the main clinically relevant MPA-PK parameters, stratifying patients for the co-administered CNI after HTx.

All these data further support the MPA TDM employment in clinical practice.

Author Contributions: Conceptualization, F.L.R., M.B. and U.L.; methodology, F.L.R., M.B. and U.L.; software, F.L.R. and A.Z.; formal analysis, F.L.R., A.Z. and J.B.; investigation, F.L.R. and M.B.; data curation, F.L.R. and A.Z.; writing—original draft preparation, F.L.R., M.B., S.S., C.N., U.L., J.A. and A.Z.; writing—review and editing, F.L.R., M.B., S.S., C.N., U.L., J.A. and A.Z.; visualization, F.L.R. and M.B.; supervision, F.L.R. and M.B.; project administration, F.L.R., M.B., S.S., C.N., U.L., J.A. and A.Z. All authors have read and agreed to the published version of the manuscript.

Funding: This research received no external funding.

Institutional Review Board Statement: The study was performed at the "S. Maria della Misericordia" University Hospital of Udine, Italy. The study was approved on 22 September 2022 by the Internal Review Board (I.R.B.) of the Commission for the Experimentation and Protection of Human Subjects of the Department of Medical Area of the University of Udine with the protocol number: 036/2020_IRB.

Informed Consent Statement: Informed consent for clinical, epidemiological research, training, and study of pathologies was obtained from all subjects involved in the study. For the 12-h MPA-PK profile, written informed consent was obtained.

Data Availability Statement: The data that support the findings of this study are available from the corresponding author upon reasonable request.

Acknowledgments: The authors thank the healthcare staff of the Clinical Pharmacology and Toxicology Institute, "S. Maria della Misericordia" University Hospital Friuli Centrale, Udine, Italy, for the collection of blood samples and for the analyses performed. The authors thank Enza Pincente for the English revision of the manuscript.

Conflicts of Interest: The authors declare no conflict of interest.

References

1. Chambers, D.C.; Cherikh, W.S.; Harhay, M.O.; Hayes, D.J.; Hsich, E.; Khush, K.K.; Meiser, B.; Potena, L.; Rossano, J.W.; Toll, A.E.; et al. The International Thoracic Organ Transplant Registry of the International Society for Heart and Lung Transplantation: Thirty-sixth adult lung and heart-lung transplantation Report-2019; Focus theme: Donor and recipient size match. *J. Heart Lung Transplant. Off. Publ. Int. Soc. Heart Transplant.* **2019**, *38*, 1042–1055. [CrossRef] [PubMed]
2. Staatz, C.E.; Tett, S.E. Clinical pharmacokinetics and pharmacodynamics of mycophenolate in solid organ transplant recipients. *Clin. Pharmacokinet.* **2007**, *46*, 13–58. [CrossRef] [PubMed]
3. Staatz, C.E.; Tett, S.E. Pharmacology and toxicology of mycophenolate in organ transplant recipients: An update. *Arch. Toxicol.* **2014**, *88*, 1351–1389. Available online: http://www.ncbi.nlm.nih.gov/pubmed/24792322 (accessed on 1 March 2022). [CrossRef] [PubMed]
4. Cattaneo, D.; Merlini, S.; Zenoni, S.; Baldelli, S.; Gotti, E.; Remuzzi, G.; Perico, N. Influence of Co-Medication with Sirolimus or Cyclosporine on Mycophenolic Acid Pharmacokinetics in Kidney Transplantation. *Am. J. Transplant.* **2005**, *5*, 2937–2944. [CrossRef]
5. Yau, W.-P.; Vathsala, A.; Lou, H.-X.; Zhou, S.; Chan, E. Mechanism-based enterohepatic circulation model of mycophenolic acid and its glucuronide metabolite: Assessment of impact of cyclosporine dose in Asian renal transplant patients. *J. Clin. Pharmacol.* **2009**, *49*, 684–699. [CrossRef]
6. Bergan, S.; Brunet, M.; Hesselink, D.A.; Johnson-Davis, K.L.; Kunicki, P.K.; Lemaitre, F.; Marquet, P.; Molinaro, M.; Noceti, O.; Pattanaik, S.; et al. Personalized Therapy for Mycophenolate: Consensus Report by the International Association of Therapeutic Drug Monitoring and Clinical Toxicology. *Ther. Drug Monit.* **2021**, *43*, 150–200. Available online: https://journals.lww.com/10.1097/FTD.0000000000000871 (accessed on 1 March 2022). [CrossRef]
7. Kuypers, D.R.J.; Le Meur, Y.; Cantarovich, M.; Tredger, M.J.; Tett, S.E.; Cattaneo, D.; Tönshoff, B.; Holt, D.W.; Chapman, J.; van Gelder, T. Consensus report on therapeutic drug monitoring of mycophenolic acid in solid organ transplantation. *Clin. J. Am. Soc. Nephrol.* **2010**, *5*, 341–358. [CrossRef]
8. Shaw, L.M.; Kaplan, B.; DeNofrio, D.; Korecka, M.; Brayman, K.L. Pharmacokinetics and concentration-control investigations of mycophenolic acid in adults after transplantation. *Ther. Drug Monit.* **2000**, *22*, 14–19. [CrossRef]
9. Yamani, M.H.; Starling, R.C.; Goormastic, M.; Van Lente, F.; Smedira, N.; McCarthy, P.; Young, J.B. The impact of routine mycophenolate mofetil drug monitoring on the treatment of cardiac allograft rejection. *Transplantation* **2000**, *69*, 2326–2330. [CrossRef]
10. Hesse, C.J.; Vantrimpont, P.; van Riemsdijk-van Overbeeke, I.C.; van Gelder, T.; Balk, A.H.; Weimar, W. The value of routine monitoring of mycophenolic acid plasma levels after clinical heart transplantation. *Transplant. Proc.* **2001**, *33*, 2163–2164. [CrossRef]

11. van Gelder, T.; Tedesco Silva, H.; de Fijter, J.W.; Budde, K.; Kuypers, D.; Arns, W.; Paul Soulillou, J.; Kanellis, J.; Zelvys, A.; Ekberg, H.; et al. Renal Transplant Patients at High Risk of Acute Rejection Benefit From Adequate Exposure to Mycophenolic Acid. *Transplantation* **2010**, *89*, 595–599. Available online: https://journals.lww.com/transplantjournal/Fulltext/2010/03150/Renal_Transplant_Patients_at_High_Risk_of_Acute.14.aspx (accessed on 1 March 2022). [CrossRef] [PubMed]
12. Woillard, J.-B.; Saint-Marcoux, F.; Monchaud, C.; Youdarène, R.; Pouche, L.; Marquet, P. Mycophenolic mofetil optimized pharmacokinetic modelling, and exposure-effect associations in adult heart transplant recipients. *Pharmacol. Res.* **2015**, *99*, 308–315. Available online: https://www.sciencedirect.com/science/article/pii/S1043661815001450 (accessed on 1 March 2022). [CrossRef] [PubMed]
13. Figurski, M.J.; Pawiński, T.; Goldberg, L.R.; DeNofrio, D.; Nawrocki, A.; Taylor, D.O.; Lake, K.D.; Chojnowski, D.; Shaw, L.M. Pharmacokinetic monitoring of mycophenolic acid in heart transplant patients: Correlation the side-effects and rejections with pharmacokinetic parameters. *Ann. Transplant.* **2012**, *17*, 68–78. [CrossRef] [PubMed]
14. Sponga, S.; Travaglini, C.; Pisa, F.; Piani, D.; Guzzi, G.; Nalli, C.; Spagna, E.; Tursi, V.; Livi, U. Does psychosocial compliance have an impact on long-term outcome after heart transplantation? *Eur. J. Cardiothorac. Surg. Off. J. Eur. Assoc. Cardiothorac. Surg.* **2016**, *49*, 64–72. [CrossRef] [PubMed]
15. Kobashigawa, J.A.; Miller, L.W.; Russell, S.D.; Ewald, G.A.; Zucker, M.J.; Goldberg, L.R.; Eisen, H.J.; Salm, K.; Tolzman, D.; Gao, J.; et al. Tacrolimus with Mycophenolate Mofetil (MMF) or Sirolimus vs. Cyclosporine with MMF in Cardiac Transplant Patients: 1-Year Report. *Am. J. Transplant.* **2006**, *6*, 1377–1386. [CrossRef]
16. Brunet, M.; van Gelder, T.; Åsberg, A.; Haufroid, V.; Hesselink, D.A.; Langman, L.; Lemaitre, F.; Marquet, P.; Seger, C.; Shipkova, M.; et al. Therapeutic Drug Monitoring of Tacrolimus-Personalized Therapy: Second Consensus Report. *Ther. Drug Monit.* **2019**, *41*, 261–307. Available online: https://journals.lww.com/drug-monitoring/Fulltext/2019/06000/Therapeutic_Drug_Monitoring_of.2.aspx (accessed on 1 March 2022). [CrossRef]
17. Shaw, L.M.; Korecka, M.; van Breeman, R.; Nowak, I.; Brayman, K.L. Analysis, pharmacokinetics and therapeutic drug monitoring of mycophenolic acid. *Clin. Biochem.* **1998**, *31*, 323–328. [CrossRef]
18. Zhang, Y.; Huo, M.; Zhou, J.; Xie, S. PKSolver: An add-in program for pharmacokinetic and pharmacodynamic data analysis in Microsoft Excel. *Comput. Methods Programs Biomed.* **2010**, *99*, 306–314. [CrossRef]
19. Xiang, H.; Zhou, H.; Zhang, J.; Sun, Y.; Wang, Y.; Han, Y.; Cai, J. Limited Sampling Strategy for Estimation of Mycophenolic Acid Exposure in Adult Chinese Heart Transplant Recipients. *Front. Pharmacol.* **2021**, *12*, 652333. [CrossRef]
20. Ting, L.S.L.; Partovi, N.; Levy, R.D.; Riggs, K.W.; Ensom, M.H.H. Pharmacokinetics of mycophenolic acid and its phenolic-glucuronide and ACYl glucuronide metabolites in stable thoracic transplant recipients. *Ther. Drug Monit.* **2008**, *30*, 282–291. [CrossRef]
21. Billingham, M.; Kobashigawa, J.A. The revised ISHLT heart biopsy grading scale. *J. Heart Lung Transplant. Off. Publ. Int. Soc. Heart Transplant.* **2005**, *24*, 1709. [CrossRef] [PubMed]
22. Dösch, A.O.; Ehlermann, P.; Koch, A.; Remppis, A.; Katus, H.A.; Dengler, T.J. A comparison of measured trough levels and abbreviated AUC estimation by limited sampling strategies for monitoring mycophenolic acid exposure in stable heart transplant patients receiving cyclosporin A-containing and cyclosporin A-free immunosuppressive. *Clin. Ther.* **2006**, *28*, 893–905. [CrossRef] [PubMed]
23. Noreikaitė, A.; Saint-Marcoux, F.; Marquet, P.; Kaduševičius, E.; Stankevičius, E. Influence of cyclosporine and everolimus on the main mycophenolate mofetil pharmacokinetic parameters: Cross-sectional study. *Medicine* **2017**, *96*, e6469. [CrossRef]
24. Zuk, D.M.; Pearson, G.J. Monitoring of mycophenolate mofetil in orthotopic heart transplant recipients-a systematic review. *Transplant. Rev.* **2009**, *23*, 171–177. [CrossRef]
25. Monchaud, C.; Marquet, P. Pharmacokinetic Optimization of Immunosuppressive Therapy in Thoracic Transplantation: Part II. *Clin. Pharmacokinet.* **2009**, *48*, 489–516. [CrossRef] [PubMed]
26. DeNofrio, D.; Loh, E.; Kao, A.; Korecka, M.; Pickering, F.W.; Craig, K.A.; Shaw, L.M. Mycophenolic acid concentrations are associated with cardiac allograft rejection. *J. Heart lung Transplant. Off. Publ. Int. Soc. Heart Transplant.* **2000**, *19*, 1071–1076. [CrossRef]
27. Baraldo, M.; Isola, M.; Feruglio, M.T.; Francesconi, A.; Franceschi, L.; Tursi, V.; Livi, U.; Furlanut, M. Therapeutic mycophenolic acid monitoring by means of limited sampling strategy in orthotopic heart transplant patients. *Transplant. Proc.* **2005**, *37*, 2240–2243. [CrossRef] [PubMed]
28. Wada, K.; Takada, M.; Kotake, T.; Ochi, H.; Morishita, H.; Komamura, K.; Oda, N.; Mano, A.; Kato, T.S.; Hanatani, A.; et al. Limited Sampling Strategy for Mycophenolic Acid in Japanese Heart Transplant Recipients. *Circ. J.* **2007**, *71*, 1022–1028. [CrossRef]
29. Kaczmarek, I.; Bigdeli, A.K.; Vogeser, M.; Mueller, T.; Beiras-Fernandez, A.; Kaczmarek, P.; Schmoeckel, M.; Meiser, B.; Reichart, B.; Ueberfuhr, P. Defining algorithms for efficient therapeutic drug monitoring of mycophenolate mofetil in heart transplant recipients. *Ther. Drug Monit.* **2008**, *30*, 419–427. [CrossRef]
30. Shaw, L.M.; Figurski, M.; Milone, M.C.; Trofe, J.; Bloom, R.D. Therapeutic Drug Monitoring of Mycophenolic Acid. *Clin. J. Am. Soc. Nephrol.* **2007**, *2*, 1062–1072. Available online: http://cjasn.asnjournals.org/content/2/5/1062.abstract (accessed on 1 March 2022). [CrossRef]

31. Pescovitz, M.D.; Guasch, A.; Gaston, R.; Rajagopalan, P.; Tomlanovich, S.; Weinstein, S.; Bumgardner, G.L.; Melton, L.; Ducray, P.S.; Banken, L.; et al. Equivalent Pharmacokinetics of Mycophenolate Mofetil in African-American and Caucasian Male and Female Stable Renal Allograft Recipients. *Am. J. Transplant.* **2003**, *3*, 1581–1586. [CrossRef] [PubMed]
32. Tornatore, K.M.; Meaney, C.J.; Wilding, G.E.; Chang, S.S.; Gundroo, A.; Cooper, L.M.; Gray, V.; Shin, K.; Fetterly, G.J.; Prey, J.; et al. Influence of sex and race on mycophenolic acid pharmacokinetics in stable African American and Caucasian renal transplant recipients. *Clin. Pharmacokinet.* **2015**, *54*, 423–434. [CrossRef] [PubMed]

pharmaceutics

MDPI

Article

Population Pharmacokinetics of Busulfan and Its Metabolite Sulfolane in Patients with Myelofibrosis Undergoing Hematopoietic Stem Cell Transplantation

Adrin Dadkhah [1,*], Sebastian Georg Wicha [2], Nicolaus Kröger [3], Alexander Müller [4], Christoph Pfaffendorf [2], Maria Riedner [5], Anita Badbaran [3], Boris Fehse [3] and Claudia Langebrake [1,3]

1 Hospital Pharmacy, University Medical Center Hamburg-Eppendorf, 20251 Hamburg, Germany; clangebrake@uke.de
2 Department of Clinical Pharmacy, Institute of Pharmacy, University of Hamburg, 20146 Hamburg, Germany; sebastian.wicha@uni-hamburg.de (S.G.W.); christoph.pfaffendorf@uni-hamburg.de (C.P.)
3 Department of Stem Cell Transplantation, University Medical Center Hamburg-Eppendorf, 20251 Hamburg, Germany; n.kroeger@uke.de (N.K.); badbaran@uke.de (A.B.); fehse@uke.de (B.F.)
4 Department of Legal Medicine, University Medical Center Hamburg-Eppendorf, 20251 Hamburg, Germany; alexander.mueller@uke.de
5 Technology Platform Mass Spectrometry, University of Hamburg, 20146 Hamburg, Germany; maria.riedner@uni-hamburg.de
* Correspondence: a.dadkhah@uke.de; Tel.: +49-40-7410-58517

Abstract: For patients with myelofibrosis, allogeneic hematopoietic stem cell transplantation (allo-HSCT) remains the only curative treatment to date. Busulfan-based conditioning regimens are commonly used, although high inter-individual variability (IIV) in busulfan drug exposure makes individual dose selection challenging. Since data regarding the IIV in patients with myelofibrosis are sparse, this study aimed to develop a population pharmacokinetic (PopPK) model of busulfan and its metabolite sulfolane in patients with myelofibrosis. The influence of patient-specific covariates on the pharmacokinetics of drug and metabolite was assessed using non-linear mixed effects modeling in NONMEM®. We obtained 523 plasma concentrations of busulfan and its metabolite sulfolane from 37 patients with myelofibrosis. The final model showed a population clearance (CL) and volume of distribution (V_d) of 0.217 L/h/kg and 0.82 L/kg for busulfan and 0.021 L/h/kg and 0.65 L/kg for its metabolite. Total body weight (TBW) and a single-nucleotide polymorphism of glutathione-S-transferase A1 (GSTA1 SNP) displayed a significant impact on volume of distribution and metabolite clearance, respectively. This is the first PopPK-model developed to describe busulfan's pharmacokinetics in patients with myelofibrosis. Incorporating its metabolite sulfolane into the model not only allowed the characterization of the covariate relationship between GSTA1 and the clearance of the metabolite but also improved the understanding of busulfan's metabolic pathway.

Keywords: busulfan; sulfolane; myelofibrosis; population pharmacokinetics

Citation: Dadkhah, A.; Wicha, S.G.; Kröger, N.; Müller, A.; Pfaffendorf, C.; Riedner, M.; Badbaran, A.; Fehse, B.; Langebrake, C. Population Pharmacokinetics of Busulfan and Its Metabolite Sulfolane in Patients with Myelofibrosis Undergoing Hematopoietic Stem Cell Transplantation. *Pharmaceutics* **2022**, *14*, 1145. https://doi.org/10.3390/pharmaceutics14061145

Academic Editor: Monica M. Jablonski

Received: 27 April 2022
Accepted: 25 May 2022
Published: 27 May 2022

1. Introduction

Myelofibrosis is a chronic myeloproliferative disorder that is characterized by a cytokine-mediated fibrosis of the bone marrow. This results in extramedullary hematopoiesis in the liver and spleen, often accompanied by enlargement of both organs [1]. Genetic aberrations of the genes JAK2, MPL and CALR were identified as the cause of this myeloproliferative disorder [2] and deemed relevant to clinical decision-making with regard to prognosis as well [3]. Since comprehensive mutational profiling has shown that most patients carry a JAKV617F mutation, initial therapy with the JAK1/JAK2 inhibitor ruxolitinib may reduce splenomegaly and improve performance status [4].

However, allogeneic hematopoietic stem cell transplantation (allo-HSCT) remains the only curative treatment to date. Prior to allo-HSCT, patients typically undergo either

reduced intensity conditioning (RIC) [5] or myeloablative conditioning (MAC) [6,7] with busulfan and fludarabine.

Regarding other neoplastic diseases, the relationship between busulfan drug exposure and patient outcome after allo-HSCT has been investigated extensively. On the one hand, under-exposure is associated with higher risks of relapse and graft rejection, and on the other hand, over-exposure more frequently results in organ toxicity, sinusoidal obstructive syndrome (SOS), acute graft-versus-host disease (aGvHD) and overall higher treatment-related mortality (TRM) [8–11]. It is also known that busulfan has a high inter-individual variability (IIV) considering the ratio of dose and drug exposure, which makes individual dose selection challenging. Therefore, to maintain the narrow therapeutic range, it is recommended to conduct therapeutic drug monitoring (TDM) for higher dose busulfan in MAC conditioning regimens [9,12].

Studies that have investigated other neoplastic diseases found that patient-specific covariates such as age, weight, body surface area or co-medication might affect the clearance (CL) or volume of distribution (Vd) of busulfan and, therefore, may explain the IIV [13–18] as well as the inter-occasion variability (IOV) [14,19,20].

Since patients with myelofibrosis have an elevated risk of hepatotoxicity and impaired liver function due to extramedullary hematopoiesis, PK parameters of busulfan might additionally be affected. However, data describing the pharmacokinetic variability of busulfan prior to allo-HSCT in patients with myelofibrosis are sparse.

Overall, the pharmacokinetics of busulfan are complex, considering that its metabolic pathway is still not fully understood. Lawson et al. describe the conjugation of busulfan with glutathione through different isoenzymes of glutathione-S-transferase (GST), which eventually results in the four major metabolites: tetrahydrothiophene (THT), THT-1-oxide, sulfolane and 3-hydroxysulfolane [21]. Two of the most prominent isoenzymes are GSTA1 and GSTM1, and therefore, their impact on busulfan CL was subject to several investigations. In every population pharmacokinetic (PopPK) model, except one [22], it was found that polymorphisms correlate with a decrease in CL [23–26].

In order to get a better understanding of busulfan's metabolic pathway, joint PK-modeling of the parent drug and its metabolite seems sensible as it might account for uncertainties in the model and consequently improve the parameter estimations [27]. Moreover, a metabolic ratio of busulfan/sulfolane $\geq$5 is associated with a higher rate of graft failure and decreased event-free survival (EFS) [28]. However, none of busulfan's metabolites have yet been incorporated into a PopPK model.

Therefore, this study aimed to develop a PopPK model of busulfan and its metabolite sulfolane by examining known and determining new patient-specific covariates to explain busulfan's inter-individual variability in patients with myelofibrosis.

2. Materials and Methods

2.1. Patients and Data Collection

Patients of both sexes aged $\geq$18 years with diagnosed myelofibrosis that were scheduled for allo-HSCT with previous reduced intensity busulfan/fludarabine conditioning therapy at the University Medical Center Hamburg–Eppendorf between November 2018 and June 2020 were included after written informed consent. We also obtained written consent from patients who already underwent allo-HSCT between October 2016 and October 2017 and met the same criteria for enrollment. The single-center, prospective and partly retrospective, observational study was approved by the local Ethics Committee of the Hamburg Chamber of Physicians on 16 October 2018 (approval number: PV5842) and registered at the German Clinical Trials Register, number DRKS00015217, on 31 October 2018.

Patient demographics and routine clinical data, such as levels of aspartate transaminase (AST), alanine transaminase (ALT), bilirubin, alkaline phosphatase (AP), results of elastography by Fibroscan, and genetic and other diagnostic markers, were obtained from the electronic patient record before busulfan administration. Scores according to the Dynamic International Prognostic Scoring System (DIPSS) for primary myelofibrosis and

myelofibrosis secondary to PV and ET (MYSEC) for post-polycythemia vera (Post-PV) and post-essential thrombocythemia (Post-ET) myelofibrosis were determined to predict patient outcomes [29–31]. Treatment-related adverse events and outcomes (mucositis, aGvHD, cGvHD, SOS, relapse, death) were evaluated for one year after allo-HSCT.

Continuous variables are reported as medians with interquartile ranges (IQR) and discrete variables as counts (percentages).

2.2. Dosing, Pharmacokinetic Sampling and Quantification

Depending on the therapy standards at the time of enrollment, patients received either 10 doses of i.v. busulfan (0.8 mg/kg) every 6 h with a 2 h infusion rate (Q6H) or were dosed with three busulfan infusions every 24 h with an initial dose of 3.2 mg/kg and a 3 h infusion rate, followed by dose adjustment if necessary to achieve a cumulative area under the curve (cAUC) of 50 mg $\times$ h/L (Q24H). Furthermore, all patients received fludarabine and anti-thymocyte globulin (ATG) as part of the conditioning chemotherapy and levetiracetam as anticonvulsant prophylaxis. Comedications that are commonly known for their drug–drug interactions with busulfan, such as phenytoin, metronidazole, or azoles, were not administered during busulfan treatment.

For Q6H, blood samples were drawn 2.08, 3, 4 and 5.5 h after the start of the first and ninth infusion with an additional trough sample 5.5 h after start of the fifth infusion. For Q24H, sampling was conducted at 3.08, 4, 5 and 6.5 h after the start of the first infusion. Blood samples were drawn into serum tubes, immediately stored at 2–8 °C and centrifuged (2000 rpm, 10 min at 4 °C) shortly after. Supernatant plasma was separated into two aliquots and stored at −80 °C until analysis.

Busulfan was quantified at the Department of Legal Medicine at the University Medical Center Hamburg–Eppendorf using a validated gas chromatography with mass spectrometric detection method. The quantification of sulfolane was conducted according to the bioanalytical method of McCune et al. using a QTRAP 5500 mass spectrometer (SCIEX, Framingham, MA, USA) coupled with a 1290 Infinity HPLC II (Agilent Technologies, Santa Clara, CA, USA) [32] at the Dept. of Clinical Pharmacy, Institute of Pharmacy, University of Hamburg. A detailed description of the bioanalytical method is provided in the Supplementary Materials.

2.3. Genotyping

DNA samples were obtained from bone marrow or peripheral blood samples before transplantation. Genotyping was performed by real-time quantitative polymerase chain reaction (PCR) on a LightCycler 480 II (Roche Diagnostics, Penzberg, Germany).

In order to find the GSTA1 * B haplotype, which was reported to have a significantly decreased promoter activity [33], we analyzed the DNA for the single-nucleotide polymorphism (SNP) −52G > A (rs3957356) according to the method published by Ansari et al. [24]. GSTM1 deletion was detected as described by Choi et al. [23]. The primer sets used for the genotyping assays are reported in the Supplementary Materials.

2.4. PopPK Analysis

PopPK modeling was carried out in NONMEM® (version 7.4.3, ICON, Gaithersburg, MD, USA) using non-linear mixed-effect modeling. First-order conditional estimation with interaction (FOCE-I) between inter-individual and residual random effects was used throughout the process. Pirana version 3.0.1 (Certara, Princeton, NJ, USA) was used as run manager [34] and R version 4.1.2 (R Foundation for Statistical Computing, Vienna, Austria) was used for the exploratory data analysis and graphical postprocessing of the NONMEM® output.

Nested models were compared using the likelihood-ratio test (alpha = 0.05, one degree of freedom), where a drop in objective function value (OFV) of 3.84 was considered as a significant improvement. Non-nested models were compared by the Akaike information criterion (AIC), for which superior models are indicated by a lower score [35]. Goodness-of-

fit (GOF) plots, such as observed vs. population-predicted (PRED) and individual-predicted concentrations (IPRED) or conditional weighted residuals vs. time after dose and PRED, as well as eta shrinkage, were used for evaluation. A shrinkage below 30% was deemed acceptable [36].

Additive and proportional residual error models, as well as a combination of both, were tested to describe residual variability of both busulfan and sulfolane. Since intra-individual variability in busulfan pharmacokinetics is frequently observed during therapy [20], we also tested IOV on both CL and Vd of busulfan and sulfolane. The L2 data item in NONMEM® was used in order to test the correlation between the parent drug and its metabolite concentration measurements.

2.5. Covariate Model

After an initial screening for physiological plausibility and subsequent visual inspection to evaluate if there were correlations with individual estimates of the PK parameters, potential covariates were incorporated into the model using linear, exponential or power functions where appropriate. Statistical evaluation was carried out by a stepwise covariate modeling approach with alpha ≤ 0.05 (ΔOFV ≥ -3.84) in the forward inclusion step and alpha ≤ 0.01 (ΔOFV ≥ 6.64) in the backward elimination step.

Categorical covariates (GSTA1 SNP, GSTM1 deletion, sex, driver mutations) were coded as 0 or 1, whereas continuous variables (age, weight, height, BSA, serum levels, Fibroscan) were centered around their median value. Missing values for Fibroscan were imputed using the population median.

Eventually, the cAUC of all patients, as well as the clearance of busulfan after the first and ninth dose, were calculated by using the individual estimates of the final model for each patient.

2.6. Model Evaluation

Evaluation of the final model was performed by using a prediction-corrected visual predictive check (pcVPC) [37] with 1000 simulations and stratification based on predicted concentrations of the parent and metabolite as well as on the dosing regimen. Subsequently, the sampling-importance resampling (SIR) method (M/m = 5000/1000) was used to evaluate model robustness and determine the 95% confidence intervals (CI) of the estimated parameters [38].

3. Results

3.1. Patients and Data

In total, 37 patients diagnosed with myelofibrosis undergoing reduced conditioning chemotherapy with busulfan prior to allo-HSCT were included in this study. Thirty patients were included in the prospective part of the study and seven more patients consented to provide their data, measured busulfan plasma concentrations and remaining DNA samples for genotyping for retrospective analysis. The study population consisted of 19 female and 18 male patients, typically aged 60 years (median, IQR 53.5–65.5 years), with a median total body weight (TBW) of 75 kg (IQR 64.05–88.25 kg). Briefly, 18 patients had primary myelofibrosis, whereas 9 and 10 patients were diagnosed with Post-ET or Post-PV myelofibrosis, respectively.

A GSTA1 SNP was found in 28 patients (75.7%), whereas a GSTM1 deletion was detected in 19 patients (51.35%), and 10 patients (27%) had a combination of both. Overall, 523 plasma concentrations of busulfan and sulfolane were included in the PK analysis, from which 282 were parent drug and 241 were metabolite concentrations. In comparison, there were more busulfan plasma concentrations available, since sulfolane plasma concentrations could only be obtained from patients in the prospective part of the study.

In total, seven plasma concentrations were excluded from the analysis due to mishandling or implausible concentrations, and 70 sulfolane plasma concentrations (13.4% of all plasma concentrations) were below the limit of quantification (BLQ, lower limit

of quantification = 0.04 mg/L). The median cAUC of busulfan was 36.06 mg × h/L (range: 25.67–61.85 mg × h/L). Individual busulfan clearance (Figure S1) decreased from 17.16 L/h after the first dose (median, range: 10.55–22.36 L/h) to 16.47 L/h (median, range: 10.05–19.27 L/h) after the ninth dose. An overview of patient characteristics and clinical data is presented in Table 1.

Table 1. Patient demographic and clinical data.

Patient Characteristics (*n* = 37)	Median [IQR] or *n* (%)
Age [years]	60 [53.5–65.5]
Sex [female/male]	19 (51.4)/18 (48.6)
Weight [kg]	75 [64.05–88.25]
Height [cm]	174 [168–181]
BSA [m^2]	1.84 [1.75–2.07]
Diagnosis	
PMF	18 (48.7)
Post-ET MF	9 (24.3)
Post-PV MF	10 (27)
Dosing regime	
Q6H	30 (81)
Q24H	7 (19)
DIPSS/MYSEC	
Intermediate-1	2 (5)/1 (3)
Intermediate-2	15 (40)/14 (38)
High Risk	1 (3)/4 (11)
Mutation	
JAK2	26 (70.3)
CALR	7 (18.9)
MPL	1 (3)
TET2	9 (24.3)
ASXL1	13 (35.1)
Blood chemistry, serum levels	
AST [U/L]	21 [15.5–31.5]
ALT [U/L]	21 [18.5–47.5]
De Ritis Ratio	0.76 [0.58–1.07]
Albumin [g/L]	37.8 [34.6–41.4]
Alkaline Phosphatase [U/L]	85 [63–115]
Bilirubin [mg/dL]	0.6 [0.5–0.8]
Fibroscan [kPa]	5.6 [4.8–7]
Missing Data	14 (37.8)
GSTA1 52G > A	28 (75.7)
GSTM1 Deletion	19 (51.35)
Mucositis Grade 1/2/3/4	10 (27)/14 (38)/1 (2.7)/1 (2.7)
aGvHD Grade 1/2/3	10 (27)/7 (19)/4 (11)
cGvHD Grade 1/2/3	12 (32)/6 (16)/1 (2.7)
SOS	2 (5.4)
Relapse	2 (5.4)
Death	5 (13.5)

aGvHD: acute graft-versus-host-disease; **ALT**: alanine transaminase; **AST**: aspartate transaminase; **cGvHD**: chronic graft-versus-host disease; **DIPSS**: Dynamic International Prognostic Scoring System; **MYSEC**: myelofibrosis secondary to PV and ET; **PMF**: primary myelofibrosis; **Post-ET MF**: post-essential thrombocythemia myelofibrosis; **Post-PV MF**: post-polycythemia vera myelofibrosis; **SOS**: sinusoidal obstructive syndrome.

3.2. Base Model

The pharmacokinetics of busulfan and its metabolite sulfolane were best described by a one-compartment (1CMT) model with first-order elimination. The addition of a second compartment (2CMT) did not significantly improve the model, as indicated by their AIC (−1956.88 for 1CMT vs. −1956.41 for 2CMT) and lack of improvement in GOF plots. A proportional error model was used to describe the residual variability, since a mixed error model led to high eta shrinkage. The co-variance between the proportional error of

busulfan (Prop. σ_{Bu}) and sulfolane (Prop. σ_{Su}) was implemented by using a sigma block employing the L2 data item. AIC dropped by 66 points when the L2 data item was used, as the concentration between parent drug and its metabolite measurements was correlated (11.8%). The inclusion of IIV on both CL (CL_{Bu} and CL_{Su}) and Vd (V_{Bu} and V_{Su}) of busulfan and sulfolane considerably improved the model. Before including IOV, each administration, followed by blood sampling, was defined as a new occasion. The implementation of IOV on CL_{Bu} further improved the model (ΔOFV −8.96). BLQ observations were included into the model and accounted for by the error model.

Overall, busulfan and sulfolane plasma concentration–time profiles were adequately described by the compartmental model presented in Figure 1.

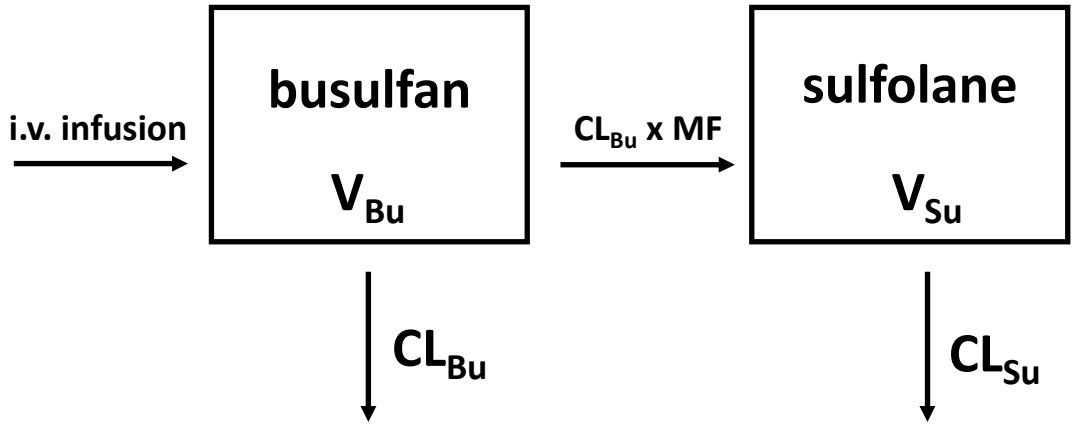

Figure 1. Compartmental model used to describe busulfan and sulfolane plasma concentration–time profiles. CL_{Bu}: busulfan clearance, representing the total clearance; V_{Bu}: volume of distribution of busulfan; MF: metabolic fraction; CL_{Su}: sulfolane clearance; V_{Su}: volume of distribution of sulfolane; formation of sulfolane as part of the total clearance.

3.3. Covariate Model

Initially, 39 demographic or clinical variables were identified as candidates for testing. Graphical exploration revealed 12 of them to be potential covariates, which then were incorporated separately into the model. Lastly, seven covariates (TBW, JAK2 mutation, GSTA1 SNP, GSTM1 deletion, De Ritis ratio, AP and bilirubin) showed a statistically significant drop in OFV (alpha ≤ 0.05) in the forward inclusion step.

Establishing a powered relationship between TBW and V_{Bu} improved the base model statistically from an OFV of −2655.3 to −2686.8 (ΔOFV −31.5), as well as graphically, and reduced the IIV on V_{Bu} from 18.5% to 10.4%. Incorporating JAK2 mutation on CL_{Su} into the model reduced the OFV by 12.6 points to −2699.4; however, parameter estimates then became physiologically implausible, and therefore, it was discarded. The exponential relationship between GSTA1 and CL_{Su} yielded in a drop by 10.7 points (OFV: −2697.5) and reduced the IIV on CL_{Su} from 136.3% to 112.8%. A further reduction by 7.61 points was achieved by including the De Ritis ratio on CL_{Bu}. However, this resulted in high relative standard errors of the PK parameters and thus the relationship was not retained in the model. An additional powered relationship between either AP or bilirubin and CL_{Bu} was statistically significant in the forward inclusion step (ΔOFV −5.56 and −5.23) but neither reduced the IIV on CL_{Bu} substantially nor showed notable improvement in GOF plots and, therefore, was eliminated within the backward elimination step.

The final covariate relationship on V_{Bu} (1) and CL_{Su} (2) can be expressed as:

$$V_{Bu} = V_{Bu-typ} \times \left(\frac{TBW}{75}\right)^{0.854} \quad (1)$$

$$\begin{array}{c} CL_{Su} = CL_{Su-typ} \times e^{1.43} \text{ (for GSTA1)} \\ CL_{Su} = CL_{Su-typ} \text{ (for non-GSTA1)} \end{array} \quad (2)$$

where $V_{Bu\text{-}typ}$ and $CL_{Su\text{-}typ}$ are the typical values of V_{Bu} and CL_{Su}, 0.854 and 1.43, and describe the effect of TBW and GSTA1 on V_{Bu} and CL_{Su}, respectively.

For the final model, the typical CL_{Bu} and V_{Bu} for a 75 kg patient were 16.3 L/h (IIV: 21.5% CV) and 61.5 L (IIV: 10% CV), respectively. CL and Vd of sulfolane were estimated to be 1.61 L/h (IIV: 112.8% CV) and 48.8 L (IIV: 77.6% CV). IOV on CL_{Bu} was 7.6%. The final model estimates and their 95% CI determined by SIR are provided in Table 2.

Table 2. Parameter estimates of the final busulfan and sulfolane PK model and SIR results.

Parameters	Final Model			SIR (M/m = 5000/1000)
	Estimate	**RSE (%)**	**Shrinkage (%)**	**95% CI**
CL_{Bu} [L/h]	16.3	3.6	-	15.18–17.35
V_{Bu} [L]	61.5	2	-	59.37–63.78
CL_{Su} [L/h]	1.61	37	-	0.84–2.24
V_{Su} [L]	48.8	35.2	-	30.75–78.46
MF	0.0704	28.6	-	0.0463–0.1029
COV_V_{Bu}_TBW [kg]	0.854	11.6	-	0.665–1.059
COV_CL_{Su}_GSTA1	1.43	43.6	-	0.63–2.40
IIV CL_{Bu} [CV%]	21.5	14.8	2	16.4–27.4
IIV V_{Bu} [CV%]	10	12	18	7.2–12.1
IIV CL_{Su} [CV%]	112.8	26.1	22	80.3–206.2
IIV V_{Su} [CV%]	77.6	14.2	18	59.2–106.4
IOV CL_{Bu} [CV%]	7.6	13.5	39	5.6–9.1
Prop. σ_{Bu} [CV%]	7.1	12.8	14	6.3–8.2
Prop. σ_{Su} [CV%]	36.2	7.2	12	32.6–40.1

CL_{Bu}: busulfan clearance; **CL_{Su}**: sulfolane clearance; **COV_CL_{Su}_GSTA1**: typical pharmacokinetic parameter for the covariate GSTA1 on CL_{Su}; **COV_V_{Bu}_TBW**: typical pharmacokinetic parameter for the covariate BTW on V_{Bu}; **CV**: coefficient of variation (%CV = sqrt(exp(OMEGA)-1) * 100); **IIV**: inter-individual variability; **IOV**: inter-occasion variability; **MF**: metabolic fraction; **OFV**: objective function value; **Prop. σ_{Bu}**: residual variability of busulfan calculated as a proportional error; **Prop. σ_{Su}**: residual variability of sulfolane calculated as a proportional error; **RSE**: relative standard error; **SIR**: sampling-importance resampling; **V_{Bu}**: volume of distribution of busulfan; **V_{Su}**: volume of distribution of sulfolane.

3.4. Model Evaluation

An overview of the GOF plots for the final model is shown in Figure 2. Plots of individual predictions (Figure 2A) as well as population predictions (Figure 2B) against observations depict an even distribution around the identity line. The conditional weighted residuals (CWRES) show a normal distribution around the *x*-axis when plotted against population predictions (Figure 2C) and time after dose (Figure 2D).

SIR was performed with a M/m ratio of 5000/1000 and revealed adequate diagnostic plots with a proposal distribution close to the true distribution (Figure S2) and a horizontal trend for the observed resampling proportion (Figure S4). The pcVPC with stratification on Q6H showed overlapping observations and predictions for both busulfan (Figure 3A) and sulfolane (Figure 3B). The pcVPC plot with stratification on Q24H is provided in the Supplementary Materials (Figure S5).

Overall, the plots indicate a good predictive performance and robustness of the final model.

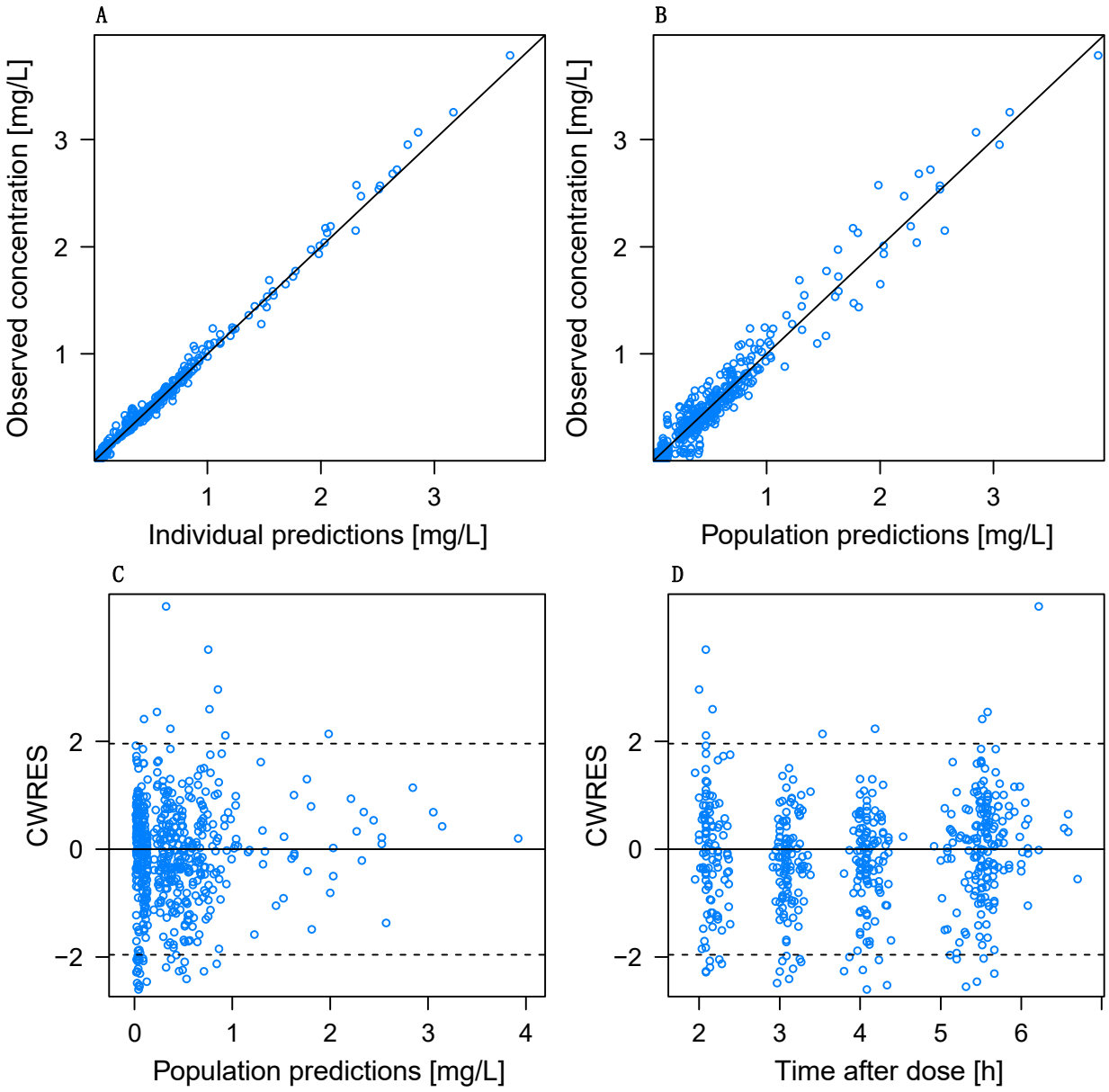

Figure 2. Goodness-of-fit (GOF) plots of the final PK model for busulfan and sulfolane. Observed concentration versus (**A**) individual predicted concentrations, and (**B**) population predicted concentrations; solid line = line of identity. Conditional weighted residuals (CWRES) versus population predicted concentration (**C**) and time after first dose (**D**).

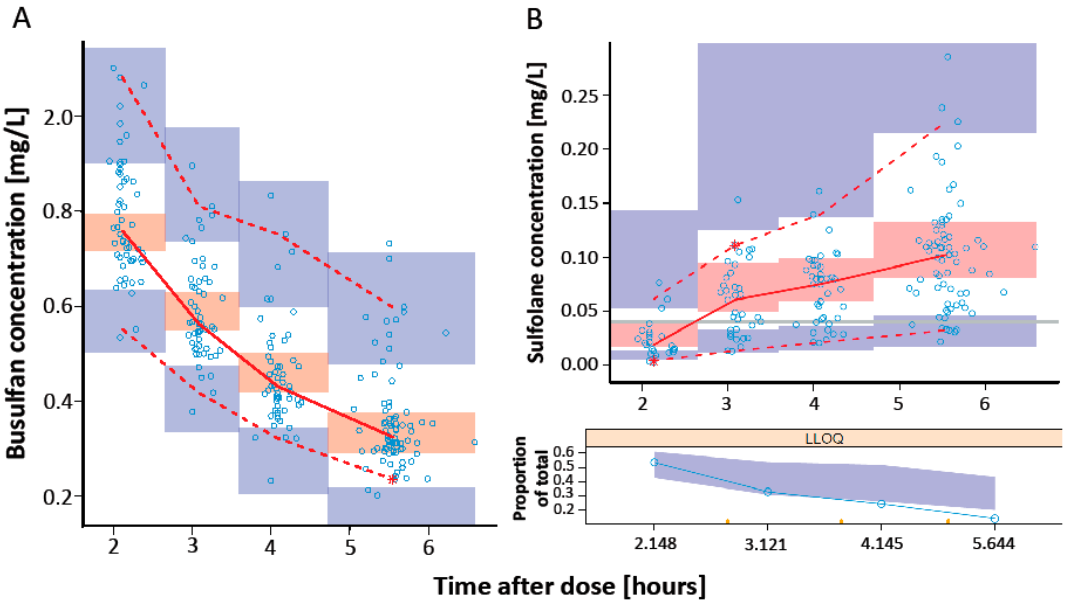

Figure 3. Prediction-corrected visual predictive check of the final model of busulfan (**A**) and sulfolane (**B**) with stratification on **Q6H**. Open dots represent prediction-corrected observed plasma concentration; solid red line = median observed concentration over time; dashed red lines = 5 and 95% quartiles of observed concentration over time; the * represent outliers at that timepoint; blue shaded area = 90% CI of 5% and 95% predictions; red shaded area = 90% CI of median predictions; horizontal grey line in (**B**) = the LLOQ of sulfolane (0.04 mg/L); lower panel in (**B**) shows the fraction of BQL sulfolane data.

4. Discussion

This is the first study to describe population pharmacokinetics of busulfan in patients with myelofibrosis undergoing allo-HSCT. Moreover, this is the first study to incorporate sulfolane into a PopPK model of busulfan in order to establish a relationship between its metabolite and patient-specific covariates.

Our data suggests that the pharmacokinetics of busulfan and its metabolite sulfolane are best described by a one-compartment model with first-order elimination. This lies in accordance with most of the published PK analyses of busulfan, even though there are few two-compartmental models for busulfan reported as well [13,26,39,40]. Most published PopPK models of busulfan set the focus either on pediatric patients as the IIV as well as the IOV of busulfan PK in children and young adults are even more difficult to predict [20,21] or on large study populations including various malignancies [11,13]. However, there is no PopPK analysis solely focused on patients with myelofibrosis to date. Considering that patients with myelofibrosis have an elevated risk of hepatotoxicity and impaired liver function due to extramedullary hematopoiesis on the one hand, and the fact that an impaired liver function is associated with adverse impact on survival on the other hand [41], determining the inter-individual pharmacokinetic variability of busulfan in patients with myelofibrosis was overdue. The range of cAUC of busulfan (25.67–61.85 mg × h/L) in our study shows a up to 2.4-fold difference in busulfan exposure and, therefore, confirms the high IIV in drug exposure that is known from the literature as well. Additionally, even though busulfan/fludarabine, as either RIC or MAC, are commonly used conditioning regimens, there is still no defined therapeutic window for myelofibrosis.

There are only a few PopPK models of busulfan that solely include adult patients. As McCune et al. showed, there is a maturation of clearance in pediatric patients [13] and, consequently, the reported range for typical values of CL in the literature is considerably wide. Our results for CL_{Bu} (16.3 L/h) and V_{Bu} (61.5 L) for a typical patient with 75 kg TBW are generally within the range of the estimates reported in the literature. However,

they differ from those of Choi et al., who found a CL of 11 L/h and V of 42.4 L for their adult patients (typical patient weighing 60 kg) [23]. Since Choi et al. included various malignancies in their analysis, the difference in population estimates might be an indicator of the necessity for more focused PK analyses on special patient populations.

Regarding patient-specific variables, body size–related covariates and GSTA1 are, similar to our findings, most often reported to have a significant impact on the PK of busulfan. However, our study is the first to incorporate sulfolane into a PopPK model of busulfan. Although our findings did not confirm that a metabolic ratio of busulfan/sulfolane $\geq$5 is associated with a higher rate of graft failure and decreased event-free survival (EFS) [28], the fact that our data indicates an IIV on CL_{Su} of 112.8% CV underlines the complexity of busulfan's metabolic pathway and calls for further investigations regarding the impact of metabolites on patient outcome as well. Moreover, the established relationship between GSTA1 and the clearance of the metabolite in our model may seem counterintuitive at first since sulfolane is not conjugated with glutathione. However, there are several intermediate metabolites within the pathway that are transitioned by different enzymes, and a change in any of the respective enzymes' activity could potentially impact the excretion of sulfolane [21].

There are a few limitations to this study that need to be kept in mind. First, the rather small cohort of 37 patients might not allow us to adequately characterize the relationships between covariates and PK parameters, in particular if the covariate effects on PK parameters are of a small effect size. In addition, using a PopPK model based on a relatively small patient cohort for model-informed precision dosing (MIPD) is not advisable since the quantitative relationship between a covariate and its respective PK parameter might be imprecise and, therefore, lead to biased estimations of drug exposure [42]. Second, due to the nature of including seven patients retrospectively, we could not obtain sulfolane plasma concentrations for those patients in order to include them in the model. Third, for technical reasons, we were unable to conduct a Fibroscan in 14 patients, and therefore, a covariate relationship could not be sufficiently investigated.

5. Conclusions

To the best of our knowledge, this is the first PopPK model developed to describe busulfan's pharmacokinetics in patients with myelofibrosis. TBW was identified as the most significant covariate. Incorporating its metabolite sulfolane into the model not only allowed us to characterize the covariate relationship between GSTA1 and the clearance of the metabolite but it also showed that there is a high inter-individual variability regarding CL_{Su} as well. Further (multi-centric) studies with larger cohorts are required in order to find further covariates that explain the high IIV of sulfolane CL and possibly determine a sensible therapeutic window for patients with myelofibrosis.

Supplementary Materials: The following supporting information can be downloaded at: https://www.mdpi.com/article/10.3390/pharmaceutics14061145/s1, Figure S1: Individual busulfan clearance after the first and ninth dose; Figure S2: SIR diagnostic plot; Figure S3: SIR diagnostic plot: Adequacy of proposal density; Figure S4: SIR diagnostic plot: Exhaustion of samples; Figure S5: pcVPC with stratification on Q24H.

Author Contributions: A.D., C.L., S.G.W. and N.K. made substantial contributions to the conception, study design and data collection. A.M. measured the busulfan blood samples using GC–MS. A.D., M.R. and C.P. measured the sulfolane blood samples using LC–MS/MS. A.D., A.B. and B.F. carried out PCR analysis for genotyping. A.D. and S.G.W. performed the pharmacometric analysis and interpretation of the PK data. C.L., S.G.W., N.K. and B.F. provided clinical input and interpretation of the data. A.D. drafted the manuscript. C.L. and S.G.W. substantively revised the manuscript. N.K., A.M., C.P., M.R., A.B. and B.F. revised the manuscript for intellectual content. All authors have read and agreed to the published version of the manuscript.

Funding: This research received no external funding.

Institutional Review Board Statement: The study was conducted in accordance with the Declaration of Helsinki and approved by the local Ethics Committee of the Hamburg Chamber of Physicians (approval number: PV5842).

Informed Consent Statement: Informed consent was obtained from all subjects involved in the study.

Data Availability Statement: The data presented in this study are available on request from the corresponding author. The data are not publicly available for reasons of privacy.

Conflicts of Interest: The authors declare no conflict of interest.

References

1. Farhadfar, N.; Cerquozzi, S.; Patnaik, M.; Tefferi, A. Allogeneic Hematopoietic Stem-Cell Transplantation for Myelofibrosis: A Practical Review. *J. Oncol. Pract.* **2016**, *12*, 611–621. [CrossRef] [PubMed]
2. Cazzola, M.; Kralovics, R. From Janus kinase 2 to calreticulin: The clinically relevant genomic landscape of myeloproliferative neoplasms. *Blood* **2014**, *123*, 3714–3719. [CrossRef] [PubMed]
3. Rumi, E.; Pietra, D.; Pascutto, C.; Guglielmelli, P.; Martínez-Trillos, A.; Casetti, I.; Colomer, D.; Pieri, L.; Pratcorona, M.; Rotunno, G.; et al. Clinical effect of driver mutations of JAK2, CALR, or MPL in primary myelofibrosis. *Blood* **2014**, *124*, 1062–1069. [CrossRef]
4. McLornan, D.P.; Malpassuti, V.; Lippinkhof-Kozijn, A.; Potter, V.; Beelen, D.; Bunjes, D.; Sengeloev, V.; Radujkovic, A.; Passweg, J.; Chalandon, Y.; et al. Outcome of allogeneic haemato-poietic stem cell transplantation in myeloproliferative neoplasm, unclassifiable: A retrospective study by the Chronic Malignancies Working Party of the EBMT. *Br. J. Haematol.* **2020**, *190*, 437–441. [CrossRef] [PubMed]
5. Kröger, N.; Holler, E.; Kobbe, G.; Bornhäuser, M.; Schwerdtfeger, R.; Baurmann, H.; Nagler, A.; Bethge, W.; Stelljes, M.; Uharek, L.; et al. Allogeneic stem cell transplantation after reduced-intensity conditioning in patients with myelofibrosis: A prospective, multicenter study of the Chronic Leukemia Working Party of the European Group for Blood and Marrow Transplantation. *Blood* **2009**, *114*, 5264–5270. [CrossRef] [PubMed]
6. Jain, T.; Kunze, K.L.; Temkit, M.; Partain, D.K.; Patnaik, M.S.; Slack, J.L.; Khera, N.; Hogan, W.J.; Roy, V.; Noel, P.; et al. Comparison of reduced intensity conditioning regimens used in patients undergoing hematopoietic stem cell transplantation for myelofibrosis. *Bone Marrow Transplant.* **2019**, *54*, 204–211. [CrossRef] [PubMed]
7. Popat, U.; Mehta, R.S.; Bassett, R.; Kongtim, P.; Chen, J.; Alousi, A.M.; Anderlini, P.; Ciurea, S.; Hosing, C.; Jones, R.B.; et al. Optimizing the Conditioning Regimen for Hematopoietic Cell Transplant in Myelofibrosis: Long-Term Results of a Prospective Phase II Clinical Trial. *Biol. Blood Marrow Transplant.* **2020**, *26*, 1439–1445. [CrossRef] [PubMed]
8. Andersson, B.S.; Thall, P.F.; Valdez, B.C.; Milton, D.R.; Alatrash, G.; Chen, J.; Gulbis, A.; Chu, D.; Martinez, C.; Parmar, S.; et al. Fludarabine with pharmacokinetically guided IV busulfan is superior to fixed-dose delivery in pretransplant conditioning of AML/MDS patients. *Bone Marrow Transplant.* **2016**, *52*, 580–587. [CrossRef]
9. Palmer, J.; McCune, J.S.; Perales, M.-A.; Marks, D.; Bubalo, J.; Mohty, M.; Wingard, J.R.; Paci, A.; Hassan, M.; Bredeson, C.; et al. Personalizing Busulfan-Based Conditioning: Considerations from the American Society for Blood and Marrow Transplantation Practice Guidelines Committee. *Biol. Blood Marrow. Transplant.* **2016**, *22*, 1915–1925. [CrossRef]
10. Perkins, J.; Field, T.; Kim, J.; Kharfan-Dabaja, M.A.; Ayala, E.; Pérez, L.; Fernandez, H.; Fancher, K.; Tate, C.; Shaw, L.M.; et al. Pharmacokinetic targeting of i.v. BU with fludarabine as conditioning before hematopoietic cell transplant: The effect of first-dose area under the concentration time curve on transplant-related outcomes. *Bone Marrow Transplant.* **2010**, *46*, 1418–1425. [CrossRef]
11. Bartelink, I.H.; Lalmohamed, A.; van Reij, E.M.L.; Dvorak, C.; Savic, R.M.; Zwaveling, J.; Bredius, R.G.M.; Egberts, T.; Bierings, M.; Kletzel, M.; et al. Association of busulfan exposure with survival and toxicity after haemopoietic cell transplantation in children and young adults: A multicentre, retrospective cohort analysis. *Lancet Haematol.* **2016**, *3*, e526–e536. [CrossRef]
12. McCune, J.S.; Holmberg, L.A. Busulfan in hematopoietic stem cell transplant setting. *Expert Opin. Drug Metab. Toxicol.* **2009**, *5*, 957–969. [CrossRef] [PubMed]
13. McCune, J.S.; Bemer, M.J.; Barrett, J.S.; Baker, K.S.; Gamis, A.S.; Holford, N. Busulfan in Infant to Adult Hematopoietic Cell Transplant Recipients: A Population Pharmacokinetic Model for Initial and Bayesian Dose Personalization. *Clin. Cancer Res.* **2013**, *20*, 754–763. [CrossRef] [PubMed]
14. Bartelink, I.H.; Boelens, J.J.; Bredius, R.G.M.; Egberts, A.C.G.; Wang, C.; Bierings, M.B.; Shaw, P.J.; Nath, C.E.; Hempel, G.; Zwaveling, J.; et al. Body Weight-Dependent Pharmacoki-netics of Busulfan in Paediatric Haematopoietic Stem Cell Transplantation Patients: Towards Individualized Dosing. *Clin. Pharmacokinet.* **2012**, *51*, 331–345. [CrossRef] [PubMed]
15. Trame, M.N.; Bergstrand, M.; Karlsson, M.O.; Boos, J.; Hempel, G. Population Pharmacokinetics of Busulfan in Children: In-creased Evidence for Body Surface Area and Allometric Body Weight Dosing of Busulfan in Children. *Clin. Cancer Res.* **2011**, *17*, 6867–6877. [CrossRef]
16. Long-Boyle, J.; Savic, R.; Yan, S.; Bartelink, I.; Musick, L.; French, D.; Law, J.; Horn, B.; Cowan, M.J.; Dvorak, C.C. Population Pharmacokinetics of Busulfan in Pediatric and Young Adult Patients Undergoing Hematopoietic Cell Transplant: A Model-Based Dosing Algorithm for Personalized Therapy and Implementation into Routine Clinical Use. *Ther. Drug Monit.* **2016**, *26*, 236. [CrossRef]

17. Takahashi, T.; Illamola, S.M.; Jennissen, C.A.; Long, S.E.; Lund, T.C.; Orchard, P.J.; Gupta, A.O.; Long-Boyle, J.R. Busulfan dose Recommendation in Inherited Metabolic Disorders: Population Pharmacokinetic Analysis. *Transplant. Cell. Ther.* **2021**, *28*, 104. [CrossRef]
18. Essmann, S.; Dadkhah, A.; Janson, D.; Wolschke, C.; Ayuk, F.; Kröger, N.M.; Langebrake, C. Iron Chelation with Deferasirox Increases Busulfan AUC During Conditioning Chemotherapy Prior to Allogeneic Stem Cell Transplantation. *Transplant. Cell. Ther.* **2021**, *28*, 115.e1–115.e5. [CrossRef]
19. Lee, J.W.; Kang, H.J.; Lee, S.H.; Yu, K.-S.; Kim, N.H.; Yuk, Y.J.; Jang, M.K.; Han, E.J.; Kim, H.; Song, S.H.; et al. Highly Variable Pharmacokinetics of Once-Daily Intravenous Busulfan When Combined with Fludarabine in Pediatric Patients: Phase I Clinical Study for Determination of Optimal Once-Daily Busulfan Dose Using Pharmacokinetic Modeling. *Biol. Blood Marrow Transplant.* **2012**, *18*, 944–950. [CrossRef]
20. Marsit, H.; Philippe, M.; Neely, M.; Rushing, T.; Bertrand, Y.; Ducher, M.; Leclerc, V.; Guitton, J.; Bleyzac, N.; Goutelle, S. Intra-individual Pharmacokinetic Variability of Intravenous Busulfan in Hematopoietic Stem Cell-Transplanted Children. *Clin. Pharmacokinet.* **2020**, *59*, 1049–1061. [CrossRef]
21. Lawson, R.; Staatz, C.E.; Fraser, C.J.; Hennig, S. Review of the Pharmacokinetics and Pharmacodynamics of Intravenous Busulfan in Paediatric Patients. *Clin. Pharmacokinet.* **2020**, *60*, 17–51. [CrossRef] [PubMed]
22. Zwaveling, J.; Press, R.R.; Bredius, R.G.M.; van Derstraaten, T.R.J.H.M.; Hartigh, J.D.; Bartelink, I.H.; Boelens, J.J.; Guchelaar, H.-J. Glutathione S-transferase Polymorphisms Are Not Associated with Population Pharmacokinetic Parameters of Busulfan in Pediatric Patients. *Ther. Drug Monit.* **2008**, *30*, 504–510. [CrossRef] [PubMed]
23. Choi, B.; Kim, M.G.; Han, N.; Kim, T.; Ji, E.; Park, S.; Kim, I.-W.; Oh, J.M. Population pharmacokinetics and pharmacodynamics of busulfan with *GSTA1* polymorphisms in patients undergoing allogeneic hematopoietic stem cell transplantation. *Pharmacogenomics* **2015**, *16*, 1585–1594. [CrossRef] [PubMed]
24. Ansari, M.; Curtis, P.H.-D.; Uppugunduri, C.R.S.; Rezgui, M.A.; Nava, T.; Mlakar, V.; Lesne, L.; Theoret, Y.; Chalandon, Y.; Dupuis, L.L.; et al. GSTA1 diplotypes affect busulfan clearance and toxicity in children undergoing allogeneic hematopoietic stem cell transplantation: A multicenter study. *Oncotarget* **2017**, *8*, 90852–90867. [CrossRef]
25. Nava, T.; Kassir, N.; Rezgui, M.A.; Uppugunduri, C.R.S.; Huezo-Diaz Curtis, P.; Duval, M.; Theoret, Y.; Daudt, L.E.; Litalien, C.; Ansari, M.; et al. Incorporation of GSTA1 genetic variations into a population pharmacokinetic model for IV busulfan in paediatric hematopoietic stem cell transplantation: GSTA1-based busulfan population pharmacokinetic model in children. *Br. J. Clin. Pharmacol.* **2018**, *84*, 1494–1504. [CrossRef]
26. Hassine, K.B.; Nava, T.; Théoret, Y.; Nath, C.E.; Daali, Y.; Kassir, N.; Lewis, V.; Bredius, R.G.M.; Shaw, P.J.; Shaw, P.J.; et al. Precision dosing of intravenous busulfan in pediatric hematopoietic stem cell transplantation: Results from a multicenter population pharmacokinetic study. *CPT Pharmacomet. Syst. Pharmacol.* **2021**, *10*, 1043–1056. [CrossRef]
27. Bertrand, J.; Laffont, C.M.; Mentré, F.; Chenel, M.; Comets, E. Development of a Complex Parent-Metabolite Joint Population Pharmacokinetic Model. *AAPS J.* **2011**, *13*, 390–404. [CrossRef]
28. Uppugunduri, C.R.S.; Rezgui, M.A.; Diaz, P.H.; Tyagi, A.K.; Rousseau, J.; Daali, Y.; Duval, M.; Bittencourt, H.; Krajinovic, M.; Ansari, M. The association of cytochrome P450 genetic polymorphisms with sulfolane formation and the efficacy of a busulfan-based conditioning regimen in pediatric patients undergoing hematopoietic stem cell transplantation. *Pharm. J.* **2013**, *14*, 263–271. [CrossRef]
29. Passamonti, F.; Cervantes, F.; Vannucchi, A.M.; Morra, E.; Rumi, E.; Pereira, A.; Guglielmelli, P.; Pungolino, E.; Caramella, M.; Maffioli, M.; et al. A dynamic prognostic model to predict survival in primary myelofibrosis: A study by the IWG-MRT (International Working Group for Myeloproliferative Neo-plasms Research and Treatment). *Blood* **2010**, *115*, 1703–1708. [CrossRef]
30. Passamonti, F.; Giorgino, T.; Mora, B.; Guglielmelli, P.; Rumi, E.; Maffioli, M.; Rambaldi, A.; Caramella, M.; Komrokji, R.; Gotlib, J.; et al. A clinical-molecular prognostic model to predict survival in patients with post polycythemia vera and post essential thrombocythemia myelofibrosis. *Leukemia* **2017**, *31*, 2726–2731. [CrossRef]
31. Gagelmann, N.; Eikema, D.-J.; de Wreede, L.C.; Koster, L.; Wolschke, C.; Arnold, R.; Kanz, L.; McQuaker, G.; Marchand, T.; Socié, G.; et al. Comparison of Dynamic International Prognostic Scoring System and MYelofibrosis SECondary to PV and ET Prognostic Model for Prediction of Outcome in Polycythemia Vera and Essential Thrombocythemia Myelofibrosis after Allogeneic Stem Cell Transplantation. *Biol. Blood Marrow Transplant.* **2019**, *25*, e204–e208. [CrossRef] [PubMed]
32. McCune, J.; Shen, D.D.; Shireman, L.; Phillips, B. *Bioanalytical Method: Tetrahydrothiophene-1-Oxide and Sulfolane and 3-Hydroxysulfolane in Plasma*; Report No.: BAM217; National Cancer Institute, University of Washington School of Pharmacy: Seattle, WA, USA, 2017.
33. Coles, B.F.; Morel, F.; Rauch, C.; Huber, W.W.; Yang, M.; Teitel, C.H.; Green, B.; Lang, N.; Kadlubar, F.F. Effect of polymorphism in the human glutathione S-transferase A1 promoter on hepatic GSTA1 and GSTA2 expression. *Pharmacogenetics* **2001**, *11*, 663–669. [CrossRef] [PubMed]
34. Keizer, R.J.; van Benten, M.; Beijnen, J.H.; Schellens, J.H.; Huitema, A.D. Piraña and PCluster: A modeling environment and cluster infrastructure for NONMEM. *Comput. Methods Programs Biomed.* **2011**, *101*, 72–79. [CrossRef] [PubMed]
35. Bonate, P.L. *Pharmacokinetic-Pharmacodynamic Modeling and Simulation*, 2nd ed.; Springer: Boston, MA, USA, 2011. [CrossRef]
36. Savic, R.M.; Karlsson, M.O. Importance of Shrinkage in Empirical Bayes Estimates for Diagnostics: Problems and Solutions. *AAPS J.* **2009**, *11*, 558–569. [CrossRef]

37. Bergstrand, M.; Hooker, A.C.; Wallin, J.E.; Karlsson, M.O. Prediction-Corrected Visual Predictive Checks for Diagnosing Nonlinear Mixed-Effects Models. *AAPS J.* **2011**, *13*, 143–151. [CrossRef]
38. Dosne, A.-G.; Bergstrand, M.; Harling, K.; Karlsson, M.O. Improving the estimation of parameter uncertainty distributions in nonlinear mixed effects models using sampling importance resampling. *J. Pharmacokinet. Pharmacodyn.* **2016**, *43*, 583–596. [CrossRef]
39. Ms, A.K.; Funaki, T.; Kim, S. Population Pharmacokinetic Analysis of Busulfan in Japanese Pediatric and Adult HCT Patients. *J. Clin. Pharmacol.* **2018**, *58*, 1196–1204. [CrossRef]
40. Neroutsos, E.; Nalda-Molina, R.; Paisiou, A.; Zisaki, K.; Goussetis, E.; Spyridonidis, A.; Kitra, V.; Grafakos, S.; Valsami, G.; Dokoumetzidis, A. Development of a Population Pharmacokinetic Model of Busulfan in Children and Evaluation of Different Sampling Schedules for Precision Dosing. *Pharmaceutics* **2022**, *14*, 647. [CrossRef]
41. Wong, K.M.; Atenafu, E.G.; Kim, D.; Kuruvilla, J.; Lipton, J.H.; Messner, H.; Gupta, V. Incidence and Risk Factors for Early Hepatotoxicity and Its Impact on Survival in Patients with Myelofibrosis Undergoing Allogeneic Hematopoietic Cell Transplantation. *Biol. Blood Marrow Transplant.* **2012**, *18*, 1589–1599. [CrossRef]
42. Broeker, A.; Nardecchia, M.; Klinker, K.; Derendorf, H.; Day, R.; Marriott, D.; Carland, J.; Stocker, S.; Wicha, S. Towards precision dosing of vancomycin: A systematic evaluation of pharmacometric models for Bayesian forecasting. *Clin. Microbiol. Infect.* **2019**, *25*, 1286.e1–1286.e7. [CrossRef]

pharmaceutics

MDPI

Article

Ganciclovir Pharmacokinetics and Individualized Dosing Based on Covariate in Lung Transplant Recipients

Eliška Dvořáčková [1], Martin Šíma [1,*], Jakub Petrus [2], Eva Klapková [2], Petr Hubáček [3], Jiří Pozniak [4], Jan Havlín [4], Robert Lischke [4] and Ondřej Slanař [1]

[1] Department of Pharmacology, First Faculty of Medicine, Charles University and General University Hospital in Prague, 128 00 Prague, Czech Republic; eliskadvorackova@seznam.cz (E.D.); ondrej.slanar@lf1.cuni.cz (O.S.)
[2] Department of Medical Chemistry and Clinical Biochemistry, Second Faculty of Medicine, Charles University in Prague and Motol University Hospital, 150 06 Prague, Czech Republic; jakubpet@gmail.com (J.P.); eva.klapkova@fnmotol.cz (E.K.)
[3] Department of Medical Microbiology, Second Faculty of Medicine, Charles University in Prague and Motol University Hospital, 150 06 Prague, Czech Republic; petr.hubacek@fnmotol.cz
[4] Prague Lung Transplant Program, 3rd Department of Surgery, First Faculty of Medicine, Charles University in Prague and Motol University Hospital, 150 06 Prague, Czech Republic; jiri.pozniak@fnmotol.cz (J.P.); jan.havlin@fnmotol.cz (J.H.); robert.lischke@fnmotol.cz (R.L.)
* Correspondence: martin.sima@lf1.cuni.cz

Abstract: The aim of this prospective study was to evaluate the pharmacokinetics of ganciclovir in lung transplant recipients, to explore its covariates, and to propose an individualized dosing regimen. Ganciclovir was administered according to the protocol in a standardized intravenous dose of 5 mg/kg twice daily. Serum ganciclovir concentrations were monitored as a trough and at 3 and 5 h after dosing. Individual ganciclovir pharmacokinetic parameters were calculated in a two-compartmental pharmacokinetic model, while regression models were used to explore the covariates. Optimal loading and maintenance doses were calculated for each patient. In lung transplant recipients (n = 40), the median (IQR) ganciclovir total volume of distribution and clearance values were 0.65 (0.52–0.73) L/kg and 0.088 (0.059–0.118) L/h/kg, respectively. We observed medium-to-high inter-individual but negligible intra-individual variability in ganciclovir pharmacokinetics. The volume of distribution of ganciclovir was best predicted by height, while clearance was predicted by glomerular filtration rate. Bodyweight-normalized clearance was significantly higher in patients with cystic fibrosis, while distribution half-life was reduced in this subgroup. On the basis of the observed relationships, practical nomograms for individualized ganciclovir dosing were proposed. The dosing of ganciclovir in patients with cystic fibrosis requires special caution, as their daily maintenance dose should be increased by approximately 50%.

Keywords: ganciclovir; lung transplant recipients; cystic fibrosis; therapeutic drug monitoring; covariates

Citation: Dvořáčková, E.; Šíma, M.; Petrus, J.; Klapková, E.; Hubáček, P.; Pozniak, J.; Havlín, J.; Lischke, R.; Slanař, O. Ganciclovir Pharmacokinetics and Individualized Dosing Based on Covariate in Lung Transplant Recipients. *Pharmaceutics* **2022**, *14*, 408. https://doi.org/10.3390/pharmaceutics14020408

Academic Editors: Barna Vasarhelyi and Gellért Balázs Karvaly

Received: 25 January 2022
Accepted: 11 February 2022
Published: 13 February 2022

1. Introduction

Ganciclovir is an antiviral agent with broad activity against herpes viruses, including cytomegalovirus. It is indicated for the prophylaxis and treatment of herpesvirus infection in immunocompromised patients, including lung transplant recipients, in whom cytomegalovirus infection is associated with premature graft failure and decreased overall survival [1,2]. In routine clinical practice, ganciclovir dosing is adjusted according to the patient's weight, renal function and indication (prophylaxis or treatment) [3]. However, this approach may vary among different institutions, depending on the dosing algorithm locally adopted. Several institutions extrapolate the results generated in studies with patients with AIDS or renal transplant recipients [4]. The method used for renal function estimation is another potential source of variability among clinical centers. Therapeutic drug monitoring

(TDM) may be helpful for dose adjustment to maintain efficacious drug levels related to viral inhibitory concentrations, although the timely availability of appropriate bioanalytical assays of antiviral drugs is limited [5]. Although there is currently little consensus on the therapeutic range that would optimally predict clinical outcomes and toxicity, subtherapeutic levels of ganciclovir may lead to the selection of resistant strains (e.g., with mutations in the UL97 gene–viral thymidine kinase) with subsequent treatment failure [6]. By contrast, high exposure to ganciclovir increases the risk of myelosuppression and neurotoxicity [7,8].

Cystic fibrosis is one of the major indications for lung transplantation [9]. Although changes in the drug disposition can be expected in these patients, no pharmacokinetic study on ganciclovir pharmacokinetics has been published apart, from observational data for C_{max}, C_{min} and AUC from 12 patients with cystic fibrosis [10]. Ganciclovir TDM may be especially beneficial for patients with highly variable pharmacokinetic profiles, such as patients with unstable renal function or cystic fibrosis.

Ganciclovir is a cyclic analogue of endogenous purine nucleoside guanosine, with an intracellular half-life of 16.5 h [11]. The drug has low protein binding (1–2%), a rapid distribution phase (0.23 h) and a terminal serum half-life of 2–4 h. Renal clearance is the dominant form of elimination. Most of the drug is eliminated via glomerular filtration, with more than 80% of the administered dose found in the urine unchanged [12].

Although ganciclovir is routinely used for prophylaxis and treatment in lung recipients, its individual pharmacokinetic parameters and covariates (sex, age, bodyweight, height, serum creatinine, serum cystatin C, liver enzymes, white blood cells, platelet count, concomitant pharmacotherapy and cystic fibrosis) have not yet been clearly addressed. Therefore, the objective of this prospective study was to evaluate the pharmacokinetics of ganciclovir in lung transplant recipients and to explore its covariates in order to propose an individualized ganciclovir dosing regimen prior to TDM.

2. Materials and Methods

2.1. Study Design

This was a prospective open-label (laboratory-blinded) pharmacokinetic study on adult patients treated with intravenous ganciclovir (Cymevene®; CHEPLAPHARM Arzneimittel GmbH, Greifswald, Germany) at the Third Department of Surgery, First Faculty of Medicine, Charles University in Prague and Motol University Hospital between January 2020 and July 2021. Patients were included if they met all the following inclusion criteria: age $\geq$18 years, had undergone lung transplantation and received antiviral prophylaxis with intravenous ganciclovir twice daily at least 48 h after transplantation. Patients treated with ganciclovir before lung transplantation, patients with combined transplantation, re-transplantation, and patients aged under 18 years were excluded from this study. All patients received basiliximab or antithymocyte globulin as induction immunosuppressive therapy. All patients also received triple drug immunosuppression with tacrolimus (Prograf®; Astellas Pharma s.r.o., Praha, Czech Republic), mycophenolate mofetil (CellCept®; Roche Registration GmbH, Grenzach-Wyhlen, Germany) and prednisone (Prednison®; Zentiva; Prague, Czech Republic)/methylprednisone (Solu-Medrol®; Pfizer, spol. s r.o., Prague, Czech Republic). Antiviral therapy for all patients was administered according to the standardized protocol. Steady-state whole-blood concentrations of ganciclovir were measured over a median of 9 days (2–28) after transplantation. The study was approved by the local Ethics Committee under No. EK- 11/20 and was conducted in accordance with the Declaration of Helsinki. Written informed consent was obtained from all subjects before any study-related procedures. Ganciclovir was initially administered at a dose of 5 mg/kg/12 h given through 60 min intravenous infusion at concentrations not exceeding 10 mg/mL. Whole-blood concentrations for pharmacokinetic analysis were taken as a trough (C_{trough}) and at 3 (C_3) and 5 h (C_5) after the infusion was completed. Patients from whom a complete concentration-time profile was not collected were excluded from the study. Whole-blood samples (5 mL) were collected into serum collecting tubes without clot activators and

immediately placed in the cold. The samples were then centrifuged at 4500× *g* for 10 min at 4 °C and serum aliquots were stored at −80 °C until analysis.

The following demographic, laboratory and clinical characteristics of the patients were recorded as potential covariates of ganciclovir pharmacokinetics: sex, age, body weight, height, serum creatinine, serum cystatin C (available only in some patients), alanine aminotransferase (ALT), gamma-glutamyl transferase (GGT), white blood cell and platelet counts, diagnosis of cystic fibrosis and co-medication with immunosuppressants (tacrolimus, mycophenolate mofetil, corticosteroids) or antimycotics (voriconazole-Vfend®; Pfizer Europe MA EEIG, Bruxelles, Belgien, fluconazole-Fluconazole®, Aurovitas, spol. s r.o., Prague, Czech Republic).

For each patient, the body mass index (BMI), body surface area (BSA) according to the DuBois formula, estimated glomerular filtration rate (eGFR) according to CKD-EPI creatinine and optionally according to CKD-EPI cystatin C equations were calculated [13–15].

2.2. Bioanalytical Assay

Liquid chromatography-mass spectrometry (LC-MS)-grade acetonitril, ammonium acetate, trifluoroacetic acid, acetic acid and trichloroacetic acid (HPLC grade) were obtained from Supelco and Honeywell (HPST, Prague, Czech Republic). Ganciclovir (reference standard) and deuterium-labelled internal standard ganciclovir-d5 were obtained from Toronto Research Chemicals Inc. (Toronto, ON, Canada). We used an Agilent Technologies 1290 Infinity II LC system, including an autosampler, binary pumps, and a thermostatted column compartment with 6470 Triple Quad (Agilent Technologies, Santa Clara, CA, USA). Other necessary equipment were MS 40+ Vacuum Products (Agilent Technologies, Santa Clara, CA, USA) and a nitrogen generator NM32LA (Peak Scientific, Inchinnan, UK). Sample separation was carried out on a reverse phase column Eclipse Plus C18, 1.8 µm, 3.0 × 50 mm (Agilent Technologies, Santa Clara, CA, USA). The column was operated at 35 °C. A chromatographic separation was achieved under gradient flow of eluents, initially in 95/5 mix of mobile phase (A) water and aqueous buffer (95/5, *v*/*v*) and (B) acetonitril and aqueous buffer (95/5, *v*/*v*). The set-up of the gradient is shown in Table 1. The autosampler was cooled at 7 °C. An aqueous buffer was prepared at this concentration (ammonium acetate 5 g/L, 2 mL/L trifluoroacetic acid, and 35 mL/L acetic acid). The total run time per sample was 4 min. For measurement, we used 10 µL of serum sample (control, calibrator) and 500 µL of internal standard (ganciclovir-d5 5 µg/L dissolved in 5% trichloroacetic acid). The sample was briefly mixed and then centrifuged 10 min at 3727 *g*. A total of 50 µL of the upper layer was then mixed with 950 µL of 5% trichloroacetic acid. A total of 5µL of prepared sample was injected into the column. The Agilent Jet Stream with electrospray ionization ion source operated in positive ion mode. The scan type used dynamic multiple reaction monitoring. The measurements used were: gas temperature at 250 °C, gas flow 8 L/min, nebulizer at 45 psi, sheath gas temperature 350 °C and sheath gas flow 11 L/min. The mass ion transitions for ganciclovir were 256.1 $m/z \rightarrow 152$ m/z and for ganciclovir-d5 were 261.1 $m/z \rightarrow 152$ *m/z*. Collision energies were 12 V for both analytes. Full validation according to the U.S. Food and Drug Administration (FDA) requirements was conducted [16]. The calibration curve was constructed by plotting the peak ratios of ganciclovir standard to the internal standard against the concentration of ganciclovir. The assay was linear (r^2 was 0.9938) across the whole range of concentrations (0.1; 0.5; 1; 2.5; 5; 10; 20 mg/L). The intra- and inter-day accuracy and precision were evaluated in three QC samples (0.5; 2.5; 10 mg/L) by multiple analysis (n = 10). The intra-day and inter-day accuracy ranged from 0.86% to 1.16% and from 3.58% to 8.32%, respectively. The ranges of intra-day and inter-day precision were 6.21% to 8.90 and 1.39% to 1.50%, respectively. The limit of quantification was 0.1 mg/L. The intra- and inter-day accuracy was expressed as the relative error in % for LLOQ (n = 10) was 2.39% and 4.54%, respectively. The intra-day and inter-day precision for LLOQ was 7.04% and 14.02%, respectively. Detailed concentrations measured in the samples at each spiking level in the intra-day and inter-day accuracy and precision study are summarized in Table 2. The sample stability of ganciclovir was

documented at room temperature or −20 °C for 7 days or 3 months, respectively. Sample stability after three freeze-thaw cycles was also evaluated. Maximal change of concentration was within ±5% during all stability tests.

Table 1. Gradient of mobile phases.

Time (min)	A (%)	B (%)	Flow (mL/min)
0	95	5	0.2
1	0	100	0.4
3	0	100	0.4
3.1	95	5	0.4
3.5	95	5	0.4

Table 2. Concentrations measured in the samples at each spiking level in the intra-day and inter-day accuracy and precision study.

Sample	QC 1 0.1 (ng/mL)	QC 2 0.5 (ng/mL)	QC 3 2.5 (ng/mL)	QC 4 10 (ng/mL)
Intra-Day Accuracy and Precision				
1	0.107	0.47	2.29	9.42
2	0.108	0.47	2.26	9.43
3	0.111	0.47	2.26	9.40
4	0.109	0.47	2.28	9.34
5	0.105	0.47	2.30	9.24
6	0.109	0.47	2.30	9.32
7	0.106	0.48	2.26	9.19
8	0.109	0.47	2.25	9.27
9	0.103	0.47	2.28	9.40
10	0.104	0.46	2.30	9.35
Mean (ng/mL)	0.107	0.47	2.28	9.34
SD (ng/mL)	0.003	0.005	0.021	0.081
CV (%)	2.39	1.16	0.91	0.86
BIAS (%)	7.04	6.21	8.92	6.64
Inter-Day Accuracy and Precision				
1	0.107	0.47	2.23	9.87
2	0.114	0.48	2.45	10.21
3	0.119	0.46	2.26	10.55
4	0.116	0.51	2.79	9.92
5	0.115	0.52	2.36	9.78
6	0.112	0.49	2.48	10.23
7	0.104	0.53	2.74	10.46
8	0.116	0.51	2.77	9.48
9	0.119	0.48	2.69	10.33
10	0.119	0.47	2.61	10.56
Mean (ng/mL)	0.114	0.49	2.54	10.14
SD (ng/mL)	0.005	0.024	0.211	0.36
CV (%)	5.54	4.81	8.32	3.58
BIAS (%)	14.02	1.50	1.50	1.39

2.3. Pharmacokinetic Analysis

Individual pharmacokinetic parameters of ganciclovir, namely central compartment volume of distribution (Vd_c), total volume of distribution (Vd), clearance (CL), distribution half-life ($t_{1/2}\alpha$), elimination half-life ($t_{1/2}\beta$), and 24 h area under the concentration-time curve (AUC_{24}) were calculated in a two-compartmental pharmacokinetic model with first-order elimination kinetics based on individual demographic and clinical data and observed ganciclovir serum levels using MWPharm^{++} software (MediWare, Prague, Czech

Republic). The ganciclovir pharmacokinetic data derived from Sommadossi et al. was used for a priori simulation of concentration-time profile in each patient [17]. These simulated pharmacokinetic profile curves were a posteriori individualized to maximize fitting with observed concentration points of each patient. The fitting was performed using the Bayesian method. The Bayesian approach defines all unknown parameters as random variables and via a large number of subsequent iterations, the variables are adapted, taking into account the physiological and substance properties to achieve maximal fitting of the simulated pharmacokinetic profile curve with the real measured concentration points in each patient. The goodness-of-fit was expressed using weighted sum of squares and root mean square values.

For patients whose set of ganciclovir levels (C_{trough}, C_3 and C_5) was measured repeatedly during hospitalization, the pharmacokinetic parameters of ganciclovir were calculated separately from each set of concentrations. Only the PK parameters from the first drug concentration triplet (C_{trough}, C_3 and C_5) were used for the analysis of covariates, while subsequent data sets were used for the analysis of intraindividual variability.

2.4. Statistical Analysis

Descriptive parameters of mean, standard deviation, coefficient of variation, median and interquartile range (IQR) were calculated using MS Excel 2010 (Microsoft Corporation, Redmond, DC, USA). The 95% confidence intervals (CI) for medians were calculated using the Bonett and Price method [18]. Mann–Whitney U-test or linear regression model were used to evaluate the relationships of individual ganciclovir pharmacokinetic parameters and categorical or continuous variables, respectively. Pharmacokinetic parameters obtained from one patient repeatedly during hospitalization were compared using Wilcoxon signed-rank test. Possible impact of immunosuppressants (taken by all patients at different doses) on ganciclovir pharmacokinetic parameters was evaluated in a dose-dependent manner using linear regression, while the effect of antimycotics (taken only by some patients) was evaluated dose-independently using the Mann–Whitney U-test, as described previously [19]. GraphPad Prism 8.2.1 software (GraphPad Inc., La Jolla, CA, USA) was used for all comparisons and p-levels < 0.05 were considered statistically significant.

2.5. Loading and Maintenance Dose Calculation

Optimal loading doses (LD) were calculated for each patient based on individual ganciclovir Vd values using the following formula: LD (mg) = ganciclovir Vd (L) × 7.75 mg/L. The maximum concentration of 7.75 mg/L was set as a midpoint of the proposed therapeutic range for peak ganciclovir levels (3–12.5 mg/L) [20].

Optimal daily maintenance doses (MD) were calculated for each patient based on individual ganciclovir CL values using the following formula: MD (mg/day) = 24 h × ganciclovir CL (L/h) × 6.75 mg/L. The steady-state concentration of 6.75 mg/L was set as a midpoint of the proposed therapeutic range for ganciclovir both at trough and peak levels (1–12.5 mg/L) [20].

3. Results

There were 54 patients enrolled in the study. Fourteen patients were excluded due to discontinuation of ganciclovir therapy, deviations in sampling times, or missing samples. Therefore, 40 patients were included in the pharmacokinetic analysis. The demographic, laboratory and clinical characteristics of the patients are summarized in Table 3. Among the patients included in the pharmacokinetic analysis, only one subject received CVVHD support, while none of the patients needed support with extracorporeal membrane oxygenation. The ganciclovir dose ranged from 100 mg/day to 1000 mg/day. All the patients were concomitantly treated with immunosuppressive drugs (tacrolimus, mycophenolate mofetil and prednisone or methylprednisolone). The median (IQR) doses of tacrolimus, mycophenolate mofetil and corticoid (expressed as prednisone equivalent dose) were 6 (0–14) mg, 1500 (250–3000) mg and 30 (20–63) mg, respectively. Four patients

were treated with voriconazole (400 mg/day) and three patients received fluconazole (400 mg/day). There were five patients with cystic fibrosis in our study group.

Table 3. Demographic and laboratory characteristics of the patients (n = 40).

	Median	**Interquartile Range**	**Range**
Age (years)	52	46–58	22–71
Body weight (kg)	76	61–86	45–117
Height (cm)	175	168–178	152–197
BSA (m^2)	1.90	1.73–2.03	1.44–2.51
BMI (kg/m^2)	25.5	21.7–27.8	15.4–34.9
eGFR creatinine ($mL/s/1.73\ m^2$)	1.66	1.39–1.84	0.28–2.58
eGFR cystatin C * ($mL/s/1.73\ m^2$)	0.83	0.56–1.01	0.30–1.88
ALT (μkat/L)	0.56	0.31–1.08	0.15–7.87
GGT (μkat/L)	0.67	0.41–1.17	0.18–15.52
White blood cell count ($\times 10^9$/L)	9.55	7.30–13.25	2.70–23.00
Platelet count ($\times 10^9$/L)	266	187–377	63–530
	Total count	**Percentage (%)**	
Sex (M/F)	28/12	70/30	

BSA—body surface area, BMI—body mass index, eGFR—estimated glomerular filtration rate according to the CKD-EPI creatinine or cystatin C equations, ALT—alanine aminotransferase, GGT—gamma-glutamyl transferase. * Analyzed only in a subgroup of 24 patients, in whom the cystatin C level was available.

In total, 132 ganciclovir serum concentrations were included in the analysis. In four patients, the ganciclovir concentration set (C_{trough}, C_3 and C_5) was measured twice during hospitalization. The ganciclovir pharmacokinetic profiles of both cystic fibrosis and non-cystic fibrosis patients are shown in Figure 1. The individual pharmacokinetic parameters of ganciclovir used in the study are summarized in Table 4. The median (IQR) weighted sum of squares and root mean square values were 4. 23 (1.19–14.04) and 0.97 (0.90–0.99), respectively. We observed medium-to-high inter-individual variability of pharmacokinetic parameters normalized per kg of body weight, as demonstrated by coefficients of variation of 19%, 59%, 52%, 68% and 79% for Vd_c, Vd, CL, $t_{1/2}\alpha$ and $t_{1/2}\beta$, respectively. By contrast, there were no significant differences in ganciclovir pharmacokinetic parameters obtained from the same patients (n = 4) repeatedly during hospitalization (p-value of 0.5000, >0.9999, >0.9999, 0.5000 and 0.8750 for Vd_c, Vd, CL, $t_{1/2}\alpha$ and $t_{1/2}\beta$, respectively), which indicates negligible intra-individual variability.

All the sampling time points (C_3, C_5 and C_{trough}) were significantly associated with ganciclovir total exposure (AUC); however, AUC was best predicted by the peak level (r^2 was 0.7720, 0.3184 and 0.2580 for C_3, C_5 and C_{trough}, respectively).

Both Vd and CL normalized by body weight were significantly and negatively related to age ($p = 0.0439$ and $p = 0.0116$, respectively). Males showed significantly higher bodyweight-normalized Vd than females (median value 0.69 vs. 0.55 L/kg; $p = 0.0330$). Vd_c was significantly related to bodyweight, height, BSA and BMI ($p < 0.0001$, $p = 0.0011$, $p < 0.0001$, and $p < 0.0001$, respectively), while total Vd increased significantly only with height ($p = 0.0297$) and BSA ($p = 0.0386$). CL was significantly related only to eGFR ($p < 0.0001$). For the patients whose cystatin C level was measured (n = 24), the predictive performance of creatinine- and cystatine C-based CKD-EPI formulas for the estimation of glomerular filtration rate was compared. In this sense, creatinine-based estimates performed slightly better numerically ($p = 0.0010$, $r^2 = 0.3952$ vs. $p = 0.0033$, $r^2 = 0.3309$). Both ALT and GGT were not significantly related to the pharmacokinetics of ganciclovir. Ganciclovir exposure (AUC_{24}) was also not associated with either white blood cell or platelet counts. Bodyweight-normalized CL was significantly higher in patients with cystic fibrosis, while distribution half-life was reduced in patients with this diagnosis (see Table 4). There was also a trend towards increased volume of distribution in the cystic fibrosis patients. We observed no dose-dependent drug interaction between immunosuppressive therapy and ganciclovir weight-normalized pharmacokinetic parameters. The dose-independent

analysis also did not show any impact of antimycotic therapy on ganciclovir disposition. The main observed relationships between ganciclovir's pharmacokinetic parameters and its covariates are showed in Figure 2.

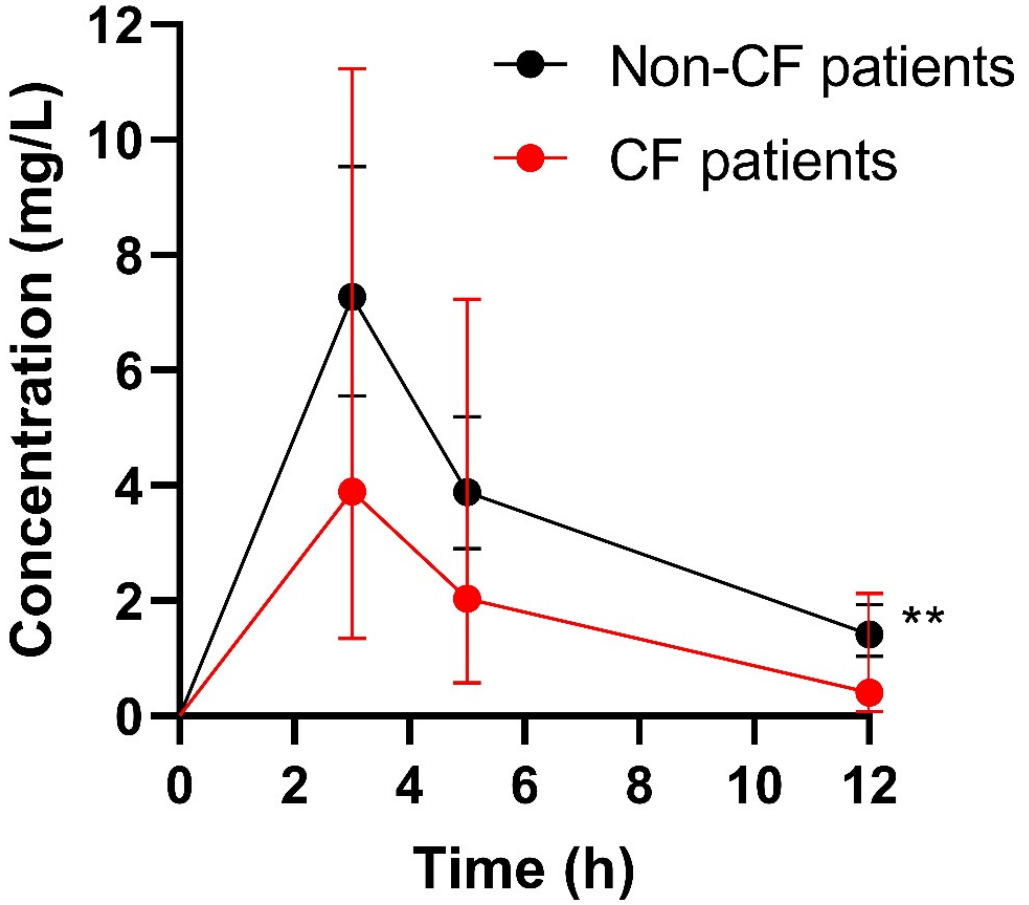

Figure 1. Ganciclovir pharmacokinetic profiles in both cystic fibrosis (CF) and non-cystic fibrosis (non-CF) patients. Data are expressed as geomeans (95% CI). ** Significantly different (p = 0.0085).

Table 4. Pharmacokinetic analysis of ganciclovir.

PK Parameter	Whole Study Population (n = 40)	CF Patients (n = 5)	Non-CF Patients (n = 35)	p-Value CF vs. Non-CF
Vd_c (L)	8.96 (7.51–10.30)	6.19 (6.05–7.65)	9.13 (8.36–10.46)	-
Vd_c (L/kg)	0.120 (0.110–0.124)	0.129 (0.121–0.130)	0.119 (0.109–0.124)	0.069
Vd (L)	51.7 (32.7–60.1)	39.5 (31.5–59.7)	52.5 (34.3–60.1)	-
Vd (L/kg)	0.65 (0.52–0.73)	0.67 (0.67–1.08)	0.65 (0.50–0.72)	0.1987
CL (L/h)	6.64 (4.27–9.20)	7.39 (6.38–9.29)	6.49 (4.04–9.14)	-
CL (L/h/kg)	0.088 (0.059–0.118)	0.125 (0.112–0.198)	0.081 (0.057–0.106)	0.0127 *
$t_{1/2}\alpha$ (h)	0.20 (0.18–0.37)	0.18 (0.16–0.18)	0.20 (0.18–0.44)	0.0318 *
$t_{1/2}\beta$ (h)	4.7 (3.6–5.8)	3.6 (2.8–3.7)	5.2 (3.7–5.9)	0.1448
AUC_{24} (mg × h/L)	104.9 (76.1–154.0)	53.8 (40.9–78.0)	114.2 (85.5–155.9)	-

Data are expressed as median (IQR). Only bodyweight-normalized and independent pharmacokinetic parameters were compared. Statistically significant * CF—cystic fibrosis, Vd_c—central volume of distribution, Vd—total volume of distribution, CL—clearance, $t_{1/2}\alpha$—distribution half-life, $t_{1/2}\beta$—elimination half-life, AUC_{24}—24 h area under the concentration time curve.

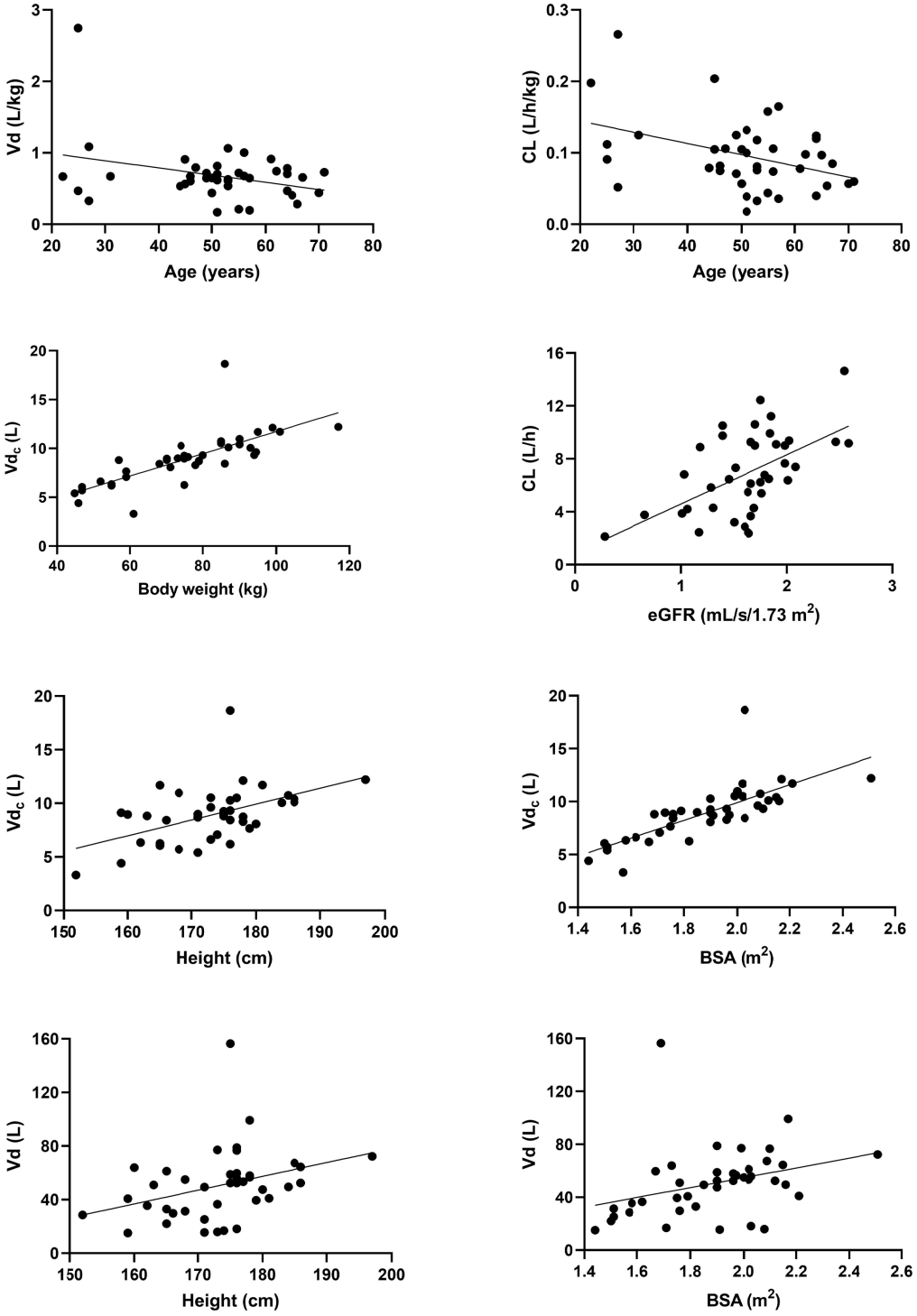

Figure 2. Relationships between ganciclovir pharmacokinetic parameters and its main covariates. Vd_c—central volume of distribution, Vd—total volume of distribution, CL—clearance, BSA—body surface area, eGFR—estimated glomerular filtration rate according to the CKD-EPI creatinine equation.

Based on the regression analysis, height was shown to be the most predictive parameter for ganciclovir Vd and, consequently, for LD. Thus, CL and MD were best predicted by eGFR according to the creatinine CKD-EPI equation. Based on these relations, the optimal estimated LD was defined according to the following equation: LD (mg) = 7.988 × height (cm)–992.1. Optimal estimated daily MD was described as: MD (mg/day) = 705.4 × eGFR (mL/s)–109.4. These relationships were used to construct the dosing nomograms for more

convenient clinical use (Figure 3). The median (95% CI) LD ganciclovir and daily MD were 2.31 (2.24–2.39) mg per cm of height and 643.88 (638.18–649.59) mg per 1 mL/s of eGFR, respectively. Subsequently, we simulated the administration of the dose recommended by the nomograms in model subjects with the pharmacokinetic data of each individual enrolled in the study. After the simulated LD administration, 32 (80%) of the patients reached the target range for ganciclovir peak concentrations (3–12.5 mg/L), 7 (17.5%) were above and 1 (2.5%) was below the range, while after the simulated administration of MD, 33 (82.5%) of the patients reached the target range for ganciclovir levels in the whole interval (1–12.5 mg/L), while 17 (17.5%) were above and none (0%) were below the range.

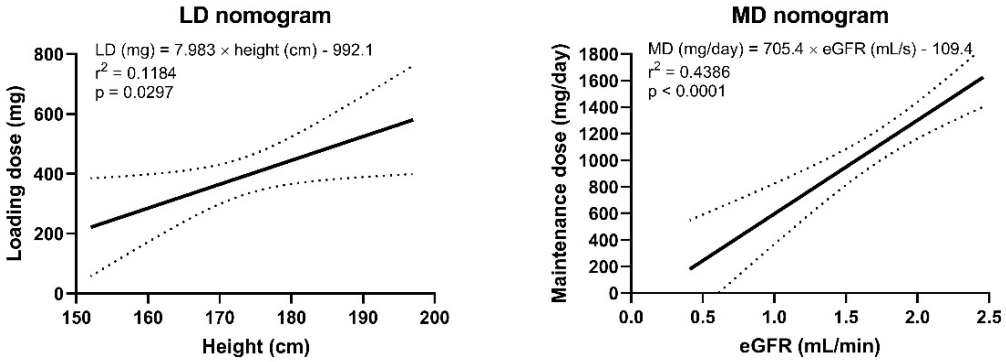

Figure 3. Nomograms for the calculation of the loading dose (LD) and the daily maintenance dose (MD) of ganciclovir according to height and estimated glomerular filtration rate according to the creatinine CKD-EPI formula, respectively. The dashed lines represent the 95% confidence interval.

4. Discussion

Cytomegalovirus is a leading cause of infection in lung transplant recipients and it is associated with significant morbidity and mortality [21]. Adequate cytomegalovirus dosing is therefore of great importance, as low serum concentrations of ganciclovir should be avoided to minimize the risk of resistance development [22]. To ensure adequate exposure to ganciclovir, TDM could be applied to optimize ganciclovir serum concentrations during treatment or prophylaxis. Although the target ganciclovir levels that should be achieved during therapy have not yet been unequivocally defined [23], the therapeutic ranges frequently used for peak and trough ganciclovir concentrations in clinical practice are 3–12 and 1–3 mg/L, respectively [20]. The monitoring of ganciclovir exposure especially, in high-risk patient groups with unpredictable pharmacokinetics, i.e., patients with unstable renal function, solid organ transplant recipients, or patients not responding to treatment as expected, has been suggested [24].

In this study, we reviewed the pharmacokinetics of ganciclovir in patients after lung transplantation, on whom TDM was performed. In total, 132 samples were received from 40 lung transplant recipients. This represents one of the largest data sets describing ganciclovir pharmacokinetics in this vulnerable population.

We observed medium-to-high inter-individual variability of pharmacokinetic parameters, which was similar to the results of Märtson et al. and Galar et al. [24,25]. By contrast, there were no significant differences in the ganciclovir pharmacokinetic parameters obtained from the same patients.

We observed an increase in ganciclovir CL of approximately 50% in patients with cystic fibrosis. Although the patients with cystic fibrosis were significantly younger than the patients not suffering from this disease and we found a negative relationship between age and bodyweight-normalized ganciclovir CL in this subgroup, we assume that the independent covariate of ganciclovir CL is cystic fibrosis, because there was no relationship between age and ganciclovir CL in the patients not suffering from cystic fibrosis. Although the pharmacokinetics of ganciclovir have not been described previously in patients with cystic fibrosis, our findings correspond well with the theoretical assumption that ganciclovir enhances the clearance of renally eliminated compounds. It was previously shown that

cystic fibrosis leads to several pharmacokinetic alterations, including the enlargement of the volume of distribution and/or enhanced clearance for most drugs [26]. The enhanced drug of drugs in cystic fibrosis is generally explained by increased glomerular filtration, increased active tubular secretion, and decreased tubular reabsorption [26,27].

Ganciclovir can be dosed on a milligram-per-kilogram of bodyweight basis as this corresponds well to ganciclovir clearance and the volume of distribution [28]. The other most clearly defined variable affecting the pharmacokinetic parameters is renal function status/creatinine clearance [25,29–31].

Based on our results, an LD of 7.988 × height (cm)–992.1 mg followed with a daily MD of 705.4 × eGFR (mL/s)–109.4 mg/day (divided into 2 doses every 12 h) should be optimal. Of course, the administration of an LD only make sense if the LD is higher than a single MD. Therefore, the condition eGFR (mL/s) < 0.023 × height (cm)–2.66 must be met. Thus, LD administration should be considered especially in patients with moderate-to-severe decrease in renal function. The daily MD deducted from the proposed nomogram should be further increased by approximately 50% in patients with cystic fibrosis.

Measured creatinine clearance is not available from most patients at the time when ganciclovir treatment is initiated. Therefore, eGFR according to the CKD-EPI equation was used to individualize ganciclovir MD. The CKD-EPI equation is an up-to-date method for estimating GFR and its superiority in the prediction of MD in other drugs excreted via kidney has been described previously [32,33].

There was no correlation between ganciclovir trough and peak serum levels, nor between hematologic toxicity and nephrotoxicity [20,34]. In our study, ganciclovir exposure (AUC_{24}) was associated neither with white blood cell count nor with platelet count. Neither ALT nor GGT were significantly related to the pharmacokinetics of ganciclovir. We also observed no impact of concomitant immunosuppressant treatment or antimycotic therapy on ganciclovir pharmacokinetics. This observation is of interest, since the co-administration of the antifungal voriconazole and ganciclovir was excluded in previous clinical studies [35].

We acknowledge a few limitations of our study. First, we enrolled only one subject with eGFR below 0.5 mL/s; therefore, our dosing recommendation may not be applicable in this subpopulation. Furthermore, the subpopulation of patients with cystic fibrosis is rather limited (n = 5); therefore, the PK and dosing estimates should be considered as pilot data only for this subpopulation.

5. Conclusions

Ganciclovir clearance is correlated with creatinine clearance; therefore, ganciclovir should be dosed according to renal function status. Significantly higher bodyweight-normalized CL and lower distribution half-life were observed in patients with cystic fibrosis. As a result, ganciclovir's daily maintenance dose should be increased by approximately 50% in cystic fibrosis patients. We did not observe any pharmacokinetic drug interactions between ganciclovir and immunosuppressive or antimycotic therapy. Large inter-individual variability of serum levels was observed. This is one of the reasons for supporting TDM. Future studies may aim to identify an appropriate group of patients for ganciclovir dosing according to our nomogram, depending on height and renal function. Our data also provide the basis for the design of a pharmacokinetic model that is needed to more accurately describe the PK/PD relationship in ganciclovir.

Author Contributions: Conceptualization: E.D., M.Š. and O.S.; methodology: M.Š., J.P. (Jakub Petrus) and E.K.; investigation: P.H., J.P. (Jiří Pozniak), J.H. and R.L.; formal analysis: M.Š. and E.D.; data curation: E.D., M.Š., J.P. (Jakub Petrus), E.K., P.H., J.P. (Jiří Pozniak) and J.H.; writing—original draft preparation: E.D., M.Š., J.P. (Jakub Petrus) and E.K.; writing—review and editing: P.H., J.P. (Jiří Pozniak), J.H., R.L. and O.S.; supervision: E.K., R.L. and O.S. All authors have read and agreed to the published version of the manuscript.

Funding: This study was supported by MH CZ-DRO (Motol University Hospital, Prague, Czech Republic 00064203) and by the Charles University Cooperatio Program (research area PHAR), grant SVV 260523.

Institutional Review Board Statement: The study was conducted in accordance with the Declaration of Helsinki, and approved by the Institutional Ethics Committee of Motol University Hospital, Prague, Czech Republic (No. EK-11/20) on 8 January 2020.

Informed Consent Statement: Written informed consent has been obtained from the patients to publish this paper.

Data Availability Statement: Data supporting the findings of this study are available from the corresponding author upon reasonable request.

Acknowledgments: The authors thank Kristyna Vyskocilova, Jan Simonek, Tereza Kotowski, Jiri Vachtenheim, Monika Svorcova, Jan Kolarik, and Rene Novysedlak for routine care for the patients in this study.

Conflicts of Interest: The authors declare no conflict of interest.

References

1. Hubacek, P.; Virgili, A.; Ward, K.N.; Pohlreich, D.; Keslova, P.; Goldova, B.; Markova, M.; Zajac, M.; Cinek, O.; Nacheva, E.P.; et al. HHV-6 DNA throughout the tissues of two stem cell transplant patients with chromosomally integrated HHV-6 and fatal CMV pneumonitis. *Br. J. Haematol.* **2009**, *145*, 394–398. [CrossRef] [PubMed]
2. Kurihara, C.; Fernandez, R.; Safaeinili, N.; Akbarpour, M.; Wu, Q.; Budinger, G.R.S.; Bharat, A. Long-Term Impact of Cytomegalovirus Serologic Status on Lung Transplantation in the United States. *Ann. Thorac. Surg.* **2019**, *107*, 1046–1052. [CrossRef] [PubMed]
3. Kotton, C.N.; Kumar, D.; Caliendo, A.M.; Huprikar, S.; Chou, S.; Danziger-Isakov, L.; Humar, A.; The Transplantation Society International CMV Consensus Group. The Third International Consensus Guidelines on the Management of Cytomegalovirus in Solid-organ Transplantation. *Transplantation* **2018**, *102*, 900–931. [PubMed]
4. Ho, S.A.; Slavin, M.; Roberts, J.A.; Yong, M. Optimization of Ganciclovir use in allogeneic hematopoietic cell transplant recipients—The role of therapeutic drug monitoring. *Expert Rev. Anti-Infect. Ther.* **2021**, *19*, 707–718. [CrossRef] [PubMed]
5. Perrottet, N.; Decosterd, L.A.; Meylan, P.; Pascual, M.; Biollaz, J.; Buclin, T. Valganciclovir in adult solid organ transplant recipients: Pharmacokinetic and pharmacodynamic characteristics and clinical interpretation of plasma concentration measurements. *Clin. Pharmacokinet.* **2009**, *48*, 399–418. [CrossRef] [PubMed]
6. Gilbert, C.; Boivin, G. Human cytomegalovirus resistance to antiviral drugs. *Antimicrob. Agents Chemother.* **2005**, *49*, 873–883. [CrossRef] [PubMed]
7. Razonable, R.R. Management strategies for cytomegalovirus infection and disease in solid organ transplant recipients. *Infect. Dis. Clin. N. Am.* **2013**, *27*, 317–342. [CrossRef]
8. Davis, C.L.; Springmeyer, S.; Gmerek, B.J. Central nervous system side effects of ganciclovir. *N. Engl. J. Med.* **1990**, *322*, 933–934.
9. Chambers, D.C.; Zuckermann, A.; Cherikh, W.S.; Harhay, M.O.; Hayes, D., Jr.; Hsich, E.; Khush, K.K.; Potena, L.; Sadavarte, A.; Singh, T.P.; et al. The International Thoracic Organ Transplant Registry of the International Society for Heart and Lung Transplantation: 37th adult lung transplantation report—2020; focus on deceased donor characteristics. *J. Heart Lung Transplant.* **2020**, *39*, 1016–1027. [CrossRef]
10. Snell, G.I.; Kotsimbos, T.C.; Levvey, B.J.; Skiba, M.; Rutherford, D.M.; Kong, D.C.; Williams, T.J.; Krum, H. Pharmacokinetic assessment of oral ganciclovir in lung transplant recipients with cystic fibrosis. *J. Antimicrob. Chemother.* **2000**, *45*, 511–516. [CrossRef]
11. Crumpacker, C.S. Ganciclovir. *N. Engl. J. Med.* **1996**, *335*, 721–729. [CrossRef] [PubMed]
12. Faulds, D.; Heel, R.C. Ganciclovir: A review of its antiviral activity, pharmacokinetic properties and therapeutic efficacy in cytomegalovirus infections. *Drugs* **1990**, *39*, 597–638. [CrossRef] [PubMed]
13. Du Bois, D.; Du Bois, E.F. A formula to estimate the approximate surface area if height and weight be known. *Nutrition* **1989**, *5*, 303–311; discussion 312–313.
14. Inker, L.A.; Schmid, C.H.; Tighiouart, H.; Eckfeldt, J.H.; Feldman, H.I.; Greene, T.; Kusek, J.W.; Manzi, J.; Van Lente, F.; Zhang, Y.L.; et al. Estimating glomerular filtration rate from serum creatinine and cystatin C. *N. Engl. J. Med.* **2012**, *367*, 20–29. [CrossRef] [PubMed]
15. Garrow, J.S. Quetelet index as indicator of obesity. *Lancet* **1986**, *1*, 1219. [CrossRef]
16. U.S. Department of Health and Human Services, Food and Drug Administration. Guidance for Industry: Bioanalytical Method Validation. U.S. 2018. Available online: https://www.fda.gov/files/drugs/published/Bioanalytical-Method-Validation-Guidance-for-Industry.pdf (accessed on 3 February 2022).

17. Sommadossi, J.P.; Bevan, R.; Ling, T.; Lee, F.; Mastre, B.; Chaplin, M.D.; Nerenberg, C.; Koretz, S.; Buhles, W.C., Jr. Clinical pharmacokinetics of ganciclovir in patients with normal and impaired renal function. *Rev. Infect. Dis.* **1988**, *10* (Suppl. 3), S507–S514. [CrossRef]
18. Bonett, D.G.; Price, R.M. Statistical inference for a linear function of medians: Confidence intervals, hypothesis testing, and sample size requirements. *Psychol. Methods* **2002**, *7*, 370–383. [CrossRef]
19. Sima, M.; Pokorna, P.; Hronova, K.; Slanar, O. Effect of co-medication on the pharmacokinetic parameters of phenobarbital in asphyxiated newborns. *Physiol. Res.* **2015**, *64*, S513–S519. [CrossRef]
20. Ritchie, B.M.; Barreto, J.N.; Barreto, E.F.; Crow, S.A.; Dierkhising, R.A.; Jannetto, P.J.; Tosh, P.K.; Razonable, R.R. Relationship of Ganciclovir Therapeutic Drug Monitoring with Clinical Efficacy and Patient Safety. *Antimicrob. Agents Chemother.* **2019**, *63*, e01855-18. [CrossRef]
21. Trachuk, P.; Bartash, R.; Abbasi, M.; Keene, A. Infectious Complications in Lung Transplant Recipients. *Lung* **2020**, *198*, 879–887. [CrossRef]
22. Lurain, N.S.; Chou, S. Antiviral drug resistance of human cytomegalovirus. *Clin. Microbiol. Rev.* **2010**, *23*, 689–712. [CrossRef]
23. Stockmann, C.; Roberts, J.K.; Knackstedt, E.D.; Spigarelli, M.G.; Sherwin, C.M. Clinical pharmacokinetics and pharmacodynamics of ganciclovir and valganciclovir in children with cytomegalovirus infection. *Expert Opin. Drug Metab. Toxicol.* **2015**, *11*, 205–219. [CrossRef]
24. Galar, A.; Valerio, M.; Catalan, P.; Garcia-Gonzalez, X.; Burillo, A.; Fernandez-Cruz, A.; Zatarain, E.; Sousa-Casasnovas, I.; Anaya, F.; Rodriguez-Ferrero, M.L.; et al. Valganciclovir-Ganciclovir Use and Systematic Therapeutic Drug Monitoring. An Invitation to Antiviral Stewardship. *Antibiotics* **2021**, *10*, 77. [PubMed]
25. Martson, A.G.; Edwina, A.E.; Burgerhof, J.G.M.; Berger, S.P.; de Joode, A.; Damman, K.; Verschuuren, E.A.M.; Blokzijl, H.; Bakker, M.; Span, L.F.; et al. Ganciclovir therapeutic drug monitoring in transplant recipients. *J. Antimicrob. Chemother.* **2021**, *76*, 2356–2363. [CrossRef] [PubMed]
26. De Sutter, P.J.; Gasthuys, E.; Van Braeckel, E.; Schelstraete, P.; Van Biervliet, S.; Van Bocxlaer, J.; Vermeulen, A. Pharmacokinetics in Patients with Cystic Fibrosis: A Systematic Review of Data Published Between 1999 and 2019. *Clin. Pharmacokinet.* **2020**, *59*, 1551–1573. [CrossRef] [PubMed]
27. Jouret, F.; Bernard, A.; Hermans, C.; Dom, G.; Terryn, S.; Leal, T.; Lebecque, P.; Cassiman, J.J.; Scholte, B.J.; de Jonge, H.R.; et al. Cystic fibrosis is associated with a defect in apical receptor-mediated endocytosis in mouse and human kidney. *J. Am. Soc. Nephrol.* **2007**, *18*, 707–718. [CrossRef] [PubMed]
28. Scott, J.C.; Partovi, N.; Ensom, M.H. Ganciclovir in solid organ transplant recipients: Is there a role for clinical pharmacokinetic monitoring? *Ther. Drug Monit.* **2004**, *26*, 68–77. [CrossRef] [PubMed]
29. Lefeuvre, S.; Chevalier, P.; Charpentier, C.; Zekkour, R.; Havard, L.; Benammar, M.; Amrein, C.; Boussaud, V.; Lillo-Le Louet, A.; Guillemain, R.; et al. Valganciclovir prophylaxis for cytomegalovirus infection in thoracic transplant patients: Retrospective study of efficacy, safety, and drug exposure. *Transpl. Infect. Dis.* **2010**, *12*, 213–219. [CrossRef] [PubMed]
30. Murray, B.M. Management of cytomegalovirus infection in solid-organ transplant recipients. *Immunol. Investig.* **1997**, *26*, 243–255. [CrossRef]
31. Palacio-Lacambra, M.E.; Comas-Reixach, I.; Blanco-Grau, A.; Sune-Negre, J.M.; Segarra-Medrano, A.; Montoro-Ronsano, J.B. Comparison of the Cockcroft-Gault, MDRD and CKD-EPI equations for estimating ganciclovir clearance. *Br. J. Clin. Pharmacol.* **2018**, *84*, 2120–2128. [CrossRef]
32. Sima, M.; Hartinger, J.; Cikankova, T.; Slanar, O. Estimation of once-daily amikacin dose in critically ill adults. *J. Chemother.* **2018**, *30*, 37–43. [CrossRef] [PubMed]
33. Sima, M.; Hartinger, J.; Stenglova Netikova, I.; Slanar, O. Creatinine Clearance Estimations for Vancomycin Maintenance Dose Adjustments. *Am. J. Ther.* **2018**, *25*, e602–e604. [CrossRef] [PubMed]
34. Wiltshire, H.; Paya, C.V.; Pescovitz, M.D.; Humar, A.; Dominguez, E.; Washburn, K.; Blumberg, E.; Alexander, B.; Freeman, R.; Heaton, N.; et al. Pharmacodynamics of oral ganciclovir and valganciclovir in solid organ transplant recipients. *Transplantation* **2005**, *79*, 1477–1483. [CrossRef] [PubMed]
35. Rousseau, A.; Monchaud, C.; Debord, J.; Vervier, I.; Estenne, M.; Thiry, P.; Marquet, P. Bayesian forecasting of oral cyclosporin pharmacokinetics in stable lung transplant recipients with and without cystic fibrosis. *Ther. Drug Monit.* **2003**, *25*, 28–35. [CrossRef] [PubMed]

pharmaceutics

MDPI

Article

Real-Life Therapeutic Concentration Monitoring of Long-Acting Cabotegravir and Rilpivirine: Preliminary Results of an Ongoing Prospective Observational Study in Switzerland

Paul Thoueille [1], Susana Alves Saldanha [1], Fabian Schaller [1], Aline Munting [2], Matthias Cavassini [2], Dominique Braun [3,4], Huldrych F. Günthard [3,4], Katharina Kusejko [3,4], Bernard Surial [5], Hansjakob Furrer [5], Andri Rauch [5], Pilar Ustero [6], Alexandra Calmy [6,7], Marcel Stoeckle [8], Manuel Battegay [8,9], Catia Marzolini [8,9,10], Pascal Andre [1], Monia Guidi [1,11,12], Thierry Buclin [1], Laurent A. Decosterd [1,*] and on behalf of the Swiss HIV Cohort Study [†]

1 Service and Laboratory of Clinical Pharmacology, Department of Laboratory Medicine and Pathology, Lausanne University Hospital and University of Lausanne, 1011 Lausanne, Switzerland; paul.thoueille@chuv.ch (P.T.); susana.alves-saldanha@chuv.ch (S.A.S.); fabian.schaller@chuv.ch (F.S.); pascal.andre@chuv.ch (P.A.); monia.guidi@chuv.ch (M.G.); thierry.buclin@chuv.ch (T.B.)
2 Service of Infectious Diseases, Department of Medicine, Lausanne University Hospital and University of Lausanne, 1011 Lausanne, Switzerland; aline.munting@chuv.ch (A.M.); matthias.cavassini@chuv.ch (M.C.)
3 Department of Infectious Diseases and Hospital Epidemiology, University Hospital Zurich, 8091 Zurich, Switzerland; dominique.braun@usz.ch (D.B.); huldrych.guenthard@usz.ch (H.F.G.); katharina.kusejko@usz.ch (K.K.)
4 Institute of Medical Virology, University of Zurich, 8057 Zurich, Switzerland
5 Department of Infectious Diseases, Inselspital, Bern University Hospital, University of Bern, 3010 Bern, Switzerland; bernard.surial@insel.ch (B.S.); hansjakob.furrer@insel.ch (H.F.); andri.rauch@insel.ch (A.R.)
6 Division of Infectious Diseases, Faculty of Medicine, Geneva University Hospitals, 1205 Geneva, Switzerland; pilar.usteroalonso@hcuge.ch (P.U.); alexandra.calmy@hcuge.ch (A.C.)
7 Department of Medicine, Faculty of Medicine, University of Geneva, 1205 Geneva, Switzerland
8 Division of Infectious Diseases and Hospital Epidemiology, University Hospital Basel, University of Basel, 4031 Basel, Switzerland; marcel.stoeckle@usb.ch (M.S.); manuel.battegay@usb.ch (M.B.); catia.marzolini@usb.ch (C.M.)
9 Faculty of Medicine, University of Basel, 4031 Basel, Switzerland
10 Department of Molecular and Clinical Pharmacology, Institute of Translational Medicine, University of Liverpool, Liverpool L69 3GF, UK
11 Centre for Research and Innovation in Clinical Pharmaceutical Sciences, Lausanne University Hospital and University of Lausanne, 1011 Lausanne, Switzerland
12 Institute of Pharmaceutical Sciences of Western Switzerland, University of Geneva, 1206 Geneva, Switzerland
* Correspondence: laurentarthur.decosterd@chuv.ch
† The Swiss HIV Cohort Study are listed in acknowledgments.

Citation: Thoueille, P.; Alves Saldanha, S.; Schaller, F.; Munting, A.; Cavassini, M.; Braun, D.; Günthard, H.F.; Kusejko, K.; Surial, B.; Furrer, H.; et al. Real-Life Therapeutic Concentration Monitoring of Long-Acting Cabotegravir and Rilpivirine: Preliminary Results of an Ongoing Prospective Observational Study in Switzerland. *Pharmaceutics* **2022**, *14*, 1588. https://doi.org/10.3390/pharmaceutics14081588

Academic Editor: Donald E. Mager

Received: 30 May 2022
Accepted: 26 July 2022
Published: 29 July 2022

Abstract: SHCS#879 is an ongoing Switzerland-wide multicenter observational study conducted within the Swiss HIV Cohort Study (SHCS) for the prospective follow-up of people living with HIV (PLWH) receiving long-acting injectable cabotegravir-rilpivirine (LAI-CAB/RPV). All adults under LAI-CAB/RPV and part of SHCS are enrolled in the project. The study addresses an integrated strategy of treatment monitoring outside the stringent frame of controlled clinical trials, based on relevant patient characteristics, clinical factors, potential drug-drug interactions, and measurement of circulating blood concentrations. So far, 91 blood samples from 46 PLWH have been collected. Most individuals are less than 50 years old, with relatively few comorbidities and comedications. The observed concentrations are globally in accordance with the available values reported in the randomized clinical trials. Yet, low RPV concentrations not exceeding twice the reported protein-adjusted 90% inhibitory concentration have been observed. Data available at present confirm a considerable between-patient variability overall. Based on the growing amount of PK data accumulated during this ongoing study, population pharmacokinetic analysis will characterize individual concentration-time profiles of LAI-CAB/RPV along with their variability in a real-life setting and their association with treatment response and tolerability, thus bringing key data for therapeutic monitoring and precision dosage adjustment of this novel long-acting therapy.

Keywords: long-acting antiretroviral therapy; cabotegravir; rilpivirine; therapeutic drug monitoring; pharmacokinetics; population pharmacokinetic modeling; pharmacokinetic simulation

1. Introduction

Following the identification of HIV as the causal agent of AIDS in the early eighties, we have witnessed a progressive improvement in the management of HIV infection, which started with the approval of the first antiretroviral therapy (ART) for HIV treatment in 1987. Since the development of highly active ARTs about 25 years ago, complex therapies have been progressively simplified to potent, once-daily, fixed-dose multidrug formulations, thereby improving tolerability, efficacy, and convenience. These treatments have transformed HIV infection from a then fatal disease to a manageable chronic condition. Recently, not only the management but also the prevention of HIV infection has entered the bright new era of long-acting (LA) antiretroviral approaches, as reviewed elsewhere [1].

Cabotegravir (CAB) and rilpivirine (RPV), an integrase inhibitor combined with a non-nucleoside reverse transcriptase inhibitor, have been recently approved as a complete dual regimen for the maintenance treatment of HIV-1 infection in adults [2]. In Europe and Switzerland, CAB and RPV are marketed as two separate injectable medicines under the brand names VOCABRIA® and REKAMBYS®, respectively, while CABENUVA®, a combined pack of CAB and RPV, is notably available in Canada and the United States. After an optional oral lead-in period of CAB 30 mg plus RPV 25 mg once daily, followed by an intramuscular (i.m.) loading dose (CAB/RPV at 600/900 mg), CAB and RPV are administered through i.m. injections either every 2 months (q8w) at 600/900 mg or monthly (q4w) at 400/600 mg. The nanosuspension technology enabled this long-acting injectable (LAI) delivery approach by increasing the apparent half-life of CAB and RPV from 41 h and 45 h to approximately 8.5 weeks and 20.5 weeks, respectively, although with substantial inter-individual variability already outlined in clinical trials [3]. Recently, LAI-CAB has also been approved by the U.S. FDA for use in at-risk adults and adolescents for pre-exposure prophylaxis (PrEP) to reduce the risk of sexually acquired HIV [4].

LA-ARTs undoubtedly have the potential to improve the treatment and prevention of HIV infection, particularly in terms of patient confidentiality, convenience, and empowerment. In addition, they will essentially contribute to overcoming the challenge of adherence. However, we hypothesize that close monitoring of the patients will probably be necessary for an optimal implementation of these revolutionary approaches. Indeed, many people living with HIV (PLWH) face complex situations, which are rarely taken into account in most clinical trials [5–8]. Concomitant initiation of treatments for comorbidities with a definite risk of drug–drug interactions (DDIs) (e.g., tuberculosis, HCV infection, cancer, and further comorbidities associated with polypharmacy) will definitely require special attention in people receiving this new LA-ART. Moreover, LAI-CAB/RPV therapy will require close monitoring in underweight or obese people and possibly in pregnant women with regard to not only efficacy but also tolerability and long-term safety. In particular, a body mass index (BMI) greater than 30 already appears to be an independent risk factor for CAB/RPV treatment failure [9].

In this context, we have launched a Swiss-wide prospective observational study within the frame of the Swiss HIV Cohort Study (SHCS) (project SHCS#879). This project aims to bring an original contribution to the monitoring of the LAI-ART by investigating the characteristics of the LAI-CAB/RPV pharmacokinetics (PK) in real-life PLWH. Despite the so far limited clinical validation of therapeutic drug monitoring (TDM) in the context of ART [10], we believe that TDM will be an important component of optimal patient follow-up in the LA-ART era. Indeed, with adherence no longer representing a confounding factor (as long as the patients do not miss their injections' appointments), physicians facing inadequate therapeutic response in patients are likely to question whether they are actually exposed to appropriate levels of antiretroviral drugs throughout the whole dosing intervals.

Although population pharmacokinetic (popPK) analyses of CAB/RPV have been conducted during phase III clinical trials [11,12], there is, to the best of our knowledge, no popPK analysis involving a real-life cohort of PLWH. The SHCS#879 observational study addresses an integrated strategy of LAI-ART treatment monitoring outside the stringent frame of controlled clinical trials, based on relevant individual characteristics, demographic/clinical factors, potential DDIs, and measurement of circulating blood concentrations. Based on the information continuously gathered during the ongoing implementation of LAI-CAB/RPV within the Swiss PLWH population, a popPK analysis will be performed to characterize the variability of concentration-time profiles of LAI-CAB/RPV and to examine the patients' covariates possibly influencing LAI-ART plasma exposure. Ultimately, the SHCS#879 project aims to develop a suitable popPK model, providing an individual prediction of the range of trough concentration (C_{min}) expected in a given PLWH, taking into account both the known variability of drug concentrations and the patient's individual characteristics. The present article gives some insights into the first observations performed during the implementation of LAI-CAB/RPV in Switzerland and examines whether they fit with our underlying hypothesis on the clinical relevance of TDM.

2. Materials and Methods

2.1. Study Design

The SHCS, established in 1988, is an ongoing multicenter, clinic-based, prospective, longitudinal, observational study including HIV-infected adults in Switzerland [13,14]. SHCS#879 is an ongoing Swiss-wide prospective observational project on LAI-CAB/RPV in a real-life cohort of PLWH. Adults (>18 years old) enrolled in the SHCS and followed up in the centers of Lausanne, Geneva, Bern, Basel, Zürich, St-Gall, and Lugano are systematically included in the SHCS#879 project if they receive the CAB-RPV regimen. At present, physicians are selecting in the first instance, PLWH who have been consistently adherent to antiretroviral therapy, although this is not an inclusion criterion, in order to avoid potential issues related to administration schedules (e.g., patients who forget or fail to show up for drug administration appointments). In addition, a one-month oral lead-in period is currently recommended in Switzerland [15,16], but its implementation occurs according to physician and patient preferences. For the most part, the samples are collected and the data are recorded at medical visits, on average every 2 months, or at one or two of the bi-yearly planned SHCS cohort visits. These cohort visits do not necessarily coincide with the day of CAB/RPV injection, resulting in samples obtained at unselected times during the entire dosing interval. In addition, to enrich the data collected during standard visits, detailed PK investigations are planned in PLWH who consent to donate a few additional blood samples. These additional investigations will allow a better characterization of the PK of early levels after i.m. injection and capture the actual C_{min} concentrations (just prior to next i.m. injection). Furthermore, considering the reported existence of secondary depots of drug nanoparticles distributed throughout the lymphatic and reticuloendothelial systems [17], CAB and RPV levels will be quantified in peripheral blood mononuclear cells (PBMC) from a subset of consenting patients.

The study data (i.e., demographic parameters, adverse events, CAB/RPV dosing regimen) are recorded using the study TDM request form, complemented with relevant clinical information (i.e., CD4 count, viremia, lab values, comedications) extracted from the national SHCS database, which contains the prospective medical records of SHCS cohort visits. In particular, the date and time of both the blood sampling and injection of LAI-CAB/RPV are carefully documented in the TDM request form, as the time lapse after the dose is necessary to interpret plasma concentrations.

Of note, some individuals were receiving CAB and RPV prior to Swiss market authorization and the start of the SHCS#879 study. Some samples were collected from PLWH receiving treatment for compassionate use, while other samples were obtained as laboratory quality control within the frame of the analytical method development. All these data

could be included in the study since these individuals are still followed in their respective SHCS centers.

2.2. Outcomes

The primary study endpoint is the quantification of CAB/RPV concentrations in plasma, and in PBMC, for the development of detailed popPK models and the characterization of the secondary depots of drug nanoparticles in PBMC, respectively. The key secondary endpoint is the quantification of CAB/RPV C_{min} in plasma as part of a validation step assessing whether the PK model is able to predict actual C_{min} based on one random sample drawn at an unselected time during the dosing interval. Other secondary endpoints include the comparison of PK characteristics from real-life patients on LAI-ART with those deduced from clinical trials submitted to registration agencies, the association of "on-target" plasma levels with treatment efficacy and tolerability, the assessment of the proportion of patients who interrupt i.m. treatment and the subsequent analysis of predictors for the interruption, and the identification of factors leading to a viral failure (defined as confirmed HIV viral load > 200 copies/mL). Targeted and detailed exploration of specific clinical situations is planned as well, such as undescribed DDIs or impact of specific comorbidities, susceptible to affect the absorption and disposition of LAI-ART. None of these endpoints of the SHCS#879 study have yet been attained at this early stage of the study, and thus, this article focuses only on preliminary results indicating whether or not they support our underlying assumption on the clinical interest of TDM.

2.3. Drug Level Measurements

The Laboratory of Clinical Pharmacology (CHUV, Lausanne, Switzerland) is equipped with a state-of-the-art platform of six instruments of high-performance chromatography coupled to tandem mass spectrometry (LC-MS/MS). It participates in International External Quality Control Proficiency Programs for CAB and RPV (Asqualab, Paris, France, https://www.asqualab.com/ accessed on 26 May 2022; KKGT, The Hague, The Netherlands, http://kkgt.nl/?lang=en accessed on 26 May 2022), certifying accurate drug level measurements. Whole blood samples are shipped immediately in a plastic transport protection coffer to the Laboratory of Clinical Pharmacology. In-house stability studies indicate that CAB and RPV are stable in the whole blood at room temperature for up to 96 h. Upon arrival, blood samples are centrifuged (2000$\times$ g, 10 min at 4 °C), and the separated plasma is frozen at −80 °C until analysis by LC-MS/MS, using a previously published validated multiplex method [18]. The CAB and RPV's lower limits of quantification are 25 ng/mL and 5 ng/mL, respectively. An analytical series for LC-MS/MS quantification is performed once a week, and the TDM results are sent within the same week to the physicians in charge.

Concerning the investigations on PBMC, the quantification of cell-associated ART levels require cell isolation immediately after blood collection using Vacutainer^{TM} Cell Preparation Tubes (CPT), using an adaptation of methods developed in our laboratory [19,20]. Cellular isolation is conducted according to the standardized procedure provided by the manufacturer [21].

2.4. Pharmacokinetic Modelling

Circulating drug concentration in plasma is the principal driver for both the efficacy and toxicity of most systemic therapies. Yet, drugs are often prescribed at standard dosages without taking into account between-patient PK variability, which can be remarkably large for some HIV drugs with a definite impact on therapeutic response. Multiple sources of variability have been identified, including demographic, environmental, clinical, pharmacological, and genetic factors. Population-based approaches represent the best way to characterize the PK profile of drugs in a cohort of patients and to capture the contribution of individual factors affecting drug levels [22,23].

The characterization of the LAI-CAB/RPV PK in PLWH enrolled in this study will be performed using compartmental methods employing non-linear mixed effects modeling

techniques. We will develop popPK models for CAB and RPV to describe their absorption and disposition after the injection of LA formulations and determine the effects of specific factors such as sex, age, body size, comorbidities, DDIs, and issues at the injection site or concomitant pathophysiological conditions. These models will be used to derive Bayesian maximum likelihood indicators of drug exposure (C_{min} levels). As most (up to 97%) of the SHCS participants have given their consent for genetic exploration, the popPK model developed for the SHCS#879 study will also be used for pharmacogenetic explorations.

At this early stage of results examination, our essential question was simply whether these first concentration data of LAI-CAB/RPV supported our underlying hypothesis of a clinical interest in TDM. The first criterion for TDM candidates is a significant between-subject PK variability associated with acceptable within-subject PK stability over time [24]. For our preliminary concentration data, this translates into statistically comparing the inter-individual variability and the within-patient variability with a one-way analysis of variance on log-transformed values, neglecting to a first approximation the influence of time lapse after dose and various covariates.

3. Preliminary Results

3.1. Study Population

At this early stage of the ongoing study (last samples collected in July 2022), 46 PLWH from Lausanne, Zürich, Bern, Geneva, and Basel have been so far included in SHCS#879. Table 1 summarizes their demographic and clinical characteristics.

To date, most of the included individuals are less than 50 years old (61%, 28 PLWH), male (83%, 38 PLWH), and Caucasian (63%, 29 PLWH), with relatively few comorbidities. In addition, seven PLWH (15%) are considered obese (BMI higher than 30 kg/m^2), while more than half (54%, 25 PLWH) are classified as overweight (BMI between 25 and 30 kg/m^2) [27]. No virologic failure, defined as confirmed HIV viral load > 200 copies/mL, occurred, but viral blips (single HIV viral load < 200 copies/mL) were observed in three patients (7%). Overall, 94% of the PLWH were undetectable (HIV viral load < 50 copies/mL), and one had missing data.

Individuals who were receiving CAB/RPV for compassionate use prior to Swiss market authorization received LAI-CAB/RPV every 4 weeks (4%, 2 PLWH), as this was the only recommended regimen at that time. However, these PLWH are to switch to the q8w regimen, with one individual having switched very recently. Participants who started the LAI treatment during the SHCS#879 study all receive the q8w regimen (96%, 44 PLWH). The oral lead-in was not initiated for every PLWH, with 17% having started directly with the i.m. loading dose. Lastly, various comedications were recorded, with five PLWH (30%) having three or more comedications. None were considered likely to cause DDIs.

Table 1. Characteristics of the PLWH included in the SHCS#879 study.

Population Characteristics Recorded at Last Cohort Visit or Last Sample Collection (n = 46)	**Median (Range) or Number (%)**	**[Missing Data, (%)]**
Demographic characteristics		
Sex:		
Male	38 (83)	
Female	8 (17)	
Ethnicity:		
Caucasian	29 (63)	
Black	6 (13)	
Hispanic American	3 (7)	
Asian	3 (7)	
Unknown	5 (10)	
Age (year)	45 (28–62)	
Body weight (kg)	83 (63–120)	
Height (cm)	177 (161–189)	
BMI (kg/m^2)	26 (19–37)	

Table 1. *Cont.*

Population Characteristics Recorded at Last Cohort Visit or Last Sample Collection (n = 46)	Median (Range) or Number (%)	[Missing Data, (%)]
Physiological characteristics		
Serum creatinine (µmol/L)	85 (46–131)	[4, (9)]
CL_{CR} (mL/min) [a]	111 (61–176)	[4, (9)]
eGFR (mL/min/1.73 m^2) [b]	92 (44–145)	[4, (9)]
CKD stage (mL/min/1.73 m^2)		
G1: ≥90	21 (46)	[4, (9)]
G2: 60–89	19 (41)	
G3a: 45–59	1 (2)	
G3b: 30–44	1 (2)	
Liver function		
Albumin (g/L)	44 (36–51)	[17, (37)]
Bilirubin (µmol/L)	7 (3–19)	[13, (28)]
AST (UI/L)	24 (13–44)	[4, (9)]
ALT (UI/L)	26 (9–67)	[4, (9)]
Heart blood pressure:		
Diastolic pressure (mmHg)	80 (60–107)	[4, (9)]
Systolic pressure (mmHg)	130 (108–180)	[4, (9)]
Malabsorption after gastrectomy	1 (2)	
HIV molecular biology		
CD4 (cells/mm^3)	667 (191–1192)	[4, (9)]
HIV RNA (copies/mL)		
<50	43 (94)	[1, (2)]
>50 and <200	2 (4)	
Previous antiretroviral therapy, no. (%):		
Bictegravir/Tenofovir alafenamide/Emtricitabine	18 (39)	
Elvitegravir/Tenofovir alafenamide/Emtricitabine/Cobicistat	6 (13)	
Dolutegravir/Lamivudine	3 (7)	[5, (10)]
Darunavir/Tenofovir alafenamide/Emtricitabine/Cobicistat	3 (7)	
Other	11 (24)	
Antiretroviral therapy, no. (%):		
Long-acting regimen		
CAB-RPV q4w	2 (4)	
CAB-RPV q8w	44 (96)	
Followed oral lead-in period	38 (83)	
Number of comedications, no. (%):		
0	15 (33)	
1	10 (22)	
2	3 (7)	
3	5 (10)	[4, (9)]
4	1 (2)	
≥5	8 (17)	

CKD: Chronic Kidney Disease; CL_{CR}: Creatinine Clearance; eGFR: estimated Glomerular Filtration Rate; AST: aspartate aminotransferase; ALT: alanine aminotransferase; q4w: every 4 weeks; q8w: every 8 weeks. [a] CL_{CR} calculated according to the Cockcroft and Gault equation [25]. [b] eGFR calculated according to the CKD-EPI equations reported by Levey et al. [26]. Note that some PLWH were recently enrolled in the SHCS, while four PLWH are in the SHCS process enrolment. Therefore, much of the data for these individuals are not yet available at this time.

3.2. Adverse Events

Table 2 presents the main categories of reported adverse events.

Table 2. Main categories of reported adverse events.

Adverse Events Categories	Number Reported in the TDM Request Forms (%) (n = 91)	Number of PLWH (%) (n = 46)
No adverse events, no. (%)	67 (74%)	32 (70%)
Any adverse event, no. (%)	20 (22%)	14 (30%)
Injection site reaction [a]	11 (12%)	8 (17%)
Pyrexia [b]	1 (1%)	1 (2%)
Fatigue [c]	5 (5%)	4 (9%)
Headache	3 (3%)	2 (4%)
Musculoskeletal pain [d]	5 (5%)	4 (9%)
Gastrointestinal disorders [e]	2 (2%)	2 (4%)
Sleep disorders [f]	2 (2%)	2 (4%)
Missing data	4 (4%)	-

[a] Includes pain/discomfort, nodules, induration, swelling, erythema, pruritis, bruising, discoloration, warmth, hematoma. [b] Includes pyrexia, feeling hot, chills, influenza-like illness, body temperature increased. [c] Includes fatigue, malaise, asthenia. [d] Includes musculoskeletal pain, musculoskeletal discomfort, back pain, myalgia, pain in extremity. [e] Includes nausea, dizziness, diarrhea.[f] Includes insomnia, poor quality sleep, somnolence.

The most common recorded adverse events were injection-site reactions (12%), reported in eight PLWH (17%). Most people did not report any side effects (70%, 32 PLWH), while seven individuals (15%) reported multiple adverse events.

3.3. Pharmacokinetics

Overall, 91 samples, of which 61 were collected during the long-acting dosing interval, were obtained from the 46 PLWH so far enrolled in the study. Thirty samples were obtained during or at the end of the oral lead-in period. Figure 1 shows the concentrations observed up to now, compared to usual ranges (approximated for illustrative purposes) reported in clinical trials [8,28–31].

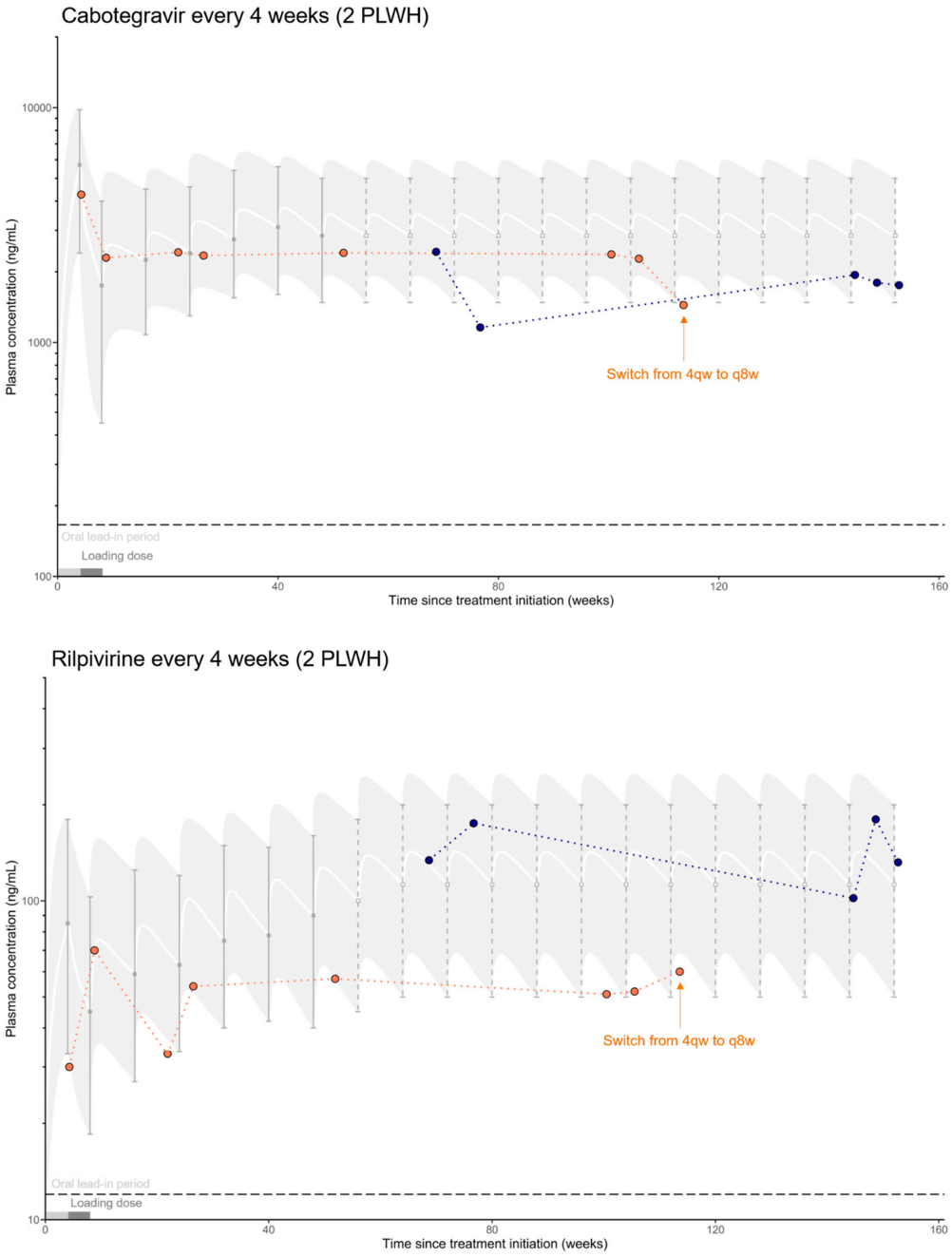

Figure 1. *Cont.*

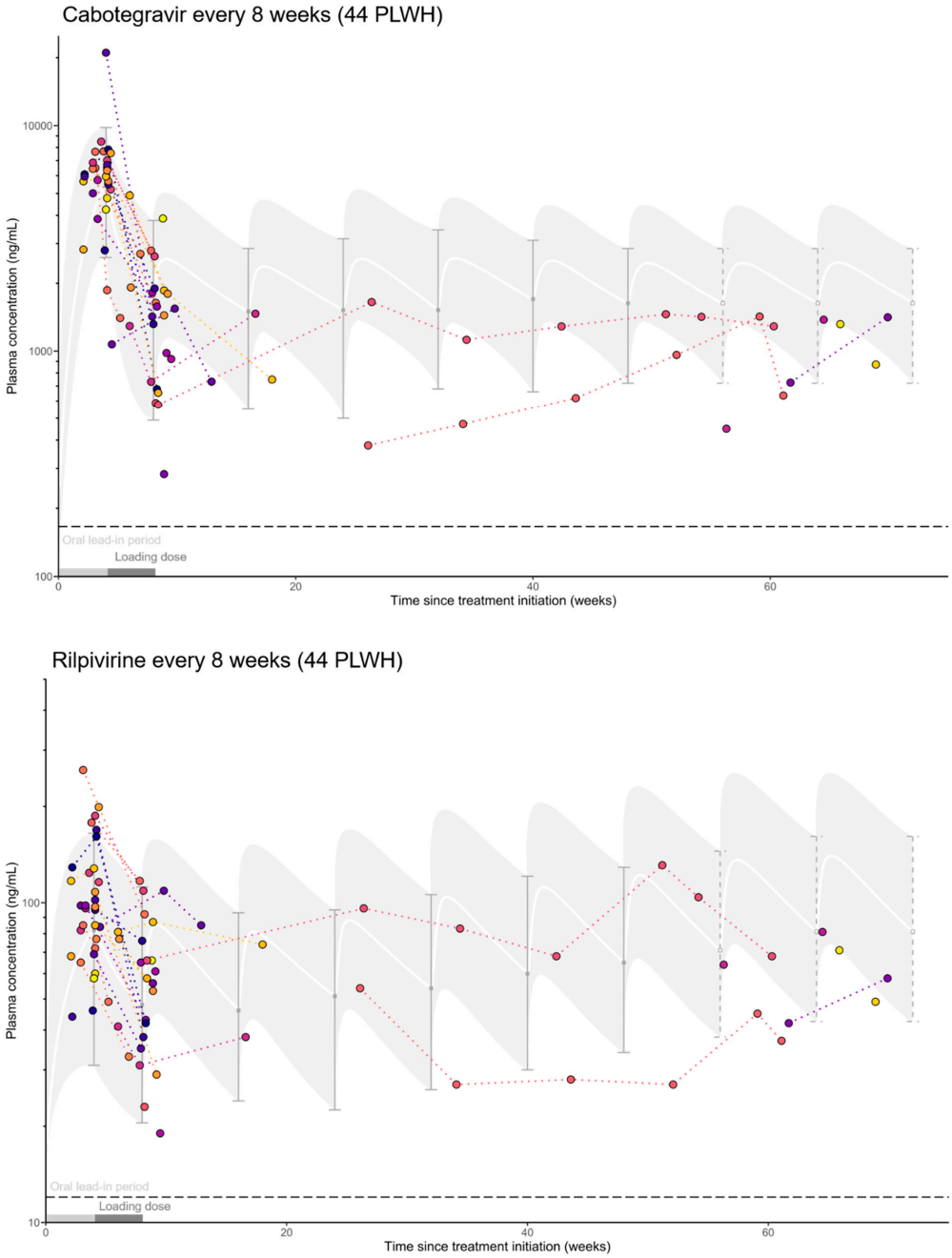

Figure 1. Observed plasma concentrations for the different dosing regimen of CAB and RPV, along with usual concentration ranges, approximated for illustrative purposes, from the ATLAS-2M trial shown as median profile and 5% and 95% percentiles [8]. Ranges are prolonged beyond 48 weeks for CAB as PK steady-state is reached after 44 weeks (dashed intervals) [29]. For RPV, 80% of the PK steady-state is achieved after 52 weeks [30], so the data were extrapolated accordingly, and showed accordance with the results of the FLAIR trial [28]. For visual purposes, dotted lines connect drug levels measurements (different color of dots for each PLWH) in the same PLWH. The horizontal dashed lines represent the protein-adjusted inhibitory concentration required for 90% inhibition ($PAIC_{90}$). $PAIC_{90}$ values are 166 ng/mL for CAB [32], and 12 ng/mL for RPV [33]. The oral lead-in period followed by the loading dose period are indicated, prior to the initiation of maintenance therapy. Finally, because concentrations from ATLAS-2M were obtained in patients who underwent a 4-week oral lead-in period, data from individuals included in this present study who started directly with injections were shifted accordingly to match the *x*-axis. PLWH: people living with HIV; q4w: every 4 weeks; q8w: every 8 weeks.

Observed concentrations confirm the hypothesis of an inter-individual variability much larger than the within-patient variability for both CAB (101% vs. 50%, $p = 0.002$) and RPV (94% vs. 27%, $p < 0.0001$). The concentrations observed are globally in accordance with the ranges already reported in the literature. However, low RPV concentrations at approximately two times the $PAIC_{90}$ were observed in six individuals (13%). One patient (receiving CAB/RPV q8w, in orange) showed a surprisingly rapid concentration decrease during the follow-up injection, without identified cause. This patient's medical records containing historic TDM results performed during its previous oral therapy indicated adequate exposure to bictegravir, also a substrate of CYP3A and UGT1A1, as are rilpivirine and cabotegravir, respectively [34]. On the other hand, this individual is young and athletic and was injecting anabolic steroids before starting LAI-CAB/RPV treatment, which might suggest undisclosed exposure to an interacting treatment. Physical activity could also result in greater absorption and, therefore, faster elimination [3]. Overall, the majority of the blood samples were collected at or close to C_{min} (85%, 77 samples). Notably, seven samples (8%) were collected between 9 and 10 weeks after the last drug administration.

4. Discussion

The population included so far in the SHCS#879 project is relatively healthy and, therefore, similar to the population observed in clinical trials. However, significant PK variability is already observed, which confirms an important prerequisite for the rational development of a TDM strategy. In particular, some RPV levels only reached about two times the reported $PAIC_{90}$ of 12 ng/mL. Such low levels of circulating RPV could be of concern in terms of efficacy and safety. In clinical practice, a minimum plasma concentration of 50 ng/mL is sometimes recommended [35,36]. Some authors even conclude that higher plasma levels should be targeted [37]. In our study, one individual had not only low levels of RPV but also low CAB for several weeks and showed a surprisingly rapid decrease over one injection interval. Various hypotheses were considered, and a preliminary investigation revealed that this individual was presumably not a rapid metabolizer of CYP3A and/or UGT1A1, which could have explained the abnormally low plasma drug levels. Despite the lack of definite clinical evidence [38–40], long-lasting physiologic or inductive effects resulting from previous or reiterated use of anabolic steroids, such as an increased intrinsic organ clearance or increased metabolic activity may last for weeks to months, and could explain, to some extent at least, the observations. In addition, depending on the type of steroid-conjugated fatty acid used, a slower release from the injected depot could also have contributed to sustained physiologic or metabolic effects [38]. Eventually, nearly a year after the start of the treatment, RPV and CAB concentrations reached levels within the reported ranges. Although the timing may be quite revealing, further investigation is needed to clearly establish the causal relationship. This case nevertheless highlights the potential importance of TDM to prevent under- or over-exposure that could lead to therapeutic failure or toxicity, respectively. In addition to the standard monitoring of viral suppression and CD4 counts, TDM might become advised for ensuring optimal therapeutic efficacy. Note that due to the small number of patients included at this time, it is difficult to determine whether lower drug levels could cause viral blips.

The initial stage of the implementation of LAI-CAB/RPV in Switzerland has already provided clinically useful information for improved patient management. In particular, at the Lausanne center, the oral lead-in period has been reduced to only 3 weeks as the oral steady-state is largely achieved after 21 days, and drug tolerability is certainly assessed. The remnant tablets spared from week 4 are then available to complete the regimen in case patients would miss or are unable to attend a scheduled i.m. appointment. On another note, it appears that CAB injection is less painful than RPV injection. It is, therefore, preferable to inject CAB first for the comfort of the patient. This recommendation is not included in the official monographs but could have an impact on the long-term acceptability of these treatments. Indeed, one of the main limitations associated with these drugs is the large volumes injected, which can be painful and for which there is currently no

alternative. Various formulations are currently being developed to address this issue and may eventually allow for longer administration intervals [41–43].

On another note, the majority of samples were, expectedly, collected at or close to C_{min}, usually at the end of the optional oral lead-in period, just prior to the loading dose, and then one month later, just prior to the first injection for the maintenance regimen. It is indeed more convenient for healthcare professionals to perform blood sampling just before the next injection. The patient is then asked to come only on the days when the drugs are to be administered, i.e., every 2 months. It might be convenient sometimes, however, to collect TDM samples at random times during the injection interval. When sufficient data are available, popPK models will be developed for CAB and RPV using parametric non-linear mixed effect modeling and validated by comparing the inferred PK-models predictions with actual LAI-ART C_{min} measured in patients. This clinical validation will also indicate whether an intervention based on TDM might improve antivirals plasma exposure in patients on LAI-ART, thereby giving indications on the potential suitability of altering the LAI-ART dosing schedule by shortening or extending dosing intervals in selected patients exhibiting lower or higher C_{min}, respectively. Considering the timely implication of LAI-ARTs in the management of HIV, the development of popPK models will help improve the implementation of a clinically-appropriate TDM for these new drugs in real-life situations.

As these are preliminary results from the implementation of LAI-CAB/RPV in Switzerland, only limited data are available at this time. As described above, physicians are at present selecting PLWH who have been consistently adherent to antiretroviral therapy. In addition, the organization, staff, and infrastructure are currently evolving to accommodate the new paradigm represented by these novel approaches. These issues limit, to some extent, the ability to enroll patients at this time. We ultimately aim at including 200–300 PLWH over the next two years, with at least five samples collected per person, thus reaching a total of more than 1000 blood samples. Our translational research collaboration encompasses state-of-the-art mass spectrometry assays, access to institutional genetic platforms, prospective capture of PK, pharmacodynamic, genetic, metabolic markers and clinical data, modeling and simulation capabilities, and clinical expertise in TDM. This setting, therefore, offers a unique opportunity for contributing to the short- and long-term optimization of LAI-ARTs at the individual patient level.

Author Contributions: Conceptualization, P.T., L.A.D. and T.B.; methodology, P.T., S.A.S., F.S. and L.A.D.; validation, L.A.D., M.C. and T.B.; formal analysis, P.T.; investigation, A.M., M.C., D.B., B.S., P.U., M.S. and P.T.; data curation, K.K.; writing—original draft preparation, P.T.; writing—review and editing, M.G., P.A., A.M., M.C., T.B., L.A.D., D.B., H.F.G., B.S., H.F., A.R., P.U., A.C., C.M., M.S. and M.B.; visualization, P.T., M.G., T.B. and P.A.; supervision, T.B. and L.A.D.; project administration, L.A.D.; funding acquisition, L.A.D. The Swiss HIV Cohort Study provided the framework of the study. All authors have read and agreed to the published version of the manuscript.

Funding: This work was supported by the Swiss National Science Foundation, grant number N° 324730_192449 (to L.A.D.).

Institutional Review Board Statement: The study was conducted in accordance with the Declaration of Helsinki, and approved by the Institutional Scientific Board of the Swiss HIV Cohort Study (protocol 879, approved on 30 September 2021).

Informed Consent Statement: Informed consent was obtained from all subjects involved in the SHCS study.

Data Availability Statement: The data presented in this study are available on request from the corresponding author.

Acknowledgments: The authors would like to thank all PLWH who agreed to participate in the study, as well as the following persons for their invaluable help and implication in blood sample collection, as study physicians, study coordinators and study nurses: Dominique Niksch, Sylvie Umwali, Rheliana Katzensteiner, Cornelia Staehlin, Elisavet Stavropoulou, Ellen Cristina Mereles

Costa, Emily West, Emeline Gauthiez, Laurence Rochat Stettler, Malela Kalubi, Sébastien Vingerhoets, Martin Yonas, Yulia Butscheid, Johannes Nemeth, Vanessa Geib and Yvan Gosmain. In addition, the authors would like to thank Jan Meier for his help with SHCS data extraction. The members of the SHCS Scientific Board: Andri Rauch (chairperson), Marcel Stöckle, Hans Hirsch, Matthias Hoffmann, Niklaus Labhardt, Karoline Leuzinger, Catia Marzolini, Dunja Nicca, Philip Tarr, Maja Weisser, Karoline Aebi-Popp, Matthias Egger, Hansjakob Furrer, Christoph Fux, Gilles Wandeler, Alexandra Calmy, Laurent Kaiser, Begona Martinez de Tejada, Matthias Cavassini, Angela Ciuffi, Jacques Fellay, Enos Bernasconi, Patrick Schmid, Christian Kahlert, Julia Notter, Michael Huber, Roger Kouyos, Karin Metzner, Johannes Nemeth, Paolo Paioni, Huldrych Günthard (president of SHCS), Katharina Kusejko (head of data center), David Haerry (patient representative), David Jackson-Perry (patient representative).

Conflicts of Interest: D.B. received honoraria for advisory board from the companies Gilead, MSD, Pfizer, and ViiV. H.F.G. has received unrestricted research grants from Gilead Sciences; fees for data and safety monitoring board membership from Merck; consulting/advisory board membership fees from Gilead Sciences, Merck, Johnson and Johnson, Novartis, and ViiV Healthcare; and grants from the Swiss National Science Foundation, the Yvonne Vontobel Foundation and from National Institutes of Health. B.S. reports support to his institution for advisory boards and travel grants from Gilead Sciences and ViiV. The institution of H.F. received educational grants from ViiV, MSD, AbbVie, Gilead, and Sandoz paid to the institution. M.S. reports advisory board paid to his institution by Gilead, MSD, and ViiV and grant to participate at conferences paid to his institution by Gilead. A.C. received a research grant from MSD, and educational grants from Gilead, MSD, and ViiV. C.M. has received speaker honoraria from ViiV and MSD unrelated to this work. The other authors declare no conflict of interest.

References

1. Thoueille, P.; Choong, E.; Cavassini, M.; Buclin, T.; Decosterd, L.A. Long-acting antiretrovirals: A new era for the management and prevention of HIV infection. *J. Antimicrob. Chemother.* **2022**, *77*, 290–302. [CrossRef] [PubMed]
2. ViiV Healthcare. Product Monograph of Vocabria and Cabenuva. 2020. Available online: https://viivhealthcare.com/content/dam/cf-viiv/viiv-healthcare/en_GB/medicines/CABENUVA-VOCABRIA-PM-26-Mar-2021.pdf (accessed on 22 April 2022).
3. Hodge, D.; Back, D.J.; Gibbons, S.; Khoo, S.H.; Marzolini, C. Pharmacokinetics and drug–drug interactions of long-acting intramuscular cabotegravir and rilpivirine. *Clin. Pharm.* **2021**, *60*, 835–853. [CrossRef] [PubMed]
4. FDA Approves First Injectable Treatment for HIV Pre-Exposure Prevention. U.S. Food & Drug Administration, 20 December 2021. Available online: https://www.fda.gov/news-events/press-announcements/fda-approves-first-injectable-treatment-hiv-pre-exposure-prevention (accessed on 28 April 2022).
5. Margolis, D.A.; Gonzalez-Garcia, J.; Stellbrink, H.J.; Eron, J.J.; Yazdanpanah, Y.; Podzamczer, D.; Lutz, T.; Angel, J.B.; Richmond, G.J.; Clotet, B.; et al. Long-acting intramuscular cabotegravir and rilpivirine in adults with HIV-1 infection (LATTE-2): 96-week results of a randomised, open-label, phase 2b, non-inferiority trial. *Lancet* **2017**, *390*, 1499–1510. [CrossRef]
6. Orkin, C.; Arasteh, K.; Górgolas Hernández-Mora, M.; Pokrovsky, V.; Overton, E.T.; Girard, P.M.; Oka, S.; Walmsley, S.; Bettacchi, C.; Brinson, C.; et al. Long-acting cabotegravir and rilpivirine after oral induction for HIV-1 infection. *N. Engl. J. Med.* **2020**, *382*, 1124–1135. [CrossRef]
7. Swindells, S.; Andrade-Villanueva, J.F.; Richmond, G.J.; Rizzardini, G.; Baumgarten, A.; Masiá, M.; Latiff, G.; Pokrovsky, V.; Bredeek, F.; Smith, G.; et al. Long-acting cabotegravir and rilpivirine for maintenance of HIV-1 suppression. *N. Engl. J. Med.* **2020**, *382*, 1112–1123. [CrossRef]
8. Overton, E.T.; Richmond, G.; Rizzardini, G.; Jaeger, H.; Orrell, C.; Nagimova, F.; Bredeek, F.; García Deltoro, M.; Swindells, S.; Andrade-Villanueva, J.F.; et al. Long-acting cabotegravir and rilpivirine dosed every 2 months in adults with HIV-1 infection (ATLAS-2M), 48-week results: A randomised, multicentre, open-label, phase 3b, non-inferiority study. *Lancet* **2021**, *396*, 1994–2005. [CrossRef]
9. Cutrell, A.G.; Schapiro, J.M.; Perno, C.F.; Kuritzkes, D.R.; Quercia, R.; Patel, P.; Polli, J.W.; Dorey, D.; Wang, Y.; Wu, S.; et al. Exploring predictors of HIV-1 virologic failure to long-acting cabotegravir and rilpivirine: A multivariable analysis. *AIDS* **2021**, *35*, 1333–1342. [CrossRef]
10. Punyawudho, B.; Singkham, N.; Thammajaruk, N.; Dalodom, T.; Kerr, S.J.; Burger, D.M.; Ruxrungtham, K. Therapeutic drug monitoring of antiretroviral drugs in HIV-infected patients. *Expert. Rev. Clin. Pharm.* **2016**, *9*, 1583–1595. [CrossRef]
11. Neyens, M.; Crauwels, H.M.; Perez-Ruixo, J.J.; Rossenu, S. Population pharmacokinetics of the rilpivirine long-acting formulation after intramuscular dosing in healthy subjects and people living with HIV. *J. Antimicrob. Chemother.* **2021**, *76*, 3255–3262. [CrossRef]
12. Han, K.; Patel, P.; Baker, M.; Margolis, D.; Spreen, W.; Ford, S. Population pharmacokinetics of cabotegravir in healthy adult subjects and HIV-1 infected patients following administration of oral tablet and long-acting Intramuscular injection. In Proceeding of the 22nd International AIDS Conference, Amsterdam, The Netherlands, 23–27 July 2018.

13. Scherrer, A.U.; Traytel, A.; Braun, D.L.; Calmy, A.; Battegay, M.; Cavassini, M.; Furrer, H.; Schmid, P.; Bernasconi, E.; Stoeckle, M.; et al. Cohort profile update: The swiss HIV cohort study (SHCS). *Int. J. Epidemiol.* **2022**, *51*, 33j–34j. [CrossRef]
14. Swiss HIV Cohort Study. Available online: http://www.shcs.ch/ (accessed on 27 May 2022).
15. Compendium.ch. VOCABRIA Depot Susp Inj 600 mg/3 mL. Approved by Swissmedic. Available online: https://compendium.ch/product/1484015-vocabria-depot-susp-inj-600-mg-3ml (accessed on 22 April 2022).
16. Compendium.ch. REKAMBYS Depot Susp Inj 900 mg/3 mL. Approved by Swissmedic. Available online: https://compendium.ch/product/1483717-rekambys-depot-susp-inj-900-mg-3ml (accessed on 22 April 2022).
17. Surve, D.H.; Jindal, A.B. Recent advances in long-acting nanoformulations for delivery of antiretroviral drugs. *J. Control. Release* **2020**, *324*, 379–404. [CrossRef]
18. Courlet, P.; Alves Saldanha, S.; Cavassini, M.; Marzolini, C.; Choong, E.; Csajka, C.; Günthard, H.F.; André, P.; Buclin, T.; Desfontaine, V.; et al. Development and validation of a multiplex UHPLC-MS/MS assay with stable isotopic internal standards for the monitoring of the plasma concentrations of the antiretroviral drugs bictegravir, cabotegravir, doravirine, and rilpivirine in people living with HIV. *J. Mass Spectrom* **2020**, *55*, e4506. [CrossRef]
19. Colombo, S.; Beguin, A.; Telenti, A.; Biollaz, J.; Buclin, T.; Rochat, B.; Decosterd, L.A. Intracellular measurements of anti-HIV drugs indinavir, amprenavir, saquinavir, ritonavir, nelfinavir, lopinavir, atazanavir, efavirenz and nevirapine in peripheral blood mononuclear cells by liquid chromatography coupled to tandem mass spectrometry. *J. Chromatogr. B Anal. Technol. Biomed. Life Sci.* **2005**, *819*, 259–276. [CrossRef]
20. Fayet Mello, A.; Buclin, T.; Franc, C.; Colombo, S.; Cruchon, S.; Guignard, N.; Biollaz, J.; Telenti, A.; Decosterd, L.A.; Cavassini, M. Cell disposition of raltegravir and newer antiretrovirals in HIV-infected patients: High inter-individual variability in raltegravir cellular penetration. *J. Antimicrob. Chemother.* **2011**, *66*, 1573–1581. [CrossRef]
21. BD Vacutainer®CPT™ Cell Preparation Tube with Sodium Citrate for the Separation of Mononuclear Cells from Whole Blood. Becton, Dickinson and Co.: Franklin Lakes, NJ, USA. Available online: https://www.bdj.co.jp/pas/products/mekkin/1f3pro00000r5drz-att/bd-cpt-manual-362760-362761.pdf (accessed on 22 April 2022).
22. Barrett, J.S.; Labbe, L.; Pfister, M. Application and impact of population pharmacokinetics in the assessment of antiretroviral pharmacotherapy. *Clin. Pharm.* **2005**, *44*, 591–625. [CrossRef]
23. Sheiner, L.B.; Ludden, T.M. Population pharmacokinetics/dynamics. *Annu. Rev. Pharm. Toxicol.* **1992**, *32*, 185–209. [CrossRef]
24. Buclin, T.; Thoma, Y.; Widmer, N.; André, P.; Guidi, M.; Csajka, C.; Decosterd, L.A. The steps to therapeutic drug monitoring: A structured approach illustrated with imatinib. *Front. Pharm.* **2020**, *11*, 177. [CrossRef]
25. Cockcroft, D.W.; Gault, M.H. Prediction of creatinine clearance from serum creatinine. *Nephron* **1976**, *16*, 31–41. [CrossRef]
26. Levey, A.S.; Stevens, L.A.; Schmid, C.H.; Zhang, Y.L.; Castro, A.F., 3rd; Feldman, H.I.; Kusek, J.W.; Eggers, P.; Van Lente, F.; Greene, T.; et al. A new equation to estimate glomerular filtration rate. *Ann. Intern. Med.* **2009**, *150*, 604–612. [CrossRef]
27. Weir, C.B.; Jan, A. BMI Classification Percentile and Cut Off Points. In *StatPearls*; StatPearls Publishing: Treasure Island, FL, USA, 2022.
28. Orkin, C.; Oka, S.; Philibert, P.; Brinson, C.; Bassa, A.; Gusev, D.; Degen, O.; García, J.G.; Morell, E.B.; Tan, D.H.S.; et al. Long-acting cabotegravir plus rilpivirine for treatment in adults with HIV-1 infection: 96-week results of the randomised, open-label, phase 3 FLAIR study. *Lancet HIV* **2021**, *8*, e185–e196. [CrossRef]
29. University of Liverpool. Cabotegravir (IM) PK Fact Sheet. Produced February 2021. Available online: https://liverpool-hiv-hep.s3.amazonaws.com/prescribing_resources/pdfs/000/000/171/original/HIV_FactSheet_CAB_IM_2021_Feb.pdf?1632406449 (accessed on 9 May 2022).
30. University of Liverpool. Rilpivirine (IM) PK Fact Sheet. Produced February 2021. Available online: www.hiv-druginteractions.org/prescribing_resources/hiv-pk-rilpivirine-im (accessed on 9 May 2022).
31. Landovitz, R.J.; Li, S.; Grinsztejn, B.; Dawood, H.; Liu, A.Y.; Magnus, M.; Hosseinipour, M.C.; Panchia, R.; Cottle, L.; Chau, G.; et al. Safety, tolerability, and pharmacokinetics of long-acting injectable cabotegravir in low-risk HIV-uninfected individuals: HPTN 077, a phase 2a randomized controlled trial. *PLoS Med.* **2018**, *15*, e1002690. [CrossRef]
32. Margolis, D.A.; Brinson, C.C.; Smith, G.H.R.; de Vente, J.; Hagins, D.P.; Eron, J.J.; Griffith, S.K.; Clair, M.H.S.; Stevens, M.C.; Williams, P.E.; et al. Cabotegravir plus rilpivirine, once a day, after induction with cabotegravir plus nucleoside reverse transcriptase inhibitors in antiretroviral-naive adults with HIV-1 infection (LATTE): A randomised, phase 2b, dose-ranging trial. *Lancet Infect. Dis.* **2015**, *15*, 1145–1155. [CrossRef]
33. Azijn, H.; Tirry, I.; Vingerhoets, J.; de Bethune, M.P.; Kraus, G.; Boven, K.; Jochmans, D.; Van Craenenbroeck, E.; Picchio, G.; Rimsky, L.T. TMC278, a next-generation nonnucleoside reverse transcriptase inhibitor (NNRTI), active against wild-type and NNRTI-resistant HIV-1. *Antimicrob. Agents Chemother.* **2010**, *54*, 718–727. [CrossRef]
34. European Medicines Agency (EMA). BIKTARVY Film-Coated Tablets. Summary of the Product Characteristics. Available online: https://www.ema.europa.eu/en/documents/product-information/biktarvy-epar-product-information_en.pdf (accessed on 4 May 2022).
35. Aouri, M.; Barcelo, C.; Guidi, M.; Rotger, M.; Cavassini, M.; Hizrel, C.; Buclin, T.; Decosterd, L.A.; Csajka, C.; Swiss, H.I.V. Cohort Study. Population pharmacokinetics and pharmacogenetics analysis of rilpivirine in HIV-1-infected individuals. *Antimicrob. Agents Chemother.* **2017**, *61*, e00899-16. [CrossRef]

36. Yapa, H.J.A.; Moyle, G.; Else, L.; Khoo, S.; Back, D.; Karolia, Z.; Higgs, C.; Boffito, M. Pharmacokinetics (PK) of tenofovir (TFV), emtricitabine (FTC), and rilpivirine (RPV) over 10 days following drug cessation. In Proceedings of the 14th European Aids Conference, Brussels, Belgium, 16–19 October 2013.
37. Néant, N.; Solas, C.; Bouazza, N.; Lê, M.P.; Yazdanpanah, Y.; Dhiver, C.; Bregigeon, S.; Mokhtari, S.; Peytavin, G.; Tamalet, C.; et al. Concentration–response model of rilpivirine in a cohort of HIV-1-infected naive and pre-treated patients. *J. Antimicrob. Chemother.* **2019**, *74*, 1992–2002. [CrossRef]
38. de Ronde, W.; Smit, D.L. Anabolic androgenic steroid abuse in young males. *Endocr. Connect.* **2020**, *9*, R102–R111. [CrossRef]
39. Kam, P.C.; Yarrow, M. Anabolic steroid abuse: Physiological and anaesthetic considerations. *Anaesthesia* **2005**, *60*, 685–692. [CrossRef]
40. Cirrincione, L.R.; Huang, K.J. Sex and gender differences in clinical pharmacology: Implications for transgender medicine. *Clin. Pharm. Ther.* **2021**, *110*, 897–908. [CrossRef]
41. Kulkarni, T.A.; Bade, A.N.; Sillman, B.; Shetty, B.L.D.; Wojtkiewicz, M.S.; Gautam, N.; Hilaire, J.R.; Sravanam, S.; Szlachetka, A.; Lamberty, B.G.; et al. A year-long extended release nanoformulated cabotegravir prodrug. *Nat. Mater.* **2020**, *19*, 910–920. [CrossRef] [PubMed]
42. Gautam, N.; McMillan, J.M.; Kumar, D.; Bade, A.N.; Pan, Q.; Kulkarni, T.A.; Li, W.; Sillman, B.; Smith, N.A.; Shetty, B.L.D.; et al. Lipophilic nanocrystal prodrug-release defines the extended pharmacokinetic profiles of a year-long cabotegravir. *Nat. Commun.* **2021**, *12*, 3453. [CrossRef] [PubMed]
43. Hilaire, J.R.; Bade, A.N.; Sillman, B.; Gautam, N.; Herskovitz, J.; Dyavar Shetty, B.L.; Wojtkiewicz, M.S.; Szlachetka, A.; Lamberty, B.G.; Sravanam, S.; et al. Creation of a long-acting rilpivirine prodrug nanoformulation. *J. Control. Release* **2019**, *311–312*, 201–211. [CrossRef] [PubMed]

pharmaceutics

MDPI

Article

Isavuconazole Pharmacokinetics and Pharmacodynamics in Children

Hirsh Elhence [1], Kanokporn Mongkolrattanothai [1,2], Sindhu Mohandas [1,2] and Michael N. Neely [1,2,3,*]

[1] Keck School of Medicine, University of Southern California, Los Angeles, CA 90027, USA
[2] Division of Infectious Diseases, Children's Hospital Los Angeles, Los Angeles, CA 90027, USA
[3] Laboratory of Applied Pharmacokinetics and Bioinformatics, The Saban Research Institute, Children's Hospital Los Angeles, Los Angeles, CA 90027, USA
* Correspondence: mneely@chla.usc.edu; Tel.: +1-(323)-361-5047

Abstract: Isavuconazole is a broad-spectrum azole anti-fungal not yet approved in children. We conducted a retrospective, single-center review of isavuconazole use and routine therapeutic drug monitoring in pediatric patients, extracting demographic, dosing, concentration, mortality and hepatoxicity data. We constructed a nonparametric population model using Pmetrics. Of 26 patients, 19 (73%) were male. The mean (SD) age and weight were 12.7 (5.5) years and 50.9 (26.8) kg. Eighty percent received between 9.7 and 10.6 mg/kg per dose. Ten (38%) subjects had proven fungal disease and eight (31%) had probable disease, mostly with *Candida* and *Aspergillus* spp. The predicted steady-state isavuconazole concentrations in our patients were similar to previous reports in children and adults, and simulations with the proposed dosing of 10 mg/kg/dose every 8 h for 2 days followed by once daily maintenance matched effective adult exposures. Attributable mortality (5 of 11 deaths) was associated with steady-state daily AUC < 60 mg∗h/L and higher AST/ALT with trough concentrations > 5 mg/L. Neither dose nor trough alone correlated well with AUC, but AUC can be estimated with one sample 10 h after the first maintenance dose or a trough concentration, if combined with a Bayesian approach or a peak and trough without a Bayesian approach.

Keywords: isavuconazole; pediatric; pharmacokinetics; pharmacodynamics; Bayesian; therapeutic drug monitoring; fungal infection; outcomes

Citation: Elhence, H.; Mongkolrattanothai, K.; Mohandas, S.; Neely, M.N. Isavuconazole Pharmacokinetics and Pharmacodynamics in Children. *Pharmaceutics* **2023**, *15*, 75. https://doi.org/10.3390/pharmaceutics15010075

Academic Editor: Neal M. Davies

Received: 15 November 2022
Revised: 7 December 2022
Accepted: 15 December 2022
Published: 26 December 2022

1. Introduction

Invasive fungal infections (IFIs) are a major source of morbidity and mortality in immunocompromised pediatric patients. The incidence of IFI in patients with acute leukemia or post stem cell transplant varied from 15–25% in one report [1]. Of these patients, estimates of mortality are wide but significant, with 10–70% dying from IFI, depending on the patient population. The most common causes of IFIs are *Candida* species, *Aspergillus* species, and organisms from the *Mucorales* family [2]. The primary therapy for invasive *Aspergillus* in children is considered to be voriconazole, which also has activity against *Candida* and many other fungi, but complex, highly variable pharmacokinetics and significant toxicities, plus lack of activity against *Mucorales*, make alternative therapy desirable [3]. Amphotericin B has a broader spectrum of activity than voriconazole, often used empirically for anti-fungal treatment or if voriconazole is not tolerated or active, but its significant nephrotoxicity and lack of oral formulation make Amphotericin B no longer the antifungal of choice for pediatric IFIs when alternatives are available.

Isavuconazole is a triazole that was FDA approved in 2015 and shown to be non-inferior to voriconazole in treating invasive aspergillosis [4]. Isavuconazole is the only other drug in addition to Amphotericin B approved by the US FDA to treat invasive mucormycosis. In adults, isavuconazole appears to be better tolerated than voriconazole, with reduced hepatobiliary, eye, and skin disorders [4]. While isavuconazole has been approved for use in adults by the FDA, and numerous case reports and series indicate

that it is likely safe and effective in pediatric populations, it is not yet approved for use in children younger than 18 years of age.

Based on a prospective study of isavuconazole pharmacokinetics (PK) in pediatric patients receiving the drug for anti-fungal prophylaxis, a pediatric dosage regimen was proposed to match isavuconazole exposures after approved dosing in adults [5]. The proposed pediatric regimen begins with a loading dose of 10 mg/kg/dose IV/PO every 8 h on days 1 and 2, followed by 10 mg/kg once daily with a maximum dosage of 372 mg. Dosing is based on the pro-drug isavuconazonium, and 372 mg of isavuconazonium is equivalent to 200 mg of isavuconazole. We wished to verify this dosage regimen in another pediatric patient population and to explore pharmacokinetic/pharmacodynamic (PK/PD) relationships.

During the first year of isavuconazole use at our hospital, we made it standard practice to measure serum drug concentrations due to the lack of an approved pediatric dose. We now report the results of our retrospective review of those initial patients at our hospital who were prescribed oral and/or intravenous isavuconazole with available measured serum concentrations. Our goals were four-fold: (1) to summarize the usage in our population; (2) to estimate isavuconazole serum concentration-time profiles and characteristics using a population approach, comparing to adult exposures and the previous pediatric study [5]; (3) to assess for relationships between serum concentrations and both mortality and hepatotoxicity (PK/PD); and (4) to devise a maximally informative, optimized sampling regimen to measure serum isavuconazole in our pediatric patients.

2. Materials and Methods

2.1. Study Design

We conducted a retrospective review of patients at the Children's Hospital Los Angeles (CHLA). The CHLA Institutional Review Board (IRB) approved the study and extraction of data between 1 January 2019 and 31 May 2020, the period during which we routinely collected blood samples for isavuconazole therapeutic drug monitoring (TDM). The IRB waived the requirement for informed consent since we only used existing clinical data, all of which was de-identified for this project.

2.2. Subjects

We searched our hospital electronic medical record system for eligible patients identified as those who met both of the following criteria: (1) received isavuconazole as part of their standard inpatient care within the study period, and (2) underwent inpatient TDM with measured serum drug concentrations of isavuconazole. We allowed inpatients who were continuing isavuconazole therapy from the outpatient setting, but we restricted our data extraction to hospital data because we could not verify outpatient isavuconazole dosing times.

2.3. Data Collection

We searched our hospital electronic medical record system for eligible patients identified as those who met both of the following criteria: (1) received isavuconazole as part of their standard inpatient care within the study period and (2) underwent inpatient TDM with measured serum drug concentrations of isavuconazole. We allowed inpatients who were continuing isavuconazole therapy from the outpatient setting, but we restricted our data extraction to hospital data because we could not verify outpatient isavuconazole dosing times.

For each included patient, we extracted demographic, dosing, concentration, and clinical data, which we stored in an Excel spreadsheet. The dosing data included isavuconazonium dose date and time, amount, and route of administration. For intravenous doses, the standard infusion time was one hour. The concentration data included date and time of the sample and the measured isavuconazole concentration. All blood samples were obtained for routine TDM. The CHLA isavuconazole TDM protocol was to obtain a trough

concentration within one hour of the next dose. However, due to the long half-life of the drug, random times were acceptable if more convenient for patient management. Samples were to be obtained after maintenance dosing commenced. The exact number of maintenance doses prior to sampling varied but generally ranged between 3 and 7 unless the patient was already receiving isavuconazole when admitted. The therapeutic serum target in the first few days of dosing was >0.5 μg/mL, since steady state was not expected until at least one week. The ultimate steady-state concentration goal was >1 μg/mL based on the lower limit of the day 7 trough reported in the SECURE study (Supplemental Data) [4]. There was no established upper safety limit for the isavuconazole concentration.

For clinical data, we recorded underlying medical conditions, details of the fungal infection including diagnostic certainty using EORTC criteria [6], location and pathogen if identified, serum alanine transaminase (ALT), aspartate aminotransferase (AST) and mortality with attributable cause as abstracted from the medical record.

2.4. Isavuconazole Measurement

The CHLA clinical laboratory sent frozen serum to Eurofins Viracor for measurement of isavuconazole. The turn-around time was 3–5 days. Eurofins Viracor used methanol protein precipitation and a validated high-performance liquid chromatography/tandem mass spectrometry (HPLC/MS/MS) assay with deuterated isavuconazole as an internal standard. The assay linear range was 0.10–10.0 μg/mL, with intra-assay imprecision of ≤3%, and inter-assay imprecision of ≤4%. The lower limit of detection was 0.041 μg/mL. The bias of low, middle and high control samples ranged from −3% to 0%.

2.5. Population Modeling

For all data analysis and figures, we used R (4.2.1, R Core Team, Vienna, Austria), including for population modeling and simulation with the Pmetrics package [7]. To pre-process the data, we first ordered doses and concentrations by date/time for each subject. When no documented loading doses were available for a given subject and hospital admission, we assumed that the isavuconazole was carried forward from outpatient dosing prior to admission and added 6 loading doses and 7 daily maintenance doses to the beginning of the record to account for concentrations measured during the first week of admission. For these prepended doses, we used the same dose amount as recorded on admission in the medical record. We included all admissions for subjects with multiple hospitalizations within the study period. Because sampling was typically very sparse, we did not attempt to estimate interoccasion variability in model parameter values. We also recorded measured weight, AST and ALT and ordered them with respect to date/time obtained and dates/times of isavuconazole doses and concentrations. We assumed weight, AST and ALT to change linearly between measurements for a given patient. We assumed height to be unchanged during each admission.

Within Pmetrics, we used the non-parametric adaptive grid algorithm [8]. We tested increasingly complex models, starting with the simplest model comprising linear absorption (Ka) from an oral bolus compartment into a central compartment with volume V, clearance (CL), intercompartmental clearance (Q) and volume of the peripheral compartment (Vp). After finding the model with a peripheral compartment to be superior, we compared it to a model parameterized with elimination, Ke, and transfer to (KCP) and from (KPC) a peripheral compartment. For both CL and Ke models, we tested inclusion of weight normalized to a reference weight of 70 kg as an allometric multiplier, using an exponent of −0.25 for rate constants, 0.75 for clearance terms and 1.0 for volume terms. In addition to these fixed exponents, we compared models with fitted allometric exponents and age-dependent exponents as suggested by Mahmood et al. [9].

For the prediction error model, NPAG uses fixed coefficients that define a polynomial equation, which in turn defines the standard deviation of any observation, such that $SD = C_0 + C_1 * [c] + C_2 * [c]^2 + C_3 * [c]^3$, where $\{C_0, \ldots, C_3\}$ are the fixed coefficients and $[c]$ is the observed drug concentration. We set $C_0 = C_1 = 0.1$, and $C_2 = C_3 = 0$,

which is an additive and proportional error model related to the measurement. Ideally, coefficient values are determined by fitting the polynomial equation to assay validation data, but the values we chose are typical when assay validation data are unavailable. We used lambda (λ) to capture additional noise related to uncertainty in the data (e.g., small misspecifications in dose amount or dose/sample times) and model misspecification, such that individual observations were fitted by NPAG with weights of the inverse of the variance, i.e., $(\lambda + SD)^{-2}$. λ was optimized over the population.

For model selection, we were particularly interested in mean posterior prediction bias (mean weighted prediction minus observation) to evaluate the models, since we were most interested in estimating individual exposures to correlate with clinical outcomes. However, because we also wished to use the model for simulation, we evaluated the Akaike Information Criterion, population bias, population/posterior imprecision (bias-adjusted, mean weighted squared prediction minus observation) and the normalized prediction distribution error (npde) method of Comets et al. [10], using the npde package (version 3.2) for R, to which Pmetrics links. Overall, we chose the model with the best performance in the largest number of these criteria.

2.6. Use of the Population Model

We had four major objectives for the accepted model: (1) to compare the exposures in our pediatric patients to reference adult exposures reported in the package insert after approved dosing and to previously reported pediatric exposures [5]; (2) to compare simulated pediatric exposures associated with the proposed dosing of 10 mg/kg every 8 h for 2 days, followed by once daily thereafter to the reference exposures; (3) to test whether average daily trough and/or 24-h area under the time-concentration profile (AUC) were associated either with mortality or with ALT/AST as markers of toxicity; and (4) to calculate the optimal time to sample for isavuconazole measurement to best estimate AUC.

For objective 1, since published reference adult values in the package insert are at steady state, we appended an additional 20 regularly timed doses administered every 24 h to the end of each patient's data file. This permitted us to analyze their individually predicted concentration-time profiles at steady state. We used the final dose and subsequent 24-h concentration profile for these calculations. We extracted each subject's projected steady-state maximum concentration (Cmax), time to Cmax (Tmax) for oral dosing and minimum (trough) concentration. We conducted non-compartmental analyses including estimation of AUC by the trapezoidal approximation and calculation of half-life (T-half) by linear regression on the final 5 predicted concentrations. We calculated clearance by the equation CL = Dose/AUC, assuming 100% bioavailability for oral doses (reported as 98% in the Cresemba package insert). However, we did adjust the dose by a factor of 0.54 for this calculation of CL to reflect that isavuconazole is supplied as the prodrug isavuconazonium, for which 372 mg = 200 mg of active compound and 200/372 = 0.54.

For objective 2, we used the simulation function in Pmetrics and the population model to estimate the exposure after 3 weeks of daily dosing following an initial two-day loading with doses every 8 h on each of the first two days (six total loading doses). All simulated doses were 10 mg/kg. Of the 2000 simulated patients, half were oral dosing and half were intravenous. We used the mean weight in our study population (50 kg) and the SD of the weight (27 kg) for the purposes of simulating the weights. We used a mean age of 10 and SD of 8 years, limiting the range to <18 years. Pmetrics maintains all population correlations between covariates and between covariates and parameters when simulating. As above, we calculated Cmax, Tmax, trough concentration, AUC, T-half and CL from the final 24 h of each simulated profile.

For objective 3, we calculated the average daily trough concentration and AUC from each subject's individual, Bayesian-posterior predicted concentration-time profiles, with predictions at one-hour intervals. To estimate only the actual subject exposures, we omitted the trailing 20 doses we had appended to predict steady state PK profiles for objective 1 above. For the average daily AUC, we calculated the total AUC for the entire study period

for each subject, divided this number by the total time in hours and multiplied by 24 to obtain the daily average. Then, by Wilcoxon rank sum for univariate testing or multiple linear regression, we tested the associations between isavuconazole trough concentration and AUC (log transformed to satisfy assumptions of normality) vs. ALT and AST AUC, calculated in a similar manner as for isavuconazole AUC but only dividing total AST/ALT AUC by total time to generate an estimate of average ALT/AST over the study period. By multiple logistic regression, we tested the association between isavuconazole trough concentration, AUC and mortality, both crude and attributable to the IFI. For all regressions, we additionally included dose, weight, height, age and sex as possible predictors. We used the "step" function in R to test predictors by forward and backward elimination.

For Objective 4, we used our multiple-model optimal (MMopt) sampling algorithm [11]. MMopt finds any number of times at which point the possible concentration time profiles arising from the discrete support points in the population model are the most separate for a given dosage regimen. This minimizes the risk of choosing a misinformative Bayesian posterior parameter value distribution for an individual by maximizing the information content of a given sample. We used the same regimen as for Objective 2. MMopt has a number of advantages over traditional D-optimal sampling [12], in particular, that the number of samples does not have to be equal to the number of model parameters, although the risk of choosing a misinformative prior drops with increasing sample number. MMopt can also be tuned or "weighted" to maximize discrimination of a particular statistic, and in this case, we chose to minimize the risk of estimating an incorrect AUC as our statistic of choice. Because we were interested in informing clinical practice, we tested only a single MMopt sample obtained in the 24-h window after the first maintenance dose from 48 to 72 h after start of therapy. The endpoint was predicted AUC from 48 to 96 h based on simulated concentrations every hour (full AUC) compared to the Bayesian posterior AUC estimates from simulated patients with only the MMopt sample available (i.e., one isavuconazole concentration or limited AUC).

3. Results

3.1. Study Population

We identified 26 patients who met the eligibility criteria, of whom 19 (73%) were male. The mean (SD) age was 12.7 (5.5) years with a range of 10.8 months to 20.3 years. Mean weight was 50.9 (26.8) kg, range 9.3 to 116.6 kg. Of the 26, 18 (69%) had pulmonary disease. The rest of the subjects suffered from either sinus or disseminated infections. Based on EORTC criteria, 10 (38%) subjects had proven disease: five were *Candida* species (one each for albicans, tropicalis, krusei, glabrata, and parapsilosis), one *Rhizomucor pusillus*, one *Absidia* sp., one mixed *Aspergillus fumigatus* and *A. terreus* and two *Mucorales* sp. Based on positive galactomannan with compatible radiographic findings in an immunocompromised host, an additional 8 (31%) had probable disease. The final 8 (31%) had possible disease. The underlying diagnosis was leukemia or lymphoma for 22 (79%) of the patients.

3.2. Therapeutic Characteristics

There were 8 episodes in 7 patients that required pre-pended doses due to outpatient dosing prior to admission. Only one patient had pre-pended doses for the first episode, i.e., the other 6 patients started isavuconazole in the hospital during a study period, were discharged and had at least one subsequent occasion/readmission while still taking isavuconazole. A median of 12 isavuconazole doses were modeled per subject, ranging from 6 to 65. Of 455 isavuconazole doses in the data, 152 (33%) were oral. For both routes of administration, 176 (39%) doses were capped at the adult dose of 372 mg in 17 (65%) of the 26 subjects. Among the subjects who received doses less than 372 mg, the mean dose was 9.8 mg/kg, with 80% between 9.7 and 10.6 mg/kg and a range between 5.9 and 11.3 mg/kg.

One sample was obtained from 18 of the subjects, two samples from three subjects, three samples from two subjects, and four to six samples from one subject each. The median

time of sampling was 17.9 h after the previous dose, with 29 (64%) of the 45 samples as trough concentrations obtained between 20 and 25 h post-dose. The full distribution of post-dose sample times is shown in Figure 1. The median trough concentration was 3.0 mg/L, ranging between 0.9 and 10.0 mg/L. The median concentration obtained within five hours after the dose (roughly a peak for oral) was 3.8 mg/L, range 3.1 to 5.6 mg/L. Note that the median peak and trough were similar, reflecting the very long half-life. Furthermore, most patients did not have early concentrations, so the range of trough concentrations was greater than the peak.

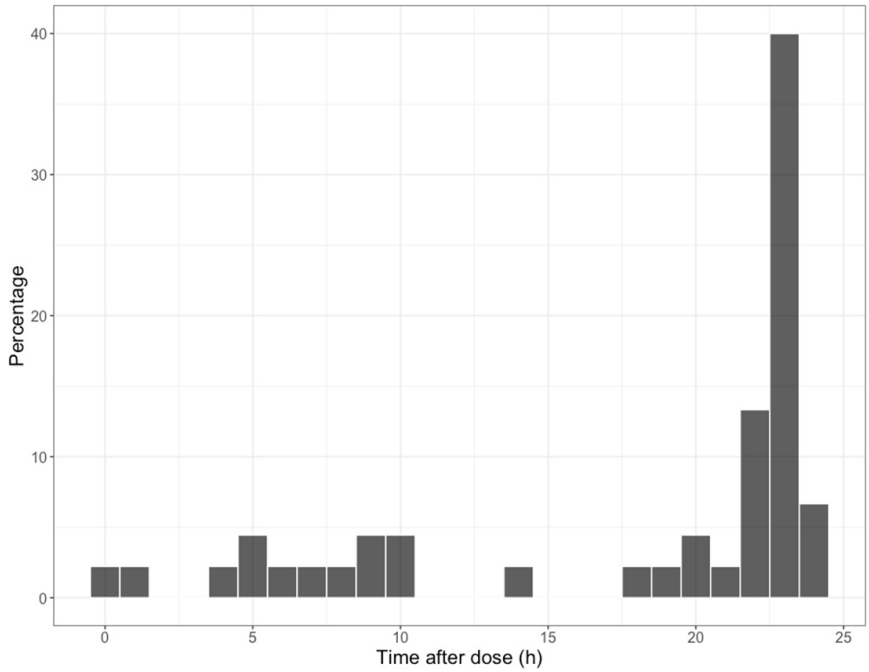

Figure 1. Distribution of blood sampling times after prior isavuconazole dose in the population. The majority were trough concentrations near the end of the dosing interval (24 h).

3.3. Model Fit

Starting with models parameterized with clearance, the best model had orally administered drug transferring from the depot compartment with a fractional absorption rate constant (Ka) to the central compartment with volume V, clearance (CL) and distribution to and from (Q), a peripheral compartment with volume Vp. Models with delayed or fixed absorption or bioavailability increased the prediction bias and decreased the likelihood, so we discarded them. Fitting the allometric exponent for weight normalized to 70 kg on CL resulted in a mean value of 0.72, very close to the theoretical value of 0.75. The age-dependent fixed exponents were not better than the theoretical value of 0.75. Therefore, we retained the constant 0.75 model. However, re-parameterizing the CL model with rate constants resulted in improved likelihood and reduced prediction bias. Therefore, our final model had drug eliminated from the central compartment (Ke) and transferred to (KCP) and from (KPC) the peripheral compartment. Weight was normalized to 70 kg and scaled to each transfer rate with a fixed exponent of −0.25. Normalized weight was scaled to V by a fixed exponent of 1.

Summaries of the final model parameters are shown in Table 1. The discrete marginal distributions and final support points for the model parameters are shown in Supplemental Figure S1 and Table S1, and observed vs. predicted plots are shown in Figure 2. The npde plot is shown in Supplemental Figure S2.

Table 1. Population parameter value summaries. Ka, absorption; KCP0, distribution from central to peripheral compartment; Ke0, elimination from central compartment; KPC0, distribution from peripheral to central compartment; V0, volume of the central compartment.

Parameter	Median (95% CI)	Range	Shrinkage
Ka (h^{-1})	12.00 (0.03–12.00)	0.01–12.00	48%
KCP0 (h^{-1})	2.42 (0.14–4.39)	0.10–6.38	41%
Ke0 (h^{-1})	0.10 (0.05–0.12)	1.52×10^{-05}–0.12	40%
KPC0 (h^{-1})	0.51 (0.13–1.34)	0.03–5.00	57%
V0 (L)	45.50 (37.27–53.92)	24.58–73.32	45%

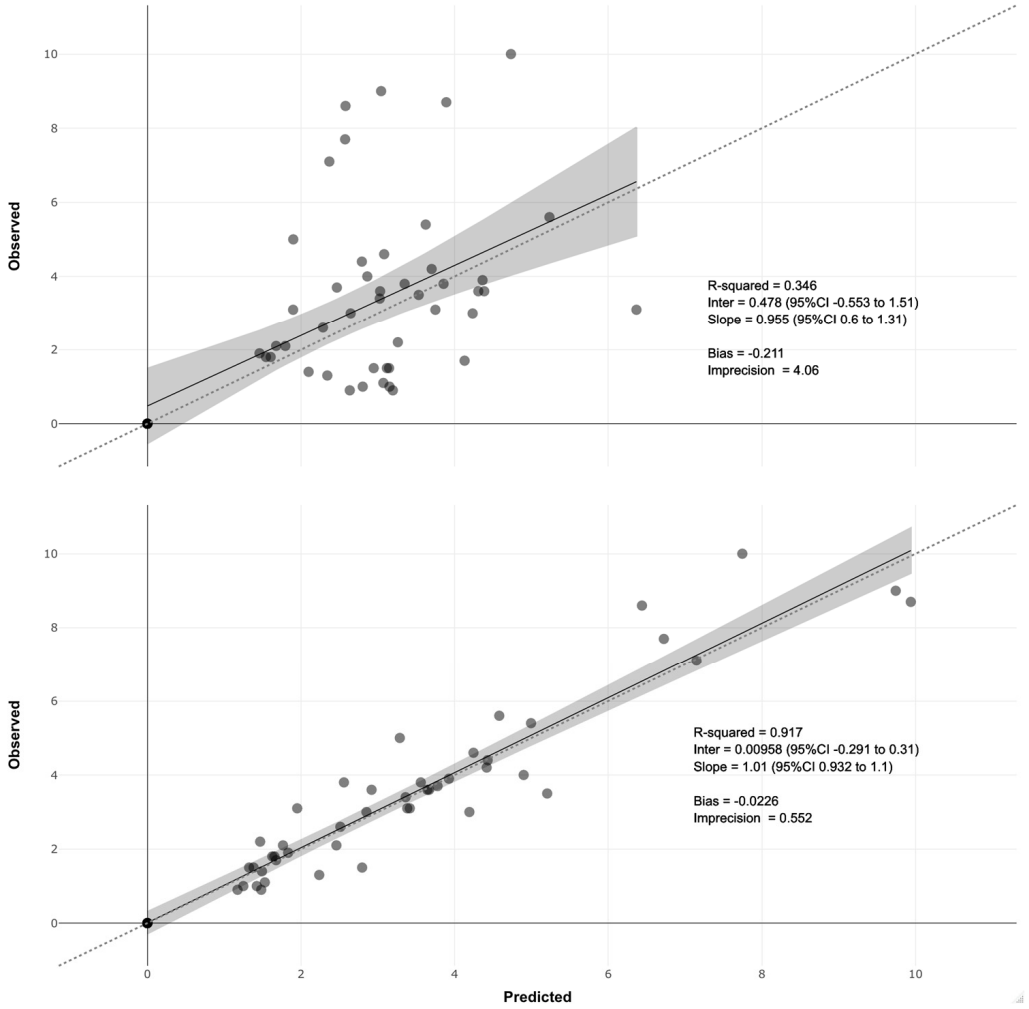

Figure 2. Observed vs. predicted plots. Predictions are based on population median parameter values in the top plot and posterior medians in the bottom plot. Bias is mean weighted prediction error, and imprecision is mean, bias-adjusted, weighted squared error. Dotted lines are identity with slope of 1 and intercept of 0. Shaded regions are 95% CI around the solid mean regression lines.

Overall, while there was considerable variability in the parameter values, based on an excellent R^2 for the posterior predictions with low bias and regression slope of close to one for both population and posterior predictions, npde in good agreement with expected distribution and moderate parameter shrinkage, we felt confident in the model to estimate individual exposures and to simulate expected exposures.

3.4. Objective 1: Steady State Pediatric Exposures Compared to Adult Benchmarks

Projected steady-state non-compartmental PK parameters in our population, given their individual dosing and body weight, and a comparison with adult values are shown in Table 2.

Table 2. Comparison between steady-state pharmacokinetic characteristics in the current study population with reference values, arranged by dosing route (IV with white and Oral with grey background). Letters correspond to Objective, but rows are arranged to facilitate comparison between individual steady state (Objective 1), simulated steady state (Objective 2), and a previously reported external dataset of pediatric patients [5]. All rows are pediatric except for Row G. Rows A, B: Projected steady state in the current study population. Except for Row G, all data are presented as median (95% ile). Rows C, D: Steady state in simulated pediatric patients with 10 mg/kg loading every 8 h on days 1 and 2, followed by a week of daily dosing. Rows E, F: Weighted median (range) in pediatric patients extracted from Table 2 in Arrieta et al. [5] by taking the weighted median across age groups. Row G: geometric mean values from the Cresemba package insert.

	Population (N)	Route	Cmax (mg/L)	Tmax (h)	Thalf (h)	AUC (mg∗h/L)	CL (L/h)
A	Current (26) (Objective 1)	IV	5.9 (4.2–18.6)	–	49.5 (8.8–2767)	70.8 (41.4–336.0)	1.6 (0.3–4.8)
C	Simulated (1000) (Objective 2)	IV	8.8 (5.8–29.1)	–	42.1 (7.9–1959.3)	115.9 (65.0–639.6)	1.7 (0.3–3.1)
E	External (45)	IV	6.6 (3.44–9.96)	–	NR	86.3 (43.0–179.0)	NR
B	Current (26) (Objective 1)	Oral	6.0 (4.0–14.6)	2.0 (0–9)	44.7 (8.7–3183)	107.3 (70.1–295.0)	1.4 (0.5–2.3)
D	Simulated (1000) (Objective 2)	Oral	6.8 (4.0–22.8)	1.0 (1.0–7.0)	37.4 (7.8–1857.2)	112.8 (62.0–532.8)	1.7 (0.4–3.2)
F	External (45)	Oral	5.6 (2.0–8.9)	4.0 (2.0–8.0)	NR	97.7 (37.6–185)	NR
G	Adult (37)	Oral	7.4	3	130	121	2

Overall, there was good agreement between pediatric and adult exposures, as summarized by Cmax, Tmax and AUC, with slightly higher median Cmax and AUC in adults. The half-life appeared to be somewhat shorter in children, but clearance was lower, implying by the relationship $t_{half} = \frac{\ln(2)}{CL} * V$ that volume of distribution was smaller in the children. Indeed, we estimated median volume at steady state (V_{ss}) to be 115 L, compared to a mean V_{ss} of 450 L in adults reported in the Cresemba package insert.

The full distributions of projected steady-state trough concentrations and AUCs are shown in Figure 3. Overall, the trough concentrations and the AUCs for children were within adult ranges, but on the lower end. Figure 4 shows the lack of relationship between isavuconazonium dose in mg/kg and average daily AUC and a marginal linear relationship between isavuconazole trough concentration and AUC. The variability around the linear regression between trough concentration and AUC was wide, such that the AUC 95% prediction interval for the median study population trough concentration of 3 mg/L was 77 to 163 mg∗h/L, more than a two-fold difference.

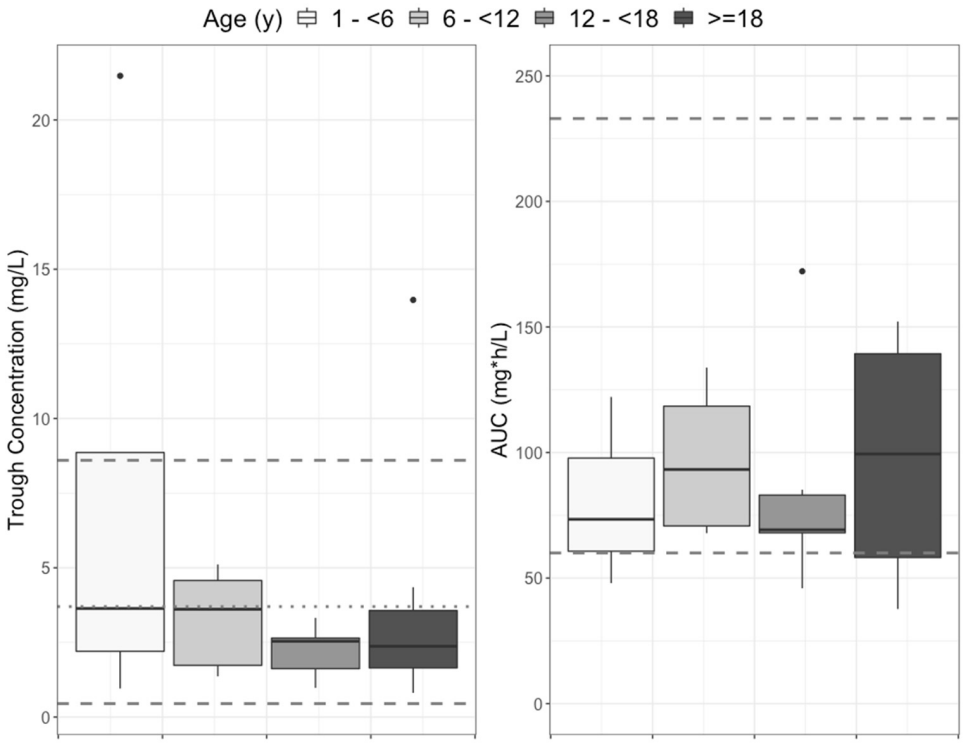

Figure 3. Distribution of projected steady-state trough concentrations (**left**) and 24-h AUC (**right**) in the current study population. For trough concentrations, dashed lines are the ranges (0.45 and 8.6 mg/L) and the dotted line is the median (3.7 mg/L) of the assumed steady state for adults, based on concentrations measured on day 14 in the SECURE study (included in their published Supplemental Data) [4]. For AUCs, the upper dashed line (233 mg∗h/L) is the minimum adult AUC in a high-dose isavuconazole study with increased toxicity, used as an upper threshold by Arietta et al. [5]. The lower dashed line (60 mg∗h/L) is the 25th percentile for adults in the SECURE study, again used by Arrieta et al. as the lower target in their pediatric study. The horizontal solid line in each box is the median, the upper and lower box margins are the interquartile range (IQR, 25th and 75th percentiles), the whiskers extend to 1.5× IQR, and points are outliers.

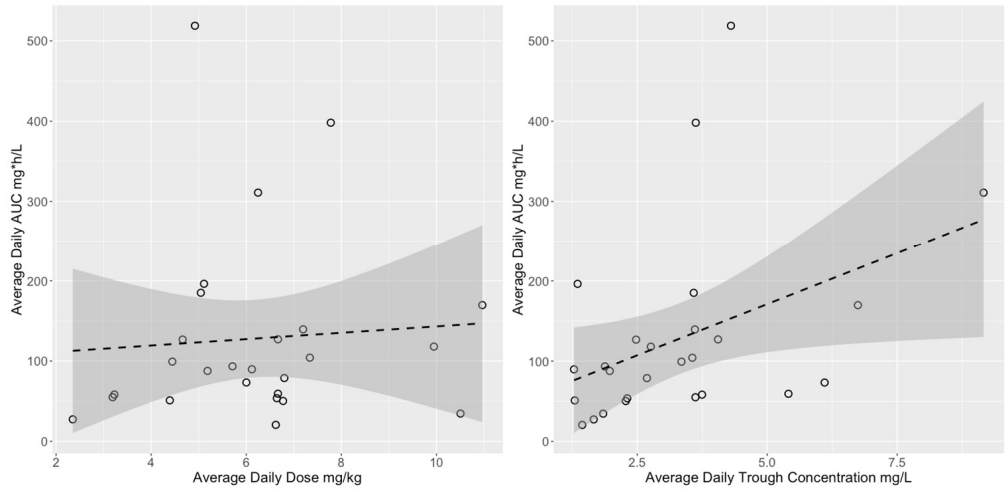

Figure 4. Relationship between average daily isavuconazole AUC and dose (**left**) or trough concentration (**right**). Dashed line is the linear regression and shaded area is the 95% confidence interval. Regression statistics for the dose were slope = 0.35, $p = 0.73$, $R^2 = 0.004$. For the trough concentration they were slope = 25.5, $p = 0.04$, $R^2 = 0.13$.

3.5. Objective 2: Simulated Pediatric Exposures from 10 mg/kg Dosing Compared to Adult Benchmarks

Table 2 includes a comparison between adult values compared with distributions in 2000 simulated pediatric patients. Dosing for the simulated patients was 10 mg/kg IV or oral, 3 times daily for two days, followed by a week of once-daily dosing. Doses were capped at the adult dose of 372 mg in accordance with the proposed regimen [5] and likely typical clinical practice. Median (range) simulated weights and ages were 47.3 (10.6–77.3) kg and 10.2 (2.2–17.2) years, with the same correlation as the study population between weight and age and between these covariates and the model parameters. As for the projected steady state metrics in our study population, overall, there was good agreement between simulated pediatric and adult exposures. Again, half-life was shorter in children.

The distributions of simulated steady-state trough concentration and AUC are shown in Figure 5. Overall, the simulated steady-state trough concentrations and AUCs for children were within adult ranges but on the lower end.

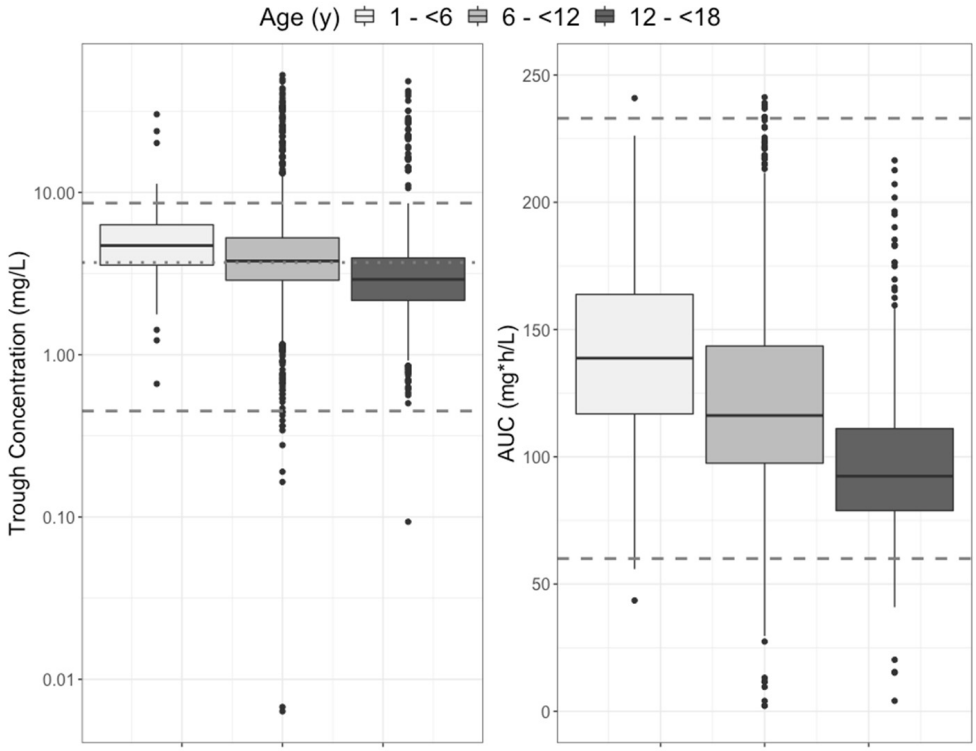

Figure 5. Distribution of steady-state trough concentrations (**left**) and 24-h AUC (**right**) in 1000 simulated patients administered isavuconazole 10 mg/kg/dose IV q8h on the first two days and then daily for a week. Reference lines are the same as for Error! Reference source not found.

3.6. Objective 3: PK/PD Relationships

3.6.1. Mortality

Of the 11 deaths in the study population, five could be attributed at least partially to their IFI (3 proven, 2 probable), and for the remaining six, it was uncertain if the IFI (2 proven, 2 probable, 2 possible) contributed to mortality. Among all patients who died (crude mortality), there was no clear relationship between death and average daily isavuconazole trough, AUC, or AUC > 91.58 mg∗h/L, which was the population median, as shown in Table 3, top half.

However, when considering mortality attributed to the IFI vs. those who survived or died from causes other than an IFI, average daily AUC was lower in those with attributed mortality, and all the patients who succumbed to their IFI had an average daily AUC < 91.58 mg∗h/L (Table 3, bottom half). By univariate analysis, median AUC

was higher in those without attributed mortality vs. those with attributed mortality (104.2 vs. 53.7, $p = 0.034$, Wilcoxon rank sum), as shown in Figure 6. Further multivariate logistic regression analysis with forward/backward elimination to predict attributed mortality identified only average daily AUC ($p = 0.058$) as a borderline significant predictor controlling for weight, age, trough concentration and dose. Although trough concentration was not a significant predictor of attributable mortality, average daily steady-state trough concentration did tend to be lower in this group. All of the four patients with a steady state daily AUC of <60 mg∗h/L (the lower threshold used by Arietta et al. [5]) had average daily steady-state trough concentrations < 2 mg/L, although 2 of the 5 with attributed mortality were above this trough threshold.

Table 3. Relationship between isavuconazole exposures and survival outcomes. Trough and AUC are within-patient average daily values. The AUC threshold of 91.58 mg∗h/L is the population median. Mortality is considered in two ways: crude (top section), and mortality attributed by treating clinicians to the invasive fungal infection (bottom section).

	Survived (*n* = 15)	**Died (*n* = 11)**	***p*-Value (Test)**
Trough (mg/L)	3.6 (1.9–6.5)	2.3 (1.2–8.2)	0.10 (Wilcox)
AUC (mg∗h/L)	93.4 (40.1–476.6)	89.8 (22.2–282.3)	0.38 (Wilcox)
AUC > 91.58	8 (53%)	5 (45%)	1 (Fisher)
	Non-attributed mortality or survived (*n* = 21)	Attributed mortality (*n* = 5)	
Trough	3.6 (1.4–7.9)	1.7 (1.3–5.1)	0.09 (Wilcox)
AUC	104.2 (27.5–458.5)	53.7 (29.7–86.7)	0.03 (Wilcox)
AUC > 91.58	13 (62%)	0 (0%)	0.04 (Fisher)

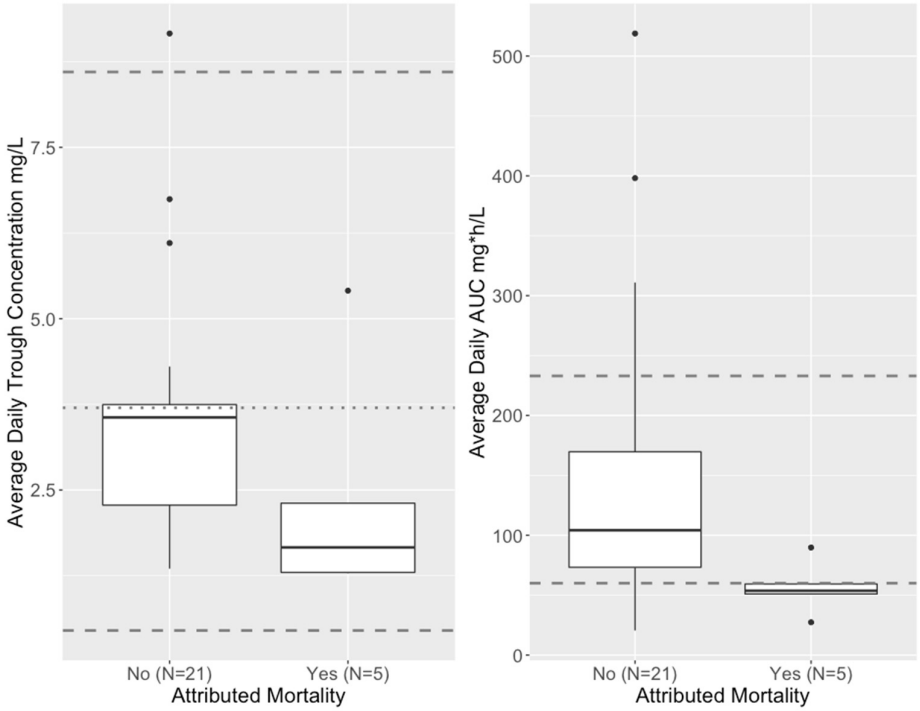

Figure 6. Distribution of isavuconazole average daily trough concentrations (**left**) and AUCs (**right**) in subjects who either survived or were not considered to have died from their IFI (attributed mortality = NO) vs. those who were considered to have died from their IFI (Attributed Mortality = YES). The same adult reference concentrations as for Table 2 are indicated by horizontal dashed lines. The median trough concentrations were 3.6 vs. 1.6, $p = 0.09$ (Wilcoxon rank sum) and median AUCs were 104.2 vs. 53.7, $p = 0.03$, Wilcoxon rank sum.

3.6.2. Hepatotoxicity

Average AST and ALT were commonly elevated above 40 IU (AST: n = 14, 54%; ALT: n = 15, 58%) in this population with polypharmacy and multiple co-morbid conditions. The maximum values observed were 1144 IU and 698 IU for AST and ALT, respectively. We defined emergent hepatoxicity as either an increase to >3× upper limit normal (ULN) for those with normal baseline AST/ALT, or 3× baseline for those with baseline abnormal enzymes (>1× ULN). For both AST and ALT, 14 (54%) of the patients had elevated values at baseline. Four (15%) had emergent toxicity by AST and ALT and an additional patient by ALT only (5 total, 19%) while taking isavuconazole. Although the ALT was improving in 3 (60%) of the 5, it had not returned to baseline by the end of the study period in any subject.

By multivariate linear regression with forward and backward elimination, a mean daily isavuconazole trough > 5 mg/L was associated with higher average daily AST (p = 0.003) and ALT (p = 0.005), controlling for mean daily isavuconazole AUC and dose. By multiple logistic regression, controlling for AUC and dose, a trough of >5 mg/L was also independently associated with occurrence of treatment-emergent elevations for AST (p = 0.03) and for ALT (p = 0.05), as shown in Figure 7.

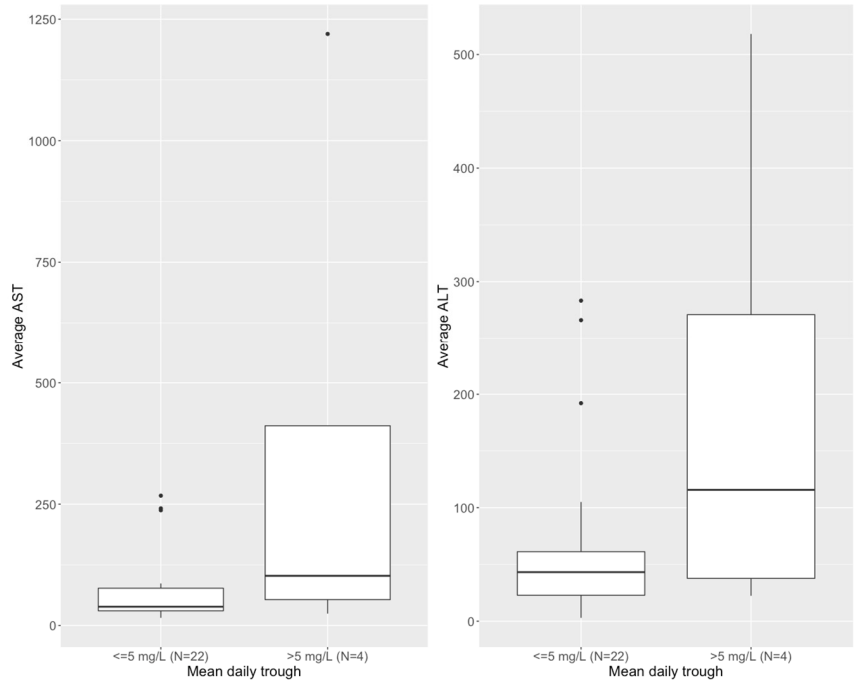

Figure 7. Distribution of average daily AST (**left**) and ALT (**right**) in study subjects, stratified by mean daily isavuconazole trough concentration.

3.7. Objective 4: Optimal Sampling

We restricted the optimal sampling window to between 48 and 72 h after start of therapy to allow for completion of all 6 loading doses and the first maintenance dose yet balance the need to assess exposure early. The single optimal sampling time for both IV and oral dosing was 58 h, i.e., 10 h after the first maintenance dose. We compared the "Full" simulated AUC from 48 to 96 h to the "Limited" AUCs calculated from the median of the Bayesian posterior parameter distributions based on the single MMopt sample in each of 200 simulated subjects (half IV dosing, half oral dosing) or based on a trough. The distributions of full vs. limited AUCs are shown in Figure 8. For IV administration, the geometric mean full AUC was 248; for MM, it was 244; and for trough, it was 229 mg∗h/L (p = 0.45, analysis of variance). For oral administration, full AUC was 225, MM was 237 and trough was 253 (p = 0.14).

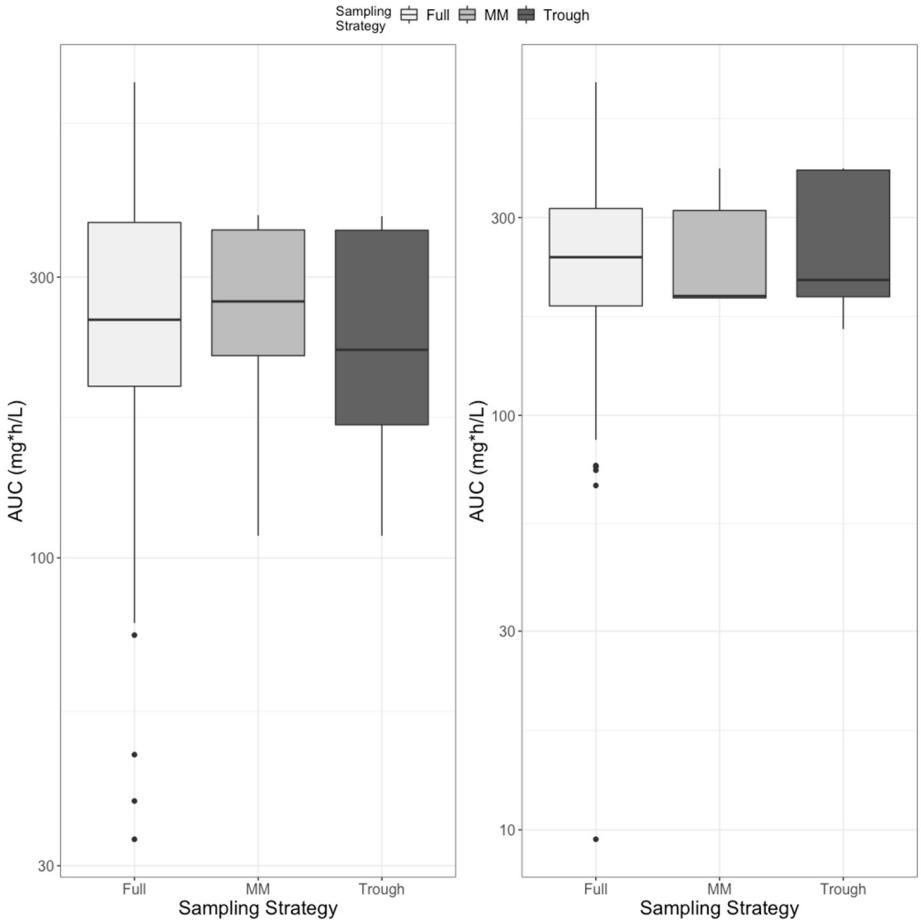

Figure 8. Distribution of AUC for IV (**left**) and oral (**right**) dosing comparing values calculated from concentrations simulated every hour (Full) or predictions from models using only a single MMopt sample (MM) at 10 h after the first maintenance dose or the trough concentration (Trough) after the first maintenance dose to generate the Bayesian posterior parameter value probability distributions.

4. Discussion

In the most comprehensive report thus far of isavuconazole PK/PD in children with possible, probable or proven invasive fungal infections (IFI), we found that the proposed dose of isavuconazonium 10 mg/kg, capped at the adult dose of 372 mg, is likely safe and effective in children, at least as an initial regimen. Our study population, who largely received this dose or close to it, had projected average steady-state trough concentrations and AUCs very similar to previously studied children given the same dose for prophylaxis [5], who in turn were very similar to adults with IFIs who were treated with isavuconazole [4]. With our population model developed from the real subjects, we demonstrated similar average exposures in a simulated population of children ranging from 2 to 18 years and 10 to 77 kg dosed according to the proposed regimen above. Nevertheless, there was considerable interpatient variability in isavuconazole concentrations.

For PK/PD relationships, we found that all 5 subjects whose deaths were attributable to their IFI had serum isavuconazole average daily AUCs below 90 mg∗h/L, and 4 of the 5 were below 60 mg∗h/L, which was a proposed lower limit in a previous pediatric study of isavuconazole PK used for prophylaxis [5]. Although the median daily trough concentration was also lower in those with IFI-attributed mortality, there was substantial heterogeneity, making it difficult to establish a threshold: three were below 2 mg/L, one was between 2 and 3 mg/L, and one was >5 mg/L on average.

A question arises whether isavuconazole trough concentrations are generally a good surrogate for AUC when AUC is the true isavuconazole target based on murine studies

of invasive candidiasis [13] and aspergillosis [14], consistent with animal studies of other azoles, as well as our own findings regarding attributable mortality. We found that while there may have been a statistically significant linear relationship between isavuconazole trough concentration and AUC, the variability around the regression line, with an R^2 value of only 0.13, forces us to conclude that isavuconazole trough concentrations do not predict AUC with enough precision to truly ensure the AUCs greater than those we found to be associated with attributed mortality. This is the same as we have found for vancomycin [15–17] and may be part of the reason why there is no clearly established trough concentration target for isavuconazole. However, we did find that when combined with our population model, a limited trough sampling strategy after the first maintenance dose predicts AUC with an accuracy that cannot be statistically distinguished from an optimally timed sample 10 h after the same dose. The similarity between trough and optimal sample is likely due to the long half-life of the drug. Nevertheless, the trough concentration only became a useful predictor of AUC when combined with a population model.

In contrast to attributable mortality, we found that the measured trough concentration was more predictive of increases in liver enzymes than AUC. There was a highly significant linear relationship between average trough concentration > 5 mg/L and either higher average AST or ALT and a borderline association with average trough concentration > 5 mg/L and emergent hepatotoxicity on treatment. Since we analyzed average trough concentration, this threshold is not meant to be one that is never exceeded but merely a suggestion that prolonged trough concentrations above this will likely increase the risk of developing some degree of enzyme elevation. As we found for voriconazole [18], many children will experience bumps in their enzymes while on azole therapy, but will regress towards or achieve baseline values without the need to stop or change therapy.

A previous secondary analysis of the relationship between isavuconazole exposure metrics and outcomes including mortality and liver enzyme elevations in adults from the SECURE study found no discernible PK/PD relationship [19]. While it is possible that the relationships we found were by chance, despite the *p*-values, given our very small population size relative to the SECURE study, there are some differences worth noting. First, we examined IFI-attributed mortality, which we believe to be more relevant in a highly co-morbid population to antifungal PK/PD rather than crude mortality as measured by Desai et al. Second, we had a higher level of liver enzyme elevation in approximately 50% of our subjects compared to their surprisingly low ~10% rate. We also estimated average AST/ALT as the area under the total concentration time profile divided by the total time, which corrects for sparse or irregular sampling, and used that as our outcome, rather than individual values. Third, the isavuconazole exposure variability (CV%) in the adult study was reported as 62%, while it was 92% based on average daily AUC in our study. This equated to a 25-fold AUC difference between the highest and lowest subjects, and the broader range may have allowed us to find PK/PD relationships not previously demonstrated. This last point has important therapeutic implications. Despite a 4.6-fold difference in dose (mg/kg) across our pediatric population, the AUC difference was much greater, and there was no correlation between dose and AUC. Clearly, the same dose, even adjusted for bodyweight, does not lead to predictable or consistent exposures in a real-world population of children with IFI.

Regarding our model, we found the best to be a central compartment with a single peripheral compartment. The prior pediatric population PK model found an additional peripheral compartment improved the predictions [5]. However, this is likely due to more intensive sampling than was available to us, and our model did not appear to suffer in its ability to predict exposures very closely in line with prior reports. On a final note about our model, there is great debate in the pharmacometric literature on whether allometric exponents should be fixed, fixed with a maturation function, fixed according to age, or fitted. We found that fitting the exponent on clearance resulted in an allometric exponent of 0.72, very close to the theoretical value of 0.75, and that age-dependent fixed values were not any better. Isavuconazole is highly bound to albumin, and it is metabolized

extensively by CYP3A4/5. For such drugs, where average CYP3A4/5 enzyme maturation is 76% of adult values by one year of age and 92% by 5 years of age (van Rongen et al., their Table 4) [20], allometry using fixed exponents without a maturation function is expected to be the preferred method of scaling (van Rongen et al., their Table 2) [20]. This is exactly what we found in our population, which had 1 subject 10.8 months, 1 subject 2.6 years old, 1 subject 3.3 years old, and the remaining 23 subjects aged 5 years and older.

The main limitation of our study is the small sample size. It was also retrospective, which means that there can be confounding factors that we were not able to control that affected outcomes, such as other contributions to mortality or to hepatoxicity. Nevertheless, despite these limitations, we believe we have shed some light on the PK/PD of isavuconazole in the pediatric population. We found that an average daily AUC of <60 mg∗h/L was associated with increased risk of mortality attributed to IFI. We also found that risk of hepatotoxicity increased with mounting isavuconazole trough concentrations and that 5 mg/L may be a reasonable threshold above which extra caution is warranted.

Finally, unlike previous conclusions in adults [19], we feel that the poor correlation between dose and serum concentrations, the wide variability of serum exposures in children, and the suggestion of exposure response relationships all merit strong consideration of optimized dosing based on measured drug concentrations in these incredibly vulnerable patients with little room for therapeutic error. As for vancomycin, AUC-guided dosing appears best for efficacy, with trough-guided dosing to avoid hepatotoxicity. Obtaining a steady-state peak concentration in addition to the trough concentration would permit estimation of AUC by fundamental PK equations, as we have outlined for vancomycin [21]. The disadvantage of this strategy is the need to wait for steady state, which is likely not until after the 5th maintenance dose (i.e., day 7 or beyond). A single steady-state trough sample of >2 mg/L may predict an AUC above a proposed lower threshold of 60 mg∗h/L [5], but we did not find either threshold to be predictive of survival. In our opinion, a better approach is to obtain either one sample 10 h after the first maintenance dose or a trough concentration combined with a Bayesian algorithm and a population model to estimate AUC, targeting a steady-state value > 100 mg∗h/L.

Supplementary Materials: The following supporting information can be downloaded at: https://www.mdpi.com/article/10.3390/pharmaceutics15010075/s1, Figure S1: Marginal probability distributions for model parameter values; Figure S2: Normalized prediction distribution error (npde); Table S1: Model support points.

Author Contributions: Conceptualization, methodology, M.N.N.; formal analysis, M.N.N. and H.E.; investigation, H.E.; data curation, K.M. and S.M.; writing—original draft preparation, M.N.N. and H.E.; writing—review and editing, all authors; supervision, M.N.N. All authors have read and agreed to the published version of the manuscript.

Funding: This research received no external funding.

Institutional Review Board Statement: Ethical review and approval were waived for this study due to use of existing, de-identified data.

Informed Consent Statement: Not applicable.

Data Availability Statement: De-identified data are available by reasonable request to corresponding author.

Conflicts of Interest: M.N. is a paid consultant to Astellas, Inc. on a separate project to assess isavuconazole use in children from national data warehouse records.

References

1. Hale, K.A.; Shaw, P.J.; Dalla-Pozza, L.; MacIntyre, C.R.; Isaacs, D.; Sorrell, T.C. Epidemiology of Paediatric Invasive Fungal Infections and a Case-Control Study of Risk Factors in Acute Leukaemia or Post Stem Cell Transplant. *Br. J. Haematol.* **2010**, *149*, 263–272. [CrossRef] [PubMed]
2. Pana, Z.D.; Roilides, E.; Warris, A.; Groll, A.H.; Zaoutis, T. Epidemiology of Invasive Fungal Disease in Children. *J. Pediatr. Infect. Dis. Soc.* **2017**, *6*, S3–S11. [CrossRef] [PubMed]

3. Hsu, A.J.; Tamma, P.D.; Fisher, B.T. Challenges in the Treatment of Invasive Aspergillosis in Immunocompromised Children. *Antimicrob. Agents Chemother.* **2022**, *66*, e0215621. [CrossRef] [PubMed]
4. Maertens, J.A.; Raad, I.I.; Marr, K.A.; Patterson, T.F.; Kontoyiannis, D.P.; Cornely, O.A.; Bow, E.J.; Rahav, G.; Neofytos, D.; Aoun, M.; et al. Isavuconazole versus Voriconazole for Primary Treatment of Invasive Mould Disease Caused by *Aspergillus* and Other Filamentous Fungi (SECURE): A Phase 3, Randomised-Controlled, Non-Inferiority Trial. *Lancet* **2016**, *387*, 760–769. [CrossRef] [PubMed]
5. Arrieta, A.C.; Neely, M.; Day, J.C.; Rheingold, S.R.; Sue, P.K.; Muller, W.J.; Danziger-Isakov, L.A.; Chu, J.; Yildirim, I.; McComsey, G.A.; et al. Safety, Tolerability, and Population Pharmacokinetics of Intravenous and Oral Isavuconazonium Sulfate in Pediatric Patients. *Antimicrob. Agents Chemother.* **2021**, *65*, e0029021. [CrossRef] [PubMed]
6. De Pauw, B.; Walsh, T.J.; Donnelly, J.P.; Stevens, D.A.; Edwards, J.E.; Calandra, T.; Pappas, P.G.; Maertens, J.; Lortholary, O.; Kauffman, C.A.; et al. Revised Definitions of Invasive Fungal Disease from the European Organization for Research and Treatment of Cancer/Invasive Fungal Infections Cooperative Group and the National Institute of Allergy and Infectious Diseases Mycoses Study Group (EORTC/MSG) Consensus Group. *Clin. Infect. Dis.* **2008**, *46*, 1813–1821. [CrossRef]
7. Neely, M.N.; van Guilder, M.G.; Yamada, W.M.; Schumitzky, A.; Jelliffe, R.W. Accurate Detection of Outliers and Subpopulations with Pmetrics, a Nonparametric and Parametric Pharmacometric Modeling and Simulation Package for R. *Ther. Drug Monit.* **2012**, *34*, 467–476. [CrossRef]
8. Yamada, W.M.; Neely, M.N.; Bartroff, J.; Bayard, D.S.; Burke, J.V.; van Guilder, M.; Jelliffe, R.W.; Kryshchenko, A.; Leary, R.; Tatarinova, T.; et al. An Algorithm for Nonparametric Estimation of a Multivariate Mixing Distribution with Applications to Population Pharmacokinetics. *Pharmaceutics* **2021**, *13*, 42. [CrossRef]
9. Mahmood, I.; Tegenge, M.A. A Comparative Study between Allometric Scaling and Physiologically Based Pharmacokinetic Modeling for the Prediction of Drug Clearance From Neonates to Adolescents. *J. Clin. Pharmacol.* **2019**, *59*, 189–197. [CrossRef]
10. Comets, E.; Brendel, K.; Mentré, F. Computing Normalised Prediction Distribution Errors to Evaluate Nonlinear Mixed-Effect Models: The Npde Add-on Package for R. *Comput. Methods Programs Biomed.* **2008**, *90*, 154–166. [CrossRef]
11. Bayard, D.S.; Neely, M. Experiment Design for Nonparametric Models Based on Minimizing Bayes Risk: Application to Voriconazole. *J. Pharmacokinet. Pharmacodyn.* **2017**, *44*, 95–111. [CrossRef]
12. D'Argenio, D.Z. Optimal Sampling Times for Pharmacokinetic Experiments. *J. Pharmacokinet. Pharmacodyn.* **1981**, *9*, 739–756. [CrossRef]
13. Lepak, A.J.; Marchillo, K.; VanHecker, J.; Diekema, D.; Andes, D.R. Isavuconazole Pharmacodynamic Target Determination for *Candida* Species in an In Vivo Murine Disseminated Candidiasis Model. *Antimicrob. Agents Chemother.* **2013**, *57*, 5642–5648. [CrossRef]
14. Lepak, A.J.; Marchillo, K.; Vanhecker, J.; Andes, D.R. Isavuconazole (BAL4815) Pharmacodynamic Target Determination in an in Vivo Murine Model of Invasive Pulmonary Aspergillosis against Wild-Type and Cyp51 Mutant Isolates of *Aspergillus* Fumigatus. *Antimicrob. Agents Chemother.* **2013**, *57*, 6284–6289. [CrossRef]
15. Lee, B.V.; Fong, G.; Bolaris, M.; Neely, M.; Minejima, E.; Kang, A.; Lee, G.; Gong, C.L. Cost-Benefit Analysis Comparing Trough, Two-Level AUC and Bayesian AUC Dosing for Vancomycin. *Clin. Microbiol. Infect.* **2021**, *27*, e1–e1346. [CrossRef]
16. Neely, M.N.; Youn, G.; Jones, B.; Jelliffe, R.W.; Drusano, G.L.; Rodvold, K.A.; Lodise, T.P. Are Vancomycin Trough Concentrations Adequate for Optimal Dosing? *Antimicrob. Agents Chemother.* **2014**, *58*, 309–316. [CrossRef]
17. Neely, M.N.; Kato, L.; Youn, G.; Kraler, L.; Bayard, D.; Van Guilder, M.; Schumitzky, A.; Yamada, W.; Jones, B.; Minejima, E. Prospective Trial on the Use of Trough Concentration versus Area under the Curve To Determine Therapeutic Vancomycin Dosing. *Antimicrob. Agents Chemother.* **2018**, *62*, e02042-17. [CrossRef]
18. Neely, M.; Rushing, T.; Kovacs, A.; Jelliffe, R.; Hoffman, J. Voriconazole Pharmacokinetics and Pharmacodynamics in Children. *Clin. Infect. Dis.* **2010**, *50*, 27–36. [CrossRef]
19. Desai, A.V.; Kovanda, L.L.; Hope, W.W.; Andes, D.; Mouton, J.W.; Kowalski, D.L.; Townsend, R.W.; Mujais, S.; Bonate, P.L. Exposure-Response Relationships for Isavuconazole in Patients with Invasive Aspergillosis and Other Filamentous Fungi. *Antimicrob. Agents Chemother.* **2017**, *61*, e01034-17. [CrossRef]
20. van Rongen, A.; Krekels, E.H.; Calvier, E.A.; de Wildt, S.N.; Vermeulen, A.; Knibbe, C.A. An Update on the Use of Allometric and Other Scaling Methods to Scale Drug Clearance in Children: Towards Decision Tables. *Expert Opin. Drug Metab. Toxicol.* **2022**, *18*, 99–113. [CrossRef]
21. Pai, M.P.; Neely, M.; Rodvold, K.A.; Lodise, T.P. Innovative Approaches to Optimizing the Delivery of Vancomycin in Individual Patients. *Adv. Drug Deliv. Rev.* **2014**, *77*, 50–57. [CrossRef] [PubMed]

pharmaceutics

MDPI

Article

Total and Unbound Pharmacokinetics of Cefiderocol in Critically Ill Patients

Noël Zahr [1,*,†], Saik Urien [2,†], Benoit Llopis [1], Gaëlle Noé [1], Nadine Tissot [1], Kevin Bihan [1], Helga Junot [3], Clémence Marin [1], Bochra Mansour [1], Charles-Edouard Luyt [4], Alexandre Bleibtreu [5] and Christian Funck-Brentano [1]

1 Pharmacokinetics and Therapeutic Drug Monitoring Unit, Department of Pharmacology, Pitié-Salpêtrière Hospital, Inserm, CIC-1901, UMR-S 1166, AP-HP Sorbonne Université, 75013 Paris, France
2 Unité de Recherche Clinique, Hôpital Necker-Enfants Malades, AP-HP, 75015 Paris, France
3 Pharmacy Department, Pitié-Salpêtrière Hospital, AP-HP Sorbonne Université, 75013 Paris, France
4 Service de Médecine Intensive Réanimation, Institut de Cardiologie, AP-HP Sorbonne-Université, Pitié-Salpêtrière Hospital, 75013 Paris, France
5 Service de Maladies Infectieuses et Tropicales, Pitié-Salpêtrière Hospital, AP-HP Sorbonne Université, 75013 Paris, France
* Correspondence: noel.zahr@aphp.fr
† These authors contributed equally to this work.

Abstract: Background: Cefiderocol is a siderophore cephalosporin antibiotic active against Gram-negative bacteria, including extended-spectrum beta-lactamase and carbapenemase-producing strains. The pharmacokinetics of cefiderocol has been studied in healthy subjects and particularly in phase II and III studies. This retrospective study investigated intravenous cefiderocol population pharmacokinetics in adult patients treated by cefiderocol. Methods: We studied 55 consecutive patients hospitalized in an intensive care unit. Cefiderocol plasma samples were obtained on different occasions during treatment. Plasma concentration was assayed using mass spectrometry. Data analysis was performed using a non-linear mixed-effect approach via Monolix 2020R1. Results: A total of 205 plasma samples were obtained from 55 patients. Eighty percent of patients received cefiderocol for ventilator-associated pneumonia due to carbapenem-resistant *Pseudomonas aeruginosa* infection. Cefiderocol concentration time-courses were best fit to a two-compartment open model with first-order elimination. Elimination clearance was positively related to renal function (estimated by the CKD formula). Adding albumin plasma binding in the model significantly improved the model assuming a ~40% unbound drug fraction given a ~40 g/L albuminemia. The final model included CKD plus cefiderocol plasma binding effects. Fat-free mass was better than total body weight to influence, via the allometric rule, clearance and volume terms, but this effect was negligible. The final clearance based on free circulating drug (CL_U) for a typical patient, CKD = 90, was 7.38 L/h [relative standard error, RSE, 22%] with a between-subject variability of 0.47 [RSE 10%] (exponential distribution). Conclusion: This study showed that albumin binding and CKD effects were significant predictors of unbound and total plasma cefiderocol concentrations. Our results indicate that individual adjustment of cefiderocol can be used to reach high minimum inhibitory concentrations based on an estimation of unbound drug concentration and optimize therapeutic efficacy.

Keywords: cefiderocol; pharmacokinetics; PK/PD; antibiotics; drug monitoring

Citation: Zahr, N.; Urien, S.; Llopis, B.; Noé, G.; Tissot, N.; Bihan, K.; Junot, H.; Marin, C.; Mansour, B.; Luyt, C.-E.; et al. Total and Unbound Pharmacokinetics of Cefiderocol in Critically Ill Patients. *Pharmaceutics* **2022**, *14*, 2786. https://doi.org/10.3390/pharmaceutics14122786

Academic Editors: Barna Vasarhelyi and Gellért Balázs Karvaly

Received: 24 October 2022
Accepted: 9 December 2022
Published: 13 December 2022

1. Introduction

Cefiderocol is a cephalosporin active against most Gram-negative bacteria, including extended-spectrum beta-lactamase and carbapenemase-producing strains such as *Pseudomonas aeruginosa*, *Acinetobacter baumannii* and *Enterobacteriales* [1]. Cefiderocol was approved by the U.S. Food and Drug Administration and the European Medicines Agency for the treatment of complicated urinary tract infections, the treatment of hospital-acquired

bacterial pneumonia and ventilator-associated bacterial pneumonia and for the treatment of infections due to aerobic Gram-negative organisms in adults with limited treatment options [2–4].

Cefiderocol approved dosage is 2 g administered every 8 h by intravenous infusion over 3 h. The dosage must be adjusted according to renal function as creatinine clearance (CrCL) was the most significant covariate in population pharmacokinetic studies [5,6]. Indeed, cefiderocol is primarily eliminated by the kidneys. Similar to other beta-lactam antibiotics, the cefiderocol efficacy target is the percentage of the dosing interval during which free drug concentrations are above the minimal inhibitory concentration (MIC) (%fT > MIC) [7]. Recommendations for optimal clinical response in intensive care patients are that residual plasma concentrations of beta-lactams antibiotics should be four to eight times the MIC [8,9].

Several studies have shown a high inter- and intra-individual variability of plasma concentrations of antibiotics, especially beta-lactam antibiotics in critically ill patients [10]. Pharmacokinetic (PK) analysis of cefiderocol has been described in healthy subjects and in patients with complicated urinary tract infections [5,6]. Cefiderocol is poorly metabolized and hepatic elimination represents a minor elimination pathway. Its protein binding, mainly to albumin, is around 40 to 60%. Cefiderocol terminal elimination half-life is about 2–3 h and its mean total and renal clearances in healthy volunteers were 5.46 L/h and 3.89 L/h, respectively [11,12]. However, data on cefiderocol PK properties in critically ill patients are currently lacking. This retrospective study was conducted to investigate individual characteristics that can influence cefiderocol pharmacokinetics in real life in order to optimize drug dosage.

2. Materials and Methods

2.1. Patients and Drug Assay

All patients included in this study were hospitalized in the intensive care units (ICU) at Pitié-Salpêtrière hospital. Patients were treated by cefiderocol in combination with other antibiotics for ventilator-associated bacterial pneumonia (VABP). As almost all patients were hospitalized in the ICU for more than a few days, all patients included in the study had ICU-induced malnutrition, as assessed by their low albumin level [13]. Blood samples were collected into lithium heparin tubes at steady state, one prior to the start of the infusion (Ctrough) and the others during and after the end of infusion. Blood samples were transferred to the laboratory within 2 h. Plasma samples were prepared by centrifuging collected blood samples for 5 min at 4500$\times$ *g* at 4 °C. All plasma samples were frozen at −80 °C until analysis. Plasma cefiderocol concentrations were assayed by an ultra-performance liquid chromatography system coupled with mass tandem spectrometry in a positive ionization mode (UPLC-MS/MS), as previously described by Llopis et al. [14]. Patients characteristics that could influence pharmacokinetics were collected retrospectively during the study.

The fat-free mass (FFM) was determined after the equation [15]:

$$FFM = WHSmax \cdot HT^2 \cdot BW / (WHS50 \cdot HT^2 + BW)$$

where WHSmax is the maximum FFM for a given height (HT, m) and WHS_{50} is the total bodyweight (BW, Kg) value when FFM is half of WHSmax. WHSmax is 42.92 and 37.99 kg/m^2 and WHS50 is 30.93 and 35.98 kg/m^2 for males and females, respectively.

The CKD (Chronic Kidney Disease Epidemiology Collaboration) equation was used to estimate glomerular filtration rate.

This retrospective study was based on data extracted from medical records and was performed in compliance with French regulations and according to the reference methodology MR-004, established by French National Commission on Informatics and Liberties (CNIL).

2.2. Data Analysis

Cefiderocol time-courses were fit to a two-compartment open model with first-order elimination. The following compartmental parameters were then derived: CL, Q, V1 and V2, which stand for the elimination and inter-compartmental clearances, central and peripheral volumes of distribution, respectively.

The nonlinear mixed effect modelling program Monolix version 2020R1 (Lixoft, Antony, France) (http://lixoft.com (accessed on 1 January 2022)) was used for the model development. The between-subject, BSV or ω and residual variabilities (square roots of the variances ω^2 and σ^2) were ascribed to an exponential distribution. The influence of demographic and clinical characteristics that could affect cefiderocol pharmacokinetics, i.e., sex, total bodyweight (BW), FFM, age and renal function (CKD equation) were investigated.

Because the drug is albumin-bound in plasma, the effect of albuminemia was also investigated after the following pharmacokinetic principles, i.e., the elimination and exchange processes are thought to depend upon the unbound drug concentration, C_U, as:

$$C_B(t) = C_U(t) \times K_{BIND} \times ALB, \text{ non-saturable binding or}$$

$$C_B(t) = C_U(t) \times ALB/(C_U(t) + Kd), \text{ saturable binding}$$

$$dA1(t)/dt = R - CL_U \times C_U(t) - k12 \times A1(t) + k21 \times A2(t) \text{ where } k_{12} = Q_U/V_{1U} \text{ and } k_{21} = Q_U/V_{2U}$$

$$dA_2(t)/dt = k_{12} \times A_1(t) - k_{21} \times A_2(t)$$

$$C_1(t) = C_U(t) + C_B(t)$$

where $A_1(t)$, $A_2(t)$ and R are the drug amounts in the 1st and 2nd compartments and infusion rate. The drug exchanges between compartments 1 (central) and 2 (peripheral) are driven by the transfer rate constants k_{12} and k_{21}. $C_B(t)$ is the albumin-bound concentration assuming a non-saturable or saturable binding to albumin with K_{BIND}, binding constant (L/g) or Kd, dissociation constant. The observed total plasma concentration is then fitted after the model predicted $C_1(t)$ and the corresponding clearance and volume terms are designed by the subscript U. Note that CL and V terms for total drug concentration kinetics are simply derived from $CL = f_U \times CL_U$ and $V = f_U \times V_U$ where $f_U = 1/(1 + K_{BIND} \times ALB)$.

The corrected Bayesian Information Criterion (cBIC) was used to test different hypotheses regarding the final model. The covariate sub-model was evaluated both via the BICc and BSV values. A covariate effect was finally retained, provided its effect could be physiologically explained. Each model was evaluated by visual inspection of goodness-of-fit plots, mainly observed-predicted (population and individual) concentration scatter plots. The normalized prediction distribution error metrics, whose mean and variance should not be different from 0 and 1 with a normal distribution, were preferred over the visual predictive checks (VPC), because the various inter-dose intervals rendered the latter difficult to interpret. Diagnostic graphics and other statistics were obtained using the R software.

3. Results

A total of 205 plasma samples were obtained from 55 patients, 37 males and 18 females. All patients were treated with cefiderocol for ventilator-associated pneumonia with carbapenem-resistant gram negative bacteria (GNB) including Pseudomonas aeruginosa (52), Stenotrophomonas maltophilia (2) and Acinetobacter baumanii (1). Patients' characteristics are summarized in Table 1. The median of residual concentration (C0), and maximal concentration (Cmax) were 35 mg/L [range 19–67] and 60 mg/L [range 40–84] respectively.

There were no concentrations below the limit of quantification. Patients received cefiderocol as 750 to 2000 mg infusions every 6, 8 or 12 h. At the time of sampling, severe renal impairment (CKD < 30 mL/min/1.73 m^2) was diagnosed in 10 (14.5%) patients. In 16 patients (29%) the value of CKD was greater than 120 mL/min/1.73 m^2 (median 150 mL/min/1.73 m^2 Interquartile range (IQR) (143–164).

Table 1. Demographic and biological characteristics of the 55 patients (37 males/18 females).

	Mean	%RSD	Median	Min	Max
Age, years	55.5	30.3	60	14	80
Total bodyweight, Kg	79.9	20.5	76	29	120
Height, m	1.75	5.76	1.78	1.52	2.01
Body mass index, Kg/m^2	26	18.5	26	25.5	39.8
Fat-free mass, Kg	55.6	17.9	53.6	23.6	79
Creatinine, µmol/L	132	113	86	17	736
CKD, mL/min/1.73 m^2	79.6	61	70	6	170
Albumin, g/L	22.6	29	22	11.5	37.9
Plasma proteins, g/L	55.6	17.3	57	37	77
ASAT, U/L	39.5	79.9	28	12	183
ALAT, U/L	36.4	137	21	6	208
CRP, mg/L	84.7	78.2	87	1	302

Abbreviations: ALAT: alanine aminotransferase, ASAT: aspartate aminotransferase, CRP: C-reactive protein, CKD (Chronic Kidney Disease Epidemiology Collaboration) %RSD: Relative standard deviation in %. All data were collected at the time of cefiderocol sampling.

The population parameters of the covariate-free model were satisfactorily estimated. Only BSV for CL and Q, ω_{CL} and ω_Q, could be estimated. Table 2 summarizes the covariates sub-models tested (only the models that produced a cBIC value lower than the base model cBIC value are shown). CKD positively influenced CL and decreased both ω_{CL} and the cBIC value. The non-saturable albumin binding effect alone was also significant (saturable binding was unidentifiable and failed to converge). The K_{BIND} value was fixed to 0.036 L/g assuming a 41% free concentration fraction for a 40.5 g/L albuminemia [16]. When clearance and volume terms were related to size effects, WT or FFM, $(SIZE/mean_{SIZE})^{p\_size}$ (p_size exponents fixed to 0.75 and 1 for clearances and volumes according to the allometric rule), only the FFM effect was significant. The final model combined the CKD and albumin binding effects (the further addition of FFM did not significantly improve this model). A sensitivity analysis on K_{BIND} assuming f_U values of 50 and 60% (K_{BIND} = 0.025 or 0.017) provided cBIC slightly greater than that of the final model. The final covariate sub-model for CL_U was then:

$$CL_U\ (L/h) = 7.38 \times (CKD/100)^{0.426}$$

or, adding the FFM effect

$$CL_U\ (L/h) = 7.33 \times (FFM/54)^{0.75} \times (CKD/100)^{0.416}$$

Table 2. Covariate sub-model building.

Model	Covariate	Parameter	Estimate	ω	cBIC
6.	#FREE + CKD	CL_U	7.38	0.467	1682
5.	#FREE + CKD + FFM	CL_U	7.33	0.464	1686
4.	#FREE + CKD + WT	CL_U	6.84	0.491	1689
3. FFM	FFM-based allometry	CL	4.03	0.459	1698
2. CKD	Effect of CKD on CL	CL	4.07	0.461	1698
1. FREE #	albumin binding, $C_T = C_U + C_B$	CL_U	6.26	0.627	1726
0	covariate free, basic	CL	3.47	0.634	1732

Abbreviations: CL or CLU, clearance or unbound drug clearance; ω, square root of between-subject variance ω^2, for CL or CLU; FFM, fat-free mass (Kg); WT, total bodyweight (Kg); CKD (mL/min/1.73 m^2), renal function index; cBIC, corrected Bayesian Information Criteria; CT, CU or CB, total, unbound or bound concentration; #FREE, model taking into account the drug binding to albumin then estimating the unbound drug pharmacokinetic parameters, CL_U, $V1_U$, etc., related to the unbound drug concentration.

Parameter estimates are summarized in Table 3. Note that the shrinkages for CL_U and Q_U were 1.84 and 81%.

Table 3. Cefiderocol population parameters estimates for the unbound drug pharmacokinetics from 205 total plasma concentrations in 55 adult patients.

Population Parameters	Estimate	RSE (%)
$V1_U$, L	17	22
CL_U, L/h per CKD = 100	7.38	6.8
Q_U, L/h	34	39
$V2_U$, L	46	12
CKD effect on CL_U	0.426	8.8
K_{BIND}, FIXED (albumin binding constant), L/g	0.036	NA
Statistical Parameters		
ωCLu	0.467	10.4
ωQu	0.706	44
log-additive residual variability	0.183	6

Abbreviations: RSE, relative standard error in %; ω, square root of between-subject variance ω^2; CKD (mL/min/1.73 m^2), renal function index; Clu = 7.38 × $(CKD/100)^{0.426}$; $f_U = 1/(1 + ALB * 0.036)$ with f_U and ALB unbound drug fraction and albumin concentration in L/g. Note that CL and V terms for total drug concentration kinetics are simply $CL = f_U \times CL_U$ and $V = f_U \times V_U$. The total concentration is $C_T = C_U \times (1 + K_{BIND} \times ALB)$ with C_U = f(Rate, CL_U, $V1_U$, Q_U, $V2_U$).

The goodness-of-fit plots for the final model shown in Figures 1 and 2 show the visual predictive checks for the cefiderocol final PK model. The observed concentration percentiles are well included in the corresponding model-predicted 90% confidence interval bands.

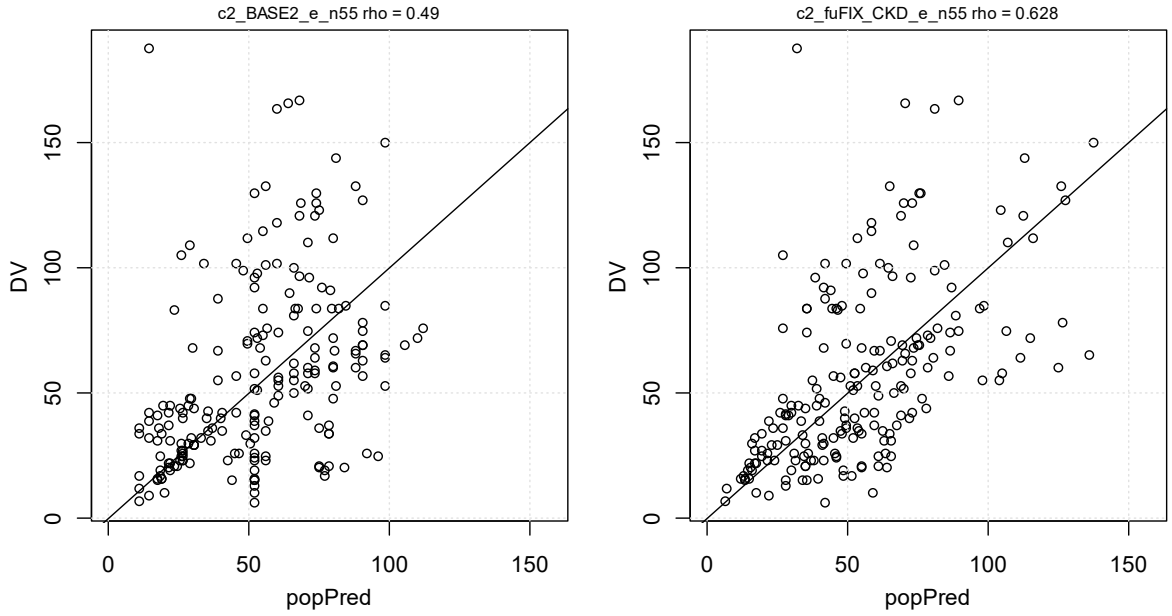

Figure 1. *Cont.*

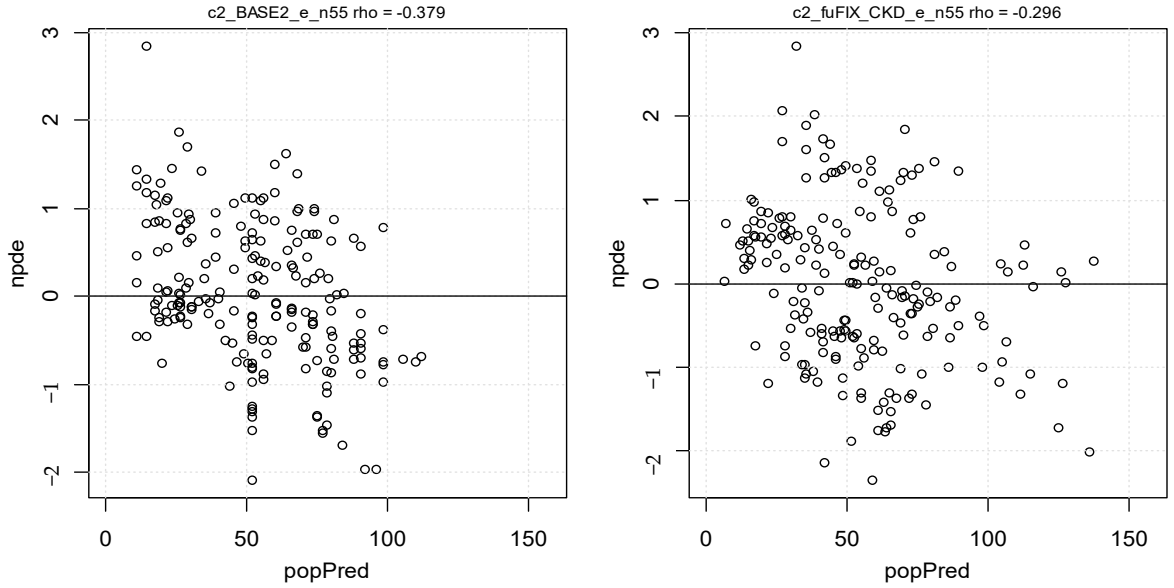

Figure 1. Goodness-of-fit plots for the base (covariate-free, **left**) and final (CKD + albumin binding, **right**) models. DV and popPred, observed and population predicted concentrations; npde, versus popPred values with the y = zero line.

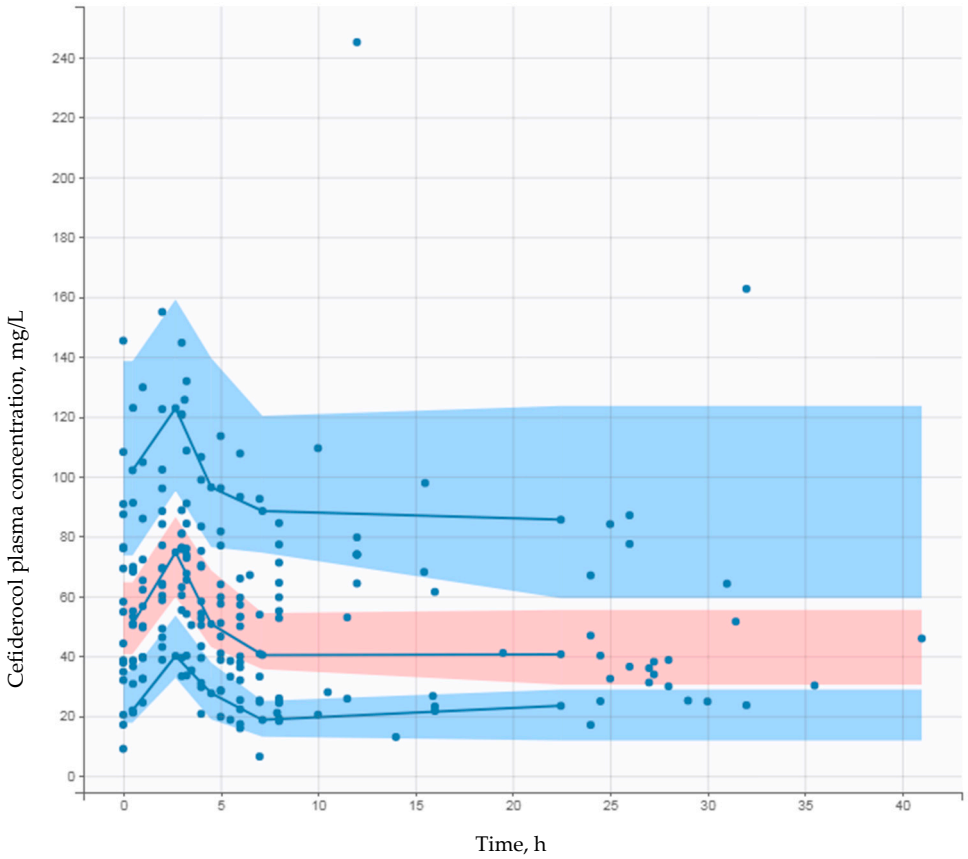

Figure 2. Prediction-corrected visual predictive check for the final cefiderocol population pharmacokinetic model. Plain (•) and blue lines stand for prediction-corrected observed concentrations and their 5th, 50th and 95th percentiles. Light blue and red bands stand for the corresponding model predicted 90% confidence intervals.

Finally, Figure 3 depicts the model curve fittings for some individuals. The mean and standard deviation of the normalized prediction distribution errors (NPDE), −0.002 and

1.15, were not significantly different from 0 and 1 ($p = 0.98$ and $p = 0.15$) with a symmetrical distribution around 0, as expected for these metrics.

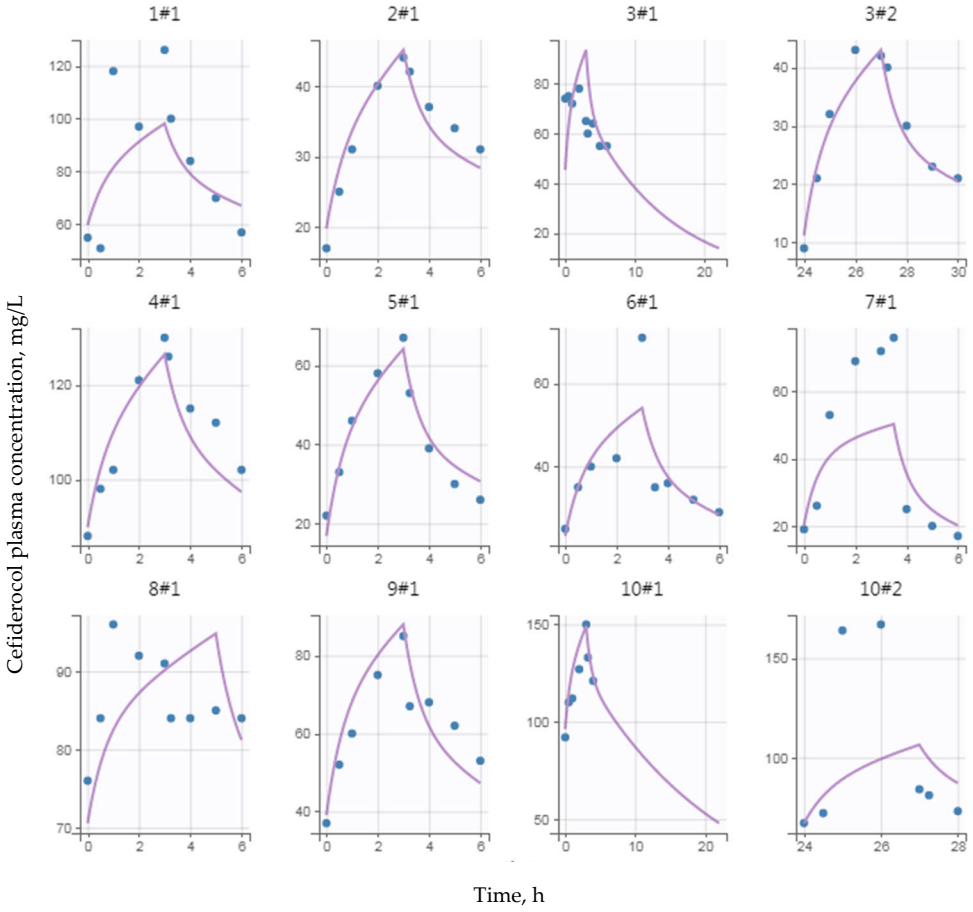

Figure 3. Representative individual curve fitting of cefiderocol (circles, observed concentration; purple solid lines, individual fits; N1#N2, *i*th subject # *i*th occasion).

Dosage Recommendations

Cefiderocol approved regimen is at a dose of 2 g every 8 h for the treatment of adult patients for whom treatment options are limited with a bacterial MIC $\leq$ 2 mg/L. Optimal clinical response of β-lactam antibiotics is obtained with a residual plasma concentration $\geq$ 4–8 times the MIC [8,9]. Positive clinical outcome was associated with increasing 100% fT > MIC ratio in infected critically ill patients [17]. The dose of cefiderocol can be directly estimated from the model-predicted unbound concentrations given the renal function index CKD. Figure 4 represents a proposal for the doses of cefiderocol to be administered according to various levels of renal function for a MIC value of 2 in situ, i.e., considering the epithelial lining fluid (ELF) where the ELF-to-C_U concentration ratio is (0.5) two hours post-end of infusion [18]. The probability of target attainment, in these intensive care patients with an undernutrition status, for > 99% fT > MIC was > 99% when MIC was 4 mg/L.

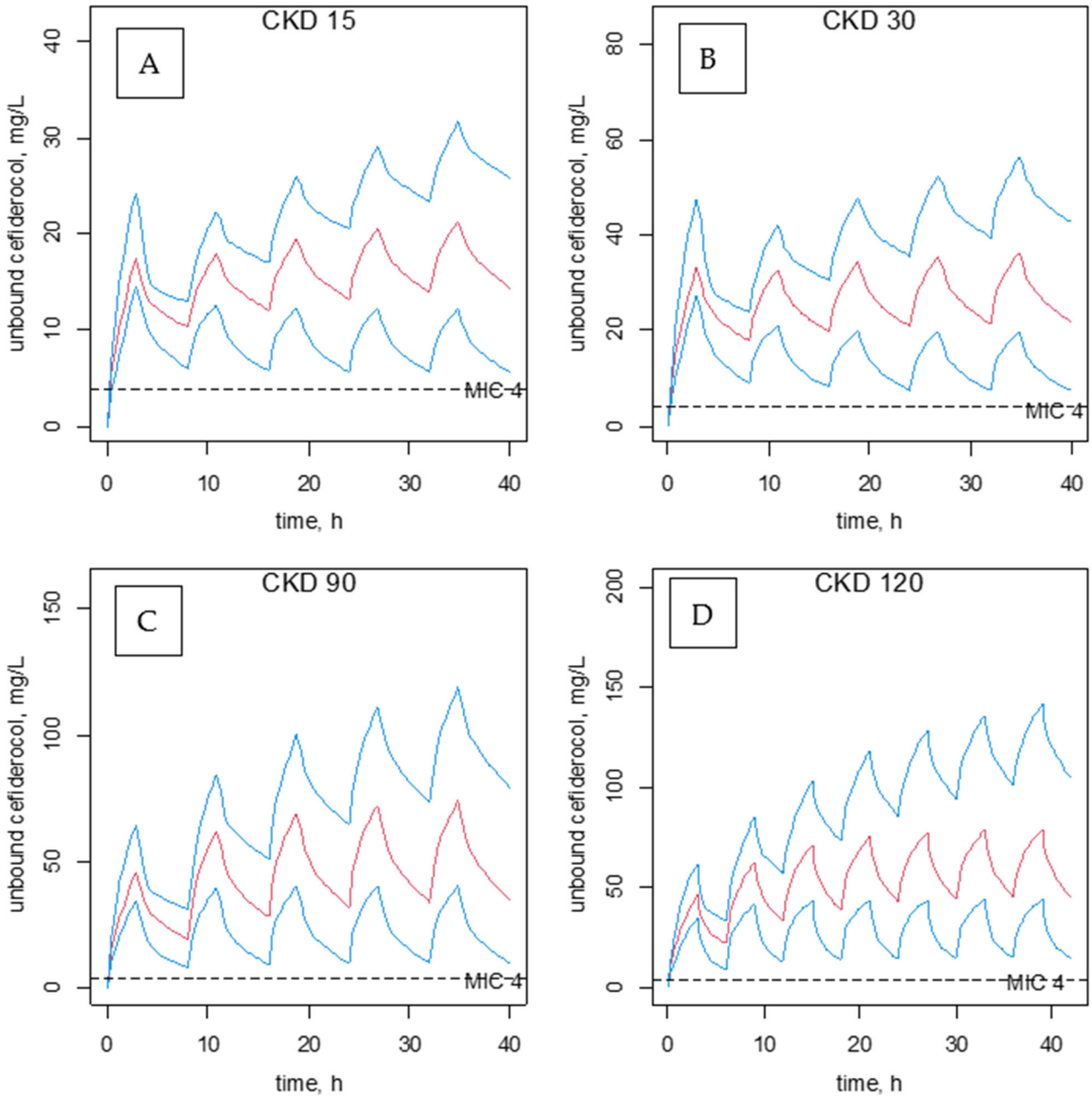

Figure 4. Unbound plasma cefiderocol concentration-time courses for 4 typical renal function (CKD = 15, CKD = 30, CKD = 90, CKD = 120), receiving doses of (1000 mg then 3 × 500 mg) panel (**A**), (2000 mg then 3 ×1000 mg) panel (**B**), (3 × 3000 mg) panel (**C**), (4 × 3000 mg) panel (**D**) by 3 h infusion, respectively. Doses are administered every 8 h except for CKD = 120, every 6 h. Note total plasma cefiderocol concentration is obtained by multiplying the unbound concentration by 2.5 assuming a 40 g/L albuminemia ($f_{U,40g/LALB}$ = 0.6). The horizontal dashed line is drawn at 4 mg/L (considering the ELF-to-CU concentration ratio is 0.5) Blue lines stand for prediction concentrations and their 5th, and 95th percentiles. Red and blue lines represent means and 5th–95th percentiles for predicted concentrations, respectively.

4. Discussion

To date, most of the pharmacokinetics parameters of cefiderocol have been generated from phase one, two and three clinical studies [19–22]. In this study, we showed that cefiderocol time-courses were well described by a two-compartment model. The limited number of patients, n = 55, allowed the estimation of only one between-subject variability

parameter, ω_{CL}. Kawaguchi et al. [6] described cefiderocol pharmacokinetics after using a three-compartment model. However, the volume of the central compartment, 0.73 L, was very small and can only be determined with a rich data sampling at early times post-infusion.

The pharmacokinetic/pharmacodynamic (PK/PD) index of cefiderocol with bactericidal activity is correlated with fraction of time for which the free drug concentration in plasma exceeds the minimum inhibitory concentration of the infecting microorganism over the dosing interval (%fT > MIC) [5,7]. In this study of patient hospitalized in intensive care unit, albumin levels were low (median 22 g/L IQR (18–24)). In this modeling, the plasma albumin binding could be accounted for, thanks to the wide variation in albuminemia observed in these patients. The output of the pharmacokinetic model was ascribed to the unbound drug concentration which is thought to be the freely exchangeable drug in the body. The result was then fitted to the total drug concentration by adding the drug-bound concentration, based on albumin concentration. Compared to the same model based on total concentration, the cBIC value dropped by 16 units. Moreover, the relative precision of CKD effect on CL_U was 8.77%, as compared to 13.3% when based on total concentration. This demonstrates that the model based on the diffusible free concentration is more appropriate, which was expected for this renally-eliminated hydrophilic drug. Figure 5 shows that, for each patient, fu is determined as a function of its albuminemia.

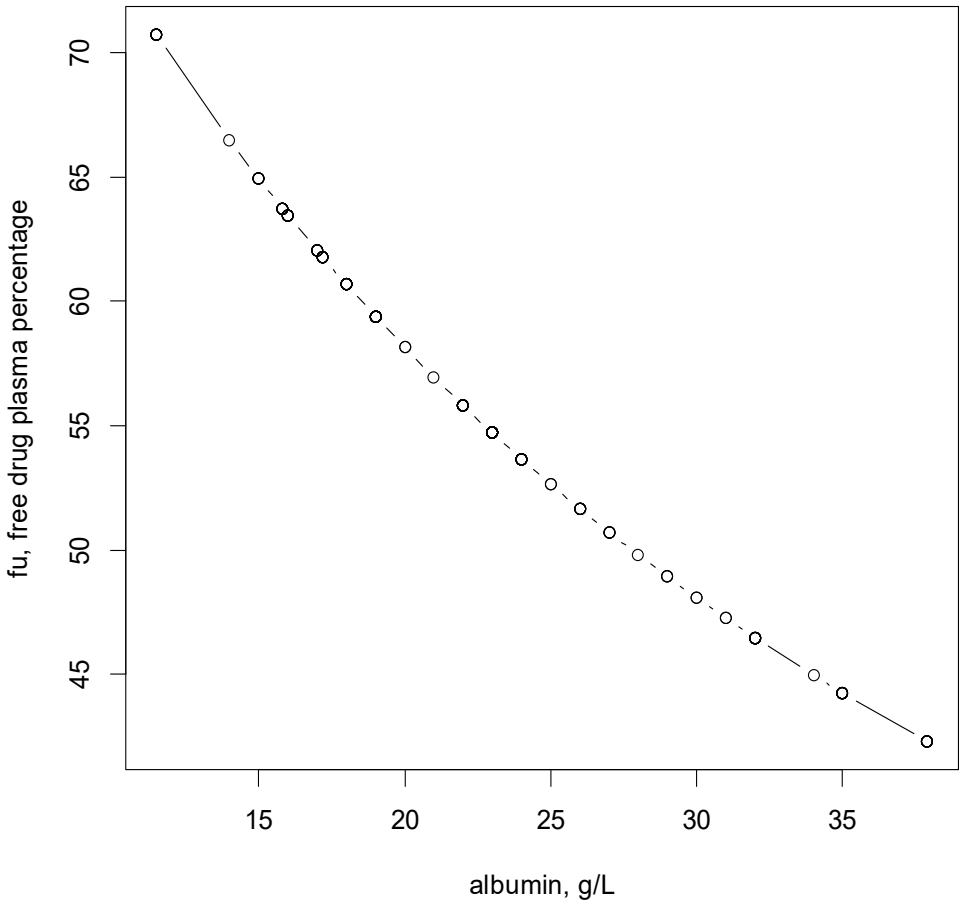

Figure 5. Relationship between f_U and the plasma albumin concentration.

The K_{BIND} value was fixed according to the f_U values observed for various albumin concentrations, as previously reported [16]. This allowed the estimation of the unbound drug's kinetic parameters. The CKD value was the main relevant covariate effect on the unbound drug clearance (CL_U) that was not unexpected because of the very hydrophilic nature of cefiderocol (logP = −2.27). There was also an effect of FFM (but not total body

weight) that was not unexpected given the hydrophilic nature of cefiderocol. However, this effect was not retained in the final model because it did not provide significant improvement. Nevertheless, in future studies, this FFM covariate should be considered instead of total body weight. The final model included the albumin-binding effect plus the renal function effect via the CKD index. Interestingly, the kinetic parameters for the unbound drug allow the prediction of the unbound, active, drug concentration, given the patient's CKD is known. The CL value relative to the total drug concentration is 2.95 L/h (0.4 × 7.38). This low value, as compared to that reported by Kawaguchi et al. [6] (i.e., 4.2 to 5.0 L/h), may result from the poor condition of the patients, presenting various degrees of malnutrition.

Our study has some limitations. The small number of patients in our study did not allow an external validation of our model. In addition to be in an ICU, these patients exhibit a significant degree of undernutrition. Note that unbound concentrations were not measured, and that total and unbound concentration have been translated into each other simply by applying multiplicative constants. Moreover, MICs of cefiderocol were not available for all samples. Due to the shrinkage level observed on Q_U, but not CL_U, a pharmacokinetic-based individualization is not advised. In addition, it is usually accepted that ICU patients' pathophysiologic state can rapidly change. New studies including ICU patients should be done for this recent antibiotic. Finally, estimates of renal function have low accuracy and precision in critically ill patients [23].

5. Conclusions

In conclusion, our study showed that albumin binding and CKD effects were significant predictors of unbound and total plasma cefiderocol concentrations. Our results indicate that individual adjustment of cefiderocol can be used to reach high minimum inhibitory concentrations based on an estimation of unbound drug concentration. Whether such an estimation results in a better therapeutic outcome remains to be determined.

Author Contributions: N.Z., A.B. and C.F.-B. conceptualized and designed the study. B.L., G.N., N.T., C.M., B.M., K.B., H.J., C.-E.L. and A.B. generated the data. N.Z., S.U. and C.F.-B. analyzed and interpreted the data. N.Z., S.U. and C.F.-B. wrote the manuscript. All authors were involved in revising the manuscript critically for intellectual contents. All authors approved the final version. All authors have read and agreed to the published version of the manuscript.

Funding: This research received no external funding.

Institutional Review Board Statement: This retrospective study was based on data extracted from medical records and was performed in compliance with French regulations and according to the reference methodology MR-004, established by French National Commission on Informatics and Liberties (CNIL).

Informed Consent Statement: Approval for data collection was obtained from the Commission Nationale de l'Informatique et des Libertés (n°1491960v0).

Data Availability Statement: The data support the findings of this study are available on request from the corresponding author upon reasonable request.

Conflicts of Interest: A.B. has received fees from Shionogi, the manufacturer of cefiderocol. Other authors have no conflicts of interest to disclose.

References

1. Parsels, K.A.; Mastro, K.A.; Steele, J.M.; Thomas, S.J.; Kufel, W.D. Cefiderocol: A novel siderophore cephalosporin for multidrug-resistant Gram-negative bacterial infections. *J. Antimicrob. Chemother.* **2021**, *76*, 1379–1391. [CrossRef] [PubMed]
2. FDA Approves New Antibacterial Drug to Treat Complicated Urinary Tract Infections as Part of Ongoing Efforts to Address Antimicrobial Resistance. Available online: https://www.fda.gov/news-events/press-announcements/fda-approves-new-antibacterial-drug-treat-complicated-urinary-tract-infections-part-ongoing-efforts (accessed on 16 December 2019).
3. Andrei, S.; Droc, G.; Stefan, G. FDA approved antibacterial drugs: 2018–2019. *Discoveries* **2019**, *7*, e102. [CrossRef] [PubMed]
4. European Medicines Agency. *Fetcroja (Cefiderocol) Product Information*; European Medicines Agency: Amsterdam, The Netherlands, 2020; Available online: https://www.ema.europa.eu/en/documents/product-information/fetcroja-epar-product-information_en.pdf (accessed on 1 January 2022).

5. Katsube, T.; Wajima, T.; Ishibashi, T.; Arjona Ferreira, J.C.; Echols, R. Pharmacokinetic/Pharmacodynamic Modeling and Simulation of Cefiderocol, a Parenteral Siderophore Cephalosporin, for Dose Adjustment Based on Renal Function. *Antimicrob. Agents Chemother.* **2017**, *61*, e01381-16. [CrossRef] [PubMed]
6. Kawaguchi, N.; Katsube, T.; Echols, R.; Wajima, T. Population Pharmacokinetic Analysis of Cefiderocol, a Parenteral Siderophore Cephalosporin, in Healthy Subjects, Subjects with Various Degrees of Renal Function, and Patients with Complicated Urinary Tract Infection or Acute Uncomplicated Pyelonephritis. *Antimicrob. Agents Chemother.* **2018**, *62*, e01391-17. [CrossRef]
7. Nakamura, R.; Ito-Horiyama, T.; Takemura, M.; Toba, S.; Matsumoto, S.; Ikehara, T.; Tsuji, M.; Sato, T.; Yamano, Y. In Vivo Pharmacodynamic Study of Cefiderocol, a Novel Parenteral Siderophore Cephalosporin, in Murine Thigh and Lung Infection Models. *Antimicrob. Agents Chemother.* **2019**, *63*, e02031-18. [CrossRef]
8. Guilhaumou, R.; Benaboud, S.; Bennis, Y.; Dahyot-Fizelier, C.; Dailly, E.; Gandia, P.; Goutelle, S.; Lefeuvre, S.; Mongardon, N.; Roger, C.; et al. Optimization of the treatment with beta-lactam antibiotics in critically ill patients-guidelines from the French Society of Pharmacology and Therapeutics (Societe Francaise de Pharmacologie et Therapeutique-SFPT) and the French Society of Anaesthesia and Intensive Care Medicine (Societe Francaise d'Anesthesie et Reanimation-SFAR). *Crit. Care* **2019**, *23*, 104. [CrossRef]
9. Scharf, C.; Liebchen, U.; Paal, M.; Taubert, M.; Vogeser, M.; Irlbeck, M.; Zoller, M.; Schroeder, I. The higher the better? Defining the optimal beta-lactam target for critically ill patients to reach infection resolution and improve outcome. *J. Intensive Care* **2020**, *8*, 86. [CrossRef]
10. Veiga, R.P.; Paiva, J.A. Pharmacokinetics-pharmacodynamics issues relevant for the clinical use of beta-lactam antibiotics in critically ill patients. *Crit. Care* **2018**, *22*, 233. [CrossRef]
11. Katsube, T.; Echols, R.; Wajima, T. Pharmacokinetic and Pharmacodynamic Profiles of Cefiderocol, a Novel Siderophore Cephalosporin. *Clin. Infect. Dis.* **2019**, *69*, S552–S558. [CrossRef]
12. Saisho, Y.; Katsube, T.; White, S.; Fukase, H.; Shimada, J. Pharmacokinetics, Safety, and Tolerability of Cefiderocol, a Novel Siderophore Cephalosporin for Gram-Negative Bacteria, in Healthy Subjects. *Antimicrob. Agents Chemother.* **2018**, *62*, e02163-17. [CrossRef]
13. Mohialdeen Gubari, M.I.; Hosseinzadeh-Attar, M.J.; Hosseini, M.; Mohialdeen, F.A.; Othman, H.; Hama-Ghareeb, K.A.; Norouzy, A. Nutritional Status in Intensive Care Unit: A Meta-Analysis and Systematic Review. *Galen Med. J.* **2020**, *9*, e1678. [CrossRef]
14. Llopis, B.; Bleibtreu, A.; Schlemmer, D.; Robidou, P.; Paccoud, O.; Tissot, N.; Noe, G.; Junot, H.; Luyt, C.E.; Funck-Brentano, C.; et al. Simple and accurate quantitative analysis of cefiderocol and ceftobiprole in human plasma using liquid chromatography-isotope dilution tandem mass spectrometry: Interest for their therapeutic drug monitoring and pharmacokinetic studies. *Clin. Chem. Lab. Med.* **2021**, *59*, 1800–1810. [CrossRef]
15. McCune, J.S.; Bemer, M.J.; Barrett, J.S.; Scott Baker, K.; Gamis, A.S.; Holford, N.H. Busulfan in infant to adult hematopoietic cell transplant recipients: A population pharmacokinetic model for initial and Bayesian dose personalization. *Clin. Cancer Res.* **2014**, *20*, 754–763. [CrossRef]
16. Katsube, T.; Echols, R.; Arjona Ferreira, J.C.; Krenz, H.K.; Berg, J.K.; Galloway, C. Cefiderocol, a Siderophore Cephalosporin for Gram-Negative Bacterial Infections: Pharmacokinetics and Safety in Subjects With Renal Impairment. *J. Clin. Pharmacol.* **2017**, *57*, 584–591. [CrossRef]
17. Roberts, J.A.; Paul, S.K.; Akova, M.; Bassetti, M.; De Waele, J.J.; Dimopoulos, G.; Kaukonen, K.M.; Koulenti, D.; Martin, C.; Montravers, P.; et al. DALI: Defining antibiotic levels in intensive care unit patients: Are current beta-lactam antibiotic doses sufficient for critically ill patients? *Clin. Infect. Dis.* **2014**, *58*, 1072–1083. [CrossRef]
18. Katsube, T.; Nicolau, D.P.; Rodvold, K.A.; Wunderink, R.G.; Echols, R.; Matsunaga, Y.; Menon, A.; Portsmouth, S.; Wajima, T. Intrapulmonary pharmacokinetic profile of cefiderocol in mechanically ventilated patients with pneumonia. *J. Antimicrob. Chemother.* **2021**, *76*, 2902–2905. [CrossRef]
19. Portsmouth, S.; van Veenhuyzen, D.; Echols, R.; Machida, M.; Ferreira, J.C.A.; Ariyasu, M.; Tenke, P.; Nagata, T.D. Cefiderocol versus imipenem-cilastatin for the treatment of complicated urinary tract infections caused by Gram-negative uropathogens: A phase 2, randomised, double-blind, non-inferiority trial. *Lancet Infect Dis.* **2018**, *18*, 1319–1328. [CrossRef]
20. Naseer, S.; Weinstein, E.A.; Rubin, D.B.; Suvarna, K.; Wei, X.; Higgins, K.; Goodwin, A.; Jang, S.H.; Iarikov, D.; Farley, J.; et al. US Food and Drug Administration (FDA): Benefit-Risk Considerations for Cefiderocol (Fetroja(R)). *Clin. Infect. Dis.* **2021**, *72*, e1103–e1111. [CrossRef]
21. Bassetti, M.; Echols, R.; Matsunaga, Y.; Ariyasu, M.; Doi, Y.; Ferrer, R.; Lodise, T.P.; Naas, T.; Niki, Y.; Paterson, D.L.; et al. Efficacy and safety of cefiderocol or best available therapy for the treatment of serious infections caused by carbapenem-resistant Gram-negative bacteria (CREDIBLE-CR): A randomised, open-label, multicentre, pathogen-focused, descriptive, phase 3 trial. *Lancet Infect. Dis.* **2021**, *21*, 226–240. [CrossRef]
22. Wunderink, R.G.; Matsunaga, Y.; Ariyasu, M.; Clevenbergh, P.; Echols, R.; Kaye, K.S.; Kollef, M.; Menon, A.; Pogue, J.M.; Shorr, A.F.; et al. Cefiderocol versus high-dose, extended-infusion meropenem for the treatment of Gram-negative nosocomial pneumonia (APEKS-NP): A randomised, double-blind, phase 3, non-inferiority trial. *Lancet Infect. Dis.* **2021**, *21*, 213–225. [CrossRef]
23. Carlier, M.; Dumoulin, A.; Janssen, A.; Picavet, S.; Vanthuyne, S.; Van Eynde, R.; Vanholder, R.; Delanghe, J.; De Schoenmakere, G.; De Waele, J.J.; et al. Comparison of different equations to assess glomerular filtration in critically ill patients. *Intensive Care Med.* **2015**, *41*, 427–435. [CrossRef] [PubMed]

pharmaceutics

Article

Modeling Pharmacokinetics in Individual Patients Using Therapeutic Drug Monitoring and Artificial Population Quasi-Models: A Study with Piperacillin

Gellért Balázs Karvaly [1,*], István Vincze [1], Michael Noel Neely [2], István Zátroch [3], Zsuzsanna Nagy [4], Ibolya Kocsis [1] and Csaba Kopitkó [3]

[1] Department of Laboratory Medicine, Semmelweis University, 1089 Budapest, Hungary; vincze.istvan@pharma.semmelweis-univ.hu (I.V.); kocsis.ibolya@med.semmelweis-univ.hu (I.K.)
[2] Laboratory of Applied Pharmacokinetics and Bioinformatics, The Saban Research Institute, University of Southern California, Los Angeles, CA 90027, USA; mneely@chla.usc.edu
[3] Central Department of Anaesthesiology and Intensive Care, Uzsoki Teaching Hospital, 1145 Budapest, Hungary; zatroch.istvan@uzsoki.hu (I.Z.); kopitko.csaba@uzsoki.hu (C.K.)
[4] Central Laboratory, Uzsoki Teaching Hospital, 1145 Budapest, Hungary; nagy.zsuzsanna@uzsoki.hu
* Correspondence: karvaly.gellert_balazs@med.semmelweis-univ.hu

Abstract: Population pharmacokinetic (pop-PK) models constructed for model-informed precision dosing often have limited utility due to the low number of patients recruited. To augment such models, an approach is presented for generating fully artificial quasi-models which can be employed to make individual estimates of pharmacokinetic parameters. Based on 72 concentrations obtained in 12 patients, one- and two-compartment pop-PK models with or without creatinine clearance as a covariate were generated for piperacillin using the nonparametric adaptive grid algorithm. Thirty quasi-models were subsequently generated for each model type, and nonparametric maximum a posteriori probability Bayesian estimates were established for each patient. A significant difference in performance was found between one- and two-compartment models. Acceptable agreement was found between predicted and observed piperacillin concentrations, and between the estimates of the random-effect pharmacokinetic variables obtained using the so-called support points of the pop-PK models or the quasi-models as priors. The mean squared errors of the predictions made using the quasi-models were similar to, or even considerably lower than those obtained when employing the pop-PK models. Conclusion: fully artificial nonparametric quasi-models can efficiently augment pop-PK models containing few support points, to make individual pharmacokinetic estimates in the clinical setting.

Keywords: therapeutic drug monitoring; piperacillin; tazobactam; nonparametric adaptive grid; Bayesian models; pharmacokinetics; model-informed precision dosing; intensive care

Citation: Karvaly, G.B.; Vincze, I.; Neely, M.N.; Zátroch, I.; Nagy, Z.; Kocsis, I.; Kopitkó, C. Modeling Pharmacokinetics in Individual Patients Using Therapeutic Drug Monitoring and Artificial Population Quasi-Models: A Study with Piperacillin. *Pharmaceutics* **2024**, *16*, 358. https://doi.org/10.3390/pharmaceutics16030358

Academic Editor: Patrick J. Sinko

Received: 28 September 2023
Revised: 6 December 2023
Accepted: 7 February 2024
Published: 4 March 2024

1. Introduction

Model-informed precision dosing (MIPD) is an emerging clinical discipline which allows the guidance of individualized drug therapies based on the therapeutic monitoring of drug concentrations and pharmacokinetic modeling. The construction of population (pop-PK) and, subsequently, individual models allows the prediction of each patient's future exposure to the monitored substance. The clinical implementation of MIPD requires an efficient laboratory assay, suitable computer modeling software, and the efforts of a multidisciplinary team consisting of clinicians, nurses, pharmacists and laboratory analysts [1–3]. This discipline has become especially useful in optimizing antibiotic treatments at intensive care units due to the very high vulnerability and, in terms of the pharmacokinetically relevant physiological functions and parameters, variability of critically ill patients [4,5].

The quality of the prediction of individual drug concentrations has a crucial impact on finding the optimal dosage regimen and, eventually, on therapeutic success. Interest

in augmenting pharmacokinetic models with the help of machine learning algorithms has recently increased because the construction of models which efficiently represent a broader set of patients has often proved to be an overwhelming task, especially in pediatric populations, as well as in populations diagnosed with rare diseases, or living with special conditions (e.g., oncological and organ-transplant recipients, or patients receiving intensive care) [6–9]. Augmented pop-PK models are expected to overcome the limitations posed by the availability of a low number of subjects and/or data points, and may therefore facilitate the implementation of MIPD [10].

In this work, a novel approach to constructing a set of fully artificial population pharmacokinetic quasi-models (QM) is put forward. The most suitable of which is then selected for each patient individually to estimate their exposure to the drug administered. The term "fully artificial quasi-model" refers to the fact that, unlike pop-PK models which are based on drug concentrations measured in the blood of human subjects, a set of data, none of which actually represent the true characteristics of any human, is generated using a computer algorithm. This does not eliminate the need to collect data from humans, which remains crucial for establishing the modeled *ranges* of the random-effect pharmacokinetic variables, but the number of subjects required can be considerably lower. The workflow for constructing the quasi-models, and applying them to make individual parameter estimates, is displayed in Figure 1.

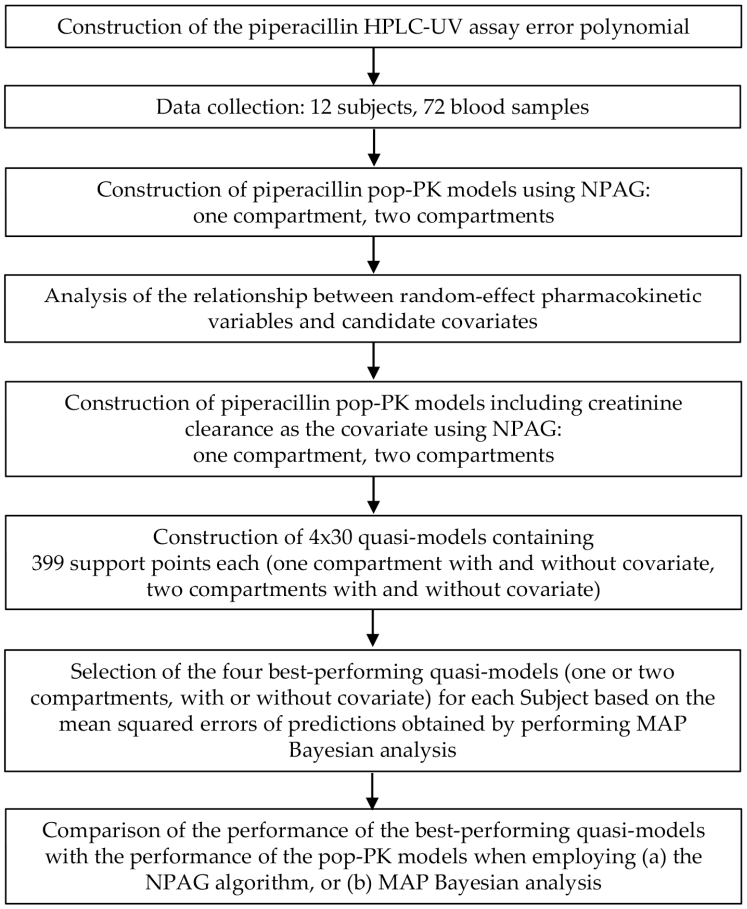

Figure 1. Overview of the workflow for constructing and applying fully artificial quasi-models to make estimates of the individual pharmacokinetic properties of piperacillin. HPLC-UV, high-performance liquid chromatography coupled with ultraviolet light absorbance detection. MAP, maximum a posteriori probability. NPAG, nonparametric adaptive grid modeling. Pop-PK: population pharmacokinetic model.

The nonparametric adaptive grid (NPAG) algorithm of Leary and Burke was employed for constructing mixed-effects pop-PK models based on the data obtained from human subjects. This iterative approach allows the nonparametric estimation of the joint population distribution of pharmacokinetic model parameter values by establishing a set of grid points of modest size, finding the maximum likelihood solution for that grid, and then refining the grid based on the optimal discrete so-called support points (i.e., vectors containing estimates of the pharmacokinetic parameter along with a probability value) and by adding a modestly sized set of new support points. The process continues until a convergence criterion defined by the modeler is reached, and no further improvement of the likelihood of the estimates of the random-effect variables can be attained [11–13].

In contrast to parametric modeling, which is based on the generation of measures of central tendency and dispersion, and the approximation of the likelihood function, NPAG relies on determining the exact likelihood function to describe the population, making the approach statistically consistent. No assumptions of the distributions of the random-effect variables are made, which makes NPAG superior in detecting subpopulations and outliers [12]. Nonparametric maximum a posteriori probability (MAP) Bayesian analysis in turn uses the pop-PK support points to find the pharmacokinetic parameters which apply to individual patients [14]. The utility of nonparametric pharmacokinetic modeling in the clinical setting has been demonstrated [15].

The modeled substance was piperacillin administered to critically ill adults diagnosed with community-acquired pneumonia, who were receiving treatment at the intensive care unit of a public hospital. This work is part of a larger clinical study conducted as described in a protocol published earlier, the overall aim of which is to establish a multidisciplinary methodology for the evaluation of pharmacological intervention in the first 5 days of the patient receiving intensive care for community-acquired pneumonia. The objectives include monitoring intra-individual changes in the pharmacokinetic properties of piperacillin and tazobactam, as well as in the concentrations of endogenous steroids and inflammatory markers which characterize the clinical status [16]. The pharmacokinetic modeling of the beta-lactamase was not performed since its serum concentrations were in strong correlation with those of piperacillin, which is in line with previous findings. There is no evidence that tazobactam concentrations should be taken into consideration when making a decision on the antibiotic regimen employed [17].

2. Materials and Methods

This investigator-initiated, unicentric, observational, one-arm study has been approved by the National Institute of Pharmacy and Nutrition (Budapest, Hungary, identifier of approval document: 261-IK/2020), the National Competent Authority of Hungary for medical research ethics. The Principal Investigator was Cs. Kopitkó. Twelve adults, admitted to the Central Department of Anesthesiology and Intensive Care, Uzsoki Teaching Hospital (Budapest, Hungary) with the diagnosis of community-acquired pneumonia, were recruited (Table 1). All subjects received standard care, including mechanical ventilation. The administration of a daily dose of 16 g (30.98 mmol) piperacillin + 2 g (6.66 mmol) tazobactam divided into four doses, given every 6 h as a 3-h intravenous infusion, was initiated empirically and immediately following admittance. No other antibiotics were given. Blood samples were collected by trained personnel in certified collection tubes (Greiner Bio-One Hungary Ltd., Budapest, Hungary) by accessing the vena cava superior, after finishing the first 8 AM infusion on the day following the day of admission, as described in [16]. Care was taken by the nurses of the Central Department of Anesthesiology and Intensive Care to adhere to all professional standards and institutional protocols, including drug administration and sample collection, as well as to document all activities and events related to the research, which was crucial for obtaining valid and credible outcomes. The sampling times, documented by the healthcare team, were 0.25 h, 0.5 h, 1 h, 1.5 h, 2 h and 2.5 h post-infusion. The samples were pretreated as necessary by the personnel of the Central Department of Anesthesiology and Intensive Care under the supervision of the

Principal Investigator, and were subsequently sent to the laboratories where the various assays were performed. Native blood samples were kept at ambient temperature for no longer than 15 min, and were centrifuged thereafter at 10 °C and 2500× *g*, for 10 min. An aliquot of 0-h serum, as well as K_3-EDTA-anticoagulated, heparinized and sodium citrate-treated whole blood samples were transferred to the Central Laboratory, Uzsoki Teaching Hospital, for routine laboratory assays, whole blood count and hematocrit measurement. A total of 250 µL serum separated for interleukin-6 measurement was frozen and sent to the Central Laboratory, Department of Laboratory Medicine, Semmelweis University (Budapest, Hungary). To 100 µL serum pipetted in a microcentrifuge tube, 20 µL Chromsystems Priming Solution (Cat. 61012) was added before freezing and transporting the samples for the evaluation of piperacillin and tazobactam concentrations at the Laboratory of Mass Spectrometry and Separation Technology, Department of Laboratory Medicine, Semmelweis University.

Table 1. Demographic properties of the subjects included in the study. Values or medians with ranges in parentheses are displayed. ICU, intensive care unit.

Characteristic	Value
Number of subjects	12
Age (years)	69.7 (45.3–86.4)
Male gender (%)	58
APACHE II score on admission to ICU (no unit)	25 (19–37)
CURB-65 mortality score on admission to ICU (no unit)	6.8 (2.7–27.8)
SAPS-E mortality score on admission to ICU (no unit)	42.3 (7.9–59.7)
SOFA mortality score on admission to ICU (no unit)	33.3 (33.3–50.0)
Body mass index on admission to ICU (kg/m^2)	29.6 (24.2–51.9)
Mean arterial pressure (mm Hg)	73.7 (56.7–120.7)
Serum creatinine (µmol/L)	98 (34–224)
Sodium (mmol/L)	137 (135–144)
Potassium (mmol/L)	4.4 (3.6–5.8)
Glucose (mmol/L)	9.1 (5.6–13.7)
Urea (mmol/L)	11.1 (2.6–41.8)
Total bilirubin (µmol/L)	15.9 (5.5–82.3)
Procalcitonin (µg/L)	0.5 (0.0–126.6)
C-reactive protein (mg/L)	129.4 (7.5–546.8)
White blood cell count ($\times 10^9$/L)	17.0 (9.0–31.1)
Thrombocyte count ($\times 10^3$/L)	274 (86–714)
Serum lactate (mmol/L)	1.8 (1.1–3.0)
Base excess (mEq/L)	5.0 (−8.4–13.7)
Hematocrit (L/L)	0.4 (0.3–0.7)
Interleukin-6 (ng/L)	32.0 (4.8–3629.0)
Pharmacokinetically relevant drugs administered on the day of blood sample collection (% of subjects):	
Dexmedetomidine	8.3
Alprazolam	16.6
Methylprednisolone	25.0
Ibuprofen	8.3
Fentanyl	8.3
Norepinephrine	66.7

Piperacillin concentrations were determined using a Jasco series 4000 robust high-performance liquid chromatograph equipped with an MD-4010 photodiode array detector (ABL&E-JASCO Hungary Ltd., Budapest, Hungary). The Chromsystems® Antibiotics in serum/plasma—HPLC in vitro diagnostic (CE-IVD) reagent kit, analytical column, multi-level calibrators and controls were employed for the analysis according to the instructions of the reagent kit manufacturer (ABL&E-JASCO Hungary Ltd., Budapest, Hungary). The analytical column was thermostatted at 30 °C, and the detection wavelength was 252 nm. The preparation of serum samples consisted of adding 200 µL of internal standard solution

(supplied with the reagent kit) to the stabilized serum, vortexing the mixture at 2000 rpm for 1 min, separating the supernatant by centrifugation (10 °C, 10,000× *g*, 5 min), and diluting 100 µL of supernatant with 100 µL of dilution buffer (also supplied with the reagent kit). Calibration equations were obtained by performing 1/concentration^2-weighted linear regression on piperacillin/internal standard peak area ratios. Internal controls were run at the beginning of each batch. In addition, the performance of the assay was tested regularly by participation in an external quality assessment scheme (#890—Antibiotics 02, Instand e.V., Düsseldorf, Germany).

The assay error polynomial (the fixed-effect component of the pop-PK models) was determined experimentally by quantitating piperacillin concentrations after spiking it in known concentrations to blank serum samples. Piperacillin was spiked at 20 different concentration levels and to 20 independent serum samples at each spiking level, in addition to the unspiked sera, all of which had been collected from different individuals for diagnostic purposes and had been left over from the laboratory tests. The de-identification of these samples had been performed, and no patient-related data were accessed by the authors. The standard deviation (SD) of measured piperacillin concentrations was calculated at each concentration level, including the blanks, and the regression of unweighted linear, second-degree and third-degree polynomials on the nominal concentration-SD data pairs was performed using Microsoft Excel to find the equation which could best describe this relationship, based on the work of Jelliffe and Tahani [18].

Nonparametric pharmacokinetic modeling was performed pursuant to the pioneering theoretical work of Roger W. Jelliffe and his co-workers, and by using the software tools they developed for this purpose. One- and two-compartment pop-PK models (#1 and #2) were constructed using 72 pieces of concentration data obtained from the 12 subjects recruited, and the NPAG algorithm incorporated into the Pmetrics^{TM} package run in the R environment (Laboratory of Applied Pharmacokinetics and Bioinformatics, University of Southern California, Los Angeles, CA, USA) [12,19]. The single-compartment models included the elimination rate constant (K) and the apparent volume of distribution (V), while the two-compartment models contained K, the rate constant of mass transfer from the central to the peripheral compartment (KCP) and of mass transfer from the peripheral to the central compartment (KPC), as well as the volume of the central compartment (V_c) as random-effect variables. Single-compartment models take into account a hypothetical, equilibrated fluid compartment without anatomic reality in which the drug is distributed evenly, and eliminated in a single process regardless of its route, with the exception of cases where relevant covariates are included in the model to account for various specific routes. Two-compartment models represent a central and a peripheral fluid compartment. The central compartment refers to the intravascular water space as well as extravascular spaces which are rapidly equilibrated with it, and into which the transport of the drug is not limited. The peripheral compartment corresponds to fluid spaces which are accessed by the drug, and which can even accumulate the drug, but which are also not well equilibrated with the central compartment. Again, elimination is considered as a single-route process unless covariates describing the impact of various routes are included in the model.

The evaluation of the models' performance was based on the strength of the correlation between predicted and observed concentrations, the slope and intercept of the regression line fit to these pairs of concentrations, as well as their weighted squared residuals (bias) and the bias-adjusted weighted squared residuals (imprecision). The performance indicators $-2 \times$ log-likelihood, and Akaike and Bayesian information criteria were also assessed. The decision to include candidate covariates or not was made by investigating their linear correlation, as well as the linear correlation of the square roots and the natural logarithms of their values, with the posteriors of the random-effect pharmacokinetic variables: K, KCP/KPC and V or V_c. A Pearson's correlation coefficient of at least 0.80 was considered strong enough for inclusion. One- and two-compartment models of piperacillin (models #3 and #4, respectively) were subsequently constructed by including creatinine clearance as a covariate, calculated as proposed by Jelliffe, and by making an estimate of the elimination

rate constant by using the function K = KI + KS × CRCL where KI is the rate constant accounting for non-renal elimination, KS is the rate constant accounting for renal elimination, and CRCL is the creatinine clearance [20,21]. KI and KS were the random-effect variables in these models.

Individual pharmacokinetic parameters (IPKP) of each subject were estimated in NPAG runs conducted using Pmetrics™ (version 2.1, IPKP-NPAG), as well as by using the BestDose™ standalone clinical pharmacokinetic modeling software (desktop version 1.127b, IPKP-NPB) which performs nonparametric maximum a posteriori probability (MAP) Bayesian analysis (Laboratory of Applied Pharmacokinetics and Bioinformatics, University of Southern California, Los Angeles, CA, USA). Fully artificial quasi-models were constructed by generating 399 random values with uniform distribution for each random-effect variable, and by creating 399 support points which contained a random value assigned to each parameter in the order they were created in, as well as a probability value of 1/399. The amount of the support points generated was the highest allowed by the BestDose™ software. The ranges the random values were generated in were made equivalent to those employed for the priors entered into the NPAG models. The dosing error, the model misspecification, and the timing error were set to 0.01. A total of 30 QMs were created for each type of PK model, and their performance was compared by calculating the mean squared errors of the predictions: $\sum(c_{obs} - c_{pred})^2/n_{dp}$, where n_{dp} stands for the number of data points; in the present work, $n_{dp} = 6$.

3. Results

3.1. Analytical Considerations

The performance of the piperacillin assay was monitored in each run. The internal control measurements yielded acceptable results in terms of the reagent kit manufacturer's specifications. A nonlinear relationship existed between the concentrations of piperacillin and their standard deviations, and was defined by the third-degree polynomial $SD = 0.255056 + 0.049873 \times c - 0.000361 \times c^2 + 0.000001 \times c^3$ with a determination coefficient of $r^2 = 0.9564$ (where c is the concentration of piperacillin, Figure 2). The correlation between piperacillin and tazobactam concentrations was strong, confirming previous findings, and could be described with the equation $c_{tazobactam} = 0.2267 \times c_{piperacillin} + 2.6802$ [17]. The slope of this equation displayed very close correspondence to 0.2150; which is the molar ratio of the administered drugs.

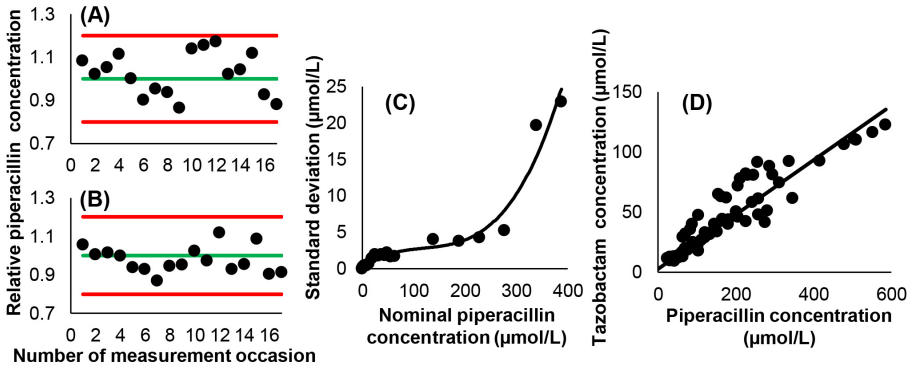

Figure 2. Characteristics of the employed piperacillin HPLC-UV assay. (**A**) Ratios of the measured and nominal concentrations of piperacillin in the low-level internal control samples. The green line corresponds to the nominal concentration, while red lines represent the limits of measurement acceptability. (**B**) Ratios of the measured and nominal concentrations of piperacillin in the high-level internal control samples. (**C**) Relationship between piperacillin concentration and the standard deviation of measurement results. (**D**) Relationship between piperacillin and tazobactam concentrations. Ordinary linear least squares regression yielded a Pearson's correlation coefficient of r = 0.9245.

3.2. Population Pharmacokinetic Models

The summary of the performance characteristics of the constructed population pharmacokinetic models #1–#4 is demonstrated in Table 2, as well as in Figures 3 and 4. All models performed well in terms of the agreement between observed and estimated posterior concentrations (slopes: 0.994–1.01, intercepts: −0.651–0.687, r^2 = 0.995–0.997), bias and imprecision. A statistically significant difference was found between one-and two-compartment models generated either without or with the inclusion of creatinine clearance as a covariate ($p < 0.001$). No statistical impact of including creatinine clearance as a covariate was identified, irrespective of the number of pharmacokinetic compartments. The posterior ranges of the random-effect pharmacokinetic variables which were subsequently considered when generating the random values for the support points of the QMs are displayed in Table 3.

Table 2. Performance of the constructed population pharmacokinetic models. AIC, Akaike information criterion. BIC, Bayesian information criterion. CRCL, creatinine clearance. LL, log-likelihood. #SP, number of support points.

Model No.	Compartments	Covariate	#SP	Bias (*p*-Value of Difference from 0)	Imprecision	−2 × LL	AIC	BIC	Shrinkage (%)
#1	1	None	12	−0.0697 (0.6591)	0.6465	478.8	485.2	491.6	0.030–0.012
#2	2	None	12	−0.1061 (0.8310)	1.3578	423.5	434.4	444.8	0.000–0.002
#3	1	CRCL	10	−0.0088 (0.8637)	0.6061	474.4	483.0	491.5	0.348–14.91
#4	2	CRCL	11	−0.0792 (0.6000)	1.3616	422.4	435.7	448.1	0.000–0.006

Table 3. Posterior ranges of the random-effect pharmacokinetic variables considered for generating the quasi-models. K, elimination rate constant. KCP, rate constant of mass transfer from the central to the peripheral compartment. KPC, rate constant of mass transfer from the peripheral to the central compartment. KI, non-renal elimination rate constant. KS, renal elimination rate constant. V, volume of distribution. V_c, volume of the central compartment.

Models with No Covariate Included					
Model No.	**Compartments**	**K (1/h)**	**V (L) or V_c (L)**	**KCP (1/h)**	**KPC (1/h)**
#1	1	0.10–0.75	10–100		
#2	2	0.10–1.70	5–35	0.05–5.00	0.05–5.00

Models with Creatinine Clearance Included as a Covariate						
Model No.	**Compartments**	**KS (1/h)**	**KI (1/h)**	**V (L) or V_c (L)**	**KCP (1/h)**	**KPC (1/h)**
#3	1	0.001–0.006	0.005–0.100	15–80		
#4	2	0.0005–0.0250	0.00–0.35	5–25	0.2–6.0	0.2–6.0

3.3. Individual Pharmacokinetic Models

Exemplary results of fitting the QMs to the individual concentration data series are displayed in Figure 5. The support points generated using random values covered the entire parameter space. When pop-PK models were used as priors, the posterior probabilities of only one or two support points were increased. When models #1 and #2 were applied, the support point with the increased probability corresponded to that generated for the given individual using NPAG. On the contrary, high posterior probabilities were obtained for several support points when applying the quasi-models, especially when two-compartment models were fitted.

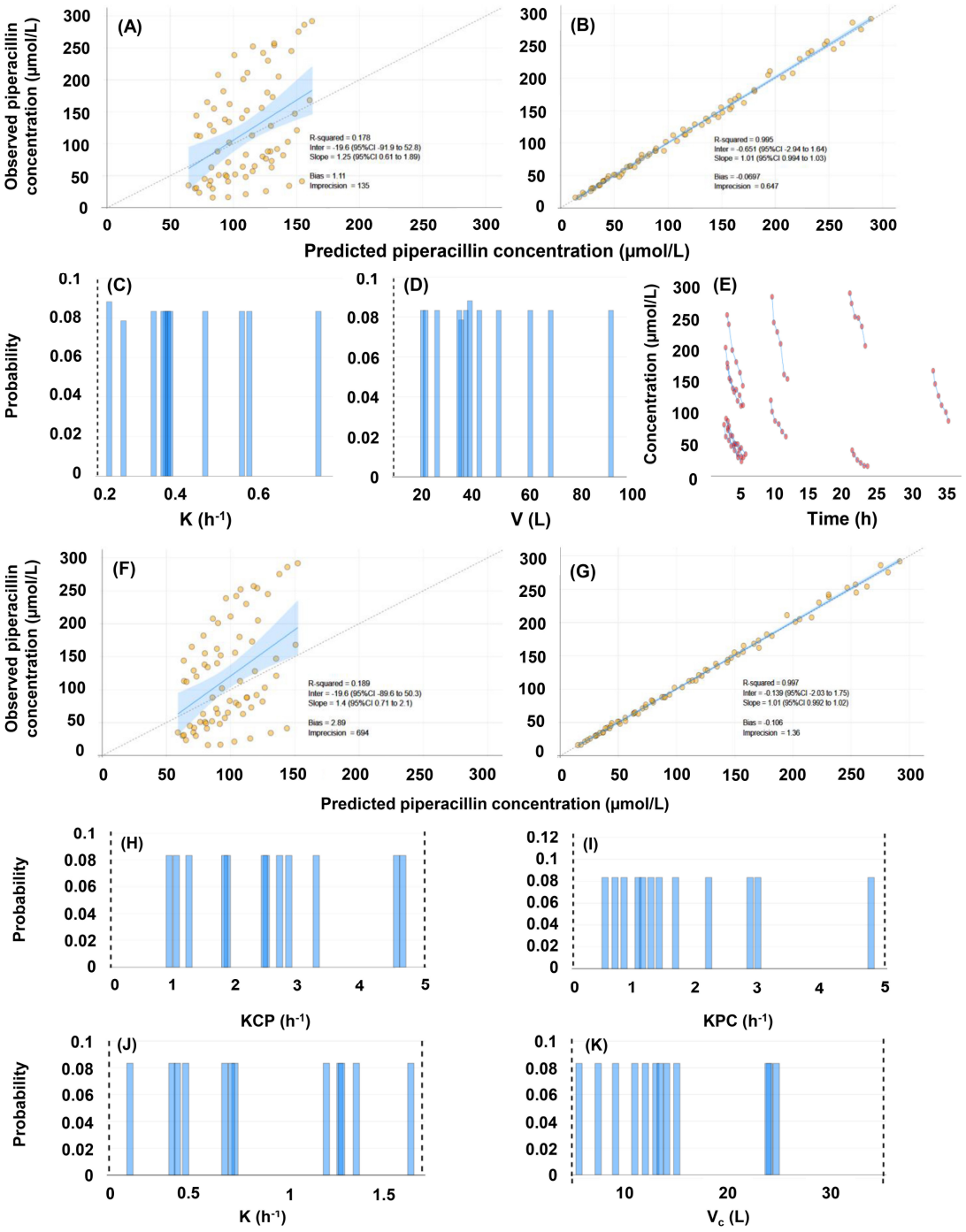

Figure 3. Evaluation of the population pharmacokinetic models of piperacillin, constructed with the inclusion of 72 concentrations obtained in 12 human subjects, and with no covariate. (**A**–**E**), evaluation of the single-compartment model (#1). (**A**) Comparison of predicted and observed concentrations based on population priors. (**B**) Comparison of predicted and observed concentrations based on individual posteriors. (**C**) Marginals of the elimination rate constant. (**D**) Marginals of the volume of distribution. (**E**) Raw concentration-time plots. (**F**–**K**), evaluation of the two-compartment model (#2). (**F**) Comparison of predicted and observed concentrations based on population priors. (**G**) Comparison of predicted and observed concentrations based on individual posteriors. (**H**–**I**) Marginals of the intercompartmental mass transfer rate constants: (**H**) central to peripheral compartment, (**I**) peripheral to central compartment. (**J**) Marginals of the elimination rate constant. (**K**) Marginals of the volume of distribution.

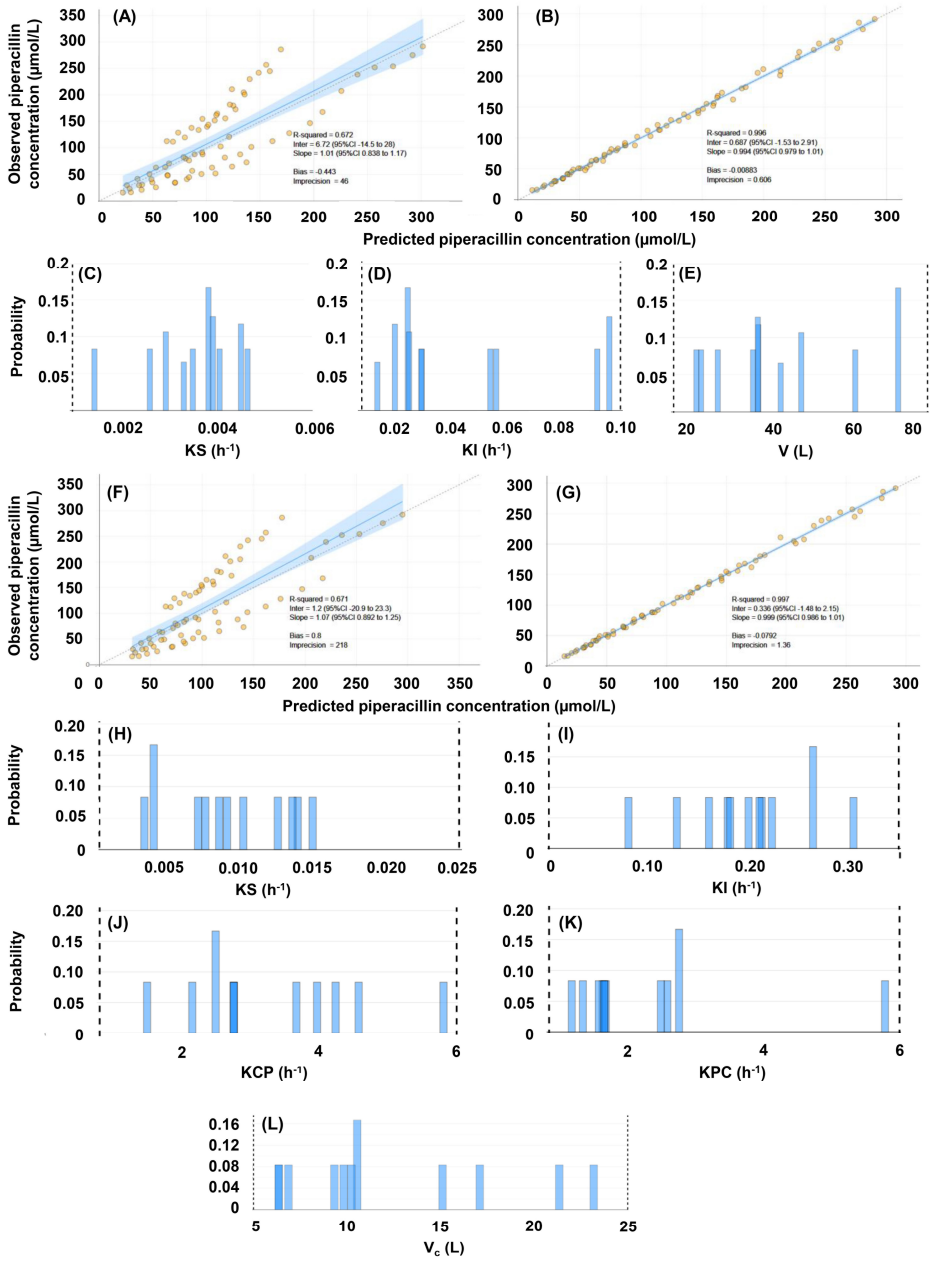

Figure 4. Evaluation of the population pharmacokinetic models of piperacillin, constructed with the inclusion of 72 concentrations obtained in 12 human subjects, and with the inclusion of creatinine clearance as a covariate. (**A**–**E**), evaluation of the single-compartment model (#3). (**A**) Comparison of predicted and observed concentrations based on population priors. (**B**) Comparison of predicted and observed concentrations based on individual posteriors. (**C**) Marginals of the renal elimination rate constant. (**D**) Marginals of the non-renal elimination rate constant. (**E**) Marginals of the volume of the central compartment. (**F**–**L**), evaluation of the two-compartment model (#4). (**F**) Comparison of predicted and observed concentrations based on population priors. (**G**) Comparison of predicted and observed concentrations based on individual posteriors. (**H**) Marginals of the renal elimination rate constant. (**J**) Marginals of the rate constant of mass transfer from the central to the peripheral compartment. (**K**) Marginals of the rate constant of mass transfer from the peripheral to the central compartment. (**L**) Marginals of the volume of the central compartment.

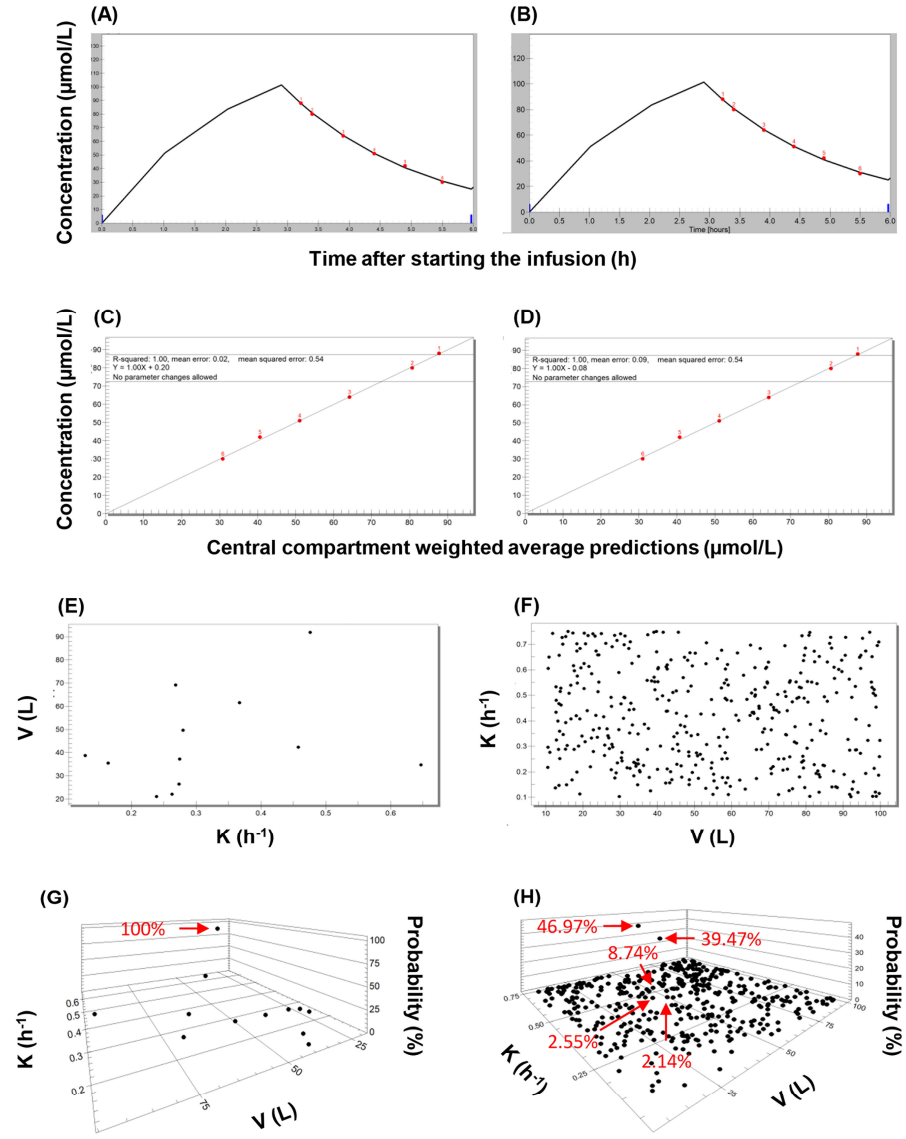

Figure 5. An overview of the main features of applying the nonparametric expectation maximization algorithm to population-based and quasi-models. The evaluation of piperacillin concentrations observed in subject 1 is shown as an illustration. (**A**) Concentration-time plot showing the observed values (red dots), and the curve fitted using the single-compartment population pharmacokinetic model with no covariate (model #1). (**B**) Concentration-time plot showing the observed values (red dots), and the curve fitted using the best-performing single-compartment quasi-model. (**C**) Correlation plot of observed piperacillin concentrations and those predicted using population pharmacokinetic model #1. (**D**) Correlation plot of observed piperacillin concentrations and those predicted using the best-performing single-compartment quasi-model. (**E**) Two-dimensional plot showing the support points of model #1. (**F**) Two-dimensional plot showing the support points of the best-performing single-compartment quasi-model employed as priors. (**G**) Three-dimensional plot of the posterior support points of model #1. (**H**) Three-dimensional plot of the posterior support points of the best-performing single-compartment quasi-model.

The mean squared errors, as well as the estimates of the random-effect pharmacokinetic variables obtained in each subject by applying the best-performing QMs, were compared to those obtained by using the support points of the pop-PK models as priors, and either the NPAG or the MAP Bayesian algorithm. The results of these comparisons are displayed in Table 4 and visualized in Figures 6 and 7. When a single-compartment model

with no covariate was employed, the MSEs obtained using the respective best-performing quasi-models ranged between 0.70 and 1.08 for 10 out of 12 subjects. The comparison of the MSEs with those obtained when using the pop-PK model support points as priors yielded IPKP-QM/IPKP-NPAG and IPKP-QM/IPKP-NPB ratios of 0.70–1.08 and 0.27–1.07, respectively. A ratio of 0.01–1.00 indicates better performance of the quasi-model-based predictions, a ratio of 1.00 corresponds to equivalence, while a ratio of >1.00 corresponds to better performance of the estimates made by using the pop-PK model support points. Each 0.01 increment corresponds to an additional 1% difference. The ratios of the individual elimination rate constants were 0.95–1.21 and 0.88–1.05, respectively, while the ratios of the volumes of distribution were 0.91–1.04 and 0.93–1.04, respectively. When creatinine clearance was included as a covariate in the single compartment model, the MSE ratios were 0.37–1.83 and 0.29–1.01, respectively. The ratios of the renal component of the elimination rate constant (KS) were 0.50–1.25 in both comparisons. The ratios of V ranged between 0.89–1.10 and 0.81–1.32, respectively, for 11 of the 12 subjects. When a two-compartment model with no covariate was applied, the MSE ratios were 0.09–111 and 0.01–1.60, respectively. The ratios of K were 0.49–1.33 in both comparisons, while the ratios of the estimated V_c were 0.75–2.45 and 0.75–2.49, respectively. The KCP/KPC ratios ranged between 0.27 and 1.80, and 0.27 and 1.66, respectively. Finally, when a two-compartment model with a creatinine clearance covariate was employed, the MSE ratios were 1.02–5.47 and 0.05–1.61, respectively (with the exception of subject 10, for whom the MSE ratios obtained were 181 and 5.33, respectively). The ratios of KS were 0.14–2.75 and 0.14–2.33, and the ratios of the estimated V_c were 0.84–3.55 and 0.83–2.56, respectively. The KCP/KPC ratios were 0.15–1.70 and 0.15–1.72, respectively. The comprehensive evaluation of the performance of QMs is provided in the Supplementary File.

Table 4. Comparison of the performance of quasi-models (QM) and population pharmacokinetic (pop-PK) models when applying nonparametric adaptive grid (NPAG) modeling, or nonparametric maximum a posteriori probability (MAP) Bayesian analysis. Ratios of the mean squared errors (MSE) and of pharmacokinetic parameters are shown. In the case of MSE, a ratio of 0.01–1.00 corresponds to the superior performance of the quasi-model-based estimation, a ratio of 1.00 corresponds to equivalence, while a ratio of >1.00 corresponds to the better performance of the pop-PK model-based estimation; each 0.01 increment corresponds to an additional 1% difference. K, elimination rate constant. KCP, rate constant of mass transfer from the central to the peripheral compartment. KPC, rate constant of mass transfer from the peripheral to the central compartment. KS, renal elimination rate constant. V, apparent volume of distribution. Vc, apparent volume of the central compartment.

Model	Comparator	Value Obtained for QM/Value Obtained for pop-PK Model, NPAG	Value Obtained for QM/Value Obtained for pop-PK Model, MAP Bayesian Analysis
#1	MSE	0.70–1.08 (Subject 4: 1.83, Subject 10: 5.67)	0.27–1.07
	K	0.95–1.21	0.88–1.05
	V	0.91–1.04	0.93–1.04
#2	MSE	0.09–111	0.01–1.60 (Subject 8: 7.40)
	K	0.49–1.33	0.49–1.33
	Vc	0.75–2.45	0.75–2.49
	KCP/KPC	0.27–1.80	0.27–1.66
#3	MSE	0.37–1.83 (Subject 9: 32.54, Subject 10: 4.89)	0.29–1.01
	KS	0.50–1.25	0.50–1.25
	V	0.89–1.10 (Subject 9: 3.55)	0.81–1.32 (Subject 9: 1.99)
#4	MSE	1.02–5.47 (Subject 10: 181)	0.05–1.61 (Subject 10: 5.33)
	KS	0.14–2.75	0.14–2.33
	Vc	0.84–3.55	0.83–2.56
	KCP/KPC	0.15–1.70	0.15–1.72

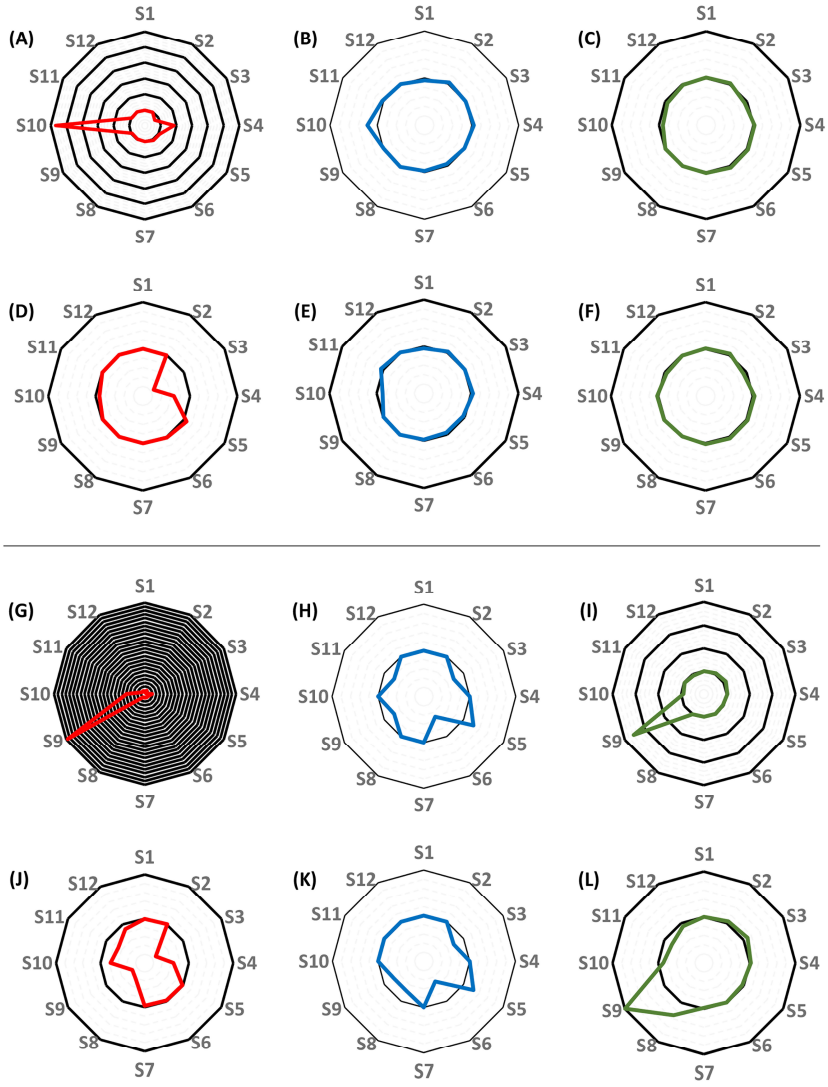

Figure 6. Radar plots showing the differences between the performance of the best-performing single-compartment quasi-models and of the single-compartment population pharmacokinetic models (#1 and #3) for each subject. (**A**–**F**), comparison of the performance of models constructed without the inclusion of creatinine clearance as a covariate. (**A**–**C**), the comparison of the mean squared errors (MSE) of predictions (**A**), the elimination rate constants (**B**), and the volumes of distribution (**C**) obtained by applying the best-performing quasi-models to the estimates obtained using non-parametric adaptive grid (NPAG) modeling and the population PK models. (**D**,**F**), the comparison of the MSE's of predictions (**D**), the elimination rate constants (**E**), and the volumes of distribution (**F**) obtained by applying the best-performing quasi-models to the estimates obtained when conducting nonparametric maximum a posteriori probability (MAP) Bayesian analysis on the population PK models. (**G**–**L**), comparison of the performance of models constructed with the inclusion of creatinine clearance as a covariate. (**G**–**I**), the comparison of the MSE's of predictions (**G**), the elimination rate constants (**H**), and the volumes of distribution (**I**) obtained by applying the best-performing quasi-models to the estimates obtained using NPAG and the population PK models. (**J**–**L**), the comparison of the MSEs of predictions (**J**), the elimination rate constants (**K**), and the volumes of distribution (**L**) obtained by applying the best-performing quasi-models to the estimates obtained when conducting MAP Bayesian analysis on the population PK models. Each black circle represents an additional 100% increase in the ratio of values obtained by applying the best-performing quasi-models and of values obtained by applying the NPAG or the MAP Bayesian algorithm to the population PK models, with the central black circle corresponding to 100% agreement.

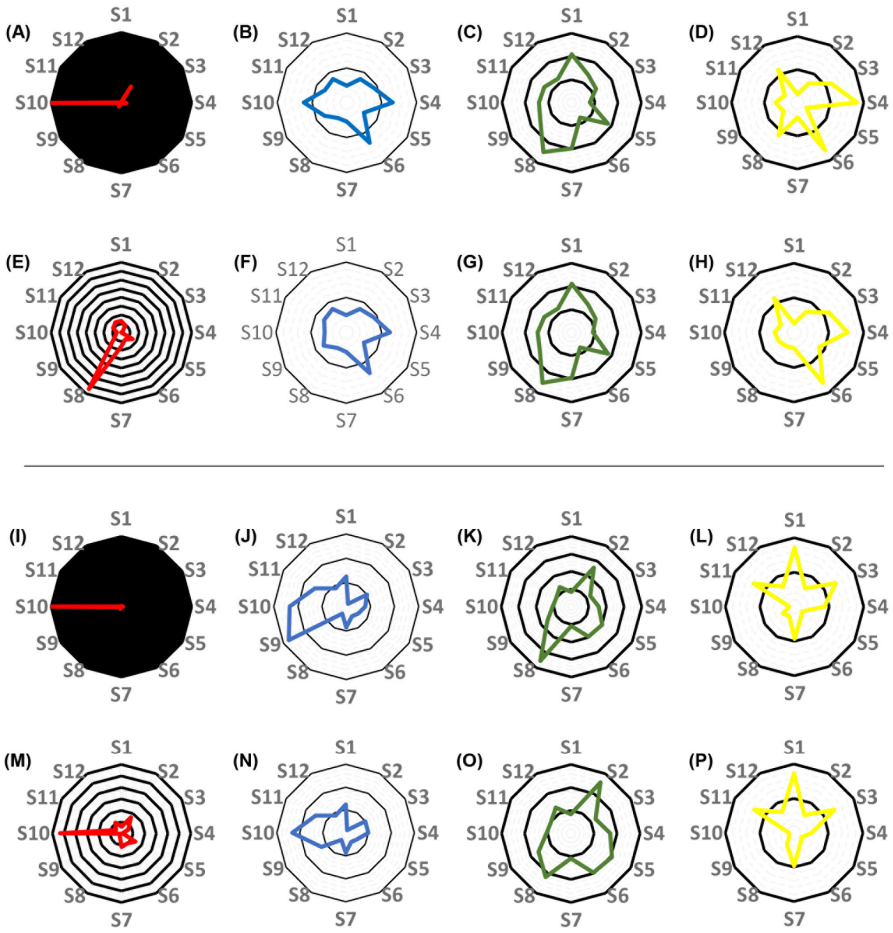

Figure 7. Radar plots showing the differences between the performance of the best-performing two-compartment quasi-models and of the two-compartment population pharmacokinetic models (#2 and #4) for each subject. (**A**–**H**), comparison of the performance of models constructed without the inclusion of creatinine clearance as a covariate. (**A**–**D**), the comparison of the mean squared errors (MSE) of predictions (**A**), the elimination rate constants (**B**), the volumes of the central compartment (**C**), and the ratios of the central-to peripheral compartment and the peripheral-to-central compartment mass transfer rate constants (KCP/KPC ratio, (**D**)) obtained by applying the best-performing quasi-models to the estimates obtained when applying nonparametric adaptive grid (NPAG) modeling and the population PK data. (**E**–**H**), the comparison of the MSEs of predictions (E), the elimination rate constants (**F**), the volumes of the central compartment (**G**), and the KCP/KPC ratios (**H**) obtained by applying the best-performing quasi-models to the estimates obtained when applying nonparametric maximum a posteriori probability (MAP) Bayesian analysis on the population PK data. (**I**–**P**), comparison of the performance of models constructed with the inclusion of creatinine clearance as a covariate. (**I**–**L**), the comparison of the MSEs of predictions (**I**), the elimination rate constants (**J**), the volumes of the central compartment (**K**), and the KCP/KPC ratios (**L**) obtained by applying the best-performing quasi-models to the estimates obtained when applying NPAG algorithm and the population PK data. (**M**–**P**), the comparison of the MSEs of predictions (**M**), the elimination rate constants (**N**), the volumes of the central compartment (**O**), and the ratios of the KCP/KPC ratios (**P**) obtained employing the best-performing quasi-models to the estimates obtained when applying MAP Bayesian analysis on the population PK data. Each black circle represents an additional 100% increase in the ratio of values obtained by applying the best-performing quasi-models and of values obtained by applying the NPAG or the MAP Bayesian algorithm to the population PK models, with the central black circle corresponding to 100% agreement.

The concentration curves fitted by nonparametric MAP Bayesian analysis using the best-performing individual QMs as priors, along with the quality of the fits, are available in the Supplementary File. The determination coefficients of the relationship between the predicted and observed piperacillin concentrations were 0.933–0.999, 0.922–0.999, 0.935–0.999 and 0.935–0.999 when applying model #1–#4, respectively. Considerable mismatches between predicted and observed concentrations were observed when two-compartment QMs were applied with no covariate for the data of subject 9. In the case of subject 10, the determination coefficients obtained when single-compartment models (model #1 and model #3) were applied were 0.831–0.834 and 0.833–0.834, respectively. The underlying reason for the weaker agreement appeared to be a single sample (sample 2) for which the measured piperacillin concentration was consistently lower than predicted. Two-compartment quasi-models were clearly not suitable for this patient, as reflected by the determination coefficients 0.292–0.568 and 0.359–0.513 obtained for models #2 and #4, respectively. The poor agreement between predicted and observed values could be traced back to the algorithm included in the nonparametric MAP Bayesian analysis; when the pop-PK models were employed as priors, running NPAG resulted in determination coefficients of 0.985–0.987, whereas the application of the MAP Bayesian algorithm resulted in coefficients of 0.136–0.831.

4. Discussion

Several piperacillin population pharmacokinetic models are available in the literature, predominantly with the consideration of single- or, more often, two-compartment models including creatinine clearance as a covariate [22–24]. Nevertheless, it has recently become apparent that the suitability of these models for making estimates of individual pharmacokinetic properties can be highly variable. A multicenter study revealed only three models which provided acceptable estimates and absolute prediction errors. Interestingly, the authors of this study concluded that the accuracy of estimates was gender-dependent [24].

Nonparametric pharmacokinetic modeling is a powerful tool for guiding individualized drug therapy. The pharmacokinetic characteristics of the individuals included in the modeling process are retained instead of constructing statistical summaries which do not show individual values. Consequently, the identification of subpopulations and individual outliers, which are often of special clinical interest, is feasible. The evaluation and comparison of nonparametric models is straightforward, and the limitations of the constructed models are transparent.

Multimodel approaches have been proposed to improve individual estimates for drugs such as tacrolimus in liver, lung and bowel transplanted patients. For each individual, a model could be selected by employing a weight-based algorithm which compared the median prediction error of each model to that of a set of nine models picked randomly from a library consisting of 70 population models [25]. Such efforts can be supported further by employing models augmented by computer algorithms. Mao et al. demonstrated the efficiency of models based on machine learning (ML), specifically of those built using an artificial neural network algorithm, to be superior to that of population pharmacokinetic models when estimating cyclosporin A concentrations [8]. Hybrid pop-PK-ML models have been shown to have a performance superior to that of pop-PK models alone with iohexol and isavuconazole [26,27]. In addition to improving modeling performance, the tremendous saving on modeling time offered by ML algorithms is an important advantage [28]. Such efforts indicate that the application of ML-based approaches, should they rely on the integrated analysis of several pop-PK models or on artificial algorithms, could be the next important step towards the implementation of personalized drug therapy.

The methodology presented in this work is similar to an earlier concept created by Jelliffe et al., and based on hybrid Bayesian analysis [29]. Jelliffe et al. proposed the augmentation of nonparametric population PK model support points with further ones, generated by the modeler. These additional support points were evenly distributed in a parameter subspace (not necessarily within the parameter space defined by the pop-PK

model), formed a symmetric grid, and were assigned equal probabilities. Our methodology relies on the generation of random support points with equal probabilities (currently within the parameter space defined by the population PK model), and on building multiple models. This approach is based on a simple computing algorithm, and is not bound by the set of support points of the pop-PK model. Instead of employing the conventional workflow of generating a population model, and then applying it to individual data, any number of such QMs can be generated and tested until a set of support points displaying acceptable performance in estimating drug exposure in the given patient is found. An important advantage of employing QMs is the simplicity and the low time-consumption of their generation, as well as the transparency of their operation. In most of our analyses, the performance of the best-performing QMs was equivalent to, or better than that of MAP Bayesian analysis or of the NPAG model; although the latter actually contained the set of the estimated pharmacokinetic properties of each individual. Two-compartment models of piperacillin were superior in performance to single-compartment models when considering statistical indicators at population level but, in view of the MSE's obtained, could not be favored in all individuals. Our results demonstrate that the type of pharmacokinetic model which provides the best performance may have to be determined for each individual. As an example, a two-compartment model could not be fitted to the data of subject 10, while a single-compartment model with creatinine clearance included as a covariate provided considerably worse fits for subject 9 in comparison to all other models employed. This indicates that flexibility in selecting the most suitable type of the PK model from a set of models in each individual case may be relevant to clinical practice, and also highlights the importance of collecting a set of blood samples from each patient which is sufficiently large for comparing the performance of various PK models (Table 5).

Table 5. Mean squared errors obtained for each subject using the best-performing quasi-model. CRCL, creatinine clearance.

	Mean Squared Errors of the Quasi-Models Showing Best Performance			
Number of Subject	**One Compartment, No Covariate**	**One Compartment, CRCL Covariate**	**Two Compartments, No Covariate**	**Two Compartments, CRCL Covariate**
1	0.538	0.534	0.679	0.629
2	22.552	22.853	15.219	16.599
3	1.623	1.727	0.755	1.196
4	66.147	65.318	9.096	13.452
5	14.362	13.305	5.292	5.968
6	49.163	47.331	46.657	46.923
7	16.046	15.458	13.018	8.677
8	22.919	22.909	28.703	24.227
9	26.125	612.196	18.442	23.742
10	25.978	25.999	455.938	743.067
11	99.281	99.798	96.929	94.461
12	10.755	10.732	6.882	5.302

Usually, the subjects are divided into a training set and a test (or validation) set when evaluating the performance of a pharmacokinetic model [30]. In the presented work, the training and testing set had to be the same due to the fact that the support points of the pop-PK models and the QMs were independent of each other. The NPAG algorithm employs several thousand support points for selecting the best fit; therefore, it is extremely reliable in making the most efficient estimates in a setting of rich sampling such as the one employed in the present work. The results show that the differences in IPKP-NPAG versus IPKP-NPB estimates were larger than those obtained for IPKP-NPB versus IPKP-QM estimates. The performance of QMs compared to that of the pop-PK models when employing the MAP Bayesian algorithm provides evidence that they are efficient alternatives to pop-PK models.

The inclusion of creatinine clearance as a covariate did not lead to the improvement of the pharmacokinetic models (Table 2). When CRCL was included in the single-compartment model #3, the shrinkage was considerably higher than that observed for model #1. Since this effect of the inclusion of the CRCL covariate was not observed in the case of two-compartment models (#2 and #4), it seems rational to conclude that the result of testing this covariate was helpful in model selection. It is rational to assume that the importance of including CRCL as a covariate may become even more apparent when the course of piperacillin pharmacokinetics is monitored over several days, considering the fact that the renal function of critically ill patients is often unstable.

Creatinine clearance was estimated using the equation described by Jelliffe, which allows calculation without measuring urinary creatinine levels. This equation was incorporated into the BestDose^{TM} software. Calculation is based on Equation (1):

$$\frac{0.4 \times BW \times (c_2 - c_1)}{T} = P_{adj} - \frac{c_1 + c_2}{2} \times CCR \times 1440 \quad (1)$$

where BW corresponds to body weight in kg, c_1 and c_2 are the first and second serum creatinine concentrations in mg/dL, respectively, P_{adj} is the adjusted creatinine production in mg and CCR is the creatinine clearance in hundreds of mL per minute [20]. It must be noted that estimating creatinine clearance by measuring serum creatinine is not an optimal approach in the critically ill, as sarcopenia or a poor clinical status influence serum creatinine concentrations [31]. Furthermore, creatinine is not only filtered, but also secreted by the kidneys [32]. The impact of changes in the clinical status on serum creatinine can be detected with a delay of 24–36 h, and only when at least half of the nephrons have ceased to function. Since the present work focused on piperacillin pharmacokinetics in the first 24 h of intensive care, these factors are not expected to have influenced our findings.

Evaluating inulin clearance is often considered as the gold standard for characterizing the glomerular filtration rate, but is impractical in the clinical setting [33]. Various biomarkers (such as cystatin C) have been proposed, and it seems that multimarker panels may be superior to single laboratory parameters in this respect [34]. An important yet challenging area of future research is the incorporation of novel biomarkers of renal function in pharmacokinetic models, especially in unstable, critically ill patients. Jelliffe's formula is valuable as it takes the instability of renal function into account, and is compatible with interacting multiple modeling, which is an efficient approach to describing even the rapidly changing pharmacokinetics of a drug in unstable patients [35]. Combined with QMs, this approach may be highly useful in detecting changes in the clinical status of critically ill patients receiving piperacillin.

The following limitations apply to the results presented: (1) the efficiency of QMs was tested only within the ranges of the random-effect pharmacokinetic variables established in the NPAG runs; (2) the number of subjects included in the study was small, and model optimization was not performed by, for example, evaluating the inclusion of covariates other than creatinine clearance; and (3) the QMs did not allow the inference of real pharmacokinetic information on the population involved in the modeling process. The goal of making efficient individual estimates was nevertheless attained; therefore, the QMs have the potential to be applicable for predicting future concentrations in individuals, which is the most important aim in the clinical setting. From a clinical standpoint, a minor limitation is that obtaining six concentration points can be difficult in real clinical scenarios. A further exploration of the performance of the QMs on sets of less richly samples patients will, therefore, be necessary.

Finally, the extensive experimental elaboration of the assay error polynomial proved to be essential for achieving the described performance of the QMs. While the options of an additive or a multiplicative error model are available when running NPAG, and the definition of a higher value for the respective constant may compensate for a less accurate assay error model, the definition of additional error terms is more complex in the BestDose^{TM} software, and the compensation may require entering unrealistic values for dosing and sampling

error, or may not be possible at all. Most often, linear equations and second-degree polynomials can be applied to describe the quantitative relationship between analyte concentration and the method standard deviation of liquid chromatography-tandem mass spectrometry methods and immunoassays, respectively. In our case, a third-degree polynomial fit was clearly appropriate for the employed HPLC-UV assay [36,37].

5. Conclusions

The joint concept of rich sampling and the use of fully artificial nonparametric quasi-models can provide an efficient augmentation tool for planning and monitoring individualized drug regimens, and may therefore be considered as an alternative to limited sampling strategies employed when a larger set of subjects is available. Nonparametric QMs can be especially useful when the number of subjects available for pop-PK modeling is small, which is a common scenario in the clinical setting, especially in the case of drugs which have been introduced to the market only recently.

The performance of two-compartment pharmacokinetic models has proved to be superior to that of single-compartment models, pointing to the benefit of rich sampling. Including creatinine clearance as a covariate did not lead to a significant improvement in model performance. Nevertheless, such models may be valuable in the future when longitudinal analyses are conducted in patients with unstable renal function.

Supplementary Materials: The following supporting information can be downloaded at: https://www.mdpi.com/article/10.3390/pharmaceutics16030358/s1, Figure S1. Individual concentration-time curves obtained when applying the best-performing quasi-models to the observed piperacillin concentrations. Each row shows the curves fitted, along with the correlation plots of the observed and predicted concentrations for a Subject (S1–S12). The horizontal and vertical axes of the fitted curve plots represent time (h) and piperacillin concentration (μmol/L), respectively. The origin (time = 0 h) corresponds to the time of the initiation of treatment with piperacillin/tazobactam. The axes of the correlation plots are predicted and observed piperacillin concentrations (μmol/L). CRCL, creatinine clearance. Table S1. Coefficients of correlation between the values of the covariates tested, and the pharmacokinetic variables modeled. K, elimination rate constant. KCP, rate constant of the mass transfer from the central to the peripheral compartmetnt. KPC, rate constant of the mass transfer from the peripheral to the central compartment. V, Volume of distribution. Vc, volume of the central compartment. Table S2: Performance of the quasi-models for Subject 1; Table S3: Performance of the quasi-models for Subject 2; Table S4: Performance of the quasi-models for Subject 3; Table S5: Performance of the quasi-models for Subject 4; Table S6: Performance of the quasi-models for Subject 5; Table S7: Performance of the quasi-models for Subject 6; Table S8: Performance of the quasi-models for Subject 7; Table S9: Performance of the quasi-models for Subject 8; Table S10: Performance of the quasi-models for Subject 9; Table S11: Performance of the quasi-models for Subject 10; Table S12: Performance of the quasi-models for Subject 11; Table S13: Performance of the quasi-models for Subject 12.

Author Contributions: Conceptualization, G.B.K., C.K., I.V. and M.N.N.; methodology, C.K., G.B.K. and I.V.; software, M.N.N.; validation, I.V. and G.B.K.; formal analysis, G.B.K., C.K. and I.V.; investigation, C.K., I.Z. and G.B.K.; resources, G.B.K., I.Z., Z.N., I.K. and C.K.; data curation, C.K., G.B.K., Z.N. and I.K.; writing—original draft preparation, G.B.K.; writing—review and editing, M.N.N., C.K., I.V., I.Z., Z.N. and I.K.; visualization, G.B.K.; supervision, C.K.; project administration, C.K. and G.B.K. All authors have read and agreed to the published version of the manuscript.

Funding: This research received no external funding.

Institutional Review Board Statement: The study was conducted in accordance with the Declaration of Helsinki, and approved by the National Institute of Pharmacy and Nutrition (Budapest, Hungary, identifier of approval document: 261-IK/2020).

Informed Consent Statement: Informed consent was obtained from all subjects involved in the study, or their closest relatives if the clinical condition of the subject did not allow the proper accomplishment of the recruitment procedure.

Data Availability Statement: All relevant data are contained in the article.

Acknowledgments: The nurses of the Department of Anesthesiology and Intensive Care, Uzsoki Teaching Hospital (Budapest, Hungary) are gratefully acknowledged for taking the highest care in adhering to professional standards and institutional protocols, as well as to the protocols of the study, which was critically important for managing and successfully processing patient samples and data. Róbert Farkas and Krisztián Bocskai are gratefully acknowledged for performing the analysis of piperacillin and tazobactam. We thank Ferenc Olajos for conducting interleukin-6 assays. József Fűrész is acknowledged for providing expert advice for the interpretation of results.

Conflicts of Interest: The authors declare no conflict of interest.

References

1. Darwich, A.S.; Polasek, T.M.; Aronson, J.K.; Ogungbenro, K.; Wright, D.F.; Achour, B.; Reny, J.-L.; Daali, Y.; Eiermann, B.; Cook, J.; et al. Model-informed precision dosing: Background, requirements, validation, implementation, and forward trajectory of individualizing drug therapy. *Ann. Rec. Pharmacol. Toxicol.* **2021**, *61*, 225–245. [CrossRef] [PubMed]
2. Pérez-Blanco, J.S.; Lanao, J.M. Model-informed precision dosing. *Pharmaceutics* **2022**, *14*, 2731. [CrossRef] [PubMed]
3. Tyson, R.J.; Park, C.C.; Powell, J.R.; Patterson, J.H.; Weiner, D.; Watkins, P.B.; Gonzalez, D. Precision dosing priority criteria: Drug, disease, and patient population variables. *Front. Pharmacol.* **2020**, *11*, 420. [CrossRef] [PubMed]
4. Wicha, S.G.; Märtson, A.-G.; Nielsen, E.I.; Koch, B.C.P.; Friberg, L.E.; Alffenaar, J.-W.; Minichmayr, I.K. From therapeutic drug monitoring to model-informed precision dsing for antibiotics. *Clin. Pharm. Ther.* **2021**, *109*, 928–941. [CrossRef] [PubMed]
5. Evans, L.; Rhodes, A.; Alhazzani, W.; Antonelli, M.; Coopersmith, C.M.; French, C.; Machado, F.R.; McIntyre, L.; Ostermann, M.; Prescott, H.C.; et al. Surviving sepsis campaign: International guidelines for management of sepsis and septic shock 2021. *Intensiv. Care Med* **2021**, *47*, 1181–1247. [CrossRef] [PubMed]
6. Visibelli, A.; Roncaglia, B.; Spiga, O.; Santucci, A. The impact of artificial intelligence in the Odyssey of rare diseases. *Biomedicines* **2023**, *11*, 887. [CrossRef]
7. Damnjanovic, I.; Tsyplakova, N.; Stefanovic, N.; Tosic, T.; Catic-Dordevic, A.; Karalis, V. Joint use of population pharmacokinetics and machine learning for optimizing antiepileptic treatment in paediatric population. *Ther. Adv. Drug Saf.* **2023**, *14*, 20420986231181336. [CrossRef]
8. Mao, J.; Chen, Y.; Xu, L.; Chen, W.; Chen, B.; Fang, Z.; Qin, W.; Zhong, M. Applying machine learning to the pharmacokinetic modeling of cyclosporine in adult renal transplant recipients: A multi-method comparison. *Front. Pharmacol.* **2022**, *13*, 1016399. [CrossRef]
9. Verhaeghe, J.; Dhaese, S.A.M.; De Corte, T.; Mijnsbrugge, D.V.; Aardema, H.; Zijlstra, J.G.; Verstraete, A.G.; Stove, V.; Colin, P.; Ongenae, F.; et al. Development and evaluation of uncertainty quantifying machine learning models to predict piperacillin plasma concentrations in critically ill patients. *BMC Med. Inform. Decis. Mak.* **2022**, *22*, 224. [CrossRef]
10. Poweleit, E.A.; Vinks, A.A.; Mizuno, T. Artificial intelligence and machine learning approaches to facilitate therapeutic drug management and model-informed precision dosing. *Ther. Drug Monit.* **2023**, *45*, 143–150. [CrossRef] [PubMed]
11. Leary, R.; Jelliffe, R.; Schumitzky, A.; Van Guilder, M. An adaptive grid non-parametric approach to pharmacokinetic and dynamic (PK/PD) population models. In Proceedings of the 14th IEEE Symposium on Computer-Based Medical Systems. CBMS 2001, Bethesda, MD, USA, 26–27 July 2001; pp. 389–394.
12. Neely, M.; van Guilder, M.; Yamada, W.; Schumitzky, A.; Jelliffe, R. Accurate detection of outliers and subpopulations with Pmetrics, a non-parametric and parametric pharmacometrics modeling and simulation package for R. *Ther. Drug Monit.* **2012**, *34*, 467–476. [CrossRef]
13. Tatarinova, T.; Neely, M.; Bartroff, J.; van Guilder, M.; Yamada, W.; Bayard, D.; Jelliffe, R.; Leary, R.; Chubatiuk, A.; Schumitzky, A. Two general methods for population pharmacokinetic modeling: Non-parametric adaptive grid and non-parametric Bayesian. *J. Pharmacokinet. Pharmacodyn.* **2013**, *40*, 189–199. [CrossRef]
14. Jelliffe, R. Using the BestDose clinical software—Examples with aminoglycosides. In *Individualized Drug Therapy for Patients. Basic Foundations, Relevant Software, and Clinical Applications*; Jelliffe, R.W., Neely, M., Eds.; Elsevier: Amsterdam, The Netherlands, 2016; pp. 59–75.
15. de Velde, F.; de Winter, B.C.M.; Neely, M.N.; Strojil, J.; Yamada, W.M.; Harbarth, S.; Huttner, A.; van Gelder, T.; Koch, B.C.P.; Miller, A.E. Parametric and nonparametric population pharmacokinetic models to assess probability of target attainment of imipenem concentrations in critically ill patients. *Pharmaceutics* **2021**, *13*, 2170. [CrossRef] [PubMed]
16. Vincze, I.; Czermann, R.; Nagy, Z.; Kovács, M.; Neely, M.N.; Farkas, R.; Kocsis, I.; Karvaly, G.B.; Kopitkó, C. Assessment of antibiotic pharmacokinetics, molecular biomarkers and clinical status in critically ill adults diagnosed with community-acquired pneumonia and receiving intravenous piperacillin/tazobactam and hydrocortisone over the first five days of intensive care: And observational study (STROBE compliant). *J. Clin. Med.* **2022**, *11*, 4140. [PubMed]
17. Wallenburg, E.; ter Heine, R.; Schouten, J.A.; Raaijmakers, J.; ten Oever, J.; Kolwijck, E.; Burger, D.M.; Pickkers, P.; Frenzel, T.; Brüggemann, R.J.M. An integral pharmacokinetic analysis of piperacillin and tazobactam in plasma and urine in critically ill patients. *Clin. Pharmacokinet.* **2022**, *61*, 907–918. [CrossRef] [PubMed]
18. Jelliffe, R.W.; Tahani, B. Pharmacoinformatics: Equations for serum drug assay error patterns; implications for therapeutic drug monitoring and dosage. *Proc. Annu. Symp. Comput. Appl. Med. Care* **1993**, 517–521.

19. R Core Team. *R: A Language and Environment for Statistical Computing*; R Foundation for Statistical Computing: Vienna, Austria, 2022. Available online: https://www.R-project.org/ (accessed on 5 December 2023).
20. Jelliffe, R. Estimation of creatinine clearance in patients with unstable renal function, without a urine specimen. *Am. J. Nephrol.* **2002**, *22*, 320–324. [CrossRef] [PubMed]
21. Jelliffe, R.W.; Iglesias, T.; Hurst, A.K.; Foo, K.A.; Rodriguez, J. Individualising gentamicin dosage regimens. A comparative review of selected models, data fitting methods and monitoring strategies. *Clin. Pharmacokinet.* **1991**, *21*, 461–478. [CrossRef]
22. Alobaid, A.S.; Wallis, S.C.; Jarret, P.; Starr, T.; Stuart, J.; Lassig-Smith, M.; Mejia, J.L.O.; Roberts, M.S.; Roger, C.; Udy, A.A.; et al. Population pharmacokinetics of piperacillin in nonobese, obese, and morbidly obese critically ill patients. *Antimicrob. Agents Chemother.* **2017**, *61*, e01276-16. [CrossRef] [PubMed]
23. Hemmersbach-Miller, M.; Balevic, S.J.; Winokur, P. Population pharmacokinetics of piperacillin/tazobactam across the adult lifespan. *Clin. Pharmacokinet.* **2023**, *62*, 127–139. [CrossRef]
24. Greppmair, S.; Brinkmann, A.; Roehr, A.; Frey, O.; Hagel, S.; Dorn, C.; Marsot, A.; El-Haffaf, I.; Zoller, M.; Saller, T.; et al. Towards model-informed precision dosing of piperacillin: Multicenter systematic external evaluation of pharmacokinetic models in critically ill adults with a focus on Bayesian forecasting. *Intensive Care Med.* **2023**, *49*, 966–976. [CrossRef]
25. Hoffert, Y.; Vanleberghe, B.T.K.; Kuypers, D.; Vos, R.; Vanuytsel, T.; Verbeek, J.; Dreesen, E. *An Automated Multi-Model Selection Algorithm to Improve Precision Dosing of Tacrolimus in Liver, Lung, and Bowel Transplant Recipients*; PAGE Meeting: A Coruna, Spain, 2023.
26. Destere, A.; Marquet, P.; Gandonniere, C.S.; Asberg, A.; Loustaud-Ratti, V.; Carrier, P.; Ehrmann, S.; Barin-Le Guellec, C.; Premaud, A.; Woillard, J.-B. A hybrid model associating population pharmacokinetics with machine learning: A case study with iohexol clearance estimation. *Clin. Pharmacokinet.* **2022**, *61*, 1157–1165. [CrossRef]
27. Destere, A.; Marquet, P.; Labriffe, M.; Drici, M.-D.; Woillard, J.-B. A hybrid algorithm combining population pharmacokinetic and machine learning for isavuconazole exposure prediction. *Pharm. Res.* **2023**, *40*, 951–959. [CrossRef]
28. Keutzer, L.; You, H.; Farnoud, A.; Nyberg, J.; Wicha, S.G.; Maher-Edwards, G.; Vlasakakis, G.; Moghaddam, G.K.; Svensson, E.M.; Menden, M.P.; et al. Machine learning and pharmacometrics for prediction of pharmacokinetic data: Differences, similarities and challenges illustrated with rifampicin. *Pharmaceutics* **2022**, *14*, 1530. [CrossRef]
29. Jelliffe, R.; Schumitzky, A.; Bayard, D.; Neely, M. Monitoring the patient: Four different Bayesian methods to make individual patient drug models. In *Individualized Drug Therapy for Patients. Basic Foundations, Relevant Software, and Clinical Applications*; Jelliffe, R.W., Neely, M., Eds.; Elsevier: Amsterdam, The Netherlands, 2016; pp. 77–90.
30. Sherwin, C.M.T.; Kiang, T.K.L.; Spigarelli, M.G.; Ensom, M.H.H. Fundamentals of population pharmacokinetic modelling. Validation methods. *Clin. Pharmacokinet.* **2012**, *51*, 573–590. [CrossRef]
31. De Rosa, S.; Greco, M.; Rauseo, M.; Annetta, M.G. The good, the bad, and the serum creatinine: Exploring the effect of muscle mass and nutrition. *Blood Purif.* **2023**, *52*, 775–785. [CrossRef]
32. Ostermann, M.; Joannidis, M. Acute kidney injury 2016: Diagnosis and diagnostic workup. *Crit Care* **2016**, *20*, 299. [CrossRef] [PubMed]
33. Hsu, C.-Y.; Bansal, N. Measured GFR as "Gold Standard"—All that glitters is not gold? *Clin. J. Am. Soc. Nephrol.* **2011**, *6*, 1813–1814. [CrossRef] [PubMed]
34. Speeckaert, M.M.; Seegmiller, J.; Glorieux, G.; Lameire, N.; Van Biesen, W.; Vanholder, R.; Delanghe, J.R. Measured glomerular filtration rate: The query for a workable golden standard technique. *J. Pers. Med.* **2021**, *11*, 949. [CrossRef] [PubMed]
35. Jelliffe, R.; Liu, J.; Drusano, G.L.; Martinez, M.N. Individualized patient care through model-informed precision dosing: Reflections on training futire practitioners. *AAPS J.* **2022**, *24*, 117. [CrossRef]
36. Jelliffe, R.W.; Schumitzky, A.; Bayard, D.; Fu, X.; Neely, M.N. Describing assay precision—Reciprocal of variance is correct, not CV percent: Its use should significantly improve laboratory performance. *Ther. Drug Monit.* **2015**, *37*, 389–394. [CrossRef] [PubMed]
37. Karvaly, G.B.; Neely, M.N.; Kovács, K.; Vincze, I.; Vásárhelyi, B.; Jelliffe, R.W. Development of a methodology to make individual estimates of the precision of liquid chromatography-tandem mass spectrometry drug assay results for use in population pharmacokinetic modeling and the optimization of dosage regimens. *PLoS ONE* **2020**, *15*, e0229873. [CrossRef] [PubMed]

pharmaceutics

MDPI

Article

Optimizing Vancomycin Therapy in Critically Ill Children: A Population Pharmacokinetics Study to Inform Vancomycin Area under the Curve Estimation Using Novel Biomarkers

Kevin J. Downes [1,2,3,4,*], Athena F. Zuppa [1,4], Anna Sharova [1,2] and Michael N. Neely [5,6]

[1] The Center for Clinical Pharmacology, Children's Hospital of Philadelphia, Philadelphia, PA 19104, USA
[2] Clinical Futures, Children's Hospital of Philadelphia, Philadelphia, PA 19104, USA
[3] Division of Infectious Diseases, Children's Hospital of Philadelphia, Philadelphia, PA 19104, USA
[4] Department of Pediatrics, Perelman School of Medicine, University of Pennsylvania, Philadelphia, PA 19104, USA
[5] Children's Hospital Los Angeles, Los Angeles, CA 90027, USA
[6] Keck School of Medicine, University of Southern California, Los Angeles, CA 90033, USA
* Correspondence: downeskj@chop.edu; Tel.: +1-215-590-4024

Abstract: Area under the curve (AUC)-directed vancomycin therapy is recommended, but Bayesian AUC estimation in critically ill children is difficult due to inadequate methods for estimating kidney function. We prospectively enrolled 50 critically ill children receiving IV vancomycin for suspected infection and divided them into model training (n = 30) and testing (n = 20) groups. We performed nonparametric population PK modeling in the training group using Pmetrics, evaluating novel urinary and plasma kidney biomarkers as covariates on vancomycin clearance. In this group, a two-compartment model best described the data. During covariate testing, cystatin C-based estimated glomerular filtration rate (eGFR) and urinary neutrophil gelatinase-associated lipocalin (NGAL; full model) improved model likelihood when included as covariates on clearance. We then used multiple-model optimization to define the optimal sampling times to estimate AUC_{24} for each subject in the model testing group and compared the Bayesian posterior AUC_{24} to AUC_{24} calculated using noncompartmental analysis from all measured concentrations for each subject. Our full model provided accurate and precise estimates of vancomycin AUC (bias 2.3%, imprecision 6.2%). However, AUC prediction was similar when using reduced models with only cystatin C-based eGFR (bias 1.8%, imprecision 7.0%) or creatinine-based eGFR (bias −2.4%, imprecision 6.2%) as covariates on clearance. All three model(s) facilitated accurate and precise estimation of vancomycin AUC in critically ill children.

Keywords: critical illness; sepsis; kidney injury; biomarkers; pediatric pharmacology; population pharmacokinetics; Bayesian estimation

Citation: Downes, K.J.; Zuppa, A.F.; Sharova, A.; Neely, M.N. Optimizing Vancomycin Therapy in Critically Ill Children: A Population Pharmacokinetics Study to Inform Vancomycin Area under the Curve Estimation Using Novel Biomarkers. *Pharmaceutics* **2023**, *15*, 1336. https://doi.org/10.3390/pharmaceutics15051336

Academic Editor: Evelyne Jacqz-Aigrain

Received: 31 March 2023
Revised: 20 April 2023
Accepted: 21 April 2023
Published: 25 April 2023

1. Introduction

Vancomycin is the drug of choice for treatment of serious Gram-positive infections in children and is one of the most frequently administered drugs in the pediatric intensive care unit [1]. Its efficacy and toxicity are most closely related to an individual's 24 h area under the curve (AUC_{24}) [2–6]. Traditionally, vancomycin therapeutic drug monitoring (TDM) relied upon measurement of trough concentrations (C_{min}), which were used as a surrogate for AUC_{24} [7]. However, with the continued maturation of Bayesian dosing software programs, AUC-based dosing using population models and limited sampling is becoming more routine [8]. Unfortunately, Bayesian AUC estimation from a single trough measurement can be inaccurate, and validated vancomycin population pharmacokinetic (popPK) models to inform Bayesian dosing and AUC estimation in critically ill children are lacking.

Vancomycin is renally eliminated, and total body clearance (CL) is correlated with glomerular filtration rate (GFR) [9]. However, direct measurement of GFR in critically ill children is impractical and biomarkers are typically used to estimate renal function in individual patients. Creatinine is the biomarker most often relied upon to estimate kidney function in children, but it is not ideal in critically ill children as serum concentrations are affected by numerous factors (medications, muscle mass, age) and are slow to change in the setting of acute kidney injury (AKI) [10]. Despite their limitations, creatinine-based GFR equations, such as the bedside Schwartz equation (Schwartz) [11], remain commonly used for dosing guidance in the critical care setting.

Newer biomarkers have been discovered that are more sensitive indicators of kidney injury and function than creatinine. Cystatin C (CysC) is a protein that is widely expressed by nucleated cells, produced at a constant rate in the body, freely filtered by the glomerulus, and not secreted by renal tubules [12]. These characteristics make plasma CysC a good biomarker of GFR [12] and studies have demonstrated its superiority over creatinine for GFR estimation and earlier AKI detection in critically ill children, including those with sepsis [13–19]. We also previously found that CysC-based eGFR was more closely associated with vancomycin clearance (CL) than creatinine-based eGFR in critically ill children using a popPK modeling approach [20]. Neutrophil gelatinase-associated lipocalin (NGAL) is another promising biomarker for the early detection of AKI in critically ill children [19,21,22]. Plasma and urinary NGAL increase prior to changes in creatinine in critically ill children with sepsis [19,23], and urinary NGAL concentrations have been described as a predictor of vancomycin-associated AKI in hospitalized adults [24]. Other urinary biomarkers, kidney injury molecule-1 (KIM-1) and osteopontin, show good correlation with vancomycin exposures (AUC_{24}, C_{max}) and are predictive of vancomycin-associated AKI in humanized rat models [25–27]. Given the known limitations of creatinine in children, we hypothesized that the clinical use of novel biomarkers can improve estimation of kidney function and vancomycin clearance in critically ill children and ultimately promote individualized vancomycin dosing via Bayesian approaches.

We aimed to develop a popPK model for intravenous (IV) vancomycin in critically ill children incorporating novel urinary and plasma biomarkers of kidney injury. From this population model, we sought to evaluate Bayesian estimation of AUC_{24} in a separate cohort of patients. Ultimately, the goal of this work was to generate and validate a population PK model of vancomycin in critically ill children that could inform Bayesian estimation of AUC_{24} using limited sampling.

2. Materials and Methods

2.1. Study Population

We performed a prospective, observational study in the Pediatric Intensive Care Unit (PICU) at the Children's Hospital of Philadelphia (CHOP) from August 2018 to July 2021. Patients aged 1–17 years old receiving intermittent dosing of intravenous (IV) vancomycin for a suspected infection, defined as performance of a microbiological culture within 24 h of vancomycin initiation, were eligible for inclusion. Eligible patients were identified as soon after initiation of vancomycin as possible. Those receiving renal replacement therapy, plasmapheresis, or extracorporeal membrane oxygenation were ineligible. To be deemed evaluable, subjects had to have $\geq$3 PK samples collected, as well as $\geq$1 urine sample and 1 plasma sample collected for biomarker measurement (see below).

After enrollment was completed, evaluable subjects were divided into model training (n = 30) and testing (n = 20) groups. To perform this, we randomly selected 20 subjects who had $\geq$4 PK samples obtained to serve as the model testing group, while the remainder were assigned to the model training group. This approach was taken to facilitate AUC_{24} estimation using noncompartmental methods within the model testing group, as described below.

The CHOP Institutional Review Board (IRB) approved the study protocol (IRB 18-014851, Approved: 20 March 2018) with a waiver of documented assent; verbal assent was

obtained, as appropriate. Documented informed consent was obtained from the patient's parent(s)/legal guardian(s).

2.2. Dosing, PK Sampling, and Biomarker Measurement

Vancomycin was ordered for clinical care in all patients, with dosages and infusion rates determined by the clinical team. Typical initial dosages were 10–15 mg/kg/dose every 6–8 h, depending on age, weight, and estimated renal function. All decisions about dosing and duration of therapy were at the discretion of the clinical team. During the study, routine TDM included collection of trough (C_{min}) concentrations, with doses adjusted to achieve a goal of 5–15 μg/mL, as appropriate. In 2020, AUC-based TDM was implemented at our hospital, such that patients requiring >48 h of vancomycin therapy had two blood samples collected (at 1 h after the end of the infusion and at C_{min}). AUC was calculated using log-linear methods and doses were adjusted to achieve an AUC of 400–600 mg h/L.

For each participant, five vancomycin concentrations (PK sampling) were obtained after ≥4 vancomycin doses during a single dosing interval at the goal times shown in Table S1; since clinical care could interfere with the precise timing of sample collection, samples were accepted outside of these windows. Sampling took place within 48 h of enrollment for all participants. Samples could be collected prior to the fourth dose if a patient had impaired renal function such that he/she did not receive vancomycin at regular dosing intervals, so long as he/she had received ≥24 h of treatment; this applied to only one participant. All samples were collected via arterial catheter, peripheral venipuncture, or venous catheter, if not used for administration of vancomycin. In addition to PK sampling, the clinical team performed therapeutic drug monitoring (TDM) according to institutional standard practice. Results of TDM samples were recorded and included in our study if collected prior to PK sampling; individuals only participated through the time of PK sampling, so dosing information and TDM results that took place after PK sampling for the study were not recorded.

All vancomycin concentrations were measured by chemiluminescent microparticle immunoassay (Abbott, Abbott Park, IL, USA) in the CHOP Chemistry Laboratory; the lower limit of quantification (LLOQ) of this assay was 3.0 μg/mL. Results of both PK sampling and TDM were made available in the subject's electronic medical record.

After enrollment, urine and blood samples were obtained for biomarker measurement. Two urine samples were collected from subjects for measurement of the following biomarkers: NGAL, KIM-1, cystatin C, osteopontin, and creatinine. These samples were obtained starting the day of enrollment in the evening (3–7 pm) and morning (6–10 am) prior to PK sampling. Collection of urine samples outside of the above windows was permitted, based on the condition and clinical care needs of the patient. Urine samples were collected via indwelling urinary catheter, clean intermittent catheterization (if performed for clinical care), cotton balls, urine cup, or urine bag. In addition to prospective urine collection, we also identified and obtained any available residual urine samples that had been collected clinically within 24 h prior to initiation of IV vancomycin. These samples served as baseline biomarker measurements when available. A single blood sample was drawn within 24 h of PK sampling for measurement of plasma biomarkers (cystatin C and NGAL), as well as creatinine if not performed clinically. We similarly identified any available residual plasma samples that had been collected clinically up to 24 h preceding initiation of IV vancomycin to serve as baseline measurement of biomarkers.

KIM-1, osteopontin, NGAL (urine and plasma), and cystatin C (urine and plasma) were measured using Quantikine® ELISA (R & D Systems, Inc., Minneapolis, MN, USA). Urine creatinine (uCr) was measured via two-point end enzymatic method on a Cobas® system (Roche Diagnostics, Basel, Switzerland). These tests were performed in the CHOP Translational Core Laboratory. Plasma creatinine was measured by two-point rate spectrophotometric method (Vitros5600™ analyzer, Ortho Clinical Diagnostics, Raritan, NJ, USA) in the CHOP Chemistry Laboratory.

2.3. Population PK Model Training

Figure 1 displays a flow diagram of our approach to population PK model training and testing. Nonparametric population PK modeling was performed using the Pmetrics package (version 1.9.7; Laboratory of Applied Pharmacokinetics and Bioinformatics, Los Angeles, CA, USA) [28] for R (version 3.6.3; R Foundation for Statistical Computing, Vienna, Austria) [29] in RStudio (v1.2.5033; RStudio, Inc., Boston, MA, USA) [30]. One- and two-compartment models were constructed using the nonparametric adaptive grid (NPAG) algorithm [31]. Parameters included V_d (volume of the distribution) and CL (total body clearance) for one-compartment models and CL (clearance), Q (intercompartmental clearance), V1 (central volume), and V2 (peripheral volume) for two-compartment models. Clearance parameters were allometrically scaled for standardized weight to a power of 0.75 and volume parameters were scaled by standardized weight (power 1); weight was standardized by the median of the subjects' weights (27 kg). The weighting function on observations was $1/(\text{gamma} * SD^2)$, where SD (standard deviation) was a combined additive and multiplicative function of the assay imprecision as a polynomial equation: $SD = C_0 + [C_1 \times \text{observed concentration}]$; C_0 had a value of 1.5 (half the LLOQ) and C_1 a value of 0.1, i.e., an assay with 10% coefficient of variation (CV%). Gamma was initially set to 1 and fitted to estimate the residual model error.

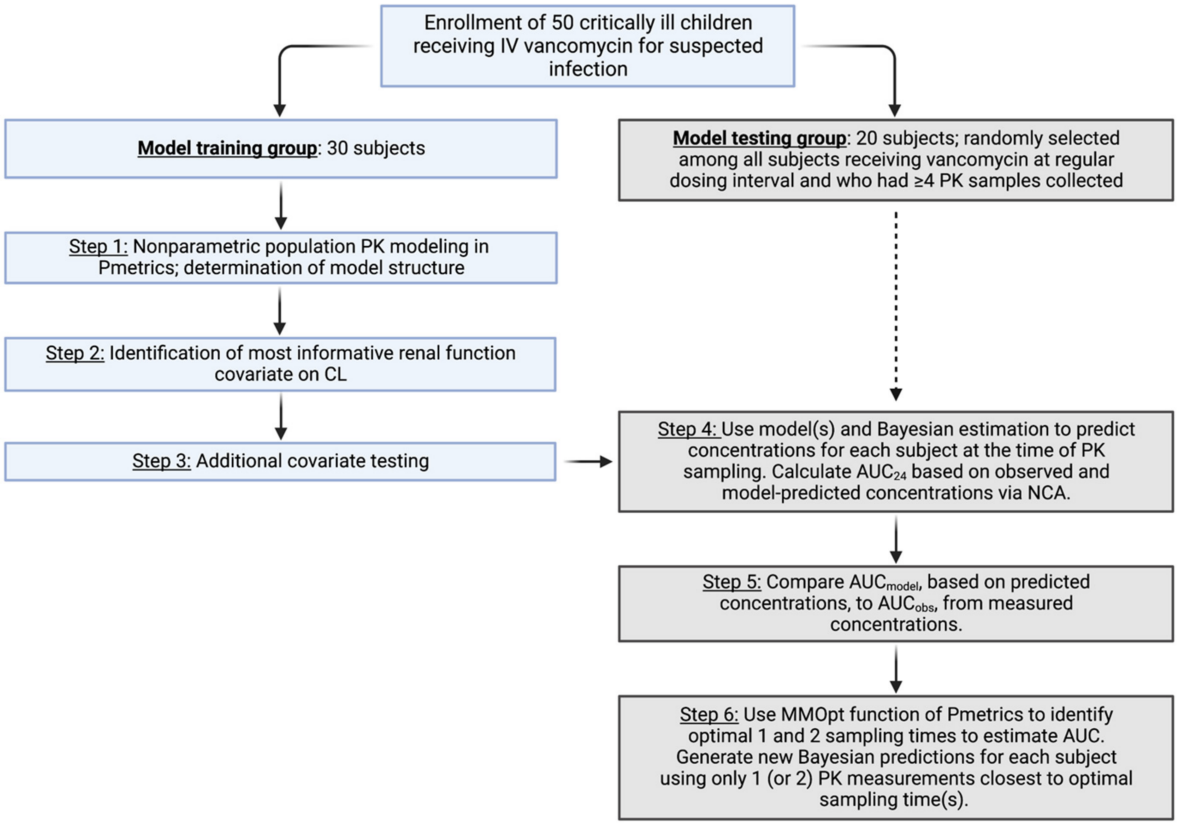

Figure 1. Flow diagram of study design. **Left**-hand side depicts how data from the 30 subjects assigned to model training were used, while **right**-hand side shows how data from the 20 subjects in the model testing group were utilized. Abbreviations: AUC, area under the concentration–time curve; AUC_{model}, area under the curve from model-predicted concentrations; AUC_{obs}, area under the curve from observed concentrations; CL, clearance; MMOpt, multiple-model optimization algorithm; NCA, noncompartmental analysis; PK, pharmacokinetic. Created with BioRender.com.

Following determination of the base model structure, covariate model selection was then performed in a two-stage process. Since vancomycin is renally eliminated, we first sought to identify the best renal function marker to include as a covariate on CL. This

included plasma biomarkers (creatinine, cystatin C (pCysC), and NGAL (pNGAL)), as well as eGFR based on these biomarkers. GFR was estimated using creatinine alone according to the bedside Schwartz equation ($Schwartz_{bed}$) [11], pCysC alone based on the Hoek equation [32], and both creatinine and pCysC based on the full age spectrum equation [33]. These cystatin C equations were chosen based on our previous evaluation of their ability to inform vancomycin CL during parametric population PK modeling [20].

Next, we evaluated additional covariates on CL and V1 using a forward selection approach. All covariates were selected based on physiologic plausibility. Binary covariates included sex, receipt of vasopressor medications, and presence of augmented renal clearance (defined as eGFR > 130 mL/min/1.73 m^2; tested on CL only) [34], while continuous covariates included age, Pediatric Index of Mortality 3 (PIM3) score [35], and the above listed plasma and urinary biomarkers (on CL only). Urinary biomarkers were normalized to urine creatinine (i.e., [biomarker]/[uCr]) to account for urine volume. Continuous covariates were normalized to the median population value with the covariate effect evaluated using a power function; age was also evaluated as a Hill function on CL [36]. Meanwhile, binary covariates were parameterized using a linear proportional approach such that the covariate effect reflects a proportion increase/decrease of the typical parameter value in the absence of the covariate.

Covariate selection was guided by the principle of parsimony and by measures of goodness-of-fit. Models were evaluated at each step by inspection of observed-versus-predicted concentration plots, as well as examination of the model's bias, imprecision, regression coefficient, log-likelihood ratio ($-2 \times$ LL), and Akaike's information criterion (AIC) value. With the addition of a covariate to a model, a difference in the log-likelihood ratio of >3.84 was considered significantly improved fit (corresponding to $p < 0.05$ for one additional degree of freedom). When comparing models with the same degrees of freedom, lower AIC, bias, and imprecision of the observed-versus-predicted concentrations guided model selection.

2.4. Model Testing via Area under the Curve Comparisons

After model training, we evaluated the ability of the full model to predict vancomycin AUC for each subject in the model testing group. We first calculated the AUC for the dosing interval during which PK sampling was performed using his/her observed concentrations and linear up-log down trapezoidal noncompartmental analysis (NCA) [37]. Because of the timing of PK sampling, the drug was assumed to be at steady state, and therefore the same minimum concentration (C_{min}) was used prior to and after a given dose in these calculations. The 24 h "true" or observed AUC (AUC_{obs}) was then computed based on the subject's anticipated number of doses in a 24 h period.

We then used Bayesian estimation to evaluate how well our full model predicted AUC_{obs}. The population joint density of the full model was employed as a Bayesian prior for each subject in the model testing group. Simulated concentration–time profiles were generated with predicted outputs each minute. The predicted concentration at the time of each measured PK sample, as well as at the start and end of his/her infusion, was recorded. The trapezoidal method was then taken, using all of the subject's predicted concentrations to calculate a predicted AUC_{24} (AUC_{full}).

Recognizing that urinary biomarkers would not be routinely available in clinical practice, we also performed Bayesian estimation using two simpler models: a model incorporating only CysC-based eGFR (from Hoek equation) on CL and a model incorporating only creatinine-based eGFR (from bedside Schwartz equation) on CL. These models were chosen as comparators because they are more parsimonious and contain covariates that are readily available at all (creatinine) or many (CysC) pediatric institutions, which we felt would allow for easier clinical implementation. As above, AUC_{24} was calculated for both the Hoek (AUC_{Hoek}) and Schwartz ($AUC_{Schwartz}$) models.

To assess the predictive performance of our models for AUC estimation, we determined the bias and imprecision of the AUC predictions from each model for each

subject. Bias was calculated as $(AUC_{pred} - AUC_{obs})/AUC_{obs} \times 100$ and imprecision as $|AUC_{pred} - AUC_{obs}|/AUC_{obs} \times 100$, where AUC_{pred} is the generic AUC_{24} predicted by our models: AUC_{full}, AUC_{Hoek}, and $AUC_{Schwartz}$. Data were then summarized as the median bias (median percentage predictive error) and imprecision (median absolute percentage predictive error) for each model, as well as the fraction of subjects whose AUC_{pred} was within 5%, 10%, 15%, and 20% of his/her AUC_{obs}. Spearman correlation between AUC_{pred} and AUC_{obs} was also determined for each model. The a priori acceptance criteria were that AUC_{pred} was within 20% of AUC_{obs} in 85% of subjects and that the correlation between AUC_{pred} and AUC_{obs} was >0.9.

2.5. Area under the Curve Estimation from Optimal Sampling

The goal of Bayesian AUC estimation in clinical practice is to accurately estimate vancomycin AUC_{24} using limited PK sampling. As such, we also sought to evaluate the ability of our model(s) to estimate AUC_{24} using one and two optimally timed PK samples per subject. To achieve this, we utilized the multiple-model optimization algorithm (MMopt) in Pmetrics, which finds the optimal times based on when all the PK curves generated by the support points in the nonparametric model are most separated (e.g., the time points that are most informative), minimizing the Bayesian risk of misclassifying an individual as the wrong set of support points [38]. For each subject in the model testing group, MMopt was used identify the one and two most informative sampling time points for Bayesian estimation of AUC. We then created a reduced dataset for each subject that contained only the one or two observed concentrations closest to the optimal sampling time(s) identified by MMopt. We repeated the processes above in 2.d. with the population joint density of each model employed as a Bayesian prior and simulated concentration–time profiles generated using only these reduced datasets. Predicted concentrations were again recorded and AUC_{24} was calculated via the trapezoidal method. Bias, imprecision, and correlation were determined for each model, this time based on predictions from limited sampling.

3. Results

3.1. Study Population

In total, 85 patients provided consent to participate. Five were deemed screen failures following consent and were excluded prior to performance of any study procedures. Meanwhile, 29 subjects were unevaluable because vancomycin was discontinued by the clinical team prior to PK sampling (n = 28) or could not undergo PK sampling (n = 1). One additional subject was excluded due to laboratory processing issues of the PK samples, making results uninterpretable (results reported out of order). As a result, 50 individuals participated in our study and were fully evaluable. Of these, 44 were eligible to be in the testing group (i.e., had $\geq$4 PK samples available), of whom we randomly chose 20. The characteristics of the model training and test groups are shown in Table 1. In general, the groups were similar, although the test group were less often on vasopressors at the start of vancomycin and received slightly larger vancomycin doses at the time of PK sampling.

Table 1. Study population characteristics.

Characteristic	Model Training Group (n = 30)	Model Testing Group (n = 20)	*p*-Value [a]
At start of vancomycin			
Age in years, median (IQR)	9.8 (3.8–11.2)	10.2 (2.9–13.2)	0.68
Weight in kg, median (IQR)	25.9 (13.9–41.8)	37.6 (14.4–57.5)	0.33
Female sex, n (%)	11 (37)	5 (25)	0.54
Serum creatinine in mg/dL, median (IQR)	0.40 (0.23–0.60)	0.40 (0.19–0.43)	0.22

Table 1. *Cont.*

Characteristic	Model Training Group (n = 30)	Model Testing Group (n = 20)	*p*-Value [a]
$eGFR_{Schwartz}$ in mL/min/1.73 m^2, median (IQR)	117 (97–154)	154 (126–185)	0.06
Receipt of vasopressors, n (%)	18 (60)	6 (30)	0.05
Vancomycin dose in mg/kg/dose, median (IQR)	14.7 (11.9–15.0)	14.5 (11.8–14.8)	0.60
At PK sampling			
Serum creatinine in mg/dL, median (IQR)	0.30 (0.20–0.48)	0.35 (0.19–0.50)	0.92
$eGFR_{Schwartz}$ in mL/min/1.73 m^2, median (IQR)	164 (114–222)	156 (134–184)	0.95
$eGFR_{Hoek}$ in mL/min/1.73 m^2, median (IQR)	143 (110–197)	130 (96–156)	0.64
Receipt of vasopressors, n (%)	14 (47)	7 (35)	0.56
PIM3 probability of death, median (IQR)	1.3% (0.5–4.3)	1.3% (0.4–4.1)	0.96
Vancomycin dose in mg/kg/dose, median (IQR)	13.2 (10.0–14.8)	15.0 (14.5–15.7)	0.005
Duration of vancomycin therapy prior to PK sampling (in hours), median (IQR)	36.4 (30.8–41.4)	36.1 (32.1–41.9)	0.68

[a] Continuous variables were compared using Wilcoxon rank sum tests and categorical variables were compared using chi-squared or Fisher's exact tests. Abbreviations: eGFR, estimated glomerular filtration rate; IQR, interquartile range; PIM3, Pediatric Index of Mortality 3.

3.2. Population PK Model Training

Thirty subjects contributed 150 vancomycin concentrations (14 clinical samples and 136 research PK samples) towards model training. The range of vancomycin concentrations was 3.9 to 67.8 μg/mL. Two concentrations were below the limit of quantification and coded as LLOQ/2 (i.e., 1.5 μg/mL). Observed concentrations vs. time after dose are plotted in Supplementary Figure S1.

Table S2 displays the model training steps. A two-compartment model best described the data (AIC 820.5 vs. 879.6 for one-compartment). When evaluating renal function covariates on vancomycin CL, cystatin C outperformed SCr (AIC difference of −14.6) and pNGAL (AIC difference of −14.3). Meanwhile, eGFR based on the Hoek equation had a lower AIC (793.3) compared to eGFR based on the Schwartz equation (807.6) or the full age spectrum equation (801.5). Incorporation of $eGFR_{Hoek}$ or pCysC on CL resulted in comparable −2 × LL, AIC, and population predicted vs. observed R^2 values. We proceeded with further model training using the $eGFR_{Hoek}$ model since clinical dosing guidance is typically based on a patient's eGFR rather than a direct biomarker result.

When evaluating the addition of other covariates on CL and V1, numerous covariates, including urinary biomarkers on CL, improved model fitness based on a reduction in −2 × LL and AIC (Table S2). However, the incorporation of the uNGAL on CL, parameterized as the natural logarithm of uNGAL/uCr, led to the largest −2 × LL and AIC reductions. The correlation between log uNGAL and $eGFR_{Hoek}$ was low (−0.27). No additional covariates were informative on vancomycin CL or V1; thus, this model constituted the full model for testing. Observed versus population and individual predicted concentration plots of the full model are shown in the Supplemental Files (Figure S2), and the population PK parameter estimates from this model are shown in Table 2.

Table 2. Population PK parameter estimates for the full PK model.

Parameter	Weighted Parameter Estimate		CV%	Shrinkage %
	Median	95th Percentile		
CL0	3.31	2.53–4.22	39.5	54.7
CL_{WT}	0.75	-	-	
CL_{HOEK}	0.85	0.22–0.90	62.8	55.6
CL_{NGAL}	0.94	0.86–1.00	10.9	50.5
V_C0	3.50	2.72–7.09	49.2	59.5
$V_{C\text{-}WT}$	1	-	-	
Q0	7.09	4.76–7.97	32.6	60.9
Q_{WT}	0.75	-	-	
V_P0	7.75	6.63–13.80	39.0	49.1
$V_{P\text{-}WT}$	1	-	-	

Full model parameterized as: $CL = CL0 \cdot (WT/27)^{CLWT} \cdot (HOEK/134)^{CLHOEK} \cdot (CL_{NGAL})^{LNGAL}$, $V1 = V_C0 \cdot (WT/27)^{VCWT}$, $Q = Q0 \cdot (WT/27)^{QWT}$, $V2 = V_P0 \cdot (WT/27)^{VPWT}$. Hoek is the estimated GFR based on the cystatin C-based Hoek equation; LNGAL is the natural logarithm of the urinary NGAL concentration normalized to urinary creatinine (uNGAL/uCr). Abbreviations: CL, clearance; Q, intercompartmental clearance; V1, central volume; V2, peripheral volume.

3.3. Area under the Curve Comparisons

Twenty subjects comprised the model testing group. These subjects were similar to the model training group in terms of age, weight, PIM3 scores at PK sampling, timing of PK sampling, and vancomycin dosages received (Table 1), although they less often received vasopressors and had higher eGFR at vancomycin initiation. Biomarker concentrations at the time of PK sampling were also similar between the two groups (Table S3).

The median AUC_{24} among the 20 subjects calculated using the trapezoidal method and observed concentrations (AUC_{obs}) was 456 mg h/L (range: 367–885). When using estimated concentrations from the individual Bayesian posteriors and our full model (AUC_{full}), the median AUC_{24} was 475 mg h/L (range: 327–907). The median bias and imprecision of AUC_{full} compared to AUC_{obs} were 2.3% and 6.2%, respectively, and the correlation between the AUC estimates was 0.939. Meanwhile, 90% of subjects' AUC_{full} estimates were with 20% of their AUC_{obs}.

The PK parameter estimates for the two simplified models (based on $eGFR_{Hoek}$ and $eGFR_{Schwartz}$) are shown in Table S4. The median bias and imprecision of AUC_{Hoek} compared to AUC_{obs} were 1.8% and 7.0%, respectively, and the correlation between AUC_{Hoek} and AUC_{obs} was 0.926. The median bias and imprecision of $AUC_{Schwartz}$ compared to AUC_{obs} were -2.4% and 6.2%, respectively, and the correlation between $AUC_{Schwartz}$ and AUC_{obs} was 0.893. Additionally, 85% and 95% of subjects' AUC estimates were with 20% of their AUC_{obs} using the Hoek and Schwartz models, respectively.

Observed versus individual predicted concentrations (i.e., Bayesian posteriors) for each of the three models are shown in Figure 2, while Table 3 displays the performance parameters of these models to estimate AUC_{24}. The optimal sampling times relative to the end of the infusion for each of the three models are shown in Table S5. When fitting all available PK samples, the three models performed similarly (with AUC_{obs} as the reference). However, when fitting the one or two PK samples closest to the MMopt optimal times, the performance of our full model declined. The imprecision of AUC_{full} more than doubled when using one or two PK samples, and fewer subjects' AUC_{24} were within 20% of AUC_{obs}. However, $\geq$85% of subjects' AUC_{24} from the Hoek and Schwartz models were within 20% of AUC_{obs} when using limited sampling.

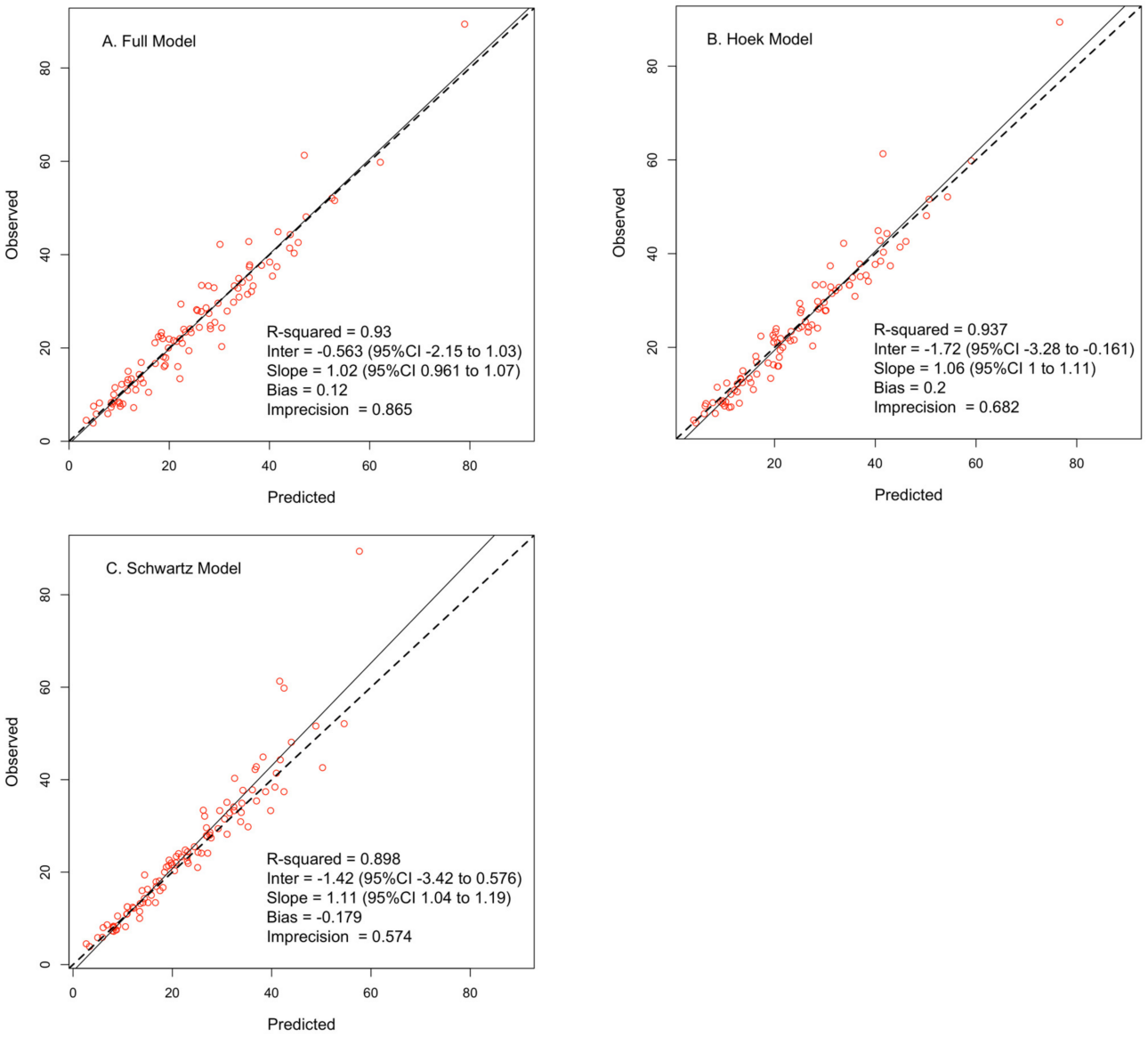

Figure 2. Observed versus posterior (individual) predicted concentrations for the full (**A**), Hoek (**B**), and Schwartz (**C**) models.

Table 3. Performance of models to estimate AUC_{24} via Bayesian estimation (AUC_{model}) compared to AUC calculated using observed concentrations (AUC_{obs}) [a].

	Full Model	Hoek Model	Schwartz Model
All available PK samples			
AUC_{24}, median (range)	475 (325–857)	488 (338–907)	501 (319–710)
Median bias [b]	2.3%	1.8%	−2.4%
Median imprecision [c]	6.2%	7.0%	6.2%
Number of subjects with AUC_{model} within 20% of AUC_{obs}	18 (90%)	17 (85%)	19 (95%)
Correlation between AUC_{model} and AUC_{obs}	0.939	0.926	0.893

Table 3. *Cont.*

	Full Model	Hoek Model	Schwartz Model
Two optimally timed PK samples			
AUC_{24}, median (range)	487 (316–968)	482 (333–832)	471 (332–714)
Median bias [b]	2.0%	1.8%	−1.2%
Median imprecision [c]	13.4%	6.0%	6.8%
Number of subjects with AUC_{model} within 20% of AUC_{obs}	15 (75%)	18 (90%)	17 (85%)
Correlation between AUC_{model} and AUC_{obs}	0.876	0.928	0.860
Single optimally timed PK sample			
AUC_{24}, median (range)	526 (284–968)	523 (283–830)	466 (353–700)
Median bias [b]	3.7%	2.5%	−0.9%
Median imprecision [c]	13.4%	11.4%	7.0%
Number of subjects with AUC_{model} within 20% of AUC_{obs}	13 (65%)	17 (85%)	17 (85%)
Correlation between AUC_{model} and AUC_{obs}	0.817	0.891	0.825

[a] All model-derived AUC estimates were compared to AUC calculated using the trapezoidal methods on observed concentrations (AUC_{obs}); median AUC_{obs}: 456 mg h/L, range: 367–885 mg h/L. [b] Bias calculated as: $(AUC_{model} - AUC_{obs})/AUC_{obs} \times 100$. [c] Imprecision calculated as: $|AUC_{model} - AUC_{obs}|/AUC_{obs} \times 100$.

4. Discussion

In this population PK study, cystatin C was superior to the traditional renal function biomarker of serum creatinine as a marker of vancomycin clearance in critically ill children. This is consistent with other studies that described better correlation between vancomycin CL and CysC-based eGFR than creatinine-based eGFR in noncritically ill and critically ill pediatric patients [20,39]. Contrary to our previous work [20], however, we found that eGFR based on CysC alone (using the Hoek equation) outperformed eGFR based on both CysC and creatinine (full age spectrum equation). This highlights the inadequacy of creatinine as a renal function marker in critically ill children and suggests that routine measurement of CysC when administering vancomycin may be a more reliable approach. As the availability of cystatin C at pediatric institutions increases, and experience with cystatin C-based eGFR equations mounts, cystatin C may replace creatinine as the biomarker to inform dosing of other renally eliminated drugs in pediatrics as well. With increased appreciation of the negative ramifications of AKI on clinical outcomes, it is crucial to provide safe doses of nephrotoxic medications such as vancomycin. Given the well-recognized limitations of creatinine in pediatric patients, particularly in the ICU setting, it may be time to move towards a better biomarker in our most vulnerable children.

A goal of this work was to explore the potential value of novel urinary biomarkers to describe vancomycin disposition in critically ill children using a popPK modeling approach. Since changes in serum creatinine and other blood markers of kidney function may be delayed in the setting of AKI [40], we hypothesized that urinary biomarkers could facilitate detection of fluctuations in vancomycin CL before blood biomarkers. In fact, urinary NGAL was an influential covariate on vancomycin CL during our full model training; other urinary biomarkers (KIM-1, CysC, osteopontin) also led to large reductions in the AIC during model training steps, although not to the same extent as NGAL. We believe that these findings are important and warrant further investigation. Rather than solely relying on blood biomarkers to signify kidney function, bedside measurement of urinary biomarkers could provide insight into which patients have subclinical kidney injury (i.e., not detected via blood biomarkers) and may require early, pre-emptive dose adjustments. Although biomarkers did not improve estimation of AUC_{24} estimation in our testing group, they could potentially be used as screening tests to identify patients at highest risk for impaired kidney function and/or toxicity.

Urinary biomarkers can detect subclinical kidney injury, but the majority of patients in our study actually had augmented renal clearance (ARC). This phenomenon describes a state of hyperfiltration and increased drug clearance, which can be detrimental in critically ill patients with severe infections, and it is unclear how reliable urinary biomarkers are in that clinical situation. Although the precise definition of ARC in children has been debated, an eGFR >130 mL/min/1.73 m^2 has been utilized in other vancomycin studies [41]. In our study, half of each of the model training and testing groups had ARC by Hoek equation calculation. This may explain why our full model failed to outperform the Schwartz and Hoek model in terms of AUC_{24} estimation, as urinary biomarkers may not perform as well in patients with ARC as they do in those with AKI. Similarly, eGFR equations are generally more accurate in patients with impaired renal function rather than in ARC. Given the small sample size of our model testing group and limited number of subjects with impaired renal function, we may have been unable to fully demonstrate the value of novel biomarkers (both urinary and plasma) when it comes to AUC estimation.

It is also possible that urinary NGAL measurement is not precise enough to substantially influence AUC_{24} estimation, particularly when using limited PK sampling. Urinary NGAL ranged from 1.4 to 2809 ng/mg creatinine in the model training group and from 7.8 to 10,034 ng/mg creatinine in the model testing group. Although measurements were not significantly different between the groups using Wilcoxon rank sum testing, this large variability in urinary biomarker values may preclude precise AUC estimation at an individual level using Bayesian methods. While we did not explore utilizing cut-points to categorize biomarker values (e.g., low, medium, high values), that is a potential avenue for future investigation.

Another goal of this study was to develop a popPK model that could be used to inform AUC-based vancomycin dosing using Bayesian estimation and limited sampling. We utilized a nonparametric popPK modeling approach, which differs from the more widely used parametric popPK methods in that it assumes that the distribution of parameter values is not necessarily described by an a priori defined continuous function (e.g., normal distribution) [42]. As a result, more commonly used statistical measures of variability in parametric popPK models (e.g., mean, standard deviation, coefficient of variation) may not fully describe the shape and structure of a nonparametric distribution and, as such, the idea of typical parameter values and interindividual variability around them does not apply. However, because nonparametric approaches allow for parameter probability distributions to take any shape, subpopulations and outliers can be detected, which is ideal in a popPK study of a highly dynamic population such as critically ill children, and methods for Bayesian estimation of individual PK parameters are robust. A more thorough review of nonparametric and parametric popPK approaches has been published [43].

At the time that this study started, AUC estimation was not standard of care. However, AUC-based dosing is now routine at our institution for anyone receiving >48 h of treatment. Clinical pharmacists implement log-linear methods to calculate AUC based on two vancomycin concentrations. To provide a distinct advantage over this approach, we felt it was important to specifically evaluate the utility of our models to inform AUC estimation based on a single, optimally timed vancomycin measurement. Both the Hoek and Schwartz models accurately estimated AUC_{24} (within 20% of AUC_{NCA}) in 85% of subjects from a single sample with a median bias of 2.5% and −0.9%, respectively. An ongoing, prospective observational study (NCT05691309) at our institution is evaluating how well Bayesian AUC using our Hoek model aligns with clinical AUC calculations (using log-linear calculations) and assessing the ways in which this would influence dosing recommendations.

There are limitations to our study. First, we did not enroll children younger than one year of age and so our model(s) cannot be applied to infants. Cystatin C values are affected by age in this group, likely due to renal maturation occurring over the first year of life; thus, infants were specifically excluded from our study. A recent popPK study in critically ill neonates found that a model including creatinine on vancomycin CL performed similarly to a model including cystatin C and age [43]; thus, cystatin C may not be a superior renal

function biomarker in the neonatal population. Second, because we required that a subject have at least four PK samples to be included in the model testing group, it is possible that our process of group assignment introduced bias; hence, the groups were different. We did not detect any statistically significant differences in the blood or urinary biomarkers between these groups, which were the covariates included in our models, but it is possible that other factors not considered covariates during model development in the training group were influential on vancomycin PK and AUC_{24} estimation within the smaller model testing group. Third, recently published data suggest that urine chemistry analytes can be affected by collection of urine using cotton balls [44]. We are unaware of studies that have evaluated this for the urinary biomarkers included in our study, but this should be explored in future studies as urine collection methods could be a potential source of variability that affect the association between biomarkers and vancomycin clearance. Lastly, urinary biomarkers are sensitive for detection of AKI and, thus, may fluctuate over time. Although we collected $\geq$2 samples per subject, it is possible that changes in biomarker concentrations occurred outside of the windows of our urine sample collection. Although understanding the fluctuations of urinary biomarkers in critically ill children would be of interest, the need to collect urine at very specific times or to collect samples more often would further limit the clinical applicability of these biomarkers to inform drug dosing.

5. Conclusions

The present study developed a two-compartment model to describe vancomycin PK in critically ill children. Plasma cystatin C and urinary NGAL were informative on vancomycin clearance in our full popPK model. However, the full popPK model was not superior for estimation of Bayesian AUC_{24} compared to simpler popPK models that included only cystatin C- or creatinine-based eGFR on clearance. Future studies will evaluate the utility of our models to inform vancomycin dosing using Bayesian estimation compared to two-point log-linear regression calculations.

Supplementary Materials: The following supporting information can be downloaded at: https://www.mdpi.com/article/10.3390/pharmaceutics15051336/s1, Table S1: Goal PK sampling times relative to end of the vancomycin infusion; Table S2: Model training steps; Table S3: Biomarker concentrations at time of PK sampling; Table S4: Population PK parameter estimates for the full model, $eGFR_{Hoek}$ model, and $eGFR_{Schwartz}$; Table S5: Summary of optimal sampling times relative to the end of the vancomycin infusion among model testing group; Figure S1: Observed concentrations versus time after dose for the model testing group; Figure S2: Observed versus population and individual predicted concentration plots of the full model.

Author Contributions: Conceptualization, K.J.D., A.F.Z. and M.N.N.; methodology, K.J.D., A.F.Z. and M.N.N.; formal analysis, K.J.D.; investigation, K.J.D. and A.S.; resources, K.J.D. and A.F.Z.; data curation, A.S. and K.J.D.; writing—original draft preparation, K.J.D.; writing—review and editing, A.F.Z., A.S. and M.N.N.; supervision, A.F.Z. and M.N.N.; funding acquisition, K.J.D. All authors have read and agreed to the published version of the manuscript.

Funding: This project was supported by the Eunice Kennedy Shriver National Institute of Child Health & Human Development of the National Institutes of Health under Award Number K23HD091365 (PI: Downes). This project was also supported, in part, by the Penn/CHOP Institutional Clinical and Translational Science Award Research Center through NIH/NCATS (National Center for Advancing Translational Sciences) Grant UL1TR001878.

Institutional Review Board Statement: The study was conducted in accordance with the Declaration of Helsinki, and approved by the CHOP Institutional Review Board (IRB) (protocol code IRB 18-014851, Approved: 20 March 2018).

Informed Consent Statement: Informed consent was obtained from all subjects' parents/legal guardians involved in the study.

Data Availability Statement: Data can be made available upon request.

Acknowledgments: We would like to thank Lauren Gianchetti and Emily Duffey for their hard work performing recruitment, data collection, and oversight of sample collection for this project.

Conflicts of Interest: A.F.Z. is currently employed by Janssen Pharmaceuticals. All work was conducted while A.F.Z. was at the Children's Hospital of Philadelphia and the University of Pennsylvania School of Medicine. Janssen had no input into the design, implementation, analysis, or interpretation of data. All other authors have no conflict of interest to disclose.

Abbreviations

ARC, augmented renal clearance; AUC, area under the concentration–time curve; CHOP, the Children's Hospital of Philadelphia; CL, clearance; CysC, cystatin C; eGFR, estimated glomerular filtration rate; KIM-1, kidney injury molecule-1; MMopt, multiple-model optimization; NCA, non-compartmental analysis; NGAL, neutrophil gelatinase-associated lipocalin; PD, pharmacodynamic(s); PK, pharmacokinetic(s); popPK, population pharmacokinetic; Q, intercompartmental clearance; TDM, therapeutic drug monitoring; V1, central volume of distribution; V2, peripheral volume of distribution.

References

1. Weiss, S.L.; Fitzgerald, J.C.; Pappachan, J.; Wheeler, D.; Jaramillo-Bustamante, J.C.; Salloo, A.; Singhi, S.C.; Erickson, S.; Roy, J.A.; Bush, J.L.; et al. Global epidemiology of pediatric severe sepsis: The sepsis prevalence, outcomes, and therapies study. *Am. J. Respir. Crit. Care Med.* **2015**, *191*, 1147–1157. [CrossRef] [PubMed]
2. Moise-Broder, P.A.; Forrest, A.; Birmingham, M.C.; Schentag, J.J. Pharmacodynamics of vancomycin and other antimicrobials in patients with Staphylococcus aureus lower respiratory tract infections. *Clin. Pharmacokinet.* **2004**, *43*, 925–942. [CrossRef]
3. Kullar, R.; Davis, S.L.; Levine, D.P.; Rybak, M.J. Impact of vancomycin exposure on outcomes in patients with methicillin-resistant Staphylococcus aureus bacteremia: Support for consensus guidelines suggested targets. *Clin. Infect. Dis.* **2011**, *52*, 975–981. [CrossRef] [PubMed]
4. Song, K.H.; Kim, H.B.; Kim, H.S.; Lee, M.J.; Jung, Y.; Kim, G.; Hwang, J.H.; Kim, N.H.; Kim, M.; Kim, C.J.; et al. Impact of area under the concentration-time curve to minimum inhibitory concentration ratio on vancomycin treatment outcomes in methicillin-resistant Staphylococcus aureus bacteraemia. *Int. J. Antimicrob. Agents* **2015**, *46*, 689–695. [CrossRef] [PubMed]
5. Jung, Y.; Song, K.H.; Cho, J.; Kim, H.S.; Kim, N.H.; Kim, T.S.; Choe, P.G.; Chung, J.Y.; Park, W.B.; Bang, J.H.; et al. Area under the concentration-time curve to minimum inhibitory concentration ratio as a predictor of vancomycin treatment outcome in methicillin-resistant Staphylococcus aureus bacteraemia. *Int. J. Antimicrob. Agents* **2014**, *43*, 179–183. [CrossRef]
6. Le, J.; Ny, P.; Capparelli, E.; Lane, J.; Ngu, B.; Muus, R.; Romanowski, G.; Vo, T.; Bradley, J. Pharmacodynamic Characteristics of Nephrotoxicity Associated with Vancomycin Use in Children. *J. Pediatr. Infect. Dis. Soc.* **2015**, *4*, e109–e116. [CrossRef]
7. Rybak, M.J.; Lomaestro, B.M.; Rotscahfer, J.C.; Moellering, R.C., Jr.; Craig, W.A.; Billeter, M.; Dalovisio, J.R.; Levine, D.P. Vancomycin Therapeutic Guidelines: A Summary of Consensus Recommendations from the Infectious Diseases Society of America, the American Society of Health-System Pharmacists, and the Society of Infectious Diseases Pharmacists. *Clin. Infect. Dis.* **2009**, *49*, 325–327. [CrossRef]
8. Rybak, M.J.; Le, J.; Lodise, T.P.; Levine, D.P.; Bradley, J.S.; Liu, C.; Mueller, B.A.; Pai, M.P.; Wong-Beringer, A.; Rotschafer, J.C.; et al. Therapeutic monitoring of vancomycin for serious methicillin-resistant Staphylococcus aureus infections: A revised consensus guideline and review by the American Society of Health-System Pharmacists, the Infectious Diseases Society of America, the Pediatric Infectious Diseases Society, and the Society of Infectious Diseases Pharmacists. *Am. J. Health Syst. Pharm.* **2020**, *77*, 835–864.
9. Gyssens, I.C. Glycopeptides. In *Fundamentals of Antimicrobial Pharmacokinetics and Pharmacodynamics*; Vinks, A.A., Derendorf, H., Mouton, J.W., Eds.; Springer: New York, NY, USA, 2014; Volume 1, pp. 279–322.
10. Fuchs, T.C.; Hewitt, P. Biomarkers for drug-induced renal damage and nephrotoxicity-an overview for applied toxicology. *AAPS J.* **2011**, *13*, 615–631. [CrossRef]
11. Schwartz, G.J.; Munoz, A.; Schneider, M.F.; Mak, R.H.; Kaskel, F.; Warady, B.A.; Furth, S.L. New equations to estimate GFR in children with CKD. *J. Am. Soc. Nephrol.* **2009**, *20*, 629–637. [CrossRef]
12. Mussap, M.; Plebani, M. Biochemistry and clinical role of human cystatin C. *Crit. Rev. Clin. Lab. Sci.* **2004**, *41*, 467–550. [CrossRef]
13. Roos, J.F.; Doust, J.; Tett, S.E.; Kirkpatrick, C.M. Diagnostic accuracy of cystatin C compared to serum creatinine for the estimation of renal dysfunction in adults and children—A meta-analysis. *Clin. Biochem.* **2007**, *40*, 383–391. [CrossRef]
14. Larsson, A.; Malm, J.; Grubb, A.; Hansson, L.O. Calculation of glomerular filtration rate expressed in mL/min from plasma cystatin C values in mg/L. *Scand. J. Clin. Lab. Investig.* **2004**, *64*, 25–30. [CrossRef]
15. Ataei, N.; Bazargani, B.; Ameli, S.; Madani, A.; Javadilarijani, F.; Moghtaderi, M.; Abbasi, A.; Shams, S.; Ataei, F. Early detection of acute kidney injury by serum cystatin C in critically ill children. *Pediatr. Nephrol.* **2014**, *29*, 133–138. [CrossRef]

16. Asilioglu, N.; Acikgoz, Y.; Paksu, M.S.; Gunaydin, M.; Ozkaya, O. Is serum cystatin C a better marker than serum creatinine for monitoring renal function in pediatric intensive care unit? *J. Trop. Pediatr.* **2012**, *58*, 429–434. [CrossRef]
17. Di Nardo, M.; Ficarella, A.; Ricci, Z.; Luciano, R.; Stoppa, F.; Picardo, S.; Picca, S.; Muraca, M.; Cogo, P. Impact of severe sepsis on serum and urinary biomarkers of acute kidney injury in critically ill children: An observational study. *Blood Purif.* **2013**, *35*, 172–176. [CrossRef]
18. Herrero-Morin, J.D.; Malaga, S.; Fernandez, N.; Rey, C.; Dieguez, M.A.; Solis, G.; Concha, A.; Medina, A. Cystatin C and beta2-microglobulin: Markers of glomerular filtration in critically ill children. *Crit. Care* **2007**, *11*, R59. [CrossRef]
19. McCaffrey, J.; Coupes, B.; Chaloner, C.; Webb, N.J.; Barber, R.; Lennon, R. Towards a biomarker panel for the assessment of AKI in children receiving intensive care. *Pediatr. Nephrol.* **2015**, *30*, 1861–1871. [CrossRef]
20. Downes, K.J.; Zane, N.R.; Zuppa, A.F. Effect of Cystatin C on Vancomycin Clearance Estimation in Critically Ill Children Using a Population Pharmacokinetic Modeling Approach. *Ther. Drug Monit.* **2020**, *42*, 848–855. [CrossRef]
21. Wheeler, D.S.; Devarajan, P.; Ma, Q.; Harmon, K.; Monaco, M.; Cvijanovich, N.; Wong, H.R. Serum neutrophil gelatinase-associated lipocalin (NGAL) as a marker of acute kidney injury in critically ill children with septic shock. *Crit. Care Med.* **2008**, *36*, 1297–1303. [CrossRef]
22. Haase, M.; Bellomo, R.; Devarajan, P.; Schlattmann, P.; Haase-Fielitz, A.; Group, N.M.-a.I. Accuracy of neutrophil gelatinase-associated lipocalin (NGAL) in diagnosis and prognosis in acute kidney injury: A systematic review and meta-analysis. *Am. J. Kidney Dis.* **2009**, *54*, 1012–1024. [PubMed]
23. Kim, H.; Hur, M.; Cruz, D.N.; Moon, H.W.; Yun, Y.M. Plasma neutrophil gelatinase-associated lipocalin as a biomarker for acute kidney injury in critically ill patients with suspected sepsis. *Clin. Biochem.* **2013**, *46*, 1414–1418. [CrossRef] [PubMed]
24. Sampaio de Souza Garms, D.; Cardoso Eid, K.Z.; Burdmann, E.A.; Marcal, L.J.; Antonangelo, L.; Dos Santos, A.; Ponce, D. The Role of Urinary Biomarkers as Diagnostic and Prognostic Predictors of Acute Kidney Injury Associated with Vancomycin. *Front. Pharmacol.* **2021**, *12*, 705636. [CrossRef] [PubMed]
25. Rhodes, N.J.; Prozialeck, W.C.; Lodise, T.P.; Venkatesan, N.; O'Donnell, J.N.; Pais, G.; Cluff, C.; Lamar, P.C.; Neely, M.N.; Gulati, A.; et al. Evaluation of Vancomycin Exposures Associated with Elevations in Novel Urinary Biomarkers of Acute Kidney Injury in Vancomycin-Treated Rats. *Antimicrob. Agents Chemother.* **2016**, *60*, 5742–5751. [CrossRef] [PubMed]
26. Fuchs, T.C.; Frick, K.; Emde, B.; Czasch, S.; von Landenberg, F.; Hewitt, P. Evaluation of novel acute urinary rat kidney toxicity biomarker for subacute toxicity studies in preclinical trials. *Toxicol. Pathol.* **2012**, *40*, 1031–1048. [CrossRef]
27. Pais, G.M.; Avedissian, S.N.; O'Donnell, J.N.; Rhodes, N.J.; Lodise, T.P.; Prozialeck, W.C.; Lamar, P.C.; Cluff, C.; Gulati, A.; Fitzgerald, J.C.; et al. Comparative Performance of Urinary Biomarkers for Vancomycin-Induced Kidney Injury According to Timeline of Injury. *Antimicrob. Agents Chemother.* **2019**, *63*. [CrossRef]
28. Neely, M.N.; van Guilder, M.G.; Yamada, W.M.; Schumitzky, A.; Jelliffe, R.W. Accurate detection of outliers and subpopulations with Pmetrics, a nonparametric and parametric pharmacometric modeling and simulation package for R. *Ther. Drug Monit.* **2012**, *34*, 467–476. [CrossRef]
29. R Foundation for Statistical Computing Team. *R: A Language and Environment for Statistical Computing*; R Foundation for Statistical Computing: Vienna, Austria, 2020.
30. RStudio. *RStudio: Integrated Development Environment for R*; RStudio, Inc.: Boston, MA, USA, 2019.
31. Yamada, W.M.; Neely, M.N.; Bartroff, J.; Bayard, D.S.; Burke, J.V.; Guilder, M.V.; Jelliffe, R.W.; Kryshchenko, A.; Leary, R.; Tatarinova, T.; et al. An Algorithm for Nonparametric Estimation of a Multivariate Mixing Distribution with Applications to Population Pharmacokinetics. *Pharmaceutics* **2020**, *13*, 42. [CrossRef]
32. Hoek, F.J.; Kemperman, F.A.; Krediet, R.T. A comparison between cystatin C, plasma creatinine and the Cockcroft and Gault formula for the estimation of glomerular filtration rate. *Nephrol. Dial. Transplant.* **2003**, *18*, 2024–2031. [CrossRef]
33. Pottel, H.; Delanaye, P.; Schaeffner, E.; Dubourg, L.; Eriksen, B.O.; Melsom, T.; Lamb, E.J.; Rule, A.D.; Turner, S.T.; Glassock, R.J.; et al. Estimating glomerular filtration rate for the full age spectrum from serum creatinine and cystatin C. *Nephrol. Dial. Transplant.* **2017**, *32*, 497–507. [CrossRef]
34. Chen, I.H.; Nicolau, D.P. Augmented Renal Clearance and How to Augment Antibiotic Dosing. *Antibiotics* **2020**, *9*, 393. [CrossRef]
35. Straney, L.; Clements, A.; Parslow, R.C.; Pearson, G.; Shann, F.; Alexander, J.; Slater, A.; ANZICS Paediatric Study Group; Paediatric Intensive Care Audit Network. Paediatric Index of Mortality 3: An Updated Model for Predicting Mortality in Pediatric Intensive Care. *Pediatr. Crit. Care Med.* **2013**, *14*, 673–681. [CrossRef]
36. Back, H.M.; Lee, J.B.; Han, N.; Goo, S.; Jung, E.; Kim, J.; Song, B.; An, S.H.; Kim, J.T.; Rhie, S.J.; et al. Application of Size and Maturation Functions to Population Pharmacokinetic Modeling of Pediatric Patients. *Pharmaceutics* **2019**, *11*, 259. [CrossRef]
37. Rowland, M.; Tozer, T.N. Appendix A: Assessment of Area. In *Clinical Pharmacokinetics: Concepts and Applications*, 2nd ed.; Lea & Febiger: Malvern, PA, USA, 1989.
38. Bayard, D.S.; Neely, M. Experiment design for nonparametric models based on minimizing Bayes Risk: Application to voriconazole. *J. Pharm. Pharm.* **2017**, *44*, 95–111. [CrossRef]
39. Oh, Y.; Park, S.; Park, E.; Lee, J.; Lee, H.; Kim, J.; Cho, J. Correlation between vancomycin clearance and cystatin C-based glomerular filtration rate in paediatric patients. *Br. J. Clin. Pharmacol.* **2021**, *87*, 3190–3196. [CrossRef]
40. Hasson, D.; Menon, S.; Gist, K.M. Improving acute kidney injury diagnostic precision using biomarkers. *Pract. Lab. Med.* **2022**, *30*, e00272. [CrossRef]

41. Hirai, K.; Ishii, H.; Shimoshikiryo, T.; Shimomura, T.; Tsuji, D.; Inoue, K.; Kadoiri, T.; Itoh, K. Augmented Renal Clearance in Patients with Febrile Neutropenia is Associated with Increased Risk for Subtherapeutic Concentrations of Vancomycin. *Ther. Drug Monit.* **2016**, *38*, 706–710. [CrossRef]
42. Goutelle, S.; Woillard, J.B.; Neely, M.; Yamada, W.; Bourguignon, L. Nonparametric Methods in Population Pharmacokinetics. *J. Clin. Pharmacol.* **2022**, *62*, 142–157. [CrossRef]
43. Leroux, S.; Biran, V.; van den Anker, J.; Gotta, V.; Zhao, W.; Zhang, D.; Jacqz-Aigrain, E.; Pfister, M. Serum Creatinine and Serum Cystatin C are Both Relevant Renal Markers to Estimate Vancomycin Clearance in Critically Ill Neonates. *Front. Pharmacol.* **2021**, *12*, 634686. [CrossRef]
44. Thomas, S.N.; Stieglitz, H.M.; Hackenmueller, S.; Suh-Lailam, B.; Pyle-Eilola, A.L. Use of Cotton Balls in Diapers for Collection of Urine Samples Impacts the Analysis of Routine Chemistry Tests: An Evaluation of Cotton Balls, Diapers, and Chemistry Analyzers. *J. Pediatr.* **2022**, *245*, 179–183.e8. [CrossRef]

pharmaceutics

MDPI

Article

Clinical Effectiveness and Pharmacokinetics of Dalbavancin in Treatment-Experienced Patients with Skin, Osteoarticular, or Vascular Infections

Giacomo Stroffolini [1,*,†], Amedeo De Nicolò [2,†], Alberto Gaviraghi [1], Jacopo Mula [2], Giuseppe Cariti [1], Silvia Scabini [1], Alessandra Manca [2], Jessica Cusato [2], Silvia Corcione [1], Stefano Bonora [1], Giovanni Di Perri [1], Francesco Giuseppe De Rosa [1,‡] and Antonio D'Avolio [2,‡]

[1] Infectious Diseases Unit, Department of Medical Sciences, University of Turin, 10149 Turin, Italy
[2] Laboratory of Clinical Pharmacology and Pharmacogenetics, Department of Medical Sciences, University of Turin, 10149 Turin, Italy
* Correspondence: giacomo.stroffolini@unito.it; Tel.: +39-0114393856; Fax: +39-0114393740
† These authors contributed equally to this work.
‡ These authors contributed equally to this work.

Abstract: Dalbavancin (DBV) is a lipoglycopeptide approved for the treatment of Gram-positive infections of the skin and skin-associated structures (ABSSSIs). Currently, its off-label use at different dosages for other infections deserves attention. This work aimed to study the clinical effectiveness and tolerability of DBV in outpatients with ABSSSIs, osteoarticular (OA), or other infections, treated with either one or two 1500 mg doses of dalbavancin, for different scheduled periods. A liquid chromatography–tandem mass spectrometry method was used to measure total DBV concentrations. PK/PD parameters and the clinical and microbiological features of this cohort were evaluated in order to investigate the best predictors of treatment success in real-life settings. Of the 76 screened patients, 41 completed the PK study. Long-term PK was comparable to previous studies and showed significant differences between genders and dosing schedules. Few adverse events were observed, and treatment success was achieved in the vast majority of patients. Failure was associated with lower PK parameters, particularly C_{max}. Concluding, we were able to describe DBV PK and predictors of treatment success in selected infections in this cohort, finding DBV C_{max} as a possible candidate for therapeutic drug-monitoring purposes, as well as highlighting the dual-dose one-week-apart treatment as the optimal choice for OA infections.

Keywords: dalbavancin; long-acting; Gram-positive; PK/PD; osteoarticular infections

Citation: Stroffolini, G.; De Nicolò, A.; Gaviraghi, A.; Mula, J.; Cariti, G.; Scabini, S.; Manca, A.; Cusato, J.; Corcione, S.; Bonora, S.; et al. Clinical Effectiveness and Pharmacokinetics of Dalbavancin in Treatment-Experienced Patients with Skin, Osteoarticular, or Vascular Infections. *Pharmaceutics* **2022**, *14*, 1882. https://doi.org/10.3390/pharmaceutics14091882

Academic Editors: Avi Domb, Barna Vasarhelyi and Gellért Balázs Karvaly

Received: 6 June 2022
Accepted: 26 August 2022
Published: 6 September 2022

1. Introduction

Dalbavancin (DBV) is a semi-synthetic, novel, long-acting lipoglycopeptide active against Gram-positive pathogens, including multi-drug resistant isolates, approved for the treatment of ABSSSIs [1]. Long elimination half-life (around 9–10 days) and good tissue penetration represent the main pharmacokinetic features of dalbavancin, allowing for its long-term efficacy despite the simplified weekly administration regimens [2]. This extremely long half-life is also due to its high percentage of binding to plasma proteins (mainly albumin), which was described to vary from nearly 98% in rats to 93% in humans. DBV exhibits peculiar PK/PD properties, with good tissue penetration and a high susceptibility rate (near 100.0%) [2–7]. The clearance of DBV is not influenced by inhibitors or inducers of cytochrome P450, and therefore, its potential for drug–drug interaction involving hepatic metabolism is very low [2]. Furthermore, in an exploratory study, patient demographic characteristics had minor impacts on the pharmacokinetic profile of DBV, while females showed slightly higher concentration values, particularly in relation to body surface area (BSA) and body mass index (BMI) [3]. The ratio between the mean

free area under the curve and the minimum inhibitory concentration (fAUC/MIC) was previously proposed as the best PK/PD parameter for its correlation with in vivo efficacy of DBV [2,3]. The 24 h fAUC/MIC values for net stasis, 1-log kill, and 2-log kill against *Staphylococcus aureus* were, respectively, 27.1, 53.3, and 111.1 [8,9]. No DBV dose adjustment is required in mild–moderate renal impairment, any degree of hepatic impairment, and for different modalities of renal replacement therapy (RRT); nevertheless, evidence in different modalities of RRT is poor, and the role of hypoalbuminemia still deserves better understanding [10], while dose reduction is suggested in patients affected by severe renal impairment. DBV exhibits a potent activity in vitro against the established biofilms due to *Staphylococcus aureus*, *Staphylococcus epidermidis*, and vancomycin-susceptible *Enterococci*, thus possibly playing a crucial role in the management of relevant infections characterised by bacterial biofilm production [11–13]. Nicolau et al. [14] reported a mean dalbavancin penetration into skin blister fluid of 59.6%, compared with plasma, after a single 1000 mg infusion, resulting in tissue concentrations well above the MIC_{90} of common Gram-positive pathogens implicated in ABSSSIs (including MRSA) for up to 7 days. In another study, Rappo et al. [15] found that, in 35 healthy subjects receiving a single infusion of 1500 mg DBV, the penetration into the epithelial-lining fluid was 36%, resulting in DBV lung concentrations exceeding the MIC90 of *Streptococcus pneumoniae* and *Staphylococcus aureus* for at least 7 days. Moreover, Dunne et al. [16] found a mean bone/plasma AUC of 13.1%, suggesting that two doses of DBV 1500 mg infusion administered one week apart may provide tissue exposure over the MIC for *Staphylococcus aureus* for 8 weeks. These findings were confirmed in two recent studies involving patients with OA infections [3,8]. Consequently, these convenient PK/PD properties make DBV a valuable alternative to daily in-hospital intravenous or daily continuous outpatient antimicrobial regimens in the treatment of long-term Gram-positive infections, posing the basis for its use beyond approved indications [4,5]. The DBV PK/PD relationship has been described to be AUC/MIC-dependent, making the application of TDM particularly difficult. In this scenario, some works suggested alternative analysis methods to the DBV quantification throughout treatment, such as the evaluation of the bactericidal activity of plasma samples [17], C_{max} values as a proxy of AUC [18], or punctual DBV concentration after 1 month [9]; recently, our group described DBV AUC over the long term in a small subset of patients with ABSSSIs or OA infections [3]. Despite all these studies, the definition of optimal PK/PD parameters with a useful TDM potential is still tricky, particularly considering patients with different clinical and microbiological features, as well as different dosing and posology. Therefore, more information is needed about DBV PK/PD and clinical effectiveness in a "real-life" context, in relation to the infection site and posological differences. The aim of this work was to better describe DBV PK in real-life settings and to characterise its PK/PD profile, for both approved and unapproved indications, treated with either a single 1500 mg dose or a double 1500 mg dose, 1 week, 2 weeks, or 3 weeks apart. Moreover, we aimed to evaluate the possible role of a TDM-based approach in optimising therapeutic choices, focusing on the most important PK/PD parameters for DBV, namely C_{max} and AUC/MIC, in different treatment periods. Ultimately, we aimed to link these PK/PD data to clinical outcomes and monitor the DBV safety profile.

2. Materials and Methods

2.1. Patient Enrolment and DBV Administration

We included patients with Gram-positive infections, with previous therapeutic failure to other antibiotic regimens or need for consolidation, and eligible for treatment with DBV, enrolled in the "Appropriatezza Farmacologica della Terapia Anti-Infettiva" (ethical approval no. 0040388 23 April 2020) clinical study. Patients stopped all their previous antibiotic therapies and were selected for a single 1500 mg or dual 1500 mg DBV infusion (1500 mg, 2 doses 1, 2, or 3 weeks apart) based on guidelines, investigator judgment, and the emerging data from the literature [19–27]. DBV was generally prescribed for patients who did not significantly benefit from previous therapies, for consolidation purposes, or

due to intolerance to other therapies; therapy was conducted as an outpatient modality, also considering the COVID-19 emergency; a therapeutic scheme of two doses one week apart was recommended mainly in the setting of osteoarticular infections based on the data from other Italian and international experiences [3,8,19]. DBV preparation and administration were performed in this study as per label indications since patients' selection and follow-up were in line with the instructions previously followed by our study group and described in an exploratory study [3]. Drug infusion was intravenously performed for 30 min. The cure was defined as the resolution of symptoms, microbiological cure, or no evidence of pathology as assessed by radiology techniques when applicable. Conversely, clinical/microbiological failure was retained if patients required additional antibiotics for their lack of response, presented new purulence, needed amputation, or died. The body surface area (BSA) was estimated using the Du Bois formula. Based on DBV administration, we identified 4 subgroups in relation to the interval that elapsed between the first and subsequent drug administration: *group 1* (1 week apart), *group 2* (2 weeks apart), and *group 3* (3 weeks apart); patients receiving a single DBV administration pertain to *group 0*.

2.2. PK and PD Evaluation

Blood sampling for the PK was performed in a 7 mL lithium/heparin tube using the following timing schedules, relatively to DBV infusion: 0 h (pre-dose), 0.5 h (end of infusion), 1 h, 1 week, 2 weeks, 3 weeks, 4 weeks, and then every 2 weeks, up to 6 months. No specific susceptibility testing was available for the direct determination of DBV MIC; therefore, surrogate categorisation of susceptibility was performed based on the MIC value for vancomycin, as previously reported and indicated by the EUCAST and Jones et al. [28]. On this basis, susceptibility to vancomycin (minimal inhibitory concentration, MIC 2 mg/L) was interpreted as a proxy of DBV MIC lower than 0.125 mg/L (nearly 97% probability from [28]), the EUCAST-suggested breakpoint for cocci. PK evaluation was performed as previously described in the literature [3,29], with an analytical kit (KIT-SYSTEM Antibiotics, CoQua Lab, Torino, Italy). Briefly, 50 µL of sample underwent protein precipitation, with the addition of isotope-labelled DBV as internal standard, and the diluted supernatants were analysed via reverse phase ultra-high performance liquid chromatography and tandem mass spectrometry (UHPLC–MS/MS). This method was associated with the mean bias and imprecision both being lower than 15%, in accordance with the EMA and FDA guidelines [29–31]. All the AUC data were calculated using a "linear-up/log-down" model by interpolating the concentration data of each patient, using the Phoenix WinNonlin software (Certara, Princeton, NJ, USA). The cumulative $AUC_{0–1w}$/MIC, $AUC_{0–2w}$/MIC, and $AUC_{0–4w}$/MIC values were calculated in this analysis, in order to compare the different dosing schedules in terms of the overall early systemic exposure, which is supposed to be the most important for microbiological and clinical success [3,8,9]. Additionally, protein-binding-adjusted (PBA) AUC/MIC values were calculated by dividing the PK parameters by the PBA breakpoint MIC 1.786 mg/L (0.125 mg/L/0.07) considering a 93% protein binding, based on the mean percentage of protein binding in humans, as reported in several works [2,3,32].

2.3. Statistical Analysis

All statistical analyses were performed through Excel and SPSS 27.0 (IBM Corp, Armonk, NY, USA). Descriptive data are reported as percentages, median, and interquartile ranges (IQRs). The correlations between continuous data were evaluated through Pearson's correlation tests. Differences between the groups were tested through the Kruskal–Wallis and Mann–Whitney non-parametric rank tests, and with an ANOVA test.

3. Results

3.1. Population Characteristics

A total of 76 patients were included in the preliminary screening and analysis. Of these, 41 completed the intensive PK study as per the Methods section (see Supplementary Materials).

The main clinical and demographic characteristics are presented in Table 1, and the main infection features are presented in Table 2. None of the involved patients was immunocompromised. Overall, chronic osteomyelitis was present in five patients. One patient dropped out because of an alternative diagnosis (tuberculous osteomyelitis). All the patients received previous antibiotic treatment except three (4%), comprising 52 patients (68%) with one single therapeutic line, 20 with two lines (26%), and 1 patient with three lines. The median duration of previous therapies was 28 days (IQR 14–56). Most commonly, patients were pre-treated with lipopeptides, glycopeptides, and beta-lactams. The reasons for treatment with DBV were: consolidation (43 patients, 56%), intolerance (2 patients, 3%), or failure (31, 41%) to other therapies. The majority of our patients (40, 54%) received two doses, while the remainder received one. The median time to cure after DBV was 56 days [28–84]. Overall, in terms of the final outcome, 58 patients (82%) were cured, 13 (17%) failed, and 4 (5%, excluded from the final analysis) were LFU patients, classified as per described in the Methods section.

Table 1. Overall patients' characteristics at the baseline.

	Overall	***Intensive PK Study (n = 41)***			
	n = 76	***Group 0 (n = 17)***	***Group 1 (n = 9)***	***Group 2 (n = 13)***	***Group 3 (n = 2)***
Variable	Value (median [IQR]/%)	-	-	-	-
Age (median [IQR])	60 [50–70.5]	60 [51–73]	67 [48–75]	60 [48–71]	40 [17–40]
Ethnicity: Caucasian (%)	100%	-	-	-	-
Sex: Male (n (%))	47 [60%]	9 [53]	7 [78]	6 [60]	1 [50]
Albumin (g/L)	43 [40–45]	44 [39–46]	44 [43–46]	43 [42–45]	45 [40–45]
BMI	24.5 [22.2-28.2]	26 [22–31]	20 [22–24]	24 [23–30]	23 [21–23]
BSA	1.7 [1.4–2.2]	1.8 [1.5–2.3]	1.6 [1.2–1.8]	1.9 [1.7–2.2]	1.2 [1–1.3]
eGFR (mL/min)	94.5 [77.3–116.2]	86 [74–104]	91 [79–126]	100 [73–118]	112 [90–113]
AEs: yes	1	1 [6%]	-	-	-
Infection control: yes (n, (%))	36 [47%]	10 [60]	3 [30]	10 [80]	1 [50]
Diabetes: yes (n, (%))	19 [25%]	4 [23]	1 [13]	3 [23]	-
Previous therapy: yes (n, (%))	73 [96%]	17 [100]	8 [89]	13 [100]	2 [100]
N. therapy lines: 1 (n, (%)); 2: (n, (%)); 3: (n, (%))	52 [75%]; 20 [26]; 1 [1]	12 [67]; 5 [33]	4 [50]; 4 [50]	5 [40]; 8 [60]	1 [50]; 1 [50]
Length of therapy before DBV (days)	14 [14–35]	14 [14–56]	35 [23–75]	35 [28–105]	35 [14–35]
Reasons for DBV (n, (%)): previous failure; consolidation; intolerance	31 [41%]; 43 [56]; 2 [3]	9 [53]; 8 [47]	5 [55]; 4 [45]	4 [30]; 7 [55]; 2 [15]	1 [50]; 1 [50]

Table 2. Main clinical and microbiological characteristics and outcomes.

	Overall (76)	***Intensive PK Study (n = 41)***			
		Group 0 (n = 17)	***Group 1 (n = 9)***	***Group 2 (n = 13)***	***Group 3 (n = 2)***
Type of infection (n, (%))	ABSSSIs: 16 [21] LVAD: 3 [4] Endocarditis: 3 [4] OAs: 54 [71] Osteomyelitis: 13 [25] Spondylodiscitis: 8 [15] Septic arthritis: 5 [11] PJI: 27 [49]	ABSSSIs: 7 LVAD: 2 Septic Arthritis: 1 Osteomyelitis: 2 Prosthetic infection: 5	Septic arthritis: 1 Osteomyelitis: 4 Spondylodiscitis: 3 Endocarditis: 1	ABSSSIs: 2 Septic arthritis: 1 Osteomyelitis: 3 Spondylodiscitis: 2 PJI: 5	Spondylodiscitis: 1 PJI: 1
Aetiology (n, (%))	MSSA: 32 [42] MRSA 23 [30] MRSE 7 [9.2] MSSE 2 [2.6] S. Lugdunensis 1 [1.3] Streptococcus spp.: 3 [4.1]	MRSA: 4 MSSA: 8 MRSE: 3	MRSA: 3 MSSA: 3 MRSE: 1 S. dysgalactiae: 1	MSSA: 8 MRSA: 4 MSSE: 1	MRSA: 2
Outcome: cure (n, (%))	58/71 [82%]	14/17 [82]	9/9 [100]	7/13 [54]	2/2 [100]
Time to cure (days)	28 [28–56]	14 [14–56]	84 [49–105]	84 [84–112]	28 [28–84]

3.2. Pharmacokinetic Results

Of these 76 screened patients, 41 had a complete PK study, with a median of 7 [5–9.5] PK evaluations throughout the study. Of these patients, 25 (60%) were male; 17 patients (41.5%) were included in the one-dose dosing group (3 failed, 14 were cured); 8 patients (19.5%) were included in the two-dose, one-week-apart dosing group (*group 1*, no failure, 8 were cured); 13 patients (31.7%) were included in the two-dose, two-week-apart dosing group (*group 2*, 6 failed, 7 were cured); and 2 (4.9%) and 1 (2.4%) patients were included in the two-dose, three-week- and four-week-apart dosing groups (*group 3* and *4*, all cured). In addition, 20 patients (49%) underwent DBV therapy for consolidation purposes, 19 (46%) for failure, and 2 (5%) because of intolerance to other therapies. Eight patients from this group (20%) had diabetes, and three (7.3%) had slight renal insufficiency. Twenty-two (53.7%) underwent infection control procedures. Overall, 32 patients (78%) were cured at the end of the study period. The median PK parameters of the first dose, the cumulative AUC in the first month of therapy, as well as the protein-binding-adjusted (PBA) AUC/MIC (PBA AUC/MIC) results, categorised by dosing groups, are presented in Table 3 and displayed in Figure 1. Moreover, the curves describing the terminal half-life and mean PK parameters in each group are displayed in Supplementary Figure S2. Second-dose AUC0–1w values were 32,810 mg/L·h [31,477–40,392]; 23,391 mg/L·h [21,930–30,780]; and 28,847 mg/L·h [28726–28847] for group 1, 2, or 3, respectively; second-dose AUC0–2w values were 45,595 mg/L·h [41,210–58,551]; 30,070 mg/L·h [29,183–40,644]; and 36,848 mg/L·h [36,636–36,848] for these same groups. Second-dose AUC0–3w values were 54,330 mg/L·h [46,317–68,054]; 40,570 mg/L·h [32,817–48,132]; and 41,124 mg/L·h [41,099–41,124] for the same groups. A significant positive correlation between Cmax at the first dose and cumulative $AUC_{0–4w}$, for both *group 0* and *group 1* ($p = 0.018$; $p = 0.041$), was observed; C_{max} at the second dose for *group 1* also significantly correlated with the cumulative $AUC_{0–4w}$ ($p = 0.039$). Moreover, C_{max} at the first dose in *group 1* was significantly correlated with

$AUC_{0–1w}$ (p = 0.015). The latter variable showed a significant positive correlation with cumulative $AUC_{0–4w}$ for that group (p = 0.043).

Table 3. Main PK and PK/PD characteristics, by dosing group, including protein-binding-adjusted (PBA) parameters. -: not applicable.

		Intensive PK Study			
Variable	**Overall**	**Group 0**	**Group 1**	**Group 2**	**Group 3**
C_{max} I dose (mg/L)	342.8 [290.5–424.0]	419.6 [306.8–477.0]	347.0 [292.4–479.2]	323.3 [305.8–385.4]	383.8 [335.5–383.8]
C_{max} II dose (mg/L)	379.5 [321.3–448.8]		420.6 [380.6–469.8]	337.0 [290.7–424.0]	432.440 [372.2–432.4]
$AUC_{0–1w}$ (mg/L·h)	-	26,693 [20,842–28,630]	25,623 [23,335–28,347]	23,924 [20,685–26,501]	28,489 [25,573–28,489]
$AUC_{0–2w}$ (mg/L·h)	-	34,168 [25,336–37,301]	-	31,686 [26,281–33,914]	35,912 [32,891–35,912]
$AUC_{0–3w}$ (mg/L·h)	-	39,270 [28,876–43,971]	= -	-	39,985 [37,045–39,985]
Cumul.$AUC_{0–4w}$ (mg/L·h)	-	41,681 [32,055–48,180]	79,486 [71,849–95,210]	62,432 [55,860–74,010]	68,835 [66,005–68,835]
PBA $AUC_{0–1w}$/MIC	-	14,946 [11,670–16,030]	14,341 [13,065–15,872]	13,395 [11,582–14,838]	15,951 [14,318–15,951]
PBA $AUC_{0–2w}$/MIC	-	-	-	17,741 [14,715–18,989]	20,107 [18,416–20,107]
PBA $AUC_{0–3w}$/MIC	-	-	-	-	22,388 [20,741–22,388]
PBA Cumul.$AUC_{0–4w}$/MIC (mg/L·h)	-	23,338 [17,948–26,976]	44,505 [40,229–53,309]	34,956 [31,277–41,439]	38,541 [36,957–38,541]
Terminal half-life	-	508	633	413	437

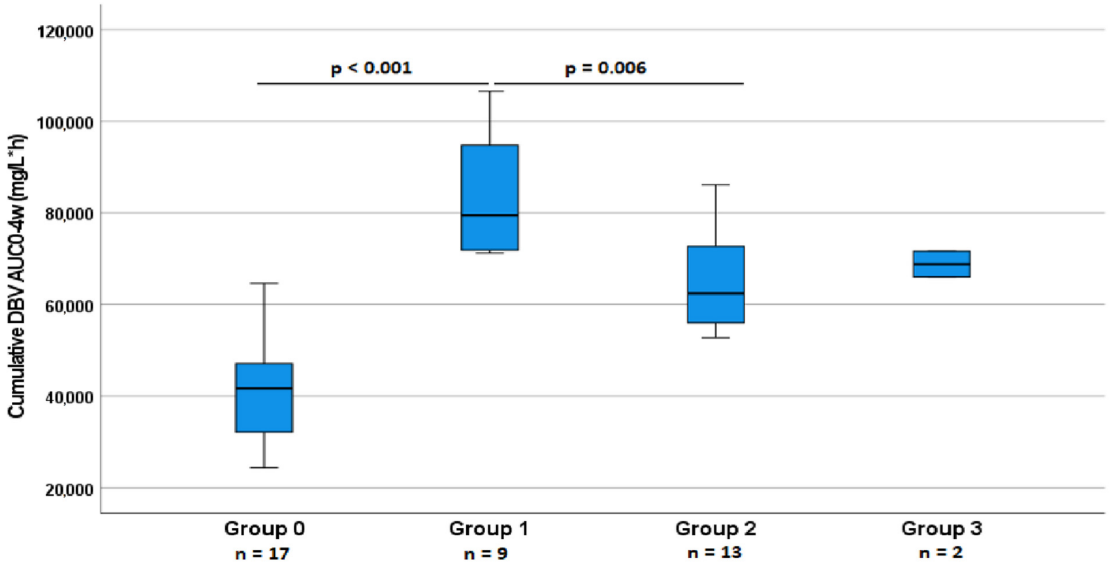

Figure 1. Cumulative $AUC_{0–4w}$ for different dosing groups. DBV levels are expressed in mg/L·h. Cumulative $AUC_{0–4w}$ of treatment was significantly higher for *group 1*, compared with all the other dosing groups.

A significant positive correlation between C_{max} at the first dose and cumulative $AUC_{0–4w}$, for both *group 0* and *group 1* ($p = 0.018$; $p = 0.041$), was observed; C_{max} at the second dose for *group 1* also significantly correlated with cumulative $AUC_{0–4w}$ ($p = 0.039$). Moreover, C_{max} at the first dose in *group 1* was significantly correlated with $AUC_{0–1w}$ ($p = 0.015$). The latter variable showed a significant positive correlation with cumulative $AUC_{0–4w}$ for that group ($p = 0.043$).

We performed the Kruskal–Wallis and Mann–Whitney non-parametric tests and found that the cumulative $AUC_{0–4w}$ of treatment was significantly higher for *group 1*, compared with all the other dosing groups ($p < 0.001$; Figure 1). Moreover, at the second dose, *group 1* also showed a significantly higher C_{max} than *group 2* ($p = 0.05$; Table 3).

3.3. Association between DBV PK and Treatment Outcomes

Among all the PK parameters which were tested for their associations with treatment outcome, C_{max} at the first dose, $AUC_{0–1w}$, and cumulative $AUC_{0–4w}$ all resulted in higher values in cured patients, although these differences were not statistically significant ($p = 0.114$, 0.063 and 0.324, respectively; Figure 2). Concurrently, the highest efficacy was highlighted in *group 1*, especially when compared with the other groups, with a solid trend toward significance ($p = 0.053$, cured vs. not cured). The same PK parameters were tested for their associations with treatment outcome, further stratifying groups by infection site. When analysing ABSSSIs, no significant association was observed. For all the other indications, PK parameters appeared slightly reduced but without reaching statistical significance. This stratified analysis was not applicable to LVAD, because all three patients failed, nor did it apply to intravascular infections and spondylodiscitis, as all patients were cured at the end of the study period.

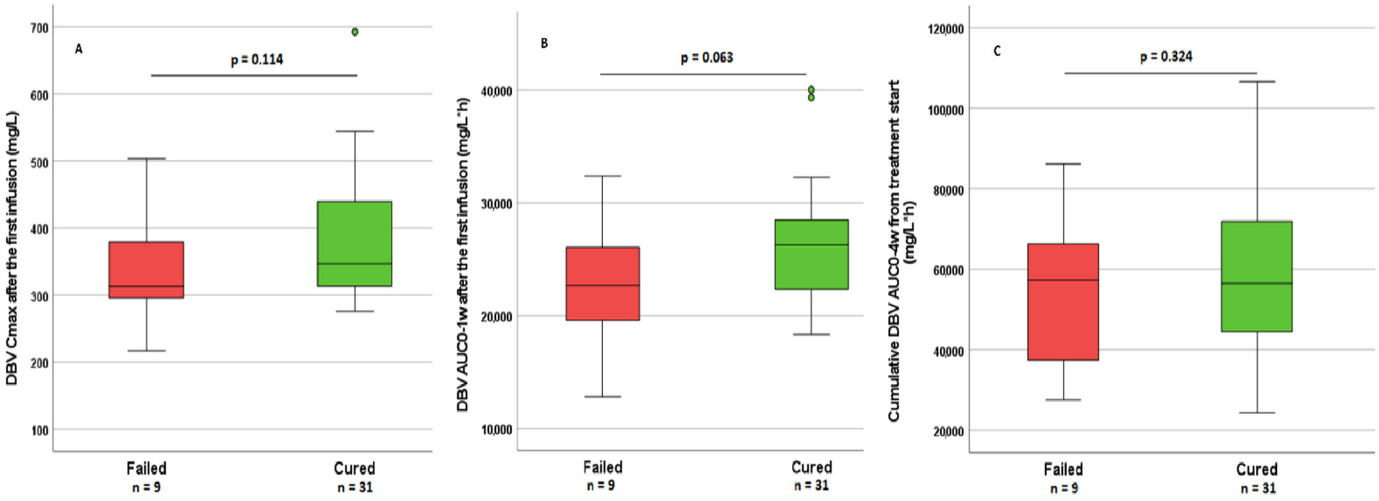

Figure 2. (**A**–**C**) distribution of DBV C_{max} after the first infusion, $AUC_{0–1w}$, cumulative $AUC_{0–4w}$, and DBV levels with regard to outcomes. Among all the PK parameters which were tested for their associations with treatment outcome, C_{max} at the first dose, $AUC_{0–1w}$, and cumulative $AUC_{0–4w}$ all resulted in higher values in cured patients, although these differences were not statistically significant.

When stratifying this analysis by reasons for treatment with DBV (previous failure, intolerance, or consolidation) and site of infection, no significant difference was observed in patients with ABSSSIs, while for all the other indications, a significantly higher value for C_{max} after the first infusion was associated with treatment success for patients treated for consolidation purposes ($p = 0.04$) but not when patients were selected for therapy with DBV because of previous failure or intolerance ($p = 0.214$, Figure 3).

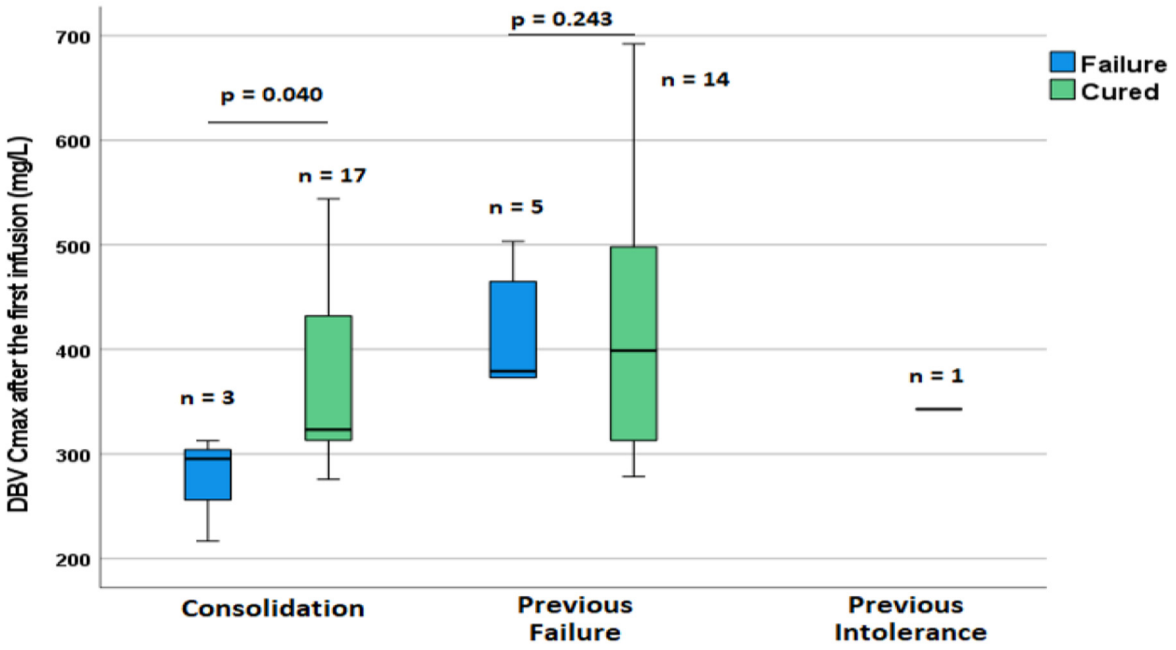

Figure 3. Differences in DBV levels between patient groups based on the reason for using DBV with regard to previous treatments and the outcome of therapy with DBV.

3.4. Correlations of DBV PK Parameters with Patient Characteristics

Overall, albumin was inversely correlated with the cumulative $AUC_{0–4w}$ ($p = 0.047$). BSA was significantly and negatively correlated with $AUC_{0–1w}$ at the first dose, C_{max} at the second dose, and the cumulative $AUC_{0–4w}$, ($p = 0.006$, 0.002, and 0.004, respectively). C_{max} at the first dose showed only a trend towards a correlation with BSA ($p = 0.091$). No other significant correlations were found between eGFR, albumin, or other variables and DBV PK parameters. The Mann–Whitney test was applied relative to PK variables and gender in the whole cohort who underwent the PK study: Significant differences were found for C_{max} at the first dose and $AUC_{0–1w}$ values with regard to gender, resulting in higher values for both variables in female patients ($p < 0.001$). Gender differences in PK parameters are depicted in Figure 4. These differences were clearly explainable by a difference in BSA, which was also significantly different between genders ($p = 0.002$). Nevertheless, these differences did not result in significant differences in outcome ($p = 0.380$), probably due to the small sample size and the low number of failures.

3.5. Predictors of Failure to DBV

In the overall population of 71 patients, in the context of off-label indications (OA and vascular infections), patients' results were more likely to indicate failure to DBV if they were treated for failure to previous regimens ($p = 0.036$) and when treated for LVAD infections ($p = 0.007$). While no significant PK predictors of treatment success were observed in patients with failure to previous treatments, in the group of patients who were treated for consolidation purposes, failure was related to significantly lower DBV C_{max} at the first dose ($p = 0.04$), with a possible utility for future TDM purposes. For this reason, a ROC curve for C_{max} after the first dose was calculated with the aim to identify a threshold value capable to identify patients at risk for failure. From this analysis, the identified value was 313 mg/L, with the potential to identify patients prone to failure, with a sensitivity of 100% and a specificity of 78% ($p = 0.035$).

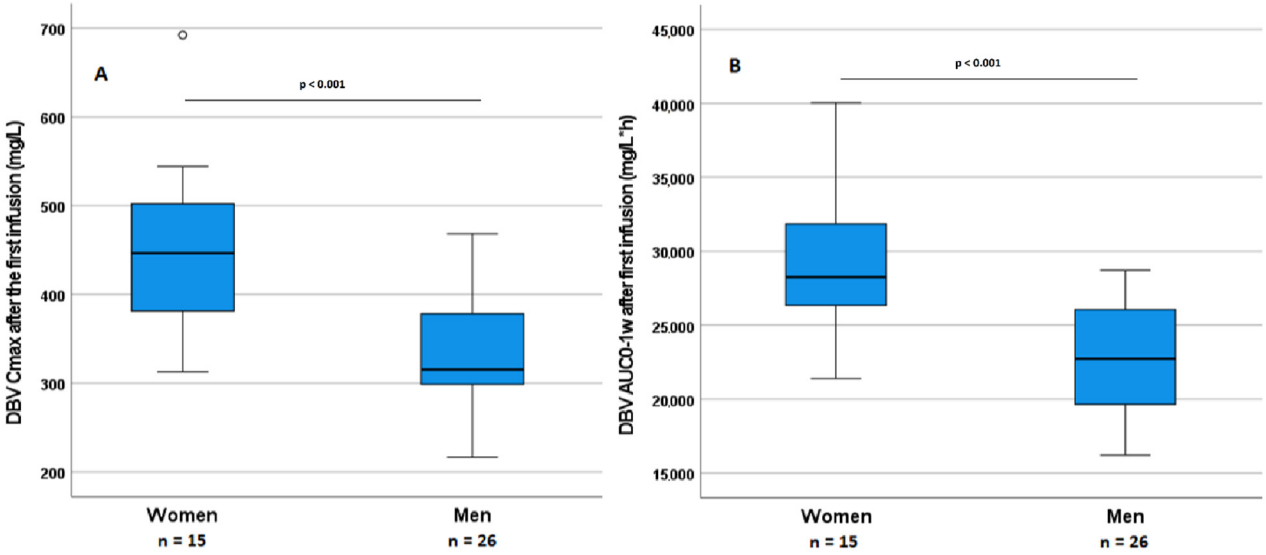

Figure 4. Differences in PK variables with regard to gender. (**A**,**B**) DBV C_{max} and DBV $AUC_{0\text{-}1w}$ differences in women and men ($p < 0.001$).

3.6. Testing Late PK Thresholds

In previous works, based on the PK/PD target attainment of an AUC/MIC ratio over 24 h after 1 month of treatment, two putative punctual threshold values were proposed for TDM purposes, 4 or 8 mg/L (in case of bacterial MIC of 0.062 or 0.125 mg/L, respectively) [8,9]. Considering these values, 7/41 and only 1/41 patients resulted below the 8 mg/L and 4 mg/L thresholds in our cohort, respectively. The latter patient experienced treatment failure. On the other hand, among patients with concentration values over the proposed 8 mg/L threshold, eight failed, while six patients with DBV concentrations below the 8 mg/L cut-off achieved treatment success. Finally, there was no statistically significant difference between DBV concentrations at week 4 with regard to outcome ($p = 0.389$).

4. Discussion

In this work, we described the PK variability and clinical performance of DBV in its real-life use, taking into account its different posology for the treatment of OA infections, ABSSSIs, and intravascular/bloodstream infections. These data were analysed for associations and/or correlations with the demographical, anthropometrical, microbiological, and clinical features of each patient; more importantly, we analysed the relationship between DBV PK and therapeutic outcome. The results of the observed PK and clinical data were concordant with previous studies [3,8,27]. Our cohort is representative of a third-level referral hub since the enrolled patients had frequently a complicated clinical history related to the management of their infections, usually with failure to one or more therapeutic approaches (multi-failed/experienced patients). Additionally, a considerable number of microbiological isolates were resistant to common first-line agents (MRSA, MRSE). Considering this setting, our results are extremely encouraging, showing an 82% cure rate, confirming the high efficacy of DBV even for its off-label alternative indications. This success is remarkable also in view of the high prevalence of comorbidities, in particular diabetes (25%). The overall propensity to the adoption of source control/surgery (47% in this cohort) is noteworthy in these contexts, highlighting the importance of surgery in complicated infections and the advantages of a combined approach. Unfortunately, our centre lacks a joint collaboration with orthopaedicians, a factor that would possibly improve the infection control tendency and outcomes. Generally speaking, few patients were lost to follow-up, and time-to-cure for patients was in line with what is expected for the infections described in this study. Cumulative exposure to DBV in the first month of

treatment (the most critical period to achieve bacterial eradication at the site of infection) revealed different results in patients in different exposure groups (close versus delayed re-administration). PK variables seemed generally higher in cured patients, although the low number of failures and variability in the clinical features of these patients led to low statistical significance. Interestingly, a context in which our molecule performed worse was the LVAD infection, for which no data are available in the literature, and in which classic long-term suppressive strategies or bridge therapies remain the treatment of choice; nevertheless, there is not an easy explanation for this phenomenon. This topic deserves a dedicated investigation in the future. On the other hand, no failures were observed for intravascular infections. The most satisfactory results from the off-label use of DBV were derived from the OA setting, with an overall 83% rate (45/54 patients), confirming the excellent suitability of DBV in this context, as already suggested in previous works [21–27]. In particular, no patient failed when treated for spondylodiscitis, and the percentages of failure were low in other OA indications. From a PK/PD perspective, the C_{max} measured at the end of the first infusion appeared to be the best PK predictor of clinical success, showing similar performance with AUC parameters, particularly in patients treated for consolidation purposes. The C_{max} was, in turn, found to be significantly different between genders and negatively correlated with BSA. Taken together, these results suggest that the therapeutic schedule for DBV could be optimised based on gender differences and anthropometric features. Specifically, the dual-dose one-week-apart schedule (*group 1*) showed both a higher proportion of treatment success, as well as a higher C_{max} value at the second administration and significantly higher cumulative AUC in the first month. In terms of the capability to predict treatment failure/success, we observed significant differences in terms of C_{max} between patients who failed in treatment for consolidation purposes (partial response to previous treatments) and those who were cured: In this context, it was possible to identify a putative cutoff value for C_{max} at the first dose of 313 mg/L, which could be predicted with good sensitivity and specificity. It is noteworthy that failures in this context happened at lower concentrations than for other subgroups (e.g., in patients with previous failures to other treatments), highlighting the cut-off value of 313 mg/L as a general threshold level for risk of failures, also in other contexts. These results provide useful information for a possible "fast-track" TDM use since the significant correlation between C_{max} and outcome suggests the possibility of using it as a proxy for early PK exposure and for the prediction of success/failure [33]. On the other hand, some previously proposed candidate markers for TDM use, such as DBV concentration after 1 month of treatment, seemed to be unrelated to the outcomes in our cohort [8,9]. Together, these observations suggest that, despite its long-acting activity, the clinical effectiveness of DBV seems greatly dependent on early exposure in the first weeks of treatment, highlighting the concept of a concentration-dependent primal effect for that molecule. It may be speculated that higher concentrations and early exposure are needed in order to reach the pharmacological sanctuaries of infection, where metabolically slow bacteria can proliferate due to being protected by biofilm, creating a pabulum for resistance, infection persistence, and incomplete cure. More data from tissues (e.g., bone and bone marrow) and intracellular (PBMCs), for which collection and measurements are challenging, may clarify these points. Importantly, additional help may come from combination therapy, the use of which still remains to be evaluated in prospective comparative studies [34–36]. To summarise, in our cohort, failures seemed to be more ascribable to worst infection characteristics (sanctuary site, lack of previous infection control/surgery, chronic infection, and comorbidities) than to PK underexposure, except for lower C_{max} when indicated for defined purposes. In this direction, we can state that DBV is not a magic bullet but certainly a game-changing molecule in the treatment of complicated Gram-positive infections. This is of much importance, especially for comorbid patients and those with multiple treatment failures who may be exposed to unnecessary infectious risks. Other advantages presented in different works [4,5] which we could not confirm due to the nature of our study pertain to the pharmacoeconomic role of this antibiotic. Other limitations of our study pertain to the generalisability of our

observations, inherent to the study design, specifically because of the lack of a prospective a priori randomised controlled schedule and the relatively low number of enrolled patients. Additionally, population modeling based on a larger population would be beneficial in predicting DBV PK parameters, and adding specific testing procedures for DBV MIC would yield additional predictive value both to the Cmax/MIC and AUC/MIC parameters. In the future, due to its microbiological and PK/PD features, it is possible to consider DBV as a first-line treatment strategy in certain indications rather than as a consolidation or step-down one [4,5,32].

5. Conclusions

In this work, we were able to show the real-life characteristics of DBV, especially PK/PD features, in terms of their correlations with anthropometric characteristics and clinical success. The high effectiveness of DBV was confirmed in a real-life cohort of treatment-experienced patients, allowing a more complete understanding of complicated OA infections. The identification of an extremely early marker as the C_{max} after the first infusion as a predictor of treatment failure could be useful for future TDM purposes. Further studies with larger and more homogeneous cohorts are needed in order to identify precise and dedicated threshold levels for DBV for each treatment indication. Finally, the observed gender-based and BSA-related differences in DBV exposure suggest the consideration of these factors for treatment optimisation.

Supplementary Materials: The following supporting information can be downloaded at: https://www.mdpi.com/article/10.3390/pharmaceutics14091882/s1. Figure S1: Flow in the selection of patients from screening to complete follow-up. DBV: dalbavancin; LFU: lost to follow-up; PK: pharmacokinetic; Figure S2: Mean PK profiles in each treatment group. Panel (a) group 0; Panel (b) Group 1; Panel (c) group 2; Panel (d) group 3. X axis = time from the first dose (weeks).

Author Contributions: Conceptualisation, G.S., G.D.P., F.G.D.R., A.D.N. and A.D.; methodology, G.S., A.G., G.C., A.D.N., F.G.D.R., G.D.P. and A.D.; software, A.D.N.; validation, A.M., J.M. and J.C.; formal analysis, J.M., A.M., J.C. and A.D.N.; investigation, G.S., G.C., A.G., S.C., S.S. and F.G.D.R.; resources, S.B., F.G.D.R., G.D.P. and A.D.; data curation, G.S., A.G., A.D.N. and J.M.; writing—original draft preparation, G.S. and A.D.N.; writing—review and editing, A.D., G.D.P., F.G.D.R., G.S., A.D.N. and S.C.; supervision, S.B., G.C., G.D.P., F.G.D.R. and A.D.; project administration, G.D.P. and F.G.D.R.; funding acquisition, A.D. All authors have read and agreed to the published version of the manuscript.

Funding: This research received no external funding.

Institutional Review Board Statement: The study was conducted according to the guidelines of the Declaration of Helsinki and approved by the Institutional Review Board of the "ASL Cittàdella Salute e della Scienza" (protocol No. 0040388 23 April 2020).

Informed Consent Statement: Written informed consent was obtained from all subjects involved in the study.

Data Availability Statement: Raw data will be provided on request. Data are contained within the article and Supplementary Materials.

Conflicts of Interest: A.D. and G.D.P. are shareholders of CoQua Lab. Other authors declare no conflict of interest.

References

1. Boucher, H.W.; Wilcox, M.; Talbot, G.H.; Puttagunta, S.; Das, A.F.; Dunne, M.W. Once-Weekly Dalbavancin versus Daily Conventional Therapy for Skin Infection. *N. Engl. J. Med.* **2014**, *370*, 2169–2179. [CrossRef]
2. Dash, R.P.; Babu, R.J.; Srinivas, N.R. Review of the pharmacokinetics of dalbavancin, a recently approved lipoglycopeptide antibiotic. *Infect. Dis.* **2017**, *49*, 483–492. [CrossRef] [PubMed]
3. De Nicolò, A.; Stroffolini, G.; Antonucci, M.; Mula, J.; De Vivo, E.D.; Cusato, J.; Palermiti, A.; Cariti, G.; Di Perri, G.; Corcione, S.; et al. Long-Term Pharmacokinetics of Dalbavancin in ABSSSI and Osteoarticular Settings: A Real-Life Outpatient Context. *Biomedicines* **2021**, *9*, 1288. [CrossRef] [PubMed]

4. Gatti, M.; Andreoni, M.; Pea, F.; Viale, P. Real-world use of dalbavancin in the era of empowerment of outpatient antimicrobial treatment: A careful appraisal beyond approved indications focusing on unmet clinical needs. *Drug Des. Dev. Ther.* **2021**, *15*, 3349–3378. [CrossRef] [PubMed]
5. Andreoni, M.; Bassetti, M.; Corrao, S.; De Rosa, F.G.; Esposito, V.; Falcone, M.; Grossi, P.; Pea, F.; Petrosillo, N.; Tascini, C.; et al. The role of dalbavancin for Gram positive infections in the COVID-19 era: State of the art and future perspectives. *Expert Rev. Anti-infective Ther.* **2021**, *19*, 1125–1134. [CrossRef]
6. Pfaller, M.; Flamm, R.K.; Castanheira, M.; Sader, H.S.; Mendes, R. Dalbavancin in-vitro activity obtained against Gram-positive clinical isolates causing bone and joint infections in US and European hospitals (2011–2016). *Int. J. Antimicrob. Agents* **2018**, *51*, 608–611. [CrossRef]
7. Sader, H.S.; Streit, J.M.; Mendes, R.E. Update on the in vitro activity of dalbavancin against indicated species (Staphylococcus aureus, Enterococcus faecalis, β-hemolytic streptococci, and Streptococcus anginosus group) collected from United States hospitals in 2017–2019. *Diagn. Microbiol. Infect. Dis.* **2021**, *99*, 115195. [CrossRef]
8. Cojutti, P.G.; Rinaldi, M.; Zamparini, E.; Rossi, N.; Tedeschi, S.; Conti, M.; Pea, F.; Viale, P. Population pharmacokinetics of dalbavancin and dosing consideration for optimal treatment of adult patients with staphylococcal osteoarticular infections. *Antimicrob. Agents Chemother.* **2021**, *65*, e02260-20. [CrossRef] [PubMed]
9. Cojutti, P.G.; Rinaldi, M.; Gatti, M.; Tedeschi, S.; Viale, P.; Pea, F. Usefulness of therapeutic drug monitoring in estimating the duration of dalbavancin optimal target attainment in staphylococcal osteoarticular infections: A proof-of-concept. *Int. J. Antimicrob. Agents* **2021**, *58*, 106445. [CrossRef]
10. Corona, A.; Agarossi, A.; Veronese, A.; Cattaneo, D.; D'Avolio, A. Therapeutic Drug Monitoring of Dalbavancin Treatment in Severe Necrotizing Fasciitis in 3 Critically Ill Patients: A Grand Round. *Ther. Drug Monit.* **2020**, *42*, 165–168. [CrossRef]
11. Silva, V.; Antão, H.S.; Guimarães, J.; Prada, J.; Pires, I.; Martins, Â.; Maltez, L.E.; Pereira, J.; Capelo, J.L.; Igrejas, G.; et al. Efficacy of dalbavancin against MRSA biofilms in a rat model of orthopaedic implant-associated infection. *J. Antimicrob. Chemother.* **2020**, *75*, 2182–2187. [CrossRef]
12. Sader, H.; Mendes, R.; Pfaller, M.; Flamm, R.K. Antimicrobial activity of dalbavancin tested against Gram-positive organisms isolated from patients with infective endocarditis in US and European medical centres. *J. Antimicrob. Chemother.* **2019**, *74*, 1306–1310. [CrossRef] [PubMed]
13. Silva, V.; Miranda, C.; Bezerra, M.; Antão, H.S.; Guimarães, J.; Prada, J.; Pires, I.; Maltez, L.; Pereira, J.E.; Capelo, J.L.; et al. Anti-biofilm activity of dalbavancin against methicillin-resistant *Staphylococcus aureus* (MRSA) isolated from human bone infection. *J. Chemother.* **2021**, *33*, 469–475. [CrossRef] [PubMed]
14. Nicolau, D.P.; Sun, H.K.; Seltzer, E.; Buckwalter, M.; Dowell, J.A. Pharmacokinetics of dalbavancin in plasma and skin blister fluid. *J. Antimicrob. Chemother.* **2007**, *60*, 681–684. [CrossRef] [PubMed]
15. Rappo, U.; Dunne, M.W.; Puttagunta, S.; Baldassarre, J.S.; Su, S.; Desai-Krieger, D.; Inoue, M. Epithelial Lining Fluid and Plasma Concentrations of Dalbavancin in Healthy Adults after a Single 1,500-Milligram Infusion. *Antimicrob. Agents Chemother.* **2019**, *63*, e01024-19. [CrossRef]
16. Dunne, M.W.; Puttagunta, S.; Sprenger, C.R.; Rubino, C.; Van Wart, S.; Baldassarre, J. Extended-duration dosing and distribution of dalbavancin into bone and articular tissue. *Antimicrob. Agents Chemother.* **2015**, *59*, 1849–1855. [CrossRef]
17. Spaziante, M.; Franchi, C.; Taliani, G.; D'Avolio, A.; Pietropaolo, V.; Biliotti, E.; Esvan, R.; Venditti, M. Serum Bactericidal Activity Levels Monitor to Guide Intravenous Dalbavancin Chronic Suppressive Therapy of Inoperable Staphylococcal Prosthetic Valve Endocarditis: A Case Report. *Open Forum Infect. Dis.* **2019**, *6*, ofz427. [CrossRef] [PubMed]
18. Bhamidipati, R.K.; Syed, M.; Mullangi, R.; Srinivas, N. Area under the curve predictions of dalbavancin, a new lipoglycopeptide agent, using the end of intravenous infusion concentration data point by regression analyses such as linear, log-linear and power models. *Xenobiotica* **2018**, *48*, 148–156. [CrossRef] [PubMed]
19. Dunne, M.W.; Puttagunta, S.; Giordano, P.; Krievins, D.; Zelasky, M.; Baldassarre, J. A Randomized Clinical Trial of Single-Dose Versus Weekly Dalbavancin for Treatment of Acute Bacterial Skin and Skin Structure Infection. *Clin. Infect. Dis.* **2016**, *62*, 545–551. [CrossRef]
20. Durante-Mangoni, E.; Gambardella, M.; Iula, V.D.; De Stefano, G.F.; Corrado, M.F.; Esposito, V.; Gentile, I.; Coppola, N. Current trends in the real-life use of dalbavancin: Report of a study panel. *Int. J. Antimicrob. Agents* **2020**, *56*, 106107. [CrossRef]
21. Bai, F.; Aldieri, C.; Cattelan, A.; Raumer, F.; Di Meco, E.; Moioli, M.C.; Tordato, F.; Morelli, P.; Borghi, F.; Rizzi, M.; et al. Efficacy and safety of dalbavancin in the treatment of acute bacterial skin and skin structure infections (ABSSSIs) and other infections in a real-life setting: Data from an Italian observational multicentric study (DALBITA study). *Expert Rev. Anti-infective Ther.* **2020**, *18*, 1271–1279. [CrossRef]
22. Thomas, G.; Henao-Martínez, A.F.; Franco-Paredes, C.; Chastain, D.B. Treatment of osteoarticular, cardiovascular, intravascular-catheter-related and other complicated infections with dalbavancin and oritavancin: A systematic review. *Int. J. Antimicrob. Agents* **2020**, *56*, 106069. [CrossRef] [PubMed]
23. Bouza, E.; Valerio, M.; Soriano, A.; Morata, L.; Carus, E.G.; Rodríguez-González, M.C.; Hidalgo-Tenorio, C.; Plata, A.; Muñoz, P.; Vena, A.; et al. Dalbavancin in the treatment of different gram-positive infections: A real-life experience. *Int. J. Antimicrob. Agents* **2018**, *51*, 571–577. [CrossRef] [PubMed]

24. Herrera-Hidalgo, L.; de Alarcón, A.; López-Cortes, L.; Luque-Márquez, R.; López-Cortes, L.; Gutiérrez-Valencia, A.; Gil-Navarro, M. *Enterococcus faecalis* Endocarditis and Outpatient Treatment: A Systematic Review of Current Alternatives. *Antibiotics* **2020**, *9*, 657. [CrossRef] [PubMed]
25. Matt, M.; Duran, C.; Courjon, J.; Lotte, R.; Le Moing, V.; Monnin, B.; Pavese, P.; Chavanet, P.; Khatchatourian, L.; Tattevin, P.; et al. Dalbavancin treatment for prosthetic joint infections in real-life: A national cohort study and literature review. *J. Glob. Antimicrob. Resist.* **2021**, *25*, 341–345. [CrossRef] [PubMed]
26. Fiore, V.; De Vito, A.; Aloisio, A.; Donadu, M.G.; Usai, D.; Zanetti, S.; Maida, I.; Madeddu, G.; Babudieri, S. Dalbavancin two dose regimen for the treatment of prosthetic joint infections: New possible options for difficult to treat infectious diseases. *Infect. Dis.* **2021**, *53*, 473–475. [CrossRef] [PubMed]
27. Rappo, U.; Puttagunta, S.; Shevchenko, V.; Shevchenko, A.; Jandourek, A.; Gonzalez, P.L.; Suen, A.; Casullo, V.M.; Melnick, D.; Miceli, R.; et al. Dalbavancin for the Treatment of Osteomyelitis in Adult Patients: A Randomized Clinical Trial of Efficacy and Safety. *Open Forum Infect. Dis.* **2018**, *6*, ofy331. [CrossRef] [PubMed]
28. Jones, R.N.; Farrell, D.J.; Flamm, R.K.; Sader, H.; Dunne, M.W.; Mendes, R. Surrogate analysis of vancomycin to predict susceptible categorization of dalbavancin. *Diagn. Microbiol. Infect. Dis.* **2015**, *82*, 73–77. [CrossRef] [PubMed]
29. Avataneo, V.; Antonucci, M.; De Vivo, E.D.; Briozzo, A.; Cusato, J.; Bermond, F.; Vitale, C.; Vitale, F.; Manca, A.; Palermiti, A.; et al. Validation and Clinical Application of a New Liquid Chromatography Coupled to Mass Spectrometry (HPLC-MS) Method for Dalbavancin Quantification in Human Plasma. *Separations* **2021**, *8*, 189. [CrossRef]
30. FDA. Bioanalytical Method Validation. Guidance for Industry. Available online: https://www.fda.gov/downloads/drugs/guidances/ucm070107.Pdf (accessed on 3 June 2022).
31. MEA/CHMP/EWP/192217/2009. Committee for Medicinal, Products for Human, Use (CHMP), Guideline on Bioanalytical, Method Validation. 2011. Available online: http://www.ema.europa.eu/docs/en_GB/document_library/Scientific_guideline/2011/08/WC500109686.pdf (accessed on 9 September 2021).
32. Molina, K.C.; Miller, M.A.; Mueller, S.W.; Van Matre, E.T.; Krsak, M.; Kiser, T.H. Clinical Pharmacokinetics and Pharmacodynamics of Dalbavancin. *Clin. Pharmacokinet.* **2022**, *61*, 363–374. [CrossRef] [PubMed]
33. Cattaneo, D.; Corona, A.; De Rosa, F.G.; Gervasoni, C.; Kocic, D.; Marriott, D.J. The management of anti-infective agents in intensive care units: The potential role of a 'fast' pharmacology. *Expert Rev. Clin. Pharmacol.* **2020**, *13*, 355–366. [CrossRef] [PubMed]
34. Baldoni, D.; Tafin, U.F.; Aeppli, S.; Angevaare, E.; Oliva, A.; Haschke, M.; Zimmerli, W.; Trampuz, A. Activity of dalbavancin, alone and in combination with rifampicin, against meticillin-resistant Staphylococcus aureus in a foreign-body infection model. *Int. J. Antimicrob. Agents* **2013**, *42*, 220–225. [CrossRef] [PubMed]
35. Žiemytė, M.; Rodríguez-Díaz, J.C.; Ventero, M.P.; Mira, A.; Ferrer, M.D. Effect of Dalbavancin on Staphylococcal Biofilms When Administered Alone or in Combination with Biofilm-Detaching Compounds. *Front. Microbiol.* **2020**, *11*, 553. [CrossRef] [PubMed]
36. Kebriaei, R.; Rice, S.A.; Stamper, K.C.; Rybak, M.J. Dalbavancin alone and in combination with ceftaroline against four different phenotypes of *staphylococcus aureus* in a simulated pharmacodynamic/pharmacokinetic model. *Antimicrob. Agents Chemother.* **2019**, *63*, e01743-18. [CrossRef] [PubMed]

pharmaceutics

MDPI

Article

Model Re-Estimation: An Alternative for Poor Predictive Performance during External Evaluations? Example of Gentamicin in Critically Ill Patients

Alexandre Duong [1,2,*], Chantale Simard [3,4], David Williamson [1,5] and Amélie Marsot [1,2,6]

1 Faculté de Pharmacie, Université de Montréal, Montreal, QC H3T 1J4, Canada; david.williamson@umontreal.ca (D.W.); amelie.marsot@umontreal.ca (A.M.)
2 Laboratoire de Suivi Thérapeutique Pharmacologique et Pharmacocinétique, Faculté de Pharmacie, Université de Montréal, Montreal, QC H3T 1J4, Canada
3 Institut Universitaire de Cardiologie et Pneumologie de Québec, Quebec, QC G1V 4G5, Canada; chantale.simard@pha.ulaval.ca
4 Faculté de Pharmacie, Université Laval, Quebec, QC G1V 0A6, Canada
5 Hôpital Sacré-Cœur de Montréal, Université de Montréal, Montreal, QC H4J 1C5, Canada
6 Centre de Recherche, CHU Sainte Justine, Montreal, QC H3T 1C5, Canada
* Correspondence: alexandre.duong.1@umontreal.ca

Abstract: Background: An external evaluation is crucial before clinical applications; however, only a few gentamicin population pharmacokinetic (PopPK) models for critically ill patients included it in the model development. In this study, we aimed to evaluate gentamicin PopPK models developed for critically ill patients. Methods: The evaluated models were selected following a literature review on aminoglycoside PopPK models for critically ill patients. The data of patients were retrospectively collected from two Quebec hospitals, the external evaluation and model re-estimation were performed with NONMEM® (v7.5) and the population bias and imprecisions were estimated. Dosing regimens were simulated using the best performing model. Results: From the datasets of 39 and 48 patients from the two Quebec hospitals, none of the evaluated models presented acceptable values for bias and imprecision. Following model re-estimations, all models showed an acceptable predictive performance. An a priori dosing nomogram was developed with the best performing re-estimated model and was consistent based on recommended dosing regimens. Conclusion: Due to the poor predictive performance during the external evaluations, the latter must be prioritized during model development. Model re-estimation may be an alternative to developing a new model, especially when most known models display similar covariates.

Keywords: gentamicin; population pharmacokinetic modeling; external evaluation; model re-estimation; dosing nomogram

Citation: Duong, A.; Simard, C.; Williamson, D.; Marsot, A. Model Re-Estimation: An Alternative for Poor Predictive Performance during External Evaluations? Example of Gentamicin in Critically Ill Patients. *Pharmaceutics* **2022**, *14*, 1426. https://doi.org/10.3390/pharmaceutics14071426

Academic Editors: José Martínez Lanao and Pedro Dorado

Received: 22 April 2022
Accepted: 6 July 2022
Published: 7 July 2022

1. Introduction

Gentamicin is a broad-spectrum antibiotic from the aminoglycoside family mostly used against life-threatening infections due to suspected Gram-negative bacteria [1,2]. The antimicrobial activity of gentamicin, along with other aminoglycosides, is concentration-dependent; therefore, its efficacy is based on the peak serum level (C_{max}) or the area under the concentration curve (AUC) related to the minimal inhibitory concentration (MIC) [3]. Moreover, due to the known potential ototoxicity and nephrotoxicity caused by aminoglycoside administration, therapeutic drug monitoring (TDM) is essential to achieve pharmacokinetic/pharmacodynamic (PK/PD) targets whilst minimizing toxicity. Considering the narrow therapeutic index of aminoglycosides, the administration of aminoglycosides has slowly shifted from a multiple daily dose (MDD) to a once-daily dose (ODD) throughout the years. The latter, also known as extended-interval dosing, has shown better signs of minimizing toxicity whilst also maintaining efficacy endpoints [4,5].

These PK/PD endpoints may be more difficult to attain in several frail populations such as critically ill patients. Due to their severe pathophysiological changes, standard dosing regimens may lead to inadequate concentrations and clinical outcomes. Therefore, the implementation of TDM based on population pharmacokinetic (PopPK) models in a clinical routine for critically ill patients should be prioritized, especially considering their high mortality rates [6].

In order to better understand aminoglycoside pharmacokinetics and the optimization of drug administration in critically ill patients, multiple PopPK models for gentamicin have been developed throughout the years [7]. Most of them did not include an external evaluation during the model development. An external evaluation, one of the most robust validation methods and a key step before the clinical application, consists of using an independent population within the final model to assess the accuracy and reproducibility of predicting the antimicrobial concentrations and clinical outcomes [8].

The primary objectives of this study were to evaluate previously published gentamicin PopPK models within a population of critically ill patients and to determine their predictive performances in order to use them during TDM in clinical settings. The subsequent objective was to determine the best performing model dosing regimens with simulations.

2. Materials and Methods

2.1. Patients

The medical records of adult ICU patients admitted to the Hôpital Sacré-Cœur de Montréal (HSCM) between 2009 and 2019 or the Institut universitaire de cardiologie et pneumologie de Québec (IUCPQ) between 2014 and 2020 and who received at least 1 dose of gentamicin and 1 serum concentration were retrospectively reviewed. Multicenter ethics approval was obtained from the Comité d'Éthique du CIUSSS-du-Nord-de-l'Île-de-Montréal (CERC-19-073-R (1) and HSCM: MP-32-2020-1904).

Data extraction from the medical records included age, sex, serum creatinine, body weight, gentamicin dose administered, gentamicin serum concentrations and infusion time dates as well as the times of all doses and concentrations, concomitant medications, medical history and admission diagnoses. Creatinine clearance based on Cockcroft–Gault (CLCG) and the glomerular filtration rate (eGFR) were estimated based on the closest time of the serum creatinine measurement according to the respective equations [9,10]:

$$\text{eGFR (mL/min)} = 186.3 \times (\text{Scr}/88.4)^{(-1.154)} \times \text{Age}^{(-0.203)} \times (1.212 \text{ if black}) \times (0.742 \text{ if female}) \quad (1)$$

$$\text{CrCl (mL/min)} = ((140 - \text{Age}) \times \text{Body weight (kg)} \times 1.23 \times (0.85 \text{ if female}))/\text{Scr} \quad (2)$$

2.2. Published Models

A literature review of aminoglycoside PopPK models for critically ill patients was previously performed. In this current study, we only aimed to externally evaluate the gentamicin PopPK models; therefore, all gentamicin PopPK models that were developed using non-linear mixed effect modeling (NONMEM) software were included in the external evaluation. Models were excluded if information on the pharmacokinetic equations of the models was missing in the respective article.

2.3. Model Evaluation

The external evaluation was conducted using NONMEM® (version 7.5: ICON Development Solutions, Ellicott City, MD, USA) and the plots were designed using R version 4.0.4. The evaluation was performed by combining both datasets (HSCM and IUCPQ).

The retained PopPK models were described based on the formulas and PK parameters reported from the final model for each publication. If a required covariate was not available within the datasets, it was assigned with the typical value of the model. No additional fitting was used during the external evaluation (the option in NONMEM was set to MAXEVAL = 0). The global fit of the PopPK models was also assessed with goodness-of-fit (GOF) plots of the predicted concentrations versus the observed concentrations. The predictive performance

of the models was evaluated with the prediction error (PE) determined by the following equation:

$$PE\ (\%) = (C_{(pred,i)} - C_{(obs,i)})/C_{(obs,i)} \times 100\% \quad (3)$$

where C_{pred} and C_{obs} correspond with the *i*th predicted concentration by the model and the observed concentration, respectively [11]. To quantify the bias and inaccuracy, the median prediction error (MDPE) and median absolute prediction error (MADPE) were used with the following equations:

- Bias: $MDPE_i$ (%) = median (PE_{ij}, j = 1, . . . , Ni)
- Inacurracy: $MADPE_i$ (%) = median ($|PE_{ij}|$, j = 1, . . . , N_i)

In order to be considered unbiased, the MDPE should be between −20 and 20% whereas to be considered accurate, the MADPE value should be ≤ 30% [12]. Finally, we used a normalized prediction distribution error (NPDE) analysis as a strategy to establish the overall fit of the PopPK model with the independent databases.

2.4. Model Re-Estimation

In the instance of an inadequate predictive performance of the models following an external evaluation based on the abovementioned criteria, the PK parameters and interindividual variability were re-estimated by NONMEM using the combined datasets of HSCM and IUCPQ. The re-estimated parameters were compared with the original values and the overall fit of the GOF plots. Normalized prediction distribution errors (NPDEs) as well as the corresponding statistical tests for normal distribution and homogeneity of variance and bootstraps were also assessed. If the re-estimated models were successfully minimized, the population and individual bias and imprecision were calculated and compared.

2.5. Simulations of C_{max}/MIC > 8–10 and C_{min} < 1 or 0.5 mg/L Following a Third Dose

Considering that the clinical efficacy of gentamicin as well as other aminoglycosides is based on C_{max}/MIC, the prediction of peak concentration following the third dose was assessed ($C_{max,3rd}$) using different dosing regimens for the best performing PopPK model. The pre-dose concentration before the fourth was also examined. These simulated PK/PD endpoints were obtained based on the covariates of the patients only (a priori prediction). The evaluation of these simulated concentrations was only completed with the best performing PopPK model in terms of the overall predictive performance (GOF plots, MDPE and MADPE).

3. Results

The medical records of 48 and 39 ICU patients from IUCPQ and HSCM, respectively, were retrieved for this study. Table 1 describes the demographic characteristics of both populations, separately and altogether. The only demographic characteristics that were statistically different between both institutions were sex and serum creatinine (Scr). Moreover, the total daily dose at HSCM appeared to be higher and more variable than at IUCPQ. In fact, IUCPQ mostly generalized their care toward people with cardiopulmonary diseases; therefore, the majority of the patients from IUCPQ included in this study suffered from endocarditis whereas the patients from HSCM suffered a variety of conditions mostly leading to sepsis.

Table 1. Demographic characteristics of the patients in the evaluated models and the external validation datasets.

Characteristics	Rea et al. [13]	Bos et al. [14]	Hodiamont et al. [15]	Hodiamont et al. [16]	HSCM	IUCPQ	Combined
Population type	Critically ill patients	Critically ill non-ICU sub-Saharan African adult patients	Critically ill patients on or off CVVH	Critically ill patients	Critically ill patients	Mostly endocarditis patients in ICU	Critically ill and endocarditis patients
Number of patients (N)	102	48	44	59	39	48	87
M/F	45/57	24/24	20/24	29/30	18/21	36/12	54/33
Age (years)	61.4 ± 16.4	40.0 (20–86)	61.0 (20–78)	60.9 ± 17.2	60.3 ± 19.2	58.7 ± 16.9	59.4 ± 17.9
Weight (kg)	81.4 ± 30.3	51.0 (33–76)	70.5 (42.0–116)	79.2 ± 22.0	79.4 ± 20.5	80.5 ± 22.4	80.0 ± 21.5
Serum creatinine (µmol/L)	194.5 ± 168	76.0 (37–1192)	115.0 (36–1719)	-	93.2 ± 91.4	99.9 ± 34.8	96.9 ± 66.0
CrCl (mL/min)	-	74.0 (4–155)	54.9 (4.0–150)	-	99.8 ± 60.6	86.0 ± 36.4	92.2 ± 48.9
eGFR (mL/min)	48.1 ± 26.5	-	-	-	73.5 ± 21.0	90.1 ± 39.9	80.9 ± 31.9
Albumin (g/L)	-	29 (13–40)	21.5 (10–36)	-	-	29.0 ± 5.6	29.0 ± 5.6
Total daily dose (mg/kg)	-	-	-	-	2.9 ± 0.9	2.0 ± 0.7	2.4 ± 1.1

The values are presented as median (range) or mean ± SD. CrCl: creatinine clearance; CVVH: continuous venovenous hemofiltration; eGFR: estimated glomerular filtration rate; HSCM: Hôpital du Sacré-Cœur de Montréal; IUCPQ: Institut universitaire de cardiologie et pneumologie de Québec; M/F: male/female; N: number. -: Not available

From our literature review of gentamicin PopPK models, eleven models were screened for inclusion [7]. Amongst them, seven were excluded due to a lack of information or if the models were not developed with NONMEM (n = 7). Therefore, the predictive performance of four models was evaluated [13–16]. The demographic characteristics are presented in Table 1. The pharmacokinetic equations of the four evaluated models are presented in Table S1. Half of them used mono-compartment models whereas the other half used bi-compartment models [13–16]. The covariates used were varied, with the use of glomerular filtration in one study, CrCl in another study, the covariates related to weight in two studies and albumin in one study. Gentamicin CL and the total volume of distribution ranged between 1.15 and 5.7 L/h and 19 and 54 L, respectively (Table S1).

The results presented in this article were from an external evaluation using combined datasets from HSCM and IUCPQ. The external evaluations were performed separately for each institution and obtained comparable results. The population-predicted versus the observed concentrations are presented in Figure S1 for each evaluated model. The models from Bos et al. and Hodiamont et al. appeared to underpredict the observed concentrations [14,16] whereas the models from Rea et al. and Hodiamont et al. tended to overpredict the observed concentrations from the validated dataset [13,15]. Following the external evaluation, the population bias and imprecision values ranged between −44.0 and 66.1% and 47.8 and 69.9%, respectively. The bias and imprecision values improved when individual characteristics were taken into consideration, with values ranging between −18.0 and 10.1% and 18.0 and 27.1%, respectively.

As presented in Table 2, all four models evaluated did not respect the targeted ranges for population bias (±20%) and imprecision (≤30%) [12]. These models were, therefore,

re-estimated in NONMEM with the combined datasets of HSCM and IUCPQ. The PK parameter coefficients in their respective PK equations are presented in Tables S1 and S2 for the external evaluation and the re-estimation, respectively. The typical PK parameters considered during the external evaluation and the re-estimated typical PK parameters as well as their respective interindividual variability are presented in Table S3.

Upon the model re-estimation, the difference between the new PK parameter values and the respective original values was generally greater for the mono-compartmental models [13,14] than for the bi-compartmental models [15,16]. For the model of Rea et al., the typical re-estimated gentamicin clearance was around 50% greater than its original value used in the external evaluation whereas the re-estimated volume of distribution was half its original value [13]. For the model of Bos et al., the typical re-estimated gentamicin clearance was slightly lower than its original value whereas the re-estimated volume of distribution was slightly higher than its original value. For the first model of Hodiamont et al. [15], both the gentamicin clearance and total volume of distribution were higher following the re-estimation compared with the original values. For the second model of Hodiamont et al. [16], both the gentamicin clearance and total volume of distribution were lower following the re-estimation compared with the original values.

The interindividual variability appeared to be generally lower with the re-estimated PopPK models. All models were successfully minimized; the population and individual bias and imprecision from these re-estimated models are presented in Table 2. The population-predicted versus the observed concentrations are presented in Figure 1 for each re-estimated model. Following the model re-estimation, the population-predicted concentrations drastically improved for each model compared with its own counterpart during the external evaluation.

Only the re-estimated model of Rea et al. was able to adequately predict the observed concentrations with an acceptable population bias and imprecision. Although the re-estimated model of Bos et al. had a population imprecision of 30.1%, its individual imprecision increased following the re-estimation from 18.0% to 20.4%. Therefore, the re-estimated model from Rea et al. was deemed to be the best performing model and was used for the therapeutic target simulations. The normalized prediction distribution errors (NPDEs) were also compared between the original and re-estimated PK parameters, as shown in Figure S2. For the original model, the statistical test results showed a normal distribution (*t*-test of 0.507), but a heterogeneity of variance (Fisher of <0.001). Although the statistical tests showed a non-normal distribution (*t*-test of 0.0371) and heterogeneity of variance (Fisher of 0.0495), the graphical representations of the NPDE (Q-Q plot and histogram) showed a better distribution and the bootstraps results were adequate (Table S4).

Both therapeutic targets ($C_{max,3rddose}$ and pre-dose before the fourth administration) were simulated for several dosing regimens (MDD and ODD). The simulations were based on two different efficacy targets: C_{max}/MIC > 8 (Table S5) and C_{max}/MIC > 10 (Table S6). Figure 2 presents the probability of target attainment (PTA) based on the MIC values and the dosing regimen used. Table S5 presents the same PTA, but displayed by total dose given per day for C_{max}/MIC > 8. Figure S3 displays the percentage for the pre-dose concentrations before the fourth administration below 1 mg/L or 0.5 mg/L. Similarly, Table S7 presents the same percentage, but displayed by dosing regimen.

For each of the eight simulated doses given per day (3 to 12 mg/kg/day), the once-daily dosing regimen was the best dosage in order to maximize the probability of target attainment for all MIC values compared with the multiple daily dosing regimen (twice or thrice daily). Similarly, for the pre-dose concentrations before the fourth administration, a higher dosing interval led to a higher probability of respecting the toxicity targets.

Table 2. Prediction error following external evaluation of the PopPK models.

Model	Population		Individual		Population (Re-Estimation)		Individual (Re-Estimation)	
	MDPE (%)	MADPE (%)	MDPE (%)	MADPE (%)	MDPE (%)	MADPE (%)	MDPE (%)	MADPE (%)
Rea et al. [13]	44.2	54.1	−18.0	27.1	2.14	28.1	−5.19	19.0
Bos et al. [14]	−44.0	47.8	−3.29	18.0	2.00	30.1	0.09	20.4
Hodiamont et al. [15]	66.1	69.9	10.1	24.0	2.20	36.9	−4.01	21.3
Hodiamont et al. [16]	−31.7	48.8	−14.7	26.8	6.03	39.2	−6.42	18.6

MDPE: median prediction error; MADPE: median absolute prediction error.

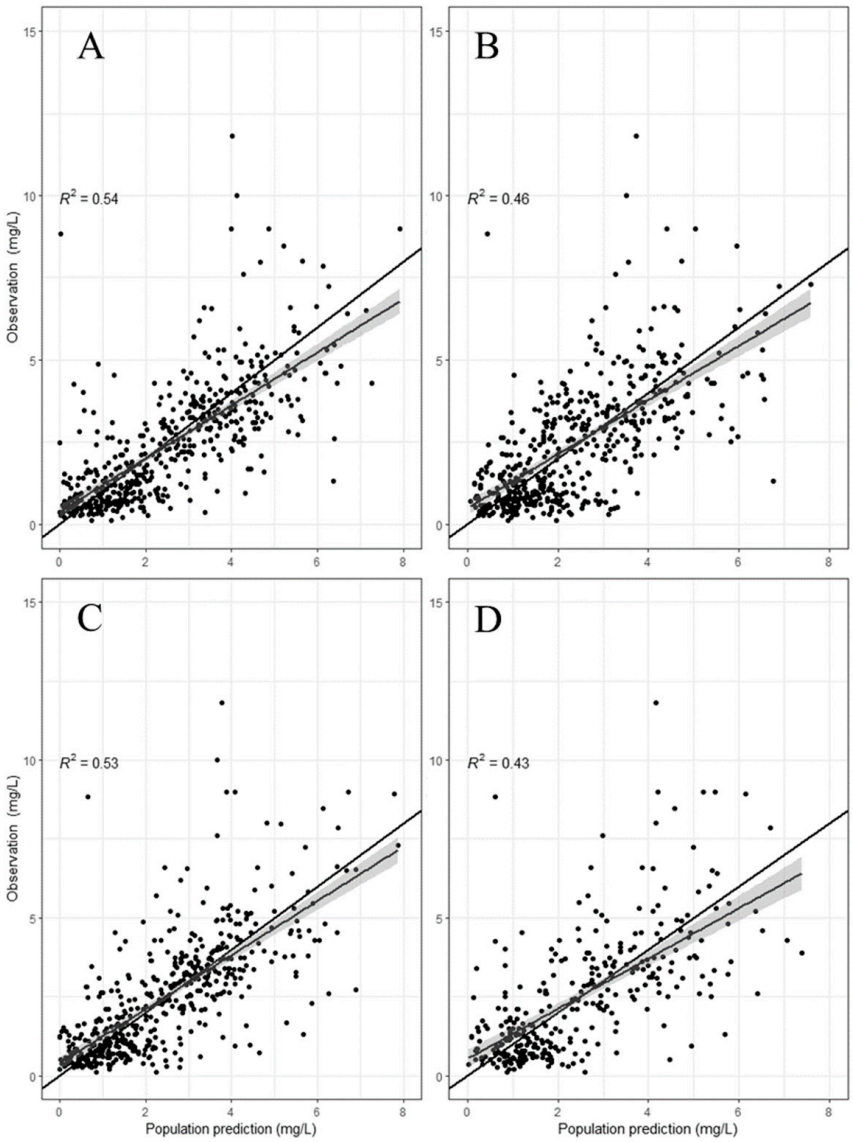

Figure 1. Population-predicted concentration versus observed concentrations for gentamicin models following re-estimation. (**A**) Bos et al. [14], (**B**) Hodiamont et al. [15], (**C**) Rea et al. [13], (**D**) Hodiamont et al. [16]. Black line with shaded area represents the trendline from the scatter points.

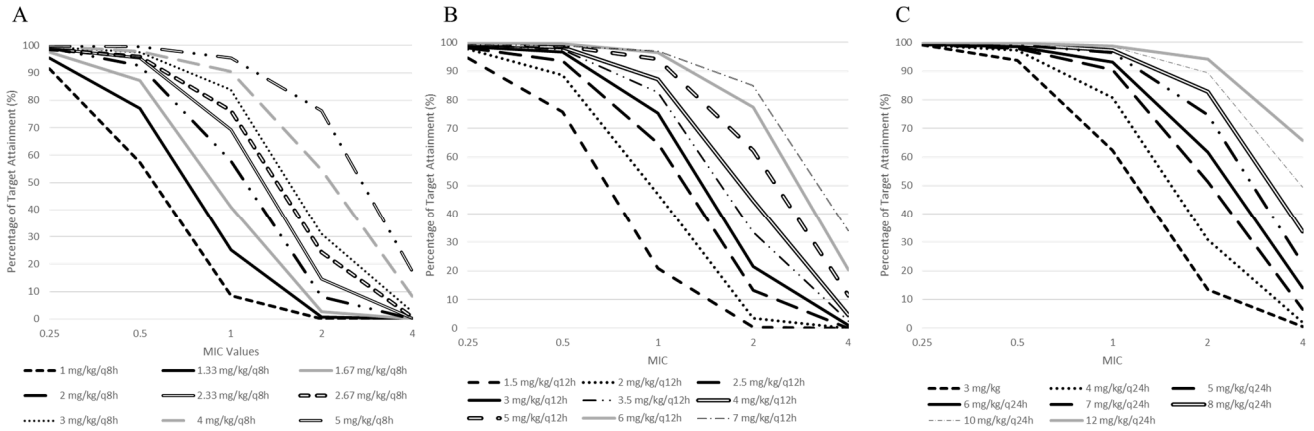

Figure 2. Probability of target attainment of C_{max}/MIC > 8 on the third dose based on different MIC values. (**A**) Dose administered thrice daily (every 8 h). (**B**) Dose administered twice daily (every 12 h). (**C**) Dose administered daily (every 24 h).

For severe infections, as per the latest MIC breakpoints from the United States Committee on Antimicrobial Susceptibility Testing (USCAST) and the European Committee on Antimicrobial Susceptibility Testing (EUCAST), *Staphylococcus* spp., *Pseudomonas* spp. and *Enterococcus* spp. present MIC values ranging from 1 to 2 mg/L. Considering these actual MIC values, only dosing regimens greater than 5 mg/kg/day had a greater PTA of 90% for an MIC value of 1 mg/L. Although these dosing regimens should reach efficacy targets of C_{max}/MIC > 8, toxicity targets should be cautiously monitored. Around 50% and 64.4% of the patients presented C_{trough} before the fourth administration greater than 1 mg/L with a dosing regimen of 5 mg/kg/day and 12 mg/kg/day, respectively (Table S7). Simulations of C_{trough} before the fourth administration for multiple daily dosing regimens (twice and thrice daily) led to poor percentages of target attainment.

4. Discussions

In the past decades, multiple PopPK models of gentamicin for critically ill patients have been developed [7]. In this current study, we evaluated the predictive performance of four models using an independent dataset with medical records from two hospitals [13–16]. The model appropriateness was evaluated based on an integrative assessment of several markers such as bias, imprecision and GOF plots. Based on the population bias and imprecision values, all four models were not within the predefined values, thereby suggesting that all four models are not directly transferable to a clinical application. Moreover, based on the observed versus the predicted concentrations from the models, the four models showed greater under- or overpredictions of the observed gentamicin concentrations. The underprediction and overprediction of actual therapeutic drug monitoring concentrations can result in a misinterpretation of efficacy and toxicity targets, respectively. This poor population prediction may have been due to the differences in the demographic characteristics and clinical conditions from the respective population of the models and the Quebec population. However, the individual prediction performance, as shown in Table 2, improved enough to be within an acceptable range, suggesting that the use of all four models may be feasible in a posteriori dosing adaptation.

If the evaluated models showed a poor predictive performance with our population, two options were considered: to develop a PopPK model with our database or to simply adjust the pre-existing models. Considering that the evaluated models included covariates that were available within our population, we opted for a re-estimation of these models. The latter method was expected to improve the predictive performance due to the adaptation of the PK parameters of each model based on our population.

Due to the differences in our population compared with the respective populations of each model, the PK parameter estimates varied following the model re-estimation. For

instance, a typical clearance value of the re-estimated model from Rea et al. was around 50% higher than its respective original value. This may be explained by the eGFR value of our combined populations (HSCM + IUCPQ) being around 60% higher than the population used to develop the model from Rea et al. [13]. Moreover, this covariate was also deemed to be significant to determine gentamicin clearance. In parallel, although the body weight was similar between Rea et al. and our study population, the re-estimated volume of distribution was half the value of the original model. Considering that critically ill patients often suffer from fluid overload caused by complications [17], this may explain the higher volume of distribution compared with the endocarditis patients from IUCPQ in our combined datasets. For the model of Bos et al., the re-estimated gentamicin clearance was lower than its original value, leading to an underprediction of the gentamicin concentration during the external evaluation. This may be due to the differences in the severity of the medical conditions and demographic characteristics between both populations. Although the population used to develop the model of Bos et al. was severely ill, it was noted that they were not in ICU whereas our patients were hospitalized in ICU settings. Moreover, the age and body weight from the sub-Saharan African population, which were both considered in the Cockcroft–Gault calculation of CrCl, were significantly lower than our population. As for the model of Hodiamont et al. [16] although the body weight was not statistically different between their respective population and our two populations, the typical volume of distribution of the re-estimated model was half than its original value. Only 7% of their population had endocarditis compared with 55% in our dataset. A higher proportion of critically ill patients where fluid overload often occurs due to sepsis may suggest the higher distribution volume observed in the study population of Hodiamont et al. [16].

Although the re-estimation of PopPK models with our population improved the predictive performance of all models, a variability remained in the prediction of the actual gentamicin concentrations as well as in the re-estimated PK parameters. Our external validation datasets formed from our two institutions consisted of patients with severe infections or endocarditis, which was comparable with the populations used to develop the evaluated models [13–16]. This variability could have been caused by several sources such as the severity of the illness, medical history and related concomitant medication. Furthermore, the origin of the study populations of the developed models was varied, with patients from the United States, Africa or Europe. The variability may also have been due to the differences between the patients of the developed PopPK model. As shown in Table S2, the interindividual and residual variabilities for the PK parameters were already high, thereby suggesting that the patients from the original dataset used in the model development were different from each other.

The variability also seen during the external evaluation may also have been due to the different study designs from the developed PopPK models. The number of patients in the validation dataset was greater than most study populations used for the model development [14–16]. Moreover, three studies had a similar sampling schedule to the validation datasets with samples from therapeutic drug monitoring [13,15,16] whereas the model from Bos et al. [14] was developed with samples collected following a prospective observational design. Alihodzic et al. demonstrated that erroneous records due to clinical routine practices may lead to an inaccurate estimation of PK parameters during PopPK model development [18].

Based on the best re-estimated performing model, we developed an a priori dosing nomogram based on the different MIC values, dosing regimens and dosing intervals. For the evaluations of C_{max} and C_{min} following the third gentamicin administration, the ODD regimen appeared to be the best option in order to maximizes the PTA of the efficacy (C_{max}/MIC > 8) and toxicity (C_{min} < 1 mg/L or C_{min} < 0.5 mg/L) targets compared with the MDD regimen. This finding was consistent with previous literature that stated that ODD regimens were able to maintain efficacy whilst minimizing the signs of toxicity [4,5].

For Gram-positive infections, the peak concentrations should be targeted at around 3 to 4 mg/L [19,20]. The latter was represented in our dosing nomogram with C_{max}/MIC > 8 con-

sidering an MIC of 0.5 mg/L (Table S5). Taken daily, a PTA over 90% is possible with any doses greater than 3 mg/kg. In terms of toxicity, the latter also represents the dosing regimen recommended for Gram-positive infections [19,20]. Although the original PopPK model of Rea et al. was not deemed to be adequate following the external evaluation, our dosing regimens simulated from its re-estimated model were in line with the literature. This finding brings to light the relevance and accuracy of the metrics generally used during an external evaluation of PopPK models.

Rea et al. also performed dosing regimen simulations with PTA based on their final model [13]. From their simulations, the probability of attaining C_{max}/MIC > 10 considering an MIC value of 0.5 mg/L with a daily dose of 7 mg/kg was 87.9%. Based on our dosing nomogram, a daily dose of 7 mg/kg with an MIC value of 0.5 mg/L led to 98.2% of our patients attaining the target of C_{max}/MIC > 10 (Table S6). Consequently, the original dosing regimens recommended by Rea et al. would be higher than needed for our population.

Several limitations should be considered in this current study. Firstly, the concentrations from the medical records from both institutions were therapeutic drug monitoring data collected during a clinical setting. Therefore, the number of samples per patient was limited. Considering the retrospective design of this study, the severity of the conditions of the patients was unobtainable from the medical records as well as other covariates of interest. Moreover, choosing NONMEM software as an inclusion criterion may have restricted the number of models to be evaluated.

5. Conclusions

In this study, we aimed to evaluate gentamicin PopPK models with two Quebec critically ill populations. Although the four evaluated models showed a poor population predictive performance, their respective predictive performances when considering the characteristics and dosing information of the patients were adequate. In the scenario of a poor predictive performance, a model re-estimation is a viable option in order to avoid the development of PopPK models similar to pre-existing ones. With the best performing re-estimated model from Rea et al., the dosing regimens were simulated with our study population. These findings suggested that the re-estimation of existing models in order to develop an a priori dosing nomogram should be considered more often and may be more suited to each population or also used for a Bayesian analysis and estimation.

Supplementary Materials: The following supporting information can be downloaded at: https://www.mdpi.com/article/10.3390/pharmaceutics14071426/s1, Table S1: Summary of the characteristics of the evaluated PopPK models; Table S2: Summary of the characteristics of the re-estimated PopPK models; Table S3: Typical values of PK parameters and variability used during external evaluation and following the re-estimation of PopPK models; Table S4: Bootstrap results of the re-estimated model from Rea et al.; Figure S1: Population-predicted concentration versus observed concentrations for gentamicin models following re-estimation: (A) Bos et al. [14], (B) Hodiamont et al. [15], (C) Rea et al. [13], (D) Hodiamont et al. [16]. Black line with shaded area represents the trendline from the scatter points; Figure S2: Normalized prediction distribution error (NPDE) plots of (A) the external evaluation and (B) following model re-estimation for Rea et al. (1) Q-Q plot of the NPDE, (2) histogram of the NPDE, (3) NPDE versus time, (4) NPDE versus predicted concentrations; Table S5: Probability of target attainment of C_{max}/MIC > 8 on the third dose based on different MIC values and MDD and ODD dosing regimens of gentamicin; Table S6: Probability of target attainment of C_{max}/MIC > 10 on the third dose based on different MIC values and MDD and ODD dosing regimens of gentamicin; Figure S3: Percentage of Ctrough following different dosage regimens and dosing intervals below (A) 1 mg/L and (B) 0.5 mg/L; Table S7: Percentage of Ctrough below 1 mg/L or 0.5 mg/L before the fourth administration following different dosage regimens and dosing interval below.

Author Contributions: Conceptualization, A.D. and A.M.; methodology, A.D. and A.M.; software, A.D.; validation, A.D. and A.M.; formal analysis, A.D. and A.M.; investigation, A.D. and A.M.; resources, C.S., D.W. and A.M.; data curation, A.D.; writing—original draft preparation, A.D.; writing—review and editing, A.D., C.S., D.W. and A.M.; visualization, A.D.; supervision, A.M.; project administration, A.M.; funding acquisition, A.M. All authors have read and agreed to the published version of the manuscript.

Funding: This project was funded by the Réseau Québécois de Recherche sur les Médicaments (RQRM) and Amélie Marsot received salary support from the Fonds de Recherche Santé Québec (FRQS).

Institutional Review Board Statement: Multicenter ethics approval was obtained for retrospective data collection from the Comité d'Éthique de l'Université de Montréal (CERC-19-073-R (1) and CIUSSS-du-Nord-de-l'Île-de-Montréal (Hôpital Sacré-Cœur de Montréal and Institut universitaire de cardiologie et pneumologie de Québec): MP-32-2020-1904).

Informed Consent Statement: Not applicable.

Data Availability Statement: Not applicable.

Conflicts of Interest: The authors declare no conflict of interest.

References

1. Krause, K.M.; Serio, A.W.; Kane, T.R.; Connolly, L.E. Aminoglycosides: An Overview. *Cold Spring Harb. Perspect. Med.* **2016**, *6*, a027029. [CrossRef] [PubMed]
2. Mingeot-Leclercq, M.-P.; Glupczynski, Y.; Tulkens, P.M. Aminoglycosides: Activity and Resistance. *Antimicrob. Agents Chemother.* **1999**, *43*, 727–737. [CrossRef] [PubMed]
3. Levison, M.E.; Levison, J.H. Pharmacokinetics and Pharmacodynamics of Antibacterial Agents. *Infect. Dis. Clin. N. Am.* **2009**, *23*, 791–815. [CrossRef] [PubMed]
4. Barclay, M.L.; Kirkpatrick, C.M.; Begg, E.J. Once Daily Aminoglycoside Therapy. *Clin. Pharmacokinet.* **1999**, *36*, 89–98. [CrossRef] [PubMed]
5. Stankowicz, M.S.; Ibrahim, J.; Brown, D.L. Once-daily aminoglycoside dosing: An update on current literature. *Am. J. Health Pharm.* **2015**, *72*, 1357–1364. [CrossRef] [PubMed]
6. Tängdén, T.; Martín, V.R.; Felton, T.W.; Nielsen, E.I.; Marchand, S.; Brüggemann, R.J.; Bulitta, J.; Bassetti, M.; Theuretzbacher, U.; Tsuji, B.T.; et al. The role of infection models and PK/PD modelling for optimising care of critically ill patients with severe infections. *Intensiv. Care Med.* **2017**, *43*, 1021–1032. [CrossRef] [PubMed]
7. Duong, A.; Simard, C.; Wang, Y.L.; Williamson, D.; Marsot, A. Aminoglycosides in the Intensive Care Unit: What Is New in Population PK Modeling? *Antibiotics* **2021**, *10*, 507. [CrossRef] [PubMed]
8. Brendel, K.; Comets, E.; Laffont, C.; Mentré, F. Evaluation of different tests based on observations for external model evaluation of population analyses. *J. Pharmacokinet. Pharmacodyn.* **2009**, *37*, 49–65. [CrossRef] [PubMed]
9. Manjunath, G.; Sarnak, M.J.; Levey, A.S. Estimating the glomerular filtration rate. *Postgrad. Med.* **2001**, *110*, 55–62. [CrossRef] [PubMed]
10. Cockcroft, D.W.; Gault, M.H. Prediction of creatinine clearance from serum creatinine. *Nephron* **1976**, *16*, 31–41. [CrossRef] [PubMed]
11. Guang, W.; Baraldo, M.; Furlanut, M. Calculating percentage prediction error: A user's note. *Pharmacol. Res.* **1995**, *32*, 241–248. [CrossRef]
12. Hara, M.; Masui, K.; Eleveld, D.; Struys, M.; Uchida, O. Predictive performance of eleven pharmacokinetic models for propofol infusion in children for long-duration anaesthesia. *Br. J. Anaesth.* **2017**, *118*, 415–423. [CrossRef] [PubMed]
13. Rea, R.S.; Capitano, B.; Bies, R.; Bigos, K.L.; Smith, R.; Lee, H. Suboptimal Aminoglycoside Dosing in Critically Ill Patients. *Ther. Drug Monit.* **2008**, *30*, 674–681. [CrossRef] [PubMed]
14. Jeannet, C.B.; Jan, M.P.; Mabor, C.M.; Nunguiane, G.; Cláudia, N.L.; José, C.B. Population Pharmacokinetics with Monte Carlo Simulations of Gentamicin in a Population of Severely Ill Adult Patients from Sub-Saharan Africa. *Antimicrob. Agents Chemother.* **2019**, *63*, e02328-18.
15. Hodiamont, C.J.; Juffermans, N.P.; Bouman, C.S.; de Jong, M.D.; Mathôt, R.A.; van Hest, R. Determinants of gentamicin concentrations in critically ill patients: A population pharmacokinetic analysis. *Int. J. Antimicrob. Agents* **2016**, *49*, 204–211. [CrossRef] [PubMed]
16. Hodiamont, C.J.; Janssen, J.M.; De Jong, M.D.; Mathôt, R.A.; Juffermans, N.P.; van Hest, R. Therapeutic Drug Monitoring of Gentamicin Peak Concentrations in Critically Ill Patients. *Ther. Drug Monit.* **2017**, *39*, 522–530. [CrossRef] [PubMed]
17. Del Granado, R.C.; Mehta, R.L. Fluid overload in the ICU: Evaluation and management. *BMC Nephrol.* **2016**, *17*, 109.
18. Alihodzic, D.; Broeker, A.; Baehr, M.; Kluge, S.; Langebrake, C.; Wicha, S.G. Impact of Inaccurate Documentation of Sampling and Infusion Time in Model-Informed Precision Dosing. *Front. Pharmacol.* **2020**, *11*, 172. [CrossRef] [PubMed]

19. Nord-de-l'Île-de-Montréal Cd. Guides Pratiques—Pharmacocinétique—Aminosides. 2021. Available online: https://www.ciusssnordmtl.ca/zone-des-professionnels/medecins/guide-dantibiotherapie-empirique/guides-pratiques-pharmacocinetique/aminosides/ (accessed on 15 February 2022).
20. Laval CdQ-U. Guide d'Utilisation de la Gentamcine et de la Tobramycine chez l'Adulte. 2016. Available online: https://www.chudequebec.ca/getmedia/89a9f1ad-41b0-40f0-a88d-f704771e1256/bulletin_23_guide_genta_tobra_adulte.aspx (accessed on 15 February 2022).

pharmaceutics

MDPI

Article

Dried Blood Spot Sampling to Assess Rifampicin Exposure and Treatment Outcomes among Native and Non-Native Tuberculosis Patients in Paraguay: An Exploratory Study

Samiksha Ghimire [1,*,†], Gladys Molinas [2,†], Arturo Battaglia [2], Nilza Martinez [2], Luis Gómez Paciello [2], Sarita Aguirre [3], Jan-Willem C. Alffenaar [4,5,6], Marieke G. G. Sturkenboom [1] and Cecile Magis-Escurra [7]

1 Department of Clinical Pharmacy and Pharmacology, University Medical Center Groningen, University of Groningen, 9712 CP Groningen, The Netherlands
2 Instituto Nacional de Enfermedades Respiratorias y del Ambiente "Juan Max Boettner", Asuncion 1430, Paraguay
3 Programa Nacional de Control de la Tuberculosis, Asuncion 1430, Paraguay
4 School of Pharmacy, Faculty of Medicine and Health, The University of Sydney, Camperdown, NSW 2006, Australia
5 Westhead Hospital, West Mead, NSW 2145, Australia
6 Sydney Institute of Infectious Diseases, The University of Sydney, Camperdown, NSW 2006, Australia
7 Department of Pulmonary Diseases, Radboud University Medical Center-TB Expert Center Dekkerswald, 6525 GA Nijmegen, The Netherlands
* Correspondence: s.ghimire@umcg.nl
† These authors contributed equally to this work.

Abstract: The aim of this study was to evaluate the difference in drug exposure of rifampicin in native versus non-native Paraguayan populations using dried blood spots (DBS) samples collected utilizing a limited sampling strategy. This was a prospective pharmacokinetic study that enrolled hospitalized tuberculosis (TB) patients from both native and non-native populations receiving oral rifampicin 10 mg/kg once-daily dosing. Steady-state DBS samples were collected at 2, 4, and 6 h after intake of rifampicin. The area under the time concentration curve 0–24 h ($AUC_{0–24}$) was calculated using a Bayesian population PK model. Rifampicin $AUC_{0–24}$ < 38.7 mg*h/L was considered as low. The probability of target attainment (PTA) was calculated using $AUC_{0–24}$/MIC > 271 as a target and estimated MIC values of 0.125 and 0.25 mg/L. In total, 50 patients were included. Native patients (n = 30) showed comparable drug exposure to the non-natives (n = 20), median $AUC_{0–24}$ 24.7 (17.1–29.5 IQR) and 21.6 (15.0–35.4 IQR) mg*h/L (p = 0.66), respectively. Among total patients, only 16% (n = 8) had a rifampicin $AUC_{0–24}$ > 38.7 mg*h/L. Furthermore, PTA analysis showed that only 12 (24%) of the patients met a target $AUC_{0–24}$ /MIC $\geq$ 271, assuming an MIC of 0.125 mg/L, which plummeted to 0% at a wild-type MIC of 0.25 mg/L. We successfully used DBS and limited sampling for the $AUC_{0–24}$ estimation of rifampicin. Currently, our group, the EUSAT-RCS consortium, is preparing a prospective multinational, multicenter phase IIb clinical trial evaluating the safety and efficacy of high-dose rifampicin (35 mg/kg) in adult subjects using the DBS technique for $AUC_{0–24}$ estimation.

Keywords: tuberculosis; rifampicin; pharmacokinetics; dried blood spots; limited-sampling strategy

Citation: Ghimire, S.; Molinas, G.; Battaglia, A.; Martinez, N.; Gómez Paciello, L.; Aguirre, S.; Alffenaar, J.-W.C.; Sturkenboom, M.G.G.; Magis-Escurra, C. Dried Blood Spot Sampling to Assess Rifampicin Exposure and Treatment Outcomes among Native and Non-Native Tuberculosis Patients in Paraguay: An Exploratory Study. *Pharmaceutics* **2023**, *15*, 1089. https://doi.org/10.3390/pharmaceutics15041089

Academic Editors: Barna Vasarhelyi and Gellért Balázs Karvaly

Received: 9 November 2022
Revised: 23 March 2023
Accepted: 25 March 2023
Published: 29 March 2023

1. Introduction

Tuberculosis (TB) remains the leading cause of death by a single infectious agent apart from COVID; being at the same time both a preventable and curable disease. Globally, the burden of TB varies greatly, with more than 60% of the newly diagnosed cases concentrated in parts of Asia and Africa [1,2]. Although the incidence of TB in South America (46.2 per 100,000) is relatively low compared to Africa (100–300 per 100,000 inhabitants), TB still remains a serious public health problem. In Paraguay, TB incidences differ significantly

among the native (350 per 100,000) and the non-native population (37.6 per 100,000) [2]. Based on limited data, the mortality rates are estimated to vary considerably with 22 deaths in native Indians compared to 4.5 per 100,000 in the rest of the population [2]. As of yet, no evidence is available to explain the reason why indigenous people have such high incidence rates of TB, why there is a higher mortality rate, and why the cure rates and relapse rates are lower. An explanation could be compliance with medication, higher prevalence of toxicity and side effects, or access to health care. Another reason might be low drug concentrations due to genetic differences (explaining differences in metabolism or toxicity) or due to food and drinking habits. None of these reasons have been studied in Paraguay so far.

Rifampicin is a key drug of standard first-line anti-TB treatment. From hollow-fiber studies and an observational cohort study [3,4], it is evident that low rifampicin blood exposures have been associated with treatment failure and the development of acquired drug resistance [5,6]. Pharmacokinetic (PK) variability, in combination with differences in drug susceptibility of *Mycobacterium tuberculosis*, explains why some patients fail the treatment [6] although the correlation with outcomes in humans has not been completely established until now. For rifampicin, the most predictive efficacy parameter is its ratio of area under the 24-h concentration-time curve ($AUC_{0–24}$) and minimum inhibitory concentration (MIC), with a suggested target exposure of $AUC_{0–24}/MIC \geq 271$ for one log CFU reduction in murine studies [5,7], whereas free $C_{max}/MIC \geq 175$ is linked to the suppression of acquired drug resistance and the post-antibiotic effect (hollow-fiber study) [5]. However, in the absence of actual MICs, clinicians often utilize an $AUC_{0–24}$ of 38.7 mg*h/L, observed with normal 8–12 mg/kg dosing in humans to make informed dosing decisions [8].

In a systematic review and meta-analysis, Stott et al. found that among 35 included studies (at steady state), 12 studies had an average $AUC_{0–24}$ between 20–30 mg*h/L, whereas, two other studies had an even lower mean $AUC_{0–24}$ of 13–14 mg*h/L [8]. There was a considerable difference in reported AUCs in the different populations (HIV status, TB status, combination therapy, intermittent dosing, diabetes status, and treatment duration) [8]. Furthermore, Stott et al. showed that by taking 38.7 mg*h/L as a mean rifampicin steady-state AUC and the epidemiological cut-off value (ECOFF) MIC of 0.5 mg/L, an AUC/MIC ratio of 77 is achieved, which is far below the optimal $AUC_{0–24}$ /MIC ≥ 271 suggested by Jayaram et al. [7,8]. However, the proposed susceptibility breakpoint MIC based on pharmacokinetic/pharmacodynamic science was much lower at 0.0078 mg/L for the standard rifampicin dose (450–600 mg once daily) [9,10].

Therapeutic drug monitoring (TDM), i.e., drug dose adjustment based on measured blood concentrations, has the potential to optimize exposure to anti-TB drugs but is not widely used in clinical practice probably due to logistic and financial challenges that arise with the conventional venous sampling [11–13]. Encouragingly, the use of alternative sampling techniques such as dried blood spots (DBS), combined with limited sampling, has led to practical solutions [14–16]. Limited sampling is drawing a limited number (usually two or three) of samples during one dosing interval to calculate $AUC_{0–24}$. DBS sampling, due to its higher stability and easy shipment to central laboratories, has overcome some of the challenges associated with conventional venous sampling [15,16]. Moreover, recent developments in the field of limited sampling strategies have enabled accurate prediction of drug exposure without the need for intensive pharmacokinetic sampling [17,18]. In Paraguayan pediatric TB patients, pharmacokinetic sampling using DBS collection utilizing limited-sampling time points (0, 2, 4, and 8 h post dose) was successful in accurately assessing the pharmacokinetics of rifampicin and pyrazinamide [18]. Although exposure to rifampicin has been extensively studied, data on rifampicin exposure in the South American adult population is lacking.

The primary aim of this study was to evaluate the differences in exposure to rifampicin in native versus non-native Paraguayans using DBS sampling. The hypothesis to study exposure of rifampicin in native vs. non-native Paraguayans stemmed from the high discrepancy in TB incidence and mortality rates among native Paraguayan patients compared to the rest of the population. Apart from the socioeconomic, cultural, educational, and

health barriers which might explain the differences in TB incidence and mortality, we were compelled to study if there were any differences in the exposure of the key anti-TB drugs, such as rifampicin, in this population. None of these reasons have been studied in Paraguay so far. Our study is the start of unraveling the differences between subgroups in the population and we decided to start to investigate exposure in the native population and compare it to another, genetically different, study population. Furthermore, it is uncertain if any related genetic differences or other biological features contributing to the differences should be considered.

1.1. Patients and Setting

The study was carried out at the hospital 'Instituto Nacional de Enfermedades Respiratorias y del Ambiente' (INERAM) in Asunción, Paraguay. The study protocol was approved by the Ethics Committee of Laboratorio Central De Salud Pública—Asunción (No: 56/160415). From July 2015 to October 2018, hospitalized adult TB patients were asked to participate in the study. Signed informed consent was obtained from all patients. New drug-susceptible TB patients, $\geq$18 years, with pulmonary or extrapulmonary involvement or patients with high clinical suspicion of TB, or starting treatment with first-line TB drugs were eligible for inclusion. Severe renal or hepatic dysfunction at the start of treatment leading to a different TB treatment regimen was excluded. For this study, a sample size of 50 hospitalized patients (30 native and 20 non-natives) was considered. In the Paraguayan national TB program, a database is available based on the Paraguayan TB epidemiology. Native Paraguayans were identified based on their indigenous identity card which also expanded on ethnic and lingual identity. Furthermore, in this database high-risk groups such as prisoners, indigenous people, and others (substance abusers, HIV, and diabetes) are indicated as such. Native Paraguayans belong to one of the 17 ethnic groups in Paraguay. Of the 17 ethnic groups, 13 live in the western region also called the Chaco of Paraguay (arid land, with very high temperatures, sometimes exceeding 50 °C, and their diet is primarily composed of the meat of wild animals). The other four ethnic groups live very close to the capital, Asuncion, and consume a similar diet to that of non-natives. The non-native population consisted of mestizo people who are of mixed Spanish and native descent.

Given the exploratory nature of the study, no formal sample size calculation was performed in this study. As PK data from the native population is lacking, we used an enrolment ratio of 1.5 to have sufficient samples to compensate for unforeseen circumstances. Patients were followed up until the completion of treatment.

1.2. TB Diagnosis, Drug Doses, Study Procedures, and Pharmacokinetic Analysis

Tuberculosis patients were verified based on the results from the sputum-smear-positive Ziehl Neelsen microscopy andculture on solid media, chest X-ray, and other molecular tests such as GeneXpert. GeneXpert was used as a confirmatory test for patients with positive sputum smears.

All patients were treated according to the WHO standard TB treatment guidelines and received once daily rifampicin (10 mg/kg, rounded to 450 or 600 mg) along with isoniazid, pyrazinamide, and ethambutol [19]. Comedication and basic demographics were recorded. Biochemical parameters were determined at baseline and on the day of PK sampling, which included hematocrit, serum creatinine, and liver enzymes. Blood samples were collected with a 10 mL syringe after disinfecting the skin with 70% alcohol. The collected blood was divided into two tubes for the collection of plasma and serum samples. The samples were immediately transferred to INERAM's laboratory for processing. At the Hospital del Indigena, the samples were collected inside the laboratory. Laboratory tests were performed at the INERAM laboratory and the Hospital del Indigena (Asuncion, Paraguay), both using the same automated Beckman equipment (German origin). The equipment used the enzymatic method for transaminases: alkaline phosphatase (ALP), alanine transaminase (ALT), and aspartate aminotransferase (AST) and the colorimetry method for bilirubins. Hemoglobin and hematocrit were analyzed by the flow-cytometry

method. The modified Jaffé kinetic method was used to analyze creatinine. The creatinine reference range was 0.7–1.3 mg/dL. The baseline laboratory tests were used to gain insights into the overall health status of the TB patients which included the patient's liver and kidney function, as well as their glucose metabolism, more as a descriptive approach. Apart from hematocrit, all other baseline parameters mentioned in Table 1 are routinely analyzed in the TB treatment centers every two to four weeks to evaluate if adverse reactions occur. In case of abnormal results, the test is repeated to take care of the adverse effects.

Table 1. Baseline characteristics of all included patients.

Patient Characteristics	Total (n = 50)	Native (n = 30)	Non-Native (n = 20)
Demographic data			
Male	33 (66)	16 (53)	17 (85)
Age (years)	35 (26–49)	35 (26–52)	40 (28–43)
Body weight (kg)	52 (47–62)	53 (44–62)	52 (49–63)
Length (cm)	167 (160–173)	164 (151–172)	169 (162–175)
Body Mass Index (kg/m^2) (n = 49)	19.5 (17.9–21.6)	20.2 (18.0–21.8)	18.9 (16.8–21.3)
Underweight (<18.5 kg/m^2)	19 (38)	10 (33)	9 (45)
Normal (18.5–25.0 kg/m^2)	31 (62)	20 (67)	11 (55)
Type of TB			
Pulmonary	46 (92)	28 (93)	18 (90)
Extrapulmonary	4 (8)	2 (7)	2 (10)
Comorbidities			
Diabetes	6 (12)	2 (10)	4 (20)
HIV	1 (2)	1 (3.3)	0 (0)
Radiological characteristics (n = 47)		(n = 27)	(n = 20)
Consolidation	36 (77)	23 (85)	13 (65)
Pleural fluid	8 (17)	7 (26)	1 (5)
Cavities	29 (62)	14 (52)	15 (75)
Atelectasis	8 (17)	5 (19)	3 (15)
Baseline Biochemical parameter			
Creatinine (umol/L), normal value 53 to 97.2 umol/L	61.9 (53.09–70.7)	61.9 (53.0–70.7)	61.9 (52.4–70.7)
ALT (U/L), normal value 10–49 U/L	27.5 (16–50.3)	35.0 (20.8–59.3)	20.5 (15.3–36.3)
AST (U/L), lower than 34 U/L	28.5 (19–46.2)	33.5 (23.8–57.5)	28.0 (19.5–34.0)
ALP (U/L), 90–360 U/L	209.0 (58.0–316.75)	233 (161.3–362.3)	232.0 (141.0–309.0)
Haemoglobin (g/dL)	10.65 (9.4–12.3)	10.1 (9.2–11.3)	11.5 (9.6–12.7)
Hematocrit (%)	33.6 (31.0–38.0)	33.1 (31.0–35.7)	36.0 (30.4–39.1)
Baseline Sputum smear (n = 49)		n = 30	n = 19
Positive	41 (83)	24 (80)	17 (89.4)
Negative	8 (16)	6 (20)	2 (10.5)
Baseline culture (n = 48)		n = 28	n = 20
Positive	33 (69)	19 (68)	14 (70)
Negative	15 (31)	9 (32)	6 (30)
GeneXpert MTB/RIF (n = 33)		n = 21	n = 12
Positive	32 (97)	20 (95)	12 (100)
Negative	1 (3)	1 (5)	0 (0)

Data are expressed as median (IQR) or n (%).

PK sampling was performed after two weeks of treatment (to ensure a steady state), at 2, 4, and 6 h after observed administration of rifampicin [20]. Patients had to remain fasted

for at least two hours prior to rifampicin intake until the second DBS sample (4 h) was taken. On the day of sampling, a trained healthcare worker collected capillary blood from a finger prick on special filter paper (Whatman® DMPK type C, Darmstadt, Germany) to produce DBS samples, and the DBS cards were dried at room temperature (20–35 °C) for at least 3 h and subsequently stored in a plastic ziplocked bag with silica enclosed. Contrary to standardized storage conditions, DBS samples were stored at room temperature before shipping them to the Netherlands. Rifampicin and its metabolite deacetyl-rifampicin were found to be stable at an ambient temperature of approximately 25 °C for 2 months, 37 °C for 10 days, and 50 °C for 3 days [21]. The shipping process to the Netherlands was in accordance with one of the stated conditions (37 °C for 10 days). The ambient temperature inside the local site was below 25 °C at all times due to the use of fans and coolers.

Rifampicin drug concentrations from these DBS samples were analyzed at the laboratory of the Department of Clinical Pharmacy and Pharmacology at the University Medical Center Groningen, Groningen, The Netherlands. The DBS samples were measured using a liquid-chromatography tandem mass-spectrometry technique (LC-MS/MS) assay validated for accuracy, precision, linearity, matrix effect, hematocrit effect, spot volume, and stability upon storage Details on the DBS assay of rifampicin have been published previously [21]. The calibration curve of rifampicin showed to be linear with a correlation coefficient (R^2) of 0.9953. Within run precision (%CV) ranged from 2.1% to 5.4% and between run precision ranged from 2.4% to 7.2%. Accuracy (bias) ranged from −1.1% to 4.0% at all tested QC levels (LLOQ, low, medium, high, and over the curve). Rifampicin was measured from the DBS cards and reported [21]. While reporting drug levels in two different matrixes (plasma and dried blood spots) there could be a systemic difference in rifampicin concentrations measured in plasma vs. DBS. We tested this in our earlier published clinical application study of venous blood and DBS samples for rifampicin [21]. Simple linear regression coefficients and Deming regression equations for rifampicin were R2 = 0.9076 (n = 28), y = 0.90x − 0.01 (95% confidence interval (CI) slope: 0.78–1.01, intercept: 0.53–0.51). The clinical application study showed no significant differences between the patient analysis of plasma and DBS for rifampicin [18,21]. Based on these results, a correction factor was deemed not applicable.

To estimate $AUC_{0–24}$ in this population, a validated one-compartmental population pharmacokinetic model with first-order absorption, lag time, and dose adaptation software was used (MW Pharm++, version 1.9.8.243; Mediware, Prague, Czech Republic) [16]. The currently applied three-point limited sampling strategy was validated in an earlier published study by Magis-Escurra et al. [20], where multiple linear regression analysis was conducted to obtain optimal sampling equations predictive of actual $AUC_{0–24}$ for rifampicin. All possible combinations of one to three time points were evaluated. The average adjusted R^2 and mean absolute percentage prediction error (MAPE) for all combinations comprising one, two, or three samples were calculated to investigate the correlation between the predicted $AUC_{0–24}$ using multiple linear regression and calculated $AUC_{0–24}$. The predictive performance of two-sampling time points and one-sampling time point fell short in terms of R^2 and MAPE [17,20]. Furthermore, a single PK sample at 2 h would not have been adequate for accurately predicting $AUC_{0–24}$, as it has been well established that Cmax cannot be estimated using C2 level [14].

1.3. Sputum-Smear Microscopy, Culture, and Statistical Evaluation

Sputum samples were collected from patients for sputum-smear microscopy and culture weeks after that following the WHO guidelines for the treatment of drug-susceptible TB (DS-TB) [19]. The culture was performed in the Löwenstein-Jensen media. All statistical analysis was performed in SPSS, version 23.0 (IBM Corp., Armonk, NY, USA). Categorical data were expressed in frequencies and percentages whereas continuous variables were presented as median and interquartile range. Nonparametric tests were used for the calculation of p-values (Mann–Whitney U test).

1.4. Treatment Outcomes

Treatment outcomes were reported following the WHO guidelines [19].

2. Results

2.1. Study Subjects

In this study, 50 hospitalized TB patients were included (length of hospitalization was about one month), of which 41 (82%) patients had positive sputum smears before starting TB treatment. The baseline characteristics of both natives (n= 30) and non-natives (n= 20) are summarized in Table 1. The median age of the native population was 35 years (26–52 interquartile range, IQR), and the non-native population was 40 years (28–43 IQR). The actual median rifampicin dose was 600 mg (IQR 525–600 mg). The national TB program provides Rifafour, a combination of the four drugs, in the intensive phase. Rifafour is a fixed-dose combination of four active TB drugs: rifampicin 150 mg, isoniazid 75 mg, pyrazinamide 400 mg, and ethambutol HCL 275 mg. Based on the BMI < 18.5 kg/m^2, 45% (9/20) of the non-native patients were underweight; and 31% (10/29) of the native patients were underweight. All 50 patients completed PK sampling using DBS; samples were taken in an average of a median 14 days (11–19 IQR) after starting treatment except in five patients who were sampled after 30 days of treatment. Of 50 patients, 10 (20%) patients who were lost to follow up after the first month of treatment were equally distributed over two groups, six (20%) from natives (n = 30) and four (20%) from the non-natives (n = 20). Of the total, one (2%) patient stopped TB treatment because in the diagnostic tests, all the results were negative for TB and the diagnosis became unlikely.

2.2. Pharmacokinetics

At 10 mg/kg once daily dosing, the median $AUC_{0–24}$ (n = 50) was 23.2 mg*h/L (16.4–32.3 IQR). Native patients showed a comparable rifampicin exposure to the non-natives; the median $AUC_{0–24}$ was 21.6 (15.0–35.4 IQR) and 24.7 (17.1–29.5 IQR), respectively (p = 0.66, Mann-Whitney U test, see Table 2).

Table 2. Rifampicin dose, AUC, and treatment outcomes.

	Native (n = 30)	**Non-Native (n = 20)**
Rifampicin dose (mg/kg)	10.74 (9.43–11.51)	10.66 (9.47–11.69)
AUC (mg*h/L)	24.7 (17.1–29.5)	21.6 (15.0–35.4)
Primary Treatment Outcomes		
- Sputum conversion (60 days, yes)	16 (94), n = 17	10 (91), n = 11
- Culture conversion (60 days, yes)	15 (94), n = 16	9 (90), n = 10
Final treatment outcomes (end of the treatment)		
- Cured	9 (30)	11 (55)
- Treatment completion	10 (34)	4 (20)
- Loss-to-follow up	6 (20)	4 (20)
- Missing data	1 (3)	1 (5)
- Not evaluated	4 (13)	-

Data are expressed as median (IQR) or n (%).

Of the total (n = 50), only eight (16%) patients had a rifampicin reference $AUC_{0–24}$ > 38.7 mg*h/L; six (20%) patients from the native population and two (10%) from the non-natives, indicating that the Paraguayan population (both native and the

non-native) are at the lower end of the AUC values that are observed in TB patients. The probability of rifampicin target attainment (PTA) was calculated (Figure 1) and showed PTA (AUC/MIC > 271) in the Y-axis plotted against the assumed MIC of rifampicin ranged from 0.00156 to 1 mg/L in the X-axis. The analysis (n = 50) showed that with once-daily dosing of 450–600 mg, only 27% of the native patients and 20% of the patients from the non-native group met the target $AUC_{0–24}$ /MIC $\geq$ 271 if MIC was assumed to be 0.125 mg/L. Furthermore, at an assumed MIC of 0.25 mg/L, PTA dropped dramatically to 0% in the total population. At present, the ECOFF MIC of rifampicin is set at 0.5 mg/L, whereas PK/PD susceptibility breakpoint is at 0.0625 mg/L [9]. This is reflected in our cohort (see Figure 1), as the PTA dropped from 100% (at MIC of 0.0625 mg/L) to 0% (MIC of 0.25 mg/L). The most prevalent MIC for rifampicin in Paraguay is 0.25 mg/L (*personal communication with the central laboratory in Asuncion, Paraguay*).

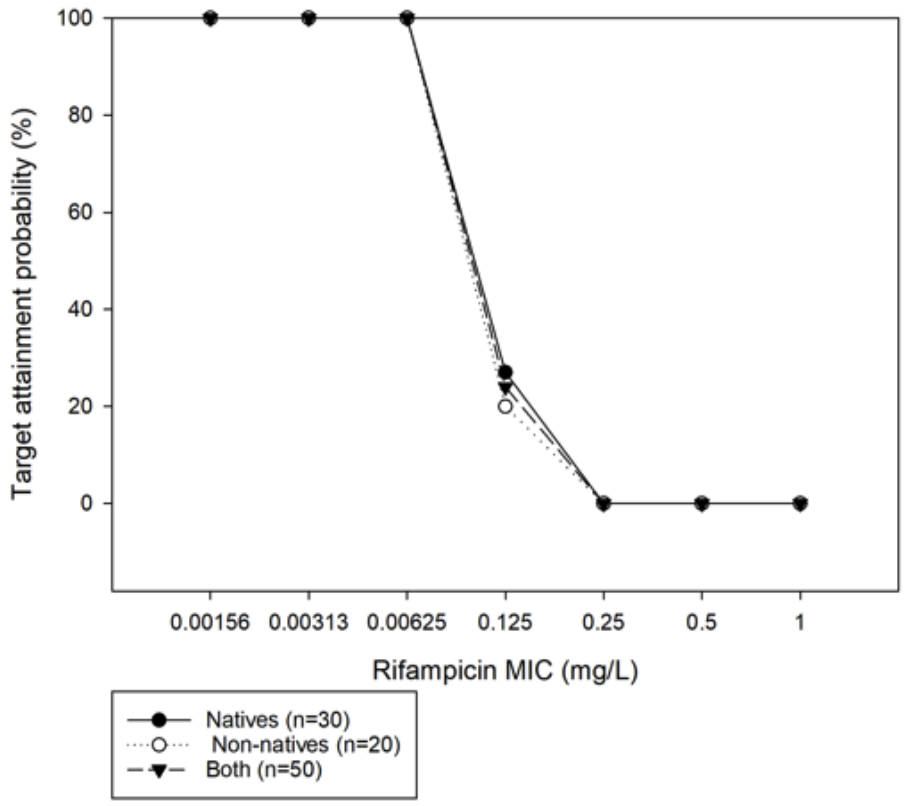

Figure 1. Probability of target attainment ($AUC_{0–24}$/MIC > 271) vs. *minimum inhibitory concentration* (MIC) in patients at assumed rifampicin MIC (ranged from 0.00156 to 1 mg/L)).

2.3. Sputum-Smear/Culture Conversion and Treatment Outcomes

The median time to sputum-smear conversion (n = 21) was 15 days (15–45 IQR) and culture conversion (n = 25) was 15 days (15–30 IQR). In the native population, the median time to sputum-smear conversion (n = 6) was 15 days (15–15 IQR), and culture conversion (n = 13) was also 15 days (15–15 IQR). In the non-native population, the median time to sputum-smear conversion (n = 15) was 15 days (15–45 IQR) and culture conversion (n = 12) was 30 days (15–60 IQR). Sputum-smear/culture conversion data at 60 days of the treatment and the final treatment outcomes of the native and non-native populations are shown in Table 2.

3. Discussion

This study evaluated the differences in drug exposure to rifampicin between native and non-native Paraguayans using DBS sampling. Rifampicin exposure in Paraguayan TB patients (natives and non-natives) was considered low as only 16% of the patients

achieved a reference $AUC_{0–24}$ > 38.7 mg*h/L [8]. There was no difference in the rifampicin doses (10 mg/kg) between the two groups (p = 0.49, see Table 2). No significant difference in rifampicin exposure was observed between the native and non-native Paraguayan population (n = 6, 20% in the native and n = 2, 10% in the non-native group met the AUC target). Both groups had rifampicin levels towards the lower AUC range (median 23.2 mg*h/L and IQR 16.4–32.3) of normal in patients receiving a dose of 10 mg/kg once daily [8]. Of note, there were higher numbers of female participants in the native group compared to the non-native group. The study by Conte et al. found that absorption of rifampicin or the plasma levels of rifampicin at 2 h and 4 h were not affected by sex [22]. Therefore, we assume that the absorption of rifampicin was comparable between males and females in our study.

Remarkably, rapid conversion in both native and non-native populations occurred despite low exposure to rifampicin. This may indicate that the current treatment during the intensive phase of treatment was adequate, which could be attributed to the combined effect of the four drugs. Several factors could have contributed to the rapid conversion. First, the MIC of rifampicin might have been low in these patients (although the most prevalent MIC for rifampicin in Paraguay is reported at 0.25 mg/L). Second, it could be that combination therapy of isoniazid, pyrazinamide, and ethambutol also contributed to the rapid response. Still, the low exposure in relation to sterilization might have resulted in the dormancy of TB bacteria rather than actually killing it as long-term follow-up data is missing, which is concerning. Therefore, our study shows that the currently used dosing of rifampicin 10 mg/kg is likely suboptimal and there is plenty of room for rifampicin dose optimization [8,23]. Furthermore, these were hospitalized patients who are often sicker than the normal TB patient population. Although other reasons for hospitalization in this study included socioeconomic reasons, patients lived far from the treatment center, were poor, or lived alone with no one to take care of them. Additionally, our study showed that pharmacokinetics can be assessed in remote settings using this strategy in adults as well as in children [18].

Our results are consistent with earlier reports on rifampicin levels in adult TB patients [8,24,25]. Seijger et al. evaluated serious adverse events in a cohort of 88 patients with severe presentations such as meningitis TB in one of our TB-expert centers, treated with high-dose rifampicin (up to 32 mg/kg) from the treatment start or after TDM [26]. Encouragingly, no serious adverse events occurred, and $AUC_{0–24}$ showed nonlinear increases at higher dosages [26]. Therefore, along with our study, the available evidence suggests that the time is now right to apply a higher dose of rifampicin in order to save lives, especially in the most difficult-to-cure patients [25]. With higher doses, not only desired AUC will be attained but also culture conversion will be reached earlier which might result in shortening the therapy duration.

This study has limitations. First, for sputum-culture conversion, a hallmark for evaluating the efficacy of the TB-treatment therapy, data were available only in half of the included patients due to several reasons such as some patients could not expectorate sputum samples, others missed the visit, some were sputum-culture negative from the start, and some had extrapulmonary TB. Second, MIC values were not measured and assumed MIC of 0.125 and 0.25 mg/L were used. Third, in our study, 20% of the patients were lost to follow up. These patients are at greater risk for developing drug resistance and further transmitting resistant forms of TB to the community. Fourth, the model was not validated separately for the native Paraguayan tuberculosis patients [16]. However, the original model was built using a heterogeneous population, with respect to ethnicity, weight, and BMI. Next to that, it was developed for the same dosing range. This model has been successfully in use to calculate AUC24 in daily patient care for almost 10 years now. Based on our vast experience with a very large range of different parameters, we are confident that the model can be applied to estimate exposure in the native population. Unfortunately, the exposures of rifampicin in routine care in the TB center are not part of this project, hence we cannot report on them, nor compare them as they are not part of the study approved by the ethics

committee. Fifth, we did not perform the genetic analysis searching for variants in the genes SLCO1B1, ABCB1, UGT1A, or PXR which have a role in the extent of gun/hepatic enzyme induction and metabolism [27]. Sixth, this exploratory study was not powered to find any differences resulting between the groups. The heterogeneity is visible in the rifampicin exposure IQR in both groups, which varied between 15.0–35.4 mg*h/L. Based on a post hoc power analysis, future studies would need a total of 95 patients to achieve 80% power (this is with 15% additional subjects included due to the non-normality of the rifampicin exposure). Therefore, this is our recommendation for any future follow-up studies of a similar nature.

Furthermore, we did not study the pharmacokinetics parameters of rifampicin as it remains outside the scope of this study due to several reasons. First, limited sampling time points (2 h, 4 h, and 6 h) are validated to estimate the exposure of rifampicin over 24 h $AUC_{0–24}$ and not other PK parameters like Cmax, Tmax, half-life, and volume of distribution [20]. To perform a full pharmacokinetics study, we need to collect multiple samples at 0 h (pre-dosing), 30 min, 1 h, 2 h, 3, 4, and 6 h postdosing. Second, since $AUC_{0–24}$ remains the first best predictor of efficacy for rifampicin, we were interested in the exposure difference between the two groups in this first prospective cohort study given the pilot character of the project. Assessing full PK parameters including genotyping and treatment-outcome data would be a follow-up study.

Finally, to address the issue of high loss to follow up, national TB treatment programs in Paraguay are currently focusing on formulating and improving health strategies. Intersectoral collaboration, sustained financing, and applying new tools and technologies such as TDM or video-based directly-observed treatment will be important to carve the path for the more efficient functioning of TB programs in Paraguay.

Future Perspectives, Next Steps

Currently, our group, the EUSAT-RCS consortium (https://www.eusattb.net/), is preparing a multinational, multicenter phase IIb clinical trial evaluating the safety and efficacy of high-dose rifampicin (35 mg/kg) in adult subjects with pulmonary or extrapulmonary DS-TB belonging to difficult to treat subgroups (such as patients older than 60 years and/or with significant comorbidities with active tuberculosis) [28]. The results from this scheduled phase II trial will generate solid evidence on if the optimized dose will be feasible in the clinical practice for the whole population.

4. Conclusions

In our cohort of 50 Paraguayan TB patients, rifampicin 10 mg/kg dosing resulted in low exposures in both native and non-native patients. Native patients showed comparable exposure to non-natives. Dried blood spot sampling was used successfully to estimate rifampicin exposure and this sampling method seems feasible in resource-limited settings.

Author Contributions: Conceptualization, G.M. and C.M.-E.; Data curation, A.B. and L.G.P.; Formal analysis, S.G. and M.G.G.S.; Funding acquisition, C.M.-E.; Investigation, G.M. and N.M.; Methodology, S.G. and G.M.; Project administration, G.M. and C.M.-E.; Supervision, S.G. and M.G.G.S.; Writing—original draft, S.G.; Writing—review & editing, S.G., A.B., L.G.P., S.A., J.-W.C.A., M.G.G.S., and C.M.-E. All authors have read and agreed to the published version of the manuscript.

Funding: Cecile Magis-Escurra received funding from Stichting Suppletiefonds Sonnevanck. Arturo Battaglia and Luis Gómez Paciello were involved in the drafting of this manuscript during their secondment to the University Medical Center Groningen for three months in 2020. Both authors received funding from Horizon 2020 as part of the secondment programme (Rise-Marie Curie, grant number 823890).

Institutional Review Board Statement: The study was carried out at the hospital 'Instituto Nacional de Enfermedades Respiratorias y del Ambiente' (INERAM) in Asunción, Paraguay. The study protocol was approved by the Ethics Committee of Laboratorio Central De Salud Pública—Asunción (No: 56/160415).

Informed Consent Statement: Informed consent was obtained from all subjects involved in the study.

Data Availability Statement: Not applicable.

Acknowledgments: We are grateful to the Paraguayan patients for their participation and thank the clinical, and laboratory staff of INERAM for their kind cooperation and assistance.

Conflicts of Interest: The authors declare no conflict of interest.

References

1. World Health Organization. *Global Tuberculosis Report*; World Health Organization: Geneva, Switzerland, 2022.
2. Centro Nacional de Tuberculosis. Implementación del Plan. Nacional del Control. de la Tuberculosis 2011–2015. 2011. Available online: https://www.mspbs.gov.py/portal/8212/incidencia-por-tuberculosis-en-paraguay-con-tendencia-decreciente.html (accessed on 8 February 2020).
3. Zheng, X.; Bao, Z.; Forsman, L.D.; Hu, Y.; Ren, W.; Gao, Y.; Li, X.; Hoffner, S.; Bruchfeld, J.; Alffenaar, J.-W. Drug Exposure and Minimum Inhibitory Concentration Predict Pulmonary Tuberculosis Treatment Response. *Clin. Infect. Dis.* **2021**, *73*, E3520–E3528.
4. Pasipanodya, J.G.; Nuermberger, E.; Romero, K.; Hanna, D.; Gumbo, T. Systematic Analysis of Hollow Fiber Model of Tuberculosis Experiments. *Clin. Infect. Dis.* **2015**, *61*, S10–S17.
5. Gumbo, T.; Louie, A.; Deziel, M.R.; Liu, W.; Parsons, L.M.; Salfinger, M.; Drusano, G.L. Concentration-dependent Mycobacterium tuberculosis killing and prevention of resistance by rifampin. *Antimicrob Agents Chemother.* **2007**, *51*, 3781–3788.
6. Dheda, K.; Gumbo, T.; Maartens, G.; Dooley, K.E.; McNerney, R.; Murray, M.; Warren, R.M. The epidemiology, pathogenesis, transmission, diagnosis, and management of multidrug-resistant, extensively drug-resistant, and incurable tuberculosis. *Lancet Respir. Med.* **2017**, *5*, 291–360.
7. Jayaram, R.; Gaonkar, S.; Kaur, P.; Suresh, B.L.; Mahesh, B.N.; Jayashree, R.; Nandi, V.; Bharat, S.; Shandil, R.K.; Kantharaj, E.; et al. Pharmacokinetics-pharmacodynamics of rifampin in an aerosol infection model of tuberculosis. *Antimicrob. Agents Chemother.* **2003**, *47*, 2118–2124.
8. Stott, K.E.; Pertinez, H.; Sturkenboom, M.G.G.; Boeree, M.J.; Aarnoutse, R.; Ramachandran, G.; Mendez, A.R.; Peloquin, C.; Koegelenberg, C.F.N.; Alffenaar, J.W.C.; et al. Pharmacokinetics of rifampicin in adult TB patients and healthy volunteers: A systematic review and meta-analysis. *J. Antimicrob. Chemother.* **2018**, *73*, 2305–2313.
9. Gumbo, T. New susceptibility breakpoints for first-line antituberculosis drugs based on antimicrobial pharmacokinetic/pharmacodynamic science and population pharmacokinetic variability. *Antimicrob. Agents Chemother.* **2010**, *54*, 1484–1491.
10. Alffenaar, J.-W.C.; Gumbo, T.; Dooley, K.E.; Peloquin, C.A.; McIlleron, H.; Zagorski, A.; Cirillo, D.M.; Heysell, S.K.; Silva, D.R.; Migliori, G.B. Integrating pharmacokinetics and pharmacodynamics in operational research to end tuberculosis. *Clin. Infect. Dis.* **2020**, *70*, 1774–1780.
11. Nahid, P.; Dorman, S.E.; Alipanah, N.; Barry, P.M.; Brozek, J.L.; Cattamanchi, A.; Vernon, A. Official American thoracic society/centers for disease control and prevention/infectious diseases society of America clinical practice guidelines: Treatment of drug-susceptible tuberculosis. *Clin. Infect. Dis.* **2016**, *63*, e147–e195.
12. Ghimire, S.; Bolhuis, M.S.; Sturkenboom, M.G.G.; Akkerman, O.W.; De Lange, W.C.M.; Van Der Werf, T.S.; Alffenaar, J.W.C. Incorporating therapeutic drug monitoring into the World Health Organization hierarchy of tuberculosis diagnostics. *Eur. Respir. J.* **2016**, *47*.
13. van der Burgt, E.P.M.; Sturkenboom, M.G.G.; Bolhuis, M.S.; Akkerman, O.W.; Kosterink, J.G.W.; de Lange, W.C.M.; Alffenaar, J.W.C. END TB by precision treatment! *Accept. Eur. Respir. J.* **2016**, *47*, 680–682.
14. Sturkenboom, M.G.G.; Märtson, A.-G.; Svensson, E.M.; Sloan, D.J.; Dooley, K.E.; van den Elsen, S.H.J.; Denti, P.; Peloquin, C.A.; Aarnoutse, R.E.; Alffenaar, J.-W.C. Population pharmacokinetics and Bayesian dose adjustment to advance TDM of anti-TB drugs. *Clin. Pharmacokinet.* **2021**, *60*, 685–710.
15. Vu, D.H.; Alffenaar, J.W.C.; Edelbroek, P.M.; Brouwers, J.R.B.J.; Uges, D.R.A. Dried blood spots: A new tool for tuberculosis treatment optimization. *Curr. Pharm. Des.* **2011**, *17*, 2931–2939.
16. Sturkenboom, M.G.G.; Mulder, L.W.; de Jager, A.; van Altena, R.; Aarnoutse, R.E.; de Lange, W.C.M.; Alffenaar, J.W.C. Pharmacokinetic Modeling and Optimal Sampling Strategies for Therapeutic Drug Monitoring of Rifampin in Patients with Tuberculosis. *Antimicrob. Agents Chemother.* **2015**, *59*, 4907–4913.
17. Saktiawati, A.M.I.; Harkema, M.; Setyawan, A.; Subronto, Y.W.; Stienstra, Y.; Aarnoutse, R.E.; Sturkenboom, M.G.G. Optimal sampling strategies for therapeutic drug monitoring of first-line tuberculosis drugs in patients with tuberculosis. *Clin. Pharmacokinet.* **2019**, *58*, 1445–1454.
18. Martial, L.C.; Kerkhoff, J.; Martinez, N.; Rodríguez, M.; Coronel, R.; Molinas, G.; Magis-Escurra, C. Evaluation of dried blood spot sampling for pharmacokinetic research and therapeutic drug monitoring of anti-tuberculosis drugs in children. *Int. J. Antimicrob. Agents* **2018**, *52*, 109–113.
19. World Health Organization. *Global Tuberculosis Control: A Short Update to the 2009 Report*; World Health Organization: Geneva, Switzerland, 2009. Available online: https://apps.who.int/iris/handle/10665/44241 (accessed on 8 February 2020).

20. Magis-Escurra, C.; Later-Nijland, H.M.; Alffenaar, J.W.; Broeders, J.; Burger, D.M.; van Crevel, R.; Aarnoutse, R.E. Population pharmacokinetics and limited sampling strategy for first-line tuberculosis drugs and moxifloxacin. *Int. J. Antimicrob. Agents* **2014**, *44*, 229–234.
21. Vu, D.H.; Koster, R.A.; Bolhuis, M.S.; Greijdanus, B.; Altena, R.V.; Nguyen, D.H.; Alffenaar, J.W.C. Simultaneous determination of rifampicin, clarithromycin and their metabolites in dried blood spots using LC–MS/MS. *Talanta* **2014**, *121*, 9–17.
22. Conte, J.E.; Golden, J.A.; Kipps, J.E.; Lin, E.T.; Zurlinden, E. Effect of sex and AIDS status on the plasma and intrapulmonary pharmacokinetics of rifampicin. *Clin. Pharmacokinet.* **2004**, *43*, 395–404.
23. Magis-Escurra, C.; Anthony, R.M.; van der Zanden, A.G.M.; van Soolingen, D.; Alffenaar, J.-W.C. Pound foolish and penny wise—When will dosing of rifampicin be optimised? *Lancet Respir. Med.* **2018**, *6*, e11–e12.
24. Boeree, M.J.; Diacon, A.H.; Dawson, R.; Narunsky, K.; du Bois, J.; Venter, A.; Phillips, P.P.J.; Gillespie, S.H.; McHugh, T.D.; Hoelscher, M.; et al. A dose-ranging trial to optimize the dose of rifampin in the treatment of tuberculosis. *Am. J. Respir. Crit. Care Med.* **2015**, *191*, 1058–1065.
25. Ruslami, R.; Ganiem, A.R.; Dian, S. Intensified regimen containing rifampicin and moxifloxacin for tuberculous meningitis: An open-label, randomised controlled phase 2 trial. *Lancet Infect. Dis.* **2013**, *13*, 12.
26. Seijger, C.; Hoefsloot, W.; Bergsma-de Guchteneire, I.; Te Brake, L.; van Ingen, J.; Kuipers, S.; Van Crevel, R.; Aarnoutse, R.; Boeree, M.; Magis-Escurra, C. High-dose rifampicin in tuberculosis: Experiences from a Dutch tuberculosis centre. *PLoS ONE* **2019**, *14*, e0213718.
27. Niemi, M.; Backman, J.T.; Fromm, M.F.; Neuvonen, P.J.; Kivistö, K.T. Pharmacokinetic interactions with rifampicin: Clinical relevance. *Clin. Pharmacokinet.* **2003**, *42*, 819–850.
28. Espinosa-Pereiro, J.; Ghimire, S.; Sturkenboom, M.G.G.; Alffenaar, J.-W.C.; Tavares, M.; Aguirre, S.; Battaglia, A.; Molinas, G.; Tórtola, T.; Akkerman, O.W.; et al. Safety of Rifampicin at High Dose for Difficult-to-Treat Tuberculosis: Protocol for RIAlta Phase 2b/c Trial. *Pharmaceutics* **2023**, *15*, 9. [CrossRef]

pharmaceutics

MDPI

Article

Implementation of Model-Based Dose Adjustment of Tobramycin in Adult Patients with Cystic Fibrosis

Jérémy Reverchon [1], Vianney Tuloup [1,2], Romain Garreau [1,2], Viviane Nave [3], Sabine Cohen [4], Philippe Reix [2,5], Stéphane Durupt [6], Raphaele Nove-Josserand [6], Isabelle Durieu [6,7], Quitterie Reynaud [6,7], Laurent Bourguignon [1,2,8], Sandrine Charles [2] and Sylvain Goutelle [1,2,8,*]

[1] Hospices Civils de Lyon, GH Nord, Service de Pharmacie, 69004 Lyon, France
[2] Univ Lyon, Université Claude Bernard Lyon 1, UMR CNRS 5558, LBBE—Laboratoire de Biométrie et Biologie Évolutive, 69622 Villeurbanne, France
[3] Hospices Civils de Lyon, Pharmacie Centrale, 69230 St. Genis Laval, France
[4] Hospices Civils de Lyon, Groupement Hospitalier Sud, Laboratoire de Pharmaco-Toxicologie, 69495 Pierre-Bénite, France
[5] Hospices Civils de Lyon, Centre de Ressources et de Compétences de la Mucoviscidose, 69500 Bron, France
[6] Hospices Civils de Lyon, Centre de Ressources et de Compétences de la Mucoviscidose (Adulte), GH Sud, Service de Médecine Interne, 69495 Pierre-Bénite, France
[7] Univ Lyon, Université Claude Bernard Lyon 1, RESHAPE, INSERM U1290, 69008 Lyon, France
[8] Univ Lyon, Université Claude Bernard Lyon 1, ISPB—Faculté de Pharmacie de Lyon, 69008 Lyon, France
* Correspondence: sylvain.goutelle@chu-lyon.fr; Tel.: +33-4-7216-8099

Abstract: Therapeutic drug monitoring (TDM) of tobramycin is widely performed in patients with cystic fibrosis (CF), but little is known about the value of model-informed precision dosing (MIPD) in this setting. We aim at reporting our experience with tobramycin MIPD in adult patients with CF. We analyzed data from adult patients with CF who received IV tobramycin and had model-guided TDM during the first year of implementation of MIPD. The predictive performance of a pharmacokinetic (PK) model was assessed. Observed maximal (Cmax) and minimal (Cmin) concentrations after initial dosing were compared with target values. We compared the initial doses and adjusted doses after model-based TDM, as well as renal function at the beginning and end of therapy. A total of 78 tobramycin courses were administered in 61 patients. After initial dosing set by physicians (mean, 9.2 $\pm$ 1.4 mg/kg), 68.8% of patients did not achieve the target Cmax $\geq$ 30 mg/L. The PK model fit the data very well, with a median absolute percentage error of 4.9%. MIPD was associated with a significant increase in tobramycin doses ($p < 0.001$) without significant change in renal function. Model-based dose suggestions were wellaccepted by the physicians and the expected target attainment for Cmax was 83%. To conclude, the implementation of MIPD was effective in changing prescribing practice and was not associated with nephrotoxic events in adult patients with CF.

Keywords: cystic fibrosis; therapeutic drug monitoring; tobramycin; pharmacokinetics; model-informed precision dosing

Citation: Reverchon, J.; Tuloup, V.; Garreau, R.; Nave, V.; Cohen, S.; Reix, P.; Durupt, S.; Nove-Josserand, R.; Durieu, I.; Reynaud, Q.; et al. Implementation of Model-Based Dose Adjustment of Tobramycin in Adult Patients with Cystic Fibrosis. *Pharmaceutics* **2022**, *14*, 1750. https://doi.org/10.3390/pharmaceutics14081750

Academic Editors: Barna Vasarhelyi, Gellért Balázs Karvaly and Antonello A. Barresi

Received: 1 July 2022
Accepted: 10 August 2022
Published: 22 August 2022

Publisher's Note: MDPI stays neutral with regard to jurisdictional claims in published maps and institutional affiliations.

1. Introduction

Pulmonary exacerbations (PE) are common infectious complications in patients with cystic fibrosis (CF) [1]. Non-fermenting gram-negative bacilli are the most retrieved agents in PE, especially *Pseudomonas aeruginosa* [2]. The recommended therapy of PE in patients with CF is the association of a beta-lactam (e.g., ceftazidime, or piperacillin/tazobactam) with an aminoglycoside, both administered by intravenous (IV) route [3]. Tobramycin is the most widely used aminoglycoside agent in this setting due to its activity against *P. aeruginosa*. As PE are recurrent, repeated courses of such antibiotic therapy are necessary in patients with CF.

Aminoglycosides have a narrow therapeutic margin, and their antibacterial effect is concentration dependent [4]. Overexposure has been associated with ototoxicity and

nephrotoxicity [5]. For initial dosing, recommended doses of tobramycin range from 10–15 mg/kg/day in CF patients [6]. However, dose individualization is required because of the narrow therapeutic margin and large interindividual pharmacokinetic (PK) variability. Therapeutic drug monitoring (TDM) has been recommended in this context to adjust the dosage and optimize the efficacy and safety in each patient [7,8].

However, TDM alone may not be an optimal approach for dose individualization of tobramycin. Traditional TDM only provides information on drug exposure to the physicians. Then, physicians have to interpret this information and use it adequately to adjust the dosage in order to achieve the pharmacokinetics/pharmacodynamics (PK/PD) target, and this process remains empirical. Limited information exists on how well TDM information is used to adjust aminoglycoside dosage in clinical routine. Model-informed precision dosing (MIPD) is an emerging approach that consists of using a pharmacokinetic model to interpret TDM results and compute the individual dose necessary to achieve a PK/PD target [9,10]. A Bayesian approach implemented in PK software is usually carried out to estimate individual PK parameter values based on both population information (population PK model) and individual information (dosing history, covariates such as renal function or body weight, and measured drug concentrations).

The objective of this study was to report our experience and first results of the implementation of an MIPD service for dosage individualization of tobramycin following TDM in adult patients with CF.

2. Materials and Methods

2.1. Tobramycin Local Dosing and Monitoring Practice

In our adult CF centre, PE were treated at home in most patients, with antibiotics administered as an outpatient parenteral antimicrobial therapy (OPAT). The initial dose was set by physicians based on previous courses. IV tobramycin was administered once daily for 14 days. A beta-lactam was commonly co-prescribed (e.g., ceftazidime or piperacillin/tazobactam). The preparation of tobramycin infusion bags was centralized in our central hospital pharmacy (Pharmacie Centrale des Hospices Civils de Lyon) and the preparations were then transported to patients' homes. Tobramycin infusion duration was set at 30 min but sometimes varied slightly in each patient. TDM was performed once during therapy, on the third or fourth day, with sampling of trough concentration (Cmin) being just before the next infusion and the peak (Cmax) being 30 min after the end of the infusion. Again, true sampling times may have varied slightly but those were precisely recorded by nurses. Blood samples were transported to the hospital pharmacology laboratory that performed tobramycin assay. Prior to MIPD implementation, the TDM results were interpreted, and the tobramycin dosages were adjusted empirically by physicians alone.

Physicians used tobramycin concentration targets recommended by the French National Drug Agency; these were Cmax of 30–40 mg/L and Cmin < 0.5 mg/L at 24 h [11]. The Cmax target is based on a Cmax/MIC (minimal inhibitory concentration) target of 8 to 10 and a putative maximal MIC of 4 mg/L, which is the tobramycin breakpoint from the Clinical and Laboratory Standards Institute (CLSI) for susceptible strains of *P. aeruginosa* [12].

MIPD of tobramycin was implemented routinely in January 2021. Clinical pharmacists interpreted the TDM results with PK software (see below) and provided a dosage recommendation to physicians. The central pharmacy responsible for infusion bag preparation was also informed and could adjust the dose to be administered, if necessary. The organization of tobramycin therapy after implementation of MIPD is depicted in Figure 1.

For the initial dose, the physicians prescribed the same dose as the post-TDM dose of the previous course. As no patient exhibited severe renal impairment at baseline (see results), once daily dosing was applied, in accordance with guidelines [13,14].

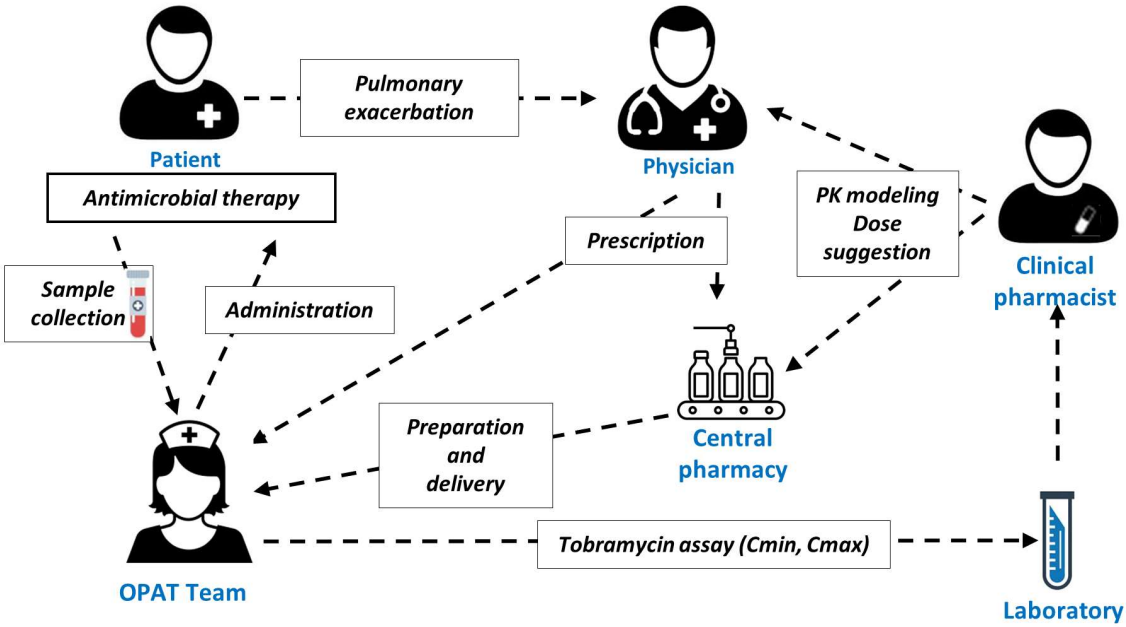

Figure 1. Organization of tobramycin therapy in our adult CF center. Abbreviations: Cmin, trough concentration; Cmax, maximal concentration; OPAT, outpatient parenteral antimicrobial therapy; PK, pharmacokinetics.

2.2. Data Collection

We performed a retrospective analysis of data from all adult patients with CF who received IV tobramycin and had TDM from January 2021 to January 2022, after MIPD implementation. As this was a non-interventional study with TDM performed as part of routine patient care, no informed consent nor ethics approval was required, in accordance with the French law on biomedical research [15].

The data collected included blood sampling times, drug administration times, intravenous infusion duration, and measured drug concentrations, as well as patient characteristics including sex, age, body weight, serum creatinine, and creatinine clearance (CL_{CR}, estimated with the Cockcroft–Gault equation) at tobramycin therapy onset and at the end of therapy. We also collected data on PK modelling (see below), including the predicted tobramycin concentrations and PK parameter values (central volume of distribution and clearance) as well as data on dosage adjustments including the tobramycin initial dose, the dose suggested by clinical pharmacists after TDM and PK modelling, and the dose set by physicians after this recommendation.

Concentrations of tobramycin were measured by using an automated immunoturbidimetry assay (PETIA). The lower limit of quantification was 0.2 mg/L. Intra- and inter-day repeatability expressed as coefficients of variation were less than 4%. The method was validated according to our national quality insurance program.

2.3. MIPD and PK Data Analysis

The TDM results were analysed by using a Bayesian PK modelling approach. We used the BestDose^{TM} software to perform Bayesian fitting of the PK model and estimation of individual PK parameters (e.g., clearance and volume of distribution) in each patient on all TDM occasions [16]. The measured Cmin < 0.2 mg/L were set at 0.1 mg/L (half the lower limit of quantification) in the Bayesian PK modeling.

Bayesian estimation of PK parameters was based on a nonparametric two-compartment population model previously developed and validated by our group in children and adolescents with CF [17]. The population distributions of PK parameters were used as prior in the Bayesian estimation. Extrapolation to adult patients was theoretically possible since this model includes the influence of physiological variables that are scalable;

the tobramycin elimination rate constant is linearly correlated with creatinine clearance (in mL/min) and the central volume of distribution is expressed in L/kg. The equations of the covariate-parameter relationships are as follows:

$$V1 = Vs. \times BW \quad (1)$$

where V1 is the tobramycin central volume of distribution (in L), Vs. is the central volume of distribution in L/kg, and BW is the body weight in kg. The symbol "S" indicates that Vs. is the slope parameter in the regression of V1 versus BW.

$$Ke = K_I + K_S \times CL_{CR} \quad (2)$$

where Ke is the tobramycin elimination rate constant (in h^{-1}), CL_{CR} is the creatinine clearance estimated by the Cockcroft-Gault equation (in mL/min), K_S is the slope parameter in the regression of Ke versus CL_{CR}, and K_I is the non-renal component of elimination (intercept parameter in the regression of Ke versus CL_{CR}).

Good predictive performance of the model in adult patients has been recently confirmed in another dataset from adult patients [18].

Once the model had been fit to the data and provided acceptable results, it was used to simulate a future once-daily dosing regimen. The dosage was computed to achieve the recommended targets cited above: Cmax of 30 to 40 mg/L and Cmin < 0.5 mg/L. Because real infusion and sampling times for Cmax could differ from the standard, the model was used to calculate Cmax 30 min after the end of a 30 min infusion ($Cmax_{mod}$), and this value was considered in the target attainment and dose adjustment.

The PK report sent to physicians included three recommended dosages for achieving the lower, mid-value, and upper bounds of the target interval (30, 35, and 40 mg/L, respectively). Due to the tobramycin presentations available in France, the dose suggestions were rounded to the next 25 mg dose.

2.4. Statistical Analysis

To assess the goodness-of-fit of the PK model, the individual predicted concentrations were compared with the observed concentrations. Target attainment after initial dosing was assessed by the proportion of Cmax, $Cmax_{mod,}$ and Cmin within the target range. We evaluated the effects of MIDP by comparing the initial dose to the dose finally selected by the physicians with the Wilcoxon signed-rank test for paired samples. To assess the effect of dose changes on renal function, baseline serum creatinine and creatinine clearance were compared with values at the end of tobramycin therapy with the same test. A *p*-value less than or equal to 0.05 was considered as significant in all tests. An increase of 50% of serum creatinine from baseline was considered as a marker of acute kidney injury (AKI).

3. Results

During the study period of one year, 78 tobramycin courses were administered in 61 patients. One patient was excluded because his age was $\leq$18 years. The characteristics of the population are presented in Table 1 and the PK results in Table 2. The tobramycin median initial dose (9.2 mg/kg) was slightly lower than the recommended dose of 10 mg/kg, and only 27% of the initial doses were within the range 10–15 mg/kg. Renal function was normal in most patients. Mild renal impairment (creatinine clearance between 60 and 90 mL/min) was observed in eighteen (23%) patients and moderate renal impairment (creatinine clearance between 30 and 60 mL/min) was observed in one (1.3%) patient. No patients had severe renal impairment.

The tobramycin PK model fit the data very well, as shown in Figure 2. The model predictions were highly correlated with the observations ($R^2 > 0.99$). The predictive performance was very good with a median (interquartile range) prediction error of −0.11 mg/L (−0.8; 0) and a median absolute percentage error of 4.9% (2.5%; 24.4%).

Table 1. Patient characteristics.

Variable	Value
Number of patients (number of women/men)	77 (53/24)
Age (years)	32.4 ± 10
Body weight (kg)	57.5 ± 12.3
Body mass index (kg/m^2)	20.9 ± 4.0
Tobramycin initial dose (mg)	518.2 ± 98.2
Tobramycin initial dose (mg/kg)	9.16 ± 1.42
Tobramycin initial dose between 10–15 mg/kg	27.3%
Baseline CL_{CR} (mL/min)	112.7 ± 28.4
CL_{CR} at the end of therapy (mL/min) [a]	112.6 ± 33.3
Difference between final and initial CL_{CR} (mL/min)	0.62 ± 17.8
Serum creatinine increase ≥50% from baseline	1.3 % (n = 1)

[a] serum creatinine at the end of therapy was not available for eight patients. Values are given as mean ± standard deviation unless otherwise stated. Abbreviations: CL_{CR}, creatinine clearance.

Table 2. Pharmacokinetic results.

Variable	Value
Infusion time (min)	35.9 ± 7.4
Cmax post-infusion sampling time (min)	32.1 ± 8.9
Measured Cmax (mg/L)	27.8 ± 5.4
Estimated Cmax (mg/L)	27.0 ± 5.2
$Cmax_{mod}$ (mg/L)	28.2 ± 4.3
$Cmax_{mod}$ < 30 mg/L	68.8%
$Cmax_{mod}$ between 30 and 40 mg/L	28.9%
$Cmax_{mod}$ > 40 mg/L (%)	1.3%
Measured Cmin at 24 h (mg/L)	0.25 ± 0.48
Estimated Cmin at 24 h (mg/L)	0.22 ± 0.19
Cmin at 24 h < 0.5 mg/L (%)	88.3%

Abbreviations: Cmax, maximal concentration; $Cmax_{mod}$, concentration estimated 30 min after the end of a 30 min infusion; Cmin, trough concentration. Values are given as mean ± standard deviation unless otherwise stated.

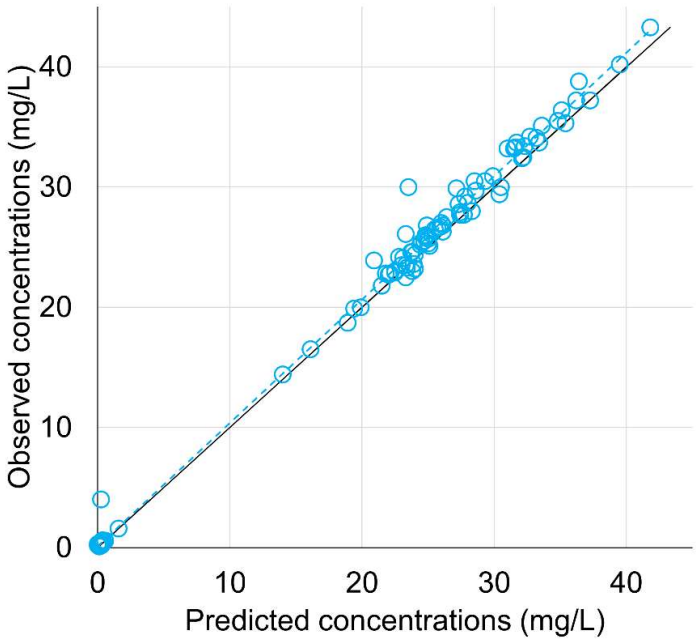

Figure 2. Observed concentrations of tobramycin versus individual model predictions. Blue circles represent observation/prediction pairs. The dashed blue line is the linear regression line. The solid line is the line of identity ($y = x$).

After initial dosing, 68.8% of patients had a $Cmax_{mod}$ value below the lower bound of the target interval (30 mg/L). Overexposure (Cmax > 40 mg/L) was observed in only one patient who received an initial dose of 9.2 mg/kg. Regarding Cmin, 88.3% of patients had values < 0.5 mg/L and 67.9% of patients had a Cmin value lower than 0.2 mg/L.

Table 3 summarizes the dose changes after model-guided TDM. Overall, the dose was unchanged in twenty-eight cases (36.4%), while it was increased in forty-six cases (59.7%) and decreased in three cases (3.9%). After the physicians' decision, 64 patients (83.1%) were expected to have tobramycin concentrations between 30 and 40 mg/L, with doses ranging from 6.1 to 14.7 mg/kg (median: 10.2 mg/kg). The comparison of the initial and adjusted doses of tobramycin is shown in Figure 3. While the initial doses were evenly distributed around a median of 500 mg, the model-guided dose adjustment resulted in a higher median dose of 550 mg ($p < 0.001$) and a larger variability, reflecting the individual dosage requirements. At the end of the antibiotic course, neither a new course nor prolongation of the cure were required for any patient, which suggests treatment efficacy.

Table 3. Dose changes after model-guided TDM according to measured concentrations.

Estimated Cmax Value (mg/L)	No Dose Change (%)	Dose Increase (Median, min–max) in mg	Dose Decrease (Median, min–max) in mg	Accepted Model-Based Dose Suggestion Targeting				Total
				30 mg/L (%)	35 mg/L (%)	Between 30 and 35 mg/L	40 mg/L (%)	
<30	12 (21.4%)	44 (100, 25–200)	0	24 (42.9%)	6 (10.7%)	14 (25%)	0 (0%)	56 (72.7%)
30–35	11 (78.6%)	2 (87.5, 75–100)	1 (75)	2 (14.3%)	1 (7.1%)	0 (0%)	0 (0%)	14 (18.2%)
35–40	4 (66.7%)	0	2 (112.5, 25–200)	1 (16.7%)	1 (16.7%)	0 (0%)	0 (0%)	6 (7.8%)
>40	1 (100%)	0	0	0 (0%)	0 (0%)	0 (0%)	0 (0%)	1 (1.3%)
Total	28 (36.4%)	46 (59.7%)	3 (3.9%)	27 (35.1%)	8 (10.4%)	14 (18.2%)	0 (0%)	77 (100%)

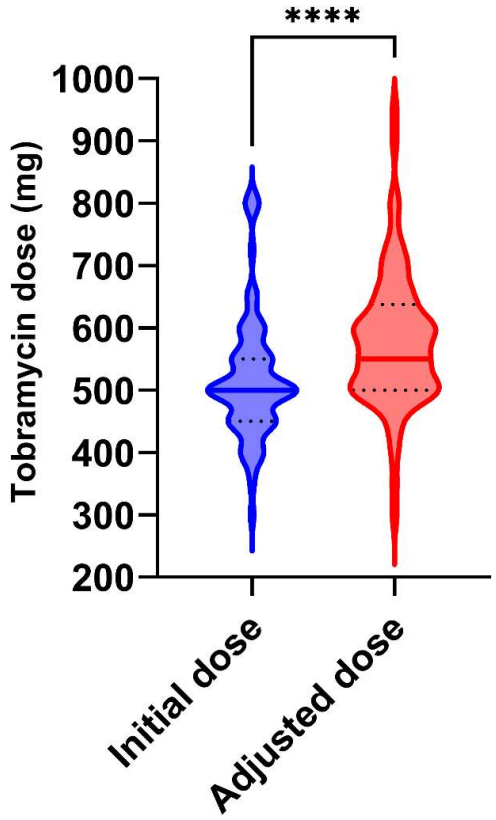

Figure 3. Violin plots of tobramycin doses before and after dose adjustment. The central solid line is the median. The black dotted lines are the quartiles (25th and 75th percentiles). Symbol **** indicates $p < 0.0001$.

Regarding the renal function under therapy, there was no statistical difference between serum creatinine at baseline and at the end of therapy (p = 0.697). Individual changes in serum creatinine during therapy are shown in Figure 4. Of note, serum creatinine at the end of therapy was not available in eight patients. Only one patient (1.3%) showed an increase in serum creatinine greater than 50% from baseline, which was considered as a marker of acute kidney injury. This patient received an initial dose of 500 mg (8.2 mg/kg), which was increased to 650 mg (10.7 mg/kg) after model-guided TDM showed a measured Cmax of 26.8 mg/L ($Cmax_{mod}$ = 24.6 mg/L). His serum creatinine increased during therapy from 76 to 139 µM.

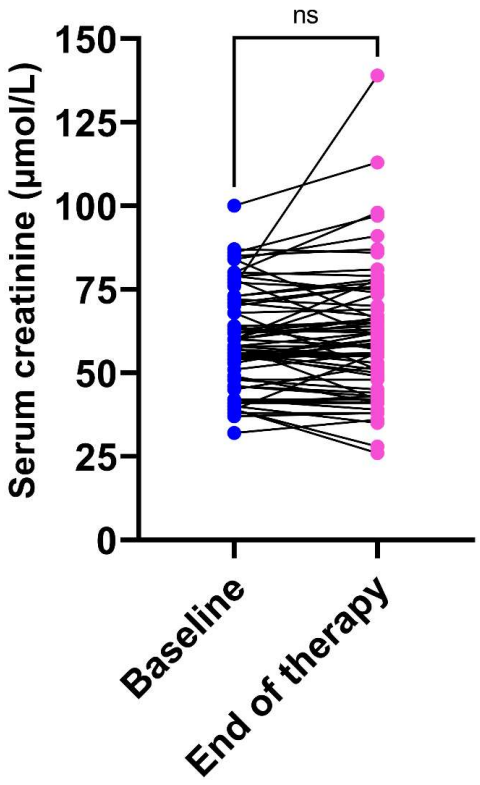

Figure 4. Individual changes in serum creatinine during tobramycin therapy (n = 69). Abbreviation: ns, non-significant.

4. Discussion

The appropriate treatment of *Pseudomonas aeruginosa* pulmonary exacerbations in CF patients has a major impact on patients' quality of life. In this context, patients are expected to receive numerous courses of antibiotics with potential side effects associated. TDM of antibiotics has been supported in numerous reports and guidelines for optimizing the efficacy and safety of antimicrobial therapy, especially in special populations [19,20]. However, TDM alone may not be an optimal approach if the interpretation of results and dose adjustments remain empirical. This was reported more than 20 years ago by van Lent-Evers et al., who showed that active model-guided TDM of aminoglycosides was associated with better concentration target attainment and clinical outcomes than standard TDM with empirical dosing [21]. In a recent study from our group, we have shown that empirical dose adjustment performed by physicians after TDM of tobramycin in CF adult patients often failed to adequately modify tobramycin dosages for achieving the Cmax target [18]. In patients with observed tobramycin Cmax lower than the target, empirical dose increases were too low for achieving the expected values in most patients. This previous study and the present one confirm that model-guided TDM, now described as MIPD, is more effective than conventional TDM in adjusting the dosage of tobramycin in goal-oriented therapy.

Considering that the initial dose represented the local dosing practice before implementation of MIPD in our cohort, our results showed that most patients (74%) received an initial tobramycin dose lower than 10 mg/kg. As a result, 68% of patients exhibited an estimated Cmax lower than the target of 30 mg/L. The MIPD approach was effective in changing clinician dosing practice and lead to a higher tobramycin dose. Those higher doses were expected to result in better target attainment. However, this could not be evaluated in the present study because TDM was not repeated during PE therapy and a second cure within the same year was rarely administered.

In our experience, the MIPD service provided by pharmacists was well accepted by physicians, with an acceptance rate of dose suggestion of 83.1%.

Physicians declined a model-based dose adjustment in n = 13 patients (16.9%) and decide to keep the initial dose despite under- or over-exposure. The main reasons were concerns about patient frailty, renal function, or pregnancy.

Importantly, there was no significant change in renal function with the dose increases suggested by MIPD. Only one patient out of sixty-nine (1.4%) showed an increase in serum creatinine over 50%. This toxicity rate is similar to the literature data [22,23]. This suggests that higher doses of once-daily tobramycin are probably safe, although further research is required to confirm this result.

Regarding the PK model and the software used for MIPD, we confirmed that a tobramycin PK model developed in children and adolescent with CF was adequate for fitting concentration in adults. Other studies reported successful model extrapolation in populations different from the one used in model building [24,25]. A strength of the BestDose^{TM} software is that it includes a hybrid-fit option, which basically consists of increasing PK parameter ranges and reducing prior information to identify parameter values out of the bounds of the original prior distribution [26,27]. This option was used in some patients of our cohort when the standard fit was not adequate (data not shown).

Another strength of model-guided TDM is the ability to interpret drug concentrations when infusion and sampling times deviate from the standards. This is especially important in the interpretation of Cmax because a small variation in sampling time can result in quite a large change in measured concentrations. In our study, the median sampling time for Cmax was 30 min, but significant deviations occurred in some patients (min, 4 min; max, 69 min).

This study has some limitations. Data were collected in routine clinical practice, so errors may have occurred in their reporting. We consider the estimated creatinine clearance as the covariate influencing tobramycin elimination, in accordance with the original model developed in children [17]. However, it would be interesting to evaluate other indices of renal function in future studies, such as other creatinine-based equations (e.g., CKD-EPI, Lund-Malmö), cystatin C-based equations, or serum cystatin C as performed elsewhere [28]. The achievement of the PK/PD objectives after dose adjustment was not evaluated because a second TDM during therapy was not routine practice in our center. The Cmax/MIC target was not based on measured MIC but on the CLSI breakpoint. Lower exposure may be adequate in the case of pathogens with a lower MIC. We did not consider a clinical endpoint of the tobramycin therapy, such as forced expiratory volume in one second (FEV) [29], because it was not performed routinely at home in our cohort. Only nephrotoxicity was considered in the safety assessment. Further clinical research with multiple efficacy and safety endpoints and a longer follow-up are necessary to confirm the value of tobramycin MIPD in patients with CF.

5. Conclusions

To conclude, in our experience in adult patients with CF, underexposure to tobramycin was frequently observed after empirical initial dosing. Implementation of an MIPD service provided by pharmacists to physicians resulted in significant increases in tobramycin doses without significant impact on renal function. Dosage adjustments were well-accepted by physicians. Further clinical evaluation is required to evaluate other potential benefits. TDM

alone is not sufficient for precision dosing of antibiotics. MIPD appears to be a promising step forward.

Author Contributions: Conceptualization, S.G.; methodology, J.R., V.T., R.G., L.B., S.C. (Sandrine Charles) and S.G.; software, J.R., V.T., R.G., L.B. and S.G.; validation, J.R. and S.G.; formal analysis, J.R. and S.G.; investigation, V.N., S.C. (Sabine Cohen), P.R., S.D., R.N.-J., I.D. and Q.R.; data curation, V.N., S.C. (Sabine Cohen), P.R., S.D., R.N.-J., I.D. and Q.R.; writing—original draft preparation, J.R. and S.G.; writing—review and editing, all authors; supervision, S.G.; project administration, J.R., S.C. (Sandrine Charles) and S.G. All authors have read and agreed to the published version of the manuscript.

Funding: This research received no external funding. It was performed as part of routine activity that is supported by Hospices Civils de Lyon and Université Lyon 1.

Institutional Review Board Statement: Ethical review and approval were waived for this study because it was an analysis of data collected in routine patient care.

Informed Consent Statement: Patient consent was waived because this was a non-interventional study with analysis of data collected in routine patient care.

Data Availability Statement: Data are available upon demand.

Conflicts of Interest: The authors declare no conflict of interest.

References

1. Klimova, B.; Kuca, K.; Novotny, M.; Maresova, P. Cystic Fibrosis Revisited—A Review. *Med. Chem.* **2017**, *13*, 102–109. [CrossRef] [PubMed]
2. Hauser, A.R.; Jain, M.; Bar-Meir, M.; McColley, S.A. Clinical significance of microbial infection and adaptation in cystic fibrosis. *Clin. Microbiol. Rev.* **2011**, *24*, 29–70. [CrossRef] [PubMed]
3. Smyth, A.R.; Bell, S.C.; Bojcin, S.; Bryon, M.; Duff, A.; Flume, P.; Kashirskaya, N.; Munck, A.; Ratjen, F.; Schwarzenberg, S.J.; et al. European Cystic Fibrosis Society Standards of Care: Best Practice guidelines. *J. Cyst. Fibros. Off. J. Eur. Cyst. Fibros. Soc.* **2014**, *13* (Suppl. S1), S23–S42. [CrossRef] [PubMed]
4. Germovsek, E.; Barker, C.I.; Sharland, M. What do I need to know about aminoglycoside antibiotics? *Arch. Dis. Child. Educ. Pract. Ed.* **2017**, *102*, 89–93. [CrossRef]
5. Prayle, A.; Watson, A.; Fortnum, H.; Smyth, A. Side effects of aminoglycosides on the kidney, ear and balance in cystic fibrosis. *Thorax* **2010**, *65*, 654–658. [CrossRef]
6. Beringer, P.M.; Vinks, A.A.T.M.M.; Jelliffe, R.W.; Shapiro, B. Pharmacokinetics of tobramycin in adults with cystic fibrosis: Implications for once-daily administration. *Antimicrob. Agents Chemother.* **2000**, *44*, 809–813. [CrossRef]
7. Castagnola, E.; Cangemi, G.; Mesini, A.; Castellani, C.; Martelli, A.; Cattaneo, D.; Mattioli, F. Pharmacokinetics and pharmacodynamics of antibiotics in cystic fibrosis: A narrative review. *Int. J. Antimicrob. Agents* **2021**, *58*, 106381. [CrossRef]
8. El Hassani, M.; Caissy, J.-A.; Marsot, A. Antibiotics in Adult Cystic Fibrosis Patients: A Review of Population Pharmacokinetic Analyses. *Clin. Pharmacokinet.* **2021**, *60*, 447–470. [CrossRef]
9. Darwich, A.S.; Ogungbenro, K.; Vinks, A.; Powell, J.R.; Reny, J.-L.; Marsousi, N.; Daali, Y.; Fairman, D.; Cook, J.; Lesko, L.J.; et al. Why Has Model-Informed Precision Dosing Not Yet Become Common Clinical Reality? Lessons From the Past and a Roadmap for the Future. *Clin. Pharmacol. Ther.* **2017**, *101*, 646–656. [CrossRef]
10. Wicha, S.G.; Märtson, A.; Nielsen, E.I.; Koch, B.C.; Friberg, L.E.; Alffenaar, J.; Minichmayr, I.K. From Therapeutic Drug Monitoring to Model-Informed Precision Dosing for Antibiotics. *Clin. Pharmacol. Ther.* **2021**, *109*, 928–941. [CrossRef]
11. Agence Française de Sécurité Sanitaire des Produits de Santé. Update on good use of injectable aminoglycosides, gentamycin, tobramycin, netilmycin, amikacin. Pharmacological properties, indications, dosage, and mode of administration, treatment monitoring. *Med. Mal. Infect.* **2012**, *42*, 301–308. [CrossRef]
12. Clinical & Laboratory Standards Institute. *Performance Standards for Antimicrobial Susceptibility Testing*, 32nd ed.; CLSI Supplement, 100; Wayne, P.A., Ed.; Clinical & Laboratory Standards Institute: Berwyn, PA, USA, 2022.
13. Zobell, J.T.; Young, D.C.; Waters, C.D.; Ampofo, K.; Stockmann, C.; Sherwin, C.M.; Spigarelli, M.G. Optimization of anti-pseudomonal antibiotics for cystic fibrosis pulmonary exacerbations: VI. Executive summary. *Pediatr. Pulmonol.* **2013**, *48*, 525–537. [CrossRef]
14. Flume, P.A.; Mogayzel, P.J., Jr.; Robinson, K.A.; Goss, C.H.; Rosenblatt, R.L.; Kuhn, R.J.; Marshall, B.C. The Clinical Practice Guidelines for Pulmonary Therapies Commit altee. Cystic fibrosis pulmonary guidelines: Treatment of pulmonary exacerbations. *Am. J. Respir. Crit. Care Med.* **2009**, *180*, 802–808. [CrossRef]
15. Michaud, M.; Michaud Peyrot, C. Réglementation de la recherche médicale en France. *Rev. Med. Interne* **2020**, *41*, 98–105. [CrossRef]

16. Neely, M.; Philippe, M.; Rushing, T.; Fu, X.; Van Guilder, M.; Bayard, D.; Schumitzky, A.; Bleyzac, N.; Goutelle, S. Accurately achieving target busulfan exposure in children and adolescents with very limited sampling and the bestdose software. *Ther. Drug Monit.* **2016**, *38*, 332–342. [CrossRef]
17. Praet, A.; Bourguignon, L.; Vetele, F.; Breant, V.; Genestet, C.; Dumitrescu, O.; Doleans-Jordheim, A.; Reix, P.; Goutelle, S. Population Pharmacokinetic Modeling and Dosing Simulations of Tobramycin in Pediatric Patients with Cystic Fibrosis. *Antimicrob. Agents Chemother.* **2021**, *65*, e00737-21. [CrossRef]
18. Praet, A.; Charles, S.; Wdowik, J.; Viviane, N.A.V.E.; Durupt, S.; Reynaud, Q.; Raphaële, N.J.; Durieu, I.; Philippe, R.E.I.X.; Bourguignon, L.; et al. Tobramycin Therapeutic Drug Monitoring in Adult patients with Cystic Fibrosis: Clinical-Based Empiric Dosing versus Model-Informed Precision Dosing. *Res. Sq.* 2022, *preprint*. [CrossRef]
19. Guilhaumou, R.; Benaboud, S.; Bennis, Y.; Dahyot-Fizelier, C.; Dailly, E.; Gandia, P.; Goutelle, S.; Lefeuvre, S.; Mongardon, N.; Roger, C.; et al. Optimization of the treatment with beta-lactam antibiotics in critically ill patients-guidelines from the French Society of Pharmacology and Therapeutics (Société Française de Pharmacologie et Thérapeutique-SFPT) and the French Society of Anaesthesia and Intensive Care Medicine (Société Française d'Anesthésie et Réanimation-SFAR). *Crit. Care* **2019**, *23*, 104. [CrossRef]
20. Cusumano, J.A.; Klinker, K.; Huttner, A.; Luther, M.K.; Roberts, J.A.; Laplante, K.L. Towards precision medicine: Therapeutic drug monitoring-guided dosing of vancomycin and β-lactam antibiotics to maximize effectiveness and minimize toxicity. *Am. J. Health Syst. Pharm. AJHP Off. J. Am. Soc. Health Syst. Pharm.* **2020**, *77*, 1104–1112. [CrossRef]
21. van Lent-Evers, N.A.E.M.; Mathôt, R.A.A.; Geus, W.P.; Van Hout, B.A.; Vinks, A. Impact of Goal-Oriented and Model-Based Clinical Pharmacokinetic Dosing of Aminoglycosides on Clinical Outcome: A Cost-Effectiveness Analysis. *Ther. Drug Monit.* **1999**, *21*, 63–73. [CrossRef]
22. Hewer, S.C.L.; Smyth, A.R.; Brown, M.; Jonets, A.P.; Hickey, H.; Kenna, D.; Ashby, D.; Thompson, A.; Williamson, P.R. Intravenous versus oral antibiotics for eradication of *Pseudomonas aeruginosa* in cystic fibrosis (TORPEDO-CF): A randomised controlled trial. *Lancet Respir. Med.* **2020**, *8*, 975–986. [CrossRef]
23. Rougier, F.; Claude, D.; Maurin, M.; Sedoglavic, A.; Ducher, M.; Corvaisier, S.; Jelliffe, R.; Maire, P. Aminoglycoside Nephrotoxicity: Modeling, Simulation, and Control. *Antimicrob. Agents Chemother.* **2003**, *47*, 1010–1016. [CrossRef]
24. Neely, M.; Jelliffe, R. Practical Therapeutic Drug Management in HIV-Infected Patients: Use of Population Pharmacokinetic Models Supplemented by Individualized Bayesian Dose Optimization. *J. Clin. Pharmacol.* **2008**, *48*, 1081–1091. [CrossRef]
25. Colin, P.J.; Eleveld, D.J.; Hart, A.; Thomson, A.H. Do Vancomycin Pharmacokinetics Differ Between Obese and Non-obese Patients? Comparison of a General-Purpose and Four Obesity-Specific Pharmacokinetic Models. *Ther. Drug Monit.* **2021**, *43*, 126–130. [CrossRef]
26. Goutelle, S.; Woillard, J.B.; Neely, M.; Yamada, W.; Bourguignon, L. Nonparametric Methods in Population Pharmacokinetics. *J. Clin. Pharmacol.* **2022**, *62*, 142–157. [CrossRef]
27. Goutelle, S.; Jay, L.; Boidin, C.; Cohen, S.; Bourguignon, L.; Bleyzac, N.; Wallet, F.; Vassal, O.; Friggeri, A. Pharmacokinetic/Pharmacodynamic Dosage Individualization of Cefepime in Critically Ill Patients: A Case Study. *Ther. Drug Monit.* **2021**, *43*, 451–454. [CrossRef]
28. Lu, J.-J.; Chen, M.; Lv, C.-L.; Zhang, R.; Lu, H.; Cheng, D.-H.; Tang, S.-Y.; Liu, T.-T. A population pharmacokinetics model for vancomycin dosage optimization based on serum cystatin C. *Eur. J. Drug Metab. Pharmacokinet.* **2020**, *45*, 535–546. [CrossRef]
29. Mouton, J.W.; Jacobs, N.; Tiddens, H.; Horrevorts, A.M. Pharmacodynamics of tobramycin in patients with cystic fibrosis. *Diagn Microbiol Infect. Dis.* **2005**, *52*, 123–127. [CrossRef]

pharmaceutics

MDPI

Review

Pharmacokinetic Boosting of Kinase Inhibitors

Niels Westra [1], Daan Touw [1,2], Marjolijn Lub-de Hooge [1], Jos Kosterink [1,3] and Thijs Oude Munnink [1,*]

[1] Department of Clinical Pharmacy and Pharmacology, University Medical Center Groningen, University of Groningen, 9713 GZ Groningen, The Netherlands
[2] Pharmaceutical Analysis, Groningen Research Institute of Pharmacy, University of Groningen, 9713 AV Groningen, The Netherlands
[3] PharmacoTherapy, Epidemiology & Economics, Groningen Research Institute of Pharmacy, University of Groningen, 9713 AV Groningen, The Netherlands
* Correspondence: t.h.oude.munnink@umcg.nl

Abstract: (1) Introduction: Pharmacokinetic boosting of kinase inhibitors can be a strategy to enhance drug exposure and to reduce dose and associated treatment costs. Most kinase inhibitors are predominantly metabolized by CYP3A4, enabling boosting using CYP3A4 inhibition. Kinase inhibitors with food enhanced absorption can be boosted using food optimized intake schedules. The aim of this narrative review is to provide answers to the following questions: Which different boosting strategies can be useful in boosting kinase inhibitors? Which kinase inhibitors are potential candidates for either CYP3A4 or food boosting? Which clinical studies on CYP3A4 or food boosting have been published or are ongoing? (2) Methods: PubMed was searched for boosting studies of kinase inhibitors. (3) Results/Discussion: This review describes 13 studies on exposure boosting of kinase inhibitors. Boosting strategies included cobicistat, ritonavir, itraconazole, ketoconazole, posaconazole, grapefruit juice and food. Clinical trial design for conducting pharmacokinetic boosting trials and risk management is discussed. (4) Conclusion: Pharmacokinetic boosting of kinase inhibitors is a promising, rapidly evolving and already partly proven strategy to increase drug exposure and to potentially reduce treatment costs. Therapeutic drug monitoring can be of added value in guiding boosted regimens.

Keywords: pharmacokinetic boosting; pharmacokinetic enhancement; ritonavir; cobicistat; kinase inhibitors; small molecule kinase inhibitors

Citation: Westra, N.; Touw, D.; Lub-de Hooge, M.; Kosterink, J.; Oude Munnink, T. Pharmacokinetic Boosting of Kinase Inhibitors. *Pharmaceutics* **2023**, *15*, 1149. https://doi.org/10.3390/pharmaceutics15041149

Academic Editors: Barna Vasarhelyi and Gellért Balázs Karvaly

Received: 28 February 2023
Revised: 21 March 2023
Accepted: 3 April 2023
Published: 5 April 2023

1. Introduction

Pharmacokinetic boosting, or pharmacokinetic enhancement, is a strategy to optimize the therapeutic properties of a drug [1]. The mechanisms for pharmacokinetic boosting can roughly be divided into four groups [1]: (1) inhibition of hepatic metabolizing enzymes, such as ritonavir inhibiting cytochrome p450 (CYP450); (2) inhibition of drug-specific enzymes, such as carbidopa-inhibiting DOPA decarboxylase; (3) inhibition of bacterial β-lactamase to enhance the antibiotic properties of β-lactam antibiotics, such as clavulanic acid-inhibiting β-lactamase; and (4) absorption enhancement with food.

The first described pharmacokinetic booster was probenecid. During World War II, there was a shortage of penicillin due to the increased demand for penicillin because of the many war casualties. To enable treating more patients with the limited available amount of penicillin, probenecid was used to increase penicillin exposure by decreasing the renal excretion of penicillin [2].

Strategies to enable treating more patients with the same amount of drug are not only of interest in situations of limited availability of drug supplies but can also be of value when drug availability is limited due to high costs. In 1989, the concomitant administration of ketoconazole and cyclosporin was investigated in renal transplant recipients to reduce the high costs associated with cyclosporin use [3]. Cyclosporin boosted with

ketoconazole resulted in a reduction of 77% in cyclosporin dosing, while maintaining the immunosuppressive effect of cyclosporin [3].

Pharmacokinetic boosting can be a strategy to enhance the pharmacokinetic profile of a drug. Ritonavir is a protease inhibitor, widely used in the treatment of human immunodeficiency virus (HIV) disease. The potent CYP450-inhibiting properties of ritonavir has led to the use of ritonavir as a pharmacokinetic booster of HIV-protease inhibitors in several HIV combination regimes [4]. In this setting, ritonavir results in a >50 fold increase in saquinavir plasma concentration, and better efficacy of saquinavir is accomplished when given concomitantly [5].

Healthcare costs have been rising worldwide, and the costs are projected to further increase at an annual rate of 3–6% [6]. In particular, newly developed drugs for the treatment of solid and hematologic malignancies are the chief contributors to these rising treatment costs [6,7]. In countries without universal healthcare insurance, the costs for drugs can become unaffordable for individual patients [6]. Pharmacokinetic boosting of expensive drugs can be a promising strategy to reduce rising treatment costs and to allow more patients to benefit from new effective treatments.

Pharmacokinetic boosting, furthermore, is of interest for anticancer drugs with low bioavailability [8–10]. In addition to pharmacokinetic boosting, exposure to anticancer drugs with low bioavailability can be increased by various changes to a formulation, such as lipid-based nanocarriers that increase bioavailability [10]. Novel anticancer drugs with better oral bioavailability have been successfully developed, such as cedazuridine/decitabine for the treatment of myeloid malignancies [11].

In the last two decades, many new kinase inhibitors and other oral targeted inhibitor drugs have been approved for treatment of malignant and auto-immune diseases. These often very expensive drugs can be attractive candidates for pharmacokinetic boosting since most are metabolized by CYP3A4 [12], and some have poor absorption that can be enhanced by food.

The aim of this narrative review is to provide answers to the following questions: (1) Which different boosting strategies can be useful in boosting kinase inhibitors? (2) Which kinase inhibitors are potential candidates for either CYP3A4 or food boosting? (3) Which clinical studies on CYP3A4 or food boosting have been published or are ongoing, and what are important lessons from these studies? Additionally, the benefits of boosting, the risks of boosting, clinical trial design and the role of therapeutic drug monitoring (TDM) in pharmacokinetic boosting are discussed.

2. Materials and Methods

The selection of potential boosting candidates was based on ATC code, as derived from the WHO ATC/DDD index [13]. Drugs with ATC code L01E, L01XK, L01XG, L01XJ, L01XK, L01XX, L04AA, L01XX52, L01XX59, L01XX62, L01XX73, L01XX77, L04AA29, L04AA32, L04AA37, L04AA44, L04AA46, L04AA49, L04AA56, L04AA59 and D11AH08 were selected to be profiled for pharmacokinetic boosting. This selection contains tyrosine kinase inhibitors, other kinase inhibitors and other oral targeted inhibitor drugs, which will collectively be described as kinase inhibitors for simplicity and recognizability. Parenterally administered drugs and drugs without FDA or EMA approval were excluded, resulting in 85 drugs to be profiled for either CYP3A4 boosting or food boosting. A QuickScan algorithm was used, followed by criteria score-based ranking (Figure 1 and Table 1). Relevant drug characteristics used for selecting candidates and the information in Tables 2–4 were retrieved from the Summary of Product Characteristics (SmPC), European Public Assessment Reports (EPAR) and UpToDate [14,15]. The known inhibitory effects of CYP3A4 inhibitors on the potential boosting candidate were retrieved from UpToDate interaction checker by entering the potential boosting candidate in combination with cobicistat [16]. To identify the kinase inhibitors used in the treatment of malignancies and auto-immune disease which are the most eligible candidates for pharmacokinetic boosting, we employed a systematic approach using predefined criteria. For CYP3A4 boosting, the target drug

needed to be a substrate for CYP3A4, excluding seven drugs. The remaining 78 drugs were systematically ranked based on criteria which are important for selecting potential boosting candidates. In the case where the boosting candidate forms active metabolites that contribute significantly to the pharmacological effect, the exposure of the active metabolites can be decreased by CYP3A4 boosting, making CYP3A4 boosting less rational. We defined three scores for the active metabolites criterium: 0—no active metabolites or unknown; 1—active metabolites with minor (<10%) contribution to effect; 2—active metabolites with major (>10%) contribution to effect. The second ranking criterium for selecting potential CYP3A4 boosting candidates is the already known effect of strong CYP3A4 inhibitors on the exposure of boosting candidates. This information is derived from drug–drug interaction studies. We defined four scores for the increase in exposure criterium: 0—>200% increase in AUC; 1—100–200% increase in AUC; 2—50–100 % increase in AUC; 5—<50% increase in AUC or unknown. Drugs with mg-based pricing or those for which only one strength of the drug is available are scored 0. Drugs with flat-based pricing for all available strengths are scored 1. As an exception to the aforementioned pricing scores, sonidegib was scored 1 because no dose reduction is possible with the one available strength of sonidegib. The therapeutic value of a drug was not taken into account; it was assumed that all kinase inhibitors have an equivalent therapeutic value.

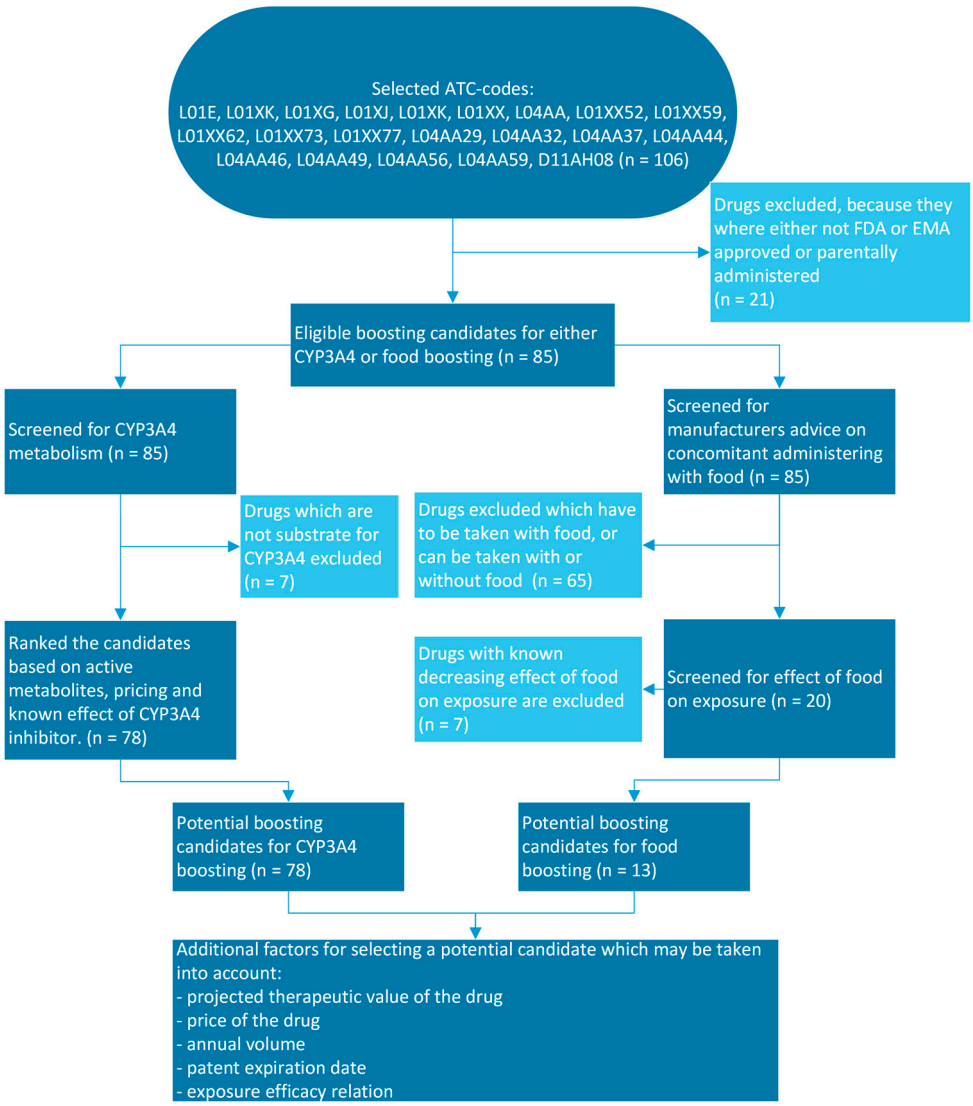

Figure 1. QuickScan algorithm for selecting either CYP3A4 or food boosting candidates.

Table 1. Scoring criteria of potential CYP3A4 boosting candidates.

Active Metabolites	Known Effect of CYP3A4 Inhibitor on AUC	Pricing of Different Drug Strengths
0—no active metabolites or unknown	0—>200% increase in AUC	0—mg-based pricing or one strength available
1—minor active metabolites (<10% responsible for efficacy)	1—100–200% increase in AUC	1—flat-based pricing for all available strengths
2—major active metabolites (>10% responsible for efficacy)	2—50–100% increase in AUC	
	5—<50% or unknown increase in AUC	

Table 2. Comparison of relevant drug properties of ritonavir and cobicistat. Relevant drug characteristics were retrieved from the Summary of Product Characteristics (SmPC), European Public Assessment Reports (EPAR) and UpToDate [14,15].

	Ritonavir	Cobicistat
Antiviral activity	Yes, HIV protease inhibitor; inhibits HIV-1 and HIV-2	No
Dosage as pharmacokinetic enhancer	100 mg or 200 mg; QD or BID	150 mg QD
Protein binding	99%	98%
Half-life	3–5 h	3–4 h
Distribution volume	20–40 L	Not known
Metabolized by	CYP3A4 and to lesser extent CYP2D6	CYP3A4 and to lesser extent CYP2D6
Inhibitor of	CYP3A4 (strong), CYP2D6 (minor), P-gp and OATP1B1	CYP3A4 (strong) CYP2D6 (minor), P-gp, BCRP, MATE1, OATP1B1, OATP1B3
Inducer of	CYP1A2, CYP2B6, CYP2C8, CYP2C9, CYP2C19, UGT	-
In vitro CYP3A4 inhibition duration	Irreversible	Irreversible

Table 3. Selection of potential CYP3A4 boosting candidates (n = 78). Drugs are ranked according to ranking score (low → high) and on alphabet within the same ranking score. Candidates with the lowest ranking score have the most potential for CYP3A4 boosting. Relevant drug characteristics were retrieved from the Summary of Product Characteristics (SmPC), European Public Assessment Reports (EPAR) and UpToDate [14,15].

Drug	Pricing of Different Strengths	Metabolism	Substrate of Transporters	Bioavailability	CYP3A4 Inhibitory Drug	Effect on AUC (Fold Change)	Effect on C_{max} (Fold Change)	Ranking Score
Adagrasib	One strength available	CYP3A4, however at steady state, adagrasib inhibits its own CYP3A4 metabolism, which allows CYP2C8, CYP1A2, CYP2B6, CYP2C9, and CYP2D6 to contribute to metabolism.	BCRP/ABCG2	-	Itraconazole	4	2.4	0
Bosutinib	Strength-based pricing	CYP3A4 to primarily inactive metabolites M2, M5 and M6	-	34% when administered with food	Ketoconazole	8.6	5.2	0
Cobimetinib	One strength available	CYP3A4	P-gp/ABCB1	46%	Itraconazole	6.7	3.2	0
Duvelisib	Strength-based pricing	CYP3A4	BCRP/ABCG2	42%	Ketoconazole	4	1.7	0
Encorafenib	One strength available	CYP3A4 and to a lesser extent by CYP2C19 and CYP2D6	P-gp/ABCB1	≥86% of the dose is absorbed	Posaconazole	3	1.7	0

Table 3. *Cont.*

Drug	Pricing of Different Strengths	Metabolism	Substrate of Transporters	Bioavailability	CYP3A4 Inhibitory Drug	Effect on AUC (Fold Change)	Effect on C_{max} (Fold Change)	Ranking Score
Fedratinib	One strength available	CYP3A4, CYP2C19, and flavin-containing monooxygenase 3 (FMO3)	OATP1B1/1B3 (SLCO1B1/1B3)	-	Ketoconazole	3.1–3.9	1.9	0
Lapatinib	One strength available	CYP3A4 and CYP3A5 and to a lesser extent by CYP2C19 and CYP2C8 to metabolites	BCRP/ABCG2 and P-gp/ ABCB1	-	Ketoconazole	3.6	2.1	0
Larotrectinib	Strength-based pricing	CYP3A4; forms a metabolite (activity unknown)	BCRP/ABCG2 and P-gp/ ABCB1	34%	Itraconazole	4.3	2.8	0
Pralsetinib	One strength available	CYP3A4 and to a lesser extent CYP2D6 and CYP1A2	BCRP/ABCG2 and P-gp/ ABCB1	-	Itraconazole	3.5	1.8	0
Zanubrutinib	One strength available	CYP3A4	-	-	Ketoconazole	3.8	2.6	0
Avacopan	One strength available	CYP3A4	-	-	Itraconazole	2.19	1.87	1
Avapritinib	Flat pricing	CYP3A4 and CYP3A5 and to lesser extent CYP2C9, which forms the metabolite M690	-	-	Itraconazole	7	-	1
Axitinib	Strength-based pricing	CYP3A4/5 and to a lesser extent CYP1A2, CYP2C19 and UGT1A1		58%	Ketoconazole	2.1	1.5	1
Brigatinib	Strength-based pricing	CYP2C8 and CYP3A4	BCRP/ABCG2 and P-gp/ ABCB1	-	Itraconazole	2.01	-	1
Ceritinib	One strength available	CYP3A4	P-gp/ABCB1	-	Ketoconazole	2.9	1.2	1
Crizotinib	Flat pricing	CYP3A4/5	P-gp/ABCB1	43%	Ketoconazole	3.2	1.7	1
Dasatinib	Strength-based pricing	CYP3A4, flavin-containing mono-oxygenase-3 (FOM-3) and UGT to an active metabolite (minor role in the efficacy)	-	-	Ketoconazole	4.8	3.6	1
Glasdegib	Strength-based pricing	CYP3A4 and to a lesser extent CYP2C8 and UGT1A9	BCRP/ABCG2	77%	Ketoconazole	2.4	1.4	1
Ibrutinib	Strength-based pricing	CYP3A and to a lesser extent CYP2D6 to form active metabolite PCI-45227(minor role in the efficacy)	-	2.9%	Ketoconazole	24	29	1
Ivosidenib	One strength available	CYP3A4 and to a lesser extent the N-dealkylation and hydrolytic pathways	P-gp/ABCB1	-	Itraconazole	2.7	No change	1
Nilotinib	Flat pricing	CYP3A4 to primarily inactive metabolites	P-gp/ABCB1	50%	Ketoconazole	3	1.8	1
Olaparib	One strength available	CYP3A4	P-gp/ABCB1	-	Itraconazole	2.7	1.4	1
Ribociclib	One strength available	CYP3A4 to metabolites M13, M4 and M1 (minor role in the efficacy)	-	-	Ritonavir	3.2	1.7	1
Selpercatinib	Strength-based pricing	CYP3A4	BCRP/ABCG2	73%	Itraconazole	2.3	1.3	1
Venetoclax	Strength-based pricing	CYP3A to form the major metabolite M27 (BCL-2 inhibitory activity 58-fold lower)	BCRP/ABCG2 and P-gp/ ABCB1	-	Ritonavir	6.1–8.1	2.3–2.4	1
Acalabrutinib	One strength available	CYP3A4 enzymes and to a lesser extent glutathione conjugation and amide hydrolysis to form active metabolite ACP-5862	BCRP/ABCG2 and P-gp/ ABCB1	25%	Itraconazole	5.1	3.7–3.9	2
Dabrafenib	Strength-based pricing	CYP2C8 and CYP3A4 to form active metabolite hydroxy-dabrafenib	BCRP/ABCG2 and P-gp/ ABCB1	95%	Ketoconazole	1.71	-	2
Erlotinib	Strength-based pricing	CYP3A4 and to a lesser extent CYP1A1, CYP1A2, and CYP1C to form metabolites (activity unknown)	-	60% without food, 100% with food	Ketoconazole	1.69	1.52	2

Table 3. *Cont.*

Drug	Pricing of Different Strengths	Metabolism	Substrate of Transporters	Bioavailability	CYP3A4 Inhibitory Drug	Effect on AUC (Fold Change)	Effect on C_{max} (Fold Change)	Ranking Score
Everolimus	Flat pricing	CYP3A4 and forms six metabolites with minor activity	P-gp/ABCB1	30%	Ketoconazole	15	3.9	2
Gefitinib	One strength available	CYP3A4 and to a lesser extent CYP2D6. Forms metabolites	BCRP/ABCG2	60%	Itraconazole	1.16–1.78	1.32–1.51	2
Gilteritinib	One strength available	CYP3A4 to form active metabolites M17, M16 and M10 (minor role in the efficacy)	P-gp/ABCB1	-	Itraconazole	2.2	1.2	2
Infigratinib	Strength-based pricing	CYP3A4 and to a lesser extent FMO3 to form active metabolites BHS697 and CQM157	BCRP/ABCG2 and P-gp/ABCB1	-	Itraconazole	7.22	2.64	2
Mobocertinib	One strength available	CYP3A to form active metabolites AP32960 and AP32914	P-gp/ABCB1	37%	Itraconazole	6.3	2.9	2
Neratinib	One strength available	CYP3A4 and flavin-containing monooxygenase to form active metabolites M3, M6, M7, and M11	P-gp/ABCB1	-	Ketoconazole	4.8	3.2	2
Pacritinib	One strength available	CYP3A4 and forms the 2 major metabolites M1 and M2 (activity unknown)	-	-	Clarithromycin	1.8	1.3	2
Pazopanib	One strength available	CYP3A4 and P-gp/ABCB1 and to a lesser extent by CYP1A2, CYP2C8 and BCRP/ABCG2	BCRP/ABCG2 and P-gp/ABCB1	-	Ketoconazole	1.66	1.45	2
Pexidartinib	One strength available	CYP3A4 and glucuronidation via UGT1A4 to form an inactive metabolite	-	-	Itraconazole	1.73	1.48	2
Sonidegib	One strength available	CYP3A4	-	<10%	Ketoconazole	2.2	1.5	2
Tofacitinib	Flat pricing	CYP3A4 and CYP2C19 to form inactive metabolites	-	74%	Itraconazole	2.04	1.15	2
Upadacitinib	Strength-based pricing	CYP3A4	-	-	Ketoconazole	1.75	1.7	2
Entrectinib	Flat pricing	CYP3A4 to form the active metabolite M5	-	-	Itraconazole	6	1.7	3
Idelalisib	Flat pricing	Aldehyde oxidase and CYP3A, which forms major metabolite GS-563117, to a lesser extent UGT1A4	BCRP/ABCG2 and P-gp/ABCB1	-	Ketoconazole	1.8	No change	3
Nintedanib	Flat pricing	Hydrolytic cleavage by esterases to inactive metabolite BIBF 1202, which is further UGT 1A1, UGT 1A7, UGT 1A8, and UGT 1A10 to BIBF 1202 glucuronide, and to a lesser extent CYP3A4	OCT1 and P-gp/ABCB1	5%	Ketoconazole	1.6	1.8	3
Palbociclib	Flat pricing	CYP3A4 and SULT2A1	-	46%	Itraconazole	1.87	1.34	3
Pemigatinib	Flat pricing	CYP3A4	BCRP/ABCG2 and P-gp/ABCB1	-	Itraconazole	1.88	1.17	3
Ponatinib	Flat pricing	CYP3A4 and to a lesser extent CYP2C8, CYP2D6, and CYP3A5	BCRP/ABCG2 and P-gp/ABCB1	-	Ketoconazole	1.78	1.47	3
Ripretinib	One strength available	CYP3A4 and to a lesser extent CYP2C8 and CYP2D6 to form active metabolite DP-5439(activity unknown)	BCRP/ABCG2 and P-gp/ABCB1	-	Itraconazole	1.99	1.36	3
Abemaciclib	Flat pricing	CYP3A4 to form active metabolites M2, M20, M18 and M1	BCRP/ABCG2 and P-gp/ABCB1	45%	Clarithromycin	2.5	-	4
Midostaurin	One strength available	CYP3A4 to form active metabolites CGP62221 and CGP52421	-	-	Ketoconazole	10.4	1.8	4
Sunitinib	Strength-based pricing	CYP3A4 to form active metabolite SU12662	-	-	Ketoconazole	1.51	1.49	4
Apremilast	One strength available	CYP3A4 and to a lesser extent CYP1A2 and CYP2A6	P-gp/ABCB1	73%	-	-	-	5
Baricitinib	Strength-based pricing	CYP3A4	BCRP/ABCG2 and P-gp/ABCB1	80%	-	-	-	5

Table 3. *Cont.*

Drug	Pricing of Different Strengths	Metabolism	Substrate of Transporters	Bioavailability	CYP3A4 Inhibitory Drug	Effect on AUC (Fold Change)	Effect on C_{max} (Fold Change)	Ranking Score
Erdafitinib	Strength-based pricing	CYP2C9 and CYP3A4	P-gp/ABCB1		Itraconazole	1.34	No change	5
Lorlatinib	Strength-based pricing	CYP3A4 and UGT1A4 and to a lesser extent CYP2C8, CYP2C19, CYP3A5 and UGT1A3	-	81%	Itraconazole	1.42	1.24	5
Selumetinib	Strength-based pricing	CYP3A4 and to a lesser extent BCRP/ABCG2, CYP1A2, CYP2A6, CYP2C19, CYP2C9, CYP2E1, CYP3A4, P-glycoprotein/ABCB1, UGT1A1 and UGT1A3	BCRP/ABCG2 and P-gp/ABCB1	62%	Itraconazole	1.49	1.19	5
Sotorasib	One strength available	CYP3A4, CYP3A5 and CYP2C8	-	-	-	-	-	5
Tucatinib	Strength-based pricing	CYP2C8 and to a lesser extent CYP3A	BCRP/ABCG2	-	-	-	-	5
Vemurafenib	One strength available	BCRP/ABCG2 and CYP3A4 and to a lesser extent P-gp/ABCB1	BCRP/ABCG2 and P-gp/ABCB1	64%	Itraconazole	1.4	1.4	5
Ruxolitinib	Flat pricing	CYP3A4 and to lesser extent CYP2C9 to form active metabolites	-	-	Ketoconazole	1.91	1.33	5
Alpelisib	Flat pricing	Chemical and enzymatic hydrolysis to form its metabolite and to a lesser extent CYP3A4	BCRP/ABCG2	-	-	-	-	6
Asciminib	Flat pricing	CYP3A4, UGT2B7 and UGT2B17	BCRP/ABCG2 and P-gp/ABCB1	-	Clarithromycin	1.36	1.19	6
Cabozantinib	Flat pricing	CYP3A4	-	-	Ketoconazole	1.36	-	6
Capmatinib	Flat pricing	CYP3A4 and aldehyde oxidase	P-gp/ABCB1	>70%	Itraconazole	1.42	No change	6
Enasidenib	Flat pricing	CYP1A2, CYP2B6, CYP2C8, CYP2C9, CYP2C19, CYP2D6, CYP3A4, UGT1A1, UGT1A3, UGT1A4, UGT1A9, UGT2B7 and UGT2B15	-	57%	-	-	-	6
Futibatinib	unknown	CYP3A, and to a lesser extent CYP2C9 and CYP2D6	BCRP/ABCG2 and P-gp/ABCB1	-	Itraconazole	1.41	1.51	6
Ixazomib	Flat pricing	CYP3A4, CYP1A2, CYP2B6, CYP2C8, CYP2D6, CYP2C19 and CYP2C9	P-gp/ABCB1	58%	-	-	-	6
Lenvatinib	Flat pricing	CYP3A4 and aldehyde oxidase	BCRP/ABCG2 and P-gp/ABCB1	-	-	-	-	6
Rucaparib	Flat pricing	CYP2D6 and to a lesser extent CYP1A2 and CYP3A4	BCRP/ABCG2 and P-gp/ABCB1	36%	-	-	-	6
Tepotinib	One strength available	CYP3A4 and CYP2C8 to form an active metabolite	P-gp/ABCB1	71.6%	-	-	-	6
Tivozanib	Flat pricing	CYP3A4	-	-	Ketoconazole	1.12	-	6
Alectinib	One strength available	CYP3A4 to form active metabolite M4	-	37%	-	-	-	7
Imatinib	Strength-based pricing	CYP3A4 and to a lesser extent CYP1A2, CYP2D6, CYP2C9 and CYP2C19 to form active metabolite CGP74588	OCT1 and P-gp/ABCB1	98%	Ketoconazole	1.4	1.26	7
Regorafenib	One strength available	CYP3A4 and UGT1A9 to form active metabolites M2 and M5	-	-	Ketoconazole	1.33	-	7
Sorafenib	One strength available	CYP3A4 and UGT1A9 to form an active metabolite	-	38–49%	Itraconazole	No change	No change	7
Vandetanib	Strength-based pricing	CYP3A4 to form active metabolites N-desmethyl vandetanib and vandetanib-N-oxide	-	-	Itraconazole	1.09	No change	7

Table 3. *Cont.*

Drug	Pricing of Different Strengths	Metabolism	Substrate of Transporters	Bioavailability	CYP3A4 Inhibitory Drug	Effect on AUC (Fold Change)	Effect on C_{max} (Fold Change)	Ranking Score
Abrocitinib	Flat pricing	CYP2C19 and to a lesser extent CYP2C9, CYP3A4 and CYP2B6 to form active metabolites 3-hydroxypropyl abrocitinib and 2-hydroxypropyl abrocitinib	OAT1/3	60%	-	-	-	8
Dacomitinib	Flat pricing	Oxidation and glutathione conjugation and by CYP2D6 and CYP3A4 to form active metabolite O-desmethyl dacomitinib	BCRP/ABCG2	80%	-	-	-	8
Osimertinib	Flat pricing	CYP3A4 to form active metabolites Z7550 and AZ5104	BCRP/ABCG2 and P-gp/ ABCB1		Itraconazole	1.24	.8	8

Table 4. Final selection of potential food boosting candidates (n = 13). Relevant drug characteristics were retrieved from the Summary of Product Characteristics (SmPC), European Public Assessment Reports (EPAR) and UpToDate [14,15].

Drug	Pricing of Different Strengths	Bioavailability	Food Effect
Avapritinib	Flat pricing	-	AUC and C_{max} increased 1.29 and 1.59-fold, respectively, when administered with a high-fat, high-calorie meal
Cabozantinib	Flat pricing	-	AUC and C_{max} increased 1.57 and 1.41-fold, respectively, when administered with a high-fat meal
Erlotinib	Strength-based pricing	60% without food	Absorption 60% in fasted state, food increases absorption to 100%
Ibrutinib	Strength-based pricing	2.9%	AUC and C_{max} increased two-fold and two- to four-fold, respectively, when administered with a high-fat, high-calorie meal
Infigratinib	Strength-based pricing	-	AUC and C_{max} increased 1.8- to 2.2-fold and 1.6- to 1.8-fold, respectively, when administered with a high-fat, high-calorie meal
Ivosidenib	One strength available	-	AUC and C_{max} increased 1.24 and 1.98-fold, respectively, when administered with a high-fat meal
Lapatinib	One strength available	-	AUC increased three- to four-fold when administered with food
Nilotinib	Flat pricing	50%	Bioavailability increased 1.82-fold when administered 30 min after a high-fat meal
Pazopanib	One strength available	-	AUC increased two-fold when administered with a high-fat or low-fat meal
Pexidartinib	One strength available	-	AUC and C_{max} increased two-fold when administered with a high-fat meal
Pralsetinib	One strength available	-	AUC and C_{max} increased 2.22 and 2.04-fold, respectively, when administered with a high-fat meal
Sonidegib	One strength available	<10%	AUC increased seven- to eight-fold when administered with a high-fat meal
Sotorasib	One strength available	-	AUC increased 1.25-fold when administered with a high-fat meal

Kinase inhibitors that are potential candidates for food boosting have been selected using a similar approach. For food boosting, the manufacturer's label administration recommendation must be to 'take without food' or must state that some specific foods cannot be taken in combination with the target drug. Drugs where food has a decreasing

effect on the exposure of the target drug are excluded. This QuickScan algorithm for selecting CYP3A4 and/or food boosting candidate is shown in Figure 1.

The PubMed database was used for reviewing available publications. For publications about CYP3A4 boosting, we used the following search query in PubMed: (abemaciclib OR abrocitinib OR acalabrutinib OR adagrasib OR afatinib OR alectinib OR alpelisib OR apremilast OR asciminib OR avacopan OR avapritinib OR axitinib OR baricitinib OR binimetinib OR bosutinib OR brigatinib OR cabozantinib OR capmatinib OR ceritinib OR cobimetinib OR crizotinib OR dabrafenib OR dacomitinib OR dasatinib OR deucravacitinib OR duvelisib OR enasidenib OR encorafenib OR entrectinib OR erdafitinib OR erlotinib OR everolimus OR fedratinib OR futibatinib OR gefitinib OR gilteritinib OR glasdegib OR ibrutinib OR idelalisib OR imatinib OR infigratinib OR ivosidenib OR ixazomib OR lapatinib OR larotrectinib OR lenvatinib OR lorlatinib OR midostaurin OR mobocertinib OR neratinib OR nilotinib OR nintedanib OR niraparib OR olaparib OR osimertinib OR pacritinib OR palbociclib OR pazopanib OR pemigatinib OR pexidartinib OR ponatinib OR pralsetinib OR regorafenib OR ribociclib OR ripretinib OR rucaparib OR ruxolitinib OR selpercatinib OR selumetinib OR sonidegib OR sorafenib OR sotorasib OR sunitinib OR talazoparib OR tepotinib OR tivozanib OR tofacitinib OR trametinib OR tucatinib OR upadacitinib OR vandetanib OR vemurafenib OR venetoclax OR vismodegib OR zanubrutinib) AND (clarithromycin OR cobicistat OR erythromycin OR itraconazole OR ketoconazole OR posaconazole OR ritonavir OR voriconazole OR grapefruit juice).

For publications about food boosting, the following search query was used in PubMed: (Avapritinib OR Cabozantinib OR Erlotinib OR Ibrutinib OR Infigratinib OR Ivosidenib OR Lapatinib OR Nilotinib OR Pazopanib OR Pexidartinib OR Pralsetinib OR Sonidegib OR Sotorasib) AND (food[Title] OR meal[Title] OR low-fat[Title] OR moderate-fat[Title] OR high-fat[Title] OR fasted[Title]).

For ongoing boosting trials, ClinicalTrials.gov was searched with the search terms 'Oncology' and 'CYP3A4' [17].

3. Results

3.1. Pharmacokinetic Boosting Strategies Potentially Useful for Kinase Inhibitors

The scope of this review focuses on pharmacokinetic boosting using inhibition of hepatic metabolic enzymes, in particular CYP3A4, and pharmacokinetic enhancement with food.

Metabolism by CYP450 is phase I metabolism that primarily produces hydrophilic structures, which are substrates for phase II metabolism and cleared more easily by the liver, kidney and small intestine [18]. CYP450 is predominantly expressed in the liver but can also be expressed in the kidney, small intestine, lung, brain and can even be found in certain tumor tissues [19,20]. CYP3A4 plays an important role in the bioavailability and exposure of its substrate drugs and is the major CYP enzyme. Approximately 50% of drugs are metabolized by CYP3A4 due to its broad substrate specificity. CYP3A4 activity has inter- and intra-patient variability, which can lead to a variable drug response within and between patients [21]. Inter- and intra-patient variability of CYP3A4 activity can have genetic and epigenetic causes and can also be affected by CYP3A4 induction or inhibition [19,22]. CYP3A5 is another important CYP enzyme, which has overlapping but not identical specificity of substrates with CYP3A4. CYP3A5 is predominantly expressed in the kidneys and lungs and can also be expressed in the liver and intestine. Genetic polymorphisms of CYP3A5 can vary greatly between different ethnic groups, with most patients being CYP3A5 non-expressors [19,23].

Inhibiting CYP3A4 metabolism can potentially lead to an increased exposure of CYP3A4 substrates. To boost the exposure of drugs which are metabolized by CYP3A4, the pharmacokinetic booster drug has to be a strong CYP3A4 inhibitor to effectively boost exposure of the substrate. Examples of strong CYP3A4 inhibitors are clarithromycin, erythromycin, ritonavir, cobicistat, itraconazole, ketoconazole, posaconazole and voriconazole [24].

Several HIV antiretroviral drugs have poor exposure and are metabolized by CYP3A. Atazanavir, darunavir, elvitegravir and lopinavir are HIV antiretroviral drugs boosted by

ritonavir or cobicistat to enhance their pharmacokinetic properties. For example, cobicistat enhances the systemic exposure of elvitegravir in the combination elvitegravir/cobicistat/emtricitabine/tenofovirdisoproxil, allowing for a once daily dosing of this single tablet regimen [14]. A more recent example of a similar boosting strategy used in another disease is ritonavir boosting of the SARS-CoV-2 inhibitor nirmatrelvir. When nirmatrelvir is administered alone, it has a $T_{1/2}$ of approximately 2 h, for which it is challenging to maintain the desired plasma concentration of several fold over the in vitro 90% effective concentration. When concomitantly administered with ritonavir, nirmatrelvir has a $T_{1/2}$ of approximately seven hours and an eight-fold increase in exposure, thus enabling a BID dosing regimen [25]. Because boosting strategies can increase the dosing interval and decrease the overall dosage of the substrate drug, boosting can also have an impact on adherence and pill burden [26]. The most widely used agents for CYP3A4 boosting are the pharmacokinetic enhancers ritonavir and cobicistat [4]. Ritonavir and cobicistat are both strong inhibitors of CYP3A4 and can therefore increase the exposure of drugs predominantly metabolized by CYP3A4.

Ritonavir, a HIV protease inhibitor, is an inhibitor of CYP3A4, CYP2D6 and the transporter P-glycoprotein (P-gp), OATP1B1 and an inductor of CYP1A2, CYP2B6, CYP2C8, CYP2C9, CYP2C19 and UGT [14,27]. Ritonavir irreversibly inhibits CYP3A4 [19]. Ritonavir, when used as a pharmacokinetic booster, is dosed 100–400 mg daily. The boosting dose of ritonavir is considered as low-dose ritonavir since therapeutic doses of ritonavir for HIV are with 600 mg BID much higher [26]. Ritonavir has a protein binding of 99%, half-life ($T_{1/2}$) of three to five hours and a distribution volume (Vd) of 20–40 L [14].

Cobicistat was initially developed as an improved version of ritonavir to better facilitate coformulation with other drugs in one tablet. This was possible because cobicistat has a higher water solubility compared to ritonavir [28]. Cobicistat is a structural analogue of ritonavir, but without antiretroviral activity [28]. Cobicistat is a strong CYP3A4 inhibitor and a weak CYP2D6 inhibitor, and furthermore inhibits P-gp, breast cancer resistance protein (BCRP), MATE1, OATP1B1 and OATP1B3. Cobicistat irreversibly inhibits CYP3A4 [29]. The cobicistat label dose is 150 mg once daily. Cobicistat has a protein binding of 98%, $T_{1/2}$ of three to four hours and is known to inhibit renal tubular secretion of creatinine, without affecting the glomerular filtration rate (GFR), which can lead to a slight decrease in the estimated creatinine clearance (CL_{cr}) [30]. A comparative overview of ritonavir and cobicistat is presented in Table 2 [14].

Cobicistat and low-dose ritonavir have good pharmacological characteristics for pharmacokinetic boosting of kinase inhibitors. Other strong CYP3A4 inhibitors such as clarithromycin, erythromycin, itraconazole, ketoconazole, posaconazole and voriconazole can also be used as a pharmacokinetic booster, but they have the disadvantage of pharmacological activity and adverse events and can be more expensive. Ketoconazole can result in QT-interval prolongation, and itraconazole is associated with liver toxicity [14]. This makes pharmacologically active CYP3A4 inhibitors less ideal to be used as pharmacokinetic boosters. Cancer patients at risk for invasive fungal disease, however, can benefit from antifungal prophylaxis. In these patients, the antifungal CYP3A4 inhibitor can serve as a two-edged sword combining pharmacokinetic booster and antifungal prophylaxis.

Food is known for its ability to alter the pharmacokinetic properties of a drug [31]. Notable examples are grapefruit juice, Coca-Cola, St. John's wort and different fasting states. Because grapefruit juice is an inhibitor of CYP3A4, it can potentially boost drugs in a similar manner to cobicistat and ritonavir [32]. Cola is known for its ability to enhance the bioavailability of drugs where low gastric pH is important for the absorption of the drug, especially when the drug is concomitantly given with a proton-pump inhibitor [33]. Different fasting states, such as low-fat meals, moderate-fat meals and high-fat meals, can have effects on the C_{max} and AUC of kinase inhibitors [32]. For the purpose of pharmacokinetic boosting, concomitant intake of certain kinase inhibitors with a high-fat meal can be considered.

3.2. Pharmacological Profiling of Candidate Kinase Inhibitors Suitable for Pharmacokinetic CYP3A4 Boosting

The ranking criteria were applied to the selected 78 CYP3A4 boosting candidates and resulted in 10 candidates with score 0 (most attractive candidates); 15 candidates with score 1; 15 candidates with score 2; 7 candidates with score 3; 3 candidates with score 4; 9 candidates with score 5; 11 candidates with score 6; 5 candidates with score 7; and 3 candidates with score 8 (least attractive candidates); see Table 3.

3.3. Pharmacological Profiling of Candidate Kinase Inhibitors Suitable for Pharmacokinetic Food Boosting

For food boosting candidates, the manufacturer's label administration recommendation must be to 'take without food' or must state that specific foods that cannot be taken in combination with the target drug. Based on this selection criterium, 65 drugs were excluded. Furthermore, drugs where food has a decreasing effect on the exposure of the target drug were excluded (n = 7). The 13 remaining drugs are potential candidates for food boosting (Table 4).

3.4. Clinical Evidence and Experience with Pharmacokinetic Boosting of Kinase Inhibitors

3.4.1. Axitinib Boosted with Cobicistat

In a case report, axitinib exposure was boosted by cobicistat [34]. A 54-year-old male, who was diagnosed with metastatic renal cell carcinoma, was previously treated with sunitinib and subsequently everolimus + pazopanib. At disease progression, the patient was switched to axitinib 5 mg BID as a last treatment option. The axitinib dose was escalated after two weeks to 10 mg BID because no serious toxicity was observed. The axitinib C_{min} was measured and was 1.4 microg/L, which is below the reported efficacy threshold of >5 microg/L [35]. Co-medication was screened for drug–drug interactions, and none were found. Screening of CYP450 polymorphisms showed CYP3A4 (*1A/*1B) polymorphism. Axitinib exposure was first boosted by grapefruit juice to inhibit intestinal CYP3A4 metabolism; however, no significant increase in axitinib exposure was seen. Grapefruit juice was subsequently switched to cobicistat 150 mg BID to boost axitinib exposure. After four weeks of axitinib 10 mg BID and cobicistat 150 mg BID, C_{2h} increased by a factor of four, and blood pressure started to slightly increase, but axitinib C_{min} was still below the >5 microg/L threshold. The axitinib and cobicistat dose was further escalated to 10 mg QID and 150 mg QID, respectively. The CT scan showed a decrease in metastasis size, no ascites drainage was needed, and albumin and hemoglobin returned to normal values, which indicates tumor response. After 15 months of ongoing response to treatment with axitinib 10 mg QID boosted by cobicistat 150 mg QID, progressive disease was detected. The patient died two months later as a result of progressive disease. The effect of CYP3A4 (*1A/*1B) polymorphism on the drug exposure of axitinib is unclear. C_{min} of pazopanib and sunitinib, by which the patient was treated initially, were also both below normal values, indicating that the patient had low exposure of pazopanib, sunitinib and axitinib. Because pazopanib, sunitinib and axitinib were all below normal values, the CYP3A4 activity can be a factor explaining the low exposure of these drugs. However, if this is the result of the CYP3A4 (*1A/*1B) polymorphism remains unclear. Based on the observed increase in axitinib concentrations, the authors conclude that boosting axitinib with cobicistat can be a promising and cost-effective strategy for patients with sub-optimal axitinib exposure.

3.4.2. Crizotinib Boosted with Cobicistat

Cobicistat-boosted crizotinib was evaluated in a phase I study in non-small cell lung cancer patients with low crizotinib exposure [36]. Crizotinib has a high interindividual variability of $C_{min,ss}$, which is associated with concentration-dependent variability in overall response rate (ORR). In the quartile with the lowest $C_{min,ss}$, the ORR is 24–47%; in the quartile with the highest $C_{min,ss}$, the ORR is 60–75%. Patients in the lower quartile versus the remaining three quartiles are associated with a higher hazard ratio of 3.2 [37]. The study

hypothesis was that patients in the lower quartile for $C_{min,ss}$ could have a better outcome when crizotinib exposure is boosted with cobicistat. Patients who received a minimum of 14 days of standard care with crizotinib and had a $C_{min,ss} \leq 310$ ng/mL were eligible. Only one patient was included because the study was prematurely terminated for ethical reasons after approval of more potent second-generation drugs. Before cobicistat 150 mg QD was added to the patient using crizotinib, blood samples for pharmacokinetic analysis were drawn. $C_{min,ss}$ was measured seven days after concurrent treatment of cobicistat with crizotinib. After 14 days of concurrent treatment of cobicistat with crizotinib, blood samples for pharmacokinetic analysis were drawn. The $AUC_{0–12h}$ and $C_{min,ss}$ increased by 78% and 164%, respectively, when crizotinib was boosted by cobicistat. No serious adverse events (AEs) were observed. The authors conclude that cobicistat can be a promising and non-expensive strategy to increase crizotinib exposure and suggest that this strategy might also be of value for other kinase inhibitors.

3.4.3. Erlotinib Boosted with Ritonavir

A phase I open-label crossover study was performed to evaluate the feasibility of erlotinib exposure boosting by ritonavir and thereby reducing the erlotinib dose to achieve cost savings [38]. Non-small cell lung cancer patients who received erlotinib 150 mg QD for a minimum of eight days were eligible for inclusion. Nine patients were included for the primary analysis of the study. After a minimum of eight days of treatment with erlotinib 150 mg QD, blood samples for pharmacokinetic analysis were drawn. The erlotinib dose was subsequently reduced to 75 mg QD, and patients were treated for seven days with the reduced dose. After these seven days, ritonavir 200 mg QD was added to erlotinib 75 mg QD, and patients were treated for seven days. Subsequently, blood samples were drawn for pharmacokinetic analysis, and patients were switched back to standard of care erlotinib 150 mg QD. The geometric mean ratio (GMR) of erlotinib 150 mg QD compared to erlotinib 75 mg + ritonavir 200 mg QD for $AUC_{0–24h}$, C_{max} and C_{min} were 0.99 (CI 95% 0.58–1.69, $p = 0.545$), 0.91 (CI 95% 0.55–1.49, $p = 0.500$) and 1.06 (CI 95% 0.59–1.93, $p = 0.150$), respectively. A statistically significant decrease in active metabolites OSI-413 and OSI-420 was observed. No grade ≥ 3 AEs were reported. The coefficient of variability (CV%) was 58–162% for erlotinib (+metabolites) and was 86–443% for ritonavir-boosted erlotinib (+metabolites). The authors expected that the CV% for erlotinib + ritonavir would be lower compared to erlotinib alone. The higher CV% for erlotinib + ritonavir could be the result of a shift in erlotinib metabolism. When erlotinib + ritonavir are concurrently administered, the main metabolism route shifts from CYP3A4 to CYP1A2 (and other isoforms), because ritonavir strongly inhibits the major CYP3A4 metabolism route. CYP1A2 expression is known to differ between patients and thus can be a factor explaining the increased CV%. Firm conclusions about the increased CV% are, however, difficult to be drawn because of the limited number of patients included in the study. The authors conclude that pharmacokinetic exposure of erlotinib 150 mg QD compared to erlotinib 75 mg QD + ritonavir 200 mg QD is equivalent, and erlotinib boosting can be a strategy to reduce an erlotinib dose by 50% and thus save treatment costs.

3.4.4. Ibrutinib Boosted with Itraconazole

In a randomized placebo-controlled crossover study with healthy volunteers, the boosting effect of itraconazole on ibrutinib exposure was evaluated [39]. The aim was to reduce the high interindividual variability of ibrutinib and to reduce treatment costs. Participants ($n = 11$) were randomly assigned to either the cohort ibrutinib 15 mg + itraconazole or ibrutinib 140 mg + placebo. Subjects were given itraconazole 200 mg BID or placebo BID on day 1, and on days 2–4 itraconazole 200 mg QD or placebo QD. On day 3, subjects who received placebo were given 140 mg ibrutinib, and subjects who received itraconazole received ibrutinib 15 mg. After a washout period of four weeks, subjects were enrolled in the crossover cohort. Ibrutinib 15 mg + itraconazole had a similar exposure when compared to ibrutinib 140 mg + placebo; the GMR of $AUC_{0-\infty}$ and C_{max} was 1.07

(CI 90% 0.77–1.49; p = 0.719) and 0.94 (CI 90% 0.68–1.30, p = 0.727), respectively. The geometric CVs of $AUC_{0-\infty}$ and C_{max} for ibrutinib 15 mg boosted with itraconazole were 0.55 and 0.53, respectively, and for ibrutinib 140 mg + placebo 1.04 and 0.99, respectively, indicating reduced interindividual variation for boosted ibrutinib. According to the manufacturer's dose recommendation when ibrutinib is concomitantly administered with a strong CYP3A4 inhibitor, the advice is to adjust the dose from 420 mg or 560 mg to 140 mg. However, the results in this study suggest a dose reduction of 90%. The authors conclude that ibrutinib boosting with itraconazole reduces interindividual variability and increases ibrutinib exposure and this enables improved dosing accuracy while achieving 90% cost savings. Annual cost savings with boosted ibrutinib in the United States are projected to be more than $10,000 per patient.

3.4.5. Imatinib Boosted with Grapefruit Juice

In an open-label, non-randomized, within-group crossover study, imatinib was boosted with grapefruit juice to ascertain if dose reduction of imatinib is feasible to reduce treatment costs [40]. Four patients with chronic myeloid leukemia (CML) who were treated with imatinib 400 mg QD for more than six months were eligible for inclusion. Blood samples for pharmacokinetic analysis were drawn when patients were using imatinib 400 mg QD. After two to three months, 250 mL Tropicana® grapefruit juice QD was added to imatinib 400 mg QD and administered for seven consecutive days. After these seven days of concurrent treatment with grapefruit juice and imatinib, blood samples for pharmacokinetic analysis were drawn. The median C_{min} was 1080 ng/mL (range: 1060–1360 ng/mL) and 1102 ng/mL (range: 772–1450 ng/mL) for imatinib 400 mg and imatinib 400 mg in combination with grapefruit juice, respectively. The median C_{max} was 2495 ng/mL (range: 2380–2680 ng/mL) and 2455 ng/mL (range: 1870–2750 ng/mL) for imatinib 400 mg and imatinib 400 mg in combination with grapefruit juice, respectively. No serious AEs were observed. Pharmacokinetics of imatinib 400 mg QD compared to imatinib 400 mg QD boosted with grapefruit juice were not significantly different. A possible explanation is that this is due to the fact grapefruit juice predominantly inhibits intestinal CYP3A4 and to a lesser extent hepatic CYP3A4. Imatinib bioavailability is almost 100%, thus only inhibiting the intestinal CYP3A4 has little effect. The study was prematurely terminated because no significant effect of grapefruit juice on imatinib exposure was observed.

3.4.6. Lapatinib Boosted with Ketoconazole

The phase I dose escalation study of lapatinib evaluated different dose-escalating strategies for lapatinib in patients with HER2 positive breast cancer to enhance the exposure of lapatinib [41]. Patients with HER2 overexpression advanced breast cancer and cardiac ejection fraction $\geq$ 50% were eligible for inclusion. The study included a total of 41 patients divided into 10 cohorts. The cohorts one to six had a predefined dose-escalating strategy without any pharmacokinetic boosting agent. After an interim analysis, it was decided that, in cohorts seven to ten, the lapatinib exposure was boosted by a pharmacokinetic enhancer. Concomitant intake with food and with or without the CYP3A4 inhibitor ketoconazole were chosen as exposure enhancement strategies. Cohorts eight to ten were concurrently treated with lapatinib BID or QID, with food and with ketoconazole 200 mg BID. A total of 12 patients were in cohorts eight to ten. Lapatinib plasma concentration blood samples were drawn at baseline and four hours after the morning dose. Food did not increase the exposure of lapatinib. Concomitant administration of lapatinib with ketoconazole increased lapatinib exposure 2.7 fold.

3.4.7. Nilotinib Boosted with Food

The NiFo study evaluated if the nilotinib dose could be reduced when concurrently administered with food to reduce the complexity of the dosing regimen and to achieve cost savings [42]. CML patients in the chronic phase (n = 15) who had had at least three months of treatment with nilotinib prior to the study were included. The first four days of the

study, patients received standard of care nilotinib 300 mg BID in fasted state, followed by seven days of nilotinib 200 mg BID concurrently administered with food. Morning meals were low-fat, evening meals were medium-fat, and on days 8 and 11, the evening dose was taken with high-fat meals. Blood samples for pharmacokinetic analysis were drawn on days 1, 3, 8 and 11. The GMR of the morning dose of $AUC_{0–12h}$, C_{max} and C_{min} was 0.89 (CI 90% 0.81–0.98), 0.90 (CI 90% 0.8–1.02) and 0.88 (CI 90% 0.84–0.92), respectively, and were within acceptance limits for bioequivalence. The GMR of the evening dose of $AUC_{0–12h}$, C_{max} and C_{min} was 0.84 (CI 90% 0.73–0.97), 0.8 (CI 90% 0.68–0.93) and 1.06 (CI 90% 0.92–1.22), respectively. The GMR of C_{min} was within acceptance limits for bioequivalence, the GMR of $AUC_{0–12h}$ and C_{max} were not. Nilotinib 200 mg BID with food was well tolerated, and patient-reported symptom burden was lower compared to nilotinib 300 mg BID standard of care. Bioequivalence for C_{min} was reached; $AUC_{0–12h}$ and C_{max} were not bioequivalent. Nilotinib efficacy is, however, associated with C_{min}; patients with a C_{min} above the threshold of $\geq$619 ng/mL have a higher major molecular response at three months [43]. Boosting nilotinib 200 mg BID with food can therefore still be a viable option, especially when guided with therapeutic drug monitoring (TDM).

3.4.8. Osimertinib Boosted with Cobicistat

The effect of cobicistat on osimertinib exposure was investigated in the proof-of-concept OSIBOOST study [44]. The aim of this study was to evaluate if osimertinib exposure could be increased by cobicistat and if the boosting effect was stable over time. Cobicistat was selected as a CYP3A4 inhibitor because of its strong inhibition of CYP3A4, lack of off-target effects and its wide use in clinical practice as a boosting agent in antiretroviral therapies. A total of 11 non-small cell lung cancer patients that had a low osimertinib exposure of $C_{min,ss} \leq 195$ ng/mL were included. Patients were initially treated with osimertinib standard of care (10 patients at 80 mg QD and 1 patient at 160 mg QD), and blood samples were drawn for pharmacokinetic analysis. After the first blood sampling day, patients were given cobicistat 150 mg QD in combination with osimertinib. The second pharmacokinetic sampling day was scheduled 22–26 days after the start of the concurrent usage of osimertinib with cobicistat 150 mg QD. After the second pharmacokinetic sampling day, patients could opt to stop the treatment of cobicistat, to continue with the concurrent use if adequate boosting was reached or to continue with the concurrent use where cobicistat was stepwise escalated to 150 mg BID or QID for patients with osimertinib $C_{min,ss} \leq 195$ ng/mL. The primary outcome was the change in $AUC_{0–24,ss}$ of osimertinib and its metabolite AZ5104 when boosted with cobicistat compared to osimertinib alone. Secondary outcomes included CYP3A4 and CYP3A5 polymorphisms, AEs and osimertinib $C_{min,ss}$ as a surrogate marker of $AUC_{0–24,ss}$ for patients who continued in the study after the first phase. During concurrent use of cobicistat, the $AUC_{0–24,ss}$ of all patients increased with a mean $AUC_{0–24,ss}$ increase of 60%. The mean $AUC_{0–24,ss}$ increase had a relatively broad range of 19–192%. The mean $AUC_{0–24,ss}$ increase in women and men was 73% and 38%, respectively. Three patients had osimertinib $C_{min} \leq 195$ ng/mL with concurrent use of cobicistat; their cobicistat dosage was consequently escalated to 150 mg BID. In one patient, osimertinib $AUC_{0–24,ss}$ decreased after cobicistat escalation, while in the other two patients the osimertinib $AUC_{0–24,ss}$ increased. In the one patient where the osimertinib $AUC_{0–24,ss}$ decreased with concurrent use of cobicistat 150 mg BID, the cobicistat dosage was further escalated to 150 mg QID. This decreased the osimertinib $AUC_{0–24,ss}$ even further to an overall increase of 1% compared to baseline. No serious AEs were observed. Concurrent use of cobicistat and osimertinib increased the exposure of osimertinib and its metabolite AZ5104 in all patients and can be an option to reduce the osimertinib dose. The added value of measuring the osimertinib metabolite AZ5104 was limited. The interindividual variation of the boosting effect of cobicistat on osimertinib exposure is challenging when composing a one-fits-all concept. Although interindividual variation of the boosting effect was relatively high, the boosting effect was constant within patients, paving the way to an integrated TDM-guided approach to cobicistat-boosted osimertinib.

3.4.9. Pazopanib Boosted with Continental Breakfast

The DIET study evaluated whether it was feasible to enhance the exposure of pazopanib with food to reduce the pazopanib dose in patients with renal cell carcinoma [45]. The study consisted of two parts. The first part was a pharmacokinetic dose-finding study to confirm bioequivalence of 800 mg QD in fasted state compared to pazopanib 600 mg QD taken with a continental breakfast. Nineteen patients were enrolled for the first part of the study. Patients received pazopanib 800 mg for 14 days in fasted state, followed by pazopanib 600 mg QD with a continental breakfast. GMR of steady state $AUC_{0–24h}$, C_{max} and C_{min} was 1.09 (CI 90% 1.02–1.17), 1.12 (CI 90% 1.04–1.20) and 1.10 (CI 90% 1.02–1.18), respectively. The second part of the study was conducted to evaluate gastrointestinal toxicity and patient preference for pazopanib 600 mg QD combined with continental breakfast compared to pazopanib 800 mg QD in a fasted state. Patients (n = 78) were initially enrolled in the second part of the study and randomly assigned to either pazopanib 800 mg QD in fasted state or pazopanib 600 mg QD with a continental breakfast. After four weeks, patients were switched to the opposite regimen. Pazopanib 600 mg QD with continental breakfast was preferred by 68% of the patients. Pazopanib 800 mg QD compared to pazopanib 600 mg QD + continental breakfast was bioequivalent; gastrointestinal AEs were comparable in both groups. Pazopanib + continental breakfast can achieve a total cost savings of approximately $8500 per patient for metastatic renal cell carcinoma and approximately $3800 per patient for soft tissue sarcoma in the Netherlands.

3.4.10. Tofacitinib Boosted with Cobicistat

The PRACTICAL study was performed to evaluate the feasibility of boosting tofacitinib exposure by cobicistat, reducing 50% of the dose and saving 50% in treatment costs [46]. The study was an open-label, non-randomized, within group crossover study, where bioequivalence of tofacitinib 5 mg QD boosted with cobicistat 150 mg QD was compared to the standard of care tofacitinib 5 mg BID. Patients with rheumatoid arthritis or psoriatic arthritis who received a minimum of 14 days of standard care with tofacitinib were eligible for inclusion. A total of 25 patients were included for the primary analysis of the study. After $\geq$14 days of tofacitinib treatment, blood samples for pharmacokinetic analysis were drawn from patients receiving tofacitinib 5 mg BID standard of care. Patients were subsequently switched to tofacitinib 5 mg QD + cobicistat 150 mg QD. Between two to six weeks after the switch to cobicistat-boosted tofacitinib, blood samples for pharmacokinetic analysis were drawn. Medication adherence was monitored in a medication diary. Patient preference was evaluated after the second pharmacokinetic sampling day. GMR of tofacitinib $C_{avg,ss}$ for tofacitinib 5 mg BID compared to tofacitinib 5 mg QD + cobicistat 150 mg QD was 0.85 (CI 90%: 0.75–0.96) and was therefore not pharmacokinetically bioequivalent according to the EMA acceptance interval. Interindividual variability expressed as relative bioavailability was 21% (residual standard error 73%) for the boosted regimen versus 32.2% (residual standard error 30.9%) for the non-boosted regimen. Disease activity remained stable, and no serious AEs were observed. The once-daily tofacitinib 5 mg QD + cobicistat 150 mg QD regimen, compared to tofacitinib 5 mg BID, was preferred by 56% of the patients. The tofacitinib 5 mg QD + cobicistat regimen can potentially achieve annual cost savings of approximately €6500 per patient in the European Union and approximately €21,500 in the United States until the patent expiry date of 2028.

3.4.11. Venetoclax and Ibrutinib Boosted with Itraconazole

In a case report, venetoclax and ibrutinib were boosted with itraconazole to save treatment costs [47]. A 22-year-old man with acute myeloid leukemia (AML) was treated with a 75% reduced dose of venetoclax 100 mg QD with itraconazole 100 mg BID as the boosting drug. No complications developed, and the patient achieved complete response, incomplete hematological recovery and a nondetectable minimal residual disease. The patient subsequently received an allogeneic stem cell transplantation. At 40 days after the stem cell transplantation, the patient developed a grade III steroid-refractory acute graft

versus host disease (GvHD) which was eventually treated with ibrutinib. The ibrutinib dose was 75% reduced compared to the normal dose and was 140 mg QD boosted with itraconazole 100 mg BID. After three weeks, the patient achieved a complete response of GvHD. After 11 months, the patient remained completely responsive, and ibrutinib was tapered. CYP3A4 boosting of venetoclax and ibrutinib to reduce treatment costs by 75% was concluded to be a promising strategy, and subsequent prospective clinical trials were initiated. A total of approximately $10,900 in cost savings was achieved in this patient by boosting venetoclax and ibrutinib.

3.4.12. Venetoclax Boosted with Posaconazole

The venetoclax–posaconazole drug–drug interaction study evaluated which dose adjustment is necessary when venetoclax is concurrently administered with posaconazole [48]. Patients (n = 12) diagnosed with AML and eligible for inclusion were included. On days one to five, patients received a venetoclax ramp-up from 20–200 mg and intravenous decitabine 20 mg/m^2. On days 6 to 20, patients received venetoclax 400 QD. On days 21 to 28, patients received a reduced venetoclax dose of either 50 mg or 100 mg in combination with posaconazole 300 mg BID on day 21, and days 22 to 28 posaconazole 300 mg QD. Six patients received the venetoclax 100 mg QD dose reduction, and five patients received the venetoclax 50 mg QD dose. The duration of the posaconazole treatment was determined to be 8 days to reach steady state. Blood samples for pharmacokinetic analysis were drawn on day 20 and day 28. In patients who received venetoclax 50 mg QD in combination with posaconazole, the mean $AUC_{0–24h}$ and C_{max} increased by 76% and 53%, respectively, when compared to venetoclax 400 mg QD alone. In patients who received venetoclax 100 mg QD in combination with posaconazole, the mean $AUC_{0–24h}$ and C_{max} increased by 155% and 93%, respectively, when compared to venetoclax 400 mg QD alone. Coadministration of posaconazole in combination with either venetoclax 50 mg QD or 100 mg QD was overall well tolerated. The venetoclax dose should be reduced by at least 75% when co-administered with posaconazole.

3.4.13. Venetoclax Boosted with Grapefruit Juice

Venetoclax was boosted with grapefruit juice in a patient with AML who could not afford the regular dose of 400 mg QD [49]. Treatment started with venetoclax 100 mg QD in combination with 200 mL grapefruit juice TID. Venetoclax C_{max} was measured weekly to ascertain adequate exposure to venetoclax and to reduce toxicity. The venetoclax C_{max} was 1440 ng/mL and 1920 ng/mL on day 7 and day 14 after receiving the combination venetoclax 100 mg QD and grapefruit juice 200 mL TID, respectively. The venetoclax C_{max} was inside the efficacy boundary, as stated by the authors, of 1000–3000 ng/mL. The patient was in remission for at least five cycles of 28 days, and no serious AEs were observed. Boosting venetoclax with grapefruit juice to make the treatment more affordable was concluded to be safe and effective for this patient. The venetoclax-associated monthly costs were reduced from 38,880 RMD yuan (approx. €5281) to 9720 RMD Yuan (approx. €1319).

The aforementioned studies are summarized in Table 5, to provide a comparative overview.

3.5. Clinical Trials Currently in Progress

Five ongoing trials were identified from ClinicalTrials.gov [17] where pharmacokinetic boosting had to be intentional and could not be a regular drug–drug interaction trial. Pharmacokinetic boosting in these ongoing trials is done to either save treatment costs or to investigate potential therapeutic benefits when the target drug is boosted. The studies evaluate efficacy of the boosted regimen with different outcomes, only the PROACTIVE study additionally include pharmacokinetic parameters as an outcome. Table 6 presents an overview of the currently ongoing boosting trials.

Table 5. Overview of kinase inhibitor boosting studies.

Target Drug	Boosting Agent	Study Aim	Study Design	Outcomes	Results	Conclusion	Reference
Axitinib	Cobicistat 150 mg QID	Boost axitinib exposure with cobicistat	Case report, one patient	C_{min}	Axitinib 10 mg QID + cobicistat 150 mg QID resulted in a 15-month stable response	Boosting axitinib with cobicistat can be a promising strategy to boost patients with sub-optimal axitinib exposure.	[34]
Crizotinib	Cobicistat 150 mg QD	Patients with low crizotinib exposure ($C_{min,ss} \leq 310$ ng/mL) were boosted with cobicistat	Open-label, non-randomized, within group crossover study, one patient	Change in $AUC_{0-24,ss}$ and $Cmin_{0-24,ss}$	The AUC and $C_{min,ss}$ increased by 78% and 164% respectively when crizotinib was boosted by cobicistat.	Cobicistat enhanced the exposure of crizotinib. Only one patient was enrolled because the next-generation ALK inhibitor alectinib was approved for the treatment of the same population with better outcomes.	[36]
Erlotinib	Ritonavir 200 mg QD	Bioequivalence of erlotinib 150 mg QD compared to erlotinib 75 mg QD + ritonavir 200 mg QD to save treatment costs	Open-label, non-randomized, within group crossover study, nine patients	GMR of AUC_{0-24h}, C_{max} and C_{min}	GMR of erlotinib 150 mg QD vs. erlotinib 75 mg + ritonavir 200 mg QD for AUC_{0-24h}, C_{max} and C_{min} were 0.99 (CI 95% 0.58–1.69, $p = 0.545$), 0.91 (CI 95% 0.55–1.49, $p = 0.500$) and 1.06 (CI 95% 0.59–1.93, $p = 0.150$), respectively.	Erlotinib 150 mg QD compared to erlotinib 75 mg + ritonavir 200 mg is bioequivalent and can be a strategy to reduce the erlotinib dosage by 50% and thus save treatment costs.	[38]
Ibrutinib	Itraconazole 200 mg BID	Evaluate exposure of Ibrutinib 15 mg + itraconazole compared to ibrutinib 140 mg + placebo	Randomized placebo-controlled crossover study with 11 healthy volunteers	GMR of $AUC_{0-\infty}$ and C_{max}	GMR of ibrutinib 15 mg + itraconazole vs. ibrutinib 140 mg + placebo $AUC_{0-\infty}$ and C_{max} were 1.07 (CI 90% 0.77–1.49; $p = 0.719$) and 0.94 (CI 90% 0.68–1.30, $p = 0.727$), respectively, the GMR CVs of $AUC_{0-\infty}$ and C_{max} for ibrutinib 15 mg boosted + itraconazole were 0.55 and 0.53, respectively, and for ibrutinib 140 mg + placebo 1.04 and 0.99, respectively.	The interindividual variability of exposure of ibrutinib is high; boosting with itraconazole and a reduced dose of ibrutinib could lower the interindividual variability. Boosting with itraconazole is cost-effective and can potentially reduce the treatment costs associate with ibrutinib by 90%. Cost savings in the United States are projected to be more than $10,000 annually per patient.	[39]
Imatinib	Grapefruit juice	Evaluate whether reduction of imatinib is feasible to reduce treatment costs with grapefruit juice	Open-label, non-randomized, within group crossover study, four patients	C_{min} and C_{max}	The median C_{min} was 1080 ng/mL (range: 1060–1360 ng/mL) and 1102 ng/mL (range: 772–1450 ng/mL) for imatinib 400 mg and imatinib 400 mg in combination with grapefruit juice, respectively. The median C_{max} was 2495 ng/mL (range: 2380–2680 ng/mL) and 2455 ng/mL (range: 1870–2750 ng/mL) for imatinib 400mg and imatinib 400mg in combination with grapefruit, juice respectively.	Pharmacokinetic of imatinib 400 mg QD compared to imatinib 400 mg QD boosted with grapefruit juice was not significantly different. The study was prematurely terminated because no significant effect of grapefruit juice on imatinib pharmacokinetics was observed.	[40]
Lapatinib	Ketoconazole 200 mg BID	Evaluate dose-escalating strategies for lapatinib	Phase I dose escalation study, 12 patients in the cohorts boosted with ketoconazole	Lapatinib concentration	Concomitant administration of lapatinib + ketoconazole increased lapatinib exposure 2.7 fold.	Lapatinib exposure can be enhanced by ketoconazole.	[41]

Table 5. *Cont.*

Target Drug	Boosting Agent	Study Aim	Study Design	Outcomes	Results	Conclusion	Reference
Nilotinib	Food; low-fat, medium-fat and high-fat meals	Evaluate whether nilotinib exposure can be enhanced with food	Open-label, non-randomized, within-group crossover study, 15 patients	GMR of AUC_{0-12h}, C_{max} and C_{min}	The GMR of the morning dose of AUC_{0-12h}, C_{max} and C_{min} was 0.89 (CI 90% 0.81–0.98), 0.90 (CI 90% 0.8–1.02) and 0.88 (CI 90% 0.84–0.92), respectively, and were within acceptance limits for bioequivalence. The GMR of the evening dose of AUC_{0-12h}, C_{max} and C_{min} was 0.84 (CI 90% 0.73–0.97), 0.8 (CI 90% 0.68–0.93) and 1.06 (CI 90% 0.92–1.22), respectively.	Bioequivalence for C_{min} was reached; AUC0–12h and C_{max} were not bioequivalent. Nilotinib efficacy is associated with C_{min}, meaning that nilotinib 200 mg BID with food can still be a viable option.	[42]
Osimertinib	Cobicistat 150 mg QD	Patients with low osimertinib exposure ($C_{min,ss} \leq 195$ ng/mL) were boosted with cobicistat	Open-label, non-randomized, within-group crossover study, 11 patients	Change in $AUC_{0-24,ss}$ (primary) and C_{min}	The mean $AUC_{0-24,ss}$ increase with cobicistat was 60%	Concurrent use of cobicistat and osimertinib increased the exposure of osimertinib and its metabolite AZ5104 in all patients and can be an option to reduce the osimertinib dose.	[44]
Pazopanib	Food; continental breakfast	Evaluate whether pazopanib exposure can be enhanced with food	Open-label, randomized, within-group crossover study, 19 patients in part 1, 78 patients in part 2	GMR of AUC_{0-24h}, C_{max}, C_{min}, gastrointestinal toxicities and patient preference	The GMR of steady state AUC_{0-24h}, C_{max} and C_{min} was 1.09 (CI 90% 1.02–1.17), 1.12 (CI 90% 1.04–1.20) and 1.10 (CI 90% 1.02–1.18), respectively.	Pazopanib 800 mg QD compared to pazopanib 600 mg QD + continental breakfast is bioequivalent, gastrointestinal AEs were comparable in both groups. Pazopanib + continental breakfast can achieve savings of approximately $8500 per patient for metastatic renal cell carcinoma and approximately $3800 per patient for soft tissue sarcoma in the Netherlands.	[45]
Tofacitinib	Cobicistat 150 mg QD	Bioequivalence of tofacitinib 5 mg BID compared to tofacitinib 5 mg QD + cobicistat 150 mg QD	Open-label, non-randomized, within-group crossover study, 25 patients	GMR of $C_{avg,ss}$	GMR of tofacitinib $C_{avg,ss}$ for tofacitinib 5 mg BID vs. tofacitinib 5 mg QD + cobicistat 150 mg QD was 85% (CI 75–96%)	Tofacitinib 5 mg BID compared to tofacitinib 5 mg QD + cobicistat 150 mg are not pharmacokinetically bioequivalent. Disease activity remained stable, indicating similar efficacy. The tofacitinib 5 mg QD + cobicistat can potentially achieve annual cost savings of approximately €6500 per patient in the European Union and approximately €21,500 in the United States until the patent expiry date of 2028.	[46]
Venetoclax and ibrutinib	Itraconazole 100 mg BID	Evaluate whether a 75% dose reduction of venetoclax and ibrutinib is feasible when co-administered with itraconazole	Case report, one patient	Efficacy	A 22-year-old man was successfully treated with a 75% reduced dose of venetoclax 100 mg QD + itraconazole 100 mg BID and ibrutinib 75% reduced dose of 140 mg QD + itraconazole 100 mg BID.	CYP3A4 boosting with itraconazole to reduce the treatment costs of venetoclax and ibrutinib can be a promising strategy. A total of approximately $10,900 in cost savings was achieved in this patient by boosting venetoclax and ibrutinib. More research to validate this hypothesis is warranted; especially prospective studies are required.	[47]
Venetoclax	Posaconazole 300 mg QD	Evaluate which dose adjustment is necessary when venetoclax is concurrently administered with posaconazole	Drug–drug interaction study, 12 patients	AUC_{0-24h} and C_{max}	Venetoclax 50 mg QD + posaconazole increased the mean AUC_{0-24h} and C_{max} by 76% and 53%, respectively, vs. venetoclax 400 mg QD alone. Venetoclax 100 mg QD + posaconazole increased the mean AUC_{0-24h} and C_{max} by 155% and 93% vs. venetoclax 400 mg QD alone.	The venetoclax dose should be reduced by at least 75% when co-administered with posaconazole.	[48]

Table 5. *Cont.*

Target Drug	Boosting Agent	Study Aim	Study Design	Outcomes	Results	Conclusion	Reference
Venetoclax	Grapefruit juice	Evaluate whether venetoclax 100 mg QD could be boosted by grapefruit juice so that the therapy becomes more affordable	Case-report, one patient	C_{max} and efficacy	The venetoclax C_{max} was 1440 ng/mL and 1920 ng/mL on day 7 and day 14 after receiving the combination venetoclax 100 mg QD and grapefruit juice 200 mL TID. The venetoclax C_{max} was inside the efficacy boundary of 1000 ng–3000 ng/mL. The patient was in remission for at least five cycles of 28 days; no serious AEs were observed.	Boosting venetoclax to make the treatment more affordable with grapefruit juice was safe and effective for this patient. The venetoclax-associated monthly costs were reduced from 38,880 RMD yuan (approx. €5281) to 9720 RMD Yuan (approx. €1319).	[49]

Table 6. Overview of currently ongoing trials on kinase inhibitor boosting (n = 5).

Study Name	Target Drug	Boosting Agent	Study Aim	Study Design	Outcomes	NCT Number
Cytochrome P450 Inhibition to Decrease Dosage of Dasatinib for Chronic Myelogenous Leukemia	Dasatinib	Ketoconazole	Investigate whether a 75% dasatinib dose reduction when boosted with ketoconazole is feasible to reduce treatment costs	Phase II open-label single-arm study with 15 participants	Primary: Cytogenetic and molecular response rates and AEs	NCT05638763
Efficacy and Safety of Low-dose Ibrutinib and Itraconazole in Chronic Graft Versus Host Disease	Ibrutinib	Itraconazole	Investigate whether a 75% ibrutinib dose reduction when boosted with Itraconazole is feasible to reduce treatment costs	Phase II open-label single-arm study with 13 participants	Primary: Overall response rate and AEs	NCT05348096
Pharmacokinetic Boosting of Olaparib to Improve Exposure, Tolerance and Cost-effectiveness (PROACTIVE)	Olaparib	Cobicistat	Ascertain bioequivalence of olaparib 300 mg BID vs. olaparib 100 mg BID + cobicistat 150 mg BID to reduce treatment costs	Part 1: bioequivalence in a cross-over olaparib vs. boosted olaparib. Part 2: non-inferiority of olaparib vs. boosted Olaparib, 160 participants	Primary: $AUC_{0–12h}$, progression-free survival, number of dose reductions as a measure of toxicity	NCT05078671
A Study of Extending Relugolix Dosing Intervals Through Addition of Itraconazole or Ritonavir in Prostate Cancer Patients	Relugolix	Itraconazole or ritonavir	Investigate safety and efficacy of relugolix when combined with itraconazole or ritonavir to extend dosing interval of relugolix to reduce treatment costs	Phase Ib in 100 participants	Primary: testosterone suppression	NCT05679388
Low-dose Venetoclax and Azacitidine as Front-line Therapy in Newly Diagnosed AML	Venetoclax	Itraconazole	Investigate whether a 75% venetoclax dose reduction when boosted with Itraconazole is feasible to reduce treatment costs	Phase II open-label single-arm study with 15 participants	Primary: number of patients who are hospitalized, number of deceased patients in predefined time frames	NCT05048615

4. Discussion

Pharmacokinetic boosting of kinase inhibitors is a rapidly evolving field, as indicated by the increasing evidence from published clinical studies and ongoing trials. Pharmacokinetic boosting can be a promising strategy for increasing exposure of anticancer drugs, which was also indicated by two previous review articles [8,9]. In the sections below, the most important aspects of the clinical boosting trials and pharmacokinetic boosting in general are discussed.

4.1. Benefits of Pharmacokinetic Boosting of Kinase Inhibitors

Increasing the bioavailability of a drug can theoretically lead to a decrease in inter-patient variability [50]. Furthermore, genetic polymorphisms of metabolizing enzymes such as CYP450 can account for variable exposure to the drug, resulting in variability in therapeutic responses between patients [44]. By inhibiting the CYP450 enzyme responsible for the metabolism of the target drug, the inter-patient variability of plasma concentrations

can theoretically decrease [26]. In the study where ibrutinib is boosted with itraconazole, the interindividual variability in exposure was decreased by pharmacokinetic boosting [39].

Boosting of expensive drugs has the potential to drastically reduce treatment costs. The high cost-saving potential of the pharmacokinetic boosting of kinase inhibitors is quantified or projected in some trials [39,45–47,49]. For some boosted kinase inhibitors, the clinical evidence for pharmacokinetic boosting safety and efficacy is already substantial. The highly reduced venetoclax dose in combination with CYP3A4 inhibitors has proven to be safe without compromising its efficacy [48], making venetoclax boosting an attractive strategy for treating patients where financial resources are limited [51].

For some kinase inhibitors, pharmacokinetic boosting can, in addition to cost savings, also result in an optimized dosing regimen. The study with cobicistat-boosted tofacitinib indicated that with pharmacokinetic boosting the standard BID tofacitinib regimen might be reduced to a once-daily regimen when tofacitinib is combined with cobicistat [46].

4.2. Risks and Disadvantages of Pharmacokinetic Boosting of Kinase Inhibitors

When drugs are intentionally off-label-boosted, this can incorporate additional risks and disadvantages compared to the standard non-boosted regimen. The exposure of the target drug can increase or decrease compared to the normal dosing regimen and can therefore increase or decrease the efficacy and toxicity of the target drug. Ascertaining bioequivalence based on the EMA bioequivalence guideline of the boosted versus non-boosted regimen is therefore important [52].

When a strong CYP3A4 inhibitor is concurrently administered with the target drug, the CYP3A4 inhibitor can also interact with the comedication of a patient. CYP3A4 inhibition of interacting comedication can lead to increased toxicity or decreased efficacy of these interacting drugs. To mitigate this risk, it is advisable to screen the comedication for drug–drug interactions before starting with the boosted regimen. When a drug–drug interaction is found, ideally an alternative for the interacting drug that is not affected by the boosting drug should be considered. When no adequate alternative is available or appropriate, a dose adjustment can be considered. When the risk of drug–drug interactions is inappropriate and no alternative or dose adjustment can be found, the patient cannot participate in a boosting regimen. When a CYP3A4 inducer is present in a patient's comedication, this can interfere with the pharmacokinetic boosting agent. Ideally the CYP3A4 inducer is switched to another drug; otherwise, the patient is unlikely to be suitable for pharmacokinetic boosting.

Inter-patient variability can decrease in a boosted regimen when compared to the non-boosted regimen. However, two clinical studies found an increased variability for boosted kinase inhibitors [38,44]. This increased variability can be due to the fact the metabolism shifts from predominantly CYP3A4-mediated metabolism to another CYP450 enzyme responsible for the metabolism with high variable activity. Unexplored causes for this increased variability have to be investigated. However, the increased variability is not necessarily a problem since some drugs do not have a strong exposure response or exposure toxicity relation. In contrast, for drugs with a known small therapeutic range, increased variability can be more problematic. To decrease the possible increased inter- and intra-individual pharmacokinetic variability, an individual TDM approach is a possibility to mitigate this risk.

Furthermore, drug-specific and disease-related risks can also be important factors. Aside from the aforementioned risks, important exclusion criteria for risk mitigation can be impairment of the gastrointestinal tract that can alter absorption, renal impairment, hepatic impairment, pregnancy and lactation and severe therapy-associated toxicity.

4.3. Factors for Selecting a Pharmacokinetic Boosting Candidate

Aside from our ranked boosting candidates as shown in Table 3, additional factors for selecting a boosting candidate have to be taken into account. Some kinase inhibitors are also substrates for transporters such as P-gp and BCRP. P-gp is expressed in multiple organs such as the small intestine, liver, kidney and the blood-brain barrier [53]. When drugs

which are substrate for P-gp are boosted with a drug that is also a P-gp inhibitor or inducer, this can cause suboptimal exposure or increased toxicity of the target drug. It is therefore important that drug transporters are also taken into account when selecting a boosting candidate. Some kinase inhibitors are inhibitors of their own metabolism (auto-inhibition) which can complicate a boosting strategy [54]. However, boosting kinase inhibitors with auto-inhibiting properties compel the need to guide therapy with TDM.

When the primary goal of pharmacokinetic boosting is to reduce treatment costs, the pricing of the target drug is an important factor that has to be taken into account. Drugs can be priced based on formulation strength or can be flat-priced with the same price for different doses [55]. Expensive drugs that are priced based on formulation strength (linear pricing) are more suitable for pharmacokinetic boosting for economic purposes than flat-priced drugs [55]. However, drug manufacturers can change the pricing structure to flat-based pricing to maximize revenues as a reaction to lower dosing regimens. This was, for example, implemented by the manufacturer of ibrutinib in the United States after a study showed equivalent efficacy of a lower ibrutinib dosing regimen [56]; however, after public objection, this decision was reversed [57]. A changed pricing structure by a manufacturer might therefore be a risk for a boosting strategy. Manipulation of dosage forms could counter the issues presented by flat-based pricing, as was performed by altering the sorafenib formulation [58]. Furthermore, it is important to consider and estimate the projected therapeutic value for upcoming years and to indicate possible shifts in overlapping indications. The study with crizotinib, for example, was prematurely terminated because the first-choice treatment option shifted from crizotinib to alectinib, making crizotinib boosting less clinically relevant [36]. In addition, factors such as total costs per patient, annual volume and the patent expiration date of the candidate drug are relevant factors when pharmacokinetic boosting is performed for economic purposes.

4.4. Clinical Trial Design of Studies Validating Pharmacokinetic Boosting

Pharmacokinetic boosting of kinase inhibitors might be applied in individual cases with low exposure at high doses and suboptimal disease control. However, for pharmacokinetic boosting of a certain drug to become more widely applied or standard-of-care, the result of pharmacokinetic boosting first has to be validated in a clinical trial. The first step in a pharmacokinetic boosting study is to determine the bioequivalent dose of the boosted regimen versus the non-boosted regimen. The kinase inhibitor dose with a booster can be estimated using pharmacokinetic or drug–drug interaction data. The best starting point is the manufacturer's recommendation for dose adjustment when co-administered with interacting drugs, such as a strong CYP3A4 inhibitor. Drug–drug interaction studies are generally available for new drugs with potential drug–drug interactions based on preclinical pharmacology. Non-linearity in drug–drug interaction studies can be an important factor for determining a good dose adjustment, such as a four-fold increase in drug exposure when concomitantly administered with a strong CYP3A4 inhibitor that does not necessarily translate to a dose reduction of 75%.

The estimated kinase inhibitor dose in combination with a booster drug has to be compared to the standard dose without booster drug for at least pharmacokinetic and safety endpoints. A bioequivalence clinical trial can be a method to compare the boosted and non-boosted regimens. The EMA bioequivalence guideline advises designing the clinical trial as a randomized, two-period, two-sequence, single-dose crossover with a wash-out period between the two periods of a minimum of five half-lives [52]. For the purpose of pharmacokinetic boosting, the EMA-recommended trial design, however, can be amended to better accommodate the specific needs of a boosting trial. Blinding the study drugs incorporates logistical issues and can complicate the clinical trial, increasing the costs of the clinical trial. Pharmaceutical companies are not keen to sponsor boosting trials because boosting potentially reduces the revenue of highly profitable drugs. Because funding of a fully blind, randomized, placebo-controlled clinical trial can be challenging, an open-label design is probably the most suitable for a clinical boosting study. For the

purpose of ascertaining bioequivalence of boosted versus non-boosted, multiple doses can be given to actual patients versus the single dose in healthy volunteers proposed by the EMA guideline [52]. The number of participants in the clinical trial should be based on the sample size calculation, with a minimum of 12. To determine bioequivalence at steady-state, the $AUC_{(0\text{-}t),ss}$, $C_{max,ss}$ and $T_{max,ss}$ have to be measured. C_{min} can also be a useful parameter to determine because it can be a surrogate marker for exposure. The acceptance level of the 90% confidence interval of the ratio of boosted versus non-boosted $AUC_{(0\text{-}t)}$ and $C_{max,ss}$ is $\geq$80% and $\leq$125%. This 80–125% acceptance interval can be tightened for drugs with a narrow therapeutic index and can be widened for drugs with high (>30%) intra-subject variability. For kinase inhibitors with no exposure–toxicity relation, it might be considered to only use the lower boundary of the acceptance interval to ensure that the boosted exposure is at least the exposure of the non-boosted dose. The T_{max} only needs to be statistically tested when a rapid onset of the tested drug is of clinical importance. When the first few participants have completed the bioequivalence trial, an interim analysis to review the preliminary bioequivalence results can be useful. When in the preliminary data of the first few participants no bioequivalence is observed and the effect of boosting is higher or lower than expected, the remaining participants can be switched to a higher or lower dose for the remainder of the bioequivalence study part. When bioequivalence is consequently ascertained for the boosted versus non-boosted regimen, the efficacy of the boosted regimen can then be compared against the standard of care.

When pharmacokinetic equivalence of the boosting regimen has been established, the second part of a boosting trial can consist of comparing the boosted regimen with the non-boosted standard of care for safety and efficacy. The level of evidence needed depends on the effect of the booster on the exposure [59]. When the boosted regimen has a bioequivalent exposure compared to the non-boosted regimen, a study on efficacy does not necessarily have to be performed [59]. However, alternative regimens where bioequivalence is already determined are rarely used in clinical practice [59]. Even if the boosted regimen is bioequivalent, further study of efficacy can be considered to strengthen the evidence so that the boosted regimen has a greater chance of being implemented in clinical practice. When efficacy evaluation is considered in a pharmacokinetic boosting trial, it has the potential to have a cost-neutral clinical trial budget when the projected high savings of the drug are realized during the trial. Patients can be randomly assigned to the boosted regimen (intervention) arm or the non-boosted standard-of-care (control) arm. Another option is to compare the boosted regimen (intervention) arm to a real-life cohort of the same population as a control arm. Outcomes that can be considered include overall survival, $AUC_{(0\text{-}t)}$, $C_{max,ss}$, and $T_{max,ss}$ for bioequivalence and possibly other pharmacokinetic parameters, efficacy endpoints based on the disease for which the drug is used, and in general quality of life and event-free survival, safety endpoints such as AEs and early mortality and exploratory endpoints such as inter- and intra-individual variability, patient preference, cost-savings and medication adherence.

4.5. Role of Therapeutic Drug Monitoring in Pharmacokinetic Boosting of Kinase Inhibitors

Therapeutic drug monitoring (TDM) is usually practiced to optimize the dose of a drug or minimize toxicity of a drug based on measured serum of plasma concentration and using estimated or calculated individual pharmacokinetic parameters. Kinase inhibitors are mainly dosed with a fixed dose derived from the maximum tolerated dose from phase I and II clinical studies [60], which focus more on toxicity and less on efficacy. Therefore, a clear exposure–response relationship cannot always be established; however, this does not necessarily mean there is no exposure-response relationship present. Drugs without exposure–response and exposure–toxicity relationships are unlikely to benefit from a TDM-guided approach in routine clinical practice because it is not clear to which extent the dose has to be adjusted.

Drugs with an exposure–response or exposure–toxicity relationship are good candidates to incorporate TDM in the boosting regimen, especially for drugs where TDM is

already proven to be of benefit [61,62]. Dose adjustments for boosting can be estimated based on the known pharmacokinetic outcomes associated with efficacy and toxicity [49]. TDM guidance can therefore help individualizing the appropriate dose and potentially reduce exposure variability. TDM guidance in this population can also lead to less toxicity because overexposure of the drug of interest is detected early, and the dose can be decreased accordingly. Drugs without a strong exposure–efficacy relationship, but with a known small exposure–toxicity relationship, can also be guided by TDM. When a patient, for example, presents with unexplainable toxicity, a drug concentration can be measured to exclude drug overexposure as a possible explanation for the observed toxicity.

In cases of boosting, bioavailability is increased and/or systemic clearance is decreased. TDM can be used to individually titrate the dose and to ascertain bioequivalence of a boosted regimen versus a non-boosted regimen. Further, it can be used to monitor medication adherence. The added value of TDM of kinase inhibitors ideally has to be established in a clinical trial, which is challenging to perform and can be expensive [63].

A drawback to implement TDM as part of the care is the required infrastructure, such as a validated analytical method for measuring drug concentrations, which can be lacking. Furthermore, the required infrastructure can be expensive to develop and maintain. It might be helpful when there is an overview of laboratories which can perform TDM on kinase inhibitors. TDM of kinase inhibitors can also introduce regulatory issues because dose adjustments based on TDM can be off-label. Still, guiding boosted kinase inhibitors with TDM can be of added value [62], but these disadvantages have to be recognized.

5. Conclusions

Pharmacokinetic boosting of kinase inhibitors is a promising, rapidly evolving and already partly proven strategy, which has the potential to reduce interindividual variability, reduce pill burden and drastically reduce treatment costs of expensive kinase inhibitors. Current evidence consists of prospective clinical trials and some case reports, and several clinical trials are ongoing. Ascertaining bioequivalence should be enough evidence to implement a boosting regimen in clinical practice. TDM in routine clinical practice can be of added value in guiding boosted regimens.

Author Contributions: Conceptualization, N.W. and T.O.M.; methodology, N.W. and T.O.M.; writing original draft preparation, N.W. and T.O.M..; writing—review and editing, T.O.M., M.L.-d.H., D.T. and J.K.; supervision, T.O.M., M.L.-d.H., D.T. and J.K. All authors have read and agreed to the published version of the manuscript.

Funding: This research received no external funding.

Institutional Review Board Statement: Not applicable.

Informed Consent Statement: Not applicable.

Data Availability Statement: Not applicable.

Conflicts of Interest: The authors declare no conflict of interest.

References

1. Krauss, J.; Bracher, F. Pharmacokinetic Enhancers (Boosters)—Escort for Drugs against Degrading Enzymes and Beyond. *Sci. Pharm.* **2018**, *86*, 43. [CrossRef] [PubMed]
2. Beyer, K.H.; Woodward, R.; Peters, L.; Verwey, W.F.; Mattis, P.A. The Prolongation of Penicillin Retention in the Body by Means of Para-Aminohippuric Acid. *Science* **1944**, *100*, 107–108. [CrossRef] [PubMed]
3. First, M.R.; Schroeder, T.J.; Weiskittel, P.; Myre, S.A.; Alexander, J.W.; Pesce, A. Concomitant administration of cyclosporin and ketoconazole in renal transplant recipients. *Lancet* **1989**, *334*, 1198–1201. [CrossRef] [PubMed]
4. Ghosn, J.; Taiwo, B.; Seedat, S.; Autran, B.; Katlama, C. HIV. *Lancet* **2018**, *392*, 685–697. [CrossRef]
5. Kempf, D.J.; Marsh, K.C.; Kumar, G.; Rodrigues, A.D.; Denissen, J.F.; McDonald, E.; Kukulka, M.J.; Hsu, A.; Granneman, G.R.; Baroldi, P.A.; et al. Pharmacokinetic enhancement of inhibitors of the human immunodeficiency virus protease by coadministration with ritonavir. *Antimicrob. Agents Chemother.* **1997**, *41*, 654–660. [CrossRef]
6. Vincent Rajkumar, S. The high cost of prescription drugs: Causes and solutions. *Blood Cancer J.* **2020**, *10*, 71. [CrossRef]

7. Glode, A.E.; May, M.B. Rising Cost of Cancer Pharmaceuticals: Cost Issues and Interventions to Control Costs. *Pharmacother. J. Hum. Pharmacol. Drug Ther.* **2017**, *37*, 85–93. [CrossRef]
8. Stuurman, F.E.; Nuijen, B.; Beijnen, J.H.; Schellens, J.H. Oral Anticancer Drugs: Mechanisms of Low Bioavailability and Strategies for Improvement. *Clin. Pharmacokinet.* **2013**, *52*, 399–414. [CrossRef]
9. Eisenmann, E.D.; Talebi, Z.; Sparreboom, A.; Baker, S.D. Boosting the oral bioavailability of anticancer drugs through intentional drug–drug interactions. *Basic Clin. Pharmacol. Toxicol.* **2022**, *130* (Suppl. S1), 23–35. [CrossRef]
10. Tucker, G.T. Pharmacokinetic considerations and challenges in oral anticancer drug therapy. *Pharm. J.* **2019**. [CrossRef]
11. Patel, A.A.; Cahill, K.; Saygin, C.; Odenike, O. Cedazuridine/decitabine: From preclinical to clinical development in myeloid malignancies. *Blood Adv.* **2021**, *5*, 2264–2271. [CrossRef] [PubMed]
12. Hakkola, J.; Hukkanen, J.; Turpeinen, M.; Pelkonen, O. Inhibition and induction of CYP enzymes in humans: An update. *Arch. Toxicol.* **2020**, *94*, 3671–3722. [CrossRef] [PubMed]
13. WHO ATC/DDD Index. Available online: https://www.whocc.no/atc_ddd_index/ (accessed on 16 January 2023).
14. European Public Assessment Reports (EPAR)—EMA. Available online: https://www.ema.europa.eu/en/medicines (accessed on 16 January 2023).
15. UpToDate. Available online: https://www.uptodate.com/contents/search (accessed on 16 January 2023).
16. UpToDate Drug Interactions. Available online: https://www.uptodate.com/drug-interactions (accessed on 16 January 2023).
17. Clinical Trials.gov. Available online: https://clinicaltrials.gov/ (accessed on 16 February 2023).
18. Zhao, M.; Ma, J.; Li, M.; Zhang, Y.; Jiang, B.; Zhao, X.; Huai, C.; Shen, L.; Zhang, N.; He, L.; et al. Cytochrome P450 Enzymes and Drug Metabolism in Humans. *Int. J. Mol. Sci.* **2021**, *22*, 12808. [CrossRef] [PubMed]
19. Loos, N.H.C.; Beijnen, J.H.; Schinkel, A.H. The Mechanism-Based Inactivation of CYP3A4 by Ritonavir: What Mechanism? *Int. J. Mol. Sci.* **2022**, *23*, 9866. [CrossRef]
20. Lolodi, O.; Wang, Y.-M.; Wright, W.C.; Chen, T. Differential Regulation of CYP3A4 and CYP3A5 and its Implication in Drug Discovery. *Curr. Drug Metab.* **2018**, *18*, 1095–1105. [CrossRef]
21. Storelli, F.; Samer, C.; Reny, J.-L.; Desmeules, J.; Daali, Y. Complex Drug–Drug–Gene–Disease Interactions Involving Cytochromes P450: Systematic Review of Published Case Reports and Clinical Perspectives. *Clin. Pharmacokinet.* **2018**, *57*, 1267–1293. [CrossRef]
22. Waring, R.H. Cytochrome P450: Genotype to phenotype. *Xenobiotica* **2020**, *50*, 9–18. [CrossRef]
23. Roy, J.-N.; Lajoie, J.; Zijenah, L.S.; Barama, A.; Poirier, C.; Ward, B.J.; Roger, M. CYP3A5 genetic polymorphisms in different ethnic populations. *Drug Metab. Dispos.* **2005**, *33*, 884–887. [CrossRef]
24. FDA. Drug Development and Drug Interactions: Table of Substrates, Inhibitors and Inducers. Available online: https://www.fda.gov/drugs/drug-interactions-labeling/drug-development-and-drug-interactions-table-substrates-inhibitors-and-inducers#table1 (accessed on 8 February 2023).
25. Singh, R.S.P.; Toussi, S.S.; Hackman, F.; Chan, P.L.; Rao, R.; Allen, R.; Van Eyck, L.; Pawlak, S.; Kadar, E.P.; Clark, F.; et al. Innovative Randomized Phase I Study and Dosing Regimen Selection to Accelerate and Inform Pivotal COVID-19 Trial of Nirmatrelvir. *Clin. Pharmacol. Ther.* **2022**, *112*, 101–111. [CrossRef]
26. Larson, K.B.; Wang, K.; Delille, C.; Otofokun, I.; Acosta, E.P. Pharmacokinetic Enhancers in HIV Therapeutics. *Clin. Pharmacokinet.* **2014**, *53*, 865–872. [CrossRef] [PubMed]
27. Eisenmann, E.D.; Garrison, D.A.; Talebi, Z.; Jin, Y.; Silvaroli, J.A.; Kim, J.-G.; Sparreboom, A.; Savona, M.R.; Mims, A.S.; Baker, S.D. Interaction of Antifungal Drugs with CYP3A- and OATP1B-Mediated Venetoclax Elimination. *Pharmaceutics* **2022**, *14*, 694. [CrossRef] [PubMed]
28. Tseng, A.; Hughes, C.A.; Wu, J.; Seet, J.; Phillips, E.J. Cobicistat Versus Ritonavir: Similar Pharmacokinetic Enhancers But Some Important Differences. *Ann. Pharmacother.* **2017**, *51*, 1008–1022. [CrossRef] [PubMed]
29. Ramanathan, S.; Mathias, A.A.; German, P.; Kearney, B.P. Clinical Pharmacokinetic and Pharmacodynamic Profile of the HIV Integrase Inhibitor Elvitegravir. *Clin. Pharmacokinet.* **2011**, *50*, 229–244. [CrossRef] [PubMed]
30. German, P.; Liu, H.C.; Szwarcberg, J.; Hepner, M.; Andrews, J.; Kearney, B.P.; Mathias, A. Effect of Cobicistat on Glomerular Filtration Rate in Subjects with Normal and Impaired Renal Function. *J. Acquir. Immune. Defic. Syndr.* **2012**, *61*, 32–40. [CrossRef]
31. Koziolek, M.; Alcaro, S.; Augustijns, P.; Basit, A.W.; Grimm, M.; Hens, B.; Hoad, C.L.; Jedamzik, P.; Madla, C.M.; Maliepaard, M.; et al. The mechanisms of pharmacokinetic food-drug interactions—A perspective from the UNGAP group. *Eur. J. Pharm. Sci.* **2019**, *134*, 31–59. [CrossRef]
32. Veerman, G.D.M.; Hussaarts, K.; Jansman, F.G.A.; Koolen, S.W.L.; van Leeuwen, R.W.F.; Mathijssen, R.H.J. Clinical implications of food–drug interactions with small-molecule kinase inhibitors. *Lancet Oncol.* **2020**, *21*, e265–e279. [CrossRef]
33. Van Leeuwen, R.W.; Peric, R.; Hussaarts, K.G.; Kienhuis, E.; Ijzerman, N.; De Bruijn, P.; Van Der Leest, C.; Codrington, H.; Kloover, J.S.; Van Der Holt, B.; et al. Influence of the Acidic Beverage Cola on the Absorption of Erlotinib in Patients with Non–Small-Cell Lung Cancer. *J. Clin. Oncol.* **2016**, *34*, 1309–1314. [CrossRef] [PubMed]
34. Lubberman, F.J.E.; Van Erp, N.P.; Ter Heine, R.; Van Herpen, C.M.L. Boosting axitinib exposure with a CYP3A4 inhibitor, making axitinib treatment personal. *Acta Oncol.* **2017**, *56*, 1238–1240. [CrossRef]
35. Tsuchiya, N.; Igarashi, R.; Suzuki-Honma, N.; Fujiyama, N.; Narita, S.; Inoue, T.; Saito, M.; Akihama, S.; Tsuruta, H.; Miura, M.; et al. Association of pharmacokinetics of axitinib with treatment outcome and adverse events in advanced renal cell carcinoma patients. *J. Clin. Oncol.* **2015**, *33*, 506. [CrossRef]

36. Hohmann, N.; Bozorgmehr, F.; Christopoulos, P.; Mikus, G.; Blank, A.; Burhenne, J.; Thomas, M.; Haefeli, W.E. Pharmacoenhancement of Low Crizotinib Plasma Concentrations in Patients with Anaplastic Lymphoma Kinase-Positive Non-Small Cell Lung Cancer using the CYP3A Inhibitor Cobicistat. *Clin. Transl. Sci.* **2021**, *14*, 487–491. [CrossRef]
37. FDA—Clinical Pharmacology and Biopharmaceutics Reviews(s)—Crizotinib. Available online: https://www.accessdata.fda.gov/drugsatfda_docs/nda/2011/202570Orig1s000ClinPharmR.pdf (accessed on 22 February 2023).
38. Boosman, R.J.; de Gooijer, C.J.; Groenland, S.L.; Burgers, J.A.; Baas, P.; van der Noort, V.; Beijnen, J.H.; Huitema, A.D.R.; Steeghs, N. Ritonavir-Boosted Exposure of Kinase Inhibitors: An Open Label, Cross-over Pharmacokinetic Proof-of-Concept Trial with Erlotinib. *Pharm. Res.* **2022**, *39*, 669–676. [CrossRef]
39. Tapaninen, T.; Olkkola, A.M.; Tornio, A.; Neuvonen, M.; Elonen, E.; Neuvonen, P.J.; Niemi, M.; Backman, J.T. Itraconazole Increases Ibrutinib Exposure 10-Fold and Reduces Interindividual Variation—A Potentially Beneficial Drug-Drug Interaction. *Clin. Transl. Sci.* **2020**, *13*, 345–351. [CrossRef]
40. Kimura, S.-I.; Kako, S.; Wada, H.; Sakamoto, K.; Ashizawa, M.; Sato, M.; Terasako, K.; Kikuchi, M.; Nakasone, H.; Okuda, S.; et al. Can grapefruit juice decrease the cost of imatinib for the treatment of chronic myelogenous leukemia? *Leuk. Res.* **2011**, *35*, e11–e12. [CrossRef]
41. Chien, A.J.; Munster, P.N.; Melisko, M.E.; Rugo, H.S.; Park, J.W.; Goga, A.; Auerback, G.; Khanafshar, E.; Ordovas, K.; Koch, K.M.; et al. Phase I Dose-Escalation Study of 5-Day Intermittent Oral Lapatinib Therapy in Patients with Human Epidermal Growth Factor Receptor 2–Overexpressing Breast Cancer. *J. Clin. Oncol.* **2014**, *32*, 1472–1479. [CrossRef]
42. Boons, C.; den Hartog, Y.M.; Janssen, J.; Zandvliet, A.S.; Vos, R.M.; Swart, E.L.; Hendrikse, N.H.; Hugtenburg, J.G. Food-effect study of nilotinib in chronic myeloid leukaemia (NiFo study): Enabling dose reduction and relief of treatment burden. *Eur. J. Haematol.* **2020**, *105*, 148–155. [CrossRef] [PubMed]
43. Fukuda, N.; Akamine, Y.; Abumiya, M.; Takahashi, S.; Yoshioka, T.; Kameoka, Y.; Takahashi, N.; Miura, M. Relationship between achievement of major molecular response or deep molecular response and nilotinib plasma concentration in patients with chronic myeloid leukemia receiving first-line nilotinib therapy. *Cancer Chemother. Pharmacol.* **2022**, *89*, 609–616. [CrossRef]
44. van Veelen, A.; Gulikers, J.; Hendriks, L.E.L.; Dursun, S.; Ippel, J.; Smit, E.F.; Dingemans, A.C.; van Geel, R.; Croes, S. Pharmacokinetic boosting of osimertinib with cobicistat in patients with non-small cell lung cancer: The OSIBOOST trial. *Lung Cancer* **2022**, *171*, 97–102. [CrossRef] [PubMed]
45. Lubberman, F.J.E.; Gelderblom, H.; Hamberg, P.; Vervenne, W.L.; Mulder, S.F.; Jansman, F.G.A.; Colbers, A.; Van Der Graaf, W.T.A.; Burger, D.M.; Luelmo, S.; et al. The Effect of Using Pazopanib With Food vs. Fasted on Pharmacokinetics, Patient Safety, and Preference (DIET Study). *Clin. Pharmacol. Ther.* **2019**, *106*, 1076–1082. [CrossRef]
46. van der Togt, C.J.T.; Verhoef, L.M.; van den Bemt, B.J.F.; den Broeder, N.; ter Heine, R.; den Broeder, A.A. Pharmacokinetic boosting to enable a once-daily reduced dose of tofacitinib in patients with rheumatoid arthritis and psoriatic arthritis (the PRACTICAL study). *Ther. Adv. Musculoskelet. Dis.* **2022**, *14*, 1759720X221142277. [CrossRef]
47. De la Garza-Salazar, F.; Colunga-Pedraza, P.R.; Gómez-Almaguer, D. Cytochrome P450 inhibition to decrease dosage and costs of venetoclax and ibrutinib: A proof-of-concept case study. *Br. J. Clin. Pharmacol.* **2023**, *89*, 898–902. [CrossRef] [PubMed]
48. Agarwal, S.K.; DiNardo, C.D.; Potluri, J.; Dunbar, M.; Kantarjian, H.M.; Humerickhouse, R.A.; Wong, S.L.; Menon, R.M.; Konopleva, M.Y.; Salem, A.H. Management of Venetoclax-Posaconazole Interaction in Acute Myeloid Leukemia Patients: Evaluation of Dose Adjustments. *Clin. Ther.* **2017**, *39*, 359–367. [CrossRef]
49. Long, Z.; Ruan, M.; Wu, W.; Zeng, Q.; Li, Q.; Huang, Z. The successful combination of grapefruit juice and venetoclax in an unfit acute myeloid leukemia patient with adverse risk: A case report. *Front. Oncol.* **2022**, *12*, 912696. [CrossRef]
50. Hellriegel, E.T.; Bjornsson, T.D.; Hauck, W.W. Interpatient variability in bioavailability is related to the extent of absorption: Implications for bioavailability and bioequivalence studies. *Clin. Pharmacol. Ther.* **1996**, *60*, 601–607. [CrossRef]
51. Chitikela, S.; Kumar, L.; Sahoo, R.K. Azacitidine and Venetoclax in AML. *New Engl. J. Med.* **2020**, *383*, 2087–2089. [CrossRef]
52. European Medicines Agency. Guideline on the Investigation of Bioequivalence (rev1). Available online: https://www.ema.europa.eu/en/documents/scientific-guideline/guideline-investigation-bioequivalence-rev1_en.pdf (accessed on 6 February 2023).
53. Glaeser, H. Importance of P-glycoprotein for Drug–Drug Interactions. *Handb. Exp. Pharmacol.* **2011**, 285–297. [CrossRef]
54. van Erp, N.P.; Gelderblom, H.; Guchelaar, H.-J. Clinical pharmacokinetics of tyrosine kinase inhibitors. *Cancer Treat. Rev.* **2009**, *35*, 692–706. [CrossRef]
55. Truong, J.; Chan, K.K.W.; Mai, H.; Chambers, A.; Sabharwal, M.; Trudeau, M.E.; Cheung, M.C. The impact of pricing strategy on the costs of oral anti-cancer drugs. *Cancer Med.* **2019**, *8*, 3770–3781. [CrossRef] [PubMed]
56. Chen, L.S.; Bose, P.; Cruz, N.D.; Jiang, Y.; Wu, Q.; Thompson, P.A.; Feng, S.; Kroll, M.H.; Qiao, W.; Huang, X.; et al. A pilot study of lower doses of ibrutinib in patients with chronic lymphocytic leukemia. *Blood* **2018**, *132*, 2249–2259. [CrossRef] [PubMed]
57. Johnson, C.Y. After Outcry, drugmakers Decide Not to Triple the Price of a Cancer Pill—The Washington Post. Available online: https://www.washingtonpost.com/news/wonk/wp/2018/05/15/after-outcry-drugmakers-decide-not-to-triple-the-price-of-a-cancer-pill/ (accessed on 15 March 2023).
58. Navid, F.; Christensen, R.; Inaba, H.; Li, L.; Chen, Z.; Cai, X.; Regel, J.; Baker, S.D. Alternative formulations of sorafenib for use in children. *Pediatr. Blood Cancer* **2013**, *60*, 1642–1646. [CrossRef]
59. Overbeek, J.K.; ter Heine, R.T.; Verheul, H.M.W.; Chatelut, E.; Rudek, M.A.; Gurney, H.; Plummer, R.; Gilbert, D.C.; Buclin, T.; Burger, D.M.; et al. Off-label, but on target: The evidence needed to implement alternative dosing regimens of anticancer drugs. *ESMO Open* **2023**, *8*, 100749. [CrossRef] [PubMed]

60. Mathijssen, R.H.; Sparreboom, A.; Verweij, J. Determining the optimal dose in the development of anticancer agents. *Nat. Rev. Clin. Oncol.* **2014**, *11*, 272–281. [CrossRef] [PubMed]
61. Groenland, S.L.; van Eerden, R.A.G.; Westerdijk, K.; Meertens, M.; Koolen, S.L.W.; Moes, D.; de Vries, N.; Rosing, H.; Otten, H.; Vulink, A.J.E.; et al. Therapeutic drug monitoring-based precision dosing of oral targeted therapies in oncology: A prospective multicenter study. *Ann. Oncol.* **2022**, *33*, 1071–1082. [CrossRef]
62. Mueller-Schoell, A.; Groenland, S.L.; Scherf-Clavel, O.; van Dyk, M.; Huisinga, W.; Michelet, R.; Jaehde, U.; Steeghs, N.; Huitema, A.D.R.; Kloft, C. Therapeutic drug monitoring of oral targeted antineoplastic drugs. *Eur. J. Clin. Pharmacol.* **2021**, *77*, 441–464. [CrossRef] [PubMed]
63. van Gelder, T. The Appropriately Designed TDM Clinical Trial: Endpoints, Pitfalls, and Perspectives. *Ther. Drug Monit.* **2023**, *45*, 6–10. [CrossRef] [PubMed]

pharmaceutics

MDPI

Review

Therapeutic Monitoring of Orally Administered, Small-Molecule Anticancer Medications with Tumor-Specific Cellular Protein Targets in Peripheral Fluid Spaces—A Review

Zoltán Köllő [1], Miklós Garami [2], István Vincze [1], Barna Vásárhelyi [1] and Gellért Balázs Karvaly [1,*]

[1] Department of Laboratory Medicine, Semmelweis University, 1089 Budapest, Hungary
[2] 2nd Department of Pediatrics, Semmelweis University, 1094 Budapest, Hungary
* Correspondence: karvaly.gellert_balazs@med.semmelweis-univ.hu

Abstract: Orally administered, small-molecule anticancer drugs with tumor-specific cellular protein targets (OACD) have revolutionized oncological pharmacotherapy. Nevertheless, the differences in exposure to these drugs in the systemic circulation and extravascular fluid compartments have led to several cases of therapeutic failure, in addition to posing unknown risks of toxicity. The therapeutic drug monitoring (TDM) of OACDs in therapeutically relevant peripheral fluid compartments is therefore essential. In this work, the available knowledge regarding exposure to OACD concentrations in these fluid spaces is summarized. A review of the literature was conducted by searching Embase, PubMed, and Web of Science for clinical research articles and case reports published between 10 May 2001 and 31 August 2022. Results show that, to date, penetration into cerebrospinal fluid has been studied especially intensively, in addition to breast milk, leukocytes, peripheral blood mononuclear cells, peritoneal fluid, pleural fluid, saliva and semen. The typical clinical indications of peripheral fluid TDM of OACDs were (1) primary malignancy, (2) secondary malignancy, (3) mental disorder, and (4) the assessment of toxicity. Liquid chromatography–tandem mass spectrometry was most commonly applied for analysis. The TDM of OACDs in therapeutically relevant peripheral fluid spaces is often indispensable for efficient and safe treatments.

Keywords: oral anticancer drugs; oncology; imatinib; precision pharmacotherapy; therapeutic drug monitoring; cerebrospinal fluid

Citation: Köllő, Z.; Garami, M.; Vincze, I.; Vásárhelyi, B.; Karvaly, G.B. Therapeutic Monitoring of Orally Administered, Small-Molecule Anticancer Medications with Tumor-Specific Cellular Protein Targets in Peripheral Fluid Spaces—A Review. *Pharmaceutics* **2023**, *15*, 239. https://doi.org/10.3390/pharmaceutics15010239

Academic Editors: Antonello Di Paolo and Haibing Zhou

Received: 11 November 2022
Revised: 29 December 2022
Accepted: 30 December 2022
Published: 10 January 2023

1. Introduction

The past two decades have seen the rise of a new era of targeted oncological pharmacotherapy. The novel treatment options have led to a tremendous increase in success rates since the first market approval of the now generic imatinib (Gleevec®, 2001), an inhibitor of the BCR-ABL oncogenic tyrosine kinase protein, and the first representative of orally administered, small-molecule anticancer drugs with specific tumor-associated cellular protein targets (OACDs). These synthetic molecules bind to proteins that are expressed excessively or even exclusively in cancer cells, resulting in the inhibition of the functions of cancer cells with a limited impact on non-malignant cells. Most OACDs are found in the subgroup L01E of the Anatomical Therapeutic Chemical (ATC) classification system (level 1: "Antineoplastic and immunomodulating agents", level 2: "Antineoplastic agents", level 3: "Protein kinase inhibitors"), and are further classified at level 4 as BCR-ABL tyrosine kinase inhibitors, epidermal growth factor receptor (EGFR) tyrosine kinase inhibitors, B-raf serine-threonine kinase (BRAF) inhibitors, anaplastic lymphoma kinase (ALK) inhibitors, mitogen-activated protein kinase (MEK) inhibitors, cyclin-dependent kinase (CDK) inhibitors, mammalian target of rapamycin (mTOR) kinase inhibitors, human epidermal growth factor receptor 2 (HER2) tyrosine kinase inhibitors, Janus-associated kinase (JAK) inhibitors, vascular endothelial growth factor receptor (VEGFR) tyrosine kinase inhibitors, Bruton's tyrosine kinase (BTK) inhibitors, phosphatidylinositol-3-kinase (Pi3K) inhibitors,

fibroblast growth factor receptor (FGFR) tyrosine kinase inhibitors, and "other" protein kinase inhibitors. Further, four OACDs are listed under level 3 code "Other antineoplastic agents" (ATC code: L01X) including histone deacetylase (HDAC) inhibitors, hedgehog pathway inhibitors, and poly-ADP-ribose polymerase inhibitors.

The changes in the treatment of malignancies brought about by OACDs have been revolutionary, considering their favorable adverse effect profiles and applicability as a regular pill medication. Indeed, targeted therapies with OACDs offer significant benefits to patients, clinicians, and the healthcare system with reduced treatment costs, milder and more tolerable adverse effects, and improved prognoses [1]. The range of malignancies that have been treated successfully keeps increasing, with regulatory agencies having granted approvals to over 80 OACDs for treating various types of cancers including central nervous system (CNS) tumors, hematological malignancies, gastrointestinal tumors, and melanoma, as well as non-small cell lung carcinoma (NSCLC), since 2001 [1,2].

Targeted oral anticancer therapy has also brought along new challenges. OACDs are most often administered in one-size-fits-all doses. Nevertheless, the remarkable inter-individual variability in their pharmacokinetic properties raises the need for the individualization of OACD regimens based on the monitoring of drug exposure [3]. Therapy adherence also influences the outcome of the treatment [1]. An increasing number of publications suggests that therapeutic drug monitoring (TDM), as well as the pharmacokinetic interpretation of TDM results, have key importance in optimizing targeted oncotherapy using OACDs [4,5]. The first consensus guideline regarding the TDM of an OACD was published on imatinib in 2021 [6].

The appearance OACDs in physiological or pathologically formed extravascular fluid compartments and in excreta has been demonstrated to bear fundamental clinical relevance. "Peripheral fluid space" is used in the current work to describe fluid compartments in which the repeated measurement of OACD concentrations bears direct therapeutic or toxicological relevance, either because they represent the availability of the drug at the site of the desired or undesired effect, or because the pathological formation of the fluid compartment as a third space alters the availability of the drug in an unpredictable manner. Two exemptions are made. Urine is a physiological excretion end product from which OACDs are not reabsorbed, presenting a fraction no longer biologically available. The appearance of OACDs in amniotic fluid may be informative, but the monitoring of drug levels is unlikely to be associated with any changes in the mater's medical care, while amniocentesis cannot be viewed as a potential intervention for optimizing OACD therapy. Therefore, we do not recommend the consideration of urine and amniotic fluid as therapeutically relevant peripheral fluid spaces in this context.

Two clinical situations highlight the need for a paradigm shift in the administration of OACDs involving their monitoring in these fluid spaces. First, reports have consistently shown that the amounts of several OACDs which pass through the blood–brain barrier are extremely low. This often leads to failure in treating CNS malignancies in spite of the attainment of sufficient systemic drug exposure [7]. Second, breastfeeding women diagnosed with malignant disorders have been observed to pass on relatively large amounts of the OACD and its metabolites with their breast milk, resulting in unknown biological effects in the lactated infant [8–10]. While the approved full prescribing information documents of several OACDs advise women not to breastfeed their infants while taking the medication, the prescription labels are neither categorical, nor consistent in this respect. Overall, it is rational to assume that, in several clinical cases, TDM- and pharmacokinetics-based therapeutic strategies will have to target exposure to OACDs in these peripheral spaces.

To facilitate further research, the aims of this review are (1) to provide a comprehensive overview of the available knowledge regarding the distribution of OACDs to the peripheral fluid spaces, and (2) to explore the methodological approaches employed for the clinical monitoring of the concentrations of OACDs in peripheral fluid spaces.

2. Materials and Methods

Due to the types of publications available, a systematic review could not be conducted; however, adhered to the applicable items of the PRISMA Guidelines [11]. The review was not registered. Only substances with per os formulations authorized for human use, identified specific oncogenic cellular protein targets, and a molecular weight not exceeding 1500 Da were assessed. The range of drugs covered is listed under the level 3 ATC code L01E, and under the level 4 codes L10XH, L10XJ, L10XK, and L10XX (as of 12 December 2022, Table 1).

Table 1. Orally taken, small-molecule anticancer medications with specific cellular protein targets which have been measured in peripheral fluid spaces to support clinical decision making. CSF, cerebrospinal fluid; PBMC, peripheral blood mononuclear cells.

ATC Code	International Nonproprietary Name	Target Cellular Protein	Monitored Peripheral Fluid	Ref.
L01EA01	Imatinib	BCR-ABL tyrosine kinase	CSF, breast milk, leukocytes, PBMC, semen	[12–26]
L01EA02	Dasatinib	BCR-ABL tyrosine kinase	CSF	[12,27,28]
L01EA03	Nilotinib	BCR-ABL tyrosine kinase	CSF, pleural fluid	[29–36]
L01EA05	Ponatinib	BCR-ABL tyrosine kinase	CSF	[37]
L01EB01	Gefitinib	Epidermal growth factor receptor tyrosine kinase	CSF, pleural fluid, peritoneal dialysis fluid	[38–46]
L01EB02	Erlotinib	Epidermal growth factor receptor tyrosine kinase	CSF, pleural fluid	[45–58]
L01EB03	Afatinib	Epidermal growth factor receptor tyrosine kinase	CSF	[59–61]
L01EB04	Osimertinib	Epidermal growth factor receptor tyrosine kinase	CSF	[62–65]
L01EB08	Icotinib	Epidermal growth factor receptor tyrosine kinase	CSF	[66,67]
L01EC01	Vemurafenib	B-raf serine-threonine kinase	CSF	[68]
L01EC02	Dabrafenib	B-raf serine-threonine kinase	CSF	[69]
L01ED01	Crizotinib	Anaplastic lymphoma kinase	CSF	[70–73]
L01ED02	Ceritinib	Anaplastic lymphoma kinase	CSF	[74]
L01ED03	Alectinib	Anaplastic lymphoma kinase	CSF	[75,76]
L01ED05	Lorlatinib	Anaplastic lymphoma kinase	CSF	[77]
L01EE01	Trametinib	Mitogen-activated protein kinase	CSF	[69]
L01EF02	Ribociclib	Cycline dependent kinase	CSF	[12,78–80]
L01EG02	Everolimus	Mammalian target of rapamycin	breast milk, saliva	[81,82]
L01EH01	Lapatinib	Human epidermal growth factor receptor 2 tyrosine kinase	CSF	[83]
L01EH02	Neratinib	Human epidermal growth factor receptor 2 tyrosine kinase	CSF	[84]
L01EL01	Ibrutinib	Bruton's tyrosine kinase	CSF	[85,86]
L01EL03	Zanubrutinib	Bruton's tyrosine kinase	CSF	[87]
L01EX01	Sunitinib	Other protein kinase	Ascitic fluid	[88]
L01EX03	Pazopanib	Other protein kinase	Ascitic fluid	[88]
L01EX05	Regorafenib	Other protein kinase	CSF	[12,89]
L01EX09	Nintedanib	Other protein kinase	CSF	[12]
L01EX21	Tepotinib	Other protein kinase	CSF	[90,91]
L01EX23	Pralsetinib	Other protein kinase	CSF	[65]
L01XH01	Vorinostat	Histone deacetylase	CSF	[12]
L01XH03	Panobinostat	Histone deacetylase	CSF	[12,92,93]
L01XJ01	Vismodegib	Hedgehog pathway proteins	CSF	[94]
L01XX52	Venetoclax	bcl-2 protein	CSF	[95,96]

2.1. Database Search

A search of the following databases was performed:

1. The database of the National Library of Medicine, National Center for Biotechnology Information (National Library of Medicine, Bethesda, MD, USA, https://pubmed.ncbi.nlm.nih.gov), keyword combination: (abemaciclib OR acalabrutinib OR afatinib OR alectinib OR alpelisib OR anagrelide OR asciminib OR avapritinib OR axitinib OR belzutifan OR binimetinib OR bosutinib OR brigatinib OR cabozantinib OR capmatinib OR ceritinib OR cobimetinib OR copanlisib OR crizotinib OR dabrafenib OR dacomitinib OR dasatinib OR duvelisib OR encorafenib OR entrectinib OR erdafitinib OR erlotinib OR everolimus OR fedratinib OR gefitinib OR gilteritinib OR glasdegib OR ibrutinib OR icotinib OR idelalisib OR imatinib OR infigratinib OR ivosidenib OR ixazomib OR lapatinib OR larotrectinib OR lenvatinib OR lorlatinib OR midostaurin OR mitotane OR neratinib OR nilotinib OR nintedanib OR niraparib OR olaparib OR osimertinib OR pacritinib OR palbociclib OR panobinostat OR pazopanib OR pemigatinib OR pexidartinib OR ponatinib OR pralsetinib OR regorafenib OR ribociclib OR ripretinib OR rucaparib OR ruxolitinib OR selinexor OR selpercatinib OR selumetinib OR sonidegib OR sorafenib OR sotorasib OR sunitinib OR

talazoparib OR tazemetostat OR tepotinib OR tivozanib OR trametinib OR tucatinib OR vandetanib OR vemurafenib OR venetoclax OR vismodegib OR vorinostat OR zanubrutinib OR tyrosine kinase inhibit OR PARP) AND (saliva OR cerebrospinal fluid OR liquor OR pleural effusion OR peritoneal dialysis OR interstitial fluid OR brain microdialysis OR semen OR follicular fluid OR tear OR breast milk OR milk OR mother's milk) AND (concentration OR chromatography OR mass spectrometry OR therapeutic drug monitoring OR levels).

2. The Web of Science (Clarivate^{TM}, Chandler, AZ, USA, https://webofscience.com) keyword combination: (abemaciclib OR acalabrutinib OR afatinib OR alectinib OR alpelisib OR anagrelide OR asciminib OR avapritinib OR axitinib OR belzutifan OR binimetinib OR bosutinib OR brigatinib OR cabozantinib OR capmatinib OR ceritinib OR cobimetinib OR copanlisib OR crizotinib OR dabrafenib OR dacomitinib OR dasatinib OR duvelisib OR encorafenib OR entrectinib OR erdafitinib OR erlotinib OR everolimus OR fedratinib OR gefitinib OR gilteritinib OR glasdegib OR ibrutinib OR icotinib OR idelalisib OR imatinib OR infigratinib OR ivosidenib OR ixazomib OR lapatinib OR larotrectinib OR lenvatinib OR lorlatinib OR midostaurin OR mitotane OR neratinib OR nilotinib OR nintedanib OR niraparib OR olaparib OR osimertinib OR pacritinib OR palbociclib OR panobinostat OR pazopanib OR pemigatinib OR pexidartinib OR ponatinib OR pralsetinib OR regorafenib OR ribociclib OR ripretinib OR rucaparib OR ruxolitinib OR selinexor OR selpercatinib OR selumetinib OR sonidegib OR sorafenib OR sotorasib OR sunitinib OR talazoparib OR tazemetostat OR tepotinib OR tivozanib OR trametinib OR tucatinib OR vandetanib OR vemurafenib OR venetoclax OR vismodegib OR vorinostat OR zanubrutinib OR 'tyrosine kinase inhibit' OR PARP) AND (saliva OR 'cerebrospinal fluid' OR liquor OR 'pleural effusion' OR 'peritoneal dialysis' OR 'interstitial fluid' OR 'brain microdialysis' OR semen OR follicular fluid OR tear OR breast milk) AND (concentration OR chromatography OR 'mass spectrometry' OR 'therapeutic drug monitoring' OR levels).

3. The Embase database (Elsevier B.V., Amsterdam, The Netherlands, https://embase.com), keyword combination: (abemaciclib OR acalabrutinib OR afatinib OR alectinib OR alpelisib OR anagrelide OR asciminib OR avapritinib OR axitinib OR belzutifan OR binimetinib OR bosutinib OR brigatinib OR cabozantinib OR capmatinib OR ceritinib OR cobimetinib OR copanlisib OR crizotinib OR dabrafenib OR dacomitinib OR dasatinib OR duvelisib OR encorafenib OR entrectinib OR erdafitinib OR erlotinib OR everolimus OR fedratinib OR gefitinib OR gilteritinib OR glasdegib OR ibrutinib OR icotinib OR idelalisib OR imatinib OR infigratinib OR ivosidenib OR ixazomib OR lapatinib OR larotrectinib OR lenvatinib OR lorlatinib OR midostaurin OR mitotane OR neratinib OR nilotinib OR nintedanib OR niraparib OR olaparib OR osimertinib OR pacritinib OR palbociclib OR panobinostat OR pazopanib OR pemigatinib OR pexidartinib OR ponatinib OR pralsetinib OR regorafenib OR ribociclib OR ripretinib OR rucaparib OR ruxolitinib OR selinexor OR selpercatinib OR selumetinib OR sonidegib OR sorafenib OR sotorasib OR sunitinib OR talazoparib OR tazemetostat OR tepotinib OR tivozanib OR trametinib OR tucatinib OR vandetanib OR vemurafenib OR venetoclax OR vismodegib OR vorinostat OR zanubrutinib OR tyrosine kinase inhibit OR PARP) AND (saliva OR cerebrospinal fluid OR liquor OR pleural effusion OR peritoneal dialysis OR interstitial fluid OR brain microdialysis OR semen OR follicular fluid OR tear OR breast milk OR milk) AND (concentration OR chromatography OR mass spectrometry OR therapeutic drug monitoring OR levels).

Scientific works published between 10 May 2001 and 31 August 2022 were evaluated. Since, to the best of the authors' knowledge, no reviews have been previously written in the same topic, the searched time range was selected to cover the entire period OACDs have been available on the market. No filtering or limiting settings were applied. In the Embase and Web of Science databases, the search was conducted in the titles and in the abstracts ("Title or Abstract").

In addition, a manual Google search was conducted using the following query terms: "name of drug" AND "therapeutic drug monitoring", "name of drug" + "milk", "name of

drug" + "liquor", "name of drug" + "cerebrospinal fluid", "name of drug" + "semen", and "name of drug" + "liquid chromatography mass spectrometry".

Each database record was evaluated by two reviewers (Z.K. and G.B.K.) who also conducted the manual research. Duplicate publications were removed by Z.K. before screening. No automation tools were employed for evaluating the eligibility of the records.

2.2. Screening Eligible Database Records

The workflow of retrieving research articles for full evaluation is shown in Figure 1. The evaluation of the records was performed by Z.K. and G.B.K.

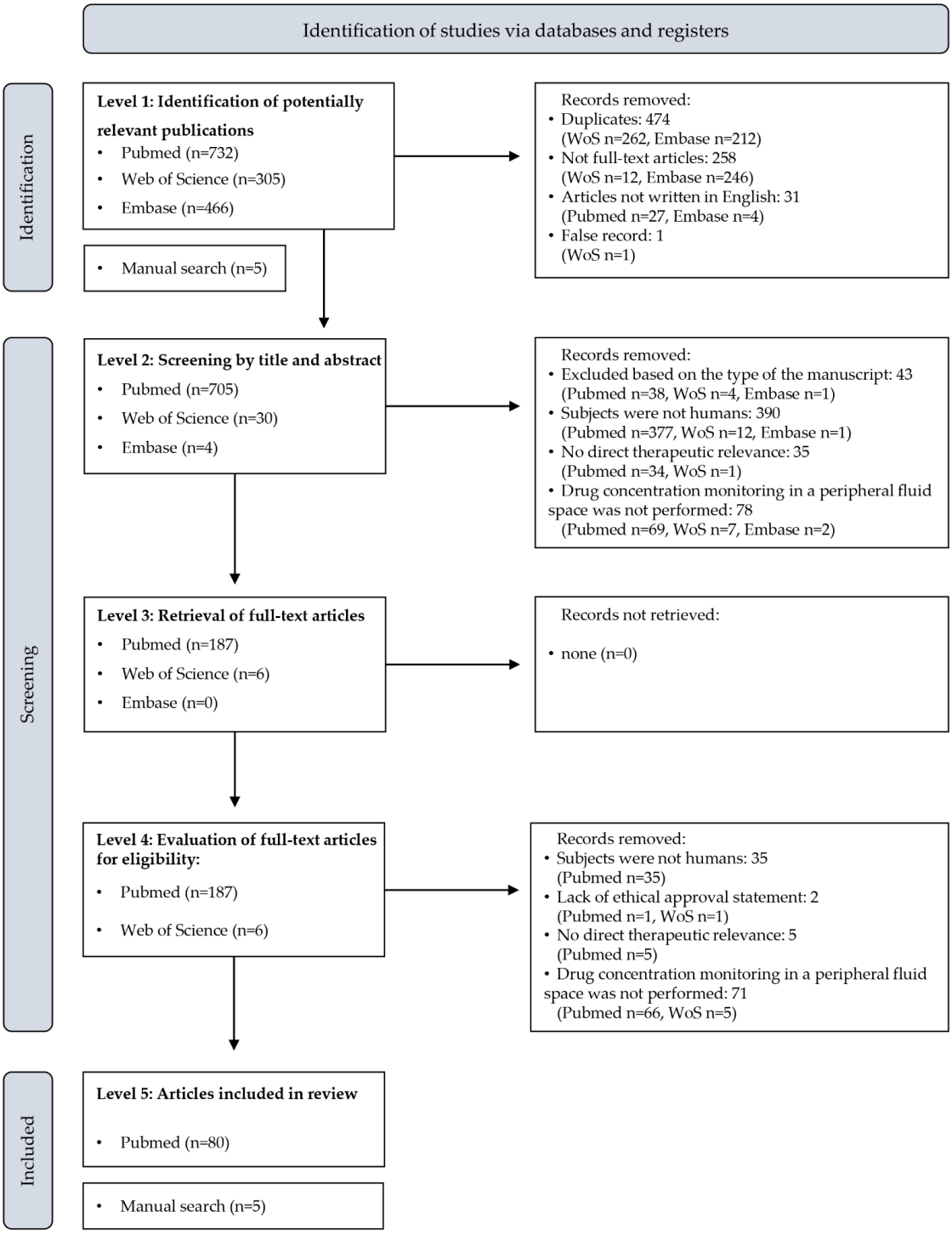

Figure 1. Flowchart of the search strategy and the article selection process. WoS, Web of Science.

First, duplicates of the PubMed records were removed from the results of the Embase and Web of Science database search. The remaining records were subsequently assessed individually for meeting basic requirements. Only peer-reviewed full manuscripts written in English, assigned an individual digital object identifier, and made available online by the publisher within the searched period were considered for further screening. Level 2 screening was based on the contents of the title and the abstract. Only records with an explicit evidence of ineligibility were removed at this level. The type of the article was the first object of assessment. Articles presenting randomized and nonrandomized registered clinical studies, non-registered, researcher-initiated clinical studies, retrospective observational studies, case series (describing 2 cases or more with the individual assessment of subjects), and individual case reports were included for further evaluation. Book chapters, comment articles, editorials, meta-analyses, practical guidelines, research protocols, scoping reviews, and systematic reviews were not considered. Second, articles describing experiments in which the subjects were not humans, i.e., in vitro experiments or in vivo animal studies, were removed. Subsequently, studies performed with the participation of human subjects, but without the aim to evaluate or to support decisions related to their medical treatment, i.e., without direct therapeutic relevance (e.g., with the inclusion of healthy volunteers, or conducted with the only aim to deliver pharmacokinetic data), or including medical intervention which, by current understanding, would not be part of the clinical practice (e.g., monitoring drug levels in cord blood or in amniotic fluid to evaluate the exposure of the fetus) were eliminated. Finally, studies explicitly performed without the monitoring of any of the drugs listed in Table 1 in a peripheral fluid space were also excluded.

In the phase of full manuscript screening, the first object of assessment was the ethical review board approval. Case reports and case series were exempt from this requirement. Articles continued to be retained if explicit evidence was found in the main text confirming that the study had been performed with direct therapeutic relevance, as described for level 2 screening. The presentation of the results of monitoring at least one drug displayed in Table 1 in a peripheral fluid space was a further requirement for inclusion. Articles not excluded in this phase were subject to full evaluation. The full manuscripts retrieved by manual search were screened in an identical manner before inclusion.

2.3. Data Evaluation and Visualization

All descriptive information on the database records and the contents of the manuscripts found were stored and processed using Microsoft Excel. The year-normalized number of publications on each drug was calculated as n_{publ}/n_{year}, where n_{publ} is the number of included publications on the drug, and n_{year} is the number of years the drug had been available on the market. The latter was defined as the period starting with the day of the first approval by the American Food and Drug Administration, and ending on 31 August 2022. Visualization was carried out using Microsoft Office applications.

3. Results

3.1. Summary of the Findings of the Literature Review

The database search yielded a set of 1503 potentially relevant articles (732, 305, and 466 hits in PubMed, Web of Science, and Embase, respectively). Four-hundred and seventy-four duplicates were removed. Of the remaining 1029 papers, 258 were presentation abstracts, and 31 were not written in English. In a single case, a record was listed with false authors. These records were also excluded. The manual search yielded five additional hits which were subsequently found in the PubMed database, but had not been listed by the automatic search. The assessment of the remaining 739 articles based on title and abstract resulted in the exclusion of further 546 publications. Forty-three articles were excluded based on their type. Three hundred and ninety works described in vitro experiments or in vivo animal studies, and 35 were conducted in humans, but without a direct therapeutic

goal. Seventy-eight studies were excluded based on evidence retrieved from the title and/or the abstract that drug concentrations were not monitored in any peripheral fluid space.

All of the 193 publications retained for full evaluation could be retrieved from the websites of the publishers. An in-depth study of these manuscripts resulted in the elimination of 113 publications. The authors of two papers failed to present evidence of the approval of an ethical review board for conducting research on humans. Thirty-five studies were not performed in humans, and five were conducted without direct therapeutic relevance. Seventy-one works were excluded because drug concentrations were not monitored in any peripheral fluid space. The remaining 80 publications were selected for the detailed review (Figure 1, Table 2). Overall, 34% of the included publications were individual case reports, 31% were registered clinical studies, 19% were case series, 13% were non-registered, researcher-initiated studies, and 3% were retrospective observational studies.

Table 2. Characteristics of the included articles. ALL, acute lymphocytic leukemia. AML, acute myeloid leukemia. CLL, chronic lymphocytic leukemia; CML, chronic myeloid leukemia; CML-BC, chronic myeloid leukemia with blast crisis; CNS, central nervous system; CSF, cerebrospinal fluid; HIV, human immunodeficiency virus; LM, leptomeningeal metastasis; NSCLC, non-small cell lung cancer; PBMC, peripheral blood mononuclear cell; PFS, peripheral fluid sample; Ph +, Philadelphia chromosome-positive.

First Author, Year	Drug	Type of Study	Patient Population	Number of Subjects Donating Samples for TDM	Period of Recruitment	Outcomes Measured	Ref.
Hoffknecht, 2015	Afatinib	Case series	2 adults with advanced NSCLC with brain metastasis or leptomeningeal disease	Blood: 2 PFS: 2	May 2010 to December 2013	Afatinib in CSF and in plasma	[59]
Kawaguchi, 2017	Afatinib	Case report	Adult (female, 41 years) with stage IV lung adenocarcinoma and cerebral metastasis	Blood: 1 PFS: 1	Not applicable	Afatinib in CSF and in plasma	[60]
Tamiya, 2017	Afatinib	Registered clinical study (UMIN000014065)	11 adults with histologically proven EGFR mutation-positive NSCLC with LMC	Blood: 11 PFS: 8	April 2014 to November 2015	Afatinib in CSF and in plasma	[61]
Gadgeel, 2014	Alectinib	Registered clinical study (NCT01588028)	47 adults with locally advanced or metastatic NSCLC with ALK gene rearrangement	Blood: 5 PFS: 5	3 May 2012 to 26 July 2013	Alectinib in CSF and in plasma	[75]
Metro, 2016	Alectinib	Case series	11 ALK-positive NSCLC patients with CNS metastasis	Blood: 2 PFS sample: 2	December 2013 to August 2015	Alectinib in CSF and in serum	[76]
Mehta, 2021	Ceritinib	Registered clinical study (NCT02605746)	10 adults with glioblastoma necessitating resection	Blood: 10 PFS: 8	Not reported	Ceritinib in CSF and in plasma	[74]
Costa, 2011	Crizotinib	Case report	Adult (male, 29 years) with stage IV NSCLC and CNS metastasis	Blood: 1 PFS: 1	Not applicable	Crizotinib in CSF and in plasma	[70]
Metro, 2015	Crizotinib	Case series	2 adults with ALK-positive advanced NSCLC and CNS metastasis	Blood: 2 PFS: 2	Not applicable	Crizotinib in CSF and in plasma	[71]
Okawa, 2018	Crizotinib	Case report	Adult (male, 60 years) with NSCLC and isolated CNS failure	Blood: 1 PFS: 1	Not applicable	Crizotinib in CSF and in plasma	[72]
Okimoto, 2019	Crizotinib	Case report	Adult (male, 61 years) with NSCLC and carcinomatous meningitis	Blood: 1 PFS: 1	Not applicable	Crizotinib in CSF and in plasma	[73]
Hottinger, 2019	Dabrafenib, trametinib	Case series	2 adults with leptomeningeal tumor	Blood: 2 PFS: 2	2017	Dabrafenib and trametinib in CSF and in plasma	[69]
Guntner, 2020	Dasatinib, imatinib, nintedanib, panobinostat, regorafenib, ribociclib, vorinostat	Case series	12 pediatric patients (ages: 7.5–20.3) with primary and secondary malignant brain tumors	Blood: 1 PFS: 9	Not reported	Imatinib, dasatinib, nintedanib, panobinostat, regorafenib, ribociclib and vorinostat in CSF	[12]
Kondo, 2014	Dasatinib	Case report	Adult (female, 58 years) with Ph + ALL and meningeal leukemia	Blood: 1 PFS: 1	Not applicable	Dasatinib in CSF and in plasma	[27]

Table 2. *Cont.*

First Author, Year	Drug	Type of Study	Patient Population	Number of Subjects Donating Samples for TDM	Period of Recruitment	Outcomes Measured	Ref.
Gong, 2021	Dasatinib	Registered clinical study (NCT02523976)	31 adults with newly diagnosed Ph + ALL	Blood: 31 PFS: 31	January 2016 to April 2018	Dasatinib in CSF and in plasma	[28]
Shriyan, 2020	Erlotinib, gefitinib	Non-registered, researcher-initiated study	20 adults with NSCLC and brain metastasis	Blood: 20 PFS: 20	August 2014 to July 2017	Erlotinib in CSF and in plasma, gefitinib in CSF and in plasma	[46]
Broniscer, 2007	Erlotinib	Case report	Pediatric patient (female, 8 years) with glioblastoma	Blood: 1 PFS: 1	Not applicable	Erlotinib in CSF and in plasma	[47]
Rogers, 2010	Erlotinib	Case report	Adult (female, 33 years) with CNS hemangioblastomatosis associated with von Hippel-Lindau disease	Blood: 1 PFS: 1	Not reported	Erlotinib in CSF and in plasma	[48]
Masago, 2011	Erlotinib	Non-registered, researcher-initiated study	9 adult patients with advanced NSCLC	Blood: 9 PFS: 9	June 2009 to December 2009	Erlotinib and OSI-420 in pleural effusate and in plasma	[49]
Masuda, 2011	Erlotinib	Case series	3 adults (NSCLC with LM)	Blood: 3 PFS: 3	Not applicable	Erlotinib in CSF and in plasma	[50]
Togashi, 2010	Erlotinib	Case series	4 adults with NSCLC and CNS metastasis	Blood: 4 PFS: 4	Not reported	Erlotinib in CSF and in plasma	[51]
Deng, 2013	Erlotinib	Non-registered, researcher-initiated study	6 adults (NSCLC)	Blood: 6 PFS: 6	March 2011 to March 2012	Erlotinib in CSF and in plasma	[52]
Sakata, 2016	Erlotinib	Case report	Adult (female, 54 years) with NSCLC and LM	Blood: 1 PFS: 1	Not applicable	Erlotinib in CSF and in plasma	[53]
Clarke, 2010	Erlotinib	Case report	Adult (female, 54 years) with stage IV NSCLC and LM	Blood: 1 PFS: 1	Not applicable	Erlotinib in CSF and in plasma	[54]
Yang, 2015	Erlotinib	Retrospective observational study	9 adults with lung adenocarcinoma and refractory CNS metastases	Blood: 6 PFS: 6	January 2011 to June 2013	Erlotinib in CSF and in plasma	[55]
Togashi, 2011	Erlotinib	Case series	9 adults with NSCLC and CNS metastasis	Blood: 9 PFS: 9	Not reported	Erlotinib in CSF and in plasma	[56]
Fukudo, 2013	Erlotinib	Non-registered, researcher-initiated study	88 adults with NSCLC	Blood: 88 PFS: 23	June 2009 to March 2012	Erlotinib in CSF and in plasma	[57]
Nosaki, 2020	Erlotinib	Registered clinical study (UMIN000007020)	21 adults (stage IV NSCLC or its recurrence with LM)	Blood: 14 PFS: 12	December 2011 to May 2015	Erlotinib in CSF and in plasma	[58]
DeWire, 2021	Everolimus, ribociclib	Registered clinical study (NCT03387020)	22 pediatric patients (ages: 3.9–20.4) with a recurrent, progressive or refractory brain tumor	Blood: 22 PFS: 5	January 2018 to April 2020	Ribociclib in CSF and in plasma, everolimus in blood	[80]
Fiocchi, 2016	Everolimus	Case report	Adult (female, 40 years) with pregnancy after undergoing heart transplant	Blood: 1 PFS: 1	Not applicable	Everolimus in breast milk (colostrum) and in plasma	[81]
Molenaar-Kuijsten, 2022	Everolimus	Registered clinical study (EudraCT 2014-004,833-25; NTR4908)	10 adults with stomatitis	Blood: 10 PFS: 10	Not reported	Everolimus in saliva and in plasma	[82]
Yamaguchi, 2015	Gefitinib	Case report	Adult (male, 72 years) lung adenocarcinoma and brain metastasis	Blood: 1 PFS: 1	Not applicable	Gefitinib in pleural effusate, peritoneal effusate dialysate, and plasma	[38]
Fukuhara, 2008	Gefitinib	Case report	Adult (male, 62 years) with stage IV lung cancer and carcinomatous meningitis	Blood: 1 PFS: 1	Not applicable	Gefitinib in CSF and in plasma	[39]
Zhao, 2013	Gefitinib	Non-registered, researcher-initiated study	22 adults (NSCLC)	Blood: 22 PFS: 22	March 2007 to December 2010	Gefitinib in CSF and in plasma	[40]
Zeng, 2015	Gefitinib	Non-registered, researcher-initiated study	28 adults with NSCLC and brain metastasis	Blood: 28 PFS: 28	October 2009 to March 2011	Gefitinib in CSF and in plasma	[41]

Table 2. *Cont.*

First Author, Year	Drug	Type of Study	Patient Population	Number of Subjects Donating Samples for TDM	Period of Recruitment	Outcomes Measured	Ref.
Zhao, 2016	Gefitinib	Case series	7 adults with NSCLC with intracranial and/or extracranial progression	Blood: 5 PFS: 5	February 2009 to May 2013	Gefitinib in CSF and in plasma	[42]
Jackman, 2015	Gefitinib	Registered clinical study (NCT00372515)	7 adults with NSCLC and LM	Blood: 7 PFS: 7	May 2006 and July 2008	Gefitinib in CSF and in plasma	[43]
Fang, 2015	Gefitinib	Case series	3 adults with lung adenocarcinoma and brain metastasis	Blood: 3 PFS: 3	Not reported	Gefitinib in CSF and in plasma	[44]
Togashi, 2012	Gefitinib, erlotinib	Non-registered, researcher-initiated study	15 adults (NSCLC with CNS metastases with EGFR mutations)	Gefitinib: Blood: 8 PFS: 8 Erlotinib: Blood: 9 PFS: 9	April 2010 to March 2012	(1) Gefitinib in CSF and in plasma; (1) Erlotinib in CSF and in plasma	[45]
Law, 2021	Ibrutinib	Case series	2 adults with Epstein–Barr virus-associated primary CNS lymphoma	Blood: 1 PFS: 1	Not applicable	Ibritunib in CSF and in plasma	[85]
Yu, 2021	Ibrutinib	Retrospective observational study	3 adults with primary central nervouos system lymphoma	Blood: 3 PFS: 1	August 2017 to May 2020	Ibrutinib in CSF and in plasma	[86]
Fan, 2015	Icotinib	Registered clinical study (NCT01514877)	20 adults with NSCLC and brain metastasis	Blood: 10 PFS: 10	February 2012 to March 2013	Icotinib in CSF and in plasma	[66]
Zhou, 2016	Icotinib	Registered clinical study (NCT01516983)	15 adults with NSCLC and brain metastasis	Blood: 15 PFS: 13	13 February 2012 to 24 July 2013	Icotinib in CSF and in plasma	[67]
Nambu, 2011	Imatinib	Non-registered, researcher-initiated study	15 adults with CML	Blood: 15 PFS: 15	2003 to 2008	Imatinib in leukocytes and in plasma	[13]
De Francia, 2014	Imatinib	Non-registered, researcher-initiated study	24 adults with Ph + CML	Blood: 24 PFS: 24	Not reported	Imatinib in PBMC's and in plasma	[14]
Petzer, 2002	Imatinib	Case report	Adult (male, 52 years) with CML with CNS relapse	Blood: 1 PFS: 1	Not applicable	Imatinib in CSF and in plasma	[15]
Takayama, 2002	Imatinib	Case report	Adult (female, 32 years) with Ph + ALL and CNS leukemia	Blood: 1 PFS: 1	Not applicable	Imatinib in CSF and in plasma	[16]
Bornhauser, 2004	Imatinib	Case report	Adult (female, 56 years) with Ph + CML and CNS leukemia	Blood: 1 PFS: 1	Not applicable	Imatinib and N-desmethyl imatinib in CSF and in plasma	[17]
le Coutre, 2004	Imatinib	Non-registered, researcher-initiated study	97 subjects with BCR/ABL + CML or BCR/ABL + ALL	Blood: 97 PFS: 17	Not reported	Imatinib and N-desmethyl imatinib in CSF and in plasma	[18]
Leis, 2004	Imatinib	Registered clinical study (CSTI5710102, CSTI15710109)	42 adults with CML in blast crisis, or Ph + ALL	Blood: 4 PFS: 4	Not reported	Imatinib in CSF and in plasma	[19]
Russell, 2007	Imatinib	Case series	2 adults with Ph + CML	Blood: 1 PFS: 1	Not applicable	Imatinib in breast milk and in plasma	[20]
Gambacorti-Passerini, 2007	Imatinib	Case report	Adult (female, 40 years) with CML	Blood: 1 PFS: 1	Not applicable	Imatinib in breast milk and in plasma	[21]
Ali, 2009	Imatinib	Case report	Adult (female, 27 years) with Ph + CML	Blood: 1 PFS: 1	Not applicable	Imatinib in breast milk and in plasma	[22]
Kronenberger, 2009	Imatinib	Case report	Adult (female, 34 years) with CML	Blood: 1 PFS: 1	Not applicable	Imatinib in breast milk and in plasma	[23]
Burwick, 2017	Imatinib	Case report	Adult (female, 29 years) with Ph + CML	Blood: 1 PFS: 1	Not applicable	Imatinib in breast milk and in plasma	[24]
Terao, 2020	Imatinib	Case report	Adult (female, 32 years) with Ph + CML	Blood: 1 PFS: 1	Not applicable	Imatinib in breast milk and in plasma	[25]
Chang, 2017	Imatinib	Non-registered, researcher-initiated study	108 males (15–51 years) with CML-CP, infertility, or controls	Blood: 48 PFS: 11	January 2010 to December 2014	Imatinib in semen and in plasma	[26]

Table 2. *Cont.*

First Author, Year	Drug	Type of Study	Patient Population	Number of Subjects Donating Samples for TDM	Period of Recruitment	Outcomes Measured	Ref.
Gori, 2014	Lapatinib	Case series	2 adults with HER2 + metastatic breast cancer	Blood: 2 PFS: 2	Not applicable	Lapatinib in CSF and in plasma	[83]
Sun, 2022	Lorlatinib	Registered clinical study (NCT01970865)	54 patients with NSCLC and suspected or confirmed leptomeningeal carcinomatosis or carcinomatous meningitis	Blood: 54 PFS: 5	Not reported	Lorlatinib in CSF and in plasma	[77]
Freedman, 2020	Neratinib	Registered clinical study (NCT01494662)	5 adults with HER2 + breast cancer and brain metastases in whom craniotomy was indicated	Blood: 2 PFS: 3	22 May 2013 to 18 October 2016	Neratinib in CSF and in plasma	[84]
Reinwald, 2014	Nilotinib	Case series	4 patients aged > 15 years with BCR-ABL + ALL or CML-BC	Blood: 4 PFS: 4	Not reported	Nilotinib in CSF and in plasma	[29]
Liu, 2019	Nilotinib	Registered clinical study (ChiCTR-ONC-12002469)	30 subjects aged > 15 years with newly diagnosed Ph + ALL	Blood: 30 PFS: 30	14 September 2011 to 21 November 2013	Nilotinib in CSF and in plasma	[30]
Satoh, 2021	Nilotinib	Case report	Adult (male, 23 years) with CML	Blood: 1 PFS: 1	Not applicable	Nilotinib in pleural effusate and in plasma	[31]
Pagan, 2016	Nilotinib	Registered clinical study (NCT02281474)	12 adults with Parkinson's disease or Dementia with Lewy Bodies	Blood: 12 PFS: 12	Not reported	Nilotinib in CSF and in plasma	[32]
Pagan, 2019	Nilotinib	Registered clinical study (NCT02954978)	75 adults with Parkinson's disease	Blood: 75 PFS: 75	Not reported	Nilotinib in CSF and in plasma	[33]
Pagan, 2020	Nilotinib	Registered clinical study(NCT02954978)	75 adults with Parkinson's disease	Blood: 75 PFS: 75	17 May 2017 to 28 April 2018	Nilotinib in CSF and in plasma	[34]
Simuni, 2021	Nilotinib	Registered clinical study (NCT03205488)	76 adults with Parkinson's disease	Blood: 41 PFS: 42	November 2017 to December 2018	Nilotinib in CSF and in plasma	[35]
Turner, 2020	Nilotinib	Registered clinical study (NCT02947893)	37 adults with Alzheimer's disease	Blood: 37 PFS: 37	Not reported	Nilotinib in CSF and in plasma	[36]
Song, 2019	Osimertinib	Case report	Adult with NSCLC and LM	Blood: 1 PFS: 1	Not applicable	Osimertinib in CSF and in plasma	[62]
Xing, 2020	Osimertinib	Registered clinical study (NCT02972333)	38 adults with refractory NSCLC and CNS metastasis	Blood: 12 PFS: 12	January 2017 to September 2017	Osimertinib in CSF and in plasma	[63]
Yamaguchi, 2021	Osimertinib	Registered clinical study (UMIN000024218, jRCTs071180017)	40 adults with confirmed NSCLC and CNS metastasis	Blood: 37 PFS: 7	27 December 2016 to 4 July 2019	Osimertinib in CSF and in plasma	[64]
Rasmussen, 2015	Panobinobstat	Registered clinical study (NCT01680094)	15 adults with HIV infection	Blood: 0 PFS: 11	September 2012 to February 2014	Panobinostat in CSF	[92]
Goldberg, 2020	Panobinostat	Registered clinical study (NCT01321346)	22 pediatric patients with relapsed or refractory acute leukemia or lymphoma	Blood: 9 PFS: not reported	3 November 2011 to 31 July 2015	Panobinostat in CSF and in plasma	[93]
Krens, 2021	Pazopanib	Case report	Adult (male, 79 years) with metastatic papillary renal cell carcinaoma and malignant ascites	Blood: 1 PFS: 1	Not applicable	Pazopanib in ascitic fluid and in plasma	[88]
Tanimura, 2021	Ponatinib	Case report	Pediatric patient (girl, 3 years) with Ph + ALL and CNS infiltration	Blood: 1 PFS: 1	Not applicable	Ponatinib in CSF and in plasma	[37]
Zhao, 2022	Pralsetinib	Case report	Adult (female, 43 years) with lung cancer and meningeal metastases	Blood: 1 PFS: 1	Not applicable	Pralsetinib in CSF and in plasma	[65]
Zeiner, 2019	Regorafenib	Retrospective observational study	21 adults with recurrent malignant glioma	Blood: 3 PFS: 3	August 2018 to July 2019	Regorafenib in CSF and in serum	[89]
Miller, 2019	Ribociclib	Registered clinical tudy (NCT02345824, IND125168)	3 adults with recurrent glioblastoma	Blood: 3 PFS: 1	First surgery dates: 29 March 2012 to 26 September 2014	Ribociclib in CSF and in plasma	[78]
Tien, 2019	Ribociclib	Registered clinical study (NCT02933736)	12 adults with a recurrent glioblastoma	Blood: 12 PFS: 12	Not reported	Ribociclib in CSF and in plasma	[79]

Table 2. *Cont.*

First Author, Year	Drug	Type of Study	Patient Population	Number of Subjects Donating Samples for TDM	Period of Recruitment	Outcomes Measured	Ref.
Tanaka, 2020	Tepotinib	Case report	Adult (male, 56 years) with with lung adenocarcinoma and LM	Blood: 1 PFS: 1	Not applicable	Tepotinib in CSF and in plasma	[90]
Ninomaru, 2021	Tepotinib	Case report	Adult (female, 77 years) with NSCLC and LM	Blood: 1 PFS: 1	Not applicable	Tepotinib in CSF and in plasma	[91]
Sakji-Dupré, 2015	Vemurafenib	Case series	6 adults with melanoma and brain metastasis	Blood: 6 PFS: 6	February 2012 to January 2013	Vemurafenib in CSF and in plasma	[68]
Reda, 2019	Venetoclax	Case report	Adult (male, 58 years) with trisomy 12, IGHV unmutated (VH4L) chronic lymphocytic leukemia	Blood: 1 PFS: 1	Not applicable	Venetoclax in CSF and in plasma	[95]
Condorelli, 2022	Venetoclax	Case report	Adult (male, 52 years) with AML and CNS leukemia	Blood: 1 PFS: 1	Not applicable	Venetoclax in CSF and in plasma	[96]
Gajjar, 2013	Vismodegib	Registered clinical study (NCT0082248)	33 pediatric patients (ages: 3.9–21 yeatrs) with recurrent, progressive or refractory medulloblastoma	Blood: 33 PFS: 3	Not reported	Vismodegib in CSF and in plasma	[94]
Zhang, 2021	Zanubrutinib	Case series	13 adults with diffuse large B-cell lymphoma and CNS involvement	Blood: 13 PFS: 13	August 2020 to December 2020	Zanubrutinib in CSF and in plasma	[87]

Thirty-two small-molecule, orally taken anticancer medications with specific cellular protein targets were monitored with a clinical indication in at least one peripheral liquid space on at least one occasion in the investigated period. This comprises 38.6% of the OACDs which had an ATC code on 31 August 2022. CSF was the most frequently monitored peripheral space (82% of all publications). The share of manuscripts on all other peripheral spaces (breast milk—8%, pleural effusate—4%, ascitic or peritoneal dialysis fluid—2%, intracellular fluid—2%, other (saliva and semen, 1 record for each)—2%) was low. In 61% of the cases, the indication for monitoring an OACD in a peripheral fluid compartment was to control a secondary malignancy. Other indications were the treatment of a primary malignancy (19%), controlling toxicity (14%), and treatment of a mental disorder (6%). In a single manuscript, an additional indication was the prevention of graft rejection [81]. Registered clinical studies, non-registered, researcher-initiated studies, case series, and case reports comprised 29.4%, 14.1%, 22.4%, and 34.1% of the included publications, respectively (Figure 2).

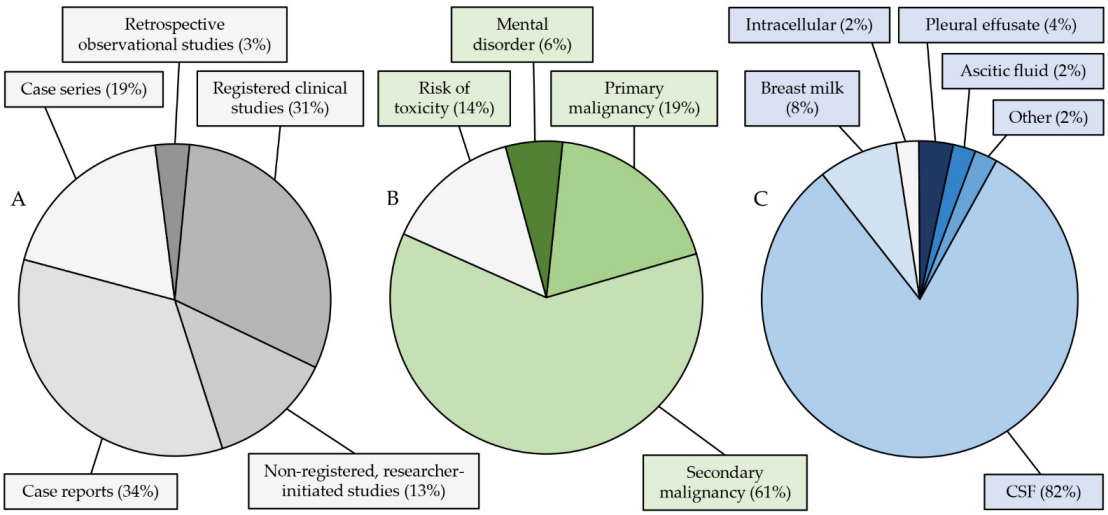

Figure 2. *Cont.*

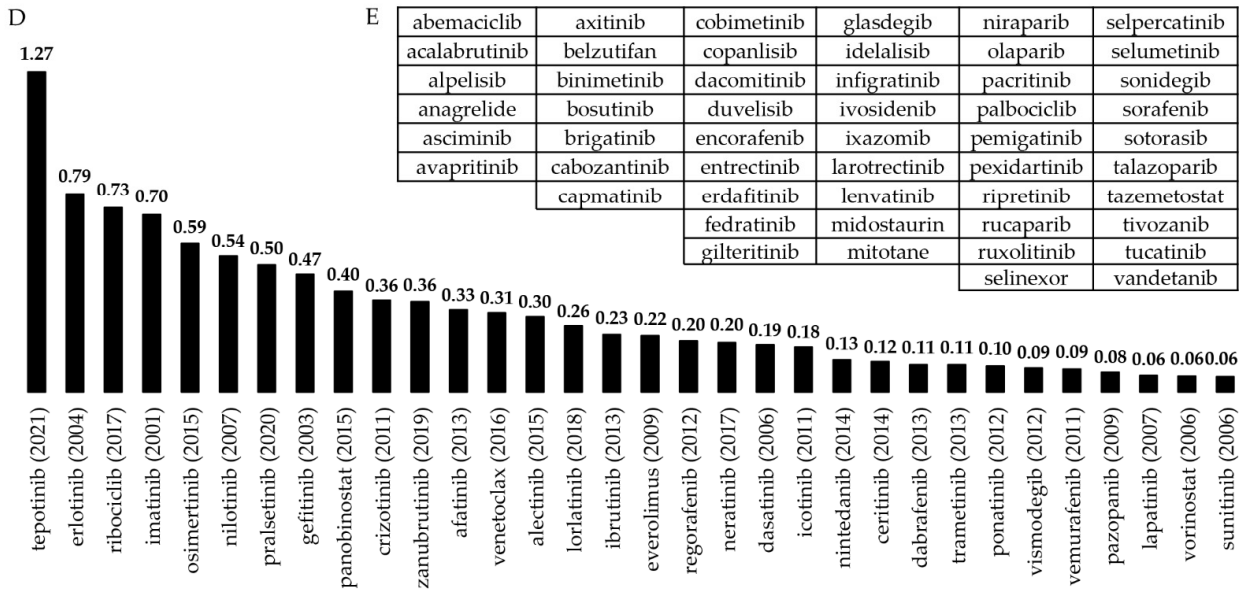

Figure 2. Summary of the results of the literature search. (**A**) Types of studies, (**B**) indications of monitoring, (**C**) monitored peripheral fluid spaces, (**D**) evaluation of clinical interest: number of manuscripts discussing the substance normalized to the number of years on the market, (**E**) marketed small-molecule, orally taken anticancer drugs with cellular protein targets without any example of being monitored in a peripheral fluid space. CSF, cerebrospinal fluid.

Based on the number of relevant publications available on a specific OACD, normalized to the number of years it has been marketed, tepotinib (Tepmetko®) triggered the largest interest, followed by erlotinib (Tarceva®), ribociclib (Kisqali®), imatinib, and osimertinib (Tagrisso®), while the OACDs receiving the least attention were lapatinib (Tyverb®), vorinostat (Zolinza®) and sunitinib (Sutent®, Figure 2, Table 3).

Table 3. Clinical background of the monitoring of OACDs in peripheral fluid spaces. ALL, acute lymphoid leukemia; AML, acute myeloid leukemia; CNS, central nervous system; CSF, cerebrospinal fluid; CLL, chronic lymphoid leukemia; CML, chronic myeloid leukemia; NSCLC, non-small cell lung cancer; PBMC, peripheral blood mononuclear cells; PCNSL, primary central nervous system lymphoma.

International Non-Proprietary Name	Peripheral Compartment	Indication of Monitoring	Pathological Condition	Ref.
Afatinib	CSF	Secondary malignancy	NSCLC with CNS metastasis and/or leptomeningeal disease	[59]
	CSF	Secondary malignancy	NSCLC with leptomeningeal carcinomatosis	[60]
	CSF	Secondary malignancy	NSCLC with leptomeningeal carcinomatosis	[61]
Alectinib	CSF	Secondary malignancy	NSCLC with CNS metastasis and systemic disease	[75]
	CSF	Secondary malignancy	NSCLC with CNS metastasis	[76]
Ceritinib	CSF	Secondary malignancy	CNS metastasis of breast tumor, head and neck tumor or melanoma, recurrent glioblastoma	[74]
Crizotinib	CSF	Secondary malignancy	NSCLC with leptomeningeal metastasis	[70]
	CSF	Secondary malignancy	NSCLC with CNS metastasis	[71]
	CSF	Secondary malignancy	NSCLC with CNS metastasis	[72]
	CSF	Secondary malignancy	NSCLC with carcinomatous meningitis	[73]
Dabrafenib	CSF	Primary malignancy	Glioma	[69]
Dasatinib	CSF	Primary malignancy	CNS tumor	[12]
	CSF	Secondary malignancy	AML with extramedullary and meningeal relapse	[27]
	CSF	Secondary malignancy	ALL and CNS leukemia prophylaxis	[28]

Table 3. *Cont.*

International Non-Proprietary Name	Peripheral Compartment	Indication of Monitoring	Pathological Condition	Ref.
Erlotinib	CSF	Secondary malignancy	NSCLC with CNS metastasis	[45]
	CSF	Secondary malignancy	NSCLC with CNS metastasis	[46]
	CSF	Primary malignancy	Glioblastoma	[47]
	CSF	Primary malignancy	CNS hemangioblastoma with von Hippel-Lindau disease	[48]
	CSF	Secondary malignancy	NSCLC with leptomeningeal metastasis	[50]
	CSF	Secondary malignancy	NSCLC with CNS metastasis	[51]
	CSF	Secondary malignancy	NSCLC with CNS metastasis	[52]
	CSF	Secondary malignancy	NSCLC with leptomeningeal metastasis	[53]
	CSF	Secondary malignancy	NSCLC with leptomeningeal meatastasis	[54]
	CSF	Secondary malignancy	NSCLC with refractory CNS metastasis	[55]
	CSF	Secondary malignancy	NSCLC with CNS metastasis	[56]
	CSF	Secondary malignancy	NSCLC with CNS metastasis	[57]
	CSF	Secondary malignancy	NSCLC with leptomeningeal metastasis	[58]
	Pleural effusate	Primary malignancy	NSCLC	[49]
Everolimus	Breastmilk	Risk of toxicity	Pregnancy in everolimus-treated heart-transplanted patient	[81]
	Saliva	Risk of toxicity	Cancer patients (breast, renal cell, neuroendocrine tumors)	[82]
Gefitinib	CSF	Secondary malignancy	NSCLC with carcinomatous meningitis	[39]
	CSF	Secondary malignancy	NSCLC with lung adenocarcinoma	[40]
	CSF	Secondary malignancy	NSCLC with CNS metastasis	[41]
	CSF	Secondary malignancy	NSCLC with leptomeningeal metastasis	[42]
	CSF	Secondary malignancy	NSCLC with leptomeningeal metastasis	[43]
	CSF	Secondary malignancy	NSCLC with CNS metastasis	[44]
	CSF	Secondary malignancy	NSCLC with CNS metastasis	[45]
	CSF	Secondary malignancy	NSCLC with CNS metastasis	[46]
	Pleural effusate, peritoneal effusate dialysate	Primary malignancy	NSCLC	[38]
Ibrutinib	CSF	Primary malignancy	Epstein–Barr associated primary CNS lymphoma	[85]
	CSF	Primary malignancy	PCNSL	[86]
Icotinib	CSF	Secondary malignancy	NSCLC with CNS metastasis	[44]
	CSF	Secondary malignancy	NSCLC with CNS metastatis	[67]
Imatinib	Breast milk	Risk of toxicity	CML during pregnancy	[20]
	Breast milk	Risk of toxicity	CML during pregnancy	[21]
	Breast milk	Risk of toxicity	CML during pregnancy and breastfeeding	[22]
	Breast milk	Risk of toxicitiy	CML during pregnancy and breastfeeding	[23]
	Breast milk	Risk of toxicity	CML in early pregnancy and breastfeedng	[24]
	Breast milk	Risk of toxicity	CML during pregnancy and breastfeeding	[25]
	CSF	Primary malignancy	CNS tumor	[12]
	CSF	Secondary malignancy	CML with lymphoid blast crisis	[15]
	CSF	Secondary malignancy	ALL with CNS leukemia	[16]
	CSF	Secondary malignancy	CML with CNS leukemia	[17]
	CSF	Secondary malignancy	CML and ALL with meningeous leukemia	[18]
	CSF	Secondary malignancy	CML with lymphoid blast crisis and AML	[19]
	Leukocytes	Primary malignancy	CML	[13]
	PBMC's	Primary malignancy	CML	[14]
	Semen	Risk of toxicity	CML	[26]
Lapatinib	CSF	Secondary malignancy	Breast cancer with CNS metastasis	[83]
Lorlatinib	CSF	Secondary malignancy	NSCLC with CNS metastasis	[77]
Neratinib	CSF	Secondary malignancy	Breast cancer with CNS metastasis	[84]
Nilotinib	CSF	Secondary malignancy	Leukemia with CNS infiltration	[29]
	CSF	Secondary malignancy	ALL and CNS leukemia prophylaxis	[30]
	CSF	Treatment of a mental disorder	Parkinson's disease, dementia	[32]
	CSF	Treatment of a mental disorder	Parkinson's disease	[33]
	CSF	Treatment of a mental disorder	Parkinson's disease	[34]
	CSF	Treatment of a mental disorder	Parkinson's disease	[35]
	CSF	Treatment of a mental disorder	Alzheimer's disease	[36]
	Pleural effusate	Risk of toxicity	CML	[31]

Table 3. *Cont.*

International Non-Proprietary Name	Peripheral Compartment	Indication of Monitoring	Pathological Condition	Ref.
Nintedanib	CSF	Primary malignancy	CNS tumor	[12]
Osimertinib	CSF	Secondary malignancy	NSCLC with leptomeningeal metastasis	[62]
	CSF	Secondary malignancy	NSCLC wth CNS metastasis	[63]
	CSF	Secondary malignancy	NSCLC with CNS metastasis	[64]
	CSF	Secondary malignancy	NSCLC with meningeal metastasis	[65]
Panobinostat	CSF	Primary malignancy	CNS tumor	[12]
	CSF	Risk of toxicity	HIV infection	[92]
	CSF	Risk of toxicity	Recurrent or refractory haematologic malignancies (leukemia and lymphoma)	[93]
Pazopanib	Ascitic fluid	Secondary malignancy	Metastatic papillary renal cell carcinoma and malignant ascites	[88]
Ponatinib	CSF	Secondary malignancy	ALL with CNS leukemia	[37]
Pralsetinib	CSF	Secondary malignancy	NSCLC with meningeal metastasis	[65]
Regorafenib	CSF	Primary malignancy	CNS tumor	[12]
	CSF	Primary malignancy	Recurrent malignant glioma	[89]
Ribociclib	CSF	Primary malignancy	CNS tumor	[12]
	CSF	Primary malignancy	Recurrent glioblastma	[78]
	CSF	Primary malignancy	Recurrent glioblastoma	[79]
	CSF	Primary malignancy	Recurrent or refractory malignant CNS tumor	[80]
Sunitinib	Ascitic fluid	Secondary malignancy	Metastatic papillary renal cell carcinoma and malignant ascites	[88]
Tepotinib	CSF	Secondary malignancy	NSCLC with leptomeningeal metastasis	[90]
	CSF	Secondary malignancy	NSCLC with leptomeningeal metastasis	[91]
Trametinib	CSF	Primary malignancy	Glioma	[69]
Vemurafenib	CSF	Secondary malignancy	Melanoma with CNS metastasis	[68]
Venetoclax	CSF	Secondary malignancy	CLL with CNS involvement	[95]
	CSF	Secondary malignancy	AML with leptomeningeal involvement	[96]
Vismodegib	CSF	Primary malignancy	Recurrent or refractory medulloblastoma	[94]
Vorinostat	CSF	Primary malignancy	CNS tumor	[12]
Zanubrutinib	CSF	Primary malignancy	CNS lymphoma	[87]

3.2. Monitoring the Concentrations of Oral Anticancer Drugs in Peripheral Fluids

3.2.1. Monitoring the Treatment of Primary Malignancies

Primary Malignant Central Nervous System Tumors

Currently, the most common indication of monitoring OACDs in a peripheral fluid space is to improve the treatment of primary and secondary CNS tumors in adults and in pediatric patients by performing measurements in the CSF. Early examples for such efforts included the assessment of erlotinib in pediatric glioblastoma and in CNS hemangioblastoma with von Hippel–Lindau disease, and of vismodegib (Erivedge®) in pediatric recurrent or refractory medulloblastoma [47,48,94]. Broniscer et al. investigated the pharmacokinetics of erlotinib in a pediatric patient by measuring the concentrations of erlotinib along with its *O*-demethylated, pharmacokinetically active metabolite OSI-420 in plasma and in CSF. Six time-matched pairs of specimens were collected. The CSF/total plasma concentration ratio (CSF-TPR) of erlotinib was 7.0%, while the ratio of drug exposure was 6.9% based on 24-h areas under the concentration-time curves. This evaluation was based on total plasma levels. Since the fraction of erlotinib bound to plasma proteins is approximately 93%, it is reasonable to assume that the unbound fraction equilibrated between plasma and CSF at a 1:1 ratio [47,97]. In a single paired measurement performed in an adult patient, a median erlotinib CSF level corresponding to 21.6% of median total plasma concentrations was found, which would be equivalent to 309% of the unbound plasma fraction [48]. In a phase 1 study conducted with pediatric patients, a total of nine paired CSF and plasma samples were collected from three subjects to evaluate vismodegib concentrations. The CSF/unbound plasma concentration ratios (CSF-UPR) attained a median of 53% (26–78%) [94].

The monitoring of OACDs in this context has gained more attention only very recently. The concentrations of regorafenib (Stivarga®) as well as its active *N*-oxide and demethylated *N*-oxide products were assessed in recurrent malignant glioma. All three substances attained detectable levels in CSF. While the concentration values were not explicitly provided by the authors, visual plots showed that the CSF-TPR's were 0.01 or higher. Approximately 99.5% of circulating regorafenib is bound to proteins, indicating that the CSF levels exceeded unbound plasma concentrations [89].

The monitoring of ceritinib (Zykadia®) and ribociclib in patients diagnosed with recurrent glioblastoma was performed [74,78,79]. The unbound fraction of ceritinib, determined using equilibrium dialysis with a 5 kDa regenerated cellulose membrane, corresponded to 1.4% (0.6–2.6%) of total levels. The unbound CSF concentrations were comparable to concentrations measured in nonenhancing tumor regions, and were tenfold higher than unbound plasma levels [74].

The ratio of ribociclib CSF/unbound plasma concentrations was 1.29 in one study and 0.6–4.4 in another. Equilibrium dialysis was employed in both works to determine the unbound fractions directly. The ratios increased over time [78,79]. Ribociclib CSF concentrations were evaluated in recurrent or refractory malignant pediatric brain tumor. The CSF-TPRs were 0.0–42.9% [80].

Dasatinib (Sprycel®), imatinib, nintedanib (Ofev®), panobinostat (Farydak®), regorafenib, ribociclib, and vorinostat were assayed in 42 CSF samples obtained from nine pediatric brain tumor patients. Nintedanib and panobinostat were undetectable in the samples. There was a correlation between blood protein levels and imatinib concentrations. In addition, imatinib and regorafenib proved to bind to CSF proteins as well, resulting in unbound fractions of 88% and 65%, respectively. These data indicate that both plasma and CSF protein concentrations may have an impact on detectable drug levels, and that the elevation of drug availability can be expected in CSF when the blood–brain barrier is not intact and CSF protein levels increase [12].

Ibrutinib (Imbruvica®) was measured in CSF in primary CNS lymphomas [85,86]. In one study, hemodialysis was conducted every other day. Six-hour post-dose CSF ibrutinib levels were about tenfold higher on hemodialysis-free days than those observed on hemodialysis days. In addition, the CSF-UPR's (with an assumed protein-bound fraction comprising 97.3% of circulating ibrutinib) were 78% and 8%, respectively [85].

Zanubrutinib (Brukinsa®) concentrations were assayed in 23 time-matched plasma and CSF samples of 13 patients, 8 of whom were diagnosed with primary CNS lymphoma, and 5 with diffuse large B-cell lymphoma. The CSF-TPR was 2.39±1.71%. With an assumed 94% protein binding rate, the authors calculated CSF-UPR's of 42.7±27.7%, and concluded that zanubrutinib was successfully transported through the blood–brain barrier [87].

Dabrafenib (Tafinlar®) and Trametinib (Mekinist®) did not reach detectable levels in CSF in patients diagnosed with V600e positive glioma [69].

Other Primary Malignancies

Other types of tumors in which OACD concentrations have been evaluated in peripheral fluid spaces include Philadelphia chromosome-positive (Ph +) chronic myeloid leukemia (CML), non-small cell lung cancer, and gastrointestinal stromal tumors.

Imatinib concentrations were monitored in patients diagnosed with Ph + CML. In a follow-up study conducted with 15 adult patients, Nambu et al. found a weak correlation between imatinib levels determined in leukocytes (buffy coat cells) and in plasma (r = 0.281). While the intracellular concentrations of the drug were not associated with the cytogenic response, there was a significant difference between groups of patients with different genotypes (SLCO1B3 334TT and 334 TG/GG) [13]. In another study conducted with adult Ph + CML subjects, peripheral blood mononuclear cells (PBMC) were isolated from anticoagulated whole blood. Again, a weak yet statistically significant positive correlation was found between imatinib concentrations observed in plasma and in PBMC (r = 0.203) [14].

In both works, intracellular imatinib concentrations were about a magnitude higher than those found in plasma.

Malignant pleural effusion is a severe condition developing as a complication of lung or breast cancer in women [98]. Masago et al. investigated erlotinib and OSI-420 concentrations in the plasma and in the pleural effusate samples of nine adult patients diagnosed with advanced NSCLC. On days 1 and 8 of the treatment, 2-h post-dose (day 1) and trough pleural effusate levels (day 8) were compared to trough plasma concentrations. They found that erlotinib and OSI-420 pleural effusate concentrations had increased considerably, with larger than 100% pleural effusate/total plasma concentration ratios obtained by day 8 [49]. In an NSCLC patient, gefitinib concentrations in pleural effusates attained approximately 30% of those observed in plasma. The penetration of gefitinib into the peritoneal third-space fluid was, on the other hand, negligible [38].

3.2.2. Monitoring the Treatment of Malignant Tumor Metastases

Central Nervous System Metastases of Myeloproliferative Malignancies

The involvement of the CNS presents a major challenge in the therapy of leukemias. Adult patients present with CNS leukemia in approximately 5% of acute leukemia cases, while CNS involvement occurs in about every third pediatric patient presenting with a relapse [99]. The risk of malignant cell penetration through the blood–brain barrier is especially high in Ph + B-cell precursor acute lymphoid leukemias (ALL) [100]. The prevention of CNS involvement in acute leukemias and the efficient treatment of established CNS leukemias are, therefore, of considerable importance and have an impact on the overall survival.

The poor penetration of the blood–brain barrier by imatinib, the first marketed tyrosine kinase inhibitor drug, was first mentioned in 2002 [15,16]. The total imatinib concentrations were 1.57 μg/mL and 0.017 μg/mL in the plasma and CSF samples of a young female adult diagnosed with Ph + ALL [16]. The size of the unbound fraction of imatinib was later established to be around 5% (4.3–6.5%) in healthy humans and in acute myeloid leukemia patients. By applying this percentage, the CSF-UPR of imatinib in this patient can be estimated as 21.7%. While the authors concluded that the distribution of imatinib into CSF was extremely poor, the consideration of the unbound fraction as the basis of the evaluation of blood–brain-barrier penetration delivers a more appreciable penetration rate [101].

On five separate days in an 11-day period, measurable imatinib concentrations were found in the CSF and plasma samples of a male Ph + CML patient who was in a lymphoid blast crisis after achieving complete cytogenic remission in the bone marrow following more than eight months of imatinib therapy, but had developed an isolated neoplastic meningitis. The authors concluded that imatinib CSF concentrations were not sufficient to inhibit 50% of BCR/ABL tyrosine kinase, and assume that the reason underlying the poor penetration of imatinib is its affinity to p-glycoprotein, a protein responsible for multi-drug resistance. Nevertheless, total imatinib concentrations were evaluated, and by calculating its unbound plasma concentrations, imatinib CSF-UPR's can be established as 7.7–56.2% [15]. Further investigations confirmed these findings. Imatinib CSF-TPR was 2.6% in a patient diagnosed with a CSF lymphoid blast crisis, while displaying a major cytogenic response in the bone marrow after 16 months of imatinib treatment. This corresponds to a calculated CSF-UPR of 52.6% [17]. In a randomized, multicenter phase 2 trial, plasma and CSF samples were collected from 17 BCR/ABL + ALL subjects with or without meningeosis and receiving imatinib. The CSF-TPRs were 1.8%. [18]. Imatinib CSF and plasma concentrations were further evaluated in parallel in four adult subjects of a multicenter clinical trial. One of the subjects was a biphenotypic Ph + CML patient, while the other three had been diagnosed with Ph + ALL. The CSF concentrations (mean: 0.044 μg/mL) were 74-fold lower than total plasma concentrations (3.27 μg/mL), corresponding to a CSF-UPR of 26.9% [19].

Dasatinib concentrations were below the detection limit in the CSF of a female adult patient treated with Ph + ALL and an extramedullary and meningeal relapse following bone marrow transplantation. The trough plasma dasatinib concentration was 32 ng/mL

(CSF-TPR: 0.23–1.5%) [27]. Following the detection of large individual variability in the systemic exposure to dasatinib, Gong et al. measured pairs of the CSF and plasma concentrations of the substance in five Ph + ALL adult patients after giving doses of 100 mg or 140 mg. Only two pairs of samples contained dasatinib in quantifiable concentrations in both media. The CSF-TPRs were 0.75% and 1.42%, while the calculated CSF-UPRs were 18.7% and 37.2% [28].

Four leukemia patients (three diagnosed with Ph + ALL and one with Ph + CML and a blast crisis), all with CNS relapse after allogeneic stem cell transplantation, received nilotinib (Tasigna®). Seventeen matched pairs of CSF and plasma samples were collected. The CSF-UPRs were calculated by taking a 98% protein binding rate into account. The calculated concentration ratios were 12%, 20%, 30%, and 68%, pointing to large individual differences in the availability of the drug [29]. In a group comprising 30 Ph + ALL patients aged 15 years or older, only non-quantifiable traces of nilotinib were found in the CSF samples collected [30].

The penetration of the selective BCL2-inhibitor venetoclax (Venclyxto®) through the blood–brain barrier was also poor; however, it corresponded to the in vitro IC_{50} of the drug in an adult, male chronic lymphocytic leukemia patient diagnosed with trisomy 12, IGHV unmutated (VH4L) chronic lymphoid leukemia and experiencing a CNS relapse. Time-matched pairs of plasma and CSF samples were assayed after their collection in steady state, after 2 h and 23 h of drug intake, with 0.23% and 2.89% concentration ratios obtained. The unbound fraction of venetoclax is smaller than 1% of the total circulating amount; therefore, the CSF concentrations corresponded to approximately 10–29% of the unbound plasma levels [95]. Venetoclax concentrations were evaluated 23, 30, and 37 days after initiating treatment in another male adult patient presenting with a complete remission in the bone marrow after hematopoietic stem cell transplant, but with a blast crisis detected in the CNS, and formerly receiving other chemotherapy. The CSF-TPRs were 0.32–0.40%, corresponding to CSF-UPRs of at least 32–40% [96].

An extremely low CSF concentration (0.1 ng/mL) of ponatinib (Iclusig®), another very heavily (> 99%) protein-bound drug, was observed in a 3-year old girl diagnosed with Ph + acute lymphoblastic leukemia which had been confirmed to have penetrated the CNS [37].

Central Nervous System Metastases of Non Small-Cell Lung Cancer

The first manuscript discussing the quantitation of OACDs in CSF for monitoring their efficacy regarding the treatment of the CNS metastases of NSCLC was published on the epidermal growth factor receptor inhibitor gefitinib (Iressa®). This was a case report presenting a Japanese male patient diagnosed with NSCLC and developing carcinomatous meningitis. Ten days after the initiation of gefitinib treatment, the drug was assayed in serum and in CSF before and 2 h after the intake of 250 mg drug. At both time points, the observed CSF concentrations were negligible, 0.9 nmol/L, while serum concentrations of 117 and 132 nmol/L were attained. Assuming a 97% protein binding rate, this corresponds to CSF/unbound serum concentration ratios of 22.7% and 25.6% [39,102]. Interestingly, significant positive linear correlations of gefitinib CSF and plasma levels were revealed in multiple research works (Figure 3) [40–42]. In contrast, the results of a phase 1 open-label trial of a novel, high-dose gefitinib treatment conducted with the involvement of seven patients diagnosed with leptomeningeal metastases of NSCLC showed that this approach did not result in an improved penetration of gefitinib into the CSF [43]. Evidence exists for supporting that the low penetration rate of gefitinib may be increased by whole-brain radiotherapy, an intervention considered to be an efficient strategy to improve blood–brain barrier permeability [41]. However, contrasting results have also been published [44]. A direct comparison of the concentrations of gefitinib and erlotinib, which have similar chemical structures, in the CSF of patients diagnosed with leptomeningeal metastases, resulted in the conclusion that erlotinib attained higher molar concentrations and a higher rate of penetration into the CNS [45].

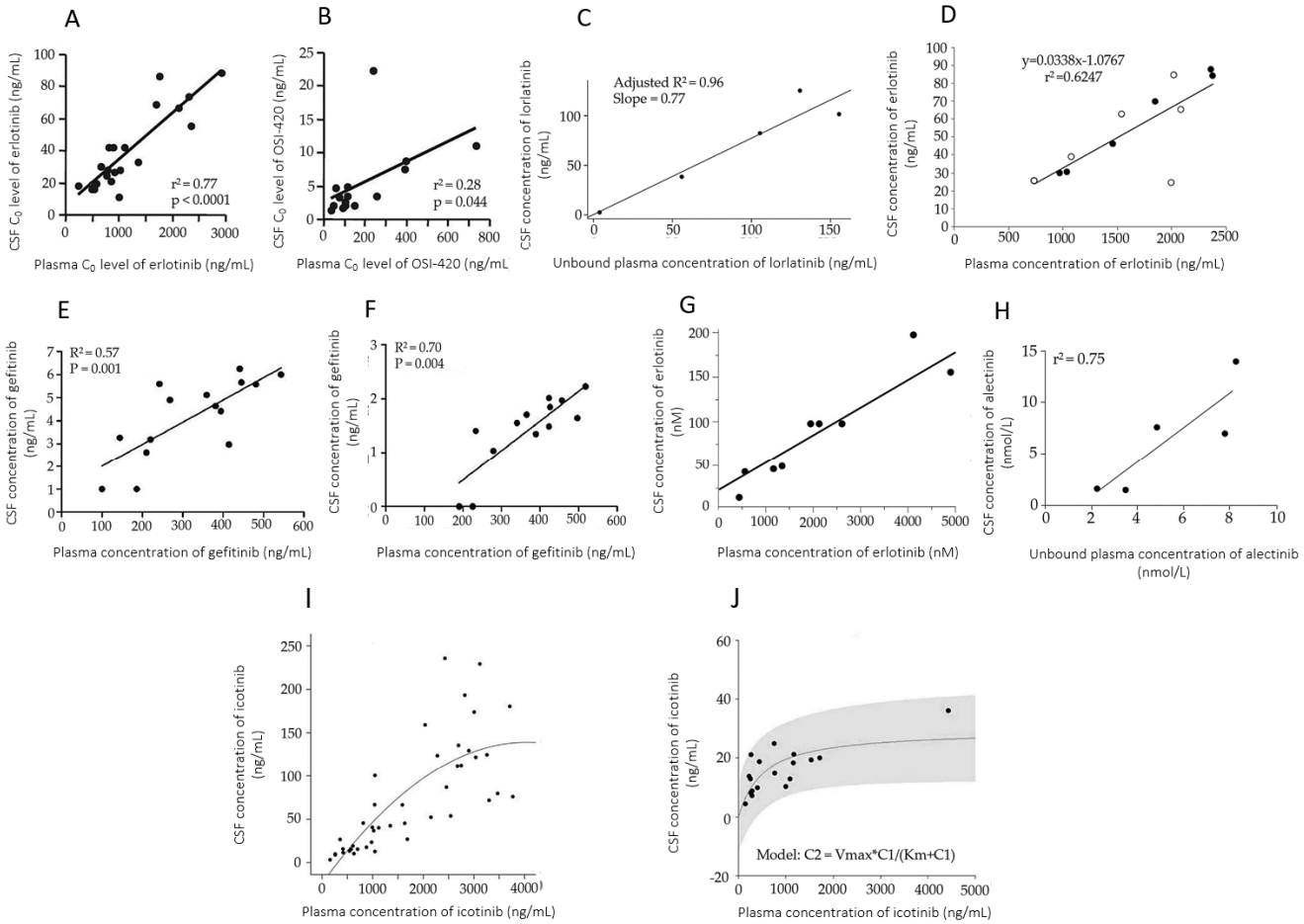

Figure 3. Relationships of the concentrations of various orally administered, small-molecule anticancer drugs with specific cellular protein targets in serum/plasma and in cerebrospinal fluid (CSF). (**A**) Erlotinib in plasma and in CSF, trough samples were drawn. (**B**) O-desmethyl-erlotinib (OSI-420) in plasma and in CSF, trough samples were drawn. (**C**) Unbound alectinib in plasma and in CSF. (**D**,**E**) Gefitinib in plasma and in CSF. (**F**) Unbound lorlatinib in plasma and in CSF. (**G**,**H**) Erlotinib in plasma and in CSF. (**I**) Gefitinib in plasma and in CSF, a Michaelis–Menten equation has been fitted to the data. (**J**) Icotinib in plasma and in CSF [50,61–64,70,77,83]. Licenses or permissions to reproduce the graphs have been granted by the copyright holders.

Two years after the publication of the first measurement of gefitinib concentrations in CSF, erlotinib concentrations were evaluated in three lung adenocarcinoma patients developing leptomeningeal metastases during gefitinib therapy. Twenty-eight days after switching to erlotinib, clinical improvement was observed, accompanied by 2.5–13.3% CSF-TPRs, corresponding to CSF-UPRs of 36–190% [50,97]. Four cases of Asian female adult NSCLC patients who had developed adenocarcinoma as a CNS metastasis and started to receive 150 mg erlotinib once daily were described by Togashi et al. Matched pairs of CSF and plasma samples were collected on day 8 of the treatment. Similar penetration of the drug and its active metabolite OSI-420 into the CSF was found. The authors provided the CSF-TPRs and the CSF concentrations, which allows the calculation of total and unbound plasma concentrations, as well as CSF-UPRs (45.7–110%). The efficiency of erlotinib to penetrate the blood–brain barrier was concluded to be higher than that of gefitinib, and allows the effective treatment of EGFR wild-type cases as well [51]. Yet another study involving six adult NSCLC patients with brain metastases confirmed that erlotinib could reach a mean penetration rate of 4.4%, corresponding to a CSF-UPR of 47.2%. The CSF concentrations of the drug were associated with the outcome, with the highest levels attained in patients showing partial response to therapy, and the lowest seen in those with

progression [52]. At steady state, the CSF penetration rate of erlotinib was determined as 5.6% (corresponding to a CSF-UPR of 77.0%) in a female patient diagnosed with stage IV lung cancer and stage I breast cancer, and receiving a combination of erlotinib and bevacizumab [53]. A considerably lower ratio of 1.15% (corresponding to a CSF-UPR of 16.4%) was observed, however, in a woman with stage IV NSCLC and leptomeningeal metastasis and receiving 1500 mg erlotinib weekly [54]. A similarly low penetration rate of erlotinib (1.6–2.6%) was identified in six Chinese adult NSCLC patients with leptomeningeal metastasis refractory to gefitinib treatment. Three patients received premetrexed and cisplatin in addition to erlotinib, while the other three received only erlotinib. There was no difference in the penetration rates between the two patient groups. The calculated CSF-UPRs were 22.8–36.6% [55]. A very strong linear correlation was identified, at the same time, between plasma and CSF erlotinib concentrations [56]. This finding was also confirmed by another study (Figure 3) [57]. A phase 2 single arm trial was conducted to reveal the efficacy of erlotinib in stage IV NSCLC with leptomeningeal metastasis (LOGIK11001) by Nosaki et al. The primary endpoint was the cytological clearance rate, and the secondary endpoints were time to disease progression, overall survival, toxicity, and quality of life. Plasma and CSF concentrations of erlotinib were determined in single steady-state samples collected from 12 participants. The mean penetration rate was 2.9–12.1%, corresponding to CSF/unbound concentration ratios of 41.9–173%. Again, a good correlation was observed between the plasma and the CSF concentrations (R^2 = 0.6247), regardless of the cytological response Figure 3 [58].

In a comparative study conducted to evaluate the penetration rate of standard (150 mg/die and 250 mg/die, respectively, administered for seven days) versus pulsatile high-dose erlotinib (1500 mg on day eight and fifteen) and gefitinib (2500 mg/die from day eight to fifteen) in NSCLC patients with brain metastases who progressed on standard doses, both drugs attained higher concentrations in the CSF as a result of high-dose administration, with a constant CSF-TPR of 2% in the case of erlotinib, and a saturable penetration rate of gefitinib with no increases in CSF levels predicted for doses of 839 mg or higher (Figure 3). In addition, those undergoing whole-brain radiotherapy attained disproportionately higher CSF concentrations of the drugs. Adverse effects were more prevalent in patients receiving erlotinib, with the high doses of gefitinib being well tolerated [46].

The next drug assayed in the CSF was crizotinib (Xalkori®), with negligible blood–brain barrier penetration rates observed. A CSF-TPR of 0.26% (corresponding to a CSF-UPR of 2.89%, assuming a 9% unbound fraction of the drug) was found in a 29-year old Caucasian male diagnosed with stage IV NSCLC and treated first with cisplatin plus pemetrexed, then with erlotinib, and finally with crizotinib. The attained CSF concentration was substantially lower than the established 50% inhibitory concentration (IC_{50}) required to inhibit mutant cell lines against which crizotinib had been tested [70,103]. In two ALK-positive male adult NSCLC patients developing brain metastases, crizotinib CSF/total serum concentration ratio was 0.06% and 0.1%, corresponding to CSF/unbound serum concentration ratios of 0.66% and 1.1%, respectively [71]. Three CSF samples of a 60-year-old male patient diagnosed with ALK-rearrangement-positive NSCLC and receiving 250 mg crizotinib twice daily after developing brain metastases were assayed for crizotinib at one-week intervals following whole brain radiotherapy (an additional sample was processed before conducting WBRT). Crizotinib was undetectable in the samples collected before and one week after WBRT, while 6.2 and 6.3 ng/mL concentrations were found after two and three weeks, respectively, accounting for 3.5% and 2.2% of the total, and for 39.0% and 24.5% unbound plasma concentrations [72]. In another male patient diagnosed with stage IIA lung adenocarcinoma and brain metastasis, a CSF-TPR of 2.6% (corresponding to a CSF-UPR of 30.4%) was achieved at a single sampling point following WBRT. The CNS symptoms diminished, and the negativity of CSF to malignant cells was confirmed. Comparing this result to earlier findings yielded the conclusion that WBRT may enhance the CNS penetration and the clinical efficacy of crizotinib [73].

In a single-arm, open-label, multicenter phase 1/2 study conducted with the involvement of adult subjects with histologically confirmed, locally advanced or metastatic NSCLC with crizotinib-resistant ALK-positive rearrangement and receiving 600 mg or 900 mg alectinib (Alecensa®) twice a day in the fixed dose phase, five matched alectinib CSF-plasma concentration pairs were obtained. The CSF concentrations not only showed positive correlation with the unbound plasma fraction of alectinib (which corresponded to 0.3% of the total amount), but were also equivalent or higher. The extrapolated trough CSF concentration exceeded the reported in vitro IC_{50} of alectinib for ALK inhibition [75]. In an institutional case series comprising eleven adult subjects diagnosed with histologically confirmed ALK-positive NSCLC and receiving 600 mg alectinib twice daily until disease progression, unacceptable toxicity or withdrawal of consent, matched CSF-serum concentration pairs were obtained in two patients in the second month of alectinib therapy. The total serum concentrations were 694 ng/mL and 707 ng/mL, both corresponding to 2.1 ng/mL unbound serum concentrations. The calculated CSF/unbound serum concentration ratios were, therefore, 100% and 30% in the two patients [76].

The evaluation of afatinib (Giotrif®) CSF levels was first described in a woman diagnosed with stage IV adenocarcinoma of the lung with an underlying mutation of the EGFR gene. Two CSF samples were assayed, and afatinib was found to attain a penetration rate lower than 1%, with a calculated CSF-UPR of 13.9% when 95% protein binding rate of the drug is assumed [59,104]. A remarkable case of a female patient diagnosed ten years earlier reporting with stage IV adenocarcinoma of the lung with an EGFR mutation was also described. Afatinib (40 mg/die, deescalated to 30 mg/die after four months) was administered as the eighth line of treatment following interchanging periods of progression and remission. Trough plasma and CSF concentrations were assayed at three, four and five months following the initiation of afatinib dosing. The CSF-TPR's were 0.28–0.40%, while the calculated CSF-UPRs are 7.5–8.8%. The total plasma concentrations were 19.0–33.4 ng/mL, which can be measured with relative convenience using liquid chromatography–tandem mass spectrometry (LC–MS/MS), but the obtained CSF levels of 0.05–0.14 ng/mL clearly indicate that assaying afatinib in the CSF is a major analytical challenge [60]. Further, a prospective multicenter trial was conducted with the involvement of 11 patients diagnosed with EGFR mutation-positive NSCLC with leptomeningeal carcinomatosis and with the aim of evaluating the CSF penetration rates and the clinical efficacy of afatinib. Participants received 40 mg afatinib once a day. On day eight, the trough concentrations were assayed in plasma and in CSF. Afatinib could be quantitated in the CSF samples of eight subjects (72.7%). The CSF-TPRs were 0.1–3.1%, with a single case of 9.3% which resulted from an unusually low plasma concentration (corresponding to 44.4% of the next value in the ranked series of the measured concentrations), accompanied by the second-highest CSF concentration. This corresponds to CSF-UPRs of 2.1–185%. It was concluded that the ability of EGFR tyrosine kinase inhibitors to penetrate the CSF should be assessed along with the efficacy of the drug against tumors with particular mutation types [61].

The penetration of icotinib (Conmana®), an OACD currently approved in China, into CSF was first evaluated in a phase 2 clinical study involving ten patients following the administration of 125 mg in a three-times-per-day regime. Meanwhile, WBRT was delivered in 3-Gy fractions once per day, five days per week, to a total dose of 30 Gy. The mean total plasma concentrations were 940.6±503.8 ng/mL (corresponding to 47.0±25.2 ng/mL unbound concentrations), while the mean CSF concentrations were 11.6±9.1 ng/mL in samples collected two hours after drug intake. The CSF-TPR was 1.4±1.1%, and the mean CSF-UPR can be calculated as 24.7% [66]. The impact of WBRT on the CSF penetration of icotinib was directly investigated in fifteen patients receiving escalating dose levels (125–352 mg) three times a day. Blood and CSF samples were collected immediately before beginning the WBRT treatment (applied in fixed doses of 37.5 Gy, five times a week, lasting for three weeks), immediately after terminating WBRT therapy, and four weeks into the follow-up period. The

CSF-TPR's of icotinib were 2.4–3.7% in a dose range of 125–500 mg (peculiarly, 6.1% at 375 mg), while the CSF-UPR can be calculated as 52.0–58.0% (130% at 375 mg) [67].

The CSF concentrations of osimertinib were first measured in an NSCLC patient with leptomeningeal metastases and EGFR-TKI resistance. A poor penetration rate (1.47%) was observed [62]. In an open-label, single-arm, multicenter, prospective study (APOLLO), twelve adult patients donated matched blood and CSF samples. The evaluation of osimertinib concentrations was based on the unbound drug fractions. A strong linear correlation was found between blood and CSF levels (r = 0.8306). Based on these calculations, the median CSF-UPR of osimertinib was 31.7% (19.8–57.8%) after six weeks of treatment [63]. In a phase 2 study involving radiotherapy-naive adult patients diagnosed with T790M EGFR mutation-positive NSCLC and CNS metastasis, who had been previously treated with EGFR tyrosine kinase inhibitors, the plasma and CSF concentrations of osimertinib and its pharmacologically active metabolite were assessed in seven participants on day twenty-two of osimertinib therapy. The CSF-TPRs of the drug and the metabolite were 0.79% (0.43–1.32%) and 0.53% (0.31–0.64%), respectively, corresponding to 15.8% (8.6–26.4%) in the case of the parent drug by assuming 99% plasma protein binding rate [64].

Tepotinib plasma and CSF concentrations were evaluated in a male adult patient diagnosed with stage IIIA lung adenocarcinoma. EGFR mutation and ALK fusion gene were not detected. Following right lung pneumonectomy, a brain metastasis was identified in the left cerebrum which later progressed to leptomeningeal metastasis and hydrocephalus in spite of treatment with cisplatin and pemetrexed. A tepotinib regimen (500 mg/die) was started. On day 20 of therapy, the tepotinib CSF-TPR achieved 1.83% in the matched samples collected four hours post-dose. The attained concentration was judged to have exceeded the IC_{50} [90]. In a female patient diagnosed with NSCLC with MET exon 14 skipping mutation and with brain metastases, and having received WBRT, remarkable clinical improvement was achieved after a 1-month treatment with tepotinib (500 mg/die). The penetration rates of tepotinib into the CSF at two, four and eight weeks of therapy were 1.19%, 1.42%, and 1.73%, respectively. By taking the 98% protein binding rate of tepotinib into account, the CSF-UPRs can be calculated as 60.0%, 71.1%, and 86.6%, respectively, based on the data described by the authors [91].

Lorlatinib (Lorviqua®) was monitored in the CSF in an ongoing, open-arm, multicenter phase 1/2 trial with the aim to further investigate the penetration of the drug into the CNS. Five patients with suspected or confirmed leptomeningeal carcinomatosis not visualized on magnetic resonance imaging, or carcinomatous meningitis, were included. Samples were collected at baseline and a later yet undefined point of the study. The CSF/plasma unbound lorlatinib concentration ratios were 61–96%, and showed very strong correlation (adjusted $r^2 = 0.96$). The CSF/total plasma lorlatinib concentration ratios were 21–33%. The results indicated that lorlatinib concentrations exceeded the minimum efficacy concentrations in all of the patients regarding wild-type anaplastic lymphoma kinase (ALK) and the L1196M ALK resistance mutation. The authors concluded that this supported the broad coverage of these mutations, and, in approximately one-third of patients, the coverage of the G1202R ALK resistance mutation [77].

The CSF concentrations of pralsetinib (Gavreto®) and osimertinib were investigated in an adult patient with an EGFR-mutant NSCLC with acquired RET fusions and meningeal metastasis after four months of co-treatment with pralsetinib and osimertinib. Pralsetinib attained concentrations of 91.3 μmol/L and 0.705 μmol/L in plasma and CSF, respectively (ratio: 0.77%, corresponding to a CSF-UPR of 15.4%). Osimertinib concentrations were 2.149 μmol/l and 0.0237 μmol/L, respectively (ratio: 1.10%, corresponding to a CSF-UPR of 110%). Despite the lower CSF/unbound concentration ratios, pralsetinib levels were judged to be sufficiently high both in plasma and in CSF to inhibit the CCDC6-RET-mutated protein, indicating that pralsetinib is more efficient than osimertinib to treat this mutation [65].

Metastases of Other Malignancies in the Central Nervous System

Lapatinib inhibits both EGFR and HER2; therefore, it has activity against brain metastases developing from HER2-positive metastatic breast cancer. This activity may be enhanced by combining lapatinib with capecitabine. Nevertheless, 0.9–1.3% of CSF-TPRs of lapatinib were observed in two adult female patients diagnosed with HER2-positive (one HR-negative and one HR-positive) ductal carcinoma yielding CNS metastases. The CSF-UPRs can be calculated as 8.6–12.9% in these two patients [83,105]. Neratinib, another HER2 tyrosine kinase inhibitor, was absent (<1.50 ng/mL) in the CSF samples of three adult HER2-positive breast cancer patients [84]. Vemurafenib was, on the other hand, quantitated successfully in the matched CSF and plasma samples of patients treated with the drug in a dose of 960 mg, given twice daily, for brain metastatic BRAF-V600 mutated melanoma. The CSF-UPRs were 28–250%, assuming a 99% protein binding rate [68,106].

Malignant Ascites

Malignant ascites is a rare condition secondary to abdominal malignancies [107]. In an elderly adult patient diagnosed with papillary renal cell carcinoma and undergoing treatment first with pazopanib (Votrient®), then with sunitinib, concentrations of the administered OACD were monitored in plasma and in ascitic fluid. The concentrations measured in the ascitic fluid were equivalent to or higher than those assayed in the systemic circulation, and, following an early phase with sufficient plasma levels, systemic concentrations became subtherapeutic [88]. The ascited fluid concentrations of the drugs remained high after discontinuation of treatment. While the underlying reason of the accumulation of these drugs in the ascitic fluid is not evident, it was proposed that it acted as a sink of the administered OACDs, while the strong binding of pazopanib and sunitinib to albumin may have facilitated the extravasation of the drugs.

3.2.3. Monitoring OACDs to Control Toxicity

Monitoring the Exposure of the Infant to the Drug during Breastfeeding

CML occurs very rarely during pregnancy, at an estimated rate of 1:750 000. Imatinib is employed for treating Ph + cases developing during pregnancy, an approach which may cause harm to the fetus and the newborn. Assaying the drug in breast milk is valuable for characterizing the exposure of the infant. The first appearance of the measurement of imatinib in breast milk was the description of a case with the imatinib concentrations being approximately 60% of the lower limit of the currently accepted blood reference range (1000–3000 ng/mL). Its pharmacologically active metabolite, however, displayed accumulation in breast milk [20]. Another patient on 400 mg once-daily imatinib donated blood and breast milk samples on a single day, 1, 2, 3, 4, and 9 h after drug intake. The concentrations of imatinib and its active metabolite in milk reached 0.5 and 0.9 of those found in plasma, respectively. The authors concluded that the maximum intake of the infant was 3 mg imatinib/day, and should be considered safe [21]. A case described two years later described a Ph + CML patient receiving the same dose resulting in complete hematological and cytogenetic remission. Blood was drawn on day 2, while breast milk was collected on days 7, 14, 15, and 16 postpartum. The imatinib concentrations measured both in plasma (2385 ng/mL) and in breast milk (1430–2623 ng/mL) were in the therapeutic range. The authors concluded that, since the long-term effects of imatinib on infants are unknown, breastfeeding is not advisable when imatinib is administered [22]. This conclusion was confirmed by the presenters of another case when imatinib treatment was initiated immediately after delivery. While the concentrations of imatinib were relatively low in breast milk, those of the active metabolite attained threefold concentrations of those measured in plasma, clearly displaying accumulation [23]. Yet in another patient, the concentrations of imatinib and the active metabolite were measured in breast milk 99 h after the last intake. The attained concentrations were 19 ng/mL and 600 ng/mL, respectively, pointing to a very significant accumulation of the metabolite in breast milk. Neonatal urine was also evaluated, with 90 ng/mL imatinib and 165 ng/mL active metabolite

concentrations detected. These results indicate that the infant was exposed to the drug, and, to an even greater extent, to the metabolite. This case raises the clinical relevance of assessing the concentrations of oral anticancer medications taken during pregnancy in neonatal urine for evaluating the potential impacts on the newborns [24]. In the most recently published case report the milk/plasma ratio of imatinib attained 0.35 at 5 days postpartum. Blood was also collected from the infant on the same day to reveal a 27-ng/mL concentration of imatinib, which was considered to be safe by the authors [25].

Everolimus is primarily administered as an immunosuppressant based on its ability to inhibit the mammalian target of rapamycin (mTOR) functional complex mTORC1. In a heart-transplanted patient, everolimus therapy was continued during pregnancy and following delivery. At 48 h postpartum, the drug was not detectable in the colostrum, indicating that the evaluation of the immunosuppression of the newborn had to be based on its prepartum administration [81].

Monitoring Other Types of Toxicity

Oral anticancer medications have serious adverse effects, including low blood cell counts, resulting in an increased susceptibility to infections and, potentially, bleeding, as well as dermal and gastrointestinal symptoms. Several of these may prompt the discontinuation of therapy. Efforts have therefore been made to identify the relationships between the presentation of the drugs in non-targeted organs and fluid compartments, and the development of adverse symptoms.

Pleural effusion may be induced by tyrosine kinase inhibitors. In a young male adult patient who had developed pleural effusion from dasatinib earlier, nilotinib therapy again led to the formation of the effusate. The measured nilotinib concentrations were 927 ng/mL and 2092 ng/mL in plasma and in the pleural effusate, respectively, clearly indicating the accumulation of nilotinib in the latter medium. Other possible causes, including malignancy, were excluded. The severity of this adverse effect is shown by the fact that, eventually, performing endotracheal intubation and left thoracic drainage was required [31].

The relationship between the occurrence of stomatitis and everolimus (Afinitor®) levels in saliva was investigated in 11 cancer patients receiving everolimus in a once-daily (10 mg) or twice-daily (2 × 5 mg) regime. Both the plasma and saliva concentrations of the drug were higher in patients with stomatitis than in those who did not develop this condition. While the statistical significance of this difference was low, this result may indicate the utility of everolimus saliva assays concerning the prevention of the occurrence of stomatitis. Of note, the rate of the penetration of everolimus into saliva was extremely low (0.8%) with high interindividual variability (67.7%) [82].

Imatinib has been demonstrated to cross the brain–testis barrier and to reach equilibrium. Imatinib concentrations reached concentrations of 1471 ± 570 ng/mL and 1397±425 ng/mL in the plasma and the semen of eleven male CML patients, respectively. The clinical relevance of the assay was confirmed by the finding that the number, the survival rate, and the activity of sperms were reduced in these patients. Reproductive hormone structures and sex hormone concentrations were unaffected [26].

Panobinostat was not detected in the CSF of patients diagnosed with human immunodeficiency virus (HIV) infection [92]. In addition, it was not present in the CSF samples of pediatric patients with refractory hematological malignancies [93]. It was concluded in these works that panobinostat did not cause CNS symptoms.

3.2.4. Monitoring the Treatment of Mental Disorders

It is increasingly acknowledged that certain OACDs may be effective against neurodegenerative and autoimmune diseases [9,108]. Nilotinib, a BCR-ABL tyrosine kinase inhibitor, has been investigated in multiple cases as a medication against mental disorders, such as Parkinson's disease and Alzheimer's disease [109,110]. The rationale of these indications is that nilotinib leads to the degradation of misfolded α-synuclein by autophagy [111]. In addition, in preclinical studies, nilotinib increased dopaminergic neuron survival in the

CNS, and improved motor and cognitive outcomes in in vivo models. Abl inhibition has been demonstrated to reduce oxidative stress, and to protect dopaminergic neurons [112].

In an open label pilot study conducted to investigate the safety and tolerability of two doses of nilotinib, the drug penetrated readily into the CSF, and remained detectable there for five hours, when administered to stage 3–5 Parkinson's disease patients in low doses (150–300 mg/die). This was accompanied by a steady increase in plasma concentrations. The CSF-TPR was higher when the lower dose was administered, with a comparable level of Abl inhibition [32]. Further research revealed that the penetration of nilotinib into CSF was dose-dependent in the dose range 150–400 mg, with 200 mg exerting optimal effects. Again, the CSF-TPR was very similar at various doses (0.5–1.0%). Nevertheless, avoiding higher doses was recommended since more side- and off-target effects were detected in the CNS [33]. A phase 2 randomized clinical trial was published with the involvement of 75 participants, 50 of whom received nilotinib. The CSF-TPR was considerably lower, 0.33% and 0.53% after applying 150 mg and 300 mg nilotinib, respectively [34].

The most recent evaluation of nilotinib delivered results which contradicted some key findings of the above works, although the safety and tolerability of low-dose nilotinib was still acceptable. The measured CSF penetration was in concert with previous findings. This was a six-month, multicenter, randomized, parallel-group, double-blind, placebo-controlled trial conducted with the involvement of 76 participants, 51 of whom received nilotinib (150 mg or 300 mg pro die). Based on the evaluation of the geometric means of measured drug concentrations, the administration of 150 mg or 300 mg resulted in 0.61–1.10 ng/mL and 1.10–1.90 ng/mL peak CSF nilotinib concentrations along with 343.3–524.4 ng/mL and 485.8–621.2 ng/mL peak serum concentrations, respectively, after three months of treatment. This corresponded to 0.16–0.23% and 0.20–0.32% CSF penetration rates, respectively. In contrast to the favorable outcomes of the earlier studies, this trial ended with the conclusion that the low penetration rates were associated with no treatment-related alterations of dopamine metabolites in the CSF. Therefore, the changes in the protein biomarkers (α-synuclein, phospho-α-synuclein, and phospho-tau) alone provided weak evidence of the clinical efficacy of nilotinib treatment [35].

In animal models of neurodegeneration, nilotinib promoted the degradation of proteins Aβ/amyloid protein and the microtubule-associated protein tau [113]. This result prompted a phase 2, randomized, double-blind, placebo-controlled study to evaluate the effects of nilotinib in mild to moderate Alzheimer's disease. The label arm received 150 mg nilotinib daily for 6 months, followed by 300 mg daily for another 6 months. The ratios of the mean CSF and plasma concentrations were 0.29% and 0.27% at 150 mg and 300 mg doses, respectively. The ratios of the areas under the concentration-time curves were 0.30% and 0.33%, respectively [36].

The above works included the detailed evaluation of quantitative changes in the pharmacodynamic variables, such as microtubule-associated protein tau or amyloid proteins. Although the penetration rate of nilotinib into the CSF was very low, these were associated with statistically significant pharmacodynamic improvement and measurable clinical efficacy.

3.3. Bioanalytical Methods of Monitoring OACD Concentrations in Peripheral Fluid Spaces

All of the described bioanalytical methods relied on chromatographic separation using high-performance or ultra-high performance liquid chromatography. Mass spectrometry was chosen for detection by most authors, but multiple examples of applying ultraviolet–visible (UV–VIS) light absorbance detection for the assessment of afatinib, erlotinib, gefitinib, imatinib, nilotinib, and vemurafenib were found.

In the majority of cases, sample pretreatment consisted of deproteinization. The removal of proteins was performed using organic solvents (acetonitrile—ceritinib [74], erlotinib [47], gefitinib [45], ibrutinib [85,86], imatinib [16,20–22], ponatinib [37], regorafenib [89], ribociclib [78,79], vemurafenib [68], venetoclax [95], zanubrutinib [86]; acetonitrile-methanol 1:1—dasatinib [27], imatinib [14], nilotinib [32–34,36]; acetonitrile-methanol 1:4—erlotinib [54];

acetonitrile-methanol 10:1—zanubrutinib [87]; methanol—alectinib [76], dabrafenib [69], dasatinib [12], erlotinib [46], nintedanib [12], panobinosat [12], regorafenib [12], ribociclib [12], trametinib [69], vorinostat [12]), and, in a single case, the aqueous dilution of perchloric acid (imatinib [18]). The deproteinization methodology was not described by Xing et al. for the monitoring of osimertinib in CSF [63]. PBMC pellets and breast milk were pretreated with acetonitrile-methanol [14] and acetonitrile [20–22], respectively, as part of the employed imatinib assays. In all other cases, deproteinization was applied to CSF samples.

Liquid–liquid extraction was applied employing methyl-*tert*-butylether for extracting afatinib [60], erlotinib [49,51,52,56,57], everolimus [82] and gefitinib [39–43]. Acetonitrile-n-butylchloride 1:4 was used for extracting erlotinib [50]. Erlotinib [45] and venetoclax [96] were extracted by applying hexane-ethylacetate 1:1. In a single case, the method of LLE was not detailed [58]. Most applications had been developed for pretreating CSF samples. Everolimus was recovered from saliva [82], while, in one case, erlotinib was extracted from pleural effusate.

Solid phase extraction with a polymeric reversed-phase sorbent was employed for extracting crizotinib from CSF [71] and imatinib from leukocytes [13]. Afatinib was recovered from CSF using an octadecyl silica loading [61]. The extraction of vismodegib from CSF was feased by employing a strong mixed-mode cation exchange sorbent [94]. Gefitinib was recovered from CSF using an unspecified cartridge [44]. Equilibrium dialysis was employed to assess the unbound concentrations of ceritinib, ribociclib, and vismodegib directly in plasma [74,78,79,84].

In addition, special pretreatment procedures were described by a few authors. Imatinib was recovered from peripheral blood mononuclear cells by sonicating the defrosted pellet in an ice-water bath, followed by centrifugation, counting cells in the supernatant, washing with acetonitrile-methanol 1:1 and solvent exchange [14]. Ribociclib was assayed in CSF after dilution with methanol-water 1:1, acidification with water containing 0.2% formic acid, and centrifugation [80]. Automated sample preparation was employed as part of the analysis of everolimus [81], imatinib [18], and nilotinib [29].

Finally, afatinib and ribociclib were assayed in CSF without any sample pretreatment [59,80].

Octadecyl silica stationary phases were selected by most authors for the liquid chromatographic separation of OACDs. Octyl silica was used for the separation of imatinib, ribociclib and vemurafenib [13,16,68,80]. There are isolated examples of the application of amide (ribociclib), polystyrol-divinylbenzene (imatinib), phenyl (gefitinib), and pentafluorophenyl (ponatinib, regorafenib) phases [18,37,40,45,69,78,79,89]. In a single case of ibrutinib measurement, a nano-high performance liquid chromatography system was employed [85].

Mass spectrometric detection was performed primarily with electrospray ionization. Nevertheless, multiple examples of applying atmospheric pressure chemical ionization for the quantitation of gefitinib [39,40,42,43], imatinib [16], and erlotinib [47] in CSF were found. Bioanalytical methods developed by Bakhtiar et al., Jones et al., and Zhao et al. were adapted in these works [114–116]. The employed mass analyzers were triple quadrupole systems and quadrupole- linear ion trap hybrids. Ibrutinib was assayed using high-resolution mass spectrometry [85]. None of the described methods mentioned the application of negative polarity mass spectrometry. Ultraviolet–visible light absorbance detection was used for the quantitation of afatinib in CSF (254 nm) [61], erlotinib in CSF (345 nm or 348 nm) [50–52,56,57] and in pleural effusate (345 nm) [49], gefitinib in CSF (344 nm) [44], imatinib in CSF (260 nm) [18] and in leukocytes (261 nm) [13], as well as nilotinib (258 nm) [29] and vemurafenib (249 nm) [68] in CSF.

Most articles reported the use of an isotopically labeled internal standard when employing mass spectrometry for detection. Non-labeled substances were chosen for assaying afatinib (internal standard: imatinib) [60], dasatinib (carbamazepine and quinoxaline) [12,27], erlotinib (midazolam and desmethyl erlotinib) [45–47], gefitinib (vandetanib) [41], ibrutinib (propranolol) [86], imatinib (carbamazepine and quinoxaline) [12,14], nintedanib, panobinostat, regorafenib and vorinostat (carbamazepine) [12], and zanubrutinib (tolbutamide) [86]. These analyses were conducted on CSF samples, except for a single

example of assaying imatinib in peripheral blood mononunclar cells [14]. The quantitation was performed without introducing an internal standard for monitoring afatinib in CSF [61], erlotinib in pleural effusate [49] and in CSF [51,52,56,57], and imatinib in breast milk [21] and in CSF [18]. UV–VIS detection was employed in all of these reports, except for one where tandem mass spectrometry was used with positive electrospray ionization [21].

Detailed information on the methods employed for monitoring OACDs in peripheral fluid spaces is provided in Table 4. Eight of the eighty-five publications (9.4%) failed to provide any methodological information or a reference to another manuscript describing the methodology employed for the quantitation of OACDs in peripheral fluid spaces. Altogether, 29 methodological publications were cited in the included manuscripts. The work of Jones et al. was cited by most included works [114]. Only five methodological works described the analysis of OACDs in peripheral fluid spaces, namely CSF (three publications), colostrum (one publication), or PBMC (one publication). The rest of the cited methodological papers described the analysis of one or more OACDs in blood.

Table 4. Analytical approaches to monitoring the concentrations of orally administered, small-molecule anticancer medications with tumor-specific cellular protein targets in peripheral fluid spaces. CSF, cerebrospinal fluid; Deprot., deproteinization; FA, formic acid; IS, internal standard; LLE, liquid–liquid extraction; NS, not specified; PBMC, peripheral blood mononuclear cells; SPE, solid phase extraction; TFA, trifluoroacetic acid.

Drug	Matrix	Internal Standard	Chromatography			Mass Spectrometry			UV–VIS (nm)	Sample Preparation	Ref.
			Stationary Phase	Mobile Phases	Type of Separation	Ioniza-tion	Analyte ions	IS Ions			
Afatinib	CSF	Isotope-labeled afatinib	Reversed phase	NS	Gradient	ESI (+)	NS	NS	Not used	None	[59]
Afatinib	CSF	Imatinib	XBridge Shield RP18 (50 × 2.1 mm, 3.5 µm)	Acetonitrile (10 mmol/L ammonium hydroxide), water (1 mmol/L ammonium hydroxide), pH = 10.5	Isocratic (70:30)	ESI (+)	486.0 > 371.3	494.1 > 394.4	Not used	LLE	[60,117]
Afatinib	CSF	None	Inertsil ODS-2 (150 × 2.1 mm, 5 µm)	Water (0.1% ammonium acetate, pH = 8.5), acetonitrile, triethy-lamine	Isocratic (55:44:0.5)	Not applicable			254	SPE	[61]
Alectinib	CSF	Liquid chromatography–mass spectrometry was used.									[75]
Alectinib	CSF	Liquid chromatography–tandem mass spectrometry was used. Sample preparation consisted of deprot. with methanol.									[76]
Ceritinib	CSF	$^{13}C_6$-ceritinib	Acquity UPLC BEH C18 (50 × 2.1 mm, 1.7 µm)	Water (0.1% FA), methanol (0.1% FA)	Gradient	ESI (+)	558.0 > 433.0	564.3 > 438.9	Not used	Deprot.	[74,118]
Crizotinib	CSF	Liquid chromatography-tandem mass spectrometry was used.									[70]
Crizotinib	CSF	$^2H_5$,$^{13}C_2$-crizotinib	Discovery C18 (50 × 2.1 mm, 5 µm)	Water (0.3% FA), methanol (0.3% FA)	Gradient	ESI (+)	450.2 > 260.2	457.2 > 267.3	Not used	SPE	[71,119]
Crizotinib	CSF	Liquid chromatography-tandem mass spectrometry was used.									[72]
Crizotinib	CSF	No details of the employed analytical methodology are disclosed.									[73]
Dabrafenib	CSF	$^2H_9$-dabrafenib	XSelect HSS T3 (75 × 2.1 mm, 3.5 µm)	Water (2 mmol/L ammonium acetate, 0.1% FA), acetonitrile (0.1% FA)	Gradient	ESI (+)	520.1 > 292.0	529.1 > 316.2	Not used	Deprot.	[69,120]
Dasatinib	CSF	Carbamazepine	Nucleoshell C18 (150 × 3 mm, 2.7 µm)	Water (0.1% FA), methanol	Gradient	ESI (+)	488.17 > 232.1 488.17 > 193.1 488.17 > 161.0	237.1 > 194.2 237.1 > 165.1 237.1 > 121.1	Not used	Deprot.	[12]
Dasatinib	CSF	Quinoxaline	Atlantis C18 (150 × 4.6 mm, 5 µm)	Water (0.05% FA), acetonitrile (0.05% FA)	Gradient	ESI (+)	487.5	313.0	Not used	Deprot.	[27,121]
Dasatinib	CSF	$^2H_8$-dasatinib	Shim-Pack XR-ODSII (50 × 2 mm, 2.2 µm)	Water (0.1% FA), acetonitrile (0.1% FA)	Gradient	ESI (+)	488.0 > 401.0	496 > 406	Not used	NS	[28]
Erlotinib	CSF	Midazolam	C18 Luna (150 × 4.6 mm, 5 µm)	Acetonitrile, 5 mmol/L ammonium acetate	Isocratic (45:55)	ESI (+)	394.1 > 278.0 394.1 > 336.0	326.2 > 291.0	Not used	LLE	[45,122]

Table 4. *Cont.*

Drug	Matrix	Internal Standard	Chromatography			Mass Spectrometry			UV–VIS (nm)	Sample Preparation	Ref.
			Stationary Phase	Mobile Phases	Type of Separation	Ioniza-tion	Analyte ions	IS Ions			
Erlotinib	CSF	Desmethyl erlotinib	Zorbax C18 (150 × 3 mm, 1.8 μm)	Acetonitrile, water (15 mmol/L ammonium acetate)	Gradient	ESI (+)	394.5 > 278.1	313.8 > 243.9	Not used	Deprot.	[46,123]
Erlotinib	CSF	Midazolam	Xterra octadecylsilica (50 × 2.1 mm, 3.5 μm)	Acetonitrile (0.1% FA), water (0.1% FA)	Isocratic (70:30)	ESI (+)	394 > 278	326 > 286.1	Not used	Deprot.	[47,116]
Erlotinib	CSF	Liquid chromatography–tandem mass spectrometry were used.									[48]
Erlotinib	CSF	OSI-597	Nova-Pak C18 (150 × 3.9 mm, 4 μm)	Acetonitrile, water (pH = 2.0)	Isocratic (60:40)	Not applicable			348	LLE	[50,124]
Erlotinib	CSF	None	Symmetry C18 (150 × 4.6 mm, 5 μm)	Acetonitrile, 0.05 mol/L aqueous potassium phosphate (0.2% triethy-lamine, pH = 4.8)	Isocratic (42:58)	Not applicable			345	LLE	[51,52,56, 57,125]
Erlotinib	CSF	High-performance liquid chromatography was used.									[53]
Erlotinib	CSF	Deprot. with methanol-acetonitrile 1:4, v/v%. Liquid chromatography-tandem mass spectrometry was used.									[54]
Erlotinib	CSF	Liquid chromatography–tandem mass spectrometry was used.									[55]
Erlotinib	CSF	Liquid–liquid extraction and high-performance liquid chromatography with mass spectrometric detection was used.									[58]
Erlotinib	pleural effusate	None	Symmetry C18 (150 × 4.6 mm, 5 μm)	Acetonitrile, 0.05 mol/L aqueous potassium phosphate (0.2% triethy-lamine, pH = 4.8)	Isocratic (42:58)	Not applicable			345	LLE	[49,125]
Everolimus	Breast milk	$^{2}H_4$-everolimus	NS	NS	Gradient	ESI (+)	975.6 > 908.5	979.6 > 912.5	Not used	Online enrichment	[81,126]
Everolimus	Saliva	$^{13}C,^{2}H_3$-everolimus	Sunfire C18	Water (20 mmol/L ammonium formate), methanol	Gradient	NS	NS	NS	Not used	LLE	[82,127]
Gefitinib	CSF	$^{2}H_8$-gefitinib	XTerra phenyl (50 × 4.6 mm, 5 μm)	Water (0.1% ammonia), acetonitrile	Isocratic (30:70)	APCI (+)	447.2 > 128.0	455.4 > 136.0	Not used	LLE	[39,40,42, 43,114, 128]
Gefitinib	CSF	Vandetanib	Intersil ODS3 (150 × 2.1 mm, 3 μm)	Water (0.02 mol/L ammonium acetate), acetonitrile.	Isocratic (70:30)	ESI (+)	447.2 > 128.1	475.6 > 112.0	Not used	LLE	[41,114]
Gefitinib	CSF	Erlotinib	Zorbax Eclipse XDB-C18 (150 × 4.6 mm, 5 μm)	Water (0.1% triethy-lamine, pH = 4.8), acetonitrile	Gradient	Not applicable			344	SPE	[44,129]
Gefitinib	CSF	$^{2}H_8$-gefitinib	Xterra octadecylsilica (50 × 2.1 mm, 3.5 μm)	Acetonitrile (0.1% FA), water (0.1% FA)	Isocratic (70:30)	ESI (+)	447.1 > 128.0	455.1 > 136.0	Not used	Deprot.	[45,130]
Gefitinib	pleural and peritoneal effusate	Liquid chromatography–tandem mass spectrometry was used.									[38]
Ibrutinib	CSF	$^{2}H_5$-ibrutinib	nLC EASY-Spray (50 cm)	NS	Gradient	Not specified (+)	441.2034 > 138.0900	446.2347 > 138.0900	Not used	Deprot.	[85]
Ibrutinib	CSF	Propranolol	Zorbax SB-C18 (150 × 2.1 mm, 5 μm)	Methanol, water (0.1% FA)	Gradient	ESI (+)	NS	NS	Not used	Deprot.	[86,131]
Icotinib	CSF	Liquid chromatography–tandem mass spectrometry was used.									[66]
Icotinib	CSF	Liquid chromatography–tandem mass spectrometry was used.									[67]
Imatinib	Breast milk	$^{2}H_8$-imatinib	Luna C18 (50 × 4.6 mm, 5 μm)	Methanol (0.1% FA), water (0.1% FA)	Gradient	ESI (+)	493.7	501.7	Not used	Deprot.	[20,132]
Imatinib	Breast milk	None	Luna C18 (50 × 4.6 mm, 5 μm)	Methanol (0.1% FA), water (0.1% FA)	Gradient	ESI (+)	494 > 394	Not used	Not used	Deprot.	[21,132]
Imatinib	Breast milk	Liquid chromatography–tandem mass spectrometry was used. Deprot. was employed as sample preparation.									[22]
Imatinib	Breast milk	No details of the employed analytical methodology are disclosed.									[23]
Imatinib	Breast milk	No details of the employed analytical methodology are disclosed.									[24]
Imatinib	Breast milk	No details of the employed analytical methodology are disclosed.									[25]
Imatinib	CSF	Carbamazepine	Nucleoshell C18 (150 × 3 mm, 2.7 μm)	Water (0.1% FA), methanol	Gradient	ESI (+)	494.27 > 394.2, 494.27 > 247.1, 494.27 > 217.2.	237.1 > 194.2 237.1 > 165.1 237.1 > 121.1	Not used	Deprot.	[12]

Table 4. *Cont.*

Drug	Matrix	Internal Standard	Chromatography			Mass Spectrometry			UV–VIS (nm)	Sample Preparation	Ref.
			Stationary Phase	Mobile Phases	Type of Separation	Ioniza-tion	Analyte ions	IS Ions			
Imatinib	CSF		Liquid chromatography–tandem mass spectrometry was used.								[15]
Imatinib	CSF	$^{2}H_{8}$-imatinib	Symmetry Shield-RP8 (50 × 4.6 mm, 3.5 µm)	Methanol (0.05% ammonium acetate), water (0.05% ammonium acetate)	Isocratic (72:28)	APCI (+)	494.3 > 394.3	502.2 > 394.3	Not used	Deprot.	[16,115]
Imatinib	CSF		No details of the analytical methodology are disclosed.								[17]
Imatinib	CSF	None	ZirChromPDB-ZrO2 (50 × 4.6 mm, 3 µm)	Water (0.01 mol/L KH_2PO_4, 0.09 mol/L K_2HPO_4), methanol	Isocratic (60:40)	Not used			260	Deprot., online enrichment	[18]
Imatinib	CSF		No details of the analytical methodology are disclosed.								[19]
Imatinib	Leukocytes	Clozapine	Symmetry Shield-RP8 (50 × 4.6 mm, 3.5 µm)	Methanol (0.05% ammonium acetate), Water (0.05% ammonium acetate)	Isocratic (72:28)	Not applicable			261	SPE	[13]
Imatinib	PBMC	Quinoxaline	Atlantis T3 C18 (150 × 2.1 mm, 3 µm)	Water (0.05% FA), acetonitrile (0.05% FA)	Gradient	ESI (+)	493.8	313.0	Not used	Deprot.	[14,133]
Imatinib	semen	NS	CAPCELLPAK-C18	Water (2 mmol/L ammonium acetate, 0.05% TFA), acetonitrile-methanol 1:1 (0.05% TFA)	NS	ESI (+)	NS	NS	Not used	NS	[26]
Lapatinib	CSF		High-performance liquid chromatography–mass spectrometry was used.								[83]
Neratinib	CSF		Liquid chromatography–tandem mass spectrometry was used.								[84]
Nilotinib	CSF	NS	Nucleosil C18 HD (125 × 2 mm, 3.5 µm)	Acetonitrile, 0.05 mol/L aqueous potassium dihydrogen-phosphate (pH = 4.03)	Isocratic (37:63)	Not applicable			258	Online enrichment	[29,134]
Nilotinib	CSF		No details of the analytical methodology are disclosed.								[30]
Nilotinib	CSF	$^{13}C,^{2}H_{3}$-nilotinib	Acquity BEH C18 (50 × 2.1 mm, 1.7 µm)	NS	NS	ESI (+)	530.27 > 289.01	NS	Not used	Deprot.	[32–34,36]
Nilotinib	CSF		High-performance liquid chromatography and tandem mass spectrometry were used. The internal standard was $^{2}H_{6}$-nilotinib.								[35]
Nilotinib	Pleural effusate		Liquid chromatography–tandem mass spectrometry was used.								[31]
Nintedanib	CSF	Carbamazepine	Nucleoshell C18 (150 × 3 mm, 2.7 µm)	Water (0.1% FA), methanol	Gradient	ESI (+)	540.26 > 113.1 540.26 > 70.2 540.26 > 42.2	237.1 > 194.2 237.1 > 165.1 237.1 > 121.1	Not used	Deprot.	[12]
Osimertinib	CSF		Liquid chromatography–tandem mass spectrometry was used.								[62]
Osimertinib	CSF		Sample pretreatment consisted of deprot. Liquid chromatography-tandem mass spectrometry was used.								[63]
Osimertinib	CSF		Liquid chromatography–tandem mass spectrometry was used.								[64]
Panobiostat	CSF	Carbamazepine	Nucleoshell C18 (150 × 3 mm, 2.7 µm)	Water (0.1% FA), methanol	Gradient	ESI (+)	350.2 > 158.2 350.2 > 143.1	237.1 > 194.2 237.1 > 165.1 237.1 > 121.1	Not used	Deprot.	[12]
Panobinostat	CSF		Liquid chromatography–tandem mass spectrometry was used.								[92]
Panobinostat	CSF		No details of the employed analytical methodology are disclosed.								[93]
Pazopanib	ascitic fluid		No details of the employed analytical methodology are disclosed.								[88]
Ponatinib	CSF	NS	Hypersil Gold PFP (100 × 2.1 mm, 1.9 µm)	Water (10 mmol/L formate ammonium buffer, 0.1% FA), acetonitrile (0.1% FA)	Gradient	ESI	NS	NS	Not used	Deprot.	[37,135]
Regorafenib	CSF	Carbamazepine	Nucleoshell C18 (150 × 3 mm, 2.7 µm)	Water (0.1% FA), methanol	Gradient	ESI (+)	483.09 > 288.1 483.09 > 270.1 483.09 > 202.0	237.1 > 194.2 237.1 > 165.1 237.1 > 121.1	Not used	Deprot.	[12]
Regorafenib	CSF	$^{2}H_{5}$-moxifloxacin	Kinetex F5 (50 × 4.6 mm, 2.5 µm)	Water (0.1% FA), methanol (0.1% FA)	Gradient	NS, (+) polarity	483.1 > 270.1	407.4 > 266.4	Not used	Deprot.	[89]
Ribociclib	CSF	Carbamazepine	Nucleoshell C18 (150 × 3 mm, 2.7 µm)	Water (0.1% FA), methanol	Gradient	ESI (+)	435.3 > 322.1 435.3 > 294.1 435.3 > 252.1	237.1 > 194.2 237.1 > 165.1 237.1 > 121.1	Not used	Deprot.	[12]

Table 4. *Cont.*

Drug	Matrix	Internal Standard	Chromatography			Mass Spectrometry			UV–VIS (nm)	Sample Preparation	Ref.
			Stationary Phase	Mobile Phases	Type of Separation	Ioniza-tion	Analyte ions	IS Ions			
Ribociclib	CSF	$^{13}C_6$-ribociclib	Xbridge Amide (100 × 4.6 mm, 3.5 µm)	Acetonitrile, water (10 mmol/L ammonium formate, pH = 3.0)	Isocratic (75:25)	ESI (+)	435.3 > 367.2	441.3 > 373.2	Not used	Deprot.	[78,79, 136]
Ribociclib	CSF	$^{2}H_6$-ribociclib	Polaris C8 (50 × 2.0 mm, 5 µm)	Water (0.1% FA), acetonitrile (0.1% FA)	Gradient	ESI (+)	435.2 > 252.1	441.2 > 252.1	Not used	Dilution, acidification, centrifugation	[80,137]
Sunitinib	ascitic fluid	No details of the employed analytical methodology are disclosed.									[88]
Tepotinib	CSF	Ultra-performance liquid chromatography was used.									[90]
Tepotinib	CSF	Liquid chromatography–tandem mass spectrometry was used.									[91]
Trametinib	CSF	$^{13}C_6$-trametinib	XSelect HSS T3 (75 × 2.1 mm, 3.5 µm)	Water (2 mmol/L ammonium acetate, 0.1% FA), acetonitrile (0.1% FA)	Gradient	ESI (+)	616.1 > 254.1 616.1 > 491.3	622.0 > 497.2	Not used	Deprot.	[69,120]
Vemurafenib	CSF	Sorafenib	XTerra C8 MS (250 × 4.6 mm, 5 µm)	Water (100 mmol/L glycine, pH = 9.0), acetonitrile	Isocratic (45:55)	Not applicable			249	Deprot.	[68,138]
Venetoclax	CSF	$^{2}H_8$-venetoclax	Atlantis C18 (50 × 2.1 mm, 3 µm)	Acetonitrile, water (0.1% FA)	Isocratic (55:45)	ESI (+)	868 > 321	876 > 329	Not used	Deprot.	[95,139]
Venetoclax	CSF	$^{2}H_8$-venetoclax	Atlantis C18 (50 × 2.1 mm, 3 µm)	Acetonitrile, water (0.1% FA)	Isocratic (55:45)	ESI (+)	868 > 321	876 > 329	Not used	LLE	[96,139]
Vismodegib	CSF	$^{2}H_5$-vismodegib	Betasil C18 (100 × 2.1 mm)	Water (0.1% FA), acetonitrile	Isocratic (40:60)	ESI (+)	421.1 > 139.2	426.1 > 139.1	Not used	SPE	[94,140]
Vorinostat	CSF	Carbamazepine	Nucleoshell C18 (150 × 3 mm, 2.7 µm)	Water (0.1% FA), methanol	Gradient	ESI (+)	265.16 > 232.1 265.16 > 77.1 265.16 > 55.1	237.1 > 194.2 237.1 > 165.1 237.1 > 121.1	Not used	Deprot.	[12]
Zanubrutinib	CSF	Tolbutamide	Zorbax SB-C18 (150 × 2.1 mm, 5 µm)	Methanol, water (0.1% FA)	Gradient	ESI (+)	NS	NS	Not used	Deprot.	[86,131]
Zanubrutinib	CSF	NS	Acquity BEH C18 (50 × 2.1 mm, 1.7 µm)	Water (0.15 FA), acetonitrile (0.1% FA)	NS	ESI (+)	NS	NS	Not used	Deprot.	[87]

4. Discussion

The rapid growth of the number of related publications reflects the increasing clinical interest in monitoring OACDs in therapeutically relevant extravascular fluids. Nevertheless, the range of substances that have been monitored in these compartments with the aim of supporting clinical decision making comprises the minor segment of marketed OACDs. Currently, imatinib is the most extensively studied drug, followed by erlotinib, gefitinib, and nilotinib. Interest in studying recently approved entities, such as dasatinib, osimertinib, panobinostat, and ribociclib, is also rising.

To date, frequently monitored peripheral fluid spaces have included cerebrospinal fluid, and, to a lesser extent, breast milk. Sporadic examples of monitoring OACDs in pleural effusion fluid, ascitic fluid, the intracellular space of peripheral blood mononuclear cells, semen, and saliva have been encountered. Collecting, handling, and processing samples originating from these fluid spaces requires expertise and, regarding CSF, pleural effusate, and ascitic fluid, specialized clinical infrastructure. Due to this limitation, as well as to the need to use specialized and resource-intensive analytical technology, it is likely that OACD monitoring in peripheral fluid spaces remains a competence of centers of excellence in oncology.

The attainment of very low OACD concentrations in CSF seems to have been unexpected by several authors. One explanation could be the poor permeability of the blood–brain barrier to these drugs, but this assumption has been contradicted by results showing that WBRT, an adjuvant intervention undertaken to increase this permeability, had not always led to increased penetration rates [67,72,91]. The application of WBRT is part of an effort to employ multimodal therapy against CNS malignancies, yet recent reports have shown that it may have detrimental adverse effects, and should not be considered as a stan-

dard measure in the therapy of NSCLC patients developing brain metastases. Experience with WBRT is also controversial regarding the treatment of primary CNS lymphomas [141]. At the same time, it has been found effective in the therapy of brain metastases of breast cancer patients, especially when combined with carboplatin injected intravenously [142]. Conventional photon radiotherapy, a similar approach with a more favorable adverse effect profile, has also been proposed for increasing the penetration rate of OACDs through the blood–brain barrier [143]. Various options of using more focal radiotherapy have also been described [144].

Another interpretation is that the CSF concentrations of OACD substances could be associated with the unbound plasma fractions. Several examples of a correlation observed between unbound serum/plasma concentrations and CSF levels confirm this assumption (Figure 3). Since the unbound fractions of various OACDs display considerable differences, it is indeed rational to judge CNS penetration based on these fractions instead of the total serum/plasma levels. The evaluation of the unbound fractions shows that the concentrations of some drugs attained in the CSF are equal to or even higher than unbound circulating concentrations. The negligible presence of everolimus in saliva, another medium accessed only by the unbound plasma fractions, confirms this rationale. No approved clinical approaches exist for establishing individual protein binding rates. Equilibrium dialysis has been used as an experimental sample pretreatment procedure for determining unbound plasma concentrations of OACDs [74,78,79,94,145]. Microdialysis has the potential to be employed for this purpose, but no examples of its application for the assessment of unbound OACD concentrations were identified. A promising sample pretreatment technology has recently become available for the rapid assessment of the extent of protein binding. The device fits into the sample preparation workflow employed by LC–MS/MS-based TDM laboratories, but there is still very limited experience regarding its use [146].

The extent of plasma protein binding may not be the only factor of the penetration of OACDs through the blood–brain barrier. Guntner et al. have shown with seven OACD substances that molecule size and the affinity of the molecule to p-glycoprotein (ABCB1 or MDR1, EC 7.6.2.2) are also key determinants. In accordance, the permeability of the blood–brain barrier to dasatinib, imatinib, regorafenib, ribociclib, and vorinostat was higher than to nintedanib or panobinostat. The comparison of experimental results to those obtained using computer models nevertheless indicated that further variables, currently unidentified, are likely to play an important role in this process [12].

In sum, more research is needed to find dosages and monitoring approaches that result in the attainment of clinically sufficient CSF concentrations in all patients. Aggressive dosing, the artificial facilitation of the penetration of drugs through the blood–brain barrier, or the administration of drug combinations containing a component which inhibits p-glycoprotein or other drug-eliminating proteins relevant to a specific OACD are potential strategies for the more efficient therapy of CNS malignancies. A methodology is also emerging to predict OACD treatment efficacy by comparing the drug concentrations measured in the target peripheral fluid to the in vitro IC_{50} established for the given malignant cell line, and based on this relationship, by creating a mathematical link between the pharmacokinetic and pharmacodynamic properties of the administered drug. In the future, this approach may prove useful in developing precision dosing schemes with pharmacokinetic–pharmacodynamic targets, in an analogy to those already employed for guiding antibiotic therapy.

In sharp contrast to the observations made in the CSF, high penetration rates or even the accumulation of OACDs were consistently described in exudates formed by pleural effusion and malignant ascites, and in excreta such as breast milk and semen. Imatinib showed considerable accumulation in buffy coat cells and in peripheral blood mononuclear cells. These findings indicate that the consideration of third spaces as pharmacokinetic compartments may be rational in patients treated with lung or breast cancer, as well as in leukemia patients.

There has been a solid consensus in relying on liquid chromatography-based analytical approaches for the therapeutic monitoring of OACDs in peripheral fluid spaces. Several early methods relied on the use of UV–VIS detectors, but LC–MS/MS has by now emerged as the primary analytical technique as a result of ensuring sufficient selectivity and sensitivity, requiring small sample volumes for the analysis, and allowing the high-throughput processing of peripheral fluid space samples. When applied for the clinical analysis of OACDs in these compartments, the main steps of these methodologies were reversed phase chromatographic separation followed by positive electrospray ionization and multiple reaction monitoring. The simple and rapid process of deproteinization was in most cases sufficient for the pretreatment of samples. A common weakness of the analytical methodologies employed in the reviewed records is that they had not undergone comprehensive validation, lowering the credibility of the presented results.

The application of equilibrium dialysis to retrieve direct clinical pharmacological information fits into a series of related emerging approaches, such as the rapid assessment of protein binding, or the partitioning between plasma and red blood cells. Such technologies are expected to facilitate the reporting of truly individualized, and, in a clinical sense, substantially more relevant information on the pharmacokinetic properties of drugs including OACDs in the future [146,147].

An important limitation of the performed evaluation is that only a minority of the retrieved publications described the outcomes of registered clinical trials. The majority of the works reported small-scale, researcher-initiated, unicentric studies, case series, or case reports. In addition, the methodologies employed for sample collection and analysis were uniquely developed by most investigators, limiting the comparability of results. Only a fraction of the subjects involved in the studies had given their consent for collecting CSF samples; consequently, the number of available CSF concentrations was small in several publications. Indeed, peripheral space drug monitoring was conducted as a collateral tool of diagnosis or patient status monitoring in several cases.

Malignancies are the leading causes of premature death worldwide, with breast and lung cancers underlying the largest number of new cases [148]. The importance of improving the treatment of these diseases is therefore beyond dispute. Therapeutic drug monitoring and research regarding model-informed precision dosing is currently based on the evaluation of drug concentrations in the systemic circulation, while evidence now shows that the monitoring of OACDs in therapeutically relevant extravascular fluid compartments can be equally important, especially for the better treatment of central nervous system malignancies. TDM laboratories providing service for large oncological centers can add a fundamental impetus by introducing suitable, validated, LC–MS/MS-based analytical methods for monitoring these drugs in peripheral fluid spaces, and in vitro approaches to determining unbound OACD concentrations. Establishing these competences is the first step for the introduction of therapy guidance based on highly relevant pharmacokinetic models and pharmacokinetic–pharmacodynamic indices, as well as for the early detection of suboptimal dosages and the risk of certain adverse effects. Since the number of available OACDs, as well as the range of their indications, is growing rapidly, the identification of further therapeutic goals and therapeutically relevant peripheral fluid spaces can be expected, maintaining a long-term need for the close cooperation of clinicians, clinical pharmacologists, and the TDM service in this field.

5. Conclusions

This review has revealed that the therapeutic monitoring of OACDs in peripheral fluid spaces is an important diagnostic tool for the assessment of the penetration of these substances into CSF and third space fluids, which is imperative for the optimization of drug administration, and of their appearance in excreta, which may convey important information on adverse effects and other forms of toxicity. LC–MS/MS is an established analytical technology for performing these measurements, with little effort required to

transfer conventional, blood-based TDM methods. Nevertheless, dedicated centers of excellence are needed to perform such measurements routinely.

A range of indications has been identified for which the TDM of OACDs in peripheral fluid spaces can provide clinically powerful information. More systematic studies with rigorous quality control are needed, however, for elucidating the pharmacokinetic properties of OACDs, for setting quantitative therapeutic targets, and for establishing standard analytical methodology. Related research in pediatric populations still remains an unmet need.

After more than 20 years of using OACDs, an alarmingly small number of these substances has ever been investigated in a clinically important peripheral fluid space. In several malignancies, the administration of these medications cannot be optimized without knowledge regarding their quantities in these fluid spaces, especially in CSF; therefore, research should be focused on gathering information on all OACDs in this respect.

Author Contributions: Conceptualization, G.B.K.; methodology, G.B.K. and Z.K.; formal analysis, Z.K. and I.V.; data curation, Z.K. and G.B.K.; writing—original draft preparation, Z.K. and G.B.K.; writing—review and editing, B.V., M.G. and I.V.; visualization, Z.K.; supervision, B.V.; project administration, Z.K. All authors have read and agreed to the published version of the manuscript.

Funding: This research received no external funding.

Institutional Review Board Statement: Not required.

Informed Consent Statement: Not applicable.

Data Availability Statement: Not applicable.

Conflicts of Interest: The authors declare no conflict of interest.

References

1. McLaughlin, A.M.; Schmulenson, E.; Teplytska, O.; Zimmermann, S.; Opitz, P.; Groenland, S.L.; Huitema, A.D.R.; Steeghs, N.; Müller, L.; Fuxius, S.; et al. Developing a nationwide infratructure for therapeutic drug monitoring of targeted oral anticancer drugs: The ON-TARGET study protocol. *Cancers* **2021**, *13*, 6281. [CrossRef] [PubMed]
2. Cohen, P.; Cross, D.; Jänne, P.A. Kinase drug discovery 20 years after imatinib: Progress and future directions. *Nat. Rev. Drug Discov.* **2021**, *20*, 551–569. [CrossRef] [PubMed]
3. Reyner, E.; Lum, B.; Jing, J.; Kagedal, M.; Ware, J.A.; Dickmann, L.J. Intrinsic and extrinsic pharmacokinetic variability of small molecule targeted cancer therapy. *Clin. Transl. Sci.* **2020**, *13*, 410–418. [CrossRef] [PubMed]
4. Verheijen, R.B.; Yu, H.; Schellens, J.H.M.; Beijnen, J.H.; Steeghs, N.; Huitema, A.D.R. Practical recommendations for therapeutic drug monitoring of kinase inhibitors in oncology. *Clin. Pharm. Ther.* **2017**, *102*, 765–776. [CrossRef]
5. Saydam, G.; Ali, R.; Demir, A.M.; Eskazan, A.E.; Guvenc, B.; Haznedaroglu, I.C.; Mehmet, A.O.; Salim, O.; Sonmez, M.; Tuglular, A.T.; et al. The effects of comorbidities on the choice of tyrosine kinase inhibitors in patients with chronic myeloid leukemia. *Int. J. Hematol. Oncol.* **2022**, *11*, IJH38.
6. Clarke, W.A.; Chatelut, E.; Fotoohi, A.K.; Larson, R.A.; Martin, J.H.; Mathijssen, R.H.J.; Salamone, S.J. Therapeutic drug monitoring in oncology: International Association of Therapeutic Drug Monitoring and Clinical Toxicology consensus guidelines for imatinib therapy. *Eur. J. Cancer* **2021**, *157*, 428–440. [CrossRef]
7. Angeli, E.; Bousquet, G. Brain metastasis treatment: The place of tyrosine kinase inhibitors and how to facilitate their diffusion across the blood-brain barrier. *Pharmaceutics* **2021**, *13*, 1446. [CrossRef]
8. Abruzzese, E.; Mauro, M.; Apperley, J.; Chelysheva, E. Tyrosine kinase inhibitors and pregnancy in chronic myeloid leukemia: Opinion, evidence, and recommendations. *Ther. Adv. Hematol.* **2020**, *11*, 2040620720966120. [CrossRef]
9. Capone, F.; Albanese, A.; Quadri, G.; Di LAzzaro, V.; Falato, E.; Cortese, A.; De Giglio, L.; Ferraro, E. Disease-modifying drugs and breastfeeding in multiple sclerosis: A narrative literature review. *Front. Neurol.* **2022**, *13*, 851413. [CrossRef]
10. Nash, P.; Kerschbaumer, A.; Dörner, T.; Dougados, M.; Fleishcmann, R.M.; Geissler, K.; McInnes, I.; Pope, J.E.; van der Heijde, D.; Stoffer-Marx, M.; et al. Points to consider for the treatment of immune-mediated inflammatory diseases with Janus kinase inhibitors: A consensus statement. *Ann. Rheum. Dis.* **2021**, *80*, 71–87. [CrossRef]
11. Page, M.J.; McKenzie, J.E.; Bossuyt, P.M.; Boutron, I.; Hoffmann, T.C.; Mulrow, C.D.; Shamseer, L.; Tetzlaff, J.M.; Akl, E.A.; Brennan, S.E.; et al. The PRISMA 2020 Statement: An updated guideline for reporting systematic reviews. *BMJ* **2021**, *372*, n71. [CrossRef] [PubMed]
12. Guntner, A.S.; Peyrl, A.; Mayr, L.; Englinger, B.; Berger, W.; Slavic, I.; Buchberger, W.; Gojo, J. Cerebrospinal fluid penetration of targeted therapeutics in pediatric tumor patients. *Acta. Neuropathol. Commun.* **2020**, *8*, 78. [CrossRef] [PubMed]

13. Nambu, T.; Hamada, A.; Nakashima, R.; Yuki, M.; Kawaguchi, T.; Mitsuya, H.; Saito, H. Association of SLCO1B3 polymorphism with intracellular accumulation of imatinib in leukocytes in patients with chronic myeloid leukemia. *Biol. Pharm. Bull.* **2011**, *34*, 114–119. [CrossRef] [PubMed]
14. De Francia, S.; D'Avolio, A.; Ariaudo, A.; Pirro, E.; Piccione, F.; Simiele, M.; Fava, C.; Calcagno, A.; Di Perri, G.; Saglio, G. Plasma and intracellular imatinib concentrations in patients with chronic myeloid leukemia. *Ther. Drug Monit.* **2014**, *36*, 410–412. [CrossRef]
15. Petzer, A.; Gunsilius, E.; Hayes, M.; Stockhammer, G.; Duba, H.C.; Schneller, F.; Grünewald, K.; Poewe, W.; Gastl, G. Low concentrations of STI571 in the cerebrospinal fluid: A case report. *Br. J. Haematol.* **2002**, *117*, 623–625. [CrossRef]
16. Takayama, N.; Sato, N.; O'Brian, S.G.; Ikeda, Y.; Okamoto, S. Imatinib mesylate has limited activity against the central nervous system invilvement of Philadelphia chromosome-positive acute lymphoblastic leukaemia due to poor penetration into cerebrospinal fluis. *Br. J. Haematol.* **2002**, *119*, 106–108. [CrossRef]
17. Bornhauser, M.; Jenke, A.; Freiberg-Richter, J.; Radke, J.; Schuler, U.S.; Mohr, B.; Ehninger, G.; Schleyer, E. CNS blast crisis of chronic myelogenous leukemia in a patient with a major cytogenic response in bone marrow associated with low levels of imatinib mesylate and its N-desmethylated metabolite in cerebral spinal fluid. *Ann. Hematol.* **2004**, *83*, 401–402. [CrossRef]
18. Le Coutre, P.; Kreuzer, K.A.; Pursche, S.; Bonin, M.V.; Leopold, T.; Baskaynak, G.; Dörken, B.; Ehningen, G.; Ottmann, O.; Jenke, A.; et al. Pharmacokinetics and cellular uptake of imatinib and its metabolite CGP74588. *Cancer Chemother. Pharmacol.* **2004**, *53*, 313–323. [CrossRef]
19. Leis, J.F.; Stepan, D.E.; Curtin, P.T.; Ford, J.M.; Peng, B.; Schubach, S.; Druker, B.J.; Maziarz, R.T. Central nervous system failure in patients with chronic myelogenous leukemia lymphoid blast crisis and Philadelphia chromosome positive acute lymphoblastic leukemia treated with imatinib (STI-571). *Leuk. Lymphoma* **2004**, *45*, 695–698. [CrossRef]
20. Russel, M.A.; Carpenter, M.W.; Akhtar, M.S.; Lagattuta, T.F.; Egorn, M.J. Imatinib mesylate and metabolite concentrations in maternal blood, umbilical cord blood, placenta and breast milk. *J. Perinatol.* **2007**, *27*, 241–243. [CrossRef]
21. Gambacorti-Passerini, C.B.; Tornaghi, L.; Marangon, E.; Franceschino, A.; Pogliani, E.M.; D'Incalci, M.; Zucchetti, M. Imatinib concentrations in human milk. *Blood* **2007**, *109*, 1790. [CrossRef]
22. Ali, R.; Ozkalemkas, F.; Kimya, Y.; Koksal, N.; Ozkocaman, V.; Gulten, T.; Yorulmaz, H.; Tunali, A. Imatinib use during pregnancy and breast feeding: A case report and review of the literature. *Arch. Gynecol. Obstet.* **2009**, *280*, 169–175. [CrossRef] [PubMed]
23. Kronenberger, R.; Schleyer, E.; Bornhäuser, M.; Ehninger, G.; Gattermann, N.; Blum, S. Imatinib in breast milk. *Ann. Hematol.* **2009**, *88*, 1265–1266. [CrossRef] [PubMed]
24. Burwick, R.M.; Kuo, K.; Brewer, D.; Druker, B.J. Maternal, Fetal, and Neonatal Imatinib Levels with Treatment of Chronic Myeloid Leukemia in Pregnancy. *Obstet. Gynecol.* **2017**, *129*, 831–834. [CrossRef] [PubMed]
25. Terao, R.; Nil, M.; Asai, H.; Nohara, F.; Okamoto, T.; Nagaya, K.; Azuma, H. Breastfeeding in a patient with chronic myeloid leukemia during tyrosine kinase inhibitor therapy. *J. Oncol. Pharm. Pract.* **2021**, *27*, 756–760. [CrossRef]
26. Chang, X.; Zhou, L.; Chen, X.; Xu, B.; Cheng, Y.; Sun, S.; Fang, M.; Xiang, Y. Impact of Imatinib on the Fertility of Male Patients with Chronic Myelogenous Leukaemia in the Chronic Phase. *Target. Oncol.* **2017**, *12*, 827–832. [CrossRef]
27. Kondo, T.; Tasaka, T.; Matsumoto, K.; Matsumoto, R.; Koresawa, L.; Sano, F.; Tokunga, H.; Matsuhashi, Y.; Nakanishi, H.; Morita, K.; et al. Philadelphia chromosome-positive acute lymphoblastic leukemia with extramedullary and meningeal relapse after allogenic hematopoietic stem cell transplantation that was successfully treated with dasatinib. *Springerplus* **2014**, *3*, 177. [CrossRef]
28. Gong, X.; Li, L.; Wei, H.; Liu, B.; Zhou, C.; Zhang, G.; Liu, K.; Lin, D.; Gong, B.; Wei, S.; et al. A higher Dose of Dasatinib May Increase the Possibility of Crossing the Blood-brain Barrier in the Treatment of Patients with Philadelphia Chromosome-positive Acute Lymphoblastic Leukemia. *Clin. Ther.* **2021**, *43*, 1265–1271. [CrossRef]
29. Reinwald, M.; Schleyer, E.; Kiewe, P.; Blau, I.W.; Baurmeister, T.; Pursche, S.; Neumann, M.; Notter, M.; Thiel, E.; Hofmann, W.K.; et al. Efficacy and pharmacologic data of second-generation tyrosine kinase inhibitor nilotinib in BCR-ABL-positive leukemia patients with central nervous system relapse after allogenic stem cell transplantation. *Biomed. Res. Int.* **2014**, *2014*, 637059. [CrossRef]
30. Liu, B.; Wang, Y.; Zhou, C.; Wei, H.; Lin, D.; Li, W.; Liu, K.; Zhang, G.; Wei, S.; Li, Y.; et al. Nilotinib combined with multi-agent chemotherapy in newly diagnosed Philadelphia chromosome-positive acute lymphoblastic leukemia: A single-center prospective study with long-term follow-up. *Ann. Hematol.* **2019**, *98*, 633–645. [CrossRef]
31. Satoh, K.; Morisawa, S.; Okuyama, M.; Nakae, H. Severe pleural effusion associated with nilotinib for chronic myeloid leukaemia: Cross-intolerance with tyrosine kinase inhibitors. *BMJ Case Rep.* **2021**, *14*, e245671. [CrossRef] [PubMed]
32. Pagan, F.; Hebron, M.; Valadez, E.H.; Torresy-Yaghi, Y.; Huang, X.; Mills, R.R.; Wilmarth, B.M.; Howard, H.; Dunn, C.; Carlson, A.; et al. Nilotinib Effects in Parkinson's disease and Dementia with Lewy bodies. *J. Parkinsons Dis.* **2016**, *6*, 503–517. [CrossRef] [PubMed]
33. Pagan, F.L.; Hebron, M.L.; Wilmarth, B.; Torres-Yaghi, Y.; Lawler, A.; Mundel, E.E.; Yusuf, N.; Starr, N.J.; Arellano, J.; Howard, H.H.; et al. Pharmacokinetics and pharmacodynamics of a single dose Nilotinib in individuals with Parkinson's disease. *Pharmacol. Res. Perspect.* **2019**, *7*, e00470. [CrossRef]
34. Pagan, F.L.; Hebron, M.L.; Wilmarth, B.; Torres-Yaghi, Y.; Lawler, A.; Mundel, E.E.; Yusuf, N.; Starr, N.J.; Anjum, M.; Arello, J.; et al. Nilotinib Effects on Safety, Tolerability, and Potential Biomarkers in Parkinson Disease: A Phase 2 Randomized Clinical Trial. *JAMA Neurol.* **2020**, *77*, 309–317. [CrossRef]

35. Simuni, T.; Fiske, B.; Merchant, K.; Coffey, C.S.; Klinger, E.; Caspell-Garcia, C.; Lafontant, D.E.; Matthews, H.; Wyse, R.K.; Brundin, P.; et al. Efficacy of Nilotinib in Patients With Moderately Advanced Parkinson Disease: A Randomized Clinical Trial. *JAMA Neurol.* **2021**, *78*, 312–320. [CrossRef] [PubMed]
36. Turner, R.S.; Hebron, M.L.; Lawler, A.; Mundel, E.E.; Yusuf, N.; Starr, J.N.; Anjum, M.; Pagan, F.; Torres-Yaghi, Y.; Shi, W.; et al. Nilotinib Effects on Safety, Tolerability, and Biomarkers in Alzheimer's Disease. *Ann. Neurol.* **2020**, *88*, 183–194. [CrossRef] [PubMed]
37. Tanimura, K.; Yamassaki, K.; Okuhiro, Y.; Hira, K.; Nitani, C.; Okada, K.; Fujisaki, H.; Matsumoto, K.; Hara, J. Monitoring Ponatinib in a Child with Philadelphia Chromosome-Positive Acute Lymphoblastic Leukemia. *Case Rep. Oncol.* **2021**, *14*, 24–28. [CrossRef] [PubMed]
38. Yamaguchi, T.; Isogai, S.; Okamura, T.; Uozu, S.; Mieno, Y.; Hoshino, T.; Goto, Y.; Hayashi, M.; Nakanishi, T.; Imaizumi, K. Pharmacokinetics of gefitinib in a patient with non-small cell lung cancer undergoing continuous ambulatory peritoneal dialysis. *Case Rep. Oncol.* **2015**, *8*, 78–82. [CrossRef]
39. Fukuhara, T.; Saijo, Y.; Sakakibara, T.; Inoue, A.; Morikawa, N.; Kanamori, M.; Nakashima, I.; Nukiwa, T. Successful treatment of carcinomatous meningitis with gefitinib in a patient with lung adenocarcinoma harboring a mutated EGF receptor gene. *Tohoku J. Exp. Med.* **2008**, *214*, 359–363. [CrossRef]
40. Zhao, J.; Chen, M.; Zhong, W.; Zhang, L.; Li, L.; Xiao, Y.; Nie, L.; Hu, P.; Wang, M. Cerebrospinal fluid concentrations of gefitinib in patients with lung adenocarcinoma. *Clin. Lung Cancer* **2013**, *14*, 188–193. [CrossRef]
41. Zeng, Y.D.; Liao, H.; Qin, T.; Zhang, L.; Wei, W.D.; Liang, J.Z.; Xu, F.; Dinglin, X.X.; Ma, S.X.; Chen, L.K. Blood-brain barrier permeability of gefitinib in patients with brain metastases from non-small-cell lung cancer before and during whole brain radiation therapy. *Oncotarget* **2015**, *6*, 8366–8367. [CrossRef] [PubMed]
42. Zhao, J.; Ye, X.; Xu, Y.; Chen, M.; Zhong, W.; Sun, Y.; Yang, Z.; Zhu, G.; Gu, Y.; Wang, M. EGFR mutation status of paired cerebrospinal fluid and plasma sample in EGFR mutant non-small cell lung cancer with leptomeningeal metastases. *Cancer Chemother. Pharmacol.* **2016**, *78*, 1305–1310. [CrossRef] [PubMed]
43. Jackman, D.M.; Cioffredi, L.A.; Jacobs, L.; Sharmeen, F.; Morse, L.K.; Lucca, J.; Plotkin, S.R.; Marcoux, P.J.; Rabin, M.S.; Lynch, T.J.; et al. A phase I trial of high dose gefitinib for patients with leptomeningeal metastases from non-small cell lung cancer. *Oncotarget* **2015**, *6*, 4527–4536. [CrossRef]
44. Fang, L.; Sun, X.; Song, Y.; Zhang, Y.; Li, F.; Xu, Y.; Ma, S.; Lin, N. Whole-brain radiation fails to boost intracerebral gefitinib concentration in patients with brain mestastatic non-small cell lung cancer: A self-controlled, pilot study. *Cancer Chemother. Pharmacol.* **2015**, *76*, 873–877. [CrossRef]
45. Togashi, Y.; Masago, K.; Masuda, S.; Mizuno, T.; Fukudo, M.; Ikemi, Y.; Sakamori, Y.; Nagai, H.; Kim, Y.H.; Katsura, T.; et al. Cerebrospinal fluid concentration of gefitinib and erlotinib in patients with non-small cell lung cancer. *Cancer Chemother. Pharmacol.* **2012**, *70*, 399–405. [CrossRef] [PubMed]
46. Shriyan, B.; Patil, D.; Gurjar, M.; Nookala, M.; Patil, A.; Kannan, S.; Patil, V.; Joshi, A.; Noronha, V.; Prabhash, K.; et al. Safety and CSF distribution of high-dose erlotinib and gefitinib in patients of non-small cell lung cancer (NSCLC) with brain mtastases. *Eur. J. Clin. Pharmacol.* **2020**, *76*, 1427–1436. [CrossRef] [PubMed]
47. Broniscer, A.; Panetta, J.C.; O'Shaunghnessy, M.; Fraga, C.; Bai, F.; Krasin, M.J.; Gajjar, A.; Stewart, C.F. Plasma and cerebrospinal fluid pharmacokinetics of erlotinib and its active metabolite OSI-420. *Clin. Cancer Res.* **2007**, *13*, 1511–1515. [CrossRef]
48. Rogers, L.R.; LoRusso, P.; Nadler, P.; Malik, G.; Shields, A.; Kaelin, W. Erlotinib therapy for central nervous system hemangioblastomatosis associated with von Hippel-Lindau disease: A case report. *J. Neurooncol.* **2011**, *101*, 307–310. [CrossRef] [PubMed]
49. Masago, K.; Togashi, Y.; Fukudo, M.; Terada, T.; Irisa, K.; Sakamori, Y.; Kim, Y.H.; Mio, T.; Inui, K.; Mishima, M. Plasma and pleural fluid pharmacokinetics of erlotinib and its active metabolite OSI-420 in patients with non-small-cell lung cancer with pleural effusion. *Clin. Lung Cancer* **2011**, *12*, 307–312. [CrossRef]
50. Masuda, T.; Hattori, N.; Hamada, A.; Iwamoto, H.; Ohshimo, S.; Kanehara, M.; Ishikawa, N.; Fujitaka, K.; Haruta, Y.; Murai, H.; et al. Erlotinib efficacy and cerebrospinal fluid concentration in patients with lung adenocarcinoma developing leptomeningeal metastases during gefiinib therapy. *Cancer Chemother. Pharmacol.* **2011**, *67*, 1465–1469. [CrossRef]
51. Togashi, Y.; Masago, K.; Fukudo, M.; Tereda, T.; Fujita, S.; Irisa, K.; Sakamori, Y.; Kim, Y.H.; Mio, T.M.; Inui, K.; et al. Cerebrospinal fluid concentration of erlotinib and its active metabolite OSI-420 in patients with central nervous system metastases of non-small cell lung cancer. *J. Thorac. Oncol.* **2010**, *5*, 950–955. [CrossRef] [PubMed]
52. Deng, Y.; Feng, W.; Wu, J.; Chen, Z.; Tang, Y.; Zhang, H.; Liang, J.; Xian, H.; Zhang, S. The concentration of erlotinib in the cerebrospinal fluid of patients with brain metastasis from non-small-cell lung cancer. *Mol. Clin. Oncol.* **2014**, *2*, 116–120. [CrossRef] [PubMed]
53. Sakata, Y.; Kawamura, K.; Shingu, N.; Ichikado, K. Erlotinib plus bevacizumab as an effective treatment for leptomeningeal metastases from EGFR mutation-positive non-small cell lung cancer. *Lung Cancer* **2016**, *99*, 120–122. [CrossRef] [PubMed]
54. Clarke, J.L.; Pao, W.; Wu, N.; Miller, V.A.; Lassman, A.B. High dose weekly erlotinib achieves therapeutic concentrations in CSF and is effective in leptomeningeal metastases from epidermal growth factor receptor mutant lung cancer. *J. Neurooncol.* **2010**, *99*, 283–286. [CrossRef] [PubMed]

55. Yang, H.; Yang, X.; Zhang, Y.; Liu, X.; Deng, Q.; Zhao, M.; Xu, X.; He, J. Erlotinib in combination with pemetrexed/cisplatin for leptomeningeal metastases and cerebrospinal fluid drug concentrations in lung adenocarcinoma patients after gefitinib failure. *Target Oncol.* **2015**, *10*, 135–140. [CrossRef] [PubMed]
56. Togashi, Y.; Masago, K.; Fukudo, M.; Tsuchido, Y.; Okuda, C.; Kim, Y.H.; Ikemi, Y.; Sakamori, Y.; Mio, T.; Katsura, T.; et al. Efficacy of increased-dose erlotinib for central nervous system metastases in non-small cell lung cancer patients with epidermal growth factor receptor mutation. *Cancer Chemother. Pharmacol.* **2011**, *68*, 1089–1092. [CrossRef] [PubMed]
57. Fukudo, M.; Ikemi, Y.; Togashi, Y.; Masago, K.; Kim, Y.H.; Mio, T.; Tereda, T.; Teramukai, S.; Mishima, M.; Inui, K.; et al. Population pharmacokinetics/pharmacodynamics of erlotinib and pharmacogenomic analysis of plasma and cerebrospinal fluid drug concentrations in Japanese patients with non-small cell lung cancer. *Clin. Pharmacokinet.* **2013**, *52*, 593–609. [CrossRef] [PubMed]
58. Nosaki, K.; Yamanaka, T.; Hamada, A.; Shiraishi, Y.; Harada, T.; Himeji, D.; Kitazaki, T.; Ebi, N.; Shimose, T.; Seto, T.; et al. Erlotinib for Non-Small Cell Lung Cancer with Leptomeningeal metastases: A Phase II Study (LOGIK1101). *Oncologist* **2020**, *25*, e1869–e1878. [CrossRef] [PubMed]
59. Hoffknecht, P.; Tufman, A.; Wehler, T.; Pelzer, T.; Wiewrodt, R.; Schütz, M.; Serke, M.; Stöhlmacher-Williams, J.; Märten, A.; Maria Huber, R.; et al. Efficacy of the irreversible ErbB family blocker afatinib in epidermal growth factor receptor (EGFR) tyrosine kinase inhibitor (TKI)-penetrated non-small-cell lung cancer patients with brain metastases or leptomeningeal disease. *J. Thorac. Oncol.* **2015**, *10*, 156–163. [CrossRef] [PubMed]
60. Kawaguchi, Y.; Hanoka, J.; Hayashi, H.; Mizusaki, N.; Iihara, H.; Itoh, Y.; Sugiyama, T. Clinical Efficacy of Afatinib Treatment for a Patient with Leptomeningeal Carcinomatosis. *Chemotherapy* **2017**, *62*, 147–150. [CrossRef]
61. Tamiya, A.; Tamiya, M.; Nishihara, T.; Shiroyama, T.; Nakao, K.; Tsuji, T.; Takeuchi, N.; Isa, S.I.; Omachi, N.; Okamoto, N.; et al. Cerebrospinal Fluid Penetration rate and Efficacy of Afatinib in Patients with EGFR Mutation-positive Non-small Cell Lung Cancer with Leptomeningeal Carcinomatosis: A Multicenter Prospective Study. *Anticancer Res.* **2017**, *37*, 4177–4182. [PubMed]
62. Song, Y.; Liu, P.; Huang, Y.; Guan, Y.; Han, X.; Shi, Y. Osimertinib Quantitative and Gene Variation Analysis in Cerebrospinal Fluid and Plasma of a Non-small Cell Lung Cancer Patient with leptomeningeal Metastases. *Curr. Cancer Drug Targets* **2019**, *19*, 666–673. [CrossRef] [PubMed]
63. Xing, L.; Pan, Y.; Shi, Y.; Shu, Y.; Feng, J.; Li, W.; Cao, L.; Wang, L.; Gu, W.; Song, Y.; et al. Biomarkers of Osimertinib Response in Patients with Refractory, EGFR-T790M-positive Non-Small Cell Lung Cancer and Central Nervous System Metastases: The APOLLO Study. *Clin. Cancer Res.* **2020**, *26*, 6168–6175. [CrossRef] [PubMed]
64. Yamaguchi, H.; Wakuda, K.; Fukuda, M.; Kenmotsu, H.; Mukae, H.; Ito, K.; Chibana, K.; Inoue, K.; Tanaka, K. A Phase II Study of Osimertinib for Radiotherapy-Naive Central Nervous System Metastasis From NSCLC: Results for the T790M Cohort of the OCEAN Study (LOGIK1603/WJOG9116L). *J. Thorac. Oncol.* **2021**, *16*, 2121–2132. [CrossRef] [PubMed]
65. Zhao, Z.; Su, C.; Xiu, W.; Wang, W.; Zeng, S.; Huang, M.; Gong, Y.; Lu, Y.; Zhang, Y. Response to Pralsetinib Observed in Meningeal-Metastatic EGFR-Mutant NSCLC With Acquired RET Fusion: A Brief Report. *JTO Clin. Res. Rep.* **2022**, *3*, 100343. [CrossRef] [PubMed]
66. Fan, Y.; Huang, Z.; Fang, L.; Miao, L.; Gong, L.; Yu, H.; Yang, H.; Lei, T.; Mao, W. A phase II study of icotinib and whole-brain radiotherapy in Chinese patients with brain metastases from non-small cell lung cancer. *Cancer Chemother. Pharmacol.* **2015**, *76*, 517–523. [CrossRef]
67. Zhou, L.; He, J.; Xiong, W.; Liu, Y.; Xiang, J.; Yu, Q.; Liang, M.; Zhou, X.; Ding, Z.; Huang, M.; et al. Impact of whole brain radiation therapy on CSF penetration ability of Icotinib in EGFR-mutated non-small cell lung cancer patients with brain metastases: Results of phase I dose-escalation study. *Lung Cancer* **2016**, *96*, 93–100. [CrossRef] [PubMed]
68. Sakji-Dupré, L.; Le Rhun, E.; Templier, C.; Desmedt, E.; Blanchet, B.; Mortier, L. Cerebrospinal fluid concentration of vemurafenib in patients treated for brain metastatic BRAF-V600 mutated melanoma. *Melanoma Res.* **2015**, *25*, 302–305. [CrossRef]
69. Hottinger, A.F.; Bensaid, D.; Micheli, R.D.; Moura, B.; Mokhtari, K.; Cardoso, E.; Idbaih, A.; Stupp, R. Leptomeningeal tumor response to combined MAPK/ERK inhibition in V600E-mutated gliomas despite undetectable CSF drug levels. *Ann. Oncol.* **2019**, *30*, 155–156. [CrossRef]
70. Costa, D.B.; Kobayashi, S.; Pandaya, S.S.; Yeo, W.; Shen, Z.; Tan, W.; Wilner, K.D. CSF concentration of the anaplastic lymphoma kinase inhibitor crizotinb. *J. Clin. Oncol.* **2011**, *29*, e443–e445. [CrossRef]
71. Metro, G.; Lunardi, G.; Floridi, P.; Pascali, J.P.; Marcomigni, L.; Chiari, R.; Ludovini, V.; Crinó, L.; Gori, S. CSF Concentration of Crizotinib in Two ALK-Positive Non-Small-Cell Lung Cancer Patients with CNS metastases Deriving Clinical Benefit from Treatment. *J. Thorac. Oncol.* **2015**, *10*, e26–e27. [CrossRef] [PubMed]
72. Okawa, S.; Shibayama, T.; Shimonishi, A.; Nishimura, J.; Ozeki, T.; Takada, K.; Kayatani, H.; Minami, D.; Sato, K.; Fujiwara, K.; et al. Success of Crizotinib Combined with Whole-Brain Radiotherapy for Brain Metastases in a Patient with Anaplastic Lymphoma Kinase Rearrangement-Positive Non-Small-Cell Lung Cancer. *Case Rep. Oncol.* **2018**, *11*, 777–783. [CrossRef]
73. Okimoto, T.; Tsubasa, Y.; Hotta, T.; Hamaguchi, M.; Nakado, M.; Hamaguchi, S.I.; Hamada, A.; Isobe, T. A Low Crizotinib Concentration in the Cerebrospinal Fluid Causes Ineffective treatment of Anaplastic Lymphoma Kinase-positive Non-small Cell Lung Cancer with Carcinomatous Meningitis. *Intern. Med.* **2019**, *58*, 703–705. [CrossRef] [PubMed]
74. Mehta, S.; Fiorelli, R.; Bao, X.; Pennington-Krygier, C.; Derogatis, A.; Kim, S.; Yoo, W.; Li, J.; Sanai, N. A Phase 0 Trial of Ceritinib in Patients with Brain Metastasis and Recurrent Glioblastoma. *Clin. Cancer Res.* **2022**, *28*, 289–297. [CrossRef] [PubMed]

75. Gadgeel, S.M.; Grandhi, L.; Riely, G.J.; Chiappori, A.A.; West, H.L.; Azada, M.C.; Morcos, P.N.; Lee, R.M.; Garcia, L.; Yu, L.; et al. Safety and activity of alectinib against systemic disease and brain metastases in patients with crizotinib-resistant ALK-rearranged non-small-cell lung cancer (AF-002JG): Results from the dose-finding portion of a phase 1/2 study. *Lancet Oncol.* **2014**, *15*, 1119–1128. [CrossRef]
76. Metro, G.; Lunardi, G.; Bennati, C.; Chiarini, P.; Sperduti, I.; Ricciuti, B.; Marcomigni, L.; Costa, C.; Crinó, L.; Floridi, P.; et al. Alectinib's activity against CNS metastases from ALK-positive non-small cell lung cancer: A single institution case series. *J. Neurooncol.* **2016**, *129*, 355–361. [CrossRef]
77. Sun, S.; Pithavala, Y.K.; Martini, Y.F.; Chen, J. Evaluation of Lorlatinib Cerebrospinal Fluid Concentrations in Relation to Target Concentrations for Anaplastic lymphoma Kinase (ALK) Inhibition. *J. Clin. Pharmacol.* **2022**, *62*, 1170–1176. [CrossRef]
78. Miller, T.W.; Traphagen, N.A.; Li, J.; Lewis, L.D.; Lopes, B.; Asthagiri, A.; Loomba, J.; de Jong, J.; Schiff, D.; Patel, S.H.; et al. Tumor pharmacokinetics and pharmacodynamics of the CDK4/6 inhibitor ribociclib in patients with recurrent glioblastoma. *J. Neurooncol.* **2019**, *144*, 563–572. [CrossRef]
79. Tien, A.; Li, J.; Bao, X.; Derogatis, A.; Kim, S.; Mehta, S.; Sanai, N. A Phase 0 Trial of Ribociclib in Recurrent Glioblastoma Patients Incorporating a Tumor Pharmacodynamic- and Pharmacokinetic-Guided Expansion Cohort. *Clin. Cancer Res.* **2019**, *25*, 5777–5786. [CrossRef]
80. DeWire, M.D.; Fuller, C.; Campagne, O.; Lin, T.; Pan, H.; Poussaint, T.Y.; Baxter, P.A.; Hwang, E.I.; Bukowinski, A.; Dorris, K.; et al. A Phase I and Surgical Study of Ribociclib and Everolimus in Children with Recurrent or Refractory Malignant Brain Tumors: A Pediatric Brain Tumor Consortium Study. *Clin. Cancer Res.* **2021**, *27*, 2442–2451. [CrossRef]
81. Fiocchi, R.; D'Elia, E.; Vittori, C.; Sebastiani, R.; Strobelt, N.; Eleftheriou, G.; Introna, M.; Freddi, C.; Crippa, A. First Report of a Successful Pregnancy in an Everolimus-Treated Hear-Transplanted Patient: Neonatal Disappearance of Immunosuppressive Drugs. *Am. J. Transplant.* **2016**, *16*, 1319–1322. [CrossRef] [PubMed]
82. Molenaar-Kuijsten, L.; Verheijen, R.B.; Jacobs, B.A.W.; Thijssen, B.; Rosing, H.; Dorlo, T.P.C.; Beijnen, J.H.; Steeghs, N.; Huitema, A.D.R. Everolimus Concentration in Saliva to Predict Stomatitis: A Feasibility Study in Patients with Cancer. *Ther. Drug Monit.* **2022**, *44*, 520–526. [CrossRef] [PubMed]
83. Gori, S.; Lunardi, G.; Inno, A.; Foglietta, J.; Cardinali, B.; Del Mastro, L.; Crinó, L. Lapatinib concentration in cerebrospinal fluid in two patients with HER2-positive metastatic breast cancer and brain metastases. *Ann. Oncol.* **2014**, *25*, 912–913. [CrossRef]
84. Freedman, R.A.; Gelman, R.S.; Agar, N.Y.R.; Santagata, S.; Randall, E.C.; Gimenez-Cassina Lopez, B.; Connolly, R.M.; Dunn, I.F.; Van Poznak, C.H.; Anders, C.K.; et al. Pre- and Postoperative Neratinib for HER2-Positive Breast Cancer Brain Metastases: Translational Breast Cancer Research Consortium 022. *Clin. Breast Cancer* **2020**, *20*, 145–151.e2. [CrossRef] [PubMed]
85. Law, S.C.; Hoang, T.; O'Rourke, K.; Tobin, J.W.D.; Gunawardana, J.; Loo-Oey, D.; Bednarska, K.; de Long, L.M.; Sabdia, M.B.; Hapgood, G.; et al. Successful treatment of Epstein-Barr virus-associated primary central nervous system lymphoma due to post-transplantation lymphoproliferative disorder, with ibrutinib and third-party Epstein-Barr virus-specific T cells. *Am. J. Transplant.* **2021**, *21*, 3465–3471. [CrossRef]
86. Yu, H.; Kong, H.; Li, C.; Dong, X.; Wu, Y.; Zhuang, Y.; Han, S.; Lei, T.; Yang, H. Bruton's tyrosine kinase inhibitors in primary central nervous system lymphoma-evaluation of anti-tumor efficacy and brain distribution. *Transl. Cancer Res.* **2021**, *10*, 1975–1983. [CrossRef] [PubMed]
87. Zhang, Y.; Li, Y.; Zhuang, Z.; Wang, W.; Wei, C.; Zhao, D.; Zhou, D.; Zhang, W. Preliminary Evaluation of Zanubrutinib-Containing Regimens in DLBCL and the Cerebrospinal Fluid Distribution of Zanubrutinib: A 13-Case Series. *Front. Oncol.* **2021**, *11*, 760405. [CrossRef] [PubMed]
88. Krens, S.D.; Mulder, S.F.; van Erp, N.P. Lost in third space: Altered tyrosine-kinase inhibitor pharmacokinetics in a patient with malignant ascites. *Cancer Chemother. Pharmacol.* **2022**, *89*, 271–274. [CrossRef] [PubMed]
89. Zeiner, P.S.; Kinzig, M.; Divé, I.; Maurer, G.D.; Filipski, K.; Harter, P.N.; Senft, C.; Bähr, O.; Hattinen, E.; Steinbach, J.P.; et al. Regorafenib CSF Penetration, Efficacy, and MRI Patterns in Recurrent Malignant Glioma Patients. *J. Clin. Med.* **2019**, *8*, 2031. [CrossRef]
90. Tanaka, H.; Taima, K.; Makiguchi, T.; Nakagawa, J.; Niiko, T.; Tasaka, S. Activity and bioavailability of tepotinib for leptomeningeal metastasis of NSCLC with MET exon skipping mutation. *Cancer Commun.* **2021**, *41*, 83–87. [CrossRef]
91. Ninomaru, T.; Okada, H.; Fujishima, M.; Irie, K.; Fukushima, S.; Hata, A. Lazarus Response to Tepotinib for Leptomeningeal metastases in a Patient with MET Exon 14 Skipping Mutation-Positive Lung Adenocarcinoma. Case Report. *JTO Clin. Res. Rep.* **2021**, *2*, 100145. [CrossRef]
92. Rasmussen, T.A.; Tolstrup, M.; Møller, H.J.; Brinkmann, C.R.; Olesen, R.; Erikstrup, C.; Laursen, A.L.; Østergaard, L.; Søgaard, O.S. Activation of latent human immunodeficiency virus by the histone deacetylase inhibitor panobinostat: A pilot study to assess effects on the central nervous system. *Open Forum Infect. Dis.* **2015**, *2*, ofv037. [CrossRef] [PubMed]
93. Goldberg, J.; Sulis, M.L.; Bender, J.; Jeha, S.; Gardner, R.; Pollard, J.; Aquino, V.; Laetsch, T.; Winick, N.; Fu, C.; et al. A phase I study of panobinostat in children with relapse and refractory hematologic malignancies. *Pediatr. Hematol. Oncol.* **2020**, *37*, 465–474. [CrossRef] [PubMed]
94. Gajjar, A.; Stewart, C.F.; Ellison, D.W.; Kaste, S.; Kun, L.E.; Packer, R.J.; Goldman, S.; Chintagumpala, M.; Wallace, D.; Takebe, N.; et al. Phase I study of vismodegib in children with recurrent or refractory medulloblastoma: A pediatric brain tumor consortium study. *Clin. Cancer Res.* **2013**, *19*, 6305–6312. [CrossRef] [PubMed]

95. Reda, G.; Cassin, R.; Dovrtelova, G.; Matteo, C.; Giannotta, J.; D'Incalci, M.; Cortelezzi, A.; Zucchetti, M. Venetoclax penetrates in cerebrospinal fluid and may be effective in chronic lymphocytic leukemia with central nervous system involvement. *Hematologica* **2019**, *104*, e222–e223. [CrossRef]
96. Condorelli, A.; Matteo, C.; Leotta, S.; Schininá, G.; Sciortino, R.; Piccolo, G.M.; Parrinello, N.L.; Proietto, M.; Camuglia, M.G.; Zucchetti, M.; et al. Venetoclax penetrates in cerebrospinal fluid of an acute myeloid leukemia patient with leptomeningeal involvement. *Cancer Chemother. Pharmacol.* **2022**, *89*, 267–270. [CrossRef]
97. Bareschino, M.A.; Schettino, C.; Troiani, T.; Martinelli, E.; Morgillo, F.; Ciardiello, F. Erlotinib in cancer treatment. *Ann. Oncol.* **2007**, *6*, 35–41. [CrossRef]
98. Psallidas, I.; Kalomenidis, I.; Porcel, J.M.; Robinson, B.W.; Stathopoulos, G.T. Malignant pleural effusion: From bench to bedside. *Eur. Respir. Rev.* **2016**, *25*, 189–198. [CrossRef]
99. Deak, D.; Gorcea-Andronic, N.; Sas, V.; Teodorescu, P.; Constantinescu, C.; Iluta, S.; Pasca, S.; Hotea, I.; Turcas, C.; Moisoiu, V.; et al. A narrative review of central nervous system involvement in acute leukemias. *Ann. Transl. Med.* **2021**, *9*, 68. [CrossRef]
100. Lenk, L.; Alsadeq, A.; Schewe, D.M. Involvement of the central nervous system in acute lymphoblastic leukemia: Opinions on molecular mechanisms and clinical implications based on recent data. *Cancer Metastasis Rev.* **2020**, *39*, 173–187. [CrossRef]
101. Kretz, O.; Weiss, H.M.; Schumacher, M.M.; Gross, G. In vitro blood distribution and plasma protein binding of the tyrosine kinase inhibitor imatinib and its active metabolite, CGP74588, in rat, mouse, dog, monkey, healthy humans and patients acute lymphatic leukaemia. *Br. J. Clin. Pharmacol.* **2004**, *58*, 212–216. [CrossRef] [PubMed]
102. Li, J.; Brahmer, J.; Messersmith, W.; Hidalgo, M.; Baker, S.D. Binding of gefitinib, an inhibitor of epidermal growth factor receptor-tyrosine kinase, to plasma proteins and blood cells: In vitro and in cancer patients. *Invest. New Drugs* **2006**, *24*, 291–297. [CrossRef] [PubMed]
103. Muller, I.B.; De Langen, A.J.; Honeywell, R.J.; Giovanni, E.; Peters, G.J. Overcoming crizotinib resistance in ALK-rearranged NSCLC with the second-generation ALK-inhibitor ceritinib. Expert Rev. *Anticancer Ther.* **2016**, *16*, 147–157. [CrossRef] [PubMed]
104. Wind, S.; Schnell, D.; Ebner, T.; Freiwald, M.; Stopfer, P. Clinical Pharmacokinetics and Pharmacodynamics of Afatinib. *Clin. Pharmacokinet.* **2017**, *56*, 235–250. [CrossRef]
105. Andreu, I.; Lence, E.; González-Bello, C.; Mayorga, C.; Cuquerella, M.C.; Vayá, I.; Miranda, M.A. Protein Binding of Lapatinib and its N- and O-Dealkylated Metabolites Interrogated by Fluorescence, Ultrafast Spectroscopy and Molecular Dynamics Simulations. *Front. Pharmacol.* **2020**, *11*, 576495. [CrossRef]
106. Zhang, W.; Heinzmann, D.; Grippo, J.F. Clinical Pharmacokinetics of Vemurafenib. *Clin. Pharmacokinet.* **2017**, *56*, 1033–1043. [CrossRef]
107. Matsusaki, K.; Aridome, K.; Emoto, S.; Kajiyama, H.; Takagaki, N.; Takahashi, T.; Tsubamoto, H.; Nagao, S.; Watanabe, A.; Shimada, H.; et al. Clinical practice guideline for the treatment of malignant ascites: Section summary in Clinical Practice Guideline for peritoneal dissemination (2021). *Int. J. Clin. Oncol.* **2022**, *27*, 1–6. [CrossRef]
108. Benn, C.L.; Dawson, L.A. Clinically precedented protein kinases: Rationale for their use in neurodegenerative disorders. *Front. Aging Neurosci.* **2020**, *12*, 242. [CrossRef]
109. Xie, X.; Yuan, P.; Kou, L.; Chen, X.; Li, J.; Li, Y. Nilotinib in Parkinson's disease: A systematic review and meta-analysis. *Front. Aging Neurosci.* **2022**, *14*, 996217. [CrossRef]
110. Ancidoni, A.; Bacigalupo, I.; Remoli, G.; Lacorte, E.; Piscopo, P.; Sarti, G.; Corbo, M.; Vanacore, N.; Canevelli, M. Anticancer drugs repurposed for Alzheimer's disease: A systematic review. *Alzheimers Res. Ther.* **2021**, *13*, 96.
111. Hebron, M.L.; Lonskaya, I.; Moussa, C. E-H. Nilotinib reverses loss of dopamine neurons and improves motor behavior via autophagic degradation of α-synuclein in Parkinson's disease models. *Hum. Mol. Genet.* **2013**, *22*, 3315–3328. [CrossRef] [PubMed]
112. La Barbera, L.; Vedele, F.; Nobili, A.; Krashia, P.; Spoleti, E.; Latagliata, E.C.; Cutuli, D.; Cauzzi, E.; Marino, R.; Viscomi, M.T.; et al. Nilotinib restores memory function by preventing dopaminergic neuron degeneration in a mouse model of Alzheimer's Disease. *Prog. Neurobiol.* **2021**, *202*, 102031. [CrossRef] [PubMed]
113. Lonskaya, I.; Hebron, M.L.; Desforges, N.M.; Schachter, J.B.; Moussa, C.E.-H. Nilotinib-induced autophagic changes increase endogenous parkin level and ubiquitination, leading to amyloid clearance. *J. Mol. Med.* **2014**, *92*, 373–386. [CrossRef] [PubMed]
114. Jones, H.K.; Stafford, L.E.; Swaisland, H.C.; Payne, R. A sensitive assay for ZD1839 (Iressa) in human plasma by liquid-liquid extraction and high performance liquid chromatography with mass spectrometric detection: Validation and use in Phase I clinical trial. *J. Pharm. Biomed. Anal.* **2002**, *29*, 221–228. [CrossRef] [PubMed]
115. Bakhtiar, R.; Lohne, J.; Ramos, L.; Khelmani, L.; Hayes, M.; Tse, F. High-throughput quantification of the anti-leukemia drug STI571 (Gleevec) and its main metabolite (CGP 74588) in human plasma using liquid chromatography-tandem mass spectrometry. *J. Chromatogr. B Analyt Technol. Biomed. Life Sci.* **2002**, *768*, 325–340. [CrossRef]
116. Zhao, M.; He, P.; Rudek, M.A.; Hidalgo, M.; Baker, S.D. Specific method for determination of OSI-774 and its metabolite OSI-420 in human plasma by using liquid chromatography-tandem mass spectrometry. *J. Chromatogr. B* **2003**, *793*, 413–420. [CrossRef]
117. Hayashi, H.; Kita, Y.; Iihara, H.; Yanase, K.; Ohno, Y.; Hirose, C.; Yamada, M.; Todoroki, K.; Kitaichi, K.; Minatoguchi, S.; et al. Simultaneous and rapid determination of gefitinib, erlotinib and afatinib plasma levels using liquid chromatography/tandem mass spectrometry in patients with non-small-cell lung cancer. *Biomed. Chromatogr.* **2016**, *30*, 1150–1154. [CrossRef]
118. Bao, X.; Wu, J.; Sanai, N.; Li, J. A liquid chromatography with tandem mass spectrometry method for quantitating total and unbound ceritinib in patient plasma and brain tumor. *J. Pharm. Biomed. Anal.* **2018**, *8*, 20–26. [CrossRef]

119. Roberts, M.S.; Turner, D.C.; Broniscer, A.; Stewart, C.F. Determination of crizotinib in human and mouse plasma by liquid chromatography electrospray ionization tandem mass spectrometry (LC-ESI-MS/MS). *J. Chromatogr. B* **2014**, *960*, 151–157. [CrossRef]
120. Cardoso, E.; Mercier, T.; Wagner, A.D.; Homicsko, K.; Michielin, O.; Ellefsen-Lavoie, K.; Cagnon, L.; Diezi, M.; Buclin, T.; Widmer, N. Quantification of the next-generation oral anti-tumor drugs dabrafenib, trametinib, vemurafenib, cobimetinib, pazopanib, regorafenib and two metabolites in human plasma by liquid chromatography-tandem mass spectrometry. *J. Chromatogr. B Analyt. Technol. Biomed. Life Sci.* **2018**, *1083*, 124–136. [CrossRef]
121. De Francia, S.; D'Avolio, A.; De Martino, F.; Pirro, E.; Baietto, L.; Siccardi, M.; Simiele, M.; Racca, S.; Saglio, G.; Di Carlo, F.; et al. New HPLC-MS method for the simultaneous quantification of the antileukemia drugs imatinib, dasatinib, and nilotonib in human plasma. *J. Chromatogr. B* **2009**, *877*, 1721–1726. [CrossRef] [PubMed]
122. Masters, A.R.; Sweeney, C.J.; Jones, D.R. The quantification of erlotinib (OSI-774) and OSI-420 in human plasma by liquid chromatography-tandem mass spectrometry. *J. Chromatogr. B* **2007**, *848*, 379–383. [CrossRef] [PubMed]
123. Thappali, S.R.S.; Varanasi, K.; Veeraraghavan, S.; Arla, R.; Chennupati, S.; Rajamanickam, M.; Vakkalanka, S.; Khagga, M. Simultaneous determination of celecoxib, erlotinib, and its metabolite desmethyl-erlotinib (OSI-420) in rat plasma by liquid chromatography/tandem mass spectrometry with positive/negative ion-switching electrospray ionisation. *Sci. Pharm.* **2012**, *80*, 633–646. [CrossRef]
124. Lepper, E.R.; Swain, S.M.; Tan, A.R.; Figg, W.D.; Sparreboom, A. Liquid-chromatographic determination of erlotinib (OSI-774), an epidermal growth factor receptor tyrosine kinase inhibitor. *J. Chromatogr. B* **2003**, *796*, 181–188. [CrossRef] [PubMed]
125. Zhang, W.; Siu, L.L.; Moore, M.J.; Chen, E.X. Simultaneous determination of OSI-774 and its major metabolite OSI-420 in human plasma by using HPLC with UV detection. *J. Chromatogr. B Analyt Technol. Biomed. Life Sci.* **2005**, *814*, 143–147. [CrossRef]
126. *Chromsystems Instruments and Chemicals G.m.b.H.: Chromsystems Instruction Manual for LC-MS/MS Analysis. MassTox Immunosuppressants in Whole Blood OneMinute Test for Automated Sample Preparation on Hamilton MassSTAR*; Order No. 93900/1200/DWP. V1.0; Chromsystems Instruments and Chemicals G.m.b.H.: Gräfelfing, Germany, 2020.
127. Verheijen, R.B.; Atrafi, F.; Schellens, J.H.M.; Beijnen, J.H.; Huitema, A.D.R.; Mathijsen, R.H.J.; Steeghs, N. Pharmacokinetic optimization of everolimus dosing in oncology: A randomized crossover trial. *Clin. Pharmacokinet.* **2018**, *57*, 637–644. [CrossRef]
128. McKillop, D.; Partridge, E.A.; Hitchison, M.; Rhead, S.A.; Parry, A.C.; Bardsley, J.; Woodman, H.M.; Swaisland, H.C. Pharmacokinetics of gefitinib, an epidermal growth factor receptor tyrosine kinase inhibitor, in rat and dog. *Xenobiotica* **2004**, *34*, 901–915. [CrossRef]
129. Fang, L.; Song, Y.; Weng, X.; Li, F.; Xu, Y.; Lin, N. Highly sensitive HPLC-DAD method for the assay of gefitinib in patient plasma and cerebrospinal fluid: Application to a blood-brain barrier penetration study. *Biomed. Chromatogr.* **2015**, *29*, 1937–1940. [CrossRef]
130. Zhao, M.; Hartke, C.; Jimeno, A.; Li, J.; He, P.; Zabelina, Y.; Hidalgo, M.; Baker, S.D. Specific method for determination of gefitinib in human plasma, mouse -plasma and tissues using high performance liquid chromatography coupled to tandem mass spectrometry. *J. Chromatogr. B* **2005**, *819*, 73–80. [CrossRef]
131. Yang, H.; Li, C.; Chen, Z.; Mou, H.; Gu, L. Determination of chidamide in rat plasma and cerebrospinal fluid. *Regul. Toxicol. Pharmacol.* **2018**, *98*, 24–30. [CrossRef]
132. Parise, R.A.; Ramanathan, R.K.; Hayes, M.J.; Egorin, M.J. Liquid chromatographic-mass spectrometric assay for quantitation of imatinib and its main metabolite (CGP 74588) in plasma. *J. Chromatogr. B* **2003**, *791*, 39–44. [CrossRef] [PubMed]
133. D'Avolio, A.; Simiele, M.; De Francia, S.; Ariaudo, A.; Baietto, L.; Cusato, J.; Fava, C.; Saglio, G.; Di Carlo, F.; Di Perri, G. HPLC-MS method for the simultaneous quantification of the antileukemia drugs imatinib, dasatinib and nilotinib in human peripheral blood mononuclear cell (PBMC). *J. Pharm. Biomed. Anal.* **2012**, *59*, 109–116. [CrossRef] [PubMed]
134. Pursche, S.; Ottmann, O.G.; Ehninger, G.; Schleyer, E. High-performance liquid chromatography method with ultraviolet detection for the quantification of the BCR-ABL inhibitor nilotinib (AMN107) in plasma, urine, culture medium and cell preparations. *J. Chromatogr. B* **2007**, *852*, 208–216. [CrossRef] [PubMed]
135. Andriamanana, I.; Gana, I.; Duretz, B.; Hulin, A. Simultaneous analysis of anticancer agents bortezomib, imatinib, nilotinib, dasatinib, erlotinib, lapatinib, sorafenib, sunitinib and vandetanib in human plasma using LC/MS/MS. *J. Chromatogr. B. Analyt. Technol. Biomed. Life Sci.* **2013**, *926*, 83–91. [CrossRef]
136. Bao, X.; Wu, J.; Sanai, N.; Li, J. Determination of total and unbound ribociclib in human plasma and brain tumor tissues using liquid chromatography coupled with tandem mass spectrometry. *J. Pharm. Biomed. Anal.* **2019**, *166*, 197–204. [CrossRef]
137. Kala, A.; Patel, Y.T.; Davis, A.; Stewart, C.F. Development and validation of LC-MS/MS methods for the measurement of ribociclib, a CDK4/6 inhibitor, in mouse plasma and Ringer's solution and its application to a cerebral microdialysis study. *J. Chromatogr. B* **2017**, *1057*, 110–117. [CrossRef]
138. Zhen, Y.; Thomas-Schoemann, A.; Sakji, L.; Boudou-Rouquette, P.; Dupin, N.; Mortier, L.; Vidal, M.; Goldwasser, F.; Blanchet, B. An HPLC-UV method for the simultaneous quantification of vemurafenib and erlotinib in plasma from cancer patients. *J. Chromatogr. B Analyt Technol. Biomed. Life Sci.* **2013**, *28*, 93–97. [CrossRef]
139. Salem, A.H.; Hu, B.; Freise, K.J.; Agarwal, S.K.; Sidhu, D.S.; Wong, S.L. Evaluation of the pharmacokinetic interaction between venetoclax, a selective BCL-2 inhibitor, and warfarin in healthy volunteers. *Clin. Drug Investig.* **2017**, *37*, 303–309. [CrossRef]

140. Ding, X.; Chou, B.; Graham, R.A.; Cheeti, S.; Percey, S.; Matassa, L.C.; Reuschel, S.A.; Meng, M.; Liu, S.; Voelker, T.; et al. Determination of GDC-0449, a small-molecule inhibitor of the Hedgehog signaling pathway, in human plasma by solid phase extraction-liquid chromatographic-tandem mass spectrometry. *J. Chromatogr. B* **2010**, *878*, 785–790. [CrossRef]
141. Seidel, C.; Viehweger, C.; Kortmann, R.-D. Is there an indication for first-line radiotherapy in primary CNS lymphoma? *Cancers* **2021**, *13*, 2580. [CrossRef]
142. Xu, K.; Huang, Y.; Yao, J.; He, X. Whole-brain radiotherapy and chemotherapy in the treatment of patients with breast cancer and brain metastases. *Int. J. Clin. Exp. Med.* **2021**, *14*, 1250–1257.
143. Hart, E.; Odé, Z.; Derieppe, M.P.P.; Groenink, L.; Heymans, M.W.; Otten, R.; Lequin, M.H.; Janssens, G.O.R.; Hoving, E.W.; van Vuurden, D.G. Blood-brain barrier permeability following conventional photon radiotherapy—A systematic review and meta-analysis of clinical and preclinical studies. *Clin. Transl. Radiat. Oncol.* **2022**, *35*, 44–55. [CrossRef] [PubMed]
144. Mantovani, C.; Gastino, A.; Cerrato, M.; Badellino, S.; Ricardi, U.; Levis, M. Brain metastases from non-small cell lung cancer: Current approaches and future directions. *Front. Oncol.* **2021**, *11*, 772789. [CrossRef] [PubMed]
145. Toh, Y.L.; Pah, Y.Y.; Shwe, M.; Kanesvaran, R.; Toh, C.K.; Chan, A.; Ho, H.K. HPLC-MS/MS coupled with equilibrium dialysis method for quantification of free drug concentration of pazopanib in plasma. *Heliyon* **2020**, *27*, e03813. [CrossRef] [PubMed]
146. Roy, K.S.; Nazdrajic, E.; Shimelis, O.I.; Ross, M.J.; Chen, Y.; Cramer, H.; Pawliszyn, J. Optimizing a high-throughtput solid-phase microextraction system to determine the plasma protein binding of drugs in human plasma. *Anal. Chem.* **2021**, *93*, 11061–11065. [CrossRef] [PubMed]
147. Mamada, H.; Iwamoto, K.; Nomura, Y.; Uesawa, Y. Predicting blood-to-plasma concentration ratios of drugs from chemical structures and volumes of distribution in humans. *Mol. Divers.* **2021**, *25*, 1261–1270. [CrossRef]
148. Cao, B.; Soerjomataram, I.; Bray, F. The burden and prevention of premature deaths from noncommunicable diseases, including cancer: A global perspective. In *World Cancer Report: Cancer Research for Cancer Prevention*; Wild, C.P., Weiderpass, E., Stewart, B.W., Eds.; International Agency for Research on Cancer, World Health Organization: Lyon, France, 2020; pp. 16–22.

pharmaceutics

MDPI

Article

External Evaluation of Population Pharmacokinetic Models of Methotrexate for Model-Informed Precision Dosing in Pediatric Patients with Acute Lymphoid Leukemia

Shengfeng Wang [1,2,3,†], Qiufen Yin [1,†], Minghua Yang [2], Zeneng Cheng [1] and Feifan Xie [1,*]

[1] Division of Biopharmaceutics and Pharmacokinetics, Xiangya School of Pharmaceutical Sciences, Central South University, Changsha 410013, China
[2] Postdoctoral Research Station of Clinical Medicine and Department of Pediatrics, The Third Xiangya Hospital, Central South University, Changsha 410013, China
[3] Department of Pharmacy, The Third Xiangya Hospital, Central South University, Changsha 410013, China
* Correspondence: feifan.xie@csu.edu.cn; Tel./Fax: +86-0731-8265-0446
† These authors contributed equally to this work and shared the first authorship.

Abstract: Background: Methotrexate (MTX) is a key immunosuppressant for children with acute lymphoid leukemia (ALL), and it has a narrow therapeutic window and relatively high pharmacokinetic variability. Several population pharmacokinetic (PopPK) models of MTX in ALL children have been reported, but the validity of these models for model-informed precision dosing in clinical practice is unclear. This study set out to evaluate the predictive performance of published pediatric PopPK models of MTX using an independent patient cohort. Methods: A PubMed literature search was performed to identify suitable models for evaluation. Demographics and measurements of the validation dataset were retrospectively collected from the medical records of ALL children who had received intravenous MTX. Predictive performance for each model was assessed by visual comparison of predictions to observations, median and mean predicted error (PE), and relative root mean squared error (RMSE). Results: Six models were identified for external evaluation, carried out on a dataset containing 354 concentrations from 51 pediatrics. Model performance varied considerably from one model to another. Different models had the median PE for population and individual predictions at −33.23% to 442.04% and −25.20% to 6.52%, mean PE for population and individual predictions at −25.51% to 780.87% and 1.33% to 64.44%, and RMSE for population and individual predictions at 62.88% to 1182.24% and 63.39% to 152.25%. All models showed relatively high RMSE. Conclusions: Some of the published models showed reasonably low levels of bias but had some problems with imprecision, and extensive evaluation is needed before model application in clinical practice.

Keywords: methotrexate; children; acute lymphoid leukemia; population pharmacokinetics; external validation

Citation: Wang, S.; Yin, Q.; Yang, M.; Cheng, Z.; Xie, F. External Evaluation of Population Pharmacokinetic Models of Methotrexate for Model-Informed Precision Dosing in Pediatric Patients with Acute Lymphoid Leukemia. *Pharmaceutics* **2023**, *15*, 569. https://doi.org/10.3390/pharmaceutics15020569

Academic Editor: Paolo Magni

Received: 30 December 2022
Revised: 5 February 2023
Accepted: 7 February 2023
Published: 8 February 2023

1. Introduction

Methotrexate (MTX), a folate reductase inhibitor, has been widely used in the treatment of autoimmune diseases and malignancies for decades [1,2]. Leukemia is a group of malignant neoplastic diseases of the hematopoietic system, and it poses a significant health risk to children. Childhood leukemia mainly includes acute lymphoid leukemia (ALL) and acute myeloid leukemia (AML). ALL is the most common childhood cancer [3], and it accounts for more than 70% of childhood leukemia in China [4]. MTX is the cornerstone of maintenance cycles in childhood ALL chemotherapy [5], and its clinical dose can be roughly classified as low (<0.5 g/m^2), intermediate (0.5–1.0 g/m^2), and high (>1.0 g/m^2) dose [6]. High-dose MTX (HD-MTX) provides the ability to target extramedullary leukemia by producing cytotoxic concentrations in sanctuary sites (e.g., cerebrospinal fluid) where low-dose MTX does not readily distribute [7]. Compared with low-dose MTX, HD-MTX

shows significantly better patient event-free survival for childhood leukemia [8,9], and the use of HD-MTX is widely accepted as the first-line therapy in consolidation for childhood ALL [10,11].

In clinical practice, administration of HD-MTX often begins with a loading dose (e.g., 10% of the total dose) infused over 0.5 h, followed immediately by a continuous titration of the remaining dose over 23.5 h. It has been described that the steady-state plasma MTX concentration ($C_{p,ss,}$ the concentration after the end of 24 h MTX infusion) is most appropriately associated with its therapeutic efficacy [12]. Depending on the risk level of cancer patients, the dose level of HD-MTX varies individually for maximizing efficacy while minimizing the toxicities [13]. For instance, a relatively high dose (e.g., 5.0 g/m^2) is suggested for ALL children with intermediate risk (IR) or high risk (HR) in order to improve the outcome [14], while the relatively low dose (e.g., 3.0 g/m^2) is adequate for low risk (LR) ALL children [10]. Age, leukocyte count, leukemic cell genotype, and minimal residual disease (MRD) are the important factors for risk classification [14,15]. The MTX dose is deemed effective if the $C_{p,ss,}$ is above 65 μmol/L (IR and HR patients) or 33 μmol/L (LR patients) [11,12], and the treatment is subtherapeutic with a high risk of relapse when the $C_{p,ss,}$ is below < 16 μmol/L. HD-MTX is associated with a variety of toxic reactions, and liver injury and nephrotoxicity are two of the serious adverse events [5,16]. It has been reported that MTX concentrations > 100 μmol/L at 24 h, >1.0 μmol/L at 48 h, and >0.1 μmol/L at 72 h are supratherapeutic and are associated with increased toxicity [10,17,18]. Therefore, the optimal use of HD-MTX is an important question for providing balanced efficacy and toxicity.

MTX has a narrow therapeutic window, and the pharmacokinetics (PK) of HD-MTX shows wide inter-individual variability (IIV) in children even under the same dosing regimen [19,20]. Routine therapeutic drug monitoring (TDM) for HD-MTX has been strongly recommended to reduce the incidence of adverse events in the target patient population [19,21]. Population pharmacokinetic (PopPK) models have the potential to improve patient care by streamlining the TDM process [22]. PopPK models are less dependent on precisely timed drug concentrations than traditional peak and/or trough concentration-based monitoring, and they provide the options to quantify PK variability and identify clinical characteristics (e.g., age and renal function) affecting the drug's PK. In particular, for the immunosuppressive agents that are typically personalized by TDM, PopPK models allow for the area under the concentration-time curve (AUC) guided monitoring using Bayesian forecasting with limited sampling. Furthermore, PopPK models can aid in accelerating the initial dose titration through a priori model-informed precision dosing (MIPD) based on the baseline covariates of the target patients. Further optimization of subsequent treatment target attainment can be performed through a posteriori MIPD based on available TDM measurements and updated covariates over time [23,24].

MIPD is an advanced quantitative approach (e.g., PopPK model) that combines prior knowledge on the drug-disease-patient system with patient data from TDM to support individualized dosing in ongoing treatment [25], which takes into account inter-individual variability in a drug's exposure. By combining the efficacy and toxicity risk targets, MIPD offers the potential to improve initial dose selection and individualized dose optimization, thereby it can minimize the duration of subtherapeutic or supratherapeutic HD-MTX doses. Before considering a PopPK model used in MIPD, model evaluation is an essential step to assess the model's accuracy and predictive performance. The most crucial question in the evaluation of a PopPK model is if it can extrapolate the model's results to patients at other institutions or forecast the drug's PK in prospective studies, especially when the goal of the model is to determine the ideal individual dose. Internal evaluation is necessary to test a model's ability to describe the population with which it has been constructed, and an external evaluation must be carried out to assess the predictive performance of the model when extrapolated. Currently, the PopPK models of HD-MTX in ALL children have been extensively reported [11,18–21,26], while the reported PK parameters and identified covariates varied significantly. Although some of the published PopPK models of MTX

in ALL children have been internally evaluated with a dataset from the same patient cohort, this does not guarantee a good prediction performance when subjected to similar patient populations from external institutions [27]. Therefore, it is important to evaluate the predictive performance of the published PopPK models of MTX using independent datasets in order to identify the best candidate model for MIPD.

The aim of this study was to provide a systemic summary of the published PopPK models of MTX in ALL children and evaluate the predictive performance of these models using an independent dataset.

2. Methods

2.1. Literature Search for the PopPK Models of MTX in ALL Children

A search of the literature data for the PopPK models of MTX in ALL children was made through PubMed (until 30 November 2022) using the following search terms: (population pharmacokinetics [Title/Abstract]) AND (methotrexate [Title/Abstract]) AND (children [Title/Abstract] OR paediatrics [Title/Abstract]). The identified studies were reviewed, and the relevant references were examined to identify other potential publications for inclusion. Published studies were included for further analysis if the PopPK of MTX was conducted in children with ALL. PopPK models of MTX were excluded from the external validation if (1) the key information (e.g., the typical PK parameters and IIVs) is inadequate for the model recompilation; and (2) the mean or median age of the patient population is beyond the age range (1.0–13.0 years) of our patient cohort for the external validation. For eligible PopPK models, the following information was extracted from the original studies: structure of the compartmental model, population PK estimates, covariate model, inter- and intra-individual variability, residual variability, and estimation method.

2.2. Dataset for External Evaluation

Data were collected retrospectively from the medical records of patients treated with HD-MTX at the Third Xiangya Hospital at Central South University from 2019 to 2022. This study was approved by the ethics committees of the hospital and was registered at the Chinese Clinical Trial Registry (Register number: ChiCTR2000035264). Throughout the study, all the procedures were carried out in accordance with the Declaration of Helsinki. ALL was diagnosed if at least 25% of lymphoblasts were present in the bone marrow [15], and we included patients with ALL who were under 18 years of age at the time of diagnosis.

Children with ALL were classified as LR, IR, and HR. The children with ALL whose MRD was <1% at 19 days or MRD < 0.01% at 46 days were placed in the LR group. Patients whose MRD was $\geq$1% at 46 days or who had leukemia blasts $\geq$ 5% without MRD markers or with mixed lineage leukemia fusion genes, age < 6 months, and WBC $\geq 300 \times 10^9$/L were placed in the HR group. All other cases are placed in the IR group. Theoretically, patients in the LR group were given an HD-MTX dose of 3.0 g/m^2, and patients in the IR or HR group were given an HD-MTX dose of 5.0 g/m^2. In practice, the actual HD-MTX dose was decided by the physicians for each patient. MTX was intravenously administered within 0.5 h for 10% of the total dose, and the remaining 90% dose was infused over 23.5 h.

Plasma samples were collected every 24 h until the MTX concentration dropped below 0.1 μmol/L. The actual sampling times were determined by the responsible nurses and may be slightly deviated from the theoretical points. MTX concentration was determined using fluorescence polarization immunoassay with a quantification limit of 0.05 μmol/L. Data were included if at least one intravenous dose of MTX and the concentration measurements were available. Data were excluded if there was any uncertainty about the time of dosing, infusion duration, or the sampling time of concentration measurements. Baseline characteristics of the ALL children were collected, including the demographics (gender, age, weight, body surface area (BSA), and height), the laboratory measurements (white blood cells, neutrophils, serum creatinine (Scr), alanine aminotransferase (ALT), and aspartate aminotransferase (AST)), and the estimated glomerular filtration rate (eGFR) based on the Bedside Schwartz formula (Equation (1)) [28]. Data collation was performed using R

version 4.2.0 (R Foundation for Statistical Computing, Vienna, Austria). No patient data in the external validation dataset had previously been included in the development of any of the PopPK models of MTX.

$$\text{eGFR} = \frac{0.413 \times \text{height}}{\text{Scr}} \quad (1)$$

2.3. Evaluation of Predictive Performance

Each selected PopPK model was separately implemented in NONMEM® software (version 7.3, Icon Development Solutions, Ellicott City, MD, USA) as described in the original article. Parameter estimates and covariate models for each PopPK model were set to those determined in the original publications. Concentration predictions were generated based on the specific PopPK models in combination with the doses, sampling times, and covariates recorded in the validation dataset. That is, the predicted concentrations were obtained based on the PopPK models using the maximum a posteriori-Bayesian estimation (MAP-BE, $ESITIMATION MAXEVAL=0 in NONMEM). Reported PK parameters were adopted for each PopPK model to calculate the predicted population and individual concentrations at sampling times identical to those of our own data. If the specified covariate in the PopPK model was not available in the evaluation dataset, the mean or median covariate value was used as stated in the original publication. In addition, a proportional error of 30% was assumed for the residual variability if the models did not report this information.

The predictive performance of the PopPK models was assessed by the use of graphics and statistical metrics. Goodness-of-fit (GOF) was assessed graphically by comparing observed concentrations (C_{obs}) to population predicted concentrations (C_{pred}) and individual predicted concentrations (C_{ipred}) to inspect potential bias (a systematic upward or downward deviation from the line of unity) and imprecision (a high degree of scattered data points around the line of unity). Furthermore, the Bland-Altman (B-A) plots were created to visualize the trends in bias for the population and individual predictions. The prediction error (PE; in percent; Equation (2)), the mean relative error (MPE; in percent; Equation (3)), and the relative root mean squared error (RMSE; in percent; Equation (4)) were calculated for population and individual predictions to quantify the predictive performance.

$$\text{PE} = \frac{C_{i,pred} - C_{obs}}{C_{obs}} \quad (2)$$

$$\text{MPE} = \frac{1}{N}\sum_{i=1}^{N}\frac{C_{i,pred} - C_{obs}}{C_{obs}} \quad (3)$$

$$\text{RMSE} = \sqrt{\frac{1}{N}\sum_{i=1}^{N}\left(\frac{C_{i,pred} - C_{obs}}{C_{obs}}\right)^2} \quad (4)$$

where N is the number of observed MTX concentrations, and $C_{i,pred}$ is the C_{ipred} or C_{pred} of MTX.

A PopPK model was deemed acceptable for our clinical settings when both the mean and median values of PE were less than 20% [27,29] and RMSE was less than or equal to 30% [29,30]. Data processing and plotting were carried out with R version 4.2.0.

3. Results

3.1. Literature Search and Summary of Published PopPK Models

The literature search identified a total of fourteen papers detailing the population pharmacokinetics of MTX in children [11,18–21,26,31–37]. Among them, six studies included ALL patients greater than 13 years or infants and were excluded for further analysis [18,31–35,37]. In addition, one PopPK study was conducted on pediatric patients with osteosarcoma and was also excluded [38]. Finally, six PopPK models of MTX in ALL children were included for the external evaluation [11,19–21,26,36]. The demographics, clinical characteristics, and doses for the patients of the included studies are summarized in

Table 1. The mean age for all the studies was 5.0–7.5 years. Three of the models evaluated were based on the data from Chinese children [19,20,26], and the others were developed for Spanish [21], American [36], and Mexican [11] children. The largest model was developed with data from 311 pediatric patients proposed by Gao et al. [19], while the smallest model was developed with data from 36 patients proposed by Hui et al. [20].

The key information (e.g., model structure and covariate model) of the included PopPK models were provided in Table 2. The disposition of MTX was described by a two-compartment model in five studies and a three-compartment model in one study [19]. Typical estimates for MTX clearance in the included studies ranged from 3.52 [36] to 7.73 [20] L/h, with the lowest value being reported in the Jonsson et al. study with a median patient age of 5.0 years old. In studies based on a two-compartment model, the typical central volume of distribution varied across different subpopulations, ranging from 7.5 [11] to 24.1 [36] L, with the lowest value being reported in a Medellin-Garibay et al. study. All models estimated the IIV associated with MTX clearance, with values ranging from 8.2% [11] to 109.0% [26]. The highest IIV in MTX clearance was reported in a Jonsson et al. [36] study. The PopPK model developed by Hui et al. study implemented an inter-individual variability on MTX clearance with an estimated effect of 14.9% [20]. Applied covariates varied among the models, but all models included body size descriptors (e.g., weight and BSA) related to clearance and/or volume of distribution. Other identified covariates were eGFR and Scr on clearance, age on clearance and volume terms [21], gender, and pre-chemotherapy alkalinization volume on clearance [26]. As for residual unexplained variability, the applied forms included additive (including the additive error on the natural log-transformed concentrations), proportional, or combined proportional and additive error models with values ranging from 19.0% to 35.4% for the proportional component and 0.0035 to 0.0872 μmol/L for the additive component.

Table 1. Demographics and clinical characteristics of the included studies and evaluation dataset of high-dose methotrexate in children with acute lymphoblastic leukemia (ALL).

Characteristics	Aumente et al. [21]	Gao et al. [19]	Hui et al. [20]	Medellin-Garibay et al. [11]	Zhang et al. [26]	Jonsson et al. [36]	Evaluation Dataset
Tumor Type	ALL	ALL	ALL	ALL	ALL	ALL	ALL
N	37	311	36	41	96	304	51
M/F	17/20	197/114	23/13	NA	66/30	NA	40/11
Age (years)	5.0 (0.5–17.0)	5.0 (0.75–15.2)	5.3 (1.3–15.8)	5.0 (1.0–15.0)	7.4 ± 3.1	5.0 (0.4–17.8)	5.5 (1.0–13.0)
Weight (kg)	24.2 (7.5–80.0)	19.0 (4.5–113.0)	18.4 (10.4–57.8)	21.2 (8.0–57.3)	26.1 ± 10.4	19.0 (5.8–93.3)	19.0 (9.5–62.0)
Height (cm)	115 (69–174)	112 (67–175)	107 (77–176)	115 ± 24	120 ± 21	110 (63–192)	113 (73–168)
BSA (m^2)	1.07 (0.30–1.90)	NA	0.74 (0.47–1.64)	0.79 (0.41–1.6)	0.97 ± 0.29	0.76 (0.31–2.19)	0.77 (0.41–1.60)
MTX dose (g/m^2)	1.23–5.23	1–5	2–5	2.89 ± 0.9	2–3.5	5–8	1–5
ALT (IU/L)	NA	16.0 (2.0–390.0)	16.5 (5.0–247.0)	19.1 (7.2–98.2)	32.7 ± 44.5	31.2 (6.0–228.6)	32.5 (4.0–250.0)
AST (IU/L)	NA	26.0 (8.0–135.0)	NA	25.8 (13.9–112.7)	45.3 ± 34.5	NA	36.0 (17.0–131.0)
Scr (mg/dL)	0.5 (0.3–0.8)	0.3 (0.1–1.5)	0.362 (0.11–1.07)	0.37 ± 0.11	0.36 ± 0.10	NA	0.31 (0.16–0.71)

The values are presented as median (range) or mean ± standard deviation. M/F: male/female; N: number of patients; ALL: acute lymphoid leukemia; BSA: body surface area; Scr: serum creatinine; MTX: methotrexate; ALT: alanine aminotransferase; AST: aspartate aminotransferase; NA: not available.

Table 2. Summary of the included population pharmacokinetics model of methotrexate for external evaluation.

Studies	Structural Model	Fixed Parameters and Covariate Models	IIV (%) (IOV (%))	RUV
Aumente et al. [21]	2 CMT	K_{12} (1/h) = 0.0155 K_{21} (1/h) = 0.0724 CL (L/h, age > 10 years) = 0.149 × Weight CL (L/h, age < 10 years) = 0.287 × $Weight^{0.876}$ V_1 (L, age > 10 years) = 0.437 × Weight V_1 (L, age < 10 years) = 0.465 × Weight	K_{12} = 20.8 K_{21} = 35.2 CL = 41.7 V_1 = 41.6	Prop = 16.2% Add = 0.0035 µmol/L
Gao et al. [19]	3 CMT	CL (L/h) = 6.9 × $(Weight/19\ kg)^{0.75}$ × (1 + (Scr-26) × (−0.0097)) × $e^{\eta_{CL}}$ V_1 (L) = 20.7 × (Weight/19 kg) V_2 (L) = 41.0 × (Weight/19 kg) × $e^{\eta_{V2}}$ Q_1 (L/h) = 0.255 × $(Weight/19\ kg)^{0.75}$ V_3 (L) = 3.17 × (Weight/19 kg) Q_2 (L/h) = 0.217 × $(Weight/19\ kg)^{0.75}$	CL = 17.9 V_1 = 26.2	Prop * = 35.4%
Hui et al. [20]	2 CMT	CL (L/h) = 7.73 × $(BSA/0.735)^{0.721}$ × $(eGFR \times 1.73/192 \times BSA)^{0.256}$ × $e^{\eta_{CL}+IOV}$ V_1 (L) = 19.0 × $(BSA/0.735)^{0.985}$ Q (L/h) = 0.283 × $(Age/5.29)^{0.278}$ V_2 (L) = 6.63 × $e^{\eta_{V2}}$	CL = 14.3 (14.9) V_2 = 34.6	Prop = 30.2%
Medellin-Garibay et al. [11]	2 CMT	CL (L/h) = 6.5 × $BSA^{0.62}$ × $e^{\eta_{CL}}$ V_1 (L) = 0.36 × Weight × $e^{\eta_{V1}}$ Q (L/h) = 0.41 V_2 (L) = 3.2 × $e^{\eta_{V2}}$	CL = 8.2 V_1 = 25.9 V_2 = 26.7	Prop = 20.1%
Zhang et al. [26]	2 CMT	CL (L/h) = (5.04 × (1 − 0.278 × Gender) × $BSA^{0.777}$ + $(OH/100)^{0.514}$) × $e^{\eta_{CL}}$ V_1 (L) = 16.1 × $e^{\eta_{V1}}$ Q (L/h) = 0.203 × $(Age/10)^{1.56}$ × e^{η_Q} V_2 (L) = 7.05 × $(Age/10)^{1.76}$ × $e^{\eta_{V2}}$	CL = 49.6 V_1 = 29.4 Q = 137.6 V_2 = 107.7	Prop = 19.0% Add = 0.0872 µmol/L
Jonsson et al. [36]	2 CMT	CL (L/h) = Weight × 0.185 × $e^{\eta_{CL}}$ V_1 (L) = Weight × 1.27 × $e^{\eta_{V1}}$ Q (L/h) = Weight × 0.017 × e^{η_Q} V_2 = Weight × 1.02 × $e^{\eta_{V2}}$	CL = 109.0 V_1 = 26.0 Q = 22.0 V_2 = 44.0	NR

* The exponential residual error model was used, in which the estimate is approximately equal to the proportional error model. CMT: number of compartments; K_{12}: transfer rate constant from central compartment to peripheral compartment; K_{21}: transfer rate constant from peripheral compartment to central compartment; CL: clearance; V_1: central volume of distribution; V_2 and V_3: volume of distribution for peripheral compartments; Q: intercompartmental clearance; Scr: serum creatinine; eGFR: estimated glomerular filtration rate: BSA: body surface area; OH: pre-chemotherapy alkalinization volume; IIV: inter-individual variability; IOV: inter-occasion variability; RUV: residual unexplained variability; Prop: proportional residual unexplained error; Add: additive residual unexplained error; NR: not reported.

3.2. Characteristics of the Evaluation Dataset

The data used for external evaluation were collected from 51 ALL pediatrics with 354 concentration measurements. The demographics and clinical features of the included patients are summarized in Table 1. The prescribed HD-MTX dose varied from 1.0 g/m^2 to 5.0 g/m^2. The median age, weight, and BSA of the pediatric population were 5.0 years, 19.0 kg, and 0.77 m^2, respectively. All the patients had normal renal function with a median eGFR of 149.9 mL/min/1.73 m^2. The concentration observations versus time after dosing are displayed in Figure 1. In general, the measurements were mainly obtained at approximately 24, 48, 72, and 96 h after the start of MTX infusion.

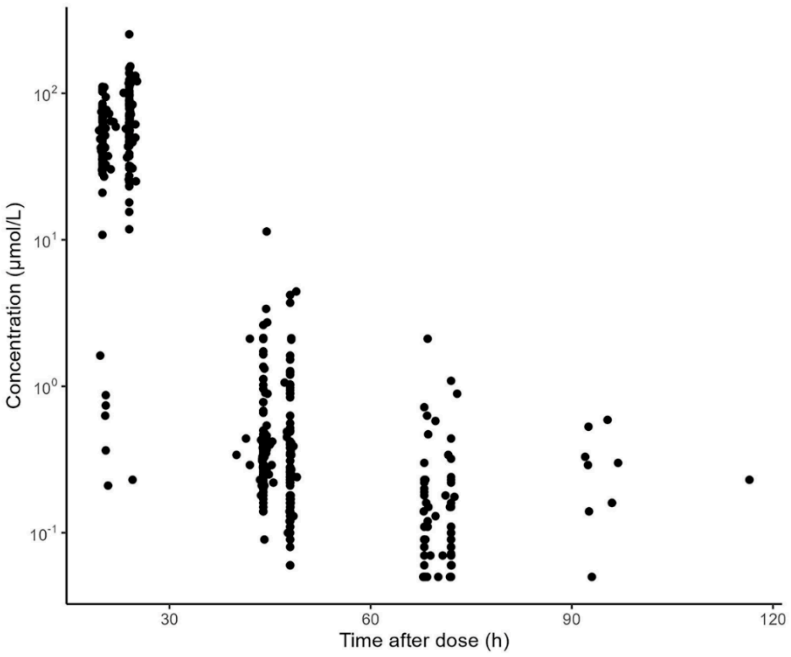

Figure 1. Methotrexate concentration versus time after dosing obtained with data available for external validation of the identified models.

3.3. Model Evaluation

The comparisons of population and individual predictions to observations for each model are shown in Figure 2. For population predictions, two of the models (Aumente et al. and Zhang et al.) had many predictions underestimated compared to the observations (Panels A and E) [21,26], while the model proposed by Jonsson et al. showed significant overpredictions (Panel F) [36]. The systematic bias of the individual predictions for the above models almost disappeared, except for the model proposed by Aumente et al. (Panel A) [21], indicating a better accuracy of individual predictions compared to the population predictions. Additionally, no systematic bias was observed for the models proposed by Gao et al., Hui et al., and Medellin-Garibay et al. in terms of the population and individual predictions (Panels B, C, and D) [11,19,20].

The prediction errors of the population and individual predictions for the evaluated models are visualized in box plots (Figure 3), and the median PE and MPE values are presented in Table 3. The median PEs of the population predictions for most of the models (except the Medellin-Garibay et al. study) were beyond ±20%, and the highest median PE (442.0%) was observed for the model proposed by Jonsson et al. [36]. Conversely, the median PE of the individual predictions for only one model (Gao et al. study) is distributed slightly over ±20% [19], and all other models showed acceptable bias. In terms of the MPE, the top three models showing good performances (<±20%) for both population and individual predictions were the Gao et al. [19], Hui et al. [20], and Zhang et al. [26] studies. Again, the model proposed by Jonsson et al. showed the worst bias with an MPE value of 780.87%. Bland-Altman plots showed that there was no apparent trend in the prediction

errors of the population (Figure 4) and individual (Figure 5) predictions for four models (Aumente et al., Medellin-Garibay et al., Zhang et al., and Jonsson et al.) [11,21,26,36] over the whole concentration range observed in our data, while obvious trends were observed for the models proposed by Gao et al. [19] and Hui et al. [20]. All models show high RMSE with determined values > 30% (Table 3). The model proposed by Gao et al. performed best in RMSE in view of both the population (72.39%) and individual (63.96%) predictions [19]. This model also showed the smallest bias, as indicated by the MPEs. In general, the high RMSEs indicate the high imprecision of the models. That is, when validated with external data, the models all showed the need for further refinement.

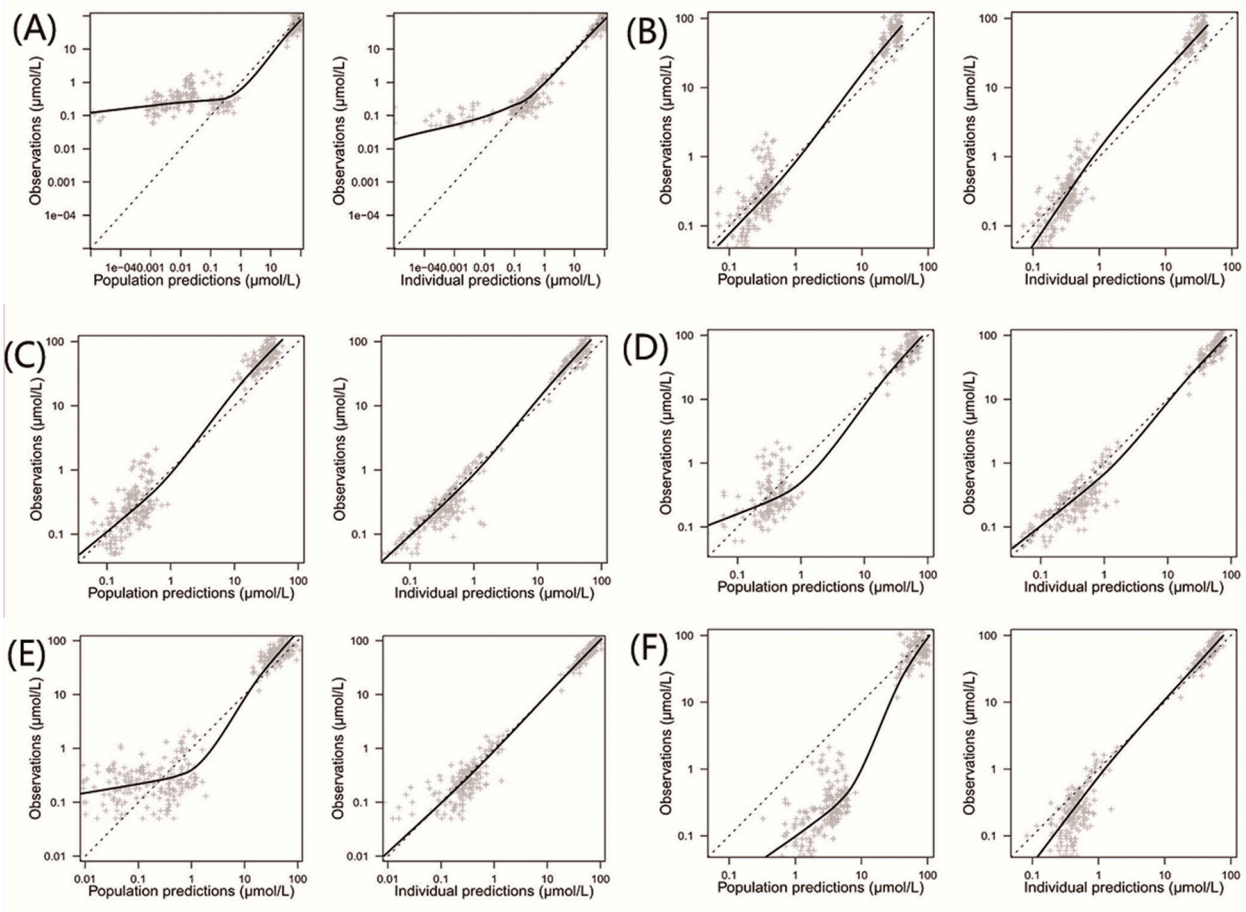

Figure 2. Observed concentrations versus population and individual predictions for the included population pharmacokinetic models of methotrexate in children with acute lymphoid leukemia. (**A**) Model proposed by Aumente et al. [21]; (**B**) model proposed by Gao et al. [19]; (**C**) model proposed by Hui et al. [20]; (**D**) model proposed by Medellin-Garibay et al. [11]; (**E**) model proposed by Zhang et al. [26]; and (**F**) model proposed by Jonsson et al. [36].

Table 3. Prediction error (PE) of the individual predictions (IPRED) and population predictions (PRED) to observations for the evaluated models.

Model	IPRED			PRED		
	Median PE (%)	MPE (%)	RMSE (%)	Median PE (%)	MPE (%)	RMSE (%)
Aumente et al. [21]	6.52	12.06	76.09	−31.70	−25.51	81.15
Gao et al. [19]	−25.20	1.33	63.96	−26.76	3.22	72.39
Hui et al. [20]	−10.43	8.78	82.96	−33.23	−8.24	62.88
Medellin-Garibay et al. [11]	−0.75	22.71	75.55	−7.56	6.39	68.33
Zhang et al. [26]	1.16	16.00	63.39	−29.92	15.62	145.92
Jonsson et al. [36]	5.25	64.44	152.25	442.04	780.87	1182.24

MPE: mean relative error, RMSE: root mean square error.

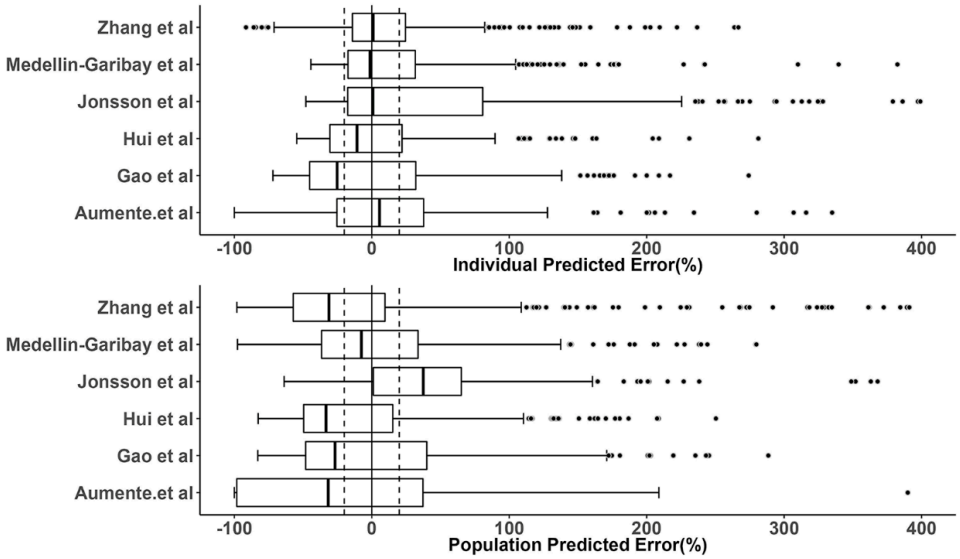

Figure 3. Prediction error (PE) distributions of the individual (upper panel) and population (bottom panel) predictions for evaluated population pharmacokinetic models of methotrexate using an independent dataset in children with acute lymphoid leukemia. In the boxplots, the lower boundary of the box indicates the 25th percentile, the line within the box marks the median, and the upper boundary of the box represents the 75th percentile. Whiskers above and below the box indicate 1.5-fold of the interquartile range below the 25th percentile and above the 75th percentile, respectively. Points above and below the whiskers are defined as outliers. The vertical black solid line represents the PE value at zero (unbiased), and the dashed black lines indicate ±20% of PE (acceptable bias) [11,19–21,26,36].

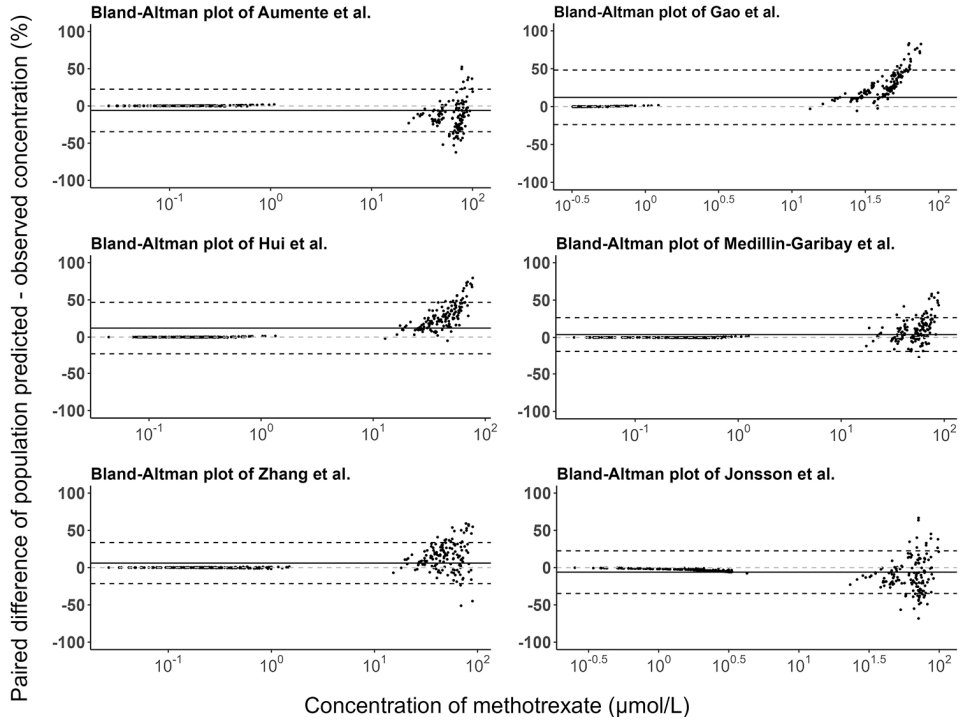

Figure 4. Bland-Altman plots of the prediction errors of population predictions for published population pharmacokinetic models of methotrexate based on an independent dataset in children with acute lymphoid leukemia. The black line is the mean of the population prediction error, and the black dashed lines are the mean ± 1.96 times the standard deviation of the population prediction error [11,19–21,26,36].

~~black dashed lines are the mean ± 1.96 times the standard deviation of the population prediction~~ error [11,19–21,26,36].

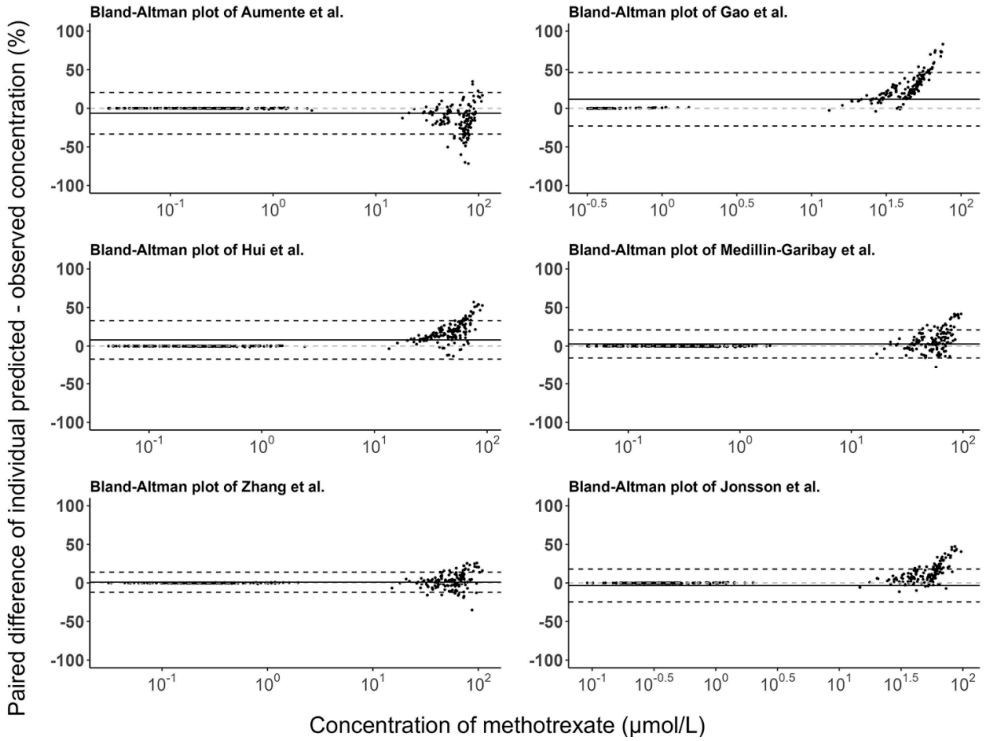

Figure 5. Bland-Altman plots of the prediction errors of individual predictions for published population pharmacokinetic models of methotrexate based on an independent dataset in children with acute lymphoid leukemia. The black line is the mean of individual prediction error, and the black dashed lines are the mean ± 1.96 times the standard deviation of the individual prediction error [11,19–21,26,36].

Figure 5. Bland-Altman plots of the prediction errors of individual predictions for published population pharmacokinetic models of methotrexate based on an independent dataset in children with acute lymphoid leukemia. The black line is the mean of individual prediction error, and the black dashed lines are the mean ± 1.96 times the standard deviation of the individual prediction error [11,19–21,26,36].

Table 3. Prediction error (PE) of the individual predictions (IPRED) and population predictions (PRED) to observations for the evaluated models.

Model	IPRED			PRED		
	Median PE (%)	MPE (%)	RMSE (%)	Median PE (%)	MPE (%)	RMSE (%)
Aumente et al. [21]	6.52	12.06	76.09	31.70	25.51	81.15
Gao et al. [19]	−25.20	1.33	63.96	−26.76	3.22	72.39
Hui et al. [20]	−10.43	8.78	82.96	−33.23	−8.24	62.88
Medellin-Garibay et al. [11]	−0.75	22.71	73.55	−7.56	6.39	68.33
Zhang et al. [26]	1.16	16.00	63.39	−29.92	15.62	145.92
Jonsson et al. [36]	5.25	64.44	152.25	442.04	780.87	1182.24

MPE: mean relative error, RMSE: root mean square error.

4. Discussion

External evaluation is a crucial step to assess the accuracy, precision, and predictive performance of a PopPK model before its application in clinical practice. This step evaluates the model's ability to describe the intended population and the impactful clinical variables related to the drug's PK. This study is the first to review the published PopPK models of MTX in ALL pediatric patients and to systematically evaluate the predictive performance of these models using a new independent dataset.

All the evaluated models incorporated the influence of body size (e.g., body weight and BSA) on either clearance or volume of distribution. As MTX distributes into extracellular fluid and tissues, it is explainable that its volume of distribution tends to increase with the patient's body size. As a predominantly renally excreted drug (80–90% of the administered dose), the descriptors of renal function (e.g., Scr and eGFR) are expected to influence MTX clearance. Of the evaluated models, only two of them included the influence of a renal function descriptor on MTX clearance [19,20]. This may be because most of the studies were based on patients with normal to moderately impaired renal function, and the impact of renal function on MTX clearance could not be detected significantly. The conflicting findings in the literature about the effect of renal function descriptors on MTX clearance might be arising from the following reasons: (1) the sample size of some studies is too small to detect the potential effect; (2) some studies only tested the effect of serum creatinine whereas eGFR is theoretically more predictive; and (3) the effect of renal function descriptors may be relatively weak in some studies and might have been blinded by other highly correlated covariates (e.g., age and body size-related covariates). Our patients in the validation dataset all had normal renal function, and the inclusion or the lack of inclusion of renal function in the PopPK model may be of little importance for the prediction.

4. Discussion

External evaluation is a crucial step to assess the accuracy, precision, and predictive performance of a PopPK model before its application in clinical practice. This step evaluates the model's ability to describe the intended population and the impactful clinical variables related to the drug's PK. This study is the first to review the published PopPK

The predictive performance of the models evaluated in our study varied considerably, and all the tested models only partially met the predefined criteria. In general, most of

the models (except the Jonsson et al. model) demonstrated good accuracy (<±20% or a bit higher, in terms of median PE and MPE) for both the population and individual predictions. This highlighted that these models would be useful for a priori dose adjustment using only the population parameters and identified covariates. However, for all models tested, the RMSEs were between 62.88–1182.24% for population predictions and 63.96–152.25% for individual predictions. This demonstrated that the use of population PK parameters and patient covariates alone without feedback concentrations from individual subjects is inadequate to make precise predictions. Incorporation of feedback measurements into the PopPK model could improve the precision of Bayesian forecasting. The PopPK models of Aumente et al. [21], Medellin-Garibay et al. [11], and Zhang et al. [26] showed the best predictive performance across all the different tests, including the graphic and numerical predictive performance assessment. All these three models were originally validated using the dataset from the patient cohort very similar to the population with which the model was developed. Although the Gao et al. [19] and Hui et al. [20] models showed comparable performance to the above models in terms of numerical assessment, they had obvious prediction bias over the concentration range, as indicated by the Bland–Altman plots. Notably, the Gao et al. [19] model was developed based on the largest dataset (311 children with 4517 measurements), but it did not show a better predictive ability. In this model, a three-compartment disposition rather than a two-compartment disposition model was used, while the residual unexplained variability of the final model is still high (35.4%). We noted that the central volume of distribution in the Gao et al. [19] model (20.7 L) is higher than in other models (Table 2), leading to an obvious underprediction for the peak concentrations of MTX (Supplementary Table S1). Similarly, significant underprediction of peak MTX concentrations was also seen with the Hui et al. model (Table S1). The worst predictive performance was observed with Jonsson et al. model, especially for the population predictions. This is because a large variability (109%) was found for MTX clearance in this model, and probably the most influential covariates were not identified to reduce the variability. As expected, a better performance was found for the individual predictions after the incorporation of the IIVs of the population parameters. The model performance could be further improved when the trough concentrations were removed (Table S1), indicating that the model is inaccurate for predictions of trough concentrations. These results highlighted that it is essential to evaluate a model in target patient populations before its application in clinical practice.

We consider that the following factors can partially explain the heterogeneous performance of the included models. First, the incorporated covariates may affect the prediction performance. Theoretically, the models including the largest number of covariates could show better results in the external evaluation, especially for the population predictions. For instance, the Jonsson et al. model only considered the effect of body weight on a drug's PK, which seems to be significantly insufficient for our data [36]. Furthermore, extrapolation of the covariate effects beyond the range of the values from the original patient population could lead to biased model predictions. Likewise, the lack of inclusion for important covariates in the PopPK models may result in high prediction errors for the population predictions (e.g., the Jonsson et al. model) [36]. Second, the differences in clinical characteristics of the external validation dataset and the patient populations in published PopPK models may influence the evaluation results. In this study, although we ensured that the mean age of the model evaluated was close to that of the validation dataset, the other patient characteristics were not considered. Differences in other parameters, such as disease severity, leucovorin rescue procedure, ethnicity and genetic polymorphisms, duration of MTX treatment, or co-medication, may alter the population parameters of the patient populations with similar age (e.g., the high central volume of distribution in Gao et al. study) [19], thus they may partly explain the models' non-applicability to our patient cohort. Third, some of the constructed models were mainly based on peak and trough concentrations [19,20], and this would lead to a biased estimation of the distribution parameters. Likewise, our validation dataset is composed of peak and trough measurements. The concentrated distribution of

such data points failed to fully assess the model prediction performance over the whole concentration-time range, potentially producing a biased evaluation.

The diverse landscape in the performance of the evaluated models observed in our study demonstrated that it is important to first execute extensive model evaluation before adopting a model in clinical facilities. Our study showed that the PopPK models of MTX failed to predict concentration-time data properly for external subjects that belong to a similar population in which the model was created. Therefore, it warns us that we should be cautious to apply the internally validated model to external institutions.

The present study has some limitations. First, the validation dataset was retrospectively collected from clinical settings, and uncertainty was associated with data records. Although we performed a data inspection by two independent persons, some random errors may still remain in the data. As the selected model is intended to be used in daily clinical practice, and the same random errors (e.g., recording errors) may also present in real situations, evaluation of the model performance using such real-world data is a meaningful and rigorous examination in order to test the robustness of the model. Second, the evaluation dataset was from a single center and consisted of centralized measurements (peak and trough), which may prevent a good appreciation of the drug's distribution. Yet, the ultimate objective of the model evaluation was to use the selected models for MIPD in daily practice with only the peak and/or trough concentrations, thus it was crucial to test the models under this real-life condition.

5. Conclusions

The present study externally evaluated six published PopPK models of MTX in ALL children with independent clinical data. Some of the published PopPK models were found to have reasonably low levels of bias for both population and individual predictions but a relatively high degree of imprecision. The fact that none of the evaluated models passed the external validation emphasized that extensive validation is required before the adoption of the model used for clinical care for ALL pediatrics.

Supplementary Materials: The following supporting information can be downloaded at: https://www.mdpi.com/article/10.3390/pharmaceutics15020569/s1, Table S1: Prediction error (PE) of the individual predictions (IPRED) and population predictions (PRED) to observations for the evaluated models for peak concentrations.

Author Contributions: **S**.W. and Q.Y. performed the model evaluations and prepared the first draft of the manuscript. M.Y. and Z.C. provided the clinical dataset. F.X. conceived the study idea, and reviewed and approved the final version of the manuscript. All authors have read and agreed to the published version of the manuscript.

Funding: This work was supported by the National Natural Science Foundation of China (grant number: 82073932 and 82202398), Hunan Provincial Natural Science Foundation of China (grant number: 2022JJ30903), Science and Technology Innovation Program of Hunan Province (grant number: 2022RC1229), and the Natural Science Foundation of Changsha City in Hunan Province of China (kq2202421).

Institutional Review Board Statement: The study was conducted in accordance with the Declaration of Helsinki, and approved by the Institutional Review Board of Third Xiangya Hospital at Central South University.

Informed Consent Statement: Informed consent was obtained from all subjects involved in the study.

Data Availability Statement: All the relevant data are shown in the manuscript.

Conflicts of Interest: The authors declare no conflict of interest.

References

1. Yazıcıoğlu, B.; Kaya, Z.; Güntekin Ergun, S.; Perçin, F.; Koçak, Ü.; Yenicesu, İ.; Gürsel, T. Influence of Folate-Related Gene Polymorphisms on High-Dose Methotrexate-Related Toxicity and Prognosis in Turkish Children with Acute Lymphoblastic Leukemia. *Turk. J. Haematol.* **2017**, *34*, 143–150. [PubMed]
2. Jolivet, J.; Cowan, K.H.; Curt, G.A.; Clendeninn, N.J.; Chabner, B.A. The pharmacology and clinical use of methotrexate. *N. Engl. J. Med.* **1983**, *309*, 1094–1104. [CrossRef] [PubMed]
3. GBD 2017 Childhood Cancer Collaborators. The global burden of childhood and adolescent cancer in 2017: An analysis of the Global Burden of Disease Study 2017. *Lancet Oncol.* **2019**, *20*, 1211–1225. [CrossRef] [PubMed]
4. Zhong, F.F.; Yang, Y.; Liu, W.J. Progress in research on childhood T-cell acute lymphocytic leukemia, Notch1 signaling pathway, and its inhibitors: A review. *Bosn. J. Basic Med. Sci.* **2021**, *21*, 136–144.
5. Mandal, P.; Samaddar, S.; Chandra, J.; Parakh, N.; Goel, M. Adverse effects with intravenous methotrexate in children with acute lymphoblastic leukemia/lymphoma: A retrospective study. *Indian J. Hematol. Blood Transfus.* **2020**, *36*, 498–504. [CrossRef]
6. Freeman, A.I.; Weinberg, V.; Brecher, M.L.; Jones, B.; Glicksman, A.S.; Sinks, L.F.; Weil, M.; Pleuss, H.; Hananian, J.; Burgert, E.O., Jr.; et al. Comparison of intermediate-dose methotrexate with cranial irradiation for the post-induction treatment of acute lymphocytic leukemia in children. *N. Engl. J. Med.* **1983**, *308*, 477–484. [CrossRef] [PubMed]
7. Bührer, C.; Henze, G.; Hofmann, J.; Reiter, A.; Schellong, G.; Riehm, H. Central nervous system relapse prevention in 1165 standard-risk children with acute lymphoblastic leukemia in five BFM trials. *Haematol. Blood Transfus.* **1990**, *33*, 500–503.
8. Pui, C.H.; Howard, S.C. Current management and challenges of malignant disease in the CNS in paediatric leukaemia. *Lancet Oncol.* **2008**, *9*, 257–268.
9. Delepine, N.; Delepine, G.; Cornille, H.; Brion, F.; Arnaud, P.; Desbois, J.C. Dose escalation with pharmacokinetics monitoring in methotrexate chemotherapy of osteosarcoma. *Anticancer Res.* **1995**, *15*, 489–494.
10. Evans, W.E.; Relling, M.V.; Rodman, J.H.; Crom, W.R.; Boyett, J.M.; Pui, C.H. Conventional compared with individualized chemotherapy for childhood acute lymphoblastic leukemia. *N. Engl. J. Med.* **1998**, *338*, 499–505. [PubMed]
11. Medellin-Garibay, S.E.; Hernández-Villa, N.; Correa-González, L.C.; Morales-Barragán, M.N.; Valero-Rivera, K.P.; Reséndiz-Galván, J.E.; Ortiz-Zamudio, J.J.; Milán-Segovia, R.d.; Romano-Moreno, S. Population pharmacokinetics of methotrexate in Mexican pediatric patients with acute lymphoblastic leukemia. *Cancer Chemother. Pharmacol.* **2020**, *85*, 21–31.
12. Pui, C.H.; Relling, M.V.; Sandlund, J.T.; Downing, J.R.; Campana, D.; Evans, W.E. Rationale and design of Total Therapy Study XV for newly diagnosed childhood acute lymphoblastic leukemia. *Ann. Hematol.* **2004**, *83* (Suppl. 1), S124–S126. [PubMed]
13. Larsen, E.C.; Devidas, M.; Chen, S.; Salzer, W.L.; Raetz, E.A.; Loh, M.L.; Mattano, L.A., Jr.; Cole, C.; Eicher, A.; Haugan, M.; et al. Dexamethasone and High-Dose Methotrexate Improve Outcome for Children and Young Adults With High-Risk B-Acute Lymphoblastic Leukemia: A Report From Children's Oncology Group Study AALL0232. *J. Clin. Oncol.* **2016**, *34*, 2380–2388. [CrossRef] [PubMed]
14. Pui, C.H.; Sallan, S.; Relling, M.V.; Masera, G.; Evans, W.E. International Childhood Acute Lymphoblastic Leukemia Workshop: Sausalito, CA, 30 November–1 December 2000. *Leukemia* **2001**, *15*, 707–715. [CrossRef] [PubMed]
15. Liu, X.; Zou, Y.; Zhang, L.; Guo, Y.; Chen, Y.; Yang, W.; Chen, X.; Wang, S.; Zhang, Y.; Ruan, M.; et al. A Novel Risk Defining System for Pediatric T-Cell Acute Lymphoblastic Leukemia From CCCG-ALL-2015 Group. *Front. Oncol.* **2022**, *12*, 841179. [CrossRef]
16. Qin, F.L.; Sang, G.Y.; Zou, X.Q.; Cheng, D.H. Drug-Induced Liver Injury during Consolidation Therapy in Childhood Acute Lymphoblastic Leukemia as Assessed for Causality Using the Updated RUCAM. *Can. J. Gastroenterol. Hepatol.* **2022**, *2022*, 5914593.
17. Widemann, B.C.; Adamson, P.C. Understanding and managing methotrexate nephrotoxicity. *Oncologist* **2006**, *11*, 694–703.
18. Beechinor, R.J.; Thompson, P.A.; Hwang, M.F.; Vargo, R.C.; Bomgaars, L.R.; Gerhart, J.G.; Dreyer, Z.E.; Gonzalez, D. The Population Pharmacokinetics of High-Dose Methotrexate in Infants with Acute Lymphoblastic Leukemia Highlight the Need for Bedside Individualized Dose Adjustment: A Report from the Children's Oncology Group. *Clin. Pharmacokinet.* **2019**, *58*, 899–910.
19. Gao, X.; Qian, X.W.; Zhu, X.H.; Yu, Y.; Miao, H.; Meng, J.H.; Jiang, J.-Y.; Wang, H.-S.; Zhai, X.-W. Population Pharmacokinetics of High-Dose Methotrexate in Chinese Pediatric Patients With Acute Lymphoblastic Leukemia. *Front. Pharmacol.* **2021**, *12*, 701452. [CrossRef]
20. Hui, K.H.; Chu, H.M.; Fong, P.S.; Cheng, W.T.F.; Lam, T.N. Population Pharmacokinetic Study and Individual Dose Adjustments of High-Dose Methotrexate in Chinese Pediatric Patients with Acute Lymphoblastic Leukemia or Osteosarcoma. *J. Clin. Pharmacol.* **2019**, *59*, 566–577. [CrossRef]
21. Aumente, D.; Buelga, D.S.; Lukas, J.C.; Gomez, P.; Torres, A.; Garcia, M.J. Population pharmacokinetics of high-dose methotrexate in children with acute lymphoblastic leukaemia. *Clin. Pharmacokinet.* **2006**, *45*, 1227–1238. [PubMed]
22. Broeker, A.; Nardecchia, M.; Klinker, K.P.; Derendorf, H.; Day, R.O.; Marriott, D.J.; Carland, J.E.; Stocker, S.L.; Wicha, S.G. Towards precision dosing of vancomycin: A systematic evaluation of pharmacometric models for Bayesian forecasting. *Clin. Microbiol. Infect.* **2019**, *25*, 1286.e1–1286.e7.
23. Zwart, T.C.; Guchelaar, H.J.; van der Boog, P.J.M.; Swen, J.J.; van Gelder, T.; de Fijter, J.W.; Moes, D.J.A.R. Model-informed precision dosing to optimise immunosuppressive therapy in renal transplantation. *Drug Discov. Today* **2021**, *26*, 2527–2546. [PubMed]
24. Keizer, R.J.; Ter Heine, R.; Frymoyer, A.; Lesko, L.J.; Mangat, R.; Goswami, S. Model-Informed Precision Dosing at the Bedside: Scientific Challenges and Opportunities. *CPT Pharmacomet. Syst. Pharmacol.* **2018**, *7*, 785–787.

25. Darwich, A.S.; Polasek, T.M.; Aronson, J.K.; Ogungbenro, K.; Wright, D.F.B.; Achour, B.; Reny, J.L.; Daali, Y.; Eiermann, B.; Cook, J.; et al. Model-Informed Precision Dosing: Background, Requirements, Validation, Implementation, and Forward Trajectory of Individualizing Drug Therapy. *Annu. Rev. Pharmacol. Toxicol.* **2021**, *61*, 225–245. [CrossRef]
26. Zhang, C.; Zhai, S.; Yang, L.; Wu, H.; Zhang, J.; Ke, X. Population pharmacokinetic study of methotrexate in children with acute lymphoblastic leukemia. *Int J. Clin. Pharmacol. Ther.* **2010**, *48*, 11–21. [CrossRef]
27. Guo, T.; van Hest, R.M.; Roggeveen, L.F.; Fleuren, L.M.; Thoral, P.J.; Bosman, R.J.; van der Voort, P.H.J.; Girbes, A.R.J.; Mathot, R.A.A.; Elbers, P.W.G. External Evaluation of Population Pharmacokinetic Models of Vancomycin in Large Cohorts of Intensive Care Unit Patients. *Antimicrob. Agents Chemother.* **2019**, *63*, e02543-18.
28. Schwartz, G.J.; Muñoz, A.; Schneider, M.F.; Mak, R.H.; Kaskel, F.; Warady, B.A.; Furth, S.L. New equations to estimate GFR in children with CKD. *J. Am. Soc. Nephrol.* **2009**, *20*, 629–637. [CrossRef]
29. Hara, M.; Masui, K.; Eleveld, D.J.; Struys, M.; Uchida, O. Predictive performance of eleven pharmacokinetic models for propofol infusion in children for long-duration anaesthesia. *Br. J. Anaesth.* **2017**, *118*, 415–423. [CrossRef]
30. Bloomfield, C.; Staatz, C.E.; Unwin, S.; Hennig, S. Assessing Predictive Performance of Published Population Pharmacokinetic Models of Intravenous Tobramycin in Pediatric Patients. *Antimicrob. Agents Chemother.* **2016**, *60*, 3407–3414.
31. Zhan, M.; Sun, Y.; Zhou, F.; Wang, H.; Chen, Z.; Yan, L.; Li, X. Population pharmacokinetics of methotrexate in paediatric patients with acute lymphoblastic leukaemia and malignant lymphoma. *Xenobiotica* **2022**, *52*, 265–273. [CrossRef] [PubMed]
32. Panetta, J.C.; Roberts, J.K.; Huang, J.; Lin, T.; Daryani, V.M.; Harstead, K.E.; Patel, Y.T.; Onar-Thomas, A.; Campagne, O.; Ward, D.A.; et al. Pharmacokinetic basis for dosing high-dose methotrexate in infants and young children with malignant brain tumours. *Br. J. Clin. Pharmacol.* **2020**, *86*, 362–371. [CrossRef] [PubMed]
33. Kawakatsu, S.; Nikanjam, M.; Lin, M.; Le, S.; Saunders, I.; Kuo, D.J.; Capparelli, E.V. Population pharmacokinetic analysis of high-dose methotrexate in pediatric and adult oncology patients. *Cancer Chemother. Pharmacol.* **2019**, *84*, 1339–1348. [PubMed]
34. Lui, G.; Treluyer, J.M.; Fresneau, B.; Piperno-Neumann, S.; Gaspar, N.; Corradini, N.; Gentet, J.-C.; Berard, P.M.; Laurence, V.; Schneider, P.; et al. A Pharmacokinetic and Pharmacogenetic Analysis of Osteosarcoma Patients Treated With High-Dose Methotrexate: Data from the OS2006/Sarcoma-09 Trial. *J. Clin. Pharmacol.* **2018**, *58*, 1541–1549. [CrossRef] [PubMed]
35. Zhang, W.; Zhang, Q.; Tian, X.; Zhao, H.; Lu, W.; Zhen, J.; Niu, X. Population pharmacokinetics of high-dose methotrexate after intravenous administration in Chinese osteosarcoma patients from a single institution. *Chin. Med. J. (Engl.).* **2015**, *128*, 111–118.
36. Jönsson, P.; Skärby, T.; Heldrup, J.; Schrøder, H.; Höglund, P. High dose methotrexate treatment in children with acute lymphoblastic leukaemia may be optimised by a weight-based dose calculation. *Pediatr. Blood Cancer* **2011**, *57*, 41–46.
37. Colom, H.; Farre, R.; Soy, D.; Peraire, C.; Cendros, J.M.; Pardo, N.; Torrent, M.; Domenech, J.; Mangues, M.-A. Population pharmacokinetics of high-dose methotrexate after intravenous administration in pediatric patients with osteosarcoma. *Ther. Drug Monit.* **2009**, *31*, 76–85. [CrossRef]
38. Shi, Z.Y.; Liu, Y.O.; Gu, H.Y.; Xu, X.Q.; Yan, C.; Yang, X.Y.; Yan, D. Population pharmacokinetics of high-dose methotrexate in Chinese pediatric patients with medulloblastoma. *Biopharm. Drug Dispos.* **2020**, *41*, 101–110.

pharmaceutics

MDPI

Article

Population Pharmacokinetics and Dose Optimization Based on Renal Function of Rivaroxaban in Thai Patients with Non-Valvular Atrial Fibrillation

Noppaket Singkham [1,2], Arintaya Phrommintikul [3], Phongsathon Pacharasupa [3], Lalita Norasetthada [3], Siriluck Gunaparn [3], Narawudt Prasertwitayakij [3], Wanwarang Wongcharoen [3,*] and Baralee Punyawudho [4,*]

1 Division of Clinical Pharmacy, Department of Pharmaceutical Care, School of Pharmaceutical Sciences, University of Phayao, Phayao 56000, Thailand
2 Unit of Excellence on Pharmacogenomic Pharmacokinetic and Pharmacotherapeutic Researches (UPPER), School of Pharmaceutical Sciences, University of Phayao, Phayao 56000, Thailand
3 Division of Cardiology, Department of Internal Medicine, Faculty of Medicine, Chiang Mai University, Chiang Mai 50200, Thailand
4 Department of Pharmaceutical Care, Faculty of Pharmacy, Chiang Mai University, Chiang Mai 50200, Thailand
* Correspondence: bwanwarang@yahoo.com (W.W.); baralee.p@cmu.ac.th (B.P.)

Abstract: Low-dose rivaroxaban has been used in Asian patients with direct oral anticoagulants (DOACs) eligible for atrial fibrillation (AF). However, there are few pharmacokinetic (PK) data in Thai patients to support precise dosing. This study aimed to develop a population PK model and determine the optimal rivaroxaban doses in Thai patients. A total of 240 Anti-Xa levels of rivaroxaban from 60 Thai patients were analyzed. A population PK model was established using the nonlinear mixed-effect modeling approach. Monte Carlo simulations were used to predict drug exposures at a steady state for various dosages. Proportions of patients having rivaroxaban exposure within typical exposure ranges were determined. A one-compartment model with first-order absorption best described the data. Creatinine clearance (CrCl) and body weight significantly affected CL/F and V/F, respectively. Regardless of body weight, a higher proportion of patients with CrCl < 50 mL/min receiving the 10-mg once-daily dose had rivaroxaban exposures within the typical exposure ranges. In contrast, a higher proportion of patients with CrCl $\geq$ 50 mL/min receiving the 15-mg once-daily dose had rivaroxaban exposures within the typical exposure ranges. The study's findings suggested that low-dose rivaroxaban would be better suited for Thai patients and suggested adjusting the medication's dose in accordance with renal function.

Keywords: population pharmacokinetic; rivaroxaban; atrial fibrillation; direct oral anticoagulants; Thai patient

Citation: Singkham, N.; Phrommintikul, A.; Pacharasupa, P.; Norasetthada, L.; Gunaparn, S.; Prasertwitayakij, N.; Wongcharoen, W.; Punyawudho, B. Population Pharmacokinetics and Dose Optimization Based on Renal Function of Rivaroxaban in Thai Patients with Non-Valvular Atrial Fibrillation. *Pharmaceutics* **2022**, *14*, 1744. https://doi.org/10.3390/pharmaceutics14081744

Academic Editors: Barna Vasarhelyi and Gellért Balázs Karvaly

Received: 9 July 2022
Accepted: 17 August 2022
Published: 21 August 2022

1. Introduction

Rivaroxaban, one of the direct Factor Xa (FXa) inhibitors, is an oral anticoagulant approved for stroke prevention in patients with direct oral anticoagulants (DOACs) eligible for atrial fibrillation (AF) [1]. The approved doses for AF are 20 and 15 mg administered once daily in patients with normal renal function and moderately impaired renal function, respectively [1]. Rivaroxaban was proved to be non-inferior to warfarin in clinical studies in Caucasians and Asians (the ROCKET AF and the Japanese ROCKET AF studies) [2,3]. High interindividual variability and the unexpected risk of bleeding caused by rivaroxaban are concerns in the Asian population [4]. Although low-dose rivaroxaban has been used based on patient-specific factors in a real-world setting among Asian patients [3–5], the precise low dose has never been established in this population. This increases the uncertainty around the clinical practice of rivaroxaban prescription. Additionally, because of the substantial interindividual variability of this medication, selecting the best dose in accordance with patient characteristics may help to increase its effectiveness and safety. However, there is a

lack of important pharmacokinetic (PK) data for choosing the right dose. As a result, it can be difficult to precisely dose rivaroxaban for Asian individuals.

Anti-Xa activity is linearly correlated with the plasma concentration of direct FXa inhibitors, including rivaroxaban [6,7], making it useful for predicting clinical outcomes. Studies have shown that individuals with AF who had a higher Anti-Xa levels of rivaroxaban measured at peak concentration reported more bleeding complications following treatment [8–10]. In addition, a previous study showed an elevated risk of thrombotic events in patients with low Anti-Xa level measured at trough concentration [11,12]. Therefore, a precise dosage of rivaroxaban would be required to provide optimum exposure. Furthermore, substantial interpatient variability in the trough concentration of rivaroxaban has been observed, which raises the risk of unexpected bleeding [13,14]. Despite the fact that therapeutic drug monitoring is not required for all patients treated with rivaroxaban in a routine clinical care setting [15], it may be useful for patients in certain clinical situations (i.e., major bleeding, surgery, renal failure, thromboembolism, and drug-drug interactions), as well as for a population at a high risk of bleeding, such as the elderly, extremely underweight, and those with renal impairment [13,16].

Previous studies showed high interindividual variabilities of rivaroxaban concentrations [17,18]. Numerous variables, including age, gender, body weight, and renal function, as well as drug-drug interactions (e.g., inhibitors or inducers of CYP3A4 and/or P-glycoprotein), may contribute to the considerable variability in rivaroxaban's PK [19,20]. Thus, dosage modification of rivaroxaban based on patient characteristics may result in optimum drug exposure and safer dose administration.

The disparities in rivaroxaban dosage needs between ethnic groups have been reported [2,3], which may be attributable to the difference in body weight and renal function [21,22]. The clinical trials in Caucasians (the global ROCKET AF) and Japanese (the Japanese ROCKET AF) demonstrated comparable clinical outcomes for stroke prevention and bleeding events [2,3], despite the fact that the Japanese patients received a lower dose of rivaroxaban (15 mg once daily for patients with normal renal function and 10 mg once daily for patients with moderately impaired renal function) [3]. Population PK studies revealed equivalent simulated area under the plasma concentration-time curve from 0–24 h ($AUC_{0–24}$) and peak plasma concentration (C_{MAX}) values for rivaroxaban at 15 mg once day in Japanese and 20 mg once daily in non-Japanese individuals [23,24]. Japanese patients taking 20 mg once daily, on the other hand, showed a larger simulated $AUC_{0–24}$ and C_{MAX} than Caucasian patients receiving the same dosage. These findings supported the use of low-dose rivaroxaban in Japanese patients with DOAC-eligible AF.

With Thai individuals sharing comparable features to Japanese patients, a lower dose of rivaroxaban may be more appropriate. A cohort study in Thai DOAC-eligible AF patients discovered that using the lower Japan-specific dose resulted in a larger proportion of patients meeting the typical exposure ranges of Anti-Xa at peak concentrations, whereas the approved dose was likely to exceed the range [25]. As a result, a lower dose of rivaroxaban is likely to be used in Thai patients. However, the rivaroxaban PK profiles in the Thai population have not been studied. The information on rivaroxaban PK derived from real-world data is required to facilitate dose optimization. Additionally, dosing based on patient characteristics could be utilized to guide the individualized rivaroxaban dose. Thus, this study aimed to develop a population PK model and evaluate factors influencing rivaroxaban PK. The developed model was then applied to design the optimal dose using Monte Carlo simulations.

2. Materials and Methods

2.1. Study Design

The analysis included data from a previous study comparing Anti-Xa levels at peak and trough between the standard dose and a Japan-specific dose of rivaroxaban in Thai patients [25]. Sixty adult patients with non-valvular AF were included in the previous study at a tertiary hospital that serves as an academic and referral center for northern

Thailand between June 2018 and January 2019. Patients with significant renal impairment (CrCl < 15 mL/min) or poor medication adherence were excluded [25].

Rivaroxaban was given to the patients based on their renal function, determined as CrCl. Two dosing strategies, including the standard doses and the Japan-specific doses, were evaluated. The standard doses were 20 mg once daily for CrCl $\geq$ 50 mL/min and 15 mg once daily for CrCl 15–49 mL/min, while the Japan-specific doses were 15 mg once daily for CrCl $\geq$ 50 mL/min and 10 mg once daily for CrCl 15–49 mL/min.

All patients were started with the standard dose of rivaroxaban for at least one week. Then the Anti-Xa were collected at peak (2–4 h after taking the dose) and trough concentrations (22–24 h after the last dose). They were then switched to the Japan-specific dose, and the Anti-Xa were measured at peak and trough concentrations after at least one week of rivaroxaban administration.

Ethical approval was given by the Institutional Review Board of the Faculty of Medicine, Chiang Mai University, Chiang Mai, Thailand, and the Institutional Review Board Committee on human research at the University of Phayao, Phayao, Thailand.

2.2. Rivaroxaban Quantification

Blood samples were collected into 3.2% sodium citrate tubes and mixed by inverting them for 8–10 min to avoid clotting. The samples were centrifuged at 3000 rpm for 10 min. Plasma was separated and stored at −70 °C until the analysis.

The Anti-Xa activity of rivaroxaban in plasma was measured with the chromogenic method using BIOPHEN^{TM} Heparin LRT kits (Dasit, Milan, Italy) and analyzed on an Automated Blood Coagulation Analyzer (Sysmex CS 2500 System, Siemens Health Care, Milan, Italy). All reagents and instruments were used in accordance with the manufacturers' instructions. The Anti-Xa was specifically calibrated and translated into values of rivaroxaban concentration [25]. The BIOPHEN^{TM} Rivaroxaban Calibrator kits were used to set the curve for the low range and standard range. These calibrators were used to establish the calibration curves for the Anti-Xa chromogenic assays of rivaroxaban in plasma. The BIOPHEN^{TM} Rivaroxaban Control kits were used to control the curve for the low range and standard range. These controls were used for the quality control of Anti-Xa chromogenic assays of rivaroxaban in plasma.

2.3. Population Pharmacokinetic Analysis

The population PK analysis of rivaroxaban was performed using nonlinear mixed effects modelling in NONMEM® software, version 7.4 (Icon Development Solution, Ellicott City, MD, USA). The first-order conditional estimation method with interaction (FOCE-I) was used throughout the model development. Model diagnostics and automated functions for model development were performed using Xpose version 4.0 [26], Pirana [27], and Perl-speaks-NONMEM (PsN; version 5.2.6) [28].

The data availability during an absorption phase was limited since the Anti-Xa activity of rivaroxaban was only obtained at steady-state peak and trough concentration on two different dosing occasions. Thus, a frequentist prior approach ($PRIOR) was implemented to stabilize model parameter estimates [29]. The typical value and inter-individual variability (IIV) of the oral absorption rate constant (ka) from a previous study [23] were applied using a frequentist prior methodology.

The PK parameters were assumed to be log-normally distributed, and their IIVs were introduced as an exponential function. The residual unexplained variability (RUV) was modeled using an additive function.

The difference in objective function value (ΔOFV) was used as a criterion for model discrimination. The ΔOFV of >3.84 and >6.63 were considered statistically significant at a *p*-Value of <0.05 and <0.01, respectively, with one degree of freedom.

The influence of patient characteristics on PK parameters was investigated using a stepwise covariate approach. During stepwise forward inclusion, the ΔOFV of >3.84 was used to include the covariate in the model, and the more stringent criterion (ΔOFV

of >6.63) was used in the stepwise backward deletion to retain the covariate in the final model. The following covariates were evaluated: age (years), body weight (kg), body mass index (kg/m^2), creatinine level (mg/dL), creatinine clearance (CrCl; mL/min, calculated according to Cockcroft and Gault equation) and sex.

Model misspecification and systematic errors were assessed using the goodness-of-fit plots. The ability to detect model misspecifications in goodness-of-fit diagnostics was evaluated using eta and epsilon shrinkages [30]. The robustness of the parameter estimated from the final model was evaluated using nonparametric bootstrap (n = 1000). The visual predictive checks (VPC) were performed using 1000 simulations. The 50th percentile of the observed data was overlaid with the simulated 90% prediction interval to evaluate the model's predictive performance.

2.4. Simulations

Monte Carlo simulations were performed using the final model to evaluate three different rivaroxaban doses, i.e., 10, 15, and 20 mg, once daily. Rivaroxaban exposures at a steady state (i.e., peak concentration; C_{MAX}, trough concentration; C_{MIN} and 24 h area under the concentration-time curve; $AUC_{0–24}$) were calculated. The 5th and 95th percentile ranges of C_{MAX} (184–343 ng/mL), C_{MIN} (12–137 ng/mL), and $AUC_{0–24}$ (1860–5434 ng·h/mL) reported in DOAC-eligible AF patients were used as the typical exposure ranges [19]. For each subgroup of patients based on CrCl and body weight (i.e., 15–29, 30–49, 50–69, 70–89, and 90–110 mL/min for CrCl and 15–29, 30–59, 60–89, and 90–119 kg for body weight), 1000 in silico patients were simulated. The percentage of patients with C_{MAX}, C_{MIN}, and $AUC_{0–24}$ values that were within the typical exposure ranges were calculated.

3. Results

3.1. Population Pharmacokinetic Analysis

A total of 240 Anti-Xa levels measured at peak and trough concentrations of rivaroxaban were obtained from 60 Thai DOAC-eligible AF patients. The summary of patient characteristics is presented in Table 1.

Table 1. Summary of patient characteristics (n = 60).

Characteristics	Value
Male, *n* (%)	38 (63.3)
Age (y), mean (SD)	69.4 (9.2)
Body weight (kg), mean (SD)	64.0 (14.1)
Body mass index (kg/m^2), median (Q_1, Q_3)	24.2 (21.5, 26.9)
Creatinine (mg/dL), mean (SD)	1.1 (0.3)
Creatinine clearance (mL/min), mean (SD)	59.0 (22.8)
$CHADS_2$ score, median (Q_1, Q_3)	2 (1, 2)
CHA_2 DS_2-VASC score, median (Q_1, Q_3)	3 (2, 4)
HAS-BLED score, median (Q_1, Q_3)	2 (1, 2)
Underlying disease, *n* (%)	
Hypertension	46 (76.7)
Dyslipidemia	35 (58.3)
Diabetes	16 (26.7)
Congestive heart failure	15 (25.0)
Ischemic heart disease	8 (13.3)
Ischemic stroke	7 (11.7)
Concomitant medications, *n* (%)	
Dronedarone	3 (5.0)
Amiodarone	1 (1.7)
Aspirin	1 (1.7)
Clopidogrel	1 (1.7)

The PK of rivaroxaban was described by a one-compartment model with first-order absorption and first-order elimination. The estimation of CL/F was 4.19 L/h with IIV of 21.9%, V/F was 37.5 L, and ka was 0.697 h-1 with IIV of 75.9%. Parameter estimates from the final model are presented in Table 2.

Table 2. Parameter estimates of rivaroxaban in Thai patients with non-valvular atrial fibrillation obtained from the final model and bootstrap analysis.

Parameters	Final Model (NONMEM)		Bootstrap Analysis (n = 1000 Samples)	
	Estimates [a] [RSE%]	95% CI *	Median [b] [RSE%]	95% CI **
CL/F (L/h)	4.19 [3.8%]	3.88–4.50	4.21 [4.08]	3.88–4.55
V/F (L)	37.5 [4.7%]	34.03–40.97	37.59 [4.62%]	34.0–40.8
ka (h^{-1})	0.697 [10.7%]	0.550–0.844	0.699 [5.06%]	0.623–0.764
CrCl on CL/F [c]	0.277 [29%]	0.120–0.434	0.277 [35.2%]	0.054–0.480
WT on V/F [d]	0.412 [35.7%]	0.124–0.70	0.413 [28.1%]	0.149–0.639
IIV of CL/F (%CV)	21.94 [21.3%]	16.67–26.24	21.24 [14.7%]	14.8–27.5
IIV of ka (%CV)	75.91 [10.1%]	66.39–85.10	75.81 [1.08%]	74.1–78.1
RUV, additive (mg/L)	0.092 [11.7%]	0.071–0.114	0.0926 [9.44%]	0.064–0.131

Abbreviations; CL/F, apparent oral clearance; V/F, apparent volume of distribution; ka, absorption rate constant; IIV, interindividual variability; RUV, residual unexplained variability; %CV, percent coefficient of variation; CI, confidence interval; SE, standard error; CrCl, creatinine clearance (mL/min); WT, body weight (kg). [a] Population mean values was estimated by NONMEM. * 95%CI = estimated value $\pm$ (1.96 $\times$ SE). [b] Median values was calculated from the non-parametric bootstrap results (n = 1000). ** 95%CI = 2.5th and 97.5th percentiles of the bootstrap parameter estimates. [c] Calculated as; $CL/F = 4.19 \times (CrCl/57.5)^{0.277}$. [d] Calculated as; $V/F = 37.5 \times (WT/63)^{0.412}$.

CrCl was a significant covariate for rivaroxaban CL/F (ΔOFV = -9.96, p-Value < 0.01). A power coefficient of 0.278 was used to define their association, showing that patients with higher CrCl have higher rivaroxaban CL/F. Additionally, body weight was a significant covariate for V/F (ΔOFV = -7.33, p-Value < 0.01) with a power coefficient of 0.412, indicating that patients with higher body weight have higher rivaroxaban V/F.

The goodness of fit plots showed that the final model adequately describes the data (Figure 1). The simulation-based diagnostic of the final model showed an adequate predictive performance (Figure 2). Eta shrinkage for CL/F (5.9%) and epsilon shrinkage (17.1%) were <20%, indicating robust individual parameter estimates [30].

3.2. Simulations

Figures 3 and 4 show the simulated C_{MAX} and C_{MIN} for different dosage regimens, stratified by CrCl and body weight. As body weight did not effect on the simulated $AUC_{0–24}$, the simulated $AUC_{0–24}$ by CrCl was displayed (Figure 5). The percentage of simulated patients with rivaroxaban exposures within the typical exposure ranges under various scenarios is summarized in Figure 6. The C_{MAX}, C_{MIN}, and $AUC_{0–24}$ values of patients who received 20 mg of rivaroxaban once daily were greater than the typical exposure ranges, particularly in those with CrCl less than 50 mL/min.

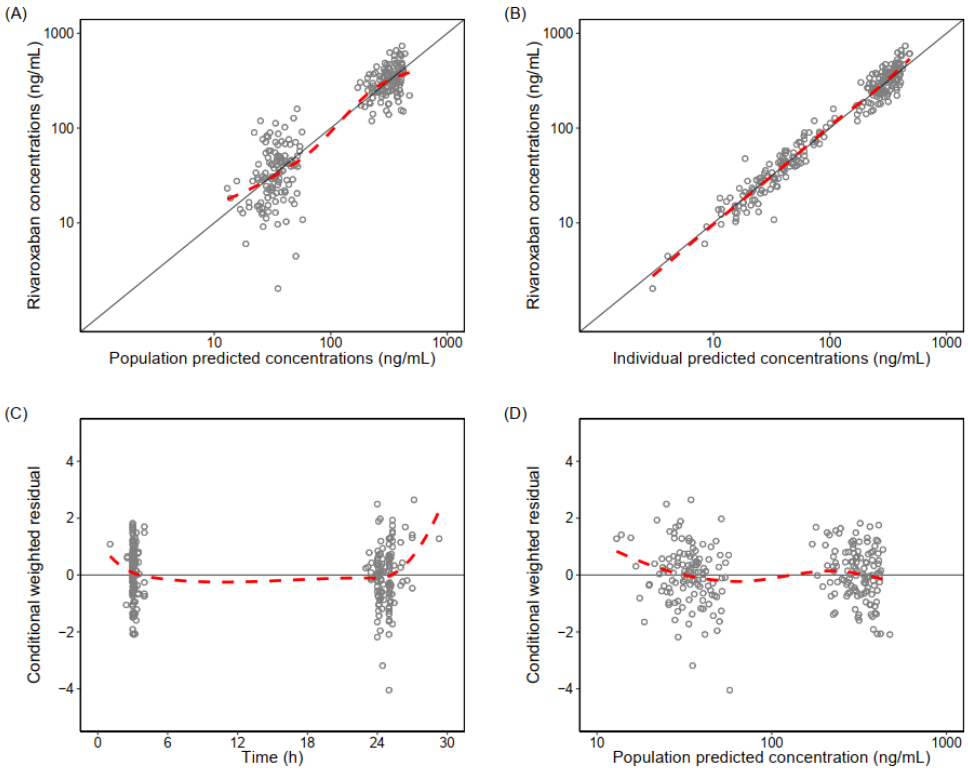

Figure 1. Goodness-of-fits of the final population pharmacokinetic model of rivaroxaban. (**A**) Observed rivaroxaban concentrations vs. population predictions, (**B**) observed rivaroxaban concentrations vs. individually predicted concentrations, (**C**) conditionally weighted residual vs. time, and (**D**) conditionally weighted residual vs. population predictions. The open circles represent the observed rivaroxaban concentrations. The solid black lines are the line of identity or zero-line. The dashed red lines are loess smooth lines (trend lines).

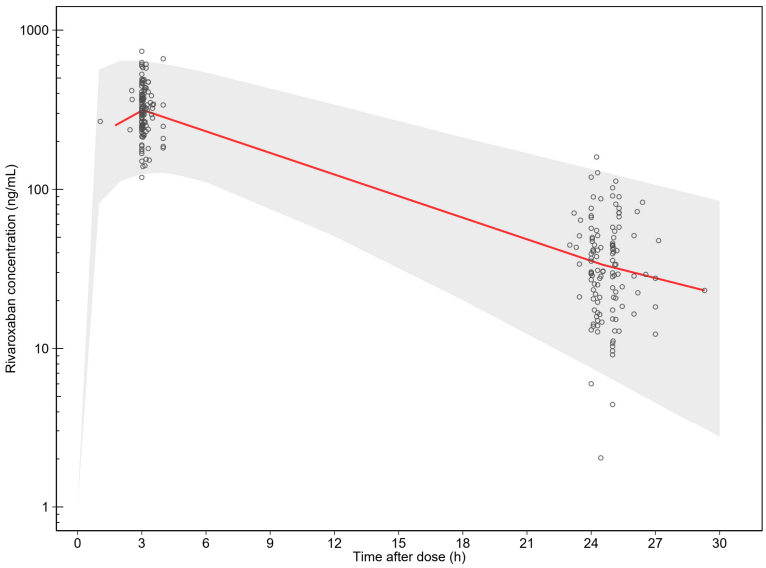

Figure 2. The simulated 90% prediction interval from the final population pharmacokinetic model of rivaroxaban. The open circles represent the observed rivaroxaban concentrations. Solid red line represents the 50th percentile of the observations. The shaded area represents the 90% prediction interval of the simulations (n = 1000).

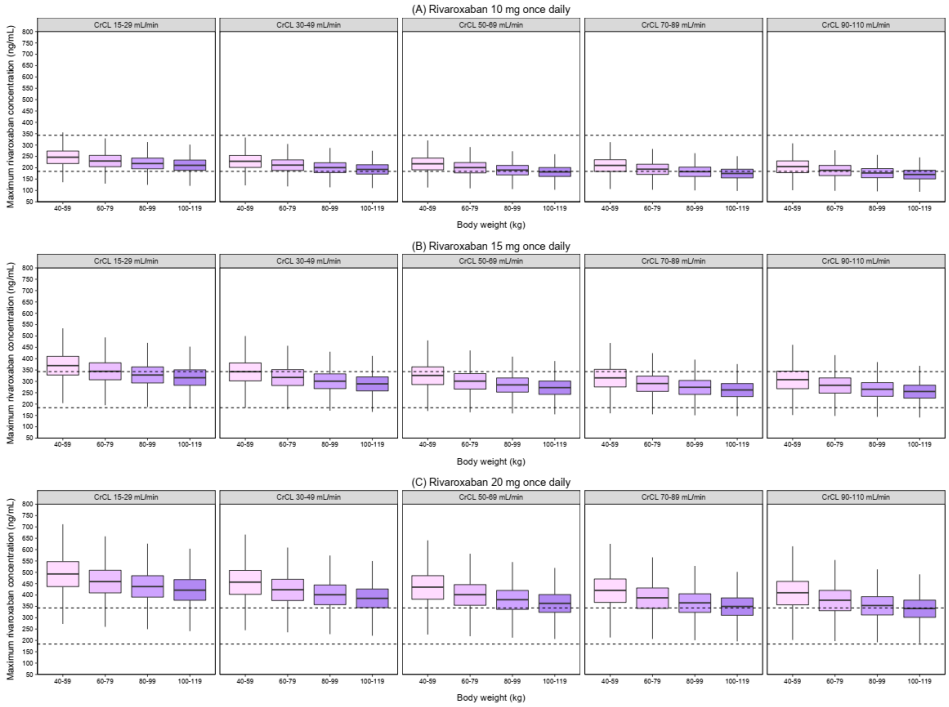

Figure 3. Simulated maximum concentration (C_{MAX}) of rivaroxaban with different dosing regimens. The boxplots represent the predicted C_{MAX} stratified by creatinine clearance and body weight. (**A**) rivaroxaban 10 mg once daily. (**B**) rivaroxaban 15 mg once daily. (**C**) rivaroxaban 20 mg once daily. The dashed lines represent the 5th and 95th percentile ranges of the typical C_{MAX} (184–343 ng/mL) reported in patients with non-valvular atrial fibrillation receiving 20 mg of rivaroxaban [19].

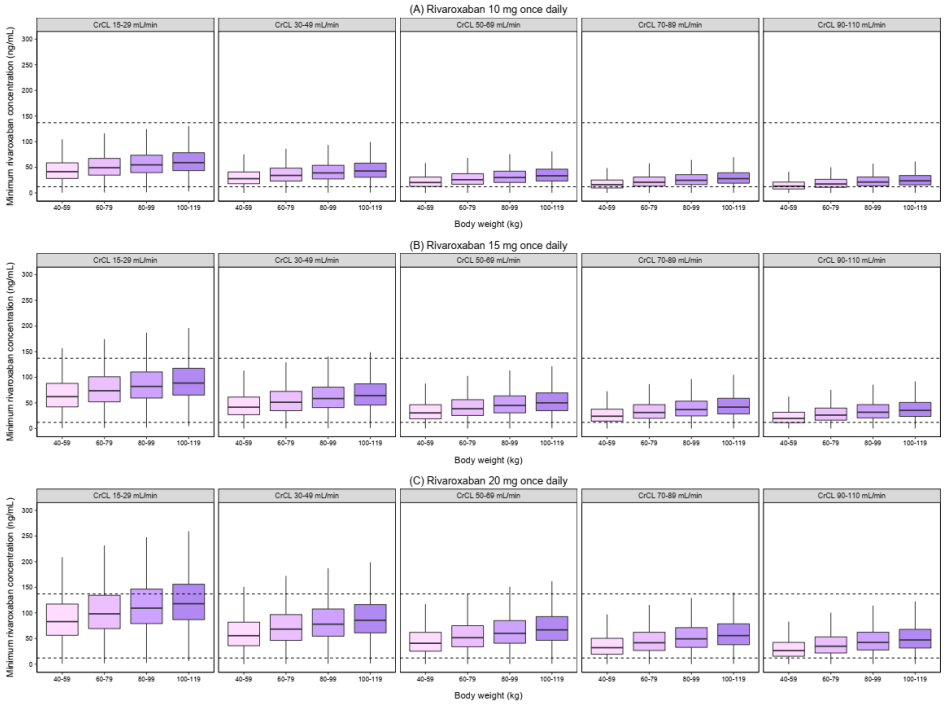

Figure 4. Simulated minimum concentration (C_{MIN}) of rivaroxaban with different dosing regimens. The boxplots represent the predicted C_{MIN} stratified by creatinine clearance and body weight. (**A**) rivaroxaban 10 mg once daily. (**B**) rivaroxaban 15 mg once daily. (**C**) rivaroxaban 20 mg once daily. The dashed lines represent the 5th and 95th percentile ranges of the typical C_{MIN} (12–137 ng/mL) reported in patients with non-valvular atrial fibrillation receiving 20 mg of rivaroxaban [19].

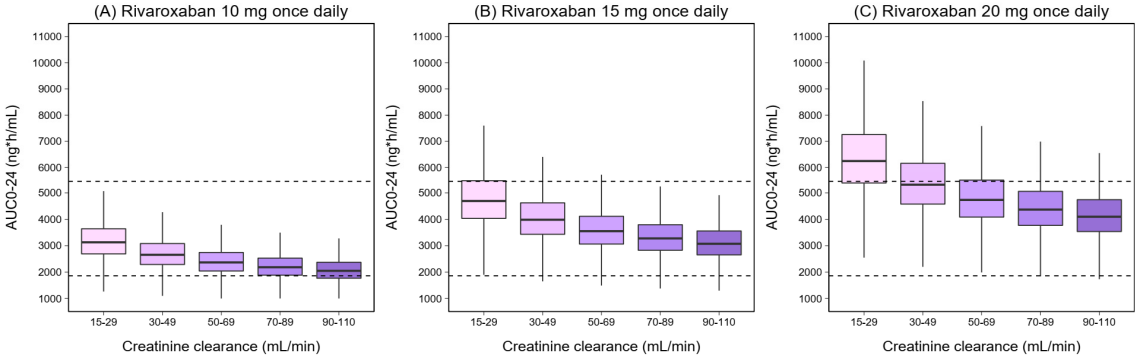

Figure 5. Simulated $AUC_{0–24}$ of rivaroxaban with different dosing regimens. The solid black lines represent the median $AUC_{0–24}$ The shaded areas represent the 90% prediction interval of the model. The dashed lines represent the 5th and 95th percentile ranges of the typical $AUC_{0–24}$ (1860–5434 ng·h/mL) reported in patients with non-valvular atrial fibrillation receiving 20 mg of rivaroxaban [19].

Figure 6. Proportion of patients having predicted C_{MAX}, C_{MIN}, and $AUC_{0–24}$ within the typical exposure ranges reported in patients with non-valvular atrial fibrillation [19] (1000 simulations per subgroup).

In comparison to the other dosing groups, the dosage of 10 mg once daily had the highest proportion of patients with C_{MAX}, C_{MIN}, and $AUC_{0–24}$ values within the typical exposure ranges for patients with CrCl between 15–29 and 30–49 mL/min, regardless of body weight. The proportion of patients with C_{MAX}, C_{MIN}, and $AUC_{0–24}$ within the typical exposure ranges was greater for patients with CrCl 50–69, 70–89, and 90–110 mL/min who took 15 mg once a day, regardless of body weight.

4. Discussion

Because of differences in patient characteristics, the Japanese patients had greater rivaroxaban concentrations when treated with the approved dosage [23,24]. The renal function of Asian patients with AF, as measured by CrCl, was lower than that of Caucasians [31,32]. As a result, it is likely that a lower dose of rivaroxaban gives enough exposure for Asians [23,24,33,34], reducing the risk of bleeding [5,35]. However, the PK data needed to optimize doses in Thai and Asian populations is scarce. Additionally, the high cost of rivaroxaban restricts access to therapy in resource-limited settings, including Thailand. Due to concerns about the risk of bleeding and cost, a lower dosage of DOACs has been prescribed for Thai patients [36]. Thus, the optimal low dose of rivaroxaban provided by this study could make rivaroxaban more accessible and safer for Thai patients. The current study developed a population PK model of rivaroxaban in Thai DOAC-eligible AF patients. To find the optimal dose of rivaroxaban, simulations were performed to predict drug exposure depending on significant covariates.

The rivaroxaban PK in Thai DOAC-eligible AF patients was adequately described by a one-compartment model with first-order absorption and elimination, consistent with previous studies in AF patients [20,23,24,33,34,37]. The estimation of CL/F (4.19 L/h) in Thai DOAC-eligible AF patients was slightly lower than that reported in other ethnicities, including Caucasians (5.58–6.10 L/h) [20,37]. When compared to other Asian populations, the CL/F in this study is comparable to Japanese (4.72–4.73 L/h) [23,24] but lower than Chinese (5.03–7.39 L/h) [33,34,38]. The estimated V/F (37.5 L) was lower than that reported in other studies (40.3–79.7 L) [23,24,33,34,37]. The discrepancies in PK values between ethnic groups might be attributable to variability in patient characteristics. Due to the small number of samples collected during the distribution phase, we were unable to determine the IIV of the V/F. The parameterized ka using a frequentist prior approach was 0.697 h^{-1}, which is closed to the value (0.600–0.617 h^{-1}) reported in Japanese [23,24].

In the covariate analysis, the final model revealed that CL/F and V/F of rivaroxaban increase by increasing CrCl and body weight, respectively. Several previous studies showed the significant effect of CrCl on rivaroxaban CL/F [20,24,34,39–42], thus, our finding confirmed this relationship. Because rivaroxaban is partly excreted through the kidneys, reduced renal function results in lower drug clearance [19]. The Cockcroft–Gault equation, which is preferably used to determine the renal function and is expressed as CrCl, is indicative of rivaroxaban dose adjustment [1,19].

Age, gender, or body weight had no influence on rivaroxaban CL/F. These results are consistent with earlier findings showing that the C_{MAX} of rivaroxaban was unaltered in patients with high body mass but increased by 24% in those with severely low body mass (50 kg), resulting in a prolonged prothrombin time [43]. A prior study indicated that elderly patients were exposed to 41 percent more rivaroxaban than young subjects [44]. However, the increasing exposure with age was mostly attributable to a lower clearance as a result of decreased renal function [37,44]. Moreover, these factors are employed in the Cockcroft-Gault equation to determine CrCl.

It has been determined that body size (i.e., lean body mass and body surface area) influences the PK characteristics of rivaroxaban [20,34,37,39]. One research involving healthy volunteers demonstrated that BMI influences the V/F of rivaroxaban [38]. Moreover, the results from previous studies showing that CrCl was the significant covariate influencing rivaroxaban CL/F, whereas other body size measurements alone were not found to significantly impact rivaroxaban CL/F [40,41]. In our study, BMI was not detected as a

significant covariate for either V/F or CL/F ($p > 0.05$) during covariate analysis. However, body weight was a significant covariate for V/F ($p < 0.01$) with an improvement in the goodness of fit. In clinical practice, body weight is more readily available than other weight measurements. Thus, using body weight as a measurement of body size would be more practical.

In our analysis, the IIV of V/F could not be estimated from the data; thus, the V/F was estimated without its IIV. Although the impact of body weight in explaining part of the IIV of V/F cannot be determined, weight was kept in the final model as a significant covariate on V/F as it showed a significantly decreased OFV and improved the overall model fit.

Rivaroxaban exposure has been associated with clinical outcomes and may aid in predicting the benefit–risk profile [13,16]. Peak Anti-Xa concentrations have been linked to bleeding complications [8–10], whereas trough concentrations have been related to the occurrence of thromboembolic events [11,12].

Based on the results from simulations, it was shown that the use of the approved dose in the Thai population resulted in higher rivaroxaban exposures. For patients with normal renal function (CrCl $\geq$ 50 mL/min) irrespective of body weight, a reduced dose of 15 mg resulted in a high proportion of patients having rivaroxaban exposure within the typical exposure ranges. This reduced dose is considered more appropriate for Thai DOAC-eligible AF patients with normal renal function, which supports the results from population PK studies in Asian patients, including Japanese [23,24] and Chinese [33,34].

Patients with renal impairment had a decrease in the CL/F, leading to increased rivaroxaban exposure [19]. Based on the simulation results, the C_{MAX}, C_{MIN}, and $AUC_{0–24}$ were higher in patients with lower CrCl, which are in line with previous findings [20,37]. Our simulation results showed that the predicted C_{MAX} was decreased with increasing body weight in the same CrCl range group. In contrast, individuals with higher body weight are more likely to have a higher predicted C_{MIN} within the same group of CrCl patients, which may be owing to an increase in V/F as body weight increases, resulting in a decrease in the elimination rate constant (ke). Similar trends in C_{MAX} and C_{MIN} alterations were seen in Chinese patients in a prior investigation [34].

A previous study, which looked at a wider range of CrCl (i.e., 15–29, 30–69, 70–159, and 160–250 mL/min) than the phase III clinical trial, showed that for individuals with CrCl of 15–29 mL/min, the dosage should be lowered from 15 to 10 mg [45]. Although rivaroxaban dosing has not been proven for patients with CrCl 15–29 mL/min [1], a dose reduction may be warranted for people in this group who require this medication. The results from our study suggested a daily dose of 10 mg for Thai DOAC-eligible AF patients with CrCl 15–29 mL/min, regardless of body weight. This recommendation is consistent with the dosage indicated for this population in previous research [45].

The previous integrated PK/PD study of rivaroxaban in Chinese patients suggested that the median peak Anti-Xa level at a dose of 10 mg was within the expected range for patients with CrCL 30–49 mL/min but not at a dose of 15 mg [38]. As a result, dosage modification based on body weight is unnecessary [38]. Results from our simulations confirmed a lower rivaroxaban dose of 10 mg should be appropriate for patients with poor renal function (CrCl of 30–49 mL/min) regardless of body weight. In summary, for patients with renal impairment, CrCL < 50 mL/min, a daily dose of 10 mg of rivaroxaban is recommended.

In this investigation, rivaroxaban concentrations were determined indirectly using commercially available Anti-Xa assays (BIOPHEN^{TM} Heparin LRT) with validated specific rivaroxaban calibrators. Despite the fact that liquid chromatography with tandem mass spectrometry (LC-MS/MS) is the gold standard approach for direct detection of rivaroxaban plasma concentrations [46], it is time-consuming, technically demanding, and not always available. The technique comparison research revealed a correlation between the BIOPHEN^{TM} Heparin LRT and LC-MS/MS test at all rivaroxaban concentrations (r^2 = 0.97) [47]. Thus, Anti-Xa tests can be used to detect rivaroxaban levels indirectly in clinical practice.

This study has some limitations. First, data during the absorption phase were limited. Thus, the prior method was used to estimate ka and its variability, which indicated the reliability of parameter estimates. Second, the number of patients concomitantly receiving inducers and inhibitors of CYP3A4 and/or P-glycoprotein was small, so the effect of the drug-drug interactions [19,20,48] could not be evaluated. Third, we did not explore other covariates (i.e., genetic polymorphisms, hepatic impairment) which can cause PK variability of rivaroxaban [34,42,49,50]. A previous study revealed that mild hepatic impairment decreased drug clearance and increased drug exposure, resulting in a prolonged prothrombin time [50]. Patients with moderate or severe hepatic impairment (Child-Pugh B and C) should thus avoid using rivaroxaban. Although a prior study determined that total bilirubin was a significant covariate for baseline prothrombin time, its effect on the PK of rivaroxaban was not identified [33,34]. Due to a lack of data, the effect of hepatic function was not explored in our study. Considering the aforementioned factors, further research should be undertaken.

Fourth, the typical exposure ranges of rivaroxaban were established from prior research on patients with non-valvular AF [19]. As the therapeutic window associated with the risk-benefit profile of rivaroxaban is unknown, the optimal dosage recommended in this study is the dose that provides equivalent rivaroxaban exposure to the typical exposure ranges, which may not be the clinically optimal dose. Finally, the impact of a reduced dose on clinical outcomes was not investigated in this study. Several previous studies found that low-dose rivaroxaban, compared to warfarin, was associated with a lower risk of stroke or systemic embolism and major bleeding [5,35,51,52]. However, there is evidence of a higher risk of ischemic stroke without a lower risk of bleeding when a lower dose of rivaroxaban was given to Asian patients [53]. Further investigations are needed to determine the clinical relevance of low-dose rivaroxaban regarding effectiveness for stroke prevention and safety.

5. Conclusions

In conclusion, a population PK model of rivaroxaban PK in Thai DOAC-eligible AF patients confirmed the effect of renal function on CL/F and the effect of body weight on V/F. Simulations suggested that low-dose rivaroxaban may be more appropriate for Thai patients, and dosages of rivaroxaban depending on renal function were proposed for Thai patients. A daily 10 mg dose was proposed for Thai DOAC-eligible AF patients with CrCl < 50 mL/min, regardless of body weight. For Thai DOAC-eligible AF patients with CrCl $\geq$ 50 mL/min, a daily dose of 15 mg was recommended.

Author Contributions: Conceptualization, N.S., A.P., W.W. and B.P.; Data curation, P.P., L.N. and S.G.; Formal analysis, N.S. and B.P.; Investigation, A.P., P.P., L.N., N.P. and W.W.; Methodology, N.S. and B.P.; Resources, A.P., P.P., L.N., S.G., N.P. and W.W.; Software, N.S.; Supervision, W.W. and B.P.; Validation, N.S.; Visualization, N.S.; Writing—original draft, N.S.; Writing—review & editing, N.S., A.P., W.W. and B.P. All authors have read and agreed to the published version of the manuscript.

Funding: This research was funded by the Thailand Science Research and Innovation Fund (grant number FF64-RIM024) and the Unit of Excellence on Pharmacogenomic Pharmacokinetic and Pharmacotherapeutic Researches (UPPER) (grant number FF65-UoE012), School of Pharmaceutical Sciences, University of Phayao, Thailand.

Institutional Review Board Statement: This study was approved by the Institutional Review Board of the Faculty of Medicine, Chiang Mai University, Chiang Mai, Thailand, and the Institutional Review Board Committee on human research at University of Phayao, Phayao, Thailand.

Informed Consent Statement: Informed consent was obtained from all subjects involved in the study.

Data Availability Statement: The data that support the findings of this study are available from the corresponding author upon request.

Acknowledgments: We thank all patients participating in the cohort study and the staff for their support.

Conflicts of Interest: The authors declare no conflict of interest. The funding source had no role in the study design, collection, analysis, and interpretation of data.

References

1. Steffel, J.; Collins, R.; Antz, M.; Cornu, P.; Desteghe, L.; Haeusler, K.G.; Oldgren, J.; Reinecke, H.; Roldan-Schilling, V.; Rowell, N.; et al. 2021 European Heart Rhythm Association Practical Guide on the Use of Non-Vitamin K Antagonist Oral Anticoagulants in Patients with Atrial Fibrillation. *Europace* **2021**, *23*, 1612–1676. [CrossRef] [PubMed]
2. Patel, M.R.; Mahaffey, K.W.; Garg, J.; Pan, G.; Singer, D.E.; Hacke, W.; Breithardt, G.; Halperin, J.L.; Hankey, G.J.; Piccini, J.P.; et al. Rivaroxaban versus warfarin in nonvalvular atrial fibrillation. *N. Engl. J. Med.* **2011**, *365*, 883–891. [CrossRef] [PubMed]
3. Hori, M.; Matsumoto, M.; Tanahashi, N.; Momomura, S.; Uchiyama, S.; Goto, S.; Izumi, T.; Koretsune, Y.; Kajikawa, M.; Kato, M.; et al. Rivaroxaban vs. warfarin in Japanese patients with atrial fibrillation–the J-ROCKET AF study-. *Circ. J.* **2012**, *76*, 2104–2111. [CrossRef] [PubMed]
4. Kim, Y.H.; Shim, J.; Tsai, C.T.; Wang, C.C.; Vilela, G.; Muengtaweepongsa, S.; Kurniawan, M.; Maskon, O.; Fern, H.L.; Nguyen, T.H.; et al. XANAP: A real-world, prospective, observational study of patients treated with rivaroxaban for stroke prevention in atrial fibrillation in Asia. *J. Arrhythm.* **2018**, *34*, 418–427. [CrossRef]
5. Chan, Y.H.; Lee, H.F.; Wang, C.L.; Chang, S.H.; Yeh, C.H.; Chao, T.F.; Yeh, Y.H.; Chen, S.A.; Kuo, C.T. Comparisons of Rivaroxaban Following Different Dosage Criteria (ROCKET AF or J-ROCKET AF Trials) in Asian Patients with Atrial Fibrillation. *J. Am. Heart Assoc.* **2019**, *8*, e013053. [CrossRef]
6. Cuker, A.; Siegal, D.M.; Crowther, M.A.; Garcia, D.A. Laboratory measurement of the anticoagulant activity of the non-vitamin K oral anticoagulants. *J. Am. Coll. Cardiol.* **2014**, *64*, 1128–1139. [CrossRef]
7. Molenaar, P.J.; Dinkelaar, J.; Leyte, A. Measuring Rivaroxaban in a clinical laboratory setting, using common coagulation assays, Xa inhibition and thrombin generation. *Clin. Chem. Lab. Med.* **2012**, *50*, 1799–1807. [CrossRef]
8. Sakaguchi, T.; Osanai, H.; Murase, Y.; Ishii, H.; Nakashima, Y.; Asano, H.; Suzuki, S.; Takefuji, M.; Inden, Y.; Sakai, K. Monitoring of anti-Xa activity and factors related to bleeding events: A study in Japanese patients with nonvalvular atrial fibrillation receiving rivaroxaban. *J. Cardiol.* **2017**, *70*, 244–249.
9. Testa, S.; Legnani, C.; Antonucci, E.; Paoletti, O.; Dellanoce, C.; Cosmi, B.; Pengo, V.; Poli, D.; Morandini, R.; Testa, R.; et al. Drug levels and bleeding complications in atrial fibrillation patients treated with direct oral anticoagulants. *J. Thromb. Haemost.* **2019**, *17*, 1064–1072. [CrossRef]
10. Jakowenko, N.; Nguyen, S.; Ruegger, M.; Dinh, A.; Salazar, E.; Donahue, K.R. Apixaban and rivaroxaban anti-Xa level utilization and associated bleeding events within an academic health system. *Thromb. Res.* **2020**, *196*, 276–282. [CrossRef]
11. Testa, S.; Paoletti, O.; Legnani, C.; Dellanoce, C.; Antonucci, E.; Cosmi, B.; Pengo, V.; Poli, D.; Morandini, R.; Testa, R.; et al. Low drug levels and thrombotic complications in high-risk atrial fibrillation patients treated with direct oral anticoagulants. *J. Thromb. Haemost.* **2018**, *16*, 842–848. [CrossRef] [PubMed]
12. Nosáľ, V.; Petrovičová, A.; Škorňová, I.; Bolek, T.; Dluhá, J.; Stančiaková, L.; Sivák, Š.; Babálová, L.; Hajaš, G.; Staško, J.; et al. Plasma levels of direct oral anticoagulants in atrial fibrillation patients at the time of embolic stroke: A pilot prospective multicenter study. *Eur. J. Clin. Pharmacol.* **2022**, *78*, 557–564. [CrossRef] [PubMed]
13. Miklič, M.; Mavri, A.; Vene, N.; Söderblom, L.; Božič-Mijovski, M.; Pohanka, A.; Antovic, J.; Malmström, R.E. Intra- and inter-individual rivaroxaban concentrations and potential bleeding risk in patients with atrial fibrillation. *Eur. J. Clin. Pharmacol.* **2019**, *75*, 1069–1075. [CrossRef] [PubMed]
14. Sennesael, A.L.; Larock, A.S.; Douxfils, J.; Elens, L.; Stillemans, G.; Wiesen, M.; Taubert, M.; Dogné, J.M.; Spinewine, A.; Mullier, F. Rivaroxaban plasma levels in patients admitted for bleeding events: Insights from a prospective study. *Thromb. J.* **2018**, *16*, 28. [CrossRef]
15. Cuker, A. Laboratory measurement of the non-vitamin K antagonist oral anticoagulants: Selecting the optimal assay based on drug, assay availability, and clinical indication. *J. Thromb. Thrombolysis* **2016**, *41*, 241–247. [CrossRef]
16. Ikeda, K.; Tachibana, H. Clinical implication of monitoring rivaroxaban and apixaban by using anti-factor Xa assay in patients with non-valvular atrial fibrillation. *J. Arrhythm.* **2016**, *32*, 42–50. [CrossRef]
17. Testa, S.; Tripodi, A.; Legnani, C.; Pengo, V.; Abbate, R.; Dellanoce, C.; Carraro, P.; Salomone, L.; Paniccia, R.; Paoletti, O.; et al. Plasma levels of direct oral anticoagulants in real life patients with atrial fibrillation: Results observed in four anticoagulation clinics. *Thromb. Res.* **2016**, *137*, 178–183. [CrossRef]
18. Gulilat, M.; Tang, A.; Gryn, S.E.; Leong-Sit, P.; Skanes, A.C.; Alfonsi, J.E.; Dresser, G.K.; Henderson, S.L.; Rose, R.V.; Lizotte, D.J.; et al. Interpatient Variation in Rivaroxaban and Apixaban Plasma Concentrations in Routine Care. *Can. J. Cardiol.* **2017**, *33*, 1036–1043. [CrossRef]
19. Mueck, W.; Stampfuss, J.; Kubitza, D.; Becka, M. Clinical pharmacokinetic and pharmacodynamic profile of rivaroxaban. *Clin. Pharmacokinet.* **2014**, *53*, 1–16.
20. Willmann, S.; Zhang, L.; Frede, M.; Kubitza, D.; Mueck, W.; Schmidt, S.; Solms, A.; Yan, X.; Garmann, D. Integrated Population Pharmacokinetic Analysis of Rivaroxaban Across Multiple Patient Populations. *CPT Pharmacomet. Syst. Pharmacol.* **2018**, *7*, 309–320. [CrossRef]
21. Gibson, C.M.; Yuet, W.C. Racial and Ethnic Differences in Response to Anticoagulation: A Review of the Literature. *J. Pharm. Pract.* **2021**, *34*, 685–693. [CrossRef] [PubMed]
22. Chao, T.F.; Joung, B.; Takahashi, Y.; Lim, T.W.; Choi, E.K.; Chan, Y.H.; Guo, Y.; Sriratanasathavorn, C.; Oh, S.; Okumura, K.; et al. 2021 Focused Update Consensus Guidelines of the Asia Pacific Heart Rhythm Society on Stroke Prevention in Atrial Fibrillation: Executive Summary. *Thromb. Haemost.* **2022**, *122*, 20–47. [CrossRef] [PubMed]

23. Tanigawa, T.; Kaneko, M.; Hashizume, K.; Kajikawa, M.; Ueda, H.; Tajiri, M.; Paolini, J.F.; Mueck, W. Model-based dose selection for phase III rivaroxaban study in Japanese patients with non-valvular atrial fibrillation. *Drug Metab. Pharmacokinet.* **2013**, *28*, 59–70. [CrossRef] [PubMed]
24. Kaneko, M.; Tanigawa, T.; Hashizume, K.; Kajikawa, M.; Tajiri, M.; Mueck, W. Confirmation of model-based dose selection for a Japanese phase III study of rivaroxaban in non-valvular atrial fibrillation patients. *Drug Metab. Pharmacokinet.* **2013**, *28*, 321–331. [CrossRef]
25. Wongcharoen, W.; Pacharasupa, P.; Norasetthada, L.; Gunaparn, S.; Phrommintikul, A. Anti-Factor Xa Activity of Standard and Japan-Specific Doses of Rivaroxaban in Thai Patients with Non-Valvular Atrial Fibrillation. *Circ. J.* **2020**, *84*, 1075–1082. [CrossRef]
26. Jonsson, E.N.; Karlsson, M.O. Xpose—An S-PLUS based population pharmacokinetic/pharmacodynamic model building aid for NONMEM. *Comput. Methods Programs Biomed.* **1999**, *58*, 51–64. [CrossRef]
27. Keizer, R.J.; van Benten, M.; Beijnen, J.H.; Schellens, J.H.; Huitema, A.D. Piraña and PCluster: A modeling environment and cluster infrastructure for NONMEM. *Comput. Methods Programs Biomed.* **2011**, *101*, 72–79. [CrossRef]
28. Lindbom, L.; Ribbing, J.; Jonsson, E.N. Perl-speaks-NONMEM (PsN)—A Perl module for NONMEM related programming. *Comput. Methods Programs Biomed.* **2004**, *75*, 85–94. [CrossRef]
29. Gisleskog, P.O.; Karlsson, M.O.; Beal, S.L. Use of prior information to stabilize a population data analysis. *J. Pharmacokinet. Pharmacodyn.* **2002**, *29*, 473–505. [CrossRef]
30. Savic, R.M.; Karlsson, M.O. Importance of shrinkage in empirical bayes estimates for diagnostics: Problems and solutions. *AAPS J.* **2009**, *11*, 558–569. [CrossRef]
31. Phrommintikul, A.; Detnuntarat, P.; Prasertwitayakij, N.; Wongcharoen, W. Prevalence of atrial fibrillation in Thai elderly. *J. Geriatr. Cardiol.* **2016**, *13*, 270–273. [PubMed]
32. Akao, M.; Chun, Y.H.; Wada, H.; Esato, M.; Hashimoto, T.; Abe, M.; Hasegawa, K.; Tsuji, H.; Furuke, K.; Fushimi, A.F.; et al. Current status of clinical background of patients with atrial fibrillation in a community-based survey: The Fushimi AF Registry. *J. Cardiol.* **2013**, *61*, 260–266. [CrossRef] [PubMed]
33. Liu, X.Q.; Zhang, Y.F.; Ding, H.Y.; Yan, M.M.; Jiao, Z.; Zhong, M.K.; Ma, C.L. Population pharmacokinetic and pharmacodynamic analysis of rivaroxaban in Chinese patients with non-valvular atrial fibrillation. *Acta Pharmacol. Sin.* **2022**. [CrossRef] [PubMed]
34. Zhang, F.; Chen, X.; Wu, T.; Huang, N.; Li, L.; Yuan, D.; Xiang, J.; Wang, N.; Chen, W.; Zhang, J. Population Pharmacokinetics of Rivaroxaban in Chinese Patients with Non-Valvular Atrial Fibrillation: A Prospective Multicenter Study. *Clin. Pharmacokinet.* **2022**, *61*, 881–893. [CrossRef]
35. Lee, H.F.; Chan, Y.H.; Tu, H.T.; Kuo, C.T.; Yeh, Y.H.; Chang, S.H.; Wu, L.S.; See, L.C. The effectiveness and safety of low-dose rivaroxaban in Asians with non-valvular atrial fibrillation. *Int. J. Cardiol.* **2018**, *261*, 78–83. [CrossRef] [PubMed]
36. Wattanaruengchai, P.; Nathisuwan, S.; Rattanavipanon, W.; Chulavatnatol, S.; Kongwatcharapong, J.; Mitsuntisuk, P.; Chaiyasothi, T.; Kritsanapipat, D.; Phrommintikul, A.; Chaiyakunapruk, N.; et al. Prescriber compliance to direct oral anticoagulant labels and impact on outcomes in Thailand. *Br. J. Clin. Pharmacol.* **2021**, *87*, 1390–1400. [CrossRef]
37. Girgis, I.G.; Patel, M.R.; Peters, G.R.; Moore, K.T.; Mahaffey, K.W.; Nessel, C.C.; Halperin, J.L.; Califf, R.M.; Fox, K.A.; Becker, R.C. Population pharmacokinetics and pharmacodynamics of rivaroxaban in patients with non-valvular atrial fibrillation: Results from ROCKET AF. *J. Clin. Pharmacol.* **2014**, *54*, 917–927. [CrossRef]
38. Zhao, N.; Liu, Z.; Xie, Q.; Wang, Z.; Sun, Z.; Xiang, Q.; Cui, Y. A Combined Pharmacometrics Analysis of Biomarker Distribution Under Treatment with Standard- or Low-Dose Rivaroxaban in Real-World Chinese Patients with Nonvalvular Atrial Fibrillation. *Front. Pharmacol.* **2022**, *13*, 814724. [CrossRef]
39. Mueck, W.; Eriksson, B.I.; Bauer, K.A.; Borris, L.; Dahl, O.E.; Fisher, W.D.; Gent, M.; Haas, S.; Huisman, M.V.; Kakkar, A.K.; et al. Population pharmacokinetics and pharmacodynamics of rivaroxaban—An oral, direct factor Xa inhibitor—In patients undergoing major orthopaedic surgery. *Clin. Pharmacokinet.* **2008**, *47*, 203–216. [CrossRef]
40. Barsam, S.J.; Patel, J.P.; Roberts, L.N.; Kavarthapu, V.; Patel, R.K.; Green, B.; Arya, R. The impact of body weight on rivaroxaban pharmacokinetics. *Res. Pract. Thromb. Haemost.* **2017**, *1*, 180–187. [CrossRef]
41. Speed, V.; Green, B.; Roberts, L.N.; Woolcombe, S.; Bartoli-Abdou, J.; Barsam, S.; Byrne, R.; Gee, E.; Czuprynska, J.; Brown, A.; et al. Fixed dose rivaroxaban can be used in extremes of bodyweight: A population pharmacokinetic analysis. *J. Thromb. Haemost.* **2020**, *18*, 2296–2307. [CrossRef] [PubMed]
42. Esmaeili, T.; Rezaee, M.; Esfahani, M.A.; Davoudian, A.; Omidfar, D.; Rezaee, S. Rivaroxaban population pharmacokinetic and pharmacodynamic modeling in Iranian patients. *J. Clin. Pharm. Ther.* **2022**. [CrossRef]
43. Kubitza, D.; Becka, M.; Zuehlsdorf, M.; Mueck, W. Body weight has limited influence on the safety, tolerability, pharmacokinetics, or pharmacodynamics of rivaroxaban (BAY 59-7939) in healthy subjects. *J. Clin. Pharmacol.* **2007**, *47*, 218–226. [CrossRef] [PubMed]
44. Kubitza, D.; Becka, M.; Roth, A.; Mueck, W. The influence of age and gender on the pharmacokinetics and pharmacodynamics of rivaroxaban—An oral, direct Factor Xa inhibitor. *J. Clin. Pharmacol.* **2013**, *53*, 249–255. [CrossRef] [PubMed]
45. Konicki, R.; Weiner, D.; Patterson, J.H.; Gonzalez, D.; Kashuba, A.; Cao, Y.C.; Gehi, A.K.; Watkins, P.; Powell, J.R. Rivaroxaban Precision Dosing Strategy for Real-World Atrial Fibrillation Patients. *Clin. Transl. Sci.* **2020**, *13*, 777–784. [CrossRef]
46. Gosselin, R.C.; Adcock, D.M.; Bates, S.M.; Douxfils, J.; Favaloro, E.J.; Gouin-Thibault, I.; Guillermo, C.; Kawai, Y.; Lindhoff-Last, E.; Kitchen, S. International Council for Standardization in Haematology (ICSH) Recommendations for Laboratory Measurement of Direct Oral Anticoagulants. *Thromb. Haemost.* **2018**, *118*, 437–450. [CrossRef]

47. Königsbrügge, O.; Quehenberger, P.; Belik, S.; Weigel, G.; Seger, C.; Griesmacher, A.; Pabinger, I.; Ay, C. Anti-coagulation assessment with prothrombin time and anti-Xa assays in real-world patients on treatment with rivaroxaban. *Ann. Hematol.* **2015**, *94*, 1463–1471. [CrossRef]
48. Mueck, W.; Kubitza, D.; Becka, M. Co-administration of rivaroxaban with drugs that share its elimination pathways: Pharmacokinetic effects in healthy subjects. *Br. J. Clin. Pharmacol.* **2013**, *76*, 455–466. [CrossRef]
49. Zdovc, J.; Petre, M.; Pišlar, M.; Repnik, K.; Mrhar, A.; Vogrin, M.; Potočnik, U.; Grabnar, I. Downregulation of ABCB1 gene in patients with total hip or knee arthroplasty influences pharmacokinetics of rivaroxaban: A population pharmacokinetic-pharmacodynamic study. *Eur. J. Clin. Pharmacol.* **2019**, *75*, 817–824. [CrossRef]
50. Kubitza, D.; Roth, A.; Becka, M.; Alatrach, A.; Halabi, A.; Hinrichsen, H.; Mueck, W. Effect of hepatic impairment on the pharmacokinetics and pharmacodynamics of a single dose of rivaroxaban, an oral, direct Factor Xa inhibitor. *Br. J. Clin. Pharmacol.* **2013**, *76*, 89–98. [CrossRef]
51. Qian, J.; Yan, Y.D.; Yang, S.Y.; Zhang, C.; Li, W.Y.; Gu, Z.C. Benefits and Harms of Low-Dose Rivaroxaban in Asian Patients with Atrial Fibrillation: A Systematic Review and Meta-analysis of Real-World Studies. *Front. Pharmacol.* **2021**, *12*, 642907. [CrossRef] [PubMed]
52. Shimokawa, H.; Yamashita, T.; Uchiyama, S.; Kitazono, T.; Shimizu, W.; Ikeda, T.; Kamouchi, M.; Kaikita, K.; Fukuda, K.; Origasa, H. The EXPAND study: Efficacy and safety of rivaroxaban in Japanese patients with non-valvular atrial fibrillation. *Int. J. Cardiol.* **2018**, *258*, 126–132. [CrossRef] [PubMed]
53. Cheng, W.H.; Chao, T.F.; Lin, Y.J.; Chang, S.L.; Lo, L.W.; Hu, Y.F.; Tuan, T.C.; Liao, J.N.; Chung, F.P.; Lip, G.Y.H.; et al. Low-Dose Rivaroxaban and Risks of Adverse Events in Patients with Atrial Fibrillation. *Stroke* **2019**, *50*, 2574–2577. [CrossRef] [PubMed]

pharmaceutics

MDPI

Article

Effect of Laparoscopic Sleeve Gastrectomy on the Pharmacokinetics of Oral Omeprazole Using a Population Approach

Kaifeng Chen [1,†], Ping Luo [2,†], Shaihong Zhu [2], Yaqi Lin [1], Nan Yang [1], Shuqi Huang [1], Qin Ding [1], Liyong Zhu [2,*] and Qi Pei [1,*]

[1] Department of Pharmacy, The Third Xiangya Hospital, Central South University, Changsha 410013, China
[2] Department of General Surgery, The Third Xiangya Hospital, Central South University, Changsha 410013, China
* Correspondence: zly8128@csu.edu.cn (L.Z.); qi.pei@csu.edu.cn (Q.P.)
† These authors contributed equally to this work.

Abstract: Omeprazole is commonly prescribed to obese patients and patients after laparoscopic sleeve gastrectomy (LSG). The pharmacokinetics of oral omeprazole after LSG are still unknown. Therefore, the aim of this study was to investigate the pharmacokinetics of oral omeprazole in obese patients before and after LSG. A total of 331 blood samples were collected from 62 obese patients preoperatively (visit 1) followed by 41 patients 7 days post-LSG (visit 2) and 20 patients 1 month post-LSG (visit 3). Population pharmacokinetic analysis was performed using NONMEM to characterize the effect of LSG on omeprazole absorption and disposition. A one-compartment model with 12 transit absorption compartments and linear elimination successfully described the data. Compared with pre-surgery, the oral omeprazole time to maximum plasma concentration (T_{max}) was reduced and maximum plasma concentration (C_{max}) was higher, but the apparent clearance (CL/F) and area under the plasma concentration–time curve (AUC) were unchanged 7 days and 1 month after surgery. In addition, the CYP2C19 genotype and liver function exhibited a significant influence on omeprazole CL/F. LSG increased the rate of omeprazole absorption but did not affect omeprazole exposure. A dose of 20 mg omeprazole once daily may be adequate for relieving gastrointestinal tract discomfort at short-term follow-up post-LSG.

Keywords: laparoscopic sleeve gastrectomy; omeprazole; population pharmacokinetic; modeling and simulation; obesity

Citation: Chen, K.; Luo, P.; Zhu, S.; Lin, Y.; Yang, N.; Huang, S.; Ding, Q.; Zhu, L.; Pei, Q. Effect of Laparoscopic Sleeve Gastrectomy on the Pharmacokinetics of Oral Omeprazole Using a Population Approach. *Pharmaceutics* **2022**, *14*, 1986. https://doi.org/10.3390/pharmaceutics14101986

Academic Editor: Thorsten Lehr

Received: 17 August 2022
Accepted: 16 September 2022
Published: 20 September 2022

1. Introduction

Obesity is defined as a body mass index (BMI) $\geq$ 30 kg/m^2, and it has become a global public health concern [1]. Obesity is considered to be a strong risk factor for various diseases, such as type 2 diabetes, hyperlipidemia, hypertension, nonalcoholic fatty liver disease, and sleep apnea syndrome [2], thereby leading to a decreased life quality and average life expectancy [3]. For most patients with severe obesity, the effects of nonsurgical treatments, such as reducing food intake, increasing physical activity, and drug therapy, are still limited and reversible [4]. To achieve sustained weight loss and improve obesity-related comorbidities, bariatric surgery is undoubtedly the most effective treatment option [5,6].

Currently, laparoscopic sleeve gastrectomy (LSG) is the most popular bariatric surgery worldwide, followed by Roux-en-Y gastric bypass (RYGB) [7]. LSG is well accepted as a restrictive procedure that mainly reduces the gastric volume, leaving only a smaller tube-shaped gastric pouch [8]. RYGB involves creating a small gastric pouch and bypassing the duodenum and proximal jejunum, which combines both restrictive and malabsorptive features [8]. Compared with RYGB, LSG is less invasive and has fewer complications [9]. However, due to the removal of most of the stomach fundus and body, intragastric pressure increases, and gastric compliance decreases post-LSG [10]. As a consequence, the majority

of patients suffer from gastrointestinal symptoms such as pantothenic acid, nausea, sore throat, chest pain, and epigastric pain [10]. Since proton pump inhibitors (PPIs) can reduce gastric acid secretion and protect the gastric wall barrier, obese patients undergoing bariatric surgery are instructed to take PPIs for several months to relieve these symptoms and prevent gastric ulcers [11–13].

Omeprazole, a first-generation PPI, is widely used for the prevention and treatment of acid-related disorders such as gastric and duodenal ulcers, gastroesophageal reflux disease, and Zollinger–Ellison syndrome [14]. Given its instability in an acidic environment, oral forms of omeprazole are usually formulated as enteric-coated preparations to prevent their early degradation in the stomach [15], e.g., as enteric-coated capsules. A previous study reported that the majority of RYGB patients receiving 40 mg of omeprazole daily to prevent gastric ulcers continued to have peptic injuries 2 months after surgery [11], suggesting that the dose was not sufficient to achieve a serum level that could effectively block the production of hydrochloric acid. Furthermore, it has been well established that LSG can increase gastric pH, accelerate gastric emptying, and reduce small intestinal transit time, etc. [16–18]; therefore, drug absorption and disposition might be altered after LSG surgery. However, currently, there is a research gap regarding the pharmacokinetic (PK) properties of omeprazole after LSG and, consequently, regarding its effectiveness in blocking acid secretion; hence, it is crucial to investigate the influence of LSG on omeprazole PK to recommend an appropriate omeprazole dose for patients undergoing LSG.

In this study, we prospectively collected data from 62 obese patients before surgery (visit 1), 41 patients 7 days post-LSG (visit 2), and 20 patients 1 month after LSG (visit 3). For this, a population PK model was established to evaluate the effect of LSG on the PK profile of omeprazole.

2. Materials and Methods

2.1. Study Population

We designed a prospective clinical trial to recruit obese patients who were potential candidates for LSG (BMI $\geq$ 30 kg/m^2). Participants with normal liver function or mild liver dysfunction were included. Mild liver dysfunction was defined as a total bilirubin (TBIL) level > 1–1.5 fold the upper limit of normal (ULN) or alanine aminotransferase (ALT) level > ULN or aspartate aminotransferase (AST) level > ULN [19], and the ULN was defined as 20.5 μmol/L, 40 U/L and 35 U/L for TBIL, ALT, and AST according to our laboratory standards. In addition, participants were excluded if they were known to have used CYP2C19 or CYP3A4 inhibitors and inducers over a period of three visits or were allergic to omeprazole. Before inclusion, all patients signed written informed consent. This study was performed at the Third Xiangya Hospital of Central South University after obtaining approval by the Ethics Committee and registered at the China Clinical Trial Registration Center with the identifier ChiCTR2100046578. All subjects were genotyped for CYP2C19 *2 (rs4244285), *3 (rs4986893), and *17 (rs12248560) using PCR-Fluorescence Probing [20] and were classified based on the updated Clinical Pharmacogenetics Implementation Consortium (CPIC) guidelines [21].

2.2. Study Design and Analytical Assay

Obese patients received a single 20 mg oral dose of omeprazole enteric-coated capsules under fasting conditions 2–3 days before surgery. Subsequently, 20 mg omeprazole was orally administered once daily to relieve gastrointestinal symptoms from the 7th day after LSG to 1 month after LSG. Consequently, this PK study was performed three times: after a single dose before surgery (visit 1), after a single dose 7 days post-LSG (visit 2), and after a repeated dose 1 month post-LSG (visit 3). Blood samples were obtained at approximately 1, 2, 4, 6, 8, and 9 h after omeprazole intake. The majority of patients had three blood samples collected before surgery, three collected 7 days after LSG and two collected 1 month post-LSG. Blood samples were centrifuged for 10 min at 4 °C at 2500$\times$ g, after which plasma was stored at -80 °C until analysis. Plasma samples were analyzed using a

validated liquid chromatogram tandem mass spectrometry method [20]. The lower limit of quantification of this assay was 1 ng/mL, and the upper limit of quantification was 2000 ng/mL. The quality control samples demonstrated that the intra-day and inter-days coefficients of variation were less than 10%.

2.3. Structural PK Model

A nonlinear mixed effects modeling program NONMEM (version 7.5; Icon Development Solutions, Ellicott City, MD, USA) was used to perform the population PK analysis, and R (version 4.2, http://www.r-project.org/, accessed on 6 January 2022) was used to visualize the data. The first-order conditional estimation method with inter- and intra-individual interactions (FOCE-I) was used throughout the model-building procedure. Different structural and statistical models were distinguished by means of comparing the objective function value (OFV). A p-value below 0.05, representing a reduction of 3.84 in the OFV, was considered statistically significant. Furthermore, goodness-of-fit (GOF) plots and visual predictive check (VPC) were used for diagnostic purposes [22]. Moreover, the accuracy and precision of the parameter estimates were used to assess the model. Sampling importance resampling (SIR) approach using 1000 replicates was used to obtain the 95% confidence intervals and to evaluate the robustness of the population PK model [23].

Initially, we tested one-compartment and two-compartment models. The delay in release of omeprazole enteric-coated capsules was captured by testing several transit compartment models. The time course of omeprazole concentrations was eventually modeled using a one-compartment model with 12 transit absorption compartments, which was consistent with our previous work [20]. The model was parameterized in terms of mean transit time (MTT) which represented the average time from oral administration of the drug to its appearance at the sampling point [24], apparent clearance (CL/F), and apparent volume of distribution (Vd/F). The inter-individual variability and inter-occasion variability (IOV) for the PK model parameters were modeled using an exponential model. A proportional residual error model was used to account for intra-individual variability. We have attached the NONMEM code as supplemental material.

2.4. Selection of Covariates

For evaluating potential relationships, covariates were plotted independently against the individual estimates of PK parameters. The following covariates were explored: visits, CYP2C19 genotype, liver function (normal liver function and mild liver dysfunction), sex, total body weight (TBW), age, lean body weight (LBW, based on the Janmahasatian formula [25]), ideal body weight (IBW, based on the Devine formula [26]), and adjusted body weight (ABW, based on a criterion defined by Schwartz [27]).

Continuous covariates, such as age, and TBW, were evaluated using a power function model, as presented in Equation (1).

$$P_i = \theta_p * \left(\frac{Cov}{Cov_{median}} \right)^{\theta_{cov}} * e^{\eta_j} \quad (1)$$

where P_i and θ_p represent the individual and typical population estimates, respectively; Cov_{median} is the median value for the covariate except that TBW was normalized to 70 kg; θ_{cov} is the estimated influential factor for the covariate; η_j is the random effect that describes the difference of the jth subject from the typical population value.

Categorical variables, such as visits and the CYP2C19 genotype, were assessed as follows (take visits as an example):

$$P_i = \theta_p * e^{\eta_j} \quad (2)$$

$$IF(Visit.EQ.2)\ \ P_i = \theta_1 * \ P_i \quad (3)$$

$$IF(Visit.EQ.3)\ \ P_i = \theta_2 * P_i \quad (4)$$

where θ_p is the typical value for obese patients before surgery, namely, at visit 1; θ_1 represents the numerical differences between visit 1 and visit 2 (7 days post-LSG); θ_2 represents the numerical differences between visit 1 and visit 3 (1 month post-LSG).

During forward inclusion, covariates that decreased the OFV by >3.84 (1 df, $p < 0.05$) were retained for the further multivariable analysis. Afterwards, these covariates could be kept only if removal of the covariates increased the OFV by >10.83 (1 df, $p < 0.001$). In addition, a reduction in inter-subject variability was also evaluated for a given parameter. The selection of the covariate model was further assessed as discussed above (see structural PK model section).

2.5. Monte Carlo Simulations

The final population PK model was used to simulate the omeprazole concentration profiles at a single dose of 20 mg omeprazole before and 7 days after surgery and at a repeated dose 1 month after surgery. The Friedman nonparametric paired test was used to compare the values of T_{max} (time to maximum plasma concentration) and C_{max} (maximum plasma concentration) obtained during the three visits. These secondary parameters on two occasions (visit 2 vs. visit 1 and visit 3 vs. visit 1) were then compared using the Wilcoxon nonparametric paired test.

3. Results

3.1. Subjects and Data

In total, 62 patients with obesity were included pre-surgery, with a median BMI of 40.3 kg/m^2 (range 30–72.8 kg/m^2). Of the 62 patients tested at visit 1, 41 completed the PK study 7 days post-LSG (visit 2), and 20 completed the PK study 1 month post-LSG (visit 3). Table 1 shows the demographic and clinical characteristics of the included patients during the three visits. DNA samples from 62 volunteers were genotyped, and we identified 26 normal metabolizers (NMs), 27 intermediate metabolizers (IMs), and 9 poor metabolizers (PMs) according to the CPIC guidelines. A total of 331 concentration–time points were obtained for the population PK analysis: 190 concentrations at visit 1; 101 concentrations at visit 2; 40 concentrations at visit 3.

Table 1. Demographic and clinical characteristics of study population.

Baseline Characteristics	Pre-Surgery (n = 62)	7 Days Post-LSG (n = 41)	1 Month Post-LSG (n = 20)
No. (%) of participants by sex			
Female	43 (69%)	29 (71%)	16 (80%)
Male	19 (31%)	12 (29%)	4 (20%)
No. (%) of participants by CYP2C19 genotype			
Normal metabolizers (NMs)	26 (42%)	17 (41.5%)	4 (20%)
Intermediate metabolizers (IMs)	27 (43.5%)	18 (44%)	12 (60%)
Poor metabolizers (PMs)	9 (14.5%)	6 (14.5%)	4 (20%)
Median (Q1~Q3) values for:			
Age (year)	31 (27~35)	28 (25~33)	28 (23~33)
Weight (kg)	110.8 (91~127)	114.6 (90.7~124.6)	* 96.2 (82.7~105.8)
Height (cm)	162.5 (158.6~167.5)	163 (158.5~169)	160.5 (158.1~166.4)
BMI (kg/m^2)	40.3 (35~46)	41.2 (34.6~45.2)	* 36.1 (31.7~39.5)
LBW (kg)	55.1 (48.9~69.6)	55.3 (47~68.5)	* 50.9 (46~54)
IBW (kg)	54.8 (50.9~60.6)	54.8 (50.8~63)	52.7 (50.5~58.3)
ABW (kg)	78.5 (68.8~89.2)	79.2 (65.5~84.6)	* 71.7 (64.4~76)
No. (%) of participants by liver function			
Normal liver function	27 (43.5%)	6 (14.6%)	7 (35%)
Mild liver dysfunction	35 (56.5%)	35 (85.4%)	13 (65%)

BMI, body mass index; LBW, lean body weight; IBW, ideal body weight; ABW, adjusted body weight. * $p < 0.001$ from a Wilcoxon nonparametric paired test (visit 3 vs. visit 1) in obese subjects who completed both visit 1 and visit 3 (n = 20).

3.2. Population PK Modeling

Based on the data, a one-compartment model with 12 transit absorption compartments and linear elimination was identified in which visits proved a significant covariate for MTT, and the CYP2C19 genotype and liver function exhibited a remarkable effect on CL/F. In addition, the data did not support estimates of inter-individual variability in Vd/F and setting the variance of this random effect to zero did not influence the OFV.

Implementation of the visits on MTT led to a 131.5 point ($p < 0.001$) reduction in OFV, and a shorter MTT was observed 7 days and 1 month post-LSG compared with preoperatively. No significant trend was found for visits and CL/F ($p = 0.075$), although omeprazole plasma concentrations reached a steady-state 1 month after surgery compared with a single omeprazole dose before surgery and 7 days post-LSG. However, IOV had a significant effect on CL/F, decreasing residual variability from 45.6% to 41.8%. Moreover, CYP2C19 IMs and PMs showed a lower CL/F relative to NMs (ΔOFV −21; $p < 0.001$). Individuals with mild liver dysfunction exhibited a lower CL/F than normal liver function (ΔOFV −5.35; $p = 0.021$). All three covariates fulfilled the criteria of the backward analysis ($p < 0.001$). No significant influence of other covariates (e.g., age, sex, TBW, LBW, ABW, IBW, and BMI) on any of the PK parameters was found.

The typical MTT population values at pre-surgery, 7 days post-LSG, and 1 month post-LSG were estimated at 1.9, 0.5, and 0.9 h, respectively. The typical CL/F population value of CYP2C19 NMs with normal liver function was 16.7 L/h. The CL/F population values of CYP2C19 IMs and PMs were 0.8 and 0.34 times that of NMs, respectively. The CL/F population values of subjects with mild liver dysfunction was 0.6 times that of normal liver function. The Vd/F was estimated at 22.1 L. The population PK parameter estimates in the final model are shown in Table 2.

Goodness-of-fit plots demonstrated that the final model appropriately described the observed data (Figure 1). Individual concentration–time curves of omeprazole at three visits were provided in the Supplementary Materials (Figure S1). The prediction-corrected VPC generally reflected a good agreement between the observations and simulations (Figure 2), indicating that the model adequately described the PK. In addition, all parameters estimates of final model fell near the median and within the 95% confidence interval of the SIR results (Table 2).

According to simulations, an important variability in T_{max} and C_{max} was observed before and after surgery (Table 3). LSG significantly affected the absorption rate of omeprazole, in which a reduced T_{max} and increased C_{max} were found 7 days and 1 month after surgery. However, omeprazole's CL/F and AUC (area under the plasma concentration–time curve) were not different prior to surgery and post-LSG.

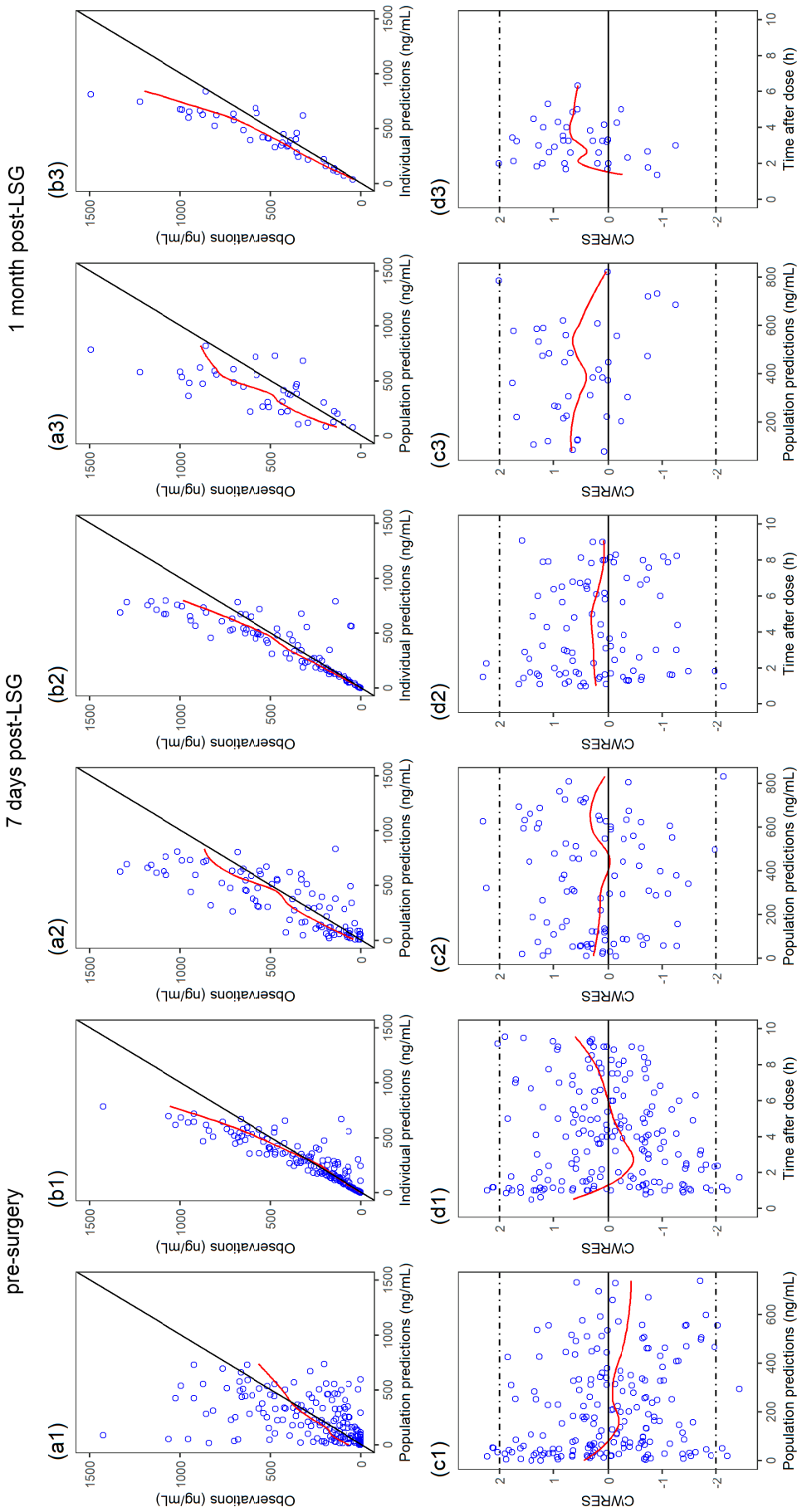

Figure 1. Goodness-of-fit plots for the final model at each visit: (**a1**,**a2**,**a3**) observations versus population predictions (PRED); (**b1**,**b2**,**b3**) observations versus individual predictions (IPRED); (**c1**,**c2**,**c3**) conditional weighted residuals (CWRES) versus PRED; (**d1**,**d2**,**d3**) CWRES versus time after dose.

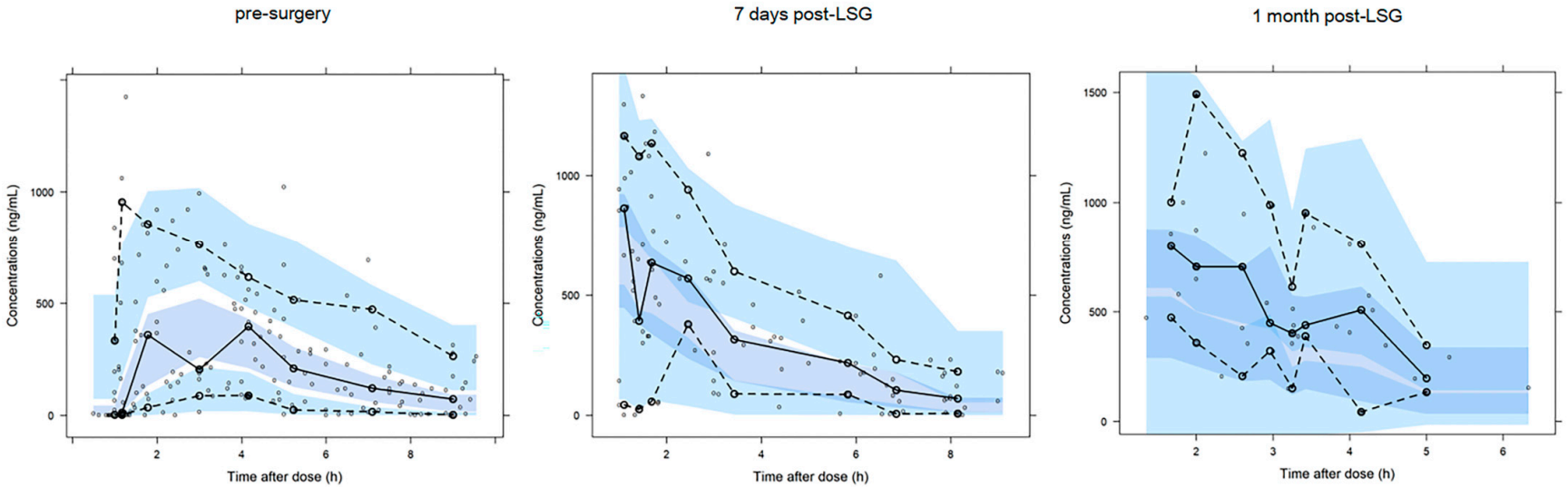

Figure 2. Prediction-corrected visual predictive check of the final model at each visit. Observed concentrations are indicated by black open circles, and the dotted and solid lines represent the 10th, 50th, and 90th percentiles of the observed data. The shaded areas represent 95% confidence intervals for the corresponding percentiles of simulated data.

Table 2. Population pharmacokinetic parameter estimates for the final model and the SIR results.

Parameter	Final Estimates	RSE (%)	SIR (Median)	RSE (%)	95% CI
Structural model					
MTT for visit 1 (h)	1.91	6	1.92	6	1.68–2.13
MTT ratio for visit 2: visit 1 (θ_1)	0.27	11.4	0.27	11.2	0.21–0.33
MTT ratio for visit 3: visit 1 (θ_2)	0.45	7.6	0.45	7.6	0.38–0.51
CL/F for normal metabolizers with normal liver function (L/h)	16.7	14.9	16.7	14.4	11.9–21.3
CL/F ratio for CYP2C19 intermediate metabolizers: normal metabolizers (θ_3)	0.8	12.4	0.8	12.3	0.6–0.98
CL/F ratio for CYP2C19 poor metabolizers: normal metabolizers (θ_4)	0.34	17.8	0.35	17.5	0.22–0.45
CL/F ratio for mild liver dysfunction: normal liver function (θ_5)	0.6	11.6	0.6	11.1	0.47–0.73
Vd/F (L)	22.1	5.5	22.2	5.4	19.7–24.5

Table 2. *Cont.*

Parameter	Final Estimates	RSE (%)	SIR (Median)	RSE (%)	95% CI
Interindividual variability					
ω^2 MTT	0.16	19.7	0.16	19.1	0.1–0.23
ω^2 CL/F	0.16	22.8	0.15	21.6	0.1–0.22
IOV on CL/F	0.05	39.3	0.05	38.7	0.01–0.09
Residual error					
σ^2 Proportional error	0.175	12.1	0.175	12.6	0.134–0.222

MTT, mean transit time; CL/F, apparent clearance; Vd/F, apparent volume of distribution; IOV, inter-occasion variability; SIR, sampling importance resampling; RSE, relative standard error; 95% CI, 95% confidence interval.

Table 3. Pharmacokinetic parameters for 20 mg omeprazole before and after LSG based on 1000 simulations.

	Pre-Surgery (N = 62)			7 Days Post-LSG (N = 41)			1 Month Post-LSG (N = 20)		
	CYP2C19 NMs	CYP2C19 IMs	CYP2C19 PMs	CYP2C19 NMs	CYP2C19 IMs	CYP2C19 PMs	CYP2C19 NMs	CYP2C19 IMs	CYP2C19 PMs
Normal liver function									
T_{max} (h)	2.3 (2~3)	2.3 (2~3.5)	2.7 (2~3.5)	* 0.8 (0.5~1)	* 0.8 (0.8~1)	* 0.8 (0.8~1)	* 1.3 (1~1.7)	* 1.3 (1~1.7)	* 1.3 (1~1.7)
C_{max} (ng/mL)	470 (386~540)	512 (427~588)	663 (595~717)	* 688 (634~738)	* 720 (660~763)	* 804 (771~830)	* 612 (547~674)	* 650 (583~709)	* 767 (720~809)
$AUC_{0\text{-}inf}$ (ng·h/mL)	1198 (876~1609)	1476 (1097~2061)	3483 (2537~4697)	1185 (881~1585)	1540 (1067~2039)	3470 (2619~4562)	1156 (894~1613)	1497 (1128~2054)	3520 (2560~4725)
CL/F (L/h)	16.7 (12.4~22.8)	13.5 (9.7~18.2)	5.7 (4.3~7.9)	16.9 (12.6~22.7)	13 (9.8~18.7)	5.8 (4.4~7.6)	17.3 (12.4~22.4)	13.3 (9.7~17.7)	5.7 (4.2~7.8)
Mild liver dysfunction									
T_{max} (h)	2.7 (2~3.5)	2.7 (2~3.5)	3 (2.3~3.5)	* 0.8 (0.8~1)	* 0.8 (0.8~1)	* 1 (0.8~1)	* 1.3 (1~1.7)	* 1.3 (1~1.7)	* 1.3 (1~1.7)
C_{max} (ng/mL)	571 (501~640)	606 (533~670)	740 (682~782)	* 752 (708~789)	* 779 (734~808)	* 840 (817~858)	* 699 (637~744)	* 725 (674~768)	* 835 (788~894)
$AUC_{0\text{-}inf}$ (ng·h/mL)	2032 (1484~2654)	2470 (1828~3242)	5948 (4376~8081)	1969 (1482~2654)	2530 (1882~3443)	5945 (4358~8258)	2027 (1519~2680)	2457 (1880~3345)	6019 (4399~8085)
CL/F (L/h)	9.8 (7.4~13.5)	8.1 (6.2~11)	3.4 (2.5~4.6)	10.2 (7.5~13.5)	7.9 (5.8~10.6)	3.4 (2.4~4.7)	9.9 (7.5~13.2)	8.1 (6~10.6)	3.3 (2.5~4.5)

Data are described as the median (Q1–Q3). NMs, normal metabolizers; IMs, intermediate metabolizers; PMs, poor metabolizers; T_{max}, time to maximum plasma concentration; C_{max}, maximum plasma concentration; $AUC_{0\text{-}inf}$, area under the plasma concentration–time curve from time zero to infinity; CL/F, apparent clearance. * $p < 0.001$ vs. pre-surgery.

4. Discussion

Herein, we report the first study to investigate the PK profile of omeprazole in patients with obesity undergoing LSG. Using population PK modeling, we found the omeprazole absorption rate increased 7 days and 1 month after LSG, but the CL/F and exposure were unchanged. In addition, the influence of CYP2C19 genotype and liver function on omeprazole CL/F were observed, which was consistent with previously published studies [20,21].

Oral dosage forms of omeprazole are usually formulated as enteric-coated capsules or tablets. Under normal physiological conditions, after passing through the acidic environment in the stomach, the enteric coating dissolves and omeprazole is absorbed. After sleeve gastrectomy surgery, the enteric coating will dissolve faster due to the increase in gastric pH caused by the decrease of acid-producing gastric parietal cells. In addition, given that the gastric volume is greatly reduced, gastric emptying is accelerated, and the residence time of omeprazole in the stomach is shorter; hence it will reach the small intestine sooner, and the absorption can be completed in a shorter time after surgery. This could be observed from a significantly shorter T_{max} postoperatively (Table 3 and Figure 3). As there was no statistical difference in BMI between visit 1 and visit 2, the higher C_{max} was presumably caused by the faster absorption of omeprazole after LSG. Our results were also similar to other drug PK studies performed in obese patients undergoing LSG, showing a reduced T_{max} and increased C_{max} in operated patients compared with nonoperated individuals [9,28].

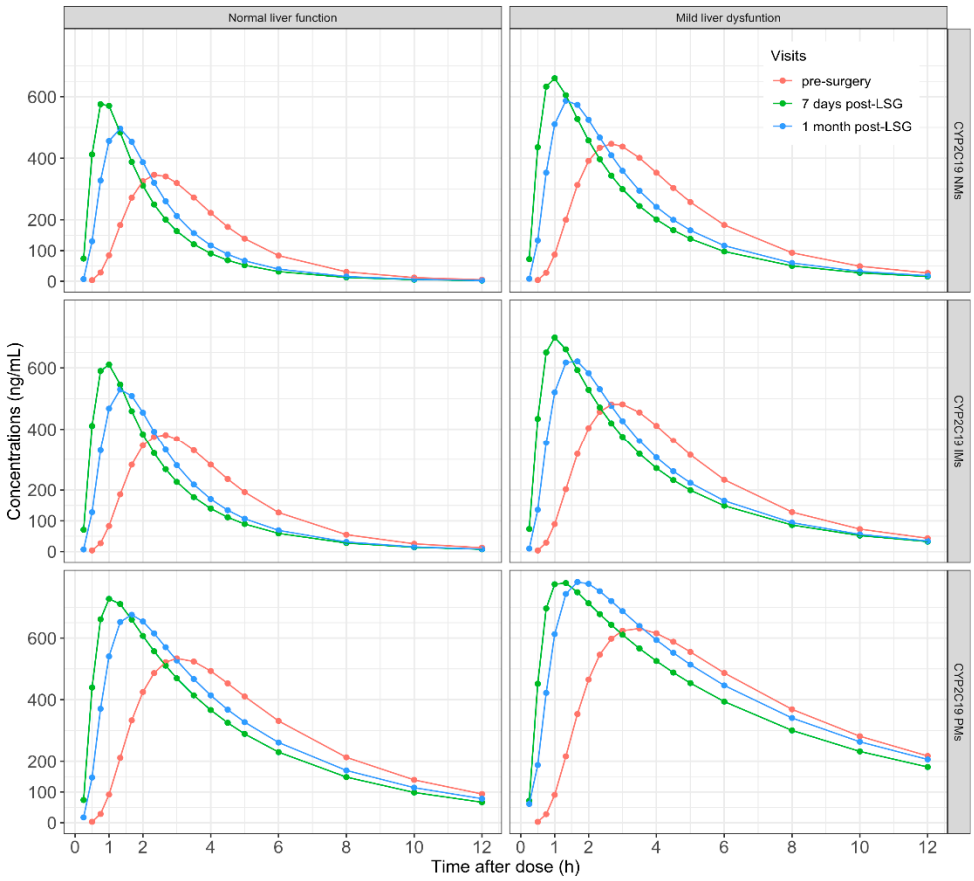

Figure 3. Mean concentration–time curves of omeprazole based on 1000 simulations stratified by liver function and CYP2C19 genotype in obese patients undergoing LSG.

No effect of weight-derived indicators (e.g., TBW, LBW, and BMI) and visits on CL/F were found. Our previous work confirmed that omeprazole CL/F was decreased in obese adults versus normal-weight adults and speculated that CYP2C19 metabolic enzyme activity might be decreased in obese individuals caused by a low-grade inflammation

state [20]. A recent research suggested that CYP2C19 activity is lower in patients with obesity versus nonobese controls and increased following RYGB-induced weight loss by measuring the plasma (3 h) 5-hydroxyomeprazole (5-OH-omeprazole)/omeprazole ratio [29]. These results indicated that the relationship between body weight and drug clearance is not always a simple allometric scaling in obese individuals. Interestingly, although we preformed PK sampling at a single dose before and 7 days after surgery and at repeat 1 month after surgery, we did not observe a difference in omeprazole CL/F between the three visits. Previous work suggested a significantly higher AUC and C_{max} after repeated omeprazole dosing in NMs but not in PMs [30,31]. This may provide some basis for explaining the unchanged clearance of omeprazole after single and multiple dosing in obese patients. As omeprazole is the inhibitor of the CYP2C19 metabolic enzyme, this leads to a decrease in first-pass effect in NMs due to auto-inhibition of CYP2C19 after repeated intake [31,32]. However, the CYP2C19 metabolic enzyme activity decreased in patients with obesity, and the auto-inhibition of CYP2C19 may be limited (similar to PMs); therefore, a comparable exposure was observed after single or repeated doses.

The CYP2C19 genotype was identified as a significant covariate for omeprazole CL/F, and a lower CL/F and higher AUC were observed in CYP2C19 IMs and PMs versus CYP2C19 NMs. Moreover, the CL/F was also found to decrease in patients with mild liver dysfunction. These results were reflected in PK parameters and concentration versus time curves obtained based on simulations (Table 3 and Figure 3). It has previously been established that the degree of acid inhibition by omeprazole was related to AUC [33,34]. However, there is no clear lower limit of efficacy at present. In the current analysis, the CL/F of omeprazole is not altered after short-term follow-up post-surgery. Furthermore, no heartburn, pantothenic acid, or other gastrointestinal symptoms were reported in patients followed up 1 month after surgery. Based on previous work, obese adults had a lower omeprazole CL/F and a higher AUC than normal adults [20]. Consequently, a 20 mg omeprazole dose daily may be adequate for obese patients undergoing LSG to relieve short-term gastrointestinal tract discomfort postoperatively.

There were some strengths and limitations in the current research. Firstly, our study had a relatively large study population, and the study design of repeated measures enabled obese subjects to act as their own control to minimize preoperative and postoperative variability. Secondly, omeprazole PK was not affected by interacting medication as we applied a specific exclusion criteria. A possible limitation was that the majority of obese patients included in the current analysis were female, but we did not observe a gender effect during model development, which was consistent with previous studies [35,36]. In addition, as the COVID-19 epidemic made it challenging to travel across provinces, quite a number of subjects could not participate in the PK follow up at visit 3. The changes in constituent ratio of CYP2C19 genotype at three visits may affect model stability; however, no statistical difference in constituent ratio of CYP2C19 genotype was observed among three visits using Fisher's exact test ($p = 0.471$). Moreover, the estimated clearance ratios (CYP2C19 IMs: NMs or CYP2C19 PMs: NMs) were also similar to those reported in the literature [31]. Furthermore, the PK profile of omeprazole at 6–8 months after LSG was not studied in patients underwent LSG due to the difficulty of follow-up during the epidemic period. Therefore, the effect of significant weight loss in the middle postoperative period on the PK of omeprazole is still unclear. Previous studies have reported that significant weight loss postoperatively can reverse the decrease in CYP3A4 activity in obese patients and restore the enzyme activity to the same level as that of normal-weight individuals [37]. In addition, a recent study reported that the CYP2C19 activity increases with weight loss in obese patients after RYGB treatment. Therefore, the clearance of the CYP2C19 substrate in LSG patients may return to normal after notable weight loss, which deserves further investigation. Overall, the current study is innovative and of clinical significance, providing a specific reference for the postoperative use of omeprazole in LSG patients.

5. Conclusions

This study adequately characterized the effect of LSG on omeprazole PK in patients with obesity using nonlinear mixed-effect modeling. Our study showed faster absorption of omeprazole after LSG, but the CL/F and exposure were not different 7 days and 1 month after LSG compared with pre-surgery. We propose the use of 20 mg omeprazole once daily to relieve short-term discomfort symptoms of gastrointestinal tract postoperatively.

Supplementary Materials: The following supporting information can be downloaded at: https://www.mdpi.com/article/10.3390/pharmaceutics14101986/s1, Figure S1: Individiual concentration-time curves of omeprazole in obese patients at three visits. Blue dots repesent observed concentrations, and grey and black lines repesent population predictions and individual predictions, respectively.

Author Contributions: Conceptualization, L.Z. and Q.P.; Data curation, K.C., P.L. and S.Z.; Formal analysis, K.C., P.L., S.Z., L.Z. and Q.P.; Funding acquisition, L.Z. and Q.P.; Investigation, P.L., Y.L., S.H. and Q.D.; Methodology, K.C. and Q.P.; Project administration, L.Z. and Q.P.; Resources, S.Z. and L.Z.; Software, Q.P.; Supervision, Q.P.; Validation, K.C., Y.L., N.Y., S.H. and Q.D.; Visualization, K.C. and N.Y.; Writing—original draft, K.C. and P.L.; Writing—review and editing, K.C., P.L., Y.L., L.Z. and Q.P. All authors have read and agreed to the published version of the manuscript.

Funding: This research was funded by the Natural Science Foundation of Hunan Province (No. 2022JJ30899), the Health Department Foundation of Hunan Province (No. 20201656), the Changsha Municipal Natural Science Foundation (No. kq2014269), and the Wisdom Accumulation and Talent Cultivation Project of the Third Xiangya Hospital of Central South University (No. YX202102).

Institutional Review Board Statement: The study was conducted in accordance with the Declaration of Helsinki and approved by the Institutional Review Board of The Third Xiangya Hospital of Central South University (protocol No. 21018, 18 April 2021) and registered at the China Clinical Trial Registration Center (www.chictr.org.cn; registration number: ChiCTR2100046578).

Informed Consent Statement: Informed consent was obtained from all subjects involved in the study. Written informed consent was obtained from the patient(s) to publish this paper.

Data Availability Statement: The data presented in this study are available upon request from the corresponding author. The data are not publicly available due to the presence of ethical reasons as per local guidelines.

Conflicts of Interest: The authors declare no conflict of interest.

References

1. WHO. Obesity and Overweight. Available online: https://www.who.int/health-topics/obesity (accessed on 28 June 2022).
2. Singh, A.K.; Singh, R. Pharmacotherapy in obesity: A systematic review and meta-analysis of randomized controlled trials of anti-obesity drugs. *Expert Rev. Clin. Pharmacol.* **2020**, *13*, 53–64. [CrossRef] [PubMed]
3. Haslam, D.W.; James, W.P.T. Obesity. *Lancet* **2005**, *366*, 1197–1209. [CrossRef]
4. Wadden, T.A.; Webb, V.L.; Moran, C.H.; Bailer, B.A. Lifestyle modification for obesity: New developments in diet, physical activity, and behavior therapy. *Circulation* **2012**, *125*, 1157–1170. [CrossRef] [PubMed]
5. Chang, S.-H.; Stoll, C.R.T.; Song, J.; Varela, J.E.; Eagon, C.J.; Colditz, G.A. The effectiveness and risks of bariatric surgery: An updated systematic review and meta-analysis, 2003–2012. *JAMA Surg.* **2014**, *149*, 275–287. [CrossRef]
6. Colquitt, J.L.; Pickett, K.; Loveman, E.; Frampton, G.K. Surgery for weight loss in adults. *Cochrane Database Syst. Rev.* **2014**, *2014*, CD003641. [CrossRef]
7. IFSO Registry. International Federation for the Surgery of Obesity and Metabolic Disorders. 2019. Available online: https://www.ifso.com/ifso-registry.php (accessed on 28 June 2022).
8. Wolfe, B.M.; Kvach, E.; Eckel, R.H. Treatment of Obesity: Weight Loss and Bariatric Surgery. *Circ. Res.* **2016**, *118*, 1844–1855. [CrossRef]
9. Porat, D.; Markovic, M.; Zur, M.; Fine-Shamir, N.; Azran, C.; Shaked, G.; Czeiger, D.; Vaynshtein, J.; Replyanski, I.; Sebbag, G.; et al. Increased Paracetamol Bioavailability after Sleeve Gastrectomy: A Crossover Pre- vs. Post-Operative Clinical Trial. *J. Clin. Med.* **2019**, *8*, 1949. [CrossRef]
10. Tan, Q.; Gao, Y.; Zhang, P.; Huo, Y.; Lu, Y.; Huang, W. Comparison of Outcomes in Patients with Obesity Between Two Administration Routes of Omeprazole After Laparoscopic Sleeve Gastrectomy: An Open-Label Randomized Clinical Trial. *Drug Des. Dev. Ther.* **2021**, *15*, 1569–1576. [CrossRef]

11. Collares-Pelizaro, R.V.A.; Santos, J.S.; Nonino, C.B.; Gaitani, C.M.; Salgado, W. Omeprazole Absorption and Fasting Gastrinemia after Roux-en-Y Gastric Bypass. *Obes. Surg.* **2017**, *27*, 2303–2307. [CrossRef]
12. Mitrov-Winkelmolen, L.; van Buul-Gast, M.-C.W.; Swank, D.J.; Overdiek, H.W.P.M.; Van Schaik, R.H.N.; Touw, D. The Effect of Roux-en-Y Gastric Bypass Surgery in Morbidly Obese Patients on Pharmacokinetics of (Acetyl)Salicylic Acid and Omeprazole: The ERY-PAO Study. *Obes. Surg.* **2016**, *26*, 2051–2058. [CrossRef]
13. Martínez-Ortega, A.J.; Olveira, G.; Pereira-Cunill, J.L.; Arraiza-Irigoyen, C.; García-Almeida, J.M.; Irles Rocamora, J.A.; Molina-Puerta, M.J.; Molina Soria, J.B.; Rabat-Restrepo, J.M.; Rebollo-Pérez, M.I.; et al. Recommendations Based on Evidence by the Andalusian Group for Nutrition Reflection and Investigation (GARIN) for the Pre- and Postoperative Management of Patients Undergoing Obesity Surgery. *Nutrients* **2020**, *12*, 2002. [CrossRef] [PubMed]
14. Savarino, V.; Marabotto, E.; Zentilin, P.; Furnari, M.; Bodini, G.; De Maria, C.; Pellegatta, G.; Coppo, C.; Savarino, E. Proton pump inhibitors: Use and misuse in the clinical setting. *Expert Rev. Clin. Pharmacol.* **2018**, *11*, 1123–1134. [CrossRef] [PubMed]
15. Strand, D.S.; Kim, D.; Peura, D.A. 25 Years of Proton Pump Inhibitors: A Comprehensive Review. *Gut Liver* **2017**, *11*, 27–37. [CrossRef]
16. Porat, D.; Vaynshtein, J.; Gibori, R.; Avramoff, O.; Shaked, G.; Dukhno, O.; Czeiger, D.; Sebbag, G.; Dahan, A. Stomach pH before vs. after different bariatric surgery procedures: Clinical implications for drug delivery. *Eur. J. Pharm. Biopharm.* **2021**, *160*, 152–157. [CrossRef]
17. Chen, K.; Lin, Y.; Luo, P.; Yang, N.; Yang, G.; Zhu, L.; Pei, Q. Effect of laparoscopic sleeve gastrectomy on drug pharmacokinetics. *Expert Rev. Clin. Pharmacol.* **2021**, *14*, 1481–1495. [CrossRef] [PubMed]
18. Melissas, J.; Leventi, A.; Klinaki, I.; Perisinakis, K.; Koukouraki, S.; de Bree, E.; Karkavitsas, N. Alterations of global gastrointestinal motility after sleeve gastrectomy: A prospective study. *Ann. Surg.* **2013**, *258*, 976–982. [CrossRef] [PubMed]
19. Shibata, S.I.; Chung, V.; Synold, T.W.; Longmate, J.A.; Suttle, A.B.; Ottesen, L.H.; Lenz, H.-J.; Kummar, S.; Harvey, R.D.; Hamilton, A.L.; et al. Phase I study of pazopanib in patients with advanced solid tumors and hepatic dysfunction: A National Cancer Institute Organ Dysfunction Working Group study. *Clin. Cancer Res.* **2013**, *19*, 3631–3639. [CrossRef]
20. Chen, K.; Luo, P.; Yang, G.; Zhu, S.; Deng, C.; Ding, J.; Lin, Y.; Zhu, L.; Pei, Q. Population pharmacokinetics of omeprazole in obese and normal-weight adults. *Expert Rev. Clin. Pharmacol.* **2022**, *15*, 461–471. [CrossRef]
21. Lima, J.J.; Thomas, C.D.; Barbarino, J.; Desta, Z.; Van Driest, S.L.; El Rouby, N.; Johnson, J.A.; Cavallari, L.H.; Shakhnovich, V.; Thacker, D.L.; et al. Clinical Pharmacogenetics Implementation Consortium (CPIC) Guideline for CYP2C19 and Proton Pump Inhibitor Dosing. *Clin. Pharmacol. Ther.* **2021**, *109*, 1417–1423. [CrossRef]
22. Wasmann, R.E.; Ter Heine, R.; van Dongen, E.P.; Burger, D.M.; Lempers, V.J.; Knibbe, C.A.J.; Brüggemann, R.J. Pharmacokinetics of Anidulafungin in Obese and Normal-Weight Adults. *Antimicrob. Agents Chemother.* **2018**, *62*, e00063-18. [CrossRef]
23. Dosne, A.G.; Bergstrand, M.; Harling, K.; Karlsson, M.O. Improving the estimation of parameter uncertainty distributions in nonlinear mixed effects models using sampling importance resampling. *J. Pharmacokinet. Pharmacodyn.* **2016**, *43*, 583–596. [CrossRef] [PubMed]
24. Savic, R.M.; Jonker, D.M.; Kerbusch, T.; Karlsson, M.O. Implementation of a transit compartment model for describing drug absorption in pharmacokinetic studies. *J. Pharmacokinet. Pharmacodyn.* **2007**, *34*, 711–726. [CrossRef] [PubMed]
25. Janmahasatian, S.; Duffull, S.B.; Ash, S.; Ward, L.C.; Byrne, N.M.; Green, B. Quantification of lean bodyweight. *Clin. Pharmacokinet.* **2005**, *44*, 1051–1065. [CrossRef] [PubMed]
26. McCarron, M.M.; Devine, B.J. Clinical pharmacy: Case studies: Case number 25 gentamicin therapy. *Drug Intell. Clin. Pharm.* **1974**, *8*, 650–655. [CrossRef]
27. Schwartz, S.N.; Pazin, G.J.; Lyon, J.A.; Ho, M.; Pasculle, A.W. A controlled investigation of the pharmacokinetics of gentamicin and tobramycin in obese subjects. *J. Infect. Dis.* **1978**, *138*, 499–505. [CrossRef]
28. Goday Arno, A.; Farré, M.; Rodríguez-Morató, J.; Ramon, J.M.; Pérez-Mañá, C.; Papaseit, E.; Civit, E.; Langohr, K.; Carbó, M.; Boix, D.B.; et al. Pharmacokinetics in Morbid Obesity: Influence of Two Bariatric Surgery Techniques on Paracetamol and Caffeine Metabolism. *Obes. Surg.* **2017**, *27*, 3194–3201. [CrossRef]
29. Kvitne, K.E.; Krogstad, V.; Wegler, C.; Johnson, L.K.; Kringen, M.K.; Hovd, M.H.; Hertel, J.K.; Heijer, M.; Sandbu, R.; Skovlund, E.; et al. Short- and long-term effects of body weight, calorie restriction and gastric bypass on CYP1A2, CYP2C19 and CYP2C9 activity. *Br. J. Clin. Pharmacol.* **2022**, *88*, 4121–4133. [CrossRef]
30. Wang, Y.; Zhang, H.; Meng, L.; Wang, M.; Yuan, H.; Ou, N.; Zhang, H.; Li, Z.; Shi, R. Influence of CYP2C19 on the relationship between pharmacokinetics and intragastric pH of omeprazole administered by successive intravenous infusions in Chinese healthy volunteers. *Eur. J. Clin. Pharmacol.* **2010**, *66*, 563–569. [CrossRef]
31. Zhang, H.-J.; Zhang, X.-H.; Liu, J.; Sun, L.-N.; Shen, Y.-W.; Zhou, C.; Zhang, H.-W.; Xie, L.-J.; Chen, J.; Liu, Y.; et al. Effects of genetic polymorphisms on the pharmacokinetics and pharmacodynamics of proton pump inhibitors. *Pharmacol. Res.* **2020**, *152*, 104606. [CrossRef]
32. Kaartinen, T.J.K.; Tornio, A.; Tapaninen, T.; Launiainen, T.; Isoherranen, N.; Niemi, M.; Backman, J.T. Effect of High-Dose Esomeprazole on CYP1A2, CYP2C19, and CYP3A4 Activities in Humans: Evidence for Substantial and Long-lasting Inhibition of CYP2C19. *Clin. Pharmacol. Ther.* **2020**, *108*, 1254–1264. [CrossRef]
33. Shirai, N.; Furuta, T.; Moriyama, Y.; Okochi, H.; Kobayashi, K.; Takashima, M.; Xiao, F.; Kosuge, K.; Nakagawa, K.; Hanai, H.; et al. Effects of CYP2C19 genotypic differences in the metabolism of omeprazole and rabeprazole on intragastric pH. Aliment. *Pharmacol. Ther.* **2001**, *15*, 1929–1937.

34. Hu, X.-P.; Xu, J.-M.; Hu, Y.-M.; Mei, Q.; Xu, X.-H. Effects of CYP2C19 genetic polymorphism on the pharmacokinetics and pharmacodynamics of omeprazole in Chinese people. *J. Clin. Pharm. Ther.* **2007**, *32*, 517–524. [CrossRef] [PubMed]
35. Marier, J.-F.; Dubuc, M.-C.; Drouin, E.; Alvarez, F.; Ducharme, M.P.; Brazier, J.-L. Pharmacokinetics of omeprazole in healthy adults and in children with gastroesophageal reflux disease. *Ther. Drug Monit.* **2004**, *26*, 3–8. [CrossRef] [PubMed]
36. Nagase, M.; Shimada, H.; Nii, M.; Ueda, S.; Higashimori, M.; Ichikawa, K.; Zhang, L.; Zhou, L.; Chen, Y.; Zhou, D.; et al. Population pharmacokinetic analysis of esomeprazole in Japanese subjects with various CYP2C19 phenotypes. *J. Clin. Pharm. Ther.* **2020**, *45*, 1030–1038. [CrossRef]
37. Rodríguez-Morató, J.; Goday, A.; Langohr, K.; Pujadas, M.; Civit, E.; Pérez-Mañá, C.; Papaseit, E.; Ramon, J.M.; Benaiges, D.; Castañer, O.; et al. Short- and medium-term impact of bariatric surgery on the activities of CYP2D6, CYP3A4, CYP2C9, and CYP1A2 in morbid obesity. *Sci. Rep.* **2019**, *9*, 20405. [CrossRef]

pharmaceutics

MDPI

Article

Pharmacokinetics of a Fixed-Dose Combination Product of Dapagliflozin and Linagliptin and Its Comparison with Co-Administration of Individual Tablets in Healthy Humans

Jin-Woo Park [1,2,3], Jong-Min Kim [1], Ji Hyeon Noh [1], Kyoung-Ah Kim [1], Hyewon Chung [4], EunJi Kim [5], Minja Kang [5] and Ji-Young Park [1,*]

[1] Department of Clinical Pharmacology and Toxicology, Korea University College of Medicine, Korea University Anam Hospital, Seoul 02841, Korea; parkzinu@korea.ac.kr (J.-W.P.); jmk157@korea.ac.kr (J.-M.K.); njh2535@korea.ac.kr (J.H.N.); kakim920@kumc.or.kr (K.-A.K.)
[2] Department of Neurology, Korea University Medical Center, Seoul 02841, Korea
[3] Division of Clinical Pharmacology, Department of Medicine, Vanderbilt University School of Medicine, Nashville, TN 37232, USA
[4] Department of Clinical Pharmacology and Toxicology, Korea University Guro Hospital, Seoul 08308, Korea; hyewonchung@korea.ac.kr
[5] HK Inno.N, Corporation, Seoul 04551, Korea; eunji.kim24@inno-n.com (E.K.); minja.kang@inno-n.com (M.K.)
* Correspondence: jypark21@korea.ac.kr; Tel.: +82-02-920-6288

Abstract: Dapagliflozin, a selective sodium–glucose co-transporter-2 inhibitor, and linagliptin, a competitive, reversible dipeptidyl peptidase-4 inhibitor, are commonly prescribed antidiabetic medications in general clinics. Since there are several merits to combining them in a fixed-dose combination product, this study investigated the pharmacokinetic equivalence between the individual component (IC) and fixed-combination drug product (FCDP) forms of dapagliflozin and linagliptin. A randomized, open-label, single-dose crossover study was conducted. All participants (n = 48) were randomly allocated to group A (period 1: ICs, period 2: FCDP) or group B (period 1: FCDP, period 2: ICs), and each group received either a single dose of IN-C009 (FCDP) or single doses of both dapagliflozin and linagliptin. There was no statistically significant difference found between the pharmacokinetic variables of FCDP and IC. The values of estimated geometric mean ratios and the 90% confidence interval for both maximum concentration and area under the plasma drug concentration–time curve were within the range of 0.8–1.25 for both dapagliflozin and linagliptin. The results of the clinical study demonstrated comparable pharmacokinetic characteristics between IC and FCDP forms of dapagliflozin and linagliptin. The combined use of dapagliflozin and linagliptin was safe and tolerable in both formulations.

Keywords: dapagliflozin; linagliptin; fixed-dose combination products; bioequivalence

Citation: Park, J.-W.; Kim, J.-M.; Noh, J.H.; Kim, K.-A.; Chung, H.; Kim, E.; Kang, M.; Park, J.-Y. Pharmacokinetics of a Fixed-Dose Combination Product of Dapagliflozin and Linagliptin and Its Comparison with Co-Administration of Individual Tablets in Healthy Humans. *Pharmaceutics* **2022**, *14*, 591. https://doi.org/10.3390/pharmaceutics14030591

Academic Editors: Barna Vasarhelyi and Gellért Balázs Karvaly

Received: 28 January 2022
Accepted: 3 March 2022
Published: 8 March 2022

1. Introduction

Dapagliflozin and linagliptin are commonly used medications for the treatment of type-2 diabetes mellitus (T2DM) [1–3]. Dapagliflozin acts by selectively inhibiting sodium–glucose co-transporter-2 (SGLT-2) protein in the kidneys, thereby reducing renal glucose reabsorption and increasing the glucose excretion via urine [3,4]. Dapagliflozin is absorbed rapidly and reaches a maximum concentration (C_{max}) within 2 h. It has a half-life ($t_{1/2}$) of 8.1–12.2 h, and approximately 65% of dapagliflozin is metabolized by uridine diphosphate glucuronosyltransferase 1A9 [1,5]. Due to its insulin-independent effects, dapagliflozin is used in combination with several other classes of antidiabetic medications [6–9].

Linagliptin is a competitive, reversible dipeptidyl peptidase (DPP)-4 inhibitor that increases the levels of active glucagon-like peptide-1 (GLP-1) [10]. GLP-1, an incretin hormone secreted by the small intestine, regulates blood glucose levels by stimulating

glucose-dependent postprandial insulin secretion and inhibiting glucagon secretion. Because it is rapidly degraded by DPP-4, the use of DPP-4 inhibitors eventually increases the GLP-1 levels and prevents high blood glucose levels [11–13]. The C_{max} of linagliptin is reached within approximately 90 min, and a steady-state level is reached within 4 days at a therapeutic dose (5 mg) [12]. Linagliptin is a known substrate for the cytochrome P450 3A4 enzyme and P-glycoprotein (P-gp) in humans, and its oral bioavailability is approximately 30% [12].

The combined use of dapagliflozin and linagliptin for managing T2DM is reasonable and attractive because of their different but complementary mechanisms of action and separate paths of degradation (i.e., metabolism), thereby avoiding possible drug interactions, which is important for harnessing drug pharmacodynamics and reducing the risk of unexpected adverse events [14–17]. Compared with a DPP-4 inhibitor, the combined use of SGLT-2 inhibitor and DPP-4 inhibitor is significantly associated with a decrease in glycemic control, body weight, and systolic blood pressure, and their advantages have already been proven for both initial combination and stepwise approaches [14,15]. However, the FCDP for dapagliflozin and linagliptin have not yet been tested.

Therefore, this study aimed to evaluate the pharmacokinetics and safety of the fixed-combination drug products (FCDPs) of dapagliflozin (10 mg) and linagliptin (5 mg), which were developed to reduce the burden of requiring multiple tablets and thus increasing compliance in healthy participants [18].

2. Materials and Methods

Sixty-three healthy male volunteers (age, 19–45 years; body weight > 50 kg) agreed to participate in the study and signed a written informed consent form. Only male participants were recruited to avoid the potential risk of pregnancy [19]. The participants were considered healthy after a detailed physical examination by physicians involving 12-lead electrocardiographs (ECG), vital sign assessments, and laboratory evaluations, including blood chemistry, hematology, and urinalysis. The exclusion criteria were a history or evidence of hepatic, renal, gastrointestinal, or hematological abnormalities; hepatitis B, hepatitis C, syphilis, or HIV infection; a history of hypersensitivity to dapagliflozin and/or linagliptin; clinically significant allergic disease; alcohol or drug abuse; heavy smoking (more than 10 cigarettes per day); and use of any medication within 30 days before the start of the study that may have affected the study results. The study protocol was approved (IRB No.2019AN0538, clinicaltrial.gov; NCT05066516) by the Institutional Review Board of Anam Hospital, Korea University Medical Center (Seoul, Korea), and all procedures were conducted following the principles described in the Declaration of Helsinki and Good Clinical Practice guidelines.

This study was conducted as a randomized, open-label, single-dose crossover study. All participants were randomly allocated to group A (period 1: individual components (ICs), period 2: FCDP) or group B (period 1: FCDP, period 2: ICs). Each group was administered a single dose of IN-C009 (FCDP, dapagliflozin 10 mg/linagliptin 5 mg) (HK Inno.N, Corporation, Seoul, Korea) or co-administered a single dose of dapagliflozin (Forxiga® 10 mg, AstraZeneca, Cambridge, UK) and linagliptin (Trajenta® 5 mg, Beringer-Ingelheim, Ingelheim, Germany) after at least 10 h of overnight fasting. After the 28-day washout period, the participants received the other treatment (group A: IN-C009; group B: dapagliflozin and linagliptin). All medications were biopharmaceutical classification system (BCS) III drugs with high solubility and low permeability. The in vitro dissolution behavior of the formulation was tested in four different pH conditions (pH 1.2, pH 4.0, pH 6.8, and aqueous water) and the results were comparable in both ICs and FCDP (greater than 80% dissolution in 30 min). For FCDP, microcrystalline cellulose and copovidone were used as major excipients. The doses of dapagliflozin and linagliptin used in this study were commercially used and the currently recommended dose for the control of T2DM was used. Previous studies have demonstrated no possible food effect on linagliptin and dapagliflozin; therefore, the food effect was not assessed in this study [20,21].

On day 1 (the day of each drug administration), serial blood samples were drawn immediately before (0 h) and 0.25, 0.5, 0.75, 1, 1.5, 2, 2.5, 3, 4, 6, 8, 12, 24, 48, and 72 h after each dosing to assess the pharmacokinetics of each drug. The collected samples were centrifuged (at 1977× *g*, 4 °C) for 15 min, and the extracted plasma samples were stored frozen at −60 °C until they were analyzed. Plasma dapagliflozin and linagliptin concentrations were determined using high-performance liquid chromatography with tandem mass spectroscopy (LC–MS/MS) described elsewhere, with minor modifications, following the Korea Ministry of Food and Drug Safety and US Food and Drug Administration guidelines [22,23].

For dapagliflozin analysis, 100 μL plasma was added to a glass tube containing an internal standard (10 μL of 1 mg/mL dapagliflozin-d_5) and 1 mL methanol. The samples were vigorously vortexed and centrifuged at 10,770× *g* for 3 min. Next, 100 μL of the upper layer was transferred to a polypropylene tube with 10 μL of internal standard (dapagliflozin-d_5, Toronto Research, Toronto, ON, Canada) and 300 μL of acetonitrile. After vigorous vortexing and centrifugation at 2191× *g* for 1 min, 200 μL of the upper layer was transferred to another polypropylene tube with 200 μL of ammonium acetate (0.1%, *w*/*v*). A 20 μL aliquot of the solution was finally injected into the LC–MS/MS system; 0.1% ammonium acetate and methanol were used for the mobile phase. The gradient elution mode was applied (methanol proportion ranging between 57.5% and 90% in 5 min) with a constant flow rate of 0.4 mL/min. Dapagliflozin was quantified using the multiple reaction monitoring (MRM) mode. The produced transitions were m/z 426.47 → 166.84 for dapagliflozin and m/z 431.50 → 166.85 for dapagliflozin-d_5. The linear function of dapagliflozin concentration ranged from 1 to 400 ng/mL with regression correlation coefficients of the calibration curves (R) greater than 0.999. The intra-day and inter-day CV values were below 15%. The lower limit of quantification (LLOQ) using this method was 1 ng/mL.

Linagliptin-^{13}C-d_3 (TLC Pharmaceutical Standards Ltd., Newmarket, ON, Canada) was used as the internal standard, and 100 μL of plasma was added to a glass tube containing the internal standard (10 μL of 1 mg/mL linagliptin-^{13}C-d_3) and 1 mL methanol. The samples were vigorously vortexed and centrifuged at 10,770× *g* for 3 min. Next, 100 μL of the upper layer was transferred to a polypropylene tube with 10 μL of the internal standard and 400 μL of methanol. After vigorous vortexing and centrifugation at 2191× *g* for 1 min, 100 μL of the upper layer was transferred to another polypropylene tube containing 300 μL of formic acid in distilled water (0.1%, *w*/*v*). A 20 μL aliquot of the solution was finally injected into the LC–MS/MS system; 0.1% ammonium formate in distilled water and acetonitrile was used as the mobile phase. The gradient elution mode was applied (acetonitrile percentage ranging between 25% and 90% in 4 min) with a constant flow rate of 0.3 mL/min. Linagliptin was quantified using MRM mode. The produced transitions were m/z 473.18 → 420.20 for linagliptin and m/z 477.20 → 420.20 for linagliptin-^{13}C-d_3. A linear function of linagliptin concentration ranged from 0.04 to 25 ng/mL with regression correlation coefficients of the calibration curves (R) greater than 0.999. The intra-day and inter-day CV values were <15%. The LLOQ with this method was 0.04 ng/mL.

The pharmacokinetic variables of dapagliflozin and linagliptin were estimated by non-compartmental methods using Phoneix® Winnolin® software (version 8.1, Certara™, Princeton, NJ, USA). The variables included were peak plasma concentration (C_{max}), area under the plasma drug concentration–time curve (AUC), time to maximal concentration, terminal elimination half-life ($t_{1/2}$), and oral clearance (CL/F). The AUC from time zero to the last measurable concentration (AUC_{last}) was obtained using the trapezoidal rule and AUC from time zero to infinity (AUC_{inf}) was calculated as $AUC_{last} + C_t/k_e$ (C_t, the last plasma concentration measured; k_e, the elimination rate constant).

SAS statistical software (version 9.4, SAS Institute, Cary, NC, USA) was used for statistical analyses. Mixed-effects models were used to compare pharmacokinetic variables, using treatment, period, and sequence as fixed effects and sequence-nested subjects as

random effects. Point estimates of GMRs and two-sided 90% CIs were calculated. The 90% CIs of GMR between 0.8 and 1.25 after comparing the log-transformed data of FCDP and ICs were considered equivalent according to the US Food and Drug Administration guidelines [24]. The safety and tolerability were assessed by vital signs, physical examinations, laboratory tests (hematology, biochemistry, and urinalysis), and 12-lead ECGs were assessed during the study period. Adverse events (AEs) were monitored based on the participants' self-reporting and general physical examinations.

3. Results

Forty-eight healthy male participants were enrolled in this study. The demographic characteristics of the study participants are summarized in Table 1. The mean age and weight of the participants were 27.3 years and 73.9 kg, respectively. Two participants dropped out due to personal reasons, and a total of 46 participants completed the study. No serious adverse events or clinically significant changes were observed through the safety parameters during the study period. Only one adverse event was reported and resolved spontaneously (myalgia).

Table 1. Baseline demographic characteristics.

Parameters	Mean ± SD	Min	Max	Median
Age (years)	27.3 ± 5.8	19	45	26
Weight (kg)	73.9 ± 10.2	53.5	99.7	72.6
Height (cm)	174.7 ± 5.2	161	185	175
BMI (kg/m^2)	24.2 ± 2.9	18.3	29.8	25.1

The mean plasma concentration versus time profile for dapagliflozin and linagliptin (both ICs and FCDP) are presented in Figure 1.

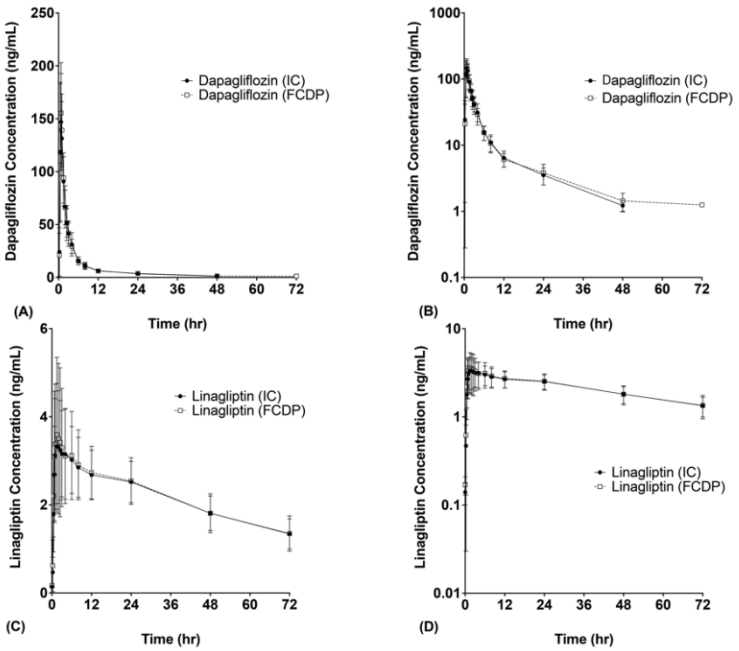

Figure 1. Mean plasma concentration–time profiles of IC (individual component) and FCDP (fixed-combination drug product) forms of dapagliflozin (**A**,**B**) and linagliptin (**C**,**D**). Linear plot, (**A**,**C**); semi-log transformed plot, (**B**,**D**) for *y*-axis.

When we compared the pharmacokinetic variables of dapagliflozin and linagliptin in different formulations, no statistically significant differences were found (Tables 2 and 3).

Table 2. Pharmacokinetic parameters of dapagliflozin in different formulations.

	IC	**FCDP**
$t_{1/2}$ (h)	11.34 ± 3.39	12.76 ± 3.84
C_{max} (ng/mL)	161.32 ± 42.05	167.59 ± 42.09
t_{max} (h)	0.75 (0.5–4)	0.75 (0.5–2.5)
AUC_{last} (ng·h/mL)	455.65 ± 92.84	465.76 ± 99.29
AUC_{inf} (ng·h/mL)	500.34 ± 93.93	516.46 ± 98.28
CL/F (L/h)	20.67 ± 3.89	20.01 ± 3.6

Notes: All values are expressed as the mean ± SD, except for t_{max}, which is shown as the median (range). Abbreviations: IC, individual component; FCDP, fixed-combination drug product; $t_{1/2}$, half-life; C_{max}, peak plasma concentration; t_{max}, time to C_{max}; AUC_{last}, area under the plasma concentration–time curve from 0 to the time of the last measurable concentration (72 h); AUC_{inf}, area under the plasma concentration–time curve from 0 to infinity; $t_{1/2}$, elimination half-life; CL/F, oral clearance.

Table 3. Pharmacokinetic variables of linagliptin in different formulations.

	IC	**FCDP**
$t_{1/2}$ (h)	54.94 ± 13.6	54.29 ± 12.26
C_{max} (ng/mL)	3.95 ± 1.42	4.2 ± 2.01
t_{max} (h)	2.5 (0.75–24)	1.5 (0.5–12)
AUC_{last} (ng·h/mL)	155.35 ± 30.35	157.37 ± 35.9
AUC_{inf} (ng·h/mL)	265.55 ± 78.74	267.97 ± 88.03
CL/F (L/h)	40.44 ± 10.50	40.81 ± 11.74

Notes: All values are expressed as the mean ± SD, except for t_{max}, which is shown as the median (range). Abbreviations: IC, individual component; FCDP, fixed-combination drug product; $t_{1/2}$, half-life; C_{max}, peak plasma concentration; t_{max}, time to C_{max}; AUC_{last}, area under the plasma concentration–time curve from 0 to the time of the last measurable concentration (72 h); AUC_{inf}, area under the plasma concentration–time curve from 0 to infinity; $t_{1/2}$, elimination half-life; CL/F, oral clearance.

The mean C_{max} values for dapagliflozin were 161.32 ng/mL (IC) and 167.59 ng/mL (FCDP) and for linagliptin, 3.95 ng/mL (IC) and 4.2 ng/mL (FCDP). The mean area under the curve $(AUC)_{last}$ values were also comparable for both dapagliflozin (IC: 455.65 ng·h/mL, FCDP: 465.76 ng·h/mL) and linagliptin (IC: 155.35 ng·h/mL, FCDP: 157.37 ng·h/mL). The estimation values of geometric mean ratios (GMRs) and 90% confidence interval (CI) for both C_{max} and AUCs were within the range of 0.8–1.25 for both dapagliflozin and linagliptin, indicating that FCDP and IC tablets are bioequivalent (Table 4). Individual comparisons of the pharmacokinetic parameters are presented in Figure 2. The intra-participant coefficient of variation (CV) (%) for dapagliflozin was 20.49% for C_{max} and 7.91% for AUC_{last}, and 27.58% and 7.96% for linagliptin, respectively.

Table 4. Point estimates and 90% CIs for log-transformed pharmacokinetic parameters (C_{max}, AUC_{last}, AUC_{inf}) of dapagliflozin and linagliptin IC vs. FCDP tablets.

Drugs	Variable	GMR (90% CI)	Intra-Participant CV%
Dapagliflozin	C_{max}	1.0413 (0.9554–1.1349)	20.49
	AUC_{last}	1.0219 (0.9885–1.0564)	7.91
	AUC_{inf}	1.0324 (1.0010–1.0648)	7.35
Linagliptin	C_{max}	1.0265 (0.9141–1.1526)	27.58
	AUC_{last}	1.0062 (0.9731–1.0404)	7.96
	AUC_{inf}	0.9996 (0.9477–1.0542)	12.67

Abbreviations: IC, individual component; FCDP, fixed-combination drug product; GMR, geometric mean ratio; CI, confidence interval; C_{max}, peak plasma concentration; AUC_{last}, area under the plasma concentration–time curve from 0 to 72 h; AUC_{inf}, area under the plasma concentration–time curve from 0 to infinity; CV, coefficient of variation.

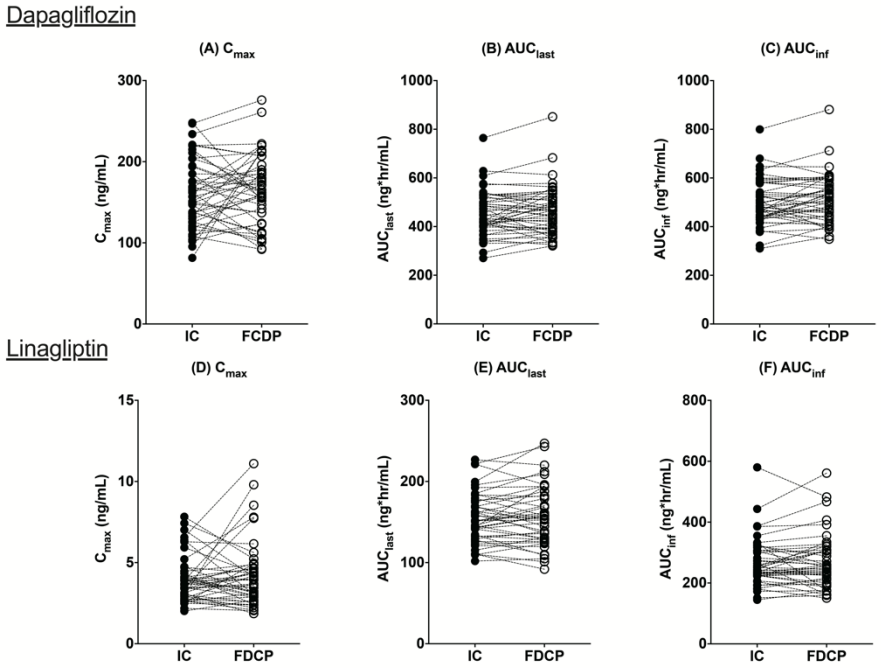

Figure 2. The comparisons of individual C_{max}, AUC_{last}, and AUC_{inf} of dapagliflozin (**A**–**C**) and linagliptin (**D**–**F**) in IC (individual component) and FCDP (fixed-combination drug product).

4. Discussion

The combination treatment using dapagliflozin and linagliptin is reasonable considering their complementary effects due to the different mechanisms of action, different metabolism, and relatively fewer adverse events, including hypoglycemia [14,25,26]. Although dapagliflozin and linagliptin are substrates of P-gp transporter, several clinical studies have already demonstrated that a combination of SGLT-2 inhibitors and DPP-4 inhibitors did not show any significant drug–drug interactions (DDI) [17,27,28]. Assuming that linagliptin and dapagliflozin have similar chemical structures, the possibility of DDI via P-gp may not be significant. Additionally, the Km of P-gp associated linagliptin transport is 187 μM and it does not inhibit P-gp at the therapeutic levels [29]. In vitro studies have shown that dapagliflozin is a weak substrate but not an inhibitor of P-gp [30] and its interaction with other P-gp substrates, including linagliptin, has not yet been reported.

A recent study suggested that dapagliflozin may have a better outcome in reducing heart failure in T2DM than empagliflozin (4.9 person-years in dapagliflozin vs. 9.0 person-years in empagliflozin) [31]. Both dapagliflozin and empagliflozin have favorable effects on heart failure; however, dapagliflozin is characterized by a longer pharmacological effect

and lower SGLT2:SGLT1 receptor selectivity (i.e., higher selectivity of SGLT1 receptors, thereby reducing postprandial blood glucose variations) than empagliflozin [31,32]. Among the DPP-4 inhibitors, linagliptin has a relatively longer half-life and higher potency of DPP-4 inhibition (approximately 90%), whereas saxagliptin has a shorter half-life (parent: 2.5 h, metabolite: 3.1 h) and lower inhibitory effect on DPP-4 (approximately 80%) [27]. Linagliptin also has an advantage over other DPP-4 inhibitors in diabetic patients with renal impairment (kidney excretion: 5%) [33–36]. Therefore, the development of FCDP for dapagliflozin and linagliptin is likely to have many advantages in the clinical management of uncontrolled T2DM.

The results of this study showed that the pharmacokinetic profiles after administration of individual dapagliflozin and linagliptin tablets were comparable to the FCDP form. In other words, the systemic exposure to IC and FCDP forms of dapagliflozin and linagliptin were similar in terms of C_{max} and AUCs. Both treatments were well-tolerated without significant adverse events and showed acceptable intra-subject variability [37]. The observed C_{max} values for dapagliflozin were 161.32 ng/mL (IC) and 167.59 ng/mL (FCDP), which were reached at 0.75 h for both, suggesting similar absorption profiles for dapagliflozin in the two formulations. The extent of absorption (i.e., AUC) too was very similar for both formulations (IC: 455.65 ng·h/mL, FCDP: 465.76 ng·h/mL). Similar results were also obtained for linagliptin (C_{max}: 3.95 ng/mL in IC and 4.2 ng/mL in FCDP, AUC_{last}: 155.35 ng·h/mL in IC and 157.37 ng·h/mL in FCDP). These results indicate the successful manufacture of the FCDP form of dapagliflozin and linagliptin combined [38].

FCDP is defined as a combination of more than two active chemicals in a single pharmaceutical administration [24,38]. The advantage of FCDP is mainly cost-effectiveness and increasing compliance by reducing the number of total medications administered at once [39]. Inappropriately manufactured FCDPs can result in reduced effectiveness or enhanced toxicity in routine clinical practice [40]. Although this study did not contain pharmacodynamic data, including blood glucose levels or HbA1c, it is believed that this FCDP should be generally comparable to its IC forms, considering that pharmacodynamic results generally correlate with pharmacokinetic variables and there were no significant adverse events related to the medication [41]. Indeed, the GMRs of the log-transformed ratio for dapagliflozin were 1.0413 (0.9554–1.1349) for C_{max} and 1.0219 (0.9885–1.0564) for AUC_{last}; those for linagliptin were 1.0265 (0.9141–1.1526) and 1.0062 (0.9731–1.0404), respectively, which were within the predefined bioequivalence range. This showed that ICs and FCDP exhibited comparable pharmacokinetic characteristics [24].

5. Conclusions

The results of this clinical study demonstrated similar pharmacokinetic characteristics between IC and FCDP forms of dapagliflozin and linagliptin at commercially used dosages of 10 mg and 5 mg, respectively. These results met the pharmacokinetic bioequivalence criteria. The combination of dapagliflozin and linagliptin was safe and tolerable in both formulations.

Author Contributions: Conceptualization, J.-Y.P. and J.-W.P.; methodology, K.-A.K.; software, J.-Y.P.: validation, E.K. and M.K.; formal analysis, J.-Y.P. and J.-W.P.; investigation, E.K. and M.K.; resources, K.-A.K.; data curation, J.-Y.P.; writing—original draft preparation, J.-W.P.; writing—review and editing, J.-Y.P., H.C., J.-M.K., E.K., M.K. and J.H.N.; visualization, J.-W.P.; supervision, J.-Y.P.; project administration, K.-A.K. All authors have read and agreed to the published version of the manuscript.

Funding: This study (study No. IN_DLC_101) was sponsored by HK Inno.N, Corporation, Seoul, Korea.

Institutional Review Board Statement: The study protocol was approved (IRB No.2019AN0538, 23 December 2019) by the Institutional Review Board of Anam Hospital, Korea University Medical Center (Seoul, Korea).

Informed Consent Statement: Informed consent was obtained from all participants involved in the study.

Data Availability Statement: The data presented in this study are available upon reasonable request from the corresponding author. The data are not publicly available because of privacy concerns.

Conflicts of Interest: E.K. and M.K. are employees of HK Inno.N, Corporation. The authors have no conflict of interest to declare.

References

1. Dhillon, S. Dapagliflozin: A Review in type 2 Diabetes. *Drugs* **2019**, *79*, 1135–1146. [CrossRef] [PubMed]
2. Jabbour, S. Durability of Response to Dapagliflozin: A Review of Long-Term Efficacy and Safety. *Curr. Med. Res. Opin.* **2017**, *33*, 1685–1696. [CrossRef] [PubMed]
3. Saleem, F. Dapagliflozin: Cardiovascular Safety and Benefits in Type 2 Diabetes Mellitus. *Cureus* **2017**, *9*, e1751. [CrossRef] [PubMed]
4. Heerspink, H.J.; Perkins, B.A.; Fitchett, D.H.; Husain, M.; Cherney, D.Z. Sodium Glucose Cotransporter 2 Inhibitors in the Treatment of Diabetes Mellitus: Cardiovascular and Kidney Effects, Potential Mechanisms, and Clinical Applications. *Circulation* **2016**, *134*, 752–772. [CrossRef]
5. Garcia-Ropero, A.; Badimon, J.J.; Santos-Gallego, C.G. The Pharmacokinetics and Pharmacodynamics of SGLT2 Inhibitors for Type 2 Diabetes Mellitus: The Latest Developments. *Expert. Opin. Drug Metab. Toxicol.* **2018**, *14*, 1287–1302. [CrossRef]
6. Coppenrath, V.A.; Hydery, T. Dapagliflozin/Saxagliptin Fixed-Dose Tablets: A New Sodium-Glucose Cotransporter 2 and Dipeptidyl Peptidase 4 Combination for the Treatment of Type 2 Diabetes. *Ann. Pharmacother.* **2018**, *52*, 78–85. [CrossRef]
7. Garnock-Jones, K.P. Saxagliptin/Dapagliflozin: A Review in Type 2 Diabetes Mellitus. *Drugs* **2017**, *77*, 319–330. [CrossRef]
8. Scheen, A.J. Dapagliflozin and Saxagliptin Tablets for Adults with type 2 Diabetes. *Expert. Rev. Clin. Pharmacol.* **2017**, *10*, 1303–1316. [CrossRef]
9. Yu, H.; Woo, V.C. Emerging Use of Combination Therapies for the Management of type 2 Diabetes—Focus on Saxagliptin and Dapagliflozin. *Diabetes Metab. Syndr. Obes.* **2017**, *10*, 317–332. [CrossRef]
10. Takayanagi, R.; Uchida, T.; Kimura, K.; Yamada, Y. Evaluation of Drug Efficacy of DPP-4 Inhibitors Based on Theoretical Analysis with Pharmacokinetics and Pharmacodynamics. *Biopharm. Drug Dispos.* **2017**, *38*, 273–279. [CrossRef]
11. Kanasaki, K. The Role of Renal Dipeptidyl Peptidase-4 in Kidney Disease: Renal Effects of Dipeptidyl Peptidase-4 Inhibitors with a Focus on Linagliptin. *Clin. Sci.* **2018**, *132*, 489–507. [CrossRef] [PubMed]
12. Ceriello, A.; Inagaki, N. Pharmacokinetic and Pharmacodynamic Evaluation of Linagliptin for the Treatment of Type 2 Diabetes Mellitus, with Consideration of Asian Patient Populations. *J. Diabetes Investig.* **2017**, *8*, 19–28. [CrossRef] [PubMed]
13. Sarashina, A.; Chiba, K.; Tatami, S.; Kato, Y. Physiologically Based Pharmacokinetic Model of the DPP-4 Inhibitor Linagliptin to Describe Its Nonlinear Pharmacokinetics in Humans. *J. Pharm. Sci.* **2020**, *109*, 2336–2344. [CrossRef] [PubMed]
14. Scheen, A.J. DPP-4 Inhibitor plus SGLT-2 Inhibitor as Combination Therapy for type 2 Diabetes: From Rationale to Clinical Aspects. *Expert. Opin. Drug Metab. Toxicol.* **2016**, *12*, 1407–1417. [CrossRef] [PubMed]
15. Molina-Vega, M.; Muñoz-Garach, A.; Fernández-García, J.C.; Tinahones, F.J. The Safety of DPP-4 Inhibitor and SGLT2 Inhibitor Combination Therapies. *Expert. Opin. Drug Saf.* **2018**, *17*, 815–824. [CrossRef]
16. Zou, H.; Zhou, B.; Xu, G. SGLT2 Inhibitors: A Novel Choice for the Combination Therapy in Diabetic Kidney Disease. *Cardiovasc. Diabetol.* **2017**, *16*, 65. [CrossRef]
17. Gu, N.; Park, S.I.; Chung, H.; Jin, X.; Lee, S.; Kim, T.E. Possibility of Pharmacokinetic Drug Interaction between a DPP-4 Inhibitor and a SGLT2 Inhibitor. *Transl. Clin. Pharmacol.* **2020**, *28*, 17–33. [CrossRef]
18. Bangalore, S.; Kamalakkannan, G.; Parkar, S.; Messerli, F.H. Fixed-Dose Combinations Improve Medication Compliance: A Meta-Analysis. *Am. J. Med.* **2007**, *120*, 713–719. [CrossRef]
19. Park, J.W.; Kim, K.A.; Choi, Y.J.; Yoon, S.H.; Park, J.Y. Effect of Glimepiride on the Pharmacokinetics of Teneligliptin in Healthy Korean Subjects. *J. Clin. Pharm. Ther.* **2019**, *44*, 720–725. [CrossRef]
20. Graefe-Mody, U.; Giessmann, T.; Ring, A.; Iovino, M.; Woerle, H.J. A randomized, open-label, crossover study evaluating the effect of food on the relative bioavailability of linagliptin in healthy subjects. *Clin. Ther.* **2011**, *33*, 1096–1103. [CrossRef]
21. Kasichayanula, S.; Liu, X.; Zhang, W.; Pfister, M.; Reele, S.B.; Aubry, A.F.; LaCreta, F.P.; Boulton, D.W. Effect of a high-fat meal on the pharmacokinetics of dapagliflozin, a selective SGLT2 inhibitor, in healthy subjects. *Diabetes Obes. Metab.* **2011**, *13*, 770–777. [CrossRef] [PubMed]
22. FDA. US Food and Drug Administration. Bioanlaytical Method Validation Guidance for Industry. Available online: https://www.fda.gov/regulatory-information/search-fda-guidance-documents/bioanalytical-method-validation-guidance-industry (accessed on 24 May 2018).
23. Korea Food & Drug Administration. Guideline for the Validation of Bioanalytical Method. Available online: http://drug.kfda.go.kr (accessed on 2 June 2017). (In Korean)
24. U.S. Department of Health and Human Services Food and Drug Administration Center for Drug Evaluation and Research (CDER). Bioequivalence Studies with Pharmacokinetic Endpoints for Drugs Submitted under an ANDA. Available online: https://www.fda.gov/regulatory-information/search-fda-guidance-documents/bioequivalence-studies-pharmacokinetic-endpoints-drugs-submitted-under-abbreviated-new-drug (accessed on 1 August 2021).

25. Scheen, A.J. Cardiovascular Effects of New Oral Glucose-Lowering Agents: DPP-4 and SGLT-2 Inhibitors. *Circ. Res.* **2018**, *122*, 1439–1459. [CrossRef] [PubMed]
26. Dey, J. SGLT2 Inhibitor/DPP-4 Inhibitor Combination Therapy—Complementary Mechanisms of Action for Management of Type 2 Diabetes Mellitus. *Postgrad. Med.* **2017**, *129*, 409–420. [CrossRef]
27. Scheen, A.J. Pharmacokinetic Drug Evaluation of Saxagliptin plus Dapagliflozin for the Treatment of type 2 Diabetes. *Expert. Opin. Drug Metab. Toxicol.* **2017**, *13*, 583–592. [CrossRef] [PubMed]
28. Scheen, A.J. Pharmacokinetic Characteristics and Clinical Efficacy of an SGLT2 Inhibitor plus DPP-4 Inhibitor Combination Therapy in type 2 Diabetes. *Clin. Pharmacokinet.* **2017**, *56*, 703–718. [CrossRef] [PubMed]
29. Ishiguro, N.; Shimizu, H.; Kishimoto, W.; Ebner, T.; Schaefer, O. Evaluation and Prediction of Potential Drug-drug Interactions of Linagliptin Using in vitro Cell Culture Methods. *Drug Metab. Dispos.* **2013**, *41*, 149–158. [CrossRef]
30. Obermeier, M.; Yao, M.; Khanna, A.; Koplowitz, B.; Zhu, M.; Li, W.; Komoroski, B.; Kasichayanula, S.; Discenza, L.; Washburn, W.; et al. In Vitro Characterization and Pharmacokinetics of Dapagliflozin (BMS-512148), a Potent Sodium-Glucose Cotransporter Type II Inhibitor, in Animals and Humans. *Drug Metab. Dispos.* **2010**, *38*, 405–414. [CrossRef]
31. Shao, S.C.; Chang, K.C.; Hung, M.J.; Yang, N.I.; Chan, Y.Y.; Chen, H.Y.; Kao Yang, Y.H.; Lai, E.C. Comparative Risk Evaluation for Cardiovascular Events Associated with Dapagliflozin vs. Empagliflozin in Real-World type 2 Diabetes Patients: A Multi-Institutional Cohort Study. *Cardiovasc. Diabetol.* **2019**, *18*, 120. [CrossRef]
32. Anker, S.D.; Butler, J. Empagliflozin, Calcium, and SGLT1/2 Receptor Affinity: Another Piece of the Puzzle. *ESC Heart Fail.* **2018**, *5*, 549–551. [CrossRef]
33. Patorno, E.; Gopalakrishnan, C.; Bartels, D.B.; Brodovicz, K.G.; Liu, J.; Schneeweiss, S. Preferential Prescribing and Utilization Trends of Diabetes Medications among Patients with Renal Impairment: Emerging Role of Linagliptin and Other Dipeptidyl Peptidase 4 Inhibitors. *Endocrinol. Diabetes Metab.* **2018**, *1*, e00005.
34. Mikov, M.; Pavlović, N.; Stanimirov, B.; Danić, M.; Goločorbin-Kon, S.; Stankov, K.; Al-Salami, H. DPP-4 Inhibitors: Renoprotective Potential and Pharmacokinetics in Type 2 Diabetes Mellitus Patients with Renal Impairment. *Eur. J. Drug Metab. Pharmacokinet.* **2020**, *45*, 1–14. [CrossRef] [PubMed]
35. Rosenstock, J.; Perkovic, V.; Johansen, O.E.; Cooper, M.E.; Kahn, S.E.; Marx, N.; Alexander, J.H.; Pencina, M.; Toto, R.D.; Wanner, C.; et al. Effect of Linagliptin vs. Placebo on Major Cardiovascular Events in Adults with type 2 Diabetes and High Cardiovascular and Renal Risk: The Carmelina Randomized Clinical Trial. *JAMA* **2019**, *321*, 69–79. [CrossRef] [PubMed]
36. Perkovic, V.; Toto, R.; Cooper, M.E.; Mann, J.F.E.; Rosenstock, J.; McGuire, D.K.; Kahn, S.E.; Marx, N.; Alexander, J.H.; Zinman, B.; et al. Effects of Linagliptin on Cardiovascular and Kidney Outcomes in People with Normal and Reduced Kidney Function: Secondary Analysis of the Carmelina Randomized Trial. *Diabetes Care* **2020**, *43*, 1803–1812. [CrossRef] [PubMed]
37. Davit, B.M.; Conner, D.P.; Fabian-Fritsch, B.; Haidar, S.H.; Jiang, X.; Patel, D.T.; Seo, P.R.; Suh, K.; Thompson, C.L.; Yu, L.X. Highly Variable Drugs: Observations from Bioequivalence Data Submitted to the FDA for New Generic Drug Applications. *AAPS J.* **2008**, *10*, 148–156. [CrossRef]
38. Rockhold, F.W.; Goldberg, M.R. An Approach to the Assessment of Therapeutic Drug Interactions with Fixed Combination Drug Products. *J. Biopharm. Stat.* **1996**, *6*, 231–240. [CrossRef]
39. Hutchins, V.; Zhang, B.; Fleurence, R.L.; Krishnarajah, G.; Graham, J. A Systematic Review of Adherence, Treatment Satisfaction and Costs, in Fixed-Dose Combination Regimens in type 2 Diabetes. *Curr. Med. Res. Opin.* **2011**, *27*, 1157–1168. [CrossRef]
40. Bell, D.S. Combine and Conquer: Advantages and Disadvantages of Fixed-Dose Combination Therapy. *Diabetes Obes. Metab.* **2013**, *15*, 291–300. [CrossRef]
41. Tadayasu, Y.; Sarashina, A.; Tsuda, Y.; Tatami, S.; Friedrich, C.; Retlich, S.; Staab, A.; Takano, M. Population Pharmacokinetic/Pharmacodynamic Analysis of the DPP-4 Inhibitor Linagliptin in Japanese Patients with Type 2 Diabetes Mellitus. *J. Pharm. Pharm. Sci.* **2013**, *16*, 708–721. [CrossRef]

pharmaceutics

MDPI

Article

A Method for Evaluating Robustness of Limited Sampling Strategies—Exemplified by Serum Iohexol Clearance for Determination of Measured Glomerular Filtration Rate

Markus Hovd [1,*], Ida Robertsen [1], Jean-Baptiste Woillard [2] and Anders Åsberg [1,3]

[1] Section for Pharmacology and Pharmaceutical Biosciences, Department of Pharmacy, University of Oslo, P.O. Box 1068 Blindern, 0316 Oslo, Norway; ida.robertsen@farmasi.uio.no (I.R.); anders.asberg@farmasi.uio.no (A.Å.)
[2] Inserm, Univ. Limoges, CHU Limoges, Pharmacology & Toxicology, U 1248, F-87000 Limoges, France; jean-baptiste.woillard@unilim.fr
[3] Department of Transplantation Medicine, Oslo University Hospital, P.O. Box 4950 Nydalen, 0424 Oslo, Norway
* Correspondence: m.h.hovd@farmasi.uio.no

Abstract: In combination with Bayesian estimates based on a population pharmacokinetic model, limited sampling strategies (LSS) may reduce the number of samples required for individual pharmacokinetic parameter estimations. Such strategies reduce the burden when assessing the area under the concentration versus time curves (AUC) in therapeutic drug monitoring. However, it is not uncommon for the actual sample time to deviate from the optimal one. In this work, we evaluate the robustness of parameter estimations to such deviations in an LSS. A previously developed 4-point LSS for estimation of serum iohexol clearance (i.e., dose/AUC) was used to exemplify the effect of sample time deviations. Two parallel strategies were used: (a) shifting the exact sampling time by an empirical amount of time for each of the four individual sample points, and (b) introducing a random error across all sample points. The investigated iohexol LSS appeared robust to deviations from optimal sample times, both across individual and multiple sample points. The proportion of individuals with a relative error greater than 15% (P15) was 5.3% in the reference run with optimally timed sampling, which increased to a maximum of 8.3% following the introduction of random error in sample time across all four time points. We propose to apply the present method for the validation of LSS developed for clinical use.

Keywords: limited sampling strategies; population pharmacokinetic modelling; semi-parametric simulation; robustness; therapeutic drug monitoring; area under the curve; AUC; glomerular filtration rate; GFR

Citation: Hovd, M.; Robertsen, I.; Woillard, J.-B.; Åsberg, A. A Method for Evaluating Robustness of Limited Sampling Strategies—Exemplified by Serum Iohexol Clearance for Determination of Measured Glomerular Filtration Rate. *Pharmaceutics* **2023**, *15*, 1073. https://doi.org/10.3390/pharmaceutics15041073

Academic Editors: Barna Vasarhelyi, Gellért Balázs Karvaly and Paolo Magni

Received: 2 February 2023
Revised: 22 March 2023
Accepted: 25 March 2023
Published: 27 March 2023

1. Introduction

The area under the plasma concentration-time curve (AUC) is a clinically useful variable for systemic drug exposure. Within several therapeutic fields, AUC-targeted therapeutic drug monitoring (TDM) is becoming more clinically acknowledged [1]. Accurate estimation of AUC either requires multiple samples within a dose interval when applying the trapezoidal method, or knowledge of the individuals' pharmacokinetic parameters, e.g., clearance. The use of the trapezoidal method in this aspect is time-consuming for both patients and healthcare professionals and not feasible in a clinical setting. However, with Bayesian estimates (BE) based on, for example, a population pharmacokinetic model or the use of a linear regression model, accurate estimates of pharmacokinetic parameters and AUC may be obtained by using a limited number of optimally timed samples [2]. Such limited sampling strategies (LSS) may reduce the number of samples and limit the length of the study visit to make AUC-targeted TDM clinically applicable [3].

In a real-life setting, it is not uncommon for actual sample times to deviate from the optimal LSS sample times. In contrast to multiple linear regression (MLR) models where

coefficients are determined for pre-defined or binned sample times, BE approaches are generally considered more flexible with regard to the timing of the samples, as long as the exact sample times are recorded [4].

According to pharmacokinetic theory, clearance of an intravenously administered drug may be determined by dividing the dose by the AUC. The glomerular filtration rate (GFR) is a clinically important marker for renal function and is typically estimated from blood concentrations of endogenous markers (eGFR). However, the most accurate metric of renal function is the measured GFR (mGFR) assessed by determining the AUC of an exogenous substance subject to clearance via filtration in the kidney [5]. The gold standard of these exogenous markers is inulin but it is difficult to obtain injection-quality inulin nowadays and the analytical assay is also somewhat challenging. Due to this, the contrast agent iohexol has become the new gold standard for mGFR as it shows high concordance with inulin-derived mGFR given optimal sampling times in relation to absolute GFR level [6]. Iohexol exhibits a low degree of protein-binding, low toxicity for the needed doses, no tubular secretion or reabsorption, and is generally stable in plasma/serum [7]. As iohexol is fully excreted by the kidneys, mGFR may be determined by measuring the clearance of iohexol. For this, both MLR- and BE-based LSS are available in the literature. Of these, BE-based methods have been shown to be more flexible and accurate than MLR [8].

We have previously demonstrated the feasibility of a BE-based 4-point LSS to accurately determine mGFR over the range of 14 to 149 mL/min using iohexol serum clearance [9]. Our LSS includes four samples within 5 h following intravenous administration of iohexol. Here, we accurately determine the iohexol serum clearance by dividing the administered dose by the AUC. As such, this method is equally viable for evaluating the effect of shifts in sample time on AUC, as well as mGFR. While the effect of a deviation in time from LSS based on MLR has been evaluated previously [10], the effect of deviations in sample time on parameter estimates in the BE-based methods has not been readily studied and is rarely considered during LSS development or their clinical use. In this work, we demonstrate a general method for evaluating the robustness of an LSS, using the iohexol model for AUC-based mGFR determination as an example. The effect of deviations in time, both across individual and multiple time points, on AUC and model estimated parameters are evaluated.

2. Materials and Methods

2.1. Population Pharmacokinetics Model and Limited Sampling Strategy of Iohexol

The population pharmacokinetic model and associated LSS for iohexol serum clearance have previously been described in detail [9]. In short, a non-parametric adaptive grid (NPAG) approach implemented in Pmetrics [11] for R [12] was used. The model consisted of two compartments, parameterized in clearance (CL) from the central compartment, the volume of central (V) and peripheral (Vp) compartments, and inter-compartmental blood flow (Q), allometrically scaled for body weight using power factors of 0.75 for CL and Q and 1 for V and Vp. The model was developed on rich data from 176 patients (1131 samples), and externally validated in a cohort of 43 patients (395 samples). The 4-point sampling strategy optimized for clinical use included samples at 10 min, 30 min, 2 h, and 5 h following intravenous administration of 3235 mg iohexol (Omnipaque 300 mg I/mL, GE Healthcare AS, Oslo, Norway). A public, web-based interface to this model was developed and is freely available at https://www.mgfr.no.

2.2. Semi-Parametric Simulation from Support Points

To evaluate the robustness of the previously developed LSS of iohexol, simulations were performed to obtain pharmacokinetic profiles from a similar parameter distribution (i.e., population) as the original dataset. Our simulation method did not include covariates, and as such, a covariate-free version of the model was used. This model was developed and evaluated using the original development and validation datasets. Model diagnostic plots and performance metrics are available in Figure S1 and Table S1.

Briefly, the NPAG algorithm estimates the joint population parameter distribution, which is used as a Bayesian prior for individual parameter estimation. The algorithm has recently been explained in detail by Yamada et al., 2020 [13]. The population parameter distribution is a discrete distribution provided as a set of support points, each a vector of length D with an associated probability, where D is the number of parameters. The discrete distribution may be transformed to a continuous distribution for the purpose of sampling a wider range of possible parameter combinations. To accomplish this, we assume a Gaussian distribution over each support point, forming a Gaussian mixture distribution. The probability density function for the multivariate Gaussian mixture is defined as

$$p(x \mid \mu, \Sigma) = N(\mu, \Sigma) \tag{1}$$

where μ and Σ are the vector of means and the matrix of variances, respectively. Values of μ are readily obtained from the individual support point vectors. In order to determine Σ, the univariate Gaussian mixture was evaluated for each parameter, the density for which is

$$p(x) = \sum_{i=1}^{K} \pi_i * N(x \mid \mu_i, \sigma_i) \quad \text{satisfying} \quad \sum_{i=1}^{K} \pi_i = 1 \tag{2}$$

where π is the weighting (or probability) for the Kth Gaussian distribution with mean μ and variance σ. For each parameter, a common σ, and thus, the proposed element of Σ, was determined by minimizing the sum of the squared distance between the simulated and observed (individual posterior) parameter distribution. Minimization was performed using the built-in optim-function in R, implementing Brent's method. Sampling from the mixture distribution is achieved by first sampling the mixture components, i.e., the support points, with replacement, weighted by their probability. Then, multivariate normal sampling of parameters was accomplished using the rtmvnorm function implemented in the tmvtnorm (version 1.5) package for R (version 4.1.3) [14]. Rejection sampling was used to respect the boundaries of the population pharmacokinetic model. A successful simulation was evaluated by the overlapping index for empirical distributions [15], for which values equal to or above 85% were considered acceptable, comparable to an error of 15%. In order to generate concentration-time profiles from the simulated parameter vectors, the population pharmacokinetic model was rewritten to be used in the mrgsolve [16] package for R (Supplementary Code S1). Simulated sampling was performed in 1 min intervals from 0 to 24 h following a dose of 3235 mg of iohexol. No systematic or random error was added to the measurements.

GFR was calculated by dividing dose by the AUC from zero to infinity ($AUC_{0\text{-}\infty}$). Simulated profiles with GFR < 15 mL/min or GFR > 115 mL/min were excluded, as they were outside the validated range of the LSS and will not be explored in this work. As such, both AUC and GFR are conversely evaluated in this work.

2.3. Deviation from Optimal Sample Times

The robustness of the 4-point sampling strategy for iohexol serum clearance was evaluated at each of the sample points with empirically selected deviations in time; 10 min (±2, 4, 5, and 6 min), 30 min (±5, 10, and 15 min), 2 h (±5, 15, 30, and 60 min), and 5 h (±5, 15, 30, 60, 120 and +180, 420, and 1140 min), in addition to a reference run with the original sample times. Each shift was run separately, with cycling, and using the support points of the covariate-free model ran on the complete dataset as a Bayesian prior, as specified in the original publication [9].

In order to evaluate the effect of deviation over multiple sample times, a random normally distributed error, centered around each respective sample point, and with a relative standard deviation (RSD) of 5, 10, 15, 20, and 25% was added to all sample points, truncated (using rejection sampling) at each point to prevent overlap; 10 min (5–15 min), 30 min (15–60 min), 2 h (1–3 h), and 5 h (3–8 h). As a measure of robustness to the aforementioned shifts in sample times, both the mean absolute prediction error in mGFR

and the proportion of individuals with relative prediction error greater than 15% (P15) were used. Here, a P15 less than 15% was considered acceptable.

2.4. Optimal Sample Windows

Based on the results of deviation in both individual and multiple sample points, two approaches to empirical sample windows were used. For deviation in individual sample time, assuming otherwise no deviation in the remaining sample points, the time intervals for which the mean error was lower than 2 mL/min may be used. For deviation across all sample times, the level of RSD associated with an acceptable P15 was used to calculate empirical sample windows for all sample points by calculating the 90% confidence interval for the normal distribution centered at each sample point, truncated to avoid overlap between samples.

3. Results

3.1. Simulated Profiles

A total of 400 pharmacokinetic profiles were simulated, of which 58 and 3 were excluded due to a simulated GFR of less than 15 mL/min or greater than 115 mL/min, respectively, yielding a total of 339 profiles used in the analysis. The variances that minimized the distance between observed and simulated parameter densities were 0.61, 2.2, 1.2, and 0.9 units, for CL, Q, V, and Vp, respectively. Simulated parameter densities demonstrated satisfactory overlap with the observed posterior parameter densities from the original population pharmacokinetic model (91, 92, 90, and 86% for CL, Q, V, and Vp, respectively) (Figure 1). Compared to the posterior, none of the simulated parameters had a difference in weighted mean greater than 15% (Table 1). The simulated profiles (n = 339) were further grouped based on the estimated mGFR in relation to the chronic kidney disease (CKD) stages; stage 4:15–29 mL/min (n = 90), stage 3B: 30–44 mL/min (n = 100), stage 3A: 45–59 mL/min (n = 57), stage 2: 60–90 mL/min (n = 73), and stage 1: >90 mL/min (n = 19).

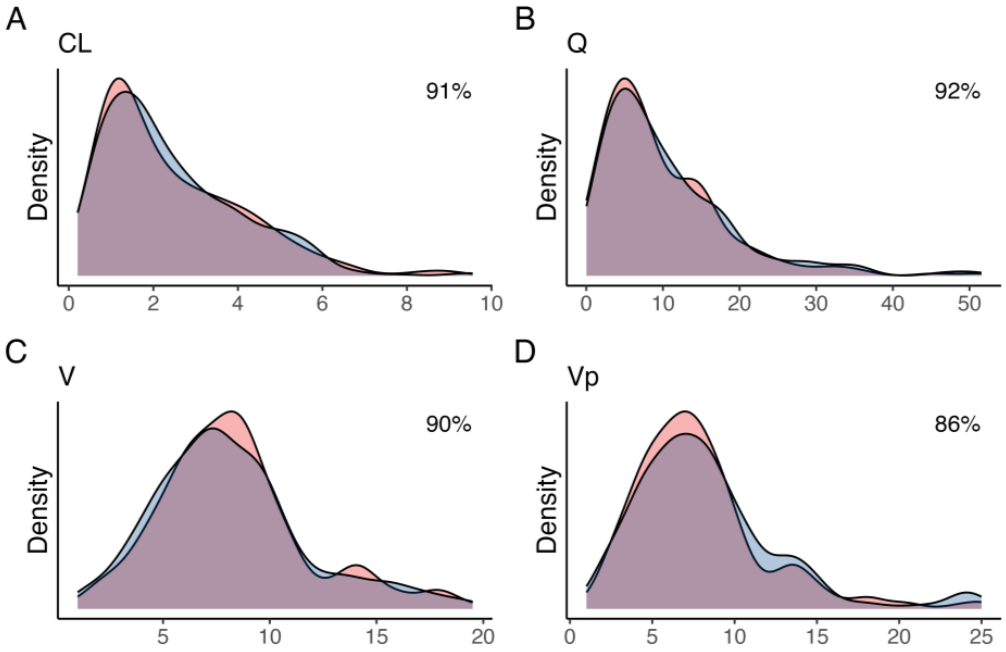

Figure 1. Kernel density estimates for the posterior (blue) and simulated (red) for (**A**) clearance from the central compartment (CL), (**B**) inter-compartmental clearance (Q), (**C**) central volume (V), and (**D**) peripheral volume (Vp). The overlap coefficient for empirical distributions between the posterior and simulated parameter distribution is shown in the top-right corner.

Table 1. Weighted mean and weighted median (95% credibility interval) of the population pharmacokinetic model parameters support points for the original and simulated dataset.

	Weighted Mean		**Weighted Median (95% Credibility Interval)**	
	Original	**Simulated**	**Original**	**Simulated**
CL (L/h)	2.89	2.84	1.95 (1.54–2.60)	2.42 (2.16–2.72)
V (L)	10.36	9.32	10.11 (9.19–10.91)	8.98 (8.25–9.57)
Vp (L)	9.20	7.98	7.95 (7.23–8.60)	7.46 (7.06–7.81)
Q (L/h)	10.65	11.37	8.03 (6.53–9.23)	8.65 (7.50–9.72)

3.2. LSS Performance on Simulated Profiles

The LSS performance on the simulated profiles was evaluated by sampling at precisely 10 min, 30 min, 2 h, and 5 h. The mean absolute and relative error in GFR were 1.5 ± 2.2 mL/min and 4.1 ± 5.5%, respectively (Table 2). In total, 6.5% of the simulated profiles demonstrated an absolute error greater than 5 mL/min, and 1.2% demonstrated an error greater than 10 mL/min. The proportion of individuals with an error larger than 15% (P15) was 5.3%, seemingly increasing with decreased GFR, as expected (Table 2).

Table 2. Limited sampling strategy performance on determining mGFR for the simulated profiles, presented as the absolute and relative error from the simulated "true" GFR. Data are presented as mean ± standard deviation.

Group	**Absolute Error (mL/min)**	**Relative Error (%)**	**P15 (%)**	***n***
All profiles	1.5 ± 2.2	4.1 ± 5.5	5.3	339
CKD Stage 4 (15–29 mL/min)	1.5 ± 1.3	6.3 ± 5.8	7.8	90
CKD Stage 3b (30–44 mL/min)	1.9 ± 2.2	5.4 ± 6.0	8.0	100
CKD Stage 3a (45–59 mL/min)	1.0 ± 1.6	2.2 ± 3.4	1.8	57
CKD Stage 2 (60–90 mL/min)	1.3 ± 3.0	1.9 ± 4.4	2.7	73
CKD Stage 1 (90–115 mL/min)	1.2 ± 2.2	1.2 ± 1.9	0.0	19

3.3. Effect of Shifts in Sample Times on Estimated GFR

A graphical representation of the effect of deviations in individual sample time on estimated GFR is shown in Figure 2. In all cases, the mean absolute error was below 4 mL/min, and the median absolute error was below 2.5 mL/min. For the 10 min sample, delays by up to 6 min increased P15 to a maximum of 9%. Sampling 5 and 6 min prior, effectively at 4 and 5 min post-dose, was not evaluable by the model, and these times were not included. In contrast, delaying the 30 min sample less than 15 min reduced P15 to 4%, while sampling up to 15 min earlier increased P15 to 16%. The 2 h sample exhibits a similar pattern, with reduced P15 for delayed samples, down to 4% at 60 min delayed. The 5 h sample was mostly unaffected by up to 7 h delay in sampling. However, delaying the sample to 24 h post iohexol administration drastically reduced the predictive performance as expected; P15 increased to 18%, and the mean absolute error was 2.9 ± 3.5 mL/min. In order to evaluate these trends for each CKD stage, the median error for each shift is shown in Figure 3.

Applying random, normally distributed noise with an RSD equal to 5 and 10% across all sample times led to a P15 of 7.7% in both cases, and a maximum P15 of 8.3% was achieved in the case of an RSD of both 20% and 25% (Figure 4). For the simulated profiles with CKD stage 1 (GFR 90–115 mL/min), P15 was 0% for all levels of RSD, and a maximum of 4.1% at 5% RSD for profiles with GFR 60–90 mL/min. In contrast, simulated profiles with GFR between 45–55 mL/min, 30–44 mL/min, and 15–15 mL/min incurred a P15 of 7%, 14%, and 10% at 25% RSD, respectively.

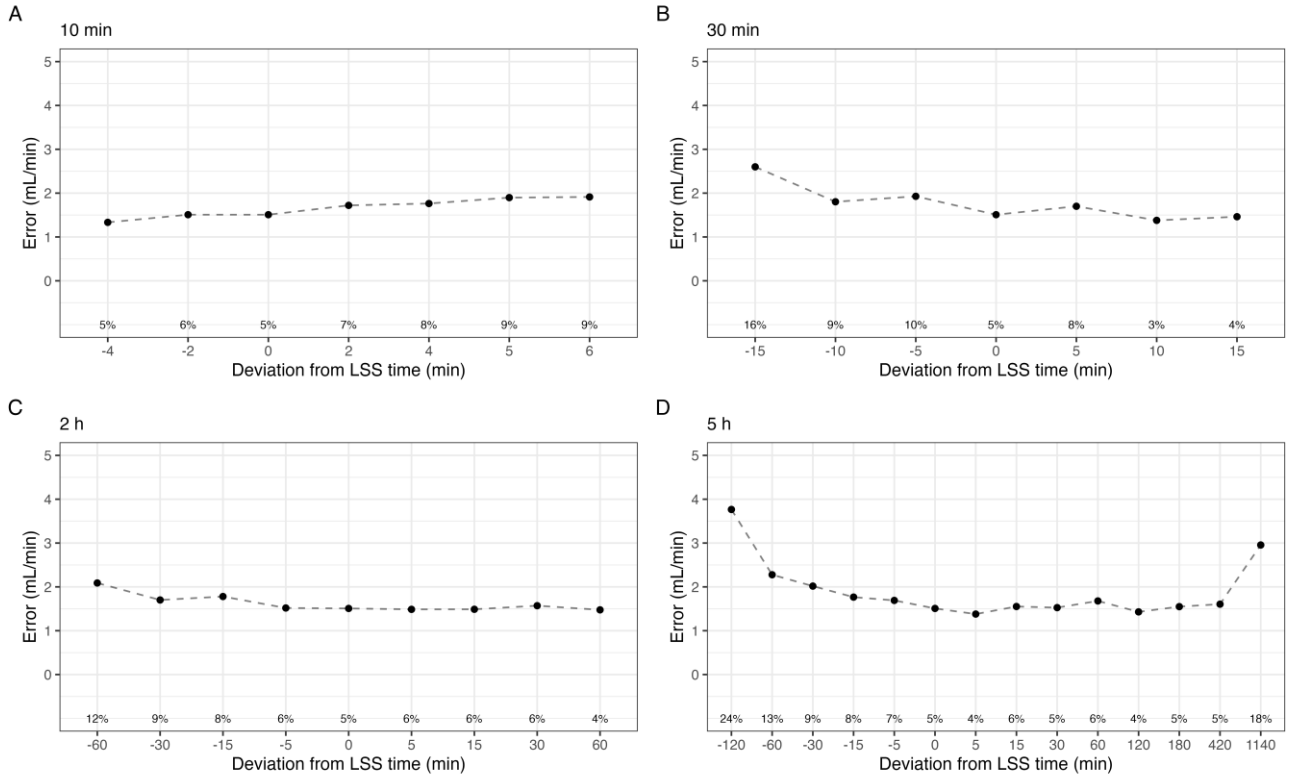

Figure 2. Mean absolute error in estimated GFR by the shift in sample time at point (**A**) 10 min, (**B**) 30 min, (**C**) 2 h, and (**D**) 5 h. Labels indicate the percentage of individuals with a relative error greater than 15% (P15).

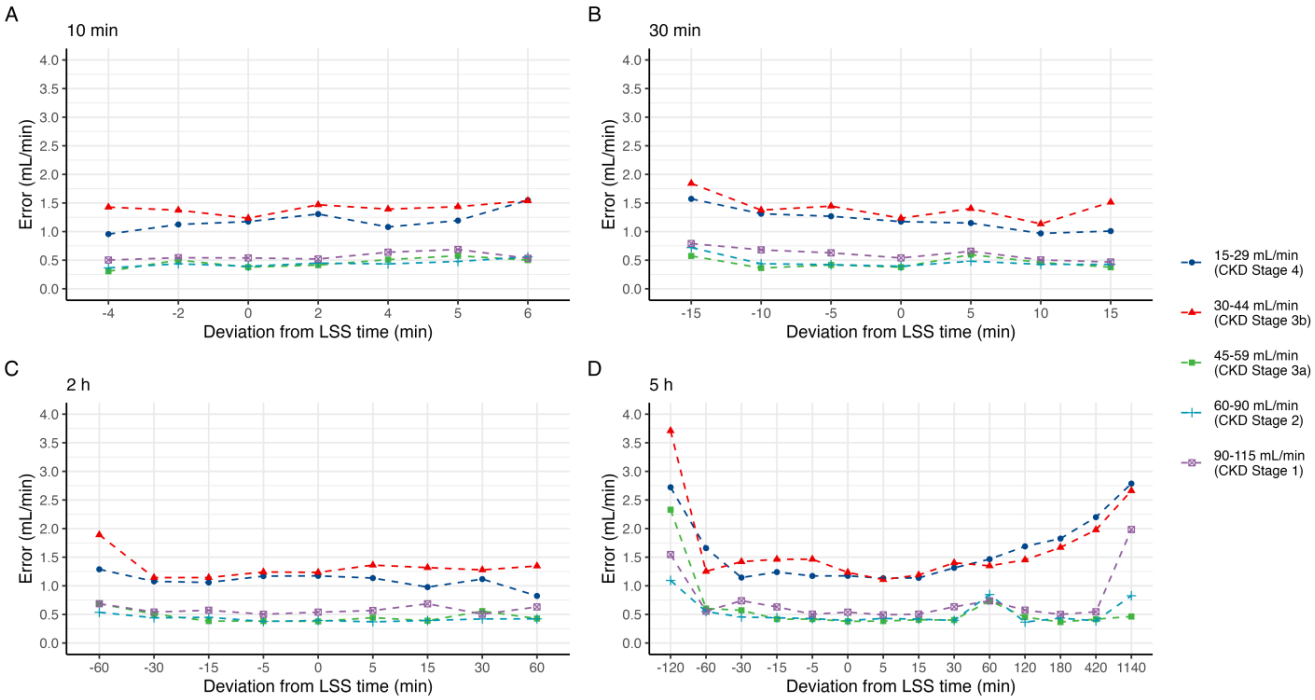

Figure 3. Median absolute error in predicted mGFR by deviation in sample time at point (**A**) 10 min, (**B**) 30 min, (**C**) 2 h, and (**D**) 5 h, grouped by CKD stage.

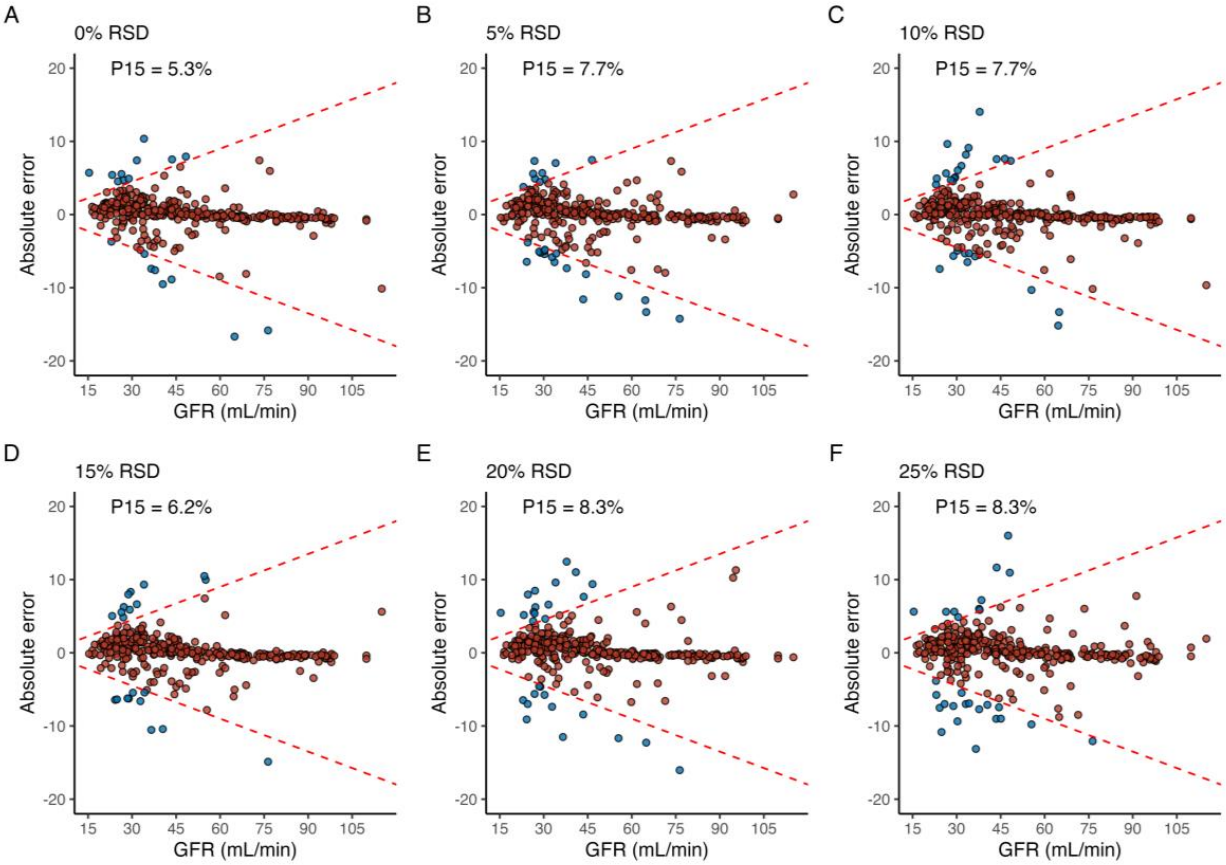

Figure 4. The effect of shifts in time over multiple sample points, where the (**A**) reference run is compared to when shifts in sample time are normally distributed around the optimal sample time with a relative standard deviation (RSD) of (**B**) 5%, (**C**) 10%, (**D**) 15%, (**E**) 20%, and (**F**) 25%. Blue and red fill indicates an individual error greater than or less than 15%, respectively. The label in the upper-left corner denotes the proportion of individuals with a relative prediction error greater than 15% (P15) for each level of RSD.

3.4. Optimal Sample Windows

The intervals around the deviation in individual optimal sample times that provide a mean error in predicted GFR less than 2 mL/min, and conversely a low error in AUC, were 6–16 min (10 min), 20–45 min (30 min), 1.5–3 h (2 h), and 4.75–12 (5 h) (Figure 5A). A careful estimate of the optimal sample window may be obtained by, e.g., the 90% confidence interval for the normal distribution with optimal sample times as the mean, and an RSD of 25%. As such, an estimate of optimal sample windows for the present LSS, without considering the absolute renal function of the patient, are 6–12 min (10 min), 18–42 min (30 min), 1–3 h (2 h), and 2.5–7.4 h (5 h) (Figure 5B), assuming no overlap.

3.5. Effect of Shifts in Sample Times on Model Parameters

Supplementary to the effect of a deviation from optimal sample time on predicted GFR, and conversely, predicted $AUC_{0\text{-inf}}$, changes in estimated model parameters were also evaluated. A graphical representation of the model-estimated parameter densities across all evaluated shifts is shown in Figure 6. When compared with the true parameter densities of the simulated data, the reference run with optimally timed samples achieved a relative error in mean population model parameter estimates in CL, V, Vp, and Q of 1.5%, 0.6%, 6.9%, and 3.8%, respectively. However, the mean individual relative errors in the same estimates in CL, V, Vp, and Q were 7.4%, 7.6%, 22.7%, and 495%.

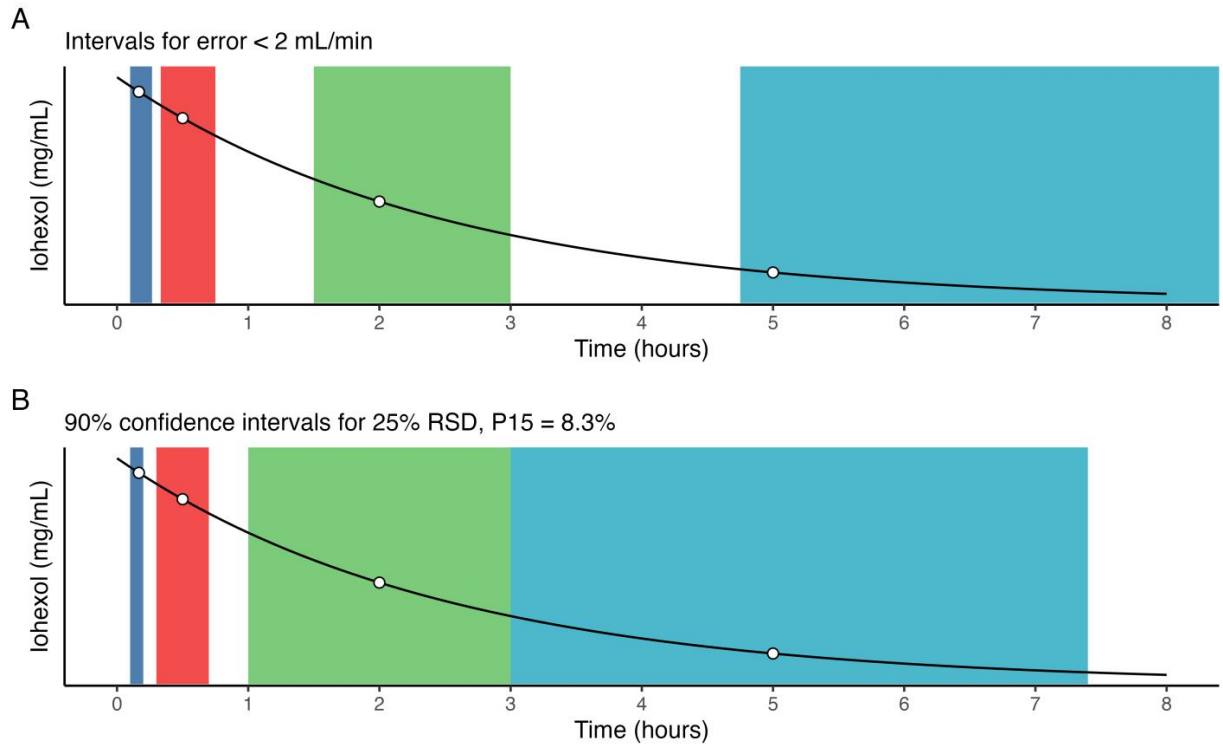

Figure 5. Empirical estimates of optimal sample windows for (**A**) deviations in individual sample times, assuming all other points are sampled optimally, resulting in mean error < 2 mL/min, and (**B**) deviations across all sample times, normally distributed around each sample point with 25% RSD, resulting in a P15 = 8.3%.

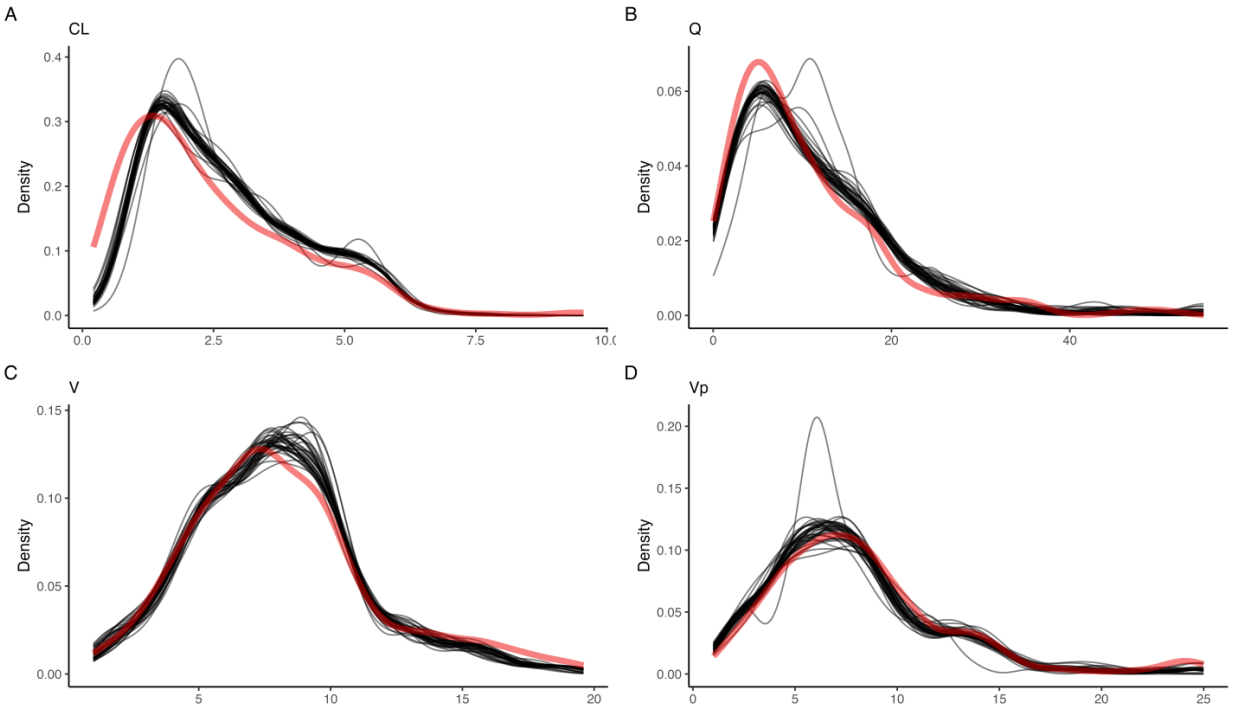

Figure 6. Kernel density estimates for all empirical deviations in time (black), compared to the observed posterior (red) for (**A**) clearance from the central compartment (CL), (**B**) inter-compartmental clearance (Q), (**C**) central volume (V), and (**D**) peripheral volume (Vp).

4. Discussion

In this work, we demonstrate an intuitive approach to evaluating the robustness of LSS, with direct clinical applications. The method was applied to a previously published model for serum iohexol clearance used for the determination of mGFR based on accurate estimates of $AUC_{0\text{-inf}}$. To our knowledge, this is the first work evaluating the robustness of LSS in such a setting. Overall, the 4-point LSS appears robust to shifts in both single and multiple sample times, especially for profiles with medium to good GFR, i.e., above 45 mL/min. An interesting finding is that the robustness is affected by patient absolute clearance or GFR, in this case, and that acceptable sample time deviations should be adapted also based on this information. This is especially useful in scenarios when a rough estimate of the patient clearance is known based on clinical history, but the exact mGFR is desired, e.g., for dose-adjustment of drugs.

In the case of LSS employing MLR, Sarem and colleagues have previously evaluated the effect of deviations in sample time on AUC only [10]. The present work applies this methodology to BE-based LSS and evaluates not only the effect of such deviations on AUC but also the effect on parameter estimates at the individual and population levels. Additionally, BE-based methods have been shown to outperform LSS based on MLR in the case of iohexol clearance for the determination of mGFR [8,9]. The BE-based method was evaluated with a restriction of sampling within standard laboratory opening hours, i.e., the whole procedure was finalized within 5 h, while the MLR-base method allowed sampling up to 24 h after dosing. The BE-based model was not only more accurate but also better adapted to clinical practice [9]. With the development of easily and freely accessible interfaces to these otherwise complicated BE-based models, such as the one we provide at https://www.mgfr.no, the barrier to implementation in a clinical setting is significantly lowered, becoming similar to that of MLR.

When evaluating deviations in sample time for individual sample points, and assuming otherwise optimal sampling, no clinically significant increase in either mean absolute error or P15 was found across shifts in the 10 min sample, and the 30 min sample may be delayed by 15 min, even favorably so. As for the 2 h and 5 h samples, either may be accelerated by up to 30 min without increasing the P15 above 10%. This may potentially save time for both the patient and healthcare personnel during AUC-guided TDM. In this work, delaying individual samples improved the predictive performance of the LSS, likely due to the abundance of simulated profiles with low GFR. Previous history or indication of the patient's AUC and/or mGFR, it is possible to make specific recommendations. For example, parameter estimation in patients with high AUC, and conversely, low mGFR, may benefit more from delayed sampling, and vice versa. A challenge is that individual pharmacokinetic parameters are subject to change over time, but a Bayesian framework compatible with the present method has previously been described by Bayard and Jelliffe [17].

The introduction of random error with an RSD of 25% was associated with a P15 of 8.3%, compared to 5.3% in the reference run. The level of RSD yielding an acceptable P15 could be viewed as a surrogate marker for LSS robustness to shifts across multiple sample times for implementation in the clinic. As demonstrated, this may be tailored to the study population as a whole, or individual sub-groups of patients with, e.g., different stages of CKD. The empirically determined optimal sample windows allow for added granularity with regard to the diligence required for sample collection. However, this does not address the minimum distance required between two given samples, which is likely to affect the accuracy of parameter estimates.

With respect to the model estimated parameters, the effect of empirical deviations in individual sample times on the population level was negligible, as indicated by a low relative error in mean parameter values and the fact that the population parameter densities mostly overlapped the simulated, true density. However, individual parameter estimates varied significantly—especially the peripheral volume and inter-compartmental clearance were often misidentified. This is not surprising, as these parameters are seldom identifiable. This misidentification did not have any effect on the predictive performance of

the model, i.e., estimates of individual $AUC_{0-\infty}$, here translated to mGFR. All runs exhibited exceptionally low mean prediction errors and relative root-mean-squared errors. This was observed during early method development and for this reason, iohexol serum clearance, and thus GFR, was calculated by dividing dose by $AUC_{0-\infty}$. This further highlights the need for a more robust evaluation of LSS, especially when model parameters are used directly. Our results demonstrate the clinical application of evaluating the robustness of BE-based LSS. Previously, the effect of a deviation in sample time was unknown but has now been quantified for the present model and population. With this information, one may look up the deviation in sample time for the relevant CKD stage and use this to decide on whether to include an additional sample, for example, which is likely to improve the accuracy of the parameter estimates. Such changes to the LSS are not possible in the case of multiple linear regression-based methods, where one is restricted to a pre-defined or binned sample space.

For simulation-based studies, it is imperative that the simulated population reflects the underlying research question. While this is implicitly assumed, it is not usually confirmed in simulation-based studies, despite its importance. In this work, we aimed to simulate profiles from a similar population, which was confirmed by evaluating the overlap in parameter densities, in addition to comparisons of weighted mean and median. A disadvantage of the proposed method for semi-parametric simulation is the lack of covariates, given that multiple model parameters were allometrically scaled in the original model. Our strategy for simulation was based on the mechanistic interpretation of the support points representing the discrete population parameter distribution from the NPAG algorithm. However, there is no direct link between the support points and the covariates. For the covariate to be included in the multivariate normal sampling, a sensible mean and variance must be provided. An initial choice would be the observed mean and variance of the covariate, which was attempted during method development, but led to poor overlap between the posterior and simulated parameter densities. Alternate approaches to include covariates in a semi-parametric simulation will be investigated in a future work. Even though the present work utilized a covariate-free version of the original model, we still believe that the proposed simulation method provides an accurate representation of the effect of deviations in LSS sample times on individual pharmacokinetic estimates, as the method for evaluating the robustness of LSS is agnostic to the process for which data is generated.

5. Conclusions

By deviating from the optimally timed sample point(s) of an LSS either empirically or randomly, the robustness of the LSS to such shifts can be approximated. Additionally, empirical optimal sample windows may be obtained for a more flexible sampling schedule. It was further revealed that despite model population parameter estimates being within 10% across all evaluated deviations, individual model parameter estimates were prone to misidentification. These findings provide additional insight into the necessary diligence required during sample collection of optimally timed samples and provide a method for evaluating LSS robustness with respect to both pharmacokinetic (i.e., AUC) and model estimated parameters. We propose the present method be applied during the development and validation of LSS for clinical use.

Supplementary Materials: The following supporting information can be downloaded at: https://www.mdpi.com/article/10.3390/pharmaceutics15041073/s1. Figure S1: Population pharmacokinetic model performance plots for the covariate-free model, including (A) observed-predicted plot, (B) weighted error across observed concentrations, and (C) weighted error across sample time. Solid black lines represent the unity line, and the solid blue lines in (B,C) indicate the loess line. Table S1: Population pharmacokinetic performance metrics for the covariate-free model. Supplementary Code S1: Implementation of the population pharmacokinetic model in mrgsolve for R.

Author Contributions: Conceptualization, M.H., I.R. and A.Å.; Methodology, M.H., I.R., J.-B.W. and A.Å.; Software, M.H. and J.-B.W.; Validation, M.H. and A.Å.; Formal Analysis, M.H.; Investigation, M.H.; Resources, I.R. and A.Å.; Data Curation, A.Å.; Writing—Original Draft Preparation, M.H.; Writing—Review & Editing, M.H., I.R., J.-B.W. and A.Å.; Visualization, M.H.; Supervision, I.R. and A.Å.; Project Administration, A.Å.; Funding Acquisition, I.R. and A.Å. All authors have read and agreed to the published version of the manuscript.

Funding: This research received no external funding.

Institutional Review Board Statement: Not applicable.

Informed Consent Statement: Not applicable.

Data Availability Statement: The data presented in this study are available on request from the corresponding author.

Conflicts of Interest: Hovd, Robertsen, Woillard, and Åsberg declare that they have no conflict of interest.

Abbreviations

P15: the proportion of individuals with an error greater than 15%.

References

1. Lim, A.S.; Foo, S.H.W.; Benjamin Seng, J.J.; Magdeline Ng, T.T.; Chng, H.T.; Han, Z. Area-Under-Curve–Guided Versus Trough-Guided Monitoring of Vancomycin and Its Impact on Nephrotoxicity: A Systematic Review and Meta-Analysis. *Ther. Drug Monit.* **2023**. [CrossRef] [PubMed]
2. van den Elsen, S.H.J.; Sturkenboom, M.G.G.; Akkerman, O.W.; Manika, K.; Kioumis, I.P.; van der Werf, T.S.; Johnson, J.L.; Peloquin, C.; Touw, D.J.; Alffenaar, J.-W.C. Limited Sampling Strategies Using Linear Regression and the Bayesian Approach for Therapeutic Drug Monitoring of Moxifloxacin in Tuberculosis Patients. *Antimicrob. Agents Chemother.* **2019**, *63*, e00384-19. [CrossRef] [PubMed]
3. Teitelbaum, Z.; Nassar, L.; Scherb, I.; Fink, D.; Ring, G.; Lurie, Y.; Krivoy, N.; Bentur, Y.; Efrati, E.; Kurnik, D. Limited Sampling Strategies Supporting Individualized Dose Adjustment of Intravenous Busulfan in Children and Young Adults. *Ther. Drug Monit.* **2020**, *42*, 427–434. [CrossRef] [PubMed]
4. van der Meer, A.F.; Marcus, M.A.; Touw, D.J.; Proost, J.H.; Neef, C. Optimal sampling strategy development methodology using maximum a posteriori Bayesian estimation. *Ther. Drug Monit.* **2011**, *33*, 133–146. [CrossRef] [PubMed]
5. Porrini, E.; Ruggenenti, P.; Luis-Lima, S.; Carrara, F.; Jiménez, A.; de Vries, A.P.J.; Torres, A.; Gaspari, F.; Remuzzi, G. Estimated GFR: Time for a critical appraisal. *Nat. Rev. Nephrol.* **2019**, *15*, 177–190. [CrossRef] [PubMed]
6. Dubourg, L.; Lemoine, S.; Joannard, B.; Chardon, L.; de Souza, V.; Cochat, P.; Iwaz, J.; Rabilloud, M.; Selistre, L. Comparison of iohexol plasma clearance formulas vs. inulin urinary clearance for measuring glomerular filtration rate. *Clin. Chem. Lab. Med.* **2021**, *59*, 571–579. [CrossRef] [PubMed]
7. Delanaye, P.; Ebert, N.; Melsom, T.; Gaspari, F.; Mariat, C.; Cavalier, E.; Björk, J.; Christensson, A.; Nyman, U.; Porrini, E.; et al. Iohexol plasma clearance for measuring glomerular filtration rate in clinical practice and research: A review. Part 1: How to measure glomerular filtration rate with iohexol? *Clin. Kidney J.* **2016**, *9*, 682–699. [CrossRef]
8. Destere, A.; Salmon Gandonnière, C.; Åsberg, A.; Loustaud-Ratti, V.; Carrier, P.; Ehrmann, S.; Barin-Le Guellec, C.; Marquet, P.; Woillard, J.B. A single Bayesian estimator for iohexol clearance estimation in ICU, liver failure and renal transplant patients. *Br. J. Clin. Pharmacol.* **2022**, *88*, 2793–2801. [CrossRef]
9. Asberg, A.; Bjerre, A.; Almaas, R.; Luis-Lima, S.; Robertsen, I.; Salvador, C.L.; Porrini, E.; Schwartz, G.J.; Hartmann, A.; Bergan, S. Measured GFR by Utilizing Population Pharmacokinetic Methods to Determine Iohexol Clearance. *Kidney Int. Rep.* **2020**, *5*, 189–198. [CrossRef]
10. Sarem, S.; Nekka, F.; Ahmed, I.S.; Litalien, C.; Li, J. Impact of sampling time deviations on the prediction of the area under the curve using regression limited sampling strategies. *Biopharm. Drug Dispos.* **2015**, *36*, 417–428. [CrossRef] [PubMed]
11. Neely, M.N.; van Guilder, M.G.; Yamada, W.M.; Schumitzky, A.; Jelliffe, R.W. Accurate detection of outliers and subpopulations with Pmetrics, a nonparametric and parametric pharmacometric modeling and simulation package for R. *Ther. Drug Monit.* **2012**, *34*, 467–476. [CrossRef] [PubMed]
12. R Core Team. *R: A Language and Environment for Statistical Computing*; R Foundation for Statistical Computing: Vienna, Austria, 2020.
13. Yamada, W.M.; Neely, M.N.; Bartroff, J.; Bayard, D.S.; Burke, J.V.; Guilder, M.V.; Jelliffe, R.W.; Kryshchenko, A.; Leary, R.; Tatarinova, T.; et al. An Algorithm for Nonparametric Estimation of a Multivariate Mixing Distribution with Applications to Population Pharmacokinetics. *Pharmaceutics* **2020**, *13*, 42. [CrossRef] [PubMed]

14. Wilhelm, S.; Manjunath, B.G. tmvtnorm: A Package for the Truncated Multivariate Normal Distribution. *R J.* **2010**, *2*, 25–29. [CrossRef]
15. Pastore, M.; Calcagni, A. Measuring Distribution Similarities Between Samples: A Distribution-Free Overlapping Index. *Front. Psychol.* **2019**, *10*, 1089. [CrossRef] [PubMed]
16. Baron, K.T. Mrgsolve: Simulate from ODE-Based Models. R package version 1.0.6. 2022. Available online: https://CRAN.R-project.org/package=mrgsolve (accessed on 1 February 2023).
17. Bayard, D.S.; Jelliffe, R.W. A Bayesian Approach to Tracking Patients Having Changing Pharmacokinetic Parameters. *J. Pharmacokinet. Pharmacodyn.* **2004**, *31*, 75–107. [CrossRef] [PubMed]

pharmaceutics

MDPI

Review

Current Status of Therapeutic Drug Monitoring in Mental Health Treatment: A Review

Filippo Pennazio [1,†], Claudio Brasso [1,*,†], Vincenzo Villari [2] and Paola Rocca [1]

[1] Department of Neuroscience "Rita Levi Montalcini", University of Turin, 10126 Turin, Italy
[2] Psychiatric Emergency Service, Department of Neuroscience and Mental Health, A.O.U. "Città della Salute e della Scienza di Torino", 10126 Turin, Italy
* Correspondence: claudio.brasso@unito.it
† The authors have contributed equally to this work and share the first authorship.

Abstract: Therapeutic drug monitoring (TDM) receives growing interest in different psychiatric clinical settings (emergency, inpatient, and outpatient services). Despite its usefulness, TDM remains underemployed in mental health. This is partly due to the need for evidence about the relationship between drug serum concentration and efficacy and tolerability, both in the general population and even more in subpopulations with atypical pharmacokinetics. This work aims at reviewing the scientific literature published after 2017, when the most recent guidelines about the use of TDM in mental health were written. We found 164 pertinent records that we included in the review. Some promising studies highlighted the possibility of correlating early drug serum concentration and clinical efficacy and safety, especially for antipsychotics, potentially enabling clinicians to make decisions on early laboratory findings and not proceeding by trial and error. About populations with pharmacokinetic peculiarities, the latest studies confirmed very common alterations in drug blood levels in pregnant women, generally with a progressive decrease over pregnancy and a very relevant dose-adjusted concentration increase in the elderly. For adolescents also, several drugs result in having different dose-related concentration values compared to adults. These findings stress the recommendation to use TDM in these populations to ensure a safe and effective treatment. Moreover, the integration of TDM with pharmacogenetic analyses may allow clinicians to adopt precise treatments, addressing therapy on an individual pharmacometabolic basis. Mini-invasive TDM procedures that may be easily performed at home or in a point-of-care are very promising and may represent a turning point toward an extensive real-world TDM application. Although the highlighted recent evidence, research efforts have to be carried on: further studies, especially prospective and fixed-dose, are needed to replicate present findings and provide clearer knowledge on relationships between dose, serum concentration, and efficacy/safety.

Keywords: therapeutic drug monitoring; treatment efficacy; medication adherence; schizophrenia spectrum and other psychotic disorders; bipolar and related disorders; depressive disorder

Citation: Pennazio, F.; Brasso, C.; Villari, V.; Rocca, P. Current Status of Therapeutic Drug Monitoring in Mental Health Treatment: A Review. *Pharmaceutics* **2022**, *14*, 2674. https://doi.org/10.3390/pharmaceutics14122674

Academic Editors: Barna Vasarhelyi and Gellért Balázs Karvaly

Received: 23 September 2022
Accepted: 26 November 2022
Published: 1 December 2022

Publisher's Note: MDPI stays neutral with regard to jurisdictional claims in published maps and institutional affiliations.

1. Introduction

Therapeutic drug monitoring (TDM) consists of measuring drug levels in biological samples, along with a clinical and pharmacological interpretation, aiming to improve prescription appropriateness. The rationale of this clinical procedure is that a relationship between drug level, clinical effects, and toxicity can be established. TDM is usually performed on blood samples, although other biologic samples or determination of endogenous compounds related to the drug activity can be used [1]. If we just think of drugs such as digoxin, we see how TDM has marked the history of several medical treatments in past decades. In psychiatry, some drugs have a relatively long history of research and clinical application of TDM (i.e., carbamazepine, clozapine, lithium), which has become a cornerstone in guiding treatment. It is impressive how current recommendations for

TDM, which are discussed below, largely overstep traditional TDM use, even if they are still too often scarcely applied in real-world clinical practice [2]. More in detail, TDM allows the determination of an individualized dose of the prescribed drug, maximizing clinical efficacy and minimizing toxicity. Appropriate clinical use of TDM requires considering both pharmacodynamic and pharmacokinetic parameters. First, under a pharmacodynamic approach, a therapeutic reference range (TRR) has to be considered for each drug, where the TRR lower limit represents the blood concentration below which a drug is unlike to have adequate clinical efficacy, while the upper limit is the concentration above which tolerability decreases or it is relatively unlikely to obtain further therapeutic improvement. Secondly, the application of another range, the dose-related reference range (DRRR), which is the expected concentration range under the prescribed dosage, permits adherence assessment and individuation of possible pharmacokinetic specificities. Thirdly, the definition of metabolite-to-parent compound ratios can be a useful tool to measure metabolizing activity.

TDM is indicated for most classes of neuropsychiatric drugs: first- and second-generation antipsychotics (i.e., haloperidol, clozapine, risperidone, olanzapine quetiapine, aripiprazole, cariprazine, etc.), mood stabilizers (i.e., lithium, valproic acid, carbamazepine, oxcarbazepine, etc.), and antidepressants (i.e., citalopram, sertraline, venlafaxine, etc.) and is recommended in a variety of clinical conditions and settings, such as suboptimal response, relapse, presence of side effects at therapeutic doses and adherence assessment. It is particularly indicated especially for drugs with a narrow therapeutic window, high inter-individual pharmacokinetic variability, or that are influenced by genetic variants of enzymes involved in drug metabolism, and in populations in which the relation between drug dose and blood level is highly unpredictable, such as limit ages, pregnancy, patients with obesity or relevant systemic diseases or treated with many different drugs [2]. In mental health, the past decades have been characterized by the introduction of several novel therapeutic interventions, comprising new drugs and an extension or more precise definition of the indications of the already existing compounds. Despite advances in the spectrum of therapeutic instruments, treatment outcomes of major psychiatric disorders remain largely perfectible. Low treatment adherence and relatively high interindividual variability of clinical efficacy and tolerability of several drugs are among the main challenges in achieving better outcomes. TDM appears to be a promising instrument to assess treatment adherence and monitor optimal drug posology. A growing body of literature supports TDM clinical implementation. Research efforts have led to an increasingly precise definition of therapeutic and dose-related reference ranges for psychotropic drugs and have highlighted the importance of combining TDM results with the evaluation of various pharmacokinetic parameters and pharmacogenetic tests [2].

Specific recommendations for TDM application in mental health have been defined, such as dose optimization, safety, adherence assessment, treatment resistance, possible drug–drug interactions (DDI), genetic alterations of drug metabolism, and physiological and clinical conditions that can lead to pharmacokinetic peculiarities. Among the latter, the main ones are limited ages (children, adolescents, and elderly), extreme body weights (i.e., obesity and severe underweight), ethnicity differences, peripartum, and pharmacokinetically relevant comorbidity (e.g., systemic infections or gastrointestinal absorption disturbances). These recommendations are summarized in the Arbeitsgemeinschaft fuer Neuropsychopharmakologie und Pharmakopsychiatrie (AGNP) Consensus Guidelines for Therapeutic Drug Monitoring in Neuro-psychopharmacology, published in 2017 [2] that represent to date the highest level of scientific evidence regarding the use of TDM in the field of mental health. TDM clinical recommendations stated in AGNP guidelines are listed in Table 1.

Specifically, AGNP guidelines propose a comprehensive evidence-based list of TRR and dose-related concentration (DRC) factors to compute DRRR for most psychoactive drugs. In addition, chronopharmacological aspects need to be considered in TDM results interpretation. TDM should be performed in the morning, before drug assumption, in order to obtain standardized and reproducible results [2]. Furthermore, a distinction between

immediate- and extended-release (IR and XR) drug formulations is needed. AGNP guidelines propose specific correction parameters for DRRR calculation according to the type of formulation (IR or XR). In any case, it has to be considered that these are population-based data and, for individual patients, optimal therapeutic response and tolerability may occur at different blood levels [2]. Therefore, the definition of patients' individual therapeutic concentration should be tailored through clinical evaluation and TDM: when a patient has reached the desired clinical outcome and no significant adverse effects are present, optimal individual drug concentration can be defined, guiding future pharmacologic treatment. In any case, TRR and DRRR enable clinicians to investigate possible causes of inadequate clinical efficacy, relapse, or adverse effects under recommended doses, comprising assessment of pseudo-resistance due to poor adherence [2].

Table 1. TDM recommendation in neuropsychopharmacological treatment.

Obligatory TDM
Dose optimization after initial prescription or after dose change for drugs with a high level of recommendation to use TDM
Drugs for which TDM is mandatory for safety reasons (e.g., lithium or carbamazepine)
Specific indications for TDM
Uncertain adherence to medication
Relapse prevention because of uncertain adherence to medication
Lack of clinical improvement under recommended doses
Relapse under maintenance treatment
Determination of optimal individual drug concentration when the patient has attained the desired clinical outcome
Recurrence of symptoms under adequate doses
Clinical improvement and adverse effects under recommended doses
Combination treatment with a drug known for its interaction potential or suspected drug interaction
Use of counterfeit medications by the patient
Presence of a genetic peculiarity concerning drug metabolism (genetic deficiency, gene multiplication)
Patients with differential ethnicity
Patients with abnormally high or low body weight
Pregnant or breastfeeding patient
Children or adolescent patient
Elderly patient (>65 y)
Patients with intellectual disability
Patients with pharmacokinetically relevant comorbidity (hepatic or renal insufficiency, cardiovascular disease)
Patients with acute or chronic inflammations or infections
Patients with restrictive gastrointestinal resection or bariatric surgery
Problems occurring after switching from an original preparation to a generic form (and vice versa)
Use of over-the-counter (OTC) drugs by the patient

TDM: therapeutic drug monitoring.

Although the undisputed potential of TDM in psychiatry, its implementation in clinical practice is still largely heterogeneous and often insufficient [3–5] even for those drugs for which it has been available for many years and is highly recommended, such as lithium, valproate, carbamazepine, and clozapine [6–10]. Therefore, following evidence-based recommendations, more extensive employment of TDM in real-world mental health practice is desirable. A contribution in enlarging TDM use may arrive from novel mini- or not invasive sampling techniques, such as dried blood spots or oral fluid analysis, which allows simple and rapid testing, with a consequent easier applicability.

We conducted this narrative review to present the state of the art in application of TDM in mental health, with particular attention to the most recent findings issued after the AGNP guidelines. The focus on findings after 2017 aimed at providing the readers with a synthesis of what is new after the issue of AGNP guidelines, enabling a clear and simple update on the topic.

To facilitate reading, we propose the following list of contents:

2. Materials

We searched the Web of Science database using the following search string: TS = (therapeutic NEAR/0 drug NEAR/0 monitoring) AND (TS = (mental health) OR TS = (psychiatry) OR TS = (mental disorder) OR TS = (schizophrenia) OR TS = (psychosis) OR TS = (bipolar disorder) OR TS = (depression) OR TS = (mood disorder) OR TS = (personality disorder) OR TS = (anxiety disorder) OR TS = (antipsychotics) OR TS = (mood stabilizers) OR TS = (antidepressants) OR TS = (benzodiazepines) OR TS = (haloperidol) OR TS = (chlorpromazine) OR TS = (perfenazine) OR TS = (chlothiapine) OR TS = (promethazine) OR TS = (clozapine) OR TS = (risperidone) OR TS = (olanzapine) OR TS = (quetiapine) OR TS = (paliperidone) OR TS = (aripiprazole) OR TS = (ziprasidone) OR TS = (asenapine) OR TS = (lurasidone) OR TS = (cariprazine) OR TS = (brexpiprazole) OR TS = (lithium) OR TS = (valproate) OR TS = (valproic acid) OR TS = (divalproex sodium) OR TS = (lamotrigine) OR TS = (carbamazepine) OR TS = (oxcarbazepine) OR TS = (fluvoxamine) OR TS = (fluoxetine) OR TS = (sertraline) OR TS = (paroxetine) OR TS = (citalopram) OR

TS = (escitalopram) OR TS = (venlafaxine) OR TS = (duloxetine) OR TS = (bupropion) OR TS = (trazodone) OR TS = (lorazepam) OR TS = (alprazolam)). A total of 2.005 records was obtained, with a date limit of 20 October 2022. The choice to search on the Web of Science (WoS) was motivated by the fact that WoS is a platform that includes several databases, including Science Citation Index Expanded and Social Science Citation Index.

The AGNP guidelines, based on a systematic literature search, were sent for publication in May 2017 and issued in 2018 [2]. Since no significant work published before 2017 and not discussed in the AGNP guidelines emerged, we focused on research data published from 2017 on, setting data limits from 1 January 2017 to 20 October 2022.

All kinds of articles were included in the search and submitted to retrieval. We excluded articles not relevant to our review by topic (i.e., articles on technical methodologies) or clinical sample (i.e., patients with epilepsy, children aged under 12) and written in languages other than English. Records were preliminarily screened by examining the title and abstract. The full text of articles that passed initial selection underwent careful examination. The selection process is shown in Figure 1.

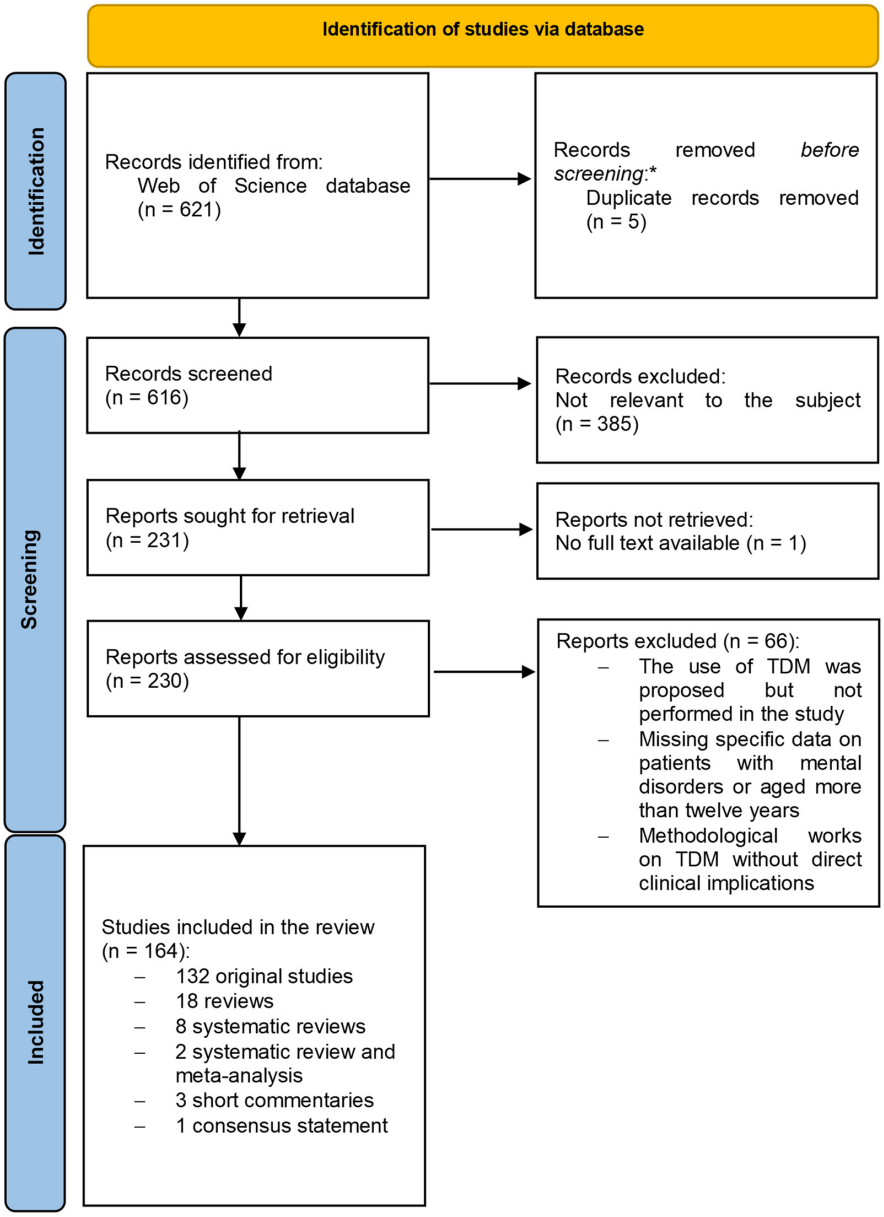

Figure 1. Identification and screening procedure of the studies included. * No automation tools were used.

3. Results and Discussion

Following the algorithm described above and reported in Figure 1, 166 records were included in the review. Sixty-six records were excluded after full-text reading for one of the following reasons: (i) the use of TDM was proposed but not performed in the study; (ii) there were no specific or separated data on patients with mental disorders or aged more than fourteen years; (iii) the record was a methodological work on TDM without direct clinical implications. The 166 included records were: 2 systematic reviews and meta-analyses; 8 systematic reviews; 18 reviews; 2 clinical trials; 108 observational studies (59 retrospective studies, 31 prospective studies, 1 retrospective and prospective study, and 17 cross-sectional studies); 2 genome-wide association study; 6 validation studies; 11 case reports; 1 consensus statement; 1 study of device efficiency testing; 1 proof-of-concept study; 1 pilot assessment of drug urinary metabolites; and 3 short commentaries.

3.1. Individual Dose Finding

Since these guidelines were issued, novel research evidence has reprised the debate on TRR and DRRR for many drugs, integrating already available data with new considerations. Literature on antipsychotics, including long-acting injection (LAI) formulation and antidepressants, was largely reviewed, and novel DRRRs were proposed for clozapine, risperidone, paliperidone, and olanzapine. The studies that we have selected are mostly based on retrospective analyses of TDM databases, comprising mainly patients treated with flexible-dosing regimens, and appear not to be suitable for the determination of therapeutically effective drug concentrations because of the flexible dosing [11–16]. Therefore, fixed-dose studies are urgently needed to determine more precise relationships between dose, blood levels, and clinical efficacy. This is in line with a recent review by Hiemke, according to which a large lack of evidence on the concentration-efficacy relationship is still present [16].

3.1.1. Clinical Efficacy

Clinical efficacy is the dimension representing the extent to which a patient benefits from a drug. Clinical response to treatment depends on complex interrelationships between demographic, clinical, and metabolic features and is not attributable to a single clinical or laboratory variable. TDM represents a valuable and still underemployed tool to understand the mechanisms involved in the interplay between such factors, both at population and individual levels, also with the potential to integrate all variables in vivo for every patient. In addition, TDM can be helpful in identifying low drug serum concentration, possibly due to individual pharmacokinetic variants (demographic, genetic, linked to concomitant diseases or treatments) as a factor involved in resistance. Since the pharmacological treatment of mental disorders is mainly carried out with oral therapies taken by the patient at home, and there are no methods to predict with certainty what will be the minimum effective dose for that patient, TDM can help to find such a dose. Consequently, it may promote the obtainment of therapeutic effects by minimizing the adverse ones, thereby reducing the risk and duration of hospitalization as well as mental health costs. This is in agreement with AGNP guidelines that indicate the TDM in relapse and recurrence prevention and management, lack of clinical improvement under recommended doses, and the determination of optimal individual drug concentration when the patient has attained the desired clinical outcome in many mental disorders [2].

Schizophrenia Spectrum Disorders

FEP is a very challenging issue for psychiatrists and a crucial period in the management of the disease: an efficient early treatment enables better long-term treatment outcomes. Although research data are still scarce and controversial, TDM appears to be a promising tool in optimizing treatment from its beginning. Additionally, for the current review, we found incoherent evidence. In particular, an observational study on 64 patients with FEP receiving second-generation antipsychotics reported no significant correlation between

serum concentrations and clinical effects, while data drawn from a large multicentric clinical trial and regarding 47 patients receiving olanzapine evidenced a role for TDM in predicting clinical efficacy after two months [17,18].

Early clinical response evaluation and dose-finding are critical issues also in schizophrenia relapse and maintenance. Data from a prospective study on aripiprazole suggest the utility of measuring the plasma level of aripiprazole and its active metabolite dehydroaripiprazole after a week of treatment, while another performed on Asian patients from Taiwan reported a higher clinical response with aripiprazole serum concentrations higher than the TRR proposed for the western population [19,20]. A recent meta-analysis suggests a high inter-individual variability and the influence of CYP2D6 genotypes in the treatment of schizophrenia spectrum disorders with aripiprazole and proposes a low daily dose approach with a starting dose of 10 mg and 5 mg for known poor metabolizers [21]. A prospective study on patients receiving second-generation antipsychotics included in a naturalistic drug-monitoring program retrieved no relationship between early clinical response and drug plasma level [22]. Another naturalistic and flexible-dose study conducted on patients treated with risperidone enlightened a possible association between risperidone active moiety (risperidone and its active metabolite 9-hydroxyrisperidone, that is paliperidone) plasma concentrations and clinical response [23]. As for FEP, available evidence on TDM in schizophrenia relapse is still sparse and heterogeneous [19–23], possibly due to the design of the studies that considered flexible, individualized dosage. However, even if real-world data are relatively lacking and highly interesting on this topic, studies with fixed-dose regimens are still awaited to define more reliable correlations between dose, blood concentration, and efficacy.

Treatment resistance in schizophrenia is a therapeutic challenge, and identifying factors associated with inadequate clinical response is often complex. TDM and early pharmacogenetic testing may help to disentangle factors underlying clozapine resistance through the analysis of genetic variants of metabolizing enzymes, blood–brain barrier transporters, and receptors of neurotransmitters [24–30]. Twelve studies focused on treatment resistance or failure in schizophrenia [17,24,30–34]. In particular, a retrospective analysis of a large sample of patients included in the Clinical Antipsychotic Trials of Intervention Effectiveness (CATIE) study and randomized to olanzapine or risperidone revealed a significant correlation between low antipsychotic blood levels and treatment failure [31]. Other retrospective data on patients evaluated as treatment-resistant by their clinician and switched to clozapine—the gold standard therapy for treatment-resistant schizophrenia—or to long-acting injectable (LAI) antipsychotics revealed a relatively high prevalence of undetectable or subtherapeutic blood levels of oral antipsychotics [32,33]. A solid correlation between clozapine serum concentration and dose-adjusted serum concentration clinical response has been confirmed by several studies [17,24,25]. On the other hand, a review assessing the clinical utility of clozapine/norclozapine ratio found no significant association with clinical response, while a subsequent clinical study on 50 patients observed an association between a higher clozapine/norclozapine ratio and clinical non-response [26,27]. Two studies demonstrated that TDM can also be useful in maintaining efficacy and safety when switching from a clozapine formulation to another, permitting a timely assessment of possible scarcely predictable intra-individual differences in blood levels due to the switch to a novel formulation [29,30]. Finally, another study showed that TDM may also assist clinicians in exploring unusual therapeutic strategies in treatment-resistant patients, such as ensuring safety in the case of prescription of off-label dosage of quetiapine [34].

Finally, since point-of-care personnel normally administer LAI antipsychotics, the role of TDM for this kind of treatment is usually underestimated and routinely less prescribed than for oral treatment, as adherence assessment is not needed. However, despite the certainty of drug assumption, the problem of not reaching adequate blood concentration due to pharmacokinetic processes concerns patients treated with LAI as well as those receiving oral treatment [12,35–39]. Furthermore, TDM can be particularly helpful during the first phase of treatment with LAI antipsychotics since, for these formulations, the

achievement of the steady state may take some months [35]. In particular, one study suggested that TDM can be useful when switching from oral to LAI formulation [11]. Another study demonstrated that under-range atypical antipsychotics serum concentrations after LAI administration predicted psychotic relapse [39]. Focusing on the first phase of treatment with paliperidone LAI formulations, an observational study reported that monthly paliperidone palmitate injection (PP1M) may take 8 months to reach the steady state and 3-month paliperidone palmitate injection (PP3M) take over 1 year [35]. Finally, four studies suggested to performed TDM with LAI formulations of antipsychotics when individual dose-finding might be difficult because of high inter-individual variability between patients [12,35–37]. This is the case of extreme age, extreme BMI, and altered cytochrome CYP2D6 activity [12,35–37].

Novel antipsychotic cariprazine pharmacokinetics needs a brief focus. Cariprazine has two active metabolites: desmethylcariprazine (DCRP) and didesmethylcariprazine (DDCRP), both pharmacologically equipotent to the maternal drug. Cariprazine and DCRP half-lives are of about 1–2 days, while DDCRP has a 2–3-week half-life, resulting in several times higher systemic exposure; cariprazine and DCRP steady states are reached on average after 2 weeks of treatment, while DDCRP steady state could need up to 8 weeks or more to be obtained, with high inter-individual variability [40]. AGNP guidelines propose TRR and dose-related concentration factors to compute DRRRs for cariprazine and its active metabolites, considering pharmacokinetic parameters, which have been subsequently reported by a specific literature review [40]. Moreover, a recent large clinical study on 2558 patients, which assessed the correlation of plasma levels of cariprazine and its active metabolites with clinical outcomes and adverse effects, confirmed the validity of the dose range recommended for schizophrenia (1.5–6 mg/d) and for bipolar mania (3–6 mg/d), in agreement with previous therapeutic drug monitoring data [41].

Bipolar Disorders

Regarding mood-stabilizing drugs, namely lithium, valproic acid, carbamazepine, and lamotrigine, TRRs are based on consolidated evidence, and TDM is highly recommended and employed for clinical decision-making [2]. Lithium stands as a singular fortunate case for which relationships between serum concentration and clinical effects are well established. A clear association between clinical response in any specific phase of bipolar disorder and blood level is defined and is of great clinical utility. Higher serum concentrations are indicated in the management of manic episodes and lower levels in depressive phases, while optimal maintenance values have to be individually determined and generally represented by low/intermediate concentration within the frame of the TRR [42]. Many atypical antipsychotics are effective in treating acute depressive or (hypo)manic episodes and as maintenance treatment and are therefore extensively prescribed for bipolar disorders. We found some evidence that TDM may help in characterizing optimal drug plasma levels according to the disease phase, as already defined for lithium [43]. In particular, about this topic, we found exclusively a prospective study conducted by Mauri and colleagues [43] on aripiprazole LAI and paliperidone LAI in patients affected by bipolar disorder type I with manic predominance. This study demonstrated that lower paliperidone plasma levels and intermediate aripiprazole plasma levels had a positive effect on depressive symptoms, which may be present and clinically relevant even in patients with this specific subtype of bipolar disorder.

Depressive Disorders

Evidence on TDM of antidepressant drugs is largely explored in the AGNP consensus guidelines [2] and in a recent meta-analysis [44], and in two reviews that extensively analyzed significant literature on most antidepressants [44,45]. Specific therapeutic reference ranges are proposed for each drug [2,45], even if a clear linear correlation between blood levels and clinical response is unclear for most available drugs [2,44,45]. Nevertheless, a prospective observational study recently demonstrated a significant bell-shaped quadratic

relationship between the efficacy of first-line antidepressants serum concentrations of those drugs, suggesting a progressive increase in antidepressants efficacy up to around the upper normalized limit of the TRR with a decrease in the antidepressant response at higher serum concentrations [46]. Furthermore, two recent works on venlafaxine conducted in a naturalistic setting showed an association between clinical response and the sum of serum concentration of venlafaxine and its active metabolite O-desmethylvenlafaxine, with a progressive increase in antidepressant efficacy up to the concentration of 400 ng/mL and a decrease at higher blood levels, suggesting that TDM, more than oral dosage, can represent the major tool for optimizing venlafaxine treatment [47,48]. Despite this recent evidence, further research with fixed doses [44] and real-world data are needed to provide clinicians with more precise and clinically relevant instruments for employing the TDM of antidepressants.

Original articles on TDM application in optimizing clinical efficacy are summarized in Table 2.

Table 2. Original articles on the use of TDM to ensure treatment efficacy.

Study	Study Design	Drugs	n	Age	Sample Characteristics	Diagnosis	Outcome
Arnaiz et al., 2021 [18]	Prospective multicentric	Olanzapine	47	26.2 ± 5.1 (mean ± SD)	Patients with FEP; ethnicity: Caucasian, other	Affective and non-affective first psychotic symptoms of at least 1-week duration	Positive association between drug C/D ratio and clinical response
Bustillo et al., 2018 [49]	Prospective multicentric	SGA	64	28.7 ± 7.3 (mean ± SD), 18–49 (range)	Patients with FEP; ethnicity: Caucasian, Hispanic	SSD and BD	Drug SC is not associated with early clinical response
Cellini et al., 2022 [46]	Prospective	Escitalopram, Duloxetine, Venlafaxine, Mirtazapine	206	58.11 ± 16.85 (mean ± SD)	Patients with current major depressive episode (HAMD-21 $\geq$ 14) treated with first-line AD ethnicity: Caucasian, other	MDD	Concentration-dependent clinical efficacy of first-line ADs with a bell-shaped quadratic function indicating a progressive increase in AD efficacy up to around the upper normalized limit of the TRR with a decrease in the AD response at higher SC.
D'Anna et al., 2022 [39]	Prospective	LAI SGA	48	44.33 ± 12.63 (mean ± SD)	Clinically stable outpatients	SSD	Under-range LAI levels predicted relapse in SSDs
Grover et al., 2022 [27]	Cross-sectional	Clozapine	50	35.7, 19–62 (mean, range)	Clozapine responders and non-responders, Asian ethnicity	Treatment-resistant schizophrenia	Association between a higher clozapine/norclozapine ratio and clinical non-response
Hyza et al., 2021 [38]	Retrospective	LAI FGA and SGA	40	45 ± 13 (mean± SD)	At least 3-month LAI treatment, ethnicity not stated	Schizophrenia and related disorders	High prevalence of subtherapeutic drug SC
Kauffmann et al., 2016 (corrigendum 2020) [22]	Prospective	SGA	87	34.7 ± 79.9 (mean ± SD), 18–58 (range)	In- and outpatients starting SGA monotherapy; ethnicity not stated	SSD	No correlation between clinical response and observed drug SC
Kylleso et al., 2021 [25]	Retrospective	Clozapine	190	Switchers: 39 ± 2 (mean ± SD); non-switchers: 43 ± 1 (mean ± SD)	Patients switching from clozapine to other AP	Schizophrenia	Association between clozapine discontinuation and low SC
Mauri et al., 2020 [43]	Prospective	LAI aripiprazole and LAI paliperidone	56	Aripiprazole: 41.92 ± 13.28 (mean ± SD); paliperidone: 40.83 ± 13.32 (mean ± SD)	Patients clinically stabilized with oral treatment, ethnicity not stated	BD with manic predominance	Lower paliperidone SC may have positive effect on depressive symptoms

Table 2. *Cont.*

Study	Study Design	Drugs	n	Age	Sample Characteristics	Diagnosis	Outcome
McCutcheon et al., 2018 [32]	Retrospective	FGA and SGA	99	Patient with SC in therapeutic range: 44.4 (median); patient with low SC: 35.7 (median)	Patients with treatment-resistant schizophrenia; ethnicity: White British, Black	Schizophrenia, schizoaffective disorder, other	Association between resistance to treatment and subtherapeutic drug SC
Melkote et al., 2018 [31]	Retrospective analysis of data from prospective RCT	Olanzapine, risperidone	316	40.9 (mean), 43 (median), 18–67(range)	Patient included in CATIE study undergoing treatment failure; ethnicity: Caucasian, African American, other	Schizophrenia	Correlation between treatment failure and antipsychotics SC below TRR
Nagai et al., 2017 [19]	Prospective	Aripiprazole	26	37.7 ± 12.8 (mean ± SD)	Japanese inpatients, early treatment phase	Schizophrenia	Optimal dose predictable through aripiprazole + dehydroaripiprazole TDM at week 1
Olmos et al., 2019 [29]	Prospective	Clozapine	98	39 (median), 20–67 (range)	Caucasian	Schizophrenia	Bioequivalence of two clozapine brands
Oloyede et al., 2020 [30]	Prospective	Clozapine	28	47 ± 11.59 (mean ± SD)	In- and outpatients; ethnicity: Asian, Black, Caucasian	Schizophrenia	Bioequivalence of two clozapine formulations
Paulzen et al., 2017 [23]	Retrospective	Risperidone	590	Responders: 46.1, 18–82 (mean, range); Non-responders: 40.9, 18–87 (mean, range)	Ethnicity not stated	Not stated	Positive association between risperidone active moiety and clinical response
Schoretsanitis et al., 2021 [36]	Retrospective	PP1M	173	Responders: 44.0, 32.0–59.0 (median, IQR); non-responders: 47.5, 39.8–58.5 (median, IQR)	Ethnicity not stated	SSD, BD, other	Possible specific patterns of clinical response according to diagnosis and SC
Schoretsanitis et al., 2022 [37]	Retrospective	PP1M	183	Control: 43.0, 33.0– 62.5 (median, IQR); Overweight: 47.0, 34.2–59.7 (median, IQR); Obese: 49.0, 39.2–57.7 (median, IQR)	Adults, elderly, normal and overweight patients	SSD, BD, other	High interindividual variability of SC, no influence of age, sex, smoking, or body weight on SC
Tien et al., 2022 [20]	Prospective	Aripiprazole	64	Aripiprazole SC: ≤300 ng/mL: 35.2 ± 14.9; >300 ng/mL: 34.3 ± 11.3 (mean ± SD)	Ethnicity; Asian—Taiwan	Schizophrenia	Higher response in terms of Clinical Global Impressions (CGI) scores with aripiprazole SC > 300 ng/mL (higher than the western population-based TRR).
Yada et al., 2021 [24]	Cross-sectional multicentric	Clozapine	131	40.1 ± 12.0 (mean ± SD), 16–72 (range)	Japanese patients	Treatment-resistant schizophrenia	Confirmed validity of AGNP clozapine TRR; doses above 1000 ng/mL are more effective but have higher toxicity risk

AP: antipsychotics; BD: bipolar disorder; C/D: concentration/dose; CATIE: Clinical Antipsychotic Trials of Intervention Effectiveness; FEP: first episode psychosis; FGA: first-generation antipsychotics; LAI: long-acting injectable; MDD: major depressive disorder; PP1M: once-monthly paliperidone palmitate; RCT: randomized clinical trial; SC: serum concentration; SGA: second-generation antipsychotics; SSD: schizophrenia spectrum disorders; TRR: therapeutic reference range.

3.1.2. Safety

As stated in the AGNP consensus guidelines, TDM is mandatory for safety reasons for drugs with a narrow therapeutic window and/or with high risk related to overdosage, such as, for example, lithium, carbamazepine, or clozapine [2]. AGNP guidelines also provide, aside from TRR values, useful laboratory alert levels for each drug, such as, for example, 1000 ng/mL for clozapine, 1.2 mmol/L for lithium, or 20 μg/mL for carbamazepine. For other drugs, in routine practice, it is often the clinician's judgment to guide dose

reduction or discontinuation because of adverse effects. However, blood levels can address proper dose-finding or appropriate discontinuation more precisely and earlier, improving treatment safety [2,11,13]. In our search, we found twelve original contributions that we present in this order: clozapine, olanzapine, other antipsychotics, and antidepressants.

Clozapine

A large real-world observational study, including 874 patients conducted after the introduction of a specific monitoring policy, showed TDM utility in individuating patients with high-risk clozapine blood concentrations [50]. Furthermore, as reported in a case report [51], easy point-of-care testing may improve clozapine TDM implementation and prevent lethal events. One study focused on the risk of neutropenia, revealing a negative relationship between norclozapine levels and neutrophil granulocyte count [52]. Regarding neurologic side effects, a multicenter cross-sectional study confirmed the validity of the TRR proposed by the AGNP guidelines and found greater efficacy when reaching clozapine serum concentrations over 1000 ng/mL, accompanied on the other hand by significantly higher central nervous system toxicity (seizures, myoclonus, sedation) [24]. Moreover, the correlation between serum concentration and seizures has also been confirmed by a recent literature review [19]. Clozapine blood levels and BMI appeared to be linked by a bi-directional relationship: on the one hand, high clozapine blood levels are associated with weight gain and insulin resistance, especially in overweight patients; on the other hand, elevated BMI, which can arise consequently to treatment, is associated with an increase in plasma concentration, probably because clozapine may deposit in body fat, leading to a consequent reduction in clearance [53]. Finally, clozapine blood concentration appeared to be positively associated with sialorrhea [54]. In conclusion, although a debate on reference range is still ongoing, TDM may also be useful in the monitoring of adverse effects [55], such as neutropenia [52], seizures [24], and sialorrhea [54].

Olanzapine, Other Antipsychotics, Antidepressants

Higher levels of olanzapine serum concentration correlated with weight gain after a two-month treatment in patients with FEP, and metabolic dysfunction was more severe and dose-dependent in drug-naive patients as compared to patients with chronic schizophrenia [18,56]. Two studies focused on the association between N-desmethyl-olanzapine (DMO), an olanzapine metabolite, and metabolic side effects [53,57], suggesting a protective role of this molecule in the development of these dangerous adverse effects. In a recent study about different drugs, higher serum antipsychotics concentrations were significantly associated with lower subjective well-being, while with paliperidone palmitate one month (PP1M), a higher serum concentration/LAI dose ratio was associated with a higher risk of developing adverse effects [58]. Focusing on specific results of this review, recent evidence demonstrated that TDM could prevent or reduce metabolic adverse effects of antipsychotics by helping to find the individual minimum effective dose in both oral and LAI treatments [45,58,59]. Regarding antidepressants, only one study was included in the present review regarding the switch from escitalopram to venlafaxine. It found a positive correlation between venlafaxine blood concentration and adverse effects, such as reduced salivation, orthostatic dizziness, and sweating [60]. All original studies presented about treatment safety are reported in Table 3.

Table 3. Original articles on the use of TDM to ensure treatment safety.

Study	Study Design	Drugs	n	Age	Sample Characteristics	Diagnosis	Outcome
An et al., 2022 [57]	Cross-sectional	Olanzapine	352	56.6 ± 14.2 (mean ± SD)	Inpatients	Schizophrenia	Negative association between plasma DMO concentrations and glucose, insulin, and triglycerides SC Positive association between plasma olanzapine concentrations and C-reactive protein and homocysteine SC

Table 3. *Cont.*

Study	Study Design	Drugs	n	Age	Sample Characteristics	Diagnosis	Outcome
Arnaiz et al., 2021 [18]	Prospective multicentric	Olanzapine	47	26.2 ± 5.1 (mean ± SD)	Patients with FEP; ethnicity: Caucasian (94.2%), other	Affective and non-affective first psychotic symptoms of at least 1-week duration	Positive correlation between drug SC and weight gain
Diaz et al., 2017 [53]	Retrospective analysis of data from RCT	Clozapine	47	45 ± 10 (mean ± SD), 28–62 (range)	Patients included in RCT; ethnicity: African Americans, Caucasians	Schizophrenia	Association between weight gain and higher SC
Engelmann et al., 2021 [60]	RCT	Venlafaxine	234	39.9 ± 12.2 (mean ± SD)	Non-responders to first-line treatment with escitalopram, ethnicity not stated	MDD	No significant correlation between venlafaxine SC and ADRs
Kang et al., 2022 [56]	Prospective	Olanzapine	117	Drug-naïve: 27.50 (24.83–30.17) Chronic: 38.82 (36.19–41.45) (Interquartile range)	First episode drug-naïf and patients with a duration of illness > 5 years ethnicity not stated	Schizophrenia	Metabolic dysfunction is more severe and dose-dependent in drug-naive patients but independent in patients with chronic schizophrenia
Kitchen et al., 2021 [50]	Retrospective	Clozapine	874	-	Patients undergoing routine TDM; ethnicity not stated	Schizophrenia, schizoaffective disorder	Reduction of patients with high-risk clozapine SC through routinary TDM implementation
Lu et al., 2018 [58]	Prospective	Olanzapine	151	41.3 ± 12.1 (mean ± SD)	In- and outpatients	Schizophrenia	Negative correlation between DMO C/D ratio and presence of metabolic syndrome. Positive correlation between olanzapine SC/DMO SC ratio and presence of metabolic syndrome. Proposal of a range for olanzapine SC/DMO SC (3–6) to maximize efficacy and reduce metabolic side effects
Schoretsanitis et al., 2021 [61]	Retrospective	PP1M	172	Patients with ADR: 50.5 (25.0) (median, IQR); patients without ADR: 47.0 (23.2) (median, IQR)	In- and outpatients, ethnicity not stated	Not stated	Paliperidone C/D ratio over 7.7 (ng/mL)/(mg/day) associated with higher ADRs risk
Schoretsanitis et al., 2021 [54]	Retrospective	Clozapine	395	Patients with hypersalivation: 41.5 (21.0) (median, IQR); patients without hypersalivation: 41.0 (22.0) (median, IQR)	In- and outpatients, ethnicity not stated	Not stated	Correlation between high clozapine SC and C/D ratio and hypersalivation
Smith et al., 2017 [52]	Retrospective	Clozapine	129	34, 20–84 (median, range)	Ethnicity not stated	Schizophrenia	Correlation between norclozapine SC and granulocyte count
Veselinović et al., 2019 [62]	Retrospective analysis of data from RCT	Aripiprazole, flupentixol, haloperidol, olanzapine, quetiapine,	69	34.8 ± 10.9 (mean ± SD)	Patients included in RCT; ethnicity not stated	Schizophrenia	Association between high SC, high D2 receptors occupancy, and low subjective well-being
Yada et al., 2021 [24]	Cross-sectional multicentric	Clozapine	131	40.1 ± 12.0 (mean ± SD), 16–72 (range)	Japanese patients	Treatment-resistant schizophrenia	Confirmed validity of AGNP clozapine TRR; doses above 1000 ng/mL are more effective but have higher toxicity risk

AD: antidepressant; ADR: adverse drug reaction; C/D: concentration/dose; DMO: N-desmethyl-olanzapine; HAMD-21: Hamilton Depression Rating Scale-21 items; MDD: major depressive disorder; PP1M: once-monthly paliperidone palmitate; RCT: randomized clinical trial; SC: serum concentration; TRR: therapeutic reference range.

3.2. Adherence

Adherence is a multidimensional phenomenon, determined by several factors related to the patient, illness, treatment, and socio-familial milieu. Treatment compliance is a major issue in mental health care, up to 70% of patients have no or only partial adherence to psychopharmacologic treatments [63–65]. Poor adherence to treatments is among the few modifiable risk factors for relapse [66], and its monitoring is therefore of crucial importance. Focusing on patients with clinical relapse presenting to emergency services, two studies found a very high prevalence of low drug plasma concentration and estimated that partial adherence or non-adherence could be hypothesized in about two-thirds of patients with schizophrenia and 50% of patients with affective disorders [67,68]. Comparable percentages were observed in a large retrospective study on psychiatric inpatients [69]. In similar samples of people acceding to inpatient emergency facilities because of a relapse of psychotic symptoms, no significant relationship has been found between subjective patient or clinician-rated adherence assessment and drug blood levels [70,71]. In patients with schizophrenia, younger age, poor clinical insight, cannabis, and substances abuse, poor premorbid functioning, the presence of specific symptoms such as paranoic thought, excitement, and lack of impulse control, and polytherapy are associated with low adherence, while the patient and familiar's positive attitude towards drugs, family involvement, and good illness insight predict adequate compliance [72,73].

Concerning outpatients, a study conducted on a very large sample observed a generally very good level of compliance, with less than 4% of the sample resulting in not adherent [74]. Higher complete non-adherence rates were found in patients receiving olanzapine compared to those receiving other antipsychotics [74]. Since both self-rated and clinician-rated adherence evaluations appear to be unreliable [70,71], TDM can be considered an essential tool in addressing adherence issues, and its use in monitoring compliance to treatment is specifically indicated by AGNP guidelines [2]. In conclusion, TDM stands as a very useful tool in distinguishing between resistance and pseudo-resistance; a larger implementation in routine care, especially in emergency services, where adherence is particularly low, can be of great clinical value. Original articles on TDM application for adherence assessment are presented in Table 4.

Table 4. Original articles on the use of TDM to ensure treatment adherence.

Study	Study Design	Drugs	n	Age	Sample Characteristics	Diagnosis	Outcome
Baldelli et al., 2020 [69]	Retrospective	AP, AD	1197	Not stated	Italian database; ethnicity not stated	Not stated	45% of patients with SC below TRR
Brasso et al., 2021 [71]	Prospective	AP, mood stabilizers	133	Patients with SSD: 43.1 ± 13.5 (mean ± SD); patients with BD: 51.9 ± 14.4 (mean ± SD)	Inpatients in a psychiatric emergency service; ethnicity: Caucasian, other	SSD, BD, and related disorders	50% of patients with SC out of TRR; no correlation between TDM and self-assessment of adherence
Geretsegger et al., 2019 [67]	Prospective	AP, AD	161	40.4 (mean)	Inpatients newly admitted to a psychiatric emergency service; ethnicity not stated	Psychotic disorders, mood disorders, other disorders	52% of patients with SC below TRR, patients with psychotic disorder are less adherent compared to patients with mood disorders
Lopez et al., 2017 [70]	Prospective	Aripiprazole, risperidone, olanzapine, paliperidone, quetiapine	97	39, 18–74 (mean, range)	Patients acceding to a psychiatric emergency service; ethnicity: African American, Asian, White, Hispanic, other	Schizophrenia, schizoaffective disorder, BD, psychotic disorder not otherwise specified	66% of patients with SC out of TRR; no correlation between TDM and clinician assessment of adherence
Silhan et al., 2018 [68]	Prospective	Citalopram, escitalopram, paroxetine, sertraline, venlafaxine	83	40.3 ± 12.2 (mean ± SD)	In- and outpatients; ethnicity not stated	Depressive disorders, anxiety disorders	37.3% of non-adherent patients in the whole sample; 56.8% of the outpatient subgroup with SC below TRR

Table 4. *Cont.*

Study	Study Design	Drugs	n	Age	Sample Characteristics	Diagnosis	Outcome
Smith et al., 2020 [72]	Retrospective	AP	24,239	44 (median), 15–106 (range)	Norwegian database; ethnicity not specified	Not stated	AP polypharmacy is associated with non-adherence
Smith et al., 2021 [74]	Retrospective	Aripiprazole, clozapine, olanzapine, quetiapine, risperidone	13,217	44.3 ± 16.0 (mean ± SD)	Norwegian database, outpatients; ethnicity not specified	Schizophrenia, other	Complete non-adherence in less than 5% of patients with psychotic symptoms; higher non-adherence in patients receiving olanzapine compared to other drugs

AD: antidepressants; AP: antipsychotics; BD: bipolar disorder; SC: serum concentration; SSD: schizophrenia spectrum disorders; TRR: therapeutic reference range.

3.3. Special Populations

Drug absorption, metabolism, distribution, and excretion are subject to relevant variation in individuals with particular conditions, such as pregnancy, limited ages, low or high body weight, and medical or surgical comorbidities. In these populations, the relationships between drug dose, blood concentration, and clinical efficacy are often highly unpredictable.

3.3.1. Peripartum

In several mental disorders, pregnancy and post-partum represent particularly critical phases for biological, psychological, and social factors and are often associated with an increased risk of relapse [75]. Pregnancy implicates alterations in pharmacokinetics, especially in drug distribution, metabolism, and excretion, leading to possibly altered blood concentration and the subsequent impact on clinical efficacy and safety. Closer clinical monitoring is needed, and TDM can play an important role, allowing a more precise dose-finding for the mother ensuring treatment efficacy and safety, and, at the same time, minimizing risks for the fetus or infant related to drug exposure via placenta or maternal milk. AGNP guidelines include pregnancy and breastfeeding as specific indications for TDM for all psychiatric drugs, with the recommendation of performing blood level testing at least once per trimester and shortly after childbirth [2]. The joint consensus statement of the American Society of Clinical Psychopharmacology and AGNP confirms such indication for antipsychotics [76].

Novel data issued in or after 2017 showed a relevant decrease over the pregnancy of serum concentrations of some first- and second-generation antipsychotics, lithium, and variations in several antidepressants' blood levels, as summarized in the following paragraphs. Focusing on antipsychotics, a large retrospective study on 110 pregnant women receiving antipsychotics revealed a relevant decrease in quetiapine and aripiprazole, up to values below 50% in the third trimester compared with the beginning of pregnancy. Increased CYP3A4 activity may explain an augmented metabolism of quetiapine, while higher CYP2D6 and CYP3A4 expression appears to implicate an increased metabolism of aripiprazole and of its active metabolite dehydroaripiprazole [12,77]. For first-generation antipsychotics, patients treated with perphenazine and haloperidol showed a trend of decreased serum concentration during pregnancy. No significant alterations were identified for olanzapine, while data on other antipsychotics were insufficient to draw relevant conclusions [78]. Focusing on LAI antipsychotic formulations, extremely low paliperidone concentrations in pregnant patients receiving 1-month paliperidone palmitate [11].

Regarding mood stabilizers, significantly lower lithium serum concentrations were observed during the third trimester compared with baseline values [79,80]. Regarding antidepressants, a systematic review and meta-analysis conducted by Schoretsanitis and colleagues searched the literature for mirror studies of comparison between drug blood levels in pregnancy and non-pregnant state in the same patient, highlighting alterations of serum concentration associated with pregnancy for the majority of drugs for which avail-

able data were found [81]. Namely, trimipramine, clomipramine, imipramine, nortriptyline, fluvoxamine, citalopram, and paroxetine showed a decrease in dose-adjusted levels, especially in the third trimester, increased concentrations were found for sertraline, whereas no significant alterations in the predicted serum concentration of fluoxetine, escitalopram and venlafaxine were detected [81]. Similar results, albeit with minor differences, were found in a recent transdiagnostic observational study of 60 pregnant women [77]. Moreover, findings from a randomized clinical trial including nine pregnant women treated with sertraline and tested for drug blood levels during the second and third trimesters, showed high interindividual variability in maternal serum concentration, stressing the need for TDM to increase treatment efficacy and safety [81]. A prospective study on breast milk concentration of three antidepressants (citalopram, sertraline, and venlafaxine) revealed that generally only a very low amount of antidepressant drug, in terms of absolute infant dose, was transmitted from mother to child, with the highest values for venlafaxine [82]. This is in line with the observational study of Leutritz et al. 2022 [77].

In conclusion, these results confirm the indication for TDM during pregnancy—especially in the third trimester—in the post-partum weeks, and in the breastfed infants, together with close clinical monitoring of psychiatric symptoms and adverse effects, in order to warrant treatment efficacy and safety of mother and child [12,79,81–84]. However, in the light of the retrieved literature in this review, as well as of studies presented in previous systematic reviews, available evidence on TDM in pregnancy and post-partum suffers from major limitations: high-quality studies based on large clinical samples are lacking on most drugs and adherence issues, drug–drug interactions and pharmacokinetics factors are often insufficiently addressed. Original articles on TDM use in peripartum considered in our review are listed in Table 5.

Table 5. Original articles on the use of TDM during peripartum.

Study	Study Design	Drugs	n	Age	Sample Characteristics	Diagnosis	Outcome
Clark et al., 2022 [80]	Prospective	Lithium	3	22–39 (range)	Women during pregnancy and post-partum; 1 Caucasian, 1 Hispanic, 1 Afro-American	BD, type I	Lithium elimination clearance increase of 63.5% by the third trimester; lithium elimination clearance was inversely related to SC; mood symptoms worsened with declines in SC; lithium elimination clearance returned to baseline at 4 to 9 weeks postpartum
Heinonen et al., 2021 [83]	RCT	Sertraline	9	24–39 (range)	Women during pregnancy and post-partum, infants; ethnicity not stated	Depression	High interindividual maternal serum concentration, low infant exposition
Leutritz et al., 2022 [77]	Retrospective and Prospective	Amitriptyline, Aripiprazole, Bupropion, Citalopram Clomipramine, Duloxetine, Escitalopram, Lamotrigine, Mirtazapine Paroxetine, Quetiapine, Sertraline, Venlafaxine	60	33.26 ± 2.45 (mean ± SD)	Outpatients during pregnancy and post-partum infants; ethnicity not stated	Major depressive disorder, Anxiety disorders, Obsessive–compulsive disorder, Bipolar disorders, Schizoaffective disorder, Adjustment disorder, Substance use disorders	↓ SC from the I to the II trimester of amitriptyline, duloxetine, escitalopram, quetiapine, and sertraline; citalopram stayed stable during pregnancy, ↑ sertraline SC from the II to the III trimester; high concentration-by-dose ratios in breastmilk for venlafaxine and lamotrigine, low for quetiapine and clomipramine
Schoretsanitis et al., 2019 [82]	Prospective	Citalopram, sertraline, venlafaxine	17	23–40 (range)	Breast-feeding women; ethnicity not stated	Depressive episode	Higher breastfed children exposure to venlafaxine

Table 5. *Cont.*

Study	Study Design	Drugs	n	Age	Sample Characteristics	Diagnosis	Outcome
Westin et al., 2017 [79]	Retrospective	Lithium	13	32.9 ± 3.8 (mean ± SD)	Pregnant women, assessment at baseline, during pregnancy, and after delivery; ethnicity not stated	BD	↓ lithium SC during III trimester
Westin et al., 2018 [84]	Retrospective	AP	103	29 (mean)	Pregnant women, assessment at baseline and during pregnancy; ethnicity not stated	Not stated	↓quetiapine and aripiprazole SC during III trimester

AP: antipsychotics; BD: bipolar disorder; RCT: randomized clinical trial; SC: serum concentration.

3.3.2. Adolescents

Adolescence is a developmental period characterized by major changes in both pharmacokinetics parameters (such as body weight and height) and central nervous system development. Several major psychiatric disorders have onset in adolescence, and psychotropic drugs are largely prescribed in this population [85,86]. However, pharmacotherapy is often associated with suboptimal treatment effects, and evidence in this population is relatively lacking [87]. Moreover, comorbidity with substance use is very common, leading to possible influence on drug metabolism and substance-drug interactions, and adherence issues are a rule more than an exception. Therefore, the dosing regimen and correlations between dose, blood concentration, clinical effects, and toxicity evidenced in adults may not be applicable to adolescents for many psychoactive drugs [88–90]. For these above-mentioned reasons, AGNP guidelines strongly recommend TDM to optimize drug treatment in adolescents suffering from mental disorders [2,76]. However, TDM is still largely unemployed in routine clinical practice. Amongst the reasons for this insufficient application of TDM, it is necessary to consider a substantial lack of clear and generally accepted age-specific data assessing the relationship between dose, drug blood levels, and clinical outcomes and defining specific therapeutic and dose-related reference ranges. In reviewing literature published after AGNP guidelines, we considered studies presenting data on patients aged from 14 on.

Only a recent prospective study focused on the relationship between daily dose, serum concentration, and treatment efficacy in adolescents. In particular, it demonstrated higher sertraline daily doses and serum concentrations are more effective in the treatment of OCD in adolescents [91]. Regarding dose-related concentration, about half of the psychotropic drugs assessed in the review by Fekete et al. [92] resulted in having different values compared to adults. Specifically, haloperidol, olanzapine, citalopram, clomipramine, fluvoxamine, and imipramine showed higher dose-related concentrations, while quetiapine, lamotrigine, oxcarbazepine, and topiramate showed lower levels compared to adults. For clozapine, risperidone, ziprasidone, aripiprazole, fluoxetine, paroxetine, sertraline, escitalopram, duloxetine, lithium, valproic acid, carbamazepine, methylphenidate, atomoxetine, guanfacine dose-concentration parameters similar to adults were observed. According to the review conducted by Kloosterboer et al. [93] in an effort to define also for adolescent patients clear blood levels/efficacy/tolerability relationships, an association between drug concentration and both efficacy and side effects was found for methylphenidate and imipramine, a concentration–efficacy relationship was evidenced for quetiapine, citalopram, fluoxetine, nortriptyline, bupropion, and lithium, while a concentration- side effects relationship was highlighted for ziprasidone, venlafaxine, and desipramine. A third recent review specifically addressed selective serotonin reuptake inhibitors (SSRI) TDM in children and adolescents, considering pharmacogenetics profiles, adherence issues, DDI, and drug–substance interactions. Adolescents with low CYP2C19 activity showed higher escitalopram and sertraline exposure and Cmax, while paroxetine clearance resulted in being highly dependent on CYP2D6 activity also for young patients. CBD and THC inhibit

CYP activity, and their chronic assumption can therefore lead to increased SSRI plasma concentrations. Oral contraceptives' effect on reducing citalopram and escitalopram serum concentrations has been observed, whereas proton-pump inhibitors can increase SSRIs blood levels [94].

The three retrospective observational studies, subsequent to the cited reviews, integrate some of the previously lacking information. In particular, Fekete et al. found lower dose-corrected serum concentrations for risperidone and venlafaxine in adolescents compared to adults [95]. The influence of sex and body weight on risperidone and aripiprazole blood levels were analyzed, finding for both drugs higher dose-adjusted concentrations in girls, lower risperidone active moiety serum concentration in lower weight patients and a positive correlation between weight and serum levels of aripiprazole [96,97]. A correlation between higher aripiprazole dose-related serum levels in adolescents and African ethnicity has been hypothesized based on preliminary data [98].

We found two systematic reviews that addressed the issue of TRR and DRRR in adolescence, proposing some novel parameters for various drugs [92,93]. Overall, these two systematic reviews found highly heterogeneous data. Finally, a recent prospective study highlighted an association between higher risperidone serum concentrations and extrapyramidal side effects, suggesting a lower TRR for this antipsychotic in adolescence [99]. In conclusion, adequate studies are lacking for several largely employed drugs in adolescents, most retrieved studies were not of sufficient quality, and most findings were not replicated. Therefore, as already hoped for in the AGNP guidelines [2], in order to better support routine TDM application in adolescents, further high-quality research on the determination of therapeutic and dose-related reference ranges, pharmacogenetic variants, substances, and drug interactions is needed to confirm and integrate present evidence.

3.3.3. Elderly Patients

Aging determines a progressive involvement of the functioning of multiple organs, with a reduction of renal and liver function, and often implies changes in weight and distribution volume. Notably, as most pharmacological clinical trials do not include patients over 65, evidence on this population is limited and based on post-marketing data. Moreover, off-label prescription of psychoactive drugs is relatively frequent. Elderly patients frequently bear the burden of physical comorbidities, are treated with polypharmacotherapy, and often display higher sensitivity to drug adverse effects. About psychotropic drugs, those with anticholinergic activity may particularly hit on elderly patients' frailty, determining an increased risk of delirium and a decrease in cognitive functions. Considering such elements, TDM in elderly patients is recommended, although evidence on specific reference ranges is still insufficient [2,76].

After the issue of AGNP guidelines, this topic has been reprised by two retrospective analyses using the same large dataset that revealed a significant impact of age on antipsychotic blood levels. In detail, Castberg et al. observed a large effect of age on clozapine, olanzapine, risperidone, and quetiapine dose-adjusted concentration, with a particularly relevant increase from 80 years of age onwards [99]. This effect was most prominent for clozapine, with a 2-fold dose-adjusted concentration for patients aged 80 and a 3-fold dose-adjusted concentration for patients aged 90 compared to patients aged 40 years. Patients treated with olanzapine, the drug for which age-related concentration increase was less prominent, had a 28% dose-adjusted concentration increase at 80 years and a 2-fold increase at 90 years. Concentrations observed in females were generally higher than in males. Jönsson and colleagues conducted analyses on the same large dataset considering patients treated with amisulpride, aripiprazole, clozapine, flupenthixol, haloperidol, olanzapine, perphenazine, quetiapine, risperidone, sertindole, zuclopenthixol, and ziprasidone [100]. For all drugs except flupenthixol and ziprasidone, higher dose-related concentrations were observed in patients over 65 compared to those under 65, with relatively lower concentration/dose ratios for higher drug doses compared to patients receiving low drug

doses for most drugs. This study confirmed the finding that in the elderly dose-adjusted concentrations are higher in females than in males.

Subsequent studies confirmed the findings of these two large retrospective analyses for oral administration of amisulpride, zuclopenthixol, olanzapine, and risperidone. Huang et al., in a study conducted on a Chinese population receiving amisulpride, observed an age-related increase in dose-adjusted concentration, leading to a possible indication of a specific age-related dosage of amisulpride (i.e., doses over 600 mg/d should not be recommended in patients over 60) [78]. Another small clinical study on eight patients of different ethnicities suggested relevant receptor occupancy and adequate clinical efficacy at relatively low amisulpride dosage in the elderly [101]. A large study on zuclopenthixol showed an age-dependent serum level increase [102]. For olanzapine, a large sample study by Tveito et al. and two studies on the Chinese population confirmed higher olanzapine dose-adjusted blood concentration and lower concentration of its metabolite desmethyl-olanzapine in the elderly [103–105]. Age and sex-related alterations for risperidone were replicated by Fekete et al., with higher dose-corrected serum concentrations of risperidone found in older patients and females [95]. With regard to LAI treatment in the elderly, interesting data showed no age effect on olanzapine LAI absorption and blood levels, in contrast with the olanzapine serum concentration increase observed for the oral formulation while a significant age-dependent increase, especially in women, was observed PP1M and zuclopenthixol, confirming data on the oral formulation, while only small effects of age emerged for fluphenazine and aripiprazole [11,35,102,103,106].

The newest studies on mood stabilizers confirmed linear age-dependent pharmacokinetics for lamotrigine, with up to 30% reduced clearance in the elderly [13,107]. Focusing on antidepressants, sertraline, citalopram, escitalopram, mirtazapine, and venlafaxine blood levels appear to be particularly influenced by age and sex, with a significant proportion of patients in real-world populations, especially elderly women, exposed to concentrations above the TRR [13,45,48,95]. Finally, focusing on the adverse effects of antidepressants in the elderly, a study demonstrated a correlation between amitriptyline and venlafaxine serum concentration and the extent of drug-induced QT prolongation [108]. Based on the studies included in this review [11,13,45,48,78,95,99–108], TDM may play an important role in optimizing treatment in aged patients, keeping in mind that the elderly, according to the reported data, should not be considered a homogenous population, with age and sex largely influencing drug blood levels. Table 6 presents original articles on TDM in adolescents and the elderly included in our review.

Table 6. Original articles on the use of TDM in adolescents and elderly patients.

	Study	Study Design	Drugs	n	Age	Sample Characteristics	Diagnosis	Outcome
Adolescents	Egberts et al., 2020 [97]	Retrospective	Aripiprazole	130	15.0 ± 2.6 (mean ± SD), 7.6–19.0 (range)	65% of the patients treated with polytherapy; ethnicity not stated	SSD, mood disorders, other	Aripiprazole TRR for adolescents similar to adults; positive correlation between weight and aripiprazole SC
	Fekete et al., 2021 [95]	Retrospective	Risperidone, venlafaxine	Total sample: 1555; patients < 18: 100	Patients < 18 treated with risperidone: 14.0; 4.0 (mean; IQR), 7–17 (range); patients < 18 treated with venlafaxine: 16.0; 2.0 (mean; IQR), 12–17 (range)	German database; ethnicity not stated	Not stated	Risperidone and venlafaxine dose-adjusted SC lower in adolescents than adults
	Piacentino et al., 2020 [96]	Retrospective	Aripiprazole, risperidone	140	14.2 ± 3.1 (mean ± SD), 5−18 (range)	Ethnicity not stated	Oppositional Defiant/Conduct Disorders	Higher aripiprazole and risperidone dose-adjusted SC in girls; lower risperidone active moiety SC in lower-weight patients

Table 6. *Cont.*

	Study	Study Design	Drugs	n	Age	Sample Characteristics	Diagnosis	Outcome
Adolescents	Taurines et al., 2022 [109]	Prospective	Risperidone	64	15.6 ± 1.7 (mean ± SD), 11–18 (range)	Inpatients and outpatients; Ethnicity not stated	SSD	Higher SC associated with a higher risk of EPS. Preliminary indications for a lower TRR in this population
	Tini et al., 2022 [91]	Prospective	Sertraline	78	14.2 ± 2.4 (mean ± SD), 7–18 (range)	Ethnicity not stated	Obsessive–compulsive and Major Depressive Disorders	Strong linear positive dose–serum concentration relationship; significant effects of weight and co-medication; no association between dose or SC and side effects; higher doses and SCs are more effective in the treatment of the OCD
Elderly	An et al., 2021 [105]	Retrospective	Olanzapine	185	18–87 (range), 67.6% of the sample aged ≥56	Chinese population	Schizophrenia	Age-related ↓ N-desmethyl olanzapine SC
	Castberg et al., 2017 [99]	Retrospective	Clozapine, olanzapine, quetiapine, risperidone	11,968	18–100 (range)	Data from Norwegian database; ethnicity not stated	Not stated	Age-related ↑ dose-adjusted SC of clozapine, olanzapine, quetiapine, risperidone, particularly in women
	Deng et al., 2020 [104]	Retrospective	Olanzapine	884	38 ± 16 (mean ± SD), 13–90 (range)	Chinese population	SSD, BD	Age-related ↑ olanzapine SC and dose-adjusted SC
	Fekete et al., 2020 [95]	Retrospective	Risperidone, venlafaxine	Total sample: 1555, patients > 60 years: 428	Patients > 60 treated with risperidone: 73.0; 11.0 (mean; IQR), 61–92 (range); Patients > 60 treated with venlafaxine: 71.0; 13.0 (mean; IQR), 60–93 (range)	German database, ethnicity not stated	Not stated	Age-related ↑ risperidone dose adjusted SC
	Hansen et al., 2017 [48]	Retrospective	Venlafaxine	1177	45 (median), 34–59 (IQR range)	Danish database, ethnicity not stated	Not stated	↑ dose-adjusted venlafaxine SC in patients over 64
	Hefner et al., 2019 [108]	Retrospective	Amitriptyline, venlafaxine	34	69.7 ± 3.5 (mean ± SD), 65–78 (range) (data referred to the whole database from which data on the 34 patients included in the study are taken from)	Ethnicity not stated	Not stated	Correlation between amitriptyline and venlafaxine SC and QT prolongation in the elderly
	Huang et al., 2021 [78]	Retrospective	Amisulpride	121	35.83 ± 13.50 (mean ± SD)	Inpatients Chinese population	Schizophrenia	Age-related ↑ dose-adjusted SC of amisulpride; proposal of 600 mg/day as the maximum dosage of amisulpride in patients over 60
	Jönsson et al., 2019 [100]	Retrospective	Amisulpride, aripiprazole, clozapine, flupenthixol, haloperidol, olanzapine, perphenazine, quetiapine, risperidone, sertindole, zuclopenthixol, ziprasidone	Different n° of patients for each drug, ranging from 11,272 (olanzapine) to 225 (sertindole)	Different ages for each drug ranging from 31 (median, sertindole) to 50 (median, haloperidol)	Data from Norwegian database; ethnicity not stated	Not stated	Age-related ↑ dose-adjusted SC of amisulpride, aripiprazole, clozapine, haloperidol, olanzapine, perphenazine, quetiapine, risperidone, sertindole, zuclopenthixol, particularly in women

Table 6. *Cont.*

	Study	Study Design	Drugs	n	Age	Sample Characteristics	Diagnosis	Outcome
Elderly	Reeves et al., 2018 [101]	Prospective	Amisulpride	8	76 ± 6 (mean ± SD)	Outpatients; Caucasian, African, Asian	Very late-onset schizophrenia-like psychosis	D2 receptor occupancy over 40% and good clinical efficacy with an amisulpride dose of 50 mg/day
	Smith et al., 2018 [107]	Retrospective	Lamotrigine	534	40 (median), 18–95 (range)	Norwegian database, ethnicity not stated	Not stated	Age-related ↑ lamotrigine dose-adjusted SC, particularly in women carrying the UGT1A4*3 allele
	Tveit et al., 2020 [45]	retrospective	Citalopram, escitalopram, mirtazapine, sertraline, venlafaxine	806 (2007 cohort); 1932 (2017 cohort)	2007 cohort, age < 65: 41, 19 (median, IQR); age ≥ 65: 76, 13 (median, IQR); 2017 cohort, age < 65: 41, 22 (median, IQR); age ≥ 65: 79, 15 (median, IQR)	Norwegian database, ethnicity not stated	Not stated	Age-related ↑ citalopram, escitalopram, mirtazapine, sertraline, venlafaxine SC, especially in women. Relevant percentage of the sample exposed to concentrations above TRR
	Tveito et al. 2021 [106]	Retrospective	Paliperidone LAI	1223	PP1M: 41.1 (mean) PP3M: 44.3 years (mean)	Norwegian database, one-third of the sample aged > 50; ethnicity not stated	Not stated	Age-related ↑ paliperidone dose-adjusted SC for paliperidone LAI users, especially in women
	Tveito et al., 2018 [103]	Retrospective	Olanzapine oral and LAI	8288	45, 18–102 (median, range)	Data from Norwegian database; ethnicity not stated	Not stated	Age-related ↑ olanzapine dose adjusted SC for oral formulation but not LAI users
	Tveito et al., 2021 [102]	Retrospective	Zuclopenthixol oral and LAI	2044	Oral subgroup: 52.3 ± 17.5 (mean ± SD); LAI subgroup: 47.3 ± 15.4 (mean ± SD)	Data from Norwegian database; ethnicity not stated	Not stated	Age-related ↑ dose-adjusted SC of zuclopenthixol for both oral and LAI formulation; LAI users over 65 and with low CYP2D6 function at risk of high SC exposure

BD: bipolar disorder; EPS: extrapyramidal side effects; LAI: long-acting injectable; PP1M: 1-month paliperidone palmitate injection; PP3M: 3-month paliperidone palmitate injection; SC: serum concentration; SSD: schizophrenia spectrum disorders; TRR: therapeutic reference range.

3.3.4. Extreme Body Weight

Weight can have a significant impact on pharmacokinetics, determining alterations, particularly in volume distribution and excretion. However, body weight impact on psychotropic drugs serum concentration is variable and often not of clinically valuable significance; therefore, no on-label specific indication for weight-adjusted dosage is reported for most drugs. Nevertheless, body weight can represent a relevant cause of scarcely predictable concentration/dose ratio, both at the population or individual levels, and abnormal weight is therefore comprised in the AGNP guidelines recommendations for TDM [2].

Obesity

A recent study by An et al. conducted on overweight patients receiving olanzapine showed that body weight significantly influences serum concentration, volume distribution, and elimination rate in the Chinese population [105]. Similarly, high BMI can relevantly impact clozapine serum concentration through the augmentation of volume distribution and hepatic enzyme activity alterations, finally resulting in a decrease in clozapine clearance and more elevated plasma levels and concentration/dose ratio [53,110]. Conversely, the concentration/dose (C/D) ratio observed in obese patients receiving PP1M was lower compared to the whole sample [35]. Recently, a clinical study on a real-world population

of patients with mania has confirmed the role of body weight in influencing sodium valproate serum concentrations, with an augmented clearance in overweight patients [111]. Similarly, a negative correlation between weight and venlafaxine C/D ratio and between BMI and venlafaxine serum concentrations has been observed [112,113]. Overall, these studies confirm the findings on which guideline recommendations are based, stressing the importance of TDM in overweight patients and over-significant weight variation in the same patient.

Low Body Weight and Eating Disorders

Low BMI and/or the presence of an eating disorder can determine highly relevant alterations in drug absorption, distribution, and metabolism. Although abnormally low body weight represents a specific indication for TDM, and its application in eating disorders comprising extremely low body weight patients is potentially beneficial, relevant literature evidence is lacking. No specific body-normalized reference ranges are available for underweight patients, and pharmacologic treatment is mostly empirically conducted [2,113]. Besides a plea for new clinical studies on TDM in low-weight patients and in eating disorders, we found only one work on this issue [112]. It included patients with BMI below 20 kg/m^2 and observed that sex, and not BMI or weight, could relevantly influence venlafaxine metabolism in the subgroup of low-weight patients, determining higher C/D levels of venlafaxine and its active moiety [112]. Original studies on the role of TDM in patients with abnormal weight are listed in Table 7.

Table 7. Original articles on the use of TDM in patients with abnormal body weight.

Study	Study Design	Drugs	n	Age	Sample Characteristics	Diagnosis	Outcome
An et al., 2021 [105]	Retrospective	Olanzapine	185	18–87 (range)	Chinese population	Schizophrenia	High body weight associated with ↓ olanzapine and n-desmethylolanzapine SC
Diaz et al., 2017 [53]	Retrospective analysis of data from RCT	Clozapine	47	45 ± 10 (mean ± SD), 28–62 (range)	Patients included in RCT; ethnicity: African Americans, Caucasians	Schizophrenia	Association between weight gain and ↑ SC
Kuzin et al., 2021 [110]	Retrospective	Clozapine	455	19–88 (range)	German database, in- and outpatients, ethnicity not stated	Not stated	High BMI associated with ↑ clozapine SC and C/D ratio
Methaneethorn et al., 2017 [111]	Retrospective	Valproic acid	206	39.3 ± 13.1 (mean ± SD)	Asian ethnicity	BD, manic episode	Reduced clearance in overweight patients
Schoretsanitis et al., 2018 [112]	Retrospective	Venlafaxine	737	45.4 ± 14.6 (mean ± SD)	German database, in- and outpatients, ethnicity not stated	SSD, mood disorders, other	Negative correlation between BMI and venlafaxine active moiety SC, O-desmethylvenlafaxine SC, and venlafaxine C/D ratio
Warrings et al., 2021 [113]	Retrospective	Amitriptyline, clozapine, doxepin, escitalopram, mirtazapine, quetiapine, risperidone, venlafaxine	1657 (whole sample)	18–92 (range)	In- and outpatients, ethnicity not stated	Not stated	Negative correlation between BMI and venlafaxine active moiety SC, O-desmethylvenlafaxine SC

BD: bipolar disorder; BMI: body mass index; C/D: concentration/dose; SC: serum concentration; SSD: schizophrenia spectrum disorders.

3.3.5. Other Medical and Surgical Conditions That Might Influence Pharmacokinetics

Systemic diseases, especially those involving gastrointestinal, renal, and hepatic systems, can significantly modify most pharmacokinetics parameters. Although renal and liver impairments are probably the most common clinical conditions that impact drug exposure, we found only one relevant review subsequent to the AGNP guidelines issue. It focuses on psychonephrology, i.e., the discipline that studies the connection between mental and kidney health, and suggests that TDM may be a useful tool for adjusting the dosage of psychotropic drugs appropriately in patients with renal disease and also in

patients undergoing dialysis [114]. Therefore, we focused on systemic inflammation, HIV infection, and post-surgical conditions, which are the topics about which recent studies provided new significant insights.

Systemic diseases characterized by acute or chronic inflammation may significantly impact drug pharmacokinetics parameters. This effect is mediated mainly through the induction of the acute phase protein α1-acid glycoprotein and variation of other circulating proteins, with consequently altered drug-binding capacity, and via the inhibition of CYP enzyme synthesis mediated by inflammatory mediators such as interleukins 6 and 1, and tumor necrosis factor α. In particular, the interrelationship between inflammation and psychosis is a very intriguing and debated topic. On the one hand, infections and immune system alterations have been implicated in the etiopathogenesis and course of schizophrenia; on the other hand, schizophrenia itself appears to possibly have an influence on the inflammatory status and immune system, with some biological parameters linked to the immune functions prospectively representing possible biomarkers of psychotic disease activity. Antipsychotics also have an impact on the immune system, their therapeutic effect could be partially mediated by immunomodulation, and some of their adverse effects are associated with immune system alterations (metabolic syndrome, myocarditis, and pericarditis) [115].

In the presence of systemic disease, on the one hand, a reduced CYP1A2 activity may increase clozapine blood levels and lead to potentially life-threatening toxicity, while on the other hand, inflammatory status with a marked increase in α1-acid glycoprotein and consequent reduction of unbound drug fraction may minimize adverse effects even in the presence of high clozapine serum concentrations. This complex interaction between inflammation and clozapine distribution and metabolism clinically results in an unstable equilibrium that can determine the occurrence of very high blood levels in the absence of relevant related symptoms [115]. This is in line with the results of our research that found two clinical studies on psychiatric patients with systemic infection showing possible clearance reduction and increased serum concentration of risperidone, clozapine, quetiapine, and aripiprazole [116–118]. Considering the above, measurement of individual drug levels over an episode of systemic inflammation, along with closer clinical monitoring of adverse effects, is highly recommended.

Focusing on HIV infection, we found an observational study conducted by Courlet et al. in HIV+ patients treated with escitalopram. It showed that over half of the patients might have serum concentration under the TRR, highlighting relevant and scarcely predictable interindividual variability, with a general tendency towards drug under-exposure, in which drug–drug interaction appears to play a minimal role [119]. Finally, gastrointestinal surgery leads to largely unpredictable alterations in drug absorption, along with subsequent possible body weight decreases and drug distribution volume variations. AGNP guidelines recommend TDM in patients with gastrointestinal resection or bariatric surgery [2]. This indication is confirmed by two studies included in the current review [120,121]. In particular, the observational study by Wallerstedt and Colleagues on patients undergoing bariatric surgery demonstrated high inter-individual variability in drug blood levels, with lower dose-adjusted serum concentrations of sertraline, mirtazapine, duloxetine, and citalopram found after the intervention compared to pre-operatory values [120]. The other work reported two cases of psychiatric patients subjected to bariatric surgery [120]. It evidenced significant antipsychotic serum concentration variations after surgery and suggested a role for long-acting antipsychotic treatment in this population [121]. Table 8 shows original articles on TDM use in patients with systemic inflammation or other relevant medical conditions.

Table 8. Original articles on the use of TDM in patients with systemic inflammation or other medical conditions.

Study	Study Design	Drugs	n	Age	Sample Characteristics	Diagnosis	Outcome
Courlet et al., 2019 [119]	Retrospective	Escitalopram	110	48, 36–56 (median, IQR)	Patients living with HIV, control group of patients not affected by HIV	Not stated	Escitalopram SC below TRR in 56% of HIV + patients; no significant DDI with antiretroviral drug identified
Scherf-Clavel et al., 2020 [117]	Retrospective	Aripiprazole, olanzapine, quetiapine, risperidone	Aripiprazole: 30, olanzapine: 24, quetiapine: 166, risperidone: 45	18–85 (range)	In- and outpatients with CRP concentration $\geq$ 0.5 mg/dL	Not stated	Positive correlation between elevated CRP and quetiapine C/D
Zhang et al., 2021 [116]	Retrospective	Aripiprazole, clozapine, quetiapine, risperidone	Aripiprazole: 13, clozapine: 42, quetiapine: 21, risperidone: 36	16–76 (range)	Inpatients with respiratory tract infections	Not stated	Higher C/D ratios during infection for all drugs considered

C/D: concentration/dose; CRP: C-reactive protein; DDI: drug–drug interaction; SC: serum concentration; TRR: therapeutic reference range.

3.4. Interactions with Psychotropic Drugs

3.4.1. Drug–Drug Interactions

In the real world, patients often receive more than one drug because they present comorbid medical diseases or need psychotropic polypharmacotherapy. In both cases, potentially relevant drug–drug interactions (DDI) may occur, especially when inhibitors or inducers of drug-metabolizing enzymes are combined with compounds that are the substrate of inhibited or induced enzymes. In these cases, TDM should support individual dosing to ensure treatment efficacy and tolerability. Significantly, in a real-world study on highly adherent patients in polypharmacotherapy, a very high rate of drugs under exposition was found, with almost half of patients having psychotropic drug levels under the therapeutic reference range. Once poor adherence risk is ruled out, polypharmacotherapy stands as a very relevant factor in determining drug exposure, with a need for close clinical monitoring and drug blood level assessment through TDM [122]. Moreover, even when a clear relationship between the coadministration of enzyme inducers and monitored drug's blood levels are known, as, in the case of lamotrigine, real-world data show that dose adjustments and TDM recommendations are rarely followed [123]. A systematic treatise of drug–drug interactions (DDI) on psychotropic treatments is already presented in previous studies [2,11,13–15] and goes beyond the scope of this article. However, we will synthetically focus on the latest evidence, providing an update to the above-cited works.

TDM studies on antipsychotics revealed significant DDI between risperidone and perazine, levomepromazine, melperone, and pipamperone [124,125]. Valproate comedication resulted in decreased olanzapine concentration of up to 40% when adjusting by dose and weight [104]. Coadministration of aripiprazole and other antipsychotics (clozapine, risperidone, quetiapine, and olanzapine) resulted in lower aripiprazole concentration/dose ratios [126]. In patients receiving valproic acid and clozapine, a significant impact on clozapine metabolism was observed, with reduced absolute and dose-adjusted norclozapine serum concentrations [127,128]. Conversely, no relevant effect of sertraline nor pantoprazole comedication was observed on clozapine metabolism [93,94]. Finally, a recent observational study demonstrated a negative relationship between vitamin D levels and dose-adjusted antipsychotic drug concentrations, particularly pronounced for drugs predominantly metabolized by the CYP3A4 (e.g., aripiprazole and quetiapine) [129]. This seems to be due to vitamin D-mediated induction of CYP3A4 [129].

Regarding antidepressants, a significant interaction between sertraline and metamizole was identified, resulting in a decrease in sertraline levels [130]. Venlafaxine metabolism appears to be reduced by quetiapine, frequently employed as augmentation therapy in depression, with higher O-desmethylvenlafaxine and venlafaxine active moiety levels observed [131]. Omeprazole and pantoprazole also showed an inhibitory effect on venlafaxine metabolism [132]. A prospective study on fluoxetine, assessing both drug concentrations

and clinical response, revealed an association between depressive symptoms and the presence of CYP2D6 inhibition due to a co-administered drug [133]. We found some studies that demonstrated specific DDIs [124–135]; however, it has to be considered that significant variations of drug blood concentrations observed in most of the reported studies are not necessarily associated with altered clinical efficacy or tolerability, and further research is needed to determine the clinical relevance of observed interactions.

3.4.2. Drug–Smoke Interaction

Although smoking habits are not directly reported in AGNP guidelines and TDM recommendations, smoke can have a large impact on drug metabolism. Smoking directly induces hepatic CYP1A2; therefore, patients receiving drugs that are CYP1A2 substrates may show reduced drug blood levels. To help clinicians' decision-making, it has to be kept in mind that an average of 10 cigarettes per day is sufficient to reach the maximum of CYP1A2 induction so that variations in smoking habits, such as passing from 5 to 10 cigarettes a day or vice versa can be of clinical relevance, whereas changes from 10 to 20 or more do not imply significant pharmacokinetic changes. Moreover, electronic cigarettes or nicotine patches do not have the same impact on CYP1AP activity, and therefore, changes in patients' habits from smoking to these products need to be considered. Other ways through which smoke can affect drug metabolism and effects have also been hypothesized, such as the effect of nicotine in altering brain-blood barrier permeability to drugs and epigenetic and microbiome modifications [115]. An indirect relationship between smoke and low drug serum concentration may also be present in psychiatric patients, as smoking is significantly related to lower cognitive performance, global functioning, economic status, and poorer prognosis [136–138]. These clinical and demographic characteristics may be associated with lower illness insight and awareness of the need for treatment and consequent poor adherence, as well as a higher prevalence of unhealthy lifestyles habits such as alcohol and substance use, with the more frequent presence of comorbidities and co-medications and possible drug–drug or drug–substance interactions [137,139]. This may finally result in lower serum concentrations of psychopharmacological treatments in smokers, as confirmed by a recent real-world study in an emergency setting [72].

The role of CYP1A2 induction is well studied for several drugs, i.e., olanzapine and clozapine, and is reported in the review cited above [115]. Nevertheless, it is worth signaling some more recent work confirming clinically relevant interactions between smoke and drug plasma levels that were not previously adequately verified in clinical samples [140–143]. Considering the direct and indirect relationships between smoke and the finding of lower drug serum concentrations found in smokers compared to non-smokers, TDM can be a very useful clinical tool for this very frequent sub-population of people with mental disorders. Studies conducted in naturalistic settings confirmed the role of smoke in reducing duloxetine levels via induction of CYP1A2 [109], found no smoke impact on paliperidone metabolism, and proved a beneficial effect of fluvoxamine augmentation in increasing clozapine blood levels in smokers, neutralizing smoke effect on CYP1A2 activity [141,142]. Finally, a retrospective naturalistic study observed reduced amitriptyline and mirtazapine serum concentrations in smokers, although CYP1A2 does not theoretically play a major role in their metabolism, enlarging the possible role of CYP2C19 e CYP3A4 induction. On the other hand, no differences between smokers and non-smokers were detected for risperidone, about which CYP3A4 induction role in reducing its concentrations is still debated [143].

3.4.3. Other Interactions

Drugs and smoke are obviously not the only factors involved in pharmacokinetic interactions. Food and alcohol intake may significantly impact drug absorption and clearance. Clinicians should be aware of food and alcohol's role in influencing drug concentrations, and food and alcohol intake habits need to be expressively addressed in clinical interviews. Food may alter drug availability influencing absorption, as in the case of lurasidone and

ziprasidone, whose absorption is increased by fatty food and through specific CYP induction or inhibition [2]. Similarly, alcohol use effects on drug metabolism may be mediated by CYP2E1 induction or indirectly via the chronic liver or gastric alterations [2]. About this topic, we found one retrospective observational study on the use of TDM for patients with major depressive disorder and alcohol use disorder treated with escitalopram [144]. According to this study, alcohol dependence alone does not lead to pharmacokinetic changes in the metabolism of escitalopram but altered liver function, in terms of elevated GGT in combination with an AST/ALT ratio ≥ 1, does [144].

3.5. Pharmacogenetics and TDM

A systematic treatise of the topic would require a specific focus that goes beyond the scope of this review. However, we provide a rapid overview of what is new after AGNP guidelines on the combined use of TDM and pharmacogenetics testing.

3.5.1. Antipsychotics

A significant impact of CYP2D6 variants, namely nonfunctional variant alleles (CYP2D6*3, *4, *4N, *5, *6, *7, *8, *11, *12, *13, *14A, *15, *36, *68) and the reduced function variant alleles (CYP2D6 *2, *9, *10, *14B, *17, *29, *41) has been observed for several first and second-generation antipsychotics [101–105]. In particular, a 3.9-fold increase in dose-adjusted serum concentration of perphenazine, a 1.5-fold increase for zuclopenthixol, 1.6-fold for risperidone, 1.4-fold for aripiprazole, and a significant increase for olanzapine in poor metabolizers (PM, i.e., patients with only null alleles) compared with normal metabolizers have been observed [145–149]. Conversely, risperidone treatment failure has been associated with a CYP2D6 variant (CYP*2A, a variant with increased metabolic activity) or multiple copies of CYP*1 or *35 (variants with normal activity) [146,150], while a higher maximum dose of aripiprazole has been proposed for ultrarapid metabolizers (UM, i.e., patients with two CYP2D6*2A alleles or three or more normal activity alleles) [149,150]. Focusing on clozapine treatment failure due to increased metabolism, we found three original contributions that adopted a pharmacogenetic approach. A genome-wide association study revealed a possible role of a non-previously considered polymorphism in modulating clozapine serum levels, namely the rs28379954 T > C polymorphism of the Nuclear Factor IB (NFIB) gene, that links to DNA and favors DNA transcription by RNA polymerase II. NFIB appears to be involved in the transcription of genes involved in clozapine metabolism, leading to reduced clozapine levels [151]. A case report found a significant role of the CYP1A2*1F variant in determining low clozapine level and clinical non-response [152], while another case report of treatment failure with low clozapine blood level detected highlighted the importance of considering clozapine metabolism as dependent on the genetic profile of various CYP genes, such as CYP1A2, CYP3A4, CYP2C19, and CYP2D6, and of UGT1A4 and ABCB1 genes [28].

3.5.2. Antidepressants and Other Psychotropic Drugs

About antidepressants, personalized dosing according to CYP2D6 and CYP2C19 variants has been proposed for several antidepressants and can be retrieved in specific guidelines and reviews [13–15,153]. CYP2D6 variants are the same as described in the antipsychotic subsection, while CYP2C19 variants are classified as follows: null activity (CYP2C19*2, *3, *4, *5, *6, *7, *8, *10, *11), decreased activity (CYP2C19*2, *3, *4, *5, *6, *7, *8, *10, *11), increased activity (CYP2C19*17). CYP2C19 PM are defined as people with two null alleles, while CYP2C19 UM as those with two increased activity alleles [149].

Studies on a very large database confirmed the role of both CYP2D6 and CYP2C19 on amitriptyline [154] and venlafaxine metabolism, with up to 13-fold dose-adjusted serum concentration in patients with PM profiles for both CYPs [155], and a very low enzyme function in CYP2D6*41 carriers has been observed [147,156]. A significant impact of CYP2D6 has also been confirmed for fluoxetine, with an increase in fluoxetine serum concentration and low norfluoxetine levels and norfluoxetine/fluoxetine ratio in PM and

intermediate metabolizers (IM, i.e., patients with one normal activity allele with one null activity allele or with two decreased activity alleles) [133,149].

Conversely, three recent studies focused on the CYP2C19*17 genetic variant that is associated with the increased metabolic activity of the CYP. In detail, lower serum concentrations of venlafaxine without variations in terms of antidepressant response in patients with one copy of the CYP2C19*17 genetic variant were found by Sherf-Clavel et al., while Zastrozhin and Collaborators reported a negative association between the CYP2C19*17 genetic variant and the antidepressant efficacy and safety of escitalopram treatment without a significant variation in the serum concentration of the drug in these subsample of patients [157,158]. Finally, a case report on a patient with scarce clinical response to bupropion revealed a previously not observed in-vivo role of an alternative metabolic pathway via CYP2C19, with UM status appearing related to low bupropion active moiety levels and low efficacy [159].

With regard to other classes of psychotropic drugs used in psychiatry, we retrieved only a study on depressed patients receiving lamotrigine as augmentation therapy that showed no relevance of UDP-glucuronosyltransferase gene polymorphism and drug plasma concentration and work on a sample of patients with anxiety disorder and alcohol use disorder, highlighting the impact of a specific polymorphism of CYP3A4 gene (99366316G > A) in determining alprazolam higher efficacy and presence of adverse effects [160,161]. In conclusion, the interplay between genetic profile, drug metabolism, C/D ratios, clinical response, and adverse effects is complex and scarcely predictable at the individual level, as it is the result of a complex multifactorial process based on genetic and non-genetic variables which multiple genes involved in drug metabolism, transcellular transport, drug receptors, and intracellular signaling need to be considered. AGNP guidelines recommend TDM in the presence of a genetic peculiarity concerning drug metabolism [2]. This agrees with the results of the studies summarized in which it has been evidenced as TDM and pharmacogenomics combined can provide useful information on the effectiveness and safety of psychoactive drugs [145–161].

3.6. Novel Approaches toward Minimally Invasive TDM

A variety of novel minimally invasive techniques receives growing interest as a promising way to increase TDM implementation in clinical practice through procedures with easy access, home or point-of-care availability, and user-friendly devices.

3.6.1. Dried Blood Spot Analysis (DBS)

Among the most studied procedures stands dried blood spot (DBS) analysis, generally carried out through a simple finger prick. Sampling can be performed by the patient himself at home or in points-of-care without the need of facilities usually needed for vena punctures. DBS is more user-friendly compared to vena puncture and can be particularly helpful in improving the elderly's access to TDM since no displacement to a health care center is required. According to the studies found in our research, DBS appears to be a reliable tool in performing TDM of clozapine, ziprasidone, lamotrigine, valproate, lithium, citalopram, fluoxetine, sertraline, venlafaxine, and vortioxetine [162–166]. Up to date, no clinical validity has been reported for DBS analyses for TDM of risperidone, aripiprazole, and pipamperone, and possible overestimation of clozapine and amitriptyline exposure through DBS TDM compared to traditional TDM has been suggested [163,167]. Overall, DBS has a generally lower sensitivity than traditional TDM based on blood levels and is more subjected to pre-analytical and analytical bias related to the variability of hematocrit values and to possible errors in remote sampling [163,167].

3.6.2. Volumetric Absorptive Microsampling (VAMS)

Novel promising microsampling techniques are emerging, such as VAMS. Its main advantages, in comparison with DBS, are a more precise and accurate collection of blood volumes, minimization of hematocrit effect on results, easier post-analytic sample manage-

ment, and reduced costs [168]. Recent validation studies suggest that volumetric absorptive microsampling (VAMS) and other microsampling procedures may be reliable and smart techniques for TDM in psychiatry. In particular, blood, plasma, and oral fluid VAMS in patients receiving, sertraline, fluoxetine, citalopram, or vortioxetine provided results in valid agreement with those obtained with routinary methods [165]. Moreover, innovative volumetric absorptive paper discs have been proposed for assessing levels of clozapine and its metabolites, demonstrating good accuracy of the new methods [162,169].

VAMS and other innovative capillary microsampling procedures [166], feasibility, accuracy, and reliability have been proven and clinically validated for several psychotropic drugs [165,166,169–171]. VAMS stands today as a very promising mini-invasive TDM procedure in terms of easy applicability and clinical reliability, making precision psychiatry closer. Nevertheless, further studies with adequate clinical validation and a clear assessment of agreement between plasma and DBS/VAMS monitoring methods are needed [163].

3.6.3. Oral Fluid Analysis

The oral fluid analysis represents another promising method toward an easily accessible TDM: the collection is non-invasive, can be carried out at home, and allows simple monitoring in patients for whom blood sampling can be problematic or undesirable. Data indicating the potential utility of saliva TDM are available for clozapine, risperidone, quetiapine, olanzapine, venlafaxine, lithium, valproate, carbamazepine, lamotrigine, and methylphenidate [162,172–174]. A single study, on the contrary, found no validity in monitoring amphetamine treatment in children and adolescents with ADHD through saliva collection [175]. In conclusion, available data are still limited and heterogeneous as saliva drug concentrations are generally lower than plasma, with consequent more complex measuring. However, oral fluid analysis emerges as a promising instrument in assessing treatment adherence for several psychotropic drugs comprising antipsychotics and antidepressants [162,172–174,176].

3.6.4. Other Non- or Mini-Invasive Procedures

A further strand of TDM development with different methods, biological samples, and intended uses has been the subject of some recent studies included in the current review [177–182]. Completely non-invasive wearable devices have been developed for TDM of lithium [177,178], and novel biosensors may constitute a reliable, cost-effective, and point-of-care disposable alternative to current laboratory techniques [180,181]. Moreover, seminal fluid TDM could be helpful in managing reduced fertility in patients receiving antipsychotics or antidepressants [181]; hair testing can be a sensitive method in assessing treatment adherence over a large timeframe, especially for lamotrigine and carbamazepine [85]; and urine metabolites dosage represents a possible tool in assessing compliance to novel antipsychotics treatment [182]. In summary, these are new technologies under development, but they may become the subject of future scientific studies and, consequently, useful tools for clinical practice.

3.7. Towards Precision Pharmacotherapy in Psychiatry

Precision medicine is a healthcare approach that considers specific characteristics of patients such as sex, age, genetics, metabolic, environment, lifestyle, etc., and of their diseases (e.g., the genetic profile of a tumor) in order to provide a tailored therapeutic intervention, maximizing treatment efficacy, minimizing toxicity and generally improving the efficiency of healthcare systems. Treatment personalization needs reliable indicators of the development and evolution of the disease and of treatment response, which can consist of measurements of different biological traits through genetic and metabolic analysis or bioimaging. The past decade has been characterized by specific efforts to achieve tailored intervention in psychiatry. A new framework to define mental disorders according to genetic, molecular, and neuronal pathways; physiological variables; and behavioral characteristics has been proposed [183]. Ongoing efforts are produced to achieve satisfying clinical

staging models for the most common and severe mental disorders in order to define disease progression, predict prognosis, and allow tailored treatment [184,185]. Large-scale genetic studies brought a growing body of information on the genetic basis of major psychiatric disorders [186,187], and progress in neuroimaging and electrophysiology allows a more exhaustive comprehension of pathological processes and of the role of treatments [188,189]. The large field of precision psychiatry comprises precision psychopharmacotherapy. Several biomarkers have been identified as related to treatment outcomes and safety, namely cytochrome P450s enzymes [190], genes, and proteins involved in DNA transcription and RNA translation or in intracellular signaling and neurotransmission [191–194]. TDM stands as a tile in this complex mosaic, enabling more precise employment of pharmacotherapy through treatment personalization, especially when performed synergically with genetic profiling, as seen in Section 3.5, in a variety of clinical conditions, such as treatment resistance or pseudo-resistance, unforeseen adverse effects, pregnancy, limit ages, abnormally high or low weight, presence of comorbidities or other pharmacological treatments. Moreover, mini-invasive TDM procedures appear to be a road to follow to extensively bring precision pharmacotherapy into everyday clinical practice.

The principal limitations of this review are the non-systematic nature of the review, which did not allow for accurate screening of the methodological quality of the included records, and the choice to search exclusively the Web of Science platform and no other databases such as PubMed. The main strength of this paper is the breadth of the topics covered that provide a summary of the literature on the use of TDM in psychiatry since the publication of the AGNP guidelines.

4. Conclusions

TDM receives growing research and clinical interest; however, it remains underemployed in the real world. Among the reasons for its relatively limited use is a lack of clear correlation between drug serum concentration and efficacy and tolerability, both in the general population and even more in patients with specificities of drug metabolism. Recent evidence, issued after the latest AGNP guidelines, help to shed light on some TDM application field still scarcely explored. In particular, some recent studies demonstrate a correlation between serum drug concentrations at the treatment start and clinical efficacy and safety, especially for antipsychotics. This might help clinicians in making decisions on early laboratory findings, possibly avoiding a trial-and-error approach. A similar result was also obtained for first-line antidepressant treatments. Concerning populations with specific pharmacokinetic characteristics, the studies included in the current review confirmed frequent alterations of serum drug concentrations in pregnant women, generally with a progressive decrease over pregnancy and a relevant dose-adjusted concentration increase in the elderly. As compared to adults, also in adolescents, several drugs result having different dose-related concentrations. Pharmacogenetic analyses combined with TDM may help clinicians in choosing more effective and safe psychopharmacologic treatments, addressing therapy on an individual pharmacometabolic basis. Mini-invasive TDM procedures may be easily performed at home or at a point-of-care level and may enhance the use of TDM on a regular basis for many psychotropic drugs in different real-world settings.

Although the recent evidence summarized in this review, research efforts have to be carried on: further studies are needed to replicate present findings and provide clearer knowledge on relationships between dose, serum concentration, and efficacy/safety. To accomplish this, prospective fixed-dose studies in the general population and in specific populations with distinctive pharmacokinetic characteristics are needed. Furthermore, a larger sample size of studies is required to obtain more accurate scientific evidence with a good balance of statistical power and significance. These goals could be achieved, for example, through consortia aimed at designing multicenter studies with a shared methodology designed to expand knowledge about TDM in psychopharmacology. In conclusion, an investment of economic resources aimed at conducting this kind of studies and an effort to diffuse the knowledge on this topic in order to train psychiatrists on the

proper use of TDM in a wider range of real-world contexts would allow clinicians and patients to benefit from this precious technique.

Author Contributions: Conceptualization, F.P. and C.B.; methodology, F.P.; writing—original draft preparation, F.P. and C.B.; writing—review and editing, V.V. and P.R.; supervision, V.V. and P.R. All authors have read and agreed to the published version of the manuscript.

Funding: This research received no external funding.

Institutional Review Board Statement: Not applicable.

Informed Consent Statement: Not applicable.

Data Availability Statement: Not applicable.

Acknowledgments: We thank Anna Carluccio and Rodolfo Sgro for their help.

Conflicts of Interest: The authors declare no conflict of interest.

References

1. Hiemke, C. Clinical Utility of Drug Measurement and Pharmacokinetics: Therapeutic Drug Monitoring in Psychiatry. *Eur. J. Clin. Pharmacol.* **2008**, *64*, 159–166. [CrossRef] [PubMed]
2. Hiemke, C.; Bergemann, N.; Clement, H.W.; Conca, A.; Deckert, J.; Domschke, K.; Eckermann, G.; Egberts, K.; Gerlach, M.; Greiner, C.; et al. Consensus Guidelines for Therapeutic Drug Monitoring in Neuropsychopharmacology: Update 2017. *Pharmacopsychiatry* **2018**, *51*, 9–62. [CrossRef]
3. Herzog, D.P.; Wagner, S.; Ruckes, C.; Tadic, A.; Roll, S.C.; Härter, M.; Lieb, K. Guideline Adherence of Antidepressant Treatment in Outpatients with Major Depressive Disorder: A Naturalistic Study. *Eur. Arch. Psychiatry Clin. Neurosci.* **2017**, *267*, 711–721. [CrossRef] [PubMed]
4. Conca, A.; Schmidt, E.; Pastore, M.; Hiemke, C.; Duffy, D.; Giupponi, G. Therapeutic Drug Monitoring in Italian Psychiatry. *Pharmacopsychiatry* **2011**, *44*, 259–262. [CrossRef] [PubMed]
5. Guo, W.; Guo, G.-X.; Sun, C.; Zhang, J.; Rong, Z.; He, J.; Sun, Z.-L.; Yan, F.; Tang, Y.-L.; Wang, C.-Y.; et al. Therapeutic Drug Monitoring of Psychotropic Drugs in China: A Nationwide Survey. *Ther. Drug Monit.* **2013**, *35*, 816–822. [CrossRef]
6. Okada, K.; Yamada, K.; Usui, K.; Ouchi, R.; Nibuya, M.; Takahashi, A.; Shito, Y.; Watanabe, Y.; Suzuki, E. Inadequate Therapeutic Drug Monitoring in Patients with Lithium Toxicity in Japan. *Psychiatry Clin. Neurosci.* **2020**, *74*, 629–631. [CrossRef] [PubMed]
7. Meehan, T.; Wang, H.; Drummond, A.; Lockman, H. Therapeutic Drug Monitoring (TDM) during Maintenance Phase Treatment at a Community Mental Health Centre. *Australas. Psychiatry* **2019**, *27*, 637–640. [CrossRef] [PubMed]
8. Nederlof, M.; Heerdink, E.R.; Egberts, A.C.G.; Wilting, I.; Stoker, L.J.; Hoekstra, R.; Kupka, R.W. Monitoring of Patients Treated with Lithium for Bipolar Disorder: An International Survey. *Int. J. Bipolar Disord.* **2018**, *6*, 12. [CrossRef] [PubMed]
9. Ooba, N.; Tsutsumi, D.; Kobayashi, N.; Hidaka, S.; Hayashi, H.; Obara, T.; Satoh, M.; Kubota, K.; Fukuoka, N. Prevalence of Therapeutic Drug Monitoring for Lithium and the Impact of Regulatory Warnings: Analysis Using Japanese Claims Database. *Ther. Drug Monit.* **2018**, *40*, 252–256. [CrossRef]
10. Ozunal, Z.G.; Ongen İpek, B. Therapeutic Drug Monitoring Characteristics in a Tertiary University Hospital in 2019. *Cureus* **2020**, *12*, e7612. [CrossRef]
11. Schoretsanitis, G.; Baumann, P.; Conca, A.; Dietmaier, O.; Giupponi, G.; Gründer, G.; Hahn, M.; Hart, X.; Havemann-Reinecke, U.; Hefner, G.; et al. Therapeutic Drug Monitoring of Long-Acting Injectable Antipsychotic Drugs. *Ther. Drug Monit.* **2021**, *43*, 79–102. [CrossRef]
12. Toja-Camba, F.J.; Gesto-Antelo, N.; Maroñas, O.; Echarri Arrieta, E.; Zarra-Ferro, I.; González-Barcia, M.; Bandín-Vilar, E.; Mangas Sanjuan, V.; Facal, F.; Arrojo Romero, M.; et al. Review of Pharmacokinetics and Pharmacogenetics in Atypical Long-Acting Injectable Antipsychotics. *Pharmaceutics* **2021**, *13*, 935. [CrossRef] [PubMed]
13. Eap, C.B.; Gründer, G.; Baumann, P.; Ansermot, N.; Conca, A.; Corruble, E.; Crettol, S.; Dahl, M.L.; de Leon, J.; Greiner, C.; et al. Tools for Optimising Pharmacotherapy in Psychiatry (Therapeutic Drug Monitoring, Molecular Brain Imaging and Pharmacogenetic Tests): Focus on Antidepressants. *World J. Biol. Psychiatry* **2021**, *22*, 561–628. [CrossRef] [PubMed]
14. Mandrioli, R.; Protti, M.; Mercolini, L. New-Generation, Non-SSRI Antidepressants: Therapeutic Drug Monitoring and Pharmacological Interactions. Part 1: SNRIs, SMSs, SARIs. *Curr. Med. Chem.* **2018**, *25*, 772–792. [CrossRef]
15. Protti, M.; Mandrioli, R.; Marasca, C.; Cavalli, A.; Serretti, A.; Mercolini, L. New-Generation, Non-SSRI Antidepressants: Drug-Drug Interactions and Therapeutic Drug Monitoring. Part 2: NaSSAs, NRIs, SNDRIs, MASSAs, NDRIs, and Others. *Med. Res. Rev.* **2020**, *40*, 1794–1832. [CrossRef] [PubMed]
16. Hiemke, C. Concentration-Effect Relationships of Psychoactive Drugs and the Problem to Calculate Therapeutic Reference Ranges. *Ther. Drug Monit.* **2019**, *41*, 174–179. [CrossRef] [PubMed]
17. Molden, E. Therapeutic Drug Monitoring of Clozapine in Adults with Schizophrenia: A Review of Challenges and Strategies. *Expert Opin. Drug Metab. Toxicol.* **2021**, *17*, 1211–1221. [CrossRef] [PubMed]

18. Arnaiz, J.A.; Rodrigues-Silva, C.; Mezquida, G.; Amoretti, S.; Cuesta, M.J.; Fraguas, D.; Lobo, A.; González-Pinto, A.; Díaz-Caneja, M.C.; Corripio, I.; et al. The Usefulness of Olanzapine Plasma Concentrations in Monitoring Treatment Efficacy and Metabolic Disturbances in First-Episode Psychosis. *Psychopharmacology* **2021**, *238*, 665–676. [CrossRef] [PubMed]
19. Nagai, G.; Mihara, K.; Nakamura, A.; Nemoto, K.; Kagawa, S.; Suzuki, T.; Kondo, T. Prediction of an Optimal Dose of Aripiprazole in the Treatment of Schizophrenia From Plasma Concentrations of Aripiprazole Plus Its Active Metabolite Dehydroaripiprazole at Week 1. *Ther. Drug Monit.* **2017**, *39*, 62–65. [CrossRef] [PubMed]
20. Tien, Y.; Huang, H.P.; Liao, D.L.; Huang, S.C. Dose-response analysis of aripiprazole in patients with schizophrenia in Taiwan. *Ther. Adv. Psychopharmacol.* **2022**, *12*, 20451253221113238. [CrossRef] [PubMed]
21. Hart, X.M.; Hiemke, C.; Eichentopf, L.; Lense, X.M.; Clement, H.W.; Conca, A.; Faltraco, F.; Florio, V.; Grüner, J.; Havemann-Reinecke, U.; et al. Therapeutic Reference Range for Aripiprazole in Schizophrenia Revised: A Systematic Review and Metaanalysis. *Psychopharmacology* **2022**, *239*, 3377–3391. [CrossRef] [PubMed]
22. Kaufmann, A.; Post, F.; Yalcin-Siedentopf, N.; Baumgartner, S.; Biedermann, F.; Edlinger, M.; Kemmler, G.; Rettenbacher, M.A.; Widschwendter, C.G.; Zernig, G.; et al. Corrigendum to "Changes in Psychopathology in Schizophrenia Patients Starting Treatment with New-Generation Antipsychotics: Therapeutic Drug Monitoring in a Naturalistic Treatment Setting". *Eur. Neuropsychopharmacol.* **2020**, *31*, 162–163. [CrossRef] [PubMed]
23. Paulzen, M.; Haen, E.; Stegmann, B.; Unterecker, S.; Hiemke, C.; Gründer, G.; Schoretsanitis, G. Clinical Response in a Risperidone-Medicated Naturalistic Sample: Patients' Characteristics and Dose-Dependent Pharmacokinetic Patterns. *Eur. Arch. Psychiatry Clin. Neurosci.* **2017**, *267*, 325–333. [CrossRef]
24. Yada, Y.; Kitagawa, K.; Sakamoto, S.; Ozawa, A.; Nakada, A.; Kashiwagi, H.; Okahisa, Y.; Takao, S.; Takaki, M.; Kishi, Y.; et al. The Relationship between Plasma Clozapine Concentration and Clinical Outcome: A Cross-Sectional Study. *Acta Psychiatr. Scand.* **2021**, *143*, 227–237. [CrossRef]
25. Kyllesø, L.; Smith, R.L.; Karlstad, Ø.; Andreassen, O.A.; Molden, E. Absolute and Dose-Adjusted Serum Concentrations of Clozapine in Patients Switching vs. Maintaining Treatment: An Observational Study of 1979 Patients. *CNS Drugs* **2021**, *35*, 999–1008. [CrossRef]
26. Schoretsanitis, G.; Kane, J.M.; Ruan, C.-J.; Spina, E.; Hiemke, C.; de Leon, J. A Comprehensive Review of the Clinical Utility of and a Combined Analysis of the Clozapine/Norclozapine Ratio in Therapeutic Drug Monitoring for Adult Patients. *Expert Rev. Clin. Pharmacol.* **2019**, *12*, 603–621. [CrossRef] [PubMed]
27. Grover, S.; Kasudhan, K.S.; Murali, N.; Patil, A.N.; Pattanaik, S.; Chakrabarti, S.; Avasthi, A. Pharmacometabolomics-Guided Clozapine Therapy in Treatment Resistant Schizophrenia: Preliminary Exploration of Future Too Near. *Asian J. Psychiatr.* **2022**, *67*, 102939. [CrossRef]
28. Whiskey, E.; Romano, G.; Elliott, M.; Campbell, M.; Anandarajah, C.; Taylor, D.; Valsraj, K. Possible Pharmacogenetic Factors in Clozapine Treatment Failure: A Case Report. *Ther. Adv. Psychopharmacol.* **2021**, *11*, 20451253211030844. [CrossRef] [PubMed]
29. Olmos, I.; Ibarra, M.; Vázquez, M.; Maldonado, C.; Fagiolino, P.; Giachetto, G. Population Pharmacokinetics of Clozapine and Norclozapine and Switchability Assessment between Brands in Uruguayan Patients with Schizophrenia. *BioMed Res. Int.* **2019**, *2019*, 3163502. [CrossRef]
30. Oloyede, E.; Dzahini, O.; Whiskey, E.; Taylor, D. Clozapine and Norclozapine Plasma Levels in Patients Switched between Different Liquid Formulations. *Ther. Drug Monit.* **2020**, *42*, 491–496. [CrossRef] [PubMed]
31. Melkote, R.; Singh, A.; Vermeulen, A.; Remmerie, B.; Savitz, A. Relationship between Antipsychotic Blood Levels and Treatment Failure during the Clinical Antipsychotic Trials of Intervention Effectiveness (CATIE) Study. *Schizophr. Res.* **2018**, *201*, 324–328. [CrossRef]
32. McCutcheon, R.; Beck, K.; D'Ambrosio, E.; Donocik, J.; Gobjila, C.; Jauhar, S.; Kaar, S.; Pillinger, T.; Reis Marques, T.; Rogdaki, M.; et al. Antipsychotic Plasma Levels in the Assessment of Poor Treatment Response in Schizophrenia. *Acta Psychiatr. Scand.* **2018**, *137*, 39–46. [CrossRef] [PubMed]
33. Kyllesø, L.; Smith, R.L.; Karlstad, Ø.; Andreassen, O.A.; Molden, E. Undetectable or Subtherapeutic Serum Levels of Antipsychotic Drugs Preceding Switch to Clozapine. *NPJ Schizophr.* **2020**, *6*, 17. [CrossRef] [PubMed]
34. Javelot, H.; Rangoni, F.; Weiner, L.; Michel, B. High-Dose Quetiapine and Therapeutic Monitoring. *Eur. J. Hosp. Pharm.* **2019**, *26*, 285–287. [CrossRef]
35. Schoretsanitis, G.; Spina, E.; Hiemke, C.; de Leon, J. A Systematic Review and Combined Analysis of Therapeutic Drug Monitoring Studies for Long-Acting Paliperidone. *Expert Rev. Clin. Pharmacol.* **2018**, *11*, 1237–1253. [CrossRef] [PubMed]
36. Schoretsanitis, G.; Haen, E.; Piacentino, D.; Conca, A.; Endres, K.; Hiemke, C.; Gründer, G.; Paulzen, M. Clinical Response in Patients Treated with Once-Monthly Paliperidone Palmitate: Analysis of a Therapeutic Drug Monitoring (TDM) Database. *Eur. Arch. Psychiatry Clin. Neurosci.* **2021**, *271*, 1437–1443. [CrossRef]
37. Schoretsanitis, G.; Haen, E.; Piacentino, D.; Conca, A.; Endres, K.; Hiemke, C.; Gründer, G.; Paulzen, M. Effects of Body Weight, Smoking Status, and Sex on Plasma Concentrations of Once-Monthly Paliperidone Palmitate. *Expert Rev. Clin. Pharmacol.* **2022**, *15*, 243–249. [CrossRef]
38. Hýža, M.; Šilhán, P.; Češková, E.; Skřont, T.; Kacířová, I.; Uřinovská, R.; Grundmann, M. Plasma Levels of Long-Acting Injectable Antipsychotics in Outpatient Care: A Retrospective Analysis. *Neuropsychiatr. Dis. Treat.* **2021**, *17*, 1069–1075. [CrossRef]

39. D'Anna, G.; Rotella, F.; Santarelli, G.; Scannerini, S.; Fanelli, A.; Ricca, V.; Ballerini, A. Therapeutic Drug Monitoring of Long-Acting Injectable Antipsychotics as a Predictor of Relapse in Schizophrenia Spectrum Disorders: A One-Year Pilot Study. *Ther. Drug Monit.* **2022**, *43*, 79–102. [CrossRef]
40. Mauri, M.C.; Paletta, S.; Di Pace, C.; Reggiori, A.; Cirnigliaro, G.; Valli, I.; Altamura, A.C. Clinical Pharmacokinetics of Atypical Antipsychotics: An Update. *EXCLI J.* **2014**, *13*, 1163–1191. [CrossRef]
41. Periclou, A.; Willavize, S.; Jaworowicz, D.; Passarell, J.; Carrothers, T.; Ghahramani, P.; Durgam, S.; Earley, W.; Kapás, M.; Khariton, T. Relationship Between Plasma Concentra-tions and Clinical Effects of Cariprazine in Patients With Schizophrenia or Bipolar Mania. *Clin. Transl. Sci.* **2020**, *13*, 362–371. [CrossRef]
42. Malhi, G.S.; Gershon, S.; Outhred, T. Lithiumeter: Version 2.0. *Bipolar Disord.* **2016**, *18*, 631–641. [CrossRef]
43. Mauri, M.C.; Reggiori, A.; Minutillo, A.; Franco, G.; Pace, C.D.; Paletta, S.; Cattaneo, D. Paliperidone LAI and Aripiprazole LAI Plasma Level Monitoring in the Prophylaxis of Bipolar Disorder Type I with Manic Predominance. *Pharmacopsychiatry* **2020**, *53*, 209–219. [CrossRef] [PubMed]
44. Funk, C.S.; Hart, X.M.; Gründer, G.; Hiemke, C.; Elsner, B.; Kreutz, R.; Riemer, T.G. Is Therapeutic Drug Monitoring Relevant for Antidepressant Drug Therapy? Implications from a Systematic Review and Meta-Analysis with Focus on Moderating Factors. *Front. Psychiatry* **2022**, *13*, 826138. [CrossRef]
45. Tveit, K.; Hermann, M.; Waade, R.B.; Nilsen, R.M.; Wallerstedt, S.M.; Molden, E. Use of Antidepressants in Older People during a 10-Year Period: An Observational Study on Prescribed Doses and Serum Levels. *Drugs Aging* **2020**, *37*, 691–701. [CrossRef]
46. Cellini, L.; De Donatis, D.; Zernig, G.; De Ronchi, D.; Giupponi, G.; Serretti, A.; Xenia, H.; Conca, A.; Florio, V. Antidepressant efficacy is correlated with plasma levels: Mega-analysis and further evidence. *Int. Clin. Psychopharmacol.* **2021**, *37*, 29–37. [CrossRef]
47. De Donatis, D.; Porcelli, S.; Zernig, G.; Mercolini, L.; Giupponi, G.; Serretti, A.; Conca, A.; Florio, V. Venlafaxine and O-Desmethylvenlafaxine Serum Levels Are Positively Associated with Antidepressant Response in Elder Depressed out-Patients. *World J. Biol. Psychiatry* **2021**, *23*, 183–190. [CrossRef] [PubMed]
48. Hansen, M.R.; Kuhlmann, I.B.; Pottegård, A.; Damkier, P. Therapeutic Drug Monitoring of Venlafaxine in an Everyday Clinical Setting: Analysis of Age, Sex and Dose Concentration Relationships. *Basic Clin. Pharmacol. Toxicol.* **2017**, *121*, 298–302. [CrossRef]
49. Bustillo, M.; Zabala, A.; Querejeta, I.; Carton, J.I.; Mentxaka, O.; González-Pinto, A.; García, S.; Meana, J.J.; Eguiluz, J.I.; Segarra, R. Therapeutic Drug Monitoring of Second-Generation Antipsychotics for the Estimation of Early Drug Effect in First-Episode Psychosis: A Cross-Sectional Assessment. *Ther. Drug Monit.* **2018**, *40*, 257–267. [CrossRef]
50. Kitchen, D.; Till, A.; Xavier, P. Routine Clozapine Assay Monitoring to Improve the Management of Treatment-Resistant Schizophrenia. *BJPsych Bull.* **2021**, *46*, 267–270. [CrossRef] [PubMed]
51. Hart, X.M.; Konietzko, R.A.A.; Hirjak, D.; Gruender, G. Case Report: Therapeutic Drug Monitoring in a Female Schizophrenia Patient with Self-Induced Clozapine Intoxication Using Point-of-Care Testing. *Eur. Neuropsychopharmacol.* **2020**, *40*, S278. [CrossRef]
52. Smith, R.L.; Haslemo, T.; Andreassen, O.A.; Eliasson, E.; Dahl, M.-L.; Spigset, O.; Molden, E. Correlation between Serum Concentrations of N-Desmethylclozapine and Granulocyte Levels in Patients with Schizophrenia: A Retrospective Observational Study. *CNS Drugs* **2017**, *31*, 991–997. [CrossRef]
53. Diaz, F.J.; Josiassen, R.C.; de Leon, J. The Effect of Body Weight Changes on Total Plasma Clozapine Concentrations Determined by Applying a Statistical Model to the Data from a Double-Blind Trial. *J. Clin. Psychopharmacol.* **2018**, *38*, 442–446. [CrossRef] [PubMed]
54. Schoretsanitis, G.; Kuzin, M.; Kane, J.M.; Hiemke, C.; Paulzen, M.; Haen, E. Elevated Clozapine Concentrations in Clozapine-Treated Patients with Hypersalivation. *Clin. Pharmacokinet.* **2021**, *60*, 329–335. [CrossRef] [PubMed]
55. Skokou, M.; Karavia, E.A.; Drakou, Z.; Konstantinopoulou, V.; Kavakioti, C.A.; Gourzis, P.; Kavakioti, C.; Gourzis, P.; Kypreos, K.E.; Andreopoulou, O. Adverse Drug Reactions in Relation to Clozapine Plasma Levels: A Systematic Review. *Pharmaceuticals* **2022**, *15*, 817. [CrossRef] [PubMed]
56. Kang, D.; Lu, J.; Liu, W.; Shao, P.; Wu, R. Association between olanzapine concentration and metabolic dysfunction in drug-naive and chronic patients: Similarities and differences. *Schizophr* **2022**, *8*, 9. [CrossRef] [PubMed]
57. An, H.; Fan, H.; Yun, Y.; Chen, S.; Qi, S.; Ma, B.; Shi, J.; Wang, Z.; Yang, F. Relationship between Plasma Olanzapine and N-Desmethyl-Olanzapine Concentration and Metabolic Parameters in Patients with Schizophrenia. *Front. Psychiatry* **2022**, *13*, 930457. [CrossRef] [PubMed]
58. Lu, M.-L.; Chen, C.-H.; Kuo, P.-T.; Lin, C.-H.; Wu, T.-H. Application of Plasma Levels of Olanzapine and N-Desmethyl-Olanzapine to Monitor Metabolic Parameters in Patients with Schizophrenia. *Schizophr Res.* **2018**, *193*, 139–145. [CrossRef] [PubMed]
59. Carli, M.; Kolachalam, S.; Longoni, B.; Pintaudi, A.; Baldini, M.; Aringhieri, S.; Fasciani, I.; Annibale, P.; Maggio, R.; Scarselli, M. Atypical Antipsychotics and Metabolic Syndrome: From Molecular Mechanisms to Clinical Differences. *Pharmaceuticals* **2021**, *14*, 238. [CrossRef] [PubMed]
60. Engelmann, J.; Wagner, S.; Solheid, A.; Herzog, D.P.; Dreimüller, N.; Müller, M.B.; Tadić, A.; Hiemke, C.; Lieb, K. Tolerability of High-Dose Venlafaxine after Switch from Escitalopram in Nonresponding Patients with Major Depressive Disorder. *J. Clin. Psychopharmacol.* **2021**, *41*, 62–66. [CrossRef] [PubMed]

61. Schoretsanitis, G.; Haen, E.; Piacentino, D.; Conca, A.; Endres, K.; Carpi, F.; Hiemke, C.; Gründer, G.; Paulzen, M. Pharmacokinetic Correlates of Once-Monthly Paliperidone Palmitate-Related Adverse Drug Reactions. *Clin. Pharmacokinet.* **2021**, *60*, 1583–1589. [CrossRef] [PubMed]
62. Veselinović, T.; Scharpenberg, M.; Heinze, M.; Cordes, J.; Mühlbauer, B.; Juckel, G.; Rüther, E.; Paulzen, M.; Haen, E.; Hiemke, C.; et al. Dopamine D2 Receptor Occupancy Estimated from Plasma Concentrations of Four Different Antipsychotics and the Subjective Experience of Physical and Mental Well-Being in Schizophrenia: Results from the Randomized NeSSy Trial. *J. Clin. Psychopharmacol.* **2019**, *39*, 550–560. [CrossRef] [PubMed]
63. Haddad, P.M.; Brain, C.; Scott, J. Nonadherence with Antipsychotic Medication in Schizophrenia: Challenges and Management Strategies. *Patient Relat. Outcome Meas.* **2014**, *5*, 43–62. [CrossRef] [PubMed]
64. Higashi, K.; Medic, G.; Littlewood, K.J.; Diez, T.; Granström, O.; De Hert, M. Medication Adherence in Schizophrenia: Factors Influencing Adherence and Consequences of Nonadherence, a Systematic Literature Review. *Ther. Adv. Psychopharmacol.* **2013**, *3*, 200–218. [CrossRef] [PubMed]
65. Murru, A.; Pacchiarotti, I.; Amann, B.L.; Nivoli, A.M.A.; Vieta, E.; Colom, F. Treatment Adherence in Bipolar I and Schizoaffective Disorder, Bipolar Type. *J. Affect. Disord.* **2013**, *151*, 1003–1008. [CrossRef] [PubMed]
66. Emsley, R.; Chiliza, B.; Asmal, L.; Harvey, B.H. The Nature of Relapse in Schizophrenia. *BMC Psychiatry* **2013**, *13*, 50. [CrossRef] [PubMed]
67. Geretsegger, C.; Pichler, E.-M.; Gimpl, K.; Aichhorn, W.; Stelzig, R.; Grabher-Stoeffler, G.; Hiemke, C.; Zernig, G. Non-Adherence to Psychotropic Medication Assessed by Plasma Level in Newly Admitted Psychiatric Patients: Prevalence before Acute Admission. *Psychiatry Clin. Neurosci.* **2019**, *73*, 175–178. [CrossRef]
68. Silhan, P.; Urinovska, R.; Kacirova, I.; Hyza, M.; Grundmann, M.; Ceskova, E. What Does Antidepressant Drug Level Monitoring Reveal about Outpatient Treatment and Patient Adherence? *Pharmacopsychiatry* **2019**, *52*, 78–83. [CrossRef]
69. Baldelli, S.; Cheli, S.; Montrasio, C.; Cattaneo, D.; Clementi, E. Therapeutic Drug Monitoring and Pharmacogenetics of Antipsychotics and Antidepressants in Real Life Settings: A 5-Year Single Centre Experience. *World J. Biol. Psychiatry* **2021**, *22*, 34–45. [CrossRef]
70. Lopez, L.V.; Shaikh, A.; Merson, J.; Greenberg, J.; Suckow, R.F.; Kane, J.M. Accuracy of Clinician Assessments of Medication Status in the Emergency Setting: A Comparison of Clinician Assessment of Antipsychotic Usage and Plasma Level Determination. *J. Clin. Psychopharmacol.* **2017**, *37*, 310–314. [CrossRef]
71. Brasso, C.; Cisotto, M.; Ghirardini, C.; Pennazio, F.; Villari, V.; Rocca, P. Accuracy of Self-Reported Adherence and Therapeutic Drug Monitoring in a Psychiatric Emergency Ward. *Psychiatry Res.* **2021**, *305*, 114214. [CrossRef] [PubMed]
72. Smith, R.L.; Tveito, M.; Kyllesø, L.; Jukic, M.M.; Ingelman-Sundberg, M.; Andreassen, O.A.; Molden, E. Impact of Antipsychotic Polypharmacy on Nonadherence of Oral Antipsychotic Drugs—A Study Based on Blood Sample Analyses from 24,239 Patients. *Eur. Neuropsychopharmacol.* **2020**, *37*, 64–69. [CrossRef] [PubMed]
73. El Abdellati, K.; De Picker, L.; Morrens, M. Antipsychotic Treatment Failure: A Systematic Review on Risk Factors and Interventions for Treatment Adherence in Psychosis. *Front. Neurosci.* **2020**, *14*, 531763. [CrossRef] [PubMed]
74. Smith, R.L.; Tveito, M.; Kyllesø, L.; Jukic, M.M.; Ingelman-Sundberg, M.; Andreassen, O.A.; Molden, E. Rates of Complete Nonadherence among Atypical Antipsychotic Drugs: A Study Using Blood Samples from 13,217 Outpatients with Psychotic Disorders. *Schizophr Res.* **2021**, *228*, 590–596. [CrossRef]
75. Jones, I.; Chandra, P.S.; Dazzan, P.; Howard, L.M. Bipolar Disorder, Affective Psychosis, and Schizophrenia in Pregnancy and the Post-Partum Period. *Lancet* **2014**, *384*, 1789–1799. [CrossRef]
76. Schoretsanitis, G.; Kane, J.M.; Correll, C.U.; Marder, S.R.; Citrome, L.; Newcomer, J.W.; Robinson, D.G.; Goff, D.C.; Kelly, D.L.; Freudenreich, O.; et al. Blood Levels to Optimize Antipsychotic Treatment in Clinical Practice: A Joint Consensus Statement of the American Society of Clinical Psychopharmacology and the Therapeutic Drug Monitoring Task Force of the Arbeitsgemeinschaft Für Neuropsychopharmakologie Und Pharmakopsychiatrie. *J. Clin. Psychiatry* **2020**, *81*, 19cs13169. [CrossRef]
77. Leutritz, A.L.; van Braam, L.; Preis, K.; Gehrmann, A.; Scherf-Clavel, M.; Fiedler, K.; Unterecker, S.; Kittel-Schneider, S. Psychotropic medication in pregnancy and lactation and early development of exposed children. *Br. J. Clin. Pharmacol.* **2022**. [CrossRef]
78. Huang, S.; Li, L.; Wang, Z.; Xiao, T.; Li, X.; Liu, S.; Zhang, M.; Lu, H.; Wen, Y.; Shang, D. Modeling and Simulation for Individualized Therapy of Amisulpride in Chinese Patients with Schizophrenia: Focus on Interindividual Variability, Therapeutic Reference Range and the Laboratory Alert Level. *Drug Des. Dev. Ther.* **2021**, *15*, 3903–3913. [CrossRef]
79. Westin, A.A.; Brekke, M.; Molden, E.; Skogvoll, E.; Aadal, M.; Spigset, O. Changes in Drug Disposition of Lithium during Pregnancy: A Retrospective Observational Study of Patient Data from Two Routine Therapeutic Drug Monitoring Services in Norway. *BMJ Open* **2017**, *7*, e015738. [CrossRef]
80. Clark, C.T.; Newmark, R.L.; Wisner, K.L.; Stika, C.; Avram, M.J. Lithium Pharmacokinetics in the Perinatal Patient with Bipolar Disorder. *J. Clin. Pharm.* **2022**, *62*, 1385–1392. [CrossRef]
81. Schoretsanitis, G.; Spigset, O.; Stingl, J.C.; Deligiannidis, K.M.; Paulzen, M.; Westin, A.A. The Impact of Pregnancy on the Pharmacokinetics of Antidepressants: A Systematic Critical Review and Meta-Analysis. *Expert Opin. Drug Metab. Toxicol.* **2020**, *16*, 431–440. [CrossRef]
82. Schoretsanitis, G.; Augustin, M.; Saßmannshausen, H.; Franz, C.; Gründer, G.; Paulzen, M. Antidepressants in Breast Milk; Comparative Analysis of Excretion Ratios. *Arch. Womens Ment. Health* **2019**, *22*, 383–390. [CrossRef]

83. Heinonen, E.; Blennow, M.; Blomdahl-Wetterholm, M.; Hovstadius, M.; Nasiell, J.; Pohanka, A.; Gustafsson, L.L.; Wide, K. Sertraline Concentrations in Pregnant Women Are Steady and the Drug Transfer to Their Infants Is Low. *Eur. J. Clin. Pharmacol.* **2021**, *77*, 1323–1331. [CrossRef]
84. Westin, A.A.; Brekke, M.; Molden, E.; Skogvoll, E.; Castberg, I.; Spigset, O. Treatment with Antipsychotics in Pregnancy: Changes in Drug Disposition. *Clin. Pharmacol. Ther.* **2018**, *103*, 477–484. [CrossRef]
85. Gogtay, N.; Vyas, N.S.; Testa, R.; Wood, S.J.; Pantelis, C. Age of Onset of Schizophrenia: Perspectives from Structural Neuroimaging Studies. *Schizophr Bull.* **2011**, *37*, 504–513. [CrossRef]
86. Bolton, S.; Warner, J.; Harriss, E.; Geddes, J.; Saunders, K.E.A. Bipolar Disorder: Trimodal Age-at-Onset Distribution. *Bipolar Disord.* **2021**, *23*, 341–356. [CrossRef]
87. Yee, C.S.; Hawken, E.R.; Baldessarini, R.J.; Vázquez, G.H. Maintenance Pharmacological Treatment of Juvenile Bipolar Disorder: Review and Meta-Analyses. *Int. J. Neuropsychopharmacol.* **2019**, *22*, 531–540. [CrossRef]
88. Krause, M.; Zhu, Y.; Huhn, M.; Schneider-Thoma, J.; Bighelli, I.; Chaimani, A.; Leucht, S. Efficacy, Acceptability, and Tolerability of Antipsychotics in Children and Adolescents with Schizophrenia: A Network Meta-Analysis. *Eur. Neuropsychopharmacol.* **2018**, *28*, 659–674. [CrossRef]
89. MacQueen, G.M.; Frey, B.N.; Ismail, Z.; Jaworska, N.; Steiner, M.; Lieshout, R.J.V.; Kennedy, S.H.; Lam, R.W.; Milev, R.V.; Parikh, S.V.; et al. Canadian Network for Mood and Anxiety Treatments (CANMAT) 2016 Clinical Guidelines for the Management of Adults with Major Depressive Disorder: Section 6. Special Populations: Youth, Women, and the Elderly. *Can. J. Psychiatry* **2016**, *61*, 588–603. [CrossRef]
90. Cipriani, A.; Zhou, X.; Del Giovane, C.; Hetrick, S.E.; Qin, B.; Whittington, C.; Coghill, D.; Zhang, Y.; Hazell, P.; Leucht, S.; et al. Comparative Efficacy and Tolerability of Antidepressants for Major Depressive Disorder in Children and Adolescents: A Network Meta-Analysis. *Lancet* **2016**, *388*, 881–890. [CrossRef]
91. Tini, E.; Smigielski, L.; Romanos, M.; Wewetzer, C.; Karwautz, A.; Reitzle, K.; Correll, C.U.; Plener, P.L.; Malzahn, U.; Heuschmann, P. Therapeutic drug monitoring of sertraline in children and adolescents: A naturalistic study with insights into the clinical response and treatment of obsessive-compulsive disorder. *Compr. Psychiatry* **2022**, *115*, 152301. [CrossRef]
92. Fekete, S.; Hiemke, C.; Gerlach, M. Dose-Related Concentrations of Neuroactive/Psychoactive Drugs Expected in Blood of Children and Adolescents. *Ther. Drug Monit.* **2020**, *42*, 315–324. [CrossRef]
93. Kloosterboer, S.M.; Vierhout, D.; Stojanova, J.; Egberts, K.M.; Gerlach, M.; Dieleman, G.C.; Hillegers, M.H.J.; Passe, K.M.; van Gelder, T.; Dierckx, B.; et al. Psychotropic Drug Concentrations and Clinical Outcomes in Children and Adolescents: A Systematic Review. *Expert Opin. Drug Saf.* **2020**, *19*, 873–890. [CrossRef]
94. Strawn, J.R.; Poweleit, E.A.; Uppugunduri, C.R.S.; Ramsey, L.B. Pediatric Therapeutic Drug Monitoring for Selective Serotonin Reuptake Inhibitors. *Front. Pharmacol.* **2021**, *12*, 749692. [CrossRef]
95. Fekete, S.; Scherf-Clavel, M.; Gerlach, M.; Romanos, M.; Kittel-Schneider, S.; Unterecker, S.; Egberts, K. Dose-Corrected Serum Concentrations and Metabolite to Parent Compound Ratios of Venlafaxine and Risperidone from Childhood to Old Age. *Pharmacopsychiatry* **2021**, *54*, 117–125. [CrossRef]
96. Piacentino, D.; Kotzalidis, G.D.; Schoretsanitis, G.; Paulzen, M.; Haen, E.; Cappelletti, S.; Giupponi, G.; Grözinger, M.; Conca, A. Plasma Risperidone-Related Measures in Children and Adolescents with Oppositional Defiant/Conduct Disorders. *Clin. Psychopharmacol. Neurosci.* **2020**, *18*, 41–48. [CrossRef]
97. Egberts, K.; Reuter-Dang, S.-Y.; Fekete, S.; Kulpok, C.; Mehler-Wex, C.; Wewetzer, C.; Karwautz, A.; Mitterer, M.; Holtkamp, K.; Boege, I.; et al. Therapeutic Drug Monitoring of Children and Adolescents Treated with Aripiprazole: Observational Results from Routine Patient Care. *J. Neural Transm.* **2020**, *127*, 1663–1674. [CrossRef]
98. Gehrmann, J.; Götz Lampe, P. Serum Level Measurements Optimize Aripriprazole Treatment in Adolescent Patients. *Z. Kinder. Jugendpsychiatr. Psychother.* **2019**, *47*, 261–264. [CrossRef]
99. Castberg, I.; Westin, A.A.; Skogvoll, E.; Spigset, O. Effects of Age and Gender on the Serum Levels of Clozapine, Olanzapine, Risperidone, and Quetiapine. *Acta Psychiatr. Scand.* **2017**, *136*, 455–464. [CrossRef]
100. Jönsson, A.K.; Spigset, O.; Reis, M. A Compilation of Serum Concentrations of 12 Antipsychotic Drugs in a Therapeutic Drug Monitoring Setting. *Ther. Drug Monit.* **2019**, *41*, 348–356. [CrossRef]
101. Reeves, S.; Eggleston, K.; Cort, E.; McLachlan, E.; Brownings, S.; Nair, A.; Greaves, S.; Smith, A.; Dunn, J.; Marsden, P.; et al. Therapeutic D2/3 Receptor Occupancies and Response with Low Amisulpride Blood Concentrations in Very Late-Onset Schizophrenia-like Psychosis (VLOSLP). *Int. J. Geriatr. Psychiatry* **2018**, *33*, 396–404. [CrossRef]
102. Tveito, M.; Smith, R.L.; Molden, E.; Høiseth, G. Impact of Age and CYP2D6 Genotype on Exposure of Zuclopenthixol in Patients Using Long-Acting Injectable versus Oral Formulation-an Observational Study Including 2044 Patients. *Eur. J. Clin. Pharmacol.* **2021**, *77*, 215–221. [CrossRef]
103. Tveito, M.; Smith, R.L.; Molden, E.; Haslemo, T.; Refsum, H.; Hartberg, C.; Correll, C.U.; Høiseth, G. Age Impacts Olanzapine Exposure Differently during Use of Oral Versus Long-Acting Injectable Formulations: An Observational Study Including 8288 Patients. *J. Clin. Psychopharmacol.* **2018**, *38*, 570–576. [CrossRef]
104. Deng, S.-H.; Wang, Z.-Z.; Lu, H.-Y.; Li, L.; Hu, J.-Q.; Zhu, X.-Q.; Xie, H.-S.; Chen, H.-Z.; Zhang, M.; Ni, X.-J.; et al. A Retrospective Analysis of Steady-State Olanzapine Concentrations in Chinese Patients Using Therapeutic Drug Monitoring: Effects of Valproate and Other Factors. *Ther. Drug Monit.* **2020**, *42*, 636–642. [CrossRef]

105. An, H.; Fan, H.; Chen, S.; Qi, S.; Ma, B.; Shi, J.; Wang, Z.; Yang, F. Effects of Dose, Age, Sex, Body Weight, and Smoking on Plasma Concentrations of Olanzapine and N-Desmethyl Olanzapine in Inpatients With Schizophrenia. *J. Clin. Psychopharmacol.* **2021**, *41*, 255–259. [CrossRef]
106. Tveito, M.; Høiseth, G.; Haslemo, T.; Molden, E.; Smith, R.L. Impact of Age and Gender on Paliperidone Exposure in Patients after Administration of Long-Acting Injectable Formulations-an Observational Study Using Blood Samples from 1223 Patients. *Eur. J. Clin. Pharmacol.* **2021**, *77*, 1201–1208. [CrossRef]
107. Smith, R.L.; Haslemo, T.; Chan, H.F.; Refsum, H.; Molden, E. Clinically Relevant Effect of UGT1A4*3 on Lamotrigine Serum Concentration Is Restricted to Postmenopausal Women—A Study Matching Therapeutic Drug Monitoring and Genotype Data From 534 Patients. *Ther. Drug Monit.* **2018**, *40*, 567–571. [CrossRef]
108. Hefner, G.; Hahn, M.; Hohner, M.; Roll, S.C.; Klimke, A.; Hiemke, C. QTc Time Correlates with Amitriptyline and Venlafaxine Serum Levels in Elderly Psychiatric Inpatients. *Pharmacopsychiatry* **2019**, *52*, 38–43. [CrossRef]
109. Taurines, R.; Fekete, S.; Preuss-Wiedenhoff, A.; Warnke, A.; Wewetzer, C.; Plener, P.; Burger, R.; Gerlach, M.; Romanos, M.; Egberts, K.M. Therapeutic drug monitoring in children and adolescents with schizophrenia and other psychotic disorders using risperidone. *J. Neural Transm.* **2022**, *129*, 689–701. [CrossRef]
110. Kuzin, M.; Haen, E.; Hiemke, C.; Bochon, B.; Bochon, K.; Gründer, G.; Paulzen, M.; Schoretsanitis, G. Body Mass Index as a Determinant of Clozapine Plasma Concentrations: A Pharmacokinetic-Based Hypothesis. *J. Psychopharmacol.* **2021**, *35*, 273–278. [CrossRef]
111. Methaneethorn, J. Population Pharmacokinetics of Valproic Acid in Patients with Mania: Implication for Individualized Dosing Regimens. *Clin. Ther.* **2017**, *39*, 1171–1181. [CrossRef] [PubMed]
112. Schoretsanitis, G.; Haen, E.; Hiemke, C.; Fay, B.; Unholzer, S.; Correll, C.U.; Gründer, G.; Paulzen, M. Sex and Body Weight Are Major Determinants of Venlafaxine Pharmacokinetics. *Int. Clin. Psychopharmacol.* **2018**, *33*, 322–329. [CrossRef] [PubMed]
113. Warrings, B.; Samanski, L.; Deckert, J.; Unterecker, S.; Scherf-Clavel, M. Impact of Body Mass Index on Serum Concentrations of Antidepressants and Antipsychotics. *Ther. Drug Monit.* **2021**, *43*, 286–291. [CrossRef] [PubMed]
114. Hashimoto, M.; Maeda, H.; Oniki, K.; Yasui-Furukori, N.; Watanabe, H.; Saruwatari, J.; Kadowaki, D. New Insight Concerning Therapeutic Drug Monitoring-The Importance of the Concept of Psychonephrology. *Biol. Pharm. Bull.* **2022**, *45*, 834–842. [CrossRef] [PubMed]
115. Moschny, N.; Hefner, G.; Grohmann, R.; Eckermann, G.; Maier, H.B.; Seifert, J.; Heck, J.; Francis, F.; Bleich, S.; Toto, S.; et al. Therapeutic Drug Monitoring of Second- and Third-Generation Antipsychotic Drugs-Influence of Smoking Behavior and Inflammation on Pharmacokinetics. *Pharmaceuticals* **2021**, *14*, 514. [CrossRef]
116. Zhang, Y.-Y.; Zhou, X.-H.; Shan, F.; Liang, J. Infection Is Associated with Elevated Serum Concentrations of Antipsychotic Drugs. *Int. Clin. Psychopharmacol.* **2021**, *36*, 264–267. [CrossRef]
117. Scherf-Clavel, M.; Weidner, A.; Deckert, J.; Menke, A.; Unterecker, S. Pathological Concentration of C-Reactive Protein Is Correlated to Increased Concentrations of Quetiapine, but Not of Risperidone, Olanzapine and Aripiprazole in a Naturalistic Setting. *Pharmacopsychiatry* **2020**, *53*, 30–35. [CrossRef]
118. Helland, A.; Habib, S.; Ulvestad, L.; Spigset, O. Systemic Inflammation Complicates the Interpretation of Therapeutic Drug Monitoring of Risperidone. *J. Clin. Psychopharmacol.* **2018**, *38*, 263–265. [CrossRef]
119. Courlet, P.; Guidi, M.; Glatard, A.; Alves Saldanha, S.; Cavassini, M.; Buclin, T.; Marzolini, C.; Eap, C.B.; Decosterd, L.A.; Csajka, C.; et al. Escitalopram Population Pharmacokinetics in People Living with Human Immunodeficiency Virus and in the Psychiatric Population: Drug-Drug Interactions and Probability of Target Attainment. *Br. J. Clin. Pharmacol.* **2019**, *85*, 2022–2032. [CrossRef]
120. Wallerstedt, S.M.; Nylén, K.; Axelsson, M.A.B. Serum Concentrations of Antidepressants, Antipsychotics, and Antiepileptics over the Bariatric Surgery Procedure. *Eur. J. Clin. Pharmacol.* **2021**, *77*, 1875–1885. [CrossRef]
121. McGrane, I.R.; Salyers, L.A.; Molinaro, J.R.; Munjal, R.C. Roux-En-Y Gastric Bypass and Antipsychotic Therapeutic Drug Monitoring: Two Cases. *J. Pharm. Pract.* **2021**, *34*, 503–506. [CrossRef] [PubMed]
122. Sutherland, J.J.; Daly, T.M.; Jacobs, K.; Khawam, E.A.; Pozuelo, L.; Morrison, R.D.; Milne, S.B.; Daniels, J.S.; Ryan, T.P. Medication Exposure in Highly Adherent Psychiatry Patients. *ACS Chem. Neurosci.* **2018**, *9*, 555–562. [CrossRef]
123. Douglas-Hall, P.; Dzahini, O.; Gaughran, F.; Bile, A.; Taylor, D. Variation in Dose and Plasma Level of Lamotrigine in Patients Discharged from a Mental Health Trust. *Ther. Adv. Psychopharmacol.* **2017**, *7*, 17–24. [CrossRef]
124. Paulzen, M.; Haen, E.; Hiemke, C.; Stegmann, B.; Lammertz, S.E.; Gründer, G.; Schoretsanitis, G. Cytochrome P450-Mediated Interaction between Perazine and Risperidone: Implications for Antipsychotic Polypharmacy. *Br. J. Clin. Pharmacol.* **2017**, *83*, 1668–1675. [CrossRef]
125. Paulzen, M.; Schoretsanitis, G.; Stegmann, B.; Hiemke, C.; Gründer, G.; Schruers, K.R.J.; Walther, S.; Lammertz, S.E.; Haen, E. Pharmacokinetic Considerations in Antipsychotic Augmentation Strategies: How to Combine Risperidone with Low-Potency Antipsychotics. *Prog. Neuropsychopharmacol. Biol. Psychiatry* **2017**, *76*, 101–106. [CrossRef]
126. Jiang, P.; Sun, X.; Ren, J.; Liu, H.; Lin, Z.; Liu, J.; Fang, X.; Zhang, C. Effects of the Combination of Second-Generation Antipsychotics on Serum Concentrations of Aripiprazole and Dehydroaripiprazole in Chinese Patients with Schizophrenia. *Gen. Psychiatr.* **2021**, *34*, e100423. [CrossRef]
127. Hommers, L.; Scharl, M.; Hefner, G.; Hohner, M.; Fischer, M.; Pfuhlmann, B.; Deckert, J.; Unterecker, S. Comedication of Valproic Acid Is Associated with Increased Metabolism of Clozapine. *J. Clin. Psychopharmacol.* **2018**, *38*, 188–192. [CrossRef]

128. Smith, R.L.; Wollmann, B.M.; Kyllesø, L.; Tran, T.T.A.; Tveito, M.; Molden, E. Effect of Valproic Acid on the Metabolic Spectrum of Clozapine in Patients with Schizophrenia. *J. Clin. Psychopharmacol.* **2022**, *42*, 43–50. [CrossRef]
129. Gaebler, A.J.; Finner-Prével, M.; Lammertz, S.; Schaffrath, S.; Eisner, P.; Stöhr, F.; Röcher, E.; Winkler, L.; Kaleta, P.; Lenzen, L.; et al. The negative impact of vitamin D on antipsychotic drug exposure may counteract its potential benefits in schizophrenia. *Br. J. Clin. Pharmacol.* **2022**, *88*, 3193–3200. [CrossRef]
130. Gaebler, A.J.; Schoretsanitis, G.; Ben Omar, N.; Haen, E.; Endres, K.; Hiemke, C.; Paulzen, M. Metamizole but Not Ibuprofen Reduces the Plasma Concentration of Sertraline: Implications for the Concurrent Treatment of Pain and Depression/Anxiety Disorders. *Br. J. Clin. Pharmacol.* **2021**, *87*, 1111–1119. [CrossRef]
131. Paulzen, M.; Schoretsanitis, G.; Hiemke, C.; Gründer, G.; Haen, E.; Augustin, M. Reduced Clearance of Venlafaxine in a Combined Treatment with Quetiapine. *Prog. Neuropsychopharmacol. Biol. Psychiatry* **2018**, *85*, 116–121. [CrossRef] [PubMed]
132. Kuzin, M.; Schoretsanitis, G.; Haen, E.; Stegmann, B.; Hiemke, C.; Gründer, G.; Paulzen, M. Effects of the Proton Pump Inhibitors Omeprazole and Pantoprazole on the Cytochrome P450-Mediated Metabolism of Venlafaxine. *Clin. Pharmacokinet.* **2018**, *57*, 729–737. [CrossRef]
133. Magalhães, P.; Alves, G.; Fortuna, A.; Llerena, A.; Falcão, A. Clinical Collaborators of the GnG-PK/PD-AD Study Pharmacogenetics and Therapeutic Drug Monitoring of Fluoxetine in a Real-World Setting: A PK/PD Analysis of the Influence of (Non-)Genetic Factors. *Exp. Clin. Psychopharmacol.* **2020**, *28*, 589–600. [CrossRef]
134. Kuzin, M.; Schoretsanitis, G.; Haen, E.; Ridders, F.; Hiemke, C.; Gründer, G.; Paulzen, M. Pharmacokinetic Interactions between Clozapine and Sertraline in Smokers and Non-Smokers. *Basic Clin. Pharmacol. Toxicol.* **2020**, *127*, 303–308. [CrossRef] [PubMed]
135. Kuzin, M.; Schoretsanitis, G.; Haen, E.; Dammann, G.; Hiemke, C.; Gründer, G.; Paulzen, M. The Effects of Co-Prescription of Pantoprazole on the Clozapine Metabolism. *Pharmacopsychiatry* **2020**, *53*, 65–70. [CrossRef]
136. Depp, C.A.; Bowie, C.R.; Mausbach, B.T.; Wolyniec, P.; Thornquist, M.H.; Luke, J.R.; McGrath, J.A.; Pulver, A.E.; Patterson, T.L.; Harvey, P.D. Current Smoking Is Associated with Worse Cognitive and Adaptive Functioning in Serious Mental Illness. *Acta Psychiatr. Scand.* **2015**, *131*, 333–341. [CrossRef]
137. Firth, J.; Solmi, M.; Wootton, R.E.; Vancampfort, D.; Schuch, F.B.; Hoare, E.; Gilbody, S.; Torous, J.; Teasdale, S.B.; Jackson, S.E.; et al. A Meta-Review of "Lifestyle Psychiatry": The Role of Exercise, Smoking, Diet and Sleep in the Prevention and Treatment of Mental Disorders. *World Psychiatry* **2020**, *19*, 360–380. [CrossRef]
138. Wang, Y.-Y.; Wang, S.; Zheng, W.; Zhong, B.-L.; Ng, C.H.; Ungvari, G.S.; Wang, C.-X.; Xiang, Y.-T.; Li, X.-H. Cognitive Functions in Smoking and Non-Smoking Patients with Schizophrenia: A Systematic Review and Meta-Analysis of Comparative Studies. *Psychiatry Res.* **2019**, *272*, 155–163. [CrossRef]
139. Prochaska, J.J.; Das, S.; Young-Wolff, K.C. Smoking, Mental Illness, and Public Health. *Annu. Rev. Public Health* **2017**, *38*, 165–185. [CrossRef]
140. Augustin, M.; Schoretsanitis, G.; Hiemke, C.; Gründer, G.; Haen, E.; Paulzen, M. Differences in Duloxetine Dosing Strategies in Smoking and Nonsmoking Patients: Therapeutic Drug Monitoring Uncovers the Impact on Drug Metabolism. *J. Clin. Psychiatry* **2018**, *79*, 17m12086. [CrossRef]
141. Schoretsanitis, G.; Haen, E.; Conca, A.; Piacentino, D.; Ridders, F.; Hiemke, C.; Gründer, G.; Paulzen, M. Lack of Smoking Effects on Pharmacokinetics of Oral Paliperidone-Analysis of a Naturalistic Therapeutic Drug Monitoring Sample. *Pharmacopsychiatry* **2021**, *54*, 31–35. [CrossRef]
142. Augustin, M.; Schoretsanitis, G.; Pfeifer, P.; Gründer, G.; Liebe, C.; Paulzen, M. Effect of Fluvoxamine Augmentation and Smoking on Clozapine Serum Concentrations. *Schizophr Res.* **2019**, *210*, 143–148. [CrossRef]
143. Scherf-Clavel, M.; Samanski, L.; Hommers, L.G.; Deckert, J.; Menke, A.; Unterecker, S. Analysis of Smoking Behavior on the Pharmacokinetics of Antidepressants and Antipsychotics: Evidence for the Role of Alternative Pathways Apart from CYP1A2. *Int. Clin. Psychopharmacol.* **2019**, *34*, 93–100. [CrossRef]
144. Hart, X.M.; Heesen, S.; Schmitz, C.N.; Dörfler, S.; Wedekind, D.; Gründer, G.; Hiemke, C.; Havemann-Reinecke, U. Concentrations of escitalopram in blood of patients treated in a naturalistic setting: Focus on patients with alcohol and benzodiazepine use disorder. *Eur. Arch. Psychiatry Clin. Neurosci.* **2022**, 1–9. [CrossRef]
145. Jukic, M.M.; Smith, R.L.; Haslemo, T.; Molden, E.; Ingelman-Sundberg, M. Effect of CYP2D6 Genotype on Exposure and Efficacy of Risperidone and Aripiprazole: A Retrospective, Cohort Study. *Lancet Psychiatry* **2019**, *6*, 418–426. [CrossRef]
146. Waade, R.B.; Solhaug, V.; Høiseth, G. Impact of CYP2D6 on Serum Concentrations of Flupentixol, Haloperidol, Perphenazine and Zuclopenthixol. *Br. J. Clin. Pharmacol.* **2021**, *87*, 2228–2235. [CrossRef]
147. Jukić, M.M.; Smith, R.L.; Molden, E.; Ingelman-Sundberg, M. Evaluation of the CYP2D6 Haplotype Activity Scores Based on Metabolic Ratios of 4,700 Patients Treated with Three Different CYP2D6 Substrates. *Clin. Pharmacol. Ther.* **2021**, *110*, 750–758. [CrossRef]
148. Miroshnichenko, I.I.; Pozhidaev, I.V.; Ivanova, S.A.; Baymeeva, N.V. Therapeutic Drug Monitoring of Olanzapine and Cytochrome P450 Genotyping in Nonsmoking Subjects. *Ther. Drug Monit.* **2020**, *42*, 325–329. [CrossRef]
149. Ji, Y.; Skierka, J.M.; Blommel, J.H.; Moore, B.E.; VanCuyk, D.L.; Bruflat, J.K.; Peterson, L.M.; Veldhuizen, T.L.; Fadra, N.; Peterson, S.E.; et al. Preemptive pharmacogenomic testing for precision medicine: A comprehensive analysis of five actionable pharmacogenomic genes using next-generation DNA sequencing and a customized CYP2D6 genotyping cascade. *J. Mol. Diagn.* **2016**, *18*, 438–445. [CrossRef]

150. Kneller, L.A.; Zubiaur, P.; Koller, D.; Abad-Santos, F.; Hempel, G. Influence of CYP2D6 Phenotypes on the Pharmacokinetics of Aripiprazole and Dehydro-Aripiprazole Using a Physiologically Based Pharmacokinetic Approach. *Clin. Pharmacokinet.* **2021**, *60*, 1569–1582. [CrossRef]
151. Smith, R.L.; O'Connell, K.; Athanasiu, L.; Djurovic, S.; Kringen, M.K.; Andreassen, O.A.; Molden, E. Correction: Identification of a Novel Polymorphism Associated with Reduced Clozapine Concentration in Schizophrenia Patients-a Genome-Wide Association Study Adjusting for Smoking Habits. *Transl. Psychiatry* **2020**, *10*, 366. [CrossRef]
152. Sangüesa, E.; Cirujeda, C.; Concha, J.; Padilla, P.P.; Ribate, M.P.; García, C.B. Implementation of Pharmacogenetics in a Clozapine Treatment Resistant Patient: A Case Report. *Pharmacogenomics* **2019**, *20*, 871–877. [CrossRef]
153. Hicks, J.K.; Sangkuhl, K.; Swen, J.J.; Ellingrod, V.L.; Müller, D.J.; Shimoda, K.; Bishop, J.R.; Kharasch, E.D.; Skaar, T.C.; Gaedigk, A.; et al. Clinical Pharmacogenetics Implementation Consortium Guideline (CPIC) for CYP2D6 and CYP2C19 Genotypes and Dosing of Tricyclic Antidepressants: 2016 Update. *Clin. Pharmacol. Ther.* **2017**, *102*, 37–44. [CrossRef]
154. Mifsud Buhagiar, L.; Casha, M.; Grech, A.; Serracino Inglott, A.; LaFerla, G. The interplay between pharmacogenetics, concomitant drugs and blood levels of amitriptyline and its main metabolites. *Pers. Med.* **2021**, *19*, 113–123. [CrossRef]
155. Kringen, M.K.; Bråten, L.S.; Haslemo, T.; Molden, E. The Influence of Combined CYP2D6 and CYP2C19 Genotypes on Venlafaxine and O-Desmethylvenlafaxine Concentrations in a Large Patient Cohort. *J. Clin. Psychopharmacol.* **2020**, *40*, 137–144. [CrossRef]
156. Haslemo, T.; Eliasson, E.; Jukić, M.M.; Ingelman-Sundberg, M.; Molden, E. Significantly Lower CYP2D6 Metabolism Measured as the O/N-Desmethylvenlafaxine Metabolic Ratio in Carriers of CYP2D6*41 versus CYP2D6*9 or CYP2D6*10: A Study on Therapeutic Drug Monitoring Data from 1003 Genotyped Scandinavian Patients. *Br. J. Clin. Pharmacol.* **2019**, *85*, 194–201. [CrossRef]
157. Scherf-Clavel, M.; Weber, H.; Wurst, C.; Stonawski, S.; Hommers, L.; Unterecker, S.; Wolf, C.; Domschke, K.; Rost, N.; Brückl, T.; et al. Effects of Pharmacokinetic Gene Variation on Therapeutic Drug Levels and Antidepressant Treatment Response. *Pharmacopsychiatry* **2022**, *55*, 246–254. [CrossRef]
158. Zastrozhin, M.S.; Skryabin, V.; Rwere, F.; Petukhov, A.E.; Pankratenko, E.P.; Pozdniakov, S.A.; Ivanchenko, V.A.; Noskov, V.V.; Zaytsev, I.A.; Vinokurova, N.V.; et al. Influence of CYP2C19*17 Genetic Polymorphism on the Steady-State Concentration of Escitalopram in Patients with Recurrent Depressive Disorder. *Psychopharmacol. Bull.* **2022**, *52*, 8–19.
159. Gaebler, A.J.; Schneider, K.L.; Stingl, J.C.; Paulzen, M. Subtherapeutic Bupropion and Hydroxybupropion Serum Concentrations in a Patient with CYP2C19*1/*17 Genotype Suggesting a Rapid Metabolizer Status. *Pharm. J.* **2020**, *20*, 840–844. [CrossRef]
160. Suzuki, T.; Mihara, K.; Nagai, G.; Kagawa, S.; Nakamura, A.; Nemoto, K.; Kondo, T. Relationship Between UGT1A4 and UGT2B7 Polymorphisms and the Steady-State Plasma Concentrations of Lamotrigine in Patients With Treatment-Resistant Depressive Disorder Receiving Lamotrigine as Augmentation Therapy. *Ther. Drug Monit.* **2019**, *41*, 86–90. [CrossRef]
161. Zastrozhin, M.S.; Skryabin, V.Y.; Smirnov, V.V.; Petukhov, A.E.; Pankratenko, E.P.; Zastrozhina, A.K.; Grishina, E.A.; Ryzhikova, K.A.; Bure, I.V.; Golovinskii, P.A.; et al. Effects of Plasma Concentration of Micro-RNA Mir-27b and CYP3A4*22 on Equilibrium Concentration of Alprazolam in Patients with Anxiety Disorders Comorbid with Alcohol Use Disorder. *Gene* **2020**, *739*, 144513. [CrossRef]
162. Zijp, T.R.; Izzah, Z.; Åberg, C.; Gan, C.T.; Bakker, S.J.L.; Touw, D.J.; van Boven, J.F.M. Clinical Value of Emerging Bioanalytical Methods for Drug Measurements: A Scoping Review of Their Applicability for Medication Adherence and Therapeutic Drug Monitoring. *Drugs* **2021**, *81*, 1983–2002. [CrossRef]
163. Martial, L.C.; Aarnoutse, R.E.; Mulder, M.; Schellekens, A.; Brüggemann, R.J.M.; Burger, D.M.; Schene, A.H.; Batalla, A. Dried Blood Spot Sampling in Psychiatry: Perspectives for Improving Therapeutic Drug Monitoring. *Eur. Neuropsychopharmacol.* **2017**, *27*, 205–216. [CrossRef]
164. Geers, L.M.; Cohen, D.; Wehkamp, L.M.; van Hateren, K.; Koster, R.A.; Fedorenko, O.Y.; Semke, A.V.; Bokhan, N.; Ivanova, S.A.; Kosterink, J.G.W.; et al. Dried Blood Spot Analysis for Therapeutic Drug Monitoring of Clozapine. *J. Clin. Psychiatry* **2017**, *78*, e1211–e1218. [CrossRef]
165. Marasca, C.; Protti, M.; Mandrioli, R.; Atti, A.R.; Armirotti, A.; Cavalli, A.; De Ronchi, D.; Mercolini, L. Whole Blood and Oral Fluid Microsampling for the Monitoring of Patients under Treatment with Antidepressant Drugs. *J. Pharm. Biomed. Anal.* **2020**, *188*, 113384. [CrossRef]
166. Protti, M.; Marasca, C.; Cirrincione, M.; Cavalli, A.; Mandrioli, R.; Mercolini, L. Assessment of Capillary Volumetric Blood Microsampling for the Analysis of Central Nervous System Drugs and Metabolites. *Analyst* **2020**, *145*, 5744–5753. [CrossRef]
167. Kloosterboer, S.M.; de Winter, B.C.M.; Bahmany, S.; Al-Hassany, L.; Dekker, A.; Dieleman, G.C.; van Gelder, T.; Dierckx, B.; Koch, B.C.P. Dried Blood Spot Analysis for Therapeutic Drug Monitoring of Antipsychotics: Drawbacks of Its Clinical Application. *Ther. Drug Monit.* **2018**, *40*, 344–350. [CrossRef]
168. Londhe, V.; Rajadhyaksha, M. Opportunities and Obstacles for Microsampling Techniques in Bioanalysis: Special Focus on DBS and VAMS. *J. Pharm. Biomed. Anal.* **2020**, *182*, 113102. [CrossRef]
169. Marasca, C.; Mandrioli, R.; Sardella, R.; Vovk, T.; Armirotti, A.; Cavalli, A.; Serretti, A.; Protti, M.; Mercolini, L. Dried volumetric microsampling approaches for the therapeutic drug monitoring of psychiatric patients undergoing clozapine treatment. *Front. Psychiatry* **2022**, *13*, 794609. [CrossRef]
170. Stern, M.; Giebels, M.; Fey, T.; Lübking, M.; Alferink, J.; Hempel, G. Validation and Clinical Application of a Volumetric Absorptive Microsampling Method for 14 Psychiatric Drugs. *Bioanalysis* **2020**, *12*, 1129–1147. [CrossRef]

171. Vincze, I.; Rudge, J.; Vásárhelyi, B.; Karvaly, G.B. Analysis of 14 Drugs in Dried Blood Mi-crosamples in a Single Workflow Using Whole Blood and Serum Calibrators. *Bioanalysis* **2020**, *12*, 1243–1261. [CrossRef]
172. Dziurkowska, E.; Wesołowski, M. Effects of Age, Drug Dose, and Sampling Time on Salivary Levels of Olanzapine, Quetiapine, and Their Metabolites. *J. Clin. Med.* **2020**, *9*, 3288. [CrossRef]
173. Parkin, G.M.; McCarthy, M.J.; Thein, S.H.; Piccerillo, H.L.; Warikoo, N.; Granger, D.A.; Thomas, E.A. Saliva Testing as a Means to Monitor Therapeutic Lithium Levels in Patients with Psychiatric Disorders: Identification of Clinical and Environmental Covariates, and Their Incorporation into a Prediction Model. *Bipolar Disord.* **2021**, *23*, 679–688. [CrossRef]
174. Ebert, K.; Maurice, E.; Lukačin, R.; Fleischhaker, C.; Schulz, E.; Ebert, D.; Clement, H.-W. Serum and Saliva Concentrations of Venlafaxine, O-Desmethylvenlafaxine, Quetiapine, and Citalopram in Psychiatric Patients. *Ther. Drug Monit.* **2018**, *40*, 351–355. [CrossRef]
175. Wohkittel, C.; Högger, P.; Fekete, S.; Romanos, M.; Gerlach, M. Relationship between Amphetamine Concentrations in Saliva and Serum in Children and Adolescents with Attention-Deficit/Hyperactivity Disorder. *Ther. Drug Monit.* **2021**, *43*, 564–569. [CrossRef]
176. Neumann, J.; Beck, O.; Dahmen, N.; Böttcher, M. Potential of Oral Fluid as a Clinical Specimen for Compliance Monitoring of Psychopharmacotherapy. *Ther. Drug Monit.* **2018**, *40*, 245–251. [CrossRef]
177. Criscuolo, F.; Cantu, F.; Taurino, I.; Carrara, S.; De Micheli, G. A Wearable Electrochemical Sensing System for Non-Invasive Monitoring of Lithium Drug in Bipolar Disorder. *IEEE Sens. J.* **2021**, *21*, 9649–9656. [CrossRef]
178. Sweilam, M.N.; Cordery, S.F.; Totti, S.; Velliou, E.G.; Campagnolo, P.; Varcoe, J.R.; Delgado-Charro, M.B.; Crean, C. Textile-Based Non-Invasive Lithium Drug Monitoring: A Proof-of-Concept Study for Wearable Sensing. *Biosens. Bioelectron.* **2020**, *150*, 111897. [CrossRef]
179. Mobed, A.; Ahmadalipour, A.; Fakhari, A.; Kazem, S.S.; Saadi, G.K. Bioassay: A Novel Approach in Antipsychotic Pharmacology. *Clin. Chim. Acta* **2020**, *509*, 30–35. [CrossRef]
180. Roda, A.; Zangheri, M.; Calabria, D.; Mirasoli, M.; Caliceti, C.; Quintavalla, A.; Lombardo, M.; Trombini, C.; Simoni, P. A Simple Smartphone-Based Thermochemiluminescent Immunosensor for Valproic Acid Detection Using 1,2-Dioxetane Analogue-Doped Nanoparticles as a Label. *Sens. Actuators B Chem.* **2019**, *279*, 327–333. [CrossRef]
181. Mazzilli, R.; Curto, M.; De Bernardini, D.; Olana, S.; Capi, M.; Salerno, G.; Cipolla, F.; Zamponi, V.; Santi, D.; Mazzilli, F.; et al. Psychotropic Drugs Levels in Seminal Fluid: A New Therapeutic Drug Monitoring Analysis? *Front. Endocrinol.* **2021**, *12*, 620936. [CrossRef]
182. Enders, J.R.; Reddy, S.G.; Strickland, E.C.; McIntire, G.L. Identification of Metabolites of Brexpiprazole in Human Urine for Use in Monitoring Patient Compliance. *Clin. Mass. Spectrom.* **2017**, *6*, 21–24. [CrossRef]
183. Insel, T.; Cuthbert, B.; Garvey, M.; Heinssen, R.; Pine, D.S.; Quinn, K.; Sanislow, C.; Wang, P. Research Domain Criteria (RDoC): Toward a New Classification Framework for Research on Mental Disorders. *Am. J. Psychiatry* **2010**, *167*, 748–751. [CrossRef]
184. Tandon, R.; Nasrallah, H.A.; Keshavan, M.S. Schizophrenia, "Just the Facts" 4. Clinical Features and Conceptualization. *Schizophr Res.* **2009**, *110*, 1–23. [CrossRef] [PubMed]
185. Kupka, R.; Duffy, A.; Scott, J.; Almeida, J.; Balanzá-Martínez, V.; Birmaher, B.; Bond, D.J.; Brietzke, E.; Chendo, I.; Frey, B.N.; et al. Consensus on Nomenclature for Clinical Staging Models in Bipolar Disorder: A Narrative Review from the International Society for Bipolar Disorders (ISBD) Staging Task Force. *Bipolar Disord.* **2021**, *23*, 659–678. [CrossRef]
186. Horwitz, T.; Lam, K.; Chen, Y.; Xia, Y.; Liu, C. A Decade in Psychiatric GWAS Research. *Mol. Psychiatry* **2019**, *24*, 378–389. [CrossRef]
187. Witt, S.H.; Streit, F.; Jungkunz, M.; Frank, J.; Awasthi, S.; Reinbold, C.S.; Treutlein, J.; Degenhardt, F.; Forstner, A.J.; Heilmann-Heimbach, S.; et al. Genome-Wide Association Study of Borderline Personality Disorder Reveals Genetic Overlap with Bipolar Disorder, Major Depression and Schizophrenia. *Transl. Psychiatry* **2017**, *7*, e1155. [CrossRef]
188. Etkin, A. A Reckoning and Research Agenda for Neuroimaging in Psychiatry. *Am. J. Psychiatry* **2019**, *176*, 507–511. [CrossRef]
189. McLoughlin, G.; Makeig, S.; Tsuang, M.T. In Search of Biomarkers in Psychiatry: EEG-Based Measures of Brain Function. *Am. J. Med. Genet. B Neuropsychiatr. Genet.* **2014**, *165B*, 111–121. [CrossRef]
190. Kam, H.; Jeong, H. Pharmacogenomic Biomarkers and Their Applications in Psychiatry. *Genes* **2020**, *11*, 1445. [CrossRef]
191. Stern, S.; Linker, S.; Vadodaria, K.C.; Marchetto, M.C.; Gage, F.H. Prediction of Response to Drug Therapy in Psychiatric Disorders. *Open Biol.* **2018**, *8*, 180031. [CrossRef] [PubMed]
192. Ziani, P.R.; Feiten, J.G.; Goularte, J.F.; Colombo, R.; Antqueviezc, B.; Géa, L.P.; Rosa, A.R. Potential Candidates for Biomarkers in Bipolar Disorder: A Proteomic Approach through Systems Biology. *Clin. Psychopharmacol. Neurosci.* **2022**, *20*, 211–227. [CrossRef] [PubMed]
193. Stevenson, J.M.; Reilly, J.L.; Harris, M.S.H.; Patel, S.R.; Weiden, P.J.; Prasad, K.M.; Badner, J.A.; Nimgaonkar, V.L.; Keshavan, M.S.; Sweeney, J.A.; et al. Antipsychotic Pharmacogenomics in First Episode Psychosis: A Role for Glutamate Genes. *Transl. Psychiatry* **2016**, *6*, e739. [CrossRef] [PubMed]
194. Lydiard, J.; Nemeroff, C.B. Biomarker-Guided Tailored Therapy. *Front. Psychiatry* **2019**, *1192*, 199–224. [CrossRef]

pharmaceutics

MDPI

Article

Pharmacokinetics of Haloperidol in Critically Ill Patients: Is There an Association with Inflammation?

Letao Li [1], Sebastiaan D. T. Sassen [1], Mathieu van der Jagt [2], Henrik Endeman [2], Birgit C. P. Koch [1] and Nicole G. M. Hunfeld [1,2,*]

[1] Department of Hospital Pharmacy, Erasmus MC-University Medical Center, Doctor Molewaterplein 40, 3015 GD Rotterdam, The Netherlands; l.li.1@erasmusmc.nl (L.L.); s.sassen@erasmusmc.nl (S.D.T.S.); b.koch@erasmusmc.nl (B.C.P.K.)

[2] Department of Intensive Care, Erasmus MC-University Medical Center, Doctor Molewaterplein 40, 3015 GD Rotterdam, The Netherlands; m.vanderjagt@erasmusmc.nl (M.v.d.J.); h.endeman@erasmusmc.nl (H.E.)

* Correspondence: n.hunfeld@erasmusmc.nl

Abstract: Haloperidol is considered the first-line treatment for delirium in critically ill patients. However, clinical evidence of efficacy is lacking and no pharmacokinetic studies have been performed in intensive care unit (ICU) patients. The aim of this study was to establish a pharmacokinetic model to describe the PK in this population to improve insight into dosing. One hundred and thirty-nine samples from 22 patients were collected in a single-center study in adults with ICU delirium who were treated with low-dose intravenous haloperidol (3–6 mg per day). We conducted a population pharmacokinetic analysis using Nonlinear Mixed Effects Modelling (NONMEM). A one-compartment model best described the data. The mean population estimates were 51.7 L/h (IIV 42.1%) for clearance and 1490 L for the volume of distribution. The calculated half-life was around 22 h (12.3–29.73 h) for an average patient. A negative correlation between C-Reactive Protein (CRP) and haloperidol clearance was observed, where clearance decreased significantly with increasing CRP up to a CRP concentration of 100 mg/L. This is the first step towards haloperidol precision dosing in ICU patients and our results indicate a possible role of inflammation.

Keywords: haloperidol; pharmacokinetics; delirium; critical ill; ICU

Citation: Li, L.; Sassen, S.D.T.; van der Jagt, M.; Endeman, H.; Koch, B.C.P.; Hunfeld, N.G.M. Pharmacokinetics of Haloperidol in Critically Ill Patients: Is There an Association with Inflammation? *Pharmaceutics* **2022**, *14*, 549. https://doi.org/10.3390/pharmaceutics14030549

Academic Editors: Barna Vasarhelyi and Gellért Balázs Karvaly

Received: 21 January 2022
Accepted: 25 February 2022
Published: 28 February 2022

1. Introduction

Delirium is quite common in intensive care unit (ICU) patients and is associated with poor clinical prognosis [1–5]. Currently the treatment of delirium may include pharmacological agents, including antipsychotics, melatonin, alpha-2 agonists (dexmedetomidine and clonidine), next to nonpharmacological interventions [6–8]. Among antipsychotics, haloperidol is the most commonly used. However, clinical evidence for the effect of haloperidol in decreasing ICU delirium is scarce [8–11]. Pharmacokinetics (PK) can play an important role in understanding the effect of haloperidol in ICU patients. Critically ill patients tend to show large differences in PK [12,13]. In the case of haloperidol, this may lead to increased variability in haloperidol blood concentrations in ICU patients, compared to non-ICU patients [14,15]. The variable PK might explain the variability in the effect, hence adjusting the dose based on individual PK parameters might improve drug efficacy. To understand more of this variability in blood concentrations, it is important to specifically study the pharmacokinetics of haloperidol in ICU patients.

Previous studies in non-ICU populations have shown that haloperidol has typical pharmacokinetic features of a lipophilic drug. It has high protein binding (90%), large volume of distribution (Vd) (1000–3000 L), and is predominantly metabolized by the liver and gut via glucuronidation (40–50%), CYP3A4 (25–30%), and CYP2D6 (25–30%) [15–18].

Previous studies have shown that CYP2D6 genetic polymorphism influences the haloperidol concentration levels in non-ICU patients [19,20]. For CYP3A4, the isoenzyme activity caused concentration changes only at higher doses [21] The glucuronidation is a major metabolism pathway of haloperidol [22], but only in vitro studies have shown that this pathway might cause inter-individual concentration variance [23]. The change in volume of distribution caused by pathophysiological changes is relatively small compared to hydrophilic drugs, but it is more susceptible to changes in drug clearance (CL) due to liver function alteration.

The available pharmacokinetic parameters related to haloperidol are mainly from studies in a healthy population or in non-critically ill patients with schizophrenia with relatively small sample sizes (less than 10 patients). Only one study on Japanese psychopaths included 218 patients [16,24–29]. Hence, the dosing strategy based on the parameters from those models might not be suitable for ICU patients. The goal of this study is to better understand the pharmacokinetics of haloperidol in critical care patients. Information on pharmacokinetics by means of population PK modelling may support further efficacy studies of haloperidol in critically ill patients.

2. Materials and Methods

2.1. Study Design

Data were collected at the adult ICU of Erasmus University Medical Centre (EMC), Rotterdam, the Netherlands, during a 3-year period (between October 2014 and April 2017) as previously described [30]. This study was conducted in accordance with the principles of the Declaration of Helsinki (version: October 2008) and approved by the Institutional Review Board (project identification code: MEC-2014-264, 21-Juli-2014, Medisch Ethische Toetsings Commissie Erasmus MC), more details see Supplementary Materials File C. Informed consent was obtained from each patients' legally authorized representative given all patients had delirium (see Supplementary Materials File D). Patients who developed delirium received 1 mg every 8 h (q8h) by intravenous bolus infusion [or 0.5 mg q8h by intravenous bolus infusion for patients aged $\geq$ 80 years or 2 mg q8h by intravenous bolus infusion in case of agitation] within 8 h of delirium detection, which constituted the routine regimen in the EMC for the treatment of ICU delirium at that time. The haloperidol dose was decreased if the Intensive Care Delirium Screening Checklist (ICDSC) score, a validated screening tool for delirium, was below or equal to 3 for more than 24 h, and was ceased if the ICDSC was below or equal to 3 for more than another 24 h.

2.2. Data Collection

Samples were collected and determined on days 2, 3, 4, 5, and 6 (end of study) each morning before haloperidol was dosed or discontinued according to protocol standards, or in participants who were discharged from ICU or transferred to another hospital.. The pharmacokinetic modeling was performed at day 2 (t = 0–1 h, t = 2–3 h, t = 4–5 h, t = 6–8 h). Serum samples were collected in EDTA tubes. Samples were collected from the arterial line in a strictly standard manner (according to ICU protocol) by ICU nursing staff and therefore we expect no infection risk. The samples were immediately sent to the laboratory of the hospital pharmacy and stored at -80 °C and then thawed at room temperature before analyzing. Levels of albumin, creatinine, urea, bilirubin, and C-reactive protein (CRP) where measured in LiHep plasma (Barricor Vacutainer, BD, Franklin Lakes, NY, USA, Belgium) on a routine chemistry analyzer (Cobas 8000, Roche Diagnostics, Basel, Switzerland). Additionally, white blood cell-(WBC) and platelet count were analyzed according to standard clinical care in the ICU in whole blood (K2EDTA Vacutainer, Franklin Lakes, NY, USA) on a routine hematology analyzer (XN9000, Sysmex, Kobe, Japan).

Serum haloperidol concentrations were analyzed via validated Liquid Chromatography tandem Mass Spectrometry (Waters Corporation, Milford, MA, USA) (see Supplementary Materials File E). We determined linearity, lower limit of quantitation (LLOQ), upper limit of quantitation (ULOQ). The method was validated according to Food and

Drug Administration(FDA)/European Medicines Agency (EMA) guidelines [31,32]. The 2.1 × 100 mm Waters Acquity UPLC BEH C18 1.7 µm column (cat no. 186002352) was used in combination with optimized chromatographic conditions. To suit the validation parameters for analytical validation, a shorter runtime of 5 min and the use of two eluents with changing percentage was tested. In addition, we optimized the method for a higher sensitivity and selectivity, according to the standard procedure for validation of our method. The LLOQ was set at 0.5 µg/L and the ULOQ at 20 µg/L. Other parameters that were collected were age, gender, ethnic origin, Body Mass Index (BMI), Acute Physiology and Chronic Health Evaluation (APACHE) III score, Intensive Care Delirium Screening Checklist (ICDSC) score at start of haloperidol, quetiapine exposure, additional drug use, CYP450 status, admission reason, length of ICU stay, amount of blood samples collected, and outcome.

2.3. Data Analysis

The pharmacokinetic analysis of haloperidol was performed using the nonlinear effects modeling approach in NONMEM® first-order conditional estimates (FOCE) with interaction [version 7.4, ICON, Development Solutions, MD, USA], Pirana version 2.9.9 (Certara, Princeton, NJ, USA), and data were further analyzed in R version 4.0.5 (R Foundation for Statistical Computing, Vienna, Austria). All the concentration data were log-transformed. A one-compartment model was fitted to the data. Subsequently, more complex models were tested. The model fit was evaluated both numerically by the precision of the estimated PK parameters and the change in the objective function values (dOFV), and visually by goodness-of-fit plots (GoF) and visual predictive checks (VPC). For the covariate analysis, the stepwise covariate modeling with forward inclusion-backward elimination method was applied [33]. In the forward process, a 3.84-point decrease in OFV for one degree of freedom was considered a significant improvement of the model with a p-value of <0.05. For the backward elimination process, the statistical criterion was set to an increase of OFV to 6.64 for covariate selection. A constant error model was used on the log transformed data to describe the residual error in the model predicted plasma concentrations. Age, gender, length, weight, BMI, BSA, CYP3A4, CYP2D6, CPR, creatinine, albumin, bilirubin, APACHE III, SOFA, ASAT, ALAT, potential interaction drugs (including erythromycin, amiodarone, metoprolol, metoclopramide, voriconazole, and fluconazole), WBC, and platelet count were tested as covariates. CYP3A4 and CYP2D6 patient genotyping was performed using Autogenomics INFINITY genotyping platform (Carlsbad, CA, USA) and relevant alleles present and gene duplication were detected. Patients were classified according to the number of active enzyme alleles present: poor metabolizers (PM; two defective alleles), intermediate metabolizers (IM, 2 decreased activity alleles or 1 active and 1 inactive allele), extensive metabolizers (EM), and ultra-rapid metabolizers (UM, gene duplication positive in the absence of a CYP2D6 null allele).

2.4. Model Simulation

To show an illustration of the covariate effect on the plasma concentrations of haloperidol, deterministic simulations were performed by using NONMEM. The haloperidol plasma concentrations under different covariates were simulated over a time course of 72 h (last dose at 72 h) and intravenous bolus doses were administered every 8 h. The median and 90% confidence interval are shown graphically.

3. Results

3.1. Study Population

An overview of all patient characteristics is presented in Table 1. A total of 22 critically ill adult patients were enrolled in the study; 54.5% of the patients were male, median age was 67 years (range from 48 to 77), median BMI was 27 (range from 18 to 39) m^2, median APACHE III score was 80.5 (range from 54 to 181), median length of ICU stay was 16 days (range from 2 to 63). Main reasons for ICU admission were surgery (n = 7; 32%), sepsis

(*n* = 3; 14%), respiratory failure (*n* = 3; 14%), and vascular aneurysm (*n* = 2; 9%). For the CYP2D6 status: extensive metabolizers (*n* = 12, 54%), intermediate metabolizers (*n* = 7, 32%), and poor metabolizers (PM) (*n* = 3, 14%). No ultra-rapid metabolizers were detected. For the CYP3A4 status: extensive metabolizers (*n* = 18, 82%) and intermediate metabolizers (*n* = 4, 18%). No ultra-rapid metabolizers or PMs were detected. Of the 22 patients, eleven patients died (50%), of which six during the ICU stay, four after ICU discharge and one after transfer to another hospital.

Table 1. Patient characteristics over the time course of the study.

Characteristics	N = 22
Age, years (median, range)	67 (48–77)
Male, *n*(%)	12 (54.5)
Female, *n*(%)	10 (45.5)
Weight, kg (median, range)	80 (52–137)
Ethnic origin, *n* (%)	
Caucasian	22 (100)
BMI (median, range)	27 (18–39)
Primary reason for ICU admission, *n* (%)	
Surgery	7 (32%)
Respiratory failure	3 (14%)
Sepsis	3 (14%)
Vascular aneurysm	2 (9%)
Blood chemistry, serum levels at admission (median, range)	
Albumin, g/L	26 (6–47)
Creatinine, µmol/L	130 (32–401)
Urea, mmol/L	13(4–46)
Bilirubin, µmol/L	14 (3–754)
CRP, mg/L	171 (4.1–368)
CYP2D6 *n* (%)	
Extensive metabolizers	12 (54%)
Intermediate metabolizers	7 (32%)
Poor metabolizers	3 (14%)
CYP3A4 *n* (%)	
Extensive metabolizers	18 (82%)
Intermediate metabolizers	4 (12%)
Quetiapine exposure *n*(%)	5 (22.7%)
APACHE III score median (range)	81 (76–99)
ICDSC baseline median (range)	4 (1–6)
Duration of stay (during using halo), days (median, range)	6.5 (3–8)
Died in ICU, *n* (%)	11 (50)
Cause of death	
Respiratory failure (During ICU)	1
Sepsis with multiple organ failure (During ICU)	4
Cardiac causes (after ICU)	2
Gastrointestinal causes (after ICU)	2
Respiratory insufficiency (transferred to another hospital)	1
Unknown (transferred to another hospital)	1
Blood samples collected, median (range)	7.5 (3–8)

APACHE: Acute Physiology and Chronic Health Evaluation, BMI: Body mass index, CRP: C-reactive protein, ICDSC: Intensive Care Delirium Screening Checklist, ICU: intensive care unit.

Total daily intravenous doses of haloperidol ranged from 1.5 to 6 mg. A total of 145 blood samples were collected and a total of 6 concentrations were censored due to sampling errors (sampling during the haloperidol infusion).

3.2. Structural Model

The logarithmic transformed concentration data were best described by a one-compartment model with an additive residual error. Inter-individual variability (IIV) was included on CL. The final structural model was used for covariate analysis. Stepwise (forward and

backward screening) model building strategies were implemented to identify potential covariates, explaining the between-subject variability in model parameters, equations, and model codes (Supplementary Materials Files A and B, respectively).

The potential covariates (age, gender, length, weight, BMI, BSA, CYP3A4, CYP2D6, CPR, creatinine, albumin, bilirubin, APACHE III, SOFA, ASAT, ALAT, potential interaction drugs (including erythromycin, amiodarone, metoprolol, metoclopramide, voriconazole and fluconazole), WBC, and platelet) were screened. For continuous variables such as WBC, CRP, and weight, we used the value divided by the median as covariate on the clearance. For categorical variables like gender, CYP3A4, and CYP2D6 polymorphism, we gave different variables a value and multiplied it with typical haloperidol clearance value. Only CRP on CL resulted in a significant improvement of model fit, with a drop in OFV of 7.533 and a decrease in IIV on CL from 40.4% to 29.9%. Adding CRP into the equation decreased the objective function value (OFV) from −49.32 to −56.81 (dOFV = −7.49), which explained 31% of the IIV on CL. An overview of all parameter estimates is given in Table 2. The clearance of haloperidol is 51.7 L/h and it has a large volume of distribution (1490 L). CRP was able to significantly decrease the variance in CL, as is shown in Figure 1. When CRP was incorporated as a covariate into the final model, the ETA decreased and became more evenly distributed.

Table 2. Population pharmacokinetic parameters for base and final models.

Parameter	Base Model	RSE%	Shrinkage%	Final Model	RSE%	Shrinkage%	Bootstrap of the Final Model		
							Median	90% Percentile (Lower)	90% Percentile (Upper)
CL (L/h)	54.6	11		51.7	12		50.64	39.65	63.74
Vd (L)	1450	29		1490	31		1522.05	893.6	2305.2
CRP				−0.23	50		−0.21	−0.02	−0.42
IIV-CL (%)	40.4%	31	15	29.9%	27	24			
Residual variability	0.457	9	6	0.461	9	5	0.446	0.382	0.54

CRP: C-reactive protein, CL: clearance, IIV-CL: inter-variability on clearance, Vd: volume of distribution.

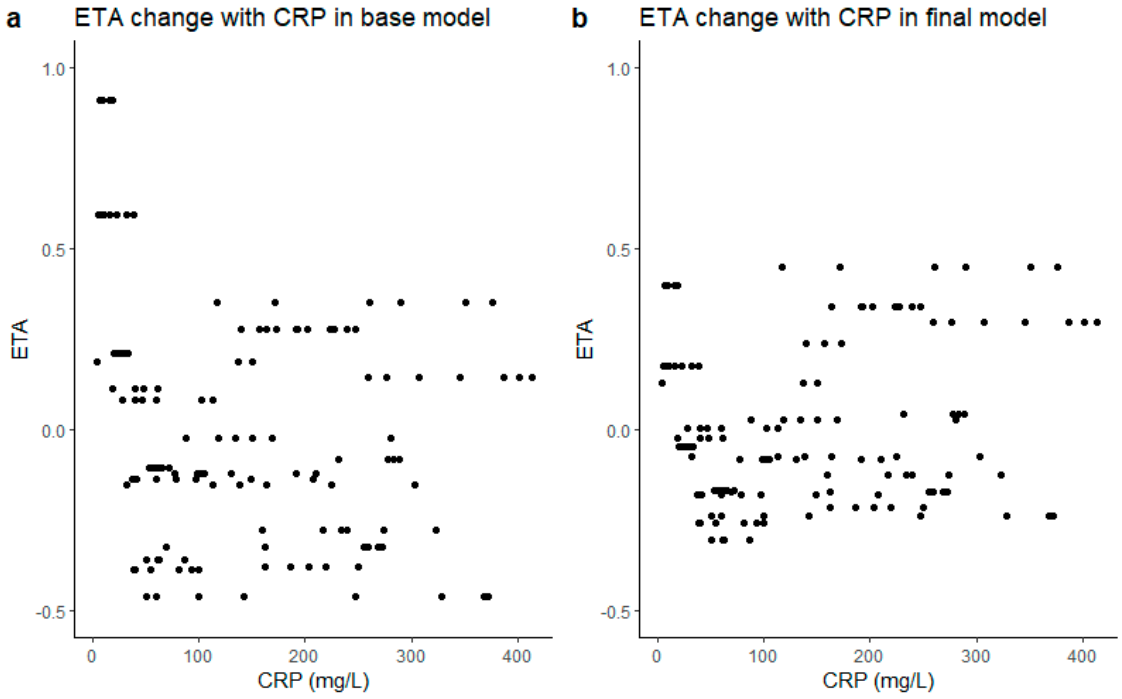

Figure 1. ETA of CL versus CRP: (**a**) ETA versus CRP in the base model; (**b**) ETA versus CRP in the final model. CRP: C−reactive protein.

3.3. Model Evaluation

Figure 2 shows that both the population predictions (PRED) and the individual predictions (IPRED) were evenly distributed around the uniform line when plotted versus observed concentrations (DV). The weighted residuals were symmetrically distributed throughout the time after dose and prediction errors were predominantly within two standard deviations. Figure 3 shows the covariate CRP on the effect of haloperidol clearance. There is a negative relationship between the clearance and CRP; the relationship disappeared with CRP above 100 mg/L.

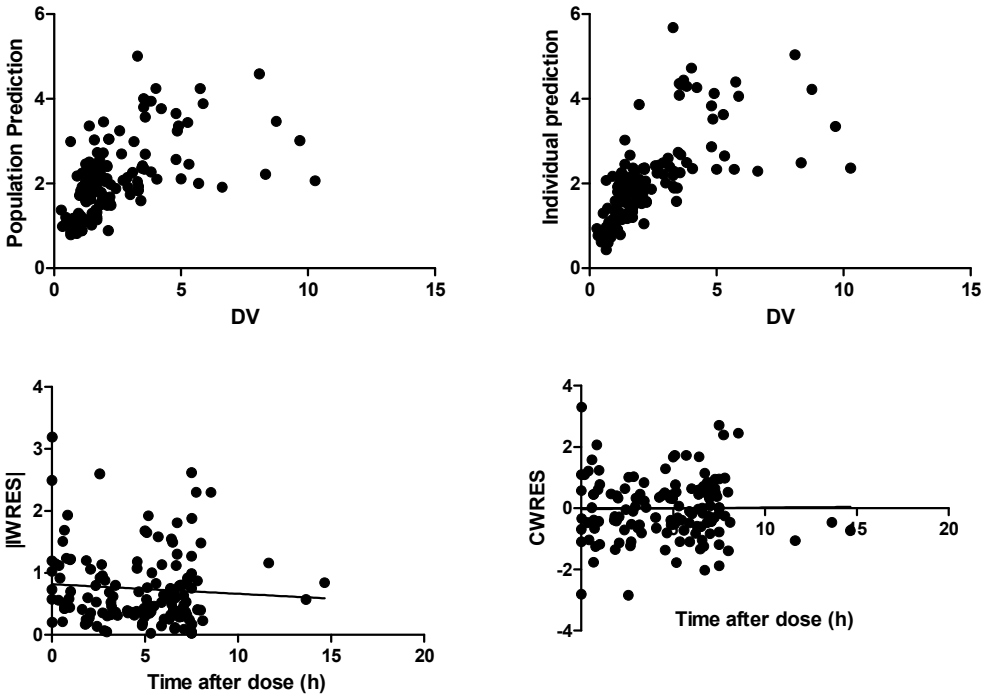

Figure 2. Basic goodness of fit plots for the final model: population predictive concentration versus observed concentration (DV) (**upper left**); individual predictive concentration versus observed concentration (DV) (**upper right**); time after dose versus individual weighted residuals (IWRES) (**lower left**); time after dose versus conditional weighted residuals (CWRES) (**lower right**). CWRES: conditional weighted residuals, DV: dependent variable, IWRES: individual weighted residuals.

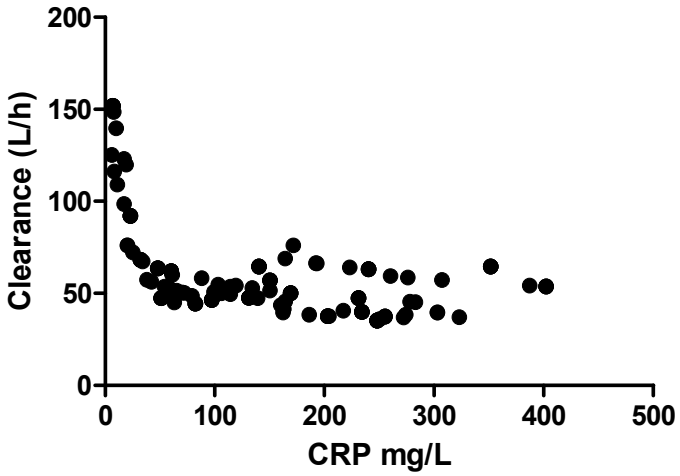

Figure 3. The relationship of inflammatory indicator CRP and haloperidol clearance. CRP: C-reactive protein.

The results of the bootstrap (n = 1000) were in accordance with the estimates of the original model data. A visual predictive check (VPC) was executed (Figure 4) to validate the model by simulating 1000 data sets, comparing the observed concentration with the distribution of simulated concentrations [34]. Figure 4 shows the VPC results and the model fitted well.

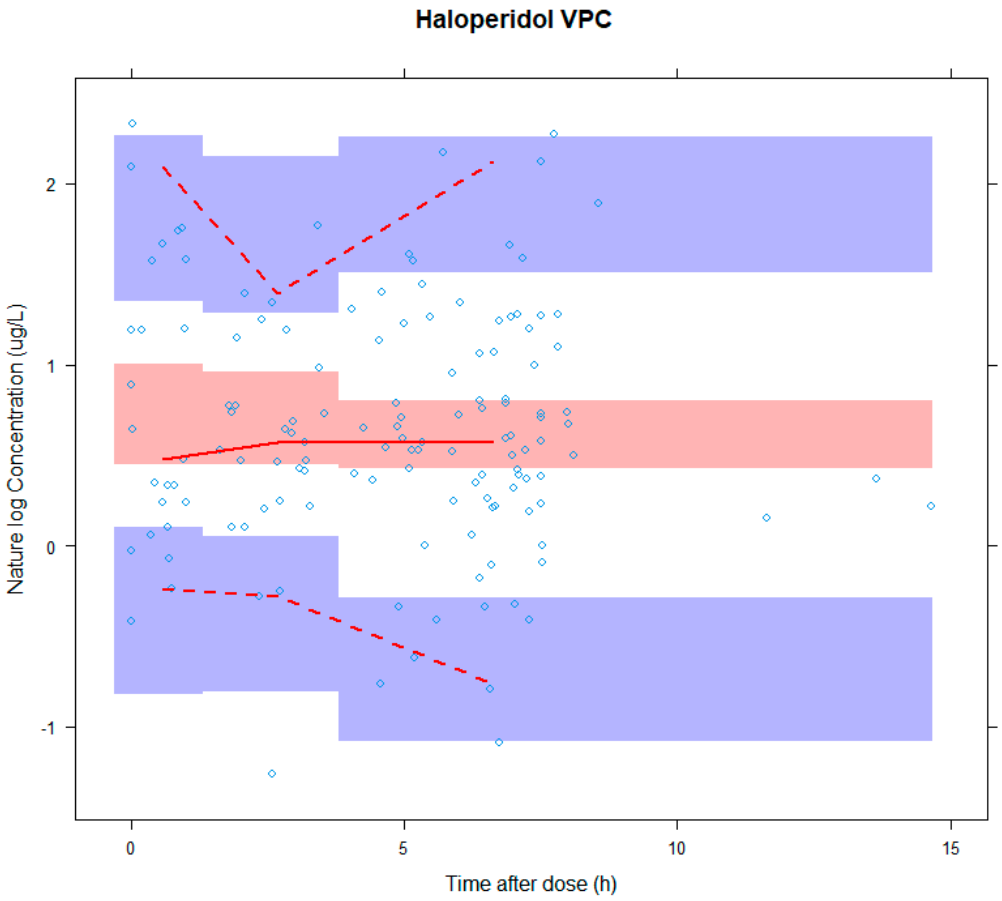

Figure 4. The visual predictive check of haloperidol. The x−axis is time (h) and y−axis is concentration of haloperidol in natural log scale. VPC: visual predictive check.

3.4. Simulations

The simulation results of the concentration under 1 mg of intravenous administered haloperidol every 8 h are shown in Figure 5. In Figure 5a, the concentration of the haloperidol increased from 1 ng/L to 2 ng/L when the CRP increased from 5 mg/L to 100 mg/L. Figure 5b shows two different simulation patients—in the left graph, a change in CRP from 5 mg/L to 100 mg/L during unaltered haloperidol dosing; the right is the opposite with CRP changing from 100 mg/L to 5 mg/L. The latter requires a longer time to reach a steady state of haloperidol concentration.

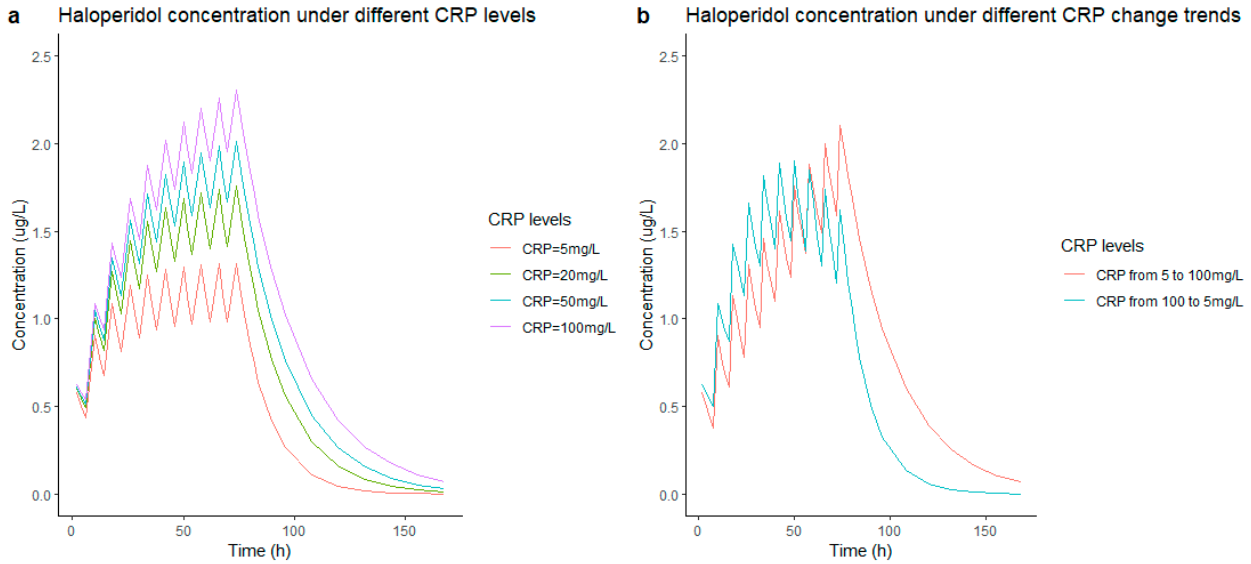

Figure 5. The simulation of the influence of CRP levels on haloperidol concentration. (**a**) is to use the final model to simulate concentration with different CRP levels (5, 20, 50, 100 mg/L), (**b**) shows two different simulations—on the left, an increase in CRP from 5 mg/L to 100 mg/L while on the right an increase in CRP from 100 mg/L to 5 mg/L; the increasing/decreasing rate is 20 mg/L per 12 h. All haloperidol simulations are performed at a dose of 1 mg q8h up until 72 h, the median concentrations are used to plot the simulation. CRP: C-reactive protein.

4. Discussion

This is the first study describing the pharmacokinetics of low dose haloperidol in adult critically ill patients. A one-compartment model adequately described the pharmacokinetics of haloperidol with good accuracy. The most interesting finding was the negative correlation between clearance and CRP levels (as long as it remained below 100 mg/L). This may indicate that a low level of inflammation may play a role in the pharmacokinetics of haloperidol.

The PK parameters of haloperidol from our final model were CL (51.7 L/h), Vd (1490 L), and t1/2 (22 h), which is similar to a previous report [29]. The negative effect of increased CRP on CL reached its maximum at around 50 mg/L to 100 mg/L after which CL did not decrease with further increasing CRP concentrations. It has been proven that inflammation influences the PK of many drugs (midazolam, irinotecan, clozapine, quetiapine, risperidone, voriconazole, perampanel) by changing the distribution of volume, influencing the enzyme activity and hepatic/renal blood flow and thus influencing the drug metabolism and excretion [35–42]. The phenomenon of CRPs negative relationship with haloperidol concentration in our study implies that inflammation can influence the clearance of haloperidol in ways other than liver function, as no significant correlation was found between clearance and liver function indicators (ASAT, ALAT, serum bilirubin), which is similar to the results of L.G. Franken et al. (28). However, other inflammatory markers such as leukocytes and platelets did not show any correlation in our study. The clearance did not further decrease with increased CRP, which is probably because the inflammation effect on clearance had reached its max effects. So far, we have no clear explanation for this phenomenon and unfortunately, there are no other data available on this topic.

The CRP could help us better estimate drug exposure and lead to more precise individual dosing. In lower levels of inflammation, generally indicating less sick patients, relatively lower CRP levels might require higher drug dosing versus higher CRP levels, given that lower CRP results in lower trough levels. This is indeed a clinically relevant signal, but requiring confirmation and external validation. Another important issue is that

the haloperidol therapeutic target concentration remains unknown with respect to delirium and requires additional research as well.

Besides the possible association between CRP and clearance, the pharmacokinetics parameters (CL = 51.7 L/h, V = 1490 L) of our study are similar to the results of previously published haloperidol models (CL range from 42.4 L/h to 88 L/h, V range from 2060 L to 3169 L) in a healthy population and studies on schizophrenia [29,43]. Furthermore, we found no correlation between clearance and other factors, such as co-medication or different CYP genotypes. However, other covariates, such as bodyweight, which were shown to be important in other studies [43,44], did not show significant associations with clearance in our study. This is most likely due to the limited number of patients, the low dose of haloperidol, and limited samples, in combination with the heterogeneous population in the ICU. On the other hand, the parameters in our study differ considerably from the parameters (CL = 29.3 L/h, V = 1260 L) of studies on terminally ill patients [28]. This difference might be explained by the impaired (reduced) liver function (liver capacity) of terminally ill patients, resulting in a decreased haloperidol clearance.

One limitation of our study was the limited number of patients, which might explain why some potential important covariates did not show significance in our model. Furthermore, the published haloperidol population models all use the two-compartment model; however, in this study, owing to the small dataset, we were unable to accurately describe a peripheral compartment and inter-compartmental clearance. However, the one-compartment model fit the data well. Furthermore, we did not look at the pharmacodynamic effect so we could not link the concentration to the haloperidol toxicity and delirium symptom relief, since the therapeutic target of haloperidol is unknown. In addition, we only detected the whole blood concentration, not the free fraction of the haloperidol. Future research should also take this into account.

It is necessary to find more accurate delirium severity related markers or clinical scores which could explore the haloperidol concentration and its effect/response relationship and whether the pharmacokinetic data could be extrapolated to higher doses/concentration range. Further studies on pharmacokinetics and pharmacodynamics of higher-dosed haloperidol in ICU patients with delirium are warranted in order to more accurately assess efficacy.

5. Conclusions

This study describes the pharmacokinetics of low dose haloperidol in critically ill patients with adequate accuracy and showed that clearance is negatively related to CRP at low levels (0–100 mg/L), which seems to indicate a role of inflammation on haloperidol pharmacokinetics.

Supplementary Materials: The following supporting information can be downloaded at: https://www.mdpi.com/article/10.3390/pharmaceutics14030549/s1. Supplementary Materials File A: The Structural model and covariate analysis equation. Supplementary Materials File B: The NONMEM codes for haloperidol modeling. Supplementary Materials File C: METC ethical approval of the research. Supplementary Materials File D: Informed Consent Statement. Supplementary Materials File E: Validation of the method for haloperidol determination.

Author Contributions: Conceptualization, L.L., S.D.T.S., B.C.P.K., N.G.M.H., H.E. and M.v.d.J.; acquisition of data, N.G.M.H. and M.v.d.J.; formal analysis, L.L. and S.D.T.S.; writing—original draft preparation, L.L.; writing—review and editing, S.D.T.S., B.C.P.K., N.G.M.H., H.E. and M.v.d.J. All authors have read and agreed to the published version of the manuscript.

Funding: This research received no external funding.

Institutional Review Board Statement: This study was conducted in accordance with the principles of the Declaration of Helsinki (version October 2008 and approved by the Institutional Review Board).

Informed Consent Statement: Informed consent was obtained from each patients' legally authorized representative, given all patients had delirium.

Data Availability Statement: The data that support the findings of this study are available from the corresponding author upon reasonable request.

Acknowledgments: Letao Li acknowledge the China Scholarship Council for the support by State Scholarship Fund No. 201908500113.

Conflicts of Interest: The authors declare no conflict of interest.

References

1. Kotfis, K.; Marra, A.; Ely, E.W. ICU delirium—A diagnostic and therapeutic challenge in the intensive care unit. *Anaesthesiol. Intensive Ther.* **2018**, *50*, 160–167. [CrossRef]
2. Adamis, D.; Treloar, A.; Martin, F.C.; Macdonald, A.J. A brief review of the history of delirium as a mental disorder. *Hist. Psychiatry* **2007**, *18*, 459–469. [CrossRef]
3. Jayaswal, A.K.; Sampath, H.; Soohinda, G.; Dutta, S. Delirium in medical intensive care units: Incidence, subtypes, risk factors, and outcome. *Indian J. Psychiatry* **2019**, *61*, 352.
4. Tilouche, N.; Hassen, M.F.; Ali, H.B.S.; Jaoued, O.; Gharbi, R.; El Atrous, S.S. Delirium in the intensive care unit: Incidence, risk factors, and impact on outcome. *Indian J. Crit. Care Med. Peer-Rev. Off. Publ. Indian Soc. Crit. Care Med.* **2018**, *22*, 144. [CrossRef]
5. Herling, S.F.; Greve, I.E.; Vasilevskis, E.E.; Egerod, I.; Bekker Mortensen, C.; Møller, A.M.; Svenningsen, H.; Thomsen, T. Interventions for preventing intensive care unit delirium in adults. *Cochrane Database Syst. Rev.* **2018**, *11*, CD009783. [CrossRef]
6. Reznik, M.E.; Slooter, A.J.C. Delirium Management in the ICU. *Curr. Treat. Options Neurol.* **2019**, *21*, 59. [CrossRef]
7. Devlin, J.W.; Skrobik, Y.; Gélinas, C.; Needham, D.M.; Slooter, A.J.C.; Pandharipande, P.P.; Watson, P.L.; Weinhouse, G.L.; Nunnally, M.E.; Rochwerg, B.; et al. Clinical Practice Guidelines for the Prevention and Management of Pain, Agitation/Sedation, Delirium, Immobility, and Sleep Disruption in Adult Patients in the ICU. *Crit. Care Med.* **2018**, *46*, e825–e873. [CrossRef]
8. Smit, L.; Dijkstra-Kersten, S.M.A.; Zaal, I.J.; van der Jagt, M.; Slooter, A.J.C. Haloperidol, clonidine and resolution of delirium in critically ill patients: A prospective cohort study. *Intensive Care Med.* **2021**, *47*, 316–324. [CrossRef]
9. van den Boogaard, M.; Slooter, A.J.C.; Brüggemann, R.J.M.; Schoonhoven, L.; Beishuizen, A.; Vermeijden, J.W.; Pretorius, D.; de Koning, J.; Simons, K.S.; Dennesen, P.J.W.; et al. Effect of Haloperidol on Survival Among Critically Ill Adults With a High Risk of Delirium: The REDUCE Randomized Clinical Trial. *JAMA* **2018**, *319*, 680–690. [CrossRef]
10. Girard, T.D.; Exline, M.C.; Carson, S.S.; Hough, C.L.; Rock, P.; Gong, M.N.; Douglas, I.S.; Malhotra, A.; Owens, R.L.; Feinstein, D.J.; et al. Haloperidol and Ziprasidone for Treatment of Delirium in Critical Illness. *N. Engl. J. Med.* **2018**, *379*, 2506–2516. [CrossRef] [PubMed]
11. Khan, B.A.; Perkins, A.J.; Campbell, N.L.; Gao, S.; Farber, M.O.; Wang, S.; Khan, S.H.; Zarzaur, B.L.; Boustani, M.A. Pharmacological Management of Delirium in the Intensive Care Unit: A Randomized Pragmatic Clinical Trial. *J. Am. Geriatr. Soc.* **2019**, *67*, 1057–1065. [CrossRef]
12. Smith, B.S.; Yogaratnam, D.; Levasseur-Franklin, K.E.; Forni, A.; Fong, J. Introduction to drug pharmacokinetics in the critically ill patient. *Chest* **2012**, *141*, 1327–1336. [CrossRef] [PubMed]
13. Blot, S.I.; Pea, F.; Lipman, J. The effect of pathophysiology on pharmacokinetics in the critically ill patient–concepts appraised by the example of antimicrobial agents. *Adv. Drug Deliv. Rev.* **2014**, *77*, 3–11. [CrossRef] [PubMed]
14. Wang, E.H.; Mabasa, V.H.; Loh, G.W.; Ensom, M.H. Haloperidol dosing strategies in the treatment of delirium in the critically ill. *Neurocrit. Care* **2012**, *16*, 170–183. [CrossRef]
15. Franken, L.G.; de Winter, B.C.; van Esch, H.J.; van Zuylen, L.; Baar, F.P.; Tibboel, D.; Mathôt, R.A.; van Gelder, T.; Koch, B.C. Pharmacokinetic considerations and recommendations in palliative care, with focus on morphine, midazolam and haloperidol. *Expert Opin. Drug Metab. Toxicol.* **2016**, *12*, 669–680. [CrossRef]
16. Cheng, Y.F.; Paalzow, L.K.; Bondesson, U.; Ekblom, B.; Eriksson, K.; Eriksson, S.O.; Lindberg, A.; Lindström, L. Pharmacokinetics of haloperidol in psychotic patients. *Psychopharmacology* **1987**, *91*, 410–414. [CrossRef]
17. Prommer, E. Role of haloperidol in palliative medicine: An update. *Am. J. Hosp. Palliat. Care* **2012**, *29*, 295–301. [CrossRef]
18. Blaschke, T.F. Protein binding and kinetics of drugs in liver diseases. *Clin. Pharm.* **1977**, *2*, 32–44. [CrossRef] [PubMed]
19. Sychev, D.A.; Zastrozhin, M.S.; Miroshnichenko, I.I.; Baymeeva, N.V.; Smirnov, V.V.; Grishina, E.A.; Ryzhikova, K.A.; Mirzaev, K.B.; Markov, D.D.; Skryabin, V.Y.; et al. Genotyping and phenotyping of CYP2D6 and CYP3A isoenzymes in patients with alcohol use disorder: Correlation with haloperidol plasma concentration. *Drug Metab. Pers. Ther.* **2017**, *32*, 129–136. [CrossRef] [PubMed]
20. Sychev, D.A.; Zastrozhin, M.S.; Smirnov, V.V.; Grishina, E.A.; Savchenko, L.M.; Bryun, E.A. The correlation between CYP2D6 isoenzyme activity and haloperidol efficacy and safety profile in patients with alcohol addiction during the exacerbation of the addiction. *Pharmgenomics Pers. Med.* **2016**, *9*, 89–95. [CrossRef]
21. Zastrozhin, M.S.; Smirnov, V.V.; Sychev, D.A.; Savchenko, L.M.; Bryun, E.A.; Matis, O.A. CYP3A4 activity and haloperidol effects in alcohol addicts. *Int. J. Risk Saf. Med.* **2015**, *27* (Suppl. S1), S23–S24. [CrossRef] [PubMed]
22. Someya, T.; Shibasaki, M.; Noguchi, T.; Takahashi, S.; Inaba, T. Haloperidol metabolism in psychiatric patients: Importance of glucuronidation and carbonyl reduction. *J. Clin. Psychopharmacol.* **1992**, *12*, 169–174. [CrossRef]
23. Kato, Y.; Nakajima, M.; Oda, S.; Fukami, T.; Yokoi, T. Human UDP-glucuronosyltransferase isoforms involved in haloperidol glucuronidation and quantitative estimation of their contribution. *Drug Metab. Dispos.* **2012**, *40*, 240–248. [CrossRef]

24. Chang, W.H.; Lam, Y.W.; Jann, M.W.; Chen, H. Pharmacokinetics of haloperidol and reduced haloperidol in Chinese schizophrenic patients after intravenous and oral administration of haloperidol. *Psychopharmacology* **1992**, *106*, 517–522. [CrossRef] [PubMed]
25. Forsman, A.; Ohman, R. Pharmacokinetic studies on haloperidol in man. *Curr. Ther. Res. Clin. Exp.* **1976**, *20*, 319–336.
26. Holley, F.O.; Magliozzi, J.R.; Stanski, D.R.; Lombrozo, L.; Hollister, L.E. Haloperidol kinetics after oral and intravenous doses. *Clin. Pharmacol. Ther.* **1983**, *33*, 477–484. [CrossRef]
27. Magliozzi, J.R.; Hollister, L.E. Elimination half-life and bioavailability of haloperidol in schizophrenic patients. *J. Clin. Psychiatry* **1985**, *46*, 20–21.
28. Franken, L.G.; Mathot, R.A.A.; Masman, A.D.; Baar, F.P.M.; Tibboel, D.; van Gelder, T.; Koch, B.C.P.; de Winter, B.C.M. Population pharmacokinetics of haloperidol in terminally ill adult patients. *Eur. J. Clin. Pharmacol.* **2017**, *73*, 1271–1277. [CrossRef]
29. Yukawa, E.; Hokazono, T.; Yukawa, M.; Ichimaru, R.; Maki, T.; Matsunaga, K.; Ohdo, S.; Anai, M.; Higuchi, S.; Goto, Y. Population pharmacokinetics of haloperidol using routine clinical pharmacokinetic data in Japanese patients. *Clin. Pharmacokinet* **2002**, *41*, 153–159. [CrossRef]
30. Trogrlić, Z.; van der Jagt, M.; Osse, R.J.; Devlin, J.W.; Nieboer, D.; Koch, B.C.P.; van Schaik, R.H.N.; Hunfeld, N.G.M. Pharmacogenomic response of low dose haloperidol in critically ill adults with delirium. *J. Crit. Care* **2020**, *57*, 203–207. [CrossRef]
31. FDA. Guidance for Industry Process Validation: General Principles and Practices: Food and Drug Administration. 2011. Available online: https://www.fda.gov/downloads/drugs/guidances/ucm070336.pdf (accessed on 1 January 2011).
32. Agency, E.E.M. Guideline on Bioanalytical Method Validation. 2011. Available online: https://www.ema.europa.eu/en/documents/scientific-guideline/guideline-bioanalytical-method-validation_en.pdf (accessed on 21 July 2011).
33. Jonsson, E.N.; Karlsson, M.O. Automated covariate model building within NONMEM. *Pharm. Res.* **1998**, *15*, 1463–1468. [CrossRef] [PubMed]
34. Bergstrand, M.; Hooker, A.C.; Wallin, J.E.; Karlsson, M.O. Prediction-corrected visual predictive checks for diagnosing nonlinear mixed-effects models. *Aaps. J.* **2011**, *13*, 143–151. [CrossRef] [PubMed]
35. Chityala, P.K.; Wu, L.; Chow, D.S.; Ghose, R. Effects of inflammation on irinotecan pharmacokinetics and development of a best-fit PK model. *Chem. Biol. Interact* **2020**, *316*, 108933. [CrossRef] [PubMed]
36. Ternant, D.; Ducourau, E.; Perdriger, A.; Corondan, A.; Le Goff, B.; Devauchelle-Pensec, V.; Solau-Gervais, E.; Watier, H.; Goupille, P.; Paintaud, G.; et al. Relationship between inflammation and infliximab pharmacokinetics in rheumatoid arthritis. *Br. J. Clin. Pharmacol.* **2014**, *78*, 118–128. [CrossRef]
37. Yamamoto, Y.; Takahashi, Y.; Horino, A.; Usui, N.; Nishida, T.; Imai, K.; Kagawa, Y.; Inoue, Y.I. nfluence of Inflammation on the Pharmacokinetics of Perampanel. *Ther. Drug Monit.* **2018**, *40*, 725–729. [CrossRef]
38. Veringa, A.; Ter Avest, M.; Span, L.F.; van den Heuvel, E.R.; Touw, D.J.; Zijlstra, J.G.; Kosterink, J.G.; van der Werf, T.S.; Alffenaar, J.C. Voriconazole metabolism is influenced by severe inflammation: A prospective study. *J. Antimicrob. Chemother.* **2017**, *72*, 261–267. [CrossRef]
39. van Wanrooy, M.J.; Span, L.F.; Rodgers, M.G.; van den Heuvel, E.R.; Uges, D.R.; van der Werf, T.S.; Kosterink, J.G.; Alffenaar, J.W. Inflammation is associated with voriconazole trough concentrations. *Antimicrob. Agents Chemother.* **2014**, *58*, 7098–7101. [CrossRef]
40. Franken, L.G.; Masman, A.D.; de Winter, B.C.M.; Baar, F.P.M.; Tibboel, D.; van Gelder, T.; Koch, B.C.P.; Mathot, R.A.A. Hypoalbuminaemia and decreased midazolam clearance in terminally ill adult patients, an inflammatory effect? *Br. J. Clin. Pharmacol.* **2017**, *83*, 1701–1712. [CrossRef]
41. Vet, N.J.; Brussee, J.M.; de Hoog, M.; Mooij, M.G.; Verlaat, C.W.; Jerchel, I.S.; van Schaik, R.H.; Koch, B.C.; Tibboel, D.; Knibbe, C.A.; et al. Inflammation and Organ Failure Severely Affect Midazolam Clearance in Critically Ill Children. *Am. J. Respir. Crit. Care Med.* **2016**, *194*, 58–66. [CrossRef]
42. Hefner, G.; Shams, M.E.; Unterecker, S.; Falter, T.; Hiemke, C. Inflammation and psychotropic drugs: The relationship between C-reactive protein and antipsychotic drug levels. *Psychopharmacology* **2016**, *233*, 1695–1705. [CrossRef]
43. Pilla Reddy, V.; Kozielska, M.; Johnson, M.; Mafirakureva, N.; Vermeulen, A.; Liu, J.; de Greef, R.; Rujescu, D.; Groothuis, G.M.; Danhof, M.; et al. Population pharmacokinetic-pharmacodynamic modeling of haloperidol in patients with schizophrenia using positive and negative syndrome rating scale. *J. Clin. Psychopharmacol.* **2013**, *33*, 731–739. [CrossRef] [PubMed]
44. Anderson, B.J.; Holford, N.H. Mechanism-based concepts of size and maturity in pharmacokinetics. *Annu. Rev. Pharmacol. Toxicol.* **2008**, *48*, 303–332. [CrossRef] [PubMed]

pharmaceutics

MDPI

Review

Therapeutic Drug Monitoring of Ivacaftor, Lumacaftor, Tezacaftor, and Elexacaftor in Cystic Fibrosis: Where Are We Now?

Eva Choong [1,*], Alain Sauty [2,3], Angela Koutsokera [3], Sylvain Blanchon [4], Pascal André [1] and Laurent Decosterd [1]

[1] Service and Laboratory of Clinical Pharmacology, Department of Laboratory Medicine and Pathology, Lausanne University Hospital and University of Lausanne, 1011 Lausanne, Switzerland
[2] Service of Pulmonology, Adult Cystic Fibrosis Unit, Pourtalès Hospital, 2000 Neuchâtel, Switzerland
[3] Unit of Adult Cystic Fibrosis Unit and CFTR-Related Disorders, Division of Pulmonology, Lausanne University Hospital and University of Lausanne, 1011 Lausanne, Switzerland
[4] Service of Pediatrics, Pediatric Pulmonology and Cystic Fibrosis Unit, Lausanne University Hospital and University of Lausanne, 1011 Lausanne, Switzerland
* Correspondence: eva.choong@chuv.ch

Abstract: Drugs modulating the cystic fibrosis transmembrane conductance regulator (CFTR) protein, namely ivacaftor, lumacaftor, tezacaftor, and elexacaftor, are currently revolutionizing the management of patients with cystic fibrosis (CF), particularly those with at least one *F508del* variant (up to 85% of patients). These "caftor" drugs are mainly metabolized by cytochromes P450 3A, whose enzymatic activity is influenced by environmental factors, and are sensitive to inhibition and induction. Hence, CFTR modulators are characterized by an important interindividual pharmacokinetic variability and are also prone to drug–drug interactions. However, these CFTR modulators are given at standardized dosages, while they meet all criteria for a formal therapeutic drug monitoring (TDM) program that should be considered in cases of clinical toxicity, less-than-expected clinical response, drug or food interactions, distinct patient subgroups (i.e., pediatrics), and for monitoring short-term adherence. While the information on CFTR drug exposure–clinical response relationships is still limited, we review the current evidence of the potential interest in the TDM of caftor drugs in real-life settings.

Keywords: TDM; therapeutic drug monitoring; plasma level; PK/PD; dose–effect relationship; cystic fibrosis; LC–MS/MS; CFTR modulators; caftor; ivacaftor; lumacaftor; tezacaftor; elexacaftor

Citation: Choong, E.; Sauty, A.; Koutsokera, A.; Blanchon, S.; André, P.; Decosterd, L. Therapeutic Drug Monitoring of Ivacaftor, Lumacaftor, Tezacaftor, and Elexacaftor in Cystic Fibrosis: Where Are We Now?*Pharmaceutics* **2022**, *14*, 1674. https://doi.org/10.3390/pharmaceutics14081674

Academic Editors: Barna Vasarhelyi and Gellért Balázs Karvaly

Received: 8 June 2022
Accepted: 23 July 2022
Published: 11 August 2022

1. Introduction

Cystic fibrosis (CF) is an autosomal recessive genetic disease caused by variants of the gene encoding the cystic fibrosis transmembrane conductance regulator (CFTR) protein, which affects about 1 of 2700 newborns [1]. The most frequent variant is *F508del*. which is found in 85% of patients [2]. Until recently, treatments of the disease were mostly symptomatic focusing on the consequences of the disease (e.g., mucolytics, antibiotics, pancreatic enzymes, etc.).

Following the discovery of the CFTR gene 30 years ago, great hopes were placed on gene therapy, which is still the subject of significant research, yet without any clinical application being planned in the near future. On the other hand, in the last decade, several molecules called "CFTR modulators" (also nicknamed "caftors"), which partially restore the activity of the CFTR protein, have been developed and are now increasingly used for alleviating the clinical conditions of many CF patients.

These drugs may remedy, in part, the intracellular destruction and/or the malfunction of the CFTR protein and reveal spectacular benefits in terms of respiratory function, nutrition, and quality of life for individuals with CF. The clinical profile is

reported to be safe, with most adverse effects being mild to moderate. These new medical breakthroughs are, however, extremely expensive (≈CHF 170.000/year/patient) and target only certain *CFTR* variants [3,4], with limitations regarding the age of the patient and the clinical severity of the disease. Their precise mechanisms of action are yet unknown, and currently, four caftors are registered, all developed by the same pharmaceutical company.

Ivacaftor (VX-770, IVA) is the first caftor and was launched in 2012, marketed as Kalydeco®. It is the only registered so-called "potentiator" and targets the *G551D* variant and other variants that affect the gating of CFTR [2]. In order for IVA to have an effect, CFTR proteins must be present on the cell surface. It binds and potentiates CFTR function by promoting decoupling between ATP hydrolysis and gating cycles [4–6]. IVA is prescribed as monotherapy for certain CFTR variants or in combination with corrector(s).

To date, three drugs designated as "correctors" are registered and used only in combination with IVA.

Lumacaftor (VX-809, LUM) is a first-generation corrector. It acts similarly to a chaperone, which influences the folding of CFTR in the *F508del*-expressing cell line, resulting in the stabilization of CFTR conformation and translocation to the surface. The combination LUM/IVA (Orkambi®) is only approved for *F508del* homozygous patients [3,7]

The second drug, tezacaftor (VX-661, TEZ), in vitro improves the processing and translocation of normal CFTR and certain variants, which leads to an increase in mature CFTR protein on the cell surface. The combination TEZ/IVA (Symkevi®, Symdeko®) is approved for homozygous and heterozygous *F508del* variants in combination with a specific "residual function" variant in the second *CFTR* allele [3,4,8].

Finally, elexacaftor (VX-445, ELX), a third-generation corrector, has only very recently become available (end of 2019 in the USA and early 2021 in Europe). It is exclusively used in a combination with TEZ and IVA. ELX in vitro improves the processing and transport of CFTR protein variants but binds to other sites of the CFTR protein than TEZ. The new three-drug combination ELX/TEZ/IVA marketed as Kaftrio® or Trikafta® has been reported to provide a more pronounced functional improvement in *F508del* and other variants than that observed with TEZ/IVA [3,4].

TEZ, ELX, and IVA are extensively metabolized by cytochromes P450 3A (CYP3A), characterized by significant variability in expression and activity levels that are notably influenced by environmental factors, and are also likely to be inhibited or induced by various drugs and xenobiotics.

Blood concentration measurement has become one of the very relevant clinical tools to optimize the therapeutic use of critical drugs through adjustment of drug exposure via a therapeutic drug monitoring (TDM) program. The criteria for drugs to be candidates for TDM include significant interindividual pharmacokinetic (PK) variability, poorly predictable from individual patients' characteristics [9,10], and plasma concentration-response and/or toxicity relationships, defining the plasma concentration ranges associated with optimal efficacy and minimal toxicity.

As the information on CFTR drug exposure–clinical response relationships is still scarce, we aimed to perform a comprehensive review of the current lines of evidence for the potential interest in TDM of caftor drugs by exploiting (i) the data on PK variability and drug exposition retrieved from registration files (Tables 1 and 2) and (ii) PK data currently reported in a limited number of publications, case series, case reports, and conference abstracts from *real-life* settings (Table 3).

Table 1. Relevant pharmacokinetics parameters for the 4 currently approved CFTR modulators [11].

	ELX	**TEZ**	**IVA**	**LUM**
T_{max} (h)	6	3	4	4
AUC fold- increased with fat containing food	1.9–2.5	1	2.5–4	2
% bound to plasma protein	99	99	99	99
Distribution volume (L)	53.7	82	293	96
Enzymes/transporters involved in metabolism	CYP3A, P–gp	CYP3A, UGT	CYP3A	(CYP3A) [c]
Active metabolites	M23–445 similar potency of ELX.	M1–TEZ similar potency of TEZ.	M1–IVA 1/6 potency of IVA.	M1–LUM 1/6 potency of LUM.
	AUC ratio metabolite/parent: 35–50%	AUC ratio metabolite/parent: 35%		
Half-life (h)	27	25	15	26
Elimination	97% faeces	72% faeces	88% faeces	51% faeces
Hepatic function [a]	Higher exposure of ELX, TEZ, IVA, LUM is expected in patients with moderate (Child–Pugh Class B, score 7 to 9), and severe hepatic impairment (Child–Pugh Class B, score 10–15).			
DDI Perpetrator [b]	n/a	n/a	Weak CYP3A and P–gp inhibitor	Strong CYP3A inducer; CYP2C9 [d], CYP2C19 [d], CYP2B6 [d] and UGT [e] inducers
Victim DDI with strong [b] CYP3A inhibitor	AUC 2.8x incr.	AUC 4.5x incr.	AUC 11x incr.	n/a
Victime DDI with strong CYP3A inducer [b]	Co-administration of strong CYP3A inducers (ex: rifampicin) is not recommended			n/a

n/a: not applicable. [a] Data available only for adult patients, [b] See "Section 3.6 Drug–Drug Interactions" for perpetrator and victim DDIs, [c] Not extensively metabolized—the majority of LUM is excreted unchanged, [d] King et al. 2022 [12], [e] Dagenais et al. 2020 [13].

Table 2. CFTR modulator exposure according to labeling information for the four current CF treatments.

Mean (±SD) PK Parameters of Ivacaftor (IVA) Monotherapy at Steady State [6]					
Age Groups (Years Old)		**PK** [a]			
		IVA			
		Dose	**C_{max} (μg/mL)**	**C_{min} (μg/mL)**	**$AUC_{0–12\ h}$ (μg·h/mL)**
2–5 yo (<14 kg) [b]		50 mg BID	n/a	n/a	10.5 (4.26)
2–5 yo (≥14 kg) [b]		75 mg BID	n/a	n/a	11.3 (3.82) [d]
6–11 yo [b]		150 mg BID	n/a	n/a	20.0 (8.33)
12–17 yo [b]		150 mg BID	n/a	n/a	9.24 (3.42) [d]
≥18 yo	Single dose [b]	150 mg QD	0.768 (0.233)	n/a	10.6 (5.26)
	Trial 809-005 [c]		1.97 (1.04)	1.06 (0.82)	17.7 (11.7)
	Trial 005 [c]		1.433 (0.296)	0.69 (0.238)	12.64 (3.72)
	Trial 008 [c]		1.39 (0.522)	0.636 (0.293)	11.6 (4.7)
	Trial 010 [c]		1.158 (0.485)	0.523 (0.303)	9.544 (4.603)
Recommended dose for CF adult		150 mg IVA BID			
Accumulation ratio		2.2–2.9			
Time to reach steady state		3–5 days			

Mean (±SD) PK Parameters of Tezacaftor (TEZ) and Ivacaftor Combination at Steady State [8]				
Age Groups (Years Old)	**PK**			
	TEZ		**IVA**	
	C_{max} (μg/mL)	**$AUC_{0–24h}$ (μg·h/mL)** [e]	**C_{max} (μg/mL)**	**$AUC_{0–12\ h}$ (μg·h/mL)** [e]
6–11 yo (<30 kg)	n/a	58.9 (17.3)	n/a	7.1 (1.95)
6–11 yo (≥30 kg)	n/a	107 (30.1)	n/a	11.8 (3.89)
12–17 yo	n/a	97.1 (35.8)	n/a	11.4 (5.5)
≥18 yo	6.52 (1.83)	82.7 (23.3)	1.28 (0.440)	10.9 (3.89)
Recommended dose for CF adult	Morning: 100 mg TEZ + 150 mg IVA. Evening: 150 mg IVA (except <30 kg/6–11 yo: TEZ 50 mg QD + IVA 75 mg BID)			
Accumulation ratio	2.3		3	
Time to reach steady state	8 days		3–5 days	

Table 2. *Cont.*

PK Parameters of Lumacaftor (LUM) and Ivacaftor Combination [7]						
Age Groups (Years Old)	**PK**					
	LUM $AUC_{0–12\ h}$ (μg·h/mL)			**IVA $AUC_{0–12\ h}$ (μg·h/mL)**		
	n	**Median (Range)**	**Mean (SD)**	***n***	**Median (Range)**	**Mean (SD)**
2–5 yo (<14 kg)	20	175 (131, 339)	180 (45.5)	19	4.64 (2.41, 22.75)	5.92 (4.61)
2–5 yo (≥14 kg)	42	212 (145, 372)	217 (48.6)	42	5.99 (3.09, 12.51)	5.90 (1.93)
6–11 yo	165	215 (108, 452)	224 (59.1)	161	5.69 (2.16, 20.04)	6.17 (2.68)
12–17 yo	98	241 (130, 496)	241 (61.4)	98	3.58 (1.78, 10.26)	3.89 (1.56)
≥18 yo	264	209 (122, 418)	217 (47.9)	264	3.41 (1.35, 17.31)	3.80 (1.94)
Recommended dose for CF adult	200 mg LUM + 125 mg IVA BID					
Accumulation ratio	1.9			n/a		
Time to reach steady state	7 days					

Mean (SD) PK Parameters of Elexacaftor (ELX), Tezacaftor and Ivacaftor [4]									
Age Groups (Years Old)	**PK**								
	ELX			**TEZ**			**IVA**		
	C_{max} (μg/mL)	**C_{min} (μg/mL)**	**AUC [f] τ (μg·h/mL)**	**C_{max} (μg/mL)**	**C_{min} (μg/mL)**	**AUC [f] τ (μg·h/mL)**	**C_{max} (μg/mL)**	**C_{min} (μg/mL)**	**AUC [f] τ (μg·h/mL)**
12 to <18 yo	8.40 (1.75)	4.048 (2.076)	149.0 (38.7)	7.00 (1.65)	2.10 (0.816)	96.0 (23.4)	1.15 (0.288)	0.626 (0.263)	10.60 (3.35)
≥18 yo	8.77 (2.16)	5.488 (2.652)	167.0 (50.5)	6.69 (1.39)	2.05 (0.81)	92.4 (23.8)	1.27 (0.353)	0.75 (0.334)	12.10 (4.17)
Recommended dose for CF adult	Morning: 200 mg ELX + 100 mg TEZ + 150 mg IVA (corresponding of 2 pills). Evening: 150 mg IVA								
Accumulation ratio	2.2			2.07			2.4		
Time to reach steady state	≤7 days			≤8 days			≤3–5 days		

n/a: not applicable, PK: Pharmacokinetics, ss: steady state, yo: years old, QD: once a day, BID: twice a day. [a] These data were the original ones retrieved from the registration file in 2011. Since then, the FDA successively approved its use in younger age, currently, the use of this product for infants as young as 4 months old was approved in September 2020, [b] These data are retrieved from the prescribing information, initial U.S. Approval: 2012, Revised: May 2017, [c] Retrieved from selected multi-dose (5–28 days) in healthy subjects from the FDA registration file, [d] Stated as similar to the mean AUC in adult patients administered 150 mg BID, [e] $AUC_{0–24h}$ for TEZ and $AUC_{0–12\ h}$ for IVA, [f] $AUC_{0–24h}$ for ELX and $AUC_{0–12\ h}$ for IVA.

Table 3. CFTR modulator multi-dose exposition from real-world setting, or trials published after the latest caftor registration (i.e., 2021), or any studies including children below the minimum age recommended in the registration file.

Drug(s)	*CFTR* Genotype	Location	Study Design	Population	Posology	PK Parameters (C_{max}, C_{min}, AUC, ss)	*n*	PK Profile	Ref.
LUM/IVA	n/a	Australia, Europe	Multiple dose, multicenter, open, observational trial reflecting a "real-life" clinical scenario	CF ≥ 12 yo	LUM 200 mg BID and IVA 125 mg BID	Median (IQR) LUM C_{max} 503 (415–1700) ng/mL Median (IQR) IVA C_{max} 59 (24–100) ng/mL	60	Yes	[14]
LUM/IVA	Homozygous F508del patients	France	Observational follow-up after starting LUM/IVA	CF ≥ 12 yo	LUM 200 mg BID and IVA 125 mg BID	Mean (SD) LUM C_{min} 1675 (75), C_{4h} 1826 (136) ng/mL Mean (SD) IVA C_{min} 72 (17), C_{4h} 151 (42) ng/mL	18	No	[15]
IVA	711 + 1G > T and S1251N mutation	Netherlands	Case report: female CF 7.5 yo patient and CF patient	CF ≥ 6 yo	IVA 150 mg BID	Observed C_{4h} range approx. 1–11 μM (392.5–4317.4 ng/mL), Mean C_{4h} 5.03 μM (1974.2 ng/mL)	16	Yes	[16]
IVA	CFTR gating mutation on at least one allele	USA UK Canada	Ongoing multicenter, phase 3, single-arm, two-part Study in CF children	4 to <6 m	IVA 25 mg BID	Median C_{min} 300 ng/mL, Median AUC 5770 ng·h/mL	6	No	[17]
				6 to <12 m	IVA 50 mg BID	Median C_{min} 365 ng/mL, Median AUC 7600 ng·h/mL	16		
				12 to <24 m	IVA 50 mg BID	Median C_{min} 383 ng/mL, Median AUC 8900 ng·h/mL	19		
				12 to <24 m	IVA 75 mg BID	Median C_{min} 451 ng/mL, Median AUC 9600 ng·h/mL	2		
TEZ/IVA	At least one Phe508del CFTR mutation	Australia Europe Israel North America	Multicenter, phase 3, 96-week, open-label study at 170 sites	CF ≥ 12 yo	TEZ 100 mg QD and IVA 150 mg BID	PK exposures to TEZ, IVA, and major metabolites were found similar to those observed in other studies, yet PK profiles or plasma levels are not shown	1044	No	[18]
IVA	CFTR gating mutation on at least one allele	USA UK Canada	Multicenter, phase 3, single-arm, two-part study of IVA in CF children	12 to <24 m	IVA 50 mg BID	Mean (SD) C_{min} 440 (212) ng/mL, Mean (SD) AUC 9050 (3050) ng·h/mL	19	No	[19]
				12 to <24 m	IVA 75 mg BID	Mean (SD) C_{min} 451 (125) ng/mL, Mean (SD) AUC 9600 (1800) ng·h/mL	2		

Table 3. *Cont.*

Drug(s)	*CFTR* Genotype	Location	Study Design	Population	Posology	PK Parameters (C_{max}, C_{min}, AUC, ss)	*n*	PK Profile	Ref.
				2 to 5 yo	IVA 50 mg BID	Mean (SD) C_{min} 577 (317) ng/mL, Mean (SD) AUC 10500 (4260) ng·h/mL	9		
				2 to 5 yo	IVA 75 mg BID	Mean (SD) C_{min} 629 (296) ng/mL, Mean (SD) AUC 11300 (3820) ng·h/mL	26		
IVA	n/a	n/a	Case report: CF patient treated with IVA for ≥3 months old	CF n/a yo	IVA 150 mg BID	Range 400–3000 ng/mL, 5/6 patients had significantly higher levels than those reported from pivotal trial for IVA	6	No	[20]
LUM/ IVA	n/a	Netherlands	CF patients sample for applicability of a developed quantification method	CF (n/a yo)	LUM 800 mg/d and IVA 500 mg/d	Plasma $C_{2.5\,h}$ IVA 554 ng/mL, LUM 29300 ng/mL Sputum $C_{2.5\,h}$ IVA 64.4 ng/mL, LUM 229 ng/mL	2	No	[21]
					TEZ 100 mg/d and IVA 300 mg/d	Plasma $C_{2\,h}$ IVA 924 ng/mL, TEZ 4540 ng/mL			
TEZ/ IVA	n/a	Netherlands	Case report: CF patient with non tuberculous mycobacterium therapy	CF 16 yo	TEZ 100 mg QD and IVA 150 mg BID	AUC TEZ 75400 ng·h/mL AUC IVA 11100 ng·h/mL	1	No	[22]

ELX: elexacaftor, IVA: ivacaftor, LUM: Lumacaftor, TEZ: tezacaftor; PK: Pharmacokinetics, ss: steady state, yo: years old, m: months old, IQR: interquartile range, n/a: not applicable.

2. Methods

For this review, we searched PubMed for publications and conference proceedings. We used the search terms "ivacaftor", "tezacaftor", "lumacaftor", "elexacaftor", "cystic fibrosis", and "CFTR modulators" in combination with the specific terms "therapeutic drug monitoring (TDM)", "area under the curve (AUC)", "plasma level", "plasma concentration", "pharmacokinetic", "dose–response", and "dose–response relationship", covering the literature from 2012 (i.e., first caftor launched) to 31 May 2022.

Besides the registration files, any studies (i.e., observational, case series, and case reports) were selected if participants received at least one marketed caftor, either from a real-life setting or trials published after the latest caftor registration (i.e., 2021), or any studies including children below the minimum recommended age in the registration file (i.e., Trikafta < 6 years). Supportive data from applications to drug registration agencies (FDA, EMA) regarding the PK, pharmacodynamics (PD), and PK/PD studies of CFTR modulators were also included.

3. Results

The PK parameters of the four currently approved caftors are given in Tables 1 and 2.

3.1. Pharmacokinetics of CFTR Modulator Drugs

In general, PK parameters are calculated based on the concentrations measured in blood or plasma, compartments that are easily accessible and minimally invasive for patients. Presently, very little information is available on the plasma exposition and steady-state plasma concentrations of caftors in monotherapy and in the different combinations (i.e., ivacaftor, ivacaftor–lumacaftor, ivacaftor−tezacaftor, and ivacaftor−tezacaftor−elexacaftor) achievable in patients under the currently recommended dosage regimens.

In fact, out of a total of 57 studies summarized in a systematic review on the real-world outcomes of IVA, the first and most studied caftor, none have analyzed IVA plasma levels as an outcome [23]. Currently, for the newest marketed combination ELX/TEZ/IVA, there are barely any published real-world observational PK studies [24,25]. Two large ongoing multicenter observational studies, namely RECOVER (Ireland and the UK) and PROMISE (USA), will shed some light on this combination. Blood collection for biomarker analyses is planned in the RECOVER study but, to the best of our knowledge, does not include caftor drug plasma levels [12]. However, the quantification of caftor levels in these collected plasma samples would be feasible, offering the opportunity to perform invaluable retrospective PK analyses for caftors, provided that the time after dose (the interval between last drug caftor intake and blood sampling) has been recorded.

The treatment outcome for caftors depends on several factors such as the severity of the disease, the presence of comorbidities, and also certainly on the circulating plasma concentrations in individuals with CF. The PK parameters for these four caftors are reported in Tables 1 and 2. An important interindividual PK variability has been reported, for instance, in patients receiving the ELX/TEZ/IVA combination (cf. standard deviation (SD) values in Table 2) [4]. Conversely, the steady state C_{max} for IVA/LUM found in a real-life setting, i.e., outside the stringent frame of clinical trials, was reported to be up to 10 times lower than that of a single-dose level in the labeling information. Moreover, the observed LUM exposure in CF patients was found to correspond to half of that measured in healthy controls (Table S2) [14,26].

While age and weight [11], for instance, in children, are known to impact the plasma concentrations of caftors, their actual area under the curve (AUC), which constitutes an index of overall plasma exposure, appears to be increased when taken with fat-containing food for all caftors, except TEZ, according to the labeling information [11]. An increase in the AUC of up to four-fold was reported for IVA when taken with fatty meals. Moreover, in their international multicentric clinical PK study, Hanafin et al. noticed notable differences in C_{max} values for IVA and LUM in the various participating centers from different continents,

but also among neighboring countries, suggesting that the type of food and socio-cultural eating habits might also modulate caftors' PK [14].

A number of drug–drug interactions (DDIs) and overlapping drug-related adverse events (AE) have already been documented for caftors. The strong CYP3A inhibitor itraconazole, an antifungal agent, increases by 4- and 15.6-fold the AUC of TEZ and IVA, respectively [27], while some moderate CYP3A inhibitors such as ciprofloxacin showed no apparent alterations in caftor plasma levels. Alternately, coadministration with the strong CYP3A inducer rifampicin significantly reduced the AUC of IVA by ≈89%. Rifampicin is also expected to reduce the exposure of the other CYP3A substrates, namely LUM, ELX, and TEZ. Such lower exposures would result in suboptimal concentrations, and thus, the manufacturer does not recommend this coadministration [4].

Further, because the four current caftors are highly bound (>99%) to plasma proteins, in vitro studies have raised concern for possible drug–drug competition for plasma protein binding sites resulting in an increase in the unbound fractions (i.e., the free pharmacologically active species circulating in plasma), thus leading to the modulation of treatment response. In vitro protein binding competition studies between IVA and albumin and α1-glycoprotein acid in the presence of common comedications, including ibuprofen, loratadine, and montelukast, showed that IVA could strongly be displaced from plasma protein sites [28].

In conclusion, the PK variability of CFTR drugs is recognizably significant, but its impact on treatments' tolerability and clinical response, the prevalence of toxicity, and the likelihood of, generally unrecognized, drug underexposure in patients remains as yet largely unknown.

3.2. Pharmacokinetics–Pharmacodynamics of CFTR Modulator Drugs

The caftor dose–response relationships with the usual CF disease parameters (i.e., body mass index (BMI), forced expiratory volume in one second (FEV1), nasal potential difference (NPD), and sweat chloride concentration) have mainly been studied in dose-escalation regimen carried out in phase II studies with adult CF patients carriers of different genotypes.

A trend of increased response with higher doses was reported for IVA, LUM, and TEZ monotherapy, while no distinct dose–response was observed for ELX over the studied 50–200 mg dosage range.

For IVA, application files to registration agencies have defined the CFTR level at the 90% maximal effect concentrations (EC_{90}) with respect to sweat chloride concentration and FEV1. A regimen of IVA 150 mg BID yielded a steady-state plasma C_{min} level of approx. 0.25 μg/mL, corresponding to values $\geq EC_{90}$ for FEV1 and $\geq EC_{84}$ for sweat chloride endpoints, respectively [6].

Conversely, the EC_{50} values of LUM and TEZ were estimated to correspond to plasma C_{min} of 4.5 and 0.5 μg/mL, respectively, using the sweat chloride concentration. A greater reduction in sweat chloride concentration with increasing LUM plasma levels has been reported in the FDA application files. Presently, no in vivo studies have evaluated the EC_{50} of ELX (in vitro EC_{50} is 0.99 μg/mL) [4].

High variability in treatment response has been found in patients with the same *CFTR* genotype and dosage regimen [29–31], suggesting that interindividual differences in pharmacokinetics per se are likely incriminated to explain, at least in part, such inconstancy in drug response.

Alternately, no association between the blood levels of IVA/LUM (at average 4 h post-dose and C_{min}) and clinical response at 6 months was found in 36 CF patients aged ≥12 years [15].

3.3. Safety and Adverse Event (AEs) of CFTR Modulator Drugs

An impressive, systematic review of the real-world safety and relation between the dosage of the first CFTR modulators (IVA, LUM) and AEs thoroughly evaluated nearly 70 studies from 2012 to 2020 [13]. The authors summarized the frequency of discontinuation

and adverse events (AEs) related to caftors with detailed patient characteristics and drug dosage regimens. The majority of studies were focused on LUM/IVA (69%), and 6% were on the latest marketed combination TEZ/ELX/IVA. Interestingly, only 16% of the studies were carried out on pediatric patients.

Intriguingly, among these considerable volumes of data and studies in patients presenting drug-related AEs, none measured caftor plasma levels. The lack of robust evidence on target levels, validated quantification methods, guidelines to monitor drug levels and poorly described indications for TDM may partly explain this observation.

Nevertheless, of these 68 articles, 10% assessed a dose reduction in the case of AE. The described AE symptoms in cohorts were related to respiratory intolerance (3/20 *F508del* homozygote CF adult patients with LUM/IVA) [32]; chest tightness (2/29 *F508del* homozygote adult CF patients with LUM/IVA [33] and 1/14 *F508del* homozygote pediatric CF patients with LUM/IVA [34]); and undescribed AE (10/116 *F508del* homozygote CF patients $\geq$12 years old (yo) with LUM/IVA [35]). Finally, a case report described elevated transaminases with subsequent normalization of symptoms (1 adult CF heterozygous for *F508del* and *R117H-7T* with IVA [36]), and in another one, a breast development was reported as a rare dose-dependent AE of treatment with IVA [16]. Alternatively, a case report concerned a CF adult who discontinued LUM/IVA for respiratory dyspnea AE despite having already a half-dose reduction [37].

In approximately two-thirds of the remaining studies, the AE led to the interruption or discontinuation of caftor treatment. The LUM/IVA AE respiratory-related events could be mitigated in some patients by decreasing the dose. Whether the other described AE of this review are dose- or concentration-dependent and whether a dose adjustment may have maintained the treatment in some of these patients are unknown.

Noticeably, certain AEs have been resolved without any dose change: A case series described respiratory symptoms within 6 weeks of LUM/IVA initiation, which returned nearly to baseline after 2 weeks without any dose change [38]. For patients with ELX/TEZ/IVA presenting testicular pain, the symptoms resolved in 1–12 days after the addition of an OTC analgesic during the continuation of their regular dose [39].

Observational studies with *real-life* CFTR modulator safety data have shown higher rates of discontinuation, as well as AE that were rarely observed or not described in the clinical trials, whereby CFTR modulators are generally well-tolerated, except for IVA/LUM associated with a higher respiratory-related AE [29]. For instance, a higher percentage of previously under-reported AE of mental health deterioration was reported in a *real-life* setting [13,40,41]. Indeed, in 266 CF adults being prescribed ELX/TEZ/IVA, 7.1% of patients reported insomnia, anxiety, mental fogginess, and mood problems. The majority of them underwent a dose reduction. While the sweat chloride (as a surrogate of CFTR function) remained corrected, in 10/13 cases, this AE was improved or resolved by dose reduction (half) and psychological support [42].

Studies in target tissues have reported a destabilization of the corrected F508del CFTR by excessive IVA concentrations [43–45], which raised the important question of the possible occurrence of supratherapeutic or toxic concentrations of IVA in some patients [13].

In preclinical studies, an IVA threshold for cataract was defined as $\geq$10 mg/kg/day in a rat model [4], and cataract also constitutes a potential risk identified with the IVA monotherapy [4,13]. The ELX/TEZ/IVA combination demonstrated an overall improved safety profile, with the most commonly reported side effects being creatine kinase (CK) increase, hepatic enzymes elevation, and rash, which were the most frequent reasons for treatment interruption in clinical studies [4]. There is a lack of information on whether these events are related to drug plasma exposure, or whether the early AE-related drug interruption is related to excessive drug concentrations.

The safety profile of the ELX/TEZ/IVA combination has demonstrated the same potential risks that have been reported for other CFTR modulators: liver function test elevation and increased blood pressure.

Relationships between early adverse drug reactions leading to treatment interruption and plasma levels remain, therefore, to be further studied, especially for the latest-generation combination of CFTR modulators.

3.4. Special Population

This is of particular concern for CF patients with altered drug metabolism and/or elimination because of drug malabsorption, hepatic or renal impairments, or for patients taking comedications for other comorbidities (i.e., anti-infective and immunosuppressive drugs) with definite risks of reciprocal DDIs, and should it occur, in case of pregnancy. Additionally, limited clinical information and little hindsight exist for elderly or young patients, especially for children with hepatic impairment. Differences in treatment response or adverse drug reactions owing to physiological and metabolic differences (i.e., differences in distribution volume (Vd), enzyme ontology, etc.) may appear in children.

All the above special situations impact drug disposition, resulting in a definite PK variability with altered drug exposition.

There is also a lack of PK information for pediatric patients below a certain age (from <12 years old (yo) for ELX/TEZ/IVA and <6 yo for LUM/IVA and TEZ/IVA to <4 months for IVA; see Table 2) and also for children with hepatic impairment, as the Child–Pugh scale is not applicable; therefore, no guideline are yet available. Moreover, studies on the drugs' long-term impact on child development are missing.

Despite the lack of data on in utero drug exposure, a case report described two babies born from mothers receiving CFTR modulators without any evidence of congenital malformations or cataracts [46,47]. Rodent models demonstrated a transfer across placenta and breastmilk of about 40% of the maternal plasma levels [48]. For the postnatal period, barely any information is available, except for the first CFTR modulators. The average LUM and IVA levels in breastmilk were 27.1 μg/l (0.06 μM) and 35.3 μg/L (0.09 μM), respectively, and the average infant plasma levels corresponded to 2.7% and 0.4%, respectively, of the maternal plasma levels [49]. A survey reported no complications in 27 infants exposed to IVA through breastmilk, although the extent of breastfeeding and exposure to caftors were not reported [50]. Besides the safety for the infant, the adequate maintenance of the drug response for pregnant mothers is sparse. Vekaria et al. studied the effect of caftors during pregnancy but without monitoring plasma levels [47]. However, alteration in drug exposition during pregnancy is due to physiological modifications in the volume distribution, clearance, inhibition, or induction of various CYPs and other enzymes. For example, in another therapeutic area, the dose of the antiepileptic drug lamotrigine should, on occasion, be tripled during pregnancy to ensure sufficient exposition [51], and benzodiazepine midazolam doubles its oral clearance during pregnancy [52].

3.5. A Case for the Therapeutic Drug Monitoring (TDM) of CFTR Drugs

Thus, current CFTR modulators are generally given at fixed standardized dosages in adults or adapted according to age/weight for children, but such a general "one-size-fits-all" approach does not account for the various factors that also contribute to the large interindividual PK variability reported for these drugs.

As previously stated, information on CFTR drug exposure in a real-life setting still remains limited, with only very few data on the actual target plasma levels (Table 3) [17–22].

The best time after dose (TAD) for blood sampling, e.g., C_{max}, C_{min} (i.e., before next dose), or AUC determination for obtaining clinically relevant TDM information remains to be formally determined. However, the multiple blood sampling required over an entire dosing interval to calculate AUC is not feasible in a routine clinical setting, even more so in an outpatient ward. Consequently, so far, no guidelines integrate TDM, despite the known PK variability reported for the newer CFTR modulators. Nevertheless, the tailored dose adjustment of these new agents may possibly improve their safety without compromising their efficacy.

TDM may prove to be a clinically useful tool to provide better care to CF patients in a number of instances, which are reviewed in Sections 3.6 and 3.7.

3.6. Drug–Drug Interactions

There are a number of alterations in exposure to caftors due to their cytochromes' P450-dependent metabolism. Many drugs commonly used in CF patients possibly inhibit CYP3A (e.g., importantly by azole antifungals such as itraconazole) or are metabolized by CYP3A (e.g., antibiotics, steroids, and hormonal contraceptives), and/or are substrates of P-gp (e.g., tacrolimus, ciclosporin, and digoxin) [27,53]. These drug associations may cause DDIs, altering thereby either the exposition of caftors (DDI victim) or the coadministered medication (DDI perpetrator) (see Tables 1 and S1).

Notably, given the very high cost of these caftor combinations, and also considering non-responder patients, a PK interaction study has been initiated by Liddy et al. aiming at increasing caftor exposure by adding a CYP3A inhibitor as a "PK booster", as conducted in the past with ritonavir for HIV protease inhibitors in antiretroviral therapies. It has been indeed demonstrated that IVA AUC was significantly increased in association with ritonavir in healthy volunteers [54].

3.7. Adherence to Caftor Treatment

The development of this new life-changing and life-saving oral medication with a simple dosing schedule provided the hope that better adherence would be a natural consequence. A former study with an electronic monitoring device that recorded adherence highlighted the fact that the IVA adherence rate was only 61% of the recommended dosing and decreased over time (n = 12 CF $\geq$ 6 yo) [55]. A mean adherence >80% for all CFTR modulators has more recently been reported [56], with a substantial improvement in the mean adherence of up to 94% (SD 12.4%) at 6 months for the newest regimen ELX/TEZ/IVA [57]. However, for those individuals with suboptimal adherence (including the remaining 6% of patients with poor adherence with ELX/TEZ/IVA), dialogue and reciprocal confidence between healthcare providers and CF patients must be improved. In that context, TDM constitutes an important tool contributing to the promotion of better adherence to these costly therapies, especially considering that the interruption of caftors can lead to withdrawal syndromes with acute deterioration [23,58].

3.8. TDM in Other Body Compartments

PK parameters are usually calculated based on concentrations measured in blood, or more generally in plasma, which are the compartments easily accessible and limitedly invasive for patients. However, the airway epithelia levels upon using the caftors were not found to be predicted by serum PK. Moreover, as the drugs act intracellularly, there may be an interest to determine their levels at the expected site of pharmacological actions. To this end, analytical methods have been developed for the quantification of IVA not only in plasma but also in epithelial cells [59,60]. An accumulation of IVA in cells as compared to plasma was observed, confirming a previous in vitro report [60]. In this case, IVA levels in the cellular compartment may be higher than those in circulating plasma, which could lead to a level of CFTR restoration distinct from what would be expected by measuring only plasma levels. Clearly, there is an exciting research area ahead for deciphering caftors' PK/PD relationships at the tissular/cellular levels.

Other analytical methods to measure caftor concentrations in alternate biological matrices including sputum and rectal organoids have also been described [21,61]. At present, the clinical relevance of, and interest in, TDM by using an alternative matrix instead of plasma for the quantification of caftors remains to be investigated.

3.9. Importance of Monitoring the Metabolites

In the TDM practice, enzyme phenotyping, namely the metabolite-to-parent drug ratio (MPR), can be used as a direct measurement of metabolizing enzyme activity (i.e., as

carried out, for instance, with midazolam MPR for CYP3A phenotyping) [62]. Unusual MPRs allow for the detection of altered CYP-mediated metabolism activity (e.g., drug–drug interactions, pharmacogenetic variants leading to defective or increased enzyme activity, or liver impairment). Except for LUM, which is marginally metabolized, the metabolites of the caftors can also be simultaneously analyzed with the parent drugs, allowing for the direct monitoring of the MPR in patients: a strong CYP3A inhibitor (e.g., azole antifungals) would lead to a marked decrease in MRP, suggestive for the requirement to adjust caftor dosage [63] (see active metabolite(s) in Table 1).

3.10. Practical Implementation of TDM for CFTR Modulator Drugs in the Clinical Setting

In the overview of our development of the TDM of imatinib, the very first oral targeted anticancer agent [64], we have already expressed that a similar TDM approach could apply to a wide range of treatments critical for the control of various life-threatening conditions, such as caftors in CF individuals. The TDM development is generally structured along five generic questions: (1) Is the concerned drug a candidate for TDM? (2) What is the usually observed or target range for the drug's concentration? (3) What is the therapeutic target for the drug's concentration? (4) How to adjust the dosage of the drug to drive concentrations close to the target? (5) Does evidence support the usefulness of TDM for this drug?

At present, the information compiled in this review provides strong arguments to support that caftor drugs fulfill most, if not all, criteria for a TDM program (question 1). There is also some information, retrieved notably from clinical studies, on the usually observed concentration ranges for caftors (question 2) (see Table 2). Alternately, there is only limited information on the plasma concentration targets of caftors for optimal therapeutic effect, and to the best of our knowledge, this would need to be formally validated clinically (question 3). For addressing question 4, the pharmacological interpretations of TDM would benefit from incoming computer tools of improved user-friendliness and performance, the development of which is underway [65,66]. For instance, the computer application Tucuxi (http://www.tucuxi.ch, accessed on 10 October 2021) aims at helping practitioners in the interpretation of drug concentration measurements by indicating whether the measured drug levels are "expected" by taking into account drug dosage, patient characteristics, intrinsic population variability, and population PK parameters, and proposes dosage adjustments when indicated. Finally, the definitive answer to question 5 "*Does evidence support the usefulness of TDM for CFTR modulator drugs*?" would be formally obtained through a randomized controlled trial comparing the clinical outcome (i.e., percentages of optimal therapeutic responses and AEs occurrence) of patients being offered a TDM-guided caftor dose adjustment versus patients receiving the currently recommended CFTR drug dosage regimens.

4. Discussion

Conceivably, the monitoring of caftors in CF patients' blood (plasma) shall allow healthcare professionals to have access without delay to information on patients' plasma exposure and, ultimately, to monitor drug plasma levels in case of drug dosage adjustment. This could be useful in case of clinical complications or toxicities. CFTR drug-dose-related adverse effects (e.g., hepatitis, rash and other skin lesions, gastrointestinal problems for some caftors), or DDI issues could also be addressed. To this end, more data on drug exposure particularly from *real-world* settings are urgently required to evaluate whether plasma levels are within the reference range. TDM has a role in preventing drug toxicity in patients unnecessarily exposed to excessive drug plasma concentrations, by adjusting drug dosage accordingly. Additionally, TDM could help to ascertain that a less-than-expected clinical response may not be due to insufficient exposure to drugs, resulting in impaired gastrointestinal absorption or imperfect treatment adherence.

This review compiled the PK data from *real-life* CF patients, which could also be balanced to those reported within the stringent framework of clinical trials in carefully selected patients who poorly reflect the complex situation of real-life patients. The sparse data on

the PK/PD relationship should also be gathered. Finally, the overall patient satisfaction, financial burden of treatments, and pharmacogenetic aspects of these treatments should be explored to even better personalize drug regimens.

5. Conclusions

In the growing movement of precision medicine, research efforts must, therefore, be pursued to improve the prescription of CFTR modulators not only with regard to clinical efficacy but also according to tolerability, long-term safety, and potential DDIs, possibly modulated by patients' pharmacogenetic traits. All the above aspects can be addressed more comprehensively by having access to information on actual caftor exposure in patients' plasma. In this regard, TDM is at the forefront of this trend to personalize treatment to best meet the needs of CF patients.

Supplementary Materials: The following supporting information can be downloaded at: https://www.mdpi.com/article/10.3390/pharmaceutics14081674/s1, Table S1: Impact of Other Drugs on Elexacaftor, Tezacaftor and/or Ivacaftor [4]; Table S2: PK parameters of ivacaftor and ivacaftor-lumacaftor standard therapy [14].

Funding: This research was funded by Cystic Fibrosis Switzerland grant number [2022], and a part of the APC was funded by the University of Lausanne.

Institutional Review Board Statement: Not applicable.

Informed Consent Statement: Not applicable.

Acknowledgments: We thank Cystic Fibrosis Switzerland, whose support made this study possible (grant 2022). We are also grateful to all collaborators of the pharmacological laboratory at Lausanne and the CF medical team at Lausanne and Neuchâtel hospitals.

Conflicts of Interest: The authors declare no conflict of interest.

References

1. Rueegg, C.S.; Kuehni, C.E.; Gallati, S.; Baumgartner, M.; Torresani, T.; Barben, J. One-Year Evaluation of a Neonatal Screening Program for Cystic Fibrosis in Switzerland. *Dtsch. Arztebl. Int.* **2013**, *110*, 356–363. [CrossRef] [PubMed]
2. Donaldson, S.H.; Pilewski, J.M.; Griese, M.; Cooke, J.; Viswanathan, L.; Tullis, E.; Davies, J.C.; Lekstrom-Himes, J.A.; Wang, L.T. Tezacaftor/Ivacaftor in Subjects with Cystic Fibrosis and F508del/F508del-Cftr or F508del/G551d-Cftr. *Am. J. Respir. Crit. Care Med.* **2018**, *197*, 214–224. [CrossRef] [PubMed]
3. Lopes-Pacheco, M. Cftr Modulators: The Changing Face of Cystic Fibrosis in the Era of Precision Medicine. *Front. Pharmacol.* **2020**, *10*, 1662. [CrossRef] [PubMed]
4. U.S. Food and Drug Administration. Center for Drug Evaluation and Research: Nda/Bla, Multi-Disciplinary Review and Evaluation, Elexacaftor/Tezacaftor/Ivacaftor. Available online: https://www.accessdata.fda.gov/drugsatfda_docs/nda/2019/212273Orig1s000MultidisciplineR.pdf (accessed on 3 June 2022).
5. Jih, K.Y.; Hwang, T.C. Vx-770 Potentiates Cftr Function by Promoting Decoupling between the Gating Cycle and Atp Hydrolysis Cycle. *Proc. Natl. Acad. Sci. USA* **2013**, *110*, 4404–4409. [CrossRef] [PubMed]
6. U.S. Food and Drug Administration. Center for Drug Evaluation and Research: Nda/Bla, Multi-Disciplinary Review and Evaluation, Ivacaftor. Available online: https://www.accessdata.fda.gov/drugsatfda_docs/nda/2012/203188Orig1s000Approv.pdf (accessed on 3 June 2022).
7. U.S. Food and Drug Administration. Center for Drug Evaluation and Research: Nda/Bla, Multi-Disciplinary Review and Evaluation, Lumacaftor/Ivacaftor. Available online: https://www.accessdata.fda.gov/drugsatfda_docs/nda/2018/211358Orig1s000Approv.pdf (accessed on 3 June 2022).
8. European Public Assessment Report. Summary of Product Characteristics. Available online: https://www.ema.europa.eu/en/documents/overview/symkevi-epar-medicine-overview_en.pdf (accessed on 3 June 2022).
9. Gross, A.S. Best Practice in Therapeutic Drug Monitoring. *Br. J. Clin. Pharmacol.* **2001**, *52* (Suppl. S1), 5S–10S. [PubMed]
10. Holford, N.H.; Buclin, T. Safe and Effective Variability-a Criterion for Dose Individualization. *Ther. Drug Monit.* **2012**, *34*, 565–568. [CrossRef] [PubMed]
11. Compendium Suisse des Médicaments. Information Sur Le Médicament. Available online: https://www.swissmedicinfo.ch/ (accessed on 3 June 2022).
12. King, J.A.; Nichols, A.-L.; Bentley, S.; Carr, S.B.; Davies, J.C. An Update on Cftr Modulators as New Therapies for Cystic Fibrosis. *Pediatr. Drugs* **2022**, *24*, 321–333. [CrossRef]

13. Dagenais, R.V.E.; Su, V.C.H.; Quon, B.S. Real-World Safety of Cftr Modulators in the Treatment of Cystic Fibrosis: A Systematic Review. *J. Clin. Med.* **2020**, *10*, 23. [CrossRef] [PubMed]
14. Hanafin, P.O.; Sermet-Gaudelus, I.; Griese, M.; Kappler, M.; Ellemunter, H.; Schwarz, C.; Wilson, J.; Tan, M.; Velkov, T.; Rao, G.G.; et al. Insights into Patient Variability during Ivacaftor-Lumacaftor Therapy in Cystic Fibrosis. *Front. Pharmacol.* **2021**, *12*, 577263. [CrossRef] [PubMed]
15. Masson, A.; Schneider-Futschik, E.K.; Baatallah, N.; Nguyen-Khoa, T.; Girodon, E.; Hatton, A.; Flament, T.; Le Bourgeois, M.; Chedevergne, F.; Bailly, C.; et al. Predictive Factors for Lumacaftor/Ivacaftor Clinical Response. *J. Cyst. Fibros.* **2018**, *18*, 368–374. [CrossRef]
16. Jeyaratnam, J.; van der Meer, R.; Berkers, G.; Heijerman, H.G.; Beekman, J.M.; van der Ent, C.K. Breast Development in a 7 Year Old Girl with Cf Treated with Ivacaftor: An Indication for Personalized Dosing? *J. Cyst. Fibros.* **2021**, *20*, e63–e66. [CrossRef] [PubMed]
17. Davies, J.C.; Wainwright, C.E.; Sawicki, G.S.; Higgins, M.N.; Campbell, D.; Harris, C.; Panorchan, P.; Haseltine, E.; Tian, S.; Rosenfeld, M. Ivacaftor in Infants Aged 4 to <12 Months with Cystic Fibrosis and a Gating Mutation. Results of a Two-Part Phase 3 Clinical Trial. *Am. J. Respir. Crit. Care Med.* **2021**, *203*, 585–593. [CrossRef] [PubMed]
18. Flume, P.A.; Biner, R.F.; Downey, D.G.; Brown, C.; Jain, M.; Fischer, R.; de Boeck, K.; Sawicki, G.S.; Chang, P.; Paz-Diaz, H.; et al. Long-Term Safety and Efficacy of Tezacaftor-Ivacaftor in Individuals with Cystic Fibrosis Aged 12 Years or Older Who Are Homozygous or Heterozygous for Phe508del Cftr (Extend): An Open-Label Extension Study. *Lancet Respir. Med.* **2021**, *9*, 733–746. [CrossRef]
19. Rosenfeld, M.; Wainwright, C.E.; Higgins, M.; Wang, L.T.; McKee, C.; Campbell, D.; Tian, S.; Schneider, J.; Cunningham, S.; Davies, J.C.; et al. Ivacaftor Treatment of Cystic Fibrosis in Children Aged 12 to <24 Months and with a Cftr Gating Mutation (Arrival): A Phase 3 Single-Arm Study. *Lancet Respir. Med.* **2018**, *6*, 545–553. [CrossRef]
20. Trittler, R.; Hug, M. Pkp-017 Monitoring of Ivacaftor Serum Levels. *Eur. J. Hosp. Pharm.* **2014**, *21* (Suppl. S1), A143.2–A144. [CrossRef]
21. Vonk, S.E.M.; van der Meer-Vos, M.; Bos, L.D.J.; Neerincx, A.H.; Majoor, C.J.; der Zee, A.H.M.; Mathot, R.A.A.; Kemper, E.M.; Group Amsterdam Mucociliary Clearance Disease Research. Quantitative Method for the Analysis of Ivacaftor, Hydroxymethyl Ivacaftor, Ivacaftor Carboxylate, Lumacaftor, and Tezacaftor in Plasma and Sputum Using Liquid Chromatography with Tandem Mass Spectrometry and Its Clinical Applicability. *Ther. Drug Monit.* **2021**, *43*, 555–563. [CrossRef] [PubMed]
22. Vonk, S.E.M.; Terheggen-Lagro, S.W.J.; Mouissie, L.M.; Mathot, R.A.A.; Kemper, E.M.; Group Amsterdam Mucociliary Clearance Disease Research. No Drug-Drug Interaction between Tezacaftor-Ivacaftor and Clofazimine: A Case Report. *J. Cyst. Fibros.* **2022**, *21*, e5–e7. [CrossRef] [PubMed]
23. Duckers, J.; Lesher, B.; Thorat, T.; Lucas, E.; McGarry, L.; Chandarana, K.; De Iorio, F. Real-World Outcomes of Ivacaftor Treatment in People with Cystic Fibrosis: A Systematic Review. *J. Clin. Med.* **2021**, *10*, 1527. [CrossRef]
24. Hong, E.; Almond, L.M.; Chung, P.S.; Rao, A.P.; Beringer, P.M. Physiologically-Based Pharmacokinetic-Led Guidance for Patients with Cystic Fibrosis Taking Elexacaftor-Tezacaftor-Ivacaftor with Nirmatrelvir-Ritonavir for the Treatment of COVID-19. *Clin. Pharmacol. Ther.* **2022**, *111*, 1324–1333. [CrossRef] [PubMed]
25. Tsai, A.; Wu, S.P.; Haseltine, E.; Kumar, S.; Moskowitz, S.M.; Panorchan, P.; Shah, K. Physiologically Based Pharmacokinetic Modeling of Cftr Modulation in People with Cystic Fibrosis Transitioning from Mono or Dual Regimens to Triple-Combination Elexacaftor/Tezacaftor/Ivacaftor. *Pulm. Ther.* **2020**, *6*, 275–286. [CrossRef]
26. Fohner, A.E.; McDonagh, E.M.; Clancy, J.P.; Whirl Carrillo, M.; Altman, R.B.; Klein, T.E. Pharmgkb Summary: Ivacaftor Pathway, Pharmacokinetics/Pharmacodynamics. *Pharm. Genom.* **2017**, *27*, 39–42. [CrossRef] [PubMed]
27. Garg, V.; Shen, J.; Li, C.; Agarwal, S.; Gebre, A.; Robertson, S.; Huang, J.; Han, L.; Jiang, L.; Stephan, K.; et al. Pharmacokinetic and Drug-Drug Interaction Profiles of the Combination of Tezacaftor/Ivacaftor. *Clin. Transl. Sci.* **2019**, *12*, 267–275. [CrossRef] [PubMed]
28. Schneider, E.; Huang, J.; Carbone, V.; Baker, M.; Azad, M.A.K.; Cooper, M.; Li, J.; Velkov, T. Drug-Drug Plasma Protein Binding Interactions of Ivacaftor. *J. Mol. Recognit.* **2015**, *28*, 339–348. [CrossRef] [PubMed]
29. Wainwright, C.E.; Elborn, J.S.; Ramsey, B.W. Lumacaftor-Ivacaftor in Patients with Cystic Fibrosis Homozygous for Phe508del Cftr. *N. Engl. J. Med.* **2015**, *373*, 1783–1784. [CrossRef] [PubMed]
30. Heijerman, H.G.M.; McKone, E.F.; Downey, D.G.; Van Braeckel, E.; Rowe, S.M.; Tullis, E.; Mall, M.A.; Welter, J.J.; Ramsey, B.W.; McKee, C.M.; et al. Efficacy and Safety of the Elexacaftor Plus Tezacaftor Plus Ivacaftor Combination Regimen in People with Cystic Fibrosis Homozygous for the F508del Mutation: A Double-Blind, Randomised, Phase 3 Trial. *Lancet* **2019**, *394*, 1940–1948. [CrossRef]
31. van der Meer, R.; Wilms, E.B.; Heijerman, H.G.M. Cftr Modulators: Does One Dose Fit All? *J. Pers. Med.* **2021**, *11*, 458. [CrossRef] [PubMed]
32. Murer, C.; Huber, L.C.; Kurowski, T.; Hirt, A.; Robinson, C.A.; Burgi, U.; Benden, C. First Experience in Switzerland in Phe508del Homozygous Cystic Fibrosis Patients with End-Stage Pulmonary Disease Enrolled in a Lumacaftor-Ivacaftor Therapy Trial—Preliminary Results. *Swiss Med. Wkly.* **2018**, *148*, w14593. [PubMed]
33. Anstead, M.; Tupayachi, G.; Murphy, D.; Autry, E.; Bulkley, V.; Kuhn, R. Lumacaftor/Ivacaftor: Real World Experience in a Cf Center. *Pediatr. Pulmonol.* **2016**, *51*, 302.

34. Flanagan, M.; Donovan, D.; Murphy, C.; Keating, E.; Jennings, R.; Shanahan, P.; Crowley, J.; Cronin, K.; Mullane, D.; Ni Chroinin, M. Orkambi: The Cork Pediatric Experience Cork University Hospital. Irish Thoracic Society Annual Scientific Meeting 2017 10th–11th November 2017, Limerick Strand Hotel, Limerick. *Ir. J. Med. Sci.* **2017**, *186* (Suppl. S10), 387–445.
35. Finnegan, R.; O'Grady, E.; Smyth, A.; Ryan, S.; Williamson, M. Evidence of Small Airways Disease and the Immediate Effects of Lumacaftor/Ivacaftor in Children with Cystic Fibrosis. *Ir. Med. J.* **2020**, *113*, 70.
36. Welsner, M.; Straßburg, S.; Taube, C.; Sutharsan, S. Use of Ivacaftor in Late Diagnosed Cystic Fibrosis Monozygotic Twins Heterozygous for F508del and R117h-7t—A Case Report. *BMC Pulm. Med.* **2019**, *19*, 76. [CrossRef] [PubMed]
37. Richards, C.J.; Sicilian, L.; Neuringer, I. Decline and Recovery of Lung Function with the Initiation and Cessation of Lumacaftor-ivacaftor. In Proceedings of the American Thoracic Society 2017 International Conference, Washington, DC, USA, 19–24 May 2017.
38. Walayat, S.; Hussain, N.; Patel, J.; Hussain, F.; Patel, P.; Dhillon, S.; Aulakh, B.; Chittivelu, S. Drug-Induced Dyspnea Versus Cystic Fibrosis Exacerbation: A Diagnostic Dilemma. *Int. Med. Case Rep. J.* **2017**, *10*, 243–246. [CrossRef] [PubMed]
39. Rotolo, S.M.; Duehlmeyer, S.; Slack, S.M.; Jacobs, H.R.; Heckman, B. Testicular Pain Following Initiation of Elexacaftor/Tezacaftor/Ivacaftor in Males with Cystic Fibrosis. *J. Cyst. Fibros.* **2020**, *19*, e39–e41. [CrossRef]
40. Tindell, W.; Su, A.; Oros, S.M.; Rayapati, A.O.; Rakesh, G. Trikafta and Psychopathology in Cystic Fibrosis: A Case Report. *J. Psychosom. Res.* **2020**, *61*, 735–738. [CrossRef]
41. Heo, S.; Young, D.C.; Safirstein, J.; Bourque, B.; Antell, M.H.; Diloreto, S.; Rotolo, S.M. Mental Status Changes During Elexacaftor/Tezacaftor/Ivacaftor Therapy. *J. Cyst. Fibros.* **2022**, *21*, 339–343. [CrossRef] [PubMed]
42. Spoletini, G.; Gillgrass, L.; Pollard, K.; Shaw, N.; Williams, E.; Etherington, C.; Clifton, I.; Peckham, D. Dose Adjustments of Elexacaftor/Tezacaftor/Ivacaftor in Response to Mental Health Side Effects in Adults with Cystic Fibrosis. *J. Cyst. Fibros.* **2022**. [CrossRef]
43. Cholon, D.M.; Quinney, N.L.; Fulcher, M.L.; Esther, C.R.; Das, J., Jr.; Dokholyan, N.V.; Randell, S.H.; Boucher, R.C.; Gentzsch, M. Potentiator Ivacaftor Abrogates Pharmacological Correction of Deltaf508 Cftr in Cystic Fibrosis. *Sci. Transl. Med.* **2014**, *6*, 246ra96. [CrossRef]
44. Avramescu, R.G.; Kai, Y.; Xu, H.; Bidaud-Meynard, A.; Schnur, A.; Frenkiel, S.; Matouk, E.; Veit, G.; Lukacs, G.L. Mutation-Specific Downregulation of Cftr2 Variants by Gating Potentiators. *Hum. Mol. Genet.* **2017**, *26*, 4873–4885. [CrossRef] [PubMed]
45. Chin, S.; Hung, M.; Won, A.; Wu, Y.-S.; Ahmadi, S.; Yang, D.; Elmallah, S.; Toutah, K.; Hamilton, C.M.; Young, R.N.; et al. Lipophilicity of the Cystic Fibrosis Drug, Ivacaftor (Vx-770), and Its Destabilizing Effect on the Major Cf-Causing Mutation: F508del. *Mol. Pharmacol.* **2018**, *94*, 917–925. [CrossRef]
46. Reyes-Ortega, F.; Qiu, F.; Schneider-Futschik, E.K. Multiple Reaction Monitoring Mass Spectrometry for the Drug Monitoring of Ivacaftor, Tezacaftor, and Elexacaftor Treatment Response in Cystic Fibrosis: A High-Throughput Method. *ACS Pharmacol. Transl. Sci.* **2020**, *3*, 987–996. [CrossRef]
47. Vekaria, S.; Popowicz, N.; White, S.W.; Mulrennan, S. To Be or Not to Be on Cftr Modulators During Pregnancy: Risks to Be Considered. *J. Cyst. Fibros.* **2019**, *19*, e7–e8. [CrossRef]
48. Qiu, F.; Habgood, M.D.; Huang, Y.; Dziegielewska, K.M.; Toll, S.; Schneider-Futschik, E.K. Entry of Cystic Fibrosis Transmembrane Conductance Potentiator Ivacaftor into the Developing Brain and Lung. *J. Cyst. Fibros.* **2021**, *20*, 857–864. [CrossRef]
49. Trimble, A.; McKinzie, C.; Terrell, M.; Stringer, E.; Esther, C.R. Measured Fetal and Neonatal Exposure to Lumacaftor and Ivacaftor During Pregnancy and While Breastfeeding. *J. Cyst. Fibros.* **2018**, *17*, 779–782. [CrossRef]
50. Nash, E.F.; Middleton, P.G.; Taylor-Cousar, J.L. Outcomes of Pregnancy in Women with Cystic Fibrosis (Cf) Taking Cftr Modulators - an International Survey. *J. Cyst. Fibros.* **2020**, *19*, 521–526. [CrossRef]
51. Petrenaite, V.; Sabers, A.; Hansen-Schwartz, J. Individual Changes in Lamotrigine Plasma Concentrations During Pregnancy. *Epilepsy Res.* **2005**, *65*, 185–188. [CrossRef] [PubMed]
52. Hebert, M.F.; Easterling, T.R.; Kirby, B.; Carr, D.B.; Buchanan, M.L.; Rutherford, T.; Thummel, K.E.; Fishbein, D.P.; Unadkat, J.D. Effects of Pregnancy on Cyp3a and P-Glycoprotein Activities as Measured by Disposition of Midazolam and Digoxin: A University of Washington Specialized Center of Research Study. *Clin. Pharmacol. Ther.* **2008**, *84*, 248–253. [CrossRef]
53. Deeks, E.D. Lumacaftor/Ivacaftor: A Review in Cystic Fibrosis. *Drugs* **2016**, *76*, 1191–1201. [CrossRef] [PubMed]
54. Liddy, A.M.; McLaughlin, G.; Schmitz, S.; D'Arcy, D.M.; Barry, M.G. The Pharmacokinetic Interaction between Ivacaftor and Ritonavir in Healthy Volunteers. *Br. J. Clin. Pharmacol.* **2017**, *83*, 2235–2241. [CrossRef] [PubMed]
55. Siracusa, C.M.; Ryan, J.; Burns, L.; Wang, Y.; Zhang, N.; Clancy, J.P.; Drotar, D. Electronic Monitoring Reveals Highly Variable Adherence Patterns in Patients Prescribed Ivacaftor. *J. Cyst. Fibros.* **2015**, *14*, 621–626. [CrossRef] [PubMed]
56. Mehta, Z.; Kamal, K.M.; Miller, R.; Covvey, J.R.; Giannetti, V. Adherence to Cystic Fibrosis Transmembrane Conductance Regulator (Cftr) Modulators: Analysis of a National Specialty Pharmacy Database. *J. Drug Assess.* **2021**, *10*, 62–67. [CrossRef] [PubMed]
57. Beswick, D.M.; Humphries, S.M.; Balkissoon, C.D.; Strand, M.; Vladar, E.K.; Ramakrishnan, V.R.; Taylor-Cousar, J.L. Olfactory Dysfunction in Cystic Fibrosis: Impact of Cftr Modulator Therapy. *J. Cyst. Fibros.* **2021**, *21*, e141–e147. [CrossRef] [PubMed]
58. Trimble, A.T.; Donaldson, S.H. Ivacaftor Withdrawal Syndrome in Cystic Fibrosis Patients with the G551d Mutation. *J. Cyst. Fibros.* **2018**, *17*, e13–e16. [CrossRef] [PubMed]
59. Guimbellot, J.S.; Ryan, K.J.; Anderson, J.; Liu, Z.; Kersh, L.; Esther, C.R.; Rowe, S.M.; Acosta, E.P. Variable Cellular Ivacaftor Concentrations in People with Cystic Fibrosis on Modulator Therapy. *J. Cyst. Fibros.* **2020**, *19*, 742–745. [CrossRef] [PubMed]
60. Lee, T.N.G.; Cholon, D.M.; Quinney, N.L.; Gentzsch, M.; Esther, C.R. Accumulation and Persistence of Ivacaftor in Airway Epithelia with Prolonged Treatment. *J. Cyst. Fibros.* **2020**, *19*, 746–751.

61. Dekkers, B.G.J.; Akkerman, O.W.; Alffenaar, J.W.C. Role of Therapeutic Drug Monitoring in Treatment Optimization in Tuberculosis and Diabetes Mellitus Comorbidity. *Antimicrob. Agents Chemother.* **2019**, *63*, e02074-18. [CrossRef] [PubMed]
62. Dahl, M.L.; Johansson, I.; Bertilsson, L.; Ingelman-Sundberg, M.; Sjoqvist, F. Ultrarapid Hydroxylation of Debrisoquine in a Swedish Population. Analysis of the Molecular Genetic Basis. *J. Pharmacol. Exp. Ther.* **1995**, *274*, 516–520. [PubMed]
63. Habler, K.; Kalla, A.S.; Rychlik, M.; Bruegel, M.; Teupser, D.; Nahrig, S.; Vogeser, M.; Paal, M. Isotope Dilution Lc-Ms/Ms Quantification of the Cystic Fibrosis Transmembrane Conductance Regulator (Cftr) Modulators Ivacaftor, Lumacaftor, Tezacaftor, Elexacaftor, and Their Major Metabolites in Human Serum. *Clin. Chem. Lab. Med.* **2022**, *60*, 82–91. [CrossRef]
64. Buclin, T.; Thoma, Y.; Widmer, N.; Andre, P.; Guidi, M.; Csajka, C.; Decosterd, L.A. The Steps to Therapeutic Drug Monitoring: A Structured Approach Illustrated with Imatinib. *Front. Pharmacol.* **2020**, *11*, 177. [CrossRef] [PubMed]
65. Dubovitskaya, A.; Buclin, T.; Schumacher, M.; Aberer, K.; Thoma, Y. Tucuxi—An Intelligent System for Personalized Medicine: From Individualization of Treatments to Research Databases and Back. In Proceedings of the 8th ACM International Conference on Bioinformatics, Computational Biology and Health Informatics, Boston, MA, USA, 20–23 August 2017; pp. 223–232.
66. Tucker, G.T. Personalized Drug Dosage—Closing the Loop. *Pharm. Res.* **2017**, *34*, 1539–1543. [CrossRef] [PubMed]

pharmaceutics

MDPI

Review

Perspectives of Therapeutic Drug Monitoring of Biological Agents in Non-Infectious Uveitis Treatment: A Review

Manuel Busto-Iglesias [1,2,†], Lorena Rodríguez-Martínez [2,†], Carmen Antía Rodríguez-Fernández [2,3,†], Jaime González-López [1,2], Miguel González-Barcia [1,2], Begoña de Domingo [4], Luis Rodríguez-Rodríguez [5,*], Anxo Fernández-Ferreiro [1,2,*] and Cristina Mondelo-García [1,2]

1 Pharmacy Department, University Clinical Hospital of Santiago de Compostela (SERGAS), 15706 Santiago de Compostela, Spain
2 Pharmacology Group, Health Research Institute of Santiago de Compostela (FIDIS), 15706 Santiago de Compostela, Spain
3 Ophthalmology Department, Bellvitge University Hospital, 08907 Barcelona, Spain
4 Ophthalmology Department, University Clinical Hospital of Santiago Compostela (SERGAS), 15706 Santiago de Compostela, Spain
5 Musculoskeletal Pathology Group, Hospital Clínico San Carlos, Instituto Investigación Sanitaria San Carlos (IdISSC), 28040 Madrid, Spain
* Correspondence: lrrodriguez@salud.madrid.org (L.R.-R.); anxordes@gmail.com (A.F.-F.)
† These authors contributed equally to this work.

Abstract: Biological drugs, especially those targeting anti-tumour necrosis factor α (TNFα) molecule, have revolutionized the treatment of patients with non-infectious uveitis (NIU), a sight-threatening condition characterized by ocular inflammation that can lead to severe vision threatening and blindness. Adalimumab (ADA) and infliximab (IFX), the most widely used anti-TNFα drugs, have led to greater clinical benefits, but a significant fraction of patients with NIU do not respond to these drugs. The therapeutic outcome is closely related to systemic drug levels, which are influenced by several factors such as immunogenicity, concomitant treatment with immunomodulators, and genetic factors. Therapeutic drug monitoring (TDM) of drug and anti-drug antibody (ADAbs) levels is emerging as a resource to optimise biologic therapy by personalising treatment to bring and maintain drug concentration within the therapeutic range, especially in those patients where a clinical response is less than expected. Furthermore, some studies have described different genetic polymorphisms that may act as predictors of response to treatment with anti-TNFα agents in immune-mediated diseases and could be useful in personalising biologic treatment selection. This review is a compilation of the published evidence in NIU and in other immune-mediated diseases that support the usefulness of TDM and pharmacogenetics as a tool to guide clinicians' treatment decisions leading to better clinical outcomes. In addition, findings from preclinical and clinical studies, assessing the safety and efficacy of intravitreal administration of anti-TNFα agents in NIU are discussed.

Keywords: non-infectious uveitis (NIU); therapeutic drug monitoring (TDM); pharmacokinetics; pharmacogenetics; biological therapy

Citation: Busto-Iglesias, M.; Rodríguez-Martínez, L.; Rodríguez-Fernández, C.A.; González-López, J.; González-Barcia, M.; de Domingo, B.; Rodríguez-Rodríguez, L.; Fernández-Ferreiro, A.; Mondelo-García, C. Perspectives of Therapeutic Drug Monitoring of Biological Agents in Non-Infectious Uveitis Treatment: A Review. *Pharmaceutics* **2023**, *15*, 766. https://doi.org/10.3390/pharmaceutics15030766

Academic Editors: Barna Vasarhelyi and Gellért Balázs Karvaly

Received: 24 January 2023
Revised: 17 February 2023
Accepted: 22 February 2023
Published: 25 February 2023

1. Introduction

Uveitis refers to a heterogeneous group of diseases characterized by inflammation of the uvea, a structure formed by the iris, the choroid, and the ciliary body. They are usually classified depending on their aetiology as infectious or non-infectious, or according to the location of the inflammation (anterior, intermediate, posterior, or panuveitis). Non-infectious uveitis (NIU) has an immune-mediated or idiopathic aetiology and usually occurs in the form of flares [1].

Traditionally, local or systemic treatment with corticosteroids has been the mainstay therapy in patients with NIU. The powerful immunosuppressive effect of corticosteroids

makes them highly effective drugs in the control of acute flares; however, long-term treatment can lead to the appearance of adverse effects or other ocular complications, especially in patients with chronic doses of prednisone equivalents over 7.5 mg per day [2]. Therefore, in many cases, it is necessary to associate other immunomodulators that allow for the reduction of the long-term adverse effects of corticosteroids while enhancing their immunosuppressive action [3]. The immunomodulatory drugs commonly used as first-line treatment in NIU are antimetabolites such as methotrexate (MTX), mycophenolate mofetil (MMF), or azathioprine (AZA), calcineurin inhibitors such as cyclosporine, or alkylating agents such as cyclophosphamide. These drugs are also known as "corticosteroid-sparing agents" since corticosteroid doses can be reduced while maintaining good control of ocular inflammation. Although treatment with immunosuppressants has led to substantial improvement in the management of NIU [3], in some cases the ocular inflammation persists. However, biological drugs have emerged in recent years as useful resources in many forms of NIU that do not respond to conventional treatment [4,5].

Numerous studies have confirmed the favourable results both in efficacy and safety of biological drugs, mainly molecules against tumour necrosis factor α (TNFα), in patients with uveitis refractory to conventional treatments. The introduction of these drugs in the treatment of NIU has been possible due to the knowledge gained about the inflammatory mediators involved in this pathology, thus allowing the use of drugs that act specifically against these molecules [4]. Despite the wide use of various biological drugs including anti-TNFα drugs for the treatment of autoimmune diseases, only adalimumab (ADA) has been approved by the Food and Drug Administration (FDA) and the European Medicines Agency (EMA) (2014 and 2016, respectively) in non-anterior NIU [6]. After the introduction of ADA for the treatment of NIU, better control of inflammation has been achieved, with improvements in visual quality and fewer complications, but there is still a high percentage of patients, around 40%, who present primary treatment failure in the first six months according to the results of VISUAL clinical trials [6,7]. However, results from a recent real-world data study showed higher drug retention rates close to 55% after the first five years, with inefficacy being the main cause of discontinuation [8]. In non-responders, treatment with ADA is not only not beneficial, but it can produce undesired adverse events. This situation highlights the need to identify factors related to treatment response with biological drugs that allow better management of patients with NIU. In this sense, the study of pharmacokinetic (PK) and pharmacogenetic (PG) parameters related to anti-TNFα drugs appears to be promising in the identification of biomarkers for treatment response.

Studies that have evaluated factors related to failure in therapy with anti-TNFα agents in the field of ophthalmology are scarce in comparison with those in immune-mediated rheumatic and gastrointestinal pathologies. This is mainly due to the short course of anti-TNFα drugs in the treatment of NIU, although the low prevalence and high heterogeneity of the disease also contribute. PK studies in other immune-mediated pathologies have revealed a significant inter-individual variability in the systemic concentrations of biological drugs. This has been related to the development of anti-drug antibodies (ADAbs), the use of concomitant immunomodulatory treatments, and alterations in biochemical parameters, among which albumin is one of the most important [9]. This variability together with the difficulty of access of the drug to the site of action may be two relevant aspects of conditioning response to treatment. From a biopharmaceutical point of view, the eye has barriers that limit the passage of high molecular weight molecules. However, the presence of inflammation can facilitate the passage of large molecules such as biologic drugs [10]. The passage of monoclonal antibodies (mAbs) through the ocular barriers toward the eye is a barely studied aspect, but it could have a great impact on the pharmacodynamic aspects of these drugs regarding the treatment of NIU. On the other hand, PG studies in immune-mediated pathologies have provided evidence of the influence of certain genetic polymorphisms in the response to biological drugs, although the relevance of these findings in NIU is currently unknown. Thus far few studies have been conducted aimed at evaluating the clinical relevance of PK and PG aspects in NIU.

Compared with classical drugs such as digoxin, mAbs used as therapeutic proteins have different pharmacokinetic characteristics due to their particular physical characteristics, generally showing a smaller volume of distribution and a longer half-life. Classic drugs are eliminated through hepatic metabolism, renal filtration, and excretion through bile or faeces. In contrast, the clearance of therapeutic antibodies is related to protein degradation and target binding. This phenomenon known as target-mediated drug disposition (TMDD), is also present in small molecules that exhibit non-linear pharmacokinetics, although it is more frequent in therapeutic proteins [11]. Although the pharmacokinetics of classical drugs and therapeutic proteins differ, in both treatment scenarios systemic drug concentrations falling within a specific therapeutic range should be achieved to maximize treatment efficacy and clinical outcomes while avoiding undesired adverse events that may arise from excessively high drug levels. However, in clinical practice, this is not achieved in all patients due to the inter-individual variability in treatment, which highlights the need for tailored therapy. Therapeutic Drug Monitoring (TDM) is a useful tool to meet this need with which treatment can be personalized to reach therapeutic concentrations.

The introduction of biological therapies has revolutionized the treatment of NIU, especially those targeting TNFα. However, NIU treatment is challenging and current strategies are sometimes insufficient to achieve adequate control of ocular inflammation. Approximately 40% of patients experience early treatment failure (primary non-response, PNR), whereas up to 20% of patients experience an initial clinical improvement followed by a loss of response 12 months after starting treatment (secondary non-response, SNR) [6]. Given the limited repertoire of effective biologic drugs available in NIU, early identification of non-response (PNR) or loss of response (SNR) is of utmost importance in clinical practice.

The therapeutic outcome of biologic drugs in immune-mediated diseases is closely related to serum drug concentration [12,13]. Whilst therapeutic failure to anti-TNFα agents is commonly associated with low or undetectable serum trough drug levels (subtherapeutic), therapeutic success is associated with trough drug levels over a specific threshold, in a range in which maximum favourable outcomes are achieved with minimal or no adverse events [14]. Hence, the implementation of therapeutic drug monitoring (TDM), consisting of measuring trough drug levels and ADAbs, is essential to assess in each patient the performance of a given biological drug and define its optimal dose ranges.

Several approaches are currently available to measure drug and anti-drug antibody concentrations. Enzyme-linked immunosorbent assay (ELISA)-based techniques and radioimmunoassay (RIA) are the most used tests compared to other assays such as Homogenous Mobility Shift Assay (HMSA) and immunological multiparameter chip technology (IMPACT) [15,16]. Each assay format has a different sensitivity, dynamic range, and cut-points, so the results obtained are not equivalent. Therefore, the method of choice to monitor drug levels and anti-drug antibodies should be reported in all studies. All assays have advantages and limitations, some of them are inherent to the specific methodology, but others are related to economic factors, the presence of adequate facilities, or qualified personnel, among others. A detailed description of the available assays, their characteristics, and their main benefits and limitations can be found elsewhere [15,16].

Ideally, anti-TNFα therapy should result in therapeutic concentrations in all patients, but this is not always achieved in clinical practice as evidenced by the large differences observed in the systemic concentration of anti-TNFα drugs [17–20]. These differences are likely explained by heterogeneous drug bioavailability in patients, which in turn is influenced by PK factors, such as drug immunogenicity [21].

Furthermore, TDM was typically considered advantageous for drugs with a large inter-individual variability in exposure with relatively low intra-individual variation, a significant exposure–efficacy relationship, a narrow therapeutic window, and the availability of a validated bioanalytical assay. It has been postulated recently that this could also represent a useful tool to individualize dosing and optimize treatment using drugs with a wide therapeutic window and high cost [22].

The purpose of this comprehensive review is to compile the available evidence on the PK, TDM, and PG monitoring of anti-TNFα drugs used in NIU, as well as to discuss the relevance of the biopharmaceutical considerations that concern drug delivery in the eye, in relation to biological drug treatment. In addition, other routes of administration used for the administration of anti-TNF, such as the intravitreal route, will be mentioned. For that purpose, an extensive review of the preclinical and clinical pharmacokinetic studies that have been published in this field was carried out. The PubMed database was searched from its inception in 2000 to September 2022, and the reference lists from the relevant studies were analysed for additional literature.

2. Biologics in Uveitis Treatment

A better understanding of ocular inflammation pathways has led to the emergence of biological therapies for the treatment of NIU [3,23] that aim to overcome the 30% failure rate obtained under classical immunosuppressive treatment [24]. Different cytokines such as TNFα, IL-6, IL-17, or IL-23 play a key role in NIU inflammatory process [25], therefore becoming very attractive as potential therapeutic targets. Bearing this in mind, randomized prospective studies have been developed in the last years to evaluate the treatment efficacy of biological drugs in NIU [6,7,26]. In this sense, the main biological drugs used in NIU treatment are depicted in Table 1.

Adalimumab: ADA is a fully human monoclonal antibody targeting TNFα, which plays a central role in ocular inflammation via reactive oxygen species, inducing angiogenesis and breakdown of blood–retinal barrier (BRB). The time to reach maximum serum concentration is 56 h, after a 40-mg subcutaneous administration to a healthy adult subject, with an average absolute bioavailability estimated at 64%. The mean terminal half-life is approximately two weeks [27]. The first report about the role of ADA in NIU was in 2008 [28], after which several studies established the effectiveness of ADA in NIU, mainly the VISUAL I and VISUAL II trials. Both were randomised and multicentric clinical trials compared with a placebo, which evaluated the efficacy and safety of ADA in active and inactive NIU [6,7]. Based on the findings of these trials, ADA was approved for its use in NIU and is currently the only biological treatment approved by FDA and EMA for this purpose [1]. Phase III extension study (VISUAL III) has shown that ADA treatment maintains disease control and provides long-term corticosteroid-sparing effects [29]. In addition, a recent meta-analysis of six randomized controlled trials (RCTs) evaluating the efficacy and safety of ADA treatment of NIU has shown that treatment failure is halved compared with placebo, as well as a reduction in visual loss and ocular inflammation [30]. Future research aims to directly compare the efficacy of ADA in monotherapy and in combination with other immunosuppressants [31].

Infliximab (IFX): IFX is a chimeric (human/mouse) monoclonal antibody targeting TNFα has a half-life of up to 9.5 days and is administered intravenously. IFX use in uveitis was first reported in 2001 [32] and has been shown to be effective for NIU in children [33] and for Behçet's disease-associated uveitis resistant to classical immunosuppressive treatment [34], although it may also be effective for the management of other ocular diseases [1,4]. The use of IFX for the treatment of patients with refractory uveoretinitis of Behçet's disease (RUBD) has been approved in Japan in 2007 [35]. Its early use is strongly recommended in patients with vision-threatening ocular manifestations of Behçet's disease and should be considered as second-line therapy in juvenile idiopathic arthritis (JIA) related uveitis [36], proven its efficacy and its safety at doses as high as 20 mg/kg successfully used in these patients [37]. Furthermore, comparable results in terms of efficacy have been reported between IFX and ADA treatments for NIU [38].

Etanercept: Etanercept is a human recombinant fusion protein consisting of the ligand-binding region of the TNF-R2 receptor coupled to the constant region of immunoglobulin G1 (IgG1-Fc), which inhibits the attachment of TNFα to endogenous TNF receptors. Its half-life is around 70 h. Etanercept is approved for use in rheumatoid arthritis (RA), psoriatic arthritis (PsA), plaque psoriasis (PS), ankylosing spondylitis, and polyarticular JIA,

whereas its use in NIU is limited to case reports and small clinical trials [4]. Paradoxically, a significant association between etanercept and the development of uveitis as a drug-associated side effect has been reported compared to ADA or IFX [39]. Therefore, it is strongly recommended that the use of either of these two anti-TNFα agents should be considered before etanercept therapy for the treatment of ocular inflammatory disease [36].

Golimumab: Golimumab, a fully human monoclonal antibody targeting TNFα, with a half-life of about 12 days, has shown potential efficacy in patients with refractory NIU to TNFα blockers [40,41], emerging as a promising therapeutic option in this disease. Nevertheless, all data were obtained from retrospective case series with small sample sizes, so additional studies on its efficacy are required.

Certolizumab: Certolizumab is a PEGylated antigen-binding fragment (Fab') of a recombinant humanized monoclonal antibody to TNFα. The conjugation of the hydrophilic polyethylene glycol (PEG) chains increases the half-life of certolizumab pegol to around two weeks. The clearance of certolizumab differs from that of other biological agents due to the absence of an fc fragment in its structure, which prevents FcRn-mediated recycling. In addition, renal excretion of certolizumab has been described due to the relatively small size of the Fab' fragments [42,43]. Data on the efficacy of certolizumab in the treatment of NIU are limited to case series showing it may be effective in the inflammatory control of refractory NIU [44].

Tocilizumab: Tocilizumab is a humanized monoclonal antibody that inhibits IL-6 signalling by preventing IL-6 from binding to its receptor. A prospective randomized trial evaluated tocilizumab safety and efficacy for the treatment of non-anterior uveitis and observed significant improvement in visual acuity and a reduction of central foveolar thickness [45]. Additionally, tocilizumab has demonstrated efficacy in managing JIA-associated uveitis refractory to anti-TNFα therapy [46], Behçet-associated uveitis [47], birdshot chorioretinopathy [48], and uveitic macular oedema [49].

Rituximab: Rituximab is a B-cell-depleting chimeric anti-CD20 monoclonal antibody. The mean terminal half-life is approximately 22 days. A growing number of reports have supported the use of rituximab in some types of NIU [50–55]. A retrospective study in JIA-associated uveitis showed a decrease in uveitis recurrences in patients who have not previously responded to other biologic therapies [50]. Additionally, rituximab treatment resulted in clinical improvement in 14 patients with Vogt–Koyanagi–Harada (VKH) disease-associated uveitis [51,52], 20 patients with severe manifestations of Behçet-associated uveitis [53] and induced remission in 20 patients with refractory ophthalmic Wegener's granulomatosis [54].

Table 1. Monoclonal antibodies used in different types of NIU.

Drug	Target	Structure	Dosage	Uveitis Type	References
Adalimumab [1]	TNF-α	mAb, fully humanized	LD: 80 mg MD: 40 mg every other week	Non-infectious non-anterior uveitis [†]	[6,7]
Infliximab	TNF-α	mAb, mouse-human chimeric	LD: 5 mg/kg at weeks 0, 4, and 6 MD: 5 mg/kg every 4 to 8 weeks Max. dose: 10mg/kg for adults, 20 mg/kg for children every 4 weeks	JIA-related uveitis, Behçet, VKH, sarcoidosis, pars planitis, birdshot retinochoroidopathy, idiopatic uveitis	[1,4,33,34,37]
Etanercept [2]	TNF-α	Human fusion protein	50 mg weekly	Behçet	[4]
Golimumab	TNF-α	mAb, fully humanized	MD: 50 mg monthly Max. dose: 100 mg monthly	Refractory uveitis	[40,41]
Certolizumab	TNF-α	mAb, fully humanized	200 mg every 2 weeks	Refractory uveitis	[44]
Tocilizumab	IL-6	mAb, fully humanized	4–12 mg/kg every 2–4 weeks	Non-infectious non-anterior uveitis, Behçet, birdshot, JIA-related uveitis	[46–49]
Rituximab	CD-20	mAb, mouse-human chimeric	LD: 500 or 1000 mg at 0, and 2 weeks. MD: Repeat at 6–12 months if needed	Refractory uveitis, JIA-related uveitis, Behçet, VKH, Wegener's granulomatosis	[50–55]

[1] Only biological drug indicated to treat non-infectious intermediate, posterior, and panuveitis. [2] Use of infliximab or adalimumab should be considered before etanercept therapy for the treatment of ocular inflammatory disease. [†] Adalimumab on-label indication. LD: loading dose, MD: maintenance dose, TNFα: tumour necrosis factor-α, IL-6: interleukin-6, CD-20: cluster of differentiation-20, mAb: monoclonal antibody.

3. Therapeutic Drug Monitoring of Anti-TNFα in NIU

3.1. Pharmacokinetics (PK) of mAbs

MAbs are glycoproteins based on the structure of γ-immunoglobulins (IgG); hence they have a high molecular weight. These drugs are administered parenterally, either intravenously (IV), subcutaneously (SC), or intramuscularly (IM). Due to their high molecular weight, mAbs are absorbed through the lymphatic system after SC or IM administration. The high molecular weight of mAbs also hinders their distribution to tissues and therefore, they are retained in vascular and interstitial spaces. Consequently, these drugs usually have small volumes of distribution [56]. mAbs are protected from lysosomal degradation by the neonatal Fc receptor (FcRn), located in a wide variety of tissues throughout the body, which explains their long half-life and low clearance [57]. The main elimination pathway of mAbs is proteolytic degradation, in contrast to low molecular weight drugs, which are usually eliminated by renal or biliary excretion or by metabolic biotransformation [56]. Antigen mass, which refers to the total amount of antigen available for mAb binding, also influences the PK of mAbs. An increase in antigen mass has been related to an increase in mAb clearance. In other words, in the presence of high antigen amounts most of the mAb molecules form antigen-antibody complexes rather than remain as free antibodies. The elimination rate of these complexes is faster than that of the free mAbs, which explains the increased clearance [58].

PK of mAbs is highly variable. A clarifying example is the inter-individual variability in the clearance of some mAbs used in RA, quantified between 17 and 44% [43]. Multiple cofactors can act as sources of this variability (Figure 1), among which the development of immunogenicity stands out [42]. This eventually translates into variability in the concentration of the mAbs, which markedly influences the therapeutic response. Accordingly, a more extensive review of the PK of mAbs is available elsewhere [21]. The present review will focus on the PK of mAbs used in the treatment of NIU.

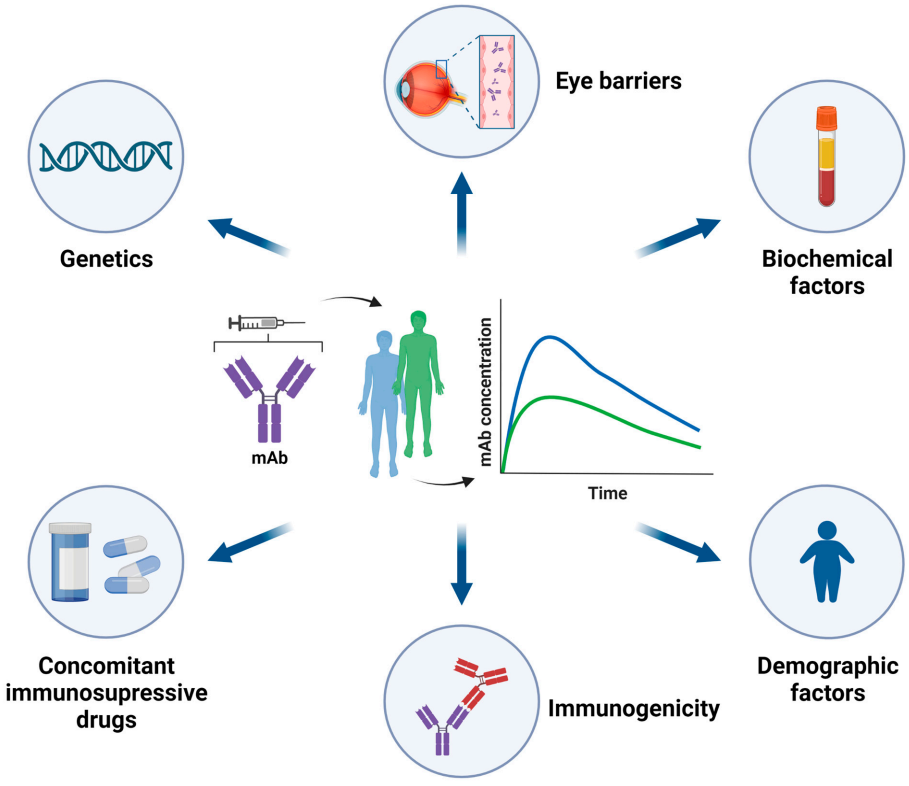

Figure 1. Factors that influence the pharmacokinetics of biologic agents in NIU. Created with biorender.com.

3.1.1. Demographic Factors

Body size and gender have an impact on the PK of mAbs and other biological drugs. An increase of clearance with body weight or body surface area has been reported for ADA [59–61] and IFX [62], but also for rituximab [63], etanercept [64], and golimumab [65]. Clearance of ADA and IFX is significantly higher in men than in women [59,60], although this may be explained by differences in body weight between gender. Despite the direct relationship between ADA and IFX clearance with body size, ADA dosage is not adjusted to weight in the adult population for the treatment of NIU, whereas IFX doses are weight-adjusted. This fact is linked to the subcutaneous administration of ADA by the patient, which limits dose adjustment by weight, in contrast to the extemporaneous preparation of IFX, enabling individualised weight adjustment at each administration. Moreover, although ADA clearance is increased in heavier patients, in VISUAL I and VISUAL II subgroup analysis by weight, ADA was favoured in all weight subgroups with standard dose [61].

3.1.2. Biochemical Factors

In inflammatory bowel disease (IBD), an inverse relationship between serum albumin levels and clearance of ADA [66] and IFX [67] was found. The reasoning behind this relationship is that low albumin levels may reflect decreased FcRn activity and thus increased clearance [43,57]. C-reactive protein (CRP) also influences the PK of IFX. Specifically, a direct correlation has been described between CRP levels and IFX clearance [68].

3.1.3. Immunogenicity of mAbs

Biological drugs are exogenous proteins, so they can induce an immune response. The development of ADAbs was more frequent in patients treated with IFX (ADAbs+: 25.3% (CI 19.5–32.2)) compared to those receiving other biological drugs (ADAbs+: <14%) according to a meta-analysis conducted in more than 14,000 patients with RA, IBD, and spondyloarthritis (SpA) [69]. The appearance of immunogenicity against the drug can lead to undesired issues such as loss of response, as well as the development of severe adverse infusion reactions [42,69]. Additionally, immunogenicity has a great impact on the PK of mAbs by increasing their clearance. In patients with NIU treated with ADA, an approximately 3-fold increase in clearance has been reported in those who developed ADAbs compared to those without ADAbs [61]. This finding is consistent with the decrease in serum levels of ADA and IFX [17,18,61,70] and with the worse clinical response observed in patients with NIU who present ADAbs [18,70] and is also in line with previously described findings in patients with immune-mediated rheumatic and gastrointestinal diseases [13,71–74].

3.1.4. Concomitant Immunosuppressive Therapy

Several studies have shown that the beneficial effect of anti-TNFα drugs is enhanced by concomitant treatment with immunosuppressants [75–80]. Although other studies have not observed any additional effect over monotherapy with biological agents [81,82], many clinical practice guidelines recommend the combined treatment of immunosuppressants and biologic drugs, in order to improve the pharmacokinetics of the biologic agent (increasing trough concentration and decreasing immunogenicity) [83]. This combined therapeutic strategy has proven superior to monotherapy treatment with ADA [75–77] and with other biological drugs [76,78–80] in patients with other immune-mediated pathologies. The superiority of combined therapy over monotherapy is reflected by significantly higher response rates or higher remission rates, improvements in inflammatory and disease activity parameters, less treatment failure or less damage to the affected tissues, and other clinical measures, without producing a higher frequency of adverse effects [75,78–80]. Potentiation of the therapeutic effect exerted by the co-administration of immunosuppressants is attributed to the higher concentration of the biological drug detected in blood compared to the absence of immunosuppressant treatment [77,84]. The association detected between co-treatment with immunosuppressants and decreased drug clearance likely explains these

findings. Specifically, the decrease in ADA clearance with concomitant immunosuppressant treatment has been estimated at 38.4% in patients with NIU [61]. It should be noted that co-treatment with immunosuppressants reduces the risk of developing immunogenicity, as well as its associated negative effects [73,77,85], which has a direct impact on the clearance of biological drugs, as already mentioned. Altogether, these findings indicate that concomitant treatment with immunosuppressants has a protective effect against the appearance of immunogenicity, which results in an increase in systemic drug levels and therefore a higher probability of clinical response.

3.2. Evidence Supporting TDM of Anti-TNFα in NIU

The inter-individual variability introduced by these and other factors in the PK parameters of anti-TNFα drugs has an impact on the individual exposure to the drug and therefore on the clinical response [21]. Evidence supporting TDM of drug levels and ADAbs of TNFα inhibitors as an effective strategy to optimize biological therapy and increase treatment response rates in immune-mediated inflammatory diseases is growing [12,14,17,73,74,86–88]. However, opposing findings have also been reported [89–91]. Given the shared similarities between these diseases and NIU regarding anti-TNFα therapy, it is reasonable to assume that TDM may also be beneficial in the management of patients with NIU. In fact, several publications support this idea, as shown in Table 2. Most of the data have been obtained from works published in the literature and have been completed with a report from the EMA.

Significantly higher trough ADA levels have been consistently reported in patients with NIU who responded to treatment compared to those non-responders. In addition, ADA trough levels have shown an inverse correlation with anti-ADA antibody levels [17,18,61,70,92]. Consequently, the presence of anti-ADA antibodies has been associated with treatment failure as assessed by a worse uveitis outcome and failure to achieve remission. This association was evaluated in more detail in two studies in which anti-ADA antibodies were classified as permanent if positive results were obtained on two or more time points during follow-up or transient if obtained on one single occasion [17,18]. In both studies, ADA trough levels were undetectable in patients with permanent anti-ADA antibodies, but not in those with transient antibodies, whose ADA trough levels did not differ from that in seronegative patients. Therefore, an inverse correlation of ADA trough levels and anti-ADA antibody levels was only observed when permanent antibodies were detected. Moreover, the presence of permanent antibodies was associated with a worse uveitis outcome and increased likelihood of non-response. In the study of Skrabl-Baumgartner et al. [17] 77.8% of non-responders developed permanent anti-ADA antibodies. In contrast, such an association was not observed in patients with transient antibodies. The authors concluded that the development of immunogenicity was the main reason for the loss of response, although other variables were not analysed. Although these results should be interpreted with caution due to the low number of patients with permanent anti-ADA antibodies analysed, which were 4 in Cordero-Coma et al. [18] and 7 in Skrabl-Baumgartner et al. [17], they derive from independent studies with different collections of patients and likely represent true rather than fortuitous findings.

Assuming this is the case, it would be of great importance to monitor ADAbs levels throughout treatment to differentiate between transient and permanent antibody positivity, since only the latter is associated with subtherapeutic drug levels and with a higher risk of treatment failure. Subsequent studies have confirmed the relationship between a worse clinical response with lower trough ADA levels, which in turn are frequently found in patients with ADAbs [17,61,70,92]. Despite most studies in NIU having shown a protective effect of immunomodulatory therapy against the development of immunogenicity [17,61,70] in accordance with previous reports in other pathologies, Cordero-Coma et al. [18] did not observe such an effect. In the work performed by Sugita et al. [93], monitoring of IFX levels showed a tendency towards higher IFX concentration in patients without uveitis flares (responders) and higher rates of treatment response in those with levels over 1 ug/mL

(Table 2), results that are in line to those observed with ADA treatment. Convincing evidence that TDM-guided optimization of ADA therapy in patients with NIU results in relevant clinical improvements has been recently reported by Sejournet et al. [92]. The authors showed that treatment adjustment in non-responders (increase in injections, dose, or change in treatment) according to TDM results, led to clinical improvement in 87% of cases, while in responders with supratherapeutic ADA levels, the reduction in the number of injections did not lead to relapse in 80% of cases (Table 2).

A question that remains to be answered is the potential utility and cost-effectiveness of proactive versus reactive TDM in the management of patients with NUI. Results obtained in IBD show greater clinical benefits and lower costs for proactive TDM compared to reactive TDM [86,94,95], probably because the proactive approach allows early intervention before a loss of response occurs and detection of immunogenicity early in treatment [96]. The potential benefits of proactive TDM of anti-TNF inhibitors in NIU need to be specifically evaluated in these patients. However, before reaching that point, some important issues remain to be clarified, such as the therapeutic range of anti-TNF drugs in NUI or the optimal frequency for monitoring [96].

Furthermore, there are reference documents on certain types of NIU that recommend using TDM to guide treatment with biologicals, such as the guide developed by the Single Hub and Access point for paediatric Rheumatology in Europe (SHARE) initiative. This document contains recommendations for the management of patients with JIA-associated uveitis [97], which indicates that increasing the dose or shortening the interval of drug administration can be considered in non-responders who do not have ADAbs but have low drug levels. Expert recommendations as well as an algorithm for the treatment of JIA-associated uveitis have also been published, which recommends adjusting treatment with ADA and IFX in non-responders or in cases of loss of response based on the results of monitoring levels of drug and ADAbs [98].

These studies show that anti-TNFα trough levels were higher in patients who responded to treatment compared to non-responders, in addition, demonstrate that ADAbs development was associated with worse NIU outcomes, and showing that treatment adjustment according to TDM results led to clinical improvement in non-responders [18,70,74,92,93]. All these data, together with expert recommendations and other reference documents, support the use of the biologic drug TDM in NIU. Despite this, the observational design of these studies added to the small size of the population studied, as well as the heterogeneity of the included NIU limits generalizations. Although we believe the data are in line with observations in other pathologies [12,14,86–88] and constitute a step forward in the difficult daily management of refractory NIU patients, they are insufficient to implement TDM in routine clinical practice.

Table 2. Relationship between anti-TNFα drug levels with ADAbs development, concomitant DMARDs, and response in NIU patients.

Authors [Ref.]	Type of Study	Treatment	Type NIU	No. Patients	Results
Cordero-Coma et al. 2016 [18]	Observational, prospective	ADA	Refractory uveitis	25 Naïve to biologics	- ADA levels: 0.6 μg/mL in non-responders vs. 9.5 μg/mL in responders ($p < 0.001$); 11.8 μg/mL in complete responders vs. 8.6 μg/mL in partial responders (p = ns). - Levels of permanent AAA (n = 4) inversely correlated with ADA levels ($p < 0.001$). - Presence of permanent AAA (n = 4) associated with worse clinical evolution of uveitis (p = 0.014).
Skrabl-Baumgartner et al. 2019 [17]	Observational, prospective	ADA	JIA related uveitis	20	- ADA trough levels inversely correlated with AAA levels in patients with permanent AAA ($p < 0.001$). - Transient AAA was not correlated with a reduction in the response. - Significantly lower use of immunosuppressants in patients with permanent AAA ($p < 0.05$).
Leinonen et al. 2017 [70]	Observational, retrospective	ADA	JIA related uveitis	31	- AAA levels $\geq$ 12 AU/mL were associated with a higher grade of uveitis ($p < 0.001$), lower ADA levels ($p <$ 0,001), and lack of concomitant MTX therapy (p = 0.043).
Sejournet et al. 2021 [92]	Observational, retrospective	ADA	JIA related uveitis	79	- Significantly higher ADA levels in responders than in non-responders (p = 0.0004). - In 24/31 cases of therapeutic adjustment in non-responders, an improvement was observed in 87% of cases.
EMA/501143/2016 [61]	Phase III studies (VISUAL I and VISUAL II)	ADA	NIU	249 (118 VISUAL I/131 VISUAL II)	- Responders had slightly higher ADA levels than non-responders after week 8. - Patients with AAA had lower ADA serum levels than those without AAA.
Sugita et al. 2011 [93]	Observational, prospective	IFX	RUBD	20	- IFX levels: 3.4 μg/mL in patients with uveitis flare (non-responders) vs. 7.3 μg/mL in patients without flare (responders), (p = ns). - Response to IFX (no development of uveitis flare): 14/16 (87.5%) with >1 μg/mL IFX vs. 1/4 (25%) with < 1 μg/mL IFX.

ADA: adalimumab, IFX: infliximab, JIA: Juvenile Idiopathic Arthritis, NIU: non-infectious uveitis, RUBD: refractory uveoretinitis of Behçet's disease, AAA: anti-adalimumab antibodies, ns: non-significant.

3.3. TDM-Based Strategies and Therapeutic trough Levels of Anti-TNFα in NIU

Overall, the aforementioned studies indicate that treatment with anti-TNFα drugs could be optimized with the implementation of TDM in the treatment decision-making process. However, it must be considered that the strength of the evidence obtained in patients with NIU is lower than in patients with other immune-mediated diseases in which the utility of TDM of biological drugs has been studied more thoroughly. The importance of optimizing biological treatment to a maximum is even more remarkable in patients with NIU who do not show a sufficient response or do not respond to ADA or IFX, in whom effective therapeutic options are even more scarce [34]. In order to prevent PNR or SNR to anti-TNFα drugs, different strategies can be adopted depending on TDM-based trough drug levels and the presence of immunogenicity. In non-responders or poor responders with low trough drug levels who do not develop immunogenicity, dose increase or interval shortening is recommended to increase drug concentration, but if immunogenicity is present, the addition of an immunomodulator or change to another anti-TNFα is a viable option. If the response to anti-TNFα is inadequate despite enough drug levels, a change to another biological drug with a different target is recommended instead [99]. Treatment should be continuously adjusted with subsequent drug concentration reappraisal until reaching the therapeutic target.

The minimum trough anti-TNFα levels that are associated with clinical response in NIU are currently unknown. The identification of a therapeutic range for anti-TNFα drugs is hampered by variability between studies and methodologies used to measure drug levels and ADAbs that generates incomparable data [100]. Prior to the implementation of TDM of ADA (or other biological drugs), a robust description of ADA PK and pharmacokinetic–pharmacodynamic (PK-PD) relationship should be obtained in patients with NIU [59], as an isolated measure of the systemic trough drug concentration does not fully explain drug exposure in a patient. The individual pharmacokinetic profile provides more accurate information on the actual systemic exposure of the drug instead. This profile is obtained by estimating the drug concentration curve (PK curve) as a function of time in each patient from measurements of the systemic trough drug levels from various samples obtained throughout the treatment. The relationship between the PK profile and the response is better known in other drugs such as antibiotics. In the case of beta-lactams, the longer their concentration (area under the curve that reflects the plasma levels of the antibiotic) is maintained above the minimum inhibitory concentration (MIC), the better response is achieved, and therefore they are considered time-dependent [101,102]. In other drugs such as aminoglycosides, in contrast, their effectiveness depends on reaching a sufficient level of maximum plasma concentration (Cmax) with respect to the MIC, and consequently, they are considered concentration-dependent [103]. In the case of anti-TNFα drugs, the influence of the PK profile on the response is unknown, i.e., it is not known whether they can be considered time- or concentration-dependent. Despite this, different dosage schedules are used in clinical practice regardless of the anti-TNFα drug to intensify treatment as discussed above [104]. However, some of these strategies may be ineffective, since the PK profile of the anti-TNF drugs determines the concentrations reached and the time they remain above a minimum value required for therapeutic action at the site of inflammation. This is especially important when the target of anti-TNFα drugs is in anatomical places that are difficult to access, such as the eye.

To our knowledge, an ADA concentration–effect relationship using PK–PD modelling of data from VISUAL I and VISUAL II phase III studies has been only described in one EMA report [61]. The mean steady-state serum ADA concentrations observed in the combined analysis of the two studies were 8–10 μg/mL, identical to that observed in patients with CD, UC, RA, and PS under the same initial and maintenance dose [61]. Strikingly, this concentration range was close to the lower level needed to prevent treatment failure based on estimated mean half maximal inhibitory concentration (IC50) values of 9.7 μg/mL (95% CI 5.5–17.4 μg/mL) and 6.4 μg/mL (95% CI 3.8–10.8 μg/mL) in VISUAL I and VISUAL II studies, respectively. Conversely, in patients with rheumatic diseases, the serum ADA

concentration range associated with clinical response is considerably lower, 2–8 μg/mL in RA 2.5–8.0 μg/mL in SpA, and 1–8 μg/mL in PsA [14,84,105]. The scenario is more complex in IBD, as reflected by the broader therapeutic thresholds (3.7- > 12 μg/mL) reported for ADA [14]. Reasonably, different optimal threshold concentrations of ADA are expected to emerge for NIU than for other immune-mediated diseases depending on disease severity, underlying inflammatory mechanisms, the target site of action, and other patient characteristics. These differences in systemic ADA levels associated with treatment response between pathologies are likely related to the heterogeneous bioavailability of ADA across different tissues.

Assuming that suboptimal steady-state ADA concentrations are achieved with the current standard doses prescribed in NIU (80 mg loading dose, followed by 40 mg every other week) [61], it is worth considering using a higher loading dose of ADA or increasing the dosing frequency to shift towards therapeutic concentrations. The former approach has already proven beneficial in Crohn's disease [19] and may also be beneficial in RA based on simulations [59]. In addition, simulations of a maintenance dose of 40 mg every week in NIU suggested that treatment failure could be reduced by up to 15% compared to the standard maintenance regimen [61]. Future studies should address whether the administration of intensified dose regiments in patients with NIU at the initiation of ADA therapy will lead to meaningful clinical benefits compared to the standard dose regimen without substantially increasing the frequency and severity of adverse events, thereby reducing the non-negligible rate of PNR and SNR. However, it should be noted that this intensification strategy may not be beneficial in some cases, for example when detectable levels of ADA are present at the time of treatment failure, indicating that molecules other than TNFα are acting as drivers of the inflammatory response. This reinforces the idea that TDM could help to individually optimise therapy to avoid unnecessary overtreatment and related adverse events and costs expenditures [86,87].

4. Implications of Ocular Drug PK

As already mentioned, target levels of anti-TNFα drugs are expected to vary among immune-mediated pathologies due, at least in part, to differences in PK parameters and biodistribution of biological drugs across ocular, intestine, and synovial tissues. The eye resides behind particularly strong blood–tissue barriers formed by endothelial-cell tight junctions and other structural specializations that selectively control the transport of molecules and have a great impact on the ocular bioavailability of the anti-TNFα drugs [10].

Anti-TNFα systemic administration: following a systemic administration, drugs can reach the choroid and then travel from the blood circulation to the ocular cavity. This process is controlled by two major barriers: the blood–aqueous barrier (BAB) and BRB, located at anterior and posterior segments respectively [106]. These barriers limit drug penetration from the blood into the eye, thus reducing its bioavailability in the target site of action [107]. Non-fenestrated endothelium of the iris vessels and the non-pigmented epithelium of the ciliary body are the main components of BAB. However, the barrier functionality of BAB is not complete, capillaries of the ciliary are fenestrated and leaky to macromolecules, allowing them to reach the aqueous humour (Figure 2). BRB consists of two types of cells, including retinal capillary endothelial and retinal pigment epithelium cells [108]. Consequently, after systemic administration of anti-TNFα, the intraocular concentration is lower than the blood concentration and therefore, patients with NIU may require elevated systemic anti-TNFα trough levels to increase intraocular bioavailability and reach a therapeutic effect.

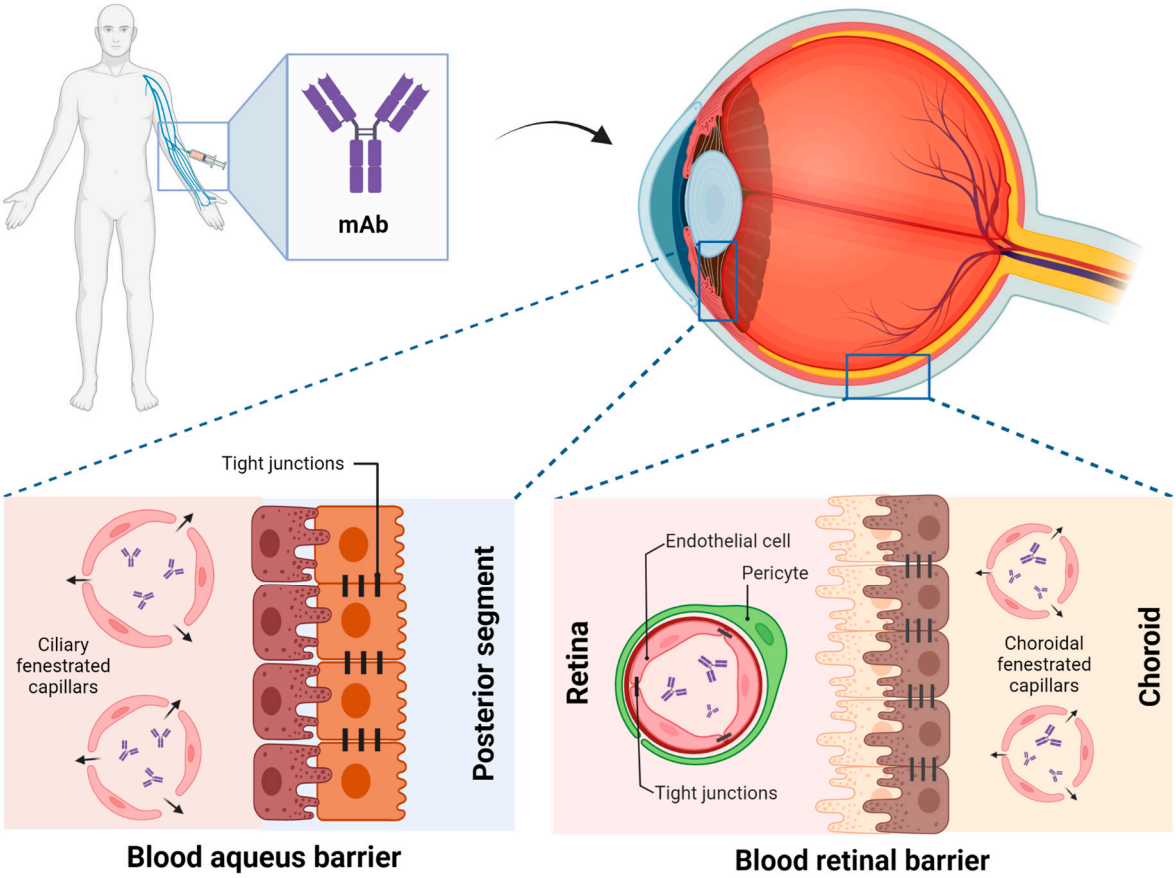

Figure 2. Ocular barriers encountered by biologic drugs to reach their ocular therapeutic target after systemic administration. Created by biorender.com.

Only a few preclinical studies have characterized the ocular PK of systemically administered mAbs, whereas ocular PK following intravitreal administration has been well described [109]. The ocular PK of rabbit Fab' fragments (rabFab, 48 kDa) after systemic administration differs from that of rabbit IgG (rabIgG, 150 kDa) [110]. In aqueous humour and vitreous humour, rabFab showed a fast absorption phase (Tmax 0.5 days) followed by a rapid decline. In contrast, rabIgG showed a relatively slow absorption (Tmax 1–4 days) followed by a slow decline. This is consistent with the accelerated clearance suffered by Fab proteins lacking an Fc fragment, whereas full-length antibodies and fusion proteins with Fc fragments have longer half-lives. Despite rabFab showing higher relative exposure between aqueous humour/serum and vitreous humour/serum and higher percent ocular partition compared to rabIgG, absolute exposure in ocular compartments was higher for rabIgG [110]. These differences may be relevant when estimating the ocular distribution of biological drugs with different structures such as ADA or IFX (IgG structure mAb) and certrolizumab (PEGylated fragment of a humanized mAb). Although informative, these parameters are derived from preclinical studies carried out under non-inflammatory conditions, and with antibodies whose pharmacological targets were not present in the animals studied. The presence of inflammation can alter the biodistribution coefficients at the tissue level. In fact, patients with uveitis experience an increase in vascular permeability due to the release of inflammatory mediators, such as TNFα, IL-6, IL-8, IL-17, or IL-23 [25,111,112]. This increase in vascular permeability has an impact on the integrity of the ocular barriers, which may play an important role in the penetration of high molecular weight drugs such as mAb in tissues with limited access like the eye [113]. Therefore, further preclinical studies are needed to accurately determine the ocular PK of mAbs under inflammatory conditions.

Anti-TNFα intravitreal injections: Following intravitreal administration, biologic drugs are distributed from the vitreous humour to the posterior (retina) and anterior (aqueous humour) segments of the eye and are eventually eliminated by disposal into the systemic circulation [114,115]. The factors that affect the drug distribution in vitreous humour are dictated by its diffusive and convective properties through the vitreous, and the possible drug interactions with the vitreous humour elements [107].

The intravitreal administration of anti-TNFα drugs such as IFX or ADA could be a potential resource to increase its bioavailability in ocular structures, thereby achieving intraocular therapeutic concentrations by minimizing its systemic absorption and toxicity, together with decreased ADAbs generation. Hence, this possibility has been raised for the treatment of inflammatory ocular diseases. Some studies that have evaluated the effect of the intravitreal administration of IFX (dose between 1 and 1.5 mg) in patients with Behçet's syndrome uveitis have observed an improvement in central macular thickness and visual acuity, without appreciating adverse events [116,117]. The reported improvement in clinical parameters places intravitreal IFX as a promising strategy in the treatment of ocular inflammation. However, previous results differ from recent findings of severe immunological reactions and a high percentage of therapeutic failure after intravitreal administration of IFX in patients with posterior uveitis associated with Behçet's disease [118]. Furthermore, evidence of an inflammatory reaction and a strong suggestion of retinotoxicity to intravitreal IFX were shown in a pilot safety study of patients with diabetic macular oedema or choroidal neovascularization secondary to age-related macular degeneration who failed conventional therapies [119].

ADA (and IFX in Japan) is the only biological drug with an approved indication for the treatment of NIU, but only under systemic administration for which its safety and efficacy have been widely demonstrated. Conversely, current evidence of the safety and efficacy of intravitreal administration of ADA is scarce and contradictory. Intravitreal ADA administration has been shown to effectively improve best-corrected visual acuity, control inflammation, limit uveitis flare and decrease cystoid macular oedema in six out of seven patients with Behçet and idiopathic uveitis. One patient failed treatment but was able to regain baseline vision with no permanent effect [120]. A retrospective study evaluated the usefulness of intravitreal ADA as a rescue treatment in flares of patients receiving chronic treatment with systemic ADA. Four patients with Behçet's disease panuveitis maintained on systemic ADA therapy prior to the panuveitis breakthrough attack were included. Of the 13 attacks documented in seven eyes, three resolved with one injection and 10 needed more than one monthly injection for resolution. This work shows that intravitreal ADA is of potential utility as a rescue therapy in patients with NIU on systemic ADA therapy that requires tighter control of the inflammation [121]. On the contrary, intravitreal ADA (monthly injections for three months) showed no efficacy in improving visual acuity or reducing central retinal thickness in eight patients with chronic uveitic macular oedema who had failed steroid treatment, although the intervention was deemed safe [122]. Evidence from preclinical studies is also inconsistent. Some studies in rabbits have reported no ocular toxicity for doses up to 5 mg of intravitreal ADA [123,124], whereas another study has reported retinal necrosis at doses of 1 mg [125]. Despite these discrepancies, a promising result of the potential utility of intravitreal administration of ADA as a strategy to increase ocular drug bioavailability has been recently obtained by García-Otero et al. [126]. These authors evaluated the pharmacokinetic profile and the biodistribution of the intravitreal administration of ^{89}Zr-adalimumab in a uveitis rat model using PET imaging and showed that ADA remained about twice as long in the vitreous of diseased rats compared to unaffected ones and that its ocular permanence was around three times higher in rats with uveitis.

Further research is required to convincingly establish the efficacy and safety of intravitreal administration of ADA before considering its approval for the treatment of ocular inflammatory diseases such as NIU. The main advantage of intravitreal administration is that ocular exposure to anti-TNFα drugs is increased using lower doses than those used

in systemic administration while avoiding its possible adverse effects. For instance, the systemic administration of anti-TNFα presents certain risks such as the reactivation of latent tuberculosis and in the case of IFX, it is contraindicated in patients suffering from congestive heart failure [127]. Nevertheless, intravitreal administration also has some drawbacks, mainly the invasiveness of the procedure and its possible complications.

5. Pharmacogenetics (PG) of Anti-TNFα in NIU

Genetic variability is one of the factors that explain the inter-individual variability in the response to treatments or in the appearance of toxicities. Unfortunately, a major limitation of PG studies on drugs used in the management of ocular inflammatory diseases is the lack of consistency due to heterogeneous study designs, different outcome measures, and small simple sizes, which possibly result in false-positive associations [128]. For this reason, PG studies focused on anti-TNFα drugs for the treatment of NIU have not been conducted. However, the treatment of NIU is very similar to that of other immune-mediated pathologies such as RA or IBD, where the influence of genetic polymorphisms on the response to biological drugs such as anti-TNFα has been evaluated [128]. Table 3 shows some of the genetic associations identified with the response to anti-TNFα agents in immune-mediated diseases that could shed light on the influence of genetics on the response to treatment in NIU. More extensive evidence of gene polymorphisms that may act as predictors of response to anti-TNFα biologic drugs in related diseases can be found in the scientific literature.

5.1. Candidate Gene Association Studies

Candidate gene association studies have described different polymorphisms that can act as predictors of response to therapy with anti-TNFα agents. These polymorphisms are located mainly in genes involved in the activation of NFkB through the metabolic pathway of Toll-like receptors (TLR), genes that regulate TNFα signalling, and cytokines regulated by NFkB and involved in the metabolic pathway of helper T cells [129]. In a meta-analysis conducted by Bek et al. [130] of 47 studies that analysed the genetic differences between patients with RA responders and non-responders to anti-TNFα therapy, six polymorphisms of six different genes were found to be involved in the response: CHUK, PTPRC, TRAF1/C5, NFKBIB, FCGR2A, and IRAK3. These were genes predominantly involved in the adaptive response, unlike others located in IBD, such as those associated with TLR, which are more involved in the innate immune response. Bank et al. [131] studied 738 patients with IBD, including CD, UC, or both, from a Danish cohort and identified 19 functional polymorphisms in 14 genes associated with response to treatment with anti-TNFα agents (TLR2, TLR4, TLR9, LY96, CD14, MAP3K14, TNFA, TNFRSF1A, TNFAIP3, IL1B, IL1RN, IL6, IL17A, and IFNG) that were implicated in the inflammatory response mediated by NFκB. These associations allowed for distinguishing not only which patients would benefit from treatment with anti-TNFα agents, but also to identify those who would benefit from treatment with an agent whose target was another cytokine such as IL-1b, IL-6 or IFN-γ, or a combination of several agents [131]. Notably, these findings have recently been replicated and extended by the same authors in a different cohort of 1045 Danish patients with IBD [132].

The possibility of identifying patients at risk of developing immunogenicity against anti-TNFα drugs, and therefore of presenting a worse response to treatment, may guide the clinician's choice of treatment towards the use of concomitant immunosuppressants associated with a lower incidence of ADAbs or the use of biological drugs with other targets. A positive association with the risk of developing ADAbs has been described for a polymorphism of the *CXCL12* gene, which is consistent with the well-known role of this chemokine in antibody affinity maturation and plasma cell survival required for antibody development. This genetic association was confirmed at the protein level. Elevated serum CXCL12 levels (dichotomized by the median value) were associated with a 2-fold increased risk of immunogenicity, although this analysis was restricted to RA patients treated with

4 different anti-TNFα agents [133]. Another factor that appears to be closely related to the development of immunogenicity is the level of IL-10. In patients with RA, the formation of ADAbs against ADA was associated with certain genetic polymorphisms and haplotypes of the promoter region of the *IL-10* gene [134]. Unfortunately, it was not specified how the associated polymorphisms/haplotypes influence IL-10 production. In another study in which IL-10 levels were measured in 17 patients with various immune-mediated diseases under IFX treatment, the absence or low IL-10 production and low IL-10/IFN-γ ratio were associated with an increased formation of ADAbs to IFX [135]. However, certain caution should be maintained toward these results due to the small number of patients and the heterogeneity of the diseases studied.

5.2. HLA Complex

A promising marker for detecting patients at higher risk of developing ADAbs, the *HLA-DQA1*05* allele, has recently been identified. Sazonovs et al. [136] found that the presence of one or two copies of the *HLA-DQA1*05* alleles conferred a 2-fold increased risk of developing immunogenicity to anti-TNFα therapy in patients with IBD, regardless of the type of anti-TNFα (ADA or IFX) or concomitant treatment with immunomodulators. This finding was replicated and extended in a multicohort prospective study of patients with multiple sclerosis (MS), RA, and IBD conducted by the European ABIRISK (Anti-Biopharmaceutical Immunization: prediction and analysis of clinical relevance to minimize the RISK) consortium [133]. This work not only confirmed the doubled risk of developing ADAbs with the presence of *HLA-DQA1*05* alleles, but also observed a 4-fold increased risk of ADAbs for patients homozygous for these alleles. Among the clinical factors evaluated, concomitant immunosuppressant treatment reduced the risk of immunogenicity, in contrast to findings from the previous study, whereas tobacco consumption showed a positive association with ADAbs development.

It has been suggested that ADAbs development against biological drugs may share common immunogenetic pathways across diseases in view of the similarities shared in dynamics of antibody production and rate of immunogenicity [133]. Since immunogenicity has a great impact on anti-TNFα drug levels, PG studies in other immune-mediated diseases could provide clues as to which genetic factors contribute to the development of ADAbs in NIU, as well as to reveal genetic factors that contribute to other pathways involved in the response to anti-TNFα treatment in these patients. Stronger evidence of the influence of PG on the response to anti-TNFα treatment in NIU can be obtained from PG studies specifically conducted in patients with this pathology. Furthermore, considering all the data shown about PG in anti-TNFα therapy, and the numerous genes involved in their response, the implementation of a genomic array encompassing all the genes involved, analogous to some used in cancer therapy [137], could be of help in interpreting PG results.

Table 3. Association between SNPs and treatment response to anti-TNFα drugs in immune-related diseases other than NIU.

Authors [Ref.]	Gene	SNP (Allele)	Effect of the SNP	Disease	Proposed Gene/Protein Function
Bek et al. 2017 [130]	*CHUK*	rs11591741 (C)	non-response	RA	Component of a cytokine-activated protein complex that inhibits NFκB.
	PTPRC	rs10919563 (A)	non-response	RA	Suppresses JAK kinases, functions as a regulator of cytokine receptor signalling.
	TRAF1/C5	rs3761847 (G)	non-response	RA	Required for TNFα-mediated activation of MAPK8/JNK and NFκB. Mediates the anti-apoptotic signals from TNF receptors.
	NFKBIB	rs9403 (C)	non-response	RA	Inhibits NFκB by complexing with and trapping it in the cytoplasm.
	FCGR2A	rs1801274 (G)	non-response	RA	Involved in the process of phagocytosis and clearing of immune complexes.
	IRAK3	rs11541076 (T)	non-response	RA	Negative regulator of Toll-like receptor signalling.
Bartelds et al. 2009 [134]	*IL10*	rs6703630, rs1800896, rs1800871 (AGC haplotype)	non-response [a]	RA	Pleiotropic cytokine with a role in immunoregulation and inflammation, enhances B cell survival, proliferation, and antibody production, can block NFκB activity, and is involved in the regulation of the JAK-STAT signalling pathway
		rs6703630, rs1800896, rs1800871 (GAT haplotype)	response [a]		
Bank et al. 2014 [131]	*TLR2*	rs4696480 (T)	non-response	Only UC	Activates inflammation through the canonical NFκB pathway.
		rs11938228 (A) [b]	non-response	IBD	
		rs1816702 (T)	response	Only CD	
		rs3804099 (C)	response	IBD	
	TLR4	rs1554973 (C) [b]	non-response	IBD	Activates inflammation through the canonical or noncanonical NFκB pathway.
		rs5030728 (A) [b]	response		
	TLR9	rs352139 (A)	non-response	IBD	Activates inflammation through the canonical NFκB pathway.
		rs187084 (C)	response		
	CD14	rs2569190 (A)	non-response	Only UC	Binds LPS and transport it to TLR4
	TNFA	rs361525 (A)	non-response	IBD	Pro-inflammatory cytokine activated by NFκB1.
	TNFAIP3	rs6927172 (G)	non-response	IBD	Inhibits NFκB activation and TNFα-mediated apoptosis.
	IL1RN	rs4251961 (C) [b]	non-response	Only UC	Inhibits IL-1β signalling.
	IL17A	rs2275913 (A)	non-response	IBD	Pro-inflammatory cytokine activated by NFκB1, induces production of IL-1β, IL-6, and TNFα.

Table 3. *Cont.*

Authors [Ref.]	Gene	SNP (Allele)	Effect of the SNP	Disease	Proposed Gene/Protein Function
	LY96	rs11465996 (G)	response	IBD	Binds to TLR2 or TLR4 and is required for their activation to LPS stimuli
	MAP3K14	rs7222094 (C)	response	IBD	Central kinase in the noncanonical NFκB pathway
	TNFRSF1A	rs4149570 (T) [b]	response	IBD	Binds TNFα and initiates a kinase cascade.
	IL1B	rs4848306 (A)	response	IBD	Pro-inflammatory cytokine activated by NFκB1.
	IL6	rs10499563 (C)	response	IBD	Pro- and anti-inflammatory cytokine activated by NFκB1.
	IFNG	rs2430561 (A)	response	IBD	Pro- and anti-inflammatory cytokine activated by NFκB1.
Bank et al. 2019 [132]	*NLRP3*	rs4612666 (T)	non-response	IBD	Member of the NLRP3 inflammasome complex, upstream activator of NFκB signalling.
	IL18	rs187238 (C)	response	Only CD	Proinflammatory cytokine of the IL-1 family, capable of stimulating IFNγ production.
		rs1946518 (T)	response	IBD	
	JAK2	rs12343867 (C)	response	IBD	Plays a central role in cytokine and growth factor signalling, downstream target of IL6
	NFKBIA	rs696 (A)	response	IBD	Complexes with REL dimers inhibit NFκB/REL complexes.
Hässler et al. 2020 [133]	*CXCL12*	rs10508884 (T)	non-response [a]	Several diseases	Plays a role in embryogenesis, immune surveillance, antibody affinity maturation, inflammation response, tissue homeostasis, and tumour growth and metastasis.
	HLA-DQ	*HLA-DQA1*05*	non-response [a]		Plays a central role in the immune system by presenting peptides from extracellular proteins.
Sazonovs et al. 2020 [136]	*HLA-DQ*	*HLA-DQA1*05*	non-response [a]	CD	Plays a central role in the immune system by presenting peptides from extracellular proteins.

[a] The genetic association with the response was indirectly ascertained through the association of the SNP with the development of ADAbs, which has been related to a worse response to anti-TNFα agents. Therefore, response represents that the SNP is negatively associated with ADAbs development, whereas non-response represents a positive association of the SNP with ADAbs development. [b] Association replicated in Bank et al. [132]. SNP: Single Nucleotide Polymorphism, RA: rheumatoid arthritis, UC: ulcerative colitis, IBD: intestinal bowel disease, CD: Crohn's disease.

6. Conclusions

The implementation of TDM of biological drugs in the field of NIU could help to optimize treatments and obtain better response rates, as already shown in other immune-mediated diseases. The clinical benefits of effective anti-TNFα treatment in NIU include better control of ocular inflammation, decrease in the number of flares, reduction in visual loss, and improvement in the quality of life for patients. However, anti-TNFα treatment can also result in adverse events, especially when supratherapeutic levels are present. Infections, congestive heart failure, demyelinating diseases, drug-induced systemic lupus erythematosus or induction of psoriasis are some of the potential adverse events associated with anti-TNFα therapy. Although the measurement of anti-TNFα and ADAbs levels is not routinely used in clinical practice in NIU, it has been shown to be useful in a series of non-randomized observational studies in patients with refractory NIU. This highlights the critical need for clinical studies to convincingly establish the usefulness and cost-effectiveness of TDM-based strategies, over empirical dose escalation strategies to guide treatment adjustment with biological drugs in the treatment of NIU and define a specific therapeutic range. Although the influence of genetic polymorphisms on the response to biological drugs has been barely explored in NIU to date, PG may be an important aspect in optimizing and predicting response to biological treatments and influencing TDM, as has been evidenced in other immune-mediated diseases. At the preclinical level, studies should further address the degree of distribution of therapeutic proteins in the eye under inflammatory conditions, in order to improve knowledge about the biopharmaceutical behaviour of mAbs in this disease.

Author Contributions: Conceptualization, M.B.-I., L.R.-M. and C.A.R.-F.; methodology, M.B.-I., L.R.-M. and C.A.R.-F.; investigation, J.G.-L., M.G.-B. and B.d.D.; writing—original draft preparation, M.B.-I., L.R.-M. and C.A.R.-F.; writing—review and editing, J.G.-L., M.G.-B. and B.d.D.; supervision, C.M.-G., L.R.-R. and A.F.-F.; project administration, C.M.-G., L.R.-R. and A.F.-F.; funding acquisition, C.M-G., L.R.-R. and A.F.-F. All authors have read and agreed to the published version of the manuscript.

Funding: C.M.-G. and A.F.-F. are grateful to ISCIII for financing in the form of the JR18/00014 and JR20/00026. This work was partially supported by Instituto de Salud Carlos III (ISCIII)/ (PI20/00719, ICI19/00020) cofounded by European Union (EU) and by Xunta de Galicia (IN607D2021/01).

Institutional Review Board Statement: Not applicable.

Informed Consent Statement: Not applicable.

Data Availability Statement: No new data were created or analyzed in this study. Data sharing is not applicable to this article.

Acknowledgments: C.M.-G. and A.F.-F. acknowledge the support of Instituto de Salud Carlos III (ISCIII) by research grants (JR20/00026 and JR18/00014).

Conflicts of Interest: The authors declare no conflict of interest.

References

1. Shahab, M.A.; Mir, T.A.; Zafar, S. Optimising Drug Therapy for Non-Infectious Uveitis. *Int. Ophthalmol.* **2019**, *39*, 1633–1650. [CrossRef]
2. Jabs, D.A. Immunosuppression for the Uveitides. *Ophthalmology* **2018**, *125*, 193–202. [CrossRef] [PubMed]
3. Leclercq, M.; Desbois, A.-C.; Domont, F.; Maalouf, G.; Touhami, S.; Cacoub, P.; Bodaghi, B.; Saadoun, D. Biotherapies in Uveitis. *J. Clin. Med.* **2020**, *9*, 3599. [CrossRef] [PubMed]
4. Thomas, A.S. Biologics for the Treatment of Noninfectious Uveitis: Current Concepts and Emerging Therapeutics. *Curr. Opin. Ophthalmol.* **2019**, *30*, 138–150. [CrossRef] [PubMed]

5. Ozguler, Y.; Leccese, P.; Christensen, R.; Esatoglu, S.N.; Bang, D.; Bodaghi, B.; Çelik, A.F.; Fortune, F.; Gaudric, J.; Gul, A.; et al. Management of Major Organ Involvement of Behçet's Syndrome: A Systematic Review for Update of the EULAR Recommendations. *Rheumatology* **2018**, *57*, 2200–2212. [CrossRef]
6. Nguyen, Q.D.; Merrill, P.T.; Jaffe, G.J.; Dick, A.D.; Kurup, S.K.; Sheppard, J.; Schlaen, A.; Pavesio, C.; Cimino, L.; Van Calster, J.; et al. Adalimumab for Prevention of Uveitic Flare in Patients with Inactive Non-Infectious Uveitis Controlled by Corticosteroids (VISUAL II): A Multicentre, Double-Masked, Randomised, Placebo-Controlled Phase 3 Trial. *Lancet* **2016**, *388*, 1183–1192. [CrossRef]
7. Jaffe, G.J.; Dick, A.D.; Brézin, A.P.; Nguyen, Q.D.; Thorne, J.E.; Kestelyn, P.; Barisani-Asenbauer, T.; Franco, P.; Heiligenhaus, A.; Scales, D.; et al. Adalimumab in Patients with Active Noninfectious Uveitis. *N. Engl. J. Med.* **2016**, *375*, 932–943. [CrossRef]
8. Llorenç, V.; Cordero-Coma, M.; Blanco-Esteban, A.; Heras-Mulero, H.; Losada-Castillo, M.-J.; Jovani-Casano, V.; Valls-Pascual, E.; Jodar-Marquez, M.; García-Aparicio, Á.; Fonollosa, A.; et al. Drug Retention Rate and Causes of Discontinuation of Adalimumab in Uveitis: Real-World Data from the Biotherapies in Uveitis (BioÚvea) Study Group. *Ophthalmology* **2020**, *127*, 814–825. [CrossRef]
9. Rodríguez-Fernández, K.; Mangas-Sanjuán, V.; Merino-Sanjuán, M.; Martorell-Calatayud, A.; Mateu-Puchades, A.; Climente-Martí, M.; Gras-Colomer, E. Impact of Pharmacokinetic and Pharmacodynamic Properties of Monoclonal Antibodies in the Management of Psoriasis. *Pharmaceutics* **2022**, *14*, 654. [CrossRef]
10. Barar, J.; Javadzadeh, A.R.; Omidi, Y. Ocular Novel Drug Delivery: Impacts of Membranes and Barriers. *Expert Opin. Drug Deliv.* **2008**, *5*, 567–581. [CrossRef]
11. An, G. Concept of Pharmacologic Target-Mediated Drug Disposition in Large-Molecule and Small-Molecule Compounds. *J. Clin. Pharmacol.* **2020**, *60*, 149–163. [CrossRef] [PubMed]
12. Papamichael, K.; Juncadella, A.; Wong, D.; Rakowsky, S.; Sattler, L.A.; Campbell, J.P.; Vaughn, B.P.; Cheifetz, A.S. Proactive Therapeutic Drug Monitoring of Adalimumab Is Associated with Better Long-Term Outcomes Compared with Standard of Care in Patients with Inflammatory Bowel Disease. *J. Crohns Colitis* **2019**, *13*, 976–981. [CrossRef]
13. Jani, M.; Chinoy, H.; Warren, R.B.; Griffiths, C.E.M.; Plant, D.; Fu, B.; Morgan, A.W.; Wilson, A.G.; Isaacs, J.D.; Hyrich, K.; et al. Clinical Utility of Random Anti–Tumor Necrosis Factor Drug–Level Testing and Measurement of Antidrug Antibodies on the Long-Term Treatment Response in Rheumatoid Arthritis. *Arthritis Rheumatol.* **2015**, *67*, 2011–2019. [CrossRef]
14. Papamichael, K.; Vogelzang, E.H.; Lambert, J.; Wolbink, G.; Cheifetz, A.S. Therapeutic Drug Monitoring with Biologic Agents in Immune Mediated Inflammatory Diseases. *Expert Rev. Clin. Immunol.* **2019**, *15*, 837–848. [CrossRef] [PubMed]
15. Meroni, P.L.; Valentini, G.; Ayala, F.; Cattaneo, A.; Valesini, G. New Strategies to Address the Pharmacodynamics and Pharmacokinetics of Tumor Necrosis Factor (TNF) Inhibitors: A Systematic Analysis. *Autoimmun. Rev.* **2015**, *14*, 812–829. [CrossRef] [PubMed]
16. Gorovits, B.; Baltrukonis, D.J.; Bhattacharya, I.; Birchler, M.A.; Finco, D.; Sikkema, D.; Vincent, M.S.; Lula, S.; Marshall, L.; Hickling, T.P. Immunoassay Methods Used in Clinical Studies for the Detection of Anti-Drug Antibodies to Adalimumab and Infliximab. *Clin. Exp. Immunol.* **2018**, *192*, 348–365. [CrossRef] [PubMed]
17. Skrabl-Baumgartner, A.; Seidel, G.; Langner-Wegscheider, B.; Schlagenhauf, A.; Jahnel, J. Drug Monitoring in Long-Term Treatment with Adalimumab for Juvenile Idiopathic Arthritis-Associated Uveitis. *Arch. Dis. Child.* **2019**, *104*, 246–250. [CrossRef]
18. Cordero-Coma, M.; Calleja-Antolín, S.; Garzo-García, I.; Nuñez-Garnés, A.M.; Álvarez-Castro, C.; Franco-Benito, M.; Ruiz de Morales, J.G. Adalimumab for Treatment of Noninfectious Uveitis. *Ophthalmology* **2016**, *123*, 2618–2625. [CrossRef]
19. Hanauer, S.B.; Sandborn, W.J.; Rutgeerts, P.; Fedorak, R.N.; Lukas, M.; MacIntosh, D.; Panaccione, R.; Wolf, D.; Pollack, P. Human Anti-Tumor Necrosis Factor Monoclonal Antibody (Adalimumab) in Crohn's Disease: The CLASSIC-I Trial. *Gastroenterology* **2006**, *130*, 323–333, quiz 591. [CrossRef]
20. Bartelds, G.M.; Wijbrandts, C.A.; Nurmohamed, M.T.; Stapel, S.; Lems, W.F.; Aarden, L.; Dijkmans, B.A.C.; Tak, P.P.; Wolbink, G.J. Clinical Response to Adalimumab: Relationship to Anti-Adalimumab Antibodies and Serum Adalimumab Concentrations in Rheumatoid Arthritis. *Ann. Rheum. Dis.* **2007**, *66*, 921–926. [CrossRef] [PubMed]
21. Thomas, V.A.; Balthasar, J.P. Understanding Inter-Individual Variability in Monoclonal Antibody Disposition. *Antibodies Basel Switz.* **2019**, *8*, 56. [CrossRef]
22. Escudero-Ortiz, V.; Domínguez-Leñero, V.; Catalán-Latorre, A.; Rebollo-Liceaga, J.; Sureda, M. Relevance of Therapeutic Drug Monitoring of Tyrosine Kinase Inhibitors in Routine Clinical Practice: A Pilot Study. *Pharmaceutics* **2022**, *14*, 1216. [CrossRef]
23. Egwuagu, C.E.; Alhakeem, S.A.; Mbanefo, E.C. Uveitis: Molecular Pathogenesis and Emerging Therapies. *Front. Immunol.* **2021**, *12*, 623725. [CrossRef]
24. Gangaputra, S.S.; Newcomb, C.W.; Joffe, M.M.; Dreger, K.; Begum, H.; Artornsombudh, P.; Pujari, S.S.; Daniel, E.; Sen, H.N.; Suhler, E.B.; et al. Comparison Between Methotrexate and Mycophenolate Mofetil Monotherapy for the Control of Noninfectious Ocular Inflammatory Diseases. *Am. J. Ophthalmol.* **2019**, *208*, 68–75. [CrossRef] [PubMed]
25. Errera, M.-H.; Pratas, A.; Fisson, S.; Manicom, T.; Boubaya, M.; Sedira, N.; Héron, E.; Merabet, L.; Kobal, A.; Levy, V.; et al. Cytokines, Chemokines and Growth Factors Profile in Human Aqueous Humor in Idiopathic Uveitis. *PLoS ONE* **2022**, *17*, e0254972. [CrossRef] [PubMed]
26. Ramanan, A.V.; Dick, A.D.; Jones, A.P.; Hughes, D.A.; McKay, A.; Rosala-Hallas, A.; Williamson, P.R.; Hardwick, B.; Hickey, H.; Rainford, N.; et al. Adalimumab in Combination with Methotrexate for Refractory Uveitis Associated with Juvenile Idiopathic Arthritis: A RCT. *Health Technol. Assess.* **2019**, *23*, 1–140. [CrossRef] [PubMed]

27. Cordero-Coma, M.; Sobrin, L. Anti–Tumor Necrosis Factor-α Therapy in Uveitis. *Surv. Ophthalmol.* **2015**, *60*, 575–589. [CrossRef]
28. Diaz-Llopis, M.; García-Delpech, S.; Salom, D.; Udaondo, P.; Hernández-Garfella, M.; Bosch-Morell, F.; Quijada, A.; Romero, F.J. Adalimumab Therapy for Refractory Uveitis: A Pilot Study. *J. Ocul. Pharmacol. Ther.* **2008**, *24*, 351–361. [CrossRef] [PubMed]
29. Suhler, E.B.; Jaffe, G.J.; Fortin, E.; Lim, L.L.; Merrill, P.T.; Dick, A.D.; Brezin, A.P.; Nguyen, Q.D.; Thorne, J.E.; Van Calster, J.; et al. Long-Term Safety and Efficacy of Adalimumab in Patients with Noninfectious Intermediate Uveitis, Posterior Uveitis, or Panuveitis. *Ophthalmology* **2021**, *128*, 899–909. [CrossRef]
30. Li, B.; Li, H.; Zhang, L.; Zheng, Y. Efficacy and Safety of Adalimumab in Noninfectious Uveitis: A Systematic Review and Meta-Analysis of Randomized Controlled Trials. *Front. Pharmacol.* **2021**, *12*, 673984. [CrossRef]
31. Rivas, A.B.; Lopez-Picado, A.; Calamia, V.; Carreño, E.; Cocho, L.; Cordero-Coma, M.; Fonollosa, A.; Francisco Hernandez, F.M.; Garcia-Aparicio, A.; Garcia-Gonzalez, J.; et al. Efficacy, Safety and Cost-Effectiveness of Methotrexate, Adalimumab or Their Combination in Non-Infectious Non-Anterior Uveitis: A Protocol for a Multicentre, Randomised, Parallel Three Arms, Active-Controlled, Phase III Open Label with Blinded Outcome Assessment Study. *BMJ Open* **2022**, *12*, e051378. [CrossRef]
32. Sfikakis, P.P.; Theodossiadis, P.G.; Katsiari, C.G.; Kaklamanis, P.; Markomichelakis, N.N. Effect of Infliximab on Sight-Threatening Panuveitis in Behçet's Disease. *Lancet Lond. Engl.* **2001**, *358*, 295–296. [CrossRef]
33. Ardoin, S.P.; Kredich, D.; Rabinovich, E.; Schanberg, L.E.; Jaffe, G.J. Infliximab to Treat Chronic Noninfectious Uveitis in Children: Retrospective Case Series with Long-Term Follow-Up. *Am. J. Ophthalmol.* **2007**, *144*, 844–849.e1. [CrossRef]
34. Markomichelakis, N.; Delicha, E.; Masselos, S.; Fragiadaki, K.; Kaklamanis, P.; Sfikakis, P.P. A Single Infliximab Infusion vs Corticosteroids for Acute Panuveitis Attacks in Behcet's Disease: A Comparative 4-Week Study. *Rheumatology* **2011**, *50*, 593–597. [CrossRef] [PubMed]
35. Ohno, S.; Umebayashi, I.; Matsukawa, M.; Goto, T.; Yano, T. Safety and Efficacy of Infliximab in the Treatment of Refractory Uveoretinitis in Behçet's Disease: A Large-Scale, Long-Term Postmarketing Surveillance in Japan. *Arthritis Res. Ther.* **2019**, *21*, 2. [CrossRef] [PubMed]
36. Levy-Clarke, G.; Jabs, D.A.; Read, R.W.; Rosenbaum, J.T.; Vitale, A.; Van Gelder, R.N. Expert Panel Recommendations for the Use of Anti–Tumor Necrosis Factor Biologic Agents in Patients with Ocular Inflammatory Disorders. *Ophthalmology* **2014**, *121*, 785–796.e3. [CrossRef]
37. Tambralli, A.; Beukelman, T.; Weiser, P.; Atkinson, T.P.; Cron, R.Q.; Stoll, M.L. High Doses of Infliximab in the Management of Juvenile Idiopathic Arthritis. *J. Rheumatol.* **2013**, *40*, 1749–1755. [CrossRef]
38. Hasegawa, E.; Takeda, A.; Yawata, N.; Sonoda, K.-H. The Effectiveness of Adalimumab Treatment for Non-Infectious Uveitis. *Immunol. Med.* **2019**, *42*, 79–83. [CrossRef]
39. Lim, L.L.; Fraunfelder, F.W.; Rosenbaum, J.T. Do Tumor Necrosis Factor Inhibitors Cause Uveitis? A Registry-Based Study. *Arthritis Rheum.* **2007**, *56*, 3248–3252. [CrossRef] [PubMed]
40. Miserocchi, E.; Modorati, G.; Pontikaki, I.; Meroni, P.L.; Gerloni, V. Long-Term Treatment with Golimumab for Severe Uveitis. *Ocul. Immunol. Inflamm.* **2014**, *22*, 90–95. [CrossRef]
41. Calvo-Río, V.; Blanco, R.; Santos-Gómez, M.; Rubio-Romero, E.; Cordero-Coma, M.; Gallego-Flores, A.; Veroz, R.; Torre, I.; Hernández, F.F.; Atanes, A.; et al. Golimumab in Refractory Uveitis Related to Spondyloarthritis. Multicenter Study of 15 Patients. *Semin. Arthritis Rheum.* **2016**, *46*, 95–101. [CrossRef]
42. Atiqi, S.; Hooijberg, F.; Loeff, F.C.; Rispens, T.; Wolbink, G.J. Immunogenicity of TNF-Inhibitors. *Front. Immunol.* **2020**, *11*, 312. [CrossRef] [PubMed]
43. Ternant, D.; Bejan-Angoulvant, T.; Passot, C.; Mulleman, D.; Paintaud, G. Clinical Pharmacokinetics and Pharmacodynamics of Monoclonal Antibodies Approved to Treat Rheumatoid Arthritis. *Clin. Pharmacokinet.* **2015**, *54*, 1107–1123. [CrossRef] [PubMed]
44. Prieto-Peña, D.; Calderón-Goercke, M.; Adán, A.; Chamorro-López, L.; Maíz-Alonso, O.; De Dios-Jiménez Aberásturi, J.R.; Veroz, R.; Blanco, S.; Martín-Santos, J.M.; Navarro, F.; et al. Efficacy and Safety of Certolizumab Pegol in Pregnant Women with Uveitis. Recommendations on the Management with Immunosuppressive and Biologic Therapies in Uveitis during Pregnancy. *Clin. Exp. Rheumatol.* **2021**, *39*, 105–114. [CrossRef] [PubMed]
45. Sepah, Y.J.; Sadiq, M.A.; Chu, D.S.; Dacey, M.; Gallemore, R.; Dayani, P.; Hanout, M.; Hassan, M.; Afridi, R.; Agarwal, A.; et al. Primary (Month-6) Outcomes of the STOP-Uveitis Study: Evaluating the Safety, Tolerability, and Efficacy of Tocilizumab in Patients with Noninfectious Uveitis. *Am. J. Ophthalmol.* **2017**, *183*, 71–80. [CrossRef]
46. Calvo-Río, V.; Santos-Gómez, M.; Calvo, I.; González-Fernández, M.I.; López-Montesinos, B.; Mesquida, M.; Adán, A.; Hernández, M.V.; Maíz, O.; Atanes, A.; et al. Anti-Interleukin-6 Receptor Tocilizumab for Severe Juvenile Idiopathic Arthritis-Associated Uveitis Refractory to Anti-Tumor Necrosis Factor Therapy: A Multicenter Study of Twenty-Five Patients. *Arthritis Rheumatol.* **2017**, *69*, 668–675. [CrossRef]
47. Atienza-Mateo, B.; Calvo-Río, V.; Beltrán, E.; Martínez-Costa, L.; Valls-Pascual, E.; Hernández-Garfella, M.; Atanes, A.; Cordero-Coma, M.; Miquel Nolla, J.; Carrasco-Cubero, C.; et al. Anti-Interleukin 6 Receptor Tocilizumab in Refractory Uveitis Associated with Behçet's Disease: Multicentre Retrospective Study. *Rheumatology* **2018**, *57*, 856–864. [CrossRef]

48. Leclercq, M.; Le Besnerais, M.; Langlois, V.; Girszyn, N.; Benhamou, Y.; Ngo, C.; Levesque, H.; Muraine, M.; Gueudry, J. Tocilizumab for the Treatment of Birdshot Uveitis That Failed Interferon Alpha and Anti-Tumor Necrosis Factor-Alpha Therapy: Two Cases Report and Literature Review. *Clin. Rheumatol.* **2018**, *37*, 849–853. [CrossRef]
49. Leclercq, M.; Andrillon, A.; Maalouf, G.; Sève, P.; Bielefeld, P.; Gueudry, J.; Sené, T.; Moulinet, T.; Rouvière, B.; Sène, D.; et al. Anti–Tumor Necrosis Factor α versus Tocilizumab in the Treatment of Refractory Uveitic Macular Edema. *Ophthalmology* **2022**, *129*, 520–529. [CrossRef]
50. Miserocchi, E.; Modorati, G.; Berchicci, L.; Pontikaki, I.; Meroni, P.; Gerloni, V. Long-Term Treatment with Rituximab in Severe Juvenile Idiopathic Arthritis-Associated Uveitis. *Br. J. Ophthalmol.* **2016**, *100*, 782–786. [CrossRef]
51. Abu El-Asrar, A.M.; Dheyab, A.; Khatib, D.; Struyf, S.; Van Damme, J.; Opdenakker, G. Efficacy of B Cell Depletion Therapy with Rituximab in Refractory Chronic Recurrent Uveitis Associated with Vogt-Koyanagi-Harada Disease. *Ocul. Immunol. Inflamm.* **2022**, *30*, 750–757. [CrossRef] [PubMed]
52. Bolletta, E.; Gozzi, F.; Mastrofilippo, V.; Pipitone, N.; De Simone, L.; Croci, S.; Invernizzi, A.; Adani, C.; Iannetta, D.; Coassin, M.; et al. Efficacy of Rituximab Treatment in Vogt-Koyanagi-Harada Disease Poorly Controlled by Traditional Immunosuppressive Treatment. *Ocul. Immunol. Inflamm.* **2022**, *30*, 1303–1308. [CrossRef] [PubMed]
53. Davatchi, F.; Shams, H.; Rezaipoor, M.; Sadeghi-Abdollahi, B.; Shahram, F.; Nadji, A.; Chams-Davatchi, C.; Akhlaghi, M.; Faezi, T.; Naderi, N. Rituximab in Intractable Ocular Lesions of Behcet's Disease; Randomized Single-Blind Control Study (Pilot Study). *Int. J. Rheum. Dis.* **2010**, *13*, 246–252. [CrossRef] [PubMed]
54. Joshi, L.; Lightman, S.L.; Salama, A.D.; Shirodkar, A.L.; Pusey, C.D.; Taylor, S.R.J. Rituximab in Refractory Ophthalmic Wegener's Granulomatosis: PR3 Titers May Predict Relapse, but Repeat Treatment Can Be Effective. *Ophthalmology* **2011**, *118*, 2498–2503. [CrossRef]
55. Ng, C.C.; Sy, A.; Cunningham, E.T. Rituximab for Non-Infectious Uveitis and Scleritis. *J. Ophthalmic Inflamm. Infect.* **2021**, *11*, 23. [CrossRef] [PubMed]
56. Datta-Mannan, A. Mechanisms Influencing the Pharmacokinetics and Disposition of Monoclonal Antibodies and Peptides. *Drug Metab. Dispos.* **2019**, *47*, 1100–1110. [CrossRef]
57. Pyzik, M.; Sand, K.M.K.; Hubbard, J.J.; Andersen, J.T.; Sandlie, I.; Blumberg, R.S. The Neonatal Fc Receptor (FcRn): A Misnomer? *Front. Immunol.* **2019**, *10*, 1540. [CrossRef]
58. Ternant, D.; Azzopardi, N.; Raoul, W.; Bejan-Angoulvant, T.; Paintaud, G. Influence of Antigen Mass on the Pharmacokinetics of Therapeutic Antibodies in Humans. *Clin. Pharmacokinet.* **2019**, *58*, 169–187. [CrossRef]
59. Ternant, D.; Ducourau, E.; Fuzibet, P.; Vignault, C.; Watier, H.; Lequerré, T.; Le Loët, X.; Vittecoq, O.; Goupille, P.; Mulleman, D.; et al. Pharmacokinetics and Concentration-Effect Relationship of Adalimumab in Rheumatoid Arthritis. *Br. J. Clin. Pharmacol.* **2015**, *79*, 286–297. [CrossRef]
60. Weisman, M.H.; Moreland, L.W.; Furst, D.E.; Weinblatt, M.E.; Keystone, E.C.; Paulus, H.E.; Teoh, L.S.; Velagapudi, R.B.; Noertersheuser, P.A.; Granneman, G.R.; et al. Efficacy, Pharmacokinetic, and Safety Assessment of Adalimumab, a Fully Human Anti-Tumor Necrosis Factor-Alpha Monoclonal Antibody, in Adults with Rheumatoid Arthritis Receiving Concomitant Methotrexate: A Pilot Study. *Clin. Ther.* **2003**, *25*, 1700–1721. [CrossRef]
61. AbbVie Ltd Humira (Adalimumab). *Extension of Indication Variation Assessment Report*; European Medicines Agency: Amsterdam, The Netherlands, 2016.
62. Matsuoka, K.; Hamada, S.; Shimizu, M.; Nanki, K.; Mizuno, S.; Kiyohara, H.; Arai, M.; Sugimoto, S.; Iwao, Y.; Ogata, H.; et al. Factors Contributing to the Systemic Clearance of Infliximab with Long-Term Administration in Japanese Patients with Crohn's Disease: Analysis Using Population Pharmacokinetics. *Int. J. Clin. Pharmacol. Ther.* **2020**, *58*, 89–102. [CrossRef]
63. Ng, C.M.; Bruno, R.; Combs, D.; Davies, B. Population Pharmacokinetics of Rituximab (Anti-CD20 Monoclonal Antibody) in Rheumatoid Arthritis Patients during a Phase II Clinical Trial. *J. Clin. Pharmacol.* **2005**, *45*, 792–801. [CrossRef]
64. Lee, H.; Kimko, H.C.; Rogge, M.; Wang, D.; Nestorov, I.; Peck, C.C. Population Pharmacokinetic and Pharmacodynamic Modeling of Etanercept Using Logistic Regression Analysis. *Clin. Pharmacol. Ther.* **2003**, *73*, 348–365. [CrossRef] [PubMed]
65. Adedokun, O.J.; Xu, Z.; Liao, S.; Strauss, R.; Reinisch, W.; Feagan, B.G.; Sandborn, W.J. Population Pharmacokinetics and Exposure-Response Modeling of Golimumab in Adults with Moderately to Severely Active Ulcerative Colitis. *Clin. Ther.* **2020**, *42*, 157–174. [CrossRef]
66. Sharma, S.; Eckert, D.; Hyams, J.S.; Mensing, S.; Thakkar, R.B.; Robinson, A.M.; Rosh, J.R.; Ruemmele, F.M.; Awni, W.M. Pharmacokinetics and Exposure-Efficacy Relationship of Adalimumab in Pediatric Patients with Moderate to Severe Crohn's Disease: Results from a Randomized, Multicenter, Phase-3 Study. *Inflamm. Bowel Dis.* **2015**, *21*, 783–792. [CrossRef]
67. Fasanmade, A.A.; Adedokun, O.J.; Blank, M.; Zhou, H.; Davis, H.M. Pharmacokinetic Properties of Infliximab in Children and Adults with Crohn's Disease: A Retrospective Analysis of Data from 2 Phase III Clinical Trials. *Clin. Ther.* **2011**, *33*, 946–964. [CrossRef] [PubMed]
68. Wolbink, G.J.; Voskuyl, A.E.; Lems, W.F.; de Groot, E.; Nurmohamed, M.T.; Tak, P.P.; Dijkmans, B.A.C.; Aarden, L. Relationship between Serum Trough Infliximab Levels, Pretreatment C Reactive Protein Levels, and Clinical Response to Infliximab Treatment in Patients with Rheumatoid Arthritis. *Ann. Rheum. Dis.* **2005**, *64*, 704–707. [CrossRef]
69. Curtis, J.R.; Chakravarty, S.D.; Black, S.; Kafka, S.; Xu, S.; Langholff, W.; Parenti, D.; Greenspan, A.; Schwartzman, S. Incidence of Infusion Reactions and Clinical Effectiveness of Intravenous Golimumab Versus Infliximab in Patients with Rheumatoid Arthritis: The Real-World AWARE Study. *Rheumatol. Ther.* **2021**, *8*, 1551–1563. [CrossRef] [PubMed]

70. Leinonen, S.T.; Aalto, K.; Kotaniemi, K.M.; Kivelä, T.T. Anti-Adalimumab Antibodies in Juvenile Idiopathic Arthritis-Related Uveitis. *Clin. Exp. Rheumatol.* **2017**, *35*, 1043–1046.
71. Imaeda, H.; Takahashi, K.; Fujimoto, T.; Bamba, S.; Tsujikawa, T.; Sasaki, M.; Fujiyama, Y.; Andoh, A. Clinical Utility of Newly Developed Immunoassays for Serum Concentrations of Adalimumab and Anti-Adalimumab Antibodies in Patients with Crohn's Disease. *J. Gastroenterol.* **2014**, *49*, 100–109. [CrossRef]
72. Ding, X.; Zhu, R.; Wu, J.; Xue, L.; Gu, M.; Miao, L. Early Adalimumab and Anti-Adalimumab Antibody Levels for Prediction of Primary Nonresponse in Ankylosing Spondylitis Patients. *Clin. Transl. Sci.* **2020**, *13*, 547–554. [CrossRef]
73. Brunelli, J.B.; Silva, C.A.; Pasoto, S.G.; Saa, C.G.S.; Kozu, K.T.; Goldenstein-Schainberg, C.; Leon, E.P.; Vendramini, M.B.G.; Fontoura, N.; Bonfa, E.; et al. Anti-Adalimumab Antibodies Kinetics: An Early Guide for Juvenile Idiopathic Arthritis (JIA) Switching. *Clin. Rheumatol.* **2020**, *39*, 515–521. [CrossRef]
74. Skrabl-Baumgartner, A.; Erwa, W.; Muntean, W.; Jahnel, J. Anti-Adalimumab Antibodies in Juvenile Idiopathic Arthritis: Frequent Association with Loss of Response. *Scand. J. Rheumatol.* **2015**, *44*, 359–362. [CrossRef]
75. Breedveld, F.C.; Weisman, M.H.; Kavanaugh, A.F.; Cohen, S.B.; Pavelka, K.; van Vollenhoven, R.; Sharp, J.; Perez, J.L.; Spencer-Green, G.T. The PREMIER Study: A Multicenter, Randomized, Double-Blind Clinical Trial of Combination Therapy with Adalimumab plus Methotrexate versus Methotrexate Alone or Adalimumab Alone in Patients with Early, Aggressive Rheumatoid Arthritis Who Had Not Had Previous Methotrexate Treatment. *Arthritis Rheum.* **2006**, *54*, 26–37. [CrossRef] [PubMed]
76. Lindström, U.; Di Giuseppe, D.; Delcoigne, B.; Glintborg, B.; Möller, B.; Ciurea, A.; Pombo-Suarez, M.; Sanchez-Piedra, C.; Eklund, K.; Relas, H.; et al. Effectiveness and Treatment Retention of TNF Inhibitors When Used as Monotherapy versus Comedication with CsDMARDs in 15 332 Patients with Psoriatic Arthritis. Data from the EuroSpA Collaboration. *Ann. Rheum. Dis.* **2021**, *80*, 1410–1418. [CrossRef] [PubMed]
77. Ducourau, E.; Rispens, T.; Samain, M.; Dernis, E.; Le Guilchard, F.; Andras, L.; Perdriger, A.; Lespessailles, E.; Martin, A.; Cormier, G.; et al. Methotrexate Effect on Immunogenicity and Long-Term Maintenance of Adalimumab in Axial Spondyloarthritis: A Multicentric Randomised Trial. *RMD Open* **2020**, *6*, e001047. [CrossRef]
78. van der Heijde, D.; Klareskog, L.; Rodriguez-Valverde, V.; Codreanu, C.; Bolosiu, H.; Melo-Gomes, J.; Tornero-Molina, J.; Wajdula, J.; Pedersen, R.; Fatenejad, S.; et al. Comparison of Etanercept and Methotrexate, Alone and Combined, in the Treatment of Rheumatoid Arthritis: Two-Year Clinical and Radiographic Results from the TEMPO Study, a Double-Blind, Randomized Trial. *Arthritis Rheum.* **2006**, *54*, 1063–1074. [CrossRef] [PubMed]
79. Chatzidionysiou, K.; Lie, E.; Nasonov, E.; Lukina, G.; Hetland, M.L.; Tarp, U.; van Riel, P.L.C.M.; Nordström, D.C.; Gomez-Reino, J.; Pavelka, K.; et al. Effectiveness of Disease-Modifying Antirheumatic Drug Co-Therapy with Methotrexate and Leflunomide in Rituximab-Treated Rheumatoid Arthritis Patients: Results of a 1-Year Follow-up Study from the CERERRA Collaboration. *Ann. Rheum. Dis.* **2012**, *71*, 374–377. [CrossRef]
80. Colombel, J.F.; Sandborn, W.J.; Reinisch, W.; Mantzaris, G.J.; Kornbluth, A.; Rachmilewitz, D.; Lichtiger, S.; D'Haens, G.; Diamond, R.H.; Broussard, D.L.; et al. Infliximab, Azathioprine, or Combination Therapy for Crohn's Disease. *N. Engl. J. Med.* **2010**, *362*, 1383–1395. [CrossRef]
81. Dulai, P.S.; Siegel, C.A.; Peyrin-Biroulet, L. Anti-Tumor Necrosis Factor-α Monotherapy versus Combination Therapy with an Immunomodulator in IBD. *Gastroenterol. Clin. N. Am.* **2014**, *43*, 441–456. [CrossRef]
82. Klein, A.; Becker, I.; Minden, K.; Foeldvari, I.; Haas, J.P.; Horneff, G. Adalimumab versus Adalimumab and Methotrexate for the Treatment of Juvenile Idiopathic Arthritis: Long-Term Data from the German BIKER Registry. *Scand. J. Rheumatol.* **2019**, *48*, 95–104. [CrossRef]
83. Feuerstein, J.D.; Isaacs, K.L.; Schneider, Y.; Siddique, S.M.; Falck-Ytter, Y.; Singh, S.; Chachu, K.; Day, L.; Lebwohl, B.; Muniraj, T.; et al. AGA Clinical Practice Guidelines on the Management of Moderate to Severe Ulcerative Colitis. *Gastroenterology* **2020**, *158*, 1450–1461. [CrossRef]
84. Pouw, M.F.; Krieckaert, C.L.; Nurmohamed, M.T.; van der Kleij, D.; Aarden, L.; Rispens, T.; Wolbink, G. Key Findings towards Optimising Adalimumab Treatment: The Concentration–Effect Curve. *Ann. Rheum. Dis.* **2015**, *74*, 513–518. [CrossRef] [PubMed]
85. Qiu, Y.; Mao, R.; Chen, B.; Zhang, S.; Guo, J.; He, Y.; Zeng, Z.; Ben-Horin, S.; Chen, M. Effects of Combination Therapy with Immunomodulators on Trough Levels and Antibodies Against Tumor Necrosis Factor Antagonists in Patients with Inflammatory Bowel Disease: A Meta-Analysis. *Clin. Gastroenterol. Hepatol.* **2017**, *15*, 1359–1372.e6. [CrossRef]
86. Yao, J.; Jiang, X.; You, J.H.S. Proactive Therapeutic Drug Monitoring of Adalimumab for Pediatric Crohn's Disease Patients: A Cost-effectiveness Analysis. *J. Gastroenterol. Hepatol.* **2021**, *36*, 2397–2407. [CrossRef] [PubMed]
87. Gómez-Arango, C.; Gorostiza, I.; Úcar, E.; García-Vivar, M.L.; Pérez, C.E.; De Dios, J.R.; Alvarez, B.; Ruibal-Escribano, A.; Stoye, C.; Vasques, M.; et al. Cost-Effectiveness of Therapeutic Drug Monitoring-Guided Adalimumab Therapy in Rheumatic Diseases: A Prospective, Pragmatic Trial. *Rheumatol. Ther.* **2021**, *8*, 1323–1339. [CrossRef]
88. Fernandes, S.R.; Bernardo, S.; Simões, C.; Gonçalves, A.R.; Valente, A.; Baldaia, C.; Moura Santos, P.; Correia, L.A.; Tato Marinho, R. Proactive Infliximab Drug Monitoring Is Superior to Conventional Management in Inflammatory Bowel Disease. *Inflamm. Bowel Dis.* **2020**, *26*, 263–270. [CrossRef]
89. Syversen, S.W.; Goll, G.L.; Jørgensen, K.K.; Sandanger, Ø.; Sexton, J.; Olsen, I.C.; Gehin, J.E.; Warren, D.J.; Brun, M.K.; Klaasen, R.A.; et al. Effect of Therapeutic Drug Monitoring vs Standard Therapy During Infliximab Induction on Disease Remission in Patients with Chronic Immune-Mediated Inflammatory Diseases: A Randomized Clinical Trial. *JAMA* **2021**, *325*, 1744–1754. [CrossRef]

90. Ricciuto, A.; Dhaliwal, J.; Walters, T.D.; Griffiths, A.M.; Church, P.C. Clinical Outcomes with Therapeutic Drug Monitoring in Inflammatory Bowel Disease: A Systematic Review with Meta-Analysis. *J. Crohns Colitis* **2018**, *12*, 1302–1315. [CrossRef] [PubMed]
91. D'Haens, G.; Vermeire, S.; Lambrecht, G.; Baert, F.; Bossuyt, P.; Pariente, B.; Buisson, A.; Bouhnik, Y.; Filippi, J.; Vander Woude, J.; et al. Increasing Infliximab Dose Based on Symptoms, Biomarkers, and Serum Drug Concentrations Does Not Increase Clinical, Endoscopic, and Corticosteroid-Free Remission in Patients with Active Luminal Crohn's Disease. *Gastroenterology* **2018**, *154*, 1343–1351.e1. [CrossRef]
92. Sejournet, L.; Kerever, S.; Mathis, T.; Kodjikian, L.; Jamilloux, Y.; Seve, P. Therapeutic Drug Monitoring Guides the Management of Patients with Chronic Non-Infectious Uveitis Treated with Adalimumab: A Retrospective Study. *Br. J. Ophthalmol.* **2021**, *106*, 1380–1386. [CrossRef] [PubMed]
93. Sugita, S.; Yamada, Y.; Mochizuki, M. Relationship between Serum Infliximab Levels and Acute Uveitis Attacks in Patients with Behcet Disease. *Br. J. Ophthalmol.* **2011**, *95*, 549–552. [CrossRef] [PubMed]
94. Assa, A.; Matar, M.; Turner, D.; Broide, E.; Weiss, B.; Ledder, O.; Guz-Mark, A.; Rinawi, F.; Cohen, S.; Topf-Olivestone, C.; et al. Proactive Monitoring of Adalimumab Trough Concentration Associated with Increased Clinical Remission in Children with Crohn's Disease Compared with Reactive Monitoring. *Gastroenterology* **2019**, *157*, 985–996.e2. [CrossRef] [PubMed]
95. Syed, N.; Tolaymat, M.; Brown, S.A.; Sivasailam, B.; Cross, R.K. Proactive Drug Monitoring Is Associated with Higher Persistence to Infliximab and Adalimumab Treatment and Lower Healthcare Utilization Compared with Reactive and Clinical Monitoring. *Crohns Colitis 360* **2020**, *2*, otaa050. [CrossRef]
96. Papamichael, K.; Cheifetz, A.S. Is It Prime Time for Proactive Therapeutic Drug Monitoring of Anti-Tumor Necrosis Factor Therapy in Inflammatory Bowel Disease? *Gastroenterology* **2019**, *157*, 922–924. [CrossRef]
97. Constantin, T.; Foeldvari, I.; Anton, J.; de Boer, J.; Czitrom -Guillaume, S.; Edelsten, C.; Gepstein, R.; Heiligenhaus, A.; Pilkington, C.A.; Simonini, G.; et al. Consensus-Based Recommendations for the Management of Uveitis Associated with Juvenile Idiopathic Arthritis: The SHARE Initiative. *Ann. Rheum. Dis.* **2018**, *77*, 1107–1117. [CrossRef]
98. Bou, R.; Adán, A.; Borrás, F.; Bravo, B.; Calvo, I.; De Inocencio, J.; Díaz, J.; Escudero, J.; Fonollosa, A.; de Vicuña, C.G.; et al. Clinical Management Algorithm of Uveitis Associated with Juvenile Idiopathic Arthritis: Interdisciplinary Panel Consensus. *Rheumatol. Int.* **2015**, *35*, 777–785. [CrossRef]
99. Kiely, P.D.W. Biologic Efficacy Optimization—A Step towards Personalized Medicine. *Rheumatology* **2016**, *55*, 780–788. [CrossRef]
100. Papamichael, K.; Cheifetz, A.S. Use of Anti-TNF Drug Levels to Optimise Patient Management. *Frontline Gastroenterol.* **2016**, *7*, 289–300. [CrossRef]
101. Hahn, A.; Burrell, A.; Chaney, H.; Sami, I.; Koumbourlis, A.C.; Freishtat, R.J.; Zemanick, E.T.; Louie, S.; Crandall, K.A. Importance of Beta-Lactam Pharmacokinetics and Pharmacodynamics on the Recovery of Microbial Diversity in the Airway of Persons with Cystic Fibrosis. *J. Investig. Med.* **2021**, *69*, 1350–1359. [CrossRef]
102. Veiga, R.P.; Paiva, J.-A. Pharmacokinetics–Pharmacodynamics Issues Relevant for the Clinical Use of Beta-Lactam Antibiotics in Critically Ill Patients. *Crit. Care* **2018**, *22*, 233. [CrossRef]
103. Bland, C.M.; Pai, M.P.; Lodise, T.P. Reappraisal of Contemporary Pharmacokinetic and Pharmacodynamic Principles for Informing Aminoglycoside Dosing. *Pharmacother. J. Hum. Pharmacol. Drug Ther.* **2018**, *38*, 1229–1238. [CrossRef]
104. Bastida, G.; Marín-Jiménez, I.; Forés, A.; García-Planella, E.; Argüelles-Arias, F.; Tagarro, I.; Fernandez-Nistal, A.; Montoto, C.; Aparicio, J.; Aguas, M.; et al. Treatment Patterns and Intensification within 5 Year of Follow-up of the First-Line Anti-TNFα Used for the Treatment of IBD: Results from the VERNE Study. *Dig. Liver Dis.* **2022**, *54*, 76–83. [CrossRef]
105. Krieckaert, C.; Hernández-Breijo, B.; Gehin, J.E.; le Mélédo, G.; Balsa, A.; Jani, M.; Mulleman, D.; Navarro-Compan, V.; Wolbink, G.; Isaac, J.; et al. Therapeutic Drug Monitoring of Biopharmaceuticals in Inflammatory Rheumatic and Musculoskeletal Disease: A Systematic Literature Review Informing EULAR Points to Consider. *RMD Open* **2022**, *8*, e002216. [CrossRef] [PubMed]
106. Gaudana, R.; Ananthula, H.K.; Parenky, A.; Mitra, A.K. Ocular Drug Delivery. *AAPS J.* **2010**, *12*, 348–360. [CrossRef] [PubMed]
107. Varela-Fernández, R.; Díaz-Tomé, V.; Luaces-Rodríguez, A.; Conde-Penedo, A.; García-Otero, X.; Luzardo-Álvarez, A.; Fernández-Ferreiro, A.; Otero-Espinar, F. Drug Delivery to the Posterior Segment of the Eye: Biopharmaceutic and Pharmacokinetic Considerations. *Pharmaceutics* **2020**, *12*, 269. [CrossRef] [PubMed]
108. Barar, J.; Aghanejad, A.; Fathi, M.; Omidi, Y. Advanced Drug Delivery and Targeting Technologies for the Ocular Diseases. *BioImpacts* **2016**, *6*, 49–67. [CrossRef]
109. Caruso, A.; Füth, M.; Alvarez-Sánchez, R.; Belli, S.; Diack, C.; Maass, K.F.; Schwab, D.; Kettenberger, H.; Mazer, N.A. Ocular Half-Life of Intravitreal Biologics in Humans and Other Species: Meta-Analysis and Model-Based Prediction. *Mol. Pharm.* **2020**, *17*, 695–709. [CrossRef] [PubMed]
110. Shivva, V.; Boswell, C.A.; Rafidi, H.; Kelley, R.F.; Kamath, A.V.; Crowell, S.R. Antibody Format and Serum Disposition Govern Ocular Pharmacokinetics of Intravenously Administered Protein Therapeutics. *Front. Pharmacol.* **2021**, *12*, 601569. [CrossRef] [PubMed]
111. Simsek, M.; Cakar Ozdal, P.; Akbiyik, F.; Citirik, M.; Berker, N.; Ozdamar Erol, Y.; Yilmazbas, P. Aqueous Humor IL-8, IL-10, and VEGF Levels in Fuchs' Uveitis Syndrome and Behçet's Uveitis. *Int. Ophthalmol.* **2019**, *39*, 2629–2636. [CrossRef]

112. Fukunaga, H.; Kaburaki, T.; Shirahama, S.; Tanaka, R.; Murata, H.; Sato, T.; Takeuchi, M.; Tozawa, H.; Urade, Y.; Katsura, M.; et al. Analysis of Inflammatory Mediators in the Vitreous Humor of Eyes with Pan-Uveitis According to Aetiological Classification. *Sci. Rep.* **2020**, *10*, 2783. [CrossRef] [PubMed]
113. Wang, Y.; Liu, C.-H.; Ji, T.; Mehta, M.; Wang, W.; Marino, E.; Chen, J.; Kohane, D.S. Intravenous Treatment of Choroidal Neovascularization by Photo-Targeted Nanoparticles. *Nat. Commun.* **2019**, *10*, 804. [CrossRef]
114. Lamminsalo, M.; Karvinen, T.; Subrizi, A.; Urtti, A.; Ranta, V.-P. Extended Pharmacokinetic Model of the Intravitreal Injections of Macromolecules in Rabbits. Part 2: Parameter Estimation Based on Concentration Dynamics in the Vitreous, Retina, and Aqueous Humor. *Pharm. Res.* **2020**, *37*, 226. [CrossRef]
115. García-Quintanilla, L.; Luaces-Rodríguez, A.; Gil-Martínez, M.; Mondelo-García, C.; Maroñas, O.; Mangas-Sanjuan, V.; González-Barcia, M.; Zarra-Ferro, I.; Aguiar, P.; Otero-Espinar, F.J.; et al. Pharmacokinetics of Intravitreal Anti-VEGF Drugs in Age-Related Macular Degeneration. *Pharmaceutics* **2019**, *11*, 365. [CrossRef] [PubMed]
116. Hamza, M.M.E.; Macky, T.A.; Sidky, M.K.; Ragab, G.; Soliman, M.M. Intravitreal Infliximab in Refractory Uveitis in Behcet's Disease: A Safety and Efficacy Clinical Study. *Retina* **2016**, *36*, 2399–2408. [CrossRef] [PubMed]
117. Farvardin, M.; Afarid, M.; Mehryar, M.; Hosseini, H. Intravitreal Infliximab for the Treatment of Sight-Threatening Chronic Noninfectious Uveitis. *Retina* **2010**, *30*, 1530–1535. [CrossRef]
118. Refaat, M.; Abdullatif, A.M.; Hamza, M.M.; Macky, T.A.; El-Agha, M.-S.H.; Ragab, G.; Soliman, M.M. Monthly Intravitreal Infliximab in Behçet's Disease Active Posterior Uveitis: A Long-Term Safety Study. *Retina* **2021**, *41*, 1739–1747. [CrossRef]
119. Giganti, M.; Beer, P.M.; Lemanski, N.; Hartman, C.; Schartman, J.; Falk, N. Adverse Events after Intravitreal Infliximab (Remicade). *Retina* **2010**, *30*, 71–80. [CrossRef]
120. Hamam, R.N.; Barikian, A.W.; Antonios, R.S.; Abdulaal, M.R.; Alameddine, R.M.; El Mollayess, G.; Mansour, A.M. Intravitreal Adalimumab in Active Noninfectious Uveitis: A Pilot Study. *Ocul. Immunol. Inflamm.* **2014**, *24*, 319–326. [CrossRef]
121. Kheir, W.J.; Mehanna, C.-J.; Abdul Fattah, M.; Al Ghadban, S.; El Sabban, M.; Mansour, A.M.; Hamam, R.N. Intravitreal Adalimumab for the Control of Breakthrough Intraocular Inflammation. *Ocul. Immunol. Inflamm.* **2018**, *26*, 1206–1211. [CrossRef]
122. Androudi, S.; Tsironi, E.; Kalogeropoulos, C.; Theodoridou, A.; Brazitikos, P. Intravitreal Adalimumab for Refractory Uveitis-Related Macular Edema. *Ophthalmology* **2010**, *117*, 1612–1616. [CrossRef]
123. Tsilimbaris, M.; Diakonis, V.F.; Naoumidi, I.; Charisis, S.; Kritikos, I.; Chatzithanasis, G.; Papadaki, T.; Plainis, S. Evaluation of Potential Retinal Toxicity of Adalimumab (Humira). *Graefes Arch. Clin. Exp. Ophthalmol.* **2009**, *247*, 1119–1125. [CrossRef]
124. Manzano, R.P.A.; Peyman, G.A.; Carvounis, P.E.; Damico, F.M.; Aguiar, R.G.; Ioshimoto, G.L.; Ventura, D.F.; Cursino, S.T.; Takahashi, W. Toxicity of High-Dose Intravitreal Adalimumab (Humira) in the Rabbit. *J. Ocul. Pharmacol. Ther.* **2011**, *27*, 327–331. [CrossRef] [PubMed]
125. Manzano, R.P.A.; Peyman, G.A.; Carvounis, P.E.; Kivilcim, M.; Khan, P.; Chevez-Barrios, P.; Takahashi, W. Ocular Toxicity of Intravitreous Adalimumab (Humira) in the Rabbit. *Graefes Arch. Clin. Exp. Ophthalmol.* **2008**, *246*, 907–911. [CrossRef]
126. García-Otero, X.; Mondelo-García, C.; Bandín-Vilar, E.; Gómez-Lado, N.; Silva-Rodríguez, J.; Rey-Bretal, D.; Victoria Otero-Espinar, M.; Adan, A.; González-Barcia, M.; Aguiar, P.; et al. PET Study of Intravitreal Adalimumab Pharmacokinetics in a Uveitis Rat Model. *Int. J. Pharm.* **2022**, *627*, 122261. [CrossRef] [PubMed]
127. Chung, E.S.; Packer, M.; Lo, K.H.; Fasanmade, A.A.; Willerson, J.T. Anti-TNF Therapy Against Congestive Heart Failure Investigators Randomized, Double-Blind, Placebo-Controlled, Pilot Trial of Infliximab, a Chimeric Monoclonal Antibody to Tumor Necrosis Factor-Alpha, in Patients with Moderate-to-Severe Heart Failure: Results of the Anti-TNF Therapy Against Congestive Heart Failure (ATTACH) Trial. *Circulation* **2003**, *107*, 3133–3140. [CrossRef] [PubMed]
128. Lima, B.R.; Nussenblatt, R.B.; Sen, H.N. Pharmacogenetics of Drugs Used in the Treatment of Ocular Inflammatory Diseases. *Expert Opin. Drug Metab. Toxicol.* **2013**, *9*, 875–882. [CrossRef]
129. Liu, B.; Sen, H.N.; Nussenblatt, R. Susceptibility Genes and Pharmacogenetics in Ocular Inflammatory Disorders. *Ocul. Immunol. Inflamm.* **2012**, *20*, 315–323. [CrossRef] [PubMed]
130. Bek, S.; Bojesen, A.B.; Nielsen, J.V.; Sode, J.; Bank, S.; Vogel, U.; Andersen, V. Systematic Review and Meta-Analysis: Pharmacogenetics of Anti-TNF Treatment Response in Rheumatoid Arthritis. *Pharmacogenomics J.* **2017**, *17*, 403–411. [CrossRef]
131. Bank, S.; Andersen, P.S.; Burisch, J.; Pedersen, N.; Roug, S.; Galsgaard, J.; Turino, S.Y.; Brodersen, J.B.; Rashid, S.; Rasmussen, B.K.; et al. Associations between Functional Polymorphisms in the NFκB Signaling Pathway and Response to Anti-TNF Treatment in Danish Patients with Inflammatory Bowel Disease. *Pharmacogenomics J.* **2014**, *14*, 526–534. [CrossRef]
132. Bank, S.; Julsgaard, M.; Abed, O.K.; Burisch, J.; Broder Brodersen, J.; Pedersen, N.K.; Gouliaev, A.; Ajan, R.; Nytoft Rasmussen, D.; Honore Grauslund, C.; et al. Polymorphisms in the NFkB, TNF-Alpha, IL-1beta, and IL-18 Pathways Are Associated with Response to Anti-TNF Therapy in Danish Patients with Inflammatory Bowel Disease. *Aliment. Pharmacol. Ther.* **2019**, *49*, 890–903. [CrossRef] [PubMed]
133. Hässler, S.; Bachelet, D.; Duhaze, J.; Szely, N.; Gleizes, A.; Hacein-Bey Abina, S.; Aktas, O.; Auer, M.; Avouac, J.; Birchler, M.; et al. Clinicogenomic Factors of Biotherapy Immunogenicity in Autoimmune Disease: A Prospective Multicohort Study of the ABIRISK Consortium. *PLoS Med.* **2020**, *17*, e1003348. [CrossRef]
134. Bartelds, G.M.; Wijbrandts, C.A.; Nurmohamed, M.T.; Wolbink, G.J.; de Vries, N.; Tak, P.P.; Dijkmans, B.A.C.; Crusius, J.B.A.; vand der Horst-Bruinsma, I.E. Anti-Adalimumab Antibodies in Rheumatoid Arthritis Patients Are Associated with Interleukin-10 Gene Polymorphisms. *Arthritis Rheum.* **2009**, *60*, 2541–2542. [CrossRef]

135. Pratesi, S.; Nencini, F.; Grosso, F.; Dies, L.; Bormioli, S.; Cammelli, D.; Maggi, E.; Matucci, A.; Vultaggio, A. ABIRISK Consortium T Cell Response to Infliximab in Exposed Patients: A Longitudinal Analysis. *Front. Immunol.* **2019**, *9*, 3113. [CrossRef]
136. Sazonovs, A.; Kennedy, N.A.; Moutsianas, L.; Heap, G.A.; Rice, D.L.; Reppell, M.; Bewshea, C.M.; Chanchlani, N.; Walker, G.J.; Perry, M.H.; et al. *HLA-DQA1*05* Carriage Associated with Development of Anti-Drug Antibodies to Infliximab and Adalimumab in Patients with Crohn's Disease. *Gastroenterology* **2020**, *158*, 189–199. [CrossRef] [PubMed]
137. Andre, F.; Ismaila, N.; Allison, K.H.; Barlow, W.E.; Collyar, D.E.; Damodaran, S.; Henry, N.L.; Jhaveri, K.; Kalinsky, K.; Kuderer, N.M.; et al. Biomarkers for Adjuvant Endocrine and Chemotherapy in Early-Stage Breast Cancer: ASCO Guideline Update. *J. Clin. Oncol.* **2022**, *40*, 1816–1837. [CrossRef] [PubMed]

MDPI AG
Grosspeteranlage 5
4052 Basel
Switzerland
Tel.: +41 61 683 77 34

Pharmaceutics Editorial Office
E-mail: pharmaceutics@mdpi.com
www.mdpi.com/journal/pharmaceutics

Academic Open
Access Publishing

mdpi.com

ISBN 978-3-7258-2022-1